Carl_G_190x270_mm_blokki_FINAL.indd 1 06-Aug-23 1:53:28 PM

SOCIETAS SCIENTIARUM FENNICA

Finska Vetenskaps-Societeten, grundad 1838, är Finlands äldsta vetenskapsakademi, som publicerar forskning, utdelar stipendier och pris, tar initiativ och håller möten med föredrag. Societeten inledde 1996 ett publiceringssamarbete med syskonakademin Suomalainen Tiedeakatemia.

Vuonna 1838 perustettu Suomen Tiedeseura on Suomen vanhin tiedeakatemia, joka julkaisee tutkimuksia, myöntää tutkimusavustuksia ja palkintoja, tekee aloitteita ja järjestää kokouksia. Seura aloitti 1996 julkaisuyhteistyön sisarjärjestönsä Suomalaisen Tiedeakatemian kanssa.

The Finnish Society of Sciences and Letters, founded in 1838, is the oldest scholarly academy of Finland. It publishes research, awards research grants and prizes, takes initiatives and organizes meetings. In 1996 the Society established cooperation with its sister organizarion the Finnish Academy of Sciences and Letters.

Redaktör – Toimittaja – Editor
Professor Mats Gyllenberg
Nadine Nousiainen
Finska Vetenskaps-Societeten/Suomen Tiedeseura/
Finnish Society of Sciences and Letters
Pohjoinen Makasiinikatu/Norra Magasinsgatan 7 A
FI-00130 Helsinki/Helsingfors

Graphic Design: Minna Etsalo

Carl_G_190x270_mm_blokki_FINAL.indd 2 06-Aug-23 1:53:28 PM

Selected Papers of
Carl G. Gahmberg

(with commentaries)

CELL MEMBRANES AND CELL ADHESION

Helsinki 2023

Carl_G_190x270_mm_blokki_FINAL.indd 3 06-Aug-23 1:53:28 PM

Carl_G_190x270_mm_blokki_FINAL.indd 4 06-Aug-23 1:53:28 PM

The articles in this book have been reprinted with permission from the following journals and publishing companies:

Biochemistry, American Chemical Society.

Biochimica et Biophysica Acta, Elsevier.

Blood, Elsevier.

Current Opinion in Cell Biology, Elsevier.

EMBO Journal, Wiley Online Library.

European Journal of Immunology, Wiley Online Library.

FEBS Letters, Wiley Online Library.

Glycobiology, Oxford University Press.

International Journal of Cancer, Wiley Online Library.

Journal of Biological Chemistry, Elsevier.

Journal of Cell Biology, Rockefeller University Press.

Journal of Experimental Medicine, Rockefeller University Press.

Journal of Immunology. Copyright 1999. The American Association of Immunologists, Inc.

Nature Biotechnology, Springer Nature.

Nature Immunology, Springer Nature.

Nature Medicine, Springer Nature.

Nature, Springer Nature.

Proceedings of the National Academy of Science USA, US National Academy of Sciences.

Scandinavian Journal of Immunology, Wiley Online Library.

Science, The American Association for the Advancement of Science.

Trends in Biochemical Sciences, Elsevier.

Virology, Elsevier.

Some of the articles are under the Creative Commons Attribution License (CC-BY) https://creativecommons.org/licenses/by/4.0/

Carl_G_190x270_mm_blokki_FINAL.indd 5 06-Aug-23 1:53:28 PM

Carl G. Gahmberg

Carl G. Gahmberg was born in Helsinki, Finland in 1942, and graduated from high school in 1961. He had excellent teachers in mathematics, physics and biology, got interested in the natural world, and began ringing birds. Another interest was collecting butterflies. He even had a muskrat one winter at home in the centre of Helsinki. Another time he had a red fox pup for a week. The family´s hunting dogs were excited, but they did it no harm. After high school, he passed the entrance course to the Medical Faculty of the University of Helsinki. Then followed the military service for 11 months and in 1962, he began the studies at the university. During the undergraduate studies, he became interested in biochemistry, and he set up paper chromatography for separation of amino acids in the bathtub at home. His mother was evidently very tolerant, permitting the strong odour of the organic solvents at home. During the student years, he was active in student organizations and acted as chairman of the Thorax Medical Students Society, and as a member of the board of the Helsinki University Student Union. The student uproars in 1968 including the occupation of their own Old Student House gave lasting memories. He finished the basic medical training in 1968. At the end of the medical studies, it was possible to spend some time in a research laboratory of the university, and he chose to work with Dr. Kai Simons. Kai also had a medical background, and he had recently returned from a postdoctoral fellowship in the USA. He was setting up a small research group at the Department of Bacteriology and Immunology, University of Helsinki. The group included Ari Helenius and Henrik Garoff. Both of them later became successful scientists. Ari and Henrik first studied serum lipoproteins, but rather soon switched to studies on Semliki

Carl_G_190x270_mm_blokki_FINAL.indd 6 06-Aug-23 1:53:28 PM

Forest Virus as a cell membrane model. Together with the research groups of Ossi Renkonen, a lipid chemist, and the virologist Leevi Kääriäinen, Kai formed a consortium, which at that time was rather unusual. The Semliki Forest virus was grown in baby hamster kidney fibroblasts (BHK21), and matures by budding at the plasma membrane. Carl´s responsibility was to isolate the plasma membrane from non-infected cells and characterize the molecular components. After finishing the doctoral thesis in 1971, he got a NIH postdoctoral fellowship and joined Professor Sen-itiroh Hakomori´s laboratory at the University of Washington in 1972. In addition to science, there was time for crayfish and crab fishing. With Roger Laine, a fellow postdoc with Finnish ancestry, they went deer and elk hunting, and were quite successful. In 1974, Carl returned to the University of Helsinki, to the Department of Bacteriology and Immunology. He early on obtained some small grants, and set up a research group. This included one technician, and two part-time students. At the same time, Leif Andersson returned to the Department of Pathology, located in the same building. He had been a postdoctoral fellow at Uppsala University in Sweden, where he worked in the group of Hans Wigzell, a famous immunologist, and later rector of the Karolinska Institute. Leif and Carl formed a close scientific collaboration, with the aim to study blood cell surfaces. In 1979, Carl got the professorship of biochemistry and pharmaceutical chemistry at the Åbo Akademi University in western Finland. Kai Simons obtained the distinguished A.I. Virtanen chair of biochemistry at the University of Helsinki, but he had already moved to the recently established EMBL laboratory in Heidelberg, Germany. He never took up the position in Helsinki, and Carl was in 1981 appointed to the professorship and head of the Department of Biochemistry, University of Helsinki. He retired from the position in 2010, but continued as professor emeritus after that. In 1988-1989, He had a visiting fellowship at the La Jolla Cancer Research Foundation in San Diego.

Carl G. Gahmberg, has won several prizes and awards. He obtained the Gustaf Komppa Prize for the best thesis in chemistry in Finland in 1971, the Norwegian Anders Jahre Prize in 1981, the 150-year Prize of the Finnish Medical Society in 1985, the Äyräpää Prize in Medicine 1997, the Runeberg Prize in 2010, and the Liv och Hälsa 75-year Prize in 2017. He became the Professor of the Year in Finland in 1995.

He is a member of EMBO since 1980, the Finnish Academy of Science and Letters (1982), the Finnish Society of Sciences and Letters (1983), World Cultural Council (1984), Academia Europaea (1989), the Royal Swedish Academy of Sciences (2007) and the Royal Society of Arts and Sciences, Gothenburg (2008). He acted as the permanent secretary of the Finnish Society of Science and Letters 1992-2018.

Carl G. Gahmberg is Commander of the Order of the Finnish Lion (2002), Chevalier d´Ordre des Palmes Académique, France (2009), Commander of the White Rose of Finland (2012), honorary member of the Finnish Medical Society (2010), and honorary member of the Finnish Society of Sciences and Letters (2018). Currently he is chancellor of Åbo Akademi University.

Carl_G_190x270_mm_blokki_FINAL.indd 7 06-Aug-23 1:53:28 PM

Contents

Preface 15

Part I
Cell surface glycoproteins 17

Introduction 18

Comments on Papers 1 to 18 19

1. Gahmberg, C.G., Simons, K., Renkonen, O. and Kääriäinen, L. (1972) Exposure of proteins and lipids in the Semliki Forest virus membrane. *Virology* **50**, 259-262.
2. Gahmberg, C.G. and Hakomori, S. (1973) External labeling of cell surface galactose and galactosamine in glycolipid and glycoprotein of human erythrocytes. *J. Biol. Chem.* **248**, 4311-4317.
3. Gahmberg, C.G. and Hakomori, S. (1973) Altered growth behavior of malignant cells associated with changes in externally labelled glycoprotein and glycolipid. *Proc. Natl. Acad. Sci. USA*. **70**, 3329-3333.
4. Gahmberg, C.G., Kiehn, D. and Hakomori, S. (1974) Changes in surface-labelled galactoprotein and in glycolipid concentrations in cells transformed by a temperature-sensitive polyoma virus mutant. *Nature* **248**, 413-415.
5. Gahmberg, C.G. (1976) External labelling of erythrocyte glycoproteins. Studies with galactose oxidase and fluorography. *J. Biol. Chem*. **251**, 510-515.
6. Gahmberg, C.G., Myllylä, G., Leikola, J., Pirkola, A. and Nordling, S. (1976) Absence of the major sialoglycoprotein in the membrane of human En(a-) erythrocytes and increased glycosylation of band 3. *J. Biol. Chem*. **251**, 6108-6116.
7. Gahmberg, C.G. and Andersson, L.C. (1977) Selective radioactive labelling of cell surface sialoglycoproteins by periodate-tritiated borohydride. *J. Biol. Chem*. **252**, 5888-5894.
8. Gahmberg, C.G., Häyry, P. and Andersson, L.C. (1976) Characterization of surface glycoproteins of mouse lymphoid cells. *J. Cell Biol*. **68**, 642-653.

Carl_G_190x270_mm_blokki_FINAL.indd 8 06-Aug-23 1:53:28 PM

9. Andersson, L.C. and Gahmberg, C.G. (1978) Surface glycoproteins of human white blood cells. Analysis by surface labelling. *Blood* **52**, 57-67.

10. Andersson, L.C., Gahmberg, C.G., Kimura, A.K. and Wigzell, H. (1978) Activated human T lymphocytes display new surface glycoproteins. *Proc. Natl. Acad. Sci. USA*. **75**, 3455-3458.

11. Gahmberg, C.G., Nilsson, K. and Andersson, L.C. (1979) Specific changes in the surface glycoprotein pattern of the human promyelocytic leukemia cell line HL-60 during morphological and functional differentiation. *Proc. Natl. Acad. Sci. USA*. **76**, 4087-4091.

12. Mustelin, T., Pessa-Morikawa, T., Autero, M., Gassman, M., Gahmberg, C.G., Andersson, L.C. and Burn, P. (1992) Regulation of the pp.59^{fyn} tyrosine kinase by the CD45 phosphotyrosine phosphatase. *Eur. J. Immunol*. **22**, 1173-1178.

13. Gahmberg, C.G. and Andersson, L.C. (1978) Leukocyte surface origin of human α1-acid glycoprotein (orosomucoid). *J. Exp. Med*. **148**, 507-521.

14. Gahmberg, C.G., Jokinen, M. and Andersson, L.C. (1978) Expression of the major sialoglycoprotein (glycophorin) on erythroid cells in human bone marrow. *Blood* **52**, 379-387.

15. Andersson, L.C., Nilsson, K. and Gahmberg, C.G. (1979) K562- a human erythroleukemic cell line. *Int. J. Cancer* **23**, 143-147.

16. Andersson, L.C., Jokinen, M. and Gahmberg, C.G. (1979) Induction of erythroid differentiation in the human leukemia cell line K562. *Nature* **278**, 364-365.

17. Jokinen, M., Gahmberg, C.G. and Andersson, L.C. (1979) Biosynthesis of the major human red cell sialoglycoprotein, glycophorin A, in a continuous cell line. *Nature* **279**, 604-607.

18. Jokinen, M., Andersson, L.C. and Gahmberg, C.G. (1985) Biosynthesis of the major human red cell sialoglycoprotein, glycophorin A: O-glycosylation. *J. Biol. Chem*. **260**, 11314-11321.

Part II
Blood group antigens 147

Introduction 148

Comments on Papers 19 to 25 148

19. Gahmberg, C.G., Ekblom, M. and Andersson, L.C. (1984) Differentiation of human erythroid cells is associated with an increased O-glycosylation of the major sialoglycoprotein, glycophorin A. *Proc. Natl. Acad. Sci. USA*. **81**, 6752-6756.

20. Karhi, K.K. and Gahmberg, C.G. (1980) Identification of blood group A-active glycoproteins in the human erythrocyte membrane. *Biochim. Biophys. Acta* **622**, 344-354.

21. Goel, S., Palmqvist, M., Moll, K., Joannin, N., Lara, P., Akhouri, R., Moradi, N., Öjemalm, K., Westman, M., Angeletti, D., Kjellin, H., Lehtiö, J., Blixt, O., Ideström, L., Gahmberg, C.G., Storry, J.R., Hult, A.K., Olsson, M.L., von Heijne, G., Nilsson, I. and Wahlgren, M. (2015) RIFINs are adhesins implicated in severe Plasmodium falciparum malaria. *Nature Med*. **21**, 314-317.

22. Tolvanen, M. and Gahmberg, C.G. (1986) In vitro attachment of mono- and oligosaccharides to surface glycoconjugates in intact cells. *J. Biol. Chem*. **261**, 9546-9551.

23. Gahmberg, C.G. (1982) Molecular identification of the human Rho(D) antigen. *FEBS Lett*. **140**, 93-97.

24. Gahmberg, C.G. (1983) Molecular characterization of the human red cell Rho(D) antigen. *EMBO J*. **2**, 223-227.

25. Gahmberg, C.G. and Tolvanen, M. (1996) Why mammalian cell surface proteins are *glyco*proteins. *Trends Biochem. Sci*. **21**, 308-311.

Part III
Integrins, discovery and characterization

Integrins, discovery and characterization 199

Introduction 200

Comments on Papers 26 to 29 201

26. Patarroyo, M., Beatty, P.G., Fabre, J.W. and Gahmberg, C.G. (1985) Identification of a cell surface protein complex mediating phorbol ester-induced adhesion (binding) among human mononuclear leukocytes. *Scand. J. Immunol*. **22**, 171-182.

27. Patarroyo, M., Beatty, P.G., Serhan, C.N. and Gahmberg, C.G. (1985) Identification of a cell surface glycoprotein mediating adhesion in human granulocytes. *Scand. J. Immunol*. **22**, 619-631.

28. Asada, M., Furukawa, K., Kantor, C., Gahmberg, C.G. and Kobata, A. (1991) Structural study of the sugar chains of human leukocyte cell adhesion molecules CD11/CD18. *Biochemistry* **30**, 1561-1571.

29. Kotovuori, P., Tontti, E., Pigott, R., Shepherd, M., Kiso, M., Hasegawa, A., Renkonen, R., Nortamo, P., Altieri, D.C. and Gahmberg, C.G. (1993) The vascular E-selectin binds to the leukocyte integrins CD11/CD18. *Glycobiology* **3**, 131-136.

Carl_G_190x270_mm_blokki_FINAL.indd 10 06-Aug-23 1:53:28 PM

Part IV
The intercellular adhesion molecules -1 to -5 247

Introduction 248

Comments on Papers 30 to 42 248

30. Gahmberg, C.G. (1997) Leukocyte adhesion. CD11/CD18 integrins and intercellular adhesion molecules. *Curr. Opin. Cell Biol*. **9**, 643-650.

31. Patarroyo, M., Clark, E.A., Prieto, J., Kantor, C. and Gahmberg, C.G. (1987) Identification of a novel adhesion molecule in human leukocytes by monoclonal antibody LB-2. *FEBS Lett*. **210**, 127-131.

32. Li, R., Nortamo, P., Valmu, L., Tolvanen, M., Huuskonen, J., Kantor, C. and Gahmberg, C.G. (1993) A peptide from ICAM-2 binds to the leukocyte integrin CD11a/CD18 and inhibits endothelial cell adhesion. *J. Biol. Chem*. **268**, 17513-17518.

33. Li, R., Nortamo, P., Kantor, C., Kovanen, P., Timonen, T. and Gahmberg, C.G. (1993) A leukocyte integrin binding peptide from intercellular adhesion molecule-2 stimulates T cell adhesion and natural killer cell activity. *J. Biol. Chem*. **268**, 21474-21477.

34. Li, R., Xie, J., Kantor, C., Koistinen, V., Altieri, D.C., Nortamo, P. and Gahmberg, C.G. (1995) A peptide derived from the intercellular adhesion molecule-2 regulates the avidity of the leukocyte integrins CD11b/CD18 and CD11c/CD18. *J. Cell Biol*. **129**, 1143-1153.

35. Kotovuori, A., Pessa-Morikawa, T., Kotovuori, P. and Gahmberg, C.G. (1999) ICAM-2 and a peptide from from its binding domain are efficient activators of leukocyte adhesion and integrin activity. *J. Immunol*. **162**, 6613-6620.

36. Koivunen, E., Ranta, T.-M., Annila, A., Taube, S., Uppala, A., Jokinen, M., van Willigen, G., Ihanus, E. and Gahmberg, C.G. (2001) Inhibition of β2 integrin-mediated leukocyte adhesion by leucine-leucine-glycine motif-containing peptides. *J. Cell Biol*. **153**, 905-916.

37. Bailly, P., Tontti, E., Hermand, P., Cartron, J.-P. and Gahmberg, C.G. (1995) The red cell LW blood group protein is an intercellular adhesion molecule which binds to CD11/CD18 integrins. *Eur. J. Immunol*. **25**, 3316-3320.

38. Ihanus, E., Uotila, L.M., Toivanen, A., Varis, M. and Gahmberg, C.G. (2007) Red-cell ICAM-4 is a ligand for the monocyte/macrophage integrin CD11c/CD18: Characterization of the binding sites on ICAM-4. *Blood* **109**, 802-810.

39. Tian, L., Yoshihara, Y., Mizuno, T., Mori, K. and Gahmberg, C.G. (1997) The neuronal glycoprotein, telencephalin, is a cellular ligand for the CD11a/CD18 leukocyte integrin. *J. Immunol*. **158**, 928-936.

40. Tian, L., Nyman, H., Kilgannon, P., Yoshihara, Y., Mori, K., Andersson, L.C., Kaukinen, S., Rauvala, H., Gallatin, W.M. and Gahmberg, C.G. (2000) Intercellular adhesion molecule-5 induces dendritic outgrowth by homophilic adhesion. *J. Cell Biol*. **150**, 243-252.

41. Tian, L., Stefanidakis, M., Ning, L., van Lint, P., Nyman-Huttunen, H., Libert, C., Itohara, S., Mishina, M., Rauvala, H. and Gahmberg, C.G. (2007) Activation of NMDA receptors

promotes dendritic spine development through MMP-mediated ICAM-5 cleavage. *J. Cell Biol*. **178**, 687-700.

42. Choi, E.Y., Chavakis, E., Czabanka, M.A., Langer, H.F., Fraemohs, L., Economopoulou, M., Kundu, R.K., Orlandi, A., Zheng, Y.Y., Prieto, D.A., Ballantyne, C.M., Constant, S.L., Aird, W.C., Papayannopoulou, T., Gahmberg, C.G., Udey, M.C., Vajkoczy, P., Quertermous, T., Dimmeler, S., Weber, C. and Chavakis, T. (2008) Del-1, an endogenous leukocyte-endothelial adhesion inhibitor, limits inflammatory cell recruitment. *Science* **322**, 1101-1104.

Part V

Regulation of integrin activity by phosphorylation 365

Introduction 366

Comments on Papers 43 to 52 366

43. Valmu, L. and Gahmberg, C.G. (1995) Treatment with okadaic acid reveals strong threonine phosphorylation of CD18 after activation of CD11/CD18 leukocyte integrin with phorbol esters or CD3 antibodies. *J. Immunol*. **155**, 1175-1183.

44. Fagerholm, S., Morrice, N., Gahmberg, C.G. and Cohen, P. (2002) Phosphorylation of the cytoplasmic domain of the integrin CD18 chain by protein kinase C isoforms in leukocytes. *J. Biol. Chem*. **277**, 1728-1738.

45. Hilden, T.J., Valmu, L., Kärkkäinen, S. and Gahmberg, C.G. (2003) Threonine phosphorylation sites in the β2 and β7 leukocyte integrin polypeptides. *J. Immunol*. **170**, 4170-4177.

46. Fagerholm, S.C., Hilden, T.J., Nurmi, S.M. and Gahmberg, C.G. (2005) Specific integrin α and β chain phosphorylations regulate LFA-1 activation through affinity-dependent and –independent mechanisms. *J. Cell Biol*. **171**, 705-715.

47. Fagerholm, S.C., Varis, M., Stefanidakis, M., Hilden, T.J. and Gahmberg, C.G. (2006) α-chain phosphorylation of the human leukocyte CD11b/CD18 (Mac-1) integrin is pivotal for integrin activation to bind ICAMs and leukocyte extravasation in vivo. *Blood* **108**, 3379-3386.

48. Takala, H., Nurminen, E., Nurmi, S.M., Aatonen, M., Strandin, T., Takatalo, M., Kiema, T., Gahmberg, C.G., Ylänne, J. and Fagerholm, S.C. (2008) β2 integrin phosphorylation on Thr758 acts as a molecular switch to regulate 14-3-3 and filamin binding. *Blood* **112**, 1853-1862.

49. Jahan, F., Madhavan, S., Rolova, T., Viazmina, L., Grönholm, M. and Gahmberg, C.G. (2018) Phosphorylation of the α-chain in the integrin LFA-1 enables β2-chain phosphorylation and α-actinin binding required for cell adhesion. *J. Biol. Chem*. **293**, 12318-12330.

Carl_G_190x270_mm_blokki_FINAL.indd 12 06-Aug-23 1:53:29 PM

50. Uotila, L.M., Jahan, F., Hinojosa, L.S., Melandri, E., Grönholm, M. and Gahmberg, C.G. (2014) Specific phosphorylations transmit signals from leukocyte β2- to β1-integrins and regulate adhesion. *J. Biol. Chem*. **289**, 32230-32242.

51. Grönholm, M., Jahan, F., Bryushkova, E.A., Madhavan, S., Aglialoro, F., Soto Hinojosa, L., Uotila, L.M. and Gahmberg, C.G. (2016) LFA-1 integrin antibodies inhibit leukocyte α4β1-mediated adhesion by intracellular signaling. *Blood* **128**, 1270-1281.

52. Gahmberg, C.G. and Grönholm, M. (2022) How integrin phosphorylations regulate cell adhesion and signaling. *Trends Biochem. Sci*. **47**, 265-278.

Part VI
Additional interactions of leukocyte integrins 481

Introduction 482

Comments on Papers 53 to 55 482

53. Koivunen, E., Arap, W., Valtanen, H., Rainisalo, A., Penate Medina, O., Heikkilä, P., Kantor, C., Gahmberg, C.G., Salo, T., Konttinen, Y.T., Sorsa, T., Ruoslahti, E. and Pasqualini, R. (1999) Tumor targeting with a selective gelatinase inhibitor. *Nature Biotech.* **17**, 768-774.

54. Orlova, V.V., Xie, C., Choi, E.Y., Chavakis, E., Ihanus, E., Ballantyne, C.M., Gahmberg, C.G., Bianchi, M.E., Nawroth, P.P. and Chavakis, T. (2007) A novel pathway of HMGB1-mediated inflammatory cell recruitment that requires the interplay between Mac-1-integrin and RAGE. *EMBO J*. **26**, 1129-1139.

55. Shulman, Z., Cohen, S.J., Roediger, B., Kalchenko, V., Jain, R., Grabosky, V., Klein, E., Shinder, V., Stoler-Barak, L., Feigelson, S.W., Nurmi, S.M., Goldstein, I., Hartley, O., Gahmberg, C.G., Etzioni, A., Weniger, W., Ben-Baruch, A. and Alon, R. (2012) Transendothelial migration of lymphocytes mediated by endothelial vesicle stores rather than by extracellular chemokine depots. *Nature Immunol*. **13**, 67-77.

Part VII
Concluding remarks 515

Acknowledgements 517

Carl_G_190x270_mm_blokki_FINAL.indd 13 06-Aug-23 1:53:29 PM

Carl_G_190x270_mm_blokki_FINAL.indd 14 06-Aug-23 1:53:29 PM

Preface

Here I have collected my most important scientific papers and written short comments on them. All my work deals with cell membranes, and I have grouped the articles into a few different topics. Most work deals with cell membrane proteins with early focus on glycoproteins, including studies on fibroblast proteins and changes in cancer, later work deals with proteins of red blood cells and leukocytes. More recently, the research focussed on functional aspects, notably on leukocyte adhesion and its regulation. It has been important to describe the knowledge, when the articles were written, and what we tried to solve. I have been fortunate in having several excellent graduate students and postdoctoral fellows, and certainly much of the results obtained have depended on them. Both my postdoctoral time in Sen Hakomori´s laboratory, and the time as visiting professor in Erkki Ruoslahti´s group, have been very important for my research. The long collaboration with Leif Andersson has been very rewarding, and the collaboration with him continues. I have, with my colleagues, written several reviews and invited articles, but the original articles in established science journals, are the most important ones and described here.

During all my time as an active researcher, I have been able to obtain grants from different bodies. This fact has enabled me to do research in addition to teaching and administration. The most important research grants, were obtained from the University of Helsinki, the Academy of Finland, the Sigrid Jusélius Foundation, the Finnish Medical Society, National Institutes of Health, the Magnus Ehrnrooth Foundation, the Finnish Society of Sciences and Letters, the Else and Wilhelm Stockmann Foundation, and the Liv och Hälsa Foundation.

Carl_G_190x270_mm_blokki_FINAL.indd 15 06-Aug-23 1:53:29 PM

Carl_G_190x270_mm_blokki_FINAL.indd 16 06-Aug-23 1:53:29 PM

Part I

CELL SURFACE GLYCOPROTEINS

Carl_G_190x270_mm_blokki_FINAL.indd 17 06-Aug-23 1:53:29 PM

Introduction

As part of my Doctor of Medical Sciences thesis, I isolated plasma membranes and endoplasmic reticulum membranes from hamster BHK21 cells, and studied their proteins by SDS gel electrophoresis. Cells were labelled using radioactive amino acids or monosaccharides (D- glucosamine, L- fucose), the membranes isolated by centrifugation and characterized using membrane markers such as Na^+K^+-ATPase for the plasma membrane. The amount of contaminating membranes and cell organelles, was estimated using enzyme markers for mitochondria, lysosomes and the endoplasmic reticulum. I realized that it was impossible to obtain membranes of high purity from cultured cells, and therefore novel techniques were important to study the composition and localization of membrane molecules. Furthermore, slab gels were not yet in use, and the resolution of proteins on cylindrical gels after slicing, was poor. Anyway, there was an increasing interest in the finding, that plasma membrane proteins, often were glycosylated, and more so than those of internal membranes.

In the early 1970,s, Mark Bretscher, working at the Laboratory of Molecular Biology in Cambridge, had developed a cell surface labelling technique, using ^{35}S- formyl methionyl sulfone methyl phosphate. The reagent does not penetrate the membrane. Using this reagent, he was able to show that the major red cell membrane glycoprotein, glycophorin A, was spanning the membrane (1). I synthesized the reagent and showed that it selectively labelled the envelope protein of Semliki Forest Virus (Paper 1). The reagent was, however, not easy to make, and never became much used. However, the results on Semliki Forest Virus got me interested in further developing methods to label cell surface molecules. In 1970, our consortium in Helsinki organized a cell membrane conference, and among the participants was Sen-itiroh Hakomori from the University of Washington in Seattle. He was an authority in the glycolipid field. I contacted him and after I succeeded in getting a NIH postdoctoral fellowship for two years, I went to Seattle with my family in September of 1972. After arriving, we discussed possible projects, and Sen got interested in the possibility of studying cell surface glycolipids and glycoproteins using radioactive surface labelling techniques. No technique for labelling of cell surface glycoconjugates, had been described. He told me that Gilbert Ashwell at NIH had used the enzyme galactose oxidase to oxidise D-galactose and N-acetyl D- galactosamine to the corresponding C-6 aldehydes in serum proteins. The aldehydes were then reduced using tritium labelled sodium borohydride back to the original sugars, resulting in tritium labelled glycoproteins. After learning this, I immediately realized that we could try the method to label intact cells. The high molecular weight of the enzyme would prevent its penetration through the plasma membrane, and only surface exposed glycoconjugates could be oxidised. After one week, I got the first positive results using red blood cells. We were very excited.

Gel electrophoresis with cylindrical gels, was laborious and the resolution was not optimal, but the new method raised a lot of interest. Soon afterwards, we applied it to normal and

Carl_G_190x270_mm_blokki_FINAL.indd 18 06-Aug-23 1:53:29 PM

transformed fibroblasts, and described the loss of a high molecular weight protein from normal cells. A great advantage of the cell surface labelling method, was that plasma membranes could be studied without previous isolation of them.

A major technical development occurred, when Bonner and Laskey introduced the use of a scintillator in gels to visualize weak radioactivity emitters such as tritium. Another important development was the introduction of slab gels.

After coming back from the US in 1974, the local university repair shop made a slab gel apparatus. I was then able to apply the new techniques to normal human red cells, and found proteins not described before. It was also interesting to study red cells carrying rare blood groups. Scientists at the Red Cross Blood Service in Helsinki, had described a red cell (En(a-)), lacking the MN-blood group antigens. After labelling the cells followed by gel analysis, it immediately became apparent, that the cells lacked the major red cell sialoglycoprotein, glycophorin A. Glycophorin A is a "classical" membrane protein, because it was the only membrane protein, which had been sequenced. Interestingly, the individual, lacking glycophorin A in his red cells, showed no hematologic problems.

With the galactose oxidase/tritiated borohydride labelling technique, we often used treatment with neuraminidase to enable labelling of penultimate galactosyl/N-acetyl galactosaminyl residues. The neuraminidase treatment changed the molecules appreciably, and therefore I began to look for alternative methods. Periodate at low concentrations, selectively oxidises sialic acids, and had been used by Ashwell for labelling of serum proteins by reduction with tritiated sodium borohydride. I found that when the oxidation was done on ice, there was no transport of periodate into cells. After reduction with tritiated borohydride, the labelling of the oxidized residues worked fine. This labelling method was easy to perform and became much used.

In the 1970,s, studies on the biosynthesis of membrane proteins were done using viral envelope proteins as models. Because of the lack of good models, little was known about mammalian membrane protein biosynthesis. We then found that the widely used K562 cell line, described as myeloid, expressed the red cell marker, glycophorin A, and actually the cells turned red after treatment with sodium butyrate. After making a crude antiserum to glycophorin A, we obtained a highly specific antiserum by absorption with the En(a-) membranes. We could then study the biosynthesis of glycophorin A, using K562 cells and ^{35}S-methionine pulse/chase labelling.

Leukocyte membrane proteins were poorly known in the 1970s. Only the transplantation antigens, had been characterized by immunologists and were best known. The development of the radioactive cell surface labelling techniques, combined with fluorography of slab gels, made it possible to study cell surface proteins at a new level. Using the new methods, we discovered several novel leukocyte glycoproteins.

Comments on Papers 1 to 18

We used ^{35}S-formyl methionyl sulfone methyl phosphate (^{35}S-FMMP) to selectively label cell surface-exposed proteins and lipids in Semliki Forest Virus (SFV). We used it as a simple membrane model. The virus buds from the host cell plasma membrane, and its envelope contains only two major envelope proteins. These were efficiently labelled with the amino group reactive ^{35}S-FMMP, whereas the core nucleocapsid protein remained unlabelled. In

Carl_G_190x270_mm_blokki_FINAL.indd 19 06-Aug-23 1:53:29 PM

addition, phosphatidyl ethanolamine was efficiently labelled, which shows that it was surface exposed. In contrast, phosphatidyl serine, was poorly labelled (Paper 1). The results show that the distribution of the viral membrane lipids, in the membrane bilayer largely reflected that of plasma membrane lipids. This paper was important for my subsequent career, because my research interest shifted to study the outer surface of the plasma membrane.

After arriving to the University of Washington, I began to develop a method for selective radioactive labelling of cell surface *glyco*proteins and *glyco*lipids. Gilbert Ashwell with co-workers, had published methods to label serum glycoproteins using galactose oxidase and tritiated sodium borohydride (2). I used human red cells as a model cell. The red cell membrane, was easy to isolate, due to the lack of other membranes in the mature erythrocyte. Notably, V.T. Marchesi had published the sequence of the major red cell sialoglycoprotein, glycophorin A (3), and Bretscher had shown that it spans the membrane (1). Galactose oxidase was commercially available, and the labelling technique worked out well. Hakomori,s laboratory was well equipped for glycolipid analysis, but not for proteins. I introduced SDS-gel electrophoresis there, and we used cylindrical gels. Then we had to get a gel slicing device, which was made in the university repair shop. The resolution of the labelled proteins on SDS-gel electrophoresis was not optimal, but the major glycoprotein, glycophorin A, was strongly labelled after neuraminidase/galactose oxidase treatment, but little label was seen when the galactose oxidase treatment was omitted. Globoside, the major red cell glycolipid, with the sequence N-acetyl galactosamine-galactose-galactose-glucose-ceramide, was strongly labelled. In addition, ceramide trihexoside, lacking the amino sugar, was labelled, whereas ceramide dihexoside was not (Paper 2).

When we mastered the galactose oxidase/ tritiated borohydride method, it became important to study the plasma membrane of normal and transformed fibroblasts. At that time, several normal fibroblast cell lines were available, as well as their tumour virus transformed counterparts. Using hamster NIL cells, we published in 1973, the presence of a major labelled high molecular weight protein in normal cells, which was lacking in transformed cells. We named the protein galactoprotein a (Paper 3). The protein was independently reported by Richard Hynes (4). He named it LETS (Large External Transformation Sensitive) protein. In addition, Antti Vaheri and Erkki Ruoslahti published the same high molecular weight protein, and named it SF- (Serum Fibroblast) antigen (5). Later, it was agreed that the protein should get the name fibronectin. We also found that ceramide penta- and tetra-saccharides were more strongly labelled in normal cells, than in the transformed fibroblasts. In contrast, the transformed cells expressed on their surfaces higher amounts of short chain glycolipids. Certainly, the finding of fibronectin was important, and it became a "classic" adhesion protein (6).

In subsequent work, we used cells, transformed with a temperature-sensitive mutant of polyoma virus. When the cells were grown at 39 °C, fibronectin was strongly expressed, whereas little label was observed in the high molecular weight region on gels of cells grown at the permissive temperature of 32 °C. In addition, ceramide dihexoside, was more strongly expressed at 32 °C than at 39 °C (Paper 4).

These findings raised a lot of interest, and several articles later appeared on the subject. Fibronectin, was later found to be secreted from cells, and deposited as a matrix protein. Transformed cells often express high protease activity, which explains the degradation of the extracellular matrix including fibronectin. Ruoslahti and co-workers later identified the minimal receptor binding sequence in fibronectin, RGD (7), and this short sequence turned out to be recognized by several integrins (8).

Carl_G_190x270_mm_blokki_FINAL.indd 20 06-Aug-23 1:53:29 PM

When slab gel electrophoresis and the use of a scintillator in gels became available, the resolution of proteins on gels was greatly improved. Therefore, it was worthwhile to return to red cells, and study their outer surface in more detail. It became apparent that the red cell contains a number of previously unknown glycoproteins. Foetal erythrocyte glycoproteins, were poorly labelled without neuraminidase treatment, which showed that they more sialylated than those of adults. When membranes were first isolated, and then labelled, no additional proteins were labelled. This finding showed that all glycosylated proteins are on the outer cell surface. Exceptions are cytoplasmic proteins containing O-glycosidic N-acetyl glucosamines (9). Furthermore, I proposed that cell surface proteins of mammalian cells *always* are *glyco*-proteins (Paper 5). This statement has largely turned out to be correct, but see the comments on the Rh_o(D) protein below.

Red cells carrying the En(a-) blood group, had been described to contain one third the normal amount of sialic acid, and weak MN-antigens (10). We obtained En(a-) cells from the Finnish Red Cross Blood Transfusion Service, and after surface labelling, it was obvious that the cells lack glycophorin A. Interestingly, the band 3 protein (anion exchange protein) of En(a-) cells, showed an increased glycosylation, due to a higher molecular weight oligosaccharide. This oligosaccharide later turned out to be polylactosamine type (11). Interestingly, the son of the proband, had red cells expressing about half the normal amount of glycophorin A, and the molecular weight of the band 3 oligosaccharide was between that of normal cells and En(a-) cells (Paper 6). We still do not know how protein glycosylation is regulated. The availability of En(a-) red cells, was crucial for the preparation of a specific anti-glycophorin A polyclonal antiserum (see below).

We modified the periodate/sodium borotritiate method (12) to be used for labelling of cell surface sialoglycoproteins. Treatment with 1-3 mM periodate for a short time at 0 °C was enough to oxidise the sialic acids at the surface of red cells. To show that the plasma membrane indeed was impermeable to periodate, we isolated red cell membranes and resealed them, with the sialic acid-rich glycoprotein fetuin inside the red cell ghosts. Little ^{3}H-label was found in fetuin after periodate oxidation and reduction with tritiated borohydride, which showed that the technique is specific for cell surface located carbohydrate (Paper 7).

This method was easy to use, and it did not need any complicated chemicals or enzymes. It soon became very popular for labelling of cell surface glycoproteins and gangliosides.

In the mid 1970,s, with exception of red cells, little was known about surface proteins of mammalian cells. Immunologists had described transplantation antigens on leukocytes, but it was obvious that the cells must contain other, unknown proteins. We began to apply the novel surface labelling methods to mouse lymphoid cells (Paper 8). The results revealed that the cells express a number of cell surface glycoproteins not described before, and the different cells showed specific surface glycoprotein patterns. In collaboration with Swedish scientists, we studied different human leukocyte cell lines. The cell surface patterns were characteristic of the different types of cell lines, and it was possible to use the patterns for diagnostic purposes (13,14). The cell surface glycoproteins of different normal human leukocytes, were studied in detail (Paper 9). We also observed major changes in T cell surface glycoproteins, when the cells, were activated to grow and differentiate (Paper 10). The same was true for B lymphocytes, B blasts Epstein-Barr virus positive and negative B lymphoid cell lines. An interesting case was the HL-60 promyelocytic cell line. The lymphoblasts expressed a rather simple surface glycoprotein pattern, with a major labelled protein of 160000 molecular weight. Upon differentiation towards granulocytes, the cells expressed in addition glycoproteins of

Carl_G_190x270_mm_blokki_FINAL.indd 21 06-Aug-23 1:53:29 PM

130000 and 90000 molecular weights. The surface glycoprotein patterns resembled those of normal granulocytes. With present knowledge, these proteins were the CD11b and CD18 subunits of the myeloid Mac-1 integrin (Paper 11).

The CD45 antigen is a major cell surface glycoprotein in leukocytes and it was originally characterized as a "common leukocyte antigen". It is differently spliced in different leukocytes. B cells expressed a major high molecular weight protein with an apparent molecular weight of 205000, whereas T cells expressed proteins of 160000-180000 (Paper 9). CD45 turned out to be a protein tyrosine phosphatase (15). We showed that it activates the Fyn tyrosine kinase by releasing the C-terminal inhibitory phosphate (Paper 12). Thus the activation of Fyn is similar to that of Lck. Together with Japanese glycobiologists we determined the structures of the CD45 N-glycosidic and O-glycosidic oligosaccharides (16,17).

We thought that some serum glycoproteins could originate from leukocytes, especially during excess white blood cell proliferation during inflammation. We found release of the serum glycoprotein, α1-acid glycoprotein from leukocytes (Paper 13). It is a marker protein of inflammation.

We also studied platelet surface proteins, and found that treatment of platelets with thrombin, released a cell surface glycoprotein fragment of around 80000 in apparent molecular weight. Another protein of higher molecular weight, was secreted without enzyme treatment (18).

As discussed above, glycophorin A was the first mammalian membrane protein that was sequenced, and it served as a model for type 1 membrane proteins. It has a relatively large external domain, a transmembrane domain, and a relatively short intracellular domain (3). We studied the expression of glycophorin A in bone marrow cells, and found expression early during red cell development, and it turned out to be a useful erythroblast marker protein (Paper 14). When screening different leukocyte cell lines, we found that the K562 cell line, considered myeloid, in fact expressed glycophorin A. The finding indicated that the cell line could be erythroid (Paper 15). Murine red cell precursor cell lines, were known to differentiate using sodium butyrate or hemin, and when K562 cells were treated with butyrate, they indeed showed a strong expression of haemoglobin (Paper 16). The cells were then shown by Rutherford et al. to express embryonic and foetal haemoglobin (19). The finding that K562 cells are erythroid, first raised some controversy, but our conclusion was confirmed. Glycophorin A from K562 cells was studied in detail and it expressed blood group MN activity. We now had a cell line expressing glycophorin A, and a specific antiserum made by absorption of a crude anti-glycophorin A antiserum with En(a-) membranes. This made it possible to study its biosynthesis in K562 cells. We used pulse-chase labelling with ^{35}S-methionine, and found that it took about 30 min for the protein to get glycosylated and reach the plasma membrane (Papers 17,18). The biosynthesis in many ways resembled that of viral membrane glycoproteins, but it was the first mammalian membrane glycoprotein studied in some detail. Later, we studied its biosynthesis in cell free systems, and its inhibition of N-glycosylation using tunicamycin (20). Glycophorin A turned out to be a useful marker of erythroleukemia (21).

Carl_G_190x270_mm_blokki_FINAL.indd 22 06-Aug-23 1:53:29 PM

References

1. Bretscher, M.S. (1971) Human erythrocyte membranes: specific labelling of surface proteins. *J. Mol. Biol*. **58**, 775-781.
2. Morell, A.G, van den Hamer, C.J., Scheinberg, I.H. and Ashwell, G. (1966) Physical and chemical studies on ceruloplasmin. IV. Preparation of radioactive, sialic acid-free cerulopasmin labeled with tritium on terminal D-galactose residues. *J. Biol. Chem*. **241**, 3745-3749.
3. Tomita, M. and Marchesi, V.T. (1975) Amino-acid sequence and oligosaccharide attachment sites of human erythrocyte glycophorin. *Proc. Natl. Acad. Sci. USA*. **72**, 2964-2968.
4. Hynes, R.O. (1973) Alteration of cell-surface proteins by viral transformation and by proteolysis. *Proc. Natl. Acad. Sci. USA*. **70**, 3170-3174.
5. Vaheri, A. and Ruoslahti, E. (1974) Disappearance of a major cell type specific surface glycoprotein antigen (SF) after transformation of fibroblasts by Rous sarcoma virus. *Int. J. Cancer* **13**, 579-586.
6. Hynes, R.O. (1986) Fibronectins. *Sci. Amer*. **254**, 42-51.
7. Ruoslahti, E. and Pierschbacher, M.D. (1986) Arg-Gly-Asp: a versatile cell recognition signal. *Cell* **44**, 517-518.
8. Ruoslahti, E. (1996) RGD and other recognition signals for integrins. *Annu. Rev. Cell Dev. Biol*. **12**, 697-715.
9. Wells, L., Vosseller, K. and Hart, G.W. (2001) Glycosylation of nucleocytoplasmic proteins: signal transduction and O-GlcNAc. *Science* **291**, 2376-2378.
10. Furuhjelm, U., Myllylä, G., Nevanlinna, H.R., Nordling, S., Pirkola, A., Gavin, J., Gooch, A., Sanger, R. and Tippett, P. (1969) The red cell phenotype En(a-) and anti-Ena: serological and physicochemical aspects. *Vox Sang*. **17**, 256-278.
11. Järnefelt, J., Rush, J., Li, Y.T. and Laine, R.A. (1978) Erythroglycan, a high molecular weight glycopeptide with the repeating structure [galactosyl-(1 leads to 4)-2-deoxy-2-acetamido-glucosyl(1 leads to 3)] comprising more than one-third of the protein-bound carbohydrate of human erythrocyte stroma. *J. Biol. Chem*. **253**, 8006-8009.
12. Van Lenten, L. and Ashwell, G. (1971) Studies on the chemical and enzymatic modification of glycoproteins. A general method for the tritiation of sialic acid-containing glycoproteins. *J. Biol. Chem*. **246**, 1889-1894.
13. Andersson, L.C., Gahmberg, C.G., Nilsson, K. and Wigzell, H. (1977) Surface glycoprotein patterns of normal and malignant human lymphoid cells. I. T cells, T blasts and leukemic T cell lines. *Int. J. Cancer* **20**, 702-707.
14. Nilsson, K., Andersson, L.C., Gahmberg, C.G. and Wigzell, H. (1977) Surface glycoprotein patterns of normal and malignant human lymphoid cells. II. B cells, B blasts and Epstein-Barr virus (EBV) positive and negative B lymphoid cell lines. *Int. J. Cancer* **20**, 708-716.
15. Charbonneau, H., Tonks, N.K., Walsh, K.A. and Fischer, E.H. (1988) The leukocyte common antigen (CD45) – A putative receptor-linked protein tyrosine phosphatase. *Proc. Natl. Acad. Sci. USA*. **85**, 7182-7186.
16. Sato, T., Furukawa, K., Autero, M., Gahmberg, C.G. and Kobata, A. (1993) Structural study of the sugar chains of human leukocyte common antigen CD45. *Biochemistry* **32**, 12694-12704.

Carl_G_190x270_mm_blokki_FINAL.indd 23 06-Aug-23 1:53:29 PM

17. Furukawa, K., Funakoshi, Y., Autero, M., Horejsi, V., Kobata, A. and Gahmberg, C.G. (1998) Structural study of the O-linked sugar chains of human leukocyte tyrosine phosphatase CD45. *Eur. J. Biochem*. **251**, 288-294.
18. Mosher, D.F., Vaheri, A., Choate, J.J. and Gahmberg, C.G. (1979) Action of thrombin on surface glycoproteins of human platelets. *Blood* **53**, 437-445.
19. Rutherford, T.R., Clegg, J.B. and Weatherall, D.J. (1979) K562 human leukaemic cells synthesise embryonic haemoglobin in response to haemin. *Nature* **280**, 164-165.
20. Gahmberg, C.G., Jokinen, M., Karhi, K.K. and Andersson, L.C. (1980) Effect of tunicamycin on the biosynthesis of the major human red cell sialoglycoprotein, glycophorin A, in the leukemia cell line K562. *J. Biol. Chem*. **255**, 2169-2175.
21. Andersson, L.C., Gahmberg, C.G., Teerenhovi, L. and Vuopio, P. (1979) Glycophorin A as a marker for early erythroid differentiation in acute leukemia. *Int. J. Cancer* **24**, 717-720.

VIROLOGY **50**, 259–262 (1972

Exposure of Proteins and Lipids in the Semliki Forest Virus Membrane

Virions of group A arboviruses comprise two components. There is a nucleocapsid core, which consists of RNA and a lysine-rich protein with a molecular weight of about 34,000 (*1*, *2*). The nucleocapsid is surrounded by a lipid-containing envelope, which the nucleocapsid acquires as it leaves the host cell by budding through the plasma membrane (*3*). Studies of the lipid composition of the viral membrane confirm that the lipids are similar to those of the host cell plasma membrane (*4*). Only one protein with an apparent molecular weight of about 50,000 and a carbohydrate content of 12% has been detected in the viral membrane by sodium dodecyl sulfate (SDS) polyacrylamide gel electrophoresis (PAGE) (*1*, *2*). This protein has recently been split into two bands using a discontinuous SDS-electrophoresis system (*5*). The structure of the viral membrane has been analyzed by X-ray diffraction methods, and it seems that the lipids are arranged into a bilayered structure (*6*). Most of the protein of the viral membrane is located outside the lipid bilayer in the form of spikes that can be removed by proteolytic enzymes (*7*).

We have studied exposure of the surface components of the Semliki Forest virus (SFV) with the reagent ^{35}S-formyl methionyl sulfone methyl phosphate (^{35}S-FMMP), designed by Bretscher (*8*). He showed that this reagent does not penetrate the red cell membrane and preferentially labels two surface proteins of the intact erythrocyte. The reagent reacts primarily with the ϵ-amino groups of lysine residues in proteins, but also with the amino groups of phosphatidylethanolamine and phosphatidylserine.

A prototype strain of Semliki Forest virus was grown and purified as described previously (*4*, *9*). ^{35}S-FMMP was synthesized exactly as described by Bretscher (*8*). SDS-PAGE was performed as described previously (*10*) in 7.5% gels. ^{3}H-Phenylalanine-labeled SFV either intact or disrupted in 1% Nonidet P40 (NP40) was reacted with ^{35}S-FMMP in the alkaline buffer described by Bretscher (*8*) in a constant volume. Excess reagent was removed by gradient centrifugation of the intact virions or by dialysis. For the fingerprinting experiments the viral envelope was isolated after NP40 disruption (9), labeled with ^{35}S-FMMP and dialyzed against 0.1 *M* ammonium bicarbonate buffer containing 1% NP40. For digestion intact SFV (500 μg protein) or SFV envelope (400 μg protein) labeled with ^{35}S-FMMP were incubated in 0.2 ml ammonium bicarbonate buffer containing 1% NP40, 250 μg bovine serum albumin and 12.5 μg each of trypsin and chymotrypsin (Worthington) at 37° for 48 hr and fingerprinted on Whatman 3 MM paper (*11*).

The lipids from the ^{35}S-FMMP-labeled virions were extracted with chloroform–methanol according to Folch *et al.* (*12*). The thin-layer chromatography plates (Kieselguhr F_{254}, E. Merck) were developed with chloroform–methanol–conc. ammonia–water (65:20:2:2 by vol.). The spots were detected by autoradiography, scraped, and counted in toluene-based scintillation fluid. The derivatives of diacyl glycerylphosphorylethanolamine (diacyl GPE) and alkenyl-acyl glycerylphosphorylethanolamine (alkenyl-acyl GPE) had identical mobilities on thin-layer chromatography, but they could be differentiated by mild acid methanolysis (*13*). This cleaves only the alkenyl-acyl derivative and gives the corresponding derivative of monoacyl GPE.

Figure 1A shows the distribution of the ^{35}S-FMMP label when an intact SFV preparation was labeled. In this SDS-PAGE system, the two membrane proteins move together. The ^{35}S-FMMP was almost totally

Copyright © 1972 by Academic Press, Inc.
All rights of reproduction in any form reserved.

Carl_G_190x270_mm_blokki_FINAL.indd 25 06-Aug-23 1:53:29 PM

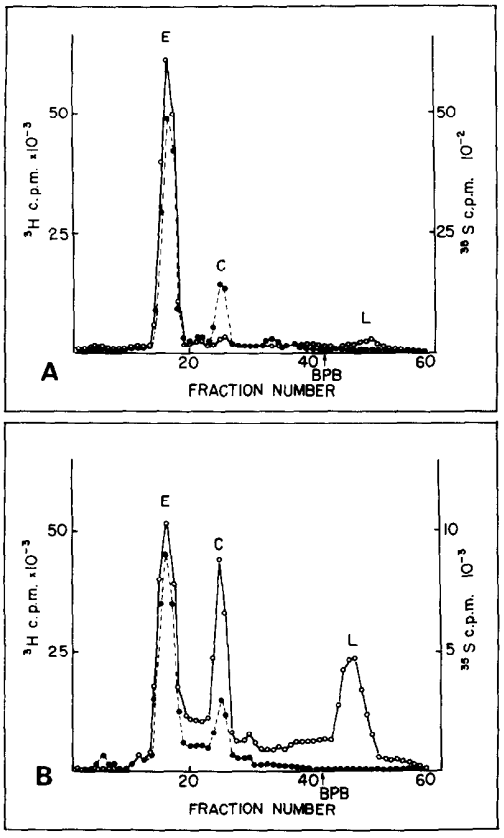

FIG. 1. (A). SDS-PAGE of intact ^{3}H-phenylalanine (●---●) labeled SFV which had been reacted with ^{35}S-FMMP (○——○). (B). SDS-PAGE of NP40 disrupted ^{3}H-phenylalanine (●---●) labeled SFV which had been allowed to react with ^{35}S-FMMP (○——○). E = envelope proteins; C = nucleocapsid protein; L = lipid fraction; BPB = bromophenol blue.

recovered from the viral membrane proteins (E). About 5% of the label was in a fast migrating fraction (L), which contains the lipids (*10*). Very little label was found in the nucleocapsid protein (C). Thus the label does not penetrate the viral membrane. The distribution of the ^{35}S-FMMP label when the virus had been disrupted with NP40 prior to labeling is shown in Fig. 1B. Results of three experiments show that 28 ± 1% of the total label was in the membrane protein peak (E), 18 ± 1% in the nucleocapsid protein peak (C) and 22 ± 3% in the L-fraction. When the virus had been treated with detergent prior to exposure to the reagent the envelope proteins contained

TABLE 1

DISTRIBUTION OF ^{35}S-FMMP LABEL IN SFV[a]

Sample	Intact SFV (cpm)	NP40 disrupted SFV (cpm)
Envelope proteins[b]	65,000	120,000
Nucleocapsid protein[b]	100	77,000
Alkenyl-acyl GPE[c]	2,050	14,100
Diacyl GPE[c]	1,100	8,650
Diacyl GPS[c]	257	4,700

[a] One of three typical experiments. The intact and disrupted preparations containing each 100 μg SFV-protein were labeled with the same amount of ^{35}S-FMMP in the same volume.

[b] From SDS-PAGE.

[c] From thin-layer plates.

85 ± 3% more label than the proteins from intact virions (Table 1).

To study whether there were qualitative differences in labeling of the membrane proteins from intact and NP40 disrupted virions, fingerprints were made of the ^{35}S-FMMP-labeled proteins. The fingerprints are shown in Fig. 2A and B. The peptide patterns were quite similar. However, two peptides marked P1 and P2 were constantly found in the fingerprints of disrupted envelope but not in the fingerprints of intact virions. These peptides must be derived from the membrane proteins as SDS-PAGE of the envelope fraction labeled with ^{35}S-FMMP showed label in the membrane proteins but not in the nucleocapsid protein.

Analysis of the Folch extracts of intact SFV revealed that diacyl GPE (about 30%), alkenyl-acyl GPE (about 60%) and diacyl glycerylphosphorylserine (diacyl GPS) (about 10%) had been labeled. These lipids are therefore exposed on the surface of the virus (cf. ref. *14*). Similar experiments with SFV that had been dissociated by NP40 before ^{35}S-FMMP labeling showed 7–8 times more label in the phospholipids (Fig. 3 and Table 1). The ratio of labeled alkenyl-acyl GPE to diacyl GPE is approximately the same in both intact and disrupted virions (Table 1). This is also the molar ratio of these molecules in the viral membrane (63% alkenyl-acyl GPE and 37% diacyl GPE) (*15*). Thus the different forms of GPE-lipids seem to be randomly distributed in the

Carl_G_190x270_mm_blokki_FINAL.indd 26 06-Aug-23 1:53:29 PM

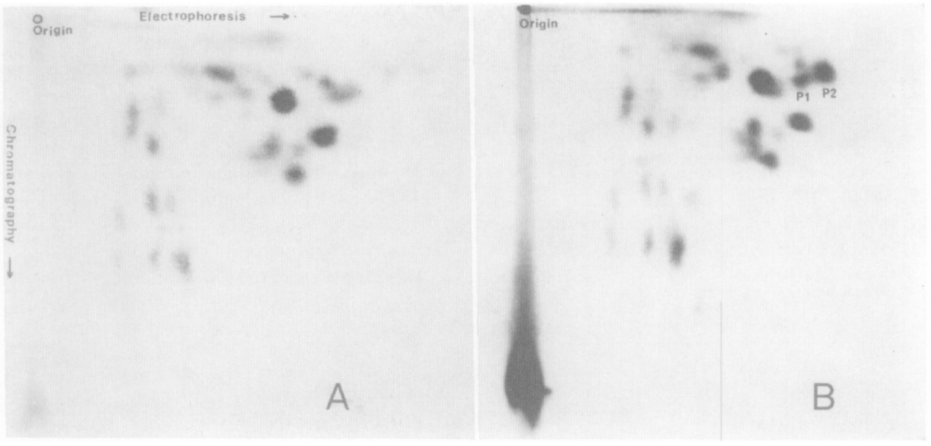

FIG. 2. (A). Trypsin-chymotrypsin fingerprint of ^{35}S-FMMP-labeled intact SFV. (B). Trypsin-chymotrypsin fingerprint of NP40-disrupted ^{35}S-FMMP-labeled SFV envelope. Anode at right.

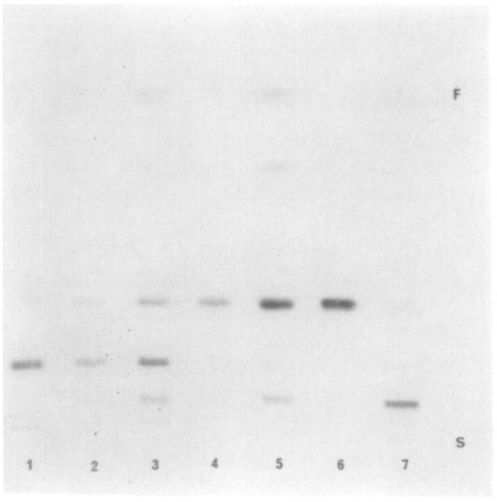

FIG. 3. Thin-layer chromatogram of ^{35}S-FMMP lipids. 1, Products of mild acid methanolysis of ^{35}S-FMMP derivative of pure alkenyl-acyl GPE; 2, products of mild acid methanolysis of ^{35}S-FMMP derivatives of the lipids of intact SFV; 3, products of mild acid methanolysis of ^{35}S-FMMP derivatives of the lipids of NP40-disrupted SFV; 4, ^{35}S-FMMP lipids of ^{35}S-FMMP-labeled intact SFV; 5, ^{35}S-FMMP lipids of NP40-treated ^{35}S-FMMP-labeled SFV; 6, ^{35}S-FMMP derivative of pure diacyl GPE; 7, ^{35}S-FMMP derivative of pure diacyl GPS.

viral membrane. We are presently studying the ^{35}S-FMMP labeling of the SFV lipids more closely to be able to decide whether protein shielding, assymetrical distribution (*16*) or other factors are causing the differences in labeling of the intact and disrupted envelope.

The present studies confirm that most of the SFV membrane protein is exposed on the outer surface of the viral envelope. The fingerprinting experiments showed the presence of two peptides from the membrane proteins which are shielded in the intact virions. Whether these are from the parts of these proteins involved in the binding to the lipid remains to be determined.

REFERENCES

1. STRAUSS, J. H., BURGE, B. W., and DARNELL, J. E., *Virology* **37**, 367 (1969).
2. SIMONS, K., and KÄÄRIÄINEN, L., *Biochem. Biophys. Res. Commun.* **38**, 981 (1970).
3. ACHESON, N. H., and TAMM, I., *Virology* **32**, 128 (1967).
4. RENKONEN, O., KÄÄRIÄINEN, L., SIMONS, K., and GAHMBERG, C. G., *Virology* **46**, 318 (1971).
5. SCHLESINGER, M. J., SCHLESINGER, S., and BURGE, B. W., *Virology* **47**, 539 (1972).
6. HARRISON, S. C., DAVID, A., JUMBLATT, J., and DARNELL, J. E., *J. Mol. Biol.* **60**, 523 (1971).
7. COMPANS, R. W., *Nature* (*London*) **229**, 114 (1971).
8. BRETSCHER, M. S., *J. Mol. Biol.* **58**, 775 (1971).
9. KÄÄRIÄINEN, L., SIMONS, K., and VON BONSDORFF, C.-H., *Ann. Med. Exp. Biol. Fenn.* **47**, 235 (1969).
10. GAHMBERG, C. G., *Biochim. Biophys. Acta* **249**, 81 (1971).

Carl_G_190x270_mm_blokki_FINAL.indd 27 06-Aug-23 1:53:29 PM

11. Bennett, J. C., *Methods Enzymol.* **11**, 330 (1967).
12. Folch, J., Lees, M., and Sloane-Stanley, G. H., *J. Biol. Chem.* **226**, 497 (1957).
13. Renkonen, O., *Biochim. Biophys. Acta* **125**, 288 (1966).
14. Friedman, R. M., and Pastan, I., *J. Mol. Biol.* **40**, 107 (1969).
15. Laine, R., Kettunen, M.-L., Gahmberg, C. G., Kääriäinen, L., and Renkonen, O., *J. Virol.*, in press.
16. Bretscher, M. S., *Nature* (*London*) **236**, 11 (1972).

Carl G. Gahmberg
Kai Simons
Ossi Renkonen
Leevi Kääriäinen
Departments of Serology and Bacteriology, Biochemistry, and Virology
University of Helsinki
Helsinki, Finland
Accepted June 28, 1972

THE JOURNAL OF BIOLOGICAL CHEMISTRY
Vol. 248, No. 12, Issue of June 25, pp. 4311–4317, 1973
Printed in U.S.A.

External Labeling of Cell Surface Galactose and Galactosamine in Glycolipid and Glycoprotein of Human Erythrocytes*

(Received for publication, January 4, 1973)

CARL GUSTAV GAHMBERG‡ AND SEN-ITIROH HAKOMORI
From the Departments of Pathobiology and Microbiology, University of Washington, Seattle, Washington 98195

SUMMARY

Treatment of erythrocytes with galactose oxidase (EC 1.1.3.9) followed by reduction with tritiated sodium borohydride (NaB^3H_4) at pH 7.4 allowed the labeling of galactosyl and *N*-acetylgalactosaminyl residues on external surfaces of cells with tritium (^3H). Labeling patterns and specific activities of galactose and galactosamine in glycolipids and glycoproteins were determined after separation with gel electrophoresis and thin layer chromatography. The labeling patterns of normal adult cells differed greatly from fetal cells, and were significantly altered when cell surfaces were modified by proteases and neuraminidase. The results of analysis indicated that (*a*) the carbohydrate moieties of two glycolipids (globoside and ceramide trihexoside) and at least three glycoproteins (molecular weight 9.5, 8.2, and 6.4 × 10^4) were exposed to the external environment, but not ceramide dihexoside, ceramide monohexoside, or other glycoproteins with higher molecular weights; (*b*) the specific activities of galactosamine in glycolipid and of galactose in glycoprotein increased after protease treatment, although total activity of glycoprotein did not change; (*c*) labeling of glycoprotein was greatly enhanced by neuraminidase treatment, while that of glycolipid was enhanced to a lesser degree; (*d*) "the relative exposures" of glycoprotein and glycolipid differed greatly between normal and fetal erythrocyte surfaces. Glycoproteins of fetal cells had a very low label as compared to glycolipid.

Enriched localization of glycoproteins and glycolipids in surface membranes of cells has been demonstrated by histochemical visualization of complex carbohydrates in the cell coat (2), by the high content of glycolipids (3–6) and protein-bound fucose and glucosamine (7) in an isolated plasma membrane, and by reactions of cell surfaces with anti-glycolipid antibodies (8, 9) and with plant agglutinin (10, 11).

* This work was supported by the National Institutes of Health Research Grants CA10909, CA12710, and by the American Cancer Society Research Grant BC-9C. A preliminary note of this paper was submitted to the Annual Meeting of the American Association of Biological Chemists, April 1973 (1).

‡ Recipient of International Fogarty Center Fellowship 1 F05 TW01885-01.

A significant role of complex carbohydrates on cell surfaces in controlling cell division and intercellular association has been predicted based on the change of chemical and organizational structures of membrane-bound carbohydrates or related enzymes in association with "contact inhibition" (12–15), cell aggregation (16), mitotic cell cycle (17), and malignant transformation (18–20). Surface-exposed carbohydrates of cells are, therefore, of great cell-sociological significance, and it has become increasingly important to elucidate the exposed chemical structures of cell surfaces. Labeling of cell surface tyrosyl residues has been developed using lactoperoxidase and radioactive iodine (21, 22), while cell surface amino groups have been labeled with ^{35}S-labeled formylmethionylsulfone methylphosphate (23) or with ^{35}S-labeled sulfanilic acid diazonium salt (24); labeling of specific surface carbohydrates, however, has been awaiting development. Very recently, labeling of surface sialyl residues by periodate and tritiated sodium borohydride was described (25), whereby sialyl residues were converted to a 3-deoxy-5-acetamidoheptulonic acid.

Although the majority of cellular glycosphingolipids are found in plasma membranes, direct evidence that the carbohydrate moiety of glycolipids is exposed to the external environment has not been provided. Also, nothing has been known about the relative exposures of glycoprotein and glycolipid or about possible change in exposure with change of surface function and with modification of cell surfaces by neuraminidase and proteases. In order to solve these problems, we have developed a method using galactose oxidase (26) and tritiated sodium borohydride (NaB^3H_4), which allowed specific labeling of surface galactose and galactosamine residues in glycolipid and glycoprotein. Application of this method to analyze the organizational state of surface carbohydrates of human erythrocytes is reported in this paper.

MATERIALS AND METHODS

Cells and Enzymes

Human adult erythrocytes (A Rh^+) were obtained from citrated blood by centrifugation and were washed with phosphate-buffered saline, pH 7.4. Fetal erythrocytes were obtained from an abortion case from the Division of Human Embryology, Department of Pediatrics, University of Washington.

Galactose oxidase of *Dactylium dendroides* (26) was obtained from Sigma Chemical Company, St. Louis, Missouri, with a described activity of 37 units per mg of protein. The enzyme

This is an Open Access article under the CC BY license.

Carl_G_190x270_mm_blokki_FINAL.indd 29 06-Aug-23 1:53:29 PM

had no contamination from protease activity, which was determined using "Azo-albumin" (Sigma Chemical Company, St. Louis, Mo.) as substrate, nor any detectable neuraminidase activity, which was determined using submaxillary mucin and disialoganglioside as substrate. Pronase (*Streptomyces griseus*, 45 units per mg) and neuraminidase (*Vibrio cholerae*, 500 units per ml) were purchased from Calbiochem, La Jolla, California. Tritiated sodium borohydride (100 mCi per mmole) was obtained from New England Nuclear Company, Boston, Massachusetts.

Cell ghosts (plasma membranes) of erythrocytes were prepared by lysing the cells in hypotonic PBS,[1] pH 7.4 (isotonic PBS diluted 1:9 with water), followed by centrifugation at 16,000 rpm for 20 min. The membranes were washed three times, after which only traces of hemoglobin remained with the ghosts.

Treatment of Cells with Trypsin—Cell suspensions in PBS, pH 7.4, were mixed with twice the volume of 0.25% trypsin solution ("Gibco" Biological Company, Berkeley, California) and incubated at 37° for 30 min with continuous shaking, transferred to an ice-water bath, and washed by centrifugation with a large volume of ice-cold PBS, pH 7.0, three times.

Treatment of Cells with Pronase—To the cells was added twice the volume of 0.5 mg per ml of pronase in PBS, pH 7.4, and the cells were incubated and washed as for trypsin treatment.

Treatment of Cells with Neuraminidase—The cells were suspended in twice the volume of 0.1 M sodium phosphate buffer, pH 6.0, and 0.05 ml of the neuraminidase solution per ml of packed cells was added. The cells were incubated and washed as for trypsin treatment.

Labeling Procedure

Erythrocytes were washed with PBS, pH 7.0, and 1 to 5 ml of packed cells were mixed with 10 to 100 μg of protein of galactose oxidase dissolved in PBS, pH 7.0. The cells were incubated for varying periods of time (optimal time 3 hours) at 37° in a water bath with gentle shaking and were washed by centrifugation in PBS, pH 7.4. To the washed packed cells was added 0.05 ml of a freshly prepared tritiated sodium borohydride solution at room temperature. The tritiated sodium borohydride solution was prepared by dissolving 1 mCi of the substance (specific activity, 100 mCi per mmole) in 0.2 ml of PBS pH 7.4. After 30 min at room temperature with occasional shaking, 1 mg of unlabeled sodium borohydride was added; the cells were diluted with 5 ml of PBS pH 7.4, shaken well, and centrifuged. Washing by centrifugation in PBS was repeated five times. Cells treated with neuraminidase and protease and isolated cell ghosts were labeled by the same procedure. No significant lysis of the cells occurred during the labeling procedure. After labeling was completed, the cells were lysed, and the ghosts isolated and washed three times in PBS. In other experiments, isolated ghosts were labeled and then washed three times in PBS.

Aliquots of the labeled cell ghosts, glycolipids, or glycoprotein fractions obtained from the labeled cells or ghosts were mixed with 0.5 ml of "NCS" solubilizer (Amersham-Searle, Arlington Heights, Illinois) containing 10% H_2O and incubated at 50° for 2 hours or more. After cooling, the vials were counted in a toluene-based scintillation fluid containing 0.4% 2,5-diphenyloxazole (PPO) and 0.01% *p*-bis[2-(5-phenyloxazolyl)]benzene (POPOP) in a Packard Tri-Carb liquid scintillation spectrometer. The efficiency for tritium counting was 43%.

Glycolipids and Glycoproteins

Glycolipids were extracted by homogenizing at room temperature for 3 min in an "Omnimixer" (Sorvall Instrument Company) with 20 to 30 volumes of chloroform-methanol (2:1, v/v) to 1 volume of cells and left at +4° overnight. One-third volume of methanol was added and the samples centrifuged to obtain the protein and glycoprotein sediment, which was then washed twice in chloroform-methanol (1:1, v/v). The glycolipid fraction was prepared from lipid extract by acetylation procedure (27); the fraction was deacetylated and separated into components by thin layer chromatography. Bands corresponding to globoside, ceramide trihexoside, and ceramide dihexoside were scraped, extracted with chloroform-methanol (2:1), filtered, and aliquots were counted. The globoside, CTH fractions, and glycoproteins were methanolyzed with 1 N methanolic HCl at 80° for 18 hours, and the sugar methyl glycosides were separated by gas-liquid chromatography according to the procedure of Sweeley and Walker (28), as modified by Laine *et al.* (29) with trimethylsilyl derivatives on an SE-30 column in a Hewlett-Packard gas chromatograph F&M (model 401). Myoinositol was used was an internal standard.

The retention times were recorded and the peaks quantified by using known amounts of galactose, *N*-acetylgalactosamine, and an internal standard. Immediately after the new aliquots were run and during the elution of galactose and *N*-acetylgalactosamine, the flame was extinguished and the derivatives collected in a capillary pipette cooled with Dry Ice. The flame was then lit again, and the inositol peak emerging last was recorded. The trimethylsilyl derivatives were eluted with chloroform-methanol (2:1) into scintillation vials, evaporated at room temperature, and the radioactivity was determined after addition of scintillation fluid.

Gel Electrophoresis

The cell ghosts were dissolved in 1% sodium dodecyl sulfate and 5% 2-mercaptoethanol and heated to 100° for 2 min. Electrophoresis was performed with bromphenol blue as tracking dye in 7.5% acrylamide gel (30). Bovine serum albumin with a molecular weight of 68,000 (31), ovalbumin with a molecular weight of 44,500 (31), and ribonuclease A with a molecular weight of 13,700 (32) were used as standards. The gels were sliced with a razor blade gel slicer, and the slices were counted in toluene-based scintillation fluid after NCS solubilization at 50° for overnight.

Autoradiography

Intact erythrocytes were labeled by the galactose oxidase method, and the total radioactivity was determined to be 25,000 cpm/0.1 ml of cells. The sample was subjected to autoradiography according to the method of Rieke *et al.* (33). The autoradiographs were studied and photographed with a Nikon inverted microscope at a magnification of × 1000.

RESULTS

Total Labeling Figure

Surface labeling of erythrocytes by the present method is indicated by the fact that a high label was found in cell

[1] The abbreviations used are: PBS, phosphate-buffered saline or isotonic phosphate buffer plus isotonic sodium chloride solution; globoside, a trivial name used as an abbreviation for a ceramide tetrasaccharide whose structure was determined as GalNAcβ1 → 3Galα1 → 4Galβ1 → 4Glc → ceramide; CTH, ceramide trihexoside Galα1 → 4Galβ1 → 4Glc → ceramide; CDH, ceramide dihexoside Galβ1 → 4Glc → ceramide.

Carl_G_190x270_mm_blokki_FINAL.indd 30 06-Aug-23 1:53:29 PM

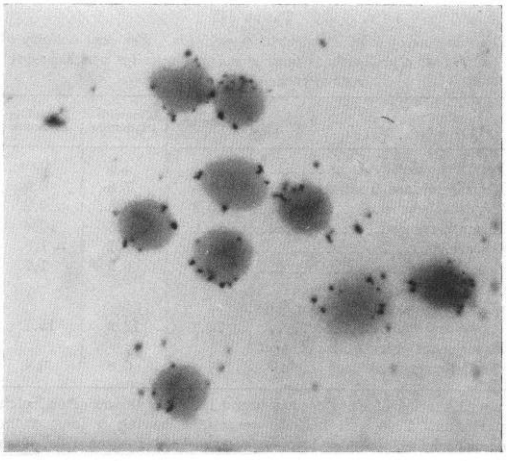

FIG. 1. Light microscopic picture of an autoradiogram of labeled intact cells. The autoradiogram was prepared according to the method of Rieke *et al.* (33) by the courtesy of Mrs. Ruth Tyler, Department of Biological Structure, University of Washington, School of Medicine. Photography by Mr. Randy Jenkins.

TABLE I

Total label in 5 ml of packed erythrocytes

Sample	Galactose oxidase	Total cpm × 10^{-4}	Protein	Lipid
	μg		% total[a]	% total[a]
Intact cells	100	24.6	62.3	37.7
Intact cells	0	3.5[b]	35.1	64.9
Neuraminidase-treated	100	141.8	86.0	14.0
Trypsin-treated	100	27.1	55.4	44.6
Pronase-treated	100	34.5	51.0	49.0
Ghost	100	101.3	54.2	45.8
Ghost	0	32.7[b]	39.8	60.2
Total label in 1 ml of packed normal and fetal cells				
Intact normal cells	50	30.1	57.5	42.5
Intact normal cells	0	4.5[b]	n.d.[c]	n.d.[c]
Intact fetal cells	50	14.8	32.3	67.7
Intact fetal cells	0	9.8[b]	33.3	66.6

[a] Determined by sodium dodecyl sulfate gel electrophoresis.

[b] Nonspecific label by tritated sodium borohydride alone (see Footnote 3 for text).

[c] n.d., not determined.

ghosts (plasma membranes)[2] and by the autoradiograph of cells (Fig. 1).

Total radioactivities of packed intact cells, of cells treated with proteases and neuraminidase, and of labeled lysed ghosts were compared and are listed in Table I.

Total labeling of erythrocytes was dependent on the quantity of galactose oxidase and was found to be linear up to 100 μg of galactose oxidase protein added per 5 ml of packed cells (Fig. 2), which indicates that most of the label is due to aldehyde groups created by galactose oxidase.

[2] Determination of the proportion of the label in surface membranes to that of total erythrocytes was difficult to perform as the total labeled activity of intact cells was impossible to determine due to chemiluminescence caused by hemoglobin.

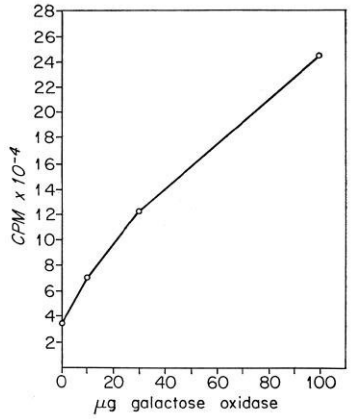

FIG. 2. Dependence of incorporation of ^3H from tritiated sodium borohydride in intact red cells on galactose oxidase concentration. Five milliliters of packed cells were labeled as described under "Materials and Methods," the cell ghosts isolated, and the radioactivity determined after NCS solubilization in toluene-based scintillation fluid.

Labeling of isolated cell ghosts resulted in a much greater label than in intact cells, especially in the lipid fraction (Table I and Fig. 4*b*).

Nonspecific Labeling

Nonspecific labeling, *i.e.* a label occurring without galactose oxidase but only with tritiated sodium borohydride, was observed (Table I); the major nonspecific label, although weak, occurred in an unidentified lipid fraction,[3] as demonstrated on gel electrophoresis (see Fig. 4*e*) and by lipid extraction, but some very weak nonspecific labels were also found in protein.[3] Nonspecific labeling was not remarkable when intact erythrocytes were labeled, but was greatly enhanced when cell ghosts were labeled (Table I, "Discussion").

Specific Labeled Activities of Galactose and Galactosamine in Glycoproteins and Glycolipids

The specific activities (counts per min per nmoles) of labeled galactose and *N*-acetylgalactosamine in glycoproteins, globoside, and CTH are shown in Table II, and the dependency of those activities on the amount of galactose residue is shown in Fig. 3. The specific activity was higher in the galactosyl residue for proteins and in the *N*-acetylgalactosaminyl residue for lipids (Fig. 3). A remarkable increase of specific activity of glycoprotein galactose was observed after treatment with proteases, although total labeling increased only slightly. The specific activities of both galactosamine and galactose in globoside increased after cells were treated with Pronase.

Labeling for both galactose and *N*-acetylgalactosamine in glycoprotein and for *N*-acetylgalactosamine in globoside increased (10 times) when the amounts of galactose oxidase added

[3] Nonspecific label without galactose oxidase in lipid fractions could be aliphatic aldehydes (plasmals), ketosphingosine, and pyridinium compounds plausibly bound to lipids. They are, however, not identified. Nonspecific label for protein is unknown, but any reducible structure as have been found in collagenous protein in the form of Schiff's base (34) can be considered. Nothing is as yet identified.

Carl_G_190x270_mm_blokki_FINAL.indd 31 06-Aug-23 1:53:29 PM

TABLE II

Specific activities labeled in galactose and N-acetylgalactosamine (cpm/nmole) of glycolipid and glycoprotein from erythrocyte membranes

The trimethylsilyl sugar derivatives were quantified by gas-liquid chromatography and the radioactivity of the peaks determined as described under "Materials and Methods."

	Glycoprotein		Globoside		CTH
	Gal	Gal-NAc	Gal	GalNAc	Gal
Intact red cells 100 μg of galactose oxidase	73.7	307	15.1	805	60
Intact red cells 0 μg of galactose oxidase	1.0	9.6	0	10.5	0
Trypsin-treated 100 μg of galactose oxidase	251	155	10.4	879	52
Pronase-treated 100 μg of galactose oxidase	183	244	31.4	1000	64

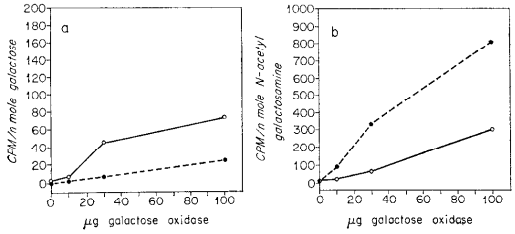

FIG. 3. Specific activities in galactose (*a*) and *N*-acetylgalactosamine (*b*) in glycoprotein (○——○) and globoside (●– – –●) obtained with varying galactose oxidase concentrations. Note that: (*a*) the specific activity of galactosamine was greater in glycolipid with a terminal *N*-acetylgalactosamine (globoside) than glycoprotein, while that of galactose was greater in glycoprotein than in glycolipid (globoside); (*b*) the specific activity of galactosamine in globoside was greatly enhanced on increase of galactose oxidase added, while that of galactose in globoside did not increase much.

were increased, while labeling for the galactosyl residue of globoside increased to a lesser degree when the amount of galactose oxidase increased (Fig. 3). No label was found in glucose.

Comparison of Specific Activities of Individual Glycolipids

Distribution of labels in various glycolipids is shown in Table III. The major label was found in globoside, followed by ceramide trihexoside, while no label was present in lactosylceramide. It is noteworthy that the label ratios for individual glycolipids (globoside-CTH-CDH) are nearly constant and are not greatly changed by treatment with neuraminidase and proteases. Some labels for ceramides with a long carbohydrate chain were also found (see footnote to Table III).

The labeling ratio between globoside, CTH, and CDH differed greatly from the actual chemical quantities of these glycolipids present in membranes (see Table III). The "degree of exposure," as expressed by counts per min per μM amount, was quite high in globoside as compared to other glycolipids.

Relative Radioactivities of Labeled Glycoproteins and Glycolipids

The labeled glycoproteins and glycolipids were separated by sodium dodecyl sulfate gel electrophoresis (7), and the relative

TABLE III

Distribution of label in neutral glycolipids. Per cent activity of individual glycolipids to total glycolipid activity[a] and exposure rate of individual glycolipids

	Globoside	Ceramide trihexoside	Ceramide dihexoside
Intact erythrocytes	95.5	4.5	0
Neuraminidase-treated	91.5	7.6	0.9
Trypsin-treated	96.3	3.5	0.2
Pronase-treated	93.0	6.6	0.4
Ghosts	91.0	7.1	1.9
Fetal erythrocytes	92.0	6.3	1.7
Chemical amounts in intact cells (molar ratio)	72.1	12.2	15.7
Exposure of glycolipids in intact cells (cpm × 10^{-3} per μmole)[b]	24	6.6	0

[a] About 1% of lipid counts found in upper layers after Folch partition. This will include ceramides having a long chain carbohydrate, ceramide hexa- to tettareskaidecasaccharide, some of which carry blood group specificities (35, and unpublished observation).

[b] Activity per μmole of glycolipid: the labeled radioactivity (cpm) of glycolipid from 1 ml of packed cells divided by the chemical quantity (μmoles) of glycolipid in 1 ml of packed cells as determined by the method of Vance and Sweeley (36).

radioactivities of the glycoprotein peaks and of the lipid peak could be determined. This pattern of activities depends on surface properties of erythrocytes and varies according to physiological state (fetal or adult) and to modification of cell surfaces by enzyme treatment.

Intact human erythrocytes were labeled, membranes were prepared, and then subjected to sodium dodecyl sulfate polyacrylamide gel electrophoresis. Under these conditions three glycoprotein Peaks a, b, and c, corresponding, respectively, to apparent molecular weights of 9.5, 8.2, and 6.4 × 10^4, and a sharp lipid peak (L) were observed (Fig. 4*a*). If the cell membranes were first prepared and then labeled, the sodium dodecyl sulfate polyacrylamide gel electrophoresis pattern was significantly different. There was a dominant Peak L and a labeled glycoprotein with high apparent molecular weight (1.5 × 10^6), in addition to Peaks a, b, and a very weak c; thus, a highly active extra peak was labeled when membranes were first prepared then labeled (Fig. 4*b* and "Discussion").

Labeling Pattern of Cells Whose Surfaces Were Modified by Enzymes

About 60% of the total label in intact cells was found in protein and 40% was in lipid. The total label was greatly increased by neuraminidase treatment but only slightly by protease treatment (Table I). After protease treatment, the label in glycolipid increased more than in glycoprotein (Table I). With trypsin treatment glycoproteins *a* and *b* lost some activity, but activity for the lipid peak (L) intensified somewhat (see Fig. 4*c*). After neuraminidase treatment an increased label was found mainly in glycoprotein with a smaller increase in glycolipid (compare Fig. 4, *a* and *d*); thus, about 85% of the total label was found in glycoprotein after treatment with neuraminidase. Neuraminidase-treated erythrocytes showed remarkable enhancement in a particular glycoprotein peak with an apparent molecular weight 8.5 × 10^4, which is probably derived from glycoprotein *a*, and the appearance of a new peak with an apparent molecular

Carl_G_190x270_mm_blokki_FINAL.indd 32 06-Aug-23 1:53:29 PM

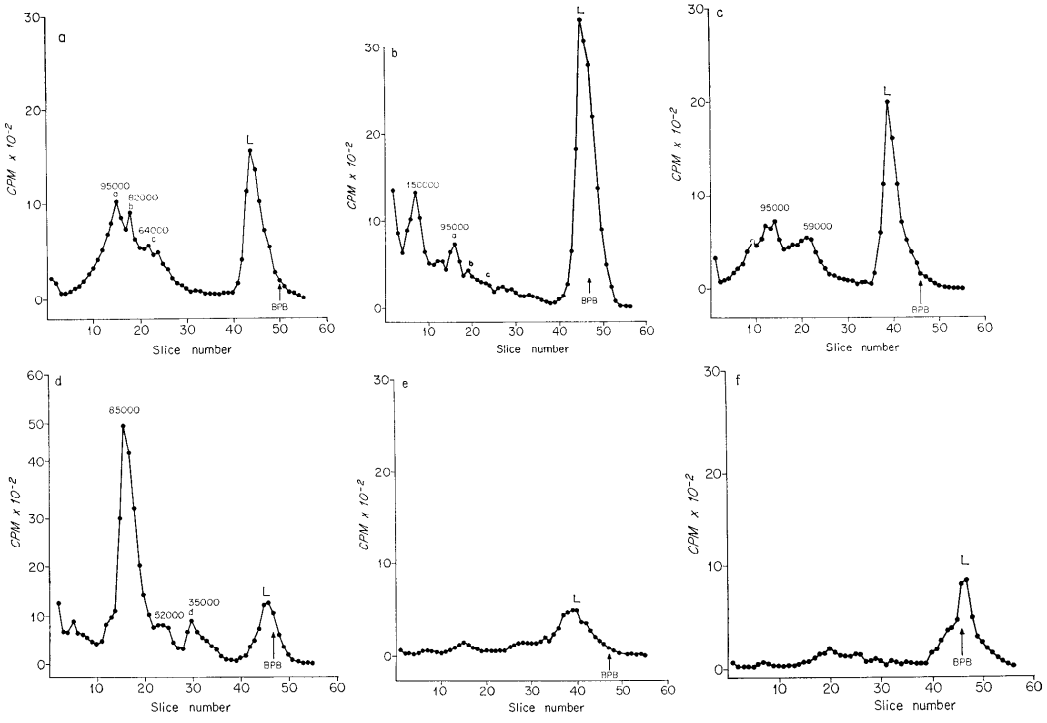

FIG. 4. Sodium dodecyl sulfate polyacrylamide gel electrophoresis of red cell ghosts, isolated from ^{3}H-labeled intact cells (*a*), ghosts isolated, then labeled (*b*), ghosts from trypsin-treated cells (*c*), from neuraminidase-treated cells (*d*), from intact cells labeled without using galactose oxidase (*e*), and from fetal cells (*f*). Apparent molecular weights are indicated. *L*, lipid peak. *BPB*, bromphenol blue tracking dye.

weight 3.5×10^4. Also, the label in the lipid peak (L) was enhanced (see Fig. 4*d*).

Comparison of Labeling Patterns of Normal Adult Erythrocytes and of Fetal Erythrocytes

Glycolipid of fetal erythrocytes obtained from 3 months gestation period was labeled less efficiently than adult erythrocytes, although the label proportions of individual glycolipids (globoside-CTH-CDH) is not greatly different in adult and fetal erythrocytes (Table I). A great deal of enhanced agglutinability by antiglobosidc antisera was demonstrated in fetal cells, however, in agreement with the previous results (9). The most remarkable label difference between normal and fetal erythrocytes was demonstrated in the ratio of activities between protein-bound carbohydrates (glycoprotein) and lipid-bound carbohydrates (glycolipid) (Table I and Fig. 4*f*). Fetal erythrocytes showed a very weak activity in the area of glycoproteins *c* and *d*. No activity corresponding to Peaks a and b was demonstrated, whereas the activity for lipid peak (L) was remarkably demonstrated.

DISCUSSION

In this study galactose oxidase from *Dactylium dendroides* has been used to obtain specific labeling of cell surface glycoproteins and glycolipids. Galactose oxidase shows a strict specificity for galactose and *N*-acetylgalactosamine, whose primary hydroxyl groups are oxidized to aldehyde groups (26). Oxidation by galactose oxidase followed by reduction with tritiated sodium borohydride has been used previously to label galactosyl and galactosaminyl residues in glycolipids (37–40) and glycoproteins (41, 42). This reaction has now been successfully applied to external labeling of galactosyl and galactosaminyl residues at the cell periphery. Lactoperoxidase with a molecular weight of 78,000 (22) is known to react exclusively at the red cell surface. Galactose oxidase has a molecular weight of 75,000 (26), which closely approximates that of lactoperoxidase. Therefore, penetration of this enzyme through the cell membrane should not occur. Surface labeling of erythrocytes was indicated by the autoradiograph of cells as seen in Fig. 1.

Cell ghosts, isolated then labeled, demonstrated a highly labeled protein with apparent molecular weight of 150,000, whereas such a protein is not seen in membranes of labeled intact cells (cells labeled then ghosts isolated) (see Fig. 4*b*). This protein, therefore, could be located on the inner surface of the plasma membrane. The results indicate that galactose oxidase cannot penetrate the cell membrane to label this protein in the intact cell.

Nonspecific labeling (see Footnote 3) was not significant in intact cells, but increased to a great extent when ghosts were labeled. Enhanced lipid labeling in ghosts as seen in Fig. 4*b*

Carl_G_190x270_mm_blokki_FINAL.indd 33 06-Aug-23 1:53:29 PM

is largely due to increased nonspecific labeling, *i.e.* the naturally occurring reducible lipid component increased when cells were lysed. The reducible materials in intact membranes can be made more accessible to borohydride by lysis of membrane, either by change of membrane conformation or by exposure of the inner surface. Although naturally occurring materials reducible by borohydride have not been identified in membrane,[3] this could be an interesting subject in membrane chemistry.

This study gives direct evidence that sugars of both glycolipids and glycoproteins are exposed on the membrane surface. Two proteins have been known to be exposed on the outer surface of human erythrocytes (22, 23, 41). One of these is the major membrane glycoprotein, which carries all demonstrable sialic acid (22–24), AB and MN blood group antigens, and receptors for influenza virus and phytoagglutinins (43). There is evidence that this protein traverses the cell membrane to the cytoplasmic surface (44). The region of protein which is exposed to the outside carries the carbohydrate portion, while the COOH-terminal end is enriched in hydrophobic amino acids and possibly serves to attach the protein to the membrane (43). This idea that membrane proteins have a hydrophobic inner end and a protease-sensitive hydrophilic outer segment is also true for cytochrome b_5 arranged in the microsomal membrane (45) and Semliki Forest virus membrane proteins (46), and it possibly has general significance. The main labeled glycoprotein peak (a) has an apparent molecular weight of 95,000 and no doubt corresponds to the multispecific glycoprotein (22, 23, 43). The major oligosaccharide portion of this protein has been proposed to have the structure NeuNAc α (2 → 3) Gal β (1 → 3) {NeuNAc α (2 → 6)} GalNAc (47). This structure could explain the more efficient labeling after neuraminidase treatment.

We have also obtained direct evidence that some glycosphingolipids of membranes are exposed directly to the external environment. Labeling of human erythrocytes was particularly remarkable in globoside, the major glycolipid of human erythrocytes with a structure GalNAcβ1 → 3Galα1 → 4Galβ1 → 4Glc → ceramide (48, 49). However, surface exposure of globoside has been doubted because of the following two findings: (*a*) treatment of intact erythrocytes by jack bean β-*N*-acetylhexosaminidase does not hydrolyze globoside in membranes, but globoside is readily hydrolyzed when an aqueous solution of globoside is treated with jack bean β-*N*-acetylhexosaminidase;[4] and (*b*) intact human erythrocytes are only slightly reactive to anti-globoside antisera (8, 9).

Human adult erythrocytes were not agglutinated nor hemolyzed by antigloboside antisera although globoside is the major glycolipid of the erythrocyte membrane. They become reactive to anti-globoside only after treatment with neuraminidase or with proteases (9). Absorption capability of anti-globoside by human erythrocytes is, in fact, increased by enzyme treatment (9).

Because human fetal erythrocytes were highly reactive to anti-globoside without enzyme treatment, globoside groups were thought to be "cryptic" in human adult erythrocytes and "exposed" in fetal erythrocytes or by enzyme treatments (9). This interpretation should be revised by the fact that globoside is highly labeled by the galactose oxidase method; the labeled activity of adult erythrocytes is not greatly different from fetal erythrocytes and is unchanged after enzyme treatment. Topological change of globoside in the membrane can be considered

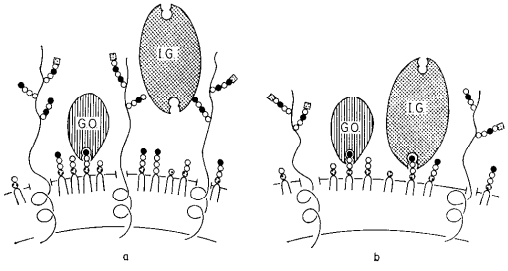

FIG. 5. An idealized version of molecular arrangement of glycolipids and glycoproteins in membranes of normal (*a*) and fetal (*b*) erythrocytes. ●, GalNAc or GlcNAc; ○, Gal; *dotted ball*, Glc; *dotted square*, sialic acid; *coiled* or *stretched lines*, peptides; *G.O.*, galactose oxidase; *I.G.*, immunoglobulin for antiglycolipid (*e.g.* antigloboside). This figure illustrates three points: (*a*) glycolipids are directly imbedded on the lipid bilayer through two hydrocarbon chains (ceramide), and glycoproteins are associated with the lipid bilayer through hydrophobic peptide regions according to Marchesi's "glycophorin" model (41); (*b*) a major carbohydrate structure bound to lipid (glycolipid) is "globoside" with a terminal GalNAc → Gal → Gal → R, whereas a major carbohydrate structure bound to protein (glycoprotein) is sialyl → Gal → GalNAc → R, although a few globosidic structures can also be found in glycoprotein (evidence proposed by the reaction of glycoprotein with antigloboside antibody).[5] Therefore, antigloboside antibody should be primarily directed to the globoside seated on the lipid bilayer; (*c*) possibly coincident to the loci of "plasma membrane particles" (48), glycoprotein and proteins are located close to each other on the lipid bilayer and form "bushes" of glycoprotein; glycolipids are located among these bushes. Galactose oxidase can penetrate between such bushes to label glycolipids, but other larger molecules like immunoglobulin cannot react with the glycolipids in normal erythrocytes as shown in *a*. In contrast, the model in *b* showed a possibility that fewer glycoproteins and proteins are present on fetal erythrocytes and therefore, not only galactose oxidase but also immunoglobulin can react with globoside on fetal cell surfaces. This model is based on a provision that glycoprotein of fetal erythrocytes are qualitatively similar to that of adult erythrocytes.

in view of a recent observation by Nicolson (11) that trypsinization can cause clustering of some phytoagglutinin reactive sites on cell surfaces.

The relevant explanation for understanding labeling pattern of globoside (and other glycolipids) and glycoprotein is that globoside may be seated directly on the lipid bilayer among "bushes" of protein and glycoprotein (see Fig. 5), and that globoside is available only to galactose oxidase but not to larger macro molecular reagents, such as immunoglobulin and β-*N*-acetylhexosaminidase. In fact, molecular weight of galactose oxidase (75,000) is smaller than immunoglobulin (mol wt 180,000) or β-*N*-acetylhexosaminidase (mol wt 100,000). Other factors such as shape and ionic charge should also be considered. On the surface of protease-treated cells, globoside is available not only to galactose oxidase but also to immunoglobulin (see Fig. 5). Lactosylceramide in the membrane was not labeled by this procedure. However, CDH alone can be easily labeled *in vitro* by this method (40), and we have shown that after Triton X-100 solubilization of the erythrocyte membranes, the labeling of CDH was greatly enhanced and comparable to the label of CTH. This indicated that the carbohydrate chain of CDH does not protrude far enough to be reached by galactose oxidase in the membrane, in agreement with immunological data that human

[4] B. Siddiqui and S. Hakomori, unpublished observations.

[5] K. Watanabe and S. Hakomori, unpublished observation.

Carl_G_190x270_mm_blokki_FINAL.indd 34 06-Aug-23 1:53:29 PM

erythrocytes are not reactive to anti-lactosylceramide even after trypsin digestion (9).

Comparative labeling of glycoprotein and glycolipid has been observed by gel electrophoresis of labeled membranes. Labeling of glycoprotein varied greatly in contrast to a rather constant labeling of glycolipid. Absence of Peaks a or b glycoprotein in fetal erythrocytes is of great interest, which indicates either of the following possibilities: (*a*) fetal glycoproteins do not have any galactosyl or galactosaminyl residues so that they are not labeled; (*b*) galactosyl or galactosaminyl residues of fetal glycoprotein could be highly substituted by other sugar residues such as sialyl or fucosyl residues so that they are not labeled; and (*c*) fetal erythrocytes have smaller number of glycoproteins; glycoproteins a or b are virtually absent. A tentative model based on the third possibility that a higher agglutinability of fetal erythrocytes to antigloboside can be ascribed to less steric hindrance due to the absence of some surface glycoprotein is shown by Fig. 5. Further extensive study is needed to correlate the surface structure revealed by external labeling to the immunological reactivity of cells surfaces. A study in progress (1) showed that this surface labeling procedure for sugars was found to be extremely useful to distinguish the surface properties of various normal and transformed cells as well.

Note Added in Proof—Since this paper was processed, at the stage of proofing, we noticed that T. L. Steck used galactose oxidase for surface labeling of erythrocytes ((1972) in *Membrane Research,* edited by C. F. Fox, p. 71 Academic Press, New York).

REFERENCES

1. Gahmberg, C. G., and Hakomori, S. (1973) *Fed. Proc.* **32,** 523
2. Rambourg, A., Neutra, M., and LeBlond, C. P. (1966) *Anat. Rec.* **154,** 41
3. Dod, B. J., and Gray, G. M. (1968) *Biochim. Biophys. Acta* **150,** 397
4. Renkonen, O., Gahmberg, C. G., Simons, K., and Kääriäinen, L. (1970) *Acta Chem. Scand.* **24,** 733
5. Weinstein, D. B., Marsh, J. B., Glick, M. C., and Warren, L. (1970) *J. Biol. Chem.* **245,** 3928
6. Klenk, H. D., and Choppin, P. W. (1970) *Proc. Nat. Acad. Sci. U. S. A.* **66,** 57
7. Gahmberg, C. G. (1971) *Biochim. Biophys. Acta* **249,** 81
8. Koscielak, J., Hakomori, S., and Jeanloz, R. W (1968) *Immunochemistry* **5,** 441
9. Hakomori, S. (1964) *Vox Sang.* **16,** 478
10. Burger, M. M. (1969) *Proc. Nat. Acad. Sci. U. S. A.* **62,** 994
11. Nicholson, G. L. (1972) *Nature New Biol.* **239,** 193
12. Hakomori, S. (1970) *Proc. Nat. Acad. Sci. U. S. A.* **67,** 1741
13. Robbins, P. W., and Macpherson, I. (1971) *Nature* **229,** 569
14. Sakiyama, H., Gross, S. K., and Robbins, P. W. (1972) *Proc. Nat. Acad. Sci. U. S. A.* **69,** 372
15. Kijimoto, S., and Hakomori, S. (1971) *Biochem. Biophys. Res. Commun.* **44,** 557
16. Roseman, S. (1971) *Chem. Phys. Lipids* **5,** 270
17. Fox, T. O., Sheppard, J. R., and Burger, M. M. (1971) *Proc. Nat. Acad. Sci. U. S. A.* **68,** 244
18. Hakomori, S., and Murakami, W. T. (1968) *Proc. Nat. Acad. Sci. U. S. A.* **59,** 254
19. Mora, P. T., Brady, R. O., Bradley, R. M., and MacFarland, V. W. (1969) *Proc. Nat. Acad. Sci. U. S. A.* **62,** 1290
20. Yogeeswaran, G., Sheinin, R., Wherrett, J. R., and Murray, R. K. (1972) *J. Biol. Chem.* **247,** 5146
21. Phillips, D. R., and Morrison, M. (1971) *Biochemistry* **10,** 1766
22. Hubbard, A. L., and Cohn, Z. A. (1972) *J. Cell Biol.* **55,** 390
23. Bretscher, M. S. (1971) *J. Mol. Biol.* **58,** 775
24. Bender, W. W., Garan, H., and Berg, H. C. (1971) *J. Mol. Biol.* **58,** 783
25. Blumenfeld, O. O., Gallop, P. M., and Liao, T. H. (1972) *Biochem. Biophys. Res. Commun.* **48,** 242
26. Avigad, G., Amaral, D., Asensio, C., and Horecker, B. L. (1962) *J. Biol. Chem.* **237,** 2736
27. Saito, T., and Hakomori, S. (1972) *J. Lipid Res.* **12,** 257
28. Sweeley, C. C., and Walker, B. (1964) *Anal. Chem.* **36,** 1461
29. Laine, R. A., Esselman, W. J., and Sweeley, C. C. (1972) *Methods Enzymol.* **28,** 159
30. Weber, K., and Osborn, M. (1969) *J. Biol. Chem.* **244,** 4406
31. Castellino, F. J., and Barker, R. (1968) *Biochemistry* **7,** 2207
32. Dayhoff, M. O., and Eck, R. V. (1967–68) *Atlas of Protein Sequence and Structure,* p. 324, National Biomedical Research Foundation, Silver Springs, Ohio
33. Rieke, W. O., Caffrey, R. W., Everett, N. B. (1963) *Blood* **22,** 674
34. Robins, S. P., and Bailey, A. J. (1972) *Biochem. Biophys. Res. Commun.* **48,** 76
35. Hakomori, S., Stellner, K., and Watanabe, K. (1972) *Biochem. Biophys. Res. Commun.* **49,** 1061
36. Vance, D. E., and Sweeley, C. C. (1967) *J. Lipid Res.* **8,** 621
37. Hajra, A. K., Bowen, D. M., Kishimoto, Y., and Radin, N. S. (1966) *J. Lipid Res.* **7,** 379
38. Radin, N. S., Hof, L., Bradley, R. M., and Brady, R. O. (1969) *Brain Res.* **14,** 497
39. Sloan, H. R., Uhlendorf, B. W., Jacobson, C. B., and Fredrickson, D. S. (1969) *Pediat. Res.* **3,** 532
40. Suzuki, Y., and Suzuki, K. (1972) *J. Lipid Res.* **13,** 687
41. Morell, A. G., van den Hamer, C. J. A., Scheinberg, I. H., and Ashwell, G. (1966) *J. Biol. Chem.* **241,** 3745
42. Morell, A. G., and Ashwell, G. (1972) *Methods Enzymol.* **28,** 205
43. Marchesi, V. T., Tillack, T. W., Jackson, R. L., Segrest, J. O., and Scott, R. E. (1972) *Proc. Nat. Acad. Sci. U. S. A.* **69,** 1445
44. Bretscher, M. S. (1971) *Nature New Biol.* **231,** 229
45. Spatz, L., and Strittmatter, P. (1971) *Proc. Nat. Acad. Sci. U. S. A.* **68,** 1042
46. Gahmberg, C. G., Utermann, G., and Simons, K. (1972) *Fed. Eur. Biochem. Soc. Lett.,* **28,** 179
47. Thomas, D. B., and Winzler, R. J. (1969) *J. Biol. Chem.* **244,** 5943
48. Yamakawa, T., Nishimura, S., and Kamimura, M. (1965) *Jap. J. Exp. Med.* **35,** 201
49. Hakomori, S., Siddiqui, B., Li, Y-T., Li, S-C., and Hellerqvist, C. G. (1971) *J. Biol. Chem.* **246,** 2271
50. Pinto da Silva, P., and Branton, D. (1970) *J. Cell Biol.* **45,** 598

Carl_G_190x270_mm_blokki_FINAL.indd 35 06-Aug-23 1:53:29 PM

Proc. Nat. Acad. Sci. USA
Vol. 70, No. 12, Part I, pp. 3329–3333, December 1973

Altered Growth Behavior of Malignant Cells Associated with Changes in Externally Labeled Glycoprotein and Glycolipid

(polyoma virus/simian virus 40/galactose oxidase)

CARL GUSTAV GAHMBERG AND SEN-ITIROH HAKOMORI

Department of Pathobiology, School of Public Health and Department of Microbiology, School of Medicine, University of Washington, Seattle, Wash. 98195

Communicated by Herman M. Kalckar, July 20, 1973

ABSTRACT **By use of galactose oxidase (EC 1.1.3.9), followed by reduction with tritiated sodium borohydride, the surface structures of transformed 3T3 and NIL cells, under ordinary growth conditions, were characterized by (*i*) deletion of the normally existing glycoprotein label and (*ii*) appearance or increase of a new glycoprotein label. NIL cells had a galactoprotein label with molecular weight 200,000 that was deleted in NIL cells transformed by polyoma virus. 3T3 cells had a glycoprotein label with molecular weight of 30,000 that was lost after transformation. Glycoproteins of transformed 3T3 cells, with molecular weight 105,000, and those of transformed NIL cells, with molecular weight 85,000, were not labeled in normal confluent cells, but became labeled after trypsin treatment. The label in glycolipids was quantitatively different in normal and transformed cells. The labeling pattern in glycoprotein and glycolipids of transformed NIL and 3T3 cells became similar to that of nontransformed cells when contact responses of transformed cells became conspicuous when cells were cultured in the presence of dextran sulfate or dibutyryl cyclic adenosine monophosphate, or in medium in which glucose was replaced with galactose.**

There is increasing evidence that the plasma membrane of tumor cells differs from that of normal cells. Increased reactivity to lectins (1) and to anti-glycolipid antibody (2), incomplete synthesis of carbohydrate chains in glycolipid (3) and glycoproteins (4), and enhanced synthesis of a specific sialylfucopeptide in transformed cells (5) are particularly noticeable. No direct evidence has been provided, however, on whether the altered glycolipid or glycoprotein components are located on the external surface of the cell membrane.

Contact response* can be restored in tumor cells by growing them under suitable conditions, such as in medium containing dextran sulfate (6) or cyclic AMP (7) or in medium in which glucose was replaced by galactose (8). Because it recently became possible to specifically label surface glycoproteins and glycolipids of cells with galactose oxidase (EC 1.1.3.9) followed by reduction with tritiated sodium borohydride (9), a technique based on the labeling of ceruloplasmin (10) and cerebroside (11), we decided to compare surface labels of cells with normal growth and of transformed cells with induced changes in growth characteristics.

Abbreviations: 3T3sv cells, mouse fibroblast 3T3 cells transformed with Simian virus 40; 3T3svpy cells, 3T3 cells doubly transformed with Simian virus 40 and polyoma virus; NILpy cells, hamster NIL cells transformed with polyoma virus; PBS, phosphate-buffered saline.

* "Contact response" collectively includes various cell contact phenomena such as contact inhibition, topoinhibition, contact orientation, and contact promotion.

EXPERIMENTAL PROCEDURE

Cells and Cell Culture. Hamster NIL cells transformed with polyoma virus (NILpy cells) were obtained after infection with polyoma virus, and one clone was isolated in November 1972. 3T3, 3T6, 3T3sv (cells transformed with simian virus 40), and 3T3svpy (cells transformed with simian virus 40 and polyoma virus) cells were cultured in Eagle's medium, modified by Dulbecco and supplemented with 10% fetal-calf serum, in a 5–6% CO_2 atmosphere. NIL and NILpy cells were cultured in Eagle's medium containing 10% calf serum in a 3% CO_2 atmosphere.

Induction of Reversed Growth Behavior. Transformed cells changed their morphology and became sensitive to contact inhibition of growth when cultured in original Eagle's medium (1 × amino acids and vitamins) and 10% calf serum, containing 10 μg (for 3T6 cells) or 4 μg (for NILpy) of dextran sulfate per ml of medium (6). The dextran sulfate (molecular weight about 50,000) was kindly provided by Dr. M. Goto, Tohoku University, Sendai, Japan. The saturation densities of 3T6 cells and NILpy cells with induced contact sensitivity were 1–1.5 × 10^5/cm² and 10^5/cm², respectively. Cells grown in regular medium reached densities as high as 5–8 × 10^5/cm².

NILpy and 3T3svpy cells were grown in the presence of 0.1 mM dibutyryl cyclic AMP and 1 mM theophyllin (12). The morphological change appeared more remarkable in NILpy cells than in 3T3svpy cells. After 2–3 days in culture, the cells appeared well contact-oriented and the size of the cells increased. Freshly transformed NILpy cells showed remarkable changes in morphology and contact orientation when cultured in Eagle's medium (twice the standard concentration of amino acids and vitamins), in which glucose was replaced with galactose and which was supplemented with 10% fetal-calf serum.

The Procedure for Surface Labeling was a slight modification of a described method (9). The cells from one plate (Falcon, 14 cm in diameter) were enough for labeling and were obtained either by scraping with a rubber policeman or by using a 0.02% EDTA solution or a 0.25% trypsin solution. The specific activity of the NaB^3H_4 was 6 Ci/mmol. For further details, see the legend to Fig. 2.

Analysis of Labeled Glycoproteins and Glycolipids: Electrophoresis was done with internal [^{14}C]formaldehyde-labeled standard proteins (13). The radioactive gels were sliced and counted as described (9). Unless otherwise indicated, the cells were harvested by treatment with 0.02% EDTA. Glycolipids were extracted and partitioned (14). The neutral glycolipid

Carl_G_190x270_mm_blokki_FINAL.indd 36 06-Aug-23 1:53:29 PM

TABLE 1. *Change of glycolipid label in NIL cells depending on growth behavior*

Cells	Growth conditions	Morphology and growth	Harvest conditions	% Distribution of Glycolipid label: % of label in glycolipid/total label*	Ceramide pentasaccharide (Forssman)	Ceramide tetrasaccharide (Globoside)	Lower glycolipid (ceramide di-, trisaccharide)
NIL	Regular Eagle's medium, confluent	Contact inhibited, oriented	scraped	4.5	19.5	71.8	8.4
			EDTA	7.2	14.2	64.0	22.6
			trypsin	4.0	18.8	65.0	15.8
NILpy	Regular Eagle's medium, confluent	Not inhibited, disoriented	scraped	8.6	6.5	20.6	72.0
			EDTA	3.4	10.0	15.0	75.1
			trypsin	1.2	10.7	19.4	70.1
NILpy	Eagle's medium Glc replaced with Gal	Not inhibited, oriented	scraped	11.4	5.4	30.8†	64.1
			EDTA	6.3	7.8	28.8†	62.9
			trypsin	6.4	6.8	30.0†	63.0
NILpy	Eagle's medium with dextran sulfate	Contact inhibited, oriented	EDTA	1.3	25.5	21.7	56.2
NILpy	Eagle's medium with cyclic AMP and theophyllin	Contact inhibited, oriented	EDTA	3.7	18.0	36.0	46.1

* The rest of the label is due to glycoprotein or nonspecific labelling.

† About 50–80% higher label in globoside in Gal-oriented NILpy cells was reproduced in three separate experiments, and the mean values are shown. Others are the mean values of two separate experiments.

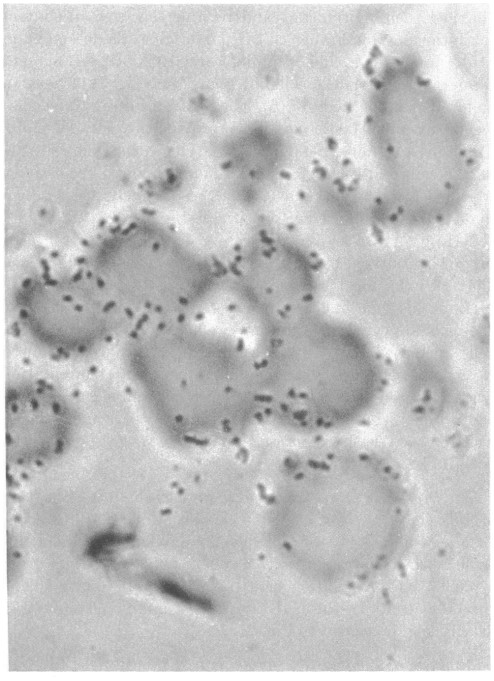

FIG. 1. Light microscopic picture of an autoradiogram of a thin section of labeled neuraminidase-treated NIL cells. Most of the label is located at the surface membrane (original magnification ×1000. The picture was prepared by Ruth Tyler, Department of Biological Structure, University of Washington.

fraction was purified from the lower phase by acetylation (15) and analyzed by thin-layer chromatography and gas chromatography as described (9).

RESULTS

Surface Localization of Label and Nonspecific Label in NIL and 3T3 Cells. The label was nearly exclusively located on cell surfaces, as shown by autoradiography of fixed and dissected cells (Fig. 1); the activity of the label was proportional to cell number. Nonspecific labels without galactose oxidase were found in some proteins and in lipids of NIL and 3T3 cells.

Peaks "c" of intact NIL and NILpy cells (Fig. 2*A* and *B*), "f" of neuraminidase-treated NIL and NILpy cells (Fig. 2*C–H*), and "e" of neuraminidase-treated transformed 3T3 cells (Fig. 3*C* and *D*) were due to nonspecific label. These proteins with nonspecific label had similar molecular weights (56,000–59,000); the label was enhanced in transformed cells.

Specific Labeling Pattern of Normal and Transformed Cells. The specific label in glycolipids was shown by the presence of radioactivity in purified glycolipid fraction by acetylation and by the presence of radioactivity in galactose and galactosamine fractions separated on gas chromatography (9). Peak "a" with an apparent molecular weight of 200,000 was found only in normal NIL cells (Fig. 2*A*), but was totally absent in transformed NIL cells (Fig. 2*B*). Without neuraminidase treatment, no appreciable glycoprotein peak was obtained for labeled 3T3 cells and their transformants.

Labeled peaks characteristic for transformed NIL and 3T3 cells were clearly demonstrated when cells were treated with neuraminidase. NILpy cells contained the enhanced peak "d" with an apparent molecular weight of 85,000 (Fig. 2*D*), and 3T3sv and 3T3svpy cells had the prominent peak "c" with

Carl_G_190x270_mm_blokki_FINAL.indd 37 06-Aug-23 1:53:29 PM

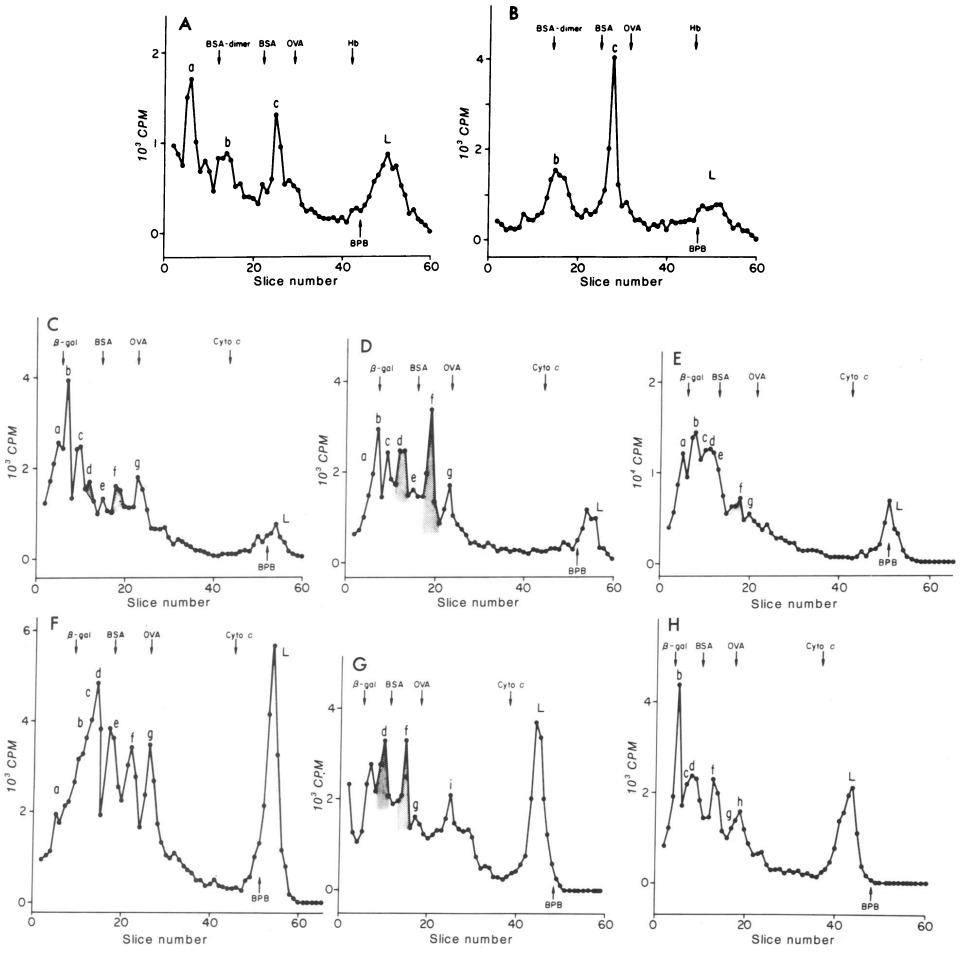

FIG. 2. Sodium dodecyl sulfate–polyacrylamide gel electrophoresis of labeled NIL cells. Cells were harvested with 0.02% EDTA solution, then treated in different ways. *A* and *B* were run in 5% polyacrylamide gels; all others (*C–H*) were run in 7.5% polyacrylamide gels. (*A*) confluent NIL cells; (*B*) NILpy cells, directly labeled without neuraminidase treatment; (*C*) confluent NIL cells; (*D*) NILpy cells, treated with neuraminidase then labeled; (*E*) NILpy cells grown in the presence of 4 μg/ml of dextran sulfate, treated with neuraminidase, then labeled; (*F*) NILpy cells grown in galactose medium (8), treated with neuraminidase, then labeled; (*G*) confluent NIL cells treated with trypsin, then with neuraminidase, then labeled; (*H*) NILpy cells grown in the presence of dibutyryl cyclic AMP, treated with neuraminidase, then labeled. Cells were washed twice by centrifugation in PBS (pH 7.0) and suspended in 0.5 ml of PBS containing 2 mM phenylmethylsulfonylfluoride (Sigma) to inhibit proteases. 100 μl of galactose oxidase dissolved in PBS (pH 7.0) containing 100 units/ml (Sigma Type III) was then added, and the cells were incubated at room temperature for 2 hr with gentle shaking. The galactose oxidase did not contain any measurable proteolytic or neuraminidase activity. In some experiments, galactose oxidase was purified by affinity chromatography on Sepharose 4B column. After incubation the cells were washed twice in PBS (pH 7.4) and suspended in 0.5 ml of PBS (pH 7.4) to which was added 50 μl of tritiated sodium borohydride solution containing 0.5–1 mCi of NaB^3H_4, specific activity 6 Ci/mmol (New England Nuclear Corp; stored in 0.01 N NaOH solution at −70). The reaction mixture was allowed to stand for 30 min at room temperature. In some experiments the cells were first incubated with 50 μl of *Vibrio cholerae* neuraminidase (Calbiochem, Type B) that contained 500 units/ml in 0.5 ml of 0.1 M phosphate buffer (pH 6.0) in the presence of protease inhibitor. Cells incubated with dibutyryl cyclic AMP were treated with *V. cholerae* neuraminidase in the presence of 1 mM dibutyryl cyclic AMP, followed by the labeling procedure. β-gal, β-galactosidase; *BSA*, bovine-serum albumin; *OVA*, ovalbumin; *cyto c*, cytochrome *c* (each labeled with [^{14}C]-formaldehyde and used as internal marker). *BPB*, peak position of bromphenol blue tracking dye. Peaks "*d*" and "*f*," which showed a remarkable change on transformation and on reverted cell behavior, are *shaded*. Peaks "*c*" of *A* and *B* and "*f*" of *C–H* were nonspecifically labeled.

Carl_G_190x270_mm_blokki_FINAL.indd 38 06-Aug-23 1:53:29 PM

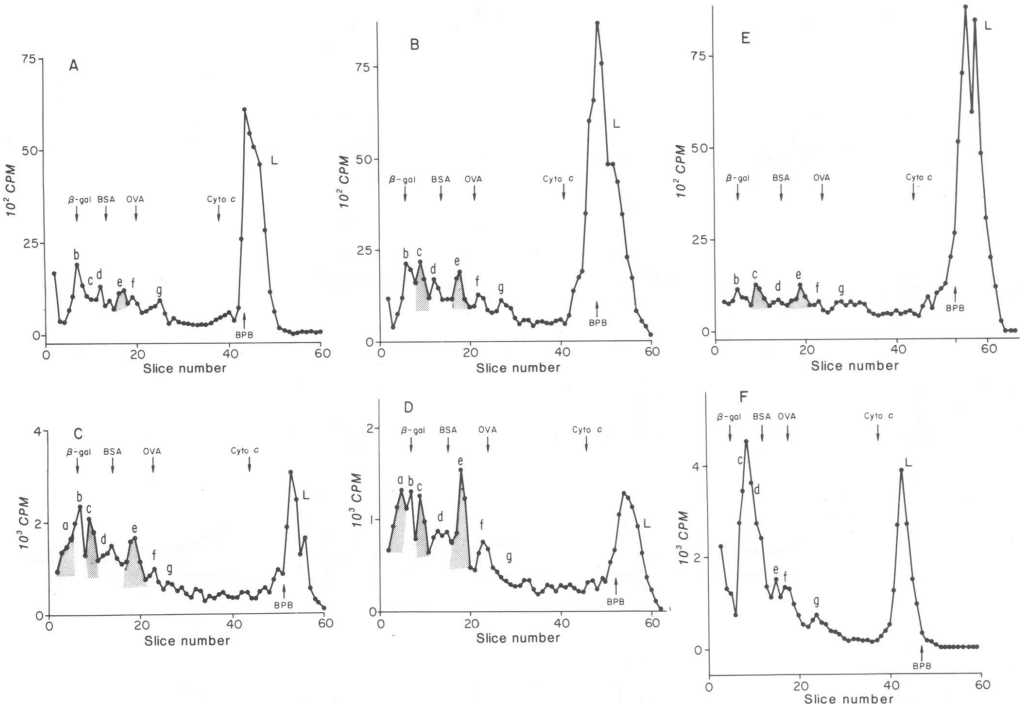

FIG. 3. Sodium dodecyl sulfate–polyacrylamide gel electrophoresis of labeled 3T3 cells and their transformants. Cells were harvested with EDTA and labeled after neuraminidase treatment. All samples were analyzed in 7.5% polyacrylamide gels. (*A*) Confluent 3T3 cells treated with neuraminidase, then labeled; (*B*) growing 3T3 cells treated with neuraminidase, then labeled; (*C*) 3T3sv cells treated with neuraminidase, then labeled; (*D*) 3T3svpy cells treated with neuraminidase, then labeled; (*E*), confluent 3T3 cells treated with trypsin, then with neuraminidase, then labeled, (*F*) 3T3svpy cells grown in the presence of dibutyryl cyclic AMP, treated with neuraminidase, then labeled. Markers and labeling procedures are the same as for Fig. 2. Peaks "c" and "e," which showed a remarkable change on transformation and on reverted cell behavior, are *shaded*. Peak "e" contained nonspecific label.

an apparent molecular weight of 105,000 (Fig. 3*C* and *D*). Actively growing 3T3 cells showed also a relatively large peak "c" (Fig. 3*B*), while confluent 3T3 cells had no detectable peak "c." Instead, the confluent 3T3 cells had more label in the "b" peak and "g" peak (Fig. 3*A*). The "g" peak was very low or not detectable in transformed cells. In either 3T3sv or 3T3svpy cells, the presence of a relatively high label at the highest molecular-weight range (peak "a" of Fig. 3*C* and *D*) was noticed.

Modified Surface Label by Trypsin and Other Reagents that Induced Altered Growth Behavior. If confluent NIL or 3T3 cells were treated with trypsin and then labeled, there appeared a greatly enlarged peak "d" for trypsinized NIL cells (Fig. 2*G*) and a peak "c" for trypsinized 3T3 cells (Fig. 3*E*), which were not markedly labeled without trypsinization. In normal 3T3 cells from either confluent or growing cultures, the label in lipid was much greater than in transformed 3T3 cells.

The relative activity of peak "b" greatly increased when contact response of NILpy cells became normal in the presence of dextran sulfate (Fig. 2*E*) or dibutyryl cyclic AMP (Fig. 2*H*, compare with *C* and *D*). 3T3svpy cells whose contact behavior was restored by cyclic AMP showed a greatly enhanced peak between "c" and "d" (Fig. 3*F*). The proportion of peaks "a"–"g" is quite characteristic for the type and physiological state of cells. The glycoprotein label profile significantly changed in NILpy cells grown in medium containing galactose (Fig. 2*F*). The glycoprotein profile of 3T6 cells resembled that of 3T3sv or 3T3svpy cells. When contact response was induced by dextran sulfate, the peaks characteristic of transformed cells disappeared, and the lipid label became prominent.

Relation of carbohydrate structures to their label and the effect of cell contact on degree of labeling were clearly seen in the labeling pattern of glycolipids. As expected, neutral glycolipids of NIL cells were strongly labeled; the label in higher glycolipids such as globoside and Forssman glycolipid decreased; the proportion of label in simpler glycolipids greatly increased in NILpy cells, in agreement with the results of chemical analysis (Table 1). A significant increase (50–80%) of globoside label and decrease of label in simpler glycolipids was observed in NILpy cells grown in galactose medium, whose contact orientation became obviously restored. Similarly, the label in Forssman glycolipid significantly increased in NILpy cells whose contact response was restored and whose contact orientation became obvious by either dextran sulfate or dibutyryl cyclic AMP (Table 1).

The label in ceramide trisaccharide increased in nontransformed NIL cells after EDTA or trypsin treatment, but was

Carl_G_190x270_mm_blokki_FINAL.indd 39 06-Aug-23 1:53:30 PM

unchanged in NILpy cells, indicating that simpler glycolipids were consistently exposed in NILpy cells.

DISCUSSION

Although several experiments using labeling with radioactive precursors have been done to distinguish membrane glycolipids and glycoproteins of normal and transformed cells (3–5), these studies were not designed to distinguish surface structural differences. Therefore, the observed differences were difficult to correlate with the function of cell surfaces. 3T3sv cells, whose contact response was partly restored by dibutyryl cyclic AMP, have a decreased level of sulfated acid mucopolysaccharides (16). Morphological change of NILpy or 3T3sv cells induced by dibutyryl cyclic AMP did not correlate with glycolipid composition (17). With the galactose oxidase labeling method, major structural differences can be seen in exposed heteroglycans in compliance with the change of growth behavior. Transformed 3T3 cells contain a labeled glycoprotein of apparent molecular weight of 105,000 (peak "c", Fig. 3), and NILpy cells contain a glycoprotein of apparent molecular weight 85,000 (peak "d," Fig. 2*F*); both glycoproteins were not labeled in the confluent normal cells but were labeled only after treatment with trypsin. Transformed 3T3 cells also contain more label in the sialylgalactoprotein *a* (Fig. 3*C* and *D*) of apparent molecular weight of 140,000. Normal NIL and 3T3 cells were characterized by higher label at peaks "a" and "b" (apparent molecular weights 200,000 and 130,000), and 3T3 cells had a peak "g" (molecular weight 30,000). These peaks were reduced or deleted in transformed cells. The presence of a galactoprotein in intact NIL cells and its complete absence in NILpy cells were well demonstrated in 5% gels (Fig. 2*A* and *B*), but not in 7.5% gels. An increase or creation of label by neuraminidase agrees with the general formula of sialoglycosides in which sialyl residue is linked to a penultimate Gal or GalNAc residue (20), detectable by *Ricinus communis* lectin (21).

In contrast to normal confluent cells, transformed cells and trypsinized normal cells are easily agglutinated by various lectins (1). This increased agglutinability was considered to be due to increased reactive sites to the agglutinins, but later work showed no essential difference in the amount of binding of agglutinins (18). This difference in agglutinability was explained by clustering of agglutinin receptors by the altered "fluid dynamic" state of the membrane of the transformed and trypsinized cells (19).

Our results show that although the total label in the glycoproteins and glycolipids of normal and transformed cells is not very different, some glycoproteins and glycolipids are much more exposed in the transformed cells, and become exposed in normal confluent cells only after trypsinization. Therefore, some of these normally cryptic specific glycoproteins could be responsible for the observed differences in agglutinability and possibly be clustered in certain regions of the cell membrane.

The label profile of transformed cells shifted towards normal when the contact response of these transformed cells was restored by dextran sulfate or by cyclic AMP. The increased label in globoside of NILpy cells, grown in a medium in which all glucose was replaced by galactose and which showed altered contact orientation, is of special interest. Previously, it was not possible to demonstrate glycolipid changes of galactose-oriented cells, compared to normally cultured cells (8). By the surface labeling technique, however, galactose-oriented cells have about 50–80% higher label in globoside, with the structure GalNAcβ1 → 3Galα1 → 3Galβ1 → 3Glc → Ceramide (22). Forssman glycolipids and globoside characteristic of normal NIL cells were much more heavily labeled in cells cultured in the presence of cyclic AMP.

These data strongly suggest that restoration of contact inhibition or the presence of contact responses observed in the cultures in the presence of dextran sulfate or dibutyryl cyclic AMP, or in galactose-oriented medium is probably due to surface structural changs. Malignantly transformed cells have a characteristic surface structure which must be the basis of their abnormal behavior, as the characteristic glycoprotein and glycolipid profile was markedly modified when cell growth behavior changed towards normal.

Supported by National Institute of Health Grants CA10909 and CA12710 and by American Cancer Society Grant BC-9C. C.G.G. was supported by International Fogarty Center Fellowship 1 F05 TW01885-01.

1. Aub, J. C., Tieslau, C. & Lankester, A. (1963) *Proc. Nat. Acad. Sci. USA* **50,** 613–619; Burger, M. M. (1969) *Proc. Nat. Acad. Sci. USA* **62,** 994–1001; Inbar, M. & Sachs, L. (1969) *Proc. Nat. Acad. Sci. USA* **63,** 1418–1425.
2. Hakomori, S., Teather, C. & Andrews, H. D. (1968) *Biochem. Biophys. Res. Commun.* **33,** 563–568.
3. Hakomori, S. & Murakami, W. T. (1968) *Proc. Nat. Acad. Sci. USA* **59,** 254–261, Brady, R. O. & Mora, P. T. (1970) *Biochim. Biophys. Acta* **218,** 308–319; Sakiyama, H., Gross, S. K. & Robbins, P. W. (1972) *Proc. Nat. Acad. Sci. USA* **69,** 872–876; Den, H., Schultz, A. M., Basu, M. & Roseman, S., (1971) *J. Biol. Chem.* **246,** 2721–2723; Critchley, D. R. & Macpherson, I. (1973) *Biochim. Biophys. Acta* **246,** 145–159.
4. Wu, H., Meezan, E., Black, P. H. & Robbins, P. W. (1969) *Biochemistry* **8,** 2518–2524; Grimes, W. J. (1970) *Biochemistry* **9,** 5083–5092, and (1973) *Biochemistry* **12,** 990–996.
5. Warren, L., Critchley, D. & Macpherson, I. (1972) *Nature* **235,** 275–278; Warren, L., Fuhrer, J. B. & Buck, C. A. (1972) *Proc. Nat. Acad. Sci. USA* **69,** 1838–1849.
6. Goto, M. & Sato, H. (1972) *Gann* **63,** 371–374.
7. Hsie, A. W. & Puck, T. T. (1971) *Proc. Nat. Acad. Sci. USA* **68,** 1648–1652; Johnson, G. S., Friedman, R M. & Pastan, I. (1971) *Proc. Nat. Acad. Sci. USA* **68,** 425–429.
8. Kalckar, H. M., Ullrey, D., Kijimoto, S. & Hakomori, S. (1973) *Proc. Nat. Acad. Sci. USA* **70,** 839–843.
9. Steck, T. L. (1972) in *Membrane Research,* ed. Fox, C. F. (Academic Press, New York), pp. 71–93; Gahmberg, C. G. & Hakomori, S. (1973) *J. Biol. Chem.* **248,** 4311–4317.
10. Morell, A. G., van der Hamer, C. J. A., Scheinberg, I. H. & Ashwell, G. (1966) *J. Biol. Chem.* **241,** 3745–3749.
11. Hajra, A. K., Bowen, D. M., Kishimoto, Y. & Radin, N. S. (1966) *J. Lipid Res.* **14,** 497.
12. Sheppard, J. R. (1971) *Proc. Nat. Acad. Sci. USA* **68,** 1316–1320.
13. Rice, R. H. & Means, G. E. (1971) *J. Biol. Chem.* **246,** 831–832.
14. Folch, T., Arsove, S. & Meath, I. (1951) *J. Biol. Chem.* **191,** 819–831.
15. Saito, T. & Hakomori, S. (1971) *J. Lipid Res.* **12,** 257–259.
16. Goggins, J. F., Johnson, G. S. & Pastan, I. (1972) *J. Biol. Chem.* **247,** 5759–5764.
17. Yogeeswaran, G., Sheinin, R., Wherrett, J. R. & Murray, R. K. (1972) *J. Biol. Chem.* **247,** 5146–5158; Sakiyama, H. & Robbins, P. W. (1973) *Arch. Biochem. Biophys.* **154,** 407–414.
18. Cline, M. J. & Livingston, D. C. (1971) *Nature New Biol.* **232,** 155–156; Ozanne, B. & Sambrook, J. (1971) *Nature New Biol.* **232,** 156–160.
19. Nicolson, G. L. (1971) *Nature New Biol.* **233,** 244–246; *Nature New Biol.* **239,** 193–197.
20. Thomas, T. B. & Winzler, R J. (1969) *J. Biol. Chem.* **244,** 5943–5946.
21. Nicolson, G. L. (1973) *J. Nat. Cancer Inst.* **50,** 1443–1451.
22. Hakomori, S., Siddiqui, B., Li, Y-T., Li, S-C. & Hellerqvist, C. G. (1971) *J. Biol. Chem.* **246,** 2271–2277.

Carl_G_190x270_mm_blokki_FINAL.indd 40 06-Aug-23 1:53:30 PM

Changes in a surface-labelled galactoprotein and in glycolipid concentrations in cells transformed by a temperature-sensitive polyoma virus mutant

In hamster cells transformed by a temperature-sensitive mutant of polyoma virus we have found that the external label in a galactoprotein disappears and the cellular concentration of lactosylceramide increases when the cells are grown at the permissive temperature. These changes can be reversed at the non-permissive temperature.

Three kinds of major membrane changes involving glycoproteins and glycolipids are associated with malignant transformation. They are (1) enhanced agglutinability of cells by some sugar-binding proteins (lectins)[1–3]; (2) blocked synthesis of gangliosides[4–10], neutral glycolipids[11–13], fucolipids[14,15] and some glycoproteins[16] with occasional accumulation of precursor glycans[4,6,10]; and (3) enhanced synthesis of sialofucoglycopeptide[17,18]. Recently a method for surface-labelling cells using galactose oxidase followed by treatment with tritiated sodium borohydride has been used to distinguished between surface galactoproteins of normal and transformed cells[19]. A galactoprotein which was labelled in normal hamster NIL cells was not labelled in polyoma-transformed NIL cells, and the introduction of label into this surface moiety seemed to be a correlative of growth control.

The enhanced agglutinability of transformed cells[1–3] has been linked directly to the control of cellular multiplication in two types of transformed cells harbouring thermosensitive mutations. In one case, what is believed to be a mutation in a cellular gene results in the restoration of regulated growth and decreased agglutinability at the restrictive temperature, while the cells seem to be transformed at the permissive temperature[20,21]. The same phenomenon is observed in cells transformed by thermosensitive polyoma virus mutant *ts*3[22,23].

We have initiated an investigation of the biochemical basis for the thermosensitive changes in the surface membrane of polyoma *ts*3-transformed BHK cells. Since topoinhibition of DNA synthesis is also rendered thermosensitive in these same cells[22], we speculate that the temperature-dependent surface alterations that we have observed may be implicated in the control of DNA synthesis.

BHK cells transformed with temperature-sensitive polyoma virus (BHKpyts3 Cl 7C), those transformed with wild type polyoma virus (BHKpywt Cl 4), and their progenitor cells (BHK Cl 13) were obtained from Dr W. Eckhart at the Salk Institute. Each cell line was grown in Dulbecco's

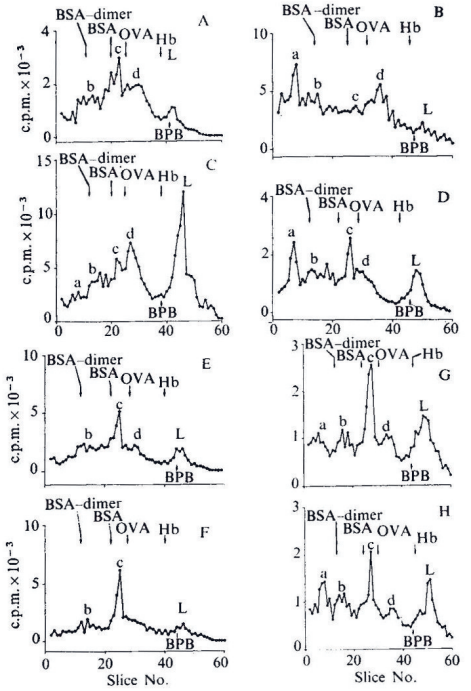

Fig. 1 Profile of external galactosyl label in baby hamster kidney fibroblasts (BHK C13) on acrylamide gel electrophoresis in sodium dodecyl sulphate. Cells were treated on the plates with 10 Worthington units of galactose oxidase for 1 h at room temperature, taken off with EDTA, and labelled as described previously[19]. Graphs show subconfluent non-transformed BHK at 32°C (A) and growing at 39°C (C); confluent non-transformed BHK at 32°C (B) and at 39°C (D); wild-type-polyoma-transformed BHK at confluency at 32°C (E) and at 39°C (F) *ts*3-transformed BHK at confluency at 32°C (G) and at 39°C (H) Acrylamide concentration was 5%; slicing, counting and preparation of internal ^{14}C-labelled standard proteins were as previously described[19]. BSA, bovine serum albumin; OVA, ovalbumin; Hb, haemoglobin; BPB, bromo-phenol blue. Note that galactoprotein a is only pronounced in confluent, non-transformed cells and in BHKpyts3 at non-permissive temperature. Peaks c and d are non-specifically labelled by sodium borotritiate alone. L = lipid label.

© 1974 Nature Publishing Group

Carl_G_190x270_mm_blokki_FINAL.indd 41 06-Aug-23 1:53:30 PM

TABLE 1 Dependence of galactoprotein a label on cell density in normal BHK cells, cells transformed with wild-type polyoma virus (BHKpywt) and with *ts*3

Cells	Temperature (°C)	Presence or absence of galactoprotein a label		
		Sparse*	Subconfluent†	Confluent‡
BHK normal	32	—	−	++
	39	−	+	++
BHKpywt	32	n.d.	−	−
	39	n.d.	−	−
BHKpyts	32	n.d.	−	−
	39	n.d.	+	++

The apparent molecular weight of galactoprotein a was approximately 200,000. −, Absent; +, obviously present; ++, present in high quantities; n.d., not determined.
* Cells growing separately without touching.
† Cells touching but not saturated.
‡ Cells at saturation density.

modified minimum essential medium containing 10% foetal calf serum at the permissive (32° C) and non-permissive (39° C) temperatures for the *ts*3 gene function.

Surface labelling was achieved on cells growing on plastic dishes by the method described previously[19]. Glycolipids were extracted with chloroform-methanol and isolated by acetylation: the glycolipids were separated on thin-layer chromatography into fractions lactosylceramide, trihexosylceramide and haematoside. Each fraction was extracted from silica gel with chloroform-methanol-water (1:1:0.1) and the extracts were methanolysed, and the sugars liberated were determined as trimethylsilyl derivatives with myo-inositol as an internal standard by gas-liquid chromatography.

As Table 1 and Fig. 1 show, in cells grown to their maximum saturation density by changing the medium frequently, a surface galactoprotein of BHK with a molecular weight of 200,000 (galactoprotein a) was not labelled in BHKpywt either at 32° C or at 39° C, nor was it labelled in BHKpyts3 at 32° C. However, galactoprotein a of BHKpyts3 was labelled when the cells were grown at 39° C, where they acquired normal morphological appearance, decreased agglutinability with lectins and increased topoinhibition of DNA synthesis.

In actively growing, sparse or subconfluent BHK cells, galactoprotein a was not labelled, whereas it was labelled when growth was inhibited at the saturation density.

As Table 2 shows, in BHKpywt the chemical concentration of lactosylceramide was obviously higher than that of normal BHK cells, and the concentration of trihexosylceramide was considerably reduced. The concentration of lactosylceramide was also sharply increased in BHKpyts3 at 32° C but not at 39° C, whereas the concentration of haematoside was depressed. It is noteworthy, however, that the concentration of trihexosylceramide was quite low at both temperatures in BHKpyts3.

Recently, Hammarström and Bjursell[24] observed that isotope incorporation from ^{14}C-palmitate into trihexosylceramide depends on cell population density and decreased considerably when the cells were transformed with wild type polyoma virus, in agreement with our previous findings[10]. Also consistent with their results, the decreased synthesis of trihexosylceramide in BHKpyts3 at the permissive temperature was not restored at the non-permissive temperature, indicating that decreased synthesis of trihexosylceramide is not essential for expression of certain aspects of the transformed phenotype. Similarly, the growth behaviour in agar and the serum requirement of BHKpyts3 are not known to be temperature-sensitive[22], although topoinhibition of DNA synthesis and agglutinability by lectins are temperature-sensitive[22,23]. Thus, although trihexosylceramide reduction accompanies transformation by polyoma virus, it is not under the control of the *ts*3 gene function and therefore does not seem to be implicated in the regulation of cell growth.

A considerable increase of lactosylceramide in some clonal isolates of BHKpywt had also been observed previously[4]. Our results suggest that increased lactosylceramide could be essential for expression of crucial aspects of the transformed phenotype, including the regulation of growth.

The inability to label galactoprotein a in the transformed state shows a good parallel with the appearance of lectin agglutinability, as demonstrated reversibly in BHKpyts3 at permissive and non-permissive temperatures[23]. The labelling of the galactoprotein in non-transformed cells at confluency is consistent with an increased reaction of galactosyl residues with *Ricinus communis* protein as observed by Nicolson[25]. Our surface labelling procedure did not label lactosylceramide of either transformed or non-transformed BHK cells, in agreement with the finding that the lactosyl moiety may not protrude towards the outside of the cells or that the length of the lactosyl moiety is too short to be externally labelled due to steric hindrance.

Perfect reversibility in the labelling of galactoprotein a and the lactosylceramide and haematoside concentrations in BHKpyts3 between permissive and non-permissive temperatures suggest that these membrane parameters are related

TABLE 2 Glycolipid concentration of BHK cells, those transformed with wild-type and with *ts*3

	Temperature (°C)	Glycolipid Concentration μmol per 100 mg dry weight*		
		Ceramide† trihexoside	Ceramide‡ dihexoside	Haematoside§
BHK normal	32°	0.070	0.218	0.46
	39°	0.075	0.161	0.93
BHKpywt	32°	0.008	0.371	0.77
	39°	0.015	0.329	0.75
BHKpyts	32°	0.040	0.725	0.12
	39°	0.015	0.120	1.21

Concentrations were determined by gas-liquid chromaography.
* Dry weight of the cell residue.
† αGal → βGal → Glc → ceramide.
‡ βGal → Glc → ceramide.
§ Sialyl 2 → 3βGal → Glc → ceramide.

© 1974 Nature Publishing Group

Carl_G_190x270_mm_blokki_FINAL.indd 42 06-Aug-23 1:53:30 PM

Nature Vol. 248 March 29 1974

to growth control in BHK cells. It is possible that deletion of galactoprotein a initiates uncontrolled DNA synthesis, as the loss of this protein has been observed after trypsin treatment of BHK and NIL cells (our unpublished observation), and since trypsin is known to induce the initiation of S-phase, and mitosis[26].

This work was supported by grants from the US Public Health Service and the American Cancer Society. C. G. G. is supported on a fellowship from the International Fogarty Center.

CARL G. GAHMBERG
DON KIEHN
SEN-ITIROH HAKOMORI

Departments of Pathobiology and Microbiology,
University of Washington,
Seattle, Washington 98195

Received November 16, 1973.

[1] Aub, J. C., and Sanford, B. H., and Wang, L., *Proc. natn. Acad. Sci. U.S.A.*, **54**, 400 (1965).
[2] Burger, M. M., *Proc. natn. Acad. Sci. U.S.A.*, **62**, 994 (1969).
[3] Inbar, M., and Sachs, L., *Proc. natn. Acad. Sci. U.S.A.*, **63**, 1418 (1969).
[4] Hakomori, S., and Murakami, W. T., *Proc. natn. Acad. Sci. U.S.A.*, **59**, 254 (1968).
[5] Brady, R. O., and Mora, P. T., *Biochim. biophys. Acta*, **218**, 308 (1970).
[6] Siddiqui, B., and Hakomori, S., *Cancer Res.*, **30**, 2930 (1970).
[7] Yogeeswaran, G., Sheinin, R., Wherrett, J., and Murray, R. K., *J. biol. Chem.*, **247**, 5146 (1972).
[8] Diringer, H., Ströbel, G., and Koch, M., *Z. physiol. Chem.*, **353**, 1769 (1972).
[9] Den, H., Schultz, A. M., Basu, M., and Roseman, S., *J. biol. Chem.*, **246**, 2721 (1971).
[10] Keenan, T. W., and Morré, D. J., *Science N.Y.*, **182**, 935 (1973).
[11] Hakomori, S., *Proc. natn. Acad. Sci. U.S.A.*, **67**, 1741 (1970).
[12] Sakiyama, H., Gross, S. K., and Robbins, P. W., *Proc. natn. Acad. Sci. U.S.A.*, **69**, 872 (1972).
[13] Critchley, D. R., and MacPherson, I., *Biochim. biophys. Acta*, **246**, 145 (1973).
[14] Steiner, S., Brennan, P. J., and Melnick, J. L., *Nature*, **245**, 19 (1973).
[15] Stellner, K., Hakomori, S., and Warner, G. A., *Biochem. biophys. Res. Commun.*, **55**, 439 (1973).
[16] Grimes, W. J., *Biochemistry*, **9**, 5083 (1970); *ibid*, **12**, 990 (1973).
[17] Warren, L., Critchley, D., and MacPherson, I., *Nature*, **235**, 275 (1972).
[18] Warren, L., Fuhrer, J. B., and Buck, C. A., *Proc. natn. Acad. Sci. U.S.A.*, **69**, 1838 (1972).
[19] Gahmberg, C. G., and Hakomori, S., *Proc. natn. Acad. Sci. U.S.A.*, **70**, 3329 (1973).
[20] Renger, H. C., and Basilico, C., *Proc. natn. Acad. Sci. U.S.A.*, **69**, 109 (1972).
[21] Noonan, K. D., Renger, H. C., Basilico, C., and Burger, M. M., *Proc. natn. Acad. Sci. U.S.A*, **70**, 347 (1973).
[22] Dulbecco, R., and Eckhart, W., *Proc. natn. Acad. Sci. U.S.A.*, **67**, 1775 (1970).
[23] Eckhart, W., Dulbecco, R., and Burger, M. M., *Proc. natn. Acad. Sci. U.S.A.*, **68**, 283 (1971).
[24] Hammarström, S., and Bjursell, G., *FEBS Lett.*, **32**, 69 (1973).
[25] Nicolson, G., and Lacorbiere, M., *Proc. natn. Acad. Sci. U.S.A.*, **70**, 1672 (1973).
[26] Burger, M. M., Bombik, B. M., Breckenridge, R. M., and Sheppard, J. R., *Nature new Biol.*, **239**, 161 (1972).

Carl_G_190x270_mm_blokki_FINAL.indd 43 06-Aug-23 1:53:30 PM

THE JOURNAL OF BIOLOGICAL CHEMISTRY
Vol. 251, No. 2, Issue of January 25, pp. 510–515, 1976
Printed in U.S.A.

External Labeling of Human Erythrocyte Glycoproteins

STUDIES WITH GALACTOSE OXIDASE AND FLUOROGRAPHY*

(Received for publication, March 28, 1975)

CARL G. GAHMBERG

From the Department of Serology and Bacteriology, University of Helsinki, Haartmaninkatu 3, 00290 Helsinki 29, Finland

Glycoproteins of the human erythrocyte membrane were labeled with tritiated sodium borohydride after oxidation of terminal galactosyl and *N*-acetylgalactosaminyl residues with galactose oxidase. After separation of the polypeptides on polyacrylamide slab gels, a scintillator was introduced into the gel, and the radioactive proteins were visualized by autoradiography (fluorography). The following results were obtained. (*a*) The erythrocyte membrane contains at least 20 glycoproteins, many of which are minor components. (*b*) The carbohydrate of all the labeled glycoproteins is exposed only to the outside, since no additional glycoproteins can be labeled in isolated unsealed ghosts. (*c*) The membrane contains two major groups of glycoproteins. The first group of proteins contains sialic acids linked to the penultimate galactosyl/*N*-acetylgalactosaminyl residues, which are efficiently labeled only after pretreatment with neuraminidase. The second group has terminal galactosyl/*N*-acetylgalactosaminyl residues which can be easily labeled without neuraminidase treatment. The glycoproteins from fetal erythrocytes all belong to the first group, whereas only five glycoproteins of erythrocytes from adults belong. (*d*) Trypsin cleaves the proteins containing sialic acids, and fragments containing carbohydrate remain tightly bound and exposed in the membrane. (*e*) Pronase cleaves Band 3 in addition to the sialic acid containing glycoproteins, but most of the glycoproteins still remain unmodified in the membrane. (*f*) No difference is seen between membrane glycoproteins from cells of different ABH blood groups.

There is increasing evidence that cell surface glycoproteins are involved in a variety of surface-mediated processes such as intercellular adhesion (1), cell recognition (2), lectin agglutinability (3–8), and ion transport (9–11). However, the molecules involved and their detailed structures are still largely unknown. This is partially due to the difficulties encountered in purifying plasma membranes from nucleated cells. By contrast, the membranes of the human erythrocyte are easy to obtain in large quantities, and many generalizations about membrane structure and function are derived from results obtained using this membrane.

One important aspect of membrane structure is the location and properties of the glycoproteins in the membranes. At least 4 major glycoproteins seem to span the membrane (12–18), the sialoglycoproteins, PAS1,[1] PAS2, and PAS3, and Band 3 (see Table II). The major sialoglycoprotein has been the most extensively studied, and it is known that the sugar-containing portion is located externally (19), the intramembranous part is hydrophobic in nature (14, 17, 20), and the COOH-terminal cytoplasmic end interacts with peripheral membrane proteins on the inside of the membrane (21, 22).

* This work was supported by the Finnish Cancer Society and the Finska Läkaresällskapet.

[1] The abbreviations used are: PAS1, PAS2, and PAS3, the periodate acid-Schiff-stained glycoproteins on gel electrophoresis; PBS, phosphate-buffered saline.

To locate external proteins, a number of techniques have recently been developed (23–28). In most of these techniques, the reagents are specific for the protein part of glycoproteins. Because most, if not all, surface proteins are glycoproteins, a technique to label this part of these molecules specifically was developed (29, 30). Terminal galactosyl or *N*-acetylgalactosaminyl residues are oxidized to the corresponding C-6 aldehydes by the enzyme galactose oxidase (31). The resulting aldehydes are then reduced under physiological conditions with tritiated borohydride. The large size of the enzyme molecule inhibits its penetration into the cell. Because sialic acids often are linked to subterminal galactosyl residues, more efficient labeling can often be achieved after pretreatment of cells with neuraminidase (29).

MATERIALS AND METHODS

Cells—Human erythrocytes from adults, obtained from citrated blood by centrifugation, were washed in phosphate-buffered saline, pH 7.4. The cells were used within 3 days of blood donation. Care was taken to remove the buffy coats. ABH blood groups were determined by standard techniques. Umbilical cord blood erythrocytes and fetal erythrocytes were obtained from the Department of Obstetrics and Gynecology, University of Helsinki.

Enzymes—Galactose oxidase with a specific activity of 130 units/mg of protein was purchased from Kabi AB, Stockholm, Sweden. It contained no neuraminidase or protease activities when measured as described previously (29). Neuraminidase (*Vibrio cholerae*, 500 units/ml) was obtained from Behringwerke AG, Marburg-Lahn, Germany.

This is an Open Access article under the CC BY license.

Carl_G_190x270_mm_blokki_FINAL.indd 44 06-Aug-23 1:53:30 PM

Pronase (*Streptomyces griseus* protease type V, 0.9 unit/mg solid) was obtained from Sigma. Crystalline trypsin was bought from Merck AG, Darmstadt, Germany.

Chemicals—Tritiated sodium borohydride (8.2 Ci/mM) was obtained from the Radiochemical Centre Ltd., Amersham, England. Two hundred fifty millicuries were dissolved in 0.5 ml of 0.01 N NaOH, divided into five tubes, and immediately frozen at −70°. Each tube was diluted with 2 ml of 0.01 N NaOH and then divided into 20 equal portions, which were immediately frozen. Usually, one of these tubes was used for the labeling experiments. When handled in this manner, the isotope remained active for at least 12 months.

Acrylamide and *N,N'*-methylenebisacrylamide were purchased from Eastman Kodak; 2,5-diphenyloxazole (PPO) and 1,4-bis[2-(5-phenyloxazolyl)]benzene (POPOP) from New England Nuclear.

Labeling Procedure—The labeling was done essentially as previously described (29, 32) but was slightly modified. Higher concentrations of galactose oxidase were used, and incubation was at room temperature. The specific activity of NaB^3H_4 was about 60 times higher than that used for erythrocytes previously. Treatment of cells with pronase, trypsin, and neuraminidase and the isolation of membranes have been described previously (29). Aliquots of the membrane preparations were counted for radioactivities in a dioxane-based scintillation fluid (33) in a Wallac liquid scintillation counter 81,000. The efficiency for tritium was 37%.

Polyacrylamide Slab Gel Electrophoresis—Electrophoresis was performed according to Laemmli (34) in 8% acrylamide gels with marker proteins in the peripheral slots. The molecular weights of the marker polypeptides were: thyroglobulin 165,000 (35), human albumin 68,000 (36), ovalbumin 43,000 (36), and hemoglobin 15,500 (36). The gels were fixed overnight in 20% sulfosalicylic acid, stained with Coomassie brilliant blue, and destained (36). At this stage, some of the gels were photographed. They were then treated with dimethylsulfoxide/2,5-diphenyloxazole according to Bonner and Laskey (37) and vacuum-dried. The dried gels were covered with Kodak RP X-Omat film, wrapped in aluminum foil, and stored at −70° in a Revco freezer for 1 to 10 days until developed. The apparent molecular weights of the polypeptides were determined according to Weber and Osborn (36).

Carbohydrate Analysis—The membrane preparations were divided into two equal portions. One part was extracted with chloroform/methanol (2/1, v/v) and partitioned according to Folch *et al.* (38). The lipid extract was dried down under nitrogen; the other portion was lyophilized. *Myo*-Inositol (10 μg) was added to the samples as an internal standard. After methanolysis at 85° for 12 hours in 1 N methanolic-HCl, the neutral sugars were analyzed as trimethylsilyl ethers according to Laine *et al.* (39). Protein-bound carbohydrate was taken as total carbohydrate minus chloroform/methanol-extractable carbohydrate.

Protein assay—The method of Lowry *et al.* (40) was used with bovine serum albumin as standard.

RESULTS

Incorporation of Label into Erythrocyte Membranes

Cells from Adults—The incorporation of label from NaB^3H_4 into erythrocyte membranes depends on the time of incubation with galactose oxidase and reaches a plateau after 1 to 2 hours (Fig. 1*A*). High concentrations of galactose oxidase suppress the labeling of the membranes (Fig. 1*B*). It is not possible to saturate the oxidized membrane with tritium fron NaB^3H_4, because after acrylamide gel analysis the stained protein pattern resembles that due to proteolysis (Ref. 30, and Footnote 2).

Initial treatment of the cells with neuraminidase results in a 3-fold increase in incorporation of label over those cells which are not treated. Pronase and trypsin remove 46% and 37%, respectively, of the radioactivity from prelabeled cells (Table I). The label in cells which are not pretreated with neuraminidase is hardly susceptible to the action of pronase or trypsin. If cells are digested with the proteolytic enzymes before labeling, less label is incorporated than when cells are digested after labeling. Control cells without galactose oxidase show very little label.

[2] Unpublished results.

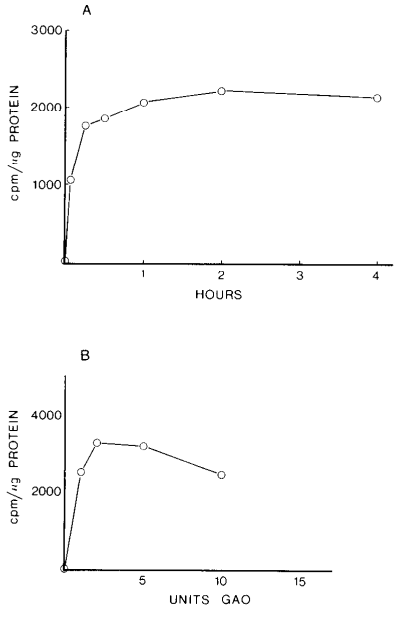

FIG. 1. *A*, effect of time of incubation with galactose oxidase on incorporation of ^3H from NaB^3H_4 into erythrocyte membranes. Packed erythrocytes (0.5 ml) were incubated in 1 ml of PBS, pH 7.0, with 5 units of galactose oxidase for the indicated time. The cells were washed three times in PBS, pH 7.4, and reduced with NaB^3H_4. After washing the cells, the membranes were isolated, and the specific radioactivities were determined. *B*, effect of concentration of galactose oxidase on incorporation of label. Packed erythrocytes (0.5 ml) were incubated in 1 ml of PBS, pH 7.0, with different concentrations of galactose oxidase for 1 hour. The cells were washed in PBS, pH 7.4, and reduced with NaB^3H_4, and washed again. The membranes were isolated, and the specific radioactivities were determined.

Umbilical Cord Blood and Fetal Cells—The membranes of these cells are not efficiently labeled with galactose oxidase/NaB^3H_4 alone. However, if the cells have been treated with neuraminidase prior to labeling, the label is strongly enhanced (Table I).

Carbohydrate Left in Membrane after Proteolytic Digestion

Chemical determinations show that even after prolonged proteolysis a substantial amount of carbohydrate, which cannot be extracted with chloroform/methanol, is left in the membrane (Fig. 2, *A* and *B*). After pronase or trypsin digestion more than 50% of the protein-bound galactose remains in the membrane.

Membrane Proteins Stained by Coomassie Blue

Fig. 3 shows the stained membrane proteins after separation on a polyacrylamide slab gel. The main components are numbered according to Fairbanks *et al.* (41). All membranes have been reduced with NaB^3H_4 after enzymatic treatments. The trypsin-treated membranes (*c* and *d*) do not show any obvious change, whereas in the pronase-treated membranes (*e* and *f*), Band 3 is cleaved and a new polypeptide P appears. This fragment has an apparent molecular weight of 64,000.

Carl_G_190x270_mm_blokki_FINAL.indd 45 06-Aug-23 1:53:30 PM

TABLE I

Total label in erythrocyte membranes

Packed cells (0.2 ml) were labeled as indicated. Neuraminidase, 25 units of neuraminidase at 37° for 30 min; galactose oxidase, 5 units galactose oxidase for 1 hour at room temperature. Pronase and trypsin digestions were performed with 0.1 mg/ml of the enzyme for 30 min at 37°. Results are expressed as percentage of neuraminidase + galactose oxidase.

Enzyme treatment	Cells from adults	Cord blood cells	Fetal cells
Neuraminidase + galactose oxidase	100	92.6	88.2
Neuraminidase + galactose oxidase + pronase	54.2		
Neuraminidase + galactose oxidase + trypsin	62.6		
Galactose oxidase	32.8	16.8	7.4
Galactose oxidase + pronase	30.2		
Galactose oxidase + trypsin	32.7		
Pronase + neuraminidase + galactose oxidase	25.8		
Trypsin + neuraminidase + galactose oxidase	26.5		
No enzyme used	0.8	1.1	1.8

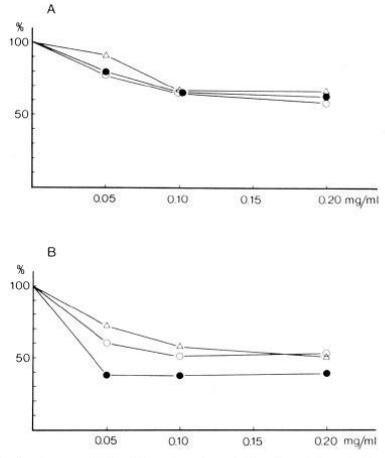

FIG. 2. *A*, removal by trypsin of protein-bound carbohydrate of erythrocyte membranes. Packed erythrocytes (2.0 ml) were incubated in 4 ml of PBS, pH 7.4 with different concentrations of trypsin for 30 min at 37°. After washing the cells three times in ice-cold PBS, pH 7.4, the membranes were isolated, and the sugars were quantitated by gas chromatography. △, D-mannose; ○, D-galactose; ●, L-fucose. Results are given in the percentage of sugar remaining in the membrane after digestion. *B*, removal by pronase of protein-bound carbohydrate of erythrocyte membranes. Details as in *A*.

Fluorography of Labeled Membranes from Adults

Tritium label could not be visualized from polyacrylamide gels by conventional autoradiography and so a scintillator was introduced into the gel before drying. Membranes from cells labeled after neuraminidase and galactose oxidase treatment show the presence of a large number of labeled polypeptides. The apparent molecular weights of these and some frequently used synonyms for the major components are given in Table II. The major components are GP7, GP8, GP13, GP14, and

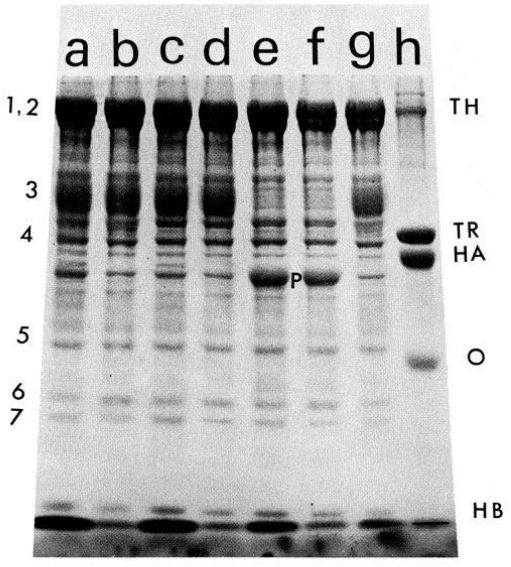

FIG. 3. Coomassie blue stained slab gel of erythrocyte membrane proteins. Samples corresponding to 10 μl of packed membranes were subjected to electrophoresis. The major components are numbered according to Fairbanks *et al.* (41). *a*, membranes from cells incubated with 25 units of neuraminidase at pH 6.0 for 30 min at 37°, and after washing incubated with 5 units of galactose oxidase in 1 ml of PBS, pH 7.0, for 1 hour at room temperature. The cells were washed and reduced with 0.5 mCi of NaB^3H_4 in 1 ml of PBS, pH 7.4, for 30 min at room temperature. The cells were then washed three times, the membranes were isolated. *b*, membranes from cells labeled with galactose oxidase only. *c*, membranes from cells treated with 0.1 mg/ml of trypsin for 30 min at 37°, then labeled after neuraminidase and galactose oxidase treatments. *d*, trypsin-treated membranes labeled with galactose oxidase only. *e*, membranes from cells treated with 0.1 mg/ml of pronase for 30 min at 37°, then labeled after neuraminidase and galactose oxidase treatments. *f*, pronase-treated membranes labeled with galactose oxidase only. *g*, membranes from cells reduced without enzymatic treatment. Note the disappearance of Band 3 in *e* and *f* and the presence of a new band (*P*). *h*, contains 25 μg of each of the marker proteins: thyroglobulin (*TH*), transferrin (*TR*), human albumin (*HA*), ovalbumin (*O*), and hemoglobin (*HB*).

GP16 (Fig. 4, *A-a*). If neuraminidase treatment is omitted, proteins GP8 and GP14 are weakly labeled, and GP13 and GP16, are not detected at all (Fig. 4, *A-b*). This indicates that in GP8, GP13, GP14, and GP16 sialic acids are linked to most of the penultimate galactosyl/*N*-acetylgalactosaminyl residues, whereas none of the other labeled glycoproteins contain neuraminidase-susceptible sialic acids. If cells are treated with trypsin before labeling, Bands GP8, GP13, and GP16 completely disappear (Fig. 4, *A-c*). Instead, Bands T1, T2, and T3 appear. These bands are not observed without pretreatment with neuraminidase. Pronase degrades Bands GP7, GP8, GP13, GP14, and GP16 (Fig. 4, *A-d*), and a strong diffuse band, PG1, appears, and in the region of the previous band, GP7, Bands $GP7_{a\text{-}d}$ appear. Bands $GP7_{a\text{-}d}$ are not fragments of larger proteins because no larger glycoproteins than GP7 are degraded. Band PG1 is very weak without pretreatment with neuraminidase (not shown). This indicates that Band PG1 is mostly derived from sialic acid-containing

Carl_G_190x270_mm_blokki_FINAL.indd 46 06-Aug-23 1:53:30 PM

TABLE II

Labeled glycoproteins, their apparent molecular weights, and synonyms used

Glycoprotein	Apparent MW × 10^{-3}	Synonym
GP1	230	
GP2	180	
GP3	160	
GP4	140	
GP5	120	
GP6	110	
GP7	100	Band 3 (41), Band a (13).
GP8	85	Major sialoglycoprotein, MN-glycoprotein (19, 20), PAS1 (41, 18), glycophorin (14), Band b (12).
GP9	73	
GP10	63	
GP11	61	
GP12	55	
GP13	50	PAS2 (41, 18)
GP14	47	PAS2 (41, 18)
GP15	29	
GP16	24	PAS3 (41, 18)
GP7a	109	
GP7b	102	
GP7c	100	
GP7d	95	
P	64	
PG1	44	
T1	62	
T2	45	
T3	22	

glycoproteins. Many of the labeled glycoproteins contain a relatively weak label. To test whether these proteins actually are glycoproteins, it was necessary to include a control where the galactose oxidase was omitted. Fig. 4, *B-a*, shows the polypeptides of membranes labeled after neuraminidase and galactose oxidase treatment; Fig. 4, *B-b*, shows the labeled polypeptides after treatment with galactose oxidase only, and Fig. 4, *B-c*, is the control where the enzymes have been omitted. No labeled bands are observed in Fig. 4, *B-c*. Thus the labeled proteins are glycoproteins.

To quantitate the amount of label in the minor glycoproteins, cells were labeled with galactose oxidase only, and the membranes were isolated and subjected to electrophoresis on cylindrical acrylamide gels. The gels were then sliced and counted as described previously (29). Twenty-four per cent of the total radioactivity in the proteins was recovered from the slices between the origin and Band 3. Band 3 contained 26%, PAS1 contained 10%, and the remaining 40% of the radioactivity was rather evenly distributed between the positions of PAS1 and the lipid peak. Thus a substantial amount of radioactivity is bound to the numerous minor glycoproteins (see Fig. 4*a* in Ref. 29).

Labeling of Umbilical Cord and Fetal Erythrocytes

Identical amounts of membranes from erythrocytes from adults, umbilical cord blood, and fetuses, labeled after neuraminidase and galactose oxidase treatments or after galactose oxidase treatment only, were subjected to electrophoresis (Fig. 5). After neuraminidase treatment, the glycoprotein patterns are similar, although some minor differences exist: GP4 and GP10 of cord blood cells are relatively strong (Fig. 5*c*). If cells are labeled without neuraminidase treatment, the fetal glycoproteins are very weakly labeled (Fig. 5*f*). This shows that in the glycoproteins of fetal erythrocytes only a few galactosyl/*N*-acetylgalactosaminyl residues are available for labeling in the native state. Instead, sialic acids are linked to penultimate galactosyl/*N*-acetylgalactosaminyl residues.

Labeling of Intact Cells and Isolated Membranes

To study the distribution of glycoproteins between the two halves of the lipid bilayer and to see whether a reorganization of the membrane can be observed after isolation, the following experiments were done. (*a*) Intact cells were treated with galactose oxidase followed by reduction with NaB^3H_4. (*b*) Intact cells were treated with galactose oxidase, and the membranes were isolated and then reduced. (*c*) The membranes were first isolated, then treated with galactose oxidase, and reduced. Table III shows the specific activities in the membranes and Fig. 6 shows the fluorography patterns of the labeled glycoproteins. The incorporation of label into intact membranes is less than that of reduced ghosts. In addition, the individual glycoproteins are less efficiently labeled than those of isolated ghosts. Other qualitative or quantitative changes are not observed. It is obvious that regardless of whether the membrane has been treated with galactose oxidase from the outside only or from both sides of the membrane, all individual glycoproteins are equally efficiently labeled. The lower label in the membranes of cells reduced while intact may be due to intracellular consumption of borohydride.

Labeling of Cells of Different ABH Blood Groups

Intact cells of the blood groups A_1, A_2, A_1B, A_2B, B, and O were labeled. The total radioactivities were similar and no obvious difference in the fluorography patterns could be observed (data not shown).

DISCUSSION

Development of the galactose oxidase method to a very high sensitivity by combining it with fluorography of slab gels permitted analysis of red cell membrane glycoproteins with a resolution previously unavailable. The labeling is very specific: galactose oxidase reacts only with galactosyl and *N*-acetylgalactosaminyl residues (29, 31). Under these conditions no labeled protein bands were observed when the galactose oxidase treatment was omitted. Therefore, the labeled proteins must represent glycoproteins. However, it is possible to label isolated proteins *in vitro* by NaB^3H_4 alone. Morell *et al.* (42) treated ceruloplasmin with NaB^3H_4, both after incubation with neuraminidase and galactose oxidase, or without enzyme treatment. After enzyme treatment, the specific radioactivity was 25 times higher. van Lenten and Ashwell (43) labeled orosomucoid with NaB^3H_4 after oxidation of sialic acids with periodate. Compared to the nonoxidized control, the specific radioactivity was 21 times higher. I have labeled, without using galactose oxidase, the glycoproteins, transferrin, and ovalbumin, and the nonglycoproteins, bovine serum albumin and hemoglobin, with NaB^3H_4. In all cases a low labeling was obtained. Therefore, it was always necessary in the membrane-labeling experiments to include a control in which no enzymes were used. In some types of cells some proteins are preferentially labeled by NaB^3H_4 alone (32).

I have separately labeled human serum proteins. Without neuraminidase treatment, no labeled protein band is observed on electrophoresis. After neuraminidase plus galactose oxidase treatment, a few proteins are labeled but they do not corre-

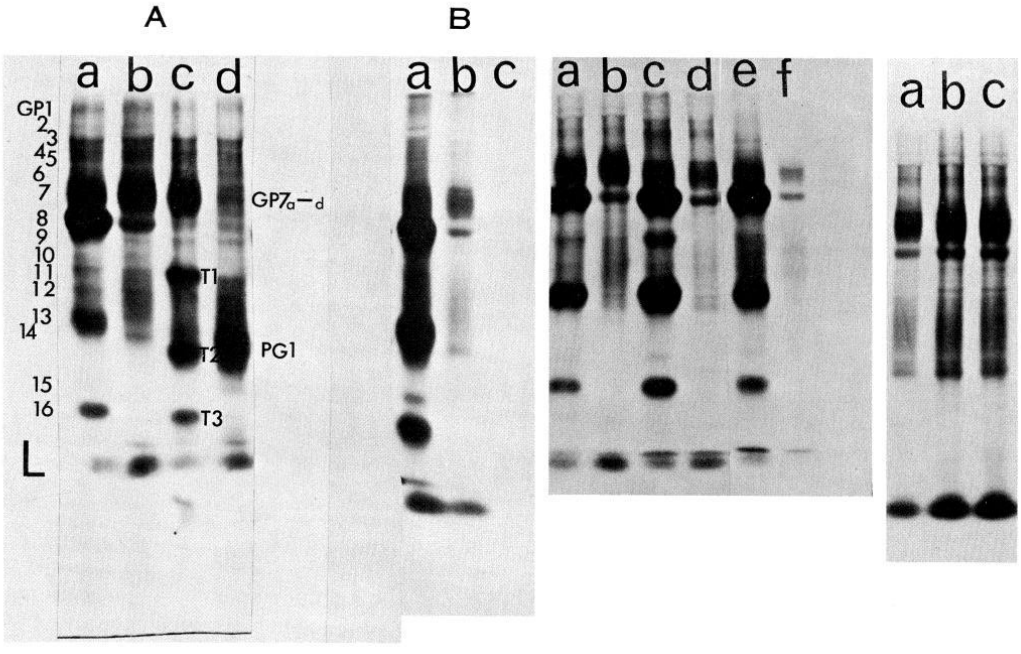

FIG. 4. *A*, Fluorography pattern of ^{3}H-labeled erythrocyte membranes. Packed erythrocytes (0.5 ml), were labeled as follows: *a*, membranes from cells labeled after treatment with neuraminidase and galactose oxidase; *b*, membranes from cells labeled with galactose oxidase only; *c*, membranes from cells first treated with trypsin and then labeled after neuraminidase and galactose oxidase treatments; *d*, membranes from cells first treated with pronase and then labeled after neuraminidase and galactose oxidase treatments. For labeling details see Fig. 3. *b*, dependency of label on enzyme treatment. Packed erythrocytes (0.5 ml) were labeled as follows: *a*, membranes from cells labeled after treatment with neuraminidase and galactose oxidase; *b*, membranes from cells labeled with galactose oxidase only; *c*, membranes from cells labeled without enzyme treatment. For labeling details see Fig. 3.

TABLE III

Total label in membranes treated with galactose oxidase from outside only or from both sides of membrane

	cpm/μg protein
Intact cells + galactose oxidase + NaB^3H_4 → membranes[a]	5275
Intact cells + galactose oxidase → membranes + NaB^3H_4[b]	10642
Intact cells → membranes + galactose oxidase + NaB^3H_4[c]	10208

[a] Packed intact cells (0.5 ml) were treated with 5 units of galactose oxidase for 1 hour in 1 ml of PBS, pH 7.0, at room temperature, and washed by centrifugations three times. The membranes were isolated and reduced with 0.5 mCi of NaB^3H_4.

[b] Packed intact cells (0.5 ml) were treated with 5 units of galactose oxidase for 1 hour in 1 ml of PBS, pH 7.0, at room temperature, and washed three times by centrifugation. The membranes were isolated and reduced with 0.5 mCi of NaB^3H_4.

[c] Membranes were isolated from 0.5-ml packed cells, treated with galactose oxidase as above, and reduced after washing by centrifugation with 0.5 mCi of NaB^3H_4.

FIG. 5 (*left*). Labeled glycoproteins from adults, cord blood, and fetuses. *a*, membranes from adults labeled after neuraminidase and galactose oxidase treatments; *b*, membranes from adults labeled with galactose oxidase only; *c*, membranes from cord blood cells labeled after neuraminidase and galactose oxidase treatments; *d*, membranes from cord blood cells labeled after galactose oxidase treatment; *e*, membranes from fetal cells labeled after neuraminidase and galactose oxidase treatments; *f*, membranes from fetal cells labeled after galactose oxidase treatment.

FIG. 6 (*right*). Membranes from cells labeled as intact or after isolation. *a*, membranes from cells treated with galactose oxidase as intact, reduced with NaB^3H_4, and then isolated; *b*, membranes from cells treated with galactose oxidase as intact, the membranes were isolated and then reduced; *c*, membranes were first isolated, then treated with galactose oxidase and reduced. In all incubations the same number of cells and identical amounts of galactose oxidase and NaB^3H_4 were used. For labeling details see Fig. 3.

spond in electrophoretic mobility to the sialic acid-containing glycoproteins of erythrocytes.

It is evident that the glycoprotein pattern of human erythrocyte membrane is unexpectedly complex. At least 20 glycoproteins are reproducibly found on the outer surface and it is reasonable to assume that there are additional glycoproteins which either do not serve as substrate for galactose oxidase, or co-migrate with other glycoproteins, or are represented by too few copies per cell to be visualized.

In contrast to the glycoproteins from erythrocytes of adults, the fetal glycoproteins are labeled with a very low efficiency if treated with galactose oxidase and NaB^3H_4 only (29). If these cells are pretreated with neuraminidase they are, however, strongly labeled. This indicates that most of the fetal glycoproteins contain penultimate galactosyl or *N*-acetylgalactosaminyl residues, which are linked to sialic acids in the native state.

The effects of proteolytic enzymes on the surface proteins of

Carl_G_190x270_mm_blokki_FINAL.indd 48 06-Aug-23 1:53:30 PM

the red cell have been extensively studied (12, 19, 26, 44). It is known that trypsin and pronase cleave the major sialoglycoprotein (PAS1) and that pronase cleaves Band 3 as well in addition to this. Chemical determinations show that approximately one-half of the nonlipid carbohydrate can be released from the membranes by pronase or trypsin. The rest of the protein-bound carbohydrate is firmly associated with the membrane and is not removed by 2 M KCl.[2] It is possible that the polypeptide backbones of these proteins are located deeper in the membrane than their constituent carbohydrate chains. The carbohydrate may then protect the proteins from proteolytic attack. No glycoproteins are more easily labeled after protease treatment, which shows that their carbohydrate always is exposed to galactose oxidase.

One major conclusion from recent erythrocyte membrane research is the asymmetrical distribution of both proteins and lipids (for recent reviews see Refs. 45 to 47). The sugar chains of both glycoprotein and glycolipid have been suggested to be located exclusively on the outer surface. Treatment of cells with neuraminidase removes all the sialic acid (48), and lectin·ferritin complexes bind only to the outer surface of isolated ghosts (49). The galactose oxidase method has been used to approach this problem before (29, 30), but the limited resolution of the glycoproteins on cylindrical gels and the low radioactivities did not permit clear-cut conclusions. The results reported here strongly confirm previous results. All of the labeled glycoprotein oligosaccharides reside on the outer surface of the cells and no extensive reorganization of the membrane seems to take place during isolation. The question then arises whether all external proteins are glycoproteins. To my knowledge all well characterized mammalian and viral surface proteins are glycoproteins. Previous work and present data indicate that no glycoproteins are located on the cytoplasmic side of the lipid bilayer. How the absolute asymmetrical distribution of the carbohydrate-containing proteins is accomplished during the biosynthesis of the membrane is not completely understood. Recently, Component 3 was implicated in anion transport (10, 11). It is also possible that many of the minor glycoproteins also span the lipid bilayer and have important functions. This problem is currently being investigated.

Acknowledgments—I thank Drs. K. Simons, O. Renkonen, A. Vaheri, and S. Hakomori for help with the preparation of the manuscript.

REFERENCES

1. Roseman, S. (1971) *Chem. Phys. Lipids* **5,** 270–297
2. Hausman, R. E., and Moscona, A. A. (1973) *Proc. Natl. Acad. Sci. U. S. A.* **70,** 3111–3114
3. Burger, M. M. (1969) *Proc. Natl. Acad. Sci. U. S. A.* **62,** 994–1001
4. Inbar, M., and Sachs, L. (1969) *Proc. Natl. Acad. Sci. U. S. A.* **63,** 1418–1425
5. Nicolson, G. L. (1971) *Nature New Biol.* **233,** 244–246
6. Gahmberg, C. G., and Hakomori, S. (1975) *J. Biol. Chem.* **250,** 2447–2451
7. Findlay, J. B. C. (1974) *J. Biol. Chem.* **249,** 4398–4403
8. Adair, W. L., and Kornfeld, S. (1974) *J. Biol. Chem.* **249,** 4696–4704
9. Kyte, J. (1972) *J. Biol. Chem.* **247,** 7642–7649
10. Cabantchik, Z. I., and Rothstein, A. (1974) *J. Membrane Biol.* **15,** 207–226
11. Ho, M. K., and Guidotti, G. (1975) *J. Biol. Chem.* **250,** 675–683
12. Bretscher, M. S. (1971) *Nature New Biol.* **231,** 229–232
13. Bretscher, M. S. (1971) *J. Mol. Biol.* **59,** 351–357
14. Marchesi, V. T., Tillack, T. W., Jackson, R. L., Segrest, J. P., and Scott, R. E. (1972) *Proc. Natl. Acad. Sci. U. S. A.* **69,** 1445–1449
15. Morrison, M., Mueller, T. J., and Huber, C. T. (1974) *J. Biol. Chem.* **249,** 2658–2660
16. Boxer, D. H., Jenkins, R. E., and Tanner, M. J. A. (1974) *Biochem. J.* **137,** 531–534
17. Segrest, J. P., Kahane, I., Jackson, R. L., and Marchesi, V. T. (1973) *Arch. Biochem. Biophys.* **155,** 167–183
18. Mueller, T. J., and Morrison, M. (1974) *J. Biol. Chem.* **249,** 7568–7573
19. Thomas, D. B., and Winzler, R. J. (1969) *J. Biol. Chem.* **244,** 5943–5946
20. Javaid, J. I., and Winzler, R. J. (1974) *Biochemistry* **13,** 3639–3642
21. Nicolson, G. L., and Painter, R. G. (1974) *J. Cell Biol.* **59,** 395–406
22. Ji, T. H., and Nicolson, G. L. (1974) *Proc. Natl. Acad. Sci. U. S. A.* **71,** 2212–2216
23. Phillips, D. R., and Morrison, M. (1971) *Biochemistry* **10,** 1766–1771
24. Hubbard, A. L., and Cohn, Z. A. (1972) *J. Cell Biol.* **55,** 390–405
25. Bretscher, M. S. (1971) *J. Mol. Biol.* **58,** 775–781
26. Bender, W. W., Garan, H., and Berg, H. C. (1971) *J. Mol. Biol.* **58,** 783–797
27. Whiteley, N. M., and Berg, H. C. (1974) *J. Mol. Biol.* **87,** 541–561
28. Staros, J. V., Haley, B. E., and Richards, F. M. (1974) *J. Biol. Chem.* **249,** 5004–5007
29. Gahmberg, C. G., and Hakomori, S. (1973) *J. Biol. Chem.* **248,** 4311–4317
30. Steck, T. L., and Dawson, G. (1974) *J. Biol. Chem.* **249,** 2135–2142
31. Avigad, G., Amaral, D., Asensio, C., and Horecker, B. L. (1962) *J. Biol. Chem.* **237,** 2736–2743
32. Gahmberg, C. G., and Hakomori, S. (1973) *Proc. Natl. Acad. Sci. U. S. A.* **70,** 3329–3333
33. Bray, G. A. (1960) *Anal. Biochem.* **1,** 279–285
34. Laemmli, U. K. (1970) *Nature* **227,** 680–685
35. DeCrombrugghe, B., Pitt-Rivers, R., and Edelhoch, H. (1966) *J. Biol. Chem.* **241,** 2766–2773
36. Weber, K., and Osborn, M. (1969) *J. Biol. Chem.* **244,** 4406–4412
37. Bonner, W. M., and Laskey, R. A. (1974) *Europ. J. Biochem.* **46,** 83–88
38. Folch, J., Lees, M., and Sloane Stanley, G. (1957) *J. Biol. Chem.* **226,** 497–509
39. Laine, R. A., Esselman, W. J., and Sweeley, C. C. (1972) *Methods Enzymol.* **28,** 159–167
40. Lowry, O. H., Rosebrough, N. J., Farr, A. L., and Randall, R. J. (1951) *J. Biol. Chem.* **193,** 265–275
41. Fairbanks, G., Steck, T. L., and Wallach, D. F. H. (1971) *Biochemistry* **10,** 2606–2617
42. Morell, A. G., van den Hamer, C. J. A., Scheinberg, I. H., and Ashwell, G. (1966) *J. Biol. Chem.* **241,** 3745–3749
43. van Lenten, L., and Ashwell, G. (1971) *J. Biol. Chem.* **246,** 1889–1894
44. Steck, T. L., Fairbanks, G., and Wallach, D. F. H. (1971) *Biochemistry* **10,** 2617–2624
45. Steck, T. L. (1974) *J. Cell Biol.* **62,** 1–19
46. Bretscher, M. S. (1973) *Science* **181,** 622–629
47. Zwaal, R. F. A., Roelofsen, B., and Colley, C. M. (1973) *Biochim. Biophys. Acta* **300,** 159–182
48. Eylar, E. H., Madoff, M. A., Brody, O. V., and Oncley, J. L. (1962) *J. Biol. Chem.* **237,** 1992–2000
49. Nicolson, G. L., and Singer, S. J. (1974) *J. Cell Biol.* **60,** 236–248

Carl_G_190x270_mm_blokki_FINAL.indd 49 06-Aug-23 1:53:30 PM

THE JOURNAL OF BIOLOGICAL CHEMISTRY
Vol. 251, No. 19, Issue of October 10, pp. 6108-6116, 1976
Printed in U.S.A.

Absence of the Major Sialoglycoprotein in the Membrane of Human En(a−) Erythrocytes and Increased Glycosylation of Band 3*

(Received for publication, February 18, 1976)

CARL G. GAHMBERG‡
From the Department of Serology and Bacteriology, University of Helsinki, Helsinki, Finland
GUNNAR MYLLYLA, JUHANI LEIKOLA, AND ANNA PIRKOLA
From the Finnish Red Cross Blood Transfusion Service, Finland
STIG NORDLING
From the Third Department of Pathology, University of Helsinki, Helsinki, Finland

The human En(a−) blood group is a rare recessive trait. These erythrocytes lack the major membrane sialoglycoprotein (PAS1, MN protein, or glycophorin) and contain a decreased amount of PAS2 as demonstrated by radiolabeling of surface proteins and chemical techniques. A third glycoprotein, Band 3, contains two labeled oligosaccharide chains; the more complex oligosaccharide has a higher molecular weight in En(a−) cells than in normal cells. A fourth glycoprotein, PAS3, is present in usual amounts in En(a−) cells. Cells heterozygous for En(a) are intermediate in these respects. The sialic acid is decreased in En(a−) cells, but the total carbohydrate is similar in the different membranes. The glycolipids are present in normal amounts but are much more exposed to galactose oxidase in En(a−) cells than in normal cells.

The human erythrocyte contains four major glycoproteins (4–8). These glycoproteins show an asymmetry in the membrane and have their carbohydrate exposed only to the outside (9–12). The sialoglycoprotein PAS1,[1] also called the MN glycoprotein and glycophorin, contains 60% carbohydrate including a large proportion of the sialic acid of the cell (4, 6, 13) and penetrates the membrane (14–16). The complete primary structure is known (17) but not the physiological function. Band 3 is also a major component of the membrane. It is a glycoprotein containing little or no sialic acid (18, 19). It also penetrates the membrane (7, 8). PAS2 and PAS3 also contain high levels of sialic acid, but these proteins have not been studied extensively.

The study of naturally occurring human erythrocyte variants should be useful in correlating membrane structure and function. One such variant is the rare blood group En(a−) (20, 21) in which there is known to be a reduction in the amount of total sialic acid (20). Therefore, homozygous and heterozygous En(a−) cells have been studied in greater detail by surface labeling and chemical techniques.

* This work was supported by the Finnish Cancer Society, the Finska Läkaresällskapet, the Academy of Finland, and the Sigrid Juselius Foundation. A preliminary report has been presented (1) and similar results were described by two other groups (2, 3).

‡ To whom correspondence should be addressed at the Department of Serology and Bacteriology, University of Helsinki, Haartmaninkatu 3, 00290 Helsinki 29, Finland.

[1] The abbreviations used are: PAS1, PAS2, and PAS3, the periodic acid-Schiff stained glycoproteins of red cell membranes; NaCl/PO_4, phosphate buffered saline; Band 3, Band 3 of the red cell membrane proteins according to the nomenclature of Fairbanks *et al.* (4).

MATERIALS AND METHODS

Cells—All erythrocytes from adults were obtained from the Finnish Red Cross Blood Transfusion Service, Helsinki. The (En(a−) cells were blood group AB, the En(a) heterozygous cells, B, and the normal cells, AB. The labeling experiments were done within 1 week after the blood was collected. The corpuscular volumes of the cells used were determined by routine methods and found to be 85 μm^3 for En(a−) cells, 87 μm^3 for En(a) heterozygous cells, and 85 μm^3 for normal cells.

Enzymes—The galactose oxidase, 130 units/mg of protein (Kabi, Stockholm, Sweden) and *Vibrio cholerae* neuraminidase (Behringwerke, Marburg-Lahn, Germany) were free from proteolytic activity (10). Lactoperoxidase (80 purpurogallin units/mg of solid) and pronase (*Streptomyces griseus* protease, type V) were obtained from Sigma, and glucose oxidase (140 units/mg of protein) from Worthington.

Isotopes—Tritiated sodium borohydride (8.2 Ci/mmol), ^{125}I, carrier free, and [^{14}C]formaldehyde (2.0 mCi/mmol) were obtained from the Radiochemical Centre, Amersham, England and handled as described (22).

Chemicals—The carbohydrate standards were: *N*-acetylneuraminic acid and *N*-acetyl-D-galactosamine (Sigma), L-fucose and *N*-acetyl-D-glucosamine (Fluka AG, Buchs, Switzerland), D-galactose, D-glucose, D-mannose, and *myo*-inositol (Merck), D-[^{14}C]glucose (3 mCi/mmol) (Radiochemical Centre). Thyroglobulin complex glycopeptide M_r = 4100) (23), was prepared by pronase digestion of bovine thyroglobulin (Sigma) and radioactively labeled by the galactose oxidase/NaB^3H_4 method. Lactodifucohexaose prepared from human milk and *O*-β-D-galactopyranosyl (1-3)*O*-β-D-galactopyranosyl (1-4)D-glucose was obtained by the courtesy of Professor O. Renkonen, Department of Biochemistry, University of Helsinki, and reduced with NaB^3H_4. All other chemicals were reagent grade or better from commercial sources.

Isolation of Membranes—Erythrocyte membranes were prepared by hypotonic lysis in 10% NaCl/PO_4 (pH 7.4) in water and washed until white (10).

Labeling Procedures—The surface labeling by using galactose oxidase has essentially been described previously (10, 12, 22). The cells were washed three times in NaCl/PO_4 and treated with 5 units of

This is an Open Access article under the CC BY license.

Carl_G_190x270_mm_blokki_FINAL.indd 50 06-Aug-23 1:53:30 PM

galactose oxidase/0.5 ml of packed cells, and when neuraminidase treatment was used with 12.5 units of neuraminidase simultaneously with the galactose oxidase in 0.5 ml of Dulbecco's phosphate-buffered saline for 30 min at 37°C. The cells were washed three times in $NaCl/PO_4$, suspended in 0.5 ml of $NaCl/PO_4$ and reduced with NaB^3H_4 (0.5 mCi/0.5 ml of cells) for 30 min at room temperature. After washing three times in $NaCl/PO_4$, the membranes were isolated.

For labeling with ^{125}I by the lactoperoxidase method (24, 25), 0.5 ml of packed cells were washed in $NaCl/PO_4$ and 1 ml of $NaCl/PO_4$ added containing 100 μCi of ^{125}I, 10 μg of D-glucose, 10 μg of glucose oxidase, and 10 μg of lactoperoxidase. After incubation at room temperature for 10 min, the cells were washed three times in $NaCl/PO_4$ and the membranes isolated. Labeling of cells by periodate/NaB^3H_4 was done as follows. To 0.5 ml of packed cells was added 1 ml of $NaCl/PO_4$ and sodium metaperiodate to a final concentration of 2 mM (26). After incubation at room temperature in the dark for 10 min, the excess periodate was removed by washing three times in $NaCl/PO_4$, 0.5 ml of $NaCl/PO_4$ added, and the cells reduced with 0.5 mCi of NaB^3H_4 for 30 min at room temperature. The cells were washed three times in $NaCl/PO_4$ and the membranes isolated.

Polyacrylamide Gel Electrophoresis—Electrophoresis in the presence of sodium dodecyl sulfate was done according to Laemmli on 8% acrylamide slab or cylindrical gels (27). After completion of the electrophoresis, the gels were fixed in 20% sulfosalicylic acid overnight, stained with Coomassie blue, and destained (28). For fluorography, the gels were treated with dimethyl sulfoxide/2,5-diphenyloxazole as described (29). Cylindrical gels were sliced with a 2-mm slicer and the radioactivity determined in a Wallac liquid scintillation counter 81000 after solubilization in NCS (Amersham/Searle) (10). Marker proteins were: thyroglobulin, transferrin, human albumin, ovalbumin, and hemoglobin. They were radioactively labeled with [^{14}C]formaldehyde as described by Rice and Means (30). ^{125}I was counted in a Wallac gamma scintillation counter.

Carbohydrate Analysis—Sialic acid was determined by the thiobarbituric acid method (31) using *N*-acetylneuraminic acid as a standard. The amino sugars were determined by the Elson-Morgan reaction (32), after hydrolysis for 16 h in 2 N HCl at 100°. *N*-Acetyl-D-glucosamine and *N*-acetyl-D-galactosamine were separated from each other using the short column of a Beckman 120 C amino acid analyzer (33, 34). Neutral sugars were determined by gas chromatography on a Perkin-Elmer F11 gas chromatography as alditol acetates, with *myo*-inositol as an internal standard (35).

Amino Acid and Protein Analysis—Amino acids were analyzed and protein content determined as described previously with norleucine as an internal standard on the amino acid analyzer (36). Protein was also determined according to Lowry *et al.* (37).

Isolation of Sialoglycoproteins—The isolation of the sialoglycoproteins was done by the chloroform/methanol extraction procedure of Hamaguchi and Cleve (38).

Isolation of Band 3—To isolated membranes was added a small amount of ^{125}I-labeled membranes from the same type of cells. After removal of peripheral proteins by extraction with hypotonic and hypertonic media (18) the membranes were solubilized by boiling in sodium dodecyl sulfate. The solubilized membranes were applied at room temperature to an Ultrogel ACA34 column (100 × 3 cm) containing 0.1% sodium dodecyl sulfate. Fractions of 4 ml were collected and the radioactivity determined. Polyacrylamide slab gel electrophoresis of the fractions was then done, and those enriched in Band 3 as seen by staining were pooled and concentrated to 2 to 3 ml by ultrafiltration. Sodium dodecyl sulfate (200 mg) and 100 μl of 2-mercaptoethanol were added to the concentrated sample (10 to 50 mg of protein) and the preparation boiled for 3 min in water. After dialysis for 12 h at room temperature against a 0.01 M sodium phosphate buffer (pH 6.4) containing 0.1% sodium dodecyl sulfate and 1 mM dithiothreitol, the sample was applied to a hydroxylapatite column (1.0 × 20 cm). After washing with 100 ml of the same buffer, the proteins were eluted with 250 ml of a linear gradient of 0.3 to 0.5 M sodium phosphate buffer (pH 6.4) containing 0.1% sodium dodecyl sulfate and 1 mM dithiothreitol. Thus, the hydroxylapatite column chromatography was done essentially according to Moss and Rosenblum (39). The phosphate molarity of the collected fractions was determined from their refraction indices. The fractions were counted in the γ counter and the position of Band 3 determined by polyacrylamide slab gel electrophoresis. Fractions containing Band 3 were pooled, dialyzed against water, lyophilized, and dissolved in a small volume of water.

Peptide Mapping—Fifty microliters of the Band 3 preparations containing 25 μg of protein were iodinated with 100 μCi of ^{125}I by the chloramine-T method, and peptide maps done exactly as described by Bray and Brownlee on Whatman 3MM paper by chromatography in butanol-1/acetic acid/water (17/5/25 by volume) followed by electrophoresis at pH 3.5 (40).

Analysis of Glycopeptides from Band 3—Intact erythrocytes were surface-labeled with the galactose oxidase method without using neuraminidase. After isolation of membranes, samples were electrophoresed on cylindrical polyacrylamide gels, which were sliced. After transfer to 5-ml plastic tubes, addition of 0.5 ml of 0.1% sodium dodecyl sulfate, the slices were incubated for 16 h at 37° with continuous shaking. Then 25-μl aliquots were counted for radioactivity in a dioxane-based scintillation fluid (41). The fractions containing Band 3 were combined and either digested with pronase or treated with hydrazine. Pronase digestion was done by adding 0.55 ml $NaCl/PO_4$ containing 2.5 mg of pronase, which had been autodigested for 1 h at 37° to destroy contaminating glycosidases, and incubated for 24 h at 60°. The samples were then lyophilized. Hydrazinolysis was done as follows. After addition of 0.3 ml of anhydrous hydrazine under nitrogen to the lyophilized samples and incubation at 100° for 30 h, 0.5 ml of toluene was added. The samples were then dried under nitrogen, 0.5 ml of toluene was added again, and the drying repeated. *N*-Acetylation was performed according to Carlson *et al.* (42) by adding 0.1 ml of saturated $NaHCO_3$ and 10 μl of acetic anhydride. The samples were left at room temperature for 10 min and lyophilized. For Bio-Gel P-10 column chromatography the samples were dissolved in 0.3 ml of 0.15 M Tris buffer (pH 7.8) containing 0.1% sodium dodecyl sulfate. Bio-Gel P-10 column (1.0 × 100 cm) was prepared in the same buffer. The samples were centrifuged at 2000 rpm for 5 min and applied to the column. After the sample had entered the gel, 0.2 ml of 1% blue dextran was immediately added. Fifty-drop fractions were collected and 0.25 ml counted in the dioxane-based scintillation fluid. The position of the blue dextran was determined in each run by the extinction at 280 nm. The apparent molecular weights of the glycopeptides were determined on a semilogarithmic scale. R_F = peak of oligosaccharide (glycopeptide)/peak of blue dextran.

Analysis of Glycolipids—Lipids were extracted with chloroform/methanol as previously described, and the glycolipids purified by column and thin layer chromatography (10). The phospholipid phosphorus was determined according to Bartlett (43). After staining with iodine the glycolipids were eluted with chloroform/methanol/water (1/10/10 by volume). Aliquots were counted for radioactivity and the rest used for chemical quantitation. The quantities of glycolipids are given as galactose after analysis of the alditol acetate derivatives.

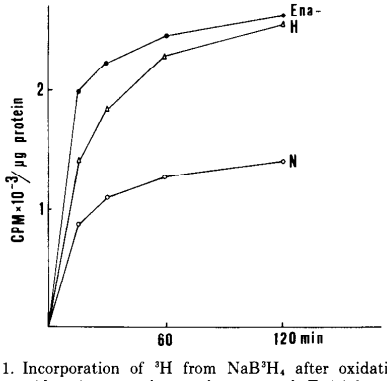

FIG. 1. Incorporation of ^3H from NaB^3H_4 after oxidation with galactose oxidase into membranes from normal, En(a) heterozygous and En(a−) cells. Packed cells (1 ml) were oxidized with 10 units of galactose oxidase for indicated times in 1 ml of Dulbecco's $NaCl/PO_4$ at 37°. After incubation, the cells were washed in $NaCl/PO_4$ two times and reduced with 0.5 mCi of NaB^3H_4 in 1 ml of $NaCl/PO_4$ for 30 min at room temperature. After washing the cells three times, the membranes were isolated and the specific radioactivities determined. *N* = normal cells, *H* = En(a) heterozygous cells, and *Ena−* = En(a−) cells.

Carl_G_190x270_mm_blokki_FINAL.indd 51 06-Aug-23 1:53:30 PM

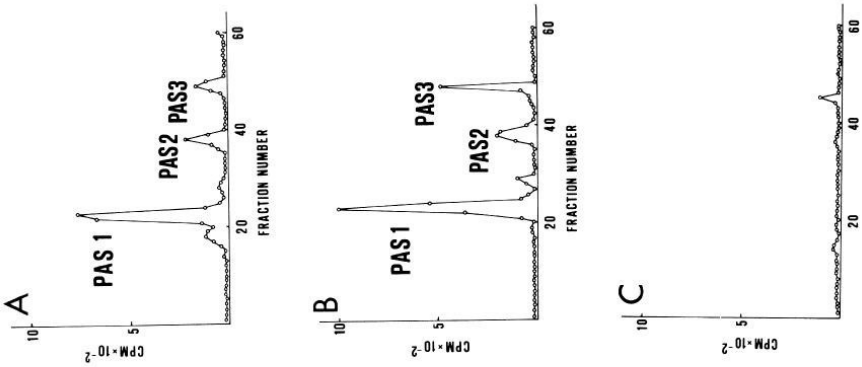

FIG. 4. Sodium dodecyl sulfate-polyacrylamide gel electrophoresis of isolated sialoglycoproteins from ^{125}I-labeled membranes *A*, normal cells; *B*, En(a) heterozygous cells; *C*, En(a−) cells.

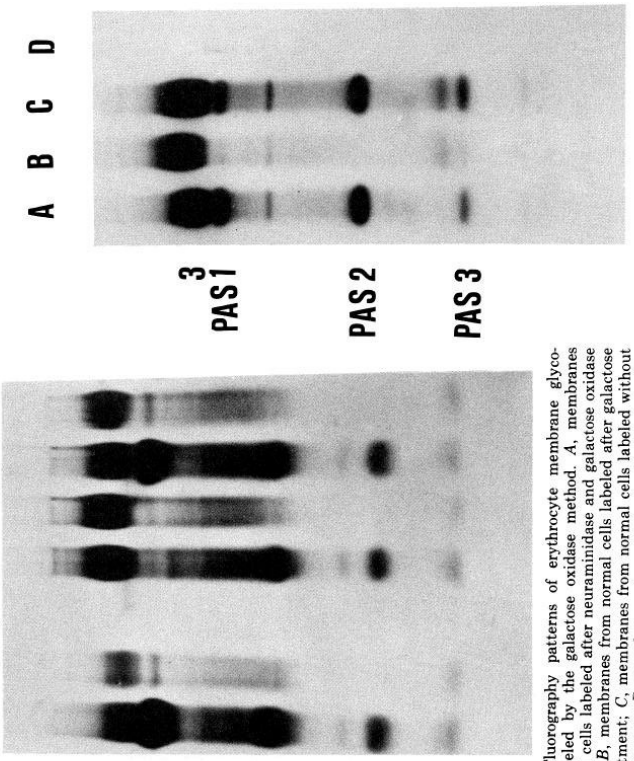

FIG. 2. Fluorography patterns of erythrocyte membrane glycoproteins labeled by the galactose oxidase method. *A*, membranes from normal cells labeled after neuraminidase and galactose oxidase treatments; *B*, membranes from normal cells labeled after galactose oxidase treatment; *C*, membranes from normal cells labeled without enzyme treatment; *D*, membranes from En(a−) cells labeled after neuraminidase and galactose oxidase treatment; *E*, membranes from En(a−) cells labeled after galactose oxidase treatment; *F*, membranes from En(a) heterozygous cells labeled after neuraminidase and galactose oxidase treatment; *G*, membranes from En(a) heterozygous cells labeled after galactose oxidase treatment. Packed cells (0.5 ml) were labeled in the same way in all cases and identical amounts of membranes electrophoresed.

FIG. 3. Fluorography patterns of ^{125}I-labeled erythrocyte membrane surface proteins. Cells were labeled with ^{125}I by the lactoperoxidase technique. *A*, membranes from normal cells; *B*, membranes from En(a−) cells; *C*, membranes from En(a) heterozygous cells; *D*, membranes from normal cells treated with ^{125}I without lactoperoxidase.

Carl_G_190x270_mm_blokki_FINAL.indd 52 06-Aug-23 1:53:30 PM

RESULTS

Surface Labeling of Cells—Normal erythrocytes take up little tritium if not pretreated with galactose oxidase. After treatment with galactose oxidase, En(a−) cells take up almost twice as much as normal cells. En(a) heterozygous cells take up somewhat less label than En(a−) cells. After about 2 h, a plateau is reached (Fig. 1). After neuraminidase treatment, which exposes new galactosyl/*N*-acetylgalactosaminyl residues, normal cells are heavily labeled in sialoglycoproteins PAS1 to 3, but (En(a−) cells do not contain a PAS1 band and PAS2 is diminished. In contrast, Band 3 is more heavily labeled in En(a−) cells and has a slightly larger apparent molecular weight. There is no difference between the two cell types in the PAS3 band. The results obtained with En(a) heterozygous cells are between those obtained with normal and En(a−) cells (Fig. 2).

Similar but not identical results are obtained with the lactoperoxidase labeling method. In En(a−) cells PAS1 and PAS2 are unlabeled compared to the strong labeling in normal cells. Band 3 labels equally well in both types of cell but has a slightly slower mobility in En(a−) cells. Again, En(a) heterozygous cells are intermediate (Fig. 3). After sialoglycoproteins from cells labeled by the lactoperoxidase method were extracted with chloroform/methanol, PAS1 to 3 could be recovered from normal and En(a) heterozygous cells, whereas very little label is obtained from En(a−) membranes (Fig. 4).

After periodate and NaB^3H_4 treatment, which labels sialic acid, PAS1 is strongly labeled in normal cells and unlabeled in En(a−) cells; En(a) heterozygous cells label intermediately (Fig. 5). The label in PAS3 is similar in all membranes.

The total amount of carbohydrate is almost the same in all types of cells with about a 10% decrease in En(a−) cells (Table

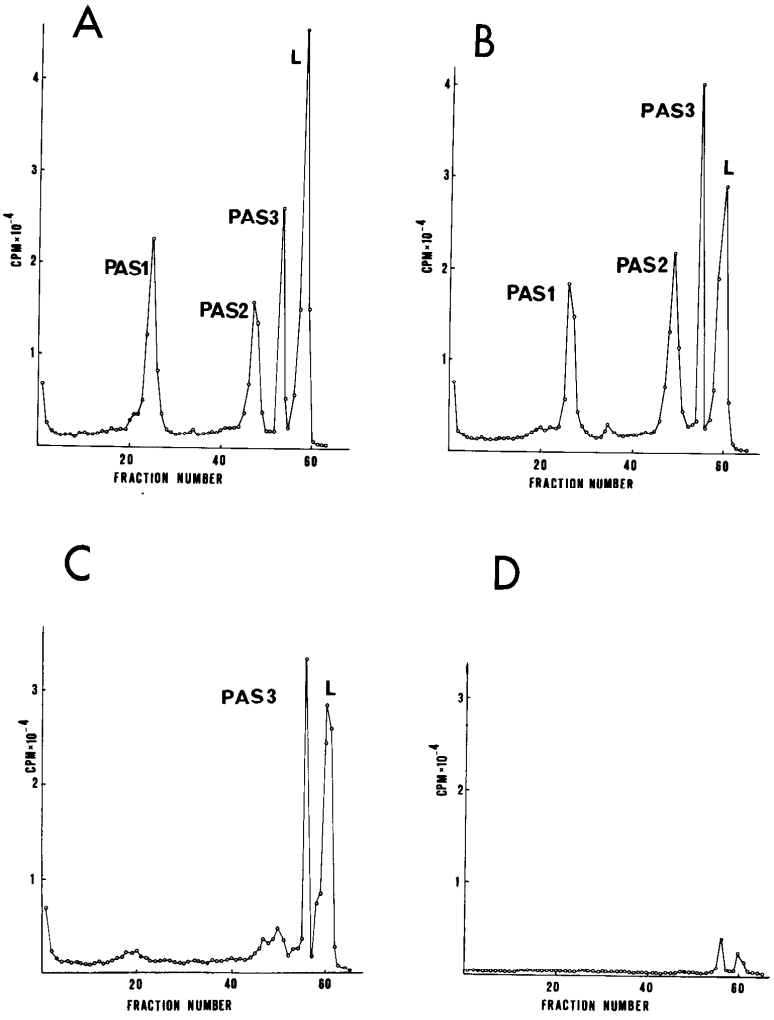

FIG. 5. Sodium dodecyl sulfate-polyacrylamide gels of periodate/NaB^3H_4-labeled membranes. *A*, normal cells; *B*, En(a) heterozygous cells; *C*, En(a−) cells; *D*, normal cells reduced with NaB^3H_4 without pretreatment with periodate.

I). However, the amount of sialic acid is markedly reduced, only 45% of normal. En(a) heterozygous cells contain 80% of the normal amount. Also, the amount of neutral sugar is somewhat decreased, whereas the amount of amino sugar is increased, especially that of *N*-acetyl-D-galactosamine which is increased by 85 and 70%, respectively. The amount of *N*-acetyl-D-glucosamine is increased by about 10%.

Properties of Band 3—On sodium dodecyl sulfate polyacrylamide gels tained with Coomassie blue, Band 3 has a slightly lower mobility in En(a−) cells. The apparent molecular weight, determined from the middle of the band, is 105,000 from normal, 110,000 from En(a) heterozygous, and 115,000 from En(a−) cells (Fig. 6). No bands not present in normal cells are seen in En(a−) cells in these gels or in gels with 12% acrylamide concentration (not shown). Also, when surface labeled with galactose oxidase without neuraminidase treatment, the labeled glycoprotein has a larger apparent molecular weight than in normal cells (Fig. 2). On Ultrogel ACA 34 columns, the elution patterns of sodium dodecyl sulfate-solubilized membranes, labeled by the lactoperoxidase method, were similar for all cell types.

Fig. 7 shows the elution pattern from normal cells. After hydroxylapatite chromatography, Band 3 is obtained almost pure in Peak 3 (Fig. 8). On polyacrylamide gel electrophoresis, some faint bands with slow mobility were seen (Fig. 9). Peak 2 contains Band 4 (nomenclature of Fairbanks *et al.* (4)). Band 3

TABLE I

Total carbohydrate in erythrocyte membranes

	Cells		
	Normal	En(a) heterozygous	En(a−)
	nmol/μg lipid phosphorus[a]		
Sialic acid	35	28	16
N-acetyl-D-glucosamine	43	49	47
N-acetyl-D-galactosamine	14	24	26
Fucose	3	2	2
Mannose	4	2	2
Galactose	29	23	24
Glucose	7	4	4
Total	135	132	121

[a] Average of three determinations.

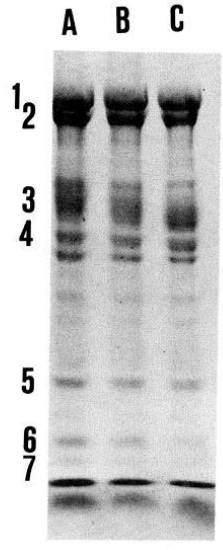

FIG. 6. Coomassie blue stained sodium dodecyl sulfate-polyacrylamide slab gel of proteins from erythrocyte membranes. Membranes were isolated from identical amounts of packed cells, solubilized with sodium dodecyl sulfate and 2-mercaptoethanol, and electrophoresed. The major bands were numbered according to Fairbanks *et al.* (4). *A*, membranes from En(a−) cells; *B*, membranes from En(a) heterozygous cells; *C*, membranes from normal cells.

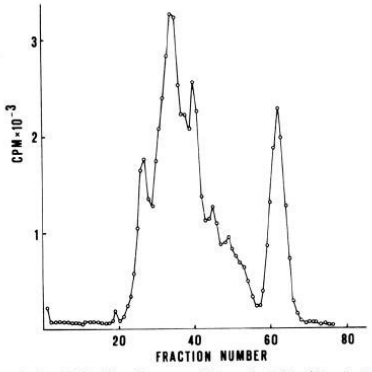

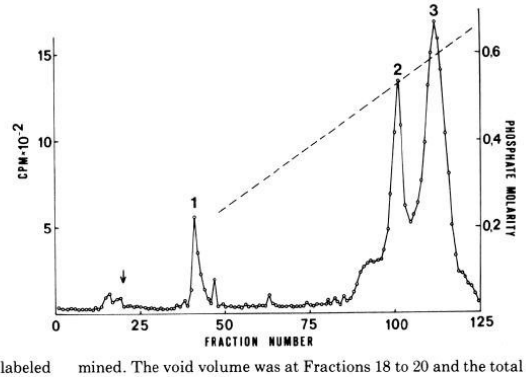

FIG. 7. (*left*). Gel filtration on Ultrogel ACA 34 of ^{125}I-labeled membranes from normal cells. ^{125}I-labeled membranes were extracted with hypotonic and hypertonic media as described under "Materials and Methods," solubilized in sodium dodecyl sulfate and 2-mercaptoethanol, and applied to the column in the presence of sodium dodecyl sulfate. Fractions (4 ml) were collected and the radioactivities determined. The void volume was at Fractions 18 to 20 and the total volume at Fractions 61 to 65.

FIG. 8. (*right*). Sodium dodecyl sulfate-hydroxylapatite column chromatography of fractions 24 to 28 from Fig. 7. Proteins were eluted with a phosphate gradient. – – –, phosphate molarity, O——O, = radioactivity per tube.

Carl_G_190x270_mm_blokki_FINAL.indd 54 06-Aug-23 1:53:30 PM

isolated from En(a−) cells contains at least twice as much carbohydrate as Band 3 from normal cells. The increase in hexose concentration is the greatest and the increase in amino sugars the smallest (Table II).

Glycopeptides obtained by pronase digestion of Band 3 isolated from En(a−) cells appear to have a slightly higher molecular weight (17,000) than the more heterogenous glycopeptides from normal cells (mean molecular weight = 9,500). The glycopeptides from En(a) heterozygous cells were intermediate both with respect to heterogeneity and molecular weight (15,000) (Fig. 10). Oligosaccharides prepared by hydrazinolysis are different. From all cells, two different oligosaccharide peaks were obtained with an apparent molecular weight of 540 for the smaller component. The larger component was largest in En(a−) cells (11,000), intermediate in En(a) heterozygous cells (8,500), and smallest in normal cells (7,500) (Fig. 11). The molecular weights of the large glycopeptides must be regarded as averages of heterogenous material. The two-dimensional peptide maps of purified Band 3 from normal and En(a−) and En(a) heterozygous cells seem to be similar (not shown).

Glycolipids—No significant differences in the amounts of neutral glycolipids exist in the different membranes (Table III) and they all look identical in thin layer chromatography. After galactose oxidase treatment, the En(a−) cells take up 4 to 5 times more label into glycolipids from NaB^3H_4 than normal cells. The uptake by heterozygous cells is even somewhat higher (Table IV).

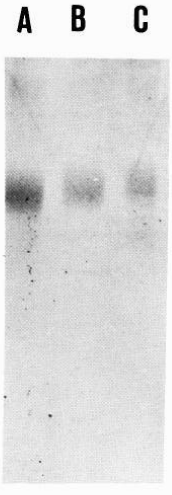

FIG. 9. Coomassie blue-stained slab gel of purified Band 3. *A*, normal cells; *B*, En(a) heterozygous cells; *C*, En(a−) cells.

TABLE II

Carbohydrate composition of Band 3

	Cells		
	Normal	En(a) heterozygous	En(a−)
		nmol/mg protein[a]	
Sialic acid	0	0	0
N-acetyl-D-glucosamine	108	66	96
N-acetyl-D-galactosamine	34	31	54
Fucose	15	21	25
Mannose	46	100	125
Galactose	52	183	298
Glucose[b]	135	244	334

[a] Average of two determinations.
[b] Not reproducible.

DISCUSSION

On sodium dodecyl sulfate-polyacrylamide gel electrophoresis of En(a−) erythrocyte membranes labeled either by the

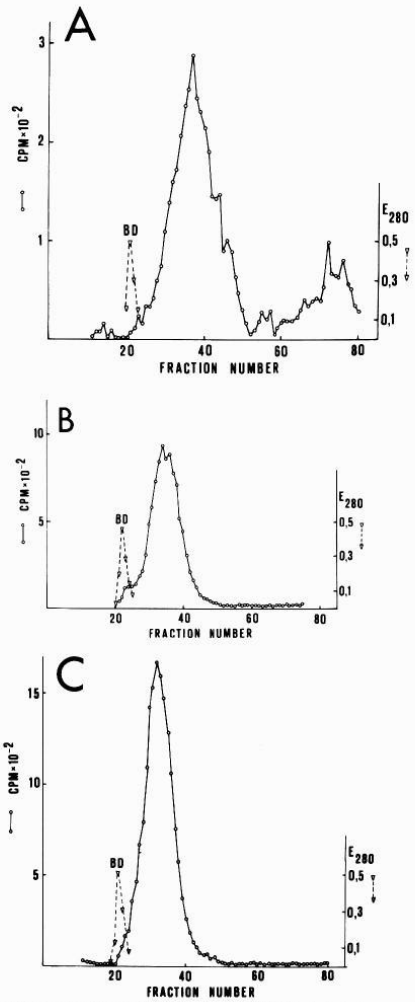

FIG. 10. Bio-Gel P-10 elution patterns of ^3H-labeled glycopeptides from Band 3 obtained by pronase digestion. *A*, normal cells; *B*, En(a) heterozygous cells; *C*, En(a−) cells.

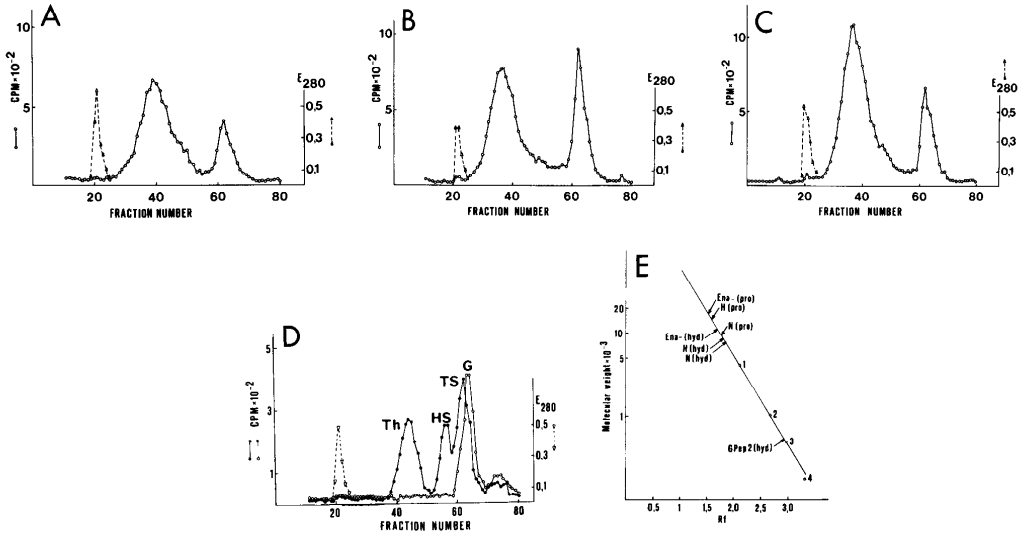

FIG. 11. Bio-Gel P-10 elution patterns of ^{3}H-labeled oligosaccharides from Band 3 obtained by hydrazinolysis. *A*, normal membranes; *B*, En(a) heterozygous membranes; *C*, En(a−) membranes; *D*, carbohydrate standards, *TH* = thyroglobulin complex glycopeptides, *HS* = hexasaccharide, *TS* = trisaccharide, *G* = glucose; *E*, calculation of the molecular weights of the glycopeptides from pronase digested samples (*pro*) and oligosaccharides obtained by hydrazinolysis (*hyd*).

TABLE III

Quantity of glycolipids in erythrocyte membranes

	Cells		
	Normal	En(a) heterozygous	En(a−)
		μg galactose/μg lipid phosphorus[a]	
Ceramide tetrasaccharide	0.26	0.22	0.20
Ceramide trisaccharide	0.04	0.03	0.04
Ceramide disaccharide	0.05	0.05	0.06

[a] Average of three determinations.

TABLE IV

Specific radioactivities in glycolipids

	Cells		
	Normal	En(a−) heterozygous	En(a−)
		cpm/μg galactose	
Ceramide tetrasaccharide	16,400	83,900	93,200
Ceramide trisaccharide	17,900	99,800	92,200
Ceramide disaccharide	20,600	92,200	59,300

galactose oxidase or the lactoperoxidase method, no label is found in the major sialoglycoprotein PAS1. This means that no terminal galactosyl or *N*-acetylgalactosaminyl residues or tyrosine residues of PAS1 are exposed to the enzymes. When cells are treated with sodium periodate and NaB^{3}H$_4$ PAS1 is strongly labeled in normal cells but no label is obtained in PAS1 from En(a−) cells. Therefore, no PAS1 molecule containing sialic acid is present in En(a−) cells. En(a) heterozygous cells contain a decreased label in PAS1. No additional band is seen after staining with Coomassie blue. These results together strongly indicate but do not prove that the whole PAS1 molecule is absent from En(a−) cells.

In normal cells, PAS2 evidently consists of two different sialoglycoproteins (12, 44, 45). One is the monomer of PAS1 and the other is a genuine PAS2. The label by NaB^{3}H$_4$ after neuraminidase and galactose oxidase treatment is markedly reduced in En(a−) cells, which probably is due to the absence of the monomer form of PAS1. After labeling with lactoperoxidase no label is found in PAS2 of En(a−) cells. This suggests that the tyrosine residues of PAS2 are more deeply embedded in the membrane in these cells than in normal cells.

After treatment with neuraminidase and galactose oxidase PAS3 is easily labeled in all cells. However, this protein is poorly labeled by the lactoperoxidase technique in both En(a−) and En(a) heterozygous cells. This must be due to a changed organization of PAS3 in the membrane of these cells.

The sialic acid content of En(a−) cells is strongly reduced. This is understandable by the absence of PAS1 and a reduced level of PAS2. However, the total carbohydrate of all cells is very similar. Therefore, other glycoproteins must contain more carbohydrate and this has been shown to be the case for Band 3. Band 3 of En(a−) cells contains twice the normal amount of carbohydrate. It shows a slightly slower mobility on sodium dodecyl sulfate gels and is enriched in galactose and mannose. It contains at least two different oligosaccharides, one of which is small and similar in all cells. The complex oligosaccharide appears to have a slightly higher molecular weight and is more homogenous in En(a−) cells than in the other cells. To our knowledge, glycopeptides with such high molecular weights have not been described previously. The molecular weight obtained after hydrazinolysis that is lower than after pronase digestion is probably due to some peptide portion that is

Carl_G_190x270_mm_blokki_FINAL.indd 56 06-Aug-23 1:53:30 PM

resistant to pronase digestion. No cleavages take place within the oligosaccharide chains by hydrazine, but the complete polypeptide portion is cleaved (46). Hydrazinolysis of ovalbumin, transferrin, and Semliki Forest virus membrane glycopeptides yield only the expected types of oligosaaccharides.[2]

From the chemical composition of Band 3, it can be calculated that there is only one copy of the complex oligosaccharide per Band 3 molecule. No difference in the composition of the glycolipids was found in the different membranes. The glycolipid label in En(a−) and En(a) heterozygous cells is, however, appreciably higher than in normal cells. The most obvious explanation is that normally the major sialoglycoprotein partially inhibits the labeling of glycolipids. However, it cannot be due simply to steric hindrance of the external portion of the molecule because protease treatment of normal cells, which removes part of the sialoglycoproteins (6, 13), does not change the label in glycolipids to the extent found in En(a−) cells (10, 11). However, the more internal part of PAS1 could somehow be associated with glycolipids. Glycolipids have been claimed to be associated with certain proteins in the erythrocyte membrane (47). It is also known that glycolipids can diffuse in the plane of the membrane (48, 49) and this diffusion may be more extensive in the cells with lower levels or absence of the major sialoglycoprotein.

A hypothetical model of the glycoproteins and glycolipids in normal and En(a−) membranes is shown in Fig. 12. In normal cells, the carbohydrate of PAS1 to 3 and Band 3 is exposed on the surface, as are tyrosine residues which can be iodinated by lactoperoxidase. The glycolipids are only partially available to the galactose oxidase molecule. Band 3 must penetrate the membrane at least twice (12, 50) because pronase digestion of intact cells removes only the smaller labeled oligosaccharide of Band 3, but the complex remains in the membrane and the 64,000 molecular weight fragment obtained by pronase digestion does not contain labeled carbohydrate (12 and footnote 3). In En(a−) cells the primary change may be the absence of PAS1. This then results in overglycosylation of the Band 3 complex oligosaccharide, because the sugar transferases have a limited capacity and normally the glycosylation of Band 3 is not complete because of the competing PAS1 substrate. The absence of PAS1 makes the glycolipids more exposed. Tyrosine residues which could act as substrates for lactoperoxidase are no longer available in PAS2 and PAS3 because of the steric hindrance by the Band 3 complex glycopeptide.

It is remarkable that neither the absence of PAS1 or the increased glycosylation of Band 3 result in any clinical symptoms (20, 21).

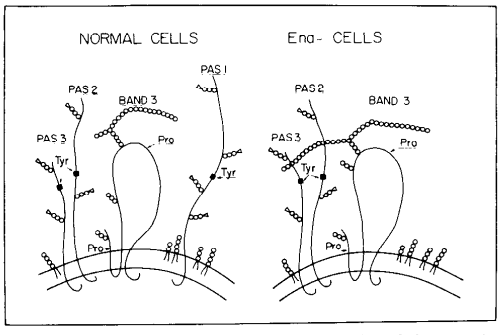

FIG. 12. A hypothetical model of the organization of glycoproteins and glycolipids in normal and En(a−) erythrocyte membranes. *Tyr* = tyrosine residue, *Pro* = cleavage point by pronase.

[2] O. Renkonen, unpublished results.
[3] Unpublished results.

Acknowledgments—The skillful technical assistance of Marja Wilkman and Kerstin Lindeberg is acknowledged.

REFERENCES

1. Gahmberg, C. G., Myllylä, G., and Nordling, S. (1975) *Abstract, 14th Congress of the International Society of Blood Transfusion, Helsinki*
2. Dahr, W., and Uhlenbruck, G. (1975) *Abstract, 14th Congress of the International Society of Blood Transfusion, Helsinki*
3. Anstee, D. J., and Tanner, M. J. A. (1975) *Abstract, 14th Congress of the International Society of Blood Transfusion, Helsinki*
4. Fairbanks, G., Steck, T. L., and Wallach, D. F. H. (1971) *Biochemistry* **10,** 2606–2617
5. Bretscher, M. S. (1971) *Nature New Biol.* **231,** 229–232
6. Marchesi, V. T., Tillack, T. W., Jackson, R. L., Segrest, J. P., and Scott, R. E. (1972) *Proc. Natl. Acad. Sci. U. S. A.* **69,** 1445–1449
7. Boxer, D. H., Jenkins, R. E., and Tanner, M. J. A. (1974) *Biochem. J.* **137,** 531–534
8. Bretscher, M. S. (1971) *J. Mol. Biol.* **59,** 351–357
9. Eylar, E. H., Madoff, M. A., Brody, O. V., and Oncley, J. L. (1962) *J. Biol. Chem.* **237,** 1992–2000
10. Gahmberg, C. G., and Hakomori, S. (1973) *J. Biol. Chem.* **248,** 4311–4317
11. Steck, T. L., and Dowson, G. (1974) *J. Biol. Chem.* **249,** 2135–2142
12. Gahmberg, C. G. (1976) *J. Biol. Chem.* **251,** 510–515
13. Thomas, D. B., and Winzler, R. J. (1969) *J. Biol. Chem.* **244,** 5943–5946
14. Morrison, M., Mueller, T. J., and Huber, C. T. (1974) *J. Biol. Chem.* **249,** 2658–2660
15. Segrest, J. P., Kahane, I., Jackson, R. L., and Marchesi, V. T. (1973) *Arch. Biochem. Biophys.* **155,** 167–183
16. Bretscher, M. S. (1975) *J. Mol. Biol.* **98,** 831–833
17. Tomita, M., and Marchesi, V. T. (1975) *Proc. Natl. Acad. Sci. U. S. A.* **72,** 2964–2968
18. Tanner, M. J. A., and Boxer, D. H. (1972) *Biochem. J.* **129,** 333–347
19. Ho, M. K., and Guidotti, G. (1975) *J. Biol. Chem.* **250,** 675–683
20. Furuhjelm, U., Myllylä, G., Nevanlinna, H. R., Nordling, S., Pirkola, A., Gavin, J., Gooch, A., Sanger, R., and Tippett, P. (1969) *Vox Sang.* **17,** 256–278
21. Darnborough, J., Dunsford, I., and Wallace, J. A. (1969) *Vox Sang.* **17,** 241–255
22. Gahmberg, C. G., Häyry, P., and Andersson, L. C. (1976) *J. Cell Biol.* **68,** 642–653
23. Spiro, R. G., (1965) *J. Biol. Chem.* **240,** 1603–1610
24. Phillips, D. R., and Morrison, M. (1971) *Biochemistry* **10,** 1766–1771
25. Hubbard, A. L., and Cohn, Z. A. (1972) *J. Cell Biol.* **55,** 390–405
26. Liao, T.-H., Gallop, P. M., and Blumenfeld, O. O. (1973) *J. Biol. Chem.* **248,** 8247–8253
27. Laemmli, U. K. (1970) *Nature* 227, 680–685
28. Weber, K. and Osborn, M. (1969) *J. Biol. Chem.* **244,** 4406–4412
29. Bonner, W. M., and Laskey, R. A. (1974) *Eur. J. Biochem.* **46,** 83–88
30. Rice, R. H., and Means, G. E. (1971) *J. Biol. Chem.* **246,** 831–832
31. Warren, L. (1959) *J. Biol. Chem.* **234,** 1971–1975
32. Gatt, R. E., and Berman, E. R. (1966) *Anal. Biochem.* **15,** 167–171
33. Bahl, O. P. (1969) *J. Biol. Chem.* **244,** 567–574
34. Laine, R., Söderlund, H., and Renkonen, O. (1973) *Intervirology* **1,** 110–118
35. Niedermeyer, W. (1971) *Anal. Biochem.* **40,** 465–475
36. Kääriäinen, L., Simons, K., and von Bonsdorff, C.-H. (1969) *Ann. Med. Exp. Biol. Fenn.* **47,** 235–248
37. Lowry, O. H., Rosebrough, N. J., Farr, A. L., and Randall, R. J. (1951) *J. Biol. Chem.* **193,** 265–275

Carl_G_190x270_mm_blokki_FINAL.indd 57 06-Aug-23 1:53:30 PM

38. Hamaguchi, H., and Cleve, H. (1972) *Biochem. Biophys. Res. Commun.* **47,** 459–464
39. Moss, B., and Rosenblum, E. N. (1972) *J. Biol. Chem.* **247,** 5194–5198
40. Bray, D., and Brownlee, S. M. (1973) *Anal. Biochem.* **55,** 213–221
41. Bray, G. A. (1960) *Anal. Biochem.* **1,** 279–285
42. Carlson, D. M., Swanson, A. L., and Roseman, S. (1964) *Biochemistry* **3,** 402–405
43. Bartlett, G. R. (1959) *J. Biol. Chem.* **234,** 466–468
44. Marton, L. S. G., and Garvin, J. S. (1973) *Biochem. Biophys. Res. Commun.* **52,** 1457–1462
45. Slutzky, G. M., and Ji, T. H. (1974) *Biochim. Biophys. Acta* **373,** 337–346
46. Bayard, B., and Roux, D. (1975) *FEBS Lett.* **55,** 206–211
47. Ji, T. H. (1974) *J. Biol. Chem.* **249,** 7841–7847
48. Révész, T., and Greaves, M. (1975) *Nature* **257,** 103–106
49. Craig, S. W., and Cuatrecasas, P. (1975) *Proc. Natl. Acad. Sci. U. S. A.* **72,** 3844–3848
50. Jenkins, R. E., and Tanner, M. J. A. (1975) *Biochem. J.* **147,** 393–399

Carl_G_190x270_mm_blokki_FINAL.indd 58 06-Aug-23 1:53:30 PM

THE JOURNAL OF BIOLOGICAL CHEMISTRY
Vol. 252, No. 16, Issue of August 25, pp. 5888–5894, 1977
Printed in U.S.A.

Selective Radioactive Labeling of Cell Surface Sialoglycoproteins by Periodate-tritiated Borohydride*

(Received for publication, December 10, 1976)

CARL G. GAHMBERG AND LEIF C. ANDERSSON

From the Department of Serology and Bacteriology, and Transplantation Laboratory, Department of Surgery IV, University of Helsinki, Haartmaninkatu 3,00290 Helsinki 29, Finland

Low concentrations of sodium metaperiodate induce specific oxidative cleavage of sialic acids between carbon 7 and carbon 8 or carbon 8 and carbon 9. The aldehydes formed can easily be reduced with NaB^3H_4 to tritiated 5-acetamido-3,5-dideoxy-L-arabino-2-heptulosonic acid or 5-acetamido-3,5-dideoxy-L-arabino-2-octulosonic acid. At 0°, the periodate anion penetrates the cell plasma membrane very slowly and only externally exposed sialic acids are oxidized. This was shown by (*a*) limited labeling of the sialoglycoproteins in a preparation of inside-out erythrocyte vesicles; (*b*) trapping ^{14}C-labeled fetuin within resealed erythrocyte ghosts; fetuin was then poorly labeled, whereas the erythrocyte sialoglycoproteins were highly labeled; (*c*) comparison of labeled glycoproteins of mouse lymphoid cells before and after treatment with neuraminidase. This simple method of specifically introducing a radioactive label into cell surface sialic acids is useful in the study of cell surface sialic acid-containing glycoproteins.

Numerous methods are available to specifically label cell surface proteins and lipids, and much of our knowledge about the molecular organization of the cell surface is based on the use of such methods (1–5). However, very few techniques have been developed to label cell surface carbohydrates, although developments in this field would be of great practical importance (see Refs. 6 and 7 for recent reviews). The galactose oxidase-NaB^3H_4 method (8, 9) for labeling cell surface galactosyl-*N*-acetylgalactosaminyl residues has proved very useful and combined with fluorography of electrophoretically separated erythrocyte surface proteins, has permitted detection of numerous minor surface glycoproteins (10).

Incubation of living cells with cytidine monophosphate-*N*-acetyl[^{14}C]neuraminic acid has been used to label cell surface sialic acid-containing glycoconjugates (11). This method, however, has some major drawbacks: (*a*) the radioactive sugar nucleotide is expensive and the specific radioactivities of the labeled products are low; (*b*) the need for sialyltransferases and the availability of suitable acceptors; and (*c*) it is possible that cytidine monophosphate-*N*-acetylneuraminic acid is hydrolyzed and the free acid penetrates into the cell where it could be used for the formation of cytidine monophosphate-*N*-acetylneuraminic acid, which in turn could cause intracellular labeling.

Mild periodate treatment of glycoproteins results in selective modification of sialic acids. After reduction with tritiated sodium borohydride, tritium-labeled 5-acetamido-3,5-dideoxy-L-arabino-2-heptulosonic acid is the major product formed (12–14). AcNeu[7] [1] is sensitive to cleavage by neuraminidase (13) and is easily released by mild acid treatment (9). Glycoproteins labeled by this technique have often been used to study their turnover in plasma (12).

This method has been used for labeling of membrane glycoproteins. Liao *et al.* (15) obtained specific labeling of human erythrocyte sialoglycoproteins and carefully characterized the labeled products. The periodate-tritiated borohydride technique has also been applied to the labeling of sialoglycoproteins of erythrocyte variants (16), and very recently, high resolution of erythrocyte sialoglycoproteins was seen after labeling with this method (17). Sialoglycoproteins of various other cells have also been studied (18, 19).

With the exception of the erythrocyte, where all the sialic acid is external, the method has not been considered to be specific for the cell surface and no careful attempts have been made to evaluate its potential use in this respect. We now report that by performing the oxidation at 0°, using short incubation times and low concentrations of periodate, the label is specific for external sialic acid-containing glycoproteins.

MATERIALS AND METHODS

Preparation of Cells

Erythrocytes – Fresh or recently outdated blood was used as source of human erythrocytes. The cells were washed by centrifugation four times in 0.15 M NaCl, 0.01 M sodium phosphate, pH 7.4 (NaCl/PO_4).

Lymphoid Cells – Mouse thymuses and spleens (CBA/HT6T6 mice) were teased apart in cold RPMI 1640 culture medium. Clumps were removed by filtration through cotton wool. Erythrocytes were lysed with an 0.83% aqueous solution of NH_4Cl and phagocytic cells were removed after incubation with carbonyl iron by treatment with a magnet (20). The spleen cell preparation contained more than 80% lymphocytes, as judged morphologically from May-Gruenwald-Giemsa-stained smears. The cells will be referred to in the text as thymocytes and lymphocytes.

Fractionation of T and B Lymphocytes

Spleen lymphocytes were fractionated into T and B cells by free flow cell electrophoresis as described previously (21). After fractiona-

* This study was supported by the Academy of Finland, the Finnish Cancer Society, the Sigrid Jusélius Foundation, and the Finska läkaresällskapet.

[1] The abbreviations used are: AcNeu[7], 5-acetamido-3,5-dideoxy-L-arabino-2-heptulosonic acid; PAS 1 to 3, the periodic acid-Schiff-positive glycoproteins of human erythrocyte membranes.

This is an Open Access article under the CC BY license.

Carl_G_190x270_mm_blokki_FINAL.indd 59 06-Aug-23 1:53:30 PM

tion more than 90% of the cells were viable as judged by trypan blue exclusion tests. The T cell fraction contained less than 5% of surface immunoglobulin-carrying cells (B cells) and the B cell fraction less than 2% of θ-antigen-carrying (T) cells (20).

Membrane Preparations

Isolation of erythrocyte membranes has been described previously (8). Resealing of erythrocyte ghosts containing fetuin was done as follows. Isolated, packed ghosts were incubated with an equal volume of 0.3 M NaCl, 0.002 M $MgCl_2$, 0.02 M sodium phosphate, pH 7.4, containing 2 mg/ml of [^{14}C]fetuin (specific activity 45,450 cpm/mg of protein). After incubation at 37° for 40 min, the membranes were washed three times in $NaCl/PO_4$, 1 mM $MgCl_2$ buffer (22). Further washings did not reduce the specific radioactivity of the [^{14}C]fetuin-containing resealed ghosts.

Inside-out erythrocyte vesicles were prepared according to Steck and Kant (22). The vesicles were fractionated on a Dextran T 110 continuous gradient, density 1.01 to 1.05 g/cc, made in 0.5 mM sodium phosphate, pH 8.0, with a Spinco SW 27 rotor at 20,000 rpm for 16 h in a Beckman L4 ultracentrifuge. The resealed inside-out vesicles were collected from the top of the gradient. The degree of contamination by right-side-out vesicles and unsealed ghosts was assayed by incubation with *Vibrio cholerae* neuraminidase in Dulbecco's $NaCl/PO_4$ containing Ca^{2+} ions either in the presence or absence of 1% Triton X-100 (22).

Chemicals

Sodium metaperiodate was from Merck AG, Darmstadt, Germany. Acrylamide and *N,N'*-methylenebisacrylamide were obtained from Eastman Kodak Co., Rochester, N. Y. 2,5-Diphenyloxazole (PPO) and *p*-bis[2-(5-phenyloxazolyl)]benzene (POPOP) were obtained from New England Nuclear, Boston, Mass. Phenylmethylsulfonyl fluoride and crystalline *N*-acetylneuraminic acid were from Sigma. Triton X-100 was purchased from British Drug Houses Chemicals Ltd., Poole, England. Bovine fetuin (99% pure) was obtained from Grand Island Biologicals. Tritiated sodium borohydride (8.2 Ci/mmol) and [^{14}C]formaldehyde (4.54 mCi/mmol) were obtained from the Radiochemical Centre Ltd., Amersham, England. The NaB^3H_4 preparation was handled as described previously (18).

Enzymes

Galactose oxidase with a specific activity of 130 units/mg of protein was purchased from Kabi AB, Stockholm, Sweden. It displayed no protease or neuraminidase activities when measured as described previously (8). *Vibrio cholerae* neuraminidase (500 units/ml) was from Behringwerke AG, Marburg-Lahn, Germany. It was free of protease activity.

Labeling of Proteins with [^{14}C]formaldehyde

This was done essentially according to Rice and Means (23). The 5 mg of fetuin or the standard proteins used for electrophoresis were dissolved in 0.05 ml of 0.5% $NaHCO_3$. Then 3 μl (6 μCi) of [^{14}C]formaldehyde was added. After 3 min at room temperature, the proteins were reduced three times with 5 μl of $NaBH_4$ (5 mg/ml) at 1 min intervals to stabilize the Schiff bases formed, 1 ml $NaCl/PO_4$ was added and the samples were dialyzed at 4° for 48 h against distilled water.

Polyacrylamide Gel Electrophoresis

Polyacrylamide gel electrophoresis in the presence of sodium dodecyl sulfate was performed according to Laemmli (24) as described previously (10, 16, 18) using either cylindrical or slab gels. The acrylamide concentration in the separating gels was 8%. The treatment of the slab gels for fluorography (25) and slicing and counting of the cylindrical gels has been described (10, 16).

Chemical Determinations

Protein was measured according to Lowry *et al.* (26) with bovine serum albumin as standard. Sialic acid was quantitated by the thiobarbituric acid method (27) with crystalline *N*-acetylneuraminic acid as standard. For determination of total sialic acid, hydrolysis was performed in 0.1 M H_2SO_4 at 80° for 1 h.

Labeling of Cells or Membranes with Periodate-tritiated Sodium Borohydride

Washed, packed erythrocytes (1 ml) or unsealed ghosts or membrane vesicles derived from 1 ml of cells were incubated in $NaCl/PO_4$ in a total volume of 2 ml either at 22° or on ice with indicated concentrations of sodium metaperiodate for different times. After incubation, 0.2 ml of 0.1 M glycerol in $NaCl/PO_4$ was added, the samples washed twice with $NaCl/PO_4$ by centrifugation, and reduced with 0.5 mCi of tritiated sodium borohydride per tube for 30 min at room temperature in a total volume of 2 ml of $NaCl/PO_4$. The cells or membranes were washed three times by centrifugation and membranes were isolated from the cells. Resealed, labeled ghosts containing fetuin were washed in $NaCl/PO_4$, 1 mM $MgCl_2$ three times, lysed in 5 mM sodium phosphate buffer, pH 8.0, and centrifuged. The supernatants were concentrated, and these and the membranes were counted for radioactivity in Bray's solution (28) in a Wallac-LKB 81000 liquid scintillation counter.

For labeling of mouse lymphoid cells 180 × 10^6 thymocytes and 90 × 10^6 T or B lymphocytes were divided into three equal aliquots. One tube of each cell type was used for labeling with the galactose oxidase method. To another tube was added 12.5 units of neuraminidase and the tubes incubated in 1 ml of Dulbecco's $NaCl/PO_4$ containing Ca^{2+} ions for 30 min at 37°. Another set of tubes was incubated in the same way but without neuraminidase. The cells were washed twice by centrifugation in $NaCl/PO_4$ and suspended in 1 ml of $NaCl/PO_4$. The cells were then treated with periodate at a final concentration of 1 mM on ice for 5 min, 0.2 ml of 0.1 M glycerol in $NaCl/PO_4$ was added to quench the reaction, and the cells were washed three times in $NaCl/PO_4$. After they were suspended in 0.5 ml of $NaCl/PO_4$, the cells were reduced with 0.5 mCi of tritiated sodium borohydride per tube for 30 min at room temperature and washed three times in $NaCl/PO_4$. At this stage, more than 90% of the cells were viable as shown by exclusion of trypan blue. Then 0.2 ml of $NaCl/PO_4$ containing 1% Triton X-100 and 2 mM phenylmethanesulfonyl fluoride (as protease inhibitor) was added on ice. After 15 min, the samples were centrifuged for 10 min at 4000 rpm at 4° to remove nuclei and the supernatants taken for counting and electrophoresis (8, 16).

Cell Surface Labeling by Galactose Oxidase Method

This was done as described previously (8, 16). Cells or membranes were incubated in 2 ml of Dulbecco's $NaCl/PO_4$ with 12.5 units of neuraminidase and 5 units of galactose oxidase for 30 min at 37°, washed, and reduced with tritiated sodium borohydride as for the periodate-oxidized samples.

Identification of Tritiated 5-Acetamido-3,5-dideoxy-L-arabino-2-heptulosonic Acid

Erythrocyte membranes, labeled by periodate-NaB^3H_4, were treated with 0.1 M H_2SO_4 at 80° for 1 h. The samples were neutralized with NaOH, centrifuged at 4000 rpm for 10 min, and the supernatants passed through Sephadex G-50 columns (1 × 20 cm) made with distilled water. Aliquots were counted for radioactivity and the radioactive fractions pooled and lyophilized. *N*-Acetylneuraminic acid standard, tritiated AcNeu[7] prepared according to Liao *et al.* (15), and the radioactive compounds from the erythrocyte samples were chromatographed on Whatman No. 3MM paper with 1-butanol:1-propanol:0.1 N HCl/water, 1:2:1 by volume (15). The *N*-acetylneuraminic acid standard was visualized after staining with alkaline silver nitrate (29). The paper strips containing the radioactive samples were cut into 1-cm pieces, placed into scintillation vials, incubated with 1 ml of water for 60 min, and the radioactivities determined using Bray's solution.

RESULTS

Labeling of Erythrocyte Membranes with NaB^3H_4 after Periodate Treatment – Labeling with NaB^3H_4 is dependent on the concentration of periodate (Fig. 1*A*). With 1 ml of packed cells, the maximal incorporation of radioactivity is obtained with 1 to 2 mM periodate which gives a 6 to 12 M ratio of periodate to sialic acids. The oxidation is rapid. There is already an appreciable oxidation after 30 s which is essentially complete after 10 min (Fig. 1*B*).

Table I shows that with low concentrations of periodate most of the radioactivity was released by 0.1 M H_2SO_4 at 80° for 60 min. Somewhat more radioactivity was released from membranes treated with periodate at 0°. All the released label comigrated with standard AcNeu[7] on paper chromatography and with an R_F value of 1.34 to 1.00 for *N*-acetylneuraminic acid.

Carl_G_190x270_mm_blokki_FINAL.indd 60 06-Aug-23 1:53:30 PM

In Fig. 2 are shown the fluorography patterns of slab gels of membrane proteins from periodate-oxidized and NaB^3H_4-reduced erythrocytes. The major bands correspond to the sialoglycoproteins PAS 1 to 3. Without periodate treatment, no radioactive band is obtained (Fig. 2*b*). High concentrations of periodate gave weaker bands (Fig. 2, *h* and *i*). Short incubation times gave weaker bands, but the differences are not very remarkable (Fig. 2, *j* to *o*).

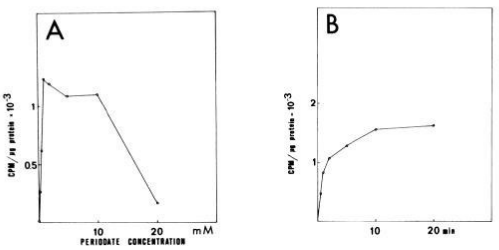

FIG. 1. *A*, incorporation of tritium from tritiated sodium borohydride into membranes of erythrocytes treated with various concentrations of periodate. The 1 ml of packed cells was incubated for 10 min at 0° with the concentrations of periodate indicated in a total volume of 2 ml. Then 0.2 ml of 0.1 M glycerol was added and the cells were washed and reduced with NaB^3H_4 (0.5 mCi/tube) for 30 min at 22°. The membranes were isolated and the specific radioactivities determined. *B*, incorporation of tritium from tritiated sodium borohydride into membranes of erythrocytes treated with periodate for different times. The 1 ml of packed cells was incubated at 0° for indicated times with 2 mM sodium metaperiodate in a total volume of 2 ml and 0.2 ml of 0.1 M glycerol was added. The cells were then washed and reduced with NaB^3H_4 (0.5 mCi/tube) for 30 min at 22°C. The membranes were then isolated and the specific radioactivities determined.

Comparison of Erythrocyte Glycoproteins Labeled by Galactose Oxidase and Periodate Techniques—Fig. 3 shows a sodium dodecyl sulfate-polyacrylamide gel electrophoresis slab gel pattern of glycoproteins labeled after galactose oxidase and periodate treatments. By the galactose oxidase technique combined with neuraminidase treatment, in addition to the sialoglycoproteins, Band 3 and the minor glycoproteins are labeled, and these are not as well labeled after periodate oxidation. A further difference is the slower mobility of PAS 2 after neuraminidase plus galactose oxidase treatment than after periodate treatment (Fig. 3, *a* and *b*).

Labeling of Fetuin by Periodate-NaB^3H_4 within Resealed Erythrocyte Membranes—Penetration of periodate through erythrocyte membranes was studied by incorporating the sialic acid-rich glycoprotein fetuin within resealed ghosts. Quantitation of trapped fetuin was possible by using ^{14}C-labeled fetuin. Table II shows the incorporation into mem-

TABLE I

Label released by weak acid from periodate-NaB^3H_4-labeled erythrocyte membranes

One milliliter of packed cells was labeled as intact, and the membranes were isolated and treated with 0.1 M H_2SO_4 at 80° for 60 min.

Periodate concentration	Labeled at 22°	Labeled at 0°
mM	*% released*	
0.1	54.5	61.8
0.5	68.2	61.0
1	67.5	68.5
2	65.2	68.5
5	51.1	70.5
10	43.0	68.5
20	41.1	59.4

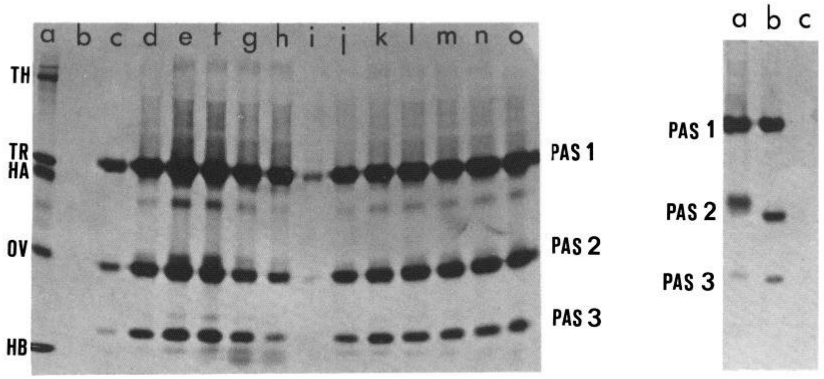

FIG. 2 (*left*). Fluorography patterns of periodate-NaB^3H_4-labeled erythrocyte membrane glycoproteins separated by slab gel electrophoresis in the presence of sodium dodecyl sulfate. *a*, ^{14}C-labeled standard protein: *TH*, thyroglobulin; *TR*, transferrin; *HA*, human albumin; *OV*, ovalbumin; *HB*, hemoglobin. *b*, pattern of membrane proteins of a 10-µl aliquot of membranes isolated from 1 ml of packed cells, which had been reduced with NaB^3H_4 without periodate treatment; *c* to *i*, patterns of labeled glycoproteins of 10-µl aliquots of membranes isolated from 1 ml of packed cells, which had been treated with different concentrations of periodate for 10 min at 0° and then reduced with NaB^3H_4; *c*, 0.1 mM periodate; *d*, 0.5 mM periodate; *e*, 1 mM periodate; *f*, 2 mM periodate; *g*, 5 mM periodate; *h*, 10 mM periodate; *i*, 20 mM periodate; *j* to *o*, patterns of labeled glycoproteins of 10-µl aliquots of membranes isolated from 1 ml of packed cells, which had been treated with 2 mM periodate at 0° for different times. *j*, 30 s; *k*, 1 min; *l*, 2 min; *m*, 5 min; *n*, 10 min; *o*, 20 min.

FIG. 3 (*right*). Fluorography patterns of erythrocyte glycoproteins labeled by the neuraminidase-galactose oxidase and periodate techniques, and separated by slab gel electrophoresis in the presence of sodium dodecyl sulfate. *a*, labeled glycoproteins of membranes isolated from 1 ml of packed cells treated with neuraminidase and galactose oxidase and reduced with NaB^3H_4; *b*, labeled glycoproteins of membranes isolated from 1 ml of packed cells treated with 2 mM periodate at 0° for 10 min; *c*, control of membranes isolated from 1 ml of packed cells, which had not been treated with enzymes or periodate but reduced with NaB^3H_4. In each case, 10 µl of packed membranes were electrophoresed.

Carl_G_190x270_mm_blokki_FINAL.indd 61 06-Aug-23 1:53:31 PM

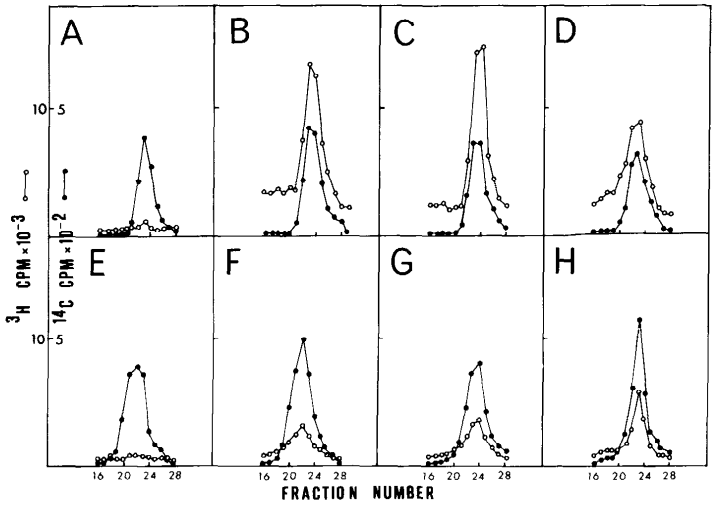

FIG. 4. Sodium dodecyl sulfate-gel electrophoresis patterns of [^{14}C]fetuin labeled by periodate-NaB^{3}H$_4$ within resealed erythrocyte ghosts. *A*, no periodate treatment at 22°; *B*, 0.2 mM periodate at 22°; *C*, 1 mM periodate at 22°; *D*, 2 mM periodate at 22°; *E*, no periodate at 0°; *F*, 0.2 mM periodate at 0°; *G*, 1 mM periodate at 0°; *H*, 2 mM periodate at 0°.

TABLE II

Incorporation of tritium from NaB^{3}H$_4$ into periodate-treated resealed membranes and trapped fetuin

Periodate concentration	Membranes	Fetuin	Fetuin/membrane
mM	*cpm/μg N-acetylneuraminic acid*		
At 22°			
0	6,080	1,520	
0.1	53,400	17,100	0.33
0.5	90,000	19,800	0.22
1	104,000	14,600	0.14
2	105,000	12,100	0.11
5	81,000	9,300	0.11
At 0°			
0	6,000	970	
0.1	26,100	3,470	0.12
0.5	52,800	4,610	0.08
1	60,000	5,090	0.08
2	64,500	6,010	0.09
5	66,400	6,420	0.09

TABLE III

Sialic acid released by neuraminidase from erythrocyte membranes

The 200 μg of membrane protein was incubated with 25 units of *Vibrio cholerae* neuraminidase for 30 min at 37° in 1 ml of Dulbecco's NaCl/PO$_4$ containing Ca^{2+} ions and the liberated sialic acid determined.

	Intact membranes	Membranes + 1% Triton X-100	Intact/disrupted
	μg/mg protein		
Inside-out vesicles	4.03	41.9	0.10
Ghosts	33.9	30.6	1.1

branes of fetuin at 22° and 0°. The specific radioactivities of the membranes are higher after treatment at 22° than at 0°. At 22°, fetuin is clearly labeled by ^{3}H after treatment with low concentrations of periodate, but at 0°, fetuin is not extensively labeled. Fig. 4 shows the sodium dodecyl sulfate-gel electrophoresis patterns of the fetuin peak fractions obtained after labeling at 22° and 0°. A clearly higher extent of labeling is seen on treatment at 22° than at 0°.

Labeling of Inside-out Erythrocyte Vesicles versus Unsealed Membranes—The inside-out erythrocyte vesicle preparation contained about 10% unsealed or right-side-out vesicles. This was indicated by the accessibility of membrane sialic acids to *Vibrio cholerae* neuraminidase in untreated as compared to Triton X-100-disrupted vesicles (Table III).

When inside-out vesicles and unsealed membranes were labeled by the galactose oxidase method combined with neuraminidase treatment, the specific radioactivity in inside-out vesicles was clearly lower than that of unsealed membranes (Table IV). The difference for the periodate-treated membranes was not that clear. With equimolar concentrations of periodate to sialic acid (0.2 μmol with 0.1 mM periodate, Table IV), most radioactivity could be released by 0.1 M H_2SO_4 at 80° for 1 h. With a 10-fold molar excess of periodate to sialic acid, much of the radioactivity was acid-resistant. The released radioactivity was all recovered as AcNeu[7]. Fig. 5, *A* to *H*, shows the corresponding sodium dodecyl sulfate-polyacrylamide gel electrophoresis patterns. Both after neuraminidase plus galactose oxidase treatment or after periodate treatment, the major labeled peaks correspond to the sialoglycoproteins PAS 1 to 3. Here it can clearly be seen that the labeling is much more pronounced in these proteins from unsealed membranes than from the inside-out vesicle preparations.

Labeling of Lymphoid Cell Glycoproteins—Mouse thymocytes and T and B lymphocytes were labeled after treatments with neuraminidase plus galactose oxidase or periodate. Cells that had been pretreated with neuraminidase were used as controls. The specific radioactivities are given in Table V. Fig. 6 shows that the most radioactive bands obtained by the two labeling techniques exactly correspond to each other. The only obvious exceptions are *bands GP9* and *GP9′* of Fig. 6, *b* and *c*, and *e* and *f*, respectively.[2] These bands have previously been shown to derive from the same protein (18). Treatment of intact cells with neuraminidase before labeling removes most

[2] For nomenclature of mouse lymphoid cell glycoproteins see Ref. 18.

Carl_G_190x270_mm_blokki_FINAL.indd 62 06-Aug-23 1:53:31 PM

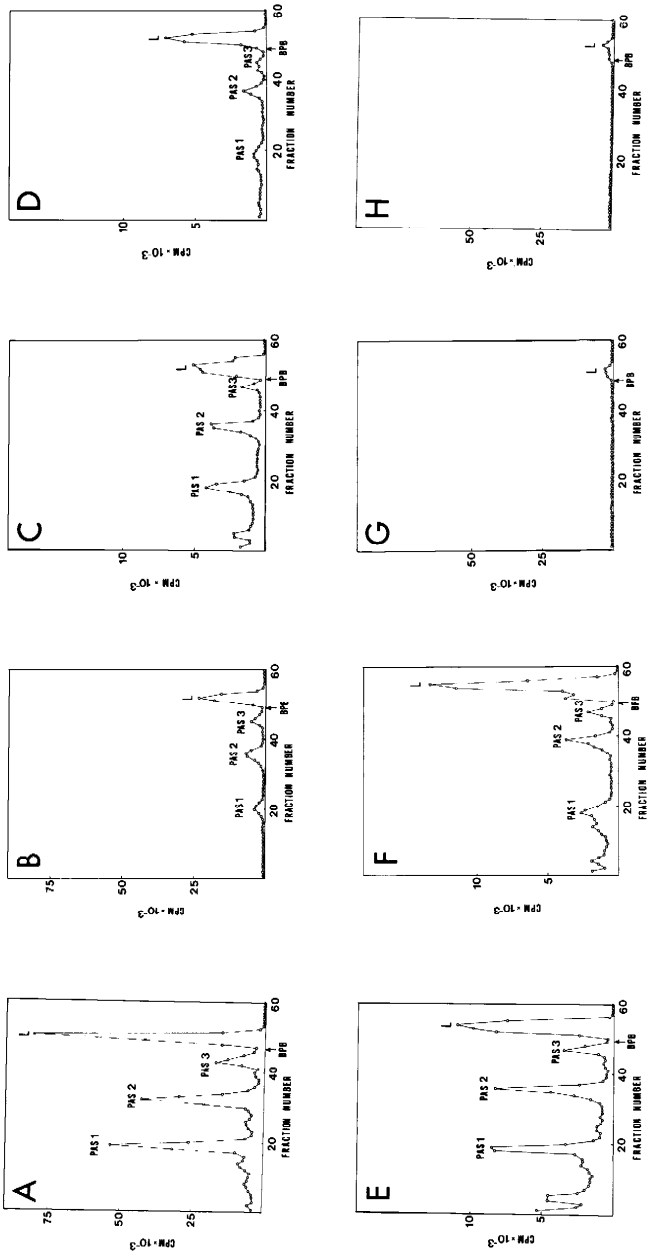

FIG. 5. Sodium dodecyl sulfate-gel electrophoresis patterns of erythrocyte membranes and resealed inside-out erythrocyte vesicles labeled by the neuraminidase-galactose oxidase and periodate techniques. Membranes or vesicles containing 72 μg of sialic acid were labeled in all cases with 0.5 mCi of NaB^3H_4 after treatment with neuraminidase plus galactose oxidase or periodate in a total volume of 2 ml. *A*, unsealed membranes labeled with NaB^3H_4 after treatment with neuraminidase plus galactose oxidase; *B*, inside-out vesicles labeled after treatment with neuraminidase plus galactose oxidase; *C*, unsealed membranes labeled after treatment with 0.1 mM periodate for 5 min at 0°; *D*, inside-out vesicles labeled after treatment with 0.1 mM periodate for 5 min at 0°; *E*, unsealed membranes labeled after treatment with 1 mM periodate for 5 min at 0°; *F*, inside-out vesicles labeled after treatment with 1 mM periodate for 5 min at 0°; *G*, unsealed membranes labeled without enzyme or periodate treatments at 0°; *H*, inside-out vesicles labeled without enzyme or periodate treatments at 0°. *BPB*, position of bromphenol blue marker dye; *L*, lipid peak.

Carl_G_190x270_mm_blokki_FINAL.indd 63 06-Aug-23 1:53:31 PM

TABLE IV

Specific radioactivities in erythrocyte membranes labeled with NaB^3H_4 after oxidation with neuraminidase plus galactose oxidase or with periodate

Membrane samples containing 72 μg of *N*-acetylneuraminic acid were treated with the enzymes or periodate in a total volume of 2 ml and labeled with 0.5 mCi of NaB^3H_4/sample.

	Neuraminidase plus galactose oxidase	Periodate			Periodate		
		0 mM	0.1 mM	1 mM	0 mM	0.1 mM	1 mM
	cpm/μg membrane sialic acid				*% radioactivity released by mild acid*[a]		
Inside-out vesicles	86,000	12,500	25,300	59,500	69.0	96.6	42.6
Ghosts	335,000	8,300	38,600	86,000	37.3	100.0	45.7

[a] Membrane samples were treated with 0.1 M H_2SO_4 for 60 min at 80°.

TABLE V

Incorporation of tritium from NaB^3H_4 into mouse lymphoid cells

Aliquots of labeled cells were precipitated with 10% trichloroacetic acid, washed, and counted after NCS solubilization (8).

	Neuraminidase plus galactose oxidase	1 mM periodate	Neuraminidase plus 1 mM periodate
		cpm/10^6 cells	
Thymocytes	3212	1775	993
T lymphocytes	6303	3441	2116
B lymphocytes	6267	3658	2496

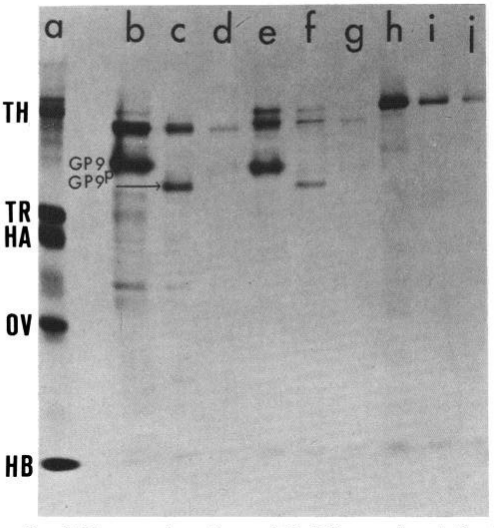

FIG. 6. Fluorography patterns of labeled mouse lymphoid cell glycoproteins separated by sodium dodecyl sulfate slab gel electrophoresis. *TH*, thyroglobulin; *TR*, transferrin; *HA*, human albumin; *OV*, ovalbumin; *HB*, hemoglobin. *a*, pattern of ^{14}C-labeled standard proteins; *b*, glycoproteins of thymocytes labeled by NaB^3H_4 after treatment with neuraminidase plus galactose oxidase; *c*, glycoproteins of thymocytes labeled after treatment with 1 mM periodate; *d*, glycoprotein of thymocytes labeled after treatment with neuraminidase and 1 mM periodate; *e*, glycoproteins of T lymphocytes labeled after treatment with neuraminidase plus galactose oxidase; *f*, glycoproteins of T lymphocytes labeled after treatment with 1 mM periodate; *g*, glycoproteins of T lymphocytes labeled after treatment with neuraminidase and 1 mM periodate; *h*, glycoproteins of B lymphocytes labeled after treatment with neuraminidase plus galactose oxidase; *i*, glycoproteins of B lymphocytes labeled after treatment with 1 mM periodate; *j*, glycoproteins of B lymphocytes labeled after treatment with neuraminidase and 1 mM periodate. The thymocyte preparations used for electrophoresis contained material derived from 7.7×10^6 cells, the T cell preparations from 3.75×10^6 cells, and the B cell preparations from 2.91×10^6 cells. The nomenclature of the labeled glycoproteins is from Ref. 18.

of the radioactive bands. In addition, *bands GP9'* shift to the positions of *bands GP9* (faintly seen).

DISCUSSION

Most, if not all cell surface proteins contain carbohydrate, and surface-associated glycoproteins and glycolipids are considered important in a variety of surface-mediated phenomena, as intercellular adhesion (30–32), growth control (33, 34), and malignancy (35–37). Therefore, development of techniques for studying these structures are of great importance.

Rather recently it became possible to specifically introduce a radioactive label into cell surface galactosyl and *N*-acetylgalactosaminyl residues of glycoproteins and glycolipids by use of galactose oxidase (8, 9). This method has proved very useful and has been applied to a large number of different cells (8, 9, 16, 18, 19). By combination with neuraminidase, sialic acid-containing surface molecules may tentatively be identified. However, it is possible that removal of sialic acids from the cell surface will change the exposure of glycoproteins and this could lead to misinterpretations. The structure of the sialoglycoproteins is also rather drastically changed by removal of sialic acids, and functional changes may occur (12).

Because of this, a more direct approach would be preferable. Low concentrations of periodate are quite specific for oxidation of sialic acids, and after reduction with tritiated borohydride radioactive AcNeu[7] is formed (12–14). This method has not been considered to be specific for the cell surface. Only in erythrocytes, where it is known that all sialic acid is external (38), there have not been problems in interpreting the labeling results. Some phospholipids are also labeled after periodate treatment, but these have not been studied (15).

The rationale of obtaining a rather specific labeling of cell surface sialic acids by the periodate-NaB^3H_4 method is based on oxidation at 0°, low concentrations of periodate, and short reaction times. At this temperature, the membrane is "frozen" and transport of anions may be relatively low. On the other hand, the oxidation of available sialic acids proceeds well at this temperature and much of the periodate should actually be consumed for oxidation at the cell surface, and never be available for transport into the cell.

To obtain appropriate controls for possible intracellular glycoprotein labeling, erythrocyte membranes were resealed with the sialic acid-rich glycoprotein fetuin inside. The structure of the fetuin oligosaccharides is known (39), and the sialic acids, linked to galactosyl residues, are all easily oxidized by periodate (14). The results show that with low concentrations of periodate at 0° the specific radioactivity in fetuin was only a few per cent of that of the cell surface glycoproteins (mainly PAS 1 to 3, Fig. 2). At 22°, the labeling of fetuin was clearly stronger. Higher concentrations of periodate result in less labeling of the membrane. The reason for this is not known but may be due to degradation of membrane polypeptides.

Compared to the labeling of unsealed membranes, the label

Carl_G_190x270_mm_blokki_FINAL.indd 64 06-Aug-23 1:53:31 PM

in the sialoglycoproteins of resealed inside-out erythrocyte vesicles is clearly smaller. In the neuraminidase plus galactose oxidase-treated membranes (Fig. 5, *A* and *B*), the difference in labeling is very clear. This is similar to the results of Steck and Dawson (9). In the periodate-treated membranes, the difference between labeling of unsealed *versus* inside-out membranes is also obvious. It is reasonable to assume that much of the label in PAS 1 to 3 in the inside-out vesicle preparation is due to the presence of contaminating vesicles with sialic acids readily available. This may be more important for periodate-treated membranes than for neuraminidase plus galactose oxidase-treated membranes because a higher ratio of periodate to available sialic acids will result in more efficient oxidation.

To show a more general application of the periodate-NaB^3H_4 method, we have labeled mouse lymphoid cells both by the galactose oxidase and periodate techniques. As previously shown, thymocytes and T and B lymphocytes show characteristic surface glycoprotein patterns when labeled by the neuraminidase-galactose oxidase technique (18). When compared to the patterns obtained after periodate labeling, they are remarkably similar. This strongly supports the surface specificity of the periodate labeling technique. The only major difference is in *bands GP9* and *GP9^v* and this is due to the neuraminidase treatment, which results in a higher apparent molecular weight. It is interesting to note that removal of sialic acids by neuraminidase increases the apparent molecular weight and this further points out the problems associated with determination of molecular weights of glycoproteins by sodium dodecyl sulfate-gel electrophoresis (40). The controls where intact cells have been pretreated with neuraminidase also show that all major glycoproteins labeled after periodate treatment most probably are surface glycoproteins because during short incubation times, the enzyme should not penetrate the cell plasma membrane extensively.

The periodate-NaB^3H_4 method could be especially useful to study cell surface glycopeptides of malignant cells which are known to be highly sialylated (41–43). It may also be possible to specifically label cell surface gangliosides by this technique. The cheap reagents, the short reaction times, and the use of chemical probes instead of more or less labile or impure enzymes are obvious advantages.

Acknowledgment—The skillful technical assistance of Marja Wilkman is acknowledged.

REFERENCES

1. Phillips, D. R., and Morrison, M. (1971) *Biochemistry* **10**, 1766–1771
2. Hubbard, A. L., and Cohn, Z. A. (1972) *J. Cell Biol.* **55**, 390–405
3. Bretscher, M. S. (1971) *J. Mol. Biol.* **58**, 775–781
4. Whiteley, N. M., and Berg, H. C. (1974) *J. Mol. Biol.* **87**, 541–561
5. Staros, J. V., Haley, B. E., and Richards, F. M. (1974) *J. Biol. Chem.* **249**, 5004–5007
6. Gahmberg, C. G., and Hakomori, S. (1976) in *Biomembranes* (Manson, L., ed) Vol. 8, pp. 131–165, Plenum Press, New York
7. Gahmberg, C. G., Itaya, K., and Hakomori, S.-i. (1976) in *Methods of Membrane Biology* (Korn, E. D., ed) Vol. 7, pp. 179–210, Plenum Press, New York
8. Gahmberg, C. G., and Hakomori, S. (1973) *J. Biol. Chem.* **248**, 4311–4317
9. Steck, T. L., and Dawson, G. (1974) *J. Biol. Chem.* **249**, 2135–2142
10. Gahmberg, C. G. (1976) *J. Biol. Chem.* **251**, 510–515
11. Datta, P. (1974) *Biochemistry* **13**, 3987–3991
12. Van Lenten, L., and Ashwell, G. (1971) *J. Biol. Chem.* **246**, 1889–1894
13. Suttajit, M., and Winzler, R. J. (1971) *J. Biol. Chem.* **246**, 3398–3404
14. Spiro, R. G. (1964) *J. Biol. Chem.* **239**, 567–573
15. Liao, T.-H., Gallop, P. M., and Blumenfeld, O. O. (1973) *J. Biol. Chem.* **248**, 8247–8253
16. Gahmberg, C. G., Myllylä, G., Leikola, J., Pirkola, A., and Nordling, S. (1976) *J. Biol. Chem.* **251**, 6108–6116
17. Mueller, T. J., Dow, A. W., and Morrison, M. (1976) *Biochem. Biophys. Res. Commun.* **72**, 94–99
18. Gahmberg, C. G., Häyry, P., and Andersson, L. C. (1976) *J. Cell Biol.* **68**, 642–653
19. Critchley, D. R., Wyke, J. A., and Hynes, R. O. (1976) *Biochim. Biophys. Acta* **436**, 335–352
20. Häyry, P., Andersson, L. C., Nordling, S., and Virolainen, M. (1972) *Transplant. Rev.* **12**, 91–140
21. Andersson, L. C., Nordling, S., and Häyry, P. (1973) *Cell. Immunol.* **8**, 235–248
22. Steck, T. L., and Kant, J. A. (1974) *Methods Enzymol.* **31**, 172–180
23. Rice, R. H., and Means, G. E. (1971) *J. Biol. Chem.* **246**, 831–832
24. Laemmli, U. K. (1970) *Nature* **227**, 680–685
25. Bonner, W. M., and Laskey, R. A. (1974) *Eur. J. Biochem.* **46**, 83–88
26. Lowry, O. H., Rosebrough, N. J., Farr, A. L., and Randall, R. J. (1951) *J. Biol. Chem.* **193**, 265–275
27. Warren, L. (1959) *J. Biol. Chem.* **234**, 1971–1975
28. Bray, G. A. (1960) *Anal. Biochem.* **1**, 279–285
29. Trevelyan, W. E., Procter, D. P., and Harrison, J. S. (1950) *Nature* **166**, 444–445
30. Roseman, S. (1970) *Chem. Phys. Lipids* **5**, 270–297
31. Merrell, R., Gottlieb, D. I., and Glaser, L. (1975) *J. Biol. Chem.* **250**, 5655–5659
32. Yamada, K. M., Yamada, S. S., and Pastan, I. (1975) *Proc. Natl. Acad. Sci. U. S. A.* **72**, 3158–3162
33. Hynes, R. O., and Bye, J. M. (1974) *Cell* **3**, 113–120
34. Vaheri, A., Ruoslahti, E., and Nordling, S. (1972) *Nature New Biol.* **85**, 211–212
35. Hakomori, S., and Murakami, W. T. (1968) *Proc. Natl. Acad. Sci. U. S. A.* **59**, 254–261
36. Gahmberg, C. G., and Hakomori, S. (1973) *Proc. Natl. Acad. Sci. U. S. A.* **70**, 3329–3333
37. Hynes, R. O. (1976) *Biochim. Biophys. Acta* **458**, 73–107
38. Eylar, E. H., Madoff, M. A., Brody, O. V., and Oncley, J. L. (1962) *J. Biol. Chem.* **237**, 1992–2000
39. Spiro, R. G. (1962) *J. Biol. Chem.* **237**, 646–652
40. Segrest, J. P., Jackson, R. L., Andrews, E. P., and Marchesi, V. T. (1971) *Biochem. Biophys. Res. Commun.* **44**, 390–395
41. Buck, C. A., Glick, M. C., and Warren, L. (1971) *Science* **172**, 169–171
42. Van Beek, W. P., Smets, L. A., and Emmelot, P. (1973) *Cancer Res.* **33**, 2913–2922
43. Andersson, L. C., Wasastjerna, C., and Gahmberg, C. G. (1976) *Int. J. Cancer* **17**, 40–46

Carl_G_190x270_mm_blokki_FINAL.indd 65 06-Aug-23 1:53:31 PM

CHARACTERIZATION OF SURFACE GLYCOPROTEINS OF MOUSE LYMPHOID CELLS

CARL G. GAHMBERG, PEKKA HÄYRY, and LEIF C. ANDERSSON

From the Departments of Serology and Bacteriology, and Third Department of Pathology, University of Helsinki, 00290 Helsinki 29, Finland

ABSTRACT

We have labeled exposed surface glycoproteins of mouse lymphoid cells by the galactose oxidase-tritated sodium borohydride technique. The labeled glycoproteins were separated by polyacrylamide slab gel electrophoresis and visualized by autoradiography (fluorography). The major thymocyte surface proteins have molecular weights of 170,000 and 125,000. Thymocytes from TL antigen-positive mouse strains showed an additional band with a molecular weight of 27,000. Highly purified T lymphocytes contain two major surface glycoproteins with molecular weights of 180,000 and 125,000. Purified B lymphocytes have one major surface glycoprotein with a molecular weight of 210,000.

When T lymphocytes are stimulated in vitro by concanavalin A or phytohemagglutinin, the major proteins characteristic of T cells are relatively weakly labeled, but new components of lower molecular weights appear on the cell surface. A similar change is seen in B lymphocytes stimulated by *Escherichia coli* lipopolysaccharide. T lymphoblasts isolated from mixed lymphocyte cultures show a slightly different surface glycoprotein pattern.

A polypeptide with a molecular weight of 57,000, which was labeled without enzymatic treatment by tritiated sodium borohydride alone, is strongly labeled in proliferating cells.

The immunobiological activities of the thymus-dependent (T)[1] and bone marrowed-derived (B) lymphocytes have been extensively studied under different in vivo and in vitro conditions. A variety of antigenic determinants and surface structures with different receptor activities have been identified. Very little, however, is known about the functional correlations between the composition of the plasma membrane and the immunological activities expressed by the lymphocyte.

The majority of the exposed plasma membrane proteins are glycoproteins (10, 11, 36). There is increasing evidence that these glycoproteins are of major importance in the maturation and regulation of the functions displayed by the lymphoid cells, since (*a*) carbohydrate-binding proteins, lectins, selectively stimulate different cells to divide (1), (*b*) mild periodate treatment, known to specifically oxidize sialic acids, or treatment with neuraminidase plus galactose oxidase, exclusively triggers T lymphocytes (29, 38), and (*c*) at least

[1] *Abbreviations used in this paper:* B blast, B lymphocyte stimulated to divide; B lymphocyte, B cell, thymus-independent, bone marrow-derived lymphocyte; Con A, concanavalin A; LPS, *E. coli* lipopolysaccharide; MLC, mixed lymphocyte culture; PBS, phosphate-buffered saline, pH 7.4; PHA, phytohemagglutinin; PPO, 2,5-diphenyloxazole; T blast, T lymphocyte stimulated to divide; T lymphocyte, T cell, thymus-dependent lymphocyte.

Carl_G_190x270_mm_blokki_FINAL.indd 66 06-Aug-23 1:53:31 PM

some of the cell-surface antigens are molecules that contain carbohydrate (33).

In order to understand the molecular basis of the lymphocyte response, it is obviously necessary to characterize the structures involved and their molecular anatomy in the plasma membrane.

One approach is selectively to label surface-exposed glycoproteins by the galactose oxidase technique (12, 37). Galactose oxidase does not penetrate the cell membrane and it oxidizes terminal galactosyl and *N*-acetyl galactosaminyl residues to the corresponding C6 aldehydes. These aldehydes are then reduced by tritiated sodium borohydride. The labeled surface glycoproteins were separated on polyacrylamide slab gels in the presence of sodium dodecyl sulfate, and the radioactive bands were visualized by modified autoradiography. By using this very sensitive technique we here show that different populations of mouse lymphoid cells have specific and characteristic surface glycoprotein patterns.

MATERIALS AND METHODS

Chemicals and Enzymes

Galactose oxidase with a specific activity of 130 U/mg protein was purchased from Kabi AB, Stockholm, Sweden. It displayed no protease or neuraminidase activity when measured as described previously (12). Neuraminidase (*Vibrio cholerae*, 500 U/ml) was obtained from Behringwerke AG, Marburg-Lahn, Germany, and was found to be free of protease activity. Concanavalin A (Con A) was kindly donated by Professor H. Wigzell, University of Uppsala, Sweden and used at the optimal concentration of 10 μg/ml. Phytohemagglutinin (PHA) was obtained from Difco Pharmaceuticals, Kalamazoo, Mich., and used at a final dilution of 1:150 of the reconstituted stock. *Escherichia coli* lipopolysaccharide (LPS) kindly given by Professor G. Möller, Stockholm, Sweden, was used at the optimal concentration of 10 μg/ml.

Tritiated sodium borohydride (8.2 Ci/mmol) was obtained from the Radiochemical Centre Ltd., Amersham, England. 250 mCi were dissolved in 0.5 ml of 0.01 N NaOH, divided among five tubes and immediately frozen at −70°C. The contents of one tube at a time were diluted with 2 ml of 0.01 NaOH and divided into 20 equal portions which were immediately frozen. Usually, one of these tubes was used for the labeling experiments. When handled in this way the isotope remained active for at least 12 mo.

Acrylamide and *N,N'*-methylenebisacrylamide were obtained from the Eastman Kodak Company, Rochester, N.Y. 2,5-diphenyloxazole (PPO) and *p*-bis/2-(5-phenyloxazolyl)/benzene (POPOP) were obtained from New England Nuclear, Boston, Mass. All other chemicals were of highest possible purity.

Mice

3–5-mo old mice of the following inbred strains were used: BALB/c, A/J, and CBA-H/T6T6. The strains originated from the Jackson Laboratories, Bar Harbor, Me., and were carried in our colony.

Preparation of Cells

Thymuses, lymph nodes (axillary, inguinal, popliteal, and mesenteric), and spleens were teased apart in cold RPMI 1640 culture medium. Clumps were removed by filtration through a loose cotton wool plug. Erythrocytes were lysed with 0.83% aqueous solution of NH_4Cl, and phagocytic cells were removed after incubation with carbonyl iron by treatment with a magnet (16). The thymus preparations contained more than 95% thymocytes. The lymph node and spleen cell preparations contained more than 98% and 80% lymphocytes, respectively, as judged morphologically from May-Gruenwald-stained smears. These cells will be referred to in the text as thymocytes, and lymph node and spleen "lymphocytes."

Cell Fractionation Procedures

PREPARATION OF T LYMPHOCYTES: Spleen cells or lymph node lymphocytes were prepurified by iron powder plus magnetic treatment (16) and passed through a Fenwall-Leukopak (Fenwall Laboratories, Division of Travenol Laboratories, Amsterdam, The Netherlands) nylon wool column as described by Julius et al. (21). The passed cell suspension contained less than 3% cells carrying surface immunoglobulin (B cells) as demonstrated by staining with polyvalent fluorescein isothiocyanate-conjugated goat anti-mouse immunoglobulin (a gift from Professor A. Fagraeus, State Bacteriological Laboratory, Stockholm, Sweden).

FRACTIONATION OF T AND B CELLS BY PREPARATIVE CELL ELECTROPHORESIS: Spleen lymphocytes of nonimmunized mice purified by iron powder plus magnet treatment were fractionated by preparative free-flow cell electrophoresis under conditions already described (3). In brief, the cells were transferred into a low ionic strength electrophoresis buffer (0.04 M potassium acetate, 0.015 M triethanolamine, 0.24 M glycine, pH 7.35, made isotonic with 0.011 M glucose and 0.03 M sucrose (3), and fractionated in the free-flow cell electrophoresis apparatus (Type FF4, Desaga GmbH, Heidelberg, Germany) at 6°C, and collected on ice. Each cell remained in the electric field (100 V/cm) for about 300 s. The cells were collected in tubes containing 10% calf serum in Eagle's minimal essential medium (Orion Pharmaceuticals, Helsinki, Finland) to minimize cell damage. After fractionation, more than 90% of the cells were viable as judged by trypan blue exclusion tests. By employing proper cuts in the electrophoresis profile

Carl_G_190x270_mm_blokki_FINAL.indd 67 06-Aug-23 1:53:31 PM

(Fig. 1) the T cell fraction was contaminated by less than 2% of surface immunoglobulin-carrying cells (B cells), and the B cell fraction by less than 2% of theta antigen-carrying (T) cells (3).

PURIFICATION OF BLASTS FROM CELL CULTURES: The blast cells were purified from the cultures by 1 *g* velocity sedimentation on a linear gradient of 15–30% fetal calf serum, phosphate-buffered saline (PBS) as described (26). The large-size blasts which sedimented rapidly were recovered from the first fractions. The cells were washed three times in PBS to remove the fetal calf serum. These fractions, containing more than 95% blast cells as judged morphologically from May-Gruenwald-Giemsa-stained smears, were used for surface labeling of activated cells.

Cell Cultures

Cultures with 20–30 × 10^6 cells were set up in 50-ml round-bottom glass tubes in 20 ml of Eagle's minimal essential medium supplemented with 5% fetal calf serum. The cultures were incubated at 37°C in a humidified atmosphere of 10% CO_2 in air. Spleen lymphocytes that had passed a nylon wool column were used as responder cells in the T cell mitogen (Con A and PHA)-stimulated cultures, whereas the B cell mitogen (LPS)-stimulated cultures were set up with unfractionated spleen lymphocytes. For the one-way mixed lymphocyte cultures (MLC), 60 × 10^6 CBA-H/T6T6 spleen T lymphocytes that had passed through a nylon wool column were stimulated with 90 × 10^6 mitomycin C-treated DBA/2 spleen cells (16). The mitogen-stimulated cultures were harvested on the 3rd day of culture and the MLC on the 6th day, at the time of the peaks of the corresponding blast responses. More than 90% of the cells in the PHA and Con A cultures and 50% in MLC were morphologically blasts. Pure (>95%) blast cell populations were recovered from the respective cultures by 1 *g* velocity sedimentation (2, 26).

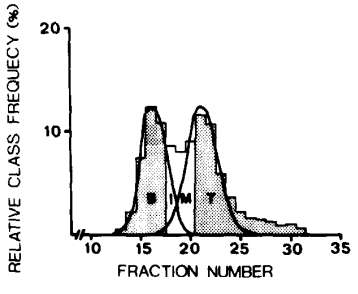

FIGURE 1 Electrophoretic distribution profile of CBA/H-T6T6 spleen lymphocytes. Higher fraction number indicates higher anodal mobility. The Gaussian distributions of the T and B cell populations are shown. Cells from the shaded fractions were used for the experiments.

Labeling Procedure

The labeling procedure was slightly modified from that previously described (12). To be able to do accurate comparisons between different cells, the labeling conditions were strictly standardized. We used 5 U of galactose oxidase with or without 12.5 U of neuraminidase for 1 h at 37°C in 1 ml of Dulbecco's PBS. 20 × 10^6 cells per tube were labeled. In control experiments the enzymes were omitted. After incubation with the enzymes the cells were washed three times by centrifugation at 4,000 rpm for 5 min in a table centrifuge in PBS, and 0.5 ml PBS finally added. Thereafter, 0.5 mCi NaB^3H_4 was added and the cells were left at room temperature for 30 min. Then the cells were washed four times in PBS, suspended in 200 μl of PBS, and an aliquot was counted for radioactivity in a dioxane-based scintillation fluid (8), with Wallac liquid scintillation counter 81000. The efficiency for tritium was 37%. The final yield of cells was >90%, and >90% were alive as shown by the trypan blue dye exclusion test.

To label mouse serum proteins, 100 μl mouse serum were diluted with 0.4 ml Dulbecco's PBS and either 12.5 U of neuraminidase plus 5 U of galactose oxidase, 5 U of galactose oxidase only, or no enzyme were added. The preparations were incubated at 37°C for 1 h, sodium dodecyl sulfate was added to a final concentration of 1%, and the samples were boiled for 1 min. 0.5 mCi NaB^3H_4 was added to each tube, and after incubation at room temperature for 30 min the samples were passed through 1 x 30-cm columns of Sephadex G25 in PBS. The fractions containing serum proteins were pooled, and samples corresponding to 10 μl serum were subjected to electrophoresis.

Polyacrylamide Slab Gel Electrophoresis

Electrophoresis was performed according to Laemmli (23) in 8% acrylamide gels. 5 × 10^6 cells (10^4–10^5 cpm) were solubilized and electrophoresed with [^{14}C]formaldehyde-labeled marker proteins in the peripheral slots (31). The molecular weights of the marker polypeptides were thyroglobulin 210,000, transferrin 78,000, human albumin 68,000, ovalbumin 44,000, and hemoglobin 17,000. The gels were fixed overnight in 20% sulfosalicylic acid, stained with Coomassie brilliant blue, and destained (43). They were then treated with dimethyl sulfoxide-PPO according to Bonner and Laskey (6) and vacuum dried. The dried gels were covered with Kodak RP X-Omat film, wrapped in aluminum foil, and kept at −70°C in a Revco freezer for 1–10 days until developed. When different gels were compared, they were kept for identical times in the deep freeze. The apparent molecular weights of the polypeptides were determined according to Weber and Osborn (43).

Periodate Oxidation

Cells were suspended in PBS and sodium metaperiodate was added to a final concentration of 2 mM. After

Carl_G_190x270_mm_blokki_FINAL.indd 68 06-Aug-23 1:53:31 PM

TABLE I

Label in Nontreated, Galactose Oxidase-Treated, Neuraminidase Plus Galactose Oxidase-Treated, and Periodate-Treated Mouse Lymphoid Cells

	Neuraminidase + galactose oxidase	Galactose oxidase	No enzymes	Periodate
		cpm/10⁶ cells		
Thymocytes	4,076 (3.46)*	2,320 (1.97)	1,178 (1.00)	—
Lymph node cells	11,214 (9.52)	5,289 (4.49)	2,803 (2.38)	—
T cells	6,778 (5.72)	4,370 (3.71)	3,333 (2.83)	6,255 (5.31)‡
B cells	6,502 (5.52)	3,604 (3.06)	2,391 (2.03).	6,361 (5.40)‡
T blasts				
(Con A)	47,332 (40.18)	25,515 (21.66)	17,811 (15.12)	—
(PHA)	30,698 (26.06)§	14,913 (12.66)§	12,168 (10.33)§	—
B blasts				
(LPS)	41,489 (35.22)	21,427 (18.19)	17,128 (14.54)	—
MLC blasts	29,768 (25.27)§	13,982 (11.87)	9,341 (7.93)	—

Average of two to four determinations.
* Relative amount of label in parentheses.
‡ Specific counts over background by NaB^3H_4 alone.
§ One determination only.

incubation for 10 min in the dark, the cells were washed three times in PBS, reduced with NaB^3H_4 as for the galactose oxidase-treated cells, and washed four times in PBS (see references 24 and 37). Spleen cells were activated to divide by the addition of 2 mM sodium metaperiodate to the medium (29).

RESULTS

Incorporation of Label

The incorporation of ^3H from NaB^3H_4 depends on galactose oxidase and is enhanced by neuraminidase treatment (Table I). Though the total label is appreciable without enzyme treatment, the gels show that very little label actually is incorporated into protein (see below). The label per cell in thymocytes is lower than that of T or B lymphocytes, whereas that of T or B blasts is considerably higher. Without enzyme treatment, some label is incorporated and is distributed among both proteins and lipids. Periodate treatment gives a higher labeling than does neuraminidase plus galactose oxidase, but the total amount of label in T or B lymphocytes is of equal magnitude.[2]

Fluorography Patterns of Labeled Glycoproteins

All experiments have been performed two to five times with very reproducible results.

[2] The molecular weights of the major labeled proteins are listed in Table II.

THYMOCYTES: In these cells we can distinguish two major surface glycoproteins with apparent molecular weights of 170,000 and 125,000 (Figs. 2 A and 3 A and B). The protein with a molecular weight of 125,000 (GP9) is not labeled without treatment with neuraminidase. GP6 can be labeled by galactose oxidase only, though more weakly (Figs. 2 B and 4 A and B). In the thymocytes derived from mouse strains A and CBA-H/T6T6 which have the TL antigen (7) expressed on their surface, an additional glycoprotein, GP15, was found (Fig. 2 D). This band was lacking from the thymocyte glycoprotein pattern of the TL-negative strain BALB/c (Fig. 2 A).

T LYMPHOCYTES: Unstimulated T lymphocytes contain two major surface glycoproteins, GP5 and GP9, and some quantitatively less-labeled glycoproteins. Both of the major components are labeled only after treatment with both neuraminidase and galactose oxidase (Fig. 3 C). Very little label is found in the glycoproteins if oxidized by galactose oxidase alone (Fig. 4 C).

B LYMPHOCYTES: Unstimulated B lymphocytes contain one major labeled surface glycoprotein, GP1 (Fig. 3 D). It is weakly labeled by galactose oxidase alone (Fig. 4 D).

MITOGEN-INDUCED T BLASTS: T blasts obtained after stimulation with Con A or PHA show an altered surface glycoprotein pattern when compared to nonstimulated T cells. The T cell-characteristic glycoproteins GP5 and GP9 are relatively less prominent, and glycoproteins with

Carl_G_190x270_mm_blokki_FINAL.indd 69 06-Aug-23 1:53:31 PM

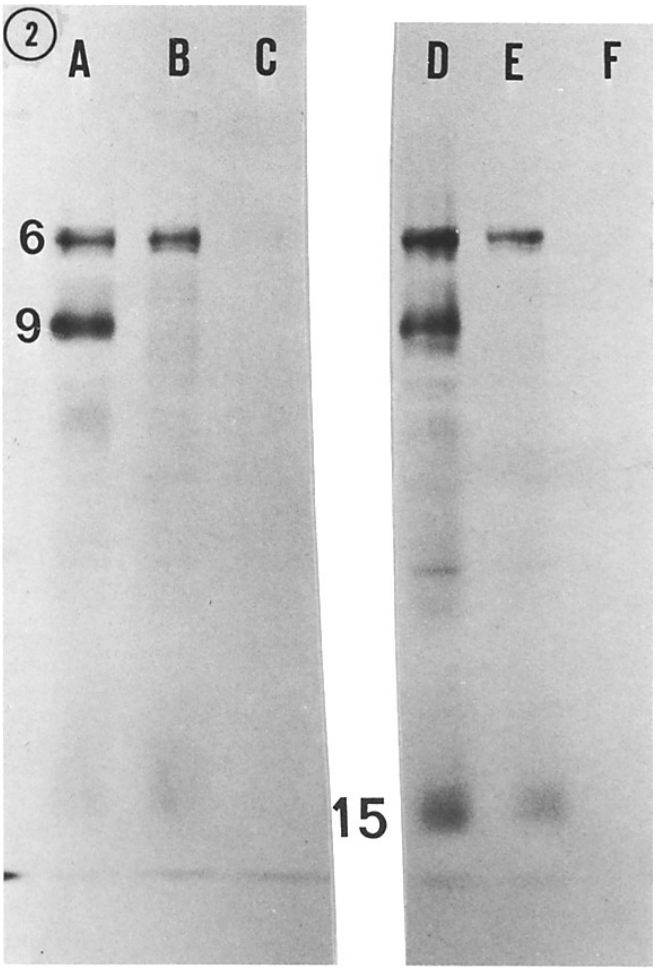

FIGURE 2 Polyacrylamide slab gel electrophoresis of mouse thymocyte glycoproteins. A, BALB/c thymocytes labeled with NaB^3H_4 after neuraminidase and galactose oxidase treatment: B, BALB/c thymocytes labeled after galactose oxidase treatment; C, BALB/c thymocytes labeled without enzyme treatment; D, A/J thymocytes labeled after neuraminidase and galactose oxidase treatment; E, A/J thymocytes labeled after galactose oxidase treatment; F, A/J thymocytes labeled without enzyme treatment.

smaller molecular weights appear instead (Figs. 3 E and F, 4 E and F).

MITOGEN-INDUCED B BLASTS: In B blasts obtained by velocity sedimentation from LPS-stimulated cultures, the B cell-specific band with a molecular weight of 210,000 was relatively weak. Instead, we observed glycoproteins similar to those stimulated T cells (Figs. 3G and 4G).

T BLASTS FROM MLC: The MLC blast population purified by velocity sedimentation showed additional bands: GP7, GP11, GP12, GP13, and GP14. GP7, GP13, and GP14 are not clearly seen in mitogen-stimulated T or B blasts.

Nonspecific Label

All cells incorporate some label without treatment with enzymes (see also reference 12). Therefore, it was always necessary to include controls in

Carl_G_190x270_mm_blokki_FINAL.indd 70 06-Aug-23 1:53:31 PM

TABLE II

Apparent Molecular Weights of Surface Glycoproteins of Mouse Lymphoid Cells

	Thymocytes	T cells	B cells	T blasts	B blasts	MLC blasts
GP 1	—	210,000	210,000		210,000	210,000
2	200,000					
3	—	190,000	—	—	—	—
4	—	—	185,000	—	—	—
5	—	180,000	—	180,000	180,000	180,000
6	170,000	170,000	—	—	—	—
7	—	—	—	—	—	165,000
8	160,000	—	—	—	—	—
9	125,000	125,000	—	125,000	125,000	125,000
10	110,000	—	—	—	—	—
11	—	—	—	86,000	86,000	86,000
12	—	—	—	77,000	77,000	77,000
13	—	—	—	—	—	72,000
14	—	—	—	—	—	58,000
15	27,000	—	—	—	—	—

Underlined values are major components.

the labeling experiments where no enzymes (but only NaB^3H_4) were used. With one exception, proteins were not appreciably labeled. This labeled protein (NS) with a molecular weight of 57,000 is weakly labeled in T or B lymphocytes, more label is observed in thymocytes, and a strong label is seen in all blast cells.

Proteins Labeled after Periodate Treatment

Fig. 5 shows the electrophoretic pattern of T and B lymphocytes reduced with NaB^3H_4 after periodate treatment. In T cells the proteins GP5 and GP9 are labeled, and in B cells GP1.

Does Neuraminidase Plus Galactose Oxidase Treatment or Periodate Treatment Change the Native Glycoprotein Pattern of T Cells?

Because neuraminidase plus galactose oxidase or periodate treatment per se has a mitogenic effect on T cells, the following experiment was done. Spleen lymphocytes were reduced with NaB^3H_4 after treatment with neuraminidase and galactose oxidase (Fig. 6 A), after periodate treatment (Fig. 6 B), kept for 2 h in culture, and then labeled after neuraminidase plus galactose oxidase (Fig. 6 C), incubated with PHA for 2 h in culture, then labeled after neuraminidase plus galactose oxidase (Fig. 6 D), or treated with periodate, cultured for 2 h, and then labeled after neuraminidase plus galactose oxidase (Fig. 6 E). The only observable effect is on GP9 which, after neuraminidase plus galctose oxidase, has a higher apparent molecular weight than if first treated with periodate. The rest of the characteristic proteins do not change. This indicates that in 2 h, which corresponds to the time it takes to label cells, no extensive change of the surface membrane glycoprotein pattern occurs. Fig. 6 F shows the control without enzyme treatment.

Labeled Mouse Serum Proteins

These proteins are shown as follows: mouse serum proteins labeled after neuraminidase plus galactose oxidase treatment (Fig. 6 G), after galactose oxidase only (Fig. 6 H), and without enzyme treatment (Fig. 6 I). Efficient glycoprotein label is only obtained after neuraminidase treatment. The major labeled proteins do not seem to correspond in electrophoretic mobility to the labeled cellular glycoproteins.

DISCUSSION

By the use of the galactose oxidase-tritiated sodium borohydride technique, we have shown that different resting as well as activated highly purified subpopulations of mouse lymphoid cells expose characteristic surface glycoproteins.

The large size of the galactose oxidase molecule inhibits its penetration into red cells (12) and fibroblasts (13), and therefore only surface-exposed terminal galactosyl and *N*-acetyl galac-

Carl_G_190x270_mm_blokki_FINAL.indd 71 06-Aug-23 1:53:31 PM

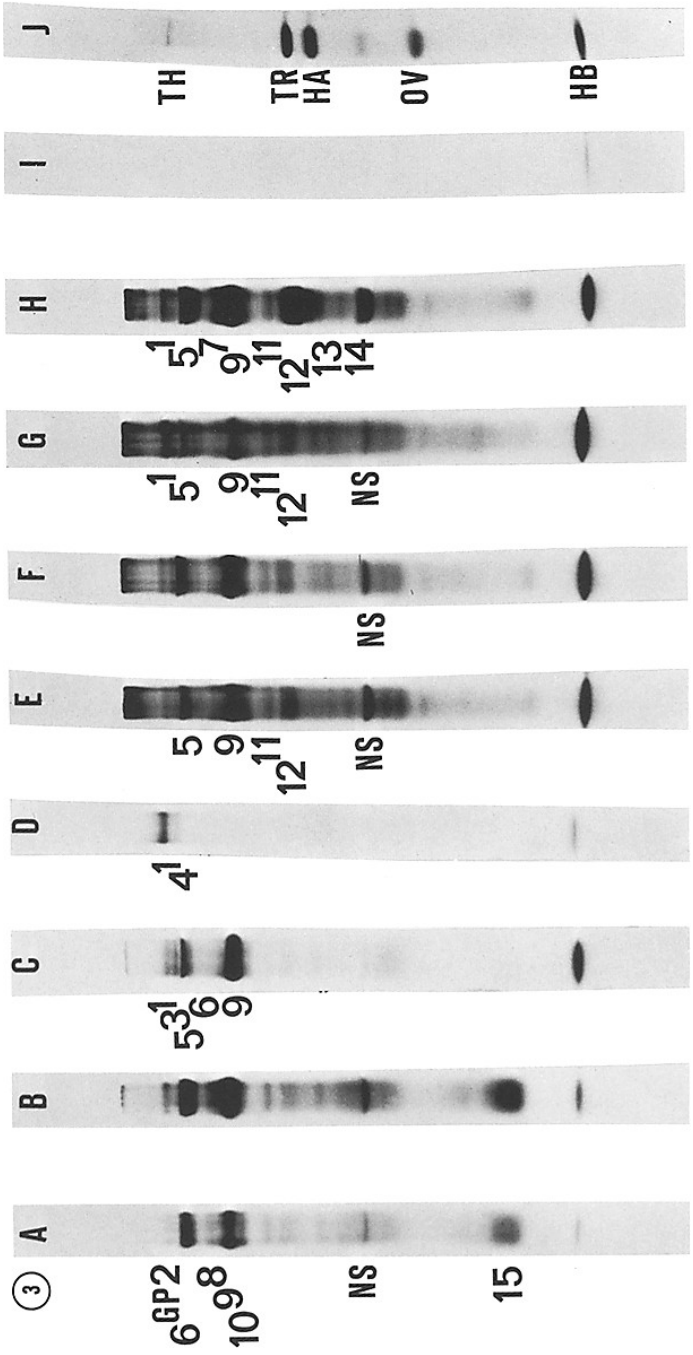

FIGURE 3 Polyacrylamide slab gel electrophoresis of surface glycoproteins of mouse lymphoid cells labeled with NaB^3H_4 after neuraminidase and galactose oxidase treatment. A, thymocytes (A/J); B, thymocytes (CBA/T6T6); C, electrophoretically purified spleen T lymphocytes; D, electrophoretically purified spleen B lymphocytes; E, T blasts from Con A-stimulated cultures; F, T blasts from PHA-stimulated cultures; G, B blasts from LPS-stimulated cultures; H, T blasts from MLC; I, T lymphocytes without enzyme treatment; J, ^{14}C-labeled standard proteins: TH, thyroglobulin; TR, transferrin; HA, human albumin; OV, ovalbumin; HB, hemoglobin. The major protein bands are numbered according to decreasing molecular weights.

Carl_G_190x270_mm_blokki_FINAL.indd 72 06-Aug-23 1:53:31 PM

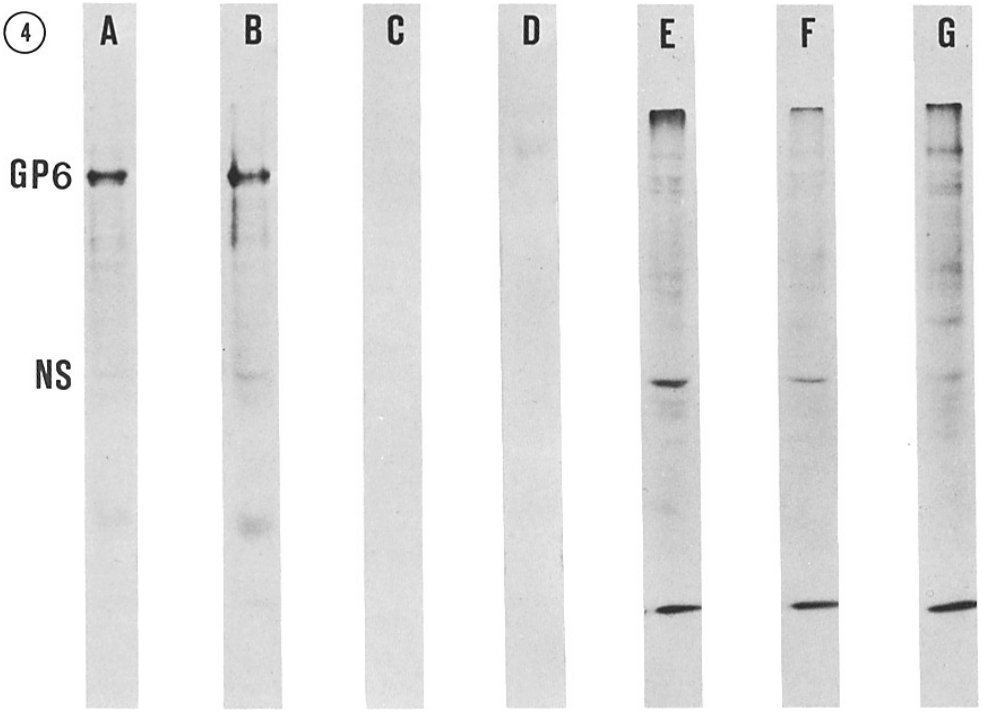

FIGURE 4 Polyacrylamide slab gel electrophoresis of surface glycoproteins of mouse lymphoid cells labeled with NaB^3H_4 after treatment with galactose oxidase only. A, thymocytes (A/J); B, thymocytes (CBA/T6T6); C, electrophoretically purified T lymphocytes; D, electrophoretically purified B lymphocytes; E, T blasts from Con A-stimulated cultures; F, T blasts from PHA-stimulated cultures; G, B blasts from LPS-stimulated cultures. The same numbers of cells were labeled, identical aliquots were electrophoresed, and the same exposure time was used as for Fig. 3.

tosaminyl residues are oxidized to the corresponding C6 aldehydes (5). We have treated intact labeled lymphocytes and thymocytes with pronase and trypsin, to verify the surface distribution of the labeled glycoproteins (not shown). Of the major labeled surface glycoproteins, GP1, GP6, and GP9 are easily degraded by the enzymes, but GP5 is degraded to a smaller extent. One could then argue that GP5 is not a surface glycoprotein. However, we think that it is, but it is for unknown reasons, resistant to the proteases. The situation is similar in hamster fibroblasts where one of the major surface glycoproteins is resistant to proteases (15). The oxidized glycoproteins are subsequently labeled by reduction with tritiated sodium borohydride. Sialic acids are often linked to penultimate galactosyl/*N*-acetyl galactosaminyl residues and, therefore, more efficient labeling is achieved by treating the cells with neuraminidase.

The resolution of autoradiography is superior to the gel slicing and counting techniques. Previously, tritium-labeled proteins could not be autoradiographically visualized from polyacrylamide gels, but recently this has become possible by the introduction of a scintillator (PPO) into the gel. This technique now enables us to define reproducibly the labeled surface glycoproteins. Because glycoproteins (9, 34) and possibly also intrinsic membrane proteins in general behave anomalously on polyacrylamide gels, the molecular weights of these proteins are only approximate.

A number of surface-labeling techniques have recently been introduced, the most popular being lactoperoxidase-catalyzed iodination (18, 25, 30).

Carl_G_190x270_mm_blokki_FINAL.indd 73 06-Aug-23 1:53:31 PM

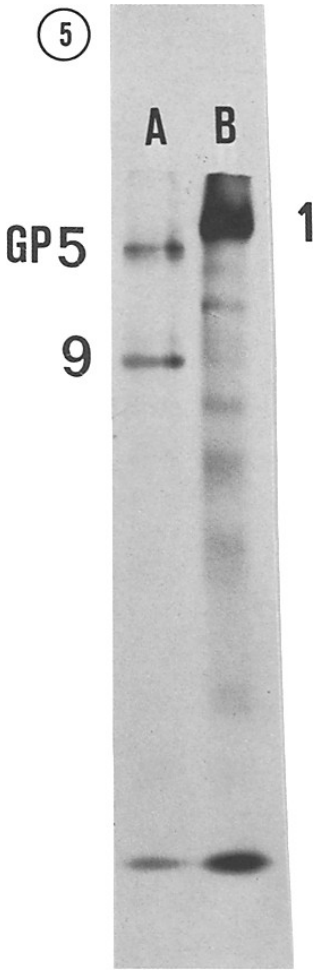

FIGURE 5 Polyacrylamide slab gel electrophoresis of electrophoretically fractionated mouse spleen T and B lymphocytes labeled with NaB^3H_4 after periodate treatment. A, T lymphocytes; B, B lymphocytes.

All labeling techniques have their drawbacks, but the galactose oxidase method enables the specific identification of glycoproteins. When the galactose oxidase method is combined with neuraminidase treatment, molecules containing sialic acid are also visualized.

The protein with a molecular weight of 170,000 from thymocytes is labeled well by galactose oxidase alone. This means that it contains a relatively large proportion of terminal galactosyl/*N*-acetyl galactosaminyl residues. This is in contrast to the glycoproteins of the lymphocytes which are labeled appreciably only if treated with neuraminidase. GP15, which is found only in strains CBA-H/T6T6 and A/J, and not in BALB/c, could correspond to the TL antigen (7).

Using the lactoperoxidase method, Trowbridge et al. (39) obtained results similar to ours and showed that mouse lymphoid cells enriched in T or B lymphocytes have characteristic surface proteins. They also found two T cell-specific proteins and one B cell-specific protein, which may well correspond to those found by us.

The B cell-specific protein with an apparent molecular weight of 210,000 shares characteristics with the major surface glycoprotein of normal fibroblasts which has a similar molecular weight (13, 17, 19, 40). This protein is absent from transformed fibroblasts, and, in mutants temperature-sensitive for transformation, it is present only at the nonpermissive temperature (14, 20, 32). Trowbridge et al. (39) also showed that the B cell-specific protein was absent from a myeloma cell line secreting immunoglobulin A, whereas the T cell-specific proteins were retained on lymphomas of T-cell origin.

Novogrodsky (29) and Thurman et al. (38) have recently shown that periodate treatment or neuraminidase plus galactose oxidase treatment selectively triggers T lymphocytes. It is reasonable to assume that the T lymphocyte-specific surface proteins that we detect by either treatment are involved in this phenomenon.

The presence of surface immunoglobulin on B lymphocytes is well established. Vitetta et al. (42) have characterized such molecules from lactoperoxidase-labeled lymphocytes. We have not definitely observed any labeled proteins corresponding to these. Quantitatively, however, these proteins constitute a rather small proportion of the total surface proteins. It is also possible that the carbohydrate of surface immunoglobulins is relatively deeply imbedded in the cell surface and therefore not available to galactose oxidase.

Both T and B blasts have an altered surface glycoprotein pattern as compared to T and B lymphocytes. This shows that major surface changes occur after triggering to proliferation. The higher label per cell is obviously partially due to the increased cellular size. The surface glycoprotein pattern from one-way MLC seems to be different from that of mitogen-stimulated cells. Quantitatively, the lymphocytes reacting to a

Carl_G_190x270_mm_blokki_FINAL.indd 74 06-Aug-23 1:53:31 PM

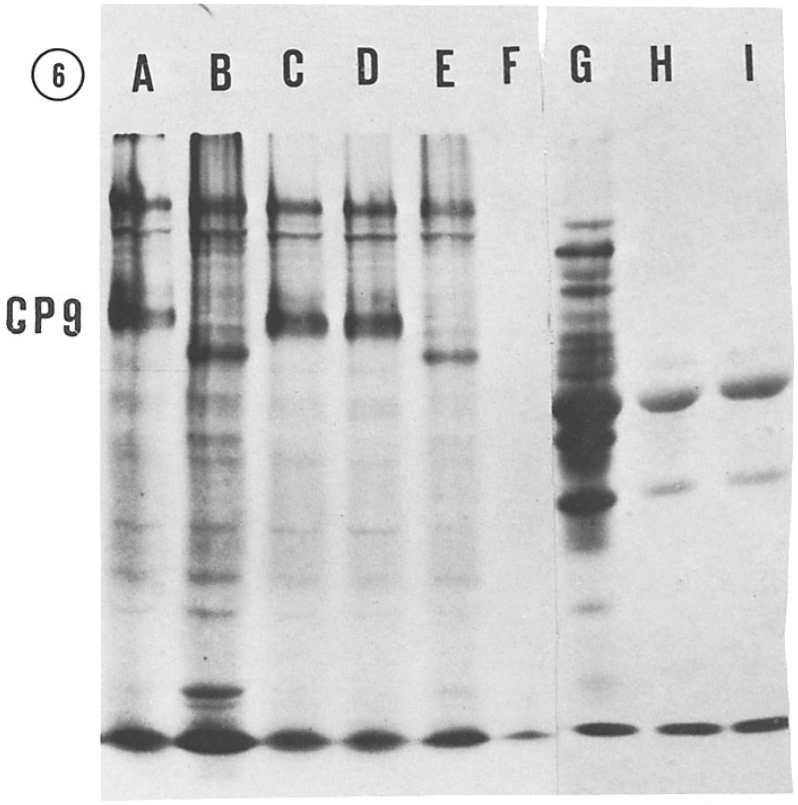

FIGURE 6 Polyacrylamide slab gel electrophoresis of labeled glycoproteins from nonstimulated and activated spleen cells, and of labeled mouse serum. A, spleen cells labeled after neuraminidase and galactose oxidase treatment; B, spleen cells labeled after periodate treatment; C, spleen cells left for 2 h in culture medium then labeled after neuraminidase and galactose oxidase treatment; D, spleen cells treated with PHA and then labeled after neuraminidase and galactose oxidase treatment; E, spleen cells treated with periodate, left for 2 h in culture, and then labeled after neuraminidase plus galactose oxidase treatment; F, control cells labeled without enzyme treatment; G, mouse serum labeled after neuraminidase plus galactose oxidase treatment; H, mouse serum labeled after galactose oxidase treatment; I, mouse serum labeled without enzyme treatment.

certain set of histocompatibility antigens constitute only a small per cent of the total T cell population (35). Whether these lymphocytes also before alloactivation in MLC have surface proteins which differ from those of the major T cell population, or whether they get their surface pattern after stimulation, is not known. An interesting possibility is that some of the additional proteins seen on MLC blasts are involved in target cell recognition. Kimura has been able to raise an antiserum reacting specifically with alloagressive killer T cells, which indicates that they express antigenic determinants not present on resting or mitogen-activated T cells (22).

The blast cells also contain a protein with an apparent molecular weight of 57,000, which is very weakly labeled in nongrowing cells. This protein is labeled without enzyme treatment by tritiated sodium borohydride alone. The nature of the reducible group is not known, but could be due to Schiff base formation between the aldehyde group and an amino group of an enzyme containing pyridoxal phosphate. Enzymes such as ornithine decarboxylase are known to be strongly activated

Carl_G_190x270_mm_blokki_FINAL.indd 75 06-Aug-23 1:53:31 PM

in growing cells (27). A similar protein is also strongly labeled in transformed fibroblasts (13) and human chronic lymphocytic leukemia cells (4).

The basis for the differences in electrophoretic mobilities of mouse T and B lymphocytes is unclear, but surface sialic acids are obviously involved since the characteristic, biphasic electrophoretic profile of T and B lymphocytes is lost after neuraminidase treatment (28). It has been difficult to determine the absolute amount of sialic acid in T and B lymphocytes because of the limited number of highly purified cells available. Therefore, we have used an indirect approach. Mild periodate treatment oxidized predominantly sialic acids, and 5-acetamido-3,5-dideoxy-L-arabino-2-heptusolonic acid was formed (24, 41). This may be reduced with sodium borohydride. Because we used a very low amount of NaB^3H_4 (about 2.5 μg) per experiment, the modified sialic acids were only partially reduced and the absolute amount of sialic acids could not be determined. Higher concentrations of NaB^3H_4 result in lower specific activities and in electrophoretic patterns resembling those of proteolysis (37).

In both T and B cells the major periodate-oxidizable proteins are similar to those labeled after neuraminidase and galactose oxidase treatments. This suggests that in B lymphocytes which have a slower electrophoretic mobility, cell surface sialic acids are less efficiently exposed at the electrophoretic plane of shear. The major sialic acid-containing surface glycoprotein (GP1) could also be covered by other surface macromolecules, such as immunoglobulin.

Received for publication 27 June 1975, and in revised form 28 October 1975.

REFERENCES

1. ANDERSSON, J., O. SJÖBERG, and G. MÖLLER. 1972. Mitogens as probes for immunocyte activation and cellular cooperation. *Transplant Rev.* **11**:131–174.
2. ANDERSSON, L. C., and P. HÄYRY. 1973. Specific priming of mouse thymus-dependent lymphocytes to allogeneic cells in vitro. *Eur. J. Immunol.* **3**:595–599.
3. ANDERSSON, L. C., S. NORDLING, and P. HÄYRY. 1973. Fractionation of mouse T and B lymphocytes by preparative cell electrophoresis. Efficiency of the method. *Cell. Immunol.* **8**:235–248.
4. ANDERSSON, L. C., C. WASASTJERNA, and C. G. GAHMBERG. 1976. Different surface glycoprotein patterns on human T, B and leukemic lymphocytes. *Int. J. Cancer. In press.*
5. AVIGAD, G., D. AMARAL, C. ASENSIO, and B. L. HORECKER. 1962. The D-galactose oxidase of *Polyporus circinatus*. *J. Biol. Chem.* **237**:2736–2743.
6. BONNER, W. M., and R. A. LASKEY. 1974. A film detection method for tritium-labelled proteins and nucleic acids in polyacrylamide gels. *Eur. J. Biochem.* **46**:83–88.
7. BOYSE, E. A., and L. J. OLD. 1969. Some aspects of normal and abnormal cell surface genetics. *Annu. Rev. Genet.* **3**:269–290.
8. BRAY, G. A. 1960. A simple efficient liquid scintillator for counting aqueous solutions in a liquid scintillation counter. *Anal. Biochem.* **1**:279–285.
9. BRETSCHER, M. S. 1971. Major human erythrocyte glycoprotein spans the cell membrane. *Nat. New Biol.* **231**:229–232.
10. BRETSCHER, M. S. 1973. Membrane structure: some general principles. *Science (Wash. D.C.).* **181**:622–629.
11. GAHMBERG, C. G. 1976. External labeling of human erythrocyte glycoproteins. Studies with galactose oxidase and fluorography. *J. Biol. Chem.* In press.
12. GAHMBERG, C. G., and S. HAKOMORI. 1973. External labeling of cell surface galactose and galactosamine in glycolipid and glycoprotein of human erythrocytes. *J. Biol. Chem.* **248**:4311–4317.
13. GAHMBERG, C. G., and S. HAKOMORI. 1973. Altered growth behavior of malignant cells associated with changes in externally labeled glycoprotein and glycolipid. *Proc. Natl. Acad. Sci. U.S.A.* **70**:3329–3333.
14. GAHMBERG, C. G., D. KIEHN, and S. HAKOMORI. 1974. Changes in surface-labelled galactoprotein and in glycolipid concentrations in cells transformed by a temperature-sensitive polyoma virus mutant. *Nature. (Lond.).* **248**:413–415.
15. GAHMBERG, C. G., and S. HAMOMORI. 1975. Surface carbohydrates of hamster fibroblasts. II. Interaction of hamster Nil cell surfaces with *Ricinus communis* lectin and concanavalin A as revealed by surface galactosyl label. *J. Biol. Chem.* **250**:2447–2451.
16. HÄYRY, P., L. C. ANDERSSON, S. NORDLING, and M. VIROLAINEN. 1972. Allograft response in vitro. *Transplant. Rev.* **12**:91–140.
17. HOGG, N. M. 1974. A comparison of membrane proteins of normal and transformed cells by lactoperoxidase labelling. *Proc. Natl. Acad. Sci. U.S.A.* **71**:489–492.
18. HUBBARD, A. L., and Z. A. COHN. 1972. The enzymatic iodination of the red cell membrane. *J. Cell Biol.* **55**:390–405.
19. HYNES, R. O. 1973. Alteration of cell surface proteins by viral transformation and by proteolysis. *Proc. Natl. Acad. Sci. U.S.A.* **70**:3170–3174.
20. HYNES, R. O., and J. A. WYKE. 1975. Alterations in surface proteins in chicken cells transformed by temperature-sensitive mutants of Rous sarcoma virus. *Virology.* **64**:492–504.
21. JULIUS, M. H., E. SIMPSON, and L. A.

Carl_G_190x270_mm_blokki_FINAL.indd 76 06-Aug-23 1:53:31 PM

HERTZENBERG. 1973. Rapid method for isolation of functional thymus derived lymphocytes. *Eur. J. Immunol.* **3**:645–651.

22. KIMURA, A. K. 1974. Inhibition of specific cell-mediated cytotoxicity by anti-T-cell receptor antibody. *J. Exp. Med.* **139**:888–901.
23. LAEMMLI, U. K. 1970. Cleavage of structural proteins during the assembly of the head of bacteriophage T4. *Nature (Lond.).* **227**:680–685.
24. LIAO, T. -H., P. M. GALLOP, and O. O. BLUMENFELD. 1973. Modification of sialyl residues of sialoglycoprotein(s) of the human erythrocyte surface. *J. Biol. Chem.* **248**:8247–8253.
25. MARCHALONIS, J. J., R. E. CONE, and V. SANTER. 1971. Enzymic iodination. A probe for accessible surface proteins of normal and neoplastic lymphocytes. *Biochem. J.* **124**:921–927.
26. MILLER, R. G., and R. A. PHILLIPS. 1969. Separation of cells by velocity sedimentation. *J. Cell. Physiol.* **73**:191–201.
27. MORRIS, D. R., and R. H. FILLINGAME. 1974. Regulation of amino acid decarboxylation. *Annu. Rev. Biochem.* **43**:303–325.
28. NORDLING, S., L. C. ANDERSSON, and P. HÄYRY. 1972. Thymus-dependent and thymus-independent lymphocyte separation: Relation to exposed sialic acid on cell surface. *Science (Wash. D.C.).* **178**:1001–1002.
29. NOVOGRODSKY, A. 1974. Selective activation of mouse T and B lymphocytes by periodate, galactose oxidase and soybean agglutinin. *Eur. J. Immunol.* **4**:646–648.
30. PHILLIPS, D. R., and M. MORRISON. 1971. Exposed protein on the intact human erythrocyte. *Biochemistry.* **10**:1766–1771.
31. RICE, R. H., and G. E. MEANS. 1971. Radioactive labeling of proteins in vitro. *J. Biol. Chem.* **246**:831–832.
32. RIEBER, M., and J. C. IRWIN. 1974. The possible correlation of growth rate and expression of transformation with temperature-dependent modification in high-molecular weight membrane glycoproteins in mammalian cells transformed by a wild-type and by a thermosensitive mutant of avian sarcoma virus. *Cancer Res.* **34**:3469–3473.
33. ROGENTINE, G. N., and B. A. PLOCINIK. 1974. Carbohydrate inhibition studies of the naturally occuring human antibody to neuraminidase-treated human lymphocytes. *J. Immunol.* **113**:848–858.
34. SEGREST, J. P., R. L. JACKSON, E. P. ANDREWS, and V. T. MARCHESI. 1971. Human erythrocyte membrane glycoprotein: a re-evaluation of the molecular weight as determined by SDS polyacrylamide gel electrophoresis. *Biochem. Biophys. Res. Commun.* **44**:390–395.
35. SIMONSEN, M. 1962. The factor of immunization: Clonal selection theory investigated by spleen assays of graft-versus-host reaction. *In* Ciba Foundation Symposium on Transplantation. G. E. W. Wolstenholme and M. D. Cameron, editors. J. & A. Churchill Ltd., London. 185–209.
36. STECK, T. L. 1974. The organization of proteins in the human red blood cell membrane. *J. Cell. Biol.* **62**:1–19.
37. STECK, T. L., and G. DAWSON. 1974. Topographical distribution of complex carbohydrates in the erythrocyte membrane. *J. Biol. Chem.* **249**:2135–2142.
38. THURMAN, G. B., B. GIOVANELLA, and A. L. GOLDSTEIN. 1974. Evidence for the T cell specificity of sodium periodate-induced lymphocyte blastogenesis. *J. Immunol.* **113**:810–812.
39. TROWBRIDGE, I. S., P. RALPH, and M. J. BEVAN. 1975. Differences in the surface proteins of mouse B and T cells. *Proc. Natl. Acad. Sci. U.S.A.* **72**:157–161.
40. VAHERI, A., and E. RUOSLAHTI. 1974. Disappearance of a major cell-type specific surface glycoprotein antigen (SF) after transformation of fibroblasts by Rous sarcoma virus. *Int. J. Cancer.* **13**:579–586.
41. VAN LENTEN, L., and G. ASHWELL. 1971. Studies on the chemical and enzymatic modification of glycoproteins. *J. Biol. Chem.* **246**:1889–1894.
42. VITETTA, E. S., S. BAUR, and J. W. UHR. 1971. Cell surface immunoglobulin. II. Isolation and characterization of immunoglobulin from mouse splenic lymphocytes. *J. Exp. Med.* **134**:242–264.
43. WEBER, K., and M. OSBORN. 1969. The reliability of molecular weight determinations by dodecyl sulfatepolyacrylamide gel electrophoresis. *J. Biol. Chem.* **244**:4406–4412.

Carl_G_190x270_mm_blokki_FINAL.indd 77 06-Aug-23 1:53:31 PM

Surface Glycoproteins of Human White Blood Cells. Analysis by Surface Labeling

By Leif C. Andersson and Carl G. Gahmberg

We labeled surface glycoproteins of normal human blood platelets, granulocytes, monocytes, T and B lymphocytes, and null cells by the galactose oxidase–NaB^3H_4 and periodate-NaB^3H_4 labeling techniques. The labeled glycoproteins were observed by fluorography after separation by polyacrylamide slab gel electrophoresis. All major types of human leukocytes showed different and characteristic surface glycoprotein patterns. These patterns evidently also include common components.

DURING THE PAST FEW YEARS A variety of surface markers characteristic for different populations of leukocytes have been recognized. Analysis of the marker profiles has, in addition to conventional morphology and enzyme histochemistry, received a wide application for identification and classification of normal and malignant blood leukocytes. Comparatively little, however, is known at the molecular level about the surface structures of different types of white blood cells (WBC).

Most, if not all, external proteins of mammalian cells are glycoproteins.[1] These comprise both various receptors and antigenic determinants.[2] The establishment of the surface glycoprotein patterns for the different types of human leukocytes would provide the basis for understanding the structural/functional relationships of the surface molecules. Comparison of the surface glycoprotein patterns of the normal leukocyte populations with those of cells in various disorders might give valuable information about the molecular changes that occur in different dysfunctional states and malignancies.

We have been studying the surface glycoproteins of different mouse and human lymphoid cells by the use of the galactose oxidase–tritiated borohydride (GO-NaB^3H_4) labeling method.[3,4] The galactosyl residues of the exposed glycoproteins are oxidized by GO and thereafter reduced with NaB^3H_4. The radioactive proteins are separated on polyacrylamide slab gels and observed by autoradiography.[5]

Another method of selective surface glycoprotein labeling was also recently described. Sialic acid residues of surface glycoproteins were labeled with NaB^3H_4 after oxidation with sodium periodate under conditions where the periodate did not penetrate the intact cell membrane.[6]

By employing various methods of cell fractionation we purified the main

From the Transplantation Laboratory, IV Department of Surgery, and the Department of Serology and Bacteriology, University of Helsinki, Helsinki, Finland.

Submitted November 18, 1977; accepted February 21, 1978.

Supported by The Academy of Finland, The Finnish Cancer Society, and The Sigrid Jusélius Foundation.

Address for reprint requests: Dr. Leif C. Andersson, Transplantation Laboratory, University of Helsinki, Haartmaninkatu 3 A, SF 00290 Helsinki 29, Finland.

© 1978 by Grune & Stratton, Inc. *ISSN 0006-4971/78/5201-2005$02.00/0.*

Carl_G_190x270_mm_blokki_FINAL.indd 78 06-Aug-23 1:53:31 PM

populations of human WBC. We report the surface glycoprotein patterns of different types of human blood leukocytes.

MATERIALS AND METHODS

Chemicals and enzymes. Sodium metaperiodate was obtained from Merck, Darmstadt, Germany, acrylamide and *N*, *N'*-methylenebisacrylamide from Eastman Kodak, Rochester, N.Y., 2,5-diphenyl oxazole (PPO) and *p*-bis-2-(5-phenyloxazolyl)-benzene (POPOP) from New England Nuclear, Boston, Mass., phenylmethylsulfonylfluoride from Sigma, St. Louis, Mo., Triton X-100 from British Drug Houses, Poole, England, and NaB^3H_4 (8.6 Ci/mmole) and ^{14}C-formaldehyde (4.54 mCi/mmole) from the Radiochemical Centre, Amersham, England. The NaB^3H_4 preparation was handled as described previously.[7]

Galactose oxidase with a specific activity of 130 U/mg protein was purchased from Kabi, Stockholm, Sweden. It displayed no protease or neuraminidase activities when measured as described.[3] *Vibrio cholerae* neuraminidase (NE) (500 U/ml) was obtained from Behringwerke, Marburg-Lahn, Germany. It was free of protease activity.

Isolation of blood cells. The following main populations of human blood leukocytes were isolated: granulocytes, platelets, monocytes, T and B lymphocytes, and null cells. These cell populations were purified from the buffy coats of blood units of 400 ml each obtained from the Finnish Red Cross Blood Transfusion Service. The buffy coats were diluted with 2 vol 0.1 *M* NaCl–0.01 *M* sodium phosphate pH 7.4 (PBS), and the platelets and the mononuclear cells were separated from the granulocytes and erythrocytes by one-step Ficoll-Isopaque (density 1.077; Pharmacia, Uppsala, Sweden) gradient centrifugation at 400 *g* for 40 min at 22°C.

Purification of granulocytes. The pellets obtained after Ficoll-Isopaque centrifugation that contained erythrocytes and granulocytes were suspended in 20 ml PBS. Then 10 ml saline containing 6% dextran was added (Macrodex 6% Leiras, Turku, Finland) and the cell suspension kept for 40 min at 37°C. The granulocyte-rich buffy coat was then collected, and contaminating erythrocytes were lysed by incubation with a Tris-buffered 0.84% aqueous solution of ammonium chloride. The leukocytes were then washed three times with PBS. This procedure yielded a cell population that contained more than 97% of granulocytes as judged from May-Grünwald-Giemsa (MGG) stained cytocentrifuged cell smears. The cell viability was close to 100% as seen in the trypan blue exclusion test.

Purification of platelets. The platelets were purified from the cell population obtained from the interphase after Ficoll-Isopaque centrifugation. This cell population was suspended in PBS and centrifuged for 10 min at 200 *g*, and the platelet-rich supernatant was recovered. This procedure was repeated once, and the platelets were then centrifuged at 400 *g* for 20 min. The purity of the platelet preparation thus obtained approached 100%, and the contamination by other blood cells was always less than 0.002%.

Purification of monocytes. The blood monocytes were separated from the cell population recovered at the interphase after Ficoll-Isopaque centrifugation. The platelets were depleted by three washes with PBS at 200 *g* for 10 min. The mononuclear cell population was mixed at the ratio of 1:50 with 2-aminoethylisothiouronium bromide (AET) (Sigma) treated sheep erythrocytes (SRBC).[8] After incubation for 15 min at 37°C the mixture was centrifuged for 10 min at 200 *g* and the T cells allowed to rosette with the AET-SRBC for 1 hr on ice. The pellet was then gently suspended in cold PBS containing 30% fetal calf serum (FCS) and the rosette-forming cells were separated from the non-rosette-forming cells by a one-step Ficoll-Isopaque density gradient centrifugation. The cell population recovered from the interphase mainly contained monocytes and non-T lymphocytes. The monocytes were then purified from the contaminating lymphocytes by a 1-*g* velocity sedimentation.[9] In this procedure cells are fractionated according to the cell size. The cells were suspended in PBS containing 5% FCS and layered onto a linear gradient of 15%–30% FCS in PBS. After sedimentation for 4 hr at 4°C the gradient was drained into fractions of 20 ml and the cell content of each fraction was analyzed from MGG-stained smears. The early fractions, which mainly contained monocytes, were pooled. The cell preparation thus obtained 90%–95% of monocytes as judged by conventional morphologic criteria. The viability always exceeded 98%. Slight contamination was caused by occasional lymphoblasts, myeloid precursor cells, and some granulocytes.

Carl_G_190x270_mm_blokki_FINAL.indd 79 06-Aug-23 1:53:31 PM

Purification of T lymphocytes. The platelet-depleted mononuclear cell population recovered from the Ficoll-Isopaque gradient centrifugation was passed over a human Ig–rabbit anti–human Ig column as described by Wigzell et al.[10] More than 95% of the column-passed lymphocyte population formed rosettes with AET-SRB and contained less than 1% of surface immunoglobulin (SIg)-bearing cells as judged by staining with fluorescein isothiocynate-conjugated polyvalent sheep anti–human ig (obtained from Professor Astrid Fagraeus, Stockholm, Sweden). The viability of the T cell population was always more than 98%.

Purification of non-T lymphocytes, null cells, and B lymphocytes. The mononuclear cells obtained after Ficoll-Isopaque centrifugation were suspended in RPMI-1640 culture medium supplemented with 10% normal human AB plasma. Carbonyl iron was added and the suspension incubated for 1 hr at 37°C. Most of the phagocytic cells were then removed with a magnet. The phagocyte-depleted cell population was allowed to rosette with AET-SRBC as described above. The T cells were depleted by centrifugation of the RFC-containing cell suspension on a Ficoll-Isopaque gradient. The cell suspension recovered from the interphase contained mainly lymphocytes and larger, monocytelike cells. The non-T lymphocytes were further purified from this population by velocity sedimentation as described above. The later fractions obtained after sedimentation for 4 hr contained mainly small lymphocytes as judged from MGG smears. These fractions were pooled, and the cell population thus obtained was contaminated by less than 3% nonlymphocytic cells. This cell population was further characterized with regard to surface markers: 2% formed rosettes with AET-SRBC and 61% were SIg positive.

This lymphocyte suspension was further fractionated by passage over an Ig/anti-Ig column at 4°C to minimize Fc binding. The passed cells, of which more than 95% had the morphology of small lymphocytes, did not bind AET-SRBC (< 3%) and lacked SIg (< 1%). These were designated null cells. The lymphocytes retained by the column were mechanically eluted by shaking the glass beads in PBS; 86% of the eluted lymphocytes stained positively for SIg and less than 2% bound AET-SRBC. This population was designated blood B lymphocytes.

Labeling of Cell Surface Glycoproteins with ^3H

Pretreatment with NE and/or GO. About 50 × 10^6 purified leukocytes, 150 μl packed platelets, or 0.5 ml packed erythrocytes were washed in PBS and divided into three equal lots. The cells were suspended in 1 ml Dulbecco's PBS (containing Ca^{2+} and Mg^{2+}), and either (1) 25 units NE plus 5 units GO or (2) GO only were added to the tubes. The third tube served as control, receiving no enzyme treatment. The tubes were incubated at 37°C for 30 min with gentle shaking. The cells were then washed twice with PBS and suspended in 0.5 ml PBS.

Pretreatment with periodate. 20–40 × 10^6 washed lymphocytes, 50 μl packed platelets, or 0.5 ml packed erythrocytes were suspended in 1 ml ice-cold PBS, and 10 μl of 0.1 *M* sodium metaperiodate was added to give a final concentration of 1 m*M* (pH 7.4). After incubation on ice for 10 min in the dark the cells were washed twice with PBS and suspended in 0.5 ml PBS.

After treatment with either enzymes or periodate, 0.5 mCi of NaB^3H_4 was added to each tube. The cells were kept for 30 min at room temperature and then washed three times with cold PBS. Then 0.2 ml PBS containing 1% Triton X-100 and 2 m*M* phenylmethylsulfonylfluoride (as protease inhibitor) was added on ice. After incubation for 5 min the tubes were centrifuged at 3000 rpm for 10 min and the supernatants recovered.

Polyacrylamide gel electrophoresis (PAGE) in the presence of sodium dodecyl sulfate (SDS) was performed according to the method of Laemmli[11] as described previously[7] using an acrylamide concentration of 8%. The treatment of the slab gels for fluorography[12] has also been described.[5] Cylindrical gels were sliced and the radioactivities counted as described previously.[3] The apparent molecular weights of the labeled proteins were calculated according to the method of Weber and Osborn.[13] The ^{14}C-labeled standard proteins were described previously.

Study of possible proteolytic degradation of surface glycoproteins during the labeling procedure. Erythrocytes (0.5 ml packed cells) labeled after NE + GO or periodate treatment were divided into two equal aliquots. To one of these were added 100 × 10^6 purified granulocytes, whereas the other remained without added cells. The mixtures were incubated at 37°C for 30 min and the erythrocyte membranes isolated.[3] Aliquots were then run on cylindrical gels to get a more quantitative estimation of possible proteolytic degradation.

Carl_G_190x270_mm_blokki_FINAL.indd 80 06-Aug-23 1:53:31 PM

RESULTS

Surface glycoprotein patterns of platelets. When platelets were labeled with NaB^3H_4 after treatment with NE + GO the following major glycoproteins were seen after slab gel electrophoresis: GP210, GP155, GP130, GP120 (the major band), GP105, GP97, GP80, GP68, GP54, GP42 (Fig. 1 A, Table 1). Selective labeling of surface sialic acid residues after periodate treatment using the same amount of platelets and the same amount of radioactivity yielded the following major labeled surface sialoglycoproteins: GP225, GP205, GP155, GP130, GP110 (major band), GP105, GP97, GP85, GP80, GP54, GP42 (Fig. 1 B, Table 1). The galactosyl-*N*-acetyl and galactosyl aminyl residues of the surface glycoproteins of the platelets apparently were heavily coated by sialic acids, since no labeling could be introduced after treatment with GO only (Fig. 2 A). The abundance of sialic acid residues on the surface proteins of platelets is further indicated by the clear reduction of the electrophoretic mobility of most of the major proteins after NE treatment (cf. Fig. 1 A and B).

Surface glycoprotein pattern of granulocytes. The following major surface glycoproteins were labeled in granulocytes after treatment with NE and GO: GP245, GP230, GP165, GP155, GP130 (major band), GP105, GP97, GP85, GP80, GP62, GP50, GP42 (Fig. 1 C). When the surface sialic acid residues were labeled after periodate treatment a fluorography pattern rather similar to that seen after NE + GO treatment was obtained. The main differences were seen in the area of GP155–GP105; GP130 was not seen after periodate treatment, while GP105 was relatively more strongly labeled than after NE + GO treatment (Fig. 1 D).

In contrast to the situation in platelets, the galactosyl and galactosylaminyl

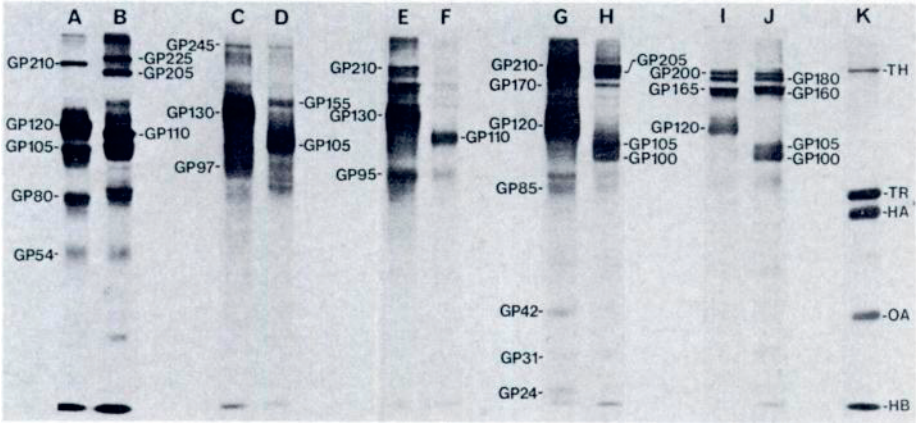

Fig 1. Fluorography patterns of tritium-labeled surface glycoproteins separated by polyacrylamide slab gel electrophoresis. (A) Platelets labeled with NaB^3H_4 after treatment with NE + GO (GP210, surface glycoprotein with an apparent molecular weight of 210,000 daltons, etc.; (B) platelets labeled after treatment with periodate; (C) granulocytes labeled after treatment with NE + GO; (D) granulocytes labeled after periodate treatment; (E) monocytes labeled after treatment with NE + GO; (F) monocytes labeled after periodate treatment; (G) non-T lymphocytes labeled after treatment with NE + GO; (H) non-T lymphocytes labeled after treatment with periodate; (I) T lymphocytes labeled after treatment with NE + GO; (J) T lymphocytes labeled after periodate treatment; (K) ^{14}C-labeled standard protein. TH, thyroglobulin; TR, transferin; HA, human albumin; OA, ovalbumin; HB, hemoglobin.

Carl_G_190x270_mm_blokki_FINAL.indd 81 06-Aug-23 1:53:31 PM

Table 1. Surface Glycoproteins of Blood Leukocytes

Apparent Mol Wt ($\times 10^{-3}$)	Platelets		Granulocytes		Monocytes		Non-T Lymphocytes		T Lymphocytes		B Lymphocytes,	Null Cells,
	NE + GO	P	NE + GO	P	NE + GO	P	NE + GO	P	NE + GO	P	NE + GO	NE + GO
GP245	–	–	+	+	–	–	–	–	–	–	–	–
GP230	–	–	+	+	–	–	–	–	–	–	–	–
GP225	–	2+	–	–	–	–	–	–	–	–	–	–
GP210	2+	–	–	–	2+	+	2+	2+	–	–	3+	3+
GP205	–	2+	–	–	+	+	2+	2+	+	+	–	–
GP200	–	–	–	–	+	–	–	–	2+	2+	–	–
GP180	–	–	–	–	–	–	+	+	2+	2+	+	2+
GP170	–	–	–	–	+	+	2+	2+	–	–	–	–
GP165	–	–	+	+	2+	+	–	–	2+	2+	–	+
GP160	–	–	–	–	–	–	–	–	+	+	–	–
GP155	+	+	2+	2+	+	+	+	+	–	–	–	–
GP120	2+	2+	3+	–	3+	–	2+	–	+	–	–	+
GP120	3+	–	–	–	–	–	3+	–	3+	–	2+	+
GP110	–	3+	–	+	–	3+	–	+	–	–	2+	+
GP105	2+	2+	2+	3+	–	–	–	3+	–	2+	–	–
GP100	+	+	–	–	–	–	–	3+	+	3+	+	+
GP97	–	–	2+	–	–	–	–	–	–	–	–	–
GP95	–	–	–	–	2+	2+	2+	+	+	+	+	+
GP85	–	+	+	+	+	+	2+	2+	+	+	+	+
GP80	2+	+	+	+	+	+	–	–	–	–	–	–
GP68	+	+	–	–	–	–	–	–	–	–	–	–
GP62	–	–	+	+	–	–	–	–	–	–	–	–
GP54	2+	2+	–	–	–	–	–	–	–	–	–	–
GP50	–	–	+	+	–	–	+	+	+	+	–	–
GP42	+	+	+	+	+	+	2+	2+	+	2+	+	+
GP31	–	–	–	–	–	–	2+	2+	–	2+	+	+
GP24	–	–	–	–	–	–	2+	2+	–	–	+	+

NE + GO, cells pretreated with neuraminidase plus galactose oxidase; P, cells pretreated with periodate. The relative labeling intensity is indicated on a scale of + to 3+.

residues of the granulocyte surface glycoproteins were relatively available to the GO directly without NE treatment. Most of the major surface proteins were labeled after treatment with GO only (Fig. 2 C). This finding and the similarities between the patterns obtained after NE + GO treatment and periodate treatment indicated that most of the surface glycoproteins with the exception of GP130 (NE + GO)/GP105 (periodate) of granulocytes are relatively poorly substituted with sialic acid residues.

Surface glycoprotein patterns of monocytes. The following major surface glycoproteins were labeled in monocytes after treatment with NE + GO: GP210, GP205, GP200, GP170, GP165, GP155, GP130 (major band), GP95, GP85, GP80, GP42 (Fig. 1 E). Labeling of the sialic acid residues after periodate treatment of the same amount of isolated monocytes yielded a pattern similar to that seen after NE + GO treatment. The main difference in the patterns were recorded in the areas of GP165-GP110; GP110 was strongly labeled after periodate treatment, while apparently the same protein showed the mobility of GP130 when labeled after NE + GO treatment (Fig. 1 E and F, Table 1).

Several glycoproteins of monocytes were labeled after treatment with GO only (Fig. 2 E). This shows that these proteins expose galactosyl/galactosaminyl residues available for the GO. The labeling intensity, however, is relatively weaker than that seen in granulocytes after treatment with GO only.

Carl_G_190x270_mm_blokki_FINAL.indd 82 06-Aug-23 1:53:31 PM

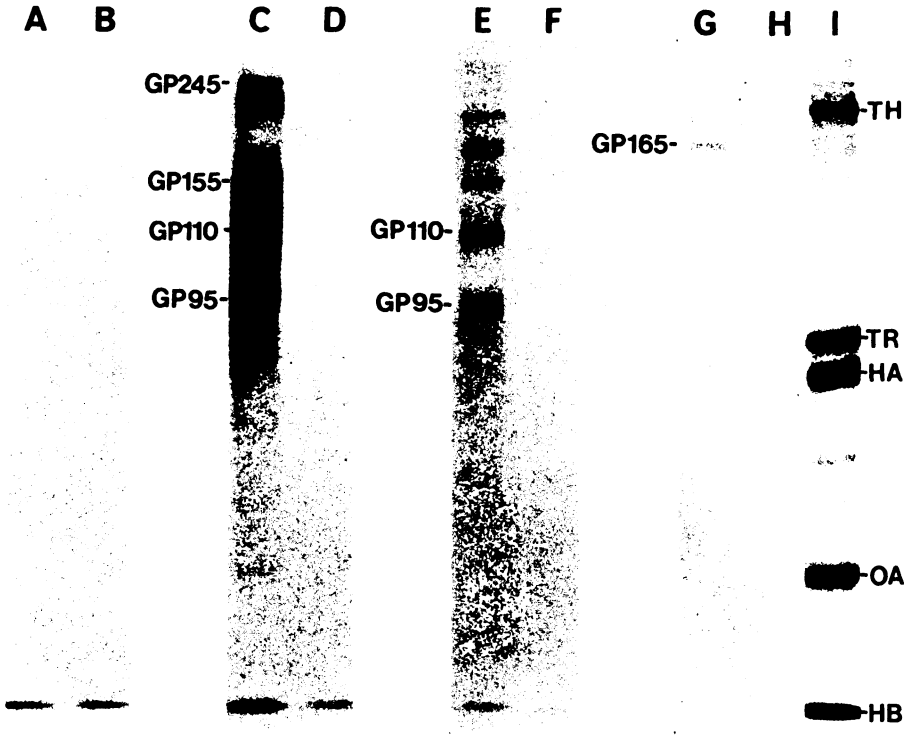

Fig. 2. Fluorography patterns of surface glycoproteins labeled after treatment with galactose oxidase only or without enzyme treatment and separated by polyacrylamide slab gel electrophoresis. (A) Platelets + GO; (B) platelets, no enzyme treatment; (C) granulocytes + GO; (D) granulocytes, no enzyme treatment; (E) monocytes + GO; (F) monocytes, no enzyme treatment; (G) T lymphocytes + GO; (H) T lymphocytes, no enzyme treatment; (I) ^{14}C-labeled standard proteins as in Fig. 1. The same amount of cells and serum borotritiate was used as for the cells in Fig. 1 and the slab exposed for the same time as that of Fig. 1.

Surface glycoprotein patterns of non-T lymphocytes. The following major glycoproteins were labeled on non-T lymphocytes after treatment with NE + GO: GP210, GP205, GP180, GP170, GP155, GP130, GP120, GP95, GP85, GP50, GP42, GP31, GP24 (Fig. 1 G). Labeling after treatment with periodate yielded a rather similar pattern. The major differences were GP105 and GP87, which were strongly labeled in the periodate-treated cells while the apparently corresponding proteins showed the mobility of GP130 and 120 in the pattern obtained after NE + GO treatment (Fig. 1 H).

Surface glycoproteins of T lymphocytes. GP200, GP180, GP165, GP160, GP130, GP120, GP97, GP95, GP85, GP50, GP42 were the major labeled glycoproteins in T cells labeled after treatment with NE + GO (Fig. 1 I, Fig. 3 A). Labeling after treatment with periodate gave a pattern similar to that seen after NE + GO treatment (Fig. 1J). There was again the typical change in the mobilities of two major bands. After NE + GO treatment they were GP130 and GP120 but were GP105 and GP97 after periodate treatment. GP31 was labeled after periodate treatment but was not seen after NE + GO treatment.

Carl_G_190x270_mm_blokki_FINAL.indd 83 06-Aug-23 1:53:31 PM

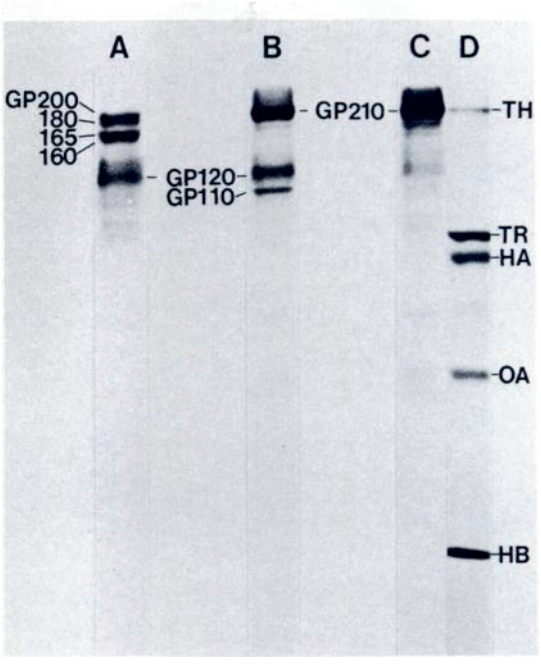

Fig. 3. Fluorography patterns of surface glycoproteins of T lymphocytes, B lymphocytes, and null cells labeled after treatment with neuraminidase and galactose oxidase and separated by polyacrylamide slab gel electrophoresis. (A) T lymphocytes; (B) B lymphocytes; (C) null cells; (D) ^{14}C-labeled standard proteins as in Fig. 1.

Surface glycoproteins of blood B lymphocytes. Figure 3 B shows the surface glycoprotein pattern of normal blood B lymphocytes labeled after NE + GO treatment. The dominating bands are GP210, GP120, and GP110. SIg, which should migrate in the 50,000-dalton region, was not seen. GP31 and GP24 were seen only after prolonged exposure.

Surface glycoproteins of blood null lymphocytes. The most strongly labeled band in null cells after NE + GO treatment was GP210. GP120 was more weakly labeled than in T or B lymphocytes (Fig. 2 C).

Absence of detectable proteolytic degradation of surface glycoproteins during the labeling procedures. When intact labeled erythrocytes were incubated with granulocytes no changes in the labeled surface glycoprotein patterns were observed (Fig. 4).

DISCUSSION

The surface glycoprotein patterns of the main populations of human blood leukocytes were analyzed by using two different methods of radiolabeling with tritium. The use of ^{3}H as a label gave an excellent resolution on the autoradiographs.

The GO-Na$B^{3}H_4$ method has received wide application in the study of surface molecules of different cells.[3,4,7] This labeling method is specific for the cell surface, since GO has a molecular weight of 75,000 daltons and apparently does not penetrate the plasma membrane of viable cells.[3] When combined with NE pretreatment, surface proteins with galactose residues covered by sialic acid may tentatively be identified. However, removal of sialic acid may cause artifactual changes in the physical or chemical properties of the sialoglycoproteins. This might affect their organization at the cell surface and is sometimes reflected by marked reductions in their electrophoretic mobilities.

Carl_G_190x270_mm_blokki_FINAL.indd 84 06-Aug-23 1:53:31 PM

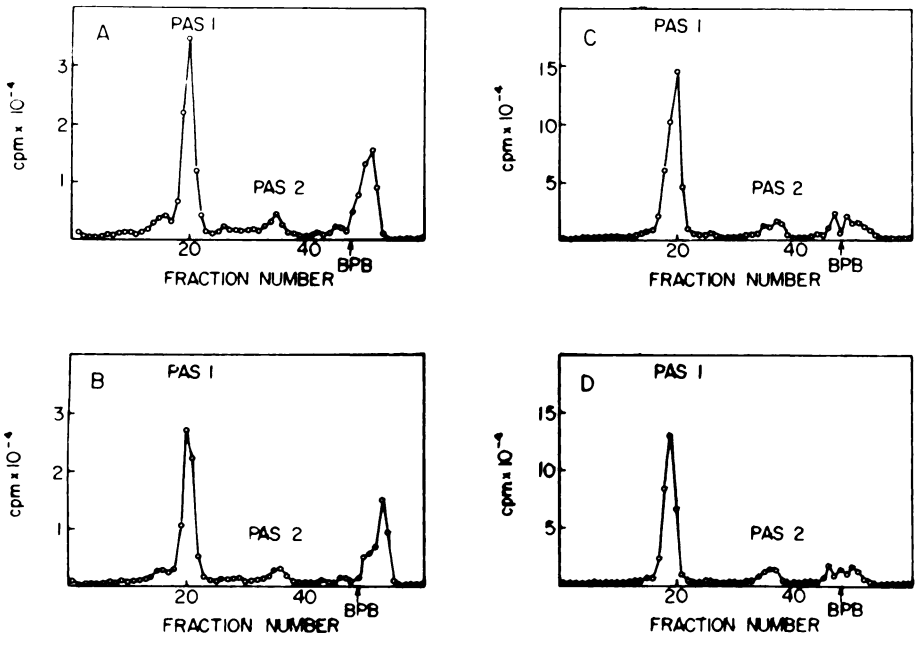

Fig. 4. Cylindrical PAGE patterns of labeled erythrocyte surface glycoproteins after incubation with or without granulocytes. (A) Surface glycoproteins of erythrocytes labeled after NE + GO treatment; (B) surface glycoproteins of erythrocytes labeled after NE + GO treatment and incubated with granulocytes; (C) surface glycoproteins of erythrocytes labeled after periodate treatment; (D) surface glycoproteins of erythrocytes labeled after periodate treatment and incubated with granulocytes. PAS 1 and PAS 2, the major labeled sialoglycoproteins; BPB, position of bromphenol blue marker dye.

Periodate in low concentrations specifically oxidizes sialic acids and after reduction with NaB^3H_4 tritium-labeled 5-acetamido-3,5-dideoxy-L-arabino-2-heptulosonic acid is the main product formed.[14,15] We recently showed this radiolabeling method to be specific for surface sialic acids under the conditions used in this study.[6] When the oxidation is carried out at 0°C with low concentrations of periodate and short reaction times the cell membrane is "frozen" and the transport of anions is low or absent.

By using these two methods of selective surface labeling we analyzed the exposed glycoproteins of the main populations of human blood leukocytes by running them on parallel slots on the same SDS-polyacrylamide slab gel. This enabled us to accurately compare the glycoprotein patterns of different cell populations and also gave information about the presence of glycoproteins of similar apparent molecular weights. Because of the anomalous electrophoretic behavior of glycoproteins on different gel systems, it should be emphasized that the figures given for the molecular weights represent only apparent weights.

In comparisons of the glycoprotein patterns obtained by the two labeling methods, all cells contained a major labeled glycoprotein with an apparent molecular weight of 100,000-130,000 daltons. Although it obviously was different in the various cells, it showed some common characteristics: it was a major labeled component, and it was obviously rich in sialic acids because it was weakly labeled with GO alone and it shifted electrophoretic mobility after

Carl_G_190x270_mm_blokki_FINAL.indd 85 06-Aug-23 1:53:31 PM

treatment with NE. Its function is unknown but it is evidently important for circulating cells.

After treatment of platelets with NE + GO, nine major labeled glycoproteins were identified. The general glycoprotein pattern seen was very similar to that recently published by Phillips and Agin[16] using the GO labeling method, although the apparent molecular weights of different components are higher throughout in their report. Labeling of the sialic acid residues after periodate treatment of platelets yielded a somewhat different electrophoretic profile. A "new" band, GP225, was seen by this technique. This finding indicates that GP225, which apparently is rich in sialic acid, either has very few galactosyl residues or has them "deeply" located and not available to the GO. The GP210 of the NE + GO profile apparently corresponds to the GP205 of the periodate profile and the GP120 to the GP110, which shows that the removal of sialic acids increases the apparent molecular weights. GP120 probably corresponds to glycocalicin,[17] and the GP68 seen after NE + GO treatment was recently showed to be the substrate for thrombin.[16]

The most strongly labeled band of granulocytes had an apparent molecular weight of 130,000 daltons (GP130). This protein is apparently rich in sialic acid residues, since its mobility was considerably higher after labeling with periodate, now recorded as GP105. Except for this protein, the general glycoprotein patterns obtained after NE + GO labeling and periodate labeling were strikingly similar. The granulocytes did not contain glycoproteins in the 160,000–200,000-dalton region. Such proteins are characteristic for lymphocytes but are also found in monocytes. The absence of glycoproteins in this region was apparently not due to proteolytic degradation, since granulocytes do not cleave labeled sialoglycoproteins of erythrocytes, which are known to be very protease sensitive[5] (Fig. 4). In contrast to the surface proteins of platelets, the galactosyl residues on the membrane proteins of granulocytes are only partially covered by sialic acid since most of the surface proteins are labeled after treatment with GO alone.

The general surface glycoprotein patterns of monocytes showed similarities to those of granulocytes but also to those of lymphocytes. After treatment with NE + GO the most strongly labeled protein was GP130. When the protein was labeled after periodate treatment it was recorded as GP110. Most of the surface molecules seen after NE + GO treatment were also labeled after periodate treatment. The surface glycoproteins of monocytes apparently carry some galactosyl residues not covered by sialic acid, since several of the major components were labeled after treatment with GO alone.

We earlier reported that according to the GO-NaB^3H_4 labeling method human blood T and B lymphocytes have different surface glycoprotein patterns.[18] Null cells resemble both T and B lymphocytes. They contain the GP210, which probably corresponds to the high molecular weight proteins of B cells. In contrast to both T and B lymphocytes, the GP120 is weak. As in granulocytes and monocytes, the major components in both T and B lymphocytes, GP120 apparently shows a higher electrophoretic mobility in the pattern obtained of surface proteins labeled after periodate treatment.

At present very few surface glycoproteins have been identified and characterized more extensively. The GP31 and GP24 of B cells are the human Ia

Carl_G_190x270_mm_blokki_FINAL.indd 86 06-Aug-23 1:53:31 PM

antigens,[19,20] and GP42 is the heavy chain of the HLA antigens.[21-23] Obviously, many of the other surface proteins are important for the physiologic functions of the white blood cells. Knowledge of the membrane glycoprotein patterns on normal blood leukocytes is fundamental for the discovery of possible molecular defects associated with various dysfunctional states.[24] Moreover, the normal patterns also provide a basis for the search for surface molecules specifically associated with malignant (leukemic) leukocytes.

ACKNOWLEDGMENT

We thank Anneli Asikainen and Liisa Räisänen for technical assistance and Leena Saraste for secretarial work.

REFERENCES

1. Gahmberg CG: Cell surface proteins. Changes during cell growth and malignant transformation, in Poste G, Nicolson GL (eds): Dynamic Aspects of Cell Surface Organization, vol 3. Amsterdam, North-Holland, 1977, p 371

2. Bretscher MS, Raff MC: Mammalian plasma-membranes. Nature 258:43-49, 1975

3. Gahmberg CG, Hakomori S: External labeling of cell surface galactose and galactosamine in glycolipid and glycoproteins of human erythrocytes. J Biol Chem 248:4311-4317, 1973

4. Steck TL, Dawson G: Topographical distribution of complex carbohydrates in the erythrocyte membrane. J Biol Chem 249: 2135-2142, 1974

5. Gahmberg CG: External labeling of human erythrocyte glycoproteins. Studies with galactose oxidase and fluorography. J Biol Chem 251:510-515, 1976

6. Gahmberg CG, Andersson LC: Selective radioactive labeling of cell surface sialoglycoproteins by periodate-tritiated borohydride. J Biol Chem 252:5888-5894, 1977

7. Gahmberg CG, Häyry P, Andersson LC: Characterization of surface glycoproteins of mouse lymphoid cells. J Cell Biol 68:642-653, 1976

8. Pellegrino MA, Ferrone S, Dierich MP, Reisfeld RA: Enhancement of sheep red blood cell human lymphocyte rosette formation by the sulfhydryl compound 2-amino ethylisothiouronium bromide. Clin Immunol Immunopathol 3:324-333, 1975

9. Häyry P, Andersson LC: Fractionation of immunocompetent cells with different physical properties. Scand J Immunol 5 [Suppl 5]:31-44, 1976

10. Wigzell H, Sundqvist YG, Yoshida TO: Separation of cells according to surface antigens by the use of antibody-coated columns. Fractionation of cells carrying immunoglobulins and blood group antigens. Scand J Immunol 1:75-87, 1972

11. Laemmli UK: Cleavage of structural proteins during the assembly of the head of bacteriophage T4. Nature 227:680-685, 1970

12. Bonner WM, Laskey RA: A film detection method for tritium labeled proteins and nucleic acids in polyacrylamide gels. Eur J Biochem 46:83-88, 1974

13. Weber K, Osborn M: The reliability of molecular weight determination by dodecyl sulfate-polyacrylamide gel electrophoresis. J Biol Chem 244:4406-4412, 1969

14. Van Lenten L, Ashwell G: Studies on chemical and enzymatic modification of glycoproteins. General methods for tritiation of sialic acid-containing glycoproteins. J Biol Chem 246:1889-1894, 1971

15. Suttajit M, Winzler RJ: Effect of modification of N-acetylneuraminic acid on the binding of glycoproteins to influenza virus and susceptibility to cleavage by neuraminidase. J Biol Chem 246:3398-3404, 1971

16. Phillips RD, Agin PP: Platelet plasma membrane glycoproteins. Identification of a proteolytic substrate for thrombin. Biochem Biophys Res Commun 75:940-947, 1977

17. Okumura T, Jamieson GA: Platelet glycocalicin. I. Orientation of glycoproteins of the human platelet surface. J Biol Chem 251:5944-5949, 1976

18. Andersson LC, Wasastjerna C, Gahmberg CG: Different surface glycoprotein patterns on human T-, B- and leukemic-lymphocytes. Int J Cancer 17:40-46, 1976

19. Klareskog L, Sandberg-Trägårdh L, Rask L, Lindblom JB, Curman B, Peterson PA: Chemical properties of human Ia antigens. Nature 265:248-251, 1977

20. Giphart MJ, Kaufman JF, Fuhs A, Albrechtsen D, Solheim BG, Bruning JW, Strominger JL: HLA-associated alloantisera

Carl_G_190x270_mm_blokki_FINAL.indd 87 06-Aug-23 1:53:31 PM

react with molecules similar to Ia antigens. Proc Natl Acad Sci USA 74:3533-3536, 1977

21. Bridgen J, Snary D, Crumpton MJ, Barnstable C, Goodfellow P, Bodmer WF: Isolation and N-terminal amino acid sequence of membrane-bound human HLA-A and HLA-B antigens. Natue 261:200-205, 1976

22. Terhorst C, Robb R, Jones C, Strominger JL: Further structural studies of the heavy chain of HLA antigens and its similarity to immunoglobulins. Proc Natl Acad Sci USA 74:4002-4006, 1977

23. Nilsson K, Andersson LC, Gahmberg CG, Wigzell H: Surface glycoprotein patterns of normal and malignant human lymphoid cells. II. B cells, B blasts and Epstein-Barr virus (EBV) positive and negative B lymphoid cell lines. Int J Cancer (in press)

24. Degos L, Tobelem G, Lethielleux P, Levy-Toledano S, Caen J, Colombani J: Molecular defect in platelets from patients with Bernard-Soulier Syndrome. Blood 50:899-903, 1977

Proc. Natl. Acad. Sci. USA
Vol. 75, No. 7, pp. 3455–3458, July 1978
Medical Sciences

Activated human T lymphocytes display new surface glycoproteins

(T-cell subsets/differentiation markers/blast transformation/killer cell antigen)

LEIF C. ANDERSSON*†, CARL G. GAHMBERG‡, ARTHUR K. KIMURA§, AND HANS WIGZELL§

* Transplantation Laboratory, † Department of Pathology, and ‡ Department of Bacteriology and Immunology, University of Helsinki, Haartmaninkatu 3, SF 00290 Helsinki 29, Finland; and § Department of Immunology, Biomedicum, Uppsala University, Uppsala, Sweden

Communicated by Werner Henle, May 8, 1978

ABSTRACT **We have analyzed the surface glycoproteins of resting and *in vitro* activated human T lymphocytes by the galactose oxidase/NaB^3H_4 and the periodate/NaB^3H_4 labeling techniques. The labeled glycoproteins were separated by polyacrylamide slab gel electrophoresis and visualized by fluorography. A "new" glycoprotein with an apparent molecular weight of 130,000 (GP130) was strongly labeled on alloantigen-activated T blasts but only weakly or not at all on mitogen-stimulated T blasts and resting T lymphocytes. These results demonstrate that human T cells, as earlier found in the mouse system, express different surface molecules in relation to the particular mode of activation and stage of differentiation.**

The functionally differentiated cells in multicellular organisms frequently carry specific surface structures which are involved in intercellular communication. A detailed characterization of such membrane molecules may allow a deeper insight to the mechanisms operating during cell-to-cell cooperation.

A number of different cells interact in the immune system to create optimal responses to various immunogenic substances. The mode and magnitude of the immune response are largely controlled by the T lymphocytes (1). Endowed with the ability to display functions like help, suppression, or killing, T lymphocytes apparently are comprised of functionally discrete subsets (2). Some of these subsets express specific differentiation antigens which, in the mouse, can be detected by appropriate alloantisera (3). Corresponding antisera specific for the subsets of human T lymphocytes are not yet available, but the surface molecules found in the murine system will most likely have their counterparts on human lymphocytes.

The surface molecules on different lymphoid cells have recently been studied by selective radiolabeling of the membrane glycoproteins (4). These investigations have disclosed that both murine and human resting T and B lymphocytes have their own, distinct, surface glycoprotein patterns (5, 6). Blast transformation and differentiation of the murine T cells *in vitro* induced changes in their surface glycoprotein patterns which were different depending on the mode of activation. T blasts from cultures stimulated with allogeneic cells in mixed lymphocyte culture (MLC) had a surface glycoprotein pattern that was different from that of mitogen-activated T cells (5). Detailed analysis revealed the expression of a unique surface glycoprotein, called T145 (molecular weight, 145,000), that appeared concomitantly with the expression of cytotoxic ability by activated T cells. The cellular distribution of this particular membrane protein indicated it to constitute a specific differentiation marker for a subset of T cells in the mouse—namely, killer cells (7).

In the present communication we report on the extension of this work to include surface glycoproteins of human T cells at various stages of differentiation. Mitogen- and alloantigen-activated (in MLC) human T blasts displayed different cell surface glycoprotein patterns compared to normal resting T lymphocytes. The MLC blasts carried a membrane glycoprotein, GP130 (molecular weight, 130,000) that appears to be a human counterpart of the murine killer T cell glycoprotein T145.

MATERIALS AND METHODS

Isolation of Blood Lymphocytes. Buffy coats from fresh human blood were obtained from the Finnish Red Cross Blood Transfusion Service. Mononuclear cells were isolated by Ficoll/Isopaque gradient centrifugation (8). Phagocytic cells were removed by treatment with iron powder and a magnet. T lymphocytes were purified by passage of the cells over a human Ig/rabbit anti-human-Ig column (9). The contamination of the T cells by surface-immunoglobulin-bearing cells was <1% as judged by immunofluorescence staining. Blood B lymphocytes and null cells (with lymphocytic morphology but lacking the typical T and B cell surface markers) were purified as reported in detail elsewhere (10).

Cultivation and Purification of T Lymphoblasts. Lymphocytes enriched for T cells were cultivated at a density of 10^6 cells per ml in RPMI-1640 culture medium supplemented with 10% normal human AB plasma for the indicated times with optimal concentrations of phytohemagglutinin (PHA) or concanavalin A (Con A). T lymphocytes were also cultivated with mitomycin C-treated allogeneic mononuclear blood cells in MLC. Blast cells were purified from the mitogen cultures and the MLC by 1-*g* velocity sedimentation (11). The blast cell populations consisted of >95% lymphoblasts as judged from May–Gruenwald–Giemsa-stained cytocentrifuged smears. More than 85% of the blasts formed rosettes with sheep erythrocytes. Viability of all cells exceeded 95% as judged by the trypan blue exclusion test.

Radiolabeling of Cell Surface Proteins. Cells were surface labeled by reduction with NaB^3H_4 after oxidation with either neuraminidase plus galactose oxidase (4) or periodate (12). About 50×10^6 cells suspended in 1 ml of Dulbecco's phosphate-buffered saline (P_i/NaCl) were incubated with 25 units of *Vibrio cholera* neuraminidase (NE) (Behringwerke, Mahrburg, Lahn) and 5 units of galactose oxidase (Kabi, Stockholm). The enzyme preparations did not contain proteolytic activity. Alternatively, the same amount of cells was suspended in 1 ml of ice-cold P_i/NaCl, 10 μl of 0.1 M sodium metaperiodate was added, and the cells were kept on ice for 10 min. After treatment with enzymes or periodate, the cells were washed with P_i/NaCl and then suspended in 0.5 ml of P_i/NaCl, and 0.5 mCi of NaB^3H_4 was added. After 30 min at room temperature, the cells were washed with cold P_i/NaCl, and 0.2

The costs of publication of this article were defrayed in part by the payment of page charges. This article must therefore be hereby marked "*advertisement*" in accordance with 18 U. S. C. §1734 solely to indicate this fact.

Abbreviations: MLC, mixed lymphocyte culture; Con A, concanavalin A; GO, galactose oxidase; NE, *Vibrio cholera* neuraminidase; PHA, phytohemagglutinin; P_i/NaCl, phosphate-buffered saline.

Carl_G_190x270_mm_blokki_FINAL.indd 89 06-Aug-23 1:53:31 PM

ml of cold P_i/NaCl containing 1% Triton X-100 and 2 mM phenylmethylsulfonyl fluoride was added. After 5 min on ice, the nuclei were pelleted and the supernatants were used for electrophoresis.

Polyacrylamide Slab Gel Electrophoresis. Electrophoresis was performed on 8% polyacrylamide gels with ^{14}C-labeled marker proteins in peripheral slots (5). The gels were fixed and treated for fluorography as described (13). Quantitative measurements of the individual fluorographic profiles were performed on a Joyce–Loebl recording densitometer.

RESULTS

Surface Glycoprotein Patterns of Resting Blood Lymphocytes. Fluorographic patterns of slab gels of surface-labeled T and B and null lymphocytes purified from normal human blood are shown in Fig. 1. The patterns of the main lymphocyte populations are clearly different. In the fluorography pattern of resting T lymphocytes, four closely spaced bands of equal labeling intensity are seen in the high molecular weight region: GP200, GP180, GP165, and GP160. B cells and null cells have one major band in this region with an apparent molecular weight of 210,000 (GP210). Both T and B lymphocytes express a major band, GP120, which is weakly labeled in null cells. The basic patterns of these lymphocyte populations were remarkably constant and did not differ between corresponding cells obtained from different donors.

Surface Glycoprotein Patterns of *In Vitro*-Generated T Blasts. T lymphoblasts recovered after activation *in vitro* with mitogens or with allogeneic cells still showed the basic glycoprotein patterns of resting T lymphocytes. On comparison of the glycoprotein patterns of T blasts isolated from mitogen-stimulated cultures with those of T blasts isolated from MLC, some apparent differences were observed. The MLC blasts expressed a major band, GP130, that was seen after 3 days in culture and was strongly labeled after 6 days in culture (Figs. 2 and 3). This was only weakly expressed on PHA- and Con A-stimulated blast cells and on T lymphocytes kept in unstimulated cultures. GP120, on the other hand, was virtually absent from MLC blasts at 6 days but was the major protein in this molecular weight range on mitogen-activated T blasts.

Another major difference between mitogen- and alloantigen-stimulated T blasts was in the labeling of the four closely spaced bands in the high molecular weight region. As shown, in Figs. 1, 2, and 3, GP200, GP180, GP165, and GP160 showed approximately identical labeling intensities on resting T lymphocytes and on T lymphocytes kept in unstimulated cultures for 6 days. GP200 and GP180 were weakly labeled on MLC-activated blasts whereas on mitogen-activated T blasts, GP180 and GP165 were relatively strongly labeled. Stimulation of lymphocytes from different individuals consistently yielded these characteristic differences between the fluorography patterns of their MLC T blasts and mitogen-induced T blasts (Fig. 4).

The different fluorography patterns of MLC and mitogen-induced T blasts obtained after labeling with the neuraminidase/galactose oxidase technique is apparently not due to differences in accessibilities of galactosyl- or *N*-acetylgalactosyl-aminyl residues, because the same principal differences were also observed after labeling of the sialic acid residues by periodate/NaB^3H_4 treatment (Fig. 5).

DISCUSSION

Analysis of exposed membrane glycoproteins by selective surface labeling (4, 12) allows the identification of certain cells and cell lineages with high accuracy (14, 15). In the present study we have shown that blast cells derived from human peripheral T lymphocytes express different surface glycoprotein patterns as a result of various cellular activations.

The most striking finding was a prominent "new" band, GP130, in the fluorography patterns of MLC blasts. GP130 was undetected in small T lymphocytes of blood and was weakly labeled in mitogen-stimulated T blasts and T lymphocytes kept in nonstimulated cultures. This difference in the expression of glycoproteins on human MLC and resting T cells parallels that reported in the mouse system, where a certain glycoprotein, called T145, was selectively found on $Ly1^-2^+$ killer T blasts (7).

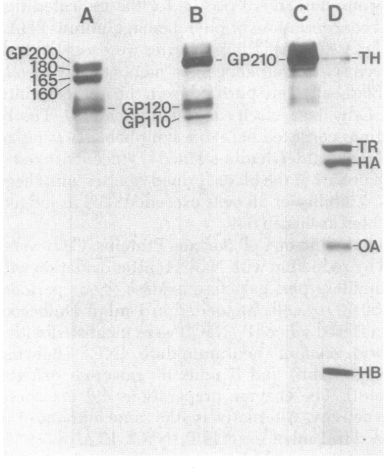

FIG. 1. Fluorography patterns of the surface glycoproteins labeled after neuraminidase/galactose oxidase treatment of human blood lymphocytes. Lanes: A, T lymphocytes; B, B lymphocytes; C, null lymphocytes; D, ^{14}C-labeled marker proteins. TH, thyroglobulin; TR, transferrin; HA, human serum albumin; OA, ovalbumin; HB, hemoglobin. GP210 indicates a glycoprotein with an apparent molecular weight of 210,000, etc. [The smaller glycoproteins (i.e., the HLA-D molecules on B lymphocytes) require longer exposure times to become apparent.]

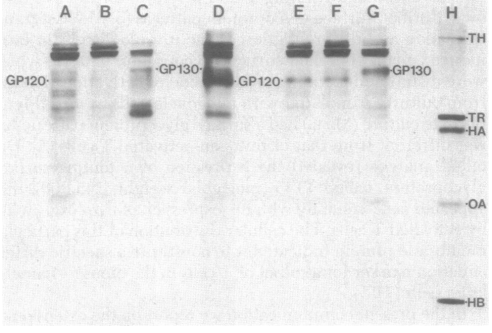

FIG. 2. Fluorography patterns of the surface glycoproteins labeled after neuraminidase/galactose oxidase treatment of T blasts and T lymphocytes cultured for different times. Lanes: A, PHA blasts, 3 days; B, Con A blasts, 3 days; C, MLC blasts, 3 days; D, T lymphocytes, kept in unstimulated cultures for 6 days; E, PHA blasts, 6 days; F, Con A blasts, 6 days; G, MLC blasts, 6 days; H, marker proteins as in Fig. 1.

Carl_G_190x270_mm_blokki_FINAL.indd 90 06-Aug-23 1:53:31 PM

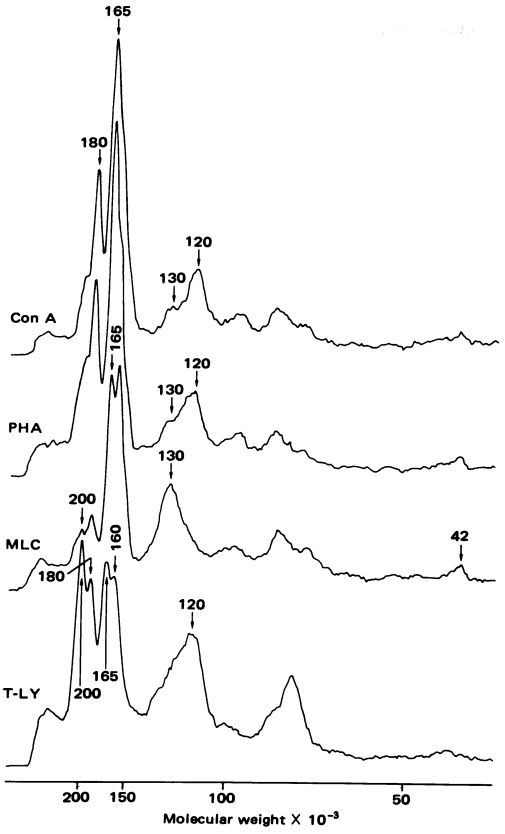

FIG. 3. Densitometric tracings of the fluorography patterns obtained with surface labeled T blasts and T lymphocytes after 6 days in culture. T-LY, T lymphocytes from nonstimulated cultures; MLC, MLC blasts; PHA, PHA blasts; Con A, Con A blasts. The major labeled proteins are indicated. The quantitative differences in the labeling intensities (GP200–GP160) and the different expressions of GP130 and GP120 are obvious. GP42, location of the heavy chain of the HLA antigen.

Although of slightly different apparent molecular weight, the behavior of this protein strongly indicates that it represents the mouse counterpart of the human GP130. The question of whether GP130 represents a marker for a functional differentiation step or is already expressed on a small, undetectable subpopulation of small T lymphocytes being strongly selected for during the MLC is yet to be answered. The kinetics for the appearance of GP130, however, are more compatible with a sequence of differentiation because, although already present on MLC blasts cultivated for 3–4 days, GP130 requires 5–7 days to reach maximal expression. Moreover, we have not found detectable expression of GP130 on thymocytes or on subpopulations of human blood, spleen, and thymocytes or on subpopulations of human blood, spleen, and tonsillar T lymphocytes selected for the presence of receptors for Fcγ, for Fcμ (16), for the ability to form "fast" or "slow" rosettes with sheep erythrocytes, etc.

On the other hand, we recently found that GP130 is a

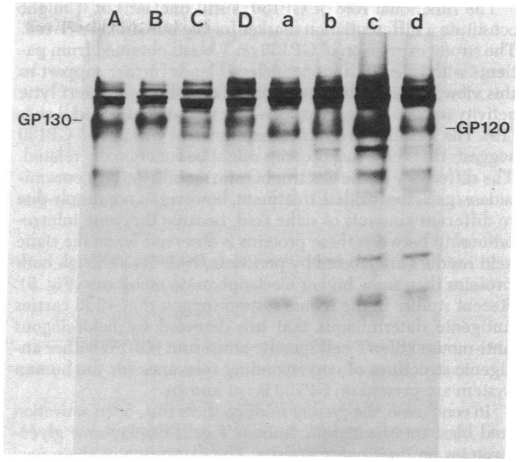

FIG. 4. Fluorography patterns of the surface glycoproteins labeled after neuraminidase/galactose oxidase treatment of MLC and PHA blasts from four different persons. Lanes: A–D, MLC blasts; a–d, PHA blasts; A and a originate from the same donor, etc.

prominent surface glycoprotein on blood T lymphoblasts from patients with acute infectious mononucleosis (17), proving that T blasts may also express this surface protein *in vivo*.

T145, which is the apparent murine counterpart of GP130, has clearly been shown to constitute a differentiation marker for the murine killer T cell. It is absent from resting spleen T lymphocytes, regardless of their Ly phenotype, but the activation of the cytotoxic capacity *in vivo* or *in vitro* coincides with the surface appearance of T145. T145 is only expressed on T killer blasts of relevant Ly phenotype but is retained on "secondary" T cells (18) that have reverted to memory lymphocytes upon prolonged culture of isolated MLC blasts in the absence of stimulator cells.

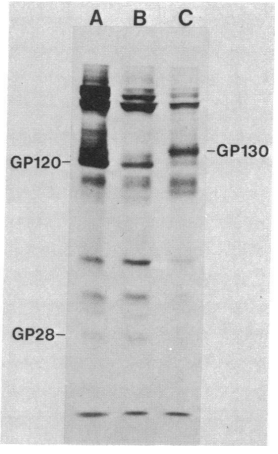

FIG. 5. Fluorography patterns of surface glycoproteins labeled by periodate/NaB^3H_4 treatment of Con A blasts (lane A), PHA blasts (lane B), and MLC blasts (lane C). The presence of negatively charged sialic acid residues gives the GP120 and GP130 higher electrophoretic mobilities compared to those seen after the enzyme treatment.

Carl_G_190x270_mm_blokki_FINAL.indd 91 06-Aug-23 1:53:32 PM

The functional role of GP130 is still unclear but it might constitute a differentiation marker for the human killer T cell. The strong expression of GP130 on T blasts obtained from patients with infectious mononucleosis lends further support to this view, because these cells have been shown to exert lytic activity *in vitro* against Epstein–Barr virus-transformed B cells (19). The seemingly reciprocal expression of GP120 and GP130 suggests that these two proteins might be functionally related. The difference in the electrophoretic mobility after neuraminidase/galactose oxidase treatment, however, is not simply due to different amounts of sialic acid, because the same interrelationship between these proteins is observed when the sialic acid residues are labeled by periodate/NaB^3H_4 although both proteins then show higher electrophoretic mobilities (Fig. 5). Recent studies in the mouse system suggest that T145 carries antigenic determinants that are detected by heterologous anti-mouse killer T cell specific antiserum (20). Whether antigenic structures of corresponding relevance for the human system are present on GP130 is not known.

In conclusion, the present findings show that, upon activation and blast transformation, human T cells display new glycoproteins on their outer surface. The expression of these new glycoproteins varies according to mode of activation and requires different time periods to achieve full expression. This suggests that these glycoproteins represent markers for subsets of T cells at different stages of differentiation.

We thank Ms. Anneli Asikainen, Ms. Liisa Räisänen, and Ms. Marja Wilkman for technical assistance and Ms. Leena Saraste for secretarial assistance. Financial support was received from the Academy of Finland, the Sigrid Jusélius Foundation, the Finnish Cancer Society, the Swedish Cancer Society, and National Institutes of Health Contract NCI-CB-74129-31.

1. Paul, W. E. & Benacerraf, B. (1977) *Science* **195,** 1293–1300.
2. Cantor, H. & Boyse, E. A. (1975) *J. Exp. Med.* **141,** 1376–1389.
3. Jandinski, J., Cantor, H., Tadakuma, T., Peavy, D. L. & Pierce, C. W. (1976) *J. Exp. Med.* **143,** 1382–1390.
4. Gahmberg, C. G. & Hakomori, S. (1973) *J. Biol. Chem.* **248,** 4311–4317.
5. Gahmberg, C. G., Häyry, P. & Andersson, L. C. (1976) *J. Cell. Biol.* **68,** 642–653.
6. Andersson, L. C., Wasastjerna, C. & Gahmberg, C. G. (1976) *Int. J. Cancer* **17,** 40–46.
7. Kimura, A. K. & Wigzell, H. (1978) *J. Exp. Med.* **147,** 1418–1434.
8. Böyum, A. (1968) *Scand. J. Clin. Lab. Invest.* **21,** Suppl. 97, 1–107.
9. Wigzell, H., Sundqvist, Y. G. & Yoshida, T. O. (1972) *Scand. J. Immunol.* **1,** 75–87.
10. Andersson, L. C. & Gahmberg, C. G. (1978) *Blood,* in press.
11. Miller, R. G. & Phillips, R. A. (1969) *J. Cell. Physiol.* **73,** 191–201.
12. Gahmberg, C. G. & Andersson, L. C. (1977) *J. Biol. Chem.* **252,** 5888–5894.
13. Bonner, W. M. & Laskey, R. A. (1974) *Eur. J. Biochem.* **46,** 83–88.
14. Andersson, L. C., Gahmberg, C. G., Nilsson, K. & Wigzell, H. (1977) *Int. J. Cancer* **20,** 702–707.
15. Nilsson, K., Andersson, L. C., Gahmberg, C. G. & Wigzell, H. (1977) *Int. J. Cancer* **20,** 708–716.
16. Moretta, L., Webb, S. R., Grossi, C. E., Lydyard, P. M. & Cooper, M. D. (1977) *J. Exp. Med.* **146,** 184–200.
17. Andersson, L. C. & Gahmberg, C. G. (1978) *Clin. Immunol. Immunopathol.* **10,** 41–46.
18. Andersson, L. C. & Häyry, P. (1975) *Transpl. Rev.* **25,** 121–162.
19. Svedmyr, E. & Jondal, M. (1972) *Proc. Natl. Acad. Sci. USA* **72,** 1622–1627.
20. Kimura, A. K., Welsh, K. I. & Wigzell, H. (1975) in *Leukocyte Membrane Determinants Regulating Immune Reactivity,* eds. Eijsvoogel, V., Roos, D. & Zeijlemaker, W. P. (Academic, New York), p. 611.

Carl_G_190x270_mm_blokki_FINAL.indd 92 06-Aug-23 1:53:32 PM

Proc. Natl. Acad. Sci. USA
Vol. 76, No. 8, pp. 4087–4091, August 1979
Medical Sciences

Specific changes in the surface glycoprotein pattern of human promyelocytic leukemic cell line HL-60 during morphologic and functional differentiation

(myeloid leukemia/hematopoietic differentiation/phagocytosis)

CARL G. GAHMBERG*, KENNETH NILSSON†, AND LEIF C. ANDERSSON‡

*Department of Bacteriology and Immunology, University of Helsinki, Finland; †The Wallenberg Laboratory, University of Uppsala, Sweden; and ‡Transplantation Laboratory, Fourth Department of Surgery and Department of Pathology, University of Helsinki, Finland

Communicated by George Klein, May 14, 1979

ABSTRACT **The human promyelocytic leukemia cell line HL-60 can be induced to undergo morphological and functional differentiation *in vitro* by various low molecular weight compounds. The cellular morphology changes from blastoid appearance to that of granulocytes and the cells acquire the ability to phagocytize. We here report that the surface glycoproteins specifically change during this differentiation, as shown by the neuraminidase/galactose oxidase/NaB^3H_4 surface-labeling technique followed by polyacrylamide slab gel electrophoresis. The most prominent change is the loss of the major glycoprotein band typical for the blast cells which has an apparent molecular weight of 160,000 and the appearance of a major surface glycoprotein band with an apparent molecular weight of 130,000. Expression of the 130,000 molecular weight band correlates with the appearance of phagocytic and chemotactic activities of the cells. It has the same molecular weight as the major surface glycoprotein of freshly isolated human blood granulocytes.**

The murine Friend erythroleukemic cells have been extensively studied and serve as a model for leukemic cell differentiation (1). These cells can be induced to differentiate by a variety of apparently unrelated low molecular weight compounds like dimethyl sulfoxide (Me_2SO) (1) and butyric acid (2). The mechanism(s) involved has remained obscure, but it may involve effects on the cell plasma membrane (3).

Very little information is available on the mechanisms operating in human hematopoietic cell differentiation. This is mainly due to the previous lack of suitable cell lines capable of maturation *in vitro*. Recently, however, Collins *et al.* (4) described a continuous human promyelocytic blastoid leukemic cell line, HL-60, that can be induced to differentiate *in vitro* by Me_2SO and other agents (5). The cells acquired both granulocyte morphology and the ability to phagocytize yeast cells.

Little is known about the cell surface changes accompanying granulocyte maturation, and the molecules involved in phagocytosis and other granulocyte functions have not been characterized. We have approached these problems by analyzing the changes in the surface glycoproteins of the HL-60 cell during its induced differentiation *in vitro*. In this report we show that the major surface glycoprotein with a molecular weight of 160,000 from HL-60 blasts can no longer be labeled in differentiated HL-60 cells. Instead, a surface glycoprotein with a molecular weight of 130,000 (GP130) is strongly labeled. Concomitant with the appearance of GP130, phagocytic activity and granulocyte morphology are acquired. Further maturation is associated with the labeling of other surface glycoproteins.

The publication costs of this article were defrayed in part by page charge payment. This article must therefore be hereby marked "*advertisement*" in accordance with 18 U. S. C. §1734 solely to indicate this fact.

MATERIALS AND METHODS

Cells. The HL-60 cell line was obtained from R. C. Gallo (National Institutes of Health). The cells were cultivated in plastic flasks (Falcon) in RPMI-1640 culture medium supplemented with 20% fetal calf serum. The cells were induced to differentiate by addition of Me_2SO to a final concentration of 1.0%. HL-60 blasts and HL-60 differentiated cells were purified by $1 \times g$ velocity sedimentation (6), and fractions exceeding 95% purity were obtained. Human granulocytes were isolated from buffy coats of normal blood units provided by the Finnish Red Cross Blood Transfusion Service as described (7). The granulocytes were >97% pure, as judged from May/Gruenwald/Giemsa-stained smears.

Chemicals and Enzymes. Me_2SO (analytical grade), sodium borohydride, and sodium metaperiodate were obtained from Merck AG (Darmstadt, West Germany). NaB^3H_4 (11.7 Ci/mmol, 1 Ci = 3.70×10^{10} becquerels) was purchased from the Radiochemical Centre (Amersham, England). The galactose oxidase (EC 1.1.3.9) (Kabi AB, Stockholm, Sweden) and *Vibrio cholerae* neuraminidase (EC 3.2.1.18) (Behringwerke, Marburg-Lahn, West Germany) were free of protease activity when assayed as described (8).

Cell Surface Labeling and Polyacrylamide Gel Electrophoresis. Cells (20×10^6) were surface labeled by use of NaB^3H_4 after treatment with either neuraminidase and galactose oxidase or periodate as described in detail (8–10). Briefly, the cells were treated with 5 units of galactose oxidase and 12 units of neuraminidase for 30 min at 37°C in Dulbecco's phosphate-buffered saline. The periodate treatment was at 0°C for 10 min with a periodate concentration of 1 mM. The cells were then washed by centrifugation and reduced with 0.5 mCi of NaB^3H_4 for 30 min at room temperature. After washing, the cells were solubilized in Triton X-100 containing buffer (11) and centrifuged at $1000 \times g$ for 10 min, and the supernatants were used for electrophoresis. Polyacrylamide gel electrophoresis in the presence of sodium dodecyl sulfate was performed on slab or cylindrical gels with an acrylamide concentration of 8% (12). The handling of the gels for fluorography (13) and the ^{14}C-labeled standard proteins have been described (10). Films were scanned with a Joyce–Loebl Chromoscan apparatus along the center of the gel lanes.

Abbreviation: Me_2SO, dimethyl sulfoxide.

Carl_G_190x270_mm_blokki_FINAL.indd 93 06-Aug-23 1:53:32 PM

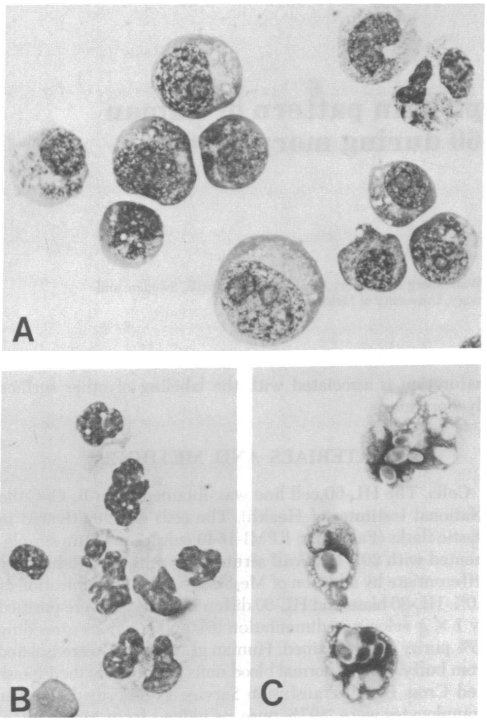

FIG. 1. Morphological and functional differentiation of HL-60 cells induced by Me_2SO. (*A*) May/Gruenwald/Giemsa-stained smears of undifferentiated HL-60 blasts. (*B*) Morphology after cultivation for 5 days in the presence of 1.0% Me_2SO. (*C*) Ingestion of *Candida albicans* cells after differentiation for 2 days.

Preparation and Analysis of Glycopeptides and Oligosaccharides from the Major Labeled Surface Glycoprotein of HL-60 Cells. Surface-labeled HL-60 cells were electrophoresed after solubilization on cylindrical polyacrylamide gels. The gels were sliced with a 2-mm gel slicer and the slices were eluted for 24 hr with 1 ml of water. The radioactivity in the aliquots was determined and the fractions containing the major labeled surface glycoprotein were pooled and lyophilized. These were then treated with Pronase (14) followed by 50 mM NaOH/1 M $NaBH_4$ for 24 hr at 45°C (15). The labeled glycopeptides and oligosaccharides were then analyzed on a Bio-Gel P6 (Bio-Rad) column prepared in 0.15 M Tris·HCl (pH 7.8) containing 0.1% sodium dodecyl sulfate.

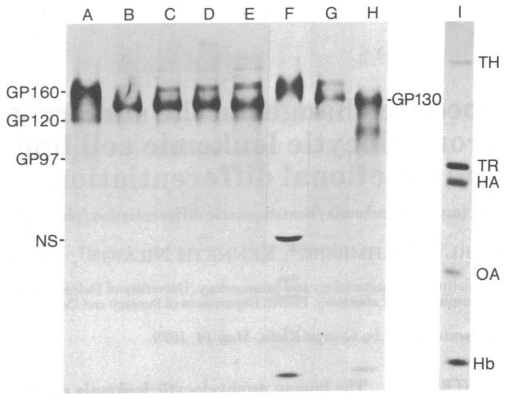

FIG. 2. Surface glycoprotein patterns of HL-60 cells and normal granulocytes labeled with ^3H after treatment with neuraminidase and galactose oxidase and separation by polyacrylamide slab gel electrophoresis. Lane A: undifferentiated HL-60 cells. Lanes B–E: HL-60 cells after cultivation in the presence of Me_2SO for 2 days (B), for 3 days (C), for 4 days (D), and for 5 days (E). Lane F: purified HL-60 blasts. Lane G: purified HL-60 granulocytes. Lane H: normal human granulocytes. Lane I: ^{14}C-labeled standard proteins (TH, thyroglobulin; TR, transferrin; HA, human albumin; OA, ovalbumin; Hb, hemoglobin). The apparent molecular weights of the labeled proteins are indicated: GP160, glycoprotein with an apparent molecular weight of 160,000, etc. NS, protein nonspecifically labeled by NaB^3H_4 alone.

Preparation of Antiserum against GP130 and Immunoprecipitation. One rabbit was immunized three times intravenously at 2-week intervals with 50×10^6 purified leukemic cells from a patient with chronic myeloid leukemia (7). Ten days after the last injection, serum was collected and 1 ml of the serum was absorbed three times for 3 hr at 0°C with 1 ml of packed normal lymphoid cells obtained by Ficoll–Isopaque centrifugation (7). After this the serum was absorbed twice with 0.5 ml of packed cells of an Epstein–Barr virus-positive lymphoblastoid cell line established from the same patient (11). Immunoprecipitations were performed from undifferentiated and differentiated Hl-60 cells that had been labeled with ^3H after treatment with neuraminidase and galactose oxidase. Briefly, equal amounts of labeled cells were dissolved in Triton X-100 containing buffer. The immunoprecipitations were done with 5 μl of either immune serum or preimmunization serum by a staphylococcal protein A technique as described in detail (11).

Phagocytosis. Phagocytic cells were quantitated by incubation of the HL-60 cells for 1 hr with opsonized *Candida albicans* cells. The cellular morphology was studied from May/Gruenwald/Giemsa-stained cytocentrifuged smears.

Table 1. Morphology and phagocytic activity of HL-60 cells during Me_2SO-induced differentiation

Day of culture	Morphology		% phagocytosing cells		
	% blasts*	% granulocytes†	Total	With 1–2 yeast particles	With 3 or more yeast particles
0	98	2	3	3	—
1	94	6	8	6	2
2	63	37	49	20	29
3	45	55	56	22	34
4	17	83	46	35	11

* Myeloblasts, promyelocytes, and myelocytes.
† Metamyelocytes and neutrophils.

Carl_G_190x270_mm_blokki_FINAL.indd 94 06-Aug-23 1:53:32 PM

RESULTS

Morphologic and Functional Differentiation Induced by Me_2SO. When HL-60 cells were grown without inducing agent, the majority of the cells showed a promyelocytic appearance with a few myelocytic and metamyelocytic cells (Fig. 1*A*). After 2 days in the presence of 1.0% Me_2SO, most of the cells showed obvious neutrophilic differentiation (Fig. 1*B*) and phagocytic activity (Fig. 1*C*). The changes in morphology and induction of phagocytosis with time in Me_2SO-containing culture are shown in Table 1.

Surface Glycoprotein Patterns of Cells Labeled by Neuraminidase/Galactose Oxidase/NaB^3H_4 Method. The surface glycoprotein profile of uninduced cells is shown in Figs. 2, lane A, and 3, curve A. The most strongly labeled glycoprotein had an apparent molecular weight of 160,000 (GP160). After 2 days in the presence of Me_2SO, the surface glycoprotein pattern was dramatically changed with a complete loss of GP160. Instead, there appeared a strongly labeled GP130 (Figs. 2, lane B, and 3, curve B). At this stage there was very little label in other surface glycoproteins. During subsequent growth in the presence of Me_2SO, the label in GP130 remained unchanged, but now GP210 and GP155 appeared (Figs. 2, lanes C–E, and 3, curves C–E). Purified HL-60 blasts contained label almost only in GP160 (Figs. 2, lane F, and 3, curve F), whereas purified differentiated HL-60 cells contained labeled GP155 and GP130 (Figs. 2, lane G, and 3, curve G). The NS band represents nonspecific label that is not dependent on enzyme treatments (16). Purified granulocytes from peripheral blood had a surface glycoprotein pattern similar to that of differentiated HL-60 cells with a dominant GP130.

Surface Glycoprotein Patterns of Periodate/NaB^3H_4-Labeled Cells. After periodate/NaB^3H_4 labeling, GP110 was the most strongly labeled protein in both undifferentiated and differentiated HL-60 cells (Fig. 4).

Glycopeptides and Oligosaccharides of Major Labeled Surface Glycoprotein. Fig. 5 shows the Bio-Gel P6 elution patterns of glycopeptides and oligosaccharides from GP110 from uninduced (Fig. 5*A*) and induced (Fig. 5*B*) HL-60 cells labeled with ^3H after periodate treatment. The patterns are remarkably similar. The apparent molecular weight of the major peak is about 2300. When the glycopeptides and oligosaccharides from GP160 and GP130 were analyzed after neuraminidase/galactose oxidase/NaB^3H_4 labeling, the patterns were similar and the major peaks had apparent molecular weights of about 600 (data not shown).

Immunoprecipitation with Antiserum against GP130. Fig. 6 shows the immunoprecipitates from uninduced and induced HL-60 cells labeled by the neuraminidase/galactose oxidase/NaB^3H_4 technique and analyzed on a polyacrylamide slab gel. A strong GP130 was obtained from induced cells (Fig. 6, lane C) and a weak GP130 from uninduced cells (Fig. 6, lane B). No GP160 was precipitated from uninduced cells with antiserum and no band was obtained with preimmune serum from induced cells (Fig. 6, lane D).

DISCUSSION

The galactose oxidase/NaB^3H_4 (8, 9) and periodate/NaB^3H_4 (10) surface-labeling techniques, combined with fluorography of polyacrylamide slab gels, have proven useful for distinguishing different normal and malignant human blood cells (7, 17) and lymphoid cell lines (18, 19). In addition we have found that, depending on the mode of activation, human T lymphoblasts have characteristic and easily distinguishable surface glycoprotein patterns that are different from those of resting T lymphocytes (20).

In contrast to the more extensive information on surface glycoprotein alterations accompanying lymphoid differentiation, very little is known about molecular changes associated with granulocyte/monocyte maturation (21–23). The surface glycoprotein patterns of normal human granulocytes and monocytes are clearly different from those of blasts from patients

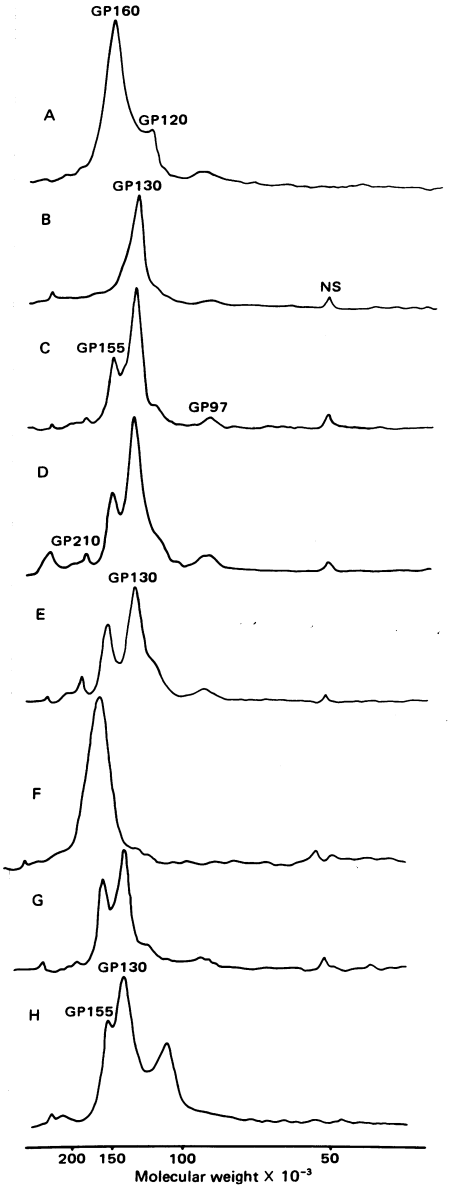

FIG. 3. Scanning patterns of HL-60 labeled surface glycoproteins (neuraminidase/galactose oxidase pretreatment) separated by slab gel electrophoresis and visualized by fluorography. Curves A–H, see legend for Fig. 2. The apparent molecular weights of the proteins are indicated.

Carl_G_190x270_mm_blokki_FINAL.indd 95 06-Aug-23 1:53:32 PM

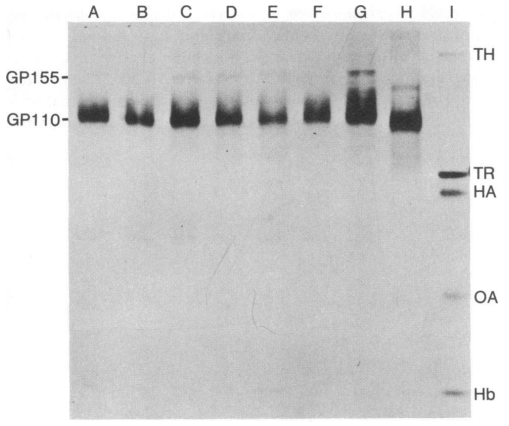

FIG. 4. Surface glycoprotein patterns of HL-60 cells and normal granulocytes labeled with ^3H after periodate treatment and separated by polyacrylamide slab gel electrophoresis. Lanes A–I, as in Fig. 2 but labeled after periodate treatment. The apparent molecular weight of the major labeled surface glycoprotein is now 110,000.

with acute or chronic myeloid leukemia (7, 17). This indicates that in the myeloblast-granulocyte lineage, surface glycoprotein changes normally occur during differentiation.

The recent establishment of the HL-60 promyelocytic cell line (4) and the successful induction of its differentiation *in vitro* (5) has made it possible to study cell surface changes at a molecular level during myeloid differentiation. When HL-60 cells were labeled by the neuraminidase/galactose oxidase/NaB^3H_4 technique, the most obvious cell surface protein change during differentiation was the loss of GP160 and the appearance of GP130. This is not a nonspecific effect of Me_2SO because the K562 cell line (originating from a patient with myeloid leukemia), which cannot be induced to differentiate by Me_2SO (5), did not show any change in its surface glycoprotein pattern after 5 days in the presence of Me_2SO (data not shown). On the other hand, this cell line can be induced to undergo erythroid differentiation by using sodium butyrate (24).

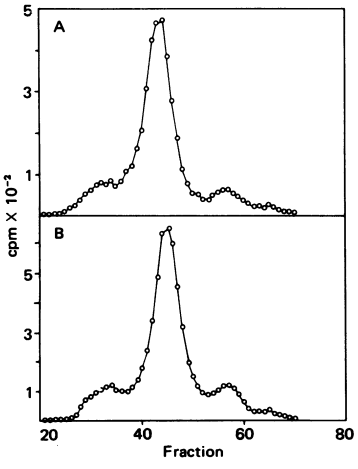

FIG. 5. Bio-Gel P6 elution patterns of periodate/NaB^3H_4-labeled GP110 glycopeptides and oligosaccharides from uninduced (*A*) and induced (*B*) HL-60 cells.

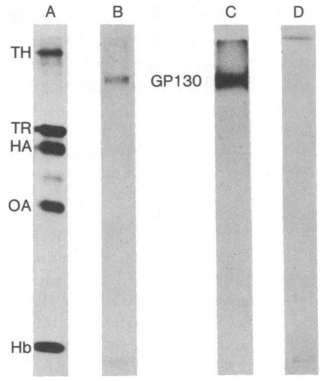

FIG. 6. Fluorography patterns of immunoprecipitates with antiserum against GP130 from neuraminidase/galactose oxidase/NaB^3H_4-labeled cells. Lane A, standard proteins as in Fig. 2; lane B, uninduced HL-60 cells with immune serum; lane C, induced HL-60 cells with immune serum; lane D, control from induced HL-60 cells with preimmune serum. Similar amounts of radioactivity were used for immunoprecipitations, and the films were exposed for identical times.

No difference between uninduced and induced HL-60 cells was seen when the cells were labeled by the periodate/NaB^3H_4 method, but all cells contained a strongly labeled GP110. We think that both GP160 and GP130 move like GP110 on polyacrylamide gel electrophoresis in the presence of sodium dodecyl sulfate when their sialic acids have not been removed by neuraminidase treatment. This is characteristic of surface glycoproteins containing *O*-glycosidic carbohydrate chains, such as the major red cell sialoglycoprotein, glycophorin, and the major T lymphocyte surface protein, which show increased electrophoretic mobilities in the presence of sodium dodecyl sulfate when their sialic acids are present (10, 20). GP160 and GP130 evidently have common features. Both are rich in apparently identical alkali-labile oligosaccharides containing sialic acids. The simultaneous appearance of GP130 with the loss of GP160 suggested the possibility of a precursor–product relationship. However, the antiserum reacting with GP130 did not react with GP160, which indicates differences in antigenicity.

Normal granulocytes contain GP130 as the most strongly labeled band (7). This protein must be closely similar to the GP130 of induced HL-60 cells because it reacts with the antiserum against GP130 (data not shown). The simultaneous appearance of GP130 in HL-60 cells with the development of phagocytic and chemotactic (unpublished results) activities could mean that this protein is involved in such functions, but no direct evidence can be provided at present. Some support for a role of this protein in chemotaxis comes from our recent studies in which it was shown that the GP130 protein is strongly reduced in granulocytes of patients with monosomy-7 (25), which have defective chemotaxis (26).

The results show that it is possible to follow human myeloid differentiation by analyzing the surface glycoprotein patterns and indicate the usefulness of this approach for investigating granulocyte structural–functional relationships. This may be particularly important when the differentiation stage of human myeloid leukemic cells is determined (17).

Carl_G_190x270_mm_blokki_FINAL.indd 96 06-Aug-23 1:53:32 PM

We thank Dr. R. C. Gallo for the HL-60 cell line. The skillful technical assistance of Anneli Asikainen and Liisa Alajoki and the secreterial help given by Leena Saraste are acknowledged. This study was supported by the Academy of Finland and the Finnish Cancer Society.

1. Friend, C., Scher, W., Holland, J. G. & Soto, T. (1971) *Proc. Natl. Acad. Sci. USA* **68,** 378–381.
2. Leder, A. & Leder, P. (1975) *Cell* **5,** 319–322.
3. Lyman, G. H., Preisler, H. D. & Papahadjopoulos, D. (1976) *Nature (London)* **262,** 360–363.
4. Collins, S. J., Gallo, R. C. & Gallagher, R. E. (1977) *Nature (London)* **270,** 347–349.
5. Collins, S. J., Ruscetti, F. W., Gallagher, R. E. & Gallo, R. C. (1978) *Proc. Natl. Acad. Sci. USA* **75,** 2458–2462.
6. Häyry, P. & Andersson, L. C. (1976) *Scand. J. Immunol. Suppl.* **5,** 31–44.
7. Andersson, L. C. & Gahmberg, C. G. (1978) *Blood* **52,** 57–67.
8. Gahmberg, C. G. & Hakomori, S. (1973) *J. Biol. Chem.* **248,** 4311–4317.
9. Gahmberg, C. G. (1978) *Methods Enzymol.* **50,** 204–206.
10. Gahmberg, C. G. & Andersson, L. C. (1977) *J. Biol. Chem.* **252,** 5888–5894.
11. Gahmberg, C. G. & Andersson, L. C. (1978) *J. Exp. Med.* **148,** 507–521.
12. Laemmli, U. K. (1970) *Nature (London)* **227,** 680–685.
13. Bonner, W. M. & Laskey, R. A. (1974) *Eur. J. Biochem.* **46,** 83–88.
14. Gahmberg, C. G., Myllylä, G., Leikola, J., Pirkola, A. & Nordling, S. (1976) *J. Biol. Chem.* **251,** 6108–6116.
15. Finne, J. (1975) *Biochim. Biophys. Acta* **412,** 317–325.
16. Gahmberg, C. G. & Hakomori, S. (1973) *Proc. Natl. Acad. Sci. USA* **70,** 3329–3333.
17. Gahmberg, C. G. & Andersson, L. C. (1978) *Ann. N. Y. Acad. Sci.* **312,** 240–255.
18. Andersson, L. C., Gahmberg, C. G., Nilsson, K. & Wigzell, H. (1977) *Int. J. Cancer* **20,** 702–707.
19. Nilsson, K., Andersson, L. C., Gahmberg, C. G. & Wigzell, H. (1977) *Int. J. Cancer* **20,** 708–716.
20. Andersson, L. C., Gahmberg, C. G., Kimura, A. K. & Wigzell, H. (1978) *Proc. Natl. Acad. Sci. USA* **75,** 3455–3458.
21. Sachs, L. (1978) *Nature (London)* **274,** 535–539.
22. Lotem, J. & Sachs, L. (1977) *Proc. Natl. Acad. Sci. USA* **74,** 5554–5558.
23. Simantov, R. & Sachs, L. (1978) *Proc. Natl. Acad. Sci. USA* **75,** 1805–1809.
24. Andersson, L. C., Jokinen, M. & Gahmberg, C. G. (1979) *Nature (London)* **278,** 364–365.
25. Gahmberg, C. G., Andersson, L. C., Ruutu, P., Timonen, T. T. T., Hänninen, A., Vuopio, P. & de la Chapelle, A. (1979) *Blood,* in press.
26. Ruutu, P., Ruutu, T., Vuopio, P., Kosunen, T. & de la Chapelle, A. (1977) *Nature (London)* **265,** 146–147.

Carl_G_190x270_mm_blokki_FINAL.indd 97 06-Aug-23 1:53:32 PM

Eur. J. Immunol. 1992. *22:* 1173–1178

Tomas Mustelin▼, Tiina Pessa-Morikawa▼, Matti Autero○, Martin Gassmann◆ Leif C. Andersson▽ Carl G. Gahmberg○, and Paul Burn◆

Department of Pathology▼, and Department of Biochemistry○, University of Helsinki, Helsinki and Department of Biology◆, PR-New Technologies, F. Hoffmann-La Roche Ltd., Basel

Regulation of the p59^{fyn} protein tyrosine kinase by the CD45 phosphotyrosine phosphatase*

Triggering of the T cell antigen receptor/CD3 (TcR/CD3) complex leads to rapid tyrosine phosphorylation of regulatory proteins that participate in initiating T cell activation and proliferation. This signal transduction event requires the presence of the TcR/CD3-associated protein tyrosine kinase p59^{fyn}. There is also evidence that the CD45 phosphotyrosine phosphatase is involved in TcR/CD3 signalling. We show here by capping experiments using double indirect immunofluorescence techniques that the receptor phosphotyrosine phosphatase CD45 and the intracellular protein tyrosine kinase p59^{fyn} specifically co-distribute in functional T lymphocytes. Furthermore, we provide evidence that isolated p59^{fyn} is a substrate for CD45 as indicated by the rapid dephosphorylation of the regulatory Tyr^{531} of p59^{fyn} by CD45. This dephosphorylation is accompanied by a severalfold increase in the catalytic activity of p59^{fyn} as measured by its autophosphorylation and phosphorylation of an exogenous substrate. We also demonstrate that CD45-mediated dephosphorylation and activation of p59^{fyn} apparently occurs at a slow basal rate in resting T cells. This represents the first identification of a physiologic regulator of p59^{fyn} and implies a mechanism for the role of CD45 in TcR/CD3 signal transduction.

1 Introduction

Triggering of the TcR/CD3 complex leads to initial and obligatory tyrosine phosphorylation events [1–3] including phosphorylation of the γ1 isoform of the phosphatidylinositol-specific phospholipase C [4, 5]. This results in enhanced hydrolysis of inositol phospholipids, activation of protein kinase C and mobilization of intracellular calcium [6].

The *src* family protein tyrosine kinase (PTK) p59^{fyn} [7, 8] was recently found to be physically associated with the TcR/CD3 complex [9, 10], and seems to be crucial for signal transduction from this receptor complex [11]. In addition to p59^{fyn}, the closely related p56^{lck} [12] is probably also involved in TcR/CD3-induced signal transduction [13–15] due to its association with the CD4 and CD8 glycoproteins, which serve as accessory molecules in antigen recognition. The relative contributions by p59^{fyn} and p56^{lck} to TcR/CD3-induced tyrosine phosphorylation, however, remain unclear and may depend on the mode of stimulation.

The catalytic activity of the *src* family of PTK is suppressed *in vivo* by phosphorylation of a C-terminal regulatory tyrosine residue [16, 17]. When the codon for this tyrosine (Tyr^{531} in p59^{fyn} or Tyr^{505} in p56^{lck}) is altered or deleted and NIH3T3 cells are transfected with the mutated cDNA the cells are transformed [16–18]. Accordingly, removal of the suppressing phosphate from the C-terminal tyrosine of p56^{lck} and p59^{fyn} by a phosphotyrosine phosphatase (PTPase) would be expected to enhance their PTK activities. We have earlier shown that the major membrane PTPase in T cells, the leukocyte common antigen (CD45), is capable of activating p56^{lck} in T cell membranes and *in vitro*, by dephosphorylating the regulatory Tyr-505 [19, 20]. Here we show that p59^{fyn} co-localizes with CD45 *in vivo* and that CD45 activates p59^{fyn} by dephosphorylating the regulatory Tyr^{531}. We infere from these results that the nonreceptor *src* family PTK p59^{fyn} and p56^{lck} are similarly regulated by CD45.

[I 10041]

* This work was supported in part, by the Academy of Finland, the Finnish Cancer Society, the Sigrid Juselius Foundation, the Finska Läkaresällskapet, J.W. Perklens Stiftelse and the Magnus Ehrnrooth Foundation

Correspondence: Tomas Mustelin, Department of Pathology, University of Helsinki, Haartmaninkatu 3, SF-00290 Helsinki, Finland

Abbreviations: **PTK:** Protein tyrosine kinase **PTPase:** Phosphotyrosine phosphatase

2 Materials and methods

2.1 Materials

A rabbit antiserum directed against a synthetic peptide corresponding to amino acid residues 29–43 of p59^{fyn} (αfynN) [21] was a kind gift of Dr. T. Kawakami (La Jolla Institute for Allergy and Immunology, La Jolla, CA), and an antiserum against amino acids 22–35 of p59^{fyn} was raised as described [10]. An antiserum against amino acid residues 39–64 of p56^{lck} was a kind gift of Dr. A. Altman (La Jolla Institute for Allergy and Immunology, La Jolla, CA). The peptide KRLIEDNEYAARQG, was synthesized using an Applied Biosystems 430 synthesizer by t-Boc chemistry and purified by HPLC. The product was found to contain the expected amino acids. [γ-^{32}P] ATP was from Amersham Int., Amersham, GB), phenylarsine oxide from Aldrich (Steinheim, FRG) and TPCK-trypsin from Worthington Biochemical Corporation (Freehold, NJ).

2.2 Cells

Human mononuclear leukocytes (PBL) were isolated from the blood of healthy volunteers by gradient centrifugation

© VCH Verlagsgesellschaft mbH, D-6940 Weinheim, 1992

0014-2980/92/0505-1173$3.50+.25/0

Carl_G_190x270_mm_blokki_FINAL.indd 98 06-Aug-23 1:53:32 PM

on Ficoll Isopaque (Pharmacia, Uppsala, Sweden). Human T lymphocyte clones were raised, maintained and cultured as described [22]. In the experiments illustrated in Fig. 1 (Sect. 3) the human $CD4^+$ T cell clone HK.L41 was used.

2.3 Immunofluorescence microscopy and capping

Capping experiments and immunofluorescence microscopy were performed as described by Gassmann et al., [10]. The following mouse and rat monoclonal antibodies were used: HLe-1, specific for human CD45 (Becton Dickinson, Montain View, CA) and YTH 81.5 specific for human LFA-1 (α chain, CD11a; Serotec, Kidlington, GB). Polyclonal rabbit antisera specific for $p59^{fyn}$ and the secondary reagents were as described [10]. All the antibodies used as secondary reagents were cross-adsorbed on appropriate rabbit, rat or mouse IgG columns to eliminate cross-species reactivities.

2.4 Western blotting

Immunoblotting was performed using PBL membranes prepared as described [19] by sonication, removal of nuclei and high-speed centrifugation (180 000 × g for 15 min in a Beckman Airfuge). Proteins were resolved by SDS-PAGE on 10 % or 12 % gels and transferred onto nitrocellulose filters. The antisera were used at 1:1000 dilution and the blots developed by a standard alkaline phosphatase method.

2.5 Immunoprecipitation

$p59^{fyn}$ was immunoprecipitated from $100 \times 10^6 - 200 \times 10^6$ PBL lysed in 1 ml of 3 % NP40, 20 mM Tris, pH 8.0, 150 mM NaCl, 1 mM Na_3VO_4, 10 μg/ml leupeptin and 10 μg/ml aprotinin. Precleared lysates were incubated for 2 h with 5–10 μl of $p59^{fyn}$ antiserum, followed by agarose-bound goat anti-rabbit Ig for 1 h. Immunocomplexes were washed three times in lysis buffer, once in lysis buffer with 0.5 M NaCl, again in lysis buffer and, finally, twice in 10 mM Hepes, pH 7.65. CD45 was immunoprecipitated as described [19, 20] from human blood lymphocytes, lysed at 50×10^6/ml in 0.2 % NP40 in PBS and protease inhibitors. Precleared lysates were incubated for 2 h with GAP 8.3 (ATCC Rockville, MD, #HB12) ascites fluid (0.3-1 μl/10^7 cell equivalents) or control antisera, followed by agarose-conjugated goat anti-mouse or anti-rabbit IgG. The precipitates were washed five times in lysis buffer.

2.6 PTK assay

Phosphorylation of the synthetic peptide, KRLIEDNEYAARQG, corresponding to the major autophosphorylation site of the *src* family kinases, was measured as described [19, 20]. In the experiments shown in Table 1 and Fig. 3, the immunoprecipitates were mixed as indicated and incubated at 30 °C for 3 min with or without 1 mM Na_3VO_4 prior to the PTK assay.

2.7 Phosphorylation and dephosphorylation of $p59^{fyn}$

For autophosphorylation of $p59^{fyn}$, the washed immunoprecipitates were incubated with 5 μCi = 185 kBq [γ-^{32}P] ATP in 50 μl of 10 mM Hepes, pH 7.65, 0.2 % Triton X-100, 10 mM $MgCl_2$, 5 mM $MnCl_2$, 5 mM 2-mercaptoethanol and 1 mM Na_3VO_4 for 10 min at 30 °C. The reaction was stopped either with trichloroacetic acid (20 % final) and the resulting precipitate washed three times in ice-cold acetone, or directly boiled in SDS sample buffer. *In situ* phosphorylation of $p59^{fyn}$ (predominantly at Tyr^{531}) was performed as described for $pp60^{c\text{-}src}$ [23]. Briefly, 50×10^6 PBL were lysed in 50 μl of 10 mM Tris-HCl, pH 7.4, 1 % Triton X-100, 2.5 mM $MnCl_2$, 150 mM NaCl, 10 μg/ml aprotinin and leupeptin and the lysate was kept on ice for 15 min and then incubated in the presence of 1 mM Na_3VO_4, 50 μCi of [γ-^{32}P] ATP, and 1 μM ATP for an additional 15 min on ice. The reaction mixture was diluted to 1 ml with ice-cold 3 % NP40, 20 mM Tris, pH 8.0, 150 mM NaCl, 1 mM Na_3VO_4 and protease inhibitors, and $p59^{fyn}$ immunoprecipitated as described above. For CD45-mediated dephosphorylation, the immunoprecipitates were washed two additional times in 50 mM imidazole, pH 7.2, 5 mM EDTA and 10 mM octyl-β-D-glucoside and suspended in 50 μl of this buffer and treated with 10 μl (1.6 μg or 1.5 Units; 1 Unit = 1 nmol/min) of the purified CD45 for 5 min at 30 °C. Phosphorylated proteins were separated on 10 % SDS polyacrylamide gels and visualized by autoradiography.

2.8 Tryptic peptide mapping

Proteins were localized in the gels by autoradiography, eluted, oxidized, digested with TPCK-trypsin and the resulting peptides separated by electrophoresis at pH 8.9 (anode to the left) and ascending chromatography as described in detail elsewhere [24]. The radiolabeled spots were identified by comparison with published results obtained with $p56^{lck}$ [16, 25] and $pp60^{c\text{-}src}$ [26, 27]. The $p59^{fyn}$ peptide containing Tyr^{420} is identical to the corresponding peptide obtained from autophosphorylated $p56^{lck}$ (Fig. 3c), which has an identical mobility on thin layer plates (data not shown).

2.9 Purification of CD45

CD45 was purified from PBL and all steps were carried out at 4 °C. Column fractions were monitored for the presence of CD45 using the monoclonal antibody MEM-28 and by measuring PTPase activity with o-phospho-L-tyrosine as substrate [19, 20]. Cells were washed in 10 mM Tris-HCl, pH 7.4, 140 mM NaCl, and lysed in 50 mM imidazole, pH 7.2, 1 % Triton X-100, 5 mM EDTA, 1 mM EGTA, 1 mM dithiotreitol, 1 mM benzamide, 5 μg/ml leupeptin and 1 μg/ml aprotinin. After centrifugation at 100 000 × g, the supernatant was passed through a DEAE-cellulose column equilibrated in the above lysis buffer. The column was washed with 50 mM imidazole, pH 7.2, 0.015 % Triton X-100, 5 mM EDTA, 1 mM EGTA, 0.1 mM dithiotreitol, 1 mM benzamide, 5 μg/ml leupeptin and 1 μg/ml aprotinin, and eluted with a gradient of KCl (0–300 mM) in the same buffer. Fractions containing CD45 were passed through a wheat germ lectin-Sepharose 4B affinity column, and the

Carl_G_190x270_mm_blokki_FINAL.indd 99 06-Aug-23 1:53:32 PM

Eur. J. Immunol. 1992. *22:* 1173–1178

column was washed extensively before eluting the bound glycoproteins with 0.2 M N-acetyl-D-glucosamine in 50 mM imidazole, pH 7.2, 0.015 % Triton X-100, 1 mM EDTA, 0.2 mM EGTA, 0.1 mM dithiotreitol. The eluate was concentrated by adsorption to DEAE-cellulose and the detergent changed to 10 mM octyl-β-D-glucoside. The preparation was further concentrated using Centricon microconcentrators (Amicon, Lexington, MA) and subjected to gel filtration through an Ultrogel AcA34 (LKB, Bromma, Sweden) column in 50 mM imidazole, pH 7.2, 200 mM KCl, 10 mM octyl-β-D-glucoside, 1 mM dithiotreitol. Fractions containing active CD45 were pooled and used in the experiments.

3 Results

3.1 p59^{fyn} and CD45 co-distribute *in vivo*

To study a possible association of p59^{fyn} and CD45 *in vivo*, the CD45 molecules on the surface of intact human T lymphocytes were collected into caps by cross-linking with specific antibodies and the capped cells were examined by double indirect immunofluorescence to determine whether intracellular p59^{fyn} was co-collected with the CD45 caps. The addition of anti-CD45 antibodies to the T cells followed by fluorescein-conjugated F(ab')$_2$ fragments of goat anti-mouse IgG, all at 4 °C, resulted in a uniform surface labeling (Fig. 1a). If the labeled cells were warmed to 37 °C, within 20 min the CD45 antigen was generally collected into a cap (Fig. 1c). Fixed and permeabilized, capped or uncapped cells were indirectly immunolabeled with p59^{fyn} followed by a rhodamine-conjugated F(ab')$_2$ fragments of goat anti-rabbit IgG. A uniform intracellular staining was observed for p59^{fyn} in uncapped cells (Fig. 1b), whereas CD45-capped cells displayed a significant co-distribution of p59^{fyn} with the CD45 caps (Fig. 1d). This was seen in >80 % of cells displaying CD45 caps. In contrast, similar capping experiments involving LFA-1 cell surface receptors (Fig. 1e) did not result in any detectable redistribution of intracellular p59^{fyn} (Fig. 1f). We have earlier shown that p59^{fyn} co-caps with TcR and CD3, while p56^{lck} co-distributes with CD4 and CD8, but not with TcR or CD3 [10] indicating further the specificity of our capping protocol. Thus, we conclude from the experiments presented here that p59^{fyn} and CD45 are specifically associated (directly or indirectly) in T lymphocytes which might indicate that p59^{fyn} is a substrate for CD45.

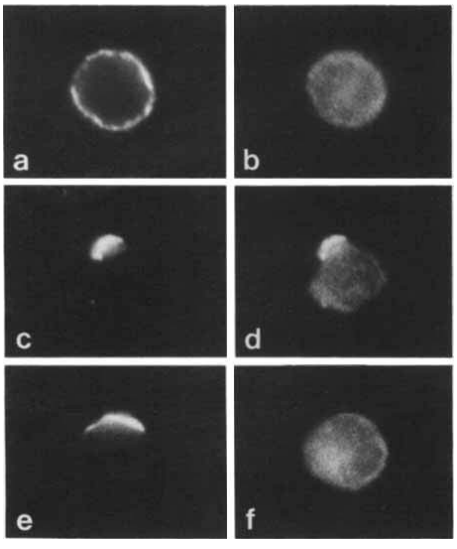

Figure 1. Double indirect immunofluorescence labeling of surface CD45 or LFA-1 and intracellular p59^{fyn} in human T lymphocytes. a) Uncapped CD45, b) p59^{fyn} in uncapped cells, c) Capped CD45, d) p59^{fyn} in CD45-capped cells, e) Capped LFA-1, and f) p59^{fyn} in LFA-1-capped cells. Note the co-localization of p59^{fyn} with the CD45 cap.

3.2 Immunoprecipitated p59^{fyn} autophosphorylates

When p59^{fyn} immunoprecipitated from resting human blood lymphocytes was incubated with [γ-^{32}P] ATP and divalent cations, two bands at 59 kDa and ~81 kDa became visible on the autoradiograms of the SDS gels (Fig. 2a, lane 1). The former corresponds to autophosphorylated p59^{fyn} and the latter might represent an associated protein.

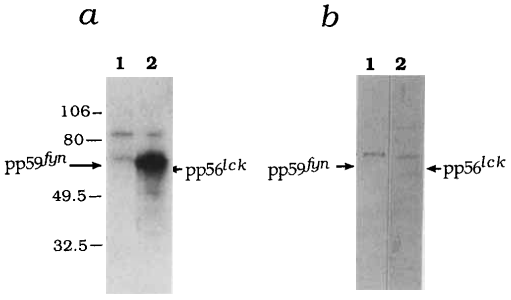

Figure 2. Comparison of p59^{fyn} and p56^{lck} from human PBL. a) Autophosphorylation of immunoprecipitated p59^{fyn} (lane 1) and p56^{lck} (lane 2). b) Immunoblotting of PBL membranes with anti-p59^{fyn} (lane 1) and anti-p56^{lck} (lane 2).

Table 1. Activation of p59^{fyn} by CD45[a)]

Immunoprecipitating antibody	Na_3VO_4 (1 mM)	PTK Activity (fmol/min/10^6 cells)	% of control
Anti-fynN	–	16.7 + 2.8 (n = 6)	100
Anti-fynN + GAP 8.3[b)]	–	66.8 + 11.6 (n = 6)	399
Anti-fynN + GAP 8.3	+	18.7 + 9.3 (n = 7)	112
Anti-fynN + OKT3[c)]	–	24.3 + 2.3 (n = 2)	145
Anti-fynN + anti-TcR ζ[d)]	–	18.7 + 0.1 (n = 2)	112

a) The two proteins were immunoprecipitated separately, mixed as indicated and incubated at 30 °C for 3 min with or without 1 mM Na_3VO_4 prior to the PTK assay (with a peptide substrate).
b) GAP8.3 is a monoclonal antibody against CD45.
c) OKT3 is a monoclonal antibody against CD3.
d) Anti-TcR ζ is a polyclonal antiserum against the TcR ζ.

Carl_G_190x270_mm_blokki_FINAL.indd 100 06-Aug-23 1:53:32 PM

Immunoprecipitated and similarly autophosphorylated p56^{lck}, run in parallel lanes, migrated as a 2–3 kDa smaller protein (Fig. 2a, lane 2). In immunoblots of human T cell membranes the anti-p59^{fyn} antiserum recognized a 59-kDa band (Fig. 2b, lane 1), slightly above the band representing p56^{lck} in the same membrane preparation (Fig. 2b, lane 2). Since two different antisera are likely to differ in affinity, the relative amounts of p56^{lck} and p59^{fyn} cannot be determined from these experiments. The immunoprecipitated p59^{fyn} also phosphorylated a synthetic tyrosine-containing peptide similar to the major autophosphorylation site of *src* family kinases (Table 1).

3.3 CD45 dephosphorylates p59^{fyn} at Tyr^{531}

Since attempts to label p59^{fyn} in PBL metabolically labeled with [^{32}P] ortho-phosphate to high enough specific activity to allow peptide mapping were unsuccessful, we used an alternative approach to study the dephosphorylation of p59^{fyn} by CD45. Schuh and Brugge [23] have established an assay in which pp60$^{c\text{-}src}$ becomes phosphorylated mainly on its C-terminal tyrosine residue, Tyr^{527} (corresponding to Tyr^{531} in p59^{fyn}). This assay can also be applied to p56^{lck} (our unpublished observation). In these experiments p59^{fyn} was labeled with [γ-^{32}P] ATP and used as a substrate for CD45. Purified CD45 rapidly dephosphorylated the labeled p59^{fyn} (Fig. 3a). When the labeled p59^{fyn} (Fig. 3A, lane 1) was eluted from the gel, oxidized and digested with TPCK-trypsin and the resulting peptides subjected to two-dimensional separation on thin layer plates, the label was mostly recovered in a doublet [27] corresponding to the Tyr^{531}-containing peptide, while the Tyr^{420}-containing peptide was barely detectable (Fig. 3b). A similar analysis of CD45-treated labeled p59^{fyn} (Fig. 3a, lane 2) did not reveal any detectable radiolabeled spots (not shown), suggesting that CD45 can dephosphorylate the regulatory Tyr^{531}. Whether the autophosphorylation site, Tyr^{420}, was dephosphorylated by CD45 remains uncertain, since it contained very low amounts of phosphate to begin with. The amino acid sequences of the labeled tryptic peptides are shown in Fig. 3c.

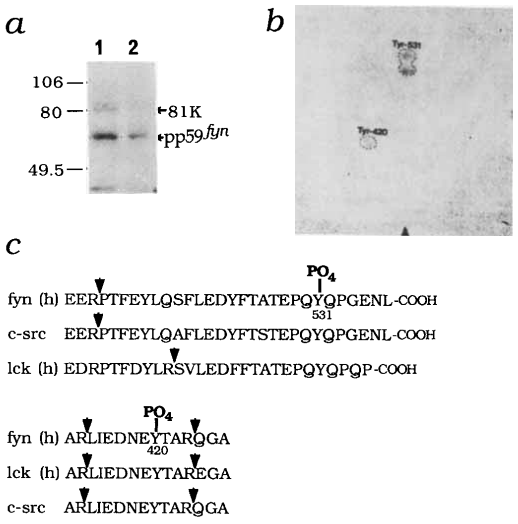

Figure 3. Dephosphorylation of p59^{fyn} by CD45. a) p59^{fyn} was labeled *in situ* with [γ-^{32}P] ATP, immunoprecipitated and treated with medium alone (lane 1) or 1.5 U (1.6 µg) or purified CD45 (lane 2), b) Tryptic peptide map of p59^{fyn} cut out from lane 1 in a). Electrophoresis was in the horizontal direction, anode to the left, and the second dimension was ascending chromatography. The arrow marks sample origin. c) Predicted tryptic phosphopeptides derived from p59^{fyn}, compared to those from p56^{lck} and pp60$^{c\text{-}src}$. The upper peptide contains Tyr^{531}, the lower peptide contains Tyr^{420}. The arrows mark the points of tryptic cleavage.

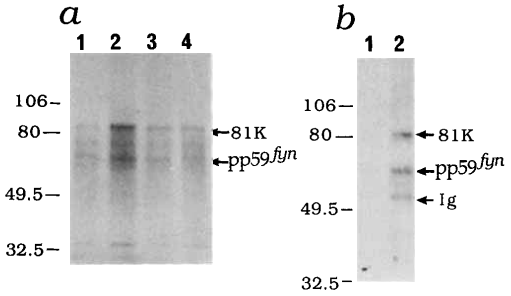

Figure 4. Activation of p59^{fyn} by CD45 measured as its subsequent autophosphorylation. a) Autophosphorylation of p59^{fyn} treated for 3 min at 30 °C with agarose-bound goat anti-mouse Ig alone (lane 1), immunoprecipitated CD45 (lane 2), immunoprecipitated CD45 + 1 mM Na_3VO_4 (lane 3) or immunoprecipitated CD3-ε (lane 4). b) Autophosphorylation of p59^{fyn} treated for 3 min at 30 °C with medium alone (lane 1) or 1.5 U (1.6 µg) of purified CD45 (lane 2).

3.4 CD45 activates p59^{fyn}

To determine the effect of CD45-mediated dephosphorylation of p59^{fyn} on its enzymatic activity we first immunoprecipitated catalytically active CD45 with the monoclonal antibody GAP 8.3 as previously described [19, 20]. When p59^{fyn} and CD45 immunoprecipitates (which did not have PTK activity) were mixed and incubated at 30 °C for 0–5 min prior to PTK activity measurement, a rapid increase in PTK activity towards the exogenous peptide substrate was observed (Table 1). The increase was about fourfold, reached a maximum within 1 min, and was completely inhibited by 1 mM Na_3VO_4, a potent inhibitor of the PTPase activity of CD45 [20]. Control immunoprecipitates (which displayed negligible PTK activity) did not influence the activity of p59^{fyn}.

Treatment of p59^{fyn} with immunoprecipitated CD45 also caused an increase in its subsequent autophosphorylation and in the phosphorylation of the co-immunoprecipitated 81-kDa protein (Fig. 4a). Other immunoprecipitated proteins did not influence the activity of p59^{fyn}, except CD3 immunoprecipitates which gave a small increase in total PTK activity. These precipitates might have contained some additional p59^{fyn} even if the conditions used did not favor co-immunoprecipitation [9].

To confirm that the observed effect of CD45 was due to this molecule and not to possible contaminating factors, we

Carl_G_190x270_mm_blokki_FINAL.indd 101 06-Aug-23 1:53:32 PM

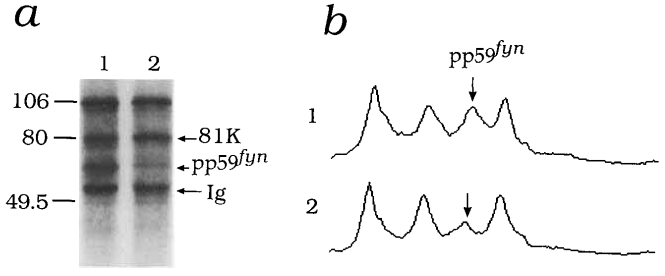

Figure 5. In vivo inactivation of p59^{fyn} using PAO, an inhibitor of CD45. p59^{fyn} was immunoprecipitated from cells treated without (lane 1) or with 30 μM (lane 2) of PAO for 60 min. The washed immunopreciptates were incubated with 5 μCi [γ-^{32}P] ATP for 10 min at 30°C. a) Autoradiogram of the gel, b) densitometric scan of the gel in a).

purified catalytically active CD45 from PBL. The final preparation contained several isoforms of CD45 as determined by immunoblotting, and a few minor contaminating proteins of lower M_r as visualized by silver staining. Using o-phospho-L-tyrosine as a substrate the specific activity of the enzyme was 0.94 μmol/min/mg at 37°C. When p59^{fyn} was treated with 1.6 μg of this purified CD45, a several fold increase in its capacity to autophosphorylate and phosphorylate Ig heavy chains and the 81-kDa protein, was observed (Fig. 4b).

3.5 PTPase regulates p59^{fyn} *in vivo*

Phosphotyrosine phosphatases can be efficiently inhibited in intact cells by treatment with submillimolar concentrations of phenylarsine oxide (PAO) [27]. This drug does not inhibit the catalytic activity of p59^{fyn} *in vitro* [28], but blocks TcR/CD3-induced tyrosine phosphorylation presumably by blocking a PTPase-mediated event [28]. When resting T cells were treated with 30 μM of PAO for 1 h, and p59^{fyn} was isolated by immunoprecipitation and allowed to autophosphorylate, it had lost most of its catalytic activity (Fig. 5). The phosphorylation of other proteins in the immunoprecipitate did not change. Whether these are substrates for p59^{fyn} is not clear and their phosphorylation does not necessarily reflect the activity of p59^{fyn} since they might be present in minor quantities. Nevertheless, our finding is compatible with the notion that a PTPase (such as CD45) constantly dephosphorylates the regulatory Tyr^{531} of p59^{fyn} and thereby keeps it at a low, but detectable, basal level of activity. When this PTPase is blocked by PAO, the dephosphorylation of Tyr^{531} ceases and the activity of p59^{fyn} declines. We cannot, however, exclude the possibility that phosphate also accumulates on Tyr^{420} during treatment of the cells with PAO. The viability of the cells was not reduced by treatment with 30 μM of PAO for 1 h and the level of p59^{fyn} did not change as determined by immunoblotting.

4 Discussion

By the means of antibody-induced capping and immunofluorescence labeling experiments, we revealed a significant and specific co-localization between the receptor PTPase CD45 and the intracellular PTK p59^{fyn} under physiologically relevant conditions in functional T lymphocytes. The nature of the interaction remains to be elucidated. In addition, our findings show that inhibition of intracellular PTPase leads to reduced kinase activity of p59^{fyn} and that p59^{fyn} can be activated by CD45-mediated dephosphorylation. Dephosphorylation most likely occurs at the regulatory tyrosine, Tyr^{531}. This tyrosine residue is implicated in suppression of the catalytic and transforming activity of p59^{fyn} [17] and is apparently phosphorylated to high stoichiometry in normal T lymphocytes [21]. Taken together, our findings suggest that CD45 is a physiologic regulator of p59^{fyn}. Apparently, CD45 keeps p59^{fyn} at a measurable basal level of activity by constantly dephosphorylating its Tyr^{531}. This pre-existing dephosphorylation and activation of p59^{fyn} is probably essential for TcR/CD3-induced T cell activation. Indeed, in a mutant T cell line lacking CD45, no tyrosine phosphorylation of cellular substrates or subsequent inositol phospholipid hydrolysis was seen after triggering of the TcR/CD3 [29, 30].

CD45 is found at high levels on all leukocytes with different isoforms expressed in leukocyte subpopulations [31]. Many members of the *src* family of PTK are also restricted to specific cells of hematopoietic origin. Thus, *lck* is expressed almost exclusively in T lymphocytes [12], *lyn* and *blk* are abundant in B lymphocytes [32, 33], *fgr* in natural killer cells [34], *hck* in mature cells of the myeloid or monocytic lineages [35] and c-*src* in platelets [36]. Since all these PTK have an analogous conserved tyrosine residue near their carboxy-terminal end and they are found in cells having high levels of CD45, it seems plausible that they all are regulated by this PTPase.

The extracellular domains of different CD45 isoforms might interact with different cellular [37] or soluble ligands. Thus, the combination of CD45 isoform and *src* family PTK present in a particular leukocyte, could have a major impact on the regulation of tyrosine phosphorylation in that cell. The CD4$^-$CD8$^-$ T cells from mice homozygous for the *lpr* gene express high levels of p59^{fyn} [38] and, aberrantly, the B cell form of CD45, B220 [39]. In these T cells the TcR ζ is constitutively tyrosine phosphorylated [40] and the cells accumulate in large numbers in the lymph nodes of the animals thereby accelerating a systemic autoimmune syndrome [39]. We and others have found that the *lpr* T cells appear to be in a preactivated state *in vivo* ([41], Coggeshall et al. submitted), as determined by their constitutively enhanced inositol phospholipid turnover and elevated tyrosine phosphorylation of a number of cellular substrates. This is compatible with the notion that p59^{fyn} is a transducer of mitogenic signals in T cells and that CD45 plays a role in the regulation of its activity.

The authors are grateful to Dr. T. Kawakami (La Jolla Institute for Allergy and Immunology, La Jolla, CA) for the kind gift of p59^{fyn} antiserum and to Dr. Vaclav Horejsi (Czechoslovak Academy of

Carl_G_190x270_mm_blokki_FINAL.indd 102 06-Aug-23 1:53:32 PM

Sciences, Prague) for the MEM-28 monoclonal antibody. We thank Ms. Aili Grundström for technical assistance and our colleagues for stimulating discussions.

Received October 29, 1991; in revised form December 30, 1991.

5 References

1 Mustelin, T., Coggeshall, K. M., Isakov, N. and Altman, A., *Science* 1990. *247:* 1584.
2 June, C. H., Fletcher, M. C., Ledbetter, J. A. and Samelson, L. E., *J. Immunol.* 1990. *144:* 1591.
3 June, C. H., Fletcher, M. C., Ledbetter, J. A., Schieven, G. L., Siegel, J. N., Phillips, A. F. and Samelson, L. E., *Proc. Natl. Acad. Sci. USA* 1990. *87:* 7722.
4 Park, D. J., Rho, H. W. and Rhee, S. G., *Proc. Natl. Acad. Sci. USA* 1991. *88:* 5453.
5 Secrist, J. P., Karnitz, L. and Abraham, R. T., *J. Biol. Chem.* 1991. *266:* 12135.
6 Berridge, M. J., *Biochem. J.* 1984. *220:* 345.
7 Semba, K., Nishizawa, M., Miyajima, N., Yoshida, M. C., Sukegawa, J., Yamanashi, Y., Sasaki, M., Yamamoto, T. and Toyoshima, K., *Proc. Natl. Acad. Sci. USA* 1986. *83:* 5459.
8 Kawakami, T., Pennington, C. Y. and Robbins, K. C., *Mol. Cell. Biol.* 1986. *6:* 4195.
9 Samelson, L. E., Phillips, A. F., Luong, E. T. and Klausner, R. D., *Proc. Natl. Acad. Sci. USA* 1990. *87:* 4358.
10 Gassmann, M., Guttinger, M., Amrein, K. E. and Burn, P., *Eur. J. Immunol.* 1992. *22:* 283.
11 Cooke, M. P., Abraham, K. M., Forbush, K. A. and Perlmutter, R. M., *Cell* 1991. *65:* 281.
12 Marth, J. D., Peet, R., Krebs, E. G. and Perlmutter, R. M., *Cell* 1985. *43:* 393.
13 Chalupny, N. J., Ledbetter, J. A. and Kavathas, P., *EMBO J.* 1991. *10:* 1201.
14 Glaichenhaus, N., Shastri, N., Littman, D. R. and Turner, J. M., *Cell* 1991. *64:* 511.
15 Abraham, N., Miceli, M. C., Parnes, J. R. and Veillette, A., *Nature* 1991. *350:* 62.
16 Marth, J. D., Cooper, J. A., King, C. S., Ziegler, S. F., Tinker, D. A., Overell, R. W., Krebs, E. G. and Perlmutter, R. M., *Mol. Cell. Biol.* 1988. *8:* 540.
17 Kawakami, T., Kawakami, Y., Aaronson, S. A. and Robbins, K. C., *Proc. Natl. Acad. Sci. USA* 1988. *85:* 3870.
18 Amrein, K. E. and Sefton, B. M., *Proc. Natl. Acad. Sci. USA* 1988. *85:* 4247.
19 Mustelin, T., Coggeshall, M. K. and Altman, A., *Proc. Natl. Acad. Sci. USA* 1989. *86:* 6302.
20 Mustelin, T. and Altman, A., *Oncogene* 1990. *5:* 809.
21 Kawakami, Y., Furue, M. and Kawakami, T., *Oncogene* 1989. *4:* 389.
22 Sinigaglia, F., Romagnoli, P., Guttinger, M., Takacs, B. and Pink, J. R. L., *Methods Enzymol.* 1991. *203:* 370.
23 Schuh, S. M. and Brugge, J. S., *Mol. Cell. Biol.* 1988. *8:* 2465.
24 Hunter, T. and Sefton, B. M., *Proc. Natl. Acad. Sci. USA* 1980. *77:* 1311.
25 Hurley, T. R. and Sefton, B. M., *Oncogene* 1989. *4:* 265.
26 Cooper, J. A., Gould, K. L., Cartwright, C. A. and Hunter, T., *Science* 1986. *231:* 1431.
27 Cheng, S. H., Piwnica-Worms, H., Harvey, R. W., Roberts, T. M. and Smith, A. E., *Mol. Cell. Biol.* 1988. *8:* 1736.
28 Garcia-Morales, P., Minami, Y., Luong, E., Klausner, R. D. and Samelson, L. E., *Proc. Natl. Acad. Sci. USA* 1990. *87:* 9255.
29 Pingel, J. T. and Thomas, M. L., *Cell* 1989. *58:* 1055.
30 Koretzky, G. A., Picus, J., Thomas, M. L. and Weiss, A., *Nature* 1990. *346:* 66.
31 Thomas, M. L., *Annu. Rev. Immunol.* 1989. *7:* 339.
32 Yamanishi, Y., Kakiuchi, T., Mizuguchi, J., Yamamoto, T. and Toyoshima, K., *Science* 1991. *251:* 192.
33 Dymecki, S. M., Niederhuber, J. E. and Desiderio, S. V., *Science* 1990. *247:* 332.
34 Inoue, K., Yamamoto, T. and Toyoshima, K., *Mol. Cell. Biol.* 1990. *10:* 1789.
35 Ziegler, S. F., Marth, J. D., Lewis, D. B. and Perlmutter, R. M., *Mol. Cell. Biol.* 1989. *7:* 2276.
36 Golden, A., Nemeth, S. P. and Brugge, J. S., *Proc. Natl. Acad. Sci. USA* 1986. *83:* 852.
37 Stamenkovic, I., Sgroi, D., Aruffo, A., Sy, M. S. and Anderson, T., *Cell* 1991. *66:* 1133.
38 Katagiri, T., Urakawa, K., Yamanashi, Y., Semba, K., Takahashi, T., Toyoshima, K., Yamamato, T. and Kano, K., *Proc. Natl. Acad. Sci. USA* 1989. *86:* 10064.
39 Theofilopoulos, A. N. and Dixon, F. J., *Adv. Immunol.* 1985. *37:* 269.
40 Samelson, W. E., Davidson, W. F., Morse, H. C. and Klausner, R. D., *Nature* 1986. *324:* 674.
41 Tomita-Yamaguchi, M. and Santoro, T. J., *J. Immunol.* 1990. *144:* 3946.

Carl_G_190x270_mm_blokki_FINAL.indd 103 06-Aug-23 1:53:32 PM

LEUKOCYTE SURFACE ORIGIN OF HUMAN α_1-ACID GLYCOPROTEIN (OROSOMUCOID)*

BY CARL G. GAHMBERG AND LEIF C. ANDERSSON

(From the Department of Bacteriology and Immunology, and the Transplantation Laboratory, Department of Surgery IV, University of Helsinki, Helsinki 29, Finland)

Human α_1-acid glycoprotein (orosomucoid) (α_1-AG)[1] constitutes the main component of the seromucoid fraction of human plasma. It belongs to the acute phase proteins, which increase under conditions such as inflammation, pregnancy, and cancer (1, 2). α_1-AG has previously been found to be synthesized in liver (3), and after removal of terminal sialic acids, it is cleared from the circulation by binding to a receptor protein on liver cell plasma membranes (4).

The structure of α_1-AG is well known. It is composed of a single polypeptide chain and contains ≅45% carbohydrate including a large amount of sialic acid. The carbohydrate is located in the first half of the peptide chain linked to asparagine residues (5, 6).

The function of α_1-AG is unclear. However, Schmid et al. (5) and Ikenaka et al. (7) and reported that the amino acid sequence of the protein shows a significant homology with human IgG. This finding and the striking increase in inflammatory and lymphoproliferative disorders made us consider the possibility that leukocytes could be directly involved in the synthesis and release of α_1-AG.

We report here the presence of a membrane form of α_1-AG, with an apparent mol wt of 52,000, on normal human lymphocytes, granulocytes, and monocytes. By the use of internal labeling with [^{3}H]leucine in vitro, we demonstrate that the membrane protein is synthesized by lymphocytes. It is apparently subsequently cleaved and released as the soluble serum form with the normal mol wt of 41,000.

Materials and Methods

Isolation of α_1-AG. α_1-AG was isolated from the urine of patients with acute infectious mononucleosis by modifications of previously published methods (8). 6 liters of urine were collected, dialyzed against tap water overnight, and lyophilized. The powder was dissolved in 0.02 M sodium phosphate, pH 7.2, and applied to a 50-ml column of DEAE-cellulose made in the same buffer. After washing, a linear 200-ml gradient of 0.02 M sodium phosphate (200 ml of 1 M NaCl, 0.02 M sodium phosphate) was applied. The α_1-AG-containing fractions, which were identified by polyacrylamide slab gel electrophoresis, eluted with an NaCl concentration of 0.05–0.15 M. These were combined, dialyzed against water, and lyophilized. The powder was dissolved in 95 ml of

* Supported by the Academy of Finland, the Finnish Cancer Society, and the Sigrid Jusélius Stiftelse.

[1] *Abbreviations used in this paper:* α_1-AG, α_1-acid glycoprotein; AET, 2-amino ethylisothiouronium bromide; buffer A, 0.15 M NaCl, 0.01 M sodium phosphate pH 7.4, 1% Triton X-100, 2 mM phenyl methyl sulfonyl fluoride, 1% ethanol; CNBr, cyanogen bromide; FITC, fluorescein isothiocyanate, LBL, lymphoblastoid B-cell line; MGG, May-Gruenwald-Giemsa stain; MLC, mixed lymphocyte culture; PBS, 0.15 M NaCl, 0.01 M sodium phosphate, pH 7.4; SDS, sodium dodecyl sulfate; SRBC, sheep erythrocytes.

J. EXP. MED. © The Rockefeller University Press · 0022-1007/78/0801-0507$1.00

Carl_G_190x270_mm_blokki_FINAL.indd 104 06-Aug-23 1:53:32 PM

H_2O, and 5 ml of 1 M sodium acetate was added. After addition of ammonium sulfate to a final concentration of 2.73 M, the mixture was left at 4°C for 16 h. After centrifugation at 12,500 rpm in a Sorvall SS-34 rotor for 15 min, the supernate was recovered. The pH of the supernate was adjusted to 4.9 with 2 N HCl, and this was left again at 4°C for 16 h. After centrifugation, the pH of the supernate was adjusted to 3.7 with 2 N HCl, and the sample was left at 4°C for 16 h. After centrifugation, the supernate was removed and the sediment was dissolved in H_2O, dialyzed against H_2O, and lyophilized. The sample was then passed through a 15-ml column of concanavalin A-Sepharose 4B (Pharmacia Fine Chemicals, Uppsala, Sweden) in 0.15 M NaCl-0.01 M sodium phosphate, pH 7.4 (PBS), and after washing it was eluted with 0.1 M α-methyl mannopyranoside (Calbiochem, San Diego, Calif.). The peak fractions eluted with the sugar were pooled, dialyzed against H_2O, and lyophilized. This sample was then passed over an Ultrogel AcA54 column (LKB Produkter, Stockholm, Sweden) in PBS, and the peak fractions were combined, dialyzed against H_2O, and lyophilized. The final yield of purified protein was 33 mg.

Isolation and Cultivation of Human Leukocytes. The following main populations of blood cells were isolated: granulocytes, monocytes, platelets, T lymphocytes, and B lymphocytes. They were isolated from buffy coats supplied by the Finnish Red Cross Blood Transfusion Service, Helsinki, Finland. The platelets and mononuclear cells were separated from the granulocytes and erythrocytes by a one-step Ficoll-Isopaque (density 1.077; Pharmacia Fine Chemicals) gradient centrifugation (9), at 400 *g* for 40 min.

Purification of Granulocytes. The pellets obtained after Ficoll-Isopaque centrifugation that contained erythrocytes and granulocytes were suspended in 20 ml of PBS. 10 ml of 0.15 M NaCl containing 6% dextran (Macrodex 6%; Leiras, Turku, Finland) was added, and the cell suspension was kept for 40 min at 37°C. The granulocyte-rich buffy coat was then collected, and contaminating erythrocytes were lysed by incubation in 0.017 M Tris-0.84% NH_4Cl, pH 7.45. The leukocytes were then washed three times with PBS. This procedure yielded a cell population which contained >97% granulocytes as judged from May-Gruenwald-Giemsa (MGG)-stained cytocentrifuged cell smears. The cell viability was close to 100%, as seen in the trypan blue exclusion test.

Purification of Platelets. The platelets were purified from the cell population obtained from the interphase after Ficoll-Isopaque centrifugation. This cell population was suspended in PBS, centrifuged for 10 min at 200 *g*, and the platelet-rich supernate was recovered. This procedure was repeated once, and the platelets were then pelleted at 400 *g* for 20 min. The purity of the platelet preparation approached 100%, and the contamination by other blood cells was always <0.002%.

Purification of Monocytes. The blood monocytes were separated from the cell population recovered at the interphase after Ficoll-Isopaque centrifugation. The platelets were depleted by three washes with PBS at 200 *g* for 10 min. The mononuclear cell population was mixed at a ratio of 1:50 with 2-amino ethylisothiouronium bromide (AET) (Sigma Chemical Co., St. Louis, Mo.) treated sheep erythrocytes (SRBC) (10). After incubation for 15 min at 37°C, the mixture was centrifuged for 10 min at 200 *g* and the T cells were allowed to rosette with the AET-SRBC for 1 h on ice. The pellet was then gently suspended in cold PBS containing 30% newborn calf serum, and the rosette-forming cells were separated from the non-rosette-forming cells by Ficoll-Isopaque centrifugation. The cell population recovered from the interphase mainly contained monocytes and non-T lymphocytes. The monocytes were then purified from the contaminating lymphocytes by a 1-*g* velocity sedimentation (11). After sedimentation for 4 h at 4°C, the gradient was drained into 20-ml fractions, and the cell content of each fraction was analyzed from MGG-stained smears. The early fractions which contained mainly monocytes were pooled. The cell preparation thus obtained contained 90–95% monocytes, as judged by conventional morphological criteria. The viability always exceeded 98%. Slight contamination was caused by occasional lymphoblasts, myeloid precursor cells, and some granulocytes.

Purification of T lymphocytes. The platelet-depleted mononuclear cell population recovered from the Ficoll-Isopaque centrifugation was passed over a human Ig–rabbit anti-human-Ig column as described by Wigzell et al. (12). The column-passed lymphocyte population contained <1% surface immunoglobulin-bearing cells, as judged by staining with fluorescein isothiocyanate (FITC)-conjugated polyvalent sheep anti-human immunoglobulin obtained from Professor Astrid Fagraeus, State Bacteriology Laboratory, Stockholm, Sweden. The viability of the T-cell population was always >98%, and >95% of the cells formed rosettes with AET-SRBC.

Purification of B Lymphocytes. The mononuclear cells obtained after Ficoll-Isopaque centrifugation were suspended into RPMI culture medium supplemented with 10% normal human AB

Carl_G_190x270_mm_blokki_FINAL.indd 105 06-Aug-23 1:53:32 PM

plasma. Carbonyl iron was added and the suspension was incubated for 1 h at 37°C. The majority of the phagocytic cells was then removed with a magnet. The phagocyte-depleted cell population was allowed to rosette with AET-SRBC as described above. The T cells were depleted by centrifugation of the rosette-forming cell-containing cell suspensions on a Ficoll-Isopaque gradient. The non-T lymphocytes recovered from the interphase were further purified by velocity sedimentation as described above. The later fractions obtained after sedimentation for 4 h contained mainly small lymphocytes, as judged from MGG-smears. These fractions were pooled and the cell population thus obtained was contaminated by <3% nonlymphocytic cells. This lymphocyte suspension was further fractionated over an Ig–anti-Ig column at 4°C to minimize Fc binding. The lymphocytes retained by the column were mechanically eluted by shaking the glass beads in PBS. 86% of the eluted lymphocytes stained positively for surface Ig, and <2% bound AET-SRBC. This preparation was designated B lymphocytes.

Establishment of Continuous B Lymphoblastoid Cell Lines (LBL) from Peripheral Blood. LBL were established by cultivation of T-lymphocyte-depleted blood leukocytes from different patients with acute infectious mononucleosis (13). The cell lines studied in this work were grown continuously for more than 4 mo before use in RPMI-1640 medium supplemented with 10% calf serum.

Mixed Lymphocyte Culture (MLC). Human blood T lymphocytes were purified and cultivated in RPMI-1640 medium supplemented with fetal calf serum or rabbit serum with mitomycin C (30 μg/ml) treated allogeneic leukocytes at an initial density of 10^6 responder cells and 2×10^6 stimulator cells/ml.

Labeling of Allogen-Activated T Lymphocytes with [^{3}H]Leucine. MLC cells obtained after 5 days in culture were washed in Dulbecco's PBS and suspended in 15 ml of leucine and serum-free Eagle's minimal essential medium. To this was added 1.5 mCi [^{3}H]L-leucine (58 Ci/mmole; The Radiochemical Centre, Amersham, England) and the cells were incubated at 37°C for 16 h. The cells were then pelleted by centrifugation and the medium was recovered. The medium was extensively dialyzed against H_2O and lyophilized. It was then dissolved in 5 ml of PBS and centrifuged at 100,000 *g* for 60 min in a Beckman L2-50 centrifuge, and the supernates were recovered. The cells were washed three times in PBS and lysed in PBS containing 1% Triton X-100, 2 mM phenyl methyl sulfonyl fluoride (Sigma Chemical Co.), 1% ethanol (buffer A). After centrifugation at 100,000 *g* for 60 min, the supernate was recovered. For subsequent immune precipitations, both the growth medium and the cell extract were passed through 2-ml columns of Lens culinaris-Sepharose, and the absorbed glycoproteins were eluted with 0.1 M α-methyl mannoside in buffer A. Lens culinaris beans were obtained from Dr. M. J. Crumpton, Medical Research Council, Mill Hill, England, and the lectins were purified by affinity chromatography on Sephadex G-50 (14) and coupled to Sepharose 4B (Pharmacia Fine Chemicals) by CNBr activation (15). Aliquots of the fractions were counted for radioactivity in a Wallac-LKB 81000 liquid scintillation counter (16). The radioactive fractions obtained after elution with the sugar hapten were pooled and used for immunoprecipitations.

Preparation of α_1-AG Antiserum. Rabbits were injected three times at 2-wk intervals with 0.5 mg of α_1-AG boiled in 1% sodium dodecyl sulfate (SDS), emulsified in Freund's adjuvant (Difco Laboratories, Detroit, Mich.), and bled 10 days after the last injection.

Surface Labeling of Cells. Cells were labeled with ^{3}H by treatment with neuraminidase and galactose oxidase followed by NaB^3H_4 (16). The labeling conditions have been described in detail previously (17). The *Vibrio cholerae* neuraminidase (500 U/ml; Behring-Werke AG, Marburg-Lahn, W. Germany) and galactose oxidase (Kabi AB, Stockholm, Sweden) preparations did not contain proteolytic activity when assayed as described (16). NaB^3H_4 (26 Ci/mmol) was obtained from The Radiochemical Centre. After labeling, the cells were dissolved in buffer A and centrifuged at 10,000 *g* for 15 min, and the supernates were recovered.

Chemical Determinations. Protein was determined according to Lowry et al. (18), with bovine serum albumin used as a standard. Amino acid analysis was performed with a Beckman 120 C amino acid analyzer (Beckman Instruments, Inc., Fullerton, Calif.) after hydrolysis in 6 N HCl under vacuum at 110°C for 22 h. No correction was made for the destruction of amino acids. Methionine and 1/2 cystine were determined after performic acid oxidation (19). Sialic acids were determined as described (20) with *N*-acetyl neuraminic acid (Sigma Chemical Co.) as a standard. Amino sugars were quantitated by the Elson-Morgan reaction (21), and the proportions of *N*-acetyl glucosamine and *N*-acetyl galactosamine were estimated by the use of the amino acid

Carl_G_190x270_mm_blokki_FINAL.indd 106 06-Aug-23 1:53:32 PM

analyzer (22). Neutral sugars were determined after hydrolysis in 4 N H_2SO_4 at 100°C for 4 h as alditol acetates (23).

Labeling of Cell Culture Medium and Purified α_1-AG with ^{125}I. MLCs carried on for 5 days in RPMI-1640 culture medium supplemented with 1% rabbit preimmunization serum were done as described above. The cells were pelleted by centrifugation, and the supernate was centrifuged at 100,000 *g* for 60 min. After dialysis against H_2O at 4°C for 24 h, 10 μl of the medium and 10 μg of purified urinary α_1-AG were iodinated by the chloramine-T method (24) using 0.5 mCi carrier-free ^{125}I (Amersham Corp.). Fractions were collected after passing through a 0.5 × 10-cm Sephadex G-25 column made in PBS and counted in a Wallac-LKB 80000 gamma sample counter.

Immunoprecipitations Using Protein A Containing Staphylococcus aureus (Strain Cowan I). Immunoprecipitations were made from Triton X-100 extracts of [^{3}H]leucine-labeled cells or [^{3}H]leucine-labeled culture medium which were eluted with sugar from the Lens culinaris columns. Immunoprecipitations were also done directly from Triton X-100 extracts of surface-labeled cells and ^{125}I-labeled culture medium. The samples were pretreated with 5 μg mouse IgG and 5 μl rabbit anti-mouse IgG (prepared by standard techniques) for 1 h at 0°C. Then, 100 μl of a 10% suspension of *S. aureus* Cowan I strain, obtained from Dr. P. Landwall of the Karolinska Institute, Stockholm, Sweden (25) was added, and the samples were further incubated at 0°C for 60 min. 100 μl of the staphylococcal suspension bound IgG from 6 μl of rabbit serum. The tubes were then centrifuged at 3,000 *g* for 10 min in a table centrifuge at 4°C, and the supernates were recovered. To identical aliquots of this supernate were added either 5 μl rabbit anti-α_1-AG antiserum, or 5 μl rabbit preimmunization serum, and the tubes were incubated at 0°C for 2 h. Then, 200 μl of the staphylococcal suspension was added, and the incubation was continued at 0°C for 1 h. The staphylococci were then washed three times by centrifugation in 0.15 M NaCl, 0.05% Triton X-100, 5 mM EDTA, 0.02% sodium azide, pH 7.4, and the absorbed antigens were eluted by boiling for 2 min in 1% SDS. The staphylococci were pelleted by centrifugation, and the supernates were recovered and used for polyacrylamide gel electrophoresis.

Radioimmunoassay of α_1-AG from Supernates of Cell Cultures. One of the lymphoblastoid B-cell lines was cultured at an initial cell density of 5 × 10^5 cells/ml in RPMI-1640 culture medium containing 10% fetal calf serum (Flow Laboratories, Glasgow, Scotland). At indicated times, 1.5-ml samples were taken, the cell number was counted, and 0.5-ml aliquots of the supernates were used for radioimmunoassay.

A radioimmunoassay standard curve was made by using 0.00001–10 μg of purified α_1-AG in 0.5 ml of the same fresh cell culture medium. 10 μl of rabbit preimmunization serum was added as carrier, and the samples were incubated with ≅ 30,000 cpm of ^{125}I-labeled α_1-AG and 0.1 μl of rabbit anti-α_1-AG antiserum for 16 h at 4°C. The antiserum was calibrated to bind ≅ 30% of the total radioactivity. Then 100 μl of sheep anti-rabbit IgG antiserum was added, and after 1 h at 4°C, the samples were centrifuged and the pellets were counted for radioactivity. The test samples were made in the same way, except that the purified α_1-AG was omitted. The standard curve was linear for 0.0005–0.5 μg of α_1-AG.

Cleavage of Proteins with Cyanogen Bromide (CNBr). ^{125}I-labeled purified α_1-AG and labeled proteins eluted from cylindrical polyacrylamide gels were cleaved by treatment with CNBr in 70% formic acid for 24 h at room temperature (26). After dilution with 20 vol of H_2O, the samples were lyophilized and run on cylindrical polyacrylamide gels.

Polyacrylamide Gel Electrophoresis. Slab and cylindrical polyacrylamide gels were run according to Laemmli (27) in the presence of SDS with an acrylamide concentration of 8%. Slab gels were stained with Coomassie brilliant blue according to Weber and Osborn (28). Cylindrical gels were sliced and counted (16). Slab gels were treated for fluorography (29) and the gels were vacuum-dried and covered with Kodak RP X-Omat film (Eastman Kodak Co., Rochester, N.Y.) and exposed for 1–14 days at −70°C. The films were photographed and scanned with a Joyce-Loebl Chromoscan (Joyce, Loebl and Co., Ltd., Gateshead-on-Tyne, England). ^{14}C-labeled standard proteins were prepared as described (30).

Indirect Immunofluorescence. To exclude nonspecific IgG binding to Fc receptors, F(AB)2 fragments were prepared from anti-α_1-AG anti-serum. 20 mg of IgG was digested with 0.5 mg of porcine pepsin (Schwarz/Mann Div. Becton, Dickinson & Co., Orangeburg, N.Y.) for 16 h at 37°C in 0.1 M sodium acetate buffer, pH 4.5, and the F(AB)2 fragments were isolated by gel filtration on Ultrogel AcA34 (LKB Produkter). The F(AB)2 preparation appeared pure on polyacrylamide gel electrophoresis.

Carl_G_190x270_mm_blokki_FINAL.indd 107 06-Aug-23 1:53:32 PM

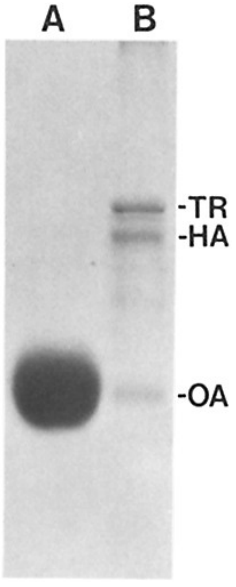

FIG. 1. Polyacrylamide gel electrophoresis of purified α_1-AG. (A), 50 μg of purified α_1-AG was run on a polyacrylamide slab gel in the presence of SDS and 2-mercaptoethanol and stained with Coomassie brilliant blue. (B), standard proteins: TR, transferrin; HA, human albumin; OA, ovalbumin.

Cells were washed and suspended in 100 μl of ice-cold PBS containing 20% fetal calf serum. 100 μg anti-α_1-AG F(AB)2, 10 μl anti-α_1-AG antiserum or 10 μl preimmunization serum were added. After 30 min on ice, the cells were washed twice with 10 ml of cold fetal calf serum in PBS and suspended in 20 μl of 1:20 diluted FITC-conjugated IgG (1 mg/ml) isolated from sheep anti-rabbit IgG antiserum. After 20–30 min on ice, the cells were washed and examined in a Zeiss Universal fluorescence microscope (Carl Zeiss, Inc., New York) equipped with epi-illuminator III RS and a high pressure mercury lamp (200 W). For capping experiments, the FITC-stained cells were incubated at 37°C.

Results

Purity, Amino Acid and Carbohydrate Compositions of Urinary α_1-AG. When α_1-AG was isolated from urine and analyzed by slab polyacrylamide gel electrophoresis, only one band was obtained with an apparent mol wt of 41,000 (Fig. 1). Our antiserum gave a single precipitation line of normal human serum on immunoelectrophoresis, and the same result was obtained with a commercially available anti-α_1-AG antiserum (Behringwerke).

Table I shows the amino acid content and the carbohydrate composition of the purified urinary protein. The amino acid composition is identical to that reported by other groups for α_1-AG.

Indirect Immunofluorescence with Anti-α_1-AG Antiserum. Isolated T and B lymphocytes, monocytes, and granulocytes showed a slightly granular membrane fluorescence pattern after staining with rabbit anti-α_1-AG F(AB)2 and FITC-conjugated sheep anti-rabbit IgG. To exclude the possibility of α_1-AG adsorption from human serum, four lymphoblastoid cell lines cultivated for

Carl_G_190x270_mm_blokki_FINAL.indd 108 06-Aug-23 1:53:32 PM

TABLE I
*Amino Acid and Carbohydrate Compositions of α_1-Acid Glycoprotein**

Amino acids	Present study‡	Calculated from amino acid sequence (5)
Lys	13.6 ± 0.2	12.8
His	3.1 ± 0.0	3.0
Arg	8.0 ± 0.4	9.5
Asx	20.3 ± 0.4	20.6
Thr	14.5 ± 0.4	14.5
Ser	6.7 ± 0.5	7.3
Glx	33.0 ± 0.8	29.5
Pro	9.4 ± 0.6	7.0
Gly	7.7 ± 0.6	7.3
Ala	9.0 ± 0.4	9.8
Val	9.2 ± 0.5	8.6
Ile	9.2 ± 0.2	9.0
Leu	14.9 ± 0.1	14.5
Tyr	9.7 ± 0.2	10.8
Phe	9.4 ± 0.1	8.8
½ cys§	4.1 ± 0.2	4.0
Met§	0.9 ± 0.0	1.3
Trp	n.d.	3.0
	Carbohydrates‖	
N-acetyl neuraminic acid		14.3
N-acetyl glucosamine		17.5
N-acetyl galactosamine		0
Fucose		7.2
Mannose		19.1
Galactose		27.2

* mol/mol, assuming a mol wt of 41,000.
‡ Mean of four determinations ± standard deviations.
§ Determined after performic acid oxidation.
‖ Mean of two determinations.

several months in the absence of human serum were also studied. All of the four cell lines had a clear membrane fluorescence, which showed redistribution or capping after incubation at 37°C (Fig. 2). No fluorescence was detected in cells treated with preimmunization rabbit serum.

Surface Labeling of Leukocytes. T and B lymphocytes, granulocytes, monocytes and MLC lymphoblasts were labeled with ^3H after treatment with neuraminidase and galactose oxidase followed by NaB^3H_4, and then run on slab gels and exposed for fluorography. The cells contain a large number of labeled characteristic surface proteins. The GP52 region is weakly labeled in all resting cells, and this protein is evidently a minor component. Immunoprecipitation of surface-labeled T lymphoblasts from MLC with anti-α_1-AG anti-serum showed one band with an apparent mol wt of 52,000 (Fig. 3, column G).

Immunoprecipitations of [^{3}H]leucine-labeled cells and culture medium with anti-α_1-AG antiserum.

To show that the cell surface antigen and the cell medium antigen which

Carl_G_190x270_mm_blokki_FINAL.indd 109 06-Aug-23 1:53:32 PM

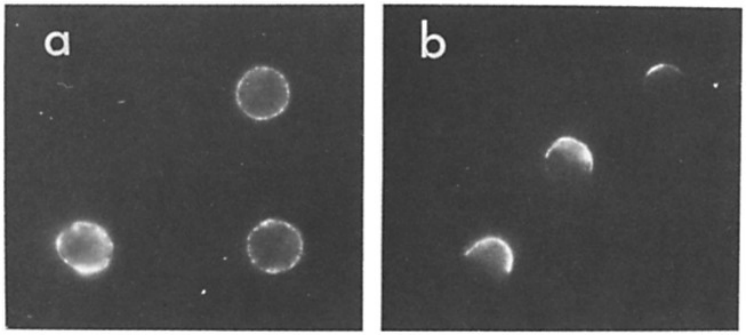

FIG. 2. Indirect immunofluorescence of cells of a lymphoblastoid line treated with rabbit anti-α_1-AG F(AB)2 and FITC-conjugated sheep anti-rabbit IgG. (a), Cells were incubated at 0°C; (b), redistribution of the fluorescence after incubation for 30 min at 37°C.

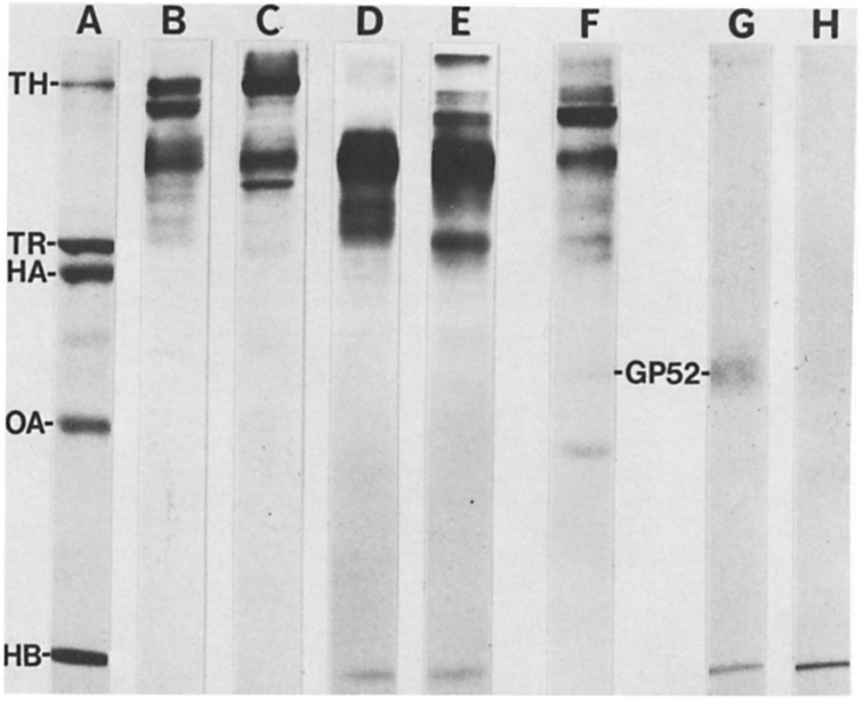

FIG. 3. Polyacrylamide gel electrophoresis patterns of surface-labeled leukocytes and leukocyte antigen precipitated with anti-α_1-AG antiserum. (A), ^{14}C-labeled standard proteins: TH, thyroglobulin; TR, transferrin; HA, human albumin; OA, ovalbumin; HB, hemoglobin. (B), T lymphocytes; (C), B lymphocytes; (D), granulocytes; (E), monocytes; (F), MLC lymphoblasts; (G), pattern of immunoprecipitation from surface-labeled MLC blasts with anti-α_1-AG antiserum; (H), control with preimmunization serum.

Carl_G_190x270_mm_blokki_FINAL.indd 110 06-Aug-23 1:53:33 PM

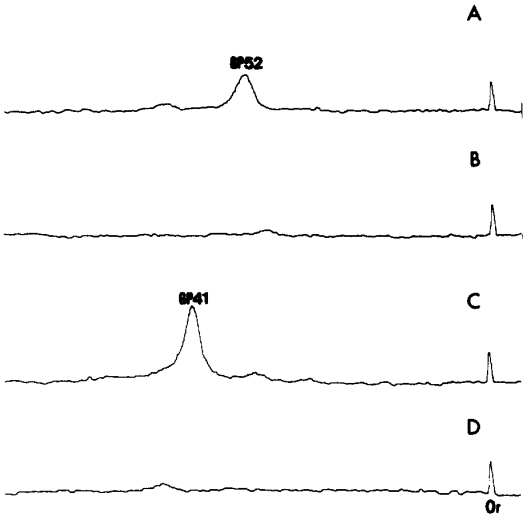

FIG. 4. Scanning patterns of immunoprecipitates obtained with anti-α_1-AG antiserum from [^{3}H]leucine-labeled MLC lymphoblasts and culture medium separated by slab gel electrophoresis and visualized by fluorography. (A), from MLC lymphoblasts with anti-α_1-AG antiserum; (B), from MLC lymphoblasts with preimmunization serum; (C), from MLC culture medium with anti-α_1-AG antiserum; (D), from MLC culture medium with preimmunization serum. Or, origin.

react with anti-α_1-AG antiserum are synthesized by lymphocytes, Triton X-100 extracts from MLC blasts labeled in culture with [^{3}H]leucine and medium from the same cultures were treated with anti-α_1-AG antiserum or preimmunization serum and staphylococci, eluted, and run on polyacrylamide gels. Fig. 4 A shows the scanning pattern of the immunoprecipitated antigen from cells. The apparent mol wt was 52,000. No radioactive band was obtained with preimmunization serum (Fig. 4 B). When the cell culture medium was treated with antiserum and staphylococci, eluted, run on gels and scanned, the pattern of Fig. 4 C was obtained. The apparent mol wt of the major peak was 41,000. Again no labeled protein was precipitated with preimmunization serum (Fig. 4 D).

Immunoprecipitations of Surface-Labeled Leukocytes. Triton X-100 extracts from surface-labeled MLC blasts were precipitated with anti-α_1-AG antiserum and staphylococci and analyzed on cylindrical gels. Two peaks were obtained with apparent mol wt of 52,000 and 41,000 (Fig. 5 A). The size of the smaller peak varied in different preparations. No peaks were obtained with preimmunization serum (Fig. 5 B). Similar patterns were obtained with labeled granulocytes (Figs. 5 C and D). Monocytes showed one major peak with a mol wt of 52,000 (Figs. 5 E and F). No detectable amounts of labeled protein could be precipitated from surface-labeled resting T and B lymphocytes, platelets, or erythrocytes.

Immunoprecipitation of ^{125}I-labeled Cell Culture Medium with Anti-α_1-AG Antiserum. To characterize the shedded antigen found in culture medium, an MLC was set up in RPMI-1640 containing rabbit preimmunization serum, the

Carl_G_190x270_mm_blokki_FINAL.indd 111 06-Aug-23 1:53:33 PM

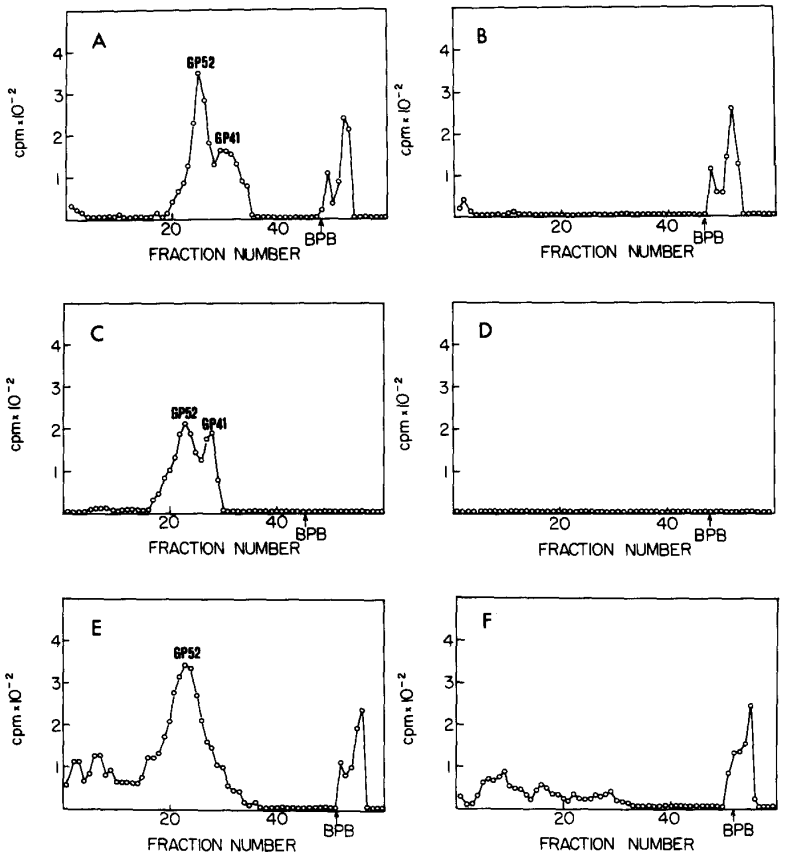

FIG. 5. Cylindrical polyacrylamide gel patterns of radioactive antigens precipitated with anti-α_1-AG antiserum from surface-labeled leukocytes. (A), MLC blasts with anti-α_1-AG antiserum; (B), MLC blasts with preimmunization serum; (C), granulocytes with anti-α_1-AG antiserum; (D), granulocytes with preimmunization serum; (E), monocytes with anti-α_1-AG antiserum; (F), monocytes with preimmunization serum. C and D were passed over a Lens culinaris column and eluted with α-methyl mannoside before immune precipitation. This procedure removed the nonspecific material of low molecular weight running in the front. BPB, position of bromphenol blue marker dye.

medium was labeled with ^{125}I, and immunoprecipitated with anti-α_1-AG antiserum. The pattern of Fig. 6 was obtained with the major peak corresponding to a mol wt of 41,000.

Accumulation of α_1-AG in the Medium of Lymphoid Cell Cultures. The rate of accumulation of α_1-AG in the culture medium during cell proliferation was studied with radioimmunoassay. For these experiments, a lymphoblastoid cell line of high viability was used to avoid contamination by α_1-AG originating from human serum and to minimize accumulation of products from disaggregating cells. Fig. 7 shows the increase of α_1-AG when determined by radioimmu-

Carl_G_190x270_mm_blokki_FINAL.indd 112 06-Aug-23 1:53:33 PM

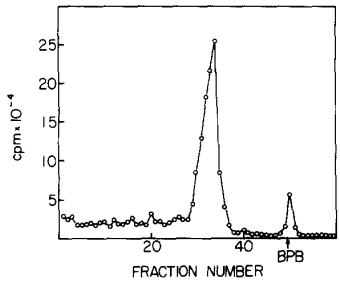

FIG. 6. Cylindrical polyacrylamide gel pattern of immune precipitated radioactive antigen obtained with anti-α_1-AG antiserum from ^{125}I-labeled MLC culture medium supplemented with rabbit preimmunization serum.

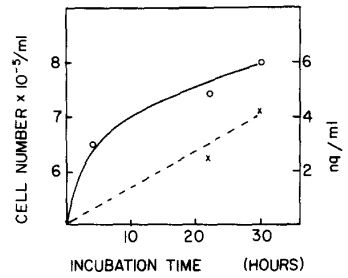

FIG. 7. Accumulation of α_1-AG in the culture medium of a B-lymphoblastoid cell line as determined by radioimmunoassay. (×- -×), cell number × 10^{-5}/ml; (O——O), ng/ml.

noassay from the culture medium. After an initial, more rapid increase, there was a slower accumulation.

Cleavage with CNBr of α_1-AG and of Molecules Recovered by Anti-α_1-AG Antiserum from Cells and Culture Medium. To prove that our anti-α_1-AG antiserum was monospecific for α_1-AG, we performed CNBr cleavage of the immunoprecipitated molecules. Purified, ^{125}I-labeled α_1-AG from urine ran on cylindrical gels as a single peak (Fig. 8 A). Cleavage of this protein with CNBr resulted in three peaks (Fig. 8 B). Cleavage of the iodinated, immunoprecipitated protein isolated from the culture medium of MLC in rabbit serum gave a pattern similar to that of CNBr-treated purified α_1-AG (Fig. 8 C). When the membrane-bound form of α_1-AG was isolated by immunoprecipitation from [^{3}H]leucine-labeled cells and cleaved by CNBr treatment, the pattern of Fig. 8 D was obtained. Again, the peaks of highest molecular weights correspond to those of CNBr-cleaved pure α_1-AG.

Discussion

We have purified α_1-AG or orosomucoid from the urine of patients with acute infectious mononucleosis. Anti-α_1-AG antiserum and its F(AB)2 fragments reacted with normal T and B lymphocytes, T lymphoblasts, granulocytes, and monocytes and lymphoblastoid B-cell lines as shown by immunofluorescence. We were not able to find this antigen on platelets, erythrocytes, or cultured

Carl_G_190x270_mm_blokki_FINAL.indd 113 06-Aug-23 1:53:33 PM

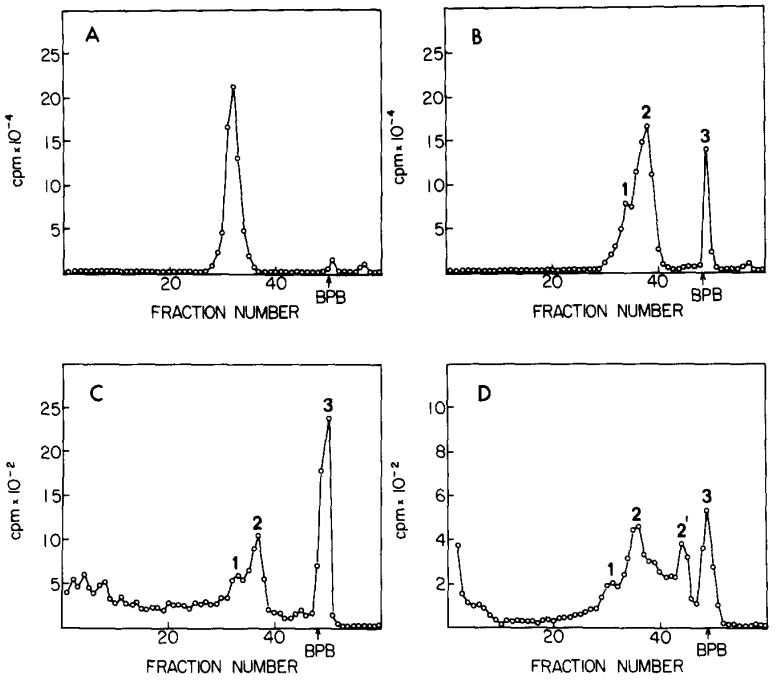

FIG. 8. Cylindrical polyacrylamide gel patterns of pure ^{125}I-labeled α_1-AG (A), its CNBr fragments (B), the CNBr fragments of the antigens precipitated with the anti-α_1-AG antiserum from ^{125}I-labeled MLC culture medium (C), and [^{3}H]leucine-labeled MLC blasts (D).

normal human fibroblasts.[2] The immunofluorescence and capping experiments indicate that the antigen is closely associated with the lipid bilayer of the membrane (31). Surface radiolabeling of cells followed by immunoprecipitation and polyacrylamide gel electrophoresis revealed that the membrane form of α_1-AG has a mol wt of 52,000. The same molecule was obtained after metabolic labeling of lymphoblasts in MLC with [^{3}H]leucine. On the other hand, the molecule isolated from the culture medium either after [^{3}H]leucine labeling or after ^{125}I-iodination of the medium, had an apparent mol wt of 41,000 which corresponds to that of α_1-AG in serum and urine. Although the α_1-AG was detectable on resting T and B lymphocytes by indirect immunofluorescence, sufficient radioactivity could not be introduced by surface labeling to yield a distinguishable band in the fluorography patterns of cells, or to allow isolation of significant amounts by immunoprecipitation. In the fluorography patterns of surface-labeled MLC T blasts and LBL (data not shown, 32), the GP 52,000 band was clearly seen and could be specifically recovered by the antiserum. This indicates that the α_1-AG constitutes only a minor component on the surface of resting lymphocytes, whereas it is more abundantly expressed on activated and

[2] C. G. Gahmberg and L. C. Andersson. Manuscript in preparation.

Carl_G_190x270_mm_blokki_FINAL.indd 114 06-Aug-23 1:53:33 PM

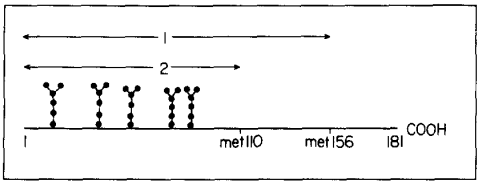

FIG. 9. Scheme of the cleavage points of α_1-AG with CNBr. The CNBr-sensitive methionine residues are at positions 110 and 156, resulting in peptides 2 and 1 (Fig. 8). The five oligosaccharide side chains are indicated.

proliferating T and B cells. The 41,000 mol wt protein found in variable amounts on freshly isolated blood granulocytes might partially represent adsorbed serum α_1-AG.

The difference seen in molecular weights between the membrane-bound and secreted molecules may be due to a hydrophobic fragment, which anchors the protein to the membrane. This would thus resemble the HLA-molecules where the membrane-bound form apparently has a hydrophobic intramembrane portion (33).

The structure of soluble α_1-AG is well known from the studies by Schmid et al. (2, 5) and Ikenaka et al. (7). It is rich in carbohydrate, containing five asparagine-linked oligosaccharide side chains. The carbohydrate is all in the first part of the molecule, and in this respect it resembles another well-studied membrane glycoprotein, the major sialoglycoprotein of human erythrocytes (34).

Elucidation of the primary structure of α_1-AG showed one constant methionine residue at position 110, and variably one more at residue 156 (5). Treatment with CNBr therefore results in cleavage at position 110 and in addition, in part of the molecules at position 156 giving large and easily distinguishable fragments. A schematic drawing of the cleavage points is shown in Fig. 9. The molecular weights of fragments 1 and 2 seen on the gels (Fig. 8) correspond to those expected from the primary structure. Fragments 1 and 2 both contain carbohydrate, which was seen after cleavage of α_1-AG labeled with ^{3}H by the galactose oxidase method.[2]

The antigen on granulocytes and monocytes with an apparent mol wt of 52,000 reacting with anti-α_1-AG antiserum had the same apparent molecular weight as that of lymphocytes. We have not studied the molecule from the nonlymphoid cells as extensively as that of lymphoid cells, but it is reasonable to assume that they are identical or nearly similar.

The elevated serum concentrations of α_1-AG under various conditions have been somewhat difficult to explain by stimulation of liver synthesis alone (2). Inflammation, major surgery, and cancer are associated with proliferation of leukocytes, and at least part of the increased serum α_1-AG may originate from such cells.

Serum α_1-AG has been shown to bind different steroids (35). The cell surface-located form of α_1-AG would also be expected to do it. Steroids have profound effects on lymphocyte functions in vivo and in vitro (36), and both T and B lymphocytes contain steroid receptors (37). Although the cytoplasmic and

Carl_G_190x270_mm_blokki_FINAL.indd 115 06-Aug-23 1:53:33 PM

nuclear binding of steroids are well documented (38), there may also be surface-located receptors.

Isoelectric focusing resolves desialylated α_1-AG from one individual into several bands, indicating heterogeneity (5). Whether these variants of serum α_1-AG are specific products of different types of cells or tissues remains to be established. α_1-AG might be important for intracellular communication and recognition by leukocytes. Such a role for α_1-AG is supported by the recent findings of Chiu et al. (39) that addition of α_1-AG to lymphocyte cultures altered the MLC response.

Summary

Specific antibodies against human α_1-acid glycoprotein reacted with human lymphocytes, granulocytes, and monocytes. The antigen on the leukocytes is an externally located integral membrane glycoprotein which is made by the cells and has an apparent mol wt of 52,000. It is released from cells in vitro to the culture medium. The mol wt of the soluble fragment is 41,000, which corresponds to that of α_1-acid glycoprotein in serum and urine. Peptide mapping confirmed that the main part of the cellular membrane antigen consists of α_1-acid glycoprotein with an additional, probably hydrophobic fragment. This finding may partially explain the increase in the serum levels of α_1-acid glycoprotein observed in many disorders involving leukocyte proliferation. In addition, the known sequence homology of α_1-acid glycoprotein with immunoglobulins can now be more easily understood by their origin in similar cell types.

The skillful technical assistance of Anneli Asikainen, Marja Wilkman, and Liisa Räisänen is acknowledged.

Received for publication 6 March 1978.

References

1. Jeanloz, R. W. 1966. α_1-acid glycoprotein. *In* Glycoproteins. A. Gottschalk, editor. Elsevier North Holland, Inc., New York. 362.
2. Schmid, K. 1975. α_1-acid glycoprotein. *In* The Plasma Proteins, Structure, Function and Genetic Control. F. W. Putnam, editor. Academic Press, Inc., New York. 1:183.
3. Sarcione, E. J. 1963. Synthesis of α_1-acid glycoprotein by the isolated perfused rat liver. *Arch. Biochem. Biophys.* 100:516.
4. Morell, A. G., C. J. A. van den Hamer, I. H. Scheinberg, and G. Ashwell. 1971. Role of sialic acid in determining survival of glycoproteins in circulation. *J. Biol. Chem.* 246:1461.
5. Schmid, K., H. Kaufmann, S. Isemura, F. Bauer, J. Emura, T. Motoyama, M. Ishiguro, and S. Nanno. 1973. Structure of α_1-acid glycoprotein. The complete amino acid sequence, multiple amino acid substitutions, and homology with the immunoglobulins. *Biochemistry.* 12:2711.
6. Schmid, K., R. B. Nimberg, A. Kimura, H. Yamaguchi, and J. P. Binette. 1977. The carbohydrate units of human plasma α_1-acid glycoprotein. *Biochim. Biophys. Acta.* 492:291.
7. Ikenaka, T., M. Ishiguro, J. Emura, J. Kaufmann, S., Isemura, W. Bauer, and K. Schmid. 1972. Isolation and partial characterization of the cyanogen bromide

Carl_G_190x270_mm_blokki_FINAL.indd 116 06-Aug-23 1:53:33 PM

fragments of α_1-acid glycoprotein and the elucidation of the amino acid sequence of the carboxy-terminal cyanogen bromide fragment. *Biochemistry*. **11**:3817.
8. Weimer, H. E., J. W. Mehl, and R. J. Winzler. 1950. Studies on the mucoproteins of human plasma. V. Isolation and characterization of a homogenous mucoprotein. *J. Biol. Chem*. **185**:561.
9. Böyum, A. 1968. Separation of leukocytes from blood and bone marrow. *Scand. J. Clin. Lab. Invest. Suppl*. **97**:1.
10. Pellegrino, M. A., S. Ferrone, M. P. Dierich, and R. A. Reisfeld. 1975. Enhancement of sheep red blood cell human lymphocyte rosette formation by the sulfhydryl compound 2-amino ethylisothiouronium bromide. *Clin. Immunol. Immunopathol*. **3**:324.
11. Häyry, P., and L. C. Andersson. 1976. Fractionation of immunocompetent cells with different physical properties. *Scand. J. Immunol. Suppl*. **5**:31.
12. Wigzell, H., Y. G. Sundqvist, and T. O. Yoshida. 1972. Separation of cells according to surface antigens by the use of antibody-coated columns. Fractionation of cells carrying immunoglobulins and blood group antigens. *Scand. J. Immunol*. **1**:75.
13. Nilsson, K., and J. Pontén. 1975. Classification and biological nature of established human hematopoietic cell lines. *Int. J. Cancer*. **15**:321.
14. Sage, H. J., and R. W. Green. 1972. Common lentil (Lens culinaris) phytohemagglutinin. *Methods Enzymol*. **28**:332.
15. Cuatracasas, P. 1970. Protein purification by affinity chromatography. Derivatizations of agarose and polyacrylamide beads. *J. Biol. Chem*. **245**:3059.
16. Gahmberg, C. G., and S. Hakomori. 1973. External labeling of cell surface galactose and galactosamine in glycolipid and glycoprotein of human erythrocytes. *J. Biol. Chem*. **248**:4311.
17. Gahmberg, C. G., P. Häyry, and L. C. Andersson. 1976. Characterization of surface glycoproteins of mouse lymphoid cells. *J. Cell Biol*. **68**:642.
18. Lowry, O. H., N. J. Rosebrough, A. L. Farr, and R. J. Randall. 1951. Protein measurement with the Folin reagent. *J. Biol. Chem*. **193**:265.
19. Hirs, C. H. W. 1967. Performic acid oxidation. *Methods Enzymol*. **11**:197.
20. Warren, L. 1959. The thiobarbituric acid assay of sialic acids. *J. Biol. Chem*. **234**:1971.
21. Gatt, R., and E. R. Berman. 1966. A rapid procedure for the estimation of amino sugars on a microscale. *Anal. Biochem*. **15**:167.
22. Bahl, O. P. 1969. Human chorionic gonadotropin. I. Purification and physicochemical properties. *J. Biol. Chem*. **244**:567.
23. Niedermeyer, W. 1971. Gas chromatography of neutral and amino sugars in glycoproteins. *Anal. Biochem*. **40**:465.
24. Greenwood, F. C., and W. M. Hunter. 1963. The preparation of ^{131}I-labelled human growth hormone of high specific radioactivity. *Biochem. J*. **89**:114.
25. Landwall, P. 1977. Dialysis cultivation of bacteria. Optimization of yields of bacteria and their products. Ph.D. Thesis. Karolinska Institute, Stockholm, Sweden.
26. Gross, E. 1967. The cyanogen bromide reaction. *Methods Enzymol*. **11**:238.
27. Laemmli, U. K. 1970. Cleavage of structural proteins during the assembly of the head of bacteriophage T4. *Nature (Lond.)*. **227**:680.
28. Weber, K., and M. Osborn. 1969. The reliability of molecular weight determination by dodecyl sulfate-polyacrylamide gel electrophoresis. *J. Biol. Chem*. **244**:4406.
29. Bonner, W. M., and R. A. Laskey. 1974. A film detection method for tritium-labeled proteins and nucleic acids in polyacrylamide gels. *Eur. J. Biochem*. **46**:83.
30. Rice, R. H., and G. E. Means. 1971. Radioactive labeling of proteins in vitro. *J. Biol. Chem*. **246**:831.

Carl_G_190x270_mm_blokki_FINAL.indd 117 06-Aug-23 1:53:33 PM

31. Bretscher, M. S., and M. C. Raff. 1975. Mammalian plasma-membranes. *Nature (Lond.)*. **258**:43.
32. Nilsson, K., L. C. Andersson, C. G. Gahmberg, and H. Wigzell. 1977. Surface glycoprotein patterns of normal and malignant human lymphoid cells. II. B cells, B blasts and Epstein-Barr virus (EBV)-positive and -negative B lymphoid cell lines. *Int. J. Cancer*. **30**:708.
33. Springer, T. A., D. L. Mann, A. L. DeFranco, and J. L. Strominger. 1977. Detergent solubilization, purification, and separation of specificities of HLA antigens from a cultured human lymphoblastoid line, RPMI 4265. *J. Biol. Chem*. **252**:4682.
34. Tomita, M., and V. T. Marchesi. 1975. Amino acid sequence and oligosaccharide attachment sites of human erythrocyte glycophorin. *Proc. Natl. Acad. Sci. U. S. A*. **72**:2964.
35. Ganguly, M., and U. Westphal. 1968. Steroid-protein interactions. XVII. Influence of solvent environment on interaction between human α_1-acid glycoprotein and progesterone. *J. Biol. Chem*. **243**:6130.
36. Lee, K.-C. 1977. Cortisone as a probe for cell interactions in the generation of cytotoxic T cells I. Effect on helper cells, cytotoxic T cell precursors, and accessory cells. J. Immunol. **119**:1836.
37. Lippmann, M., and R. Barr. 1977. Glucocorticoid receptors in purified subpopulations of human peripheral blood lymphocytes. *J. Immunol*. **118**:1977.
38. Yamamoto, K. R., and B. M. Alberts. 1976. Steroid receptors: elements for modulation of eukaryotic transcription. *Annu. Rev. Biochem*. **45**:721.
39. Chiu, K. M., R. F. Mortensen, A. P. Osmand, and H. Gewurz. 1977. Interactions of alpha$_1$-acid glycoprotein with the immune system. I. Purification and effects upon lymphocyte responsiveness. *Immunology*. **32**:997.

Carl_G_190x270_mm_blokki_FINAL.indd 118 06-Aug-23 1:53:33 PM

Expression of the Major Sialoglycoprotein (Glycophorin) on Erythroid Cells in Human Bone Marrow

By Carl G. Gahmberg, Mikko Jokinen, and Leif C. Andersson

The major sialoglycoprotein of human erythrocyte membranes (glycophorin) is one of the most-studied membrane proteins. Although the structure is relatively well known, almost nothing is known about its expression in erythroid cells. To study this we raised an antiserum that reacted specifically with this protein. This was accomplished by immunization of rabbits with a preparation of glycophorin followed by absorption with En(a−) erythrocyte membranes, which lack glycophorin. By use of this antiserum and a staphylococcus protein A technique we could establish that only bone marrow cells of erythrocyte lineage express glycophorin at the cell surface. This occurs in basophilic normoblasts and later stages of erythrocyte differentiation, whereas pronormoblasts do not seem to contain glycophorin.

HUMAN ERYTHROCYTE MEMBRANE has been extensively studied and serves as a model for plasma membranes in general.[1-3] The proteins are asymmetrically distributed, so that the integral glycoproteins of the membrane have their carbohydrates exposed only to the exterior,[4-6] and they are firmly embedded in the lipid bilayer.

The major sialoglycoprotein (glycophorin, MN-glycoprotein, PAS 1)[7,8] is one of the best-characterized integral membrane glycoproteins. It contains about 60% carbohydrate[7,9] and penetrates the membrane.[10-12] The amino acid sequence has been established and shows some interesting features:[9] the NH_2 terminal is hydrophilic and is located on the outside, the middle portion of the polypeptide is hydrophobic, and the COOH terminal is again enriched in hydrophilic amino acids. Glycophorin possibly interacts with peripheral proteins on the cytoplasmic surface of the membrane.[13,14]

In contrast to the large body of information on the structure of glycophorin, almost nothing is known about its synthesis and expression in bone marrow cells. It is not known which cells in the erythrocyte lineage actively synthesize the protein.

Recently we and others have found that erythrocytes of the rare human blood group En(a−) lack glycophorin.[15-17] We took advantage of this fact to produce a specific antiglycophorin antiserum. Rabbits were immunized with a crude preparation of glycophorin and the resulting antiserum absorbed with erythrocyte membranes of the En(a−) blood group. This antiserum was em-

From the Department of Bacteriology and Immunology and the Transplantation Laboratory, Department of Surgery IV, University of Helsinki, Helsinki, Finland.

Submitted February 10, 1978; accepted April 10, 1978.

Supported by the Academy of Finland, the Sigrid Jusélius Stiftelse, and the Finnish Cancer Society.

Address for reprint requests: Carl G. Gahmberg, M.D., Dept. of Bacteriology and Immunology, University of Helsinki, Haartmaninkatu 3, 00290 Helsinki 29, Finland.

© 1978 by Grune & Stratton, Inc. 0006-4971/78/5202-0415$01.00/0

Carl_G_190x270_mm_blokki_FINAL.indd 119 06-Aug-23 1:53:34 PM

ployed to study (by a staphylococcal protein A technique) at which stage of erythrocyte differentiation glycophorin appears at the cell plasma membrane.

MATERIALS AND METHODS

Chemicals and enzymes. Acrylamide and *N,N'*-methylenebisacrylamide were obtained from Eastman Kodak, Rochester, N.Y. NaB^3H_4 (8.6 Ci/mmole) was purchased from the Radiochemical Centre, Amersham, England. Neuraminidase (*Vibrio cholerae,* 500 U/ml) was obtained from Behringwerke, Marburg-Lahn, Germany. Galactose oxidase (200 U/ml) was obtained from Kabi, Stockholm, Sweden. The neuraminidase and galactose oxidase preparations did not contain measurable proteolytic activities when assayed as described previously.[18]

Cells. Normal human erythrocytes (AB Rh+) and En(a−) erythrocytes, from patient G.W. (AB Rh+), were obtained through the Finnish Red Cross Blood Transfusion Service, Helsinki. Bone marrow aspirates from patients with nonmalignant diseases with no obvious disturbances in erythropoiesis were obtained from Helsinki University Hospital through Dr. P. Vuopio.

The suspension of bone marrow cells was depleted from most of the erythrocytes and mature granulocytes by centrifugation on a one-step Ficoll-Isopaque density gradient.[19] The cells used for surface radiolabeling were further incubated with a 0.84% aqueous solution of NH_4Cl–0.017 *M* Tris pH 7.45 for 10 min at 37°C to remove contaminating erythrocytes. After this treatment no mature erythrocytes were left.

Protein A–containing Staphylococcus aureus strain Cowan I was obtained from Dr. P. Landwall (Statens Bakteriologiska Laboratorium, Stockholm, Sweden) and cultivated as previously described.[20] The bacteria were collected immediately after the logarithmic growth phase, heat killed at 80°C for 10 min, and washed three times in 0.15 *M* NaCl–0.01 *M* sodium phosphate pH 7.4 (PBS). They were then fixed by heating in 5% trichloroacetic acid at 70°C for 10 min and washed three times in PBS. The bacteria were stored in PBS–0.02% sodium azide at 4°C. Before use they were washed in 0.05% Triton X-100–0.15 *M* NaCl–5 m*M* EDTA 0.02% sodium azide pH 7.4 (buffer A) and suspended as a 10% suspension in this buffer. One hundred microliters of the preparation bound IgG from 6 μl of rabbit serum.

Cell surface labeling and solubilization of membranes. Erythrocytes (0.5 ml packed cells) or 100×10^6 bone marrow cells were washed three times in PBS and suspended in 1 ml of Dulbecco's PBS containing Ca^{2+}. Then 25 μl of the neuraminidase and 25 μl of the galactose oxidase preparations were added to the tubes; these were incubated at 37°C with continuous gentle shaking. Control tubes received no enzymes. The cells were then washed twice with PBS and suspended in 1 ml PBS. To each tube 0.5 mCi NaB^3H_4 was added, and the samples were incubated at room temperature for 30 min. The cells were subsequently washed three times in PBS. Membranes were isolated from the erythrocytes as previously described.[18] Samples for immune precipitations were obtained by dissolving the labeled erythrocyte membranes or bone marrow cells in PBS containing 1% Triton X-100–1% ethanol and 2 m*M* phenylmethylsulfonylfluoride (as a protease inhibitor) at 0°C followed by centrifugation at 2000 *g* for 10 min. Aliquots were counted for radioactivity in a Wallac-LKB Liquid Scintillation Counter model 81000.

Production of antiglycophorin antiserum. A glycophorin preparation was isolated from normal erythrocytes by chloroform-methanol extraction.[21] One major band was present on gel electrophoresis in the presence of sodium dodecyl sulfate (SDS) with an apparent molecular weight of 85,000 daltons. Rabbits were immunized subcutaneously with 0.5 mg of this preparation in 0.5 ml PBS emulsified with 1 ml Freund adjuvant (Difco) with 2-wk intervals. Ten days after the last injection the rabbits were bled and the serum collected; 1 ml of this serum was absorbed three times with 1 ml of packed En(a−) erythrocyte membranes at 4°C for 24 hr. After the last absorption the serum was centrifuged at 100,000 *g* for 1 hr and stored at 4°C with 0.02% sodium azide.

Immunoprecipitation. To aliquots of Triton X-100–solubilized ^3H-labeled normal or En(a−) erythrocyte membranes and bone marrow cells was added 5 μg mouse IgG and 5 μl rabbit anti–mouse IgG prepared by standard techniques. All subsequent incubations were done at 0°C. After 1 hr, 100 μl of the staphylococcal suspension was added and the tubes incubated for 30 min. These were then centrifuged and the supernatant solutions recovered. To identical amounts of supernatant solutions were added either 5 μl antiglycophorin antiserum or preimmunization

Carl_G_190x270_mm_blokki_FINAL.indd 120 06-Aug-23 1:53:34 PM

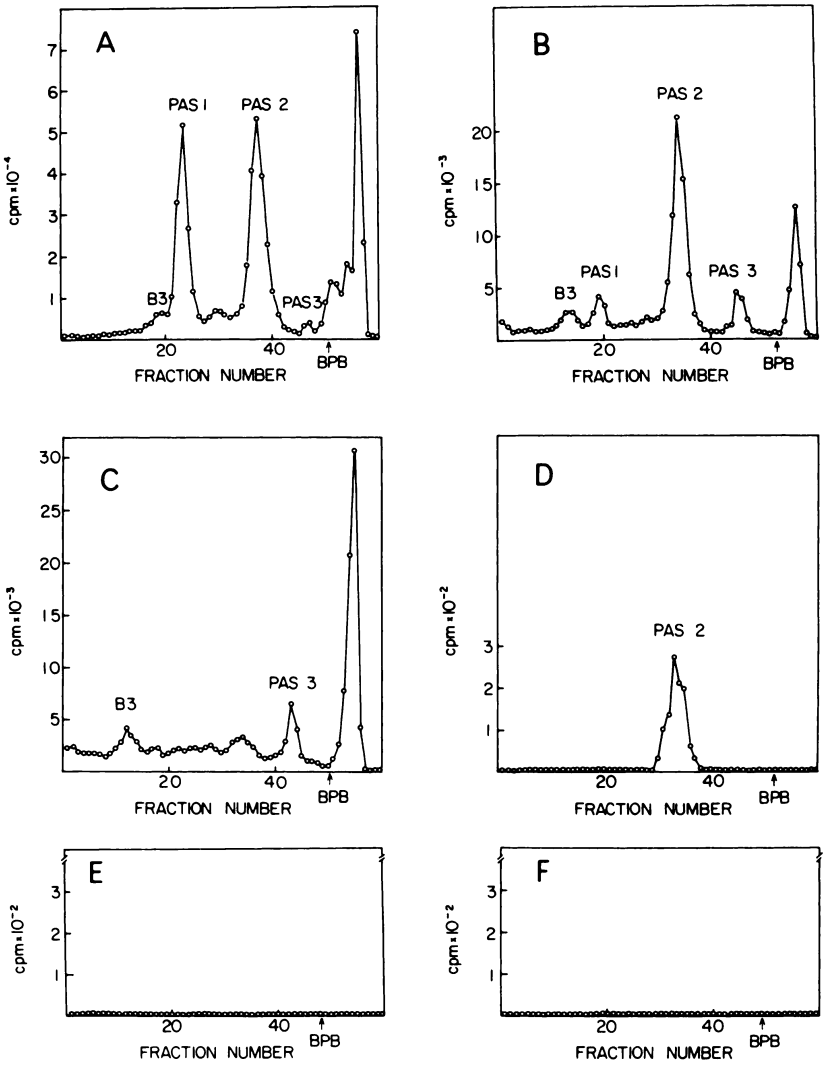

Fig. 1. PAGE patterns of ^{3}H-labeled erythrocyte membranes and immunoprecipitations with antiglycophorin antiserum. (A) Pattern of normal erythrocytes labeled after treatment with neuraminidase and galactose oxidase (25 μg protein). (B) Pattern of the same sample as in A but containing 5 μg protein. (C) Pattern of membranes from En(a−) erythrocytes, labeled after treatment with neuraminidase and galactose oxidase. (D) Pattern obtained from normal erythrocyte membranes after treatment with antiglycophorin antiserum and protein A–containing staphylococci. (E) Pattern obtained from En(a−) membranes after treatment with antiglycophorin antiserum and protein A–containing staphylococci. (F) Pattern obtained from normal erythrocyte membranes after treatment with preimmunization serum and staphylococci. BPB, position of the marker dye bromphenol blue. B3, position of band 3.[8]

Carl_G_190x270_mm_blokki_FINAL.indd 121 06-Aug-23 1:53:34 PM

serum, and the tubes were incubated for 2 hr. Then 0.2 ml of the staphylococcal suspension was added, and the incubation was continued for 1 hr. The bacteria were then washed three times in buffer A and the proteins eluted from the staphylococci by boiling in 1% SDS.

Polyacrylamide gel electrophoresis (PAGE). Samples for electrophoresis were prepared by boiling in the sample buffer of Laemmli.[22] Cylindrical gels were run in the presence of SDS with 8% acrylamide in the separating gel. The gels were then sliced into 2-mm slices and treated with NCS (Amersham/Searle) solubilizer and the slices counted in a toluene-based scintillation fluid.[18]

Incubation of bone marrow cells and erythrocytes with antiglycophorin antiserum and protein A-containing staphylococci. Bone marrow cells or erythrocytes ($20–50 \times 10^6$) were suspended in 0.1 ml cold HEPES buffered Hanks' basic salt solution (HBSS) containing 0.02% sodium azide and 1% bovine serum albumin. Then 10 μl antiglycophorin antiserum or 10 μl preimmunization serum from the same rabbit was added. After 30 min on ice, the cells were washed twice with 10 ml HBSS and suspended in 0.1 ml of the same medium; then 5 μl packed staphylococci were added. After incubation for 30 min at room temperature with intermittent shaking, the suspension was washed three times at 600 *g* for 5 min to remove loose bacteria, and cell smears were prepared by use of a Shandon cytocentrifuge. Cells binding five or more staphylococci at their cell surfaces were considered positive. The smears were stained with the Lephene modification of the peroxidase reaction[23] to detect cells containing hemoglobin and counterstained with May-Grünwald-Giemsa stain.

RESULTS

Reaction of antiglycophorin antiserum with surface-labeled erythrocytes. When normal erythrocytes were labeled with ^3H after treatment with neuraminidase and galactose oxidase, the membranes isolated, solubilized in SDS, and run on PAGE, three major protein peaks corresponding to the major carbohydrate-containing sialoglycoproteins were obtained (Fig. 1A). Other glycoproteins contain much less galactose/*N*-acetylgalactosamine and were therefore relatively weakly labeled.[6] The dimer of glycophorin migrates as peak PAS 1 and the monomer in peak PAS 2.[24] When a smaller amount of membrane is electrophoresed, PAS 2 becomes the dominating peak (Fig. 1B). In contrast to normal erythrocytes, En(a−) erythrocytes do not contain glycophorin (Fig. 1C). When normal labeled erythrocyte membranes were solubilized with Triton X-100 and precipitated with antiglycophorin antiserum and staphylococci and run on PAGE, the pattern of Fig. 1D was obtained; only the PAS 2 peak was seen. No peak was obtained from En(a−) membranes with antiglycophorin antiserum (Fig. 1E) or from normal membranes with preimmunization serum (Fig. 1F).

Reaction of antiglycophorin antiserum with surface-labeled bone marrow cells. When a mixture of bone marrow cells from which all mature erythrocytes had been removed by hypotonic treatment was labeled with ^3H after treatment with neuraminidase and galactose oxidase and precipitated with antiglycophorin antiserum, one major peak corresponding to PAS 2 was obtained (Fig. 2A). The pattern obtained with preimmunization serum is shown in Fig. 2B. The nature of the nonspecifically precipitated material running in the front is not known.

Visualization of bone marrow cells expressing surface glycophorin with S. aureus *Cowan I rosettes.* The erythrocytes and normoblasts in bone marrow pretreated with the antiglycophorin antiserum were heavily coated with staphylococci (Fig. 3). When the bone marrow smears were stained for hemo-

Carl_G_190x270_mm_blokki_FINAL.indd 122 06-Aug-23 1:53:34 PM

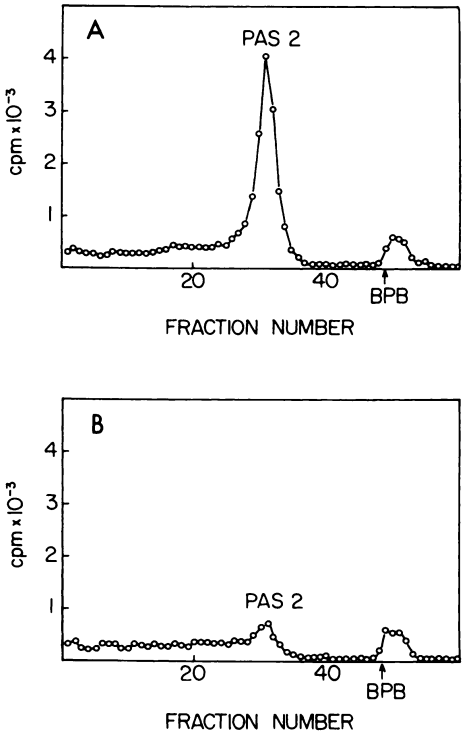

Fig. 2. PAGE patterns of ^{3}H-labeled bone marrow cell proteins obtained after treatment with antiglycophorin antiserum and protein A–containing staphylococci. (A) Pattern obtained from bone marrow cells with antiglycophorin antiserum. (B) Pattern obtained from bone marrow cells with preimmunization serum.

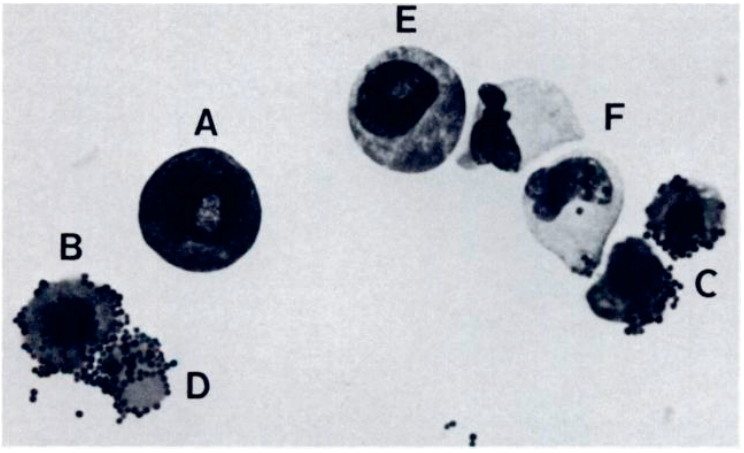

Fig. 3. Cytocentrifuged smear of bone marrow cells pretreated with antiglycophorin antiserum and *S. aureus* Cowan I. Smear was stained for hemoglobin with Lephene's peroxidase reaction and counterstained with May-Grünwald-Giemsa stain. It was photomicrographed using a red interference filter to accentuate the green benzidine reaction. A, pronormoblast; B, basophilic normoblast; C, oxyphilic normoblasts; D, mature erythrocytes; E, myelocyte; F, metamyelocytes. Strong binding of staphylococci to B, C, and D is clearly seen. B, C, and D were stained green. The few staphylococci bound to the cell F represents nonspecific binding, which was occasionally seen with both antiserum and preimmunization serum.

Carl_G_190x270_mm_blokki_FINAL.indd 123 06-Aug-23 1:53:34 PM

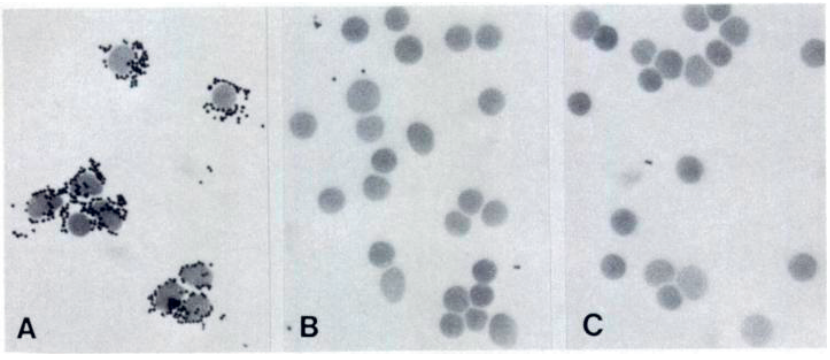

Fig. 4. Specificity of staphylococcal rosette technique. Cytocentrifuged smears stained and photomicrographed as described for Fig. 3. A, normal erythrocytes plus antiglycophorin antiserum; B, normal erythrocytes plus rabbit preimmunization serum; C, En(a−) erythrocytes plus antiglycophorin antiserum.

globin with the peroxidase-benzidine reaction and counterstained with May-Grünwald-Giemsa stain and analyzed, the surface expression of glycophorin apparently coincided with the presence of hemoglobin in the erythroid cell lineage. The pronormoblasts were negative for hemoglobin staining and did not form rosettes. The basophilic normoblasts showed weak hemoglobin reaction and binding of staphylococci. Strong binding could be seen on cells representing the subsequent stages of erythrocyte maturation. No rosettes were found in bone marrows pretreated with normal rabbit serum (Table 1). Significant binding of staphylococci to bone marrow cells outside the erythrocyte lineage was not observed. Cells of the monocyte and granulocyte series, which are rich in IgG Fc receptors, showed only occasional binding of staphylococci (Fig. 3F), presumably because of aggregated IgG present in the sera. These experiments were repeated four times with different bone marrow samples, and each time more than 100 erythroid cells were examined. Pronormoblasts were consistently negative, whereas the subsequent stages of erythroid differentiation were always positive.

Table 1. Surface Binding of Staphylococci Cowan I to Erythroid Cells in Bone Marrow After Treatment With Antiglycophorin Antiserum or With Preimmunization Serum

Cell Type	No. of Surface-bound Staphylococci	
	Antiglycophorin Antiserum (Staphylococci/Cell ± SD*)	Preimmunization Serum (Staphylococci/100 Cells)
Erythrocytes (normocytes + reticulocytes)	19.3 ± 5.8	4
Oxyphilic normoblasts	14.1 ± 3.2	8
Polychromatic normoblasts	12.3 ± 3.0	5
Basophilic normoblasts	10.0 ± 5.3	7
Pronormoblasts	0.3 ± 0.7	5

*More than 20 cells of each type were scored.

Carl_G_190x270_mm_blokki_FINAL.indd 124 06-Aug-23 1:53:34 PM

DISCUSSION

We labeled surface glycoproteins of normal and En(a−) erythrocytes by the neuraminidase-galactose oxidase/NaB^3H_4 technique.[5,6,18] The major protein peaks obtained from normal erythrocytes corresponded to the sialoglycoproteins PAS 1, PAS 2 and PAS 3.[7] By use of labeled cells we could establish the specificity of the antiglycophorin antiserum. Interestingly, only the monomer form of glycophorin (PAS 2) is seen on PAGE in the presence of SDS[24] owing to efficient disaggregation of the glycophorin dimer (PAS 1) at low concentrations of protein (see Figs. 1A and 1B).

It has been established that the NH_2-terminal portion of glycophorin is located outside the lipid bilayer.[7,9] This part of the polypeptide contains the MN antigens and receptors for influenza virus and various lectins.[2] The specific antiglycophorin antiserum obtained after absorption with En(a−) membranes clearly reacts with the external part of the glycophorin polypeptide and is different from the antiserum of Cotmore et al.,[25] which was made against the COOH-terminal portion of glycophorin and in fact reacted only with the cytoplasmic surface of the membrane.[25]

To the best of our knowledge no studies have been made on the synthesis of glycophorin. As a first step in this direction we used antiglycophorin antiserum to establish which cells in the human bone marrow express glycophorin on their surfaces. For this purpose we adapted a rosette technique using *S. aureus* Cowan I strain, which contains surface-bound protein A. Protein A has a high affinity for the Fc portion of IgG.[26,27] The great advantage of this technique as compared to, e.g., immunofluorescence staining is that this can be combined with conventional staining and histochemistry, which allows the identification of the particular surface antigen-carrying cell from permanent preparations. The presence of almost any surface antigen could probably be analyzed in this way. One additional advantage with the rosette technique is that the large size of the cell-staphylococci complexes should allow the selective recovery of the antigen-containing cell by size and/or density fractionation methods. The sensitivity of this technique is similar to that of direct immunofluorescence.[28]

From this study it is clear that the basophilic normoblasts contain glycophorin at their surface. These cells also contain hemoglobin. Glycophorin is abundantly present in the later stages of erythrocyte differentiation. The pronormoblasts, however, do not form rosettes, nor do they contain hemoglobin as detected by the peroxidase reaction. Thus the onset of hemoglobin synthesis and the expression of glycophorin at the cell surface seem to occur at the same stage of erythroid differentiation.

Bone marrow cells of other cell lineages never contain glycophorin at their surface, as shown by the absence of specific staphylococcal binding. This protein is evidently specific for the erythrocyte lineage.

The molecular mechanisms involved in the biosynthesis of glycophorin are unknown. The possibility exists that it is synthesized as a precursor before it is expressed on the cell surface. By use of monospecific antisera such aspects are now amenable to analysis.

Carl_G_190x270_mm_blokki_FINAL.indd 125 06-Aug-23 1:53:34 PM

ACKNOWLEDGMENT

The skilful technical assistance of Anneli Asikainen and Liisa Räisänen is acknowledged.

REFERENCES

1. Steck TL: The organization of proteins in the human red blood cell membrane. J Cell Biol 62:1–19, 1974

2. Marchesi VT, Furthmayr H, Tomita M: The red cell membrane. Annu Rev Biochem 45: 667–698, 1976

3. Gahmberg CG: Cell surface proteins: Changes during cell growth and malignant transformation, in Poste G, Nicolson GL (eds): Dynamic Aspects of Cell Surface Organization. Amsterdam, North-Holland, 1977, pp 371–421

4. Nicolson GL, Singer SJ: Distribution and asymmetry of mammalian cell surface saccharides utilizing ferritin-conjugated plant agglutinins as specific saccharide stains. J Cell Biol 60:236–248, 1974

5. Steck TL, Dawson G: Topographical distribution of complex carbohydrates in the erythrocyte membrane. J Biol Chem 249:2135–2142, 1974

6. Gahmberg CG: External labeling of human erythrocyte glycoproteins. Studies with galactose oxidase and fluorography. J Biol Chem 251:510–515, 1976

7. Marchesi VT, Tillack TW, Jackson RL, Segrest JP, Scott RE: Chemical characterization and surface orientation of the major glycoprotein of the human erythrocyte membrane. Proc Natl Acad Sci USA 69:1445–1449, 1972

8. Fairbanks G, Steck TL, Wallach DFH: Electrophoretic analysis of the major polypeptides of the human erythrocyte membrane. Biochemistry 10:2606–2617, 1971

9. Tomita M, Marchesi VT: Amino acid sequence and oligosaccharide attachment sites of human erythrocyte glycophorin. Proc Natl Acad Sci USA 72:2964–2968, 1975

10. Bretscher MS: Major human erythrocyte glycoprotein spans the cell membrane. Nature 231:229–232, 1971

11. Mueller TJ, Morrison M: The transmembrane proteins in the plasma membrane of normal human erythrocytes. J Biol Chem 249:7568–7573, 1974

12. Bretscher MS: C-terminal region of the major erythrocyte sialoglycoprotein is on the cytoplasmic side of the membrane. J Mol Biol 98:831–833, 1975

13. Nicolson GL, Painter RG: Anionic sites of human erythrocyte membranes. II. Antispectrin induced transmembrane aggregation of the binding sites for positively charged colloidal particles. J Cell Biol 59:395–406, 1973

14. Gahmberg CG, Virtanen I, Wartiovaara J: Crosslinking of erythrocyte membrane proteins by periodate and intramembrane particle distribution. Biochem J 171:683–686, 1978

15. Gahmberg CG, Myllylä G, Leikola J, Pirkola A, Nordling S: Absence of the major sialoglycoprotein in the membrane of human En(a–) erythrocytes and increased glycosylation of band 3. J Biol Chem 251:6108–6116, 1976

16. Dahr W, Uhlenbruck G, Leikola J, Wagstaff W, Landfried K: Studies on the membrane glycoprotein defect of En(a–) erythrocytes. I. Biochemical aspects. J Immunogenet 3:329–346, 1976

17. Tanner MJA, Anstee DJ: Membrane change in En(a–) human erythrocytes. Absence of major sialoglycoprotein. Biochem J 155:701–703, 1976

18. Gahmberg CG, Hakomori S: External labeling of cell surface galactose and galactosamine in glycolipid and glycoprotein of human erythrocytes. J Biol Chem 248:2135–2142, 1973

19. Böyum A: Separation of leukocytes from blood and bone marrow. Scand J Clin Lab Invest 21 [Suppl 97]: 1–107, 1968

20. Landwall P: Dialysis cultivation of bacteria. Optimization of yields of bacteria and their products. Thesis, Karolinska Institute, Stockholm, 1977

21. Hamaguchi H, Cleve H: Solubilization and comparative analysis of mammalian erythrocyte membrane glycoproteins. Biochem Biophys Res Commun 47:459–464, 1972

22. Laemmli UK: Cleavage of structural proteins during the assembly of the head of bacteriophage T4. Nature 227:680–685, 1970

23. Pearse AGE: Histochemistry, Theoretical and Applied, vol 2. Edinburgh, Churchill Livingstone, 1972

24. Marton LSG, Garvin JS: Subunit structure of human erythrocyte glycoprotein. Depolymerization by heating ghosts with sodium dodecyl sulfate. Biochem Biophys Res Commun 52:1457–1462, 1973

25. Cotmore SF, Furthmayr H, Marchesi VT: Immunochemical evidence for the transmembrane orientation of glycophorin A. Localization of ferritin-antibody conjugates in intact cells. J Mol Biol 113:539–553, 1977

Carl_G_190x270_mm_blokki_FINAL.indd 126 06-Aug-23 1:53:34 PM

26. Forsgren A, Sjöquist J: "Protein A" from S. aureus. I. Pseudo-immune reaction with human γ-globulin. J Immunol 97:822–827, 1966

27. Kronvall G, Williams RC: Differences in anti-protein A activity among IgG subgroups. J Immunol 103:828–833, 1969

28. Ranki A, Tötterman TH, Häyry P: Identification of resting human T and B lymphocytes by acid α-naphtyl acetate esterase staining combined with rosette formation with Staphylococcus aureus strain Cowan I. Scand J Immunol 5:1129–1138, 1976

Carl_G_190x270_mm_blokki_FINAL.indd 127 06-Aug-23 1:53:34 PM

Int. J. Cancer: **23**, 143-147 (1979)

K562—A HUMAN ERYTHROLEUKEMIC CELL LINE

Leif C. ANDERSSON [1], Kenneth NILSSON [2], and Carl G. GAHMBERG [3]

[1] *Transplantation Laboratory and Department of Pathology, University of Helsinki, Finland;* [2] *The Wallenberg Laboratory, University of Uppsala, Sweden; and* [3] *Department of Bacteriology and Immunology, University of Helsinki, Finland*

We have studied the surface membrane properties of the human leukemic cell line K562 which previously has been reported to represent an early stage of granulocyte maturation. The surface glycoprotein pattern of the K562 cells obtained after galactose oxidase-NaB[^{3}H]$_4$ labelling and slab gel electrophoresis shows striking similarities with that of normal erythrocytes but is completely different from the patterns of normal and malignant cells of various stages of the myeloblast to granulocyte differentiation. Moreover, the K562 cell expressed the major red cell sialoglycoprotein, glycophorin, on its surface as shown by immunofluorescence and by immuneprecipitation from labelled membrane preparations. As glycophorin is exclusively found on erythroid cells in human bone marrow we conclude that the K562 is a human erythroleukemic line.

The continuous cell line K562 was originally established by Lozzio and Lozzio (1975) from the pleural effusion of a patient with chronic myeloid leukemia (CLM) in terminal blast crisis. K562 has been reported to carry the Philadelphia chromosome marker and was considered to represent the outgrowth of a CML clone (Lozzio and Lozzio, 1975). Other detailed studies on the biological properties have failed to detect convincing properties characteristic of myeloid differentiation but the absence of lymphoid features has nevertheless suggested an origin from an immature cell of the myeloid differentiation lineage (Klein *et al.*, 1976; Drew *et al.*, 1977; Minowada *et al.*; 1977, 1978; Janossy *et al.*, 1978). The cell line has attained widespread use as a highly sensitive *in vitro* target for the natural killer cell assay (Ortaldo *et al.*, 1977; Saksela *et al.*, 1978).

During our previous analysis of the surface glycoprotein patterns of a large panel of human hematopoietic cell lines, and of freshly isolated populations of normal leukocytes and of leukemic cells, we have noticed that the surface glycoprotein profile (GP) of K562 is completely different from those obtained with malignant and benign cells representing various stages of the myeloblast to granulocyte maturation sequence (Andersson *et al.*, 1977; Nilsson *et al.*, 1977; Andersson and Gahmberg, 1978; Gahmberg and Andersson, 1978*a*). Moreover, we recently observed that rabbit anti-K562 antiserum, after extensive absorptions with established cell lines and blood leukocytes to non-reactivity against normal myeloblasts and blood leukocytes, still showed strong reactivity with erythrocytes and erythroid precursor cells. These findings prompted us to investigate the biology of the K562 cell line in greater detail. We report here evidence indicating that K562 in fact represents a human erythroleukemic cell line.

MATERIAL AND METHODS

Cells

The K562 cell line was kindly provided by Dr. G. Klein, Stockholm. The myeloid cell line HL-60 (Collins *et al.*, 1977) was obtained from Dr. R. Gallo, Bethesda, Maryland. The cells were grown in RPMI-1640 medium supplemented with 10% newborn calf serum. Normal human erythrocytes and buffy coat cells were obtained through the Finnish Red Cross Blood Transfusion Service, Helsinki. Blood samples from patients with CML, acute myeloid leukemia, and acute promyelocytic leukemia were obtained by Dr. P. Vuopio, Helsinki University Hospital. Normal granulocytes and leukemic cells were isolated as described in detail (Andersson and Gahmberg, 1978).

Cell surface labelling and solubilization of membranes

Cell surface glycoproteins were radiolabelled using the galactose oxidase-NaB[^{3}H]$_4$ method as described (Gahmberg and Hakomori, 1973; Gahmberg *et al.*; 1976*a*). Erythrocyte membranes were isolated as described previously (Gahmberg and Hakomori, 1973). The labelled cells or cell membranes were solubilized at 0° C in phosphate-buffered saline (PBS) containing 1% Triton X-100, 1% ethanol and 2 mM phenylmethylsulphonyl fluoride as a protease inhibitor. Cell nuclei were pelleted by centrifugation at 2,000 *g* for 10 min and the supernatant was used for electrophoresis and immune precipitation.

Anti-glycophorin antiserum

The production and specificity of the anti-glycophorin antiserum have been described (Gahmberg *et al.*, 1978). Briefly, rabbits were immunized repeatedly with the major sialoglycoprotein, glycophorin, isolated from normal erythrocyte membranes (Hamaguchi and Cleve, 1972). The antiserum was rendered specific by absorption with En (a-) erythrocyte membranes which lack glycophorin (Gahmberg *et al.*, 1976*b*; Tanner and Anstee, 1976; Dahr *et al.*, 1976). Preimmune sera from the same rabbits were used as controls.

Immuneprecipitation

Immuneprecipitations from the Triton X-100—solubilized, labelled membrane preparations were

Received: November 13, 1978

Carl_G_190x270_mm_blokki_FINAL.indd 128 06-Aug-23 1:53:34 PM

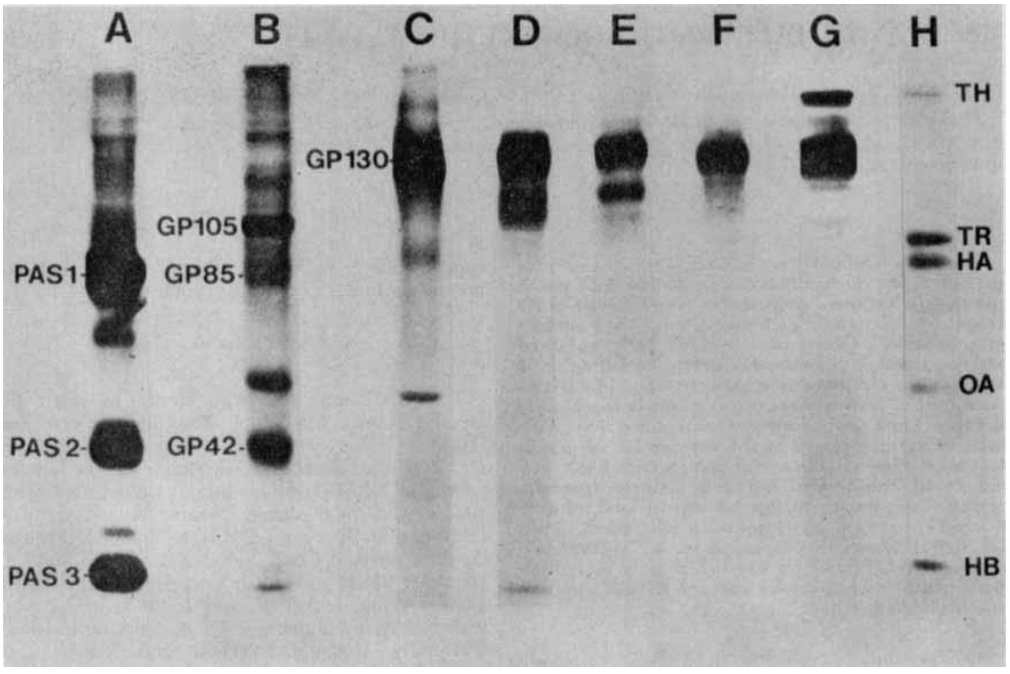

FIGURE 1 — Surface glycoprotein patterns obtained by labelling with NaB[^{3}H]$_4$ after neuraminidase and galactose oxidase treatments of *a:* normal red cells; *b:* the K562 cell line; *c:* the HL-60 cell line; *d:* normal granulocytes; *e:* leukemic cells from a patient with Ph' positive chronic granulocytic leukemia; *f:* cells from a patient with acute promyelocytic leukemia; *g:* cells from a patient with undifferentiated acute myeloid leukemia; *h:* ^{14}C-labelled standard proteins. TH: thyroglobulin, TR: transferrin, HA: human albumin, OA: ovalbumin, HB: hemoglobin. PAS1-PAS3 are the major red cell sialoglycoprotein bands, GP130 = a glycoprotein with an apparent molecular weight of 130,000 etc.

performed using the protein-A containing *Staphylococcus aureus* Cowan I strain as described (Gahmberg and Andersson, 1978*b*).

Indirect immunofluorescence

To exclude non-specific IgG binding to the Fc receptors present on K562 cells (Klein *et al.*, 1976) F(ab)$_2$ fragments were prepared from the anti-glycophorin antiserum. Twenty mg of IgG were digested with 0.5 mg of porcine pepsin for 16 h at +37° C in 0.1 M sodium acetate buffer, pH 4.5, and the F(ab)$_2$ fragments were isolated by filtration over an Ultrogel AcA34 column. The F(ab)$_2$ preparation appeared pure on polyacrylamide gel electrophoresis.

Cells were washed and suspended in ice-cold PBS containing 20% fetal calf serum. Ten μg of anti-glycophorin F(ab)$_2$ or 10 μl preimmune serum were added. After 30 min at 0° C the cells were washed twice with 10 ml of PBS containing 10% fetal calf serum, and suspended in 20 μl of 1:20 diluted fluorescein isothiocyanate-conjugated IgG (1 mg/ml) isolated from sheep anti-rabbit Ig antiserum. After 20 min in the cold, the cells were washed and examined under a Zeiss Universal fluorescence microscope (Gahmberg and Andersson, 1978*b*). For capping experiments the FITC-stained cells were incubated at +37° C.

Polyacrylamide slab gel electrophoresis

Samples were prepared by boiling in the Laemmli sample buffer (Laemmli, 1970) and run on 8% polyacrylamide slab gels as described (Andersson and Gahmberg, 1978) with ^{14}C-labelled marker proteins in the peripheral slots (Gahmberg *et al.*, 1976*a*). The radioactive proteins were visualized by fluorography (Bonner and Laskey, 1974).

RESULTS

Polyacrylamide slab gel electrophoresis patterns of of surface-labelled cells

Samples of surface-labelled erythrocytes, K562 and HL-60 cells, normal granulocytes and cells from patients with chronic myeloid leukemia and acute promyelocytic leukemia were run in parallel slots on the same slab gel. The fluorography patterns are shown in Figure 1. The HL-60 line has a glycoprotein pattern which is very similar to that of granulocytes, CML cells and AML cells with the strongest labelled proteins in the molecular weight region of 130,000 (GP130). The glycoprotein

Carl_G_190x270_mm_blokki_FINAL.indd 129 06-Aug-23 1:53:34 PM

pattern of K562 (Fig. 1*g*), on the other hand, is completely different from these but instead shows a striking similarity to that obtained with normal erythrocytes. GP42 is strongly expressed on K562 cells and corresponds in electrophoretic mobility to the monomer of glycophorin (PAS2, Marchesi *et al.*, 1976).

Studies using the anti-glycophorin antiserum

Immunofluorescence. K562 cells incubated in the cold with the $F(ab)_2$ preparation of the anti-glycophorin antiserum and FITC-conjugated sheep anti-rabbit ItG antiserum showed a strong membrane fluorescence (Fig. 2*b*) as did normal erythrocytes (not shown). No significant staining of HL-60, or CML cells was obtained, neither did the pre-immune serum stain cells of either line. After incubation of stained cells for 30 min at +37° C a partial redistribution of the fluorescein label was seen in some cells (Fig. 2*c*). This indicates that the anti-glycophorin antiserum reacts with integral membrane protein(s) of K562 cells.

Immuneprecipitation. Immuneprecipitation was performed with anti-glycophorin antiserum and with preimmune serum from Triton X-100 lysates of labelled K562 and normal erythrocytes. The precipitated material was run on parallel slots on slab gels. As shown in Figure 3, the antiserum precipitated the PAS1 (glycophorin dimer) and PAS2 (glycophorin monomer) from normal erythrocyte membranes and the corresponding proteins GP85 and GP42 were obtained from the K562 cells. No specific precipitations were obtained with the preimmune serum.

DISCUSSION

The Philadelphia-chromosome-positive K562 cell line was derived from a patient with CML in acute blast crisis. The original suggestion by Lozzio and Lozzio (1975) and Klein *et al.* (1976) that K562 represents a leukemic cell of the granulocytic series has become questionable since Greaves *et al.* (1977) recently reported that the blast crisis in CML often represents the clonal outgrowth of an immature lymphoid cell resembling that of acute lymphoblastic leukemia. K562 cells do not, however, express markers characteristic for ALL cells, like common ALL antigen, Ia-like antigen or the enzymes deoxynucleotidyl transferase and hexosaminidase. Therefore the K562 line has been thought not to represent a lymphoid but some undefined immature myeloid type of cell (Janossy *et al.*, 1978; Minowada *et al.*, 1978). The previously reported presence of the Philadelphia chromosome marker in the K562 line does not prove the granulocytic origin of the cell since this chromosomal aberration is encountered not only in myeloid cells but also in megakaryocytes and cells of the erythroid lineage during CML (for review see Mark, 1977).

The present study favors the assumption that K562 originates neither from a myeloid nor from a lymphoid but rather from an erythroid cell clone. Firstly, the surface glycoprotein pattern of K562 is very different from that of benign or malignant cells belonging to the granulocytic series. The pattern is also clearly dissimilar to that of a number of common ALL cell lines recently studied by the same surface labelling technique (Andersson *et al.*, 1977). On the other hand, many of the labelled proteins of normal erythrocyte membranes are apparently expressed on the K562 cells. This finding not only indicates an erythroid nature of this cell line but also further emphasizes the usefulness of the analysis of the surface glycoprotein profile as a tool for the identification and characterization of benign and malignant cells.

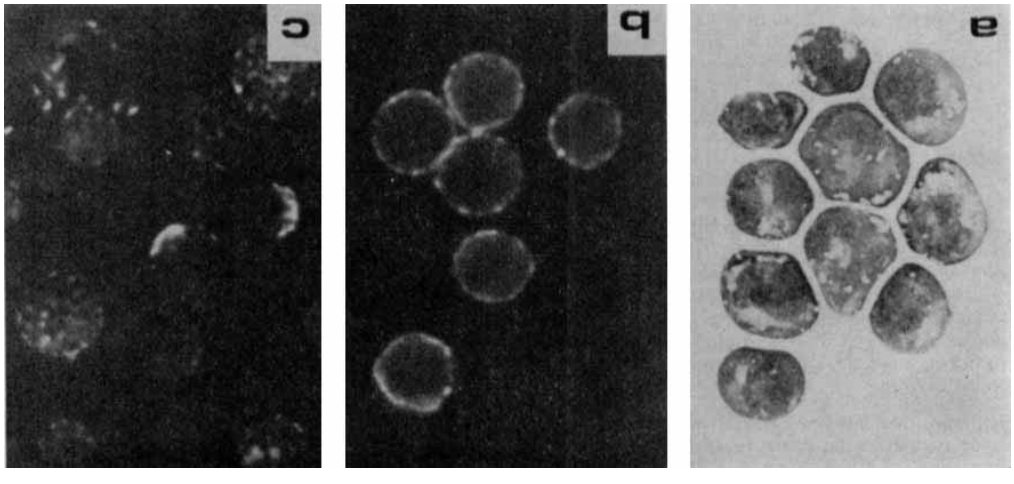

FIGURE 2 — *(a)* Microphotograph of the K562 cells. May-Grünwald-Giemsa stained cytocentrifuged smears. *(b)* Membrane fluorescence of K562 cells stained by $F(ab)_2$ preparation of anti-glycophorin antiserum. *(c)* Redistribution of the anti-glycophorin fluorescence after incubation of the stained cells for 30 min at +37° C.

Carl_G_190x270_mm_blokki_FINAL.indd 130 06-Aug-23 1:53:34 PM

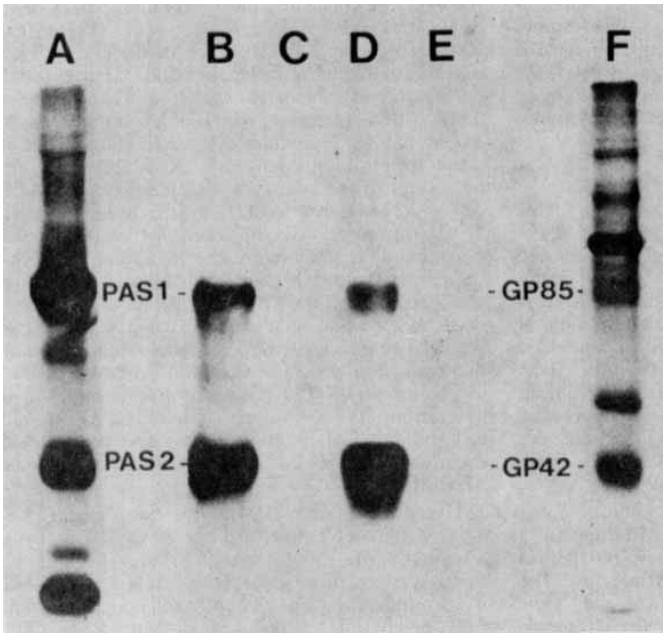

FIGURE 3 — Immunepreciptation with anti-glycophorin antiserum from surface-labelled red cells and K562 cells. *a:* Surface glycoprotein pattern of red cells; *b:* precipitation of glycophorin from red cell membranes with antiserum; *c:* with pre-immunization serum; *d:* precipitation from K562 cells with antiserum; *e:* with preimmunization serum; *f:* surface glycoprotein pattern of K562 cells.

Secondly, the erythroid origin of K562 is suggested by its synthesis and surface expression of glycophorin. Glycophorin (MN-glycophorin, PAS1) is one of the best characterized integral membrane glycoproteins and is the major sialoglycoprotein of human erythrocytes. It contains about 60% carbohydrate and penetrates the cell membrane (Marchesi *et al.*, 1976). The amino acid sequence has been established (Tomita and Marchesi, 1975). Glycophorin is known to carry the MN blood group antigens, but its involvement in normal erythrocyte function and/or maturation is unknown. The occurrence of the rare human blood group En (a-), which lacks glycophorin, has enabled us to produce monospecific antibodies against the molecule. Using this antiserum, we previously showed that glycophorin is specific to erythroid cells in the normal human bone marrow and is expressed on basophilic normoblasts and in later stages of erythroid differentiation (Gahmberg *et al.*, 1978). Although a large body of information is available on the structure of glycophorin, nothing is so far known about the biosynthesis of this membrane protein. The availability of K562 will now permit studies of such aspects.

Some previous findings with K562 also seem to be compatible with an erythroid nature of K562. The morphology of the K562 cells with the basophilic cytoplasma and the absence of intracytoplasmic granules resembles that of cells in the early stages of erythroid maturation in normal human bone marrow. Moreover, the reported absence of surface expression of the HLA-antigen is also well compatible with an erythroid origin (Drew *et al.*, 1977).

The high sensitivity of K562 natural killer cell-induced cytotoxicity is also highly compatible with its erythroid origin. The human natural killer cell expresses strong lytic activity against heterologous erythrocytes (chicken erythrocytes) and against the K562 line (Saksela *et al.*, 1978). The reason for this is unknown but the K562 line might represent the proliferative stage of a cell which *in vivo* comprises a physiological target for the natural killer cells.

The demonstration that K562 expresses erythroid markers has some important implications regarding the natural history of CML. Obviously, this disease includes the stem cell as demonstrated by previous studies employing chromosome (Mark, 1977) and G-6-PD isoenzyme (Fialkow *et al.*, 1977) markers. The erythroid features of K562 presented here suggest that, during blast crisis, the neoplastic stem cell has the potential to differentiate not only to immature myeloid or lymphoid cells but also along the erythroid differentiation lineage.

ACKNOWLEDGEMENTS

Our study was supported by the Academy of Finland and the Finnish and Swedish Cancer Societies. The skillful technical assistance of Ms. Liisa Alajoki, Ms. Anneli Asikainen, and Ms. Leena Saraste is acknowledged.

Carl_G_190x270_mm_blokki_FINAL.indd 131 06-Aug-23 1:53:34 PM

K562 — UNE LIGNÉE DE CELLULES ÉRYTHROLEUCÉMIQUES HUMAINES

Nous avons étudié les propriétés de la membrane de surface de la lignée de cellules leucémiques humaines K562 qui, comme on l'a déjà signalé, représente un stade précoce de la maturation des granulocytes. Le tableau des glycoprotéines de la surface des cellules K562 obtenu après marquage à la galactose oxydase-NaB[^{3}H]$_4$ et électrophorèse sur gel présente des similitudes frappantes avec celui des érythrocytes normaux mais est totalement différent de celui des cellules normales et malignes à divers stades de la différenciation des myéloblastes en granulocytes. De plus, la cellule K562 exprime à sa surface la sialoglycoprotéine majeure des globules rouges, la glycophorine, comme le montrent l'immunofluorescence et l'immunoprécipitation à partir de préparations de membranes marquées. La glycophorine n'étant présente que sur les cellules érythroïdes de la moelle osseuse humaine, nous en concluons que la lignée K562 est une lignée érythroleucémique humaine.

REFERENCES

ANDERSSON, L. C., and GAHMBERG, C. G., Surface glycoproteins of human white blood cells. Analysis by surface labelling. *Blood*, **52**, 57-67 (1978).

ANDERSSON, L. C., GAHMBERG, C. G., NILSSON, K., and WIGZELL, H., Surface glycoprotein patterns of normal and malignant human lymphoid cells. I. T cells, T blasts and leukemic T cell lines. *Int. J. Cancer*, **20**, 702-707 (1977).

BONNER, W. M., and LASKEY, R. A., A film detection method for tritium-labelled proteins and nucleic acids in polyacrylamide gels. *Europ. J. Biochem.*, **46**, 83-88 (1974).

COLLINS, S. J., GALLO, R. G., and GALLAGHER, R. E., Continuous growth and differentiation of human myeloid leukaemic cells in suspension culture. *Nature (Lond.)*, **270**, 347-349 (1977).

DAHR, W., UHLENBRUCK, G., LEIKOLA, J., WAGSTAFF, W., and LANDFRIED, K., Studies on the membrane glycoprotein defect of En(a-) erythrocytes. I. Biochemical aspects. *J. Immunogenet.*, **3**, 329-346 (1976).

DREW, S. I., TERASAKI, P. I., BILLING, R. J., BERGH, O. J., MINOWADA, J., and KLEIN, E., Group-specific human granulocyte antigens on a chronic myelogenous leukemia cell line with a Philadelphia chromosome marker. *Blood*, **49**, 715-718 (1977).

FIALKOW, P. J., JACOBSON, R. J., and PAPAYANNOPOULOU, T., Chronic myelocytic leukemia: clonal origin in a stem cell common to the granulocyte, erythrocyte, platelet and monocyte/macrophage. *Amer. J. Med.*, **63**, 125-130 (1977).

GAHMBERG, C. G., and ANDERSSON, L. C., Identification and characterization of normal and malignant human blood leukocytes by surface glycoprotein patterns. *Ann. N.Y. Acad. Sci.*, **312**, 240-255 (1978*a*).

GAHMBERG, C. G., and ANDERSSON, L. C., Leukocyte surface origin of human α_1-acid glycoprotein (orosomucoid) *J. exp. Med.*, **148**, 507-521 (1978*b*).

GAHMBERG, C. G., HÄYRY, P., and ANDERSSON, L. C., Characterization of surface glycoproteins of mouse lymphoid cells. *J. Cell Biol.*, **68**, 642-653 (1976*a*).

GAHMBERG, C. G., and HAKOMORI, S., External labelling of cell surface galactose and galactosamine in glycolipid and glycoproteins of human erythrocytes. *J. biol. Chem.*, **248**, 4311-4317 (1973).

GAHMBERG, C. G., JOKINEN, M., and ANDERSSON, L. C., Expression of the major sialoglycoprotein (glycophorin) on erythroid cells in human bone marrow. *Blood*, **52**, 379-387 (1978).

GAHMBERG, C. G., MYLLYLÄ, G., LEIKOLA, J., PIRKOLA, A., and NORDLING, S., Absence of the major sialoglycoprotein in the membrane of human En (a—) erythrocytes and increased glycosylation of band 3. *J. biol. Chem.*, **251**, 6108-6116 (1976*b*).

GREAVES, M. F., JANOSSY, G., ROBERTS, M., RAPSON, N. T., ELLIS, R. B., CHESSELS, J., LISTER, T. A., and CATOVSKY, D., Membrane phenotyping: diagnosis, monitoring and classification of acute lymphoid leukemias. *In:* S. Thierfelder, H. Rodt, and E. Thiel (ed.), *Immunological diagnosis of leukemias and lymphomas*, pp. 61-75, Springer-Verlag, Berlin (1977).

HAMAGUCHI, H., and CLEVE, H., Solubilization and comparative analysis of mammalian erythrocyte membrane glycoproteins. *Biochem. Biophys. Res. Commun.*, **47**, 459-464 (1972).

JANOSSY, G., GREAVES, M. F., CAPELLARO, D., MINOWADA, J., and ROSENFELD, C., Membrane antigens on leukaemic cells and lymphoid cell lines. *In:* H. Peeters (ed.) *Protides of the biological fluids (Proc. 25th Colloquium)*, pp. 591-600, Pergamon Press, Oxford and New York (1978).

KLEIN, E., BEN-BASSAT, H., NEUMANN, H., RALPH, P., ZEUTHEN, J., POLLIACK, A., and VANKY, F., Properties of the K562 cell line, derived from a patient with chronic myeloid leukemia. *Int. J. Cancer*, **18**, 421-431 (1976).

LAEMMLI, U. K., Cleavage of structural proteins during the assembly of the head of bacteriophage T4. *Nature (Lond.)*, **227**, 680-685 (1970).

LOZZIO, C. B., and LOZZIO, B. B., Human chronic myelogenous leukemia cell-line with positive Philadelphia chromosome. *Blood.*, **45**, 321-334 (1975).

MARCHESI, V. T., FURTHMAYR, H., and TOMITA, M., The red cell membrane. *Ann. Rev. Biochem.*, **45**, 667-698 (1976).

MARK, J., Chromosomal abnormalities and their specificity in human neoplasms: an assessment of recent observations by banding techniques. *Advanc. Cancer Res.*, **24**, 165-222 (1977).

MINOWADA, J., Markers of human leukaemia-lymphoma cell lines reflect haematopoietic cell differentiation. *In:* B. Serrou and C. Rosenfeld (ed.) *Human lymphocyte differentiation: its application to cancer*, pp. 337-344, INSERM Symp. No. 8, Elsevier/North Holland Biomed. Press (1978).

MINOWADA, J., TSUBOTA, T., NAKAZAWA, S., STRIVASTAVA, B. I. S., HUANG, C. C., OSHIMURA, M., SONTA, S., HAN, T., SINKS, L. F., and SANDBERG, A. A., Establishment and characterization of leukemic T-cell lines, B-cell lines and null-cell line: a progress report on surface antigen study of fresh lymphatic leukemias in man. *In:* S. Thierfelder, H. Rodt and E. Thiel (ed.), *Immunological diagnosis of leukemias and lymphomas*, pp. 241-251, Springer-Verlag, Berlin (1977).

NILSSON, K., ANDERSSON, L. C., GAHMBERG, C. G., and WIGZELL, H., Surface glycoprotein patterns of normal and malignant human lymphoid cells. II. B cells, B blasts and Epstein-Barr virus (EBV)-positive and -negative B lymphoid cell lines. *Int. J. Cancer*, **20**, 708-716 (1977).

ORTALDO, J. R., OLDHAM, R. K., CANNON, G. C., and HERBERMAN, R. B., Specificity of natural cytotoxic reactivity of normal human lymphocytes against a myeloid leukemia cell line. *J. nat. Cancer Inst.*, **59**, 77-83 (1977).

SAKSELA, E., TIMONEN, T., RANKI, A., and HÄYRY, P., Morphological and functional characterization of isolated effector cells responsible for human natural killer activity to fetal fibroblasts and to cultured cell line targets. *Immun. Rev.*, in press (1978).

TANNER, M. J. A., and ANSTEE, D. J., Membrane change in En(a-) human erythrocytes. Absence of major sialoglycoprotein. *Biochem. J.*, **155**, 701-703 (1976).

TOMITA, M., and MARCHESI, V. T., Amino acid sequence and oligosaccharide attachment sites of human erythrocyte glycophorin. *Proc. nat. Acad. Sci. (Wash.)*, **72**, 2964-2968 (1975).

Carl_G_190x270_mm_blokki_FINAL.indd 132 06-Aug-23 1:53:34 PM

364 Nature Vol. 278 22 March 1979

Induction of erythroid differentiation in the human leukaemia cell line K562

MURINE erythroleukaemic cell lines can be induced by various low molecular weight compounds to differentiate *in vitro*[1]. Corresponding human cell lines have not previously been described but we now report that human leukaemic cells of the K562 cell line can be induced to red cell differentiation *in vitro*.

Table 1 Accumulation of erythrocyte-like, benzidine-positive particles in sodium butyrate treated cultures

	Per cent of benzidine positive particles*				
Days in culture	0	1	2	3	4
1 mM Na-butyrate	1.4	3.9	12	35	48
Control	1.4	0.9	0.9	1.1	1.4

*Cytocentrifuged smears were stained with benzidine-Giemsa. Percentages were calculated by counting more than 300 cells.

The K562 line was originally established by Lozzio and Lozzio from the pleural effusion of a patient with chronic myelogenous leukaemia in terminal blast crisis[2]. This cell line, which has been considered to represent an early differentiation stage of the granulocyte lineage[3], is commonly used as a sensitive target cell in the human natural killer cell assay[4].

We have recently analysed the surface glycoprotein patterns of various established human haematopoietic cell lines[5,6] and those of isolated populations of normal and leukaemic leukocytes[7–9]. The surface glycoprotein pattern of K562 cells was found to be clearly different from those of benign and malignant cells representing various stages of the myeloblast to granulocyte differentiation sequence. In contrast, we observed several common features of normal erythrocytes and K562 cells. These observations led us to investigate more closely the K562 cells.

The cells were cultivated in RPMI 1640 culture medium supplemented with 10% newborn-calf serum. K562 cells carry on their surface[10] and synthesise[11] glycophorin A, which is the major sialoglycoprotein on human red cells[12]. This provides additional evidence for the erythroid nature of the K562 cells, as glycophorin A is known to be expressed exclusively on basophilic normoblasts and on later stages of the red cell differentiation in human bone marrow[13]. The K562 cells evidently also contain spectrin as seen by indirect immunofluorescence using rabbit anti-spectrin antibodies on acetone-fixed smears (data not shown).

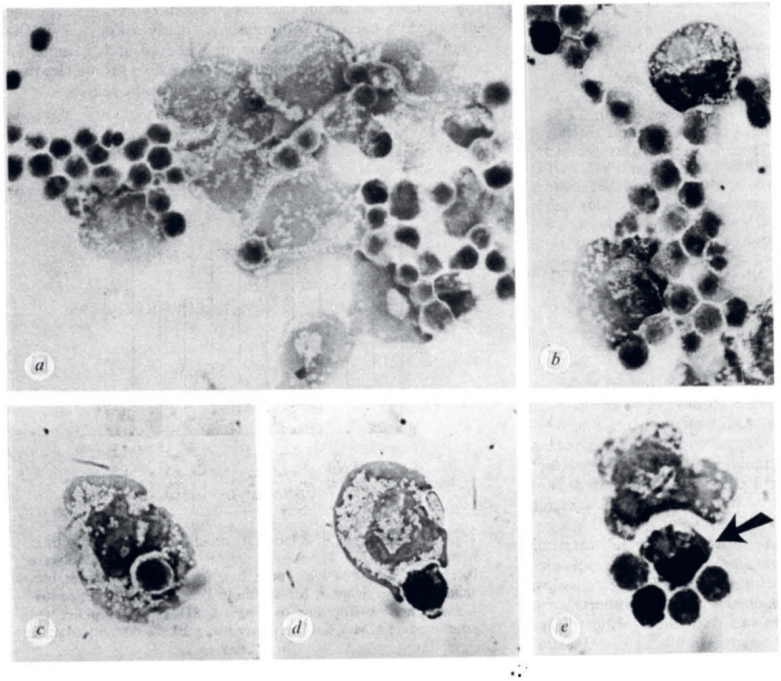

Fig. 1 Microphotographs of cytocentrifuged smears of K562 cells cultivated for 4 days in the presence of 1 mM sodium butyrate. *a*, Stained with Giemsa-eosin and photographed using a green filter. *b*, Stained with Lephene's benzidine method–Giemsa and photographed using a red filter. *c–e*, Details of the apparent sequence of generation of erythrocyte-like particles in butyrate induced K562 cultures. The arrow indicates a normoblast-like cell. These were stained with Giemsa–eosin and photographed with a green filter.

0028–0836/79/0278—0364$01.00

© Macmillan Journals Ltd 1979

Carl_G_190x270_mm_blokki_FINAL.indd 133 06-Aug-23 1:53:34 PM

Nature Vol. 278 22 March 1979

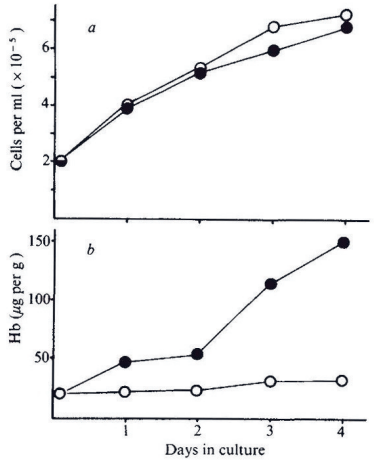

Fig. 2 *a*, Cell counts from K562 cultures treated with 1 mM sodium butyrate (●) and from control cultures without inducer (○). Each point represents the average from duplicate determinations. *b*, Synthesis of haemoglobin in sodium butyrate induced K562 cells as determined by radioimmunoassay. K562 cells were cultivated at an initial density of 0.2×10^6 cells per ml in the presence of 1 mM sodium butyrate (●) or without inducer (○) (the same cultures as in (*a*)) and aliquots taken on indicated days. After washing the cells three times in phosphate-buffered saline, aliquots were removed for protein determination[15]. The rest of the samples were solubilised in Triton X-100 containing buffer and used for radioimmunoassay. Anti-haemoglobin antiserum was prepared in rabbits and anti-rabbit IgG in sheep. Haemoglobin was radioiodinated with ^{125}I by the chloramine T method[16]. The antibody concentration was calibrated to bind approximately 30% of the radioactivity and more than 95% of the binding was inhibited by nonradioactive haemoglobin. The preparation of antisera and the radioimmunoassay will be described in detail elsewhere. The results are given as μg haemoglobin per g of protein and each point represents the average of duplicate analyses.

As the cultures of K562 cells were found to contain occasional benzidine-positive particles (Table 1) the differentiation capacity of this cell line was further investigated. Because the commonly used inducing agent dimethyl sulphoxide[1] did not cause obvious erythroid differentiation, sodium butyrate was used as inducer[14]. When K562 cells were cultivated for 4 days in the presence of 1 mM sodium butyrate (optimal concentration 1–3 mM) differentiation was observed. This amount of sodium butyrate did not significantly affect the growth rate of the K562 cells (Fig. 2*a*). Eosinophilic particles resembling erythrocytes accumulated in the cultures. These particles were surrounded by a membrane and showed positive staining reaction with benzidine (Table 1) indicating the presence of haemoglobin (Fig. 1). The induction of haemoglobin synthesis was confirmed by radioimmunoassay (Fig. 2*b*).

The mode of generation of the erythrocyte-like particles seems to be unusual. Although occasional normoblast-like cells were seen (Fig. 1*e*), most of the erythrocyte-like particles are apparently generated intracytoplasmatically (Fig. 1*c*). As shown in Fig. 1*c–e* this seems to start with an accumulation of cytoplasmic eosinophilic inclusions which condense to one or several erythrocyte-like particles which are subsequently expelled. Scanning electron microscopy shows the erythrocyte-like particles to be spherical with a smooth surface resembling spherocytes (in preparation). The mechanism may be similar to the platelet generation by megakaryocytes. The phenomenon of *in vitro* erythrocyte generation by this cell line is being further studied using time-lapse cinematography.

The findings presented here not only prove the erythroid character of the K562 cell line, but also further emphasise that malignant transformation of human haematopoietic cells does not necessarily mean irreversible loss of differentiation capacity. After 8 years in culture *in vitro*, the K562 cell line has retained its ability to react to appropriate stimuli by undergoing erythroid differentiation. The effect of sodium butyrate on human erythroid leukaemic cells might have interesting clinical implications.

This study was supported by the Academy of Finland and by the Finnish Cancer Society. We thank Liisa Alajoki and Anneli Asikainen for technical assistance. K562 cell lines were obtained from Dr G. Klein (Karolinska Institute, Stockholm) and Dr K. Nilsson (Uppsala).

LEIF C. ANDERSSON

Transplantation Laboratory,
Fourth Department of Surgery
and Department of Pathology,
University of Helsinki

MIKKO JOKINEN
CARL G. GAHMBERG

Department of Bacteriology and Immunology,
University of Helsinki,
Helsinki, Finland

Received 21 November 1978; accepted 12 February 1979.

1. Friend, C., Scher, W., Holland, J. G. & Soto, T. *Proc. natn. Acad. Sci. U.S.A.* **68,** 378–381 (1971).
2. Lozzio, C. B. & Lozzio, B. B. *Blood* **45,** 321–334 (1975).
3. Klein, E. *et al. Int. J. Cancer* **18,** 421–431 (1976).
4. Ortaldo, J. R., Oldham, R. K., Cannon, G. C. & Herberman, R. B. *J. natn. Cancer Inst.* **59,** 77–83 (1977).
5. Andersson, L. C., Gahmberg, C. G., Nilsson, K. & Wigzell, H. *Int. J. Cancer* **20,** 702–707 (1977).
6. Nilsson, K., Andersson, L. C., Gahmberg, C. G. & Wigzell, H. *Int. J. Cancer* **20,** 708–716 (1977).
7. Andersson, L. C. & Gahmberg, C. G. *Blood* **52,** 57–67 (1978).
8. Gahmberg, C. G. & Andersson, L. C. *Ann. N.Y. Acad. Sci.* **312,** 240–255 (1978).
9. Andersson, L. C., Gahmberg, C. G., Siimes, M., Teerenhovi, L. & Vuopio, P. *Int. J. Cancer* (in the press).
10. Andersson, L. C., Nilsson, K. & Gahmberg, C. G. *Int. J. Cancer* **23,** 143–147 (1979).
11. Gahmberg, C. G., Jokinen, M. & Andersson, L. C. *J. biol. Chem.* (in the press).
12. Marchesi, V. T., Tillack, T. W., Jackson, R. L., Segrest, J. P. & Scott, R. E. *Proc. natn. Acad. Sci. U.S.A.* **69,** 1445–1449 (1972).
13. Gahmberg, C. G., Jokinen, M. & Andersson, L. C. *Blood* **52,** 379–387 (1978).
14. Leder, A. & Leder, P. *Cell* **5,** 319–322 (1975).
15. Lowry, O. H., Rosebrough, N. J., Farr, A. L. & Randall, R. J. *J. biol. Chem.* **193,** 265–275 (1951).
16. Greenwood, F. C., Hunter, W. M. & Glover, J. S. *Biochem. J.* **89,** 114–123 (1963).

0028–0836/79/0278—0365$01.00

© Macmillan Journals Ltd 1979

Carl_G_190x270_mm_blokki_FINAL.indd 134 06-Aug-23 1:53:34 PM

604 Nature Vol. 279 14 June 1979

Biosynthesis of the major human red cell sialoglycoprotein, glycophorin A, in a continuous cell line

Mikko Jokinen & Carl G. Gahmberg
Department of Bacteriology and Immunology, University of Helsinki, Haartmaninkatu 3, SF 00290 Helsinki 29, Finland
Leif C. Andersson
Transplantation Laborátory, and Department of Pathology, University of Helsinki

During biosynthesis of glycophorin A in K562 cells a precursor is rapidly transferred through the endoplasmic reticulum membrane with the COOH-terminal remaining in the cytoplasm. This is glycosylated within the cell and appears at the cell surface after about 30 min. The biosynthetic pathway resembles that described for viral membrane glycoproteins.

MOST, if not all, surface proteins of mammalian cells are glycoproteins[1,2]. Their peptide portions often span the lipid bilayer membrane[3,4] and their carbohydrate is exposed to the external milieu[5–7]. The biosynthetic assembly of the peptide and sugar portions and the mechanisms leading to the appropriate membrane disposition of these proteins raise intriguing questions.

Studies on virus-coded proteins have provided us with most of our more detailed knowledge of integral membrane protein biosynthesis. The polypeptides are synthesised on membrane-bound ribosomes and transferred as nascent chains through the endoplasmic reticulum membrane; glycosylation takes place on the luminal side[8–10]. The attachment of the core portions of the oligosaccharides may occur, through lipid-linked intermediates, even before the polypeptide chains have been completely synthesised. As the virus proteins use the host cell machinery for their biosynthesis, similar mechanisms may be anticipated for mammalian surface proteins.

Most of our information on cell membrane structure is derived from studies on the easily available human erythrocyte membrane[2,13,14]. Its major sialic acid-rich glycoprotein, glycophorin A (refs 15, 16), is the best characterised integral membrane protein. Glycophorin A spans the membrane with its NH_2-terminus on the outside and its COOH-terminus in the cytoplasm[3,4], and has a molecular weight (MW) of 31,000. On polyacrylamide gel electrophoresis in the presence of SDS it shows a higher apparent MW because of its 60% carbohydrate content[3,17]. Determination of its amino acid sequence[18,19] indicates that it has 15 serine/threonine-linked oligosaccharides and one asparagine-linked complex oligosaccharide on the external surface of the erythrocyte.

We have produced specific anti-glycophorin A antiserum[20] by immunising rabbits with a crude preparation of glycophorin followed by absorption with En(a−) red cell membranes, which lack glycophorin[16,21–23]. The availability of this specific reagent for glycophorin A and our extensive knowledge of the molecular structure of this glycoprotein provide a potentially useful system for elucidating the pathways involved in mammalian plasma membrane glycoprotein biosynthesis.

We have previously observed that the human continuous leukaemia cell line K562 (ref. 24) is erythroid, and synthesises and expresses glycophorin A on its surface[25,26]. In this report we outline the biosynthesis of glycophorin A from a precursor form, its insertion into the endoplasmic reticulum membrane, its subsequent glycosylation and its migration to the plasma membrane.

Identification of a precursor for glycophorin A

For studies on the biosynthesis of glycophorin A, K562 cells were labelled with ^{35}S-methionine for 5 min and chased with medium containing non-radioactive methionine. The labelled cells were solubilised in buffer containing Triton X-100 and immune precipitation was carried out with anti-glycophorin A antiserum or control serum and protein A-containing staphylococci[20]. The precipitates were analysed by polyacrylamide slab gel electrophoresis in the presence of SDS followed by fluorography. After 5 min of labelling a single protein was specifically precipitated. It had an apparent MW of 37,000 and was designated GP_a (Fig. 1*a*, B). The use of internal labelling meant that a high background radioactivity could not be avoided and therefore the appearance of the specifically precipitated protein could only be followed by using controls with preimmunisation serum. When chased for 10 min (Fig. 1*a*, D) the final glycophorin A molecule (designated GP_c), with an apparent MW of 39,000, became visible, and its concentration relative to that of GP_a increased during chase for 25–60 min (Fig. 1*a*, F–J).

Appearance of glycophorin A at the cell surface

As surface-exposed glycophorin A can be cleaved by trypsin[15,26] the time course of its externalisation was followed by trypsin treatment of labelled intact cells. After labelling for 5 min followed by chase for 10 min, neither the precursor protein, GP_a, nor the completed glycophorin A (GP_c) had reached the cell surface, as indicated by their insensitivity to trypsinisation (Fig. 1*b*, E, G). After 25 and 45 min chase no GP_c was seen in trypsin-treated cells, but GP_a was still detected (Fig. 1*b*, I, K). In the absence of trypsin treatment the GP_c band was stronger than the GP_a band at these time points (compare Fig. 1*a*, F, H). This shows that after 25 min glycophorin A had appeared at the cell surface but that GP_a had not become exposed.

Glycophorin A precursor is incompletely glycosylated

We followed the sequence of glycosylation using lectin columns of known specificity. The glycophorin A precursor, GP_a, already contained glucose/mannose-like residues because it bound to lentil lectin–Sepharose and could be eluted with α-methyl mannoside (Fig. 2B). However, the following results indicate that GP_a does not contain significant amounts of galactose or

0028-0836/79/0279—0604$01.00

© Macmillan Journals Ltd 1979

Carl_G_190x270_mm_blokki_FINAL.indd 135 06-Aug-23 1:53:34 PM

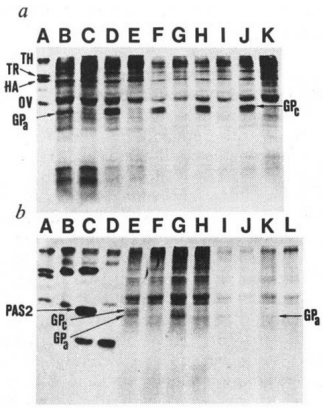

Fig. 1 *a*, Fluorography of a polyacrylamide slab gel of immune precipitates obtained from pulse-chased ^{35}S-methionine-labelled K562 cells with anti-glycophorin A antiserum and control serum. K562 cells (80×10^6) were grown in RPMI-1640 culture medium (GIBCO) containing 10% newborn calf serum. After washing three times with 0.15 M NaCl and 0.01 M sodium phosphate, *p*H 7.4 (PBS), at 37 °C, the cells were suspended in 5 ml of methionine-free Eagle's minimal essential medium (MEM) containing 0.2% bovine serum albumin (Sigma). The cells were incubated with gentle shaking in a CO_2-atmosphere for 30 min at 37 °C and 1.2 mCi of ^{35}S-methionine (Radiochemical Centre, 1,130 Ci mmol^{-1}) added. After 5 min 1 ml of the suspension was withdrawn to ice-cold PBS and the cells immediately washed three times with PBS at 0 °C. The rest of the pulse-labelled cells were rapidly washed at 37 °C with MEM containing a 50-fold excess of cold methionine and suspended in 4 ml of this medium. After incubation for 10, 25, 45 and 60 min 1-ml aliquots were removed and the cells washed at 0 °C as above. All washed cell samples were then suspended in 4 ml of PBS at 0 °C and 1 ml from each taken for trypsinisation (see *b* below). The rest of the samples were centrifuged and the cells dissolved at 0 °C in PBS containing 1% Triton X-100, 1% ethanol and 2 mM phenylmethylsulphonylfluoride (Sigma) as a protease inhibitor (buffer A). Aliquots of the Triton X-100 extracts were taken for immune precipitation experiments using 5 μl anti-glycophorin A antiserum or control serum and the *Staphylococcus aureus* protein A technique as described in detail previously[20,26]. The immune precipitates were studied by polyacrylamide slab gel electrophoresis in the presence of SDS[34] using a 12% acrylamide concentration in the separating gel. The treatment of the slab gels for fluorography[35] and the ^{14}C-labelled[36] standard proteins have been described earlier[37]. A, ^{14}C-labelled standard proteins: TH = thyroglobulin; TR = transferrin, HA = human albumin, OV = ovalbumin; B, immune precipitate obtained with anti-glycophorin A antiserum from K562 cells labelled for 5 min with ^{35}S-methionine; C, with preimmune serum; D, immune precipitate obtained with antiserum from cells labelled for 5 min with ^{35}S-methionine followed by chase for 10 min; E, with preimmune serum; F, immune precipitate obtained with antiserum from cells after 25 min chase; G, with preimmune serum; H, immune precipitate obtained with antiserum from cells after 45 min chase; I, with preimmune serum; J, immune precipitate obtained with antiserum from cells after 60 min chase; K, with preimmune serum. *b*, Fluorography of a polyacrylamide slab gel of labelled erythrocyte membranes and immune precipitates obtained from trypsin-treated K562 cells labelled with ^{35}S-methionine. Part of the ^{35}S-methionine-labelled cells obtained from the experiment described for *a* were treated with 0.1 mg ml^{-1} trypsin (Merck, Darmstadt) for 10 min at 37 °C. The samples were then immediately washed with PBS at 0 °C and solubilised in buffer A. Immune precipitations and polyacrylamide slab gel electrophoresis were carried out as described in *a*. A, ^{14}C-labelled standard proteins (same as in *a*); B, surface glycoprotein pattern of erythrocyte membranes labelled with ^{3}H after treatment of erythrocytes with neuraminidase and galactose oxidase followed by NaB^3H_4 (ref. 6); C, surface glycoprotein pattern of erythrocyte membranes obtained after labelling erythrocytes by the periodate/NaB^3H_4 method[27], PAS 2 = predominantly glycophorin A monomer; D, surface glycoprotein pattern of periodate/NaB^3H_4-labelled membranes after treatment of labelled intact erythrocytes with 0.1 mg ml^{-1} trypsin for 10 min at 37 °C; E, immune precipitate obtained with anti-glycophorin A antiserum from trypsinised K562 cells that had been labelled with ^{35}S-methionine for 5 min; F, with preimmune serum; G, immune precipitate obtained with antiserum from cells labelled for 5 min with ^{35}S-methionine followed by chase for 10 min; H, with preimmune serum; I, immune precipitate with antiserum from cells after 25 min chase; J, with preimmune serum; K, immune precipitate with antiserum from cells after 45 min chase; L, with preimmune serum.

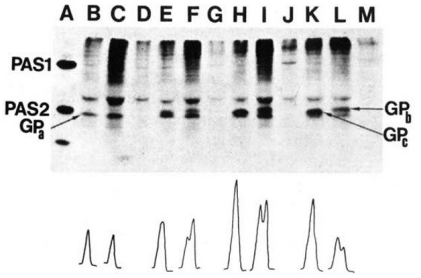

Fig. 2 Fluorography of a polyacrylamide slab gel of glycophorin molecules bound to lentil lectin–Sepharose and the effect of neuraminidase on their electrophoretic mobilities. K562 cells were labelled with ^{35}S-methionine as described in Fig. 1*a* legend, washed at 0 °C with PBS, solubilised in buffer A and applied to lentil lectin–Sepharose columns. *Lens culinaris* lectin was prepared by affinity chromatography[38] and coupled to CNBr-activated Sepharose 4B as described in detail previously[37]. The material eluted with 0.1 M α-methyl mannoside (Calbiochem) was pooled and concentrated by vacuum dialysis to 3 ml. To 1-ml aliquots from each sample was added 0.3 ml of Dulbecco's PBS containing Ca^{2+} and Mg^{2+} and 100 units of *Vibrio cholerae* neuraminidase (Behringwerke). The neuraminidase preparation did not contain proteolytic activity when assayed as described previously[6]. Two other identical aliquots did not receive neuraminidase. All samples were incubated for 10 min at 37 °C. After incubation one control sample and the neuraminidase-treated sample were incubated with 5 μl anti-glycophorin A antiserum and the third tube with preimmune serum followed by protein A-containing staphylococci. The immune precipitates were then analysed by polyacrylamide slab gel electrophoresis as described above. A, surface glycoprotein pattern of periodate/NaB^3H_4-labelled erythrocyte membranes; B, immune precipitate obtained with anti-glycophorin A antiserum from the glycoprotein fraction of K562 cells labelled for 5 min with ^{35}S-methionine; C, immune precipitate with antiserum from the neuraminidase-treated glycoprotein fraction of cells labelled for 5 min; D, with preimmune serum; E, immune precipitate obtained with antiserum from the glycoprotein fraction of cells labelled for 5 min followed by 10 min chase; F, immune precipitate with antiserum from the neuraminidase-treated glycoprotein fraction of cells labelled for 5 min followed by 10 min chase; G, with preimmune serum; H, immune precipitate obtained with antiserum after 25 min chase; I, immune precipitate with antiserum of the 25-min chase sample treated with neuraminidase; J, with preimmune serum; K, immune precipitate obtained with antiserum after 60 min chase; L, immune precipitate with antiserum of the 60-min chase sample treated with neuraminidase; M, with preimmune serum. The corresponding scanning patterns of the glycophorin regions are shown below and were obtained with a Joyce–Loebl Chromoscan apparatus.

sialic acids. First, it did not bind to *Ricinus communis* lectin–Sepharose columns specific for β-D-galactose (data not shown). Second, as it is known that neuraminidase treatment of erythrocyte glycophorin A reduces its mobility on SDS-gel electrophoresis this phenomenon was used to determine the presence of sialic acids[27]. Part of the ^{35}S-methionine-labelled eluates from the lentil lectin columns were treated with neuraminidase before immune precipitation. GP_a mobility on SDS-gel electrophoresis did not change after neuraminidase treatment, but instead of final glycophorin A, a molecule, designated GP_b, with an apparent MW of 41,000, was detected. This demonstrates that GP_c contains sialic acids. GP_c could be adsorbed not only to lentil lectin–Sepharose but also to *R. communis* lectin–Sepharose columns, indicating that it contains terminal β-D-galactosyl residues. This experiment also indicates that at this stage GP_a does not contain the penultimate galactosyl residues because its mobility would then have corresponded to that of GP_b.

The NH_2-terminal portion of glycophorin A precursor is rapidly incorporated into microsomes

The incorporation of the glycophorin A precursor into endoplasmic reticulum was studied by labelling K562 cells for 5 min with ^{35}S-methionine. The labelled cells were then immediately

©1979 Nature Publishing Group

Carl_G_190x270_mm_blokki_FINAL.indd 136 06-Aug-23 1:53:34 PM

cooled to 0 °C, homogenised and a microsomal fraction prepared. Half of this fraction was treated with trypsin. The untreated and the trypsin-treated samples were solubilised in buffer A (see Fig. 1*a* legend) and passed through lentil lectin columns; the glycoproteins were eluted with α-methyl mannoside and immune precipitated with anti-glycophorin A antiserum. The immune precipitates from the trypsin-treated and untreated samples were electrophoresed on parallel slots of a polyacrylamide slab gel. Complete, 37,000 MW, glycophorin precursor, GP_a, was recovered from untreated microsomes (Fig. 3B) but the molecule (GP_{at}) obtained from the trypsin-treated microsomes had an apparent MW of 34,000 (Fig. 3C). This shows that a fragment of approximate MW 3,000 could be cleaved off by trypsin at this stage.

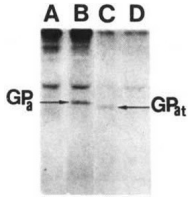

Fig. 3 Fluorography patterns of immune precipitates from K562 microsomes analysed by polyacrylamide slab gel electrophoresis. K562 cells (170×10^6) were labelled for 5 min with ^{35}S-methionine as described in Fig. 1*a* legend. They were then rapidly washed three times with PBS at 0 °C and suspended for 10 min in 15 ml of 10 mM KCl, 10 mM Tris and 1.5 mM $MgCl_2$, *p*H 7.4, at 0 °C. The cells were then homogenised in a tight-fitting Dounce homogeniser with 20 strokes and the nuclei removed by centrifugation at 1,000*g* for 10 min. The supernatant was centrifuged at 50,000*g* for 90 min at 4 °C in a Spinco rotor 30 and the microsomal pellet obtained suspended in 1 ml of Dulbecco's PBS. Half of this material was incubated with 0.01 mg ml^{-1} trypsin for 10 min at 37 °C. The control sample was handled in the same way except that trypsin was omitted. After incubation 0.5 mg of soybean trypsin inhibitor (Sigma) was added to both samples. These were then dissolved in buffer A, both divided into two and immune precipitated with either 5 μl anti-glycophorin A antiserum or preimmune serum. The immune precipitates were then analysed on a 12% polyacrylamide slab gel. A, Control microsomes + preimmune serum; B, control microsomes + anti-glycophorin A antiserum; C, trypsin-treated microsomes + anti-glycophorin A antiserum; D, trypsin-treated microsomes + preimmune serum. Note the decrease in the apparent MW of trypsin-treated GP_a.

Discussion

We recently showed that glycophorin A is expressed not only on mature red cells but also on nucleated precursor cells in human bone marrow[20]. This finding prompted us to look for cell lines synthesising glycophorin A. Our observation that the human continuous cell line K562 is erythroid[25] was the basis for the present experiments. The cells expressed 10^6 copies per cell of a surface glycoprotein which is indistinguishable from erythrocyte glycophorin A. The K562 protein has an apparent MW identical to that of glycophorin A from red cells, it dimerises easily—a characteristic of the erythrocyte protein—it reacts with anti-glycophorin A antiserum, contains MN blood group activity, gives rise to CNBr fragments and contains glycopeptides/oligosaccharides which closely resemble those of glycophorin A (ref. 26). Furthermore, treatment of K562 cells with sodium butyrate induces erythroid differentiation including haemoglobin synthesis and the generation of erythrocyte-like particles[28].

A schematic model of the way in which we consider the biosynthesis of glycophorin A to occur is shown in Fig. 4. Three forms of glycophorin A can be recognised, GP_a, GP_b and GP_c. GP_c is the final glycophorin A molecule which is synthesised completely within the cell and is present at the cell surface after 35 min of pulse labelling. (This includes the 10 min required for trypsinisation.) This glycoprotein contains the terminal sialic acid residues and the penultimate galactosyl residues[26] and has an apparent MW of 39,000 on 12% polyacrylamide gels. The presence of sialic acids gives it a higher electrophoretic mobility in the presence of SDS than after removal of these residues[27] (Fig. 2). GP_b, which can be obtained from GP_c only after neuraminidase treatment, has an apparent MW of 41,000.

GP_a is obviously a precursor of glycophorin A. It reacts with anti-glycophorin A antiserum and the precursor/product relationship is evident from the pulse-chase experiments (Fig. 1*a*). It has an apparent MW of 37,000, does not adsorb to *R. communis* lectin–Sepharose and does not contain sialic acids (Fig. 2B,C). The 4,000 MW difference between desialylated glycophorin A (GP_b) and GP_a should correspond to approximately 20 monosaccharides. This cannot be accounted for solely by the completion of the complex oligosaccharide at Asn 26 but must involve the addition of galactosyl groups to the 15 alkali-labile chains. Apparently, the sialic acids are then rapidly added because a precursor form corresponding to desialylated glycophorin A (GP_b) is never observed during the pulse-chase experiments. The addition of galactosyl and sialic acid residues is known to occur late in the biosynthesis of glycoproteins, mainly in Golgi membranes[29].

GP_a is found after 5 min of labelling in microsomes when the carbohydrate is protected from the action of trypsin (Fig. 3). Trypsin treatment decreases its apparent MW by 3,000 and the released peptide should correspond to residues 101(102)–131 of erythrocyte glycophorin A or tryptic peptide T_4 (ref. 19) located at the COOH-terminal end. When sealed, everted erythrocyte ghosts are treated with trypsin no reduction in the apparent MW of glycophorin A is observed[30]. One possibility is that proteolytic cleavage does occur, but the 3,000 MW difference is not seen because glycophorin A gives a broad and diffuse band on electrophoresis of ghosts. Another, and more likely, possibility is that the COOH-terminal portion of newly synthesised glycophorin A in microsomes is more easily accessible to proteases than the molecule in the finished erythrocyte membrane where it may be covered by other proteins. Treatment of intact cells with trypsin releases much more from the NH_2-terminal end of the polypeptide in soluble form[15,31]. This indicates that the COOH-terminal part already in the endoplasmic reticulum has a similar location in the red cell membrane.

The biosynthetic pathway of glycophorin A corresponds well to that described for the glycoprotein (G protein) of vesicular stomatitis virus. Glycophorin A has a more complex carbohydrate composition than the viral protein, involving two types of quite different oligosaccharides. The glycosylation of glycophorin A probably involves both lipid intermediates for the synthesis of the *N*-glycosidic oligosaccharide[12] and direct glyco-

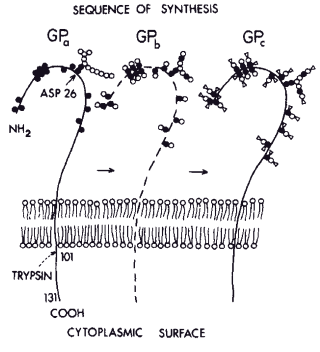

Fig. 4 Our schematic view of the biosynthesis of glycophorin A. GP_a, glycophorin A precursor; GP_b, glycophorin A treated with neuraminidase to demonstrate the stage before addition of sialic acid residues; GP_c, final glycophorin A. ● = hexosamine, ○ = neutral hexose, ▽ = sialic acid. The trypsin cleavage site of GP_a in microsomes is shown. The asparagine-linked oligosaccharide located at residue 26 in the polypeptide chain is shown in GP_a in an 'untrimmed' form from the structure described by Li *et al.*[12].

©1979 Nature Publishing Group

Carl_G_190x270_mm_blokki_FINAL.indd 137 06-Aug-23 1:53:34 PM

sylation of the serine/threonine residues from UDP-*N*-acetyl-D-galactosamine[32]. However, similar times are required for insertion into the endoplasmic reticulum membrane, glycosylation and appearance at the cell surface. Whether glycophorin A contains an additional NH_2-terminal signal sequence found in most glycoprotein precursors[33] is not known and is being investigated.

We thank Anneli Asikainen, Marja Wilkman and Liisa Alajoki for assistance. K562 cells were obtained from Dr K. Nilsson. This study was supported by the Academy of Finland, the Finnish Cancer Society and Lääke Oy.

Received 12 February; accepted 8 May 1979.

1. Bretscher, M. S. & Raff, M. C. *Nature* **258,** 43–49 (1975).
2. Gahmberg, C. G. in *Dynamic Aspects of Cell Surface Organization* (eds Poste, G. & Nicolson, G. L.) 371–421 (North-Holland, Amsterdam, 1977).
3. Bretscher, M. S. *Nature new Biol.* **231,** 229–232 (1971).
4. Bretscher, M. S. *J. molec. Biol.* **98,** 831–833 (1975).
5. Nicolson, G. L. & Singer, S. J. *J. Cell Biol.* **60,** 236–248 (1974).
6. Gahmberg, C. G. & Hakomori, S. J. *J. biol. Chem.* **248,** 4311–4317 (1973).
7. Steck, T. L. & Dawson, G. *J. biol. Chem.* **249,** 2135–2142 (1974).
8. Rothman, J. E. & Lodish, H. F. *Nature* **269,** 775–780 (1977).
9. Katz, F. N., Rothman, J. E., Knipe, D. M. & Lodish, H. F. *J. supramolec. Struct.* **7,** 353–370 (1977).
10. Garoff, H., Simons, K. & Dobberstein, B. *J. molec. Biol.* **124,** 587–600 (1978).
11. Rothman, J. E., Katz, F. N. & Lodish, H. F. *Cell* **15,** 1447–1454 (1978).
12. Li, E., Tabas, I. & Kornfeld, S. *J. biol. Chem.* **253,** 7762–7770 (1978).
13. Steck, T. L. *J. Cell Biol.* **62,** 1–19 (1974).
14. Marchesi, V. T., Furthmayr, H. & Tomita, M. *A. Rev. Biochem.* **45,** 667–698 (1976).
15. Marchesi, V. T., Tillack, T. W., Jackson, R. L., Segrest, J. P. & Scott, R. E. *Proc. natn. Acad. Sci. U.S.A.* **69,** 1445–1449 (1972).
16. Furthmayr, H. *Nature* **271,** 519–524 (1978).
17. Segrest, J. P., Jackson, R. L., Andrews, E. P. & Marchesi, V. T. *Biochem. biophys. Res. Commun.* **44,** 390–395 (1971).
18. Tomita, M. & Marchesi, V. T. *Proc. natn. Acad. Sci. U.S.A.* **72,** 2964–2968 (1975).
19. Tomita, M., Furthmayr, H. & Marchesi, V. T. *Biochemistry* **17,** 4756–4770 (1978).
20. Gahmberg, C. G., Jokinen, M. & Andersson, L. C. *Blood* **52,** 379–387 (1978).
21. Tanner, M. J. A. & Anstee, D. J. *Biochem. J.* **155,** 701–703 (1976).
22. Dahr. W., Uhlenbruck, G., Leikola, J., Wagstaff, W. & Landfield, K. *J. Immunogenet.* **3,** 329–346 (1976).
23. Gahmberg, C. G., Myllylä, G., Leikola, J., Pirkola, A. & Nordling, S. *J. biol. Chem.* **251,** 6108–6116 (1976).
24. Lozzio, C. B. & Lozzio, B. B. *Blood* **45,** 321–334 (1975).
25. Andersson, L. C., Nilsson, K. & Gahmberg, C. G. *Int. J. Cancer* **23,** 143–147 (1979).
26. Gahmberg, C. G., Jokinen, M. & Andersson, L. C. *J. biol. Chem.* (in the press).
27. Gahmberg, C. G. & Andersson, L. C. *J. biol. Chem.* **252,** 5888–5894 (1977).
28. Andersson, L. C., Jokinen, M. & Gahmberg, C. G. *Nature* **278,** 364–365 (1979).
29. Schachter, H. *et al. J. biol. Chem.* **245,** 1090–1100 (1970).
30. Steck, T. L. in *Membrane Research* (ed. Fox, C. F.) (Academic, New York, 1972).
31. Gahmberg, C. G. *J. biol. Chem.* **251,** 510–515 (1976).
32. McGuire, E. J. & Roseman, S. *J. biol. Chem.* **242,** 3745–3747 (1967).
33. Blobel, G. & Dobberstein, B. *J. Cell Biol.* **67,** 835–851, 852–867 (1975).
34. Laemmli, U. K. *Nature* **227,** 680–685 (1970).
35. Bonner, W. M. & Laskey, R. A. *Eur. J. Biochem.* **46,** 83–88 (1974).
36. Rice, R. H. & Means, G. E. *J. biol. Chem.* **246,** 831–832 (1971).
37. Gahmberg, C. G. & Andersson, L. C. *J. exp. Med.* **148,** 507–521 (1978).
38. Sage, J. H. & Green, R. W. *Meth. Enzym.* **28,** 332–339 (1972).

Carl_G_190x270_mm_blokki_FINAL.indd 138 06-Aug-23 1:53:34 PM

THE JOURNAL OF BIOLOGICAL CHEMISTRY
Vol. 260, No. 20, Issue of September 15, pp. 11314–11321, 1985
Printed in U.S.A.
© 1985 by The American Society of Biological Chemists, Inc.

Biosynthesis of the Major Human Red Cell Sialoglycoprotein, Glycophorin A

O-GLYCOSYLATION*

(Received for publication, February 26, 1985)

Mikko Jokinen‡, Leif C. Andersson§, and Carl G. Gahmberg‡

From the ‡Department of Biochemistry and the §Department of Pathology, University of Helsinki, Finland

The biosynthesis of the major human red cell sialoglycoprotein, glycophorin A, was studied in the erythroleukemia cell line K562 with emphasis on *O*-glycosylation. The cells were pulse-chase labeled with [^{35}S] methionine, and either directly immune precipitated with anti-glycophorin A antiserum or detergent-solubilized extracts first passed through columns containing the *N*-acetylgalactosamine-specific lectin from *Helix pomatia* or the glucose/mannose specific lectin from lentil beans. From the sugar-eluted fractions anti-glycophorin A antiserum was used to identify precursor molecules. After 5 min of labeling the first glycophorin A precursors were seen. The largest had an apparent molecular weight of 37,000, and bound to lentil lectin-Sepharose, but not to *H. pomatia* lectin-Sepharose. The lentil lectin-reactive glycophorin A molecules increased to M_r = 39,000 during chase and obtained sialic acids after 9 min of chase reflecting terminal *N*- and *O*-glycosylation. After 5–6 min of labeling two *H. pomatia*-interacting glycophorin A precursors with apparent molecular weights of 24,000 and 30,000 were obtained. These did not bind to lentil lectin-Sepharose. During chase also these molecules increased in size to M_r = 39,000. The immune precipitation of all anti-glycophorin A-reactive precursor molecules was inhibited by purified red cell glycophorin A.

The carboxylic ionophore, monensin, caused the accumulation of incompletely *O*-glycosylated glycophorin A molecules, which bound to *H. pomatia* lectin-Sepharose. These were degraded by treatment with endo-β-*N*-acetylglucosaminidase H reflecting incomplete processing of the *N*-glycosidic oligosaccharide.

The biosynthesis of asparagine-linked oligosaccharides has been extensively studied. It is initiated by the transfer of a high mannose-type oligosaccharide from the dolichol-PP derivative to the polypeptide. The oligosaccharide is then processed by the action of glycosidases and glycosyltransferases to the complete form on its way from the rough endoplasmic reticulum to the Golgi apparatus (1).

The biosynthesis of *O*-linked oligosaccharides has not been studied to a comparable extent. It is generally believed to take place post-translationally in the Golgi apparatus by the action of glycosyltransferases utilizing nucleotide-sugar derivatives (2–4), although co-translational glycosylation also has been proposed (5).

The major human red cell sialoglycoprotein, glycophorin A, is one of the best characterized membrane proteins. Its amino acid sequence is known, and it contains one *N*-glycosidic oligosaccharide at asparagine 26 and 15 *O*-glycosidic oligosaccharides linked to serine and threonine residues in the NH_2-terminal portion of the molecule (6). The structures of the major *O*-glycosidic and the *N*-glycosidic oligosaccharides have been determined (7, 8).

The well-known molecular structure of glycophorin A should make it an excellent model system for elucidating the pathways involved in membrane glycoprotein biosynthesis. In particular, the presence of the large number of *O*-linked oligosaccharides in glycophorin A makes it an attractive model for studies on the mechanism of *O*-glycosylation.

We have earlier shown that the human leukemic cell line K562 synthesizes a surface membrane glycoprotein which was identified as glycophorin A. This protein could be immune precipitated with specific anti-glycophorin A antiserum both from surface-labeled and metabolically labeled K562 cells. Cyanogen bromide peptides of glycophorin A from erythrocytes and the corresponding protein from K562 cells were identical and the glycopeptides and oligosaccharides obtained from Pronase and mild alkaline borohydride treatments were closely similar (9). The glycophorin A molecules from K562 cells were less *O*-glycosylated than those from red cells (10).

The biosynthesis of glycophorin A has been studied in considerable detail. Using glycophorin mRNA from K562 cells a 19,500 molecular weight molecule was obtained in a cell-free protein synthesizing system in the absence of membranes (11). When dog pancreatic membranes were included the apparent molecular weight increased to 37,000 (11). An evidently identical precursor molecule was obtained *in vivo* after a short pulse with [^{35}S]methionine (12). After chase its glycosylation was completed in about 10 min. The precursor molecule interacted with the mannose/glucose-specific lectins from *Lens culinaris* but not with the *N*-acetylgalactosamine-specific lectins from *Helix pomatia*. Tunicamycin prevented the *N*-glycosylation of glycophorin A, but not its *O*-glycosylation (13). It had no effect on the intracellular migration of glycophorin A to the cell surface.

In this article we have studied temporal aspects of *O*-glycosylation. We have now found two "new" glycophorin A precursor molecules with apparent molecular weights of 24,000 and 30,000. These precursors were found early during biosynthesis and they contained *N*-acetylgalactosamines as shown by their interactions with the *N*-acetylgalactosamine-specific lectin from *H. pomatia*. After chase the mature M_r = 39,000 glycophorin A molecules were obtained, and both the

* These studies were supported by the Academy of Finland, the Sigrid Jusélius Foundation, the Association of Finnish Life Insurance Companies, the von Platen Foundation, the Finska Läkaresällskapet, and National Cancer Institute Grant 5 R01 CA 26294-05. The costs of publication of this article were defrayed in part by the payment of page charges. This article must therefore be hereby marked "*advertisement*" in accordance with 18 U.S.C. Section 1734 solely to indicate this fact.

This is an Open Access article under the CC BY license.

Carl_G_190x270_mm_blokki_FINAL.indd 139 06-Aug-23 1:53:35 PM

lentil lectin- and *H. pomatia* lectin-reactive glycophorin A molecules contained *O*-glycosidic carbohydrates. The results show that part of the glycophorin A molecules became *O*-glycosylated at an early stage and part at a late stage of biosynthesis. The carboxylic ionophore monensin inhibited the terminal glycosylations of glycophorin A, but the *O*-glycosylations were already initiated.

MATERIALS AND METHODS

Cells—K562 cells were cultivated in RPMI 1640 culture medium supplemented with 10% newborn calf serum. Normal and En(a−) red cells were obtained from the Finnish Red Cross Blood Transfusion Service, Helsinki, Finland.

Chemicals—The sources of the chemicals were: acrylamide *N,N′*-methylenebisacrylamide (Eastman Kodak Co., Rochester, NY); 2,5-diphenyloxazole and 1,4-bis[2-(5-phenyloxazolyl)]benzene (New England Nuclear); sodium metaperiodate, $NaBH_4$ (Merck AG, Darmstadt, Federal Republic of Germany); *N*-acetylgalactosamine, sodium dodecyl sulfate (SDS[1]), sodium deoxycholate, bovine serum albumin (BSA), ovalbumin, human transferrin, and bovine submaxillary mucin (Sigma); methyl-α-D-mannopyranoside (Calbiochem-Behring); Triton X-100 (British Drug House Ltd., Poole, United Kingdom); monensin and tunicamycin (Eli Lilly & Co., Indianapolis, IN). The concentration used for monensin was 10 μM. Higher concentrations clearly inhibited the protein synthesis. The concentration of tunicamycin was 20 μg/ml as described previously (13). Lentil and wheat germ lectins were isolated as described (14, 15) and 5 mg of protein was coupled to Sepharose 4B by the cyanogen bromide method (16). *H. pomatia* lectin-Sepharose was obtained from Pharmacia (Uppsala, Sweden).

Isotopes—Tritiated sodium borohydride (11.7 Ci/mmol), [^{35}S]methionine (1130 Ci/mmol), ^{125}I- (carrier free), and ^{14}C-labeled standard proteins were obtained from the Radiochemical Centre, Amersham, United Kingdom.

Enzymes—Endoglycosidase H (*Streptomyces griseus*) was from Seikagaku Kogyo Co., Tokyo, Japan, α-*N*-acetylgalactosaminyl-oligosaccharidase (*Clostridium perfringens*) was from Bethesda Research Laboratories, neuraminidase (*Vibrio cholerae*) from Koch-Light Laboratories (Coinbrook Berks, United Kindgom) and *S. griseus* protease (Pronase) from Sigma.

Radioactive Cell Surface Labeling of Erythrocytes—Erythrocytes and K562 cells were labeled with ^{3}H using the periodate/NaB[^{3}H]$_4$ surface-labeling technique as described in detail previously (17). Lactoperoxidase-catalyzed iodination (18), and the isolation of erythrocyte membranes (19) were done as described.

Preparation of ^{125}I-labeled Proteins—A glycophorin A preparation was isolated from lactoperoxidase-^{125}I-labeled erythrocyte membranes after chloroform/methanol extraction and partition with water (20). ^{125}I-labeling of BSA, ovalbumin, transferrin, and bovine submaxillary mucin was done by the chloramine-T method (21) using 10 μg of the proteins. Part of the glycophorin A preparation and all of the other ^{125}I-labeled proteins were treated with 10 milliunits of neuraminidase in 0.3 ml of Dulbecco's phosphae buffer for 30 min at 37 °C.

Isolation of Red Cell Glycophorin A–Nonradioactive glycophorin A was isolated from red cell membranes by chloroform/methanol extraction (20), followed by chromatography on wheat germ lectin-Sepharose. The glycoproteins eluted with 0.1 M acetylglucosamine were finally fractionated on Sepharose 4B in 0.05 M Tris, pH 8.2, 0.1% deoxycholate.

Radioactive Metabolic Labeling of K562 Cells—K562 cells were washed three times in 0.15 M NaCl, 0.01 M sodium phosphate, pH 7.4 (NaCl/PO_4), and preincubated for 30 min with or without 10 μg of monensin in 5 ml of Eagle's essential medium lacking methionine but containing 0.2% BSA. The media were then supplemented with 0.5 mCi of [^{35}S]methionine. After incubation for 1 h the cells were transferred to NaCl/PO_4 at 0 °C, washed three times in the buffer, and lysed in NaCl/PO_4 containing 1% Triton X-100, 1% ethanol, and 2 mM phenylmethylsulfonyl fluoride (buffer A). After centrifugation at 1000 × *g* for 10 min the supernatants were recovered and used for subsequent studies.

For pulse-chase experiments, K562 cells, preincubated as above with or without 10 μM monensin, were labeled for 5 min with 0.5 mCi of [^{35}S]methionine, rapidly washed with normal Eagle's minimal essential medium at 37 °C, and transferred to culture bottles in normal Eagle's minimal essential medium. At indicated times, cell aliquots were removed, immediately cooled to 0 °C, and the cells washed three times in NaCl/PO_4. The labeled cells were solubilized in buffer A and cleaned by centrifugation as above.

Lectin-Sepharose Affinity Chromatographies—The [^{35}S]methionine-labeled cell extracts and the ^{125}I-labeled proteins were passed in buffer A through 2 ml of lectin-Sepharose columns and the adsorbed material eluted with buffer A containing 0.05 M of α-methylmannopyranoside for the lentil lectin columns, and 0.01 M *N*-acetylgalactosamine for the *H. pomatia* lectin columns (13). Aliquots were counted for radioactivity and the radioactive peak fractions eluted with sugar were pooled and subjected to immune precipitation.

Periodate/NaB[^{3}H]$_4$-labeled K562 cells were solubilized in buffer A and passed through a lentil lectin-Sepharose column. The adsorbed glycoproteins were eluted with 0.05 M α-methylmannopyranoside in buffer A. The passed-through fraction was applied to another lentil lectin-Sepharose column to ensure that all adsorbable glycoproteins had been removed. The sugar-eluted fraction was recovered, and the passed-through fraction applied to a wheat germ lectin-Sepharose column. The adsorbed proteins were eluted with 0.1 M *N*-acetyl-D-glucosamine in buffer A. The sugar-eluted fractions were then immune precipitated with anti-glycophorin A antiserum.

Preparation of Anti-glycophorin A Antiserum and Immune Precipitation—Anti-glycophorin A antiserum was prepared as described in detail (22). In short, a rabbit anti-glycophorin A antiserum was extensively absorbed with En(a−) red cell membranes, which lack glycophorin A. The labeled samples from lectin columns were immune precipitated in Triton X-100-containing buffer using the staphylococcal protein A technique as described previously (22). Direct immune precipitation from labeled cell extracts was performed in NaCl/PO_4 containing 0.5% Triton X-100, 0.25% deoxycholate, 0.25% SDS, and 5 mg/ml BSA to decrease nonspecific adsorption. To prove the identity of glycophorin A precursor glycoproteins, cells were labeled with [^{35}S]methionine, and the glycoproteins eluted from lectin-Sepharose columns. The eluates were used for immune precipitation with 5 μl of anti-glycophorin A antiserum in the abence or presence of 25 μg of purified red cell glycophorin A.

Treatment of [^{35}S]Methionine-labeled Glycophorin A Precursors with Endo-β-N-acetylglucosaminidase H, α-N-Acetylgalactosaminyl-oligosaccharidase and Neuraminidase—The radioactive precursor molecules obtained after immune precipitation with anti-glycophorin A antiserum were treated with endo-β-*N*-acetylglucosaminidase H as described (23). The treatment with α-*N*-acetylgalactosaminyl-oligosaccharidase was carried out in 0.05 M K-phosphate, pH 6.5, for 18 h at 37 °C. The neuraminidase treatments were done either before the *H. pomatia* lectin-Sepharose affinity chromatographies or after the immune precipitations as described previously (Refs. 12 and 24; see figure legends).

Polyacrylamide Slab Gel Electrophoresis—Polyacrylamide slab gel electrophoresis in the presence of SDS was performed according to Laemmli (25). The acrylamide concentration was 12% if not otherwise indicated. The apparent molecular weights of the proteins were obtained using ^{14}C-labeled phosphorylase *b*, BSA, ovalbumin, carbonic anhydrase, and lysozyme (11). The treatment of gels for fluorography was done according to Bonner and Laskey (26). Gels were stained for protein with Coomassie Brilliant Blue.

Analysis of Glycopeptides/Oligosaccharides—^{3}H surface labeled glycophorin A molecules were isolated from the lentil lectin and wheat germ lectin-Sepharose columns run in series by immune precipitation. The precipitates were treated with 0.5% Pronase at 60 °C for 24 h, lyophilized, and the alkali-labile oligosaccharides released as described (27). The labeled glycopeptides/oligosaccharides were analyzed on Bio-Gel P-6 columns in 0.1 M NH_4HCO_3, 0.1% SDS.

RESULTS

Specificity of H. pomatia lectin for α-N-Acetylgalactosamine/D-galactose-β(1–3)N-acetylgalactosamine-containing Glycoproteins—Crucial for the demonstration of the presence of *N*-acetylgalactosamine residues in glycophorin A precursors was the establishment of a reliable test system for glycoproteins containing this sugar. *H. pomatia* lectin is known to interact most strongly with *N*-acetylgalactosamine and D-galactose-β(1–3)*N*-acetylgalactosamine structures (28). This was con-

[1] The abbreviations used are: SDS, sodium dodecyl sulfate; BSA, bovine serum albumin.

Carl_G_190x270_mm_blokki_FINAL.indd 140 06-Aug-23 1:53:35 PM

firmed using ^{125}I-labeled BSA, ovalbumin, transferrin, bovine submaxillary mucin, and glycophorin A.

^{125}I-labeled and neuraminidase-treated BSA, ovalbumin, and transferrin showed no binding to *H. pomatia* lectin-Sepharose (Fig. 1, *A–C*). Neuraminidase-treated ^{125}I-bovine submaxillary mucin, which contains *O*-glycosidic oligosaccharides, showed partial binding (Fig. 1*D*). Native glycophorin A showed some binding (Fig. 1*E*), which substantially increased when using neuraminidase-treated glycophorin A (Fig. 1*F*).

Pulse-Chase Labeling of K562 Cells—K562 cells were pulse-chase labeled with radioactive methionine, and solubilized in Triton X-100 containing buffer. Immune precipitation with anti-glycophorin A antiserum followed by polyacrylamide gel electrophoresis, and fluorography (Fig. 2) showed three weakly labeled anti-glycophorin A reactive bands after a 5-min pulse (GPA_{HI}, GPA_{H2}, and GPA_a). The apparent molecular weights of these were 24,000, 30,000, and 37,000 (Fig. 2*C*). After chase, the glycophorin A GP_c becme stronger and the GPA_{H1}, GPA_{H2}, and GPA_a gradually disappeared (Fig. 2, *D–G*). The strongly labeled band above GP_c is actin, which also was obtained using preimmune serum (Fig. 2, *H* and *I*). To demonstrate the presence of specific carbohydrate in glycophorin A precursors the detergent extracts were treated for 5 min with neuraminidase to ensure the exposure of galactose/*N*-acetylgalactosamine residues. The extracts were then applied to *H. pomatia* lectin-Sepharose columns and eluates obtained with *N*-acetylgalactosamine were immune precipitated with anti-glycophorin A antiserum. The precipitates were analyzed by polyacrylamide gel electrophoresis. After a 5-min pulse, the precursor molecule GPA_{H1} with an apparent molecular weight of 24,000 was faintly seen and the dimer of GPA_{H2} (Fig. 3*A*). When chased for 3 min the GPA_{H2} molecule with the apparent molecular weight of 30,000 increased (Fig. 3*C*). After a 9-min chase the complete glycophorin A monomer and dimer appeared (GPA_d, GPA_d-D, Fig. 3*G*).

In parallel K562 cells were pulse-chase labeled with [^{35}S] methionine and the detergent-solubilized extracts passed through lentil lectin-Sepharose columns reactive with glucose/mannose residues. The sugar eluates were immune precipitated with anti-glycophorin A antiserum and half of the samples were treated for 10 min with neuraminidase. The antiserum precipitated the 37,000 molecular weight protein GPA_a from pulse-chase labeled cells (Fig. 4*A*) and this increased in size with time to GPA_c (Fig. 4*G*). It is apparent

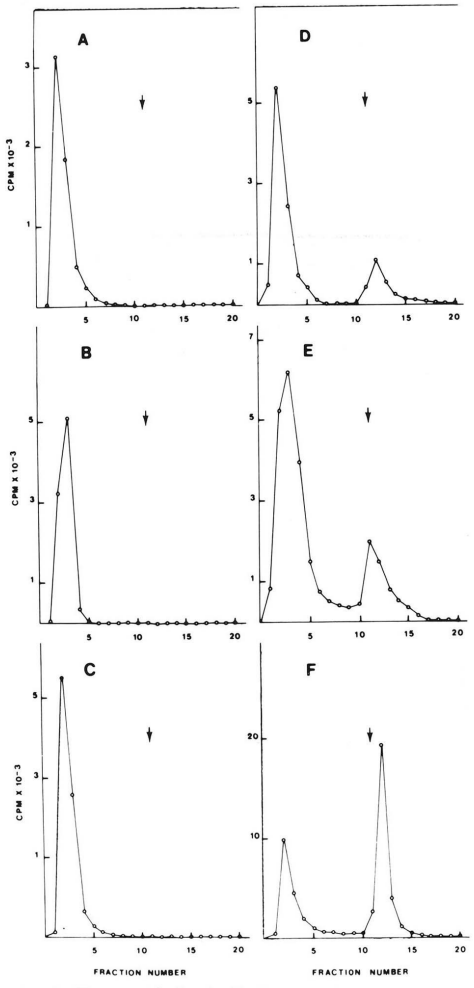

FIG. 1. ***H. pomatia* lectin-Sepharose chromatographies of ^{125}I-labeled proteins.** ^{125}I-BSA, ^{125}I-ovalbumin, ^{125}I-transferrin, ^{125}I-bovine submaxillary mucin, and ^{125}I-glycophorin A were chromatographed on *H. pomatia* lectin-Sepharose columns after treatment with neuraminidase. Glycophorin A was also run without neuraminidase treatment. *A*, neuraminidase-treated ^{125}I-BSA, *B*, neuraminidase-treated ^{125}I-ovalbumin; *C*, neuraminidase-treated ^{125}I-transferrin; *D*, neuraminidase-treated ^{125}I-bovine submaxillary mucin; *E*, ^{125}I-glycophorin A; *F*, neuraminidase-treated ^{125}I-glycophorin A. The *arrows* show the addition of α-*N*-acetylgalactosamine.

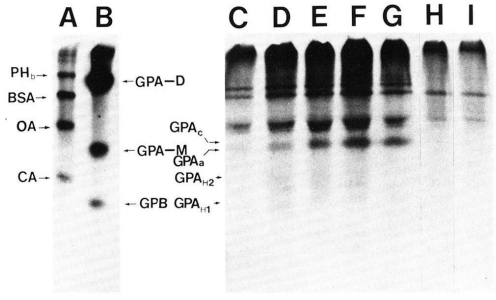

FIG. 2. **Fluorography pattern of a polyacrylamide slab gel of pulse-chase labeled glycophorin A molecules.** K562 cells were labeled for 5 min with [^{35}S]methionine and chased with nonradioactive medium. After detergent solubilization the glycophorin A molecules were immune precipitated with anti-glycophorin A antiserum. *A*, pattern of ^{14}C-labeled standard proteins. *PH_b*, phosphorylase *b*; *BSA*, bovine serum albumin; *OA*, ovalbumin; *CA*, carbonic anhydrase. *B*, pattern of periodate/NaB[^{3}H]$_4$-labeled red cell membranes. *C*, pattern obtained with antiserum after a 5-min pulse with [^{35}S]methionine. *D*, pattern obtained with antiserum after a 3-min chase. *E*, pattern obtained with antiserum after a 6-min chase. *F*, pattern obtained with antiserum after a 9-min chase. *G*, pattern obtained with antiserum after a 12-min chase. *H*, pattern obtained with preimmune serum after a 5-min pulse. *I*, pattern obtained with preimmune serum after a 12-min chase. GPA-D, glycophorin A dimer, *GPA-M*, glycophorin A monomer; *GPB*, glycophorin B; *GPA_c*, mature glycophorin A; *GPA_a*, glycophorin A precursor with apparent molecular weight of 37,000, *GPA_{H1}*, glycophorin A precursor with apparent molecular weight of 24,000; *GPA_{H2}*, glycophorin A precursor with apparent molecular weight of 30,000.

Carl_G_190x270_mm_blokki_FINAL.indd 141 06-Aug-23 1:53:35 PM

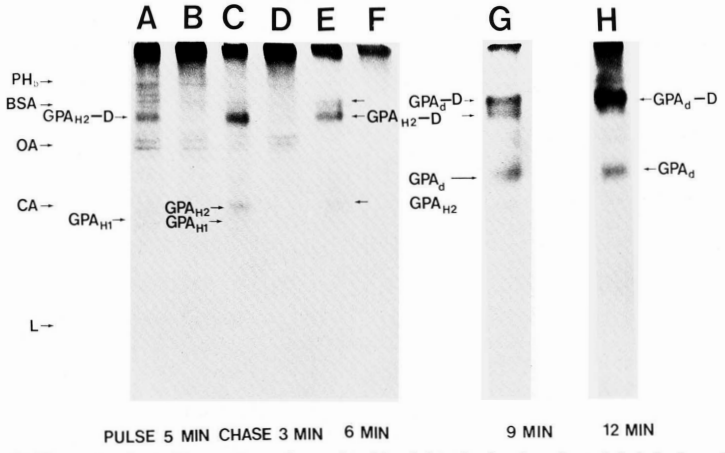

FIG. 3. **Fluorography pattern of a polyacrylamide slab gel of pulse-chase labeled glycophorin A molecules bound to *H. pomatia* lectin.** K562 cells were labeled for 5 min with [^{35}S]methionine and chased as indicated. Detergent extracts were treated with neuraminidase for 5 min to expose *N*-acetylgalactosamines before applying to *H. pomatia* lectin-Sepharose columns. Eluates obtained with α-*N*-acetylgalactosamine were immune precipitated with anti-glycophorin A antiserum and subjected to polyacrylamide slab gel electrophoresis prior to fluorography. *A*, immune precipitate obtained with antiserum from K562 cells labeled for 5 min with [^{35}S] methionine; *B*, with preimmune serum; *C*, as *A* but followed by a 3-min chase; *D*, with preimmune serum; *E*, as *A* but followed by a 6-min chase; *F*, with preimmune serum; *G*, as *A* but followed by a 9-min chase; *H*, as *A* but followed by a 12-min chase. *GPA$_d$*, mature glycophorin A treated with neuraminidase; *GPA$_{H2}$-D* and *GPA$_d$-D*, dimers of GPA$_{H2}$ and GPA$_d$. Positions of standard proteins are marked: see legend to Fig. 2. L, lysozyme.

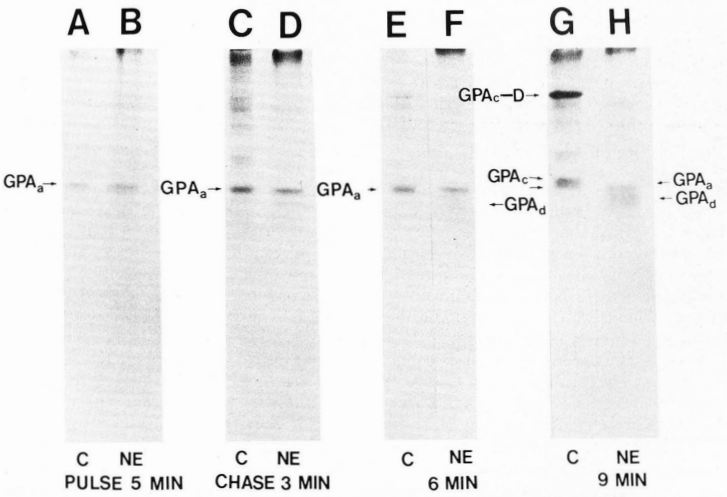

FIG. 4. **Fluorography pattern of a polyacrylamide slab gel of pulse-chase labeled glycophorin A bound to lentil lectin.** K562 cells were labeled for 5 min with [^{35}S]methionine and chased as indicated. Detergent extracts were applied to lentil lectin-Sepharose columns and eluates were immune precipitated with anti-glycophorin A antiserum. Aliquots of the immune precipitates were treated with neuraminidase (*NE*) for 10 min followed by polyacrylamide slab gel electrophoresis and fluorography. *A*, immune precipitate obtained with antiserum from K562 cells labeled for 5 min with [^{35}S]methionine; *B*, as *A* but treated with neuraminidase; *C*, as *A* but followed by a 3-min chase; *D*, as *C* but treated with neuraminidase; *E*, as *A* but followed by a 6-min chase; *F*, as *E* but treated with neuraminidase; *G*, as *A* but followed by a 9-min chase; *H*, as *G* but treated with neuraminidase. *C*, control. *GPA$_c$-D*, dimer of mature glycophorin A.

Carl_G_190x270_mm_blokki_FINAL.indd 142 06-Aug-23 1:53:35 PM

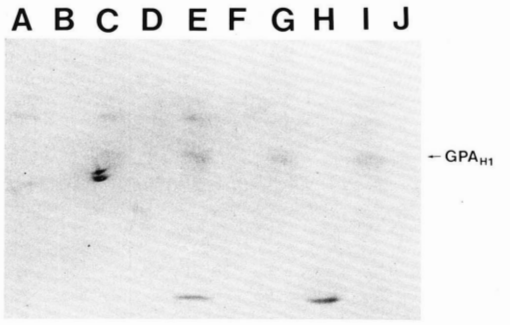

FIG. 5. **Fluorography pattern of a polyacrylamide slab gel of pulse-chase labeled glycophorin A in the presence of monensin.** K562 cells were labeled in the presence of 10 μM monensin for 5 min with [^{35}S]methionine, and chased as indicated. Detergent extracts were applied to *H. pomatia* lectin-Sepharose columns, sugar eluates were immune precipitated with anti-glycophorin A antiserum, and subjected to polyacrylamide slab gel electrophoresis followed by fluorography. *A*, immune precipitate obtained with antiserum from monensin-treated K562 cells labeled for 5 min with [^{35}S]methionine; *B*, with preimmune serum; *C*, as *A* but followed by a 3-min chase; *D*, with preimmune serum; *E*, as *A* but followed by a 6-min chase; *F*, with preimmune serum; *G*, as *A* but followed by a 9-min chase; *H*, with preimmune serum; *I*, as *A* but followed by a 12-min chase; *J*, with preimmune serum. The identities of the upper weakly labeled bands are uncertain.

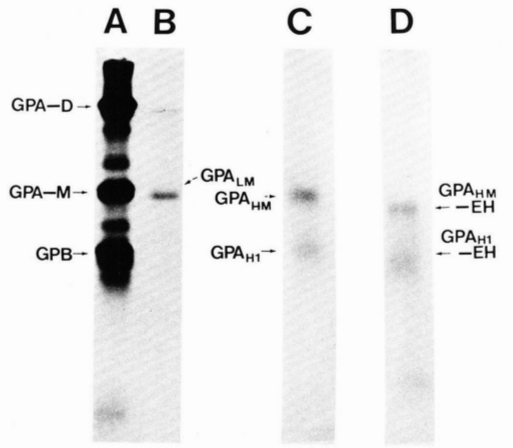

FIG. 6. **Treatment with endo-*N*-acetylglucosaminidase H of glycophorin A molecules synthesized in the presence of monensin.** K562 cells were labeled with [^{35}S]methionine for 1 h in the presence of 10 μM monensin and detergent extracts applied either to lentil lectin-Sepharose or to *H. pomatia* lectin-Sepharose columns and sugar eluates immune precipitated with anti-glycophorin A antiserum. Aliquots of immune precipitates obtained from *H. pomatia* lectin-Sepharose columns were treated with endo-*N*-acetylglucosaminidase H. All samples were then analyzed by polyacrylamide slab gel electrophoresis followed by fluorography. *A*, pattern of periodate/NaB[^{3}H]$_4$-labeled red cell proteins; *B*, immune precipitate obtained with antiserum from material bound to and eluted from lentil lectin-Sepharose; *C*, immune precipitate obtained with antiserum from material bound to *H. pomatia* lectin-Sepharose; *D*, as *C* but treated with endo-*N*-acetylglucosaminidase H. *GPA$_{LM}$*, glycophorin A precursor synthesized in the presence of monensin and bound to lentil lectin-Sepharose; *GPA$_{H1}$* and *GPA$_{HM}$*, glycophorin A precursors synthesized in the presence of monensin and bound to *H. pomatia* lectin-Sepharose; GPA$_{HM}$-EH and GPA$_{H1}$-EH, GPA$_{HM}$ and GPA$_{H1}$ treated with endo-*N*-acetylglucosaminidase H.

that the *N*-acetylneuraminic acids appeared in glycophorin A after a 9-min chase because neuraminidase treatment decreased the apparent molecular weight of the protein (Fig. 4*H*). Samples obtained with preimmune serum did not contain any specific material (data not shown). The GPA$_{H1}$ and GPA$_{H2}$ molecules did not bind to the lentil lectin columns.

Effect of Monensin on Glycophorin A Synthesis—Monensin is a carboxylic ionophore and is known to inhibit the intracellular migration of newly synthesized membrane proteins (29). When K562 cells were pulse-chase labeled with [^{35}S] methionine in the presence of 10 μM monensin, but without neuraminidase treatment, the GPA$_{H1}$ precursor molecule accumulated (Fig. 5). The identity of the bands which move more slowly is not certainly known.

When monensin-treated cells were labeled for 1 h with [^{35}S] methionine the *H. pomatia* lectin-bound precursor GPA$_{H1}$ was partially processed to the GPA$_{HM}$ molecule (Fig. 6*C*). Both proteins were incompletely processed since their *N*-linked oligosaccharides remained sensitive to endo-β-*N*-acetylglucosaminidase H treatment (Fig. 6*D*). Fig. 6*B* shows the corresponding glycophorin A molecule (GPA$_{LM}$) bound to lentil lectin from monensin-treated cells after labeling with [^{35}S] methionine. The protein is smaller than normal glycophorin A (*cf.* Fig. 10*E*), and seems to be incompletely processed. The GPA$_{LM}$ and GPA$_{HM}$ molecules are evidently the same because both the lentil lectin-Sepharose column and the *H. pomatia* lectin-Sepharose column were able to absorb all glycophorin A molecules in this molecular weight region. In the presence of monensin the glycophorin A molecules did not reach the cell surface, since they were not degraded by trypsin treatment (12, 13) of intact cells (data not shown).

Partial Characterization of the Glycophorin A Molecules—Crucial for the interpretation of the results were the demonstrations of the identity of the different molecules reacting with anti-glycophorin A antiserum. For this purpose we extensively purified glycophorin A from red cell membranes, and used the purified molecules in competitive experiments during immune precipitation. Fig. 7 shows the purified glycophorin A stained with Coomassie Blue. It shows two closely spaced bands. This is always seen using discontinuous gel systems. Two glycophorin bands are also seen in surface-labeled membranes (see, for example, Fig. 8*B*). When K562 cells were pulse-chase labeled for 6 min with [^{35}S]methionine, and the detergent extracts run on *H. pomatia*-Sepharose, the GPA$_{H1}$ and GPA$_{H2}$ molecules were obtained from the sugar chains by immune precipitation (Fig. 8*C*). When an identical sample contained 25 μg of pure glycophorin A no GPA$_{H1}$ and GPA$_{H2}$ bands were obtained (Fig. 8*D*). Similarly, the immune precipitation, of the GPA$_a$ molecule, obtained from lentil lectin eluates, was completely inhibited by purified glycophorin A (Fig. 8, *E* and *F*). When cells were labeled for 1 h, and the detergent extract passed through lentil lectin-Sepharose, the GPA$_c$ was immune precipitated from the eluate (Fig. 8*G*). Again, cold glycophorin A inhibited the precipitation (Fig. 8*H*).

To show that both the lentil lectin and *H. pomatia* lectin-reactive glycophorin A molecules really contained *O*-glycosidic carbohydrate, K562 cells were surface-labeled by the periodate/NaB[^{3}H]$_4$ technique. The cells were solubilized in Triton X-100 containing buffer and chromatographed on lentil lectin-Sepharose (Fig. 9*A*). From the sugar eluate glycophorin A was immune precipitated, digested with Pronase, and subjected to alkaline borohydride treatment. The liberated glycopeptides/oligosaccharides were analyzed by gel fil-

Carl_G_190x270_mm_blokki_FINAL.indd 143 06-Aug-23 1:53:35 PM

tration on Bio-Gel P-6 (Fig. 9*D*). Peak 1 corresponds to the position of the *N*-glycosidic oligosaccharide, peak 2 to the *O*-glycosidic tetrasaccharide, and peak 3 to the *O*-glycosidic trisaccharides (24). The passed-through fraction was once more chromatographed on lentil lectin-Sepharose (Fig. 9*B*), and the glycopeptides/oligosaccharides analyzed by gel filtration (Fig. 9*E*). Almost no glycophorin A molecules were obtained. When the passed-through fraction from the second lentil lectin column was added to a wheat germ lectin column, a clear peak was eluted by sugar (Fig. 9*C*). Immune precipitation gave a glycophorin A molecule, which contained the normal glycopeptides/oligosaccharides (Fig. 9*F*).

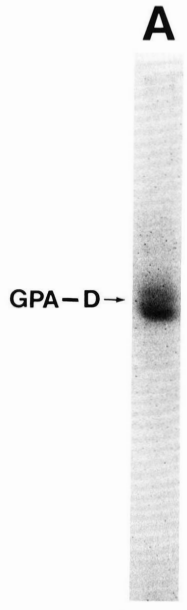

FIG. 7. **Polyacrylamide gel pattern of purified red cell glycophorin A.** Purified glycophorin A (25 μg) was run on an 8% polyacrylamide gel, and the gel stained for protein with Coomassie Blue. Only the dimer form of glycophorin A is seen.

To obtain further information on the presence of *O*-glycosidic oligosaccharides, and the electrophoretic behavior of partially de-*O*-glycosylated glycophorin A, we treated the protein with neuraminidase and α-*N*-acetylgalactosaminyl-oligosaccharides. ^{125}I-labeled glycophorin A from red cells was degraded to a lower molecular weight protein by the enzymes (Fig. 10*C*). The protein obtained by lentil lectin chromatography from control K562 cells was degraded, although less efficiently (Fig. 10*F*), but that from tunicamycin-treated cells degraded to a 22,000 molecular weight protein (Fig. 10*H*). This protein is in the same region of the gel as GPA_{H1}.

DISCUSSION

In many respects the biosynthesis of the major red cell sialoglycoprotein, glycophorin A, resembles that of other mammalian and viral glycoproteins (30). Glycophorin A is evidently synthesized with a signal peptide which is cleaved co-translationally. Simultaneously *N*-glycosylation occurs (11). It takes about 10 min for the protein to reach the Golgi apparatus, and 25 min for it to appear at the cell surface (12). Tunicamycin inhibited the synthesis of the *N*-glycosidic oligosaccharide, but had no effect on the *O*-glycosylation, and the intracellular migration of the protein (13).

The most interesting aspect of the biosynthesis of glycophorin A and the advantage to use it as a model for biosynthetic studies is to elicudate the mechanism of *O*-glycosylation and the subcellular location of this process. For such investigations glycophorin A is excellent because it contains a large number of *O*-linked oligosaccharides (6).

The glycophorin A molecules of K562 cells are similar although not identical to those of red cells. They differ in the

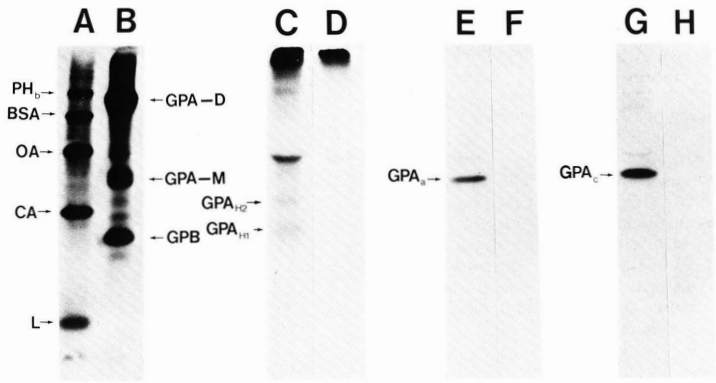

FIG. 8. **Inhibition of immune precipitation of [^{35}S]methionine-labeled glycophorin A molecules by purified glycophorin A.** The immune precipitates were visualized by fluorography. *A*, pattern of ^{14}C-labeled standard proteins; *B*, pattern of periodate/NaB[^{3}H]$_4$-labeled red cell membranes; *C*, pattern obtained with 5 μl of anti-glycophorin A antiserum from the sugar eluate of a *H. pomatia* lectin-Sepharose column of cells labeled for 6 min with [^{35}S]methionine; *D*, same as in *C*, but in the presence of 25 μg of purified glycophorin A; *E*, pattern obtained with 5 μl of anti-glycophorin A antiserum from the sugar eluate of a lentil lectin-Sepharose column of cells labeled for 6 min with [^{35}S]methionine, *F*, same as in *E* but in the presence of 25 μg of purified glycophorin A; *G*, pattern obtained with 5 μl of anti-glycophorin A antiserum from sugar eluates of a lentil lectin-Sepharose column of cells labeled for 60 min with [^{35}S]methionine; *H*, same as in *G* but in the presence of 25 μg of purified glycophorin A.

Carl_G_190x270_mm_blokki_FINAL.indd 144 06-Aug-23 1:53:35 PM

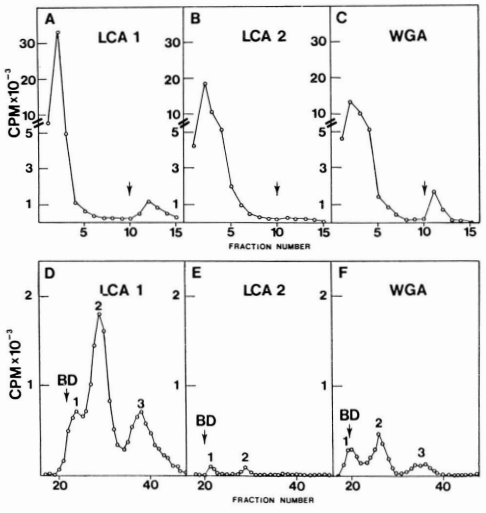

FIG. 9. **Lectin-Sepharose and Bio-Gel P-6 chromatographies of periodate/NaB[^{3}H]$_4$-labeled K562 cells and glycophorin A glycopeptides/oligosaccharides.** *A*, lentil lectin-Sepharose chromatography of ^{3}H-labeled K562 cell extract; *B*, lentil lectin-Sepharose chromatography of the passed-through fraction of sample shown in *A*; *C*, wheat germ lectin-Sepharose chromatography of the passed-through sample shown in *B*. The *arrows* indicate the additions of competing monosaccharide. Five-μl samples of a total of 2 ml were counted for radioactivity; *D*, Bio-Gel P-6 gel filtraiton of glycopeptides/oligosaccharides of glycophorin A obtained from the sugar eluate of *A* with anti-glycophorin A antiserum; *E*, as in *D* but from sugar eluate of *B*; *F*, as in *D* but from sugar eluate of *C*. *BD*, position of Blue Dextran 2000; *1*, position of *N*-glycosidic oligosaccharide; *2*, position of *O*-glycosidic tetrasaccharide; *3*, position of *O*-glycosidic trisaccharides. Only one-third of the immune precipitate was analyzed in *F*.

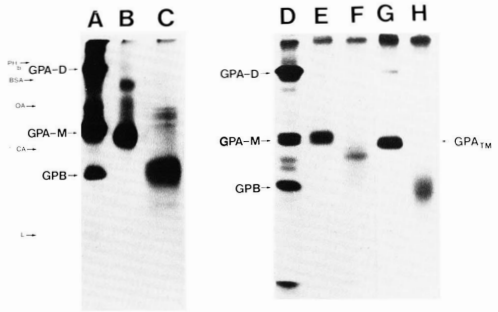

FIG. 10. **Effect of α-*N*-acetylgalactosaminyl-oligosaccharidase on glycophorin A.** K562 cells were labeled for 1 h with [^{35}S] methionine with or without 20 μg/ml of tunicamycin. Detergent extracts were applied either to lentil lectin-Sepharose or wheat germ lectin-Sepharose columns and sugar eluates immune precipitated with anti-glycophorin A antiserum. Aliquots of immune precipitates were treated with α-*N*-acetylgalactosaminyl-oligosaccharidase after pretreatment with neuraminidase. All samples were then analyzed by polyacrylamide slab gel electrophoresis followed by fluorography. *A*, pattern of ^{125}I-labeled red cell membranes; *B*, immune precipitate with antiserum from ^{125}I-labeled red cell membranes; *C*, as *B* but treated with the enzyme; *D*, pattern of periodate/NaB[^{3}H]$_4$-labeled red cell membranes; *E*, immune precipitate obtained with antiserum from K562 cell extract bound to lentil lectin-Sepharose; *F*, as *E* but treated with enzyme; *G*, immune precipitate obtained with antiserum from K562 cells grown in the presence of tunicamycin and bound to wheat germ lectin-Sepharose; *H*, as *G* but treated with enzyme. *GPA$_{TM}$*, glycophorin A synthesized in the presence of tunicamycin. The positions of the standard proteins are marked.

degree of glycosylation. The majority of the *O*-glycosidic oligosaccharides have the same structure in K562 cells and red cells (9, 10), but the K562 cell glycophorin A contains less of them (10).

It is a well-known fact that glycophorin A easily forms dimers in the presence of SDS and 2-mercaptoethanol (31, 32). Many of the polyacrylamide slab gel patterns show varying levels of glycophorin A dimerization. The reason for this is not well understood. Buffers containing Tris (like the electrophoretic sample buffer) enhance the dimer formation (33). Furthermore, dimers are more easily formed with increasing concentrations of glycophorin A. It is possible that poorly glycosylated glycophorin A molecules being relatively more hydrophobic lead to an increased dimerization. On the other hand, neuraminidase treatment lead to increased monomerization. Using molecular weight standard proteins and red cell glycophorin A molecules as markers, the identification of the monomer and dimer forms is, however, easy.

We previously identified after a short pulse with [^{35}S] methionine the GPA$_a$ glycophorin A precursor which interacted with lentil lectin (12). This fact and its endo-*N*-acetylglucosaminidase H sensitivity showed that it contained the single *N*-glycosidic oligosaccharide located at asparagine 26 (13). Whether it is *O*-glycosylated is not known, but the apparent molecular weight substantially exceeds that of the apoprotein. The protein did not, however, interact with the *N*-acetylgalactosamine-specific lectin from *H. pomatia*.

The specificity of the *H. pomatia* lectins for α-*N*-acetylgalactosamine/D-galactose-β(1–3)*N*-galactosamine was tested using ^{125}I-labeled proteins with different types of glycan structures. The proteins were treated with neuraminidase to ensure the exposure of penultimate galactosyl/*N*-acetylgalactosaminyl residues.

BSA is not a glycoprotein and did not interact. Ovalbumin mainly contains high mannose-type oligosaccharides and showed no binding, neither did transferrin, which contains complex-type oligosaccharide chains. In contrast, bovine submaxillary mucin, containing α-*N*-acetylgalactosamine linked to serine and threonine residues, showed binding. Neuraminidase-treated glycophorin A bound most efficiently. It is known that the affinity of the lectin for D-galactose-β(1–3)*N*-acetylgalactosamine is higher than that for *N*-acetylgalactosamine (28).

We have now found two glycophorin A precursors, GPA$_{H1}$ and GPA$_{H2}$, which interact with this lectin. Because the molecules bind it is obvious that they contain *N*-acetylgalactosamine residues. Interestingly, these molecules did not bind to lentil lectin-Sepharose. It is, however, known that some high mannose-type chains, which may arise during trimming of *N*-glycosidic oligosaccharides do not bind to lentil lectin (34).

Immune precipitation of GPA$_a$, GPA$_c$, GPA$_{H1}$, and GPA$_{H2}$ was inhibited by purified red cell glycophorin A. The antiserum was rendered specific for glycophorin A by absorption with En(a−) membranes, but the inhibition of precipitation by the purified red cell glycophorin A further proved that the precipitated proteins were indeed glycophorin A precursors.

From the pulse-chase experiments it became apparent that some of the glycophorin A molecules were synthesized with GPA$_a$ as precursor, and some through the GPA$_{H1}$ and GPA$_{H2}$ intermediates. The GPA$_{H1}$ and GPA$_{H2}$ molecules contained

Carl_G_190x270_mm_blokki_FINAL.indd 145 06-Aug-23 1:53:35 PM

N-acetylgalactosaminyl residues, whereas GPA_a did not seem to. The *O*-glycosylation through GPA_{H1}-GPA_{H2} is an early biosynthetic event occurring before completion of *N*-glycosylation. This was supported by the monensin experiments. Monensin resulted in the accumulation of the GPA_{H1} protein in a partially glycosylated form and it did not reach the cell surface. Some GPA_{HM} protein was also obtained. Whether this results from GPA_{H1}-GPA_{H2} or GPA_a is not known. The subcellular site of monensin action is not known exactly, but most studies indicate that it is somewhere in the Golgi region (29). Monensin may, however, also directly affect the processing of *N*-glycosidic oligosaccharides (35) and this may vary in different cells.

In contrast, the additon of *N*-acetylgalactosaminyl residues to GPA_a was much slower and took about 9 min of chase (Fig. 4). Analysis of the mature surface-labeled glycophorin A molecules showed that they all contained *O*-glycosidic oligosaccharides, but all of them never acquired the activity to bind to lentil lectin-Sepharose. The presence of *O*-glycosidic oligosaccharides was also demonstrated by the decrease in molecular weight after treatment with α-*N*-acetylgalactosaminyl-oligosaccharidase. Cummings *et al.* (36) has reported that *O*-glycosylation of the low density lipoprotein receptor occurs before the terminal glycosylation in the Golgi apparatus. This seems to be similar to the biosynthetic route of glycophorin A through the GPA_{H1} and GPA_{H2} intermediates.

On the other hand some viral glycoproteins, which contain *O*-glycosidic oligosaccharides seem to acquire them relatively late (4, 37), and no *O*-glycosylation was observed in the presence of monensin (4, 37).

These results show that the mechanisms and subcellular sites of *O*-glycosylation may be more complex than commonly believed.

Acknowledgments—We thank U. Katajarinne and M. Vaalle for technical assistance and B. Björnberg for secretarial help.

REFERENCES

1. Hubbard, S. C., and Ivatt, R. J. (1981) *Annu. Rev. Biochem.* **50,** 555–583
2. Hanover, J. A., Lennarz, W. J., and Young, J. D. (1980) *J. Biol. Chem.* **255,** 6713–6716
3. Hanover, J. A., Elting, J., Minz, G. R., and Lennarz, W. J. (1982) *J. Biol. Chem.* **257,** 10172–10177
4. Johnson, D. L., and Spear, P. G. (1983) *Cell* **32,** 987–997
5. Strous, G. J. A. M. (1979) *Proc. Natl. Acad. Sci. U. S. A.* **76,** 2694–2698
6. Tomita, M., and Marchesi, V. T. (1975) *Proc. Natl. Acad. Sci. U. S. A.* **72,** 2964–2968
7. Thomas, D. B., and Winzler, R. J. (1969) *J. Biol. Chem.* **244,** 5943–5946
8. Yoshima, H., Furthmayr, H., and Kobata, A. (1980) *J. Biol. Chem.* **255,** 9713–9718
9. Gahmberg, C. G., Jokinen, M., and Andersson, L. C. (1979) *J. Biol. Chem.* **254,** 7442–7448
10. Gahmberg, C. G., Ekblom, M., and Andersson, L. C. (1984) *Proc. Natl. Acad. Sci. U. S. A.* **81,** 6752–6756
11. Jokinen, M., Ulmanen, I., Andersson, L. C., Kääriäinen, L., and Gahmberg, C. G. (1981) *Eur. J. Biochem.* **114,** 393–397
12. Jokinen, M., Gahmberg, C. G., and Andersson, L. C. (1979) *Nature* **279,** 604–607
13. Gahmberg, C. G., Jokinen, M., Karhi, K. K., and Andersson, L. C. (1980) *J. Biol. Chem.* **255,** 2169–2175
14. Sage, H. J., and Green, R. W. (1972) *Methods Enzymol.* **28,** 332–339
15. Marchesi, V. T. (1972) *Methods Enzymol.* **28,** 354–356
16. Cuatrecasas, P. (1970) *J. Biol. Chem.* **245,** 3059–3065
17. Gahmberg, C. G., and Andersson, L. C. (1977) *J. Biol. Chem.* **252,** 5888–5894
18. Hubbard, A. L., and Cohn, Z. A. (1972) *J. Cell Biol.* **55,** 390–405
19. Gahmberg, C. G., and Hakomori, S. (1973) *J. Biol. Chem.* **248,** 4311–4317
20. Hamaguchi, H., and Cleve, H. (1972) *Biochem. Biophys. Res. Commun.* **47,** 459–464
21. Greenwood, F. C., Hunter, W. M., and Glover, J. S. (1963) *Biochem. J.* **89,** 114–123
22. Gahmberg, C. G., Jokinen, M., and Andersson, L. C. (1978) *Blood* **52,** 379–387
23. Tarentino, A. L., Plummer, T. H., Jr., and Maley, F. (1974) *J. Biol. Chem.* **249,** 818–824
24. Gahmberg, C. G., and Andersson, L. C. (1982) *Eur. J. Biochem.* **122,** 581–586
25. Laemmli, U. K. (1970) *Nature* **227,** 680–685
26. Bonner, W. M., and Laskey, R. A (1974) *Eur. J. Biochem.* **46,** 83–88
27. Carlson, D. (1966) *J. Biol. Chem.* **241,** 2984–2986
28. Hammarström, S. (1972) *Methods Enzymol.* **28,** 368–383
29. Tartakoff, A. M. (1983) *Cell* **32,** 1026–1028
30. Blobel, G. (1980) *Proc. Natl. Acad. Sci. U. S. A.* **77,** 1496–1500
31. Steck, T. L. (1974) *J. Cell Biol.* **62,** 1–19
32. Silverberg, M., and Marchesi, V. T. (1978) *J. Biol. Chem.* **253,** 95–98
33. Marton, L. S. G., and Garvin, J. E. (1973) *Biochem. Biophys. Res. Commun.* **59,** 352–360
34. Kornfeld, K., Reitman, M. L., and Kornfeld, R. (1981) *J. Biol. Chem.* **256,** 6633–6640
35. Strous, G. J. A. M., Willemsen, R., van Kerkhof, P., Slot, J. W., Geuze, H. J., and Lodish, H. F. (1983) *J. Cell Biol.* **97,** 1815–1822
36. Cummings, R. D., Kornfeld, S., Schneider, W., Hobgood, K. K., Tolleshaug, H., Brown, M. S., and Goldstein, J. L. (1983) *J. Biol. Chem.* **258,** 15261–15273
37. Niemann, H., Boschek, B., Evans, D., Rosing, M., Tamura, T., and Klenk, H.-D. (1982) *EMBO J.* **1,** 1499–1504

Carl_G_190x270_mm_blokki_FINAL.indd 146 06-Aug-23 1:53:35 PM

Part II

BLOOD GROUP ANTIGENS

Carl_G_190x270_mm_blokki_FINAL.indd 147 06-Aug-23 1:53:35 PM

Introduction

Landsteiner and others did pioneering work on blood group antigens already in the early 1900s. However, the chemical nature of the various antigens long remained poorly known. The best known were the ABO antigens and the MN antigens.

Glycolipids, carrying ABH antigens, were characterized by several groups including, that of S.-i. Hakomori (1). Whether red cell membrane proteins also carry ABH blood group activity, was unsettled. Actually, few membrane proteins had been isolated, and their purity was not good enough. However, the development of the analytical methods changed the situation. Many blood group antigens are minor components, which made their biochemical analysis challenging.

The Rh-antigen system, were described by Levine and Stetson (2) and Landsteiner and Wiener (3), but their molecular nature long remained unclear. The availability of excellent antisera, and improved blood group typing, finally made it possible to identify and characterize the antigens. The Rh system is complex, but clinically the most important antigen is Rh_o(D).

Comments on Papers 19 to 25

Above, I described studies on the expression and biosynthesis of glycophorin A. The mature red cell carries the MN antigens, which need complete O-linked oligosaccharides in the NH_2-terminal of glycophorin A for activity. However, the M/N specificity is due to the amino acid polymorphism at positions 1 and 5. M type glycophorin A has serine and glycine, whereas N type has leucine and glutamic acid. Glycophorin A was incompletely O-glycosylated in immature red cells, and concomitantly with maturation, it became more O-glycosylated and MN positive (Paper 19).

ABO blood group antigens, were first chemically studied from soluble mucins, but red cell expressing antigens had not been much studied. To be able to study red cell ABO antigens, we isolated the blood group A-specific lectin from *Vicia cracca* seeds (4), and used it for affinity chromatography of lactoperoxidase/^{125}I and galactose oxidase/NaB^3H_4 and periodate/ NaB^3H_4 labelled erythrocyte membranes of different ABO blood groups. The labelled proteins were analysed by gel electrophoresis (Paper 20). Mature red cells expressed blood group A activity on the band 3 protein and on diffusely migrating protein bands of 40000-60000 apparent molecular weights. The glycophorins were blood group A- negative. We then studied the expression of blood group A- antigens in bone marrow cells. After adding the *Vicia cracca* lectin, the cells were incubated with an antiserum to the lectin, followed by protein A- expressing staphylococci. After cytological staining, we identified the blood group expressing cells. Only cells of the erythroid lineage were positive from the basophilic normoblast to more differentiated

Carl_G_190x270_mm_blokki_FINAL.indd 148 06-Aug-23 1:53:35 PM

cells (5). Further work showed that A and B blood group active oligosaccharides were located on different glycosyl peptides from AB red blood cells (6). We later collaborated with Swedish scientists to study the binding of RIFINs in *Plasmodium falciparum* infected red cells, to red cells. Interestingly, there was a preferential binding to blood group- A cells (Paper 21).

We were also interested in the possibility to change the structure of oligosaccharides on cells by chemical means. After oxidation of cell surface glycoconjugates by treatment with galactose oxidase or periodate, we added oligosaccharide-hydrazines to the oxidized cells. This treatment resulted in covalent bonds between the added oligosaccharides and the cellular oxidized sugars. In this way we obtained blood group- A and -B active red cells from O cells (Paper 22).

The molecular nature of the important Rh blood group antigens long remained controversial. A molecular weight of 7000 was reported in 1979 for the Rh_o(D) antigen (7), and later the band 3 protein with an apparent molecular weight of 90000, was proposed to carry the antigen activity (8). I wondered how it is possible that the researchers could end up with such different results, and I decided to study the Rh_o(D) antigen. I first tried to immune precipitate the antigen from galactose oxidase/NaB^3H_4 labelled red cell membranes, but without success. However, when Rh_o(D) positive red cells were labelled by the ^{125}I-lactoperoxidase method, several protein bands were seen, but only a minor protein band of 28000-33000 apparent molecular weight was specifically obtained from Rh_o(D) positive cells (Paper 23). It was obvious that the previously reported findings were due to either degraded proteins or lipids running on gels in the front, and the quantitatively dominating band 3 protein. Stephen Moore and co-workers independently obtained a similar result (9). Convincing proof of the size of the antigen was obtained from –D-/-D- (" super-D") red cells, which express high amounts of the Rh_o(D) antigen (Paper 24). Importantly, when a detergent extract from the red cell membranes was passed over a column containing the galactose binding lectin from *Ricinus communis* lectin, the Rh_o(D) protein bound. However, the purified protein, did not bind. The results indicated that the Rho(D) protein was in complex with a glycoprotein. Later studies have shown that the Rh_o(D) antigen indeed contains no sugar, and a Rh-associated glycoprotein was described which explains the results (10).

I earlier proposed that mammalian cell surface proteins always are *glycoproteins* (Paper 5). Although, the Rh_o(D) polypeptide does not contain sugar, it is bound with the Rh-associated glycoprotein, and the complex is thus a glycoprotein. In that sense it resembles MHC type I transplantation antigens, in which the heavy chains are glycosylated and form a dimer with β2 microglobulin, which does not contain carbohydrate. In a review we discussed why surface proteins are glycoproteins (Paper 25). The importance of being glycosylated, may be due to the fact that during biosynthesis, it is important for the polypeptides to have enough time to fold, and associate with other polypeptides in a proper way. The proteins can be retained within the cells by interaction with intracellular chaperons like calnexin and calreticulin (11-13). Certainly, the cell surface carbohydrate often has receptor functions, but this fact does not explain that *all* cell surface proteins are glycoproteins.

It could be mentioned that Peter Agre and Jean-Pierre Cartron began to study the Rh_o(D) protein (14). When Agre was purifying the protein, he ended up with a contaminant. This turned out to be a water transport protein, which he named aquaporin (15). Aquaporin has a similar molecular weight as the Rh_o(D) protein. Like aquaporin, the Rh_o(D) is very hydrophobic, and it passes twelve times through the plasma membrane. This fact explains the finding that the Rh_o(D) protein, was poorly solubilized using Triton X-100, and the majority remained bound to the cytoskeleton (16).

Carl_G_190x270_mm_blokki_FINAL.indd 149 06-Aug-23 1:53:35 PM

The LW (Landsteiner-Wiener) blood group was initially confused with the Rh blood group. $Rh_o(D)$ cells expresses more of the LW-antigen than $Rh_o(D^-)$cells, and Rh^{null} cells lack the LW antigen. When the LW antigen was cloned and sequenced, it turned out that it shows homology with the intercellular adhesion molecules (ICAM) (17). We then showed that it binds to β2-integrins, and renamed it ICAM-4 (see below).

References

1. Stellner, K., Watanabe, K. and Hakomori, S. (1973) Isolation and characterization of glycosphingolipids with blood group H specificity from membranes of human erythrocytes. *Biochemistry* **12**, 656-661.
2. Levine, P. and Stetson, R.E. (1939) An unusual case of intragroup agglutination. *J. Am. Med. Assoc*. **113**, 126-127.
3. Landsteiner, K. and Wiener, A.S. (1940) An agglutinable factor in human blood recognized by immune sera for rhesus blood. *Proc. Soc. Exp. Biol. Med*. **43**, 223.
4. Karhi, K.K. and Gahmberg, C.G. (1980) Isolation and characterization of the blood group A-specific lectin from *Vicia cracca. Biochim. Biophys. Acta* **622**, 337-343.
5. Karhi, K.K., Andersson, L.C., Vuopio, P. and Gahmberg, C.G. (1981) Expression of blood group A antigens in human bone marrow cells. *Blood* **57**, 147-151.
6. Viitala, J., Karhi, K.K., Gahmberg, C.G., Finne, J., Järnefelt, J., Myllylä, G., and Krusius, T. (1981) Blood group A and B determinants are located in different polyglycosyl peptides isolated from human blood group AB erythrocytes. *Eur. J. Biochem*. **113**, 259-265.
7. Plapp, F.V., Kowalski, M.M., Tilzer, L., Brown, P.J., Evans, B.J. and Chiga, M. (1979) Partial purification of the Rho(D) antigen from Rh positive and negative erythrocytes. *Proc. Natl. Acad. Sci. USA*. **76**, 2964-2968.
8. Victoria, E.J., Mahan, L.C. and Masouredis, S.P. (1981) Anti-$Rh_o(D)$ IgG binds to band 3 glycoprotein of the human erythrocyte membrane. *Proc. Natl. Acad. Sci. USA*. **78**, 2898-2902.
9. Moore, S., Woodrow, C.F. and McClelland, D.B. (1982) Isolation of membrane components associated with human red cell antigens Rh(D), (c), (E) and Fy. *Nature* **295**, 529-531.
10. Avent, N.D. and Reid, M.E. (2000) The Rh blood group system: a review. *Blood* **95**, 375-387.
11. Ou, W.J., Cameron, P.H., Thomas, D.Y. and Bergeron, J.J. (1993) Association of folding intermediates of glycoproteins with calnexin during protein maturation. *Nature* **364**, 771-776.
12. Hebert, D.N., Foellmer, B. and Helenius, A. (1995) Glucose trimming and reglucosylation determine glycoprotein association with calnexin in the endoplasmic reticulum. *Cell* **81**, 425-433.
13. Fiedler, K. and Simons, K. (1995) The role of N-glycans in the secretary pathway. *Cell* **81**, 309-312.
14. Agre, P. and Cartron, J.-P. (1991) Molecular biology of the Rh antigens. *Blood* **78**, 551-563.
15. Agre, P. (2004) Aquaporin water channels (Nobel lecture). *Angew. Chem*. **43**, 4278-4290.

Carl_G_190x270_mm_blokki_FINAL.indd 150 06-Aug-23 1:53:35 PM

16. Gahmberg, C.G. and Karhi, K.K. (1984) Association of Rh_o(D) polypeptides with the membrane skeleton in Rh_o(D)-positive human red cells. *J. Immunol*. **133**, 334-337.
17. Bailly, P., Hermand, P., Callebout, I., Sonneborn, H.H., Khamlichi, S., Mornon, J.-P. and Cartron, J.-P. (1994) The LW blood group glycoprotein is homologous to intercellular adhesion molecules. *Proc. Natl. Acad. Sci. USA*. **91**, 5306-5310.

Carl_G_190x270_mm_blokki_FINAL.indd 151 06-Aug-23 1:53:35 PM

Carl_G_190x270_mm_blokki_FINAL.indd 152 06-Aug-23 1:53:35 PM

Proc. Natl. Acad. Sci. USA
Vol. 81, pp. 6752–6756, November 1984
Cell Biology

Differentiation of human erythroid cells is associated with increased *O*-glycosylation of the major sialoglycoprotein, glycophorin A

(erythrocyte differentiation/malaria/erythroleukemia)

CARL G. GAHMBERG*, MARJA EKBLOM,† AND LEIF C. ANDERSSON†

*Department of Biochemistry, University of Helsinki, 00170 Helsinki 17, Finland; and †Department of Pathology and Transplantation Laboratory, University of Helsinki, 00290 Helsinki 29, Finland

Communicated by Robert L. Hill, July 13, 1984

ABSTRACT **Glycophorin A, the major human erythrocyte sialoglycoprotein, is found exclusively on cells of the erythroid lineage. The amino acid sequence is known, and glycophorin A isolated from mature erythrocytes contains a single *N*-glycosidic and 15 *O*-glycosidic oligosaccharides. Monoclonal antibodies against erythrocyte glycophorin A reacted weakly with erythroid precursors while a monospecific rabbit antiserum reacted strongly with immature and mature red cells. Glycophorin A was isolated from cells representing various stages of erythropoiesis in normal bone marrow, from blood cells of neonates with erythroblastosis fetalis, and from the erythroleukemic cell lines K562 and HEL before and after induced differentiation. Analysis of the oligosaccharides showed less *O*-glycosylation of glycophorin A in erythroid precursors. The degree of glycosylation increased concomitantly with differentiation.**

The major sialoglycoprotein of human erythrocytes, glycophorin A (GPA), consists of 131 amino acids distributed in three separate domains: at the cell surface, within the lipid bilayer, and in the cytoplasm (1). The external NH_2-terminal portion is highly glycosylated, containing one *N*-glycosidic oligosaccharide at Asn-26 and 15 *O*-glycosidic oligosaccharides. The structure of the *N*-glycosidic oligosaccharide has been determined (2). Most *O*-glycosidic oligosaccharides have the structure Neu5Acα2-3Galβ1-3(Neu5Acα2-6)GalNAc (ref. 3; Neu5Ac, *N*-acetylneuraminic acid; see ref. 4 for the condensed symbolism for oligosaccharide chains).

It was shown that GPA is confined to the erythroid cell lineage and appears at the basophilic normoblast stage of erythropoiesis (5, 6). GPA is also found on the erythroleukemia cell lines K562 (7) and HEL (8, 9). The biosynthesis of the protein has been extensively studied in K562 cells and its *N*- and *O*-glycosylations have been elucidated (10–12).

We have now isolated GPA from normal bone marrow precursor cells and from the K562 and HEL cell lines before and after induction of differentiation, and we have studied its oligosaccharides. Our results show that, during differentiation of red cells, the GPA molecules become increasingly *O*-glycosylated. This change in structure of a major membrane molecule may be important to the understanding of cellular interactions and of the relationship between cellular differentiation and membrane protein glycosylation.

MATERIALS AND METHODS

Cells. Normal and En(a−) erythrocytes were obtained from the Red Cross Blood Transfusion Service, Helsinki. Bone marrow was recovered from pieces of ribs, which were resected during open thorax surgery at the Helsinki University Hospital. The cells were subjected to Ficoll-Isopaque centrifugation, and the interphase cells were collected. Fractionation according to cell size was accomplished using $1 \times g$ velocity sedimentation (13). Blood from neonatal patients with erythroblastosis fetalis was obtained from the Department of Pediatrics, Helsinki University Hospital, and the mononuclear cells were isolated. K562 cells were obtained from G. Klein, Karolinska Institute, Stockholm, and HEL cells from E. Papayannopoulou, University of Washington, Seattle.

Induction of Differentiation in K562 and HEL Cells. K562 cells and HEL cells were grown in RPMI 1640 medium containing 10% fetal calf serum. Cells were induced to differentiate for 1-6 days with 1.5 mM sodium butyrate, 0.1 μM retinoic acid, 10 nM phorbol 12-myristate 13-acetate (PMA), or 25–50 μM hemin as described (14–16). The degree of differentiation was estimated from May–Grünwald–Giemsa-stained smears, and cultures containing differentiated cells were harvested for further studies.

Antisera. Rabbit anti-GPA antisera were produced by immunizing with purified GPA (17). The antisera were adsorbed with En(a−) red cell membranes, which lack GPA (18–20), as described (5). Monoclonal anti-GPA antisera R10 and R18, and VIE-G4 were obtained from P. A. W. Edwards (21) and W. Knapp (22), respectively.

Binding of Protein A-Containing Staphylococci to Anti-GPA-Treated Bone Marrow Cells. The presence of GPA in bone marrow cells was assessed with a quantitative staphylococcal rosetting assay of anti-GPA antiserum-treated cells (5).

Radioactive Labeling. Cell surface glycoconjugates were radioactively labeled using the periodate/NaB^3H_4 technique (23). Radiolabeled red cell membranes were isolated as described (24). Labeled nucleated cells and red cell membranes were solubilized in 1% Triton X-100/0.01 M sodium phosphate/0.15 M NaCl, pH 7.4, at 0°C and centrifuged at $5000 \times g$ for 10 min, and the supernatants were recovered. For labeling with [^{35}S]methionine and ^{3}H, 3×10^7 uninduced cells or K562 cells induced with hemin for 3 days were incubated for 90 min with [^{35}S]methionine (10), washed, and labeled by the periodate/NaB^3H_4 method. After solubilization in detergent, the extracts were passed through lentil lectin-Sepharose columns and the radioactive glycoproteins were eluted with α-methylmannoside (10, 11).

Immunoprecipitation. Labeled cell extracts were subjected to immune precipitation using the staphylococcal protein A technique (25). When monoclonal antibodies were used, rabbit anti-mouse IgG antiserum (Dako, Copenhagen) was used as a second antibody.

Polyacrylamide Slab Gel Electrophoresis. Polyacrylamide slab gel electrophoresis in the presence of sodium dodecyl sulfate was done using 8% acrylamide gels (26). The gels were fixed with 5% sulfosalicyclic acid and treated for fluorography (27).

The publication costs of this article were defrayed in part by page charge payment. This article must therefore be hereby marked "*advertisement*" in accordance with 18 U.S.C. §1734 solely to indicate this fact.

Abbreviations: GPA, glycophorin A; PMA, phorbol 12-myristate 13-acetate.

Carl_G_190x270_mm_blokki_FINAL.indd 153 06-Aug-23 1:53:35 PM

Table 1. Binding of protein A-containing *Staphylococcus aureus* cells to anti-GPA-treated bone marrow cells

Cell type	mAb R10		mAb control		Rabbit anti-GPA		Rabbit preimmune IgG	
	N	Binding	*N*	Binding	*N*	Binding	*N*	Binding
Pronormoblasts	64	1.03 ± 3.98	56	0.13 ± 0.81	76	7.99 ± 10.39	50	2.88 ± 7.96
Basophilic normoblasts	66	2.30 ± 4.43	50	0.06 ± 0.31	76	15.43 ± 10.99	51	1.47 ± 2.16
Polychromatic normoblasts	53	11.83 ± 10.14	50	0.04 ± 0.20	63	21.60 ± 11.24	53	3.92 ± 7.73
Orthochromatic normoblasts	59	17.80 ± 12.54	50	0.04 ± 0.20	63	21.27 ± 10.52	61	2.46 ± 2.71
Mature erythrocytes	76	16.84 ± 10.91	50	0 0	50	22.30 ± 8.99	50	1.48 ± 1.84

Binding of staphylococci to bone marrow cells that had been treated with the indicated antisera was determined by a rosetting assay (5). Values are given as the mean and SD of the number of bacteria bound per bone marrow cell. *N*, number of marrow cells examined; mAb R10, a monoclonal antibody specific for GPA; mAb control, a monoclonal antibody of unrelated specificity.

Preparation and Analysis of Glycopeptides/Oligosaccharides. ^{3}H-labeled GPAs isolated by immune precipitation were treated with 5 mg of *Streptomyces griseus* protease (Pronase, Sigma) per ml of 0.15 M NaCl/0.01 M sodium phosphate, pH 7.4/0.1% sodium dodecyl sulfate at 60°C for 24 hr. After lyophilization, the samples were dissolved in 0.25 ml of 0.05 M NaOH/1 M $NaBH_4$ and incubated at 45°C for 16 hr to liberate *O*-glycosidic oligosaccharides (28). One drop of glacial acetic acid was then added and the samples were lyophilized. The samples were dissolved in 0.1 M NH_4HCO_3/0.1% sodium dodecyl sulfate and applied to a 1 × 80 cm Bio-Gel P-6 column equilibrated in the same buffer. The void volume was determined each time using Blue Dextran 2000 (Pharmacia). Radioactivity in eluate fractions was measured in a Triton X-114-based scintillation fluid using an LKB–Wallac 1210 Ultrobeta counter.

RESULTS

Reactivity of GPA from Normal Erythroid Cells and K562 Cells with Monoclonal Anti-GPA-Antibodies and Heteroantiserum. Results obtained using the staphylococcal rosetting assay to detect reactivity with monoclonal (R10) and heteroanti-GPA antiserum in normal bone marrow cells are shown in Table 1. The monoclonal antibody reacted poorly with pronormoblasts and basophilic normoblasts whereas polychromatic normoblasts and cells at later stages of differentiation showed a strong reaction. In contrast, rabbit anti-GPA antiserum showed a strong reactivity even with pronormoblasts and basophilic normoblasts.

Surface-labeled blood erythrocyte membranes were subjected to immune precipitation using the R10 monoclonal anti-GPA antibody. Fractionation by polyacrylamide gel electrophoresis revealed heavily labeled GPA monomer (GPA-M) and dimer bands (GPA-D) (Fig. 1, lane A). A similar pattern was obtained using the rabbit antiserum (Fig. 1, lane B).

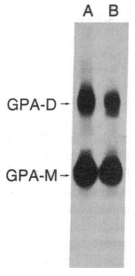

FIG. 1. Fluorogram of a polyacrylamide slab gel after electrophoresis of immunoprecipitates obtained from equal numbers of surface-labeled erythrocytes using monoclonal antibody R10 (lane A) or rabbit anti-GPA antiserum (lane B). GPA-D, GPA dimer; GPA-M, GPA monomer.

The surface glycoprotein patterns of K562 cells before and after hemin-induction are shown in Fig. 2 (lanes C and D). There was a relative increase in radioactivity in the position of GPA from induced cells. Rabbit antiserum precipitated GPA molecules from uninduced cells (Fig. 2, lane E) but no precipitate was seen with the R10 antibody (Fig. 2, lane F). However, after hemin-induced differentiation, the monoclonal antibody also precipitated GPA (Fig. 2, lane H). Flow cytometry (FACS IV, Becton Dickinson) gave similar results: K562 and HEL cells showed increased reactivity with the monoclonal antibodies R10 and R18 after induced differentiation (results not shown).

Polyacrylamide Slab Gel Electrophoresis Patterns of GPA from Bone Marrow Cells and Blasts from Patients with Erythroblastosis Fetalis. Erythroid cells from bone marrow were size-fractionated and surface-radiolabeled, and GPA was isolated by immunoprecipitation with rabbit antiserum. The

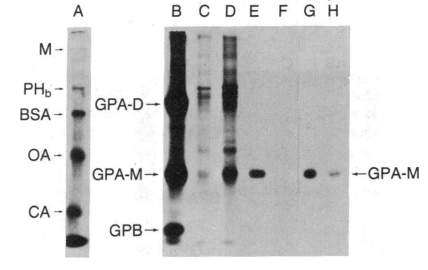

FIG. 2. Fluorogram of a polyacrylamide slab gel after electrophoresis of extracts of surface-labeled uninduced and induced K562 cells and of immunoprecipitates obtained with anti-GPA antisera. Lane A: ^{14}C-labeled standard proteins (M, myosin; PH_b, phosphorylase b; BSA, bovine serum albumin; OA, ovalbumin; CA, carbonic anhydrase). Lanes B–D: extracts of surface-labeled erythrocytes (B), uninduced K562 cells (C), and hemin-induced K562 cells (D). Lanes E–H: immunoprecipitates obtained using rabbit anti-GPA antiserum and uninduced cells (E), monoclonal antibody R10 and uninduced cells (F), rabbit anti-GPA antiserum and induced cells (G), and monoclonal antibody R10 and induced cells (H). The cells were allowed to differentiate for 3 days, and similar amounts of radioactivity were used for the immunoprecipitations.

Carl_G_190x270_mm_blokki_FINAL.indd 154 06-Aug-23 1:53:35 PM

Table 2. Erythroid cell composition of bone marrow fractions

Fraction*	% of total cells				
	Pro-normoblasts	Basophilic normoblasts	Polychromatic normoblasts	Orthochromatic normoblasts	Erythrocytes
1	20	45	20	15	0
2	5	15	17	63	0
3	3	2	5	55	35

*Cells were fractionated according to size by unit-gravity velocity sedimentation (13).

erythroid cell compositions of the three cell fractions isolated are shown in Table 2. Fraction 1 was enriched in the early precursor cells, fraction 2 consisted of a mixed cell population, and fraction 3 contained erythrocytes and late normoblasts. From fraction 1, two weakly labeled bands were observed after polyacrylamide gel electrophoresis, one in the position of the GPA monomer and the other, designated GP-26, with an apparent molecular weight of 26,000 (Fig. 3, lane B). The GPA monomer was the major species precipitated from fraction 2 cells, but GP-26 was also obtained (Fig. 3, lane C). Only the species corresponding to GPA monomers and dimers were precipitated from fraction 3 (Fig. 3, lane D). GPA-M and GP-26 were both recovered from nucleated blood cells of patients with erythroblastosis fetalis (Fig. 3, lane G).

Electrophoretic Mobilities of GPA Molecules Obtained from K562 and HEL Cells Before and After Induction. Induction of differentiation of K562 cells with sodium butyrate or hemin decreased the electrophoretic mobilities of the GPA molecules (Fig. 4, lanes A, C, and E and lanes G–J, respectively). Treatment of HEL cells with retinoic acid or PMA did not result in any major change in the apparent molecular weights of the GPA molecules (results not shown).

Analysis of Glycopeptides/Oligosaccharides of GPA Molecules. Gel filtration of ^{3}H-labeled Pronase/alkaline borohydride-treated GPA molecules obtained by immune precipitation was used to determine relative degrees of glycosylation. We know (29) that the *N*-glycosidic glycopeptide appears in the void volume (peak 1) of Bio-Gel P-6 columns, followed by the *O*-glycosidic tetrasaccharide (peak 2) and the *O*-glycosidic trisaccharides (peak 3). Fig. 5*A* shows that GPA from blasts of patients with erythroblastosis fetalis were labeled mainly in the *N*-glycosidic oligosaccharide (peak 1). In GPA from the most immature bone marrow cells (fraction 1, see Table 2), there was more label in the *O*-glycosidic tetrasaccharide and some in the trisaccharide region (Fig. 5*B*). GPA from fraction 2 was highly *O*-glycosylated (Fig. 5*C*) and had a labeling pattern similar to that of GPA from fraction 3, the fraction which contained late normoblasts and erythrocytes (Fig. 5*D*).

GPA isolated from uninduced K562 cells contained a relatively small amount of *O*-glycosidic oligosaccharides, and the tetrasaccharide/trisaccharide ratio was lower than in GPA from bone marrow cells (Fig. 6*A*). A very small amount of radioactivity was precipitated with the monoclonal antibody R10 (Fig. 6*B*) After differentiation induced by hemin the relative amount of tetrasaccharide increased (Fig. 6*C*). The GPA molecules from induced cells reacted with the monoclonal antibodies to give a glycopeptide/oligosaccharide pattern (Fig. 6*D*) similar to that obtained using the rabbit antiserum. Treatment with sodium butyrate gave a small relative increase in tetrasaccharides (results not shown).

To get a semiquantitative value for the change in glycosylation, uninduced and hemin-induced K562 cells were labeled with both [^{35}S]methionine and periodate/NaB^{3}H$_4$. The GPA molecules were isolated and the ^{3}H/^{35}S ratios were determined. The ratios were 1.51 for uninduced cells and 2.01 for induced cells.

The glycosylation of HEL cell GPA molecules also changed after treatment with inducing agents. After cultivation in the presence of retinoic acid, the relative level of tetrasaccharides increased (Fig. 7*B*); PMA treatment had the opposite effect (Fig. 7*C*).

DISCUSSION

There are few examples of polypeptides whose carbohydrate structures vary depending on the tissue localization or the developmental stage of the cells of origin. Best known are the ABO and Ii blood-group antigens, which in the red cell are associated predominantly with the band 3 and band 4.5 proteins (30, 31). Fetal cells contain simple, essentially unbranched i-active oligosaccharides whereas erythrocytes from adults contain high molecular weight branched I-active oligosaccharides (32). The rodent Thy-1 glycoproteins from brain, thymocytes, and T-lymphocytes are also differently glycosylated (33–35).

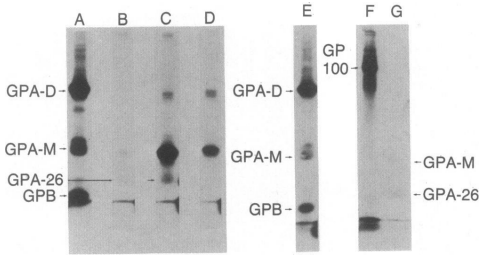

FIG. 3. Fluorograms of polyacrylamide slab gels after electrophoresis of extracts of surface-labeled erythrocytes (lanes A and E) and of immunoprecipitates obtained using rabbit anti-GPA antiserum and bone marrow blast cells (fraction 1) (lane B), bone marrow cells (fraction 2) (lane C), bone marrow cells (fraction 3) (lane D), and nucleated precursor cells from a patient with erythroblastosis fetalis (lane G). Also shown is the extract of the surface-labeled cells of the patient (lane F). GPA-26, GPA molecule with an apparent molecular weight of 26 000; GPB, glycophorin B; GP-100, glycoprotein with an apparent molecular weight of 100,000. The GPA-26 bands are barely seen in lanes B and G.

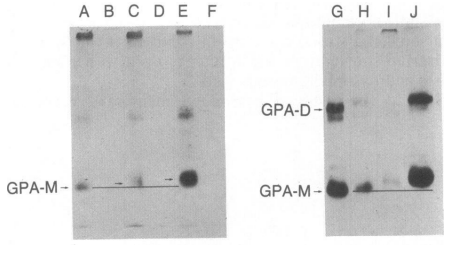

FIG. 4. Fluorograms of polyacrylamide slab gels after electrophoresis of immunoprecipitates obtained using rabbit anti-GPA antiserum and K562 cells before and after induction of differentiation with sodium butyrate or hemin. Lanes A–F: patterns obtained from uninduced cells with antiserum (A) and preimmune serum (B); patterns obtained from cells induced with sodium butyrate for 3 days with antiserum (C) and preimmune serum (D); patterns obtained from cells induced with sodium butyrate for 6 days with antiserum (E) and preimmune serum (F). Note the decreased mobility of the GPA monomer from induced cells. Lanes G–J: patterns obtained with antiserum and cells that were uninduced (G) or grown in the presence of hemin for 1 day (H), 3 days (I), or 6 days (J). The mobilities of the GPA monomer (GPA-M) and dimer (GPA-D) bands show a decrease with increased time of induction.

Carl_G_190x270_mm_blokki_FINAL.indd 155 06-Aug-23 1:53:35 PM

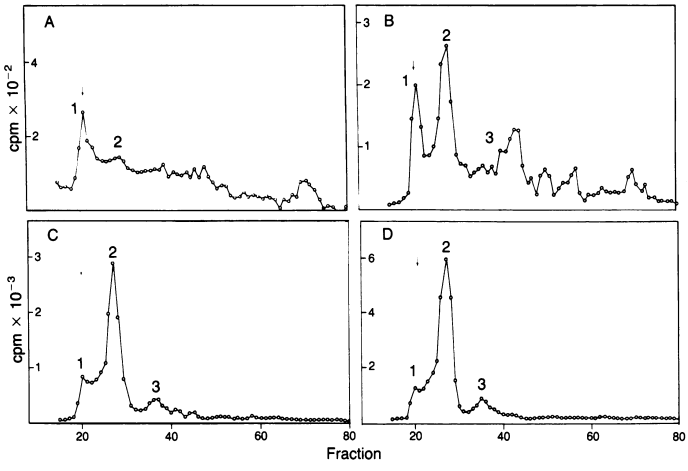

FIG. 5. Bio-Gel P-6 chromatography of ^{3}H-labeled glycopeptides/oligosaccharides from GPA molecules immunoprecipitated with rabbit anti-GPA antiserum. (*A*) Pattern obtained from GPA of erythroid precursor cells from a patient with erythroblastosis fetalis. (*B*) Pattern from GPA of bone marrow cells (fraction 1, Table 2). (*C*) Pattern from GPA of bone marrow cells (fraction 2). (*D*) Pattern from GPA of bone marrow cells (fraction 3). Peak 1 corresponds to the *N*-glycosidic glycopeptide, peak 2 to the *O*-glycosidic tetrasaccharide, and peak 3 to the *O*-glycosidic trisaccharide. All cells were surface-labeled using periodate/NaB^{3}H$_4$. Arrow indicates the void volume.

The type of variation in the glycosylation of GPA is quite different. GPA acquires an increased number of *O*-glycosidic chains when the erythroid cells differentiate. This was true for GPA both from normal precursor cells and from erythroleukemia cell lines induced to differentiate. The changes in glycosylation were detected after labeling cell surface sialoglycoconjugates by the periodate/NaB^{3}H$_4$ method, which is specific for sialic acids (23). The results were essentially the same for cells labeled using the galactose oxidase/NaB^{3}H$_4$ technique (24) to detect terminal galactose/N-acetyl galactosaminyl residues. The increased ^{3}H/^{35}S ratio of [^{35}S]methionine/periodate/NaB^{3}H$_4$ labeled GPA molecules from hemin-induced cells also indicates that the number of *O*-glycosidic oligosaccharides increased during differentiation. The GP-26 band seen in some precursor cell preparations apparently represents GPA molecules with a very low level of *O*-glycosylation because a similar molecule was obtained when erythrocyte GPA was partially deglycosylated with endo-*N*-acetylgalactosaminidase (12).

GPA is not important for the mature red cell because En(a−) individuals, lacking glycophorin A (18–20), do not show any signs of erythrocyte malfunction. On the other hand, it is possible that GPA is needed at earlier stages of erythrocyte differentiation. GPA and its incompletely glycosylated precursor molecules could function as receptors in cellular recognition; β-galactosyl-binding lectins have been found in several vertebrates (36).

GPA has recently been shown to act as a receptor for the malarial parasite *Plasmodium falciparum* (37, 38). The differentiation-related structural changes in the *O*-glycosidic oligosaccharide composition of GPA reported here could explain the well-known restriction in infectibility of the *P. falciparum* merozoites to mature red cells (39) and the inhibition of merozoite binding by carbohydrate (40).

The change in GPA structure during erythroid differentiation is also reflected in its reaction with monoclonal anti-GPA antibodies. The R10 antibody reacts with an epitope in the middle part of the polypeptide chain, the R18 antibody reacts with a region close to the lipid bilayer (21), and the VIE-G4 antibody needs sialic acid for reactivity (22). All of these antibodies reacted weakly with the GPA molecules from immature cells. This indicates that the carbohydrate

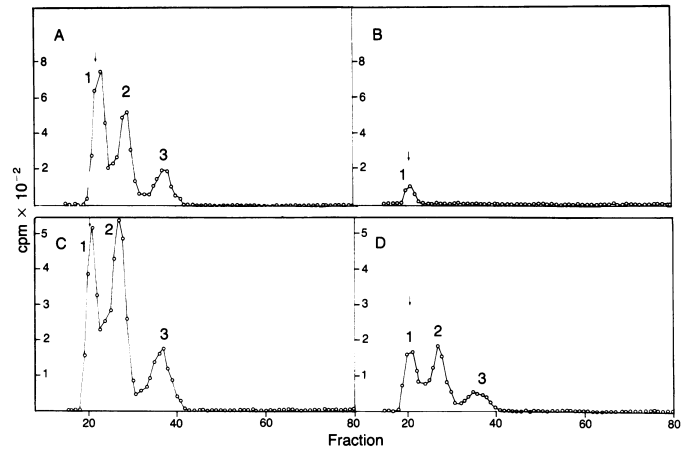

FIG. 6. Bio-Gel P-6 chromatography patterns of ^{3}H-labeled glycopeptides/oligosaccharides of immunoprecipitated GPA from K562 cells. Shown are results obtained using uninduced cells and rabbit anti-GPA antiserum (*A*), uninduced cells and monoclonal antibody R10 (*B*), cells treated with hemin for 2 days and rabbit anti-GPA antiserum (*C*), and cells treated with hemin for 2 days and monoclonal antibody R10 (*D*). Arrow indicates the void volume.

Carl_G_190x270_mm_blokki_FINAL.indd 156 06-Aug-23 1:53:35 PM

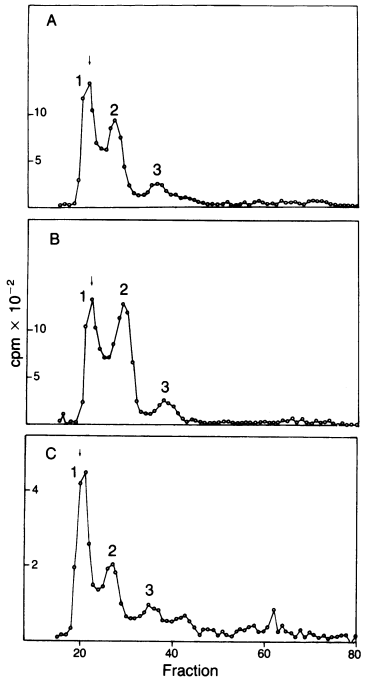

FIG. 7. Bio-Gel P-6 chromatography patterns of ^{3}H-labeled glycopeptides/oligosaccharides of GPA molecules isolated from HEL cells using rabbit anti-GPA antiserum. Patterns were obtained from digests of GPA from uninduced cells (*A*), from cells treated with retinoic acid for 3 days (*B*), and from cells treated with PMA for 3 days (*C*). Arrow indicates the void volume.

contributes to the conformation of the antigenic determinants of GPA.

We have earlier reported that the malignant blasts in a significant proportion (≤10%) of undifferentiated acute leukemias carry surface structures that react with rabbit anti-GPA antiserum (41). Using monoclonal antibodies to GPA for the phenotyping of leukemic cells, only occasional reactivity is found (22, 42). This discrepancy might be explained by the differentiation-related structural changes in GPA.

We thank Drs. P. A. W. Edwards and W. Knapp for monoclonal antibodies, U. Katajarinne for assistance, and B. Björnberg for secretarial help. This research was supported by National Cancer Institute Grant 2 R01 CA26294-04, the Sigrid Jusélius Foundation, and the Academy of Finland.

1. Tomita, M. & Marchesi, V. T. (1975) *Proc. Natl. Acad. Sci. USA* **72,** 2964–2968.
2. Yoshima, H., Furthmayr, K. & Kobata, A. (1980) *J. Biol. Chem.* **255,** 9713–9718.
3. Thomas, D. B. & Winzler, R. J. (1969) *J. Biol. Chem.* **244,** 5943–5946.
4. IUB-IUPAC Joint Commission on Biochemical Nomenclature (JCBN) (1982) *J. Biol. Chem.* **257,** 3347–3351.
5. Gahmberg, C. G., Jokinen, M. & Andersson, L. C. (1978) *Blood* **52,** 379–387.
6. Robinson, J., Sieff, C., Delia, D., Edwards, P. A. W. & Greaves, M. (1981) *Nature (London)* **289,** 68–71.
7. Gahmberg, C. G., Jokinen, M. & Andersson, L. C. (1979) *J. Biol. Chem.* **254,** 7442–7448.
8. Martin, P. & Papayannopoulou, T. (1982) *Science* **216,** 1233–1234.
9. Papayannopoulou, T., Yohochi, T., Nakamoto, B. & Martin, P. (1983) *Globin Gene Expression and Hematopoietic Differentiation* (Liss, New York), pp. 277–292.
10. Jokinen, M., Gahmberg, C. G. & Andersson, L. C. (1979) *Nature (London)* **279,** 604–607.
11. Gahmberg, C. G., Jokinen, M., Karhi, K. K. & Andersson, L. C. (1980) *J. Biol. Chem.* **255,** 2169–2175.
12. Gahmberg, C. G., Jokinen, M. & Andersson, L. C. (1983) *Red Cell Membrane Glycoconjugates and Related Genetic Markers*, eds. Cartron, J.-P., Rouger, P. & Salmon, C. (Librarie Arnette, Paris), pp. 51–63.
13. Häyry, P. & Andersson, L. C. (1976) *Scand. J. Immunol.* **5,** 31–44.
14. Andersson, L. C., Jokinen, M. & Gahmberg, C. G. (1979) *Nature (London)* **278,** 364–365.
15. Rutherford, T. R., Clegg, J. B. & Weatherall, D. J. (1979) *Nature (London)* **280,** 164–165.
16. Benz, E. J., Murnane, M. J., Tonkonow, B. L., Berman, B. W., Mazur, E. M., Cavallesco, C., Jenko, T., Snyder, E. L., Forget, B. G. & Hoffman, R. (1980) *Proc. Natl. Acad. Sci. USA* **77,** 3509–3513.
17. Hamaguchi, H. & Cleve, H. (1972) *Biochem. Biophys. Res. Commun.* **47,** 459–464.
18. Gahmberg, C. G., Myllylä, G., Leikola, J., Pirkola, A. & Nordling, S. (1976) *J. Biol. Chem.* **251,** 6108–6116.
19. Dahr, W., Uhlenbruck, G., Leikola, J., Wagstaff, W. & Landfried, K. (1976) *J. Immunogenet.* **3,** 329–346.
20. Tanner, M. J. A. & Anstee, D. J. (1976) *Biochem. J.* **155,** 701–703.
21. Anstee, D. J. & Edwards, P. A. W. (1982) *Eur. J. Immunol.* **12,** 228–232.
22. Liszka, K., Majdic, O., Bettelheim, P. & Knapp, W. (1983) *Am. J. Hematol.* **15,** 219–226.
23. Gahmberg, C. G. & Andersson, L. C. (1977) *J. Biol. Chem.* **252,** 5888–5894.
24. Gahmberg, C. G. & Hakomori, S. (1973) *J. Biol. Chem.* **248,** 4311–4317.
25. Gahmberg, C. G. & Andersson, L. C. (1978) *J. Exp. Med.* **148,** 507–521.
26. Laemmli, U. K. (1970) *Nature (London)* **227,** 680–685.
27. Bonner, W. M. & Laskey, R. A. (1974) *Eur. J. Biochem.* **46,** 83–88.
28. Carlson, D. (1966) *J. Biol. Chem.* **241,** 2984–2986.
29. Gahmberg, C. G. & Andersson, L. C. (1982) *Eur. J. Biochem.* **122,** 581–586.
30. Karhi, K. K. & Gahmberg, C. G. (1980) *Biochim. Biophys. Acta* **622,** 344–354.
31. Finne, J. (1980) *Eur. J. Biochem.* **104,** 181–189.
32. Hakomori, S. (1981) *Semin. Hematol.* **18,** 39–62.
33. Barclay, A. N., Letarte-Muirhead, M., Williams, A. F. & Faulkes, R. A. (1976) *Nature (London)* **263,** 563–567.
34. Hoessli, D., Bron, C. & Pink, J. R. L. (1980) *Nature (London)* **283,** 576–578.
35. Carlsson, S. R. & Stigbrand, T. I. (1983) *J. Immunol.* **130,** 1837–1842.
36. Barondes, S. H. (1981) *Annu. Rev. Biochem.* **50,** 207–231.
37. Perkins, M. (1981) *J. Cell Biol.* **90,** 563–567.
38. Pasvol, G., Wainscoat, J. S. & Weatherall, D. J. (1981) *Nature (London)* **297,** 64–67.
39. Tanner, M. J. A. (1982) *Trends Biochem. Sci.* **7,** 231.
40. Jungery, M., Boyle, D., Patel, T., Pasvol, G. & Weatherall, D. J. (1983) *Nature (London)* **301,** 704–705.
41. Andersson, L. C., Gahmberg, C. G., Teerenhovi, L. & Vuopio, P. (1979) *Int. J. Cancer* **24,** 717–720.
42. Greaves, M. F., Sieff, C. & Edwards, P. A. W. (1983) *Blood* **61,** 645–651.

Carl_G_190x270_mm_blokki_FINAL.indd 157 06-Aug-23 1:53:35 PM

344

Biochimica et Biophysica Acta, 622 (1980) 344—354
© Elsevier/North-Holland Biomedical Press

BBA 38386

IDENTIFICATION OF BLOOD GROUP A-ACTIVE GLYCOPROTEINS IN THE HUMAN ERYTHROCYTE MEMBRANE

KIMMO K. KARHI and CARL G. GAHMBERG *

Department of Bacteriology and Immunology, University of Helsinki, Haartmaninkatu 3, SF-00290 Helsinki 29 (Finland)

(Received April 13th, 1979)
(Revised manuscript received September 7th, 1979)

Key words: Glycoprotein; Blood group A; (Erythrocyte membrane)

Summary

Normal human erythrocytes of blood groups A_1, A_2, B and O, and En (a—) erythrocytes lacking glycophorin A, but with A_1B-activity, were surface-labeled with tritiated sodium borohydride after oxidation of terminal galactosyl and *N*-acetylgalactosaminyl residues with galactose oxidase. A_1 cells were also labeled by lactoperoxidase catalyzed iodination. After solubilization in Triton X-100, the blood group A-active glycoconjugates were isolated using the A-specific lectin from *Vicia cracca* coupled to Sepharose. No radioactivity was bound from erythrocytes of B and O blood groups. The glycoconjugates from A cell membranes which bound to the lectin and were eluted with 0.01 M *N*-acetyl-D-galactosamine were analyzed using cylindrical or slab gel electrophoresis in the presence of sodium dodecyl sulfate. The A-active glycoproteins included the major integral glycoprotein, band 3, and many minor, previously poorly defined components. Glycophorins A and B did not contain A-activity.

Introduction

The ABO blood group determinants are known to reside in the carbohydrate portion of various glycoconjugates, and *N*-acetyl-D-galactosamine $\alpha 1 \rightarrow 3$ (L-fucose $\alpha 1 \rightarrow 2$) D-galactose is the antigenic determinant of A-active substances [1,2]. Most of the original chemical work on the structure of ABO blood group substances was done with glycoprotein from various body fluids [1]. The current concept on the nature of ABO-active glycoconjugates of the human eryth-

* To whom correspondence should be addressed.

Carl_G_190x270_mm_blokki_FINAL.indd 158 06-Aug-23 1:53:35 PM

rocyte membrane has, however, remained in a confused state. It is well established that some low molecular weight glycolipids contain ABO-activity and several such lipids have been isolated and their structures determined [3,4]. It has also become evident that 'macroglycolipids' containing up to 60 monosaccharides per ceramide show ABO-activity [5—7].

Whether ABO-active glycoproteins exist in erythrocyte membranes has been a more difficult question and a matter of much dispute [2,7]. Takasaki and Kobata observed incorporation of *N*-acetyl[^{14}C]galactosamine from UDP-*N*-acetyl[^{14}C]galactosamine into several erythrocyte membrane proteins in vitro [8]. More convincing proof for the presence of ABO-active glycoproteins in the erythrocyte membrane was recently obtained by direct chemical analysis of isolated glycopeptides and oligosaccharides [9—11]. No information has, however, been available from which glycoproteins these structures originate.

The human erythrocyte membrane has been extensively studied [12—14] and more than twenty integral glycoproteins have been identified [15]. The major components are band 3 (for nomenclature see Ref. 16) and the major sialoglycoproteins, glycophorin A and B [13].

We have approached the problem of which erythrocyte glycoproteins contain blood group A-activity by using the A-specific lectin from *Vicia cracca* [17—19] for the isolation of the A-active molecules. Erythrocyte glycoconjugates were first radioactively labeled by the galactose oxidase method [20], in which the terminal galactosyl and *N*-acetylgalactosaminyl residues are reduced with tritiated sodium borohydride after oxidation with galactose oxidase. After elution from the *V. cracca* lectin-Sepharose columns with *N*-acetylgalactosamine, the A-active glycoconjugates were separated by polyacrylamide gel electrophoresis in the presence of sodium dodecyl sulfate. We show here that blood group A-activity is confined to several glycoproteins including band 3. The glycophorin molecules do not seem to contain A-activity.

Materials and Methods

Erythrocytes. Fresh normal human erythrocytes and En (a—) erythrocytes, were obtained from the Finnish Red Cross Blood Transfusion Service, Helsinki. The cells were washed in 0.15 M NaCl/0.01 M sodium phosphate, pH 7.4 (Buffer I) by centrifugation. ABO blood groups and secretor status were determined by standard techniques. When needed, erythrocytes were counted in a hemocytometer.

Chemicals and enzymes. Acrylamide and *N,N'*-methylenebisacrylamide were obtained from Eastman Kodak Co., Rochester, NY. Sodium dodecyl sulfate was purchased from Pierce Chemical Co., Rockford, IL. 2,5-diphenyloxazole (PPO) and 1,4-bis[2-(5-phenyloxazolyl)]benzene (POPOP) were from New England Nuclear, Boston, MA. *N*-acetyl-D-galactosamine, D-glucose and bovine serum albumin were from Sigma Chemical Co., St. Louis, MO, and ethyl chlorformate from Fluka AG, Buchs, Switzerland. Tritiated sodium borohydride (8.2 Ci/mol) and [^{14}C]formaldehyde (2.0 Ci/mol) were purchased from the Radiochemical Centre, Amersham, U.K. ^{125}I, carrier free, (100 mCi/ml) were obtained from New England Nuclear, Boston, MA. Galactose oxidase, 130 units/mg protein, was purchased from Kabi AB, Stockholm, Sweden. It was

Carl_G_190x270_mm_blokki_FINAL.indd 159 06-Aug-23 1:53:35 PM

free from neuraminidase and protease activities when measured as described previously [20]. Pronase (Streptomyces griseus protease type V, 0.9 unit/mg solid) and lactoperoxidase were from Sigma. Glucose oxidase was from Worthington, Freehold, NJ.

Isolation and immobilization of the blood group A-specific lectin from Vicia cracca. The A-specific lectin from *V. cracca* was isolated by affinity chromatography on immobilized porcine A/H substance as described in detail in the accompanying paper [21]. 20 mg of the lectin was coupled to 2 g (dry weight) of CNBr-activated Sepharose 4B (Pharmacia Fine Chemicals, Uppsala, Sweden), according to the manufacturer for 1 h at room temperature in the presence of 10 mM *N*-acetyl-D-galactosamine.

Radioactive labeling of purified Vicia cracca lectin. 50 μg of *V. cracca* lectin was labeled in 50 μl Buffer I/0.05 M *N*-acetyl-D-galactosamine with 0.5 mCi of ^{125}I by the chloramine T (Merck AG, Darmstadt, F.R.G.) method [22]. ^{125}I was counted in a Wallac-LKB 80000 gamma sample counter.

Binding of Vicia cracca lectin to erythrocytes. ^{125}I-labeled lectin was mixed with unlabeled lectin to a specific activity of 2770 cpm/μg protein. Incubation of 10^8 erythrocytes (blood groups A_1, A_2 and O) with 1—100 μg of lectin was performed in plastic test tubes in the final volume of 1.1 ml Buffer I containing 1% bovine serum albumin. After incubation for 3 h at room temperature with gentle shaking, the cells were washed twice with Buffer I. The cell pellets were counted for radioactivity. Control studies were performed with all reactants except erythrocytes, to correct for nonspecific binding of lectin to the tubes. This was less than 3% of that bound to A_1 erythrocytes. Control studies were also done in the presence of 10 mM *N*-acetyl-D-galactosamine to determine nonspecific binding to erythrocytes. It was negligible. The apparent association constant K and the saturation binding were calculated from a Scatchard plot [23]. The slope and the intercept of the linear regression line were calculated with the aid of a desk computer.

Radioactive surface labeling of cells. Erythrocytes were labeled by the galactose oxidase method [15,20]. No pretreatment with neuraminidase was done. After washing three times in Buffer I, the membranes were isolated [20]. For affinity chromatography the membranes were solubilized in Buffer I/0.5% Triton X-100 and cleared by centrifugation at $3000 \times g$ for 10 min. Erythrocytes were labeled by the periodate/NaB^3H_4 method as described [24], using a final concentration of 1 mM sodium metaperiodate (Merck AG. Darmstadt, F.R.G.). After washing the membranes were isolated as above.

Surface labeling with ^{125}I was done essentially according to Hubbard and Cohn [25]. A_1 erythrocytes (0.5 ml packed cells) were incubated for 30 min at room temperature in 5 ml of Buffer I containing 5 mM D-glucose, 0.5 mCi ^{125}I, 10 μg glucose oxidase and 50 μg lactoperoxidase. After incubation the cells were washed three times in Buffer I and the membranes isolated.

Isolation of blood group A-active glycoconjugates by affinity chromatography. For affinity chromatography, labeled membranes from 0.5 ml of packed erythrocytes (all samples containing approximately $2—3 \cdot 10^6$ cpm) were dissolved in 0.5% Triton X-100/Buffer I, and incubated for 20 min with 10 ml of the affinity column at 20°C. Thereafter the column was washed with the same buffer, fractions of 3 ml were collected at an elution rate of 60 ml per h, and

Carl_G_190x270_mm_blokki_FINAL.indd 160 06-Aug-23 1:53:35 PM

the A-active glycoconjugates eluted with 0.01 M *N*-acetyl-D-galactosamine in 0.05% Triton X-100/Buffer I. Aliquots of the tritium labeled material were counted in a dioxane-based scintillation fluid [26] and the ^{125}I in the gamma counter. The ^{3}H-labeled glycoconjugates were concentrated by precipitation with 10% trichloroacetic acid at 0°C after addition of 50 μg bovine serum albumin as a carrier.

Treatment with pronase. A_1-active material isolated from galactose oxidase/NaB^3H_4-labeled membranes by lectin affinity chromatography was dialyzed for 24 h against water at 4°C and lyophilized. Pronase treatment was performed in 0.004 M sodium phosphate, (pH 7.4)/0.1% sodium dodecyl sulfate, at 60°C for 17 h. The solution was made 0.1% with respect to pronase, and the same amount of enzyme was added after 9 h.

Polyacrylamide gel electrophoresis. Electrophoresis in the presence of sodium dodecyl sulfate was done according to Laemmli [27] on 8% acrylamide cylindrical or slab gels. Cylindrical gels were sliced with a 2 mm slicer and the radioactivities determined using a toluene-based scintillation fluid after solubilization in NCS-water (9 : 1) (Amersham, Searle), for 2 h at 50°C. The slab gels were fixed after completion of the electrophoresis in 20% sulfosalicyclic acid overnight. The gels were treated for fluorography as described [28] and vacuum-dried. The dried gels were covered with Kodak RP X-Omat film, wrapped in alluminium foil, and stored at −70°C in a Revco freezer for 1—8 days until developed. Standard proteins were: thyroglobulin, transferrin, human albumin, ovalbumin and hemoglobin. They were radioactively labeled with [^{14}C]formaldehyde as described [29].

Isolation of macroglycolipids. A macroglycolipid fraction was isolated from labeled erythrocyte membranes according to Dejter-Juszynski et al. [7], but the dialysis step to remove low molecular weight glycolipids, was shortened to 1 day.

Gel filtration of blood group A-active glycopeptides. An eluate of A_1 cells labeled by the galactose oxidase/NaB^3H_4 method was obtained from the *V. cracca*-Sepharose column using *N*-acetyl-D-galactosamine. Half of the sample was applied directly to a Biogel P-10 column (1 × 90 cm) (Bio-Rad, Richmond, CA) made in 0.15 M Tris-HCl (pH 7.8)/0.1% sodium dodecyl sulfate. Blue dextran 2000 (Pharmacia, Uppsala, Sweden) was added to each sample to determine the void volume. The column was calibrated using thyroglobulin glycopeptide (M_r 4100), the oligosaccharide (galactose β(1—4) *N*-acetylglucosamine β(1—2) mannose)$_2$ α(1—3) (1—6) mannose β(1—4) *N*-acetylglucosamine (M_r 1434) and a triose (M_r 504) as standards [21]. The rest of the sample was digested with pronase and then applied to the same Biogel P-10 column. Aliquots were counted for radioactivity in Bray's solution [26].

Identification of labeled monosaccharides. For neutral sugar analysis, an eluate from *V. cracca*-Sepharose of A_1 erythrocytes labeled by the galactose oxidase/NaB^3H_4 treatment containing about 12 000 cpm, was hydrolyzed in 2 N H_2SO_4 at 100°C for 5 h. For amino sugar analysis, an identical sample was hydrolyzed in 2 N HCl for 16 h at 100°C. The amino sugar sample was neutralized with silver carbonate and reacetylated at room temperature for 30 min using 50 μl of acetic anhydride in 0.3 ml of 1/3 saturated $NaHCO_3$. The hydrolyzates were passed through Dowex-1 columns (formate and H^+ forms) in water.

Carl_G_190x270_mm_blokki_FINAL.indd 161 06-Aug-23 1:53:35 PM

The samples were lyophilized and the monosaccharides analyzed by thin-layer chromatography on silica gel plates in ethylacetate/pyridine/acetic acid/water (5 : 5 : 1 : 3, v/v). Standard monosaccharides were visualized using the anilin-diphenylamine reagent [30]. The plates were scraped and the radioactivities of galactose and *N*-acetyl-D-galactosamine determined by liquid scintillation counting.

Protein analysis. Protein was determined according to Lowry et al. [31] with bovine serum albumin as a standard.

Results

Binding of Vicia cracca lectin to erythrocytes

Agglutination tests with A_1, A_2, B and O erythrocytes showed that *V. cracca* lectin was specific for A cells, the agglutinating activity being 2—4 fold higher with A_1 cells as compared to A_2 cells.

The binding of lectin was performed with A_1 (secretors and non-secretors), A_2 and O erythrocytes. The binding was strongest to A_1 cells, lower to A_2 cells and negligible to O cells. Binding to A_1 cells from secretors and non-secretors was identical (data not shown). The amount of lectin bound at saturation was determined using a Scatchard plot. When the lectin is taken to be tetrameric, with a molecular weight of 100 000 [21], the number of molecules bound per cell at saturation is $4 \cdot 10^5$. From the slope ($-K$) of the line, the association constant K was calculated to $5 \cdot 10^6$ M^{-1}. The plot was linear indicating homogeneity of the lectin-binding groups.

Vicia cracca lectin-Sepharose affinity chromatography

Fig. 1 shows the fractionation of galactose oxidase/NaB^3H_4-labeled erythrocyte membranes using *V. cracca* lectin-Sepharose affinity columns. Only A_1 and A_2 erythrocytes (Fig. 1 A—C) showed specific binding, while no binding was obtained using B and O erythrocytes (Fig. 1D). The yield of radioactivity recovered from the column was always greater than 90%.

A control experiment was performed with a mixture containing labeled O cell material and unlabeled A_1 cell material. No radioactivity was bound to the affinity column. This indicates that all material retained by the column is due to specific interaction between the lectin and the A-active molecules. When the affinity chromatography was performed at 0°C, the yield of A-active material was considerably smaller but qualitatively similar. The addition of 2 mM phenylmethylsulfonyl fluoride as a protease inhibitor in the buffers did not change the results.

The labeled monosaccharides of A_1 cell glycoconjugates, retained by the *V. cracca* lectin-Sepharose column, included both galactose (93.7%) and *N*-acetyl-D-galactosamine (6.3%).

Analysis by cylindrical polyacrylamide gel electrophoresis

Part of the radioactive materials eleuted from the affinity columns were separated after concentration on cylindrical polyacrylamide gels (Fig. 2). Most of the radioactivity was recovered from the front representing low molecular weight molecules and in the molecular weight range above 40 000. No obvious qualitative difference between the A_1 and A_2 glycoconjugates was detected.

Carl_G_190x270_mm_blokki_FINAL.indd 162 06-Aug-23 1:53:35 PM

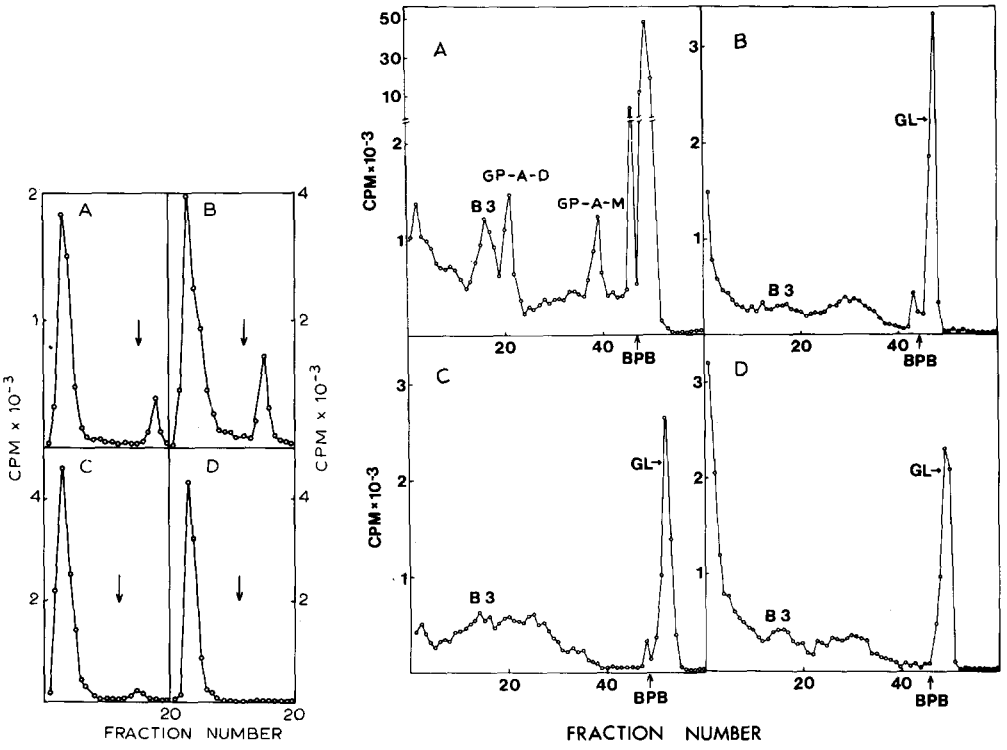

Fig. 1. Isolation of A-active glycoconjugates by *V. cracca*-lectin affinity chromatography. Fractionation of galactose oxidase/NAB^{3}H$_4$-labeled erythrocyte membranes was performed using *V. cracca*-Sepharose affinity column in the presence of 0.05% Triton X-100. The arrow shows the addition of 0.01 M *N*-acetyl-D-galactosamine. A, A_1 cells (secretor); B, A_1 cells (nonsecretor); C, A_2 cells; D, O cells.

Fig. 2. Cylindrical polyacrylamide gel electrophoresis of galactose oxidase/NaB^{3}H$_4$-labeled A-active glycoconjugates. A, A_1 erythrocyte membranes; B, eluted A-active glycoconjugates from A_2 cells; C, eluted A-active glycoconjugates from A_1 cells (secretor); D, eluted A-active glycoconjugates from A_1 cells (nonsecretor). B3, band 3; GP-A-D, glycophorin A dimer; GP-A-M, predominantly glycophorin A monomer; GL, glycolipid peak; BPB, bromphenol blue marker dye.

Analysis by polyacrylamide slab gel electrophoresis

Fig. 3 shows the fluorography patterns of erythrocyte membranes labeled by the galactose oxidase/NaB^{3}H$_4$ method and the patterns of blood A-active glycoconjugates. The slots are derived from several different experiments and corresponding amounts of radioactivities were analyzed. Radioactive molecules were retained by the lectin affinity columns only from A_1 and A_2 erythrocytes (Fig. 3D and E) and from En (a—) cells of blood group A_1B (Fig. 3K).

When blood group A glycoconjugates from normal cells were analyzed after labeling with galactose oxidase/NaB^{3}H$_4$, many A-active glycoproteins were visualized but no clearly dominating band was observed (Fig. 3D and E). En (a—) membranes had a strongly labeled A-active band 3 (Fig. 3K). Blood group A activity in band 3 from normal A cells was, however, clearly demonstrated: (1) After lactoperoxidase-catalyzed iodination, band 3 was the dominating band retained by the lectin columns (Fig. 4B) and (2), the materials that passed directly through the lectin columns after lactoperoxidase iodination (Fig. 4C)

Carl_G_190x270_mm_blokki_FINAL.indd 163 06-Aug-23 1:53:35 PM

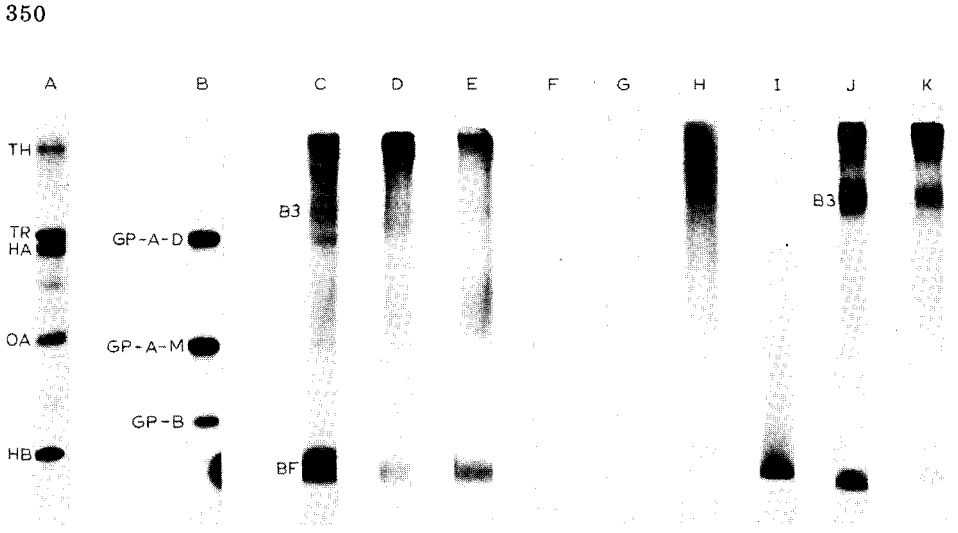

Fig. 3. Fluorography patterns of ^{3}H-labeled erythrocyte membranes and the radioactive glycoconjugates eluted from the affinity columns and separated by polyacrylamide slab gel electrophoresis. A, ^{14}C-labeled standard proteins. TH, thyroglobulin M_r 210 000; TR, transferrin M_r 78 000; HA, human albumin M_r 68 000; OA, ovalbumin M_r 43 000; HB, hemoglobin M_r 17 000. B, erythrocyte membranes labeled by the periodate/NaB^{3}H$_4$ method. C, A_1 erythrocyte membranes labeled by the galactose oxidase/NaB^{3}H$_4$ method. D, eluted A-active glycoconjugates from A_1 cells (nonsecretor). E, eluted A-active glycoconjugates from A_2 cells; F, eluted glycoconjugates from B cells; G, eluted glycoconjugates from O cells; H, eluted A-active glycoconjugates from A_1 cells and digested with pronase; I, 'macroglycolipids' isolated from A_1 erythrocytes; J, En(a—) erythrocyte membranes labeled by the galactose oxidase method; K, eluted A-active glycoconjugates from En (a—) A_1 B cells. GP-A-D, glycophorin A dimer; GP-A-M, glycophorin A monomer, predominantly; GP-B, glycophorin B; B3, band 3. BF, buffer front.

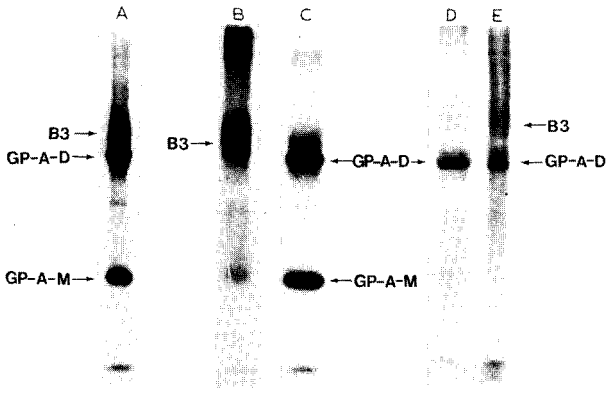

Fig. 4. Fluorography pattern of a polyacrylamide slab gel of ^{125}I and galactose oxidase/NaB^{3}H$_4$-labeled A_1 erythrocyte membranes and radioactive A_1-active and nonactive glycoconjugates. A, ^{125}I-labeled A_1 erythrocyte membranes; B, eluted A_1 active proteins from ^{125}I-labeled membranes; C, proteins from A_1-active ^{125}I-labeled membranes not interacting with the lectin-Sepharose columns; D, glycoproteins from A_1 active galactose oxidase/NaB^{3}H$_4$-labeled membranes not interacting with the lectin-Sepharose column F; original galactose oxidase/NaB^{3}H$_4$-labeled A_1 erythrocyte membranes. Labels as in Fig. 2.

Carl_G_190x270_mm_blokki_FINAL.indd 164 06-Aug-23 1:53:35 PM

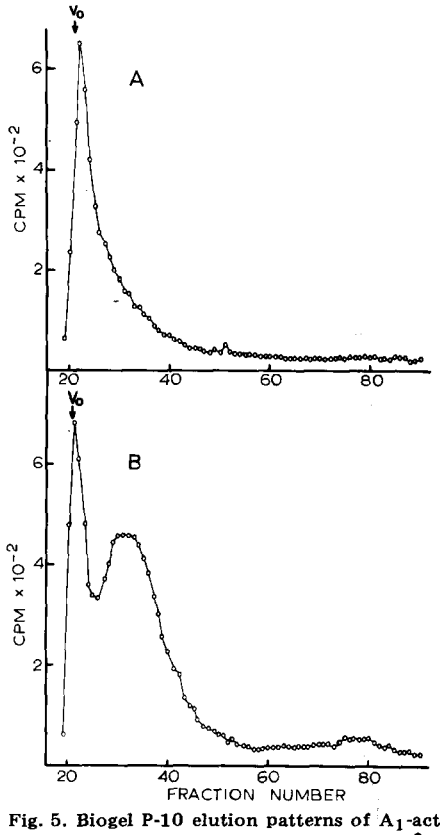

Fig. 5. Biogel P-10 elution patterns of A_1-active glycoconjugates before and after pronase treatment. A, elution pattern of galactose oxidase/NaB^3H_4-labeled A-active glycoconjugates. B, elution pattern of pronase-treated A_1-active glycoconjugates. Fractions of 1 ml were collected and the total volume of the column was 80 ml. V_0, void volume.

or galactose oxidase/NaB^3H_4 treatment (Fig. 4D) were depleted of the characteristic band 3 bands.

Substantial A-specific radioactivity was located in the diffuse area in the molecular weight range 40 000—60 000. Many weakly labeled glycoproteins were also observed in the high molecular weight region above band 3.

The glycoprotein nature of these components was further strengthened using pronase digestion which removed most radioactive material below band 3 (Fig. 3H). The diffuse radioactivity in the high molecular weight area must be due to slowly migrating glycopeptides which bind little sodium dodecyl sulfate. By gel filtration on Biogel P-10 columns, most of the radioactivity of blood group A glycoconjugates labeled by galactose oxidase/NaB^3H_4 treatment, emerged in the void volume (Fig. 5A). However, after treatment of this material with pronase, a major included peak was observed with an apparent molecular weight of 8300—10 400 (fractions 28—35, Fig. 5B).

The material running in the front on gel electrophoresis (BF) must mainly represent low molecular weight glycolipids (Fig. 3C, E) and part of the diffuse area in the 40 000—60 000 molecular weight region may be macroglycolipids

Carl_G_190x270_mm_blokki_FINAL.indd 165 06-Aug-23 1:53:35 PM

(Fig. 3I) [7]. The glycophorin molecules did not attach to the affinity column from any cell and apparently do not contain A-activity.

Discussion

The problems involved in purification of integral membrane proteins, have created difficulties in identification of ABO blood group-active glycoproteins in the human erythrocyte membrane. The question whether ABO-active oligosaccharides really are attached to proteins has therefore remained controversial. Significant progress has, however, recently been made by analyzing glycopeptides obtained after pronase digestion of the membrane [9—11]. Such glycopeptides showed ABO blood group activity and contained insignificant levels of sphingosine and fatty acids. The molecular weight of these glycopeptides ranged from 7000—12 000, and they evidently have unusual structures containing a repeating disaccharide unit. There was no information available from which glycoproteins these glycopeptides originate.

We have approached the problem of identifying the A-active glycoconjugates by first introducing tritium into terminal *N*-acetylgalactosaminyl and galactosyl residues of erythrocyte membranes by the galactose oxidase method [20]. A-active cells were also labeled by lactoperoxidase-catalyzed iodination [25]. Previously, analysis of whole galactose oxidase/NaB^3H_4-labeled erythrocyte membranes of different ABO blood groups by polyacrylamide gel electrophoresis, did not show any obvious differences [15]. This is now understood by the small amount of radioactivity specifically incorporated into A-specific *N*-acetylgalactosamine. Here we have used the A-specific lectin from *V. cracca* to isolated the A blood group-active molecules. By combining these techniques with the high resolution of polyacrylamide gel electrophoresis in the presence of sodium dodecyl sulfate, the identification of A-active glycoproteins was accomplished.

The isolated lectin from *V. cracca* showed absolute A blood group specificity, and the binding studies gave the saturation value of 400 000 lectin molecules bound per A_1 erythrocyte; assuming a molecular weight of 100 000 [21], this figure is in agreement with previous studies on the number of A receptor sites [32].

The gels showed a weakly-labeled band in the band 3 region from normal A cells. Gels stained for protein with Coomassie blue gave a similar pattern (data not shown). During the concentration of the lectin-Sepharose eluates of ^3H-labeled membranes, some irreversible aggregation of band 3 occurred. This was clearly seen using ^{125}I-labeled A_1 material. In this case, there was enough radioactivity for direct gel electrophoretic analysis, which showed the presence of band 3 (Fig. 4B). Concentration of this sample resulted in partial loss of band 3 (data not shown). The samples passed through the lectin-Sepharose columns were obviously depleted of band 3.

Band 3 contains one major oligosaccharide chain per molecule with a molecular weight of approximately 7500 [33], which must contain the A-activity. In En (a—) erythrocytes which lack glycophorin A [33—36], band 3 has an even larger sugar chain [33], which results in the slower mobility of the protein on polyacrylamide gel electrophoresis in the presence of sodium dodecyl

Carl_G_190x270_mm_blokki_FINAL.indd 166 06-Aug-23 1:53:35 PM

sulfate [33]. The A-activity of band 3 from En (a—) cells was obvious.

There are many A-active glycoproteins with apparent molecular weights of 40 000—60 000 and greater than 100 000. These glycoproteins have been observed before using galactose oxidase/NaB^3H_4 labeling [15] and *Ricinus communis* lectin affinity chromatography [37].

Our results also show that the glycophorin molecules have no A-activity, and this is in agreement with structural studies [13]. Dejter-Juszynski et al. [7] showed that the A-activity of the 'glycoprotein fraction' extracted according to Hamaguchi and Cleve [38] was due to macroglycolipids and not to glycophorin A, and claimed that glycoproteins do not contain significant ABO activity. However, most glycoproteins should remain at the interphase using chloroform/methanol/water partition and were never included in this fraction.

It should be emphasized that it is not possible with these methods to quantitate accurately the distribution of A blood group activity among the membrane glycoconjugates, because the labeling efficiency is probably not comparable between different molecules, and the quantity of large glycoconjugates containing different types of labeled oligosaccharide structures can be overestimated. Non-covalent stable associations between different surface glycoproteins in the presence of Triton X-100 cannot either be excluded, and could lead to co-purification of glycoproteins not containing A-activity with those containing this activity. No such interactions between surface glycoproteins are, however, known for the erythrocyte membrane. In any case, it is clear that A-activity contributed by glycoproteins is significant and it is interesting to note that this does not depend on the secretor status of the individuals.

Acknowledgements

This study was supported by the Academy of Finland and the Finnish Cancer Society.

References

1 Watkins, W.M. (1966) Science 152, 172—181
2 Hakomori, S. and Kobata, A. (1974) in The Antigens (Sela, M., ed.), Vol. 2, pp. 80—140, Academic Press, New York
3 Hakomori, S. and Strycharz, G.D. (1968) Biochemistry 7, 1279—1286
4 Stellner, K., Watanabe, K. and Hakomori, S. (1973) Biochemistry, S. (1973) Biochemistry 12, 656—661
5 Kóscielak, J., Miller-Podraza, H., Krauze, R. and Piasek, A. (1976) Eur. J. Biochem. 71, 9—18
6 Gardas, A. (1976) Eur. J. Biochem. 68, 177—183
7 Dejter-Juszynski, M., Harpaz, N., Flowers, H.M. and Sharon, N. (1978) Eur. J. Biochem. 83, 363—373
8 Takasaki, S. and Kobata, A. (1976) J. Biol. Chem. 251, 3610—3615
9 Finne, J., Krusius, T., Rauvala, H., Kekomäki, R. and Myllylä, G. (1978) FEBS Lett. 89, 111—115
10 Järnefelt, J., Rush, J., Li, Y.-T. and Laine, R.A. (1978) J. Biol. Chem. 253, 8006—8009
11 Takasaki, S., Yamashita, K. and Kobata, A. (1978) J. Biol. Chem. 253, 6086—6091
12 Steck, T.L. (1974) J. Cell Biol. 62, 1—19
13 Marchesi, V.T., Furthmayr, H. and Tomita, M. (1976) Annu. Rev. Biochem. 45, 667—698
14 Gahmberg, C.G. (1977) in Dynamic Aspects of Cell Surface Organization, (Poste, G. and Nicolson, G.L., eds.), pp. 371—421, North-Holland, Amsterdam
15 Gahmberg, C.G. (1976) J. Biol. Chem. 251, 510—515
16 Fairbanks, G., Steck, T.L. and Wallach, D.F.H. (1971) Biochemistry 10, 2606—2617
17 Mäkelä, O. (1957) Ann. Med. Exp. Biol. Fenn. 35, (Suppl. 11) 1—133
18 Aspberg, K., Holmén, H. and Porath, J. (1968) Biochim. Biophys. Acta 160, 116—117

Carl_G_190x270_mm_blokki_FINAL.indd 167 06-Aug-23 1:53:35 PM

19 Rüdiger, H. (1977) Eur. J. Biochem. 72, 317—322
20 Gahmberg, C.G. and Hakomori, S. (1973) J. Biol. Chem. 248, 4311—4317
21 Karhi, K.K. and Gahmberg, C.G. (1980) Biochim. Biophys. Acta 622, 337—343
22 Greenwood, F.C., Hunter, W.M. and Glover, J.S. (1963) Biochem. J. 89, 114—123
23 Scatchard, G. (1949) Ann. N.Y. Acad. Sci. 51, 660—672
24 Gahmberg, C.G. and Andersson, L.C. (1977) J. Biol. Chem. 252, 5888—5894
25 Hubbard, A.L. and Cohn, Z.A. (1972) J. Cell Biol. 55, 390—405
26 Bray, G.A. (1960) Anal. Biochem. 1, 279—285
27 Laemmli, U.K. (1970) Nature 227, 680—685
28 Bonner, W.M. and Laskey, R.A. (1974) Eur. J. Biochem. 46, 83—88
29 Rice, R.H. and Means, G.E. (1971) J. Biol. Chem. 246, 831—832
30 Krebs, K.G., Heusser, D. and Wimmer, H. (1967) in Dünnschichtchromatographie, (Stahl, E., ed.), pp. 813—859, Springer-Verlag, Berlin
31 Lowry, O.H., Rosebrough, N.J., Farr, A.L. and Randall, R.J. (1951) J. Biol. Chem. 193, 265—275
32 Economidou, J., Hughes-Jones, N.C. and Gardner, B. (1967) Vox Sang. 12, 321—328
33 Gahmberg, C.G., Myllylä, G., Leikola, J., Pirkola, A. and Nordling, S. (1976) J. Biol. Chem. 251, 6108—6116
34 Tanner, M.J.A. and Anstee, D.J. (1976) Biochem. J. 155, 701—703
35 Dahr, W., Uhlenbruck, G., Leikola, J., Wagstaff, W. and Landfried, K. (1976) J. Immunogenet. 3, 329—346
36 Furthmayr, H. (1978) Nature 271, 519—524
37 Adair, W.L. and Kornfeld, S. (1974) J. Biol. Chem. 249, 4696—4704
38 Hamaguchi, H. and Cleve, H. (1972) Biochem. Biophys. Res. Commun. 47, 459—464

Carl_G_190x270_mm_blokki_FINAL.indd 168 06-Aug-23 1:53:35 PM

BRIEF COMMUNICATIONS

nature medicine

RIFINs are adhesins implicated in severe *Plasmodium falciparum* malaria

Suchi Goel[1,8], Mia Palmkvist[1,8], Kirsten Moll[1,8], Nicolas Joannin[1], Patricia Lara[2], Reetesh R Akhouri[1], Nasim Moradi[2], Karin Öjemalm[2], Mattias Westman[1], Davide Angeletti[1], Hanna Kjellin[3], Janne Lehtiö[3], Ola Blixt[4], Lars Ideström[5], Carl G Gahmberg[6], Jill R Storry[7], Annika K Hult[7], Martin L Olsson[7], Gunnar von Heijne[2], IngMarie Nilsson[2] & Mats Wahlgren[1]

Rosetting is a virulent *Plasmodium falciparum* phenomenon associated with severe malaria. Here we demonstrate that *P. falciparum*–encoded repetitive interspersed families of polypeptides (RIFINs) are expressed on the surface of infected red blood cells (iRBCs), bind to RBCs—preferentially of blood group A—to form large rosettes and mediate microvascular binding of iRBCs. We suggest that RIFINs have a fundamental role in the development of severe malaria and thereby contribute to the varying global distribution of ABO blood groups in the human population.

Sequestration and rosetting in individuals with severe *Plasmodium falciparum* malaria has been attributed to *P. falciparum* erythrocyte membrane protein 1 (PfEMP1)[1–8]. However, antibodies to PfEMP1 disrupt rosettes of parasites grown only in blood group O RBCs, not group A RBCs. Notably, the majority of *P. falciparum* strains and fresh, clinical isolates prefer group A RBCs for rosetting[9–11] (**Supplementary Fig. 1**). We found that enzymatic removal of PfEMP1 from the iRBC surface reduced rosetting in blood group O but not blood group A, indicating that PfEMP1 may not be the only molecule responsible for RBC binding and rosette formation (**Supplementary Fig. 1a**). A second family of antigens has been found at the iRBC surface: RIFINs[12–14]. These polypeptides are encoded by 150 *rif* genes and comprise the largest family of antigenically variable molecules in *P. falciparum*. Given that the function of RIFINs is unknown and that they are resistant to enzyme degradation and upregulated in rosetting parasites[12,13] (**Supplementary Fig. 1b–d**), we speculated that they contribute to the rosetting and sequestration of *P. falciparum* mediated by blood group A antigen.

To study the function of the RIFINs, we investigated their primary structures and found that the majority (~70%) belong to subgroup A (hereafter referred to as A-RIFIN) and possess an insertion of 25 amino acids at the N terminus (indel) that the B-RIFINs lack[15]. Transmembrane helix prediction software generated inconsistent results for the RIFINs because of a hydrophobic patch present in their central region (**Supplementary Figs. 2** and **3**). Therefore, it has been unclear whether the RIFINs pass through the erythrocyte membrane once, which would expose a large portion to the outside of the iRBC, or twice, which would only expose a minor, variable fragment extracellularly[15,16]. This ambiguity led us to study the topology and orientation of several A- and B-RIFINs. From experiments using an *in vitro* transcription and translation system supplemented with endoplasmic reticulum–derived vesicles[17], we conclude that only a C-terminal segment of the RIFINs is stably inserted into the membrane (**Fig. 1** and **Supplementary Fig. 4**). We also transfected Chinese hamster ovary (CHO) cells with hemagglutinin A (HA)- and Myc-tagged *rif* genes and found that both tags were exposed to the outside of the CHO cells (**Supplementary Fig. 5**). The results of both sets of experiments demonstrate that the RIFINs have only one transmembrane segment near the C terminus (**Supplementary Fig. 3**), allowing the N terminus to be exposed to the outside of the RBC.

We analyzed the ability of *rif* gene–transfected CHO cells to bind RBCs. A-RIFIN CHO cells bound large numbers of group A RBCs (up to ~25 RBCs per CHO cell), whereas the binding of group O RBCs was less pronounced (**Fig. 1c**,**d** and **Supplementary Fig. 5c**) and similar to that of CHO cells expressing the N-terminal domain of PfEMP1 (DBL1α; IT4var60, not shown). This suggests that the group A antigen is a major receptor for A-RIFINs. RBC binding was negligible with B-RIFIN CHO cells or CHO cells expressing PfEMP1 (DBL1α of PfEMP1-FCR3S1.2var1) (control). To confirm the group A specificity, we removed the terminal α3 *N*-acetylgalactosamine (GalNAc) residue of the group A oligosaccharides from RBCs by treating them with an enzyme that converts group A RBCs into group O RBCs by exposing the underlying blood group H antigen[18]. Binding of enzyme-treated RBCs to A-RIFIN CHO cells was low compared to mock-treated or control group A RBCs and similar to that of group O RBCs (**Fig. 1d**). Similarly, when we added enzyme-treated group A RBCs (hereafter referred to as 'Azyme' RBCs) to *P. falciparum* cultures (FCR3S1.2 strain), they formed small rosettes of a size comparable to those formed by group O RBCs (**Fig. 1e**). A-antigen expression is used to define subgroups for group A RBCs, and A_1 RBCs express approximately five times more A antigen on the surface than A_2 RBCs on a per-cell basis[18]. The amount of RBC binding to both A-RIFIN CHO cells and FCR3S1.2 iRBCs correlated with the level of group A antigen expression because group A_1 RBCs bound significantly better than group A_2 RBCs (**Fig. 1d**,**e**).

We expressed and purified recombinant A-RIFIN (gene no. PF3D7_0100400) of the 3D7 strain of *P. falciparum* from *E. coli* to confirm

[1]Center for Infectious Disease Research, Department of Microbiology, Tumor and Cell Biology, Karolinska Institutet, Stockholm, Sweden. [2]Center for Biomembrane Research, Department of Biochemistry and Biophysics, Stockholm University, Stockholm, Sweden. [3]SciLifeLab, Departments of Oncology, Pathology, Molecular Medicine, and Surgery, Karolinska Institutet, Stockholm, Sweden. [4]Department of Chemistry, Faculty of Science, University of Copenhagen, Fredriksberg, Denmark. [5]Department of Medical Physics, Karolinska University Hospital, Stockholm, Sweden. [6]Department of Biosciences, Division of Biochemistry and Biotechnology, University of Helsinki, Helsinki, Finland. [7]Hematology and Transfusion Medicine, Department of Laboratory Medicine, Lund University, Lund, Sweden. [8]These authors contributed equally to this work. Correspondence should be addressed to M.W. (mats.wahlgren@ki.se).

Received 6 October 2014; accepted 29 January 2015; published online 9 March 2015; doi:10.1038/nm.3812

Carl_G_190x270_mm_blokki_FINAL.indd 169 06-Aug-23 1:53:36 PM

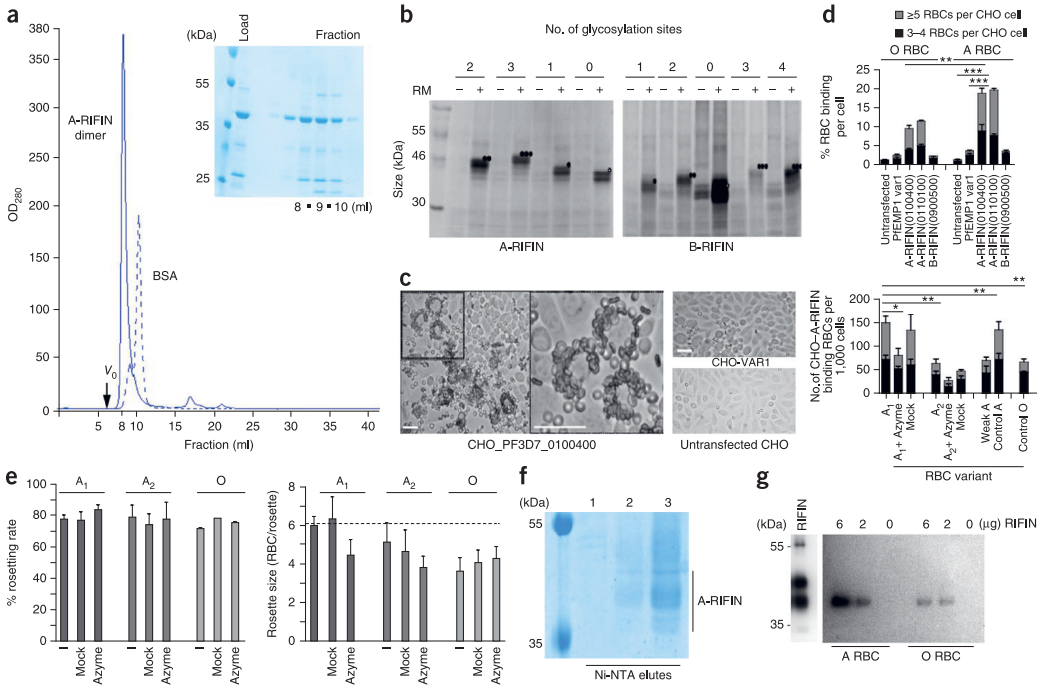

Figure 1 A-RIFINs form dimers and preferentially bind blood group A RBCs. (**a**) Size-exclusion chromatograph of A-RIFIN (solid line) and BSA (dashed line; void volume (V_0) is 7.625 ml) and SDS–PAGE gel of peak fractions. Black squares, 8.5 and 9.5 mls, respectively. (**b**) Topological analysis of A- and B-RIFINs using an *in vitro* transcription and translation system supplemented with endoplasmic reticulum–derived vesicles[17]. *rif* genes encoding A-RIFINs (one natural glycosylation site) and B-RIFINs (two) were engineered to have respectively three or four glycosylation sites. SDS–PAGE analysis of the *rif* gene products show that both A- and B-RIFINs are glycosylated at three sites, except for a site in the C terminus of B-RIFIN, indicating that the RIFINs have a single transmembrane domain ($n = 3$). Dots, number of glycosylations (**Supplementary Fig. 4**). (**c**) Bright-field images of group A RBCs binding to CHO cells expressing PF3D7_0100400 (A-RIFIN) or untransfected CHO cells or CHO cells expressing DBL1α of PfEMP1-FCR3S1.2-var1 (CHO-VAR1). Scale bars, 20 μm. (**d**) Percent binding of RBCs to CHO transfectants. The RBCs included groups A, O, A_1 (high A), A_2 (low A), weak A (low A) and Azyme (low A); $n = 3$ for each group. Comparison between RBC group and the binding of ≥5 RBCs and 3–4 RBCs was analyzed using two-way analysis of variance (ANOVA) and Bonferroni post-test; $^*P < 0.05$, $^{**}P < 0.01$, $^{***}P < 0.001$; error bars, mean + s.e.m. Numbers in parentheses are RIFIN gene IDs. (**e**) Rosetting rates and rosette sizes of FCR3S1.2 parasites in O, A_1, A_2 or Azyme RBCs; $n = 4$; error bars, mean + s.d. (**f**) SDS–PAGE of A-RIFIN purified from *Drosophila* S2 cells. The fractions are the first three eluates (1, 2, 3) containing A-RIFIN after TALON chromatography (Ni-nitrilotriacetic acid (NTA) resin). (**g**) Immunoblotting of SDS–PAGE-separated recombinant A-RIFIN after binding and elution from group O or A RBCs ($n = 3$).

its group A RBC–binding specificity, but it could only be purified as a monodisperse protein in the presence of a detergent (*n*-dodecyl-β-D-maltopyranoside; DDM), probably because of the hydrophobic nature of RIFINs. Size-exclusion chromatography revealed that A-RIFINs exist as homodimers in the presence of DDM, indicating this to be the stable RIFIN unit (**Fig. 1a**). Spaced glycine residues present in the hydrophobic patch may facilitate dimerization of A-RIFIN. Because A-RIFIN is only soluble in the presence of DDM, which is not amenable to erythrocyte-binding studies, we switched to *Drosophila* cells for expression and purification under more physiological conditions. SDS–PAGE, immunoblotting and LC-MS/MS showed that purified A-RIFIN, in the reduced state, exists as multiple species much as it does in *P. falciparum* (**Fig. 1f**). We observed that only the fastest-migrating species of recombinant A-RIFIN bound to both group O and A RBCs, and binding to group A RBCs was concentration dependent and showed higher avidity compared to group O (**Fig. 1g**).

To identify the RIFIN expressed in FCR3S1.2-strain parasites in which PfEMP1 was first identified, we performed RNA-seq analysis of iRBCs at 10 h, 20 h, 30 h and 40 h after merozoite invasion. We found a single *rif* gene (PFIT_bin05750; 11,200 reads) that was highly expressed and another 84 *rif* genes that were transcribed at lower levels (0–2,000 reads); these RNA-seq results were confirmed by qPCR (**Supplementary Fig. 6**). These data suggest that the expression of *rif* genes is allelically excluded, as are the genes that encode PfEMP1 (ref. 19), at least within each subgroup, and the previously noted microheterogeneity of the RIFINs[12] is probably due to post-translational modifications rather than expression of several RIFINs in the same parasite.

The RIFIN of parasite clone FCR3S1.2 was found to be similar to the A-RIFIN of 3D7 (PF3D7_0100400, **Supplementary Fig. 2**), and, as expected, anti-RIFIN IgG generated to the A-RIFIN of 3D7 cross-reacted with the heterologous RIFIN of FCR3S1.2 in both immunoblotting and immunofluorescence analysis (**Fig. 2a–d**).

BRIEF COMMUNICATIONS

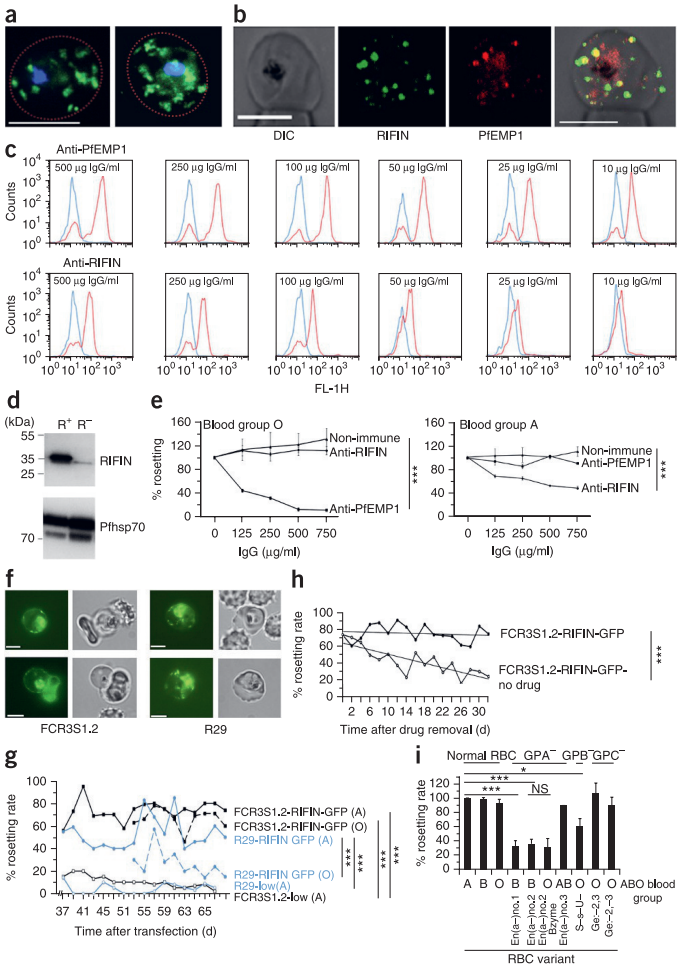

Figure 2 Expression of RIFINs at the iRBC surface and involvement in rosetting. (**a**) Indirect immunofluorescence analysis of air-dried FCR3S1.2 iRBCs using purified IgG raised in goat against full length A-RIFIN (green, Alexa Fluor 488). DAPI (blue), stained nuclei of parasites. Scale bar, 5 µm. (**b**) Confocal microscopy of live FCR3S1.2 iRBCs with anti-RIFIN IgG (green) or anti-PfEMP1 serum (red). Scale bars, 5 µm. (**c**) Surface expression of RIFIN (bottom) or PfEMP1 (top) as observed by FACS on live iRBCs using anti-RIFIN (red, bottom), anti-PfEMP1 (red, top) or non-immune IgG (blue) at various concentrations. FL-1H, channel used to detect Alexa Fluor 488 or GFP (emission wavelength, 515–545 nm). (**d**) Immunoblotting of SDS extracts of high (R^+)- and low (R^-)-rosetting FCR3S1.2 using anti-A-RIFIN and anti-Pfhsp70-IgG ($n = 4$ for each group). (**e**) Disruption of rosettes formed by FCR3S1.2 when grown in A or O RBCs after addition of anti-RIFIN, anti-PfEMP1, or non-immune IgG. The rosetting rates were calculated with respect to a control where no antibody was added ('0' on the *x* axis). $n = 5$; $^{***}P < 0.001$, Student's *t*-test, Error bars, s.e.m. (**f**) Direct fluorescence of *rif-gfp* gene–transfected parasites. Image shows live iRBC with no prior staining. 100× magnification; $n = 3$; scale bars, 5 µm. (**g**) Rosetting rates of FCR3S1.2-low, FCR3S1.2-RIFIN-GFP, R29-low, and R29-RIFIN-GFP in group A or O RBCs. Growth of transfectants in O RBCs commenced at day 53 after transfection. (**h**) Gradual loss of rosetting of FCR3S1.2-RIFIN-GFP iRBCs upon removal of the drug used for selection of the transfected parasite. The trend line suggests significant loss of rosetting upon removal of the drug. $^{***}P < 0.001$; Student's *t*-test; error bars, s.e.m. (**i**) Rosetting rate of FCR3S1.2-RIFIN-GFP with glycophorin A (En(a–))-, glycophorin B (S–s–U–)-, or glycophorin C (Ge:–2,3 and Ge:–2,–3)-deficient RBCs. $n = 3$; Student's *t*-test; $^{*}P < 0.05$, $^{***}P < 0.001$; NS, not significant; error bars, mean + s.e.m. Bzyme, enzyme-treated B RBCs converted into O RBCs.

We found that the RIFINs localized to the parasitophorous vacuole, Maurer's clefts and to the membrane of iRBCs; we also found that live, unfixed iRBCs stained in a punctate pattern similar to that obtained with antibodies to PfEMP1 (**Fig. 2a**). Staining patterns were only partially overlapping, which may suggest that the RIFINs are exported and exposed at the iRBC surface in a manner different from that of PfEMP1. In addition, semiquantitative analysis with FACS suggested that the percentage of RIFIN and PfEMP1 surface-positive iRBCs correlated with one another as well as with the rosetting rates (**Fig. 2c** and data not shown). The expression of the two molecules gradually decreased in parasite FCR3S1.2 when it was not enriched for rosetting, whereas both RIFINs and PfEMP1 were upregulated upon selection for rosetting (**Supplementary Fig. 1d**). Neither control IgG, anti-IgG–Alexa Fluor 488 conjugate alone nor antibodies to the cytoplasmic C-terminal part of RIFIN stained the iRBC surface, and RIFIN antibodies did not cross-react with the iRBC surface of other rosetting parasites (TM284S2, PAvarOvar1, R29-IT4var9, data not shown). Furthermore, RIFIN-specific IgG disrupted rosettes of FCR3S1.2 parasites when cultured in group A RBCs but did not affect group O rosetting by the same parasite (**Fig. 2e**). Conversely, PfEMP1-specific IgG did not show any effect on group A rosetting but disrupted rosettes formed by group O RBCs (**Fig. 2e** and **Supplementary Fig. 1b**). These data suggest that A-RIFINs mediate group A rosetting, whereas group O rosetting is primarily mediated by PfEMP1. However, RIFINs may also bind group O RBCs.

The human microvasculature expresses ABO blood group antigens on endothelial cells, RBCs, and serum proteins. To establish the role of RIFINs in microvascular sequestration of iRBCs, we transfected two strains of *P. falciparum* parasites selected for low rosetting (FCR3S1.2-low and R29-low) with a FCR3S1.2 *rif* gene (PFIT_bin05750) in frame with a gene encoding green fluorescent protein (GFP, **Supplementary Fig. 7a**). Immunoblotting with anti-GFP mAb or direct GFP fluorescence detected high expression of the RIFINs in both parasites (**Fig. 2f** and **Supplementary Fig. 7b**).

The R29-RIFIN-GFP strain showed higher RIFIN expression than the FCR3S1.2-RIFIN-GFP strain, but a larger fraction of the fluorescence was observed within the parasite, suggesting incomplete RIFIN transport to the iRBC surface in the R29-RIFIN-GFP compared to the FCR3S1.2-RIFIN-GFP strain, in which most of the fluorescence was observed at the iRBC-membrane (**Fig. 2f**). The FCR3S1.2-RIFIN-GFP strain displayed a ~60–80% rosetting rate, whereas control parasites (FCR3S1.2-low) grown in parallel under identical conditions remained low in rosetting (~10–20%; **Fig. 2g**). R29-low parasites transfected with the *rif* gene induced a higher rosetting rate when grown in group A than in group O RBCs (**Fig. 2g**). Removal of drug pressure from the transfected parasites led to loss of the episomally expressed plasmids and a concomitant loss of rosetting to the levels of the control parasites (**Fig. 2h**). To study the role of the RIFINs in *in vivo* sequestration of iRBCs, we injected FCR3S1.2-RIFIN-GFP parasites cultured in group A human RBCs into Sprague-Dawley rats. We found that the iRBCs bound in the microvasculature significantly more than FCR3S1.2-low or normal human RBCs ($P < 0.01$; **Supplementary Fig. 8**). This suggests a role for the RIFINs in the microvascular binding of *P. falciparum* iRBCs.

RIFIN-transfected FCR3S1.2 propagated in group A RBCs often formed large or giant rosettes comprising 10 or more RBCs. By contrast, small rosettes were common with group O RBCs (**Supplementary Fig. 9**). We found that RIFIN binding of O RBCs was mediated by sialic acid expressed on glycophorin A (GPA) because the binding was sensitive to neuraminidase and trypsin, but not chymotrypsin, and it could be inhibited with soluble sialic acid (**Supplementary Fig. 10**). Furthermore, human En(a–) RBCs devoid of GPA[20] only rosetted weakly as compared to normal RBCs or RBCs lacking glycophorin B (GPB) or glycophorin C (GPC) (**Fig. 2i** and **Supplementary Fig. 11**). Notably, En(a–) RBCs expressing the group A antigen bound avidly to iRBCs, suggesting that binding to group A supersedes GPA binding and that group A is the major receptor used by RIFINs to mediate rosetting.

In conclusion, our findings suggest that RIFINs may be central to the pathogenesis of severe *P. falciparum* malaria and to mediating PfEMP1-independent vascular sequestration of iRBCs, predominantly through binding to the blood group A antigen. Previous studies have indicated that in African children, blood group A predisposes to severe malaria[10]. Taken together with our present observations, this may imply that RIFINs contribute to the varying global distribution of ABO blood groups in favor of blood group O.

METHODS

Methods and any associated references are available in the online version of the paper.

Note: Any Supplementary Information and Source Data files are available in the online version of the paper.

ACKNOWLEDGMENTS

We thank B. Dobberstein (Ruprecht-Karls-Universität, Heidelberg) for providing dog pancreas microsomes and O. Puijalon (Pasteur Institute, France) for the gift of mAb D15-50. 3-α-N-acetylgalactosaminidase (Azyme) and 3-α-galactosidase (Bzyme) were kindly provided by Henrik Clausen (Copenhagen Center for Glycomics). This study was supported by the Swedish Strategic Foundation to I.M.N. and M.W., the EU Sixth- and Seventh-Framework Programs (MEST-CT-2004-8475 and EviMalar Network of Excellence to I.M.N. and M.W.), the Swedish Research Council (VR/2012-2014/521-2011-3377 to M.W., VR/2011-2018/14251 to M.L.O.), the Söderberg Foundation and Swedish Academy of Sciences, Swedish governmental ALF grants to Lund University Healthcare to J.R.S. and M.L.O., and a Distinguished Professor Award from Karolinska Institutet to M.W. The funders had no role in the study design, data collection and analysis, decision to publish, or preparation of the manuscript.

AUTHOR CONTRIBUTIONS

S.G., M.P., K.M., N.J., R.R.A., D.A., M. Westman and H.K. carried out the parasite culturing, protein expression in *E. coli* and S2-cells, mRNA and nucleic acid preparation, RNA-seq, PCR, plasmid construction, rosette-disruption experiments, FACS experiments, and CHO adhesion experiments, and they participated in the design of the study and writing of the manuscript. L.I. assisted with the sequestration experiments in rats. O.B., C.G.G., J.R.S., A.K.H. provided sialic acid-, Azyme- and Bzyme-treated RBCs and GPA-, GPB- and GPC-RBCs. N.J., P.L., N.M., K.Ö. and I.M.N. carried out transmembrane predictions, *in vitro* transcription and translation experiments and participated in the design of the study and writing of the manuscript. M. Wahlgren, J.L., G.v.H. and M.L.O. participated in the study design and in the writing of the manuscript.

COMPETING FINANCIAL INTERESTS

The authors declare competing financial interests: details are available in the online version of the paper.

Reprints and permission information is available online at http://www.nature.com/reprints/index.html.

1. Scherf, A., Lopez-Rubio, J.J. & Riviere, L. *Annu. Rev. Microbiol.* **62**, 445–470 (2008).
2. Miller, L.H., Ackerman, H.C., Su, X. & Wellems, T.E. *Nat. Med.* **19**, 156–167 (2013).
3. Carlson, J. *et al. Lancet* **336**, 1457–1460 (1990).
4. Rowe, A., Obeiro, J., Newbold, C.I. & Marsh, K. *Infect. Immun.* **63**, 2323–2326 (1995).
5. Rowe, J.A., Moulds, J.M., Newbold, C.I. & Miller, L.H. *Nature* **388**, 292–295 (1997).
6. Chen, Q. *et al. J. Exp. Med.* **187**, 15–23 (1998).
7. Vigan-Womas, I. *et al. PLoS Pathog.* **8**, e1002781 (2012).
8. Carlson, J., Nash, G.B., Gabutti, V., al-Yaman, F. & Wahlgren, M. *Blood* **84**, 3909–3914 (1994).
9. Carlson, J. & Wahlgren, M. *J. Exp. Med.* **176**, 1311–1317 (1992).
10. Rowe, J.A. *et al. Proc. Natl. Acad. Sci. USA* **104**, 17471–17476 (2007).
11. Cserti, C.M. & Dzik, W.H. *Blood* **110**, 2250–2258 (2007).
12. Fernandez, V. *et al. J. Exp. Med.* **190**, 1393–1404 (1999).
13. Kyes, S.A. *et al. Proc. Natl. Acad. Sci. USA* **96**, 9333–9338 (1999).
14. Petter, M. *et al. Mol. Biochem. Parasitol.* **156**, 51–61 (2007).
15. Joannin, N., Abhiman, S., Sonnhammer, E.L. & Wahlgren, M. *BMC Genomics* **9**, 19 (2008).
16. Lavazec, C., Sanyal, S. & Templeton, T.J. *Nucleic Acids Res.* **34**, 6696–6707 (2006).
17. Hessa, T. *et al. Nature* **433**, 377–381 (2005).
18. Liu, Q.P. *et al. Nat. Biotechnol.* **25**, 454–464 (2007).
19. Chen, Q. *et al. Nature* **394**, 392–395 (1998).
20. Gahmberg, C.G., Myllyla, G., Leikola, J. & Pirkola, A. *J. Biol. Chem.* **251**, 6108–6116 (1976).

ONLINE METHODS

Transmembrane region predictions. We used 10 methods to predict transmembrane regions and protein topology of the RIFINS with gene IDs: PF3D7_0100400, PF3D7_1101100, and PF3D7_0900500 proteins. These included different methodologies: hydrophobicity[21] (TOPPRED), Hidden Markov Model (HMM)[22–24] (Phobius, TMHMM2.0, HMMTOP2.1[23]), Artificial Neural Network (ANN)[25] (PHDhtm), Support Vector Machine (SVM) (MEMSAT-SVM, Nugent 2009), a mix of HMM and ANN (Octopus) and consensus methods (ConPred II (ref. 26, TOPCONS[27]). We also used the SignalP3.0 signal prediction method[28].

Parasite culture, RNA extraction and reverse transcription. *P. falciparum* parasites clone 3D7S8.4[29], clone FCR3S1.2 and strain R29 were cultivated *in vitro* according to standard procedures[30,31]. Cultures were routinely tested for the presence of mycoplasma. Late ring or early trophozoite–stage parasites (10, 20, 30 h post invasion (p.i.)) as well as schizont stage parasites (40 h p.i.) were used to isolate RNA using the RNeasy Mini Kit (Qiagen, Germany) according to the manufacturer's instructions. Samples were DNase treated (Turbo DNase, Ambion, Texas, USA) and reverse transcribed (Superscript III RNase H reverse transcriptase, Invitrogen, California, USA) using a mix of random hexamers and oligo(dT)12–18 (300 ng/ml and 25 ng/ml, respectively) at 25 °C for 10 min, 50 °C for 2 h and 70 °C for 15 min. The cDNA was subsequently used to perform real-time reverse-transcription (RT)-PCR analysis. The PCR mix was prepared by addition of 1 µl of cDNA, 200 µM of gene-specific primers or fructose bisphosphate primers, 1× SYBR green mix (Invitrogen, USA) and DNase- and RNase-free water was added to a final volume of 10 µl. The reaction was set up at 95 °C for 15 s, 50× at 95 °C for 10 s, 60 °C for 45 s with data recorded at the elongation step. The threshold cycles were calculated and the data was analyzed based on the $2^{-\Delta\Delta Ct}$ method.

RNA-seq. Total RNA was isolated at 10 h, 20 h, 30 h and 40 h after merozoite invasion and isolated using the TRIzol method[30]. Briefly, 100 µL pellets of FCR3S1.2 of IT4 origin (~20% parasitemia) were suspended in 1 ml of TRIzol (Invitrogen) and extracted with 200 µL of chloroform. The total RNA in the aqueous phase was precipitated with 0.5 ml of isopropanol, and washed with 75% ethanol. The RNA was air-dried, dissolved in DNase- and RNase-free water. 5 µg of RNA for each time point was used to prepare cDNA libraries using a poly-A adaptor at the 3′ end. The libraries were sequenced using high throughput Illumina sequencing technology. The resulting reads were assembled and analyzed by aligning with the genome sequence of the parasite IT4. The expression was represented either as FPKM (fragment per kilobase of exon per million fragments) or counts.

Trypsin treatment of the iRBC surface. MACS-purified iRBCs[30] were treated with trypsin at various concentrations at 37 °C for 10 min. Trypsin was inhibited with soybean trypsin inhibitor, followed by washing of iRBCs with RPMI. iRBCs were resuspended in RPMI containing 10% A^+ human serum (purchased from Karolinska Hospital, Stockholm, Sweden) and blood group A or O RBCs were added and incubated for 1 h at 37 °C. The rosetting rates were estimated with respect to a mock-treated control and Student's *t*-test for unpaired samples was used to study the significance of the data (see ref. 32 for more details).

Blood group preference in the formation of rosettes. iRBCs with parasites older than 24 h p.i. were enriched by MACS[30] and resuspended in malaria-complete medium with 10% human serum (MCM). Non-parasitized RBC of blood groups A and O were each labeled with a PKH Fluorescent Cell Linker (Sigma, USA) using PKH67 for green and PKH26 for red labeling. 1 µl of packed RBC was washed twice with RPMI, mixed with 125 µl of Diluent C and subsequently a mixture of 0.5 µl of PKH67 or PKH26 in 125 µl of Diluent C. The mixture was incubated for 5 min at room temperature (RT; 25 °C). 250 µl of PBS with 3% fetal calf serum (FCS) was added and the cells were subsequently washed twice with RPMI. The group O or A RBCs (labeled in the different colors) were resuspended in MCM to a 5% hematocrit and mixed in equal amounts. Purified iRBCs were subsequently added to generate a final parasitemia of 10%. The MACS-enriched iRBCs were passed through a needle directly before addition to the labeled, non-infected RBCs in order to mechanically brake rosettes and autoagglutinates. Rosettes were allowed to re-form for 60 min at RT and the percentage of blood group A or O RBCs bound to each iRBCs was determined via microscope by scoring 100 individual rosettes.

Preparation of parasite extracts and immunoblotting. Whole cultures of FCR3S1.2 parasite at 20–25 h p.i. (parasitemia, ~8%) were lysed using saponin at a final concentration of 0.05% and the parasite pellet obtained after centrifugation was washed once with PBS. The parasite proteins were subsequently extracted with 0.5% Triton X-100 and centrifuged at 10,000 *g* for 5 min. The insoluble proteins in the pellet obtained after centrifugation were further extracted with 2% SDS. The total amount of protein in the 2% SDS extract was measured using a Bradford reagent (Bio-Rad, USA).

For immunoblotting, 8 µg of total parasite protein was resolved in 4–15% SDS–PAGE gradient gels (Invitrogen, USA). The proteins from the gel were transferred onto a nitrocellulose membrane and the membrane was blocked with 3% milk in PBS with 0.05% Tween 20 (PBST) at 4 °C overnight. The membrane was subsequently incubated with purified anti-goat RIFIN IgG against the full-length A-RIFIN protein PF3D7_0100400 or to a peptide of the C-terminal region of the RIFIN (RYRRKMKLKKKLQYIKLLEE; in rabbit) at concentrations of 10 µg/ml for 2 h at RT. After washing the blot three times with PBS-Tween 20, the blot was incubated with HRP-conjugated anti-goat IgG (catalog no. 81-6129, Invitrogen, USA) or anti-rabbit IgG (catalog no. NA934V, ECL Biosciences) at a dilution of 1:5000 for 1 h at RT. Anti-rabbit PfHsp70 at a dilution of 1:1000 was used as a loading control (catalog no. SPC-186D, StressMarq Biosciences Inc., USA). The blots were washed and developed with chemoluminescence reagents (ECL, Thermo Scientific, USA).

RIFIN purification from *E. coli*. The sequence of the A-RIFIN PF3D7_0100400 was optimized for expression in *E. coli* (DNA 2.0) and the gene was amplified between 114–987 bp using forward and reverse (**Supplementary Table 1**) primers with NdeI and XhoI restriction sites for cloning into pJ414 vector. The vector and the PCR-amplified product were digested with NdeI and XhoI and ligation was performed. The ligation mix was transformed and the colonies were PCR-screened for the presence of the *rif* genes. The positive clones were further confirmed through DNA sequencing. A positive clone was transformed into SHuffle T7 cells and expression of RIFIN was performed and studied. Briefly, 1% of overnight culture of *E. coli*–RIFIN was inoculated in Terrific Broth at 30 °C and cells were grown to an OD_{600} of 0.4–0.6. The cells were then induced with 0.4 mM IPTG for 15–16 h at 16 °C. The cells were pelleted and lysed in 20 mM Tris (pH 8.0) and 150 mM NaCl (TBS) buffer by sonication. After centrifugation at 16000 r.p.m. for 1 h, the pellet was solubilized in TBS with 5× critical micelle concentration (CMC) of DDM (Anagrade, Affymetrix, CA, USA) for 5 h at 4 °C and centrifuged at 18000 r.p.m. for 1 h. The pellet obtained was solubilized again in TBS containing 50× CMC of DDM overnight at 4 °C. After centrifugation, the supernatant was loaded on a MonoQ resin (GE Healthcare Life Sciences, USA) and washed with TBS. The protein was subsequently eluted with a gradient of TBS and 20 mM Tris containing 1 M NaCl. The fractions were analyzed by SDS–PAGE and the fractions containing the protein were pooled. The pooled fractions were loaded onto a 24-ml Superdex S75 10/300 GL column (GE Healthcare Life Sciences, USA) in TBS with 1× CMC of DDM. The peak fractions were analyzed using SDS–PAGE.

PCR and plasmid construction. All PCR amplifications were done with Pfu Turbo DNA polymerase (Stratagene, California, USA) and purified using the QIAquick gel extraction kit (Qiagen, Germany). All DNA sequencing was performed using BigDye Terminator v3.1 and an ABI Prism 3130xL Genomic Analyzer capillary sequencer (Applied-Biosystems, California, USA). We used primers that target full-length genes to amplify Pf3D7_0100400 and Pf3D7_0900500 from a mix of cDNA from late-ring, early trophozoite and schizont 3D7S8.4 parasites. The PCR products were cloned into pCR 2.1 TOPO vector (Invitrogen, California, USA) and verified by sequencing. We subsequently amplified the genes from cloned plasmids with a second round of PCR amplification in which we modified the genes (i) by the introduction of an XbaI site, and (ii) by changing the context of the region immediately upstream of the initiator ATG codon to a Kozak consensus ribosome binding sequence, GCCACCATGG (refs. 33,34); both changes were encoded within the 5′ PCR primer. The reverse

Carl_G_190x270_mm_blokki_FINAL.indd 173 06-Aug-23 1:53:38 PM

primer encoded the 3′ end of the genes including the stop codon and a SmaI site for cloning. The genes were cloned into pGEM1 downstream of the SP6 promoter as an XbaI–SmaI fragment. Restriction enzymes were from New England Biolabs, Inc. (Massachusetts, USA).

Additionally, we modified each gene by site-specific mutagenesis to introduce or remove glycosylation acceptor sites, i.e. we modified one or more appropriately positioned codons for the acceptor tripeptide NX (S/T). Site-specific mutagenesis was performed using the QuickChange Site-Directed Mutagenesis kit (Stratagene, California, USA). All mutants were confirmed by sequencing of plasmids. Primers are listed in **Supplementary Table 1**.

***In vitro* expression with dog-pancreas microsomes.** DNA template for *in vitro* transcription was prepared[35]. Briefly, transcription with SP6 RNA polymerase of the relevant pGEM1-derived plasmids was performed for 1 h at 37 °C. We performed mRNA translation in nuclease-treated reticulocyte lysate supplemented with [^{35}S]Met and rough microsomes from dog pancreas as described[17] at 30 °C for 1 h. Samples were analyzed by SDS-PAGE, and proteins were visualized in a Fuji FLA-3000 phosphorimager (Japan) using the Image Reader V1.8J/Image Gauge V3.45 software.

Cloning and expression of RIFINs in CHO cells. Genes encoding A-RIFINs PF3D7_0100400, PF3D7_1101100, and B-RIFIN PF3D7_0900500 were PCR amplified from amino acid 38 to 329 and cloned into BglII and SalI sites in a pDisplay vector (Invitrogen, USA). Proteins expressed from the pDisplay vector were fused at the N terminus to the mouse Ig κ-chain leader sequence, to direct the protein to the secretory pathway, and at the C terminus to the platelet-derived growth factor receptor (PDGFR) transmembrane domain, which anchors the protein to the plasma membrane, displaying it on the extracellular side. The expression construct held sequences encoding a hemagglutinin A tag (HA) at the N terminus and a MYC tag at the C terminus of the RIFINs. All the constructs were confirmed by sequencing using Big Dye Terminator v3.1 and ABI Prism 3130xL Genomic Analyzer capillary sequencer (Applied Biosystems, California, USA). The pDisplay constructs containing genes encoding A-RIFINs PF3D7_0100400, PF3D7_1101100, or B-RIFIN PF3D7_0900500 were transfected into CHO cells using Fugene (Roche biosciences, Switzerland) according to the manufacturer's protocol. Briefly, CHO cells were plated in 6-well plates 16–18 h before transfection. Fugene was diluted in 100 µl of incomplete RPMI and incubated for 5 min, followed by addition of DNA to maintain a Fugene to DNA ratio of 6:1. After incubation at RT for 30 min, the DNA–Fugene complex was added to the cells. CHO cells were maintained with the complex at 37 °C. The transfection media was removed after 48 h and cells were selected by the addition of the drug G418 at 1 mg/ml. The surface expression of the proteins was analyzed by FACS using antibodies against the HA (N terminus) and MYC (C terminus) epitopes. Briefly, the cells were washed twice with PBS and scraped loose in PBS/0.5mM EDTA with a rubber policeman (on ice), centrifuged and blocked with PBS holding 10% FCS for 30 min (on ice). The cells were incubated with rabbit anti-HA (catalog no. H6908, Sigma-Aldrich, USA) or anti-MYC (catalog no. C3956, Sigma-Aldrich, USA) antibodies at a dilution of 1:100 for 1 h, washed followed by 30 min incubation with anti-rabbit IgG coupled to Alexa Fluor 488 (1:100, catalog no. A11070, Invitrogen, USA). CHO cells expressing the RIFINs were repeatedly enriched during prolonged cultivation using the HA-specific antibody conjugated to anti-rabbit IgG–coated micro-beads and subjected to magnetic cell sorting (Miltenyi Biotec, Bergisch Gladbach, Germany).

RBC binding to CHO cells. Transfected or control cells were seeded in 6- or 12-well culture plates overnight and grown until they were 40–50% confluent. Aliquots of blood group A or O RBC were washed twice in PBS and added to the cells at 2% hematocrit in complete growth media. The cells were incubated with erythrocytes at 37 °C in a CO_2 incubator for either 5 or 15 h and subsequently washed extensively three times with RPMI to remove unbound RBCs. Binding was assessed by microscopy (Diaphot 300, Nikon, Japan). The binding was calculated as the percentage of CHO cells that bound RBC. Further, binding was also estimated as to the number of RBC bound (3–4 or >5) per 1,000 cells using a Nikon Diaphot 300 (Japan) microscope at a magnification of 100×. 3-α-N-acetylgalactosaminidase (Azyme) and 3-α-galactosidase (Bzyme) were used for the conversion of blood group A and B, respectively, to blood group O (ref. 18).

RIFIN purification from S2 cells. The A-RIFIN gene sequence PF3D7_0100400 optimized for the *Drosophila* expression system (Genscript, USA) was amplified from bps 114 to 987 for cloning into the insect expression vector pMT/BiP/V5-His A. The gene encoding A-RIFIN was PCR amplified using primers for BglII and XhoI sites (**Supplementary Table 1**). The PCR-amplified fragment and the vector pMT/BiP/V5-His A were digested with the above enzymes and ligated together. The ligation mix was transformed in XL10 gold–competent cells and positive clones were selected and confirmed by sequencing. The clones were then transfected into Schneider 2 (S2) *Drosophila* cells. S2 cells were maintained in S2 media with 10% FCS. The cells were transfected using manufacturer's protocol (Invitrogen, USA). Briefly, 1×10^6 cells were plated into 24-well plates. The transfection mix was prepared by adding a mix of 2 M $CaCl_2$ (36 µl), DNA (19 µg) and pCoBlast (1 µg) to a final volume of 300 µl to an equal volume of 2× HEPES–buffered saline (50 mM HEPES, 1.5 mM Na_2HPO_4, 280 mM NaCl (pH 7.1)) and incubated at RT for 30–40 min. The transfection mix was placed onto the S2 cells and complete S2 media was added after 24 h. After 48 h, blasticidin (25 µg/ml) was added to transfected S2 cells. After S2 cells were stable in the blasticidin, they were induced with $CuSO_4$ and the supernatant was tested for expression of A-RIFIN.

For expression of A-RIFIN PF3D7_0100400, S2 cells stably transfected with A-RIFIN were cultured at a 1–2-liter scale and induced with 0.6 mM $CuSO_4$ for 48 h. The supernatant was collected, concentrated using diafiltration (Millipore, USA) and dialyzed against TBS (20 mM Tris and 150 mM NaCl (pH 8.0)). The dialyzed medium containing 10 mM imidazole was loaded onto a column with cobalt beads (TALON, GE healthcare, USA). The column was washed with 10 mM imidazole in TBS and the protein was eluted with 150 mM imidazole in TBS. The fractions were analyzed using SDS–PAGE and the fractions containing the A-RIFIN were pooled and dialyzed against TBS. The purified protein was used for RBC binding assay.

RIFIN-RBC binding assays. The purified RIFIN protein from S2 cells holding a 6× His tag and a V5 tag was used for RBC binding assays. Blood group A and O RBCs were washed three times with PBS containing 2% human serum. 10 µl of RBC at 1% in PBS with 2% human serum added were incubated with various concentrations of the protein for 1 h at RT. The RBCs were washed three times with PBS with 2% human serum and the protein that bound to the RBCs was eluted with 1.2 M NaCl. The eluates were run in SDS–PAGE, followed by immunoblotting with an anti-V5 antibody (catalog no. R960-25, Invitrogen, USA) to detect the RIFIN. The blots were developed using a chemiluminescence reagent (Thermoscientific, USA).

Generation of immune sera. *E. coli*–purified A-RIFIN (PF3D7_0100400) was used to repeatedly immunize rats, rabbits and a goat using Freund´s incomplete adjuvants (Agrisera, Vännäs, Sweden). The C-terminal region of the RIFIN (RYRRKMKLKKKLQYIKLLEE) coupled to KLH was used to immunize rabbits using Freund's incomplete adjuvant. The sera were collected after the fourth immunization and the IgGs were purified and used in the various assay. For polyclonal goat IgG (anti-PfEMP1-DBL1α-ITvar60, anti-PfEMP1-DBL1α-PAvarO, anti-PfEMP1-DBL1α-ITvar9) and mAbs specific for PfEMP1 please see refs. 32,36.

Analysis of antibody-surface reactivity of iRBCs. Reactivity of antibodies with the iRBC surface was tested with FACS as described previously[36] or by laser-scanning confocal microscopy using a Zeiss LSM 700 microscope. Briefly, iRBCs of ~24–30 h p.i. were incubated with the polyclonal goat IgG to RIFIN (PF3D7_0100400) or to PfEMP1 (NTS-DBL1α) (10–500 µg/ml) or with rat sera to NTS-DBL1-α of PfEMP1-ITvar60 (final dilution 1:10) for 30 min followed by a 30 min incubation with species-specific anti-IgG antibodies coupled to Alexa Fluor 488 (catalog no. A110006; Invitrogen, USA) or Alexa Fluor 594 (catalog no. A10545, dilution 1:100, Invitrogen). The antibodies were diluted in PBS with 2% FCS. Negative controls were treated the same way, using non-immune goat IgG (catalog no. 005-000-003, Chromapure) or non-immune rat serum (catalog no. 012-000-003, Chromapure, USA) as the primary antibodies.

Carl_G_190x270_mm_blokki_FINAL.indd 174 06-Aug-23 1:53:39 PM

For all experiments, goat IgG was pre-absorbed on blood group O RBCs. In brief, goat IgG at a concentration of 500 µg/ml was mixed with packed RBCs at 1/15th of the volume and incubated at RT for 1 h, the procedure was repeated once and the supernatant was used for the experiments. For nuclear staining, ethidium bromide was added at a final concentration of 2.5 µg/ml; cell acquisition was done using flow cytometry (FACSCalibur, BD Bioscience, USA) in which 2,500 iRBCs were counted. The analysis was performed using FlowJo software. Normal, non-immune goat IgG or pre-immune rat sera were used as controls in all experiments at identical concentrations. For confocal microscopy the unfixed, labeled iRBCs were immobilized on glass slides at a 0.5% hematocrit in Matrigel (BD Matrigel Basement Membrane Matrix; phenol and LDEV-free) and allowed to solidify 30 min at RT under 0.17 mm borosilicate cover slips (Marienfeld Borosilicate glass D 263 M, hydrolytic class 1). Samples were subsequently viewed in a Zeiss LSM 700 laser scanning confocal microscope, Observer.Z1 stage and C-Apochromat 40×/1.2-W Korr ∞/0.14-0.19 UV-visible-IR objective. Images were acquired through Zen 2010 V6.0.0.309 using a 36-µm pinhole, 0.02 µm *XY* scaling, 23.06 µm *XY* stack size and 6.9 times scan zoom in one plane.

Enrichment of specific IgG on RIFIN- or PfEMP1-coupled beads. To purify A-RIFIN- or PfEMP1-specific IgG from the total IgG preparations, recombinant A-RIFIN (PF3D7_0100400) or PfEMP1, purified from bacteria, were coupled to AminoLink Coupling gel (Thermoscientific, USA). The conjugation was carried out by mixing the AminoLink Coupling gel (1 ml) with 3 mg of RIFIN or PfEMP1 (NTS-DBL1α-CIDR1γ, PfIT4var60), and adding 25 µl of cyanoborohydride solution per ml of the reaction volume and incubating the mixtures overnight at 4 °C. The gels were washed once with 1 M Tris to stop the coupling reaction and then an equal volume of 1 M Tris and 50 µl of cyanoborohydride per ml of gel was added and incubated for 30 min at RT. The gels were washed several times with 1 M NaCl for complete removal of uncoupled protein and stored in PBS at 4 °C. A-RIFIN- or NTS-DBL1α-CIDRγ-coupled gels were incubated, respectively, with A-RIFIN- or PfEMP1-specific IgGs for 2 h at RT, followed by washing with 10 column-volumes of PBS. The bound IgG was eluted using 100 mM glycine (pH 2.5) and the pH was rapidly adjusted to 7.0 by the addition of Tris base. The eluted fractions were pooled and dialyzed extensively against PBS. The concentration of IgG used for rosette disruption assays was measured using Bradford reagent (Bio-Rad, USA).

Rosette disruption assays. Various dilutions of purified goat IgG (anti-RIFIN, anti-PfEMP1-ITvar60, anti-PfEMP1-PAvarO, anti-PfEMP1-ITvar9)[32,36] or non-immune IgG (no. 005-000-003, Chromapure, USA) were prepared to a final volume of 20 µl and added to 20 µl of parasite culture at 4% hematocrit to yield final concentrations of 125 µg/ml, 250 µg/ml, 500 µg/ml or 750 µg/ml. The mixtures were incubated for 1 h at RT and the rosettes were counted after staining the parasites with acridine orange[30]. The rosetting rate is presented as the percentage of number of rosettes formed by the total number of late-stage iRBCs and the inhibition of rosetting was expressed with respect to rosetting in the control cultures where no antibody was added. Rosette disruption assays using *N*-acetylneuraminic acid (sialic acid) were similarly performed as above.

Transfection of *P. falciparum* with *rif* genes. Total RNA was isolated 20 h after invasion from FCR3S1.2 culture. The cDNA was prepared and the PFIT_bin05750 gene was amplified using forward and reverse primers using XhoI and restriction sites respectively for cloning into pARL-2-GFP vector such that the *GFP* gene was in frame with PFIT_bin05750. The positive clones were also confirmed by sequencing and used for transfection of FCR3S1.2 and R29 parasites. For transfection into parasites, an erythrocyte DNA-loading protocol was followed[30]. Briefly, 350 µl of RBCs at 50% hematocrit were washed once with incomplete Cytomix[30]. The RBCs were resuspended in RPMI containing 75 µg of pARL-2-5750-GFP and the final volume was up to 400 µl and transferred to 0.2 cm cuvette (Bio-Rad, USA). The cells were electroporated with 0.31 kV, 960 µFD and the time constant was in the range of 10–14 ms. The cells were taken out of the cuvette and resuspended in complete RPMI and centrifuged. In the meantime, parasites selected for low rosetting (FCR3S1.2-low or R29-low) were diluted 1:10 and DNA-loaded erythrocytes were added to the culture and incubated at 37 °C. The drug pyrimethamine was added to the culture after 48 h and fresh medium was subsequently added every 2 d until parasites appeared.

Enzyme treatment of RBCs and rosette re-formation assay. 100 µl of RBCs were washed three times with incomplete RPMI and incubated for 1 h with 67 mU/ml of neuraminidase, 100 µg/ml of trypsin or 100 µg/ml of chymotrypsin. The RBCs were subsequently washed three times with incomplete RPMI and resuspended at a 4% hematocrit in complete RPMI.

The trophozoite-stage parasites were MACS purified (~95–99% purity) and incubated with normal or enzyme-treated RBCs for 1.5 h at 37 °C for rosettes to re-form. The rosettes formed were counted on a Nikon microscope (Diaphot 300, Nikon, Japan) after acridine orange staining of the parasites.

For rosette reformation with En(a–), S–s–U–, Ge:–2,3 or Ge:–2,–3 RBCs the RBC variants were washed three times with incomplete RPMI and resuspended in complete RPMI at 4% hematocrit. Similarly purified trophozoites (~95–99% purity) were incubated with equal numbers of RBC variants for 1.5 h at 37 °C. Rosettes were counted in the Nikon microscope after rosette re-formation and acridine orange staining.

Animals. 8 male Sprague-Dawley rats (B&K, Sweden) of 3–6 months of age were kept either in the of the Fagraeus animal facility or in the animal facility of the Microbiology and Tumor Biology Centre at Karolinska Institutet. All animal experiments were performed in compliance with ethical regulations (Swedish Board of Agriculture; http://jordbruksverket.se/) and with the permission of Northern Stockholm (permission no. N159/14) and Centuri ET no. 39862. Goats and rabbits were maintained by the company Agrisera AB (http:// www.agrisera.se), following the same ethical regulations as laid out by the Swedish Board of Agriculture.

^{99m}Technetium labeling and *in vivo* sequestration assay. Uninfected or MACS-purified iRBCs were labeled with ^{99m}Tc according to Petterson *et al*[37]. Briefly, purified iRBC or uninfected RBCs were labeled with 1000 MBq^{99m}Tc /ml for 20 min at 37 °C. After washing three times with RPMI, the iRBCs and RBCs were resuspended in RPMI, the level of ^{99m}Tc labeling was measured, and the labeled cells were injected into the rats. The sample size was based on results of previous sets of experiment[37].

Rats were chosen for each sample in a random manner and were sedated by a subcutaneous injection of midazolam (Dormicum, Roche) and placed on a heat pad located in a double-headed gamma camera. ^{99m}Tc-labeled iRBCs or RBCs (0.3–0.5ml, 2×10^7 to 5×10^7 cells) were injected into the tail vein, and dynamic, whole-body images were acquired for 30 min at a rate of one frame per second. The rats were subsequently killed via injection of pentobarbital sodium (60 mg/ml) and the lungs were removed and fixed in a 0.2% paraformaldehyde solution. The counts of the dissected lungs were similarly measured in a double-headed gamma camera. Acquired images were analyzed by merging the frames and calculating regions of interest (ROIs) in images in whole body as well as ROIs in dissected lungs. The percentage of sequestered parasites in the lungs was determined by calculating counts retained in the lungs over total counts injected in the respective rats[37].

Statistical analysis. Each experiment was performed three to five times and the data are plotted as mean values ± standard error of means (sem). All statistical analysis was performed using GraphPad Prism software 3.0 and included two-tailed Student's *t*-test or one-way ANOVA for comparing the means of two or multiple groups. $P < 0.05$ was considered statistically significant. No data were excluded in any of the experiments. For performing *in vivo* experiments, rats were assigned into different groups without any bias and each group consisted of three rats. The experiment in which sequestration of parasites was scored in the lungs of rats was done by an independent researcher (L.I) who was blinded to the treatment conditions.

21. Claros, M.G. & von Heijne, G. *Comput. Appl. Biosci.* **10**, 685–686 (1994).
22. Tusnády, G.E. & Simon, I. *Bioinformatics* **17**, 849–850 (2001).
23. Krogh, A., Larsson, B., von Heijne, G. & Sonnhammer, E.L.J. *Mol. Biol.* **305**, 567–580 (2001).
24. Käll, L. & Sonnhammer, E.L. *FEBS Lett.* **532**, 415–418 (2002).
25. Rost, B., Fariselli, P. & Casadio, R. *Protein Sci.* **5**, 1704–1718 (1996).
26. Bernsel, A., Viklund, H., Hennerdal, A. & Elofsson, A. *Nucleic Acids Res.* **37**, W465–W468 (2009).

27. Arai, M. *et al. Nucleic Acids Res.* **32**, W390–W393 (2004).
28. Bendtsen, J.D., Nielsen, H., von Heijne, G. & Brunak, S. *J. Mol. Biol.* **340**, 783–795 (2004).
29. Mok, B.W. *et al. Mol. Biochem. Parasitol.* **151**, 184–192 (2007).
30. Moll, K., Kaneko, A., Scherf, A. & Wahlgren, M. *Methods in Malaria Research*. 6th edn. (EviMalaR, Glasgow, UK & MR4/ATCC, Manassas, VA, USA, 2013).
31. Trager, W. & Jensen, J.B. *Science* **193**, 673–675 (1976).
32. Angeletti, D. *et al. PLoS ONE* **7**, e50758 (2012).
33. Kozak, M. *Cell* **44**, 283–292 (1986).
34. Johansson, H.E., Sproat, B.S. & Melefors, Ö. *Nucleic Acids Res.* **21**, 2275–2276 (1993).
35. Lundin, C. *et al. FEBS Lett.* **580**, 2281–2284 (2006).
36. Angeletti, D., Albrecht, L., Wahlgren, M. & Moll, K. *Malar. J.* **12**, 32 (2013).
37. Pettersson, F. *et al. Infect. Immun.* **73**, 7736–7746 (2005).

Carl_G_190x270_mm_blokki_FINAL.indd 176 06-Aug-23 1:53:40 PM

THE JOURNAL OF BIOLOGICAL CHEMISTRY
Vol. 261, No. 20, Issue of July 15, pp. 9546–9551, 1986
Printed in U.S.A.
© 1986 by The American Society of Biological Chemists, Inc.

In Vitro Attachment of Mono- and Oligosaccharides to Surface Glycoconjugates of Intact Cells*

(Received for publication, December 11, 1985)

Martti Tolvanen and Carl G. Gahmberg

From the Department of Biochemistry, University of Helsinki, Helsinki, Finland

We have synthesized glycosylhydrazines of various mono- and oligosaccharides and coupled these to periodate- or galactose oxidase-treated human red cells and K562 erythroleukemia cells. The optimal conditions for this carbohydrate modification of cells have been established. This method makes it possible to specifically elongate oligosaccharide chains of cell surface glycoconjugates with desired carbohydrates. In this way, new antigenic and receptor properties can be conferred to cells, and the functional roles of carbohydrates in cell surface glycoconjugates can be studied. The method has been used to make red cells of blood group O reactive with anti-A and anti-B sera, and in rendering K562 cells or red cells of blood group O agglutinable with the α-*N*-acetylgalactosamine-specific *Helix pomatia* lectin.

Cell surface carbohydrates are known to act as receptors for microbes and various ligands (1, 2), to constitute blood group antigens (3), and to be involved in intercellular adhesion (4), but, in general, their functions have remained poorly understood. The molecular diversity of these structures indicates, however, that they could be responsible for several specific functions.

In principle, it should be possible to gain insight into the functions of cell surface carbohydrates by inhibiting their synthesis, by modifying their structures, or by introducing new attachment sites on polypeptide backbones. Modifications can be achieved either by interfering with cellular biosynthetic routes or by attaching new carbohydrates to the cell surface glycoconjugates.

The biosynthesis of *N*-glycosidic oligosaccharides can be inhibited by tunicamycin, 2-deoxyglucose, glucosamine, and other agents (5). Such experiments have shown that the inhibition of the synthesis of *N*-glycosidic carbohydrate prevents the intracellular migration of some proteins (6) and, in certain instances, renders the proteins more susceptible to proteolytic enzymes (7). By site-directed mutagenesis, it has been shown that elimination of the site of oligosaccharide attachment on a polypeptide chain may affect profoundly its intracellular migration and that the exact location of the attachment site is not crucial (8). When inhibitors of the "trimming" reactions that are involved in the biosynthesis of *N*-glycosidic oligosaccharides are used, carbohydrate structures corresponding to intermediate stages of biosynthesis accumulate (9). In this way, it has been shown, for example, that altered cell surface carbohydrates are important for recognition in the mixed lymphocyte reaction (10).

Another approach is to study mutant cells which lack specific glycosyltransferases. This has made it possible to draw important conclusions about the biosynthesis and functions of cellular glycoconjugates (11, 12).

Most of the modification systems have in common the fact that they result in diminution of the normally occurring oligosaccharides; the possibilities to add structural elements are limited. Furthermore, the modified structures are not exclusively on the cell surface, but are also present intracellularly, which may cause different effects. One solution is to use glycosyltransferases and nucleotide sugars to add terminal monosaccharides externally, but, due to strict substrate specificities, more extensive modifications have not been possible.

Because of these limitations, we have begun to explore other possibilities to externally introduce "new" carbohydrate structures specifically into cell surface glycoproteins and glycolipids. Hydrazine derivatives are strongly reactive with aldehyde groups, and glycosylhydrazines of reducing mono- and oligosaccharides are easily synthesized. Using galactose oxidase or periodate treatments, aldehyde groups can specifically be generated in cell surface galactose/*N*-acetylgalactosamine (13, 14) and sialic acid residues (15), and here we have investigated the conditions for introducing glycosylhydrazines into oxidized cell surface glycoconjugates. The results show that different mono- and oligosaccharides can specifically be covalently attached to cell surface glycoproteins and glycolipids. This method thus enables the modification of cell surface glycoconjugates in principle by any available carbohydrate which contains a reducing group.

EXPERIMENTAL PROCEDURES AND RESULTS[1]

DISCUSSION

In several systems, glycoconjugate changes have been observed associated with cellular differentiation and malignant transformation (30–33). The galactose oxidase/NaB^3H_4 (13) and periodate/NaB^3H_4 (15) labeling methods, specific for cell surface galactose/*N*-acetylgalactosamine- and sialic acid-containing glycoconjugates, respectively, have proven extremely useful for studying such changes. The direct role, if any, of

* This work was supported by the Academy of Finland, the Sigrid Juselius Foundation, the Finska Läkaresällskapet, and National Cancer Institute Grant 5 R01-CA 26294-05. The costs of publication of this article were defrayed in part by the payment of page charges. This article must therefore be hereby marked "*advertisement*" in accordance with 18 U.S.C. Section 1734 solely to indicate this fact.

[1] Portions of this paper (including "Experimental Procedures," "Results," Figs. 1–10, and Table I) are presented in miniprint at the end of this paper. The abbreviations used are: $NaCl/PO_4$, 0.135 M NaCl, 0.01 M sodium phosphate buffer; Fuc, L-fucose; Gal, D-galactose; GalNAc, *N*-acetyl-D-galactosamine; Glc, D-glucose; GlcNAc, *N*-acetyl-D-glucosamine; Cer, ceramide. Miniprint is easily read with the aid of a standard magnifying glass. Full size photocopies are available from the Journal of Biological Chemistry, 9650 Rockville Pike, Bethesda, MD 20814. Request Document No. 85M-4028, cite the authors, and include a check or money order for $6.40 per set of photocopies. Full size photocopies are also included in the microfilm edition of the Journal that is available from Waverly Press.

This is an Open Access article under the CC BY license.

Carl_G_190x270_mm_blokki_FINAL.indd 177 06-Aug-23 1:53:40 PM

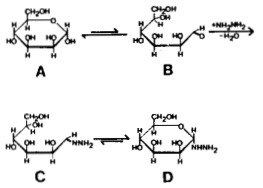

FIG. 11. **Formation of mannosylhydrazine from mannose and hydrazine.** *A*, α-D-mannopyranose; *B*, D-mannose; *C*, hydrazone of D-mannose; *D*, D-mannosylhydrazine.

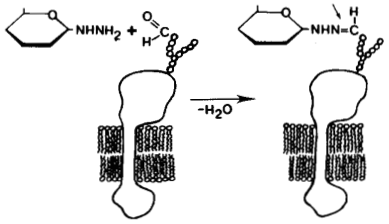

FIG. 12. **A schematic drawing of the reaction of glycosylhydrazine with an oxidized cell surface oligosaccharide.** *Arrow* points to the reducible hydrazone linkage.

cell surface oligosaccharides in these events has, however, remained unclear. To tackle this problem more directly, we have developed a method for attaching mono- and oligosaccharides specifically to cell surface oligosaccharides. Sugars which contain reducing groups can be changed into their hydrazine derivatives (Fig. 11). The glycosylhydrazine and hydrazone forms are at equilibrium with each other (Fig. 11, *C* and *D*), the glycosylhydrazine being predominant in aqueous solutions (34). Therefore, the term "glycosylhydrazine" has been used when referring to these reagent preparations in this work. The glycosylhydrazines can subsequently be attached to aldehyde-containing cell surface oligosaccharides as outlined schematically in Fig. 12.

In the present work, we have studied the optimal conditions for glycosylhydrazine modification of cell surface glycoconjugates using the well characterized human red cell membrane as a model system. As expected, both glycoproteins and glycolipids reacted with glycosylhydrazines, and the reaction was absolutely dependent on previous membrane oxidation. In addition to [^{3}H]mannosylhydrazine and glycosylhydrazines of transferrin ^{3}H-oligosaccharides, we have used glycosylhydrazines of [^{14}C]galactose, [^{3}H]sialyllactose (periodate/NaB^{3}H$_4$-labeled), and ^{3}H-oligosaccharides prepared from α_1-acid glycoprotein and fetuin. The results are similar to those described for the model compounds.

It was important to find reaction conditions gentle enough to keep the cells viable and thus useful for subsequent studies. Modification of surface oxidized cells with glycosylhydrazines at pH 7.0 and 37 °C for 1 h under isotonic conditions was a compromise between the effects of pH, temperature, and time of incubation. The method is gentle for biologically active oligosaccharides, as the blood group A- and B-active oligosaccharides were shown to retain their receptor activities for lectins and blood group antibodies when attached to the cell surface.

We have previously used methionyl sulfone hydrazide to label oxidized cell surface glycoproteins (35). The labeling was enhanced by Mn^{2+}, but, with carbohydrate hydrazines, no enhancement of labeling was observed (results not shown). Other hydrazine derivatives have previously been used to introduce functional groups in oxidized cell surface glycoconjugates including biotin hydrazide (36), ferritin hydrazide (37), various fluorescent hydrazides (38), and acylhydrazides (39). Also mannosyl-*S*-$(CH_2)_5$-$CONHNH_2$ has been coupled to red cells resulting in increased reactivity with concanavalin A (40). This type of hydrazine derivative of a saccharide is, however, more difficult to synthesize, and the structural change at the cell surface is more extensive due to the long hydrocarbon chain.

Neoglycoconjugates have previously been prepared by several methods by which carbohydrate derivatives have been coupled to amino groups in proteins and lipids (41–44). These have proven extremely useful for a number of purposes. However, they have not been applied to living cells.

The present method should have several useful applications in studies on the function of carbohydrates in glycoconjugates. As shown, altered antigenic properties and changed cellular reactivities with lectins, carbohydrate-binding toxins, or other ligands can be easily achieved. Whether these modifications will result in any physiological responses seems worth examining.

Acknowledgments—We thank Professor P. Sinaÿ for the B-active trisaccharide, A. Lampio for the glycolipid preparations, and L. Peltokorpi for endo-β-*N*-acetylglucosaminidase F.

REFERENCES

1. Sharon, N. (1984) *Trends Biochem. Sci.* **9,** 198–202
2. Morell, A. G., Gregoriadis, G., Scheinberg, I. H., Hickman, J., and Ashwell, G. (1971) *J. Biol. Chem.* **246,** 1461–1467
3. Hakomori, S.-i., and Kobata, A. (1974) in *The Antigens* (Sela, M., ed) Vol. 2, pp. 79–140, Academic Press, New York
4. Rutishauser, U., Watanabe, M., Silver, J., Troy, F. A., and Vimr, E. R. (1984) *J. Cell Biol.* **101,** 1842–1849
5. Schwarz, R. T., and Datema, R. (1980) *Trends Biochem. Sci.* **5,** 65–67
6. Hickman, S., Kulczycki, A., Jr., Lynch, R. G., and Kornfeld, S. (1977) *J. Biol. Chem.* **252,** 4402–4408
7. Schwarz, R. T., and Datema, R. (1982) *Adv. Carbohydr. Chem. Biochem.* **40,** 287–379
8. Guan, J.-L., Machamer, C. E., and Rose, J. K. (1985) *Cell* **42,** 489–496
9. Fuhrmann, U., Bause, E., and Ploegh, H. (1985) *Biochim. Biophys. Acta* **825,** 95–110
10. Powell, L. D., Bause, E., Legler, G., Molyneux, R. J., and Hart, G. W. (1985) *J. Immunol.* **135,** 714–724
11. Stanley, P. (1984) *Annu. Rev. Genet.* **18,** 525–552
12. Rothman, J. E., Urbani, L. J., and Brands, R. (1984) *J. Cell Biol.* **99,** 248–259
13. Gahmberg, C. G., and Hakomori, S. (1973) *J. Biol. Chem.* **248,** 4311–4317
14. Steck, T. L., and Dawson, G. (1974) *J. Biol. Chem.* **249,** 2135–2142
15. Gahmberg, C. G., and Andersson, L. C. (1977) *J. Biol. Chem.* **252,** 5888–5894
16. Elder, H. E., and Alexander, S. (1982) *Proc. Natl. Acad. Sci. U. S. A.* **79,** 4540–4544
17. Hammarström, S. (1972) *Methods Enzymol.* **28,** 368–383
18. Gahmberg, C. G., and Andersson, L. C. (1978) *J. Exp. Med.* **148,** 507–521
19. van Lenten, L., and Ashwell, G. (1972) *Methods Enzymol.* **28,** 209–211
20. Takasaki, S., Mizuochi, T., and Kobata, A. (1982) *Methods Enzymol.* **83,** 263–268
21. Reading, C. L., Penhoet, E. E., and Ballou, C. E. (1978) *J. Biol. Chem.* **253,** 5600–5612
22. Carlson, D. M. (1966) *J. Biol. Chem.* **241,** 2984–2986
23. Andersson, L. C., Nilsson, K., and Gahmberg, C. G. (1979) *Int. J. Cancer* **23,** 143–147
24. Lowry, O. H., Rosebrough, N. J., Farr, A. L., and Randall, R. J. (1951) *J. Biol. Chem.* **193,** 265–275
25. Laemmli, U. K. (1970) *Nature* **227,** 680–685

Carl_G_190x270_mm_blokki_FINAL.indd 178 06-Aug-23 1:53:40 PM

26. Bonner, W. M., and Laskey, R. A. (1974) *Eur. J. Biochem.* **46,** 83–88
27. Hakomori, S.-i., Siddiqui, B., Li, Y.-T., Li, S.-C., and Hellerqvist, C. G. (1971) *J. Biol. Chem.* **246,** 2271–2277
28. Siddiqui, B., and Hakomori, S. (1971) *J. Biol. Chem.* **246,** 5766–5769
29. Hudson, L., and Hay, F. C. (1980) *Practical Immunology*, pp. 11–12, 2nd Ed, Blackwell Scientific Publications, Oxford
30. Feizi, T., and Childs, R. A. (1985) *Trends Biochem. Sci.* **10,** 24–29
31. Gahmberg, C. G., and Andersson, L. C. (1982) *Biochim. Biophys. Acta* **651,** 65–83
32. Hakomori, S. (1981) *Annu. Rev. Biochem.* **50,** 733–764
33. Gahmberg, C. G., Ekblom, M., and Andersson, L. C. (1984) *Proc. Natl. Acad. Sci. U. S. A.* **81,** 6752–6756
34. Saeed, M. S., and Williams, J. M. (1980) *Carbohydr. Res.* **84,** 83–94
35. Itaya, K., Gahmberg, C. G., and Hakomori, S. (1975) *Biochem. Biophys. Res. Commun.* **64,** 1028–1035
36. Heitzmann, H., and Richards, F. M. (1974) *Proc. Natl. Acad. Sci. U. S. A.* **71,** 3537–3541
37. Roffman, E., Spiegel, Y., and Wilchek, M. (1980) *Biochem. Biophys. Res. Commun.* **97,** 1192–1198
38. Lee, J. A., and Fortes, P. A. G. (1985) *Biochemistry* **24,** 322–330
39. Rando, R. R., and Bangerter, F. W. (1979) *Biochim. Biophys. Acta* **557,** 354–362
40. Orr, G. A., and Rando, R. R. (1978) *Nature* **272,** 722–725
41. Lee, Y. C., Stovell, C. P., and Krantz, M. J. (1976) *Biochemistry* **15,** 3956–3963
42. McBroom, C. R., Samanen, C. H., and Goldstein, I. J. (1972) *Methods Enzymol.* **28,** 212–219
43. Ashwell, G. (1972) *Methods Enzymol.* **28,** 219–222
44. Tang, P. W., Gooi, H. C., Hardy, M., Lee, Y. C., and Feizi, T. (1985) *Biochem. Biophys. Res. Commun.* **132,** 474–480

SUPPLEMENTARY MATERIAL

In Vitro Attachment of Mono- and Oligosaccharides To Surface Glycoconjugates of Intact Cells

Martti Tolvanen and Carl G. Gahmberg

EXPERIMENTAL PROCEDURES

Isotopes

NaB^3H_4 (22.3 Ci/mmol), [2-^{3}H]mannose (13.4 Ci/mmol), [1-^{14}C]-D-galactose (60 mCi/mmol), [1-^{14}C]-D-galactosamine-HCl (48 mCi/mmol), [D-glucose-1-^{14}C]lactose (57.6 mCi/mmol) and [1-^{14}C]acetic anhydride (20 mCi/mmol) were obtained from The Radiochemical Centre, Amersham, U. K.

Enzymes

Galactose oxidase from Dactylium dendroides was purchased from Kabi Ltd., Stockholm, Sweden, and neuraminidase from Vibrio cholerae from Koch-Light Ltd., Haverhill, U. K. Endo-β-N-acetylglucosaminidase F was purified from the culture medium of Flavobacterium meningosepticum, a strain obtained from The American Type Culture Collection (16).

Other reagents

Anti-A and anti-B blood group antisera were obtained from the Finnish Red Cross Blood Service. Helix pomatia lectin, purified as described (17), was donated by S. Hammarström, University of Stockholm, Sweden. The blood group A active heptasaccharide GalNAcα1-3(Fucα1-2)Galβ1-3(Fucα1-4)GlcNAcβ1-3Galβ1-4Glc was obtained from BioCarb Chemicals, Lund, Sweden. The blood group B active synthetic trisaccharide Galβ1-3(Fucα1-2)Gal was a generous gift from Professor P. Sinaÿ, University of Orleans, France. α_1-Acid glycoprotein was purified from human urine (18). Human transferrin, bovine serum albumin, fluorescein isothiocyanate and sialyl lactose were purchased from Sigma, St. Louis, MO., USA, Blue Dextran 2000 from Pharmacia Fine Chemicals, Uppsala, Sweden, and sodium metaperiodate and sodium borohydride from E. Merck AG, Darmstadt, FRG. Anhydrous hydrazine (Sigma) was kept desiccated under nitrogen at 4 °C. Once opened, the same hydrazine bottle was not used for longer than three months.

Preparation of labeled oligosaccharides from human transferrin

Human transferrin was labeled at the sialic acid residues by the periodate/NaB^3H_4 method (19). After the oxidation and reduction steps, the protein was separated from the remaining reagents by gel filtration on Sephadex G-25 (Pharmacia) equilibrated in water. The sugar chains were liberated with endo-β-N-acetylglucosaminidase F (16) or by hydrazinolysis at 105 °C for 16 h (20). Oligosaccharides from unlabeled transferrin (10 mg) were obtained by hydrazinolysis at 105 °C, which results in de-N-acetylation (20). The oligosaccharides were isolated by gel filtration on the 1 x 95 cm column of Bio-Gel P-10 (Bio-Rad Laboratories, Richmond, CA., USA) equilibrated in 0.1 M pyridine-acetate buffer pH 5.0 containing 0.02 % NaN_3. The peak fractions of the ^{3}H-labeled samples were identified by liquid scintillation counting of aliquots using a Triton-X-114 based scintillation fluid and an LKB 1210 Ultrobeta liquid scintillation counter. The corresponding fractions were pooled from the sample of non-radioactive oligosaccharides. The unlabeled deacetylated oligosaccharides were re-N-acetylated (21) using 50 μCi of [1-^{14}C]acetic anhydride and the reaction was completed with non-radioactive acetic anhydride. The ^{14}C-labeled oligosaccharides were purified by gel filtration as above. After lyophilization the oligosaccharides were further purified by gel filtration on a Bio-Gel P-2 column equilibrated in water.

Alkaline borohydride treatment

For liberating O-linked oligosaccharides, isolated membranes were incubated in 0.05 M NaOH - 1 M $NaBH_4$ at 45 °C for 16 h (22).

Synthesis of glycosylhydrazines

The appropriate monosaccharides or oligosaccharides (up to 100 μg) were incubated with 0.1 ml of anhydrous NH_2NH_2 at room temperature for 16 h. After incubation the hydrazine was evaporated at reduced pressure. Some toluene was added and evaporated under nitrogen flow.

Oxidation of red blood cells

Red cells were isolated from fresh heparinized human blood by centrifugation and washed twice with 0.01 M sodium phosphate- 0.15 M NaCl buffer ($NaCl/PO_4$), pH 7.4. The periodate oxidation was performed as described (15) using a final concentration of 2 mM $NaIO_4$. Treatments with galactose oxidase or galactose oxidase plus neuraminidase were performed as described previously (13). After oxidation the cells were washed three times with $NaCl/PO_4$, pH 7.4.

Coupling of glycosylhydrazines to erythrocytes and K562 cells

Oxidized red cells (10^9) were suspended in 0.5 ml of $NaCl/PO_4$ and the labeled glycosylhydrazine, dissolved in 5–30 μl of $NaCl/PO_4$, was added. The reaction mixtures were normally incubated at 37 °C for 60 min with gentle shaking. After incubation the cells were washed three times with ice-cold $NaCl/PO_4$, pH 7.4, and lysed by adding ice-cold 5 mM Tris-HCl buffer, pH 8.0. The cell membranes were isolated by centrifugation at 20,000 x g for 20 min. and washed twice with the Tris buffer. The incorporation of the labeled mono/oligosaccharides was assayed by liquid scintillation counting of an aliquot or the whole membrane sample in a Triton-X-114-based scintillation fluid. All experiments were carried out with duplicate cell samples and the results are mean values.

Glycosylhydrazines of the blood group A active heptasaccharide and the blood group B active trisaccharide (about 100 μg) were coupled to periodate-oxidized red cells of blood group O using 2 x 10^8 cells per sample in 100 μl of $NaCl/PO_4$, pH 7.0. The reaction mixtures were incubated at 37 °C for 1 h and the cells were washed three times before agglutination tests.

K562 cells (23) were grown in RPMI 1640 medium (Flow Laboratories, Irvine, U. K.) supplemented with 10 % fetal calf serum (Flow Laboratories). Washed cells were treated with 2 mM periodate at 0 °C. Glycosylhydrazine of the blood group A active heptasaccharide was allowed to react with 8 x 10^6 cells as described above but using incubation at 25 °C.

Stability of glycosylhydrazine on cell surface

Periodate/[^{3}H]mannosylhydrazine and neuraminidase plus galactose oxidase/[^{3}H]-mannosylhydrazine treated red blood cells were prepared. A part of both samples was reduced with $NaBH_4$ (2 mg/ml) for 30 min. at 25 °C. The resulting four samples were washed three times with $NaCl/PO_4$, pH 7.4, and suspended in the same buffer at a concentration of 5 x 10^9 cells/ml. The suspensions were incubated at 37 °C, and duplicate samples of 200 μl were taken at indicated times. The membranes were isolated for protein (24) and radioactivity determinations.

Cell surface labeling by periodate/NaB^3H_4 and galactose oxidase/NaB^3H_4

Red cells were labeled by the periodate/NaB^3H_4, galactose oxidase/NaB^3H_4 and neuraminidase plus galactose oxidase/NaB^3H_4 methods as described in detail previously (13, 15).

Polyacrylamide slab gel electrophoresis

The membrane glycoproteins were separated on polyacrylamide slab gels in the presence of sodium dodecyl sulfate and 2-mercaptoethanol using 8 % acrylamide gels (25). After electrophoresis the gels were fixed in 5 % sulfosalicylic acid and treated for fluorography (26). ^{14}C-Labeled standard proteins (Amersham) were used as molecular weight markers.

Analysis of labeled glycolipids

After treating one ml of packed red blood cells sequentially with galactose oxidase and [^{3}H]mannosylhydrazine, the membranes were isolated and the lipids extracted with chloroform-methanol (2:1). The lower phase was washed three times with the theoretical upper phase and evaporated under nitrogen. The residue was applied to a thin-layer plate (20 x 20 cm DC-Fertigplatten, Kieselgel 60, Merck) and chromatographed using chloroform-methanol-water (60:30:5). Purified globoside, GalNAcβ1-3Galα1-4-Galβ1-4Glc 1-1Cer, (27) and Forssman antigen, GalNAcα1-3-GalNAcβ1-3Galα1-4-Galβ1-4Glc 1-1Cer, (28), and galactose oxidase/[^{3}H]mannosylhydrazine treated purified globoside were run on separate lanes. The distribution of radioactivity on the plate was determined by scraping 0.5 cm bands of the silica gel into scintillation fluid. The non-radioactive standards were detected by staining with iodine vapour.

Agglutination tests

Blood group properties were tested by a slide test using a drop of red cell suspension (2 % cells in $NaCl/PO_4$, pH 7.4) and a drop of standard anti-A or anti-B serum mixed together. Helix pomatia lectin reactivities were assayed on a microtiter plate with 50 μl of a 2 % red cell suspension and 50 μl of lectin dilution (1:2 serial dilution starting with a concentration of 0.1 mg lectin/ml).

Fluorescence microscopy

Helix pomatia lectin reactivity was verified using fluorescence microscopy. Fluorescein isothiocyanate was conjugated with the lectin as described (29). Cells were incubated with the fluorescent lectin in $NaCl/PO_4$, pH 7.4, containing 0.5 % bovine serum albumin for 30 min. at 0 °C in dark, washed twice and suspended in $NaCl/PO_4$, pH 7.4, containing 3 % paraformaldehyde. The fluorescence micrographs were taken of suspended cells using a Leitz Orthoplan microscope equipped with 200W/4 Ultrahigh Pressure Mercury Lamp; a filter system consisting of an exciter filter BP 450-490 nm, reflection short pass filter RKP 510 nm and barrier filter LP 515 nm; an attached Leitz camera with Kodak TX 5063 film; and an exposure control unit Wild MPS 45. The ordinary light micrographs were taken on Agfapan 25 film.

RESULTS

A number of variables were studied to establish the most favorable conditions for attaching carbohydrate hydrazines to cell surface glycoproteins and glycolipids.

Carl_G_190x270_mm_blokki_FINAL.indd 179 06-Aug-23 1:53:40 PM

Effect of pH on incorporation of glycosylhydrazines

Glycosylhydrazines were most efficiently incorporated in red cell membranes at pH 6.0 (Fig. 1). No lysis of cells occurred. The incorporation rate at pH 6.0 was approximately twice that observed at pH 7.0. In most cases pH 7.0 was used to approach physiological conditions.

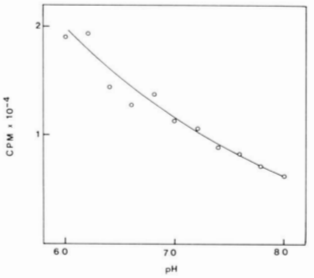

Fig. 1

The effect of pH on the coupling of [^{3}H]mannosylhydrazine to periodate-oxidized red cells. Samples of 10^7 cells in 0.5 ml of NaCl/PO_4 of indicated pH values were incubated for 5 min. at 37 °C. After incubation the cells were washed, the membranes isolated, and the membrane-bound radioactivities determined.

Effect of temperature on incorporation

The temperature-dependence of the reaction of carbohydrate hydrazines with surface oxidized cells is shown in Table I. 37 °C was adopted in routine use because of the considerably higher incorporation rate.

Table I

Effect of temperature on the incorporation of [^{3}H]mannosylhydrazine in red cell membranes.
10^8 cells in 0.5 ml of NaCl/PO_4, pH 7.0, were incubated at 37 °C for 1 h with [^{3}H]mannosylhydrazine.

T (°C)	Membrane-bound radioactivity (cpm)
0	1700
23	4300
37	6000

Time course of incorporation

Red cells oxidized by treatments with periodate, neuraminidase plus galactose oxidase or galactose oxidase only were incubated at 37 °C for various times with [^{3}H]mannosylhydrazine in NaCl/PO_4, pH 7.0. After incubation, the membranes were isolated and the radioactivities determined.

The incorporation of label in oxidized membranes was essentially complete after 60 min. (Fig. 2). The maximal incorporation in this experiment was 3.2 % of added radioactivity, corresponding to 420 molecules per cell. Without prior oxidation the membrane-associated label was less than 1/500 of that of periodate-treated cells.

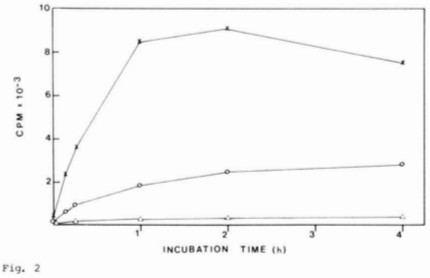

Fig. 2

Time course of incorporation of [^{3}H]mannosylhydrazine into oxidized red cells. The cells were incubated for indicated times at 37 °C, pH 7.0. After incubation the membranes were isolated and the radioactivities determined. x - x = periodate-oxidized cells; o - o = neuraminidase plus galactose oxidase-treated cells; △-△ = galactose oxidase-treated cells.

Stability of incorporated [^{3}H]mannosylhydrazine

The specific radioactivity of membranes was determined during a 20 h incubation in NaCl/PO_4, pH 7.4, at 37 °C. Fig. 3 shows that the radioactivity slowly declined in membranes of both periodate/[^{3}H]mannosylhydrazine and neuraminidase plus galactose oxidase/[^{3}H]mannosylhydrazine labeled cells. Treatment with $NaBH_4$ in order to reduce the Schiff's base formed between the glycosylhydrazine and the cellular carbohydrate (Fig. 12) did not improve the stability of the linkage (data not shown). Furthermore, the reduction resulted in increased hemolysis.

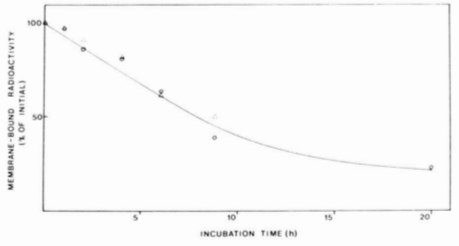

Fig. 3

Stability of [^{3}H]mannosylhydrazine in periodate-oxidized and neuraminidase plus galactose oxidase-treated red cells during incubation at 37 °C in NaCl/PO_4, pH 7.4. Samples were taken at indicated times, the membranes were isolated and the specific radioactivities (per mg of protein in membranes) were determined. o - o = periodate and △-△ = neuraminidase plus galactose oxidase treatment. The values are given in per cent of the initial specific radioactivities.

The effect of pH was studied using 4 h incubations at 37 °C. At pH 6.4, 7.0 and 8.0 the radioactivities remaining in the membranes, compared to that of the cells incubated at pH 7.4, were 74 %, 94 % and 105 %, respectively.

Lowering the temperature resulted in considerably slower release of radioactivity from the cells. After a 48 h incubation at 0 °C the specific radioactivity of the membranes was still 66 % of the initial value.

Polyacrylamide slab gel electrophoresis of [^{3}H]mannosylhydrazine-labeled red cell membranes

Fig. 4 shows a polyacrylamide slab gel of ^{3}H-labeled red cell membranes. Fig. 4 B shows the pattern of periodate/NaB^3H_4 labeled membranes and Fig. 4 C the pattern of neuraminidase plus galactose oxidase/NaB^3H_4 labeled membranes. In Fig. 4 D it can be seen that [^{3}H]mannosylhydrazine primarily labeled the glycophorin A dimers and monomers in periodate-oxidized cells. A similar pattern was obtained after neuraminidase-galactose oxidase treatment (Fig. 4 E). As expected, relatively little label was incorporated in proteins of galactose oxidase-treated membranes (Fig. 4 F). Prolonged exposure showed labeling in the position of Band 3. No labeled band was obtained from unoxidized membranes (Fig. 4 G).

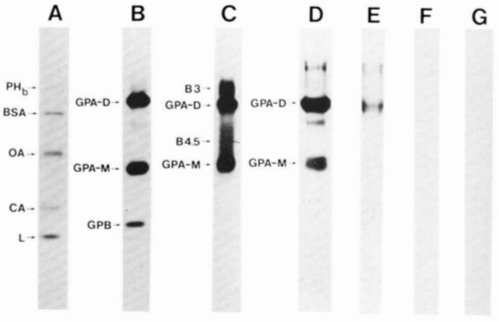

Fig. 4

Fluorogram of a polyacrylamide slab gel of labeled red cell membranes. A, standard ^{14}C-methylated protein mixture: PH_b = phosphorylase b, BSA = bovine serum albumin, OA = ovalbumin, CA = carbonic anhydrase, and L = lysozyme; B, periodate/NaB^3H_4 labeled membranes: GPA-D = glycophorin A dimer, GPA-M = glycophorin A monomer, GPB = glycophorin B; C, neuraminidase-galactose oxidase/NaB^3H_4 labeled membranes; B3 = band 3, B4.5 = band 4.5; D, periodate/[^{3}H]mannosylhydrazine labeled membranes; E, neuraminidase-galactose oxidase/[^{3}H]mannosylhydrazine labeled membranes; F, galactose oxidase/[^{3}H]mannosylhydrazine labeled membranes; G, control, [^{3}H]mannosylhydrazine treatment without prior oxidation.

In this experiment the incorporation of radioactivity was 10 % of the added amount corresponding to 77 000 molecules per cell.

Labeling of red cell glycolipids with [^{3}H]mannosylhydrazine

Red cells were treated with galactose oxidase and [^{3}H]mannosylhydrazine and the membranes extracted with chloroform-methanol. About 13 % of the incorporated radioactivity was recovered in the lipid extract. Thin layer chromatography showed that the major radioactive peak comigrated with galactose oxidase/[^{3}H]-mannosylhydrazine-treated standard globoside (Fig. 5).

Carl_G_190x270_mm_blokki_FINAL.indd 180 06-Aug-23 1:53:40 PM

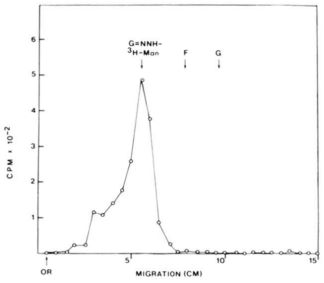

Fig. 5

Thin layer chromatography of membrane lipids from galactose oxidase/[^{3}H]-mannosylhydrazine-treated red cells. OR = sample origin, G = position of standard globoside, F = position of standard Forssman antigen, G=NNH-^{3}H-Man = position of galactose oxidase/[^{3}H]mannosylhydrazine-treated standard globoside.

Attachment of transferrin oligosaccharides to red cell membranes

^{3}H-labeled transferrin complex-type oligosaccharides were prepared by hydrazinolysis or endo-ß-N-acetylglucosaminidase F treatment. After derivatization with hydrazine, the oligosaccharides were attached to periodate-treated red cells. The incorporation of radioactivity in the membranes using the standard conditions of pH 7.0, 37 °C and 1 h of incubation was 1.3 - 3 % of the added label. (In comparison, glycosylhydrazines of monosaccharides were incorporated with yields between 3 % and 15 %.)

The modified membranes were subjected to alkaline borohydride treatment to liberate O-linked oligosaccharides. Analysis by gel filtration showed broadening of the peak towards left relative to the void volume (Fig. 6), which indicates that a major part of the glycosylhydrazines of transferrin oligosaccharides had been incorporated in alkali-labile oligosaccharides, evidently mainly derived from glycophorin A.

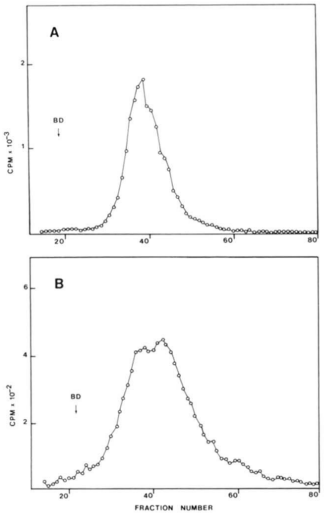

Fig. 6

Bio-Gel P-10 gel filtration patterns (A) of glycosylhydrazines of ^{3}H-labeled transferrin oligosaccharides, and (B) of their derivatives released from red cell membranes by alkaline borohydride treatment (B). BD = elution position of Blue Dextran 2000.

Stability of N-acetyl groups in glycosylhydrazine synthesis

Hydrazinolysis at 105 °C is known to deacetylate N-acetyl hexosamines (20). In contrast, the hydrazine treatment at room temperature, which was used in our synthesis of glycosylhydrazines, did not result in any appreciable deacetylation of ^{14}C-acetylated transferrin oligosaccharides as shown by the gel filtration pattern (Fig. 7 A). On the other hand, treatment at 105 °C resulted in nearly complete liberation of [^{14}C]acetate (Fig. 7 B).

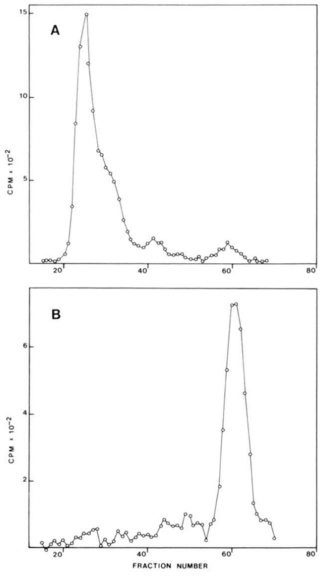

Fig. 7

Bio-Gel P-6 gel filtration patterns of derivatives of ^{14}C-acetylated transferrin oligosaccharides. A, sample incubated in hydrazine for 22 h at 24 °C; B, sample incubated in hydrazine for 22 h at 105 °C. The position of the void volume is at fraction 20.

Transfer of blood group antigen epitopes

When periodate-oxidized red cells of blood group O were modified with glycosylhydrazines of the blood group A or B active oligosaccharides, the cells became reactive with anti-A and anti-B blood group antisera, respectively (Fig. 8). No positive reactions were observed with the original cells, periodate-oxidized cells, or with cells incubated with the A or B active glycosylhydrazines without prior oxidation.

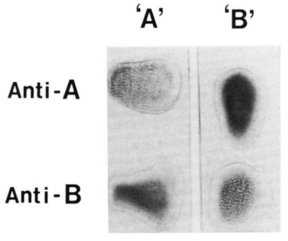

Fig. 8

Reactions of blood group antisera with red cells modified with blood group active saccharides. 'A', periodate-oxidized red cells of blood group O treated with glycosylhydrazine of A active heptasaccharide; 'B', idem, but treated with glycosylhydrazine of B active trisaccharide. Anti-A and Anti-B, the blood group antisera.

Because the blood group A active heptasaccharide contains non-reducing terminal α-N-acetyl galactosamine, which is recognized by the Helix pomatia lectin, the lectin reactivity of cells was tested after modification with this glycosylhydrazine. Red cells of blood group O were rendered even more agglutinable than authentic blood group A cells (Fig. 9). Lectin binding to K562 cells was visualized with fluorescent Helix pomatia lectin (Fig. 10). Bright fluorescence and enhanced aggregation af K562 cells can be seen. All the control samples in the lectin experiments (original cells, periodate-oxidized cells, and unoxidized cells treated with the glycosylhydrazine) were negative.

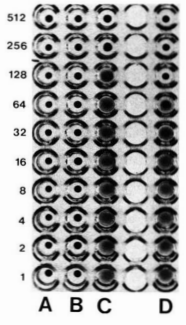

Fig. 9

Agglutination of red cells with Helix pomatia lectin. A, red cells of blood group O; B, periodate-oxidized red cells of blood group O; C, periodate-oxidized red cells of blood group O treated with the glycosylhydrazine of the A-active heptasaccharide; D, red cells of blood group A. The reciprocal dilutions of the lectin are indicated on the left.

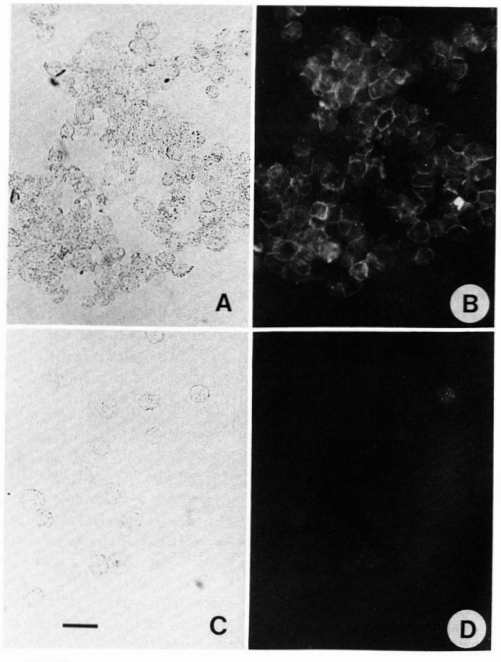

Fig. 10

Micrographs of K562 cells incubated with fluorescent Helix pomatia lectin. A, light micrograph of periodate/A-active glycosylhydrazine-treated cells; B, same cells seen by fluorescence microscopy; C, light micrograph of unoxidized cells treated with the glycosylhydrazine; D, same cells seen by fluorescence microscopy. The micrograph was obtained with the same exposure as in B. Bar in C represents 30 μm.

Carl_G_190x270_mm_blokki_FINAL.indd 182 06-Aug-23 1:53:40 PM

Volume 140, number 1 FEBS LETTERS April 1982

MOLECULAR IDENTIFICATION OF THE HUMAN $Rh_o(D)$ ANTIGEN

Carl G. GAHMBERG

Department of Biochemistry, University of Helsinki, Unioninkatu 35, 00170 Helsinki 17, Finland

Received 21 January 1982

1. Introduction

The molecular nature of the $Rh_o(D)$ antigen of the human erythrocyte blood group has remained most controversial. Although several studies agree that the antigen is an integral membrane protein, M_r estimates vary from 7000–180 000 [1–4]. We have now radioactively surface-labeled $Rh_o(D)$ positive and negative erythrocytes using the ^{125}I/lactoperoxidase method. The labeled membrane proteins were solubilized in Triton X-100-containing buffer and immunoprecipitated with anti-$Rh_o(D)$ antisera. The precipitates were analysed by sodium dodecyl sulfate (SDS)–polyacrylamide slab gel electrophoresis. The results show that only from $Rh_o(D)$ positive membranes a single minor polypeptide with app. M_r 28 000–33 000 could be precipitated specifically. Its behavior during electrophoresis indicated a hydrophobic nature. It may lack carbohydrate because it was not labeled using carbohydrate-specific surface labeling techniques.

2. Materials and methods

Human red cells were $Rh_o(D)$ typed by standard techniques. The red cells and the anti-$Rh_o(D)$ specific antisera were obtained from the Finnish Red Cross Blood Transfusion Centre, Helsinki. The red cells were radioactively labeled by lactoperoxidase-catalyzed iodination in the presence of D-glucose and glucose oxidase [5]. The membranes were isolated [6] and solubilized in 0.15 M NaCl–0.01 M sodium phosphate (pH 7.4)–1% Triton X-100–1% ethanol–2 mM phenylmethylsulfonyl fluoride at 0°C. All subsequent operations until denaturation with SDS were done at 0–4°C. After centrifugation at 5000 rev./min for 10 min, the supernatants were recovered and subjected to immunoprecipitations. These were performed using protein A-containing *Staphylococcus aureus* cells as detailed in [7]. SDS–polyacrylamide slab gel electrophoresis was done as in [8]. After electrophoresis the gels were fixed, treated for fluorography [9] and exposed to Kodak RP X-Omat film. ^{14}C-Labeled standard proteins were obtained from the Radiochemical Centre, Amersham. The app. M_r of the $Rh_o(D)$ antigen was determined as in [10]. Red cells were labeled by the periodate/NaB^3H_4 and neuraminidase–galactose oxidase/NaB^3H_4 methods as in [6,11].

3. Results

Fig.1 shows a polyacrylamide slab gel of erythrocyte surface proteins and immunoprecipitates obtained with anti-$Rh_o(D)$ antiserum. A surface-labeled protein (marked with the heavy arrow) was specifically precipitated from the $Rh_o(D)$ positive membranes (fig.1D,F,H) with antiserum. Non-immune sera did not precipitate the polypeptide (fig.1E,G,I), neither did antiserum from $Rh_o(D)$ negative membranes (fig.1J,L). The app. M_r of the $Rh_o(D)$ antigen on 12% acrylamide gel was 33 000. When immunoprecipitates were analyzed using 8% acrylamide gels, the app. M_r was 28 000 (fig.2D). An identical polypeptide was obtained from En(a–) $Rh_o(D)$ positive membranes (fig.2F), which lack glycophorin A and contain an overglycosylated band 3 [12–14].

The $Rh_o(D)$ antigen is evidently a minor component of the membrane. When ^{125}I-labeled membranes were directly analyzed by polyacrylamide slab-gel electrophoresis followed by fluorography no labeled polypeptide was seen in the position of the $Rh_o(D)$ antigen after a relatively short exposure to X-ray film (fig.3B).

Published by Elsevier Biomedical Press
00145793/82/0000–0000/$02.75 © 1982 Federation of European Biochemical Societies

Carl_G_190x270_mm_blokki_FINAL.indd 183 06-Aug-23 1:53:40 PM

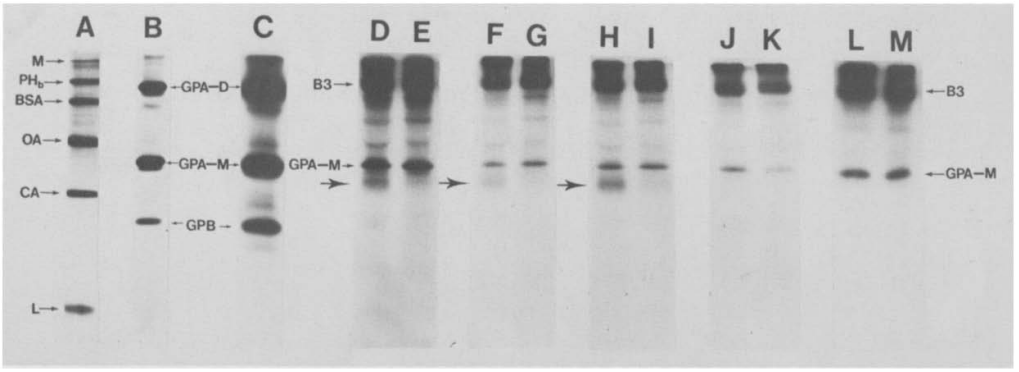

Fig.1. Fluorography pattern of a 12% polyacrylamide slab gel of immunoprecipitated $Rh_o(D)$ antigens from ^{125}I-labeled red cell membranes: (A) ^{14}C-labeled standard proteins [M, myosin; PH_b, phosphorylase *b*; BSA, bovine serum albumin; OA, ovalbumin; CA, carbonic anhydrase; L, lysozyme]; (B) pattern of periodate/NaB^3H_4-labeled red cell membranes [GPA-D, glycophorin A dimer; GPA-M, glycophorin A monomer; GPB, glycophorin B]; (C) pattern of ^{125}I-labeled red cell membranes; (D,F,H) patterns obtained by immunoprecipitation with anti-$Rh_o(D)$ antiserum from $Rh_o(D)$ positive red cell membranes; B3, band 3 (nomenclature from [23]). Heavy arrow points to the position of the $Rh_o(D)$ antigen; (E,G,I) patterns obtained with non-immune sera from identical samples as in (D,F,H); (J,L) patterns obtained with antiserum from $Rh_o(D)$ negative red cell membranes; (K,M) patterns obtained with non-immune serum from identical samples as in (J,L).

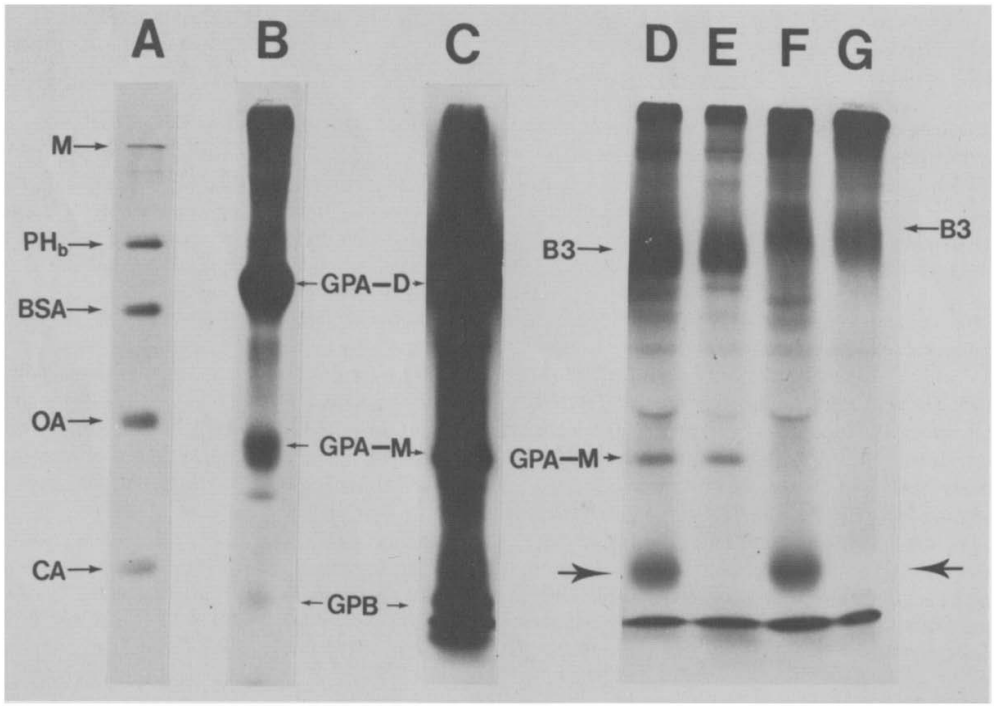

Fig.2.

Carl_G_190x270_mm_blokki_FINAL.indd 184 06-Aug-23 1:53:40 PM

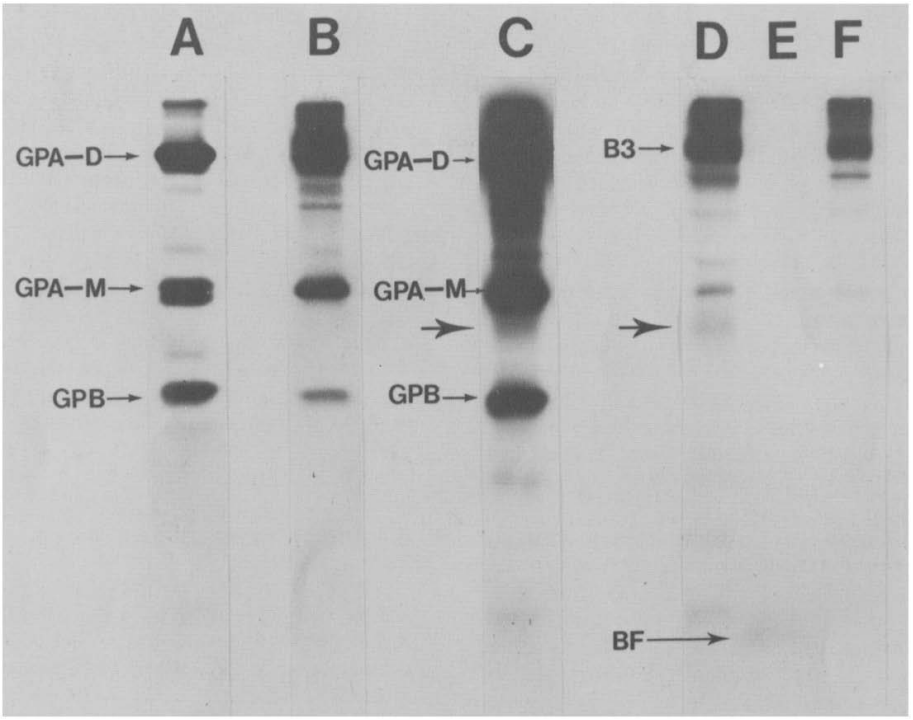

Fig.3. Fluorography pattern of a 12% slab gel of surface-labeled red cells and $Rh_o(D)$ antigen treated with pronase: (A) pattern of periodate/NaB^3H_4-labeled red cell membranes; (B) pattern of ^{125}I-labeled $Rh_o(D)$ positive red cell membranes; (C) as in (B) but exposed to X-ray film for a longer time; (D) patterns obtained with anti-$Rh_o(D)$ antiserum from $Rh_o(D)$ positive ^{125}I-labeled membranes; (E) an identical immunoprecipitate as in (D) which was treated subsequently with 1% pronase in 1% SDS for 1 h at 37°C; (F) pattern obtained with non-immune serum from an identical sample as in (D). Symbols as in legend to fig.1; (➡) $Rh_o(D)$ antigen.

A longer exposure visualized a labeled component in that position (fig.3C, arrow). The protein nature of the antigen was ascertained by protease digestion. Fig.3D shows the immunoprecipitated antigen, and it was completely degraded by pronase (fig.3E). Only some low M_r peptides remained in the region of the buffer front (BF).

4. Discussion

Here I have shown that a surface-exposed polypeptide with an app. M_r 28 000–33 000 was specifically immunoprecipitated from $Rh_o(D)$ positive red cell membranes using anti-$Rh_o(D)$ antiserum. The polypeptide has now been immunoprecipitated from

Fig.2. Fluorography pattern of an 8% polyacrylamide slab gel of $Rh_o(D)$ antigens immunoprecipitated from normal ^{125}I-labeled $Rh_o(D)$ positive red cell membranes and $Rh_o(D)$ positive En(a–) red cell membranes: (A) standard proteins, see legend to fig.1; (B) pattern of periodate/NaB^3H_4-labeled red cell membranes; (C) pattern of ^{125}I-labeled $Rh_o(D)$ positive red cell membranes; (D) pattern obtained with anti-$Rh_o(D)$ antiserum from $Rh_o(D)$ positive red cell membranes; (E) pattern obtained with non-immune serum from an identical sample as in (D); (F) pattern obtained with antiserum from $Rh_o(D)$ positive En(a–) red cell membranes; (G) pattern obtained with non-immune serum from an identical sample as in (F). Symbols as in legend to fig.1. (➡) $Rh_o(D)$ antigen. The weakly labeled band just above GPA-M in D and F is actin, which non-specifically may bind to immunoprecipitates.

Carl_G_190x270_mm_blokki_FINAL.indd 185 06-Aug-23 1:53:41 PM

>20 $Rh_o(D)$ positive cell samples but has never been obtained from $Rh_o(D)$ negative cells. Several polypeptides were non-specifically adsorbed to the Staphylococci, among them glycophorin A and a protein migrating in the band 3 position. These are the most strongly labeled surface polypeptides of red cells and evidently represent 'background' radioactivity.

The app. M_r of the $Rh_o(D)$ polypeptide was 28 000 using an 8% acrylamide slab gel whereas the app. M_r was 33 000 using a 12% gel. The major red cell sialoglycoprotein, glycophorin A, which binds relatively low amounts of SDS [15,16] and is relatively hydrophilic due to its 60% content of carbohydrate gave a higher app. M_r on the 8% acrylamide gel than on the 12% gel (cf. fig.1D,2D). Thus the $Rh_o(D)$ antigen migrated near the glycophorin A monomer on 12% gels but much faster on 8% gels. This indicated that the $Rh_o(D)$ antigen binds relatively more SDS and is more hydrophobic [17].

The antigen is weakly labeled in the intact cell which indicates that it is a minor component. Previous quantitation has given values of 20 000–32 000 antigenic sites/cell [18]. In contrast some major components like glycophorin A and band 3 are found in 10^6 copies/cell [19,20]. But the $Rh_o(D)$ antigen may well be deeply embedded in the membrane and thus rather inaccessible to external reagents. In fact, protease treatment does not destroy the antigen in intact cells [21,22], whereas the isolated polypeptide was readily degraded.

We have performed immunoprecipitations with anti-$Rh_o(D)$ antisera from solubilized red cell membranes labeled by the galactose oxidase/NaB^3H_4 or periodate/NaB^3H_4 surface-labeling techniques, but no labeled band was obtained. It may be that the protein, although surface-located, does not contain carbohydrate.

Previous work on the molecular characterization of the $Rh_o(D)$ antigen has given variable results. Early work was hampered by the lack of suitable techniques for the characterization of integral membrane proteins. In [3] an antigenically active fraction was isolated by elution from anti-$Rh_o(D)$ IgG–Sepharose columns. After staining with Coomassie brilliant blue they observed a diffuse band migrating near the buffer front on SDS gel electrophoresis. The est. M_r was 7000. Unfortunately, the affinity chromatography was performed at room temperature, which could have resulted in proteolysis. Another possibility is that the eluate indeed contained the intact antigen, but it was not stained due to its hydrophobic nature.

In [4] it was claimed that the anion transport protein band 3 carries the $Rh_o(D)$ antigen activity. Their conclusion was based on the adsorption of band 3 molecules to anti-$Rh_o(D)$ IgG columns. The results are difficult to interpret because the band 3 polypeptides were extensively fragmented. In addition it is known that band 3 is easily aggregated [23,24] and a diminution in the gel profile of the eluted controls is not conclusive. Furthermore, the number of band 3 molecules found per cell does not agree with the estimation of the number of $Rh_o(D)$ antigenic sites.

This identification of the $Rh_o(D)$ polypeptide should facilitate its large scale purification. Antiserum production by immunization with the purified antigen would be highly desirable and may then become possible.

Acknowledgements

I thank Anneli Asikainen for technical assistance and Barbara Björnberg for secretarial help. This study was supported by the Academy of Finland, the Association of Finnish Life Insurance Companies and the National Cancer Institute grant 5 R01-CA26294-02.

References

[1] Abraham, C. V. and Bakerman, S. (1975) Clin. Chim. Acta 60, 33–43.
[2] Folkerd, E. J., Ellory, J. C. and Hughes-Jones, N. C. (1977) Immunochemistry 14, 529–531.
[3] Plapp, F. V., Kowalski, M. M., Tilzer, L., Brown, P. J., Evans, J. and Chiga, M. (1979) Proc. Natl. Acad. Sci. USA 76, 2964–2968.
[4] Victoria, E. J., Mahan, L. C. and Masouredis, S. P. (1981) Proc. Natl. Acad. Sci. USA 78, 2898–2902.
[5] Hubbard, A. L. and Cohn, Z. A. (1972) J. Cell Biol. 55, 390–405.
[6] Gahmberg, C. G. and Hakomori, S.-i. (1973) J. Biol. Chem. 248, 4311–4317.
[7] Gahmberg, C. G. and Andersson, L. C. (1978) J. Exp. Med. 148, 507–521.
[8] Laemmli, U. K. (1970) Nature 227, 680–685.
[9] Bonner, W. M. and Laskey, R. A. (1974) Eur. J. Biochem. 46, 83–88.
[10] Weber, K. and Osborn, M. J. (1969) J. Biol. Chem. 244, 4406–4412.
[11] Gahmberg, C. G. and Andersson, L. C. (1977) J. Biol. Chem. 252, 5888–5894.
[12] Tanner, M. J. A. and Anstee, D. J. (1976) Biochem. J. 153, 271–277.

Carl_G_190x270_mm_blokki_FINAL.indd 186 06-Aug-23 1:53:41 PM

[13] Dahr, W., Uhlenbruck, G., Leikola, J., Wagstaff, W. and Landfried, K. (1976) J. Immunogenet. 3, 329–346.
[14] Gahmberg, C. G., Myllylä, G., Leikola, J., Pirkola, A. and Nordling, S. (1976) J. Biol. Chem. 251, 6108–6116.
[15] Mimms, L. T. and Glasgow, L. R. (1980) Fed. Proc. FASEB 39, 2515.
[16] Leach, B. S., Collawn, J. F. and Fish, W. W. (1980) Biochemistry 19, 5734–5741.
[17] Helenius, A. and Simons, K. (1975) Biochim. Biophys. Acta 415, 29–79.
[18] Masouredis, S. P., Sudora, E. J., Mahan, L. and Victoria, E. J. (1976) Transfusion 16, 94–106.
[19] Gahmberg, C. G., Jokinen, M. and Andersson, L. C. (1979) J. Biol. Chem. 254, 7442–7448.
[20] Steck, T. L. (1978) J. Supramol. Struct. 8, 311–324.
[21] Victoria, E. J., Muchmore, E. A., Sudora, E. J. and Masouredis, S. P. (1975) J. Clin. Invest. 56, 292–301.
[22] Green, F. A. (1972) J. Biol. Chem. 247, 881–887.
[23] Steck, T. L. (1974) J. Cell Biol. 62, 1–19.
[24] Karhi, K. K. and Gahmberg, C. G. (1980) Biochim. Biophys. Acta 622, 344–354.

Carl_G_190x270_mm_blokki_FINAL.indd 187 06-Aug-23 1:53:41 PM

The EMBO Journal Vol.2 No.2 pp.223–227, 1983

Molecular characterization of the human red cell $Rh_o(D)$ antigen

Carl G. Gahmberg

Department of Biochemistry, University of Helsinki, Unioninkatu 35, SF-00170 Helsinki 17, Finland

Communicated by C.G. Gahmberg
Received on 29 November 1982

Human red cells of Rh blood groups -D-/-D- ('super-D'), ---/--- (Rh_{null}) and normal $Rh_o(D)+$ cells were radioactively surface-labeled using the lactoperoxidase ^{125}I method. Polyacrylamide gel electrophoresis in the presence of SDS followed by fluorography showed a strong enrichment of a polypeptide with an apparent mol. wt. of 28 0000–33 000 in the ^{125}I-labeled -D-/-D- membranes. This polypeptide was specifically immune precipitated with anti-$Rh_o(D)$ antiserum. Treatment of intact cells with trypsin or Pronase did not digest the protein. The Rh_o polypeptide migrated identically on polyacrylamide gel electrophoresis under reducing and non-reducing conditions. It was not phosphorylated after *in vitro* incubation of red cells with ^{32}P. When whole labeled membranes were solubilized in neutral detergent and applied to lectin-Sepharose columns the $Rh_o(D)$ polypeptide adsorbed to *Ricinus communis* lectin but not to wheat germ lectin or *Lens culinaris* lectin. The purified molecule did not adsorb to *R. communis* lectin-Sepharose. Treatment of the $Rh_o(D)$ antigen with endo-N-acetyl glucosaminidase H, endo-β-galactosidase or mild alkali did not lower its apparent mol. wt.

Key words: membrane proteins/red cell membrane/$Rh_o(D)$ antigen

Introduction

The molecular identification and characterization of the human red cell $Rh_o(D)$ antigen (Levine and Stetson, 1939; Landsteiner, 1940) has been controversial and slow. Most results indicate that it is a membrane protein and it may need lipid for full activity (Green, 1972). But the mol. wt. estimates vary from 7000 to 174 000 (Abraham and Bakerman, 1975; Folkerd *et al.*, 1977; Plapp *et al.*, 1979; Victoria *et al.*, 1981). Recently Gahmberg (1982) and Moore *et al.* (1982) showed that a surface-located polypeptide with an apparent mol. wt. of 28 000–33 000 was specifically immune precipitated from ^{125}I-labeled $Rh_o(D)+$ cells. But the relatively low number of antigens per cell (20 000–32 000) (Masouredis *et al.*, 1976) and their hydrophobic nature made further characterization difficult.

I have taken advantage of the rare -D-/-D- ('super-D') phenotype (Hughes-Jones *et al.*, 1971). The protein with a mol. wt. of 28 000–33 000 was strongly enriched on -D-/-D- cells. Using specific antiserum it was purified to radioactive homogeneity. Using the ^{125}I-labeled antigen preliminary structural studies have become possible. Although a surface protein, the $Rh_o(D)$ antigen seems to lack carbohydrate. It is not phosphorylated *in vitro* and it is not disulfide-bound to other molecules.

Results

[^{125}I]Lactoperoxidase labeling of red cells and identification of the $Rh_o(D)$ antigen

Figure 1B–D shows the SDS-gel electrophoresis patterns of ^{125}I-labeled-D-/-D-, normal $Rh_o(D)+$ and Rh_{null} erythrocyte membrane proteins separated on a 12% acrylamide gel. The patterns were similar with two notable exceptions. The super-D cells (Figure 1B) contained a strongly labeled protein band (RH) with an apparent mol. wt. of 33 000. The corresponding band was weaker in normal $Rh_o(D)+$ cells (Figure 1C) and essentially absent in Rh_{null} cells (Figure 1D). In addition, the super-D cells contained a strongly labeled band with an apparent mol. wt. of 66 000 (P66) (Figure 1B). Immune precipitation with anti-$Rh_o(D)$ antiserum for super-D cells resulted in one major band (RH, Figure 1E) corresponding in mol. wt. to the labeled band strongly enriched in super-D cells.

On 12% acrylamide gels the $Rh_o(D)$ protein migrated just below the glycophorin A monomer (GPA-M) and more slowly than the carbonic anhydrase standard, but on 8% acrylamide gels it moved relatively faster (Figure 1G, H). Here the apparent mol. wt. was 28 000.

Protease treatment of intact cells

When red cells are treated with Pronase or trypsin several externally located proteins are cleaved (Steck, 1974). Pronase cleaved the anion transport protein, band 3, to a 64 000 mol. wt. fragment (B3-F) (Figure 2D, E), but the $Rh_o(D)$ protein was not affected. Neither did trypsin treatment of intact cells change its apparent mol. wt. (Figure 2F).

Electrophoresis under reducing and non-reducing conditions

The presence of interchain disulfide bridges was studied by omitting the 2-mercaptoethanol from the sample buffer. This modification did not change the apparent mol. wt. of the $Rh_o(D)$ polypeptide (Figure 3).

Radioactive labeling of cell surface carbohydrates

When super-D red cells were labeled by the periodate/NaB$[^3H]_4$ and neuraminidase + galactose oxidase/NaB$[^3H]]_4$ surface labeling techniques to label sialic acids and D-galactose/D-N-acetylgalactosamine residues, respectively, no labeled protein band was observed in the position of the $Rh_o(D)$ protein on electrophoresis (Figure 4D, F). Immune precipitation also gave negative results (Figure 4E, G) although the protein was readily labeled in a control experiment by lactoperoxidase-catalyzed iodination (Figure 4B, C).

Interaction of the $Rh_o(D)$ antigen with lectins

Solubilized ^{125}I-labeled -D-/-D- membranes were chromatographed on *R. communis* lectin-Sepharose. Most of the labeled proteins including the $Rh_o(D)$ polypeptide adsorbed to the column and were eluted with D-galactose (Figure 5C). In contrast, all or most of the $Rh_o(D)$ protein/P66 passed through the wheat germ lectin- and lentil-Sepharose columns (Figure 5D, F). When the ^{125}I-labeled $Rh_o(D)$ polypeptide was purified by cylindrical polyacrylamide gel electrophoresis and then subjected to affinity chromatography, ~40% of the

© IRL Press Limited, Oxford, England.

Carl_G_190x270_mm_blokki_FINAL.indd 188 06-Aug-23 1:53:41 PM

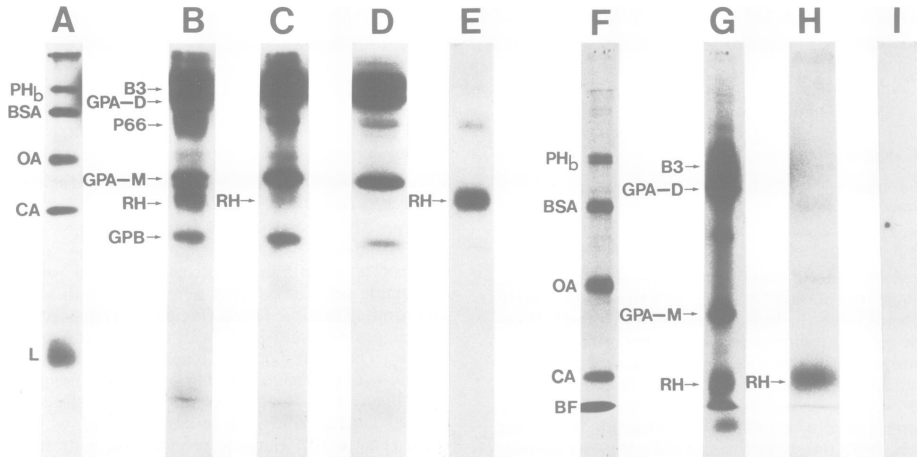

Fig. 1. Polyacrylamide gel electrophoresis patterns of ^{125}I-labeled red cells and immune precipitates obtained with anti-Rh_o(D) antiserum. **A**–**E** are run on a 12% acrylamide gel, and **F**–**I** on an 8% acrylamide gel. **A**, pattern of ^{14}C-labeled standard proteins. PH_b = phosphorylase b, BSA = bovine serum albumin, OA = ovalbumin, CA = carbonic anhydrase, L = lysozyme; **B**, pattern of -D-/-D- membranes. B3 = Band 3, GPA-D = glycophorin A dimer, P66 = protein with an apparent mol. wt. of 66 000, GPA-M = glycophorin A monomer, RH = the Rh_o(D) polypeptide, GPB = glycophorin B; **C**, pattern of normal Rh_o(D)+ membranes; **D**, pattern of Rh_{null} membranes; **E**, immune precipitate obtained from ^{125}I-labeled -D-/-D- membranes with Rh_o(D) antiserum; **F**, ^{14}C-labeled standard proteins; **G**, pattern of -D-/-D- membranes; **H**, immune precipitate obtained with anti-Rh_o(D) antiserum from ^{125}I-labeled -D-/-D-membranes; **I**, immune precipitate obtained with control serum from ^{125}I-labeled -D-/-D- membranes.

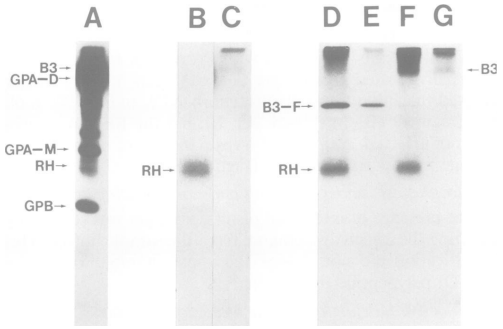

Fig. 2. Polyacrylamide gel electrophoresis patterns of ^{125}I-labeled normal Rh_o(D)+ membranes, and immune precipitates obtained with anti-Rh_o(D) antiserum from such membranes and from protease-treated ^{125}I-labeled membranes. **A**, pattern of ^{125}I-labeled Rh_o(D) membranes. Abbreviations as in legend to Figure 1; **B**, immune precipitate obtained with antiserum from normal Rh_o(D)+ membranes; **C**, immune precipitate obtained with control serum from Rh_o(D)+ membranes; **D**, immune precipitate obtained with antiserum from Pronase-treated Rh_o(D)+ cells. B3-F = fragment of Band 3; **E**, immune precipitate obtained with control serum from an identical sample as in **D**; **F**, immune precipitate obtained with antiserum from trypsin-treated Rh_o(D)+ cells; **G**, immune precipitate obtained with control serum from an identical sample as in **F**. The acrylamide concentration was 12%.

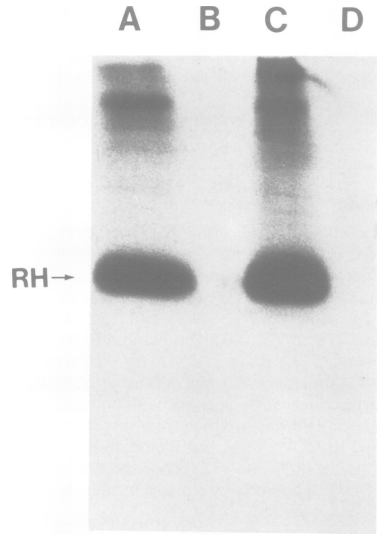

Fig. 3. Polyacrylamide gel electrophoresis patterns of the ^{125}I-labeled Rh_o(D) protein run under reducing and non-reducing conditions. **A**, immune precipitate obtained with antiserum under reducing conditions; **B**, immune precipitate obtained with control serum under reducing conditions; **C**, immune precipitate obtained with antiserum under non-reducing conditions; **D**, immune precipitate obtained with control serum under non-reducing conditions. The acrylamide concentration was 12%.

protein passed through the wheat germ lectin column (Figure 5I) (observe the relative enrichment of the contaminating GPB protein) and all through the *R. communis* lectin column (Figure 5J).

Endo-glycosidase and mild alkaline treatment of the Rh_o(D) protein

No change in the apparent mol. wt. of the Rh_o(D) protein occurred when it was digested with endo-N-acetylglucosaminidase H or endo-β-galactosidase (Figure 6C, D). Mild alkaline treatment partially resulted in higher mol. wt. forms (Figure 6E).

Carl_G_190x270_mm_blokki_FINAL.indd 189 06-Aug-23 1:53:41 PM

Phosphorylation of red cell proteins in vitro

Incubation of -D-/-D- cells with ^{32}P resulted in labeling of several red cell proteins. No obvious label was, however, observed in the position of the $Rh_o(D)$ proteins (Figure 7C) and no labeled band was obtained by immune precipitation (Figure 7D).

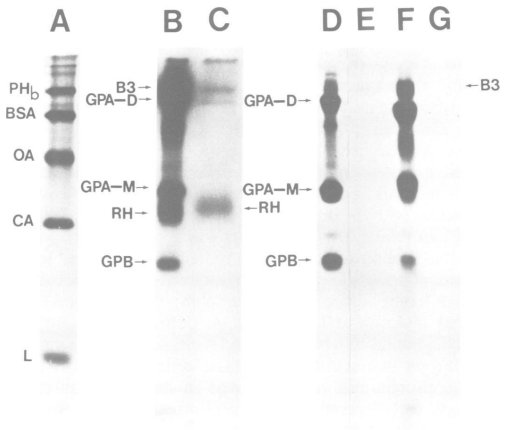

Fig. 4. Polyacrylamide gel electrophoresis patterns of lactoperoxidase/^{125}I-, periodate/NaB$[^3H]_4$- and neuraminidase + galactose/NaB$[^3H]_4$-labeled -D-/-D- erythrocyte membranes and immune precipitates obtained from them. **A**, pattern of ^{14}C-labeled standard proteins; **B**, pattern of ^{125}I-labeled membranes; **C**, immune precipitate obtained with anti-$Rh_o(D)$ antiserum from ^{125}I-labeled membranes; **D**, pattern of periodate/NaB$[^3H]_4$-labeled membranes; **E**, immune precipitate obtained with antiserum from periodate/NaB$[^3H]_4$-labeled membranes; **F**, pattern of neuraminidase + galactose oxidase/NaB$[^3H]_4$-labeled membranes; **G**, immune precipitate obtained with antiserum from neuraminidase + galactose oxidase/NaB$[^3H]_4$-labeled membranes. The acrylamide concentration was 12%.

Discussion

A large amount of work has been done on the identification of the $Rh_o(D)$ antigen, but the results have largely been conflicting. Early work was hampered by the lack of suitable methods for isolating integral membrane proteins (Green, 1972; Abraham and Bakerman, 1975; Lorusso and Green, 1975). More recently, affinity chromatography using anti-$Rh_o(D)$ antibodies and unlabeled membranes gave mol. wt. estimates of the $Rh_o(D)$ antigen of 7000 (Plapp *et al.*, 1979) and 90 000 (Victoria *et al.*, 1981). The former result may be due to proteolysis because the affinity chromatography was done at room temperature. Using affinity chromatography with unlabeled membranes and protein staining of the polyacrylamide gels we have confirmed that protein bands are seen in the band 3 region (mol. wt. = 90 000) (unpublished results), but these apparently do not represent external red cell proteins.

Recently Moore *et al.* (1982) and Gahmberg (1982) using ^{125}I-labeled membranes could show that a surface protein with an apparent mol. wt. of 28 000 – 33 000 was specifically immune precipitated from $Rh_o(D)+$ membranes. No labeled protein was precipitated from $Rh_o(D)-$ membranes. In addition, Evans *et al.* (1982) using SDS-polyacrylamide gel electrophoresis followed by incubation with anti-$Rh_o(D)$ antibodies, obtained a mol. wt. value of 13 000 – 30 000. The strong expression of the $Rh_o(D)$ polypeptide in -D-/-D- cells and its virtual absence in Rh_{null} cells gives additional evidence that this indeed represents the $Rh_o(D)$ antigen.

Routinely, red cell agglutination induced by anti-$Rh_o(D)$ antiserum is performed on protease-treated cells. The present results show that the $Rh_o(D)$ protein was not degraded by Pronase or by trypsin treatment of intact cells. On the other hand, the isolated molecule was readily degraded by Pronase (Gahmberg, 1982). Probably the protein is relatively deeply embedded in the membrane lipid bilayer and thus rather inaccessible to external proteases.

The labeling of the $Rh_o(D)$ protein by lactoperoxidase-

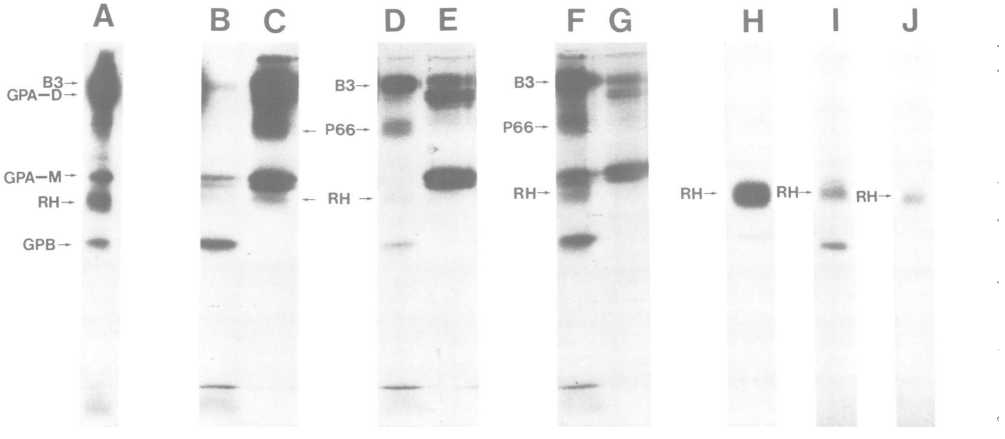

Fig. 5. Polyacrylamide gel electrophoresis patterns of fractions from lectin-Sepharose affinity chromatographies of ^{125}I-labeled -D-/-D- membranes and purified ^{125}I-labeled $Rh_o(D)$ protein. **A**, pattern of ^{125}I-labeled membranes; patterns of passed-through peak (**B**) and sugar-eluted peak (**C**) of ^{125}I-labeled membrane proteins separated on *R. communis* lectin-Sepharose; patterns of passed-through peak (**D**) and sugar-eluted peak (**E**) of ^{125}I-labeled membrane proteins separated on wheat germ lectin-Sepharose; patterns of passed-through peak (**F**) and sugar-eluted peak (**G**) of ^{125}I-labeled membrane proteins separated on lentil lectin-Sepharose; **H**, pattern of purified $Rh_o(D)$ protein; **I**, pattern of passed-through peak of purified $Rh_o(D)$ protein on wheat germ lectin-Sepharose; **J**, pattern of passed-through peak of purified $Rh_o(D)$ protein on *R. communis* lectin-Sepharose. The acrylamide concentration was 12%.

Carl_G_190x270_mm_blokki_FINAL.indd 190 06-Aug-23 1:53:41 PM

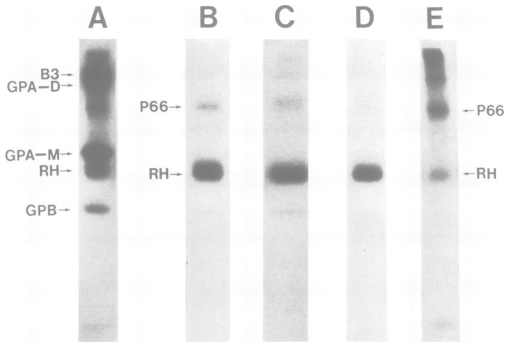

Fig. 6. Polyacrylamide gel electrophoresis patterns of ^{125}I-labeled $Rh_o(D)$ protein before and after treatment with glycosidases or milk alkali. **A**, pattern of ^{125}I-labeled -D-/-D- membranes; **B**, pattern of immune precipitated $Rh_o(D)$ protein; **C**, pattern obtained after digestion with endo-N-acetyl-glucosaminidase H; **D**, pattern obtained after digestion with endo-β-galactosidase; **E**, pattern obtained after treatment with mild alkali. The acrylamide concentration was 12%.

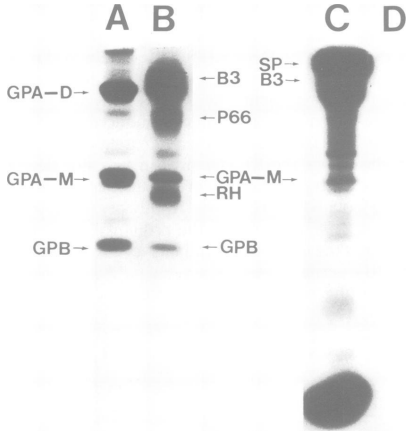

Fig. 7. Phosphorylation of -D-/-D- red cell membranes. **A**, pattern of periodate/NaB[^{3}H]$_4$-labeled membranes; **B**, pattern of ^{125}I-labeled membranes; **C**, pattern of ^{32}P-labeled membranes; **D**, immune precipitate with anti-$Rh_o(D)$ antiserum from ^{32}P-labeled membranes.

catalyzed iodination of intact cells shows that part of it is cell surface-exposed. It may be quite hydrophobic as shown indirectly by its behavior on polyacrylamide gel electrophoresis in the presence of SDS. This was most clearly seen when compared to the behavior of glycophorin A. Whereas glycophorin A, which binds relatively low amounts of SDS (Mimms and Glasgow, 1980), showed a higher apparent mol. wt. on 8% acrylamide gels than on 12% gels, the $Rh_o(D)$ protein showed the opposite behavior (cf. Figure 1B and G). Also, compared to the standard protein, the $Rh_o(D)$ protein showed a relatively increased migration on gels with a lower degree of cross-linking. This could be due to high binding of SDS (Helenius and Simons, 1975).

The $Rh_o(D)$ polypeptide is apparently not covalently bound to other surface-exposed polypeptides because it was the only major band obtained by immune precipitation. In addition, reduction of disulfide bonds had no effect on its electrophoretic migration. The P66 band, often seen after immune precipitation with anti-$Rh_o(D)$ antibodies, most probably represents a dimer of the $Rh_o(D)$ monomer. It was enriched in super-D cells, its apparent mol. wt. was twice that of the RH-band and it was increased when urea was omitted from the gel samples. Such a monomer/dimer equilibrium resembles that of glycophorin A which also easily forms dimers (Marton and Garvin, 1973).

Interestingly, the protein may lack carbohydrate. It has become almost a rule that mammalian cell surface proteins are glycoproteins (Gahmberg, 1976; Singer and Nicolson, 1972; Gahmberg, 1981). But the $Rh_o(D)$ protein was not labeled by the carbohydrate-specific surface labeling techniques, it was not degraded by endo-glycosidase treatments nor by mild alkali. Furthermore, it showed no, or only weak interaction with the different types of lectin columns. When a whole membrane detergent extract was applied to *R. communis* lectin-Sepharose, the $Rh_o(D)$ protein clearly bound to the column. This could be due to indirect binding occurring through some other membrane component, because the isolated molecule did not bind. A portion of the isolated molecule bound to wheat germ lectin-Sepharose. This may be due to ionic interactions to the basic lectin protein. Obviously, the protein has to be isolated in larger amounts and chemical carbohydrate analysis performed to verify the possible absence of sugar. Furthermore, in contrast to most red cell membrane proteins, which are phosphorylated (Johnson *et al.*, 1982), the $Rh_o(D)$ antigen seems to lack phosphate.

The molecular basis for the diversity of the Rh-complex remains unclear. However, the identification and preliminary characterization of the $Rh_o(D)$ protein should facilitate studies on other Rh-antigens (Moore *et al.*, 1982). Furthermore, a large scale purification of the $Rh_o(D)$ antigen may now become possible. This would be highly desirable for the production of monospecific antisera to be used in blood group typing and prevention of hemolytic disease of the newborn.

Materials and methods

Cells

Normal human $Rh_o(D)$ positive erythrocytes were obtained from the Finnish Red Cross Blood Transfusion Service, Helsinki, Finland. -D-/-D- cells were obtained through Professor G. Sirchia, Milano, Italy and Rh_{null} (---/---) cells through Professor S. Seidl, Frankfurt am Main, FRG. The cells were washed three times in 0.15 M NaCl-0.01 M sodium phosphate, pH 7.4 ($NaCl/PO_4$) before further studies. Erythrocyte membranes were isolated as described previously (Gahmberg and Hakomori, 1973).

Chemicals and isotopes

The sources of the chemicals were: acrylamide, N,N′-methylene bisacrylamide and cyanogen bromide (Eastman), 2,5-diphenyloxazole and 1,4 bis[2-(5-phenyloxazolyl)] benzene (New England Nuclear), phenylmethane sulfonyl fluoride (PMSF, Sigma), α-methylmannoside (Calbiochem), D-galactose and sodium metaperiodate (Merck) and N-acetyl D-glucosamine (Fluka). Tritiated sodium borohydride (24 Ci/mmol), ^{125}I (carrier-free), ^{32}P (carrier free) and ^{14}C-labeled protein standards were obtained from Amersham International, Amersham, UK. The NaB[^{3}H]$_4$ preparation was handled as described previously (Gahmberg, 1978).

Antisera and enzymes

Anti-$Rh_o(D)$ antisera and control sera were obtained from the Finnish Red Cross Blood Transfusion Service, Helsinki. *Vibrio cholerae* neuraminidase (500 units/ml) was from Koch-Light. Galactose oxidase (130 units/mg protein) was purchased from Kabi AB, Stockholm, Sweden. Both the neuraminidase and galactose oxidase preparations were free of protease activities when assayed as described previously (Gahmberg and Hakomori, 1973). Crystalline bovine trypsin (3.5 units/mg) was from Merck and *Streptomyces griseus* pro-

Carl_G_190x270_mm_blokki_FINAL.indd 191 06-Aug-23 1:53:41 PM

tease (Pronase) from Sigma. Endo-N-acetylglucosaminidase H (*S. griseus*) and endo-β-galactosidase (*Escherichia freundii*) were purchased from Seikagaku Kogyo Co., Tokyo, Japan.

Protease treatment of intact erythrocytes

Ten per cent suspensions in $NaCl/PO_4$ of $Rh_o(D)+$ cells were incubated with 0.1 mg/ml of Pronase or trypsin at 37°C for 30 min. After incubation the cells were washed three times in $NaCl/PO_4$ and ^{125}I-labeled.

Radioactive surface-labeling of erythrocytes

Intact or protease-treated red cells were ^{125}I-labeled using the lactoperoxidase-glucose oxidase method (Hubbard and Cohn, 1972). Cells were labeled by the neuraminidase + galactose oxidase/$NaB[^3H]_4$ surface-labeling technique (Gahmberg and Hakomori, 1973) as described in detail previously (Gahmberg, 1976) or by the periodate/$NaB[^3H]_4$ technique (Gahmberg and Andersson, 1977) using a final concentration of 1 mM periodate. After labeling the membranes were isolated.

Immune precipitation

Radioactively labeled membranes (0.1 ml) were incubated with 10 μl of anti-$Rh_o(D)$ antiserum or control serum overnight in $NaCl/PO_4$ at 0°C. The membranes were then washed in ice-cold $NaCl/PO_4$ and dissolved in 200 μl of $NaCl/PO_4$ containing 1% ethanol, 1% Triton X-100 and 2 mM PMSF (Buffer A). Care was taken to keep the temperature at 0–4°C during all operations until final elution with SDS. After centrifugation at 100 000 *g* for 15 min the supernatants were recovered and 0.2 ml of a 10% suspension of protein A-containing *Staphylococcus aureus* cells was added (Gahmberg and Andersson, 1978). After 1 h on ice the bacteria were subsequently washed with $NaCl/PO_4$-0.05% SDS-1% Triton X-100, 0.5 M NaCl-0.05% Triton X-100-5 mM EDTA, 0.15 M NaCl-0.05% Triton X-100-5 mM EDTA and finally with H_2O. Adsorbed proteins were eluted by boiling in 1% SDS for 1 min and the samples centrifuged. The supernatants were lyophilized and used for further analysis.

Endo-glycosidase and mild alkaline treatments

The ^{125}I-labeled $Rh_o(D)$ antigen was isolated by immune precipitation and eluted with a small volume of 1% SDS. For endo-N-acetylglucosaminidase H digestion ~10 000 c.p.m. of the antigen was digested in 0.1 ml of 0.125 M sodium citrate, pH 5.8-0.05% SDS with 10 mU of enzyme for 24 h at 37°C. Endo-β-galactosidase digestion was performed on an identical sample in 0.1 ml of 0.2 M sodium acetate, pH 5.8-0.05% SDS with 5 mU of enzyme for 24 h at 37°C. Mild alkaline degradation was performed in 0.05 M NaOH-0.05% SDS for 30 min at 80°C. This treatment is known to liberate the O-glycosidic oligosaccharides of glycophorin A (unpublished results). After incubation the sample was neutralized with HCl. All samples were then dialyzed against distilled water at 4°C and lyophilized.

Affinity chromatographies on lectin-Sepharose columns

Lentil lectin (*Lens culinaris*) was isolated by affinity chromatography on Sephadex G-50 in $NaCl/PO_4$ and eluted with 0.05 M D-glucose essentially as described (Sage and Green, 1972). Castor bean lectins (*Ricinus communis*) were isolated by affinity chromatography on unsubstituted Sepharose 4B in $NaCl/PO_4$ and eluted with 0.1 M D-galactose as described (Nicolson and Blaustein, 1972). Wheat germ lectin (*Triticum vulgaris*) was isolated on ovomucoid-Sepharose 4B as described (Marchesi, 1972) using 0.1 M acetic acid as the eluting agent. Purified lectins were coupled to Sepharose 4B (2 mg of lectin/ml of packed gel) activated with cyanogen bromide in the presence of a 0.1 M concentration of the appropriate sugar hapten (Cuatrecasas, 1970).

Affinity chromatographies were performed on ^{125}I-labeled -D-/-D- membranes solubilized in Buffer A and ^{125}I-labeled $Rh_o(D)$ antigen isolated by preparative cylindrical polyacrylamide gel electrophoresis. The radioactive samples were applied in Buffer A to the lectin-Sepharose columns at 4°C, washed extensively with Buffer A and eluted with 0.1 M of α-methylmannoside (lentil lectin-Sepharose) and D-N-acetylglucosamine (wheat germ lectin-Sepharose). The passed-through and eluted peak fractions were pooled, dialyzed against water and concentrated by lyophilization.

Labeling with ^{32}P

One ml of packed -D-/-D- cells was incubated with 2 mCi of ^{32}P at room temperature for 18 h as described (Johnson *et al.*, 1982). After incubation the cells were washed and the membranes isolated.

Polyacrylamide gel electrophoresis

Polyacrylamide gel electrophoresis in the presence of SDS was performed on cylindrical or slab gels according to Laemmli (1970) using acrylamide concentrations of 8% or 12%. Urea (3 M) was included in the samples. The treatment of the gels for fluorography was carried out as described (Bonner and Laskey, 1974). The apparent mol. wts. of the proteins were determined using the ^{14}C-labeled proteins as mol. wt. standards.

Acknowledgements

I thank Anneli Asikainen for technical assistance, Barbara Björnberg for secretarial help, and E. Haahti, A. Pirkola, G. Sirchia and S. Seidl for red blood cells and antisera. This work was supported by the Academy of Finland, the Association of Finnish Life Insurance Companies and the National Cancer Institute grant 5 R01-CA26294-03.

References

Abraham,C.V. and Bakerman,S. (1975) *Clin. Chim. Acta,* **60**, 33-43.
Bonner,W.M. and Laskey,R.A. (1974) *Eur. J. Biochem.,* **46**, 83-88.
Cuatrecasas,P. (1979) *J. Biol. Chem.,* **249**, 4398-4403.
Evans,J.P., Sinor,L.T., Brown,P.J., Tilzer,L.L. and Plapp,F.V. (1982) *Mol. Immunol.,* **19**, 671-675.
Fairbanks,G., Steck,T.L. and Wallach,D.F.H. (1971) *Biochemistry (Wash.),* **10**, 2606-2617.
Folkerd,E.J., Ellory,J.C. and Hughes-Jones,N.C. (1977) *Immunochemistry,* **14**, 529-531.
Gahmberg,C.G. (1976) *J. Biol. Chem.,* **251**, 510-515.
Gahmberg,C.G. (1978) *Methods Enzymol.,* **50**, 204-206.
Gahmberg,C.G. (1981) in Finean,J.B. and Michell,R.H. (eds.), *Comprehensive Biochemistry*, Elsevier, Amsterdam, pp. 127-160.
Gahmberg,C.G. (1982) *FEBS Lett.,* **140**, 93-97.
Gahmberg,C.G. and Andersson,L.C. (1977) *J. Biol. Chem.,* **252**, 5888-5894.
Gahmberg,C.G. and Andersson,L.C. (1978) *J. Exp. Med.,* **148**, 507-521.
Gahmberg,C.G. and Hakomori,S. (1973) *J. Biol. Chem.,* **248**, 4311-4317.
Green,F.A. (1972) *J. Biol. Chem.,* **247**, 881-887.
Helenius,A. and Simons,K. (1975) *Biochim. Biophys. Acta,* **415**, 29-79.
Hubbard,A.L. and Cohn,Z.A. (1972) *J. Cell Biol.,* **55**, 390-405.
Hughes-Jones,N.C., Gardner,B. and Lincoln,P.J. (1971) *Vox Sang.,* **21**, 210-216.
Johnson,R.M., McGowan,M.W., Morse,P.D.,II and Dzander,J.K. (1982) *Biochemistry (Wash.),* **21**, 3599-3604.
Laemmli,U.K. (1970) *Nature,* **227**, 680-685.
Landsteiner,K. (1940) *Proc. Soc. Exp. Biol. Med.,* **43**, 223.
Levine,P. and Stetson,R.E. (1939) *J. Am. Med. Assoc.,* **113**, 126-127.
Lorusso,D.J. and Green,F.A. (1975) *Science (Wash.),* **188**, 66-67.
Marchesi,V.T. (1972) *Methods Enzymol.,* **28**, 354-356.
Marton,L.S.G. and Garvin,J.S. (1973) *Biochem. Biophys. Res. Commun.,* **52**, 1457-1462.
Masouredis,S.P., Sudora,E.J., Mahan,L. and Victoria,E.J. (1976) *Transfusion,* **16**, 94-106.
Mimms,L.T. and Glasgow,L.R. (1980) *Fed. Proc.,* **39**, 2515.
Moore,S., Woodrow,C.F. and McClelland,D.B.L. (1982) *Nature,* **295**, 529-531.
Nicolson,G.L. and Blaustein,J. (1972) *Biochim. Biophys. Acta,* **266**, 543-547.
Plapp,F.V., Kowalski,M.M., Tilzer,L., Brown,P.J., Evans,J. and Chiga,M. (1979) *Proc. Natl. Acad. Sci. USA,* **76**, 2964-2968.
Sage,J.H. and Green,R.W. (1972) *Methods Enzymol.,* **28**, 332-339.
Singer,S.J. and Nicolson,G.L. (1972) *Science (Wash.),* **175**, 720-731.
Steck,T.L. (1974) *J. Cell Biol.,* **62**, 1-19.
Victoria,E.J., Mahan,L.C. and Masouredis,S.P. (1981) *Proc. Natl. Acad. Sci. USA,* **78**, 2898-2902.

Carl_G_190x270_mm_blokki_FINAL.indd 192 06-Aug-23 1:53:41 PM

i An update to this article is included at the end

REVIEWS

TIBS 21 – *AUGUST 1996*

(1995) *Biochem. Biophys. Res. Commun.* 214, 576–581
37 Muscatelli, F. *et al.* (1994) *Nature* 372, 672–676
38 Bardoni, B. *et al.* (1994) *Nat. Genet.* 7, 497–501
39 King, V. *et al.* (1995) *Curr. Biol.* 5, 37–39
40 Ryner, L. C. and Swain, A. (1995) *Cell* 81, 483–493
41 Sockanathan, S., Cohen-Tannoudji, M., Colignon, J. and Lovell-Badge, R. (1993) *Genet. Res.* 61, 149
42 Kamachi, Y. *et al.* (1995) *EMBO J.* 14, 3510–3519
43 Denny, P. *et al.* (1992) *EMBO J.* 11, 3705–3712
44 van de Wetering, M., Oosterwegel, M., van Norren, K. and Clevers, H. (1993) *EMBO J.* 12, 3847–3854
45 Affara, N. A. *et al.* (1993) *Nucleic Acids Res.* 2, 785–789
46 Harley, V. R. *et al.* (1992) *Science* 255, 453–456
47 Braun, A. *et al.* (1993) *Am. J. Hum. Genet.* 52, 578–585
48 Zeng, Y. *et al.* (1993) *J. Med. Genet.* 30, 655–657
49 Poulat, F. *et al.* (1994) *Hum. Mutat.* 3, 200–204

Why mammalian cell surface proteins are glycoproteins

Carl G. Gahmberg and Martti Tolvanen

Most proteins presented at the external surface of mammalian cells contain carbohydrate. The reason for this is not fully understood, but recent work has shown that such carbohydrate has two major functions. Inside the cell, it helps proteins fold and assemble correctly in the endoplasmic reticulum, and it might also act as a signal for the correct migration of glycoproteins. Outside the cell, it provides specific recognition structures for interaction with a variety of external ligands.

EARLY WORK IN the 1960s on the morphology of mammalian cells showed that the external surface of the plasma membrane is rich in carbohydrate, whereas the inner side is devoid of conventional-type oligosaccharides[1]. Until recently, it was unclear whether the carbohydrate was confined to few or many different cell surface glycoconjugates[2], and the development of radioactive techniques in particular has allowed the carbohydrate portions of exposed cell surface glycoproteins and glycolipids to be labeled[3,4]. It was then possible to study the larger number of glycoconjugates specifically presented at the surface of various cells. Also, it became apparent that cell membranes contain a multitude of glycoproteins, many more than previously thought[5,6].

In 1976, after studying human erythrocytes and other cells, it was proposed that cell surface proteins are always glycoproteins[5]. A similar proposal was made independently by Bretscher and Raff[2]. As more and more mammalian cell membrane proteins and the genes encoding them have been characterized, cloned and sequenced, this proposal has turned out to be largely correct.

Most glycoproteins are *N*-glycosylated, i.e. they contain asparagine-linked oligosaccharides located at the peptide sequence(s) NxS/T (where x stands for any amino acid except for proline) at the external aspect of the membrane. Some membrane proteins are *O*-glycosylated, with the carbohydrate chains attached to serine or threonine residues, which are often clustered in distinct regions of the polypeptides. Most *O*-glycosylated proteins also contain one or more *N*-glycosidic oligosaccharides[7]. The importance and requirements for *O*-glycosylation have yet to be elucidated.

Exceptions to the rule

Early searches of the literature for unglycosylated surface proteins in mammalian cells met with little success. However, in 1982, the human red cell Rh(D) (Rhesus) protein, with an apparent molecular weight of 30–32 kDa, was identified[8,9]. Importantly, no evidence for the presence of carbohydrate was found[10], and subsequent cloning and sequencing of its cDNA and that of other polypeptides belonging to the Rh-blood group system, showed that they do indeed lack *N*-glycosylation sequences[11,12]. Thus, this protein seemed to be an exception to the glycosylation rule.

However, more recent work has shown that this is not the case. There is now evidence that the Rh-polypeptides form part of a large glycopolypeptide complex, including among others the Rh50 glycoproteins and the Landsteiner–Wiener (LW) blood group glycoprotein (intercellular adhesion molecule 4) (Refs 13, 14). This situation is similar to that of β2-microglobulin in class I transplantation antigens, where the unglycosylated protein associates with the heavy chains of the transplantation antigens. The importance of the association of the Rh-polypeptide with other glycosylated proteins is underscored by the fact that it has not yet been possible to express the Rh cDNA in any mammalian cell expression system.

In a recent survey of the SWISS-PROT database (release 33.0, April 1996) we found 1823 complete animal protein entries with reported extracellular features, of which 1671 (91.7%) were described as 'glycoproteins' in the keyword field; 1630 of these 1671 contained the *N*-glycosylation peptide sequence NxS/T. The remaining 8.3%, representing 152 potentially non-glycosylated plasma-membrane proteins, contained 116 proteins with multiple transmembrane regions, 15 proteins that are known to associate with glycosylated subunits in a complex such as CD3 chains and the Rhesus D-polypeptide, and seven that contained 5–38 potential *N*-glycosylation sites, i.e. polypeptides highly likely to be glycosylated, yet not marked as glycoproteins. This leaves only 14 sequences (0.7%) that are candidates for non-glycosylated, non-complexed plasma membrane proteins with a single transmembrane domain.

In another survey, we assessed whether this high representation of the *N*-glycosylation tripeptide sequence is more than should be found by chance alone*. To do this, we extracted all sequence features marked as extracellular domains from animal proteins in SWISS-PROT 33.0, which resulted in 4259 stretches of sequence from 1933

C. G. Gahmberg and **M. Tolvanen** are at the Department of Biosciences, Division of Biochemistry, P.O. Box 56, Viikinkaari 5, FIN-00014, University of Helsinki, Finland.

© 1996, Elsevier Science Ltd

PII: S0968-0004(96)10034-7

Carl_G_190x270_mm_blokki_FINAL.indd 193 06-Aug-23 1:53:41 PM

proteins. By chance alone, this material is expected to contain 3343 potential *N*-glycosylation sites, but it actually contains 6725 sites, an over-representation of more than twofold. This high frequency of potential *N*-glycosylation sites in extracellular domains might reflect recent gene duplication and shuffling events as well as a possible evolutionary pressure to enrich for glycosylation sites.

For comparison we analysed all reported cytoplasmic sequences in animal proteins in the same way. This material contained 1656 occurrences of the *N*-glycosylation sequence versus 1727 expected occurrences.

Glycosylation is essential in the endoplasmic reticulum

It has been difficult to understand why the glycosylation machinery, especially that of *N*-glycosylation, is so remarkably complex[15]. Is Nature wasteful? Briefly, dolichol-containing glycolipids are used to donate the initial glucose$_3$-mannose$_9$-*N*-acetylglucosamine$_2$ oligosaccharide to asparagine residues in the lumen of the endoplasmic reticulum (ER) (Fig. 1). The peripheral glucose residues are subsequently removed by α-glucosidases I and II, followed by α-mannosidase removing α-mannosyl residues; the final oligosaccharides (Fig. 2) are formed by the action of various glycosyltransferases. If the protein is still unfolded after removal of the glucose residues, reglucosylation takes place by the ER enzyme UDPglucose: glycoprotein glucosyl transferase[16] (Fig. 1). Importantly, this enzyme acts only on denatured or unfolded substrates. The subsequent glycosylation reactions take place during the transport of the glycoproteins through the ER and Golgi apparatus *en route* to the cell surface.

Using glycosylation mutants, Stanley and co-workers have convincingly shown that, whereas *N*-glycosylation is essential for the viability of cells, hybrid and complex oligosaccharides are not an absolute necessity[17]. They are, however, required for the whole organism to develop normally[17]. Thus, mice with inactivated *N*-acetylglucosamine transferase I die at mid-gestational age. This transferase is the key enzyme in the initiation of complex- and hybrid-type *N*-linked oligosaccharide biosynthesis.

It is still poorly understood how the biosynthesis of membrane oligosaccharides is regulated. Evidently, the activity of the glycosyl transferases and also the availability of nucleotide sugars are of key importance. The following example might illustrate this: human En(a–) red cells lack the gene that encodes for glycophorin A, the major erythrocyte sialoglycoprotein[18], but the cell compensates for this loss by making a larger-than-normal Band 3 (anion transport protein) oligosaccharide of the polylactosamine type. Individuals heterozygous for the glycophorin A defect (containing 50% the normal amount of glycophorin A) synthesize a Band 3 oligosaccharide with a size between that of normal and En(a–) cells[18]. Although the carbohydrate chains in this example are profoundly different, the findings indicate that there is competition for activated sugars, and the lack of one major polypeptide acceptor gives others the opportunity to get more carbohydrate.

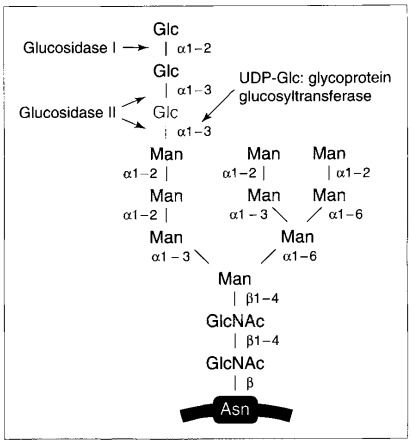

Figure 1
Structure of untrimmed *N*-glycosidic oligosaccharide. This oligosaccharide is later modified in the endoplasmic reticulum (ER) by removal of the peripheral glucose by glucosidase I and of the other two glucose residues by glucosidase II. The innermost glucose residue is essential for the interaction with calnexin and calreticulin. UDPglucose: glycoprotein glucosyltransferase, which acts on unfolded proteins, can restore it. Abbreviations used: Glc, D-glucose; GlcNAc, *N*-acetyl-D-glucosamine; Man, D-mannose.

Calnexin and calreticulin

The realization that calnexin and calreticulin, both ER proteins and molecular chaperones, recognize and bind to the carbohydrate portions (specifically to the innermost glucose residue) of newly synthesized glycoproteins is of fundamental importance[19–23]. Whereas the biosynthesis of the polypeptides is relatively quick, their subsequent folding and the association of subunits are much slower processes. By binding to newly synthesized glycopolypeptides, calnexin anchors the polypeptides in the ER until they have achieved their

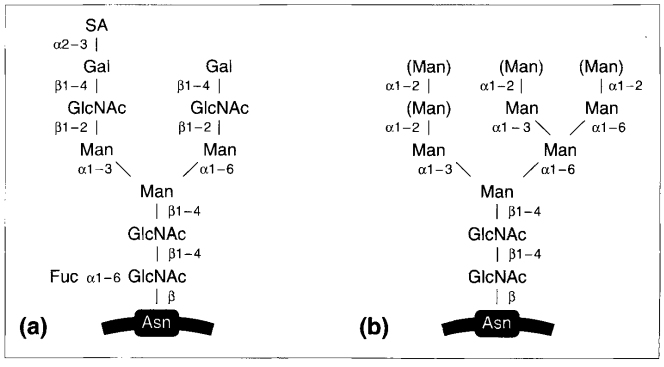

Figure 2
(a) Complex-type and **(b)** high-mannose-type *N*-glycosidic oligosaccharides. Many complex-type oligosaccharides are important for cell–ligand interactions, but also high-mannose-type structures can function as lectin and microbial ligands. Abbreviations used: Fuc, L-fucose; Gal, D-galactose; Glc, D-glucose; GlcNAc, *N*-acetyl-D-glucosamine; Man, D-mannose; SA, sialic acid.

*If the probability of a given tripeptide being an *N*-glycosylation sequence (*N*-gs) is P_{Ngs}, a sequence of n residues is considered as n – 2 tripeptides and a binomial distribution is assumed for the number of glycosylation sites in this population of tripeptides, the expectation value of the number of glycosylation sites, $\mu = P_{Ngs} \times (L - 2N)$ for N sequences of total length L. The assumption of a binomial distribution is fair when P_{Ngs} is small, but it gives a slight overestimation for the number of sites.

Carl_G_190x270_mm_blokki_FINAL.indd 194 06-Aug-23 1:53:41 PM

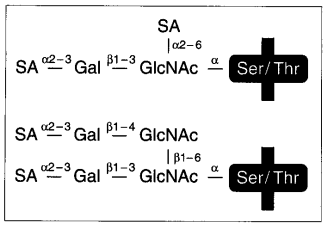

Figure 3
Structures of *O*-glycosidic oligosaccharides. *O*-glycosidic oligosaccharides are found in mucin-type glycoproteins, often in large numbers. The multi-valency is probably important in increasing their avidity for various interactions. A large number of sugar chains might also have protective functions against proteolysis. Abbreviations used: Gal, D-galactose; GalNAc, *N*-acetyl-D-galactosamine; SA, sialic acid.

correct folding conformation and, where appropriate, associated with other polypeptides into supramolecular complexes. However, if deglycosylation is prevented by glucosidase inhibitors like castanospermine and deoxynojirimycin, the proteins remain bound to calnexin and calreticulin, their transport is delayed in the ER and the proteins are subsequently degraded. Treatment with tunicamycin, which completely inhibits the *N*-glycosylation machinery, blocks calnexin and calreticulin interactions with their substrates, resulting in incorrectly folded polypeptides, protein degradation and mislocalization of newly synthesized proteins. These findings do not exclude the fact that other molecular chaperones such as BiP (binding protein) are also important.

In addition to these glycoprotein chaperones, a few proteins have been identified that can act as intracellular lectins (chaperones?) later in the biosynthetic pathway. These include the ERGIC-53 protein and VIP36, which are homologous to plant lectins and can bind high-mannose type oligosaccharides[24].

Little is known about the importance of *O*-glycosylation, but because those cell surface proteins that are *O*-glycosylated (Fig. 3) are often heavily so, they influence strongly the three-dimensional structure of these mucin-type membrane glycoproteins. Furthermore, *O*-glycosylation efficiently protects such proteins from proteolysis. *O*-linked oligosaccharides might extend surface proteins into rod-like structures, which could be important in mediating or preventing cell–cell interactions. Moreover, carbohydrate–carbohydrate interactions[25] can be important during various stages of glycoconjugate biosynthesis, but little is known about their significance.

Exit from the cell

It has been argued that plasma membrane glycoproteins do not need any 'exit signal', but migrate by bulk flow without specific retention. This would mean that glycoproteins remain at the same concentration in the transport vesicles during intracellular migration. Wieland *et al.*[26] used an ^{125}I-labeled, formylated *N*-glycosylation consensus sequence tripeptide (NYS), which was taken up by intact cells, glycosylated and then secreted in 5–10 min. Whether this sequence employed the physiological migration route through the Golgi apparatus is not known. The fast, intracellular migration by this simple molecule was interpreted to mean that secretion involves neither any specific retention signals, nor any signals that would target the tripeptide to the cell surface.

However, one could also interpret the results to suggest that the oligosaccharide of the *N*-glycosylated tripeptide in fact gives the molecule a positive migration signal. Support for such a function of oligosaccharides has been obtained using a recombinant chimeric membrane protein based on rat growth hormone. The soluble protein is normally not glycosylated, and when a membrane-anchored form was engineered it remained intracellular[27]. However, the introduction of *N*-glycosylation sites resulted in its glycosylation, and presentation at the cell surface. Interestingly, the same glycosylated protein showed apical sorting in Madin–Darby canine kidney cells, whereas the non-glycosylated growth hormone was secreted from both the apical and basolateral membranes[28].

Oligosaccharide function at the cell surface

A number of carbohydrate-specific functions occur at the cell surface, many of which involve recognition events. These include cell adhesion, interactions between cells and soluble ligands, and between cells and various microbes. Such interactions often involve carbohydrate-binding lectins.

Although the presence of mammalian cell lectins has been known for a number of years, their importance was initially largely neglected. This was owing to the fact that rather few specificities were found, and the lectins were considered important only in a few special cases. Only a few examples of specific carbohydrate–plasma membrane glycoprotein interactions can be mentioned here, and the reader is referred to more extensive recent reviews for additional reading[29,30].

The finding of a hepatocyte lectin for de-sialylated serum glycoproteins opened the field[31]. This lectin, presented at the surface of liver epithelial cells, binds to serum glycoproteins that have lost terminal sialic acids, resulting in exposure of galactosyl/*N*-acetylgalactosaminyl residues. A corresponding macrophage activity involving binding of mannose-containing proteins was subsequently described. But more widespread interest in the importance of glycoprotein oligosaccharides arose when leukocyte adhesion was found to involve initial carbohydrate–ligand interactions. Several studies have shown that 'rolling' of neutrophils and monocytes along capillary endothelia results from reversible interactions between selectins presented on endothelial cells and leukocytes, and

Carl_G_190x270_mm_blokki_FINAL.indd 195 06-Aug-23 1:53:41 PM

specific carbohydrate structures on the counter-ligand cells. These selectins[32,33] bind to sialyl Le^x, sialyl Le^a (Fig. 4), sulfatides and related carbohydrate structures. L-selectin is found on nucleated blood cells, whereas E- and P-selectins are mainly found on endothelial cells (P-selectins are also found on platelets).

Interestingly, many selectin receptors are cell surface proteins rich in *O*-glycosidic oligosaccharides. These include glycosylation-dependent cell adhesion molecule 1 (GlyCAM-1), CD34, mucosal vascular addressin cell adhesion molecule 1 (MAdCAM-1) and P-selectin glycoprotein ligand 1 (PSGL-1) (Ref. 34). The selectin-mediated 'rolling' phenomenon is essential for subsequent stronger binding, and for tissue migration of leukocytes involving integrins and ligands of the immunoglobulin superfamily [intercellular adhesion molecule (ICAM) and vascular cell adhesion molecule (VCAM)].

Additional leukocyte carbohydrate-binding proteins have recently been described; among them is the B lymphocyte surface protein CD22, which binds α2-6 sialic acid–galactosyl structures, and the macrophage sialo-adhesin with specificity for α2-3 sialic acid-containing glycoconjugates[35]. Of particular interest is the binding of sperm to zona pellucida glycoproteins through α-galactosyl residues[33], although this field is still controversial and is probably more complex than currently thought.

However, it is anticipated that this list of important surface glycoproteins will grow over the next few years, along with the elucidation of their binding specificities. In fact, the carbohydrate structures of only a few cell surface glycoproteins are currently known. This is, of course, largely owing to the fact that it is difficult to purify native glycoproteins from mammalian cell membranes in sufficient quantities. However, it is already evident that cell surface proteins originating from the same cell can have very different oligosaccharide compositions. On one hand, CD45, a major cell surface glycoprotein of leukocytes, which contains tyrosine phosphatase activity on the inner aspect of the membrane, is enriched in α2-6 sialic acid–galactosyl residues. On the other hand, the leukocyte CD11/CD18 integrins contain α2-3 sialic acid–galactose structures, but no α2-6 sialic acid. These facts are reflected in their binding specificities. Thus, CD22 binds to CD45 (and to some other proteins), but not to the integrins, whereas the opposite is true for E-selectin[36].

Currently, a large number of binding specificities of cell surface carbohydrate are known for unphysiological ligands such as bacteria, viruses, toxins etc. Although clinically important, these activities are obviously not physiological, but reflect evolutionary adaptations of various microbes.

Concluding remarks

The main purpose of this short review is to point out the requirement of cell surface proteins for carbohydrate. For successful biosynthesis, folding and intracellular migration, cell surface proteins (and most secreted proteins) need to be glycosylated or, we postulate, linked to a glycosylated protein. The few exceptions to this rule include cell surface proteins that span the membrane several times. Intracellular lectins such as calnexin and calreticulin are responsible for retaining glycoproteins on the ER until the time is right for their migration to the membrane, but carbohydrates might also be important as positive plasma membrane signals. However, many of the specific functions of mature cell surface glycoprotein oligosaccharides are physiologically important, but not always essential for the protein function.

Although this research area is still largely in its infancy, it is rapidly developing. Whether most (or all) carbohydrate structures present at the cell surfaces eventually will turn out to be important in interactions with surrounding cells, soluble ligands and infecting microbes remains to be seen.

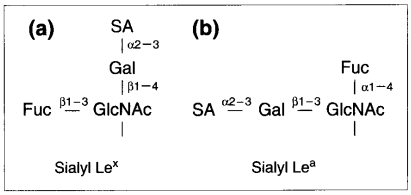

Figure 4
Structures of the selectin ligands **(a)** sialyl Le^x and **(b)** sialyl Le^a. These oligosaccharides are important ligands for selectins and are found as terminal structures in several different oligosaccharides, both in glycoproteins and glycolipids. Abbreviations used: Fuc, L-fucose; Gal, D-galactose; GlcNAc, *N*-acetyl-D-glucosamine; SA, sialic acid.

Acknowledgements

The original research from the authors' laboratory was supported by the Academy of Finland, the Sigrid Jusélius Foundation and the Finnish Cancer Society. We thank K. Simons (European Molecular Biology Laboratory) for useful comments on the manuscript, and Yvonne Heinilä for secretarial assistance.

References

1 Rambourg, A., Neutra, M. and LeBlond, C. P. (1966) *Anat. Rec.* 154, 41–71
2 Bretscher, M. S. and Raff, M. C. (1975) *Nature* 258, 43–49
3 Gahmberg, C. G. and Hakomori, S. (1973) *J. Biol. Chem.* 248, 4311–4317
4 Gahmberg, C. G. and Andersson, L. C. (1977) *J. Biol. Chem.* 252, 5888–5894
5 Gahmberg, C. G. (1976) *J. Biol. Chem.* 251, 510–515
6 Gahmberg, C. G., Häyry, P. and Andersson, L. C. (1976) *J. Cell Biol.* 68, 642–653
7 Kornfeld, R. and Kornfeld, S. (1976) *Annu. Rev. Biochem.* 45, 217–237
8 Gahmberg, C. G. (1982) *FEBS Lett.* 140, 93–97
9 Moore, S., Woodrow, C. F. and McClelland, D. B. L. (1982) *Nature* 295, 529–531
10 Gahmberg, C. G. (1983) *EMBO J.* 2, 223–227
11 Cherif-Zahar, B. *et al.* (1990) *Proc. Natl. Acad. Sci. U. S. A.* 87, 6243–6247
12 Avent, N. D., Ridgwell, K., Tanner, M. J. A. and Anstee, D. J. (1990) *Biochem. J.* 271, 821–825
13 Moore, S. and Green, C. (1987) *Biochem. J.* 244, 735–741
14 Agre, P. and Cartron, J-P. (1992) In *Protein Blood Group Antigens of the Human Red Cell* (Agre, P. and Cartron, J-P., eds), pp. 20–52, Johns Hopkins University Press
15 Kornfeld, R. and Kornfeld, S. (1985) *Annu. Rev. Biochem.* 54, 631–664
16 Parodi, A. J., Mendelzon, D. H., Lederkremer, G. Z. and Martin-Barrientos, J. (1984) *J. Biol. Chem.* 259, 6351–6357
17 Stanley, P. and Ioffe, E. (1995) *FASEB J.* 9, 1436–1444
18 Gahmberg, C. G. *et al.* (1976) *J. Biol. Chem.* 251, 6108–6116
19 Degen, E. and Williams, D. B. (1991) *J. Cell Biol.* 112, 1099–1115
20 Ou, W-J., Cameron, P. H., Thomas, D. Y. and Bergeron, J. J. M. (1993) *Nature* 364, 771–776
21 Hammond, C., Braakman, I. and Helenius, A. (1994) *Proc. Natl. Acad. Sci. U. S. A.* 91, 913–917
22 Hebert, D. N., Foellmer, B. and Helenius, A. (1995) *Cell* 81, 425–433
23 Fiedler, K. and Simons, K. (1995) *Cell* 81, 309–312
24 Fiedler, K. and Simons, K. (1994) *Cell* 77, 625–626
25 Eggens, I. *et al.* (1989) *J. Biol. Chem.* 264, 9476–9484
26 Wieland, F. T., Gleason, M. L., Serafini, T. A. and Rothman, J. E. (1987) *Cell* 50, 289–300
27 Guan, J-L., Machamer, C. E. and Rose, J. K. (1985) *Cell* 42, 489–496
28 Scheiffele, P., Peränen, J. and Simons, K. (1995) *Nature* 378, 96–98
29 Paulson, J. C. (1989) *Trends Biochem. Sci.* 14, 272–276
30 Varki, A. (1993) *Glycobiology* 3, 97–130
31 Ashwell, G. and Harford, J. (1982) *Annu. Rev. Biochem.* 51, 531–554
32 Bevilacqua, M. P. and Nelson, R. M. (1993) *J. Clin. Invest.* 91, 379–387
33 Gahmberg, C. G., Kotovuori, P. and Tontti, E. (1992) *Acta Pathol. Microbiol. Immunol. Scand.* 100, 39–52
34 McEver, R. P., Moore, K. L. and Cummings, R. D. (1995) *J. Biol. Chem.* 270, 11025–11028
35 Kelm, S. *et al.* (1994) *Curr. Biol.* 4, 965–972
36 Kotovuori, P. *et al.* (1993) *Glycobiology* 3, 131–136

Carl_G_190x270_mm_blokki_FINAL.indd 196 06-Aug-23 1:53:41 PM

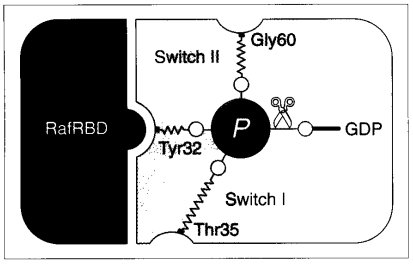

Figure 3
Schematic view of the hydrolysis-induced conformational change and its result on the Ras–Raf interface. Tyr32, Thr35 of switch I and Gly60 of switch II are suggested to be bound to the γ-phosphate by spring-like connections, which release after GTP hydrolysis and dissociation of inorganic phosphate. RBD, Ras-binding domain.

RafRBD, as, for example, the RafRBD structure is similar to that of ubiquitin, which has no sequence similarity to RafRBD either.

Outlook

Although only one three-dimensional structure for a complex between a GTP-binding protein and its effector is available at the moment, the fact that many new effector proteins for Ras and the other subfamily members have been identified, guarantees that we will see a number of additional such structures in the near future. Will they be similar to the Ras–Raf structure? As residues involved in nucleotide binding are conserved amongst GTP-binding proteins and mutations such as those homologous to Q61L and S17N in Ras produce similar biological responses, it was not surprising to find that other Ras-like proteins such as Arf[27,28], Ran[29] and Rab (P. Metcalf, unpublished) have the same overall topology. As mutations in the effector region of other Ras-related proteins block binding or biological effect, it is likely that the basic area of interaction will be similar for the different Ras-related proteins. Studies with Ras[30–32] and with Rho/Rac[33] have shown that, in addition to the effector region, other parts of the protein are involved in the interaction with full-length effectors. In Ran it has been shown that the carboxy-terminal end of the molecule, located far away from the effector site in the three-dimensional structure[29], is involved in binding to the Ran-binding protein 1 (Ref. 34). It has also been found that the activity of Ran-GAP towards Ran is stimulated by the additional binding of the effector Ran-BP1 (Refs 34, 35), whereas on Ras and Rap, the binding of effectors and the respective GAPs are mutually exclusive[15,36]. Some of the Rho effectors and a Ral effector have been predicted to be α-helical proteins and not α,β proteins such as the Ras-binding domain of Raf, or other Raf effectors[36]. Thus, we might anticipate some common and some variable features in the molecular architecture of complexes of GTP-binding proteins with their effectors.

Acknowledgements

We thank F. Schmitz for help with the graphical presentations, R. Mittal for carefully reading the manuscript and G. Horn for her ideas on Fig. 3. We apologize to our colleagues for not citing their original work, owing to space limitations.

References

1 Wittinghofer, A. and Pai, E. (1991) *Trends Biochem. Sci.* 16, 382–387
2 Schweins, T. *et al.* (1995) *Nat. Struct. Biol.* 2, 36–44
3 Downward, J. *et al.* (1990) *Nature* 346, 719–723
4 DePaolo, D. *et al.* (1996) *Mol. Cell. Biol.* 16, 1450–1457
5 Schürmann, A. *et al.* (1996) *J. Biol. Chem.* 270, 28982–28988
6 Block, C. *et al.* (1996) *Nat. Struct. Biol.* 3, 244–251
7 White, M. A. *et al.* (1995) *Cell* 80, 1–20
8 Qiu, R. G. *et al.* (1995) *Nature* 374, 457–459
9 Khosravi-Far, R. *et al.* (1995) *Mol. Cell. Biol.* 15, 6443–6453
10 Joneson, T., White, M. A., Wigler, M. H. and Bar-Sagi, D. (1996) *Science* 271, 810–812
11 Kim, S-H., Privé, G. G. and Milburn, M. V. (1993) in *GTPases in Biology I* (Dickey, B. F. and Birnbaumer, L., eds), pp. 177–194 Springer-Verlag
12 Hall, A. (1994) *Science* 264, 1413–1414
13 Nobes, C. D. and Hall, A. (1995) *Cell* 81, 53–62
14 Feig, L. A. and Cooper, G. M. (1988) *Mol. Cell. Biol.* 8, 2472–2478
15 Wittinghofer, A. and Herrmann, C. (1995) *FEBS Lett.* 369, 52–56
16 Daum, G. *et al.* (1994) *Trends Biochem. Sci.* 19, 474–480
17 Emerson, S. D. *et al.* (1996) *Biochemistry* 34, 6911–6918
18 Nassar, N. *et al.* (1995) *Nature* 375, 554–560
19 Herrmann, C., Martin, G. A. and Wittinghofer, A. (1995) *J. Biol. Chem.* 270, 2901–2905
20 Marais, R., Light, Y., Paterson, H. F. and Marshall, C. J. (1995) *EMBO J.* 14, 3136–3145
21 Dent, P., Reardon, D. B., Morrison, D. K. and Sturgill, T. W. (1995) *Mol. Cell. Biol.* 15, 4125–4135
22 Yamamori, B. *et al.* (1995) *J. Biol. Chem.* 270, 11723–11726
23 Nassar, N. *et al.* (1996) *Nat. Struct. Biol.* 3, 723–729
24 Geyer, M. *et al.* (1996) *Biochemistry* 35, 10308–10320
25 Feig, L. A., Urano, T. and Cantor, S. (1996) *Trends Biochem. Sci.* 21, 438–441
26 Wolthuis, R. M. F. *et al.* (1996) *Oncogene* 12, 353–362
27 Amor, J. C., Harrison, D. H., Kahn, R. A. and Ringe, D. (1994) *Nature* 372, 704–708
28 Greasley, S. E. *et al.* (1995) *Nat. Struct. Biol.* 2, 797–806
29 Scheffzek, K. *et al.* (1995) *Nature* 374, 378–381
30 Brtva, T. R. *et al.* (1995), *J. Biol. Chem.* 270, 9809–9812
31 Hu, C-D. *et al.* (1995), *J. Biol. Chem.* 270, 30274–30277
32 Shirouzu, M. *et al.* (1994), *Oncogene* 9, 2153–2157
33 Diekmann, D. *et al.* (1995), *EMBO J.* 14, 5297–5305
34 Richards, S. A., Lounsbury, K. M. and Macara, I. G. (1995) *J. Biol. Chem.* 270, 14405–14411
35 Bischoff, F. R. *et al.* (1995) *EMBO J.* 14, 705–715
36 McCormick, F. and Wittinghofer A. (1996) *Curr. Opin. Biotechnol.* 7, 449–456

Erratum

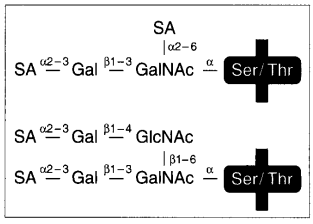

In the August 1996 issue, we published the article entitled 'Why mammalian cell surface proteins are glycoproteins' by Carl Gahmberg and Martti Tolvanen (*TiBS* 21, 308–311). It has been brought to our attention that an error was accidentally introduced during redrawing of Fig. 3. In the structure of both sidechains, the link to the Ser/Thr residue should have been through *N*-acetyl-D-galactosamine (GalNAc) and not through *N*-acetyl-D-glucosamine (GlcNAc). The corrected figure is shown here.

We apologize to the authors and to our readers for this mistake.

Carl_G_190x270_mm_blokki_FINAL.indd 197 06-Aug-23 1:53:41 PM

Carl_G_190x270_mm_blokki_FINAL.indd 198 06-Aug-23 1:53:41 PM

Part III

INTEGRINS, DISCOVERY AND CHARACTERIZATION

Carl_G_190x270_mm_blokki_FINAL.indd 199 06-Aug-23 1:53:41 PM

Introduction

The research projects on cellular changes in transformed fibroblasts, resulted in the discovery of fibronectin in 1973. Later, research groups found that fibronectin is an adhesion molecule (1). This finding led to search for cellular fibronectin receptors in fibroblasts and other cells (2,3). In parallel, studies on platelet (4), and leukocyte adhesion molecules took place. The research groups used a number of techniques to identify the receptors including protein chemistry, affinity chromatography, induction of cell aggregation or adhesion, radioactive surface labelling techniques, and the use of polyclonal and monoclonal antibodies.

In the early part of the 1980,s, I realized that it was important to shift my research from the mere identification and characterization of cell surface proteins to functional aspects. After the discovery of fibronectin and its role in cell adhesion, an obvious possibility was to begin to study leukocyte surface molecules, and their involvement in cell - cell interactions. The collaboration with Leif Andersson was very important. He had an impressive knowledge of leukocyte biology, and knew how to isolate different leukocytes. Early studies on the cell surface glycoproteins of human leukocytes, showed that the cells express a number of previously unknown surface glycoproteins (Paper 9). The promyelocytic cell line HL-60, was functionally relatively inactive, but when differentiated towards granulocytes, it acquired phagocytic and chemotactic activities, and the concomitant expression of cell surface proteins similar to those of normal granulocytes (Paper 11). Other groups identified leukocyte surface proteins, associated with various leukocyte functions, and lacking from leukocytes of patients with genetically determined immunologic deficiencies. LFA-1 and Mac-1 were protein that were found to be involved in a number of functions, but the reason for the malfunctions was not clear (5,6). Several groups studied the same proteins, but under various names, and this is still a problem. We used the name Leu-Cam (Leukocyte cell adhesion molecule) to point out the function, and immunologists preferred the CD (Cluster of Differentiation) nomenclature. The following names are used: CD11a/CD18 (LFA-1, $\alpha L\beta 2$), CD11b/CD18 (Mac-1, $\alpha M\beta 2$), CD11c/CD18 (p150/95, $\alpha X\beta 2$) and CD11d/CD18 ($\alpha D\beta 2$).

Manuel Patarroyo introduced the use of phorbol esters to induce leukocyte aggregation (7). He joined my group as a postdoctoral fellow, and we tested a large number of monoclonal antibodies, reacting with intact leukocytes, whether any could inhibit the phorbol ester induced aggregation. One of the tested antibodies (60.3) (8), efficiently inhibited the induced aggregation of T cells and granulocytes. Immunoprecipitation of surface labelled cells resulted in the Leu-Cam protein dimers. These experiments definitely showed that the molecules identified were cell adhesion proteins.

It soon became apparent that the receptors in different cells including fibroblasts, leukocytes and platelets were similar. After cloning and sequencing, a new protein family was identified. Richard Hynes named the receptors *integrins*, according to their ability to functionally and structurally

Carl_G_190x270_mm_blokki_FINAL.indd 200 06-Aug-23 1:53:41 PM

connect their cell surface domains with the cytoplasmic domains (9). The integrins are large protein heterodimers consisting of α- and β-chains. Several reviews on integrins, have been written (9-15). Structural studies showed that in resting cells, the integrin head is turned towards the membrane and upon activation, the integrins straighten out and finally open the binding site (16).

Comments on Papers 26 to 29

I was initially sceptical of using phorbol ester induced aggregation of leukocytes, to identify adhesion receptors. Perhaps the clumping of cells was just due to an unspecific artefact. However, I was wrong. We tested a number of monoclonal antibodies obtained from scientists all over the world. One of the antibodies (60.3) turned out indeed to efficiently prevent adhesion. Because we had the radioactive surface labelling techniques in use, we soon discovered that the antibody target molecules were protein dimers. In 1985, we published the identification of a glycoprotein complex with apparent molecular weights of 160000/90000 from blood mononuclear leukocytes (Paper 26). Soon thereafter, we identified a similar dimer from granulocytes (Paper 27). The same year, and the year after, there began to appear similar findings from other groups using different cells (2-4). B lymphocytes, expressed a similar protein complex as T cells (17). In collaboration with Jim Schröder we made an integrin β2-chain monoclonal antibody, which turned out excellent for purification of large amounts of leukocyte integrins (18). This was possible because we got several kilograms of packed leukocytes, which were used for interferon production at the Finnish Red Cross Blood Centre. The purified integrins, were used for making new monoclonal antibodies. One of them (7E4) turned out to efficiently inhibit leukocyte adhesion, and another one (1D10) was excellent for blotting analysis of the β2-chain (19). Using lymphocyte hybrids between a mouse thymoma and human lymphocytes, we assigned the gene for β2 to chromosome 21 (20). In collaboration with Japanese scientists, we studied the carbohydrate chains of the leukocyte β2-integrins (Paper 28). The N-glycosidic oligosaccharides included both high mannose chains and complex type chains. We then found that E-selectin in fact binds to the sugar chains of β2-integrins (Paper 29). The fact that E-selectin binds to leukocyte integrins is interesting, but whether the binding is functionally important, we still do not know.

References

1. Akiyama, S.K., Yamada, K.M. and Hayashi, M. (1981) The structure of fibronectin and its role in cellular adhesion. *J. Supramol. Struct. Cell Biochem.* **16**, 345-348.
2. Pytela, R., Pierschbacher, M.D. and Ruoslahti, E. (1985) Identification and isolation of a 140 kD cell surface glycoprotein with properties expected of a fibronectin receptor. *Cell* **40**, 191-198.
3. Tamkun, J.W., DeSimone, D.W., Fonda, D., Patel, R.S., Buck, C., Horwitz, A.F. and Hynes, R.O. (1986) Structure of integrin, a glycoprotein involved in the transmembrane linkage between fibronectin and actin. *Cell* **46**, 271-282.
4. Charo, I.F., Fitzgerald, L.A., Steiner, B., Rall, S.C.Jr., Bekeart, L.S. and Phillips, D.R. (1986) Platelet glycoproteins IIb and IIIa: Evidence for a family of immunologically and structurally related glycoproteins in mammalian cells. *Proc. Natl. Acad. Sci. USA.* **83**, 8351-8355.

Carl_G_190x270_mm_blokki_FINAL.indd 201 06-Aug-23 1:53:41 PM

5. Sanchez-Madrid, F., Nagy, J.A., Robbins, E., Simon, P.A. and Springer, T.A. (1983) A human leukocyte differentiation antigen family with distinct alpha subunits and a common beta subunit. The lymphocyte function associated antigen (LFA-1), the C3bi complement receptor (OKM1/Mac-1), and the p150,95 molecule. *J. Exp. Med*. **158**, 1785-1803.
6. Dana, N., Todd, R.F. III, Pitt, J., Springer, T.A. and Arnaout, M.A. (1984) Deficiency of a granulocyte surface glycoprotein (Mo1) in man. *J. Clin. Invest*. **73**, 153-159.
7. Patarroyo, M., Yogeeswaran, G., Biberfeld, P., Klein, E. and Klein, G. (1982) Morphological changes, cell aggregation and cell membrane alterations caused by phorbol 12,13-dibutyrate in human blood lymphocytes. *Int. J. Cancer* **30**, 707-717.
8. Beatty, P.G., Ledbetter, J.A., Martin, P.S., Price, T.H. and Hansen, J.A. (1983) Definition of a common leukocyte cell-surface antigen (Lp 95-150) associated with diverse cell-mediated immune functions. *J. Immunol*. **131**, 2913-2918.
9. Hynes, R.O. (1987) Integrins: a family of cell surface receptors. *Cell* **48**, 549-554.
10. Arnaout, M.A. (1990) Structure and function of the leukocyte adhesion molecules CD11/CD18. *Blood* **75**, 1037-1050.
11. Springer, T.A. (1990) Adhesion receptors of the immune system. *Nature* **346**, 425-434.
12. Gahmberg, C.G., Tolvanen, M. and Kotovuori, P. (1997) Leukocyte adhesion. Structure and function of human leukocyte β2-integrins and their cellular ligands. *Eur. J. Biochem*. **245**, 215-232.
13. Moser, M., Legate, K.R., Zent, R. and Fässler, R. (2009) The tail of integrins, talin and kindlins. *Science* **324**, 895-899.
14. Bachmann, M., Kukkurainen, S., Hytönen, V.P. and Wehrle-Haller, B. (2019) Cell adhesion by integrins. *Physiol. Rev*. **99**, 1655-1699.
15. Gahmberg, C.G., Grönholm, M., Madhavan, S., Jahan, F., Mikkola, E., Viazmina, L. and Koivunen, E. (2019) Regulation of cell adhesion- a collaborative effort of integrins, their ligands, cytoplasmic actors and phosphorylation. *Quarterly Rev. Biophys*. **52**:e10,1-24.
16. Xiong, J.-P., Stehle, T., Diefenbach, B., Zhang, R., Dunker, R., Scott, D.I., Joachimiak, A., Goodman, S.L. and Arnaout, M.A. (2001) Crystal structure of the complete integrin αVβ3. *Science* **294**, 339-345.
17. Patarroyo, M., Beatty, P.G., Nilsson, K. and Gahmberg, C.G. (1986) Identification of a cell surface glycoprotein mediating cell adhesion in EBV immortalized normal B cells. *Int. J. Cancer* **38**, 539-547.
18. Kantor, C., Suomalainen-Nevanlinna, H., Patarroyo, M., Österlund, K., Bergman, T., Jörnvall, H., Schröder, J. and Gahmberg, C.G. (1988) Purification in large scale and characterization of the human leukocyte adhesion glycoprotein GP90 (CD18). *Eur. J. Biochem*. **170**, 653-659.
19. Nortamo, P., Patarroyo, M., Kantor, C., Suopanki, J. and Gahmberg, C.G. (1988) Immunological mapping of the human leukocyte adhesion glycoprotein gp90 (CD18) by monoclonal antibodies. *Scand. J. Immunol*. **28**, 537-546.
20. Suomalainen, H.A., Gahmberg, C.G., Patarroyo, M., Beatty, P.G. and Schröder, J. (1986) Genetic assignment of GP90, leukocyte adhesion glycoprotein to human chromosome 21. *Somat. Cell Mol. Genet*. **12**, 297-302.

Carl_G_190x270_mm_blokki_FINAL.indd 202 06-Aug-23 1:53:41 PM

Scand. J. Immunol. **22,** 171–182, 1985

Identification of a Cell Surface Protein Complex Mediating Phorbol Ester-Induced Adhesion (Binding) among Human Mononuclear Leukocytes

M. PATARROYO, P. G. BEATTY, J. W. FABRE & C. G. GAHMBERG

Department of Immunology, Karolinska Institute, Stockholm, Sweden; Fred Hutchinson Cancer Research Center, University of Washington, Seattle, Washington, USA; Blond McIndoe Centre, Queen Victoria Hospital, East Grinstead, West Sussex, UK; and Department of Biochemistry, University of Helsinki, Helsinki, Finland

Patarroyo, M., Beatty, P.G., Fabre, J.W. & Gahmberg, C.G. Identification of a Cell Surface Protein Complex Mediating Phorbol Ester-Induced Adhesion (Binding) among Human Mononuclear Leukocytes. *Scand. J. Immunol.* **22,** 171–182, 1985.

Phorbol esters rapidly induce aggregation of human mononuclear leukocytes in vitro. Previous studies have indicated that cell surface proteins are involved. We report now that the monoclonal antibody 60.3, either as purified IgG or as Fab′ fragments, to an antigen common to leukocytes completely inhibited the phorbol ester-induced intercellular adhesion (binding). No inhibition of cell aggregation was observed with monoclonal antibodies to common leukocyte antigen T 200, T-cell-associated antigen, monocyte–granulocyte antigen, brain granulocyte–T-lymphocyte antigen, transferrin receptor, mature T-cell antigens (mol.wt either 67,000 or 19,000/29,000), T helper/inducer cell antigen, sheep erythrocyte receptor, class I or class II antigens, or T cytotoxic/suppressor cell antigen. The antibody 60.3 did not inhibit stimulation of the cells since the characteristic phorbol ester-induced morphological changes and phorbol ester-enhanced cap formation of membrane glycoproteins were readily observed. Two major cell surface polypeptides with apparent molecular weights of 90,000 and 160,000 were immunoprecipitated. We conclude that this protein complex, or at least one of its components, mediates adhesion among mononuclear leukocytes.

Manuel Patarroyo, Department of Immunology, Karolinska Institute, S-104 01 Stockholm 60, Sweden

Intercellular adhesion (binding) is a fundamental process in the physiology of multicellular organisms [39]. In the immune system interactions between mononuclear leukocytes, mainly lymphocytes and monocytes/macrophages, are essential for function and regulation. Some of these interactions are mediated by soluble factors such as interleukins and immunoglobulins, but in other cases interaction requires physical contact and adhesion between the cells, a phenomenon that is poorly understood [4].

Phorbol esters, such as tetradecanoyl phorbol acetate (TPA) and phorbol dibutyrate ($P(Bu)_2$), have been shown to affect the morphology and physiology of lymphocytes and monocytes [38]. In general, these compounds induce or modulate growth, maturation, and various functions of the cells, and have the plasma membrane as a major target [13, 30, 57].

In a previous study it was observed that TPA increased adhesion between human blood lymphocytes and cells from lymphoblastoid lines [45]. Similarly, nanomolar concentrations of $P(Bu)_2$ were found to induce morphological changes and aggregation of human blood mononuclear cells (a T-cell-enriched population with few monocytes suspended in serum-free medium) within a few minutes of treatment [49]. These observations resulted in an experimental model that was developed to analyse adhesion among mononuclear leukocytes. Further studies indicated that phorbol ester-induced intercellular binding was energy- and temperature-dependent and required extracellular divalent cations

Carl_G_190x270_mm_blokki_FINAL.indd 203 06-Aug-23 1:53:41 PM

(mainly Mg^{2+} but also Ca^{2+}), functional microfilaments, and the possible participation of an esterase (protease) and protein kinase C. Cell surface proteins but not protein synthesis was needed. Calmodulin-dependent processes, microtubules, phospholipid methylation, intracellular levels of cAMP or cGMP, or protein secretion did not seem to be involved. Interestingly, not all lymphoid subpopulations participated simultaneously, and adhesion among lymphocytes and lymphocytes-monocytes was usually observed [18, 46, 48; Patarroyo *et al.*, to be published]. Since mediation of a passive bridging between the cells by $P(Bu)_2$ could be ruled out, it was concluded that phorbol esters were inducing a cell-adhesive (binding) phenotype in certain mononuclear leukocytes and that cell surface structures such as cell adhesion (binding) molecules were mediating the intercellular binding.

Adhesion among other cell types has been studied by various groups. Different cell adhesion molecules have been identified in slime mould [40] and in several tissues of vertebrate organisms [5, 42, 56, 58]. Among these cell surface proteins the neural cell adhesion molecule (N-CAM) and the liver cell adhesion molecule (L-CAM) are the best characterized [17]. Antibodies to cell surface structures enabled these molecules to be identified by blocking the intercellular binding. In the present study a similar approach was used to identify cell adhesion molecules of mononuclear leukocytes by testing the effect of monoclonal antibodies on cell surface proteins. Only the antibody 60.3, which reacts with a cell surface antigen expressed by most peripheral blood and bone marrow leukocytes [6], completely inhibited the intercellular adhesion without affecting stimulation of the cells by phorbol esters. Since this antibody precipitated two major cell surface polypeptides with apparent molecular weights of 90,000 and 160,000, we conclude that this protein complex or at least one of its components mediates adhesion among mononuclear leukocytes.

MATERIALS AND METHODS

Monoclonal antibodies and other reagents. The antibodies used are described in Table I. Antibodies T 29/33 and TA-1 were obtained from Hybritech Inc. (San Diego, Calif., USA); OKM1 and OKT9 were purchased from Ortho Diagnostic Systems (Raritan, N.J., USA); NEI-015, NEI-039, and NEI-037 from New England Nuclear (Boston, Mass., USA); anti-Leu 3a, anti-Leu 5, and anti-HLA-DR from Becton Dickinson (Mechelen, Belgium); and W 6/32 from Sera-Lab (London, UK). Monoclonal antibodies 60.3 and F 10-44-2 were produced as previously described [6, 14]. All antibodies were dialysed against water for 48 h at 4°C to remove NaN_3. Thereafter they were lyophilized and resuspended in phosphate-buffered saline (PBS) to obtain a stock concentration of 400 μg/ml. 4β-Phorbol 12,13-dibutyrate ($P(Bu)_2$) (Sigma Chemical Co., St Louis, Mo., USA) was dissolved in dimethyl sulphoxide (DMSO) and stored at −20°C. $P(Bu)_2$ was added to cells to a final concentration of 60 nM. The final concentration of DMSO was less than 0.05%.

Mononuclear leukocyte preparation. A T-lymphocyte-enriched fraction from heparinized blood of healthy donors was used. This population consisted of 90% T cells, most with the helper/inducer phenotype, and a few monocytes (Table I). Less than 1% of the cells were B lymphocytes (data not shown). After Ficoll (Pharmacia, Uppsala, Sweden)–Isopaque (Nyegaard & Co., Norway) separation [11] and passage through a nylon wool column [26], the cells were resuspended in RPMI 1640 medium (Grand Island Biological Co., Grand Island, N.Y., USA).

Measurement of cell aggregation. Cell suspension aliquots of 0.5 ml (10×10^6 cells/ml) in 24-well tissue culture plates (Costar, Cambridge, Mass., USA) were rotated in a gyratory shaker (Model G 2, New Brunswick Scientific Co., Edison, N.J., USA) at 100 rpm at 37°C. After a 10-min delay to enable warming of the cells, $P(Bu)_2$ (60 nM was added. Twenty minutes later, the cell suspension was briefly inspected in an inverted microscope (Diavert, Leitz, Mainz, FRG) and suspended by pipetting ten times before the percentage of aggregated cells was determined in a hemocytometer with a Laborlux K microscope (Leitz) at ×400 magnification. The suspension was also inspected before treatment, and a control sample was incubated without $P(Bu)_2$. At least 5×10^2 cells were counted in each sample. $P(Bu)_2$-induced intercellular adhesion ($P(Bu)_2$ aggr) was calculated as the percentage of aggregated cells in the $P(Bu)_2$-treated sample minus the percentage of aggregated cells in the control sample, both read after 20 min. The effect of 13 monoclonal antibodies on the cell aggregation was tested. The cells were incubated with antibody (either IgG or Fab′ fragments) at concentrations ranging from 2 ng to 20 μg/ml for 20 min at room temperature and for 10 min more at 37°C before being shaken and treated with phorbol ester. Unbound antibodies were also present during $P(Bu)_2$ treatment. The effect of the antibodies (inhibition) was expressed as:

$$\frac{\%\ P(Bu)_2\ \text{aggr in control sample} - P(Bu)_2\ \text{aggr in presence of antibody}}{\%\ P(Bu)_2\ \text{aggr in control sample}} \times 100.$$

Usually, percentage $P(Bu)_2$ aggr in the control sample was around 30%. Each antibody was tested at least twice.

Carl_G_190x270_mm_blokki_FINAL.indd 204 06-Aug-23 1:53:42 PM

TABLE I. List and characteristics of monoclonal antibodies and their reactivity with mononuclear leukocytes

Monoclonal antibody	Murine IgG subclass	Human cell surface antigen	Molecular weight of immunoprecipitated proteins (daltons)	Antigen-positive cells (%; mean±SD)	References
T 29/33	IgG2b	Common leukocyte antigen (T 200)†	200,000	98.7±0.5	43
TA-1	IgG2a	T-cell-associated antigen	170,000/95,000	96.0±1.6	34
OK M1	IgG2b	Monocyte/granulocyte antigen	165,000/95,000	7.0±2.9‡	10
60.3	IgG2a	Common leukocyte surface antigen (Lp 95-150)	95,000/130,000/150,000	98.0±0.8	6
F 10-44-2	IgG2a	Brain granulocyte T-lymphocyte antigen	105,000	98.3±0.5	14
OKT9	IgG1	Transferrin receptor	94,000	1±0.0	55
NEI-015	IgG2a	Mature T-cell antigen (T1)	67,000	88.3±8.1	37
Anti-Leu 3a	IgG1	Leu 3a (T4), T helper/inducer cell antigen	55,000	65.0±5.0	19
Anti-Leu 5	IgG1	Leu 5 (T11) or sheep erythrocyte receptor	45,000–50,000	93.7±1.7	24
W 6/32	IgG2a	HLA-A, -B, -C shared determinant (class I antigen)	43,000	99.0±0.0	44
NEI-039	IgG2a	Cytotoxic/suppresor T cell (antigen T8)	32,000–45,000	40.7±10.7	35
Anti-HLA-DR	IgG2a	HLA-DR, nonpolymorphic (class II antigen)	28,000–34,000	9.3±1.9	32
NEI-037	IgG	Mature T-cell antigen (T3)	19,000–29,000	89.3±3.1	35
None	–	–	–	<1	

*Apparent molecular weight under reducing conditions. †Other names given to the immunoprecipitated molecule are in parentheses.
‡A very weak staining was also observed in 20% of the cells.

Preparation of Fab fragments. Univalent antibody fragments were prepared from the F 10-44-2 and 60.3 antibodies by papain digestion as follows. The enzyme (P 3125; Sigma Chemical Co.) was incubated with the antibody in a 1:100 ratio for 4 h at 37°C in the presence of 10 mM cysteine (Sigma) and 2 mM ethylenediaminetetraacetic acid (EDTA) (Kebo, Stockholm, Sweden) in 0.1 M phosphate buffer, pH 8.0. To inactivate any papain left, cysteine and EDTA were removed by dialysis against 0.005 M phosphate buffer for 48 h at 4°C. After additional dialysis against 0.1 M phosphate buffer, pH 8.0, the dialysate was applied to a protein A-Sepharose column (Pharmacia) previously equilibrated with the same buffer to remove Fc fragments or undigested IgG. The eluted fraction was thereafter lyophilized and resuspended in PBS to a concentration of 400 μg/ml.

Indirect immunofluorescence and morphological studies. Cells were stained with the antibodies by indirect immunofluorescence by using either fluorescein-conjugated rabbit anti-mouse Ig or goat anti-mouse IgG (Fc) (Nordic Immunology, Tilburg, The Netherlands) as the second step reagent. Incubation with the antibodies was done at room temperature. After being stained the cells were treated with glycerol and observed in a Leitz Fluorescence microscope (Schott, FRG). Morphological changes were studied by light microscopy at magnifications higher than ×320. To study the effect of antibody 60.3 on the phorbol ester-induced morphological changes, the cells were preincubated with 20 μg/ml of Fab′ fragment from the antibody and treated with $P(Bu)_2$ in the presence of the antibody. Photomicrographs were taken with a Wild microscope camera (Heerbrugg, Switzerland), using a Plus X pan (Kodak, Rochester, N.Y., USA) film.

Measurement of cap formation. Ten million cells in 1 ml of medium were preincubated with 20 μg of Fab′ fragments from antibody 60.3 at room temperature for 20 min. After 10 min of warming at 37°C the cell suspension was exposed to fluorescein-conjugated concanavalin A (Con A) (50 μg/ml; Sigma) and divided into two fractions. $P(Bu)_2$ (60 nM) was added to one of them, and both fractions were incubated at 37°C for 20 min. When antibody T 29/23 was used as a ligand, unbound antibody was removed by washing the cells twice, and goat anti-mouse IgG (Fc) was used as the second step reagent. The capping reaction was terminated by fixing the cells with 10% formaldehyde (Merck, Darmstad, FRG) for 10 min at 37°C. The cells were then washed twice with PBS containing 10% formaldehyde and examined microscopically. The distribution of fluorescent Con A or antibodies on the cell was observed in a Leitz fluorescence microscope. At least 200 cells were counted per sample at ×1250 magnification. Cells exhibiting polar fluorescence were scored as capped cells (% capped cells). $P(Bu)_2$-enhanced capping (%$P(Bu)_2$ capping) was calculated as the percentage capped cells in the $P(Bu)_2$-treated sample minus the percentage capped cells in the untreated sample, both read after 20 min.

Cell surface labelling, immunoprecipitation, and gel electrophoresis. Cells were surface-labelled with ^{125}I by the glucose oxidase–lactoperoxidase procedure [25] or

Carl_G_190x270_mm_blokki_FINAL.indd 205 06-Aug-23 1:53:42 PM

with ^{3}H after periodate oxidation [20]. Immunoprecipitation was performed as described previously, using rabbit anti-mouse Ig (Dako, Copenhagen, Denmark) in the second step [21]. Polyacrylamide slab gel electrophoresis in the presence of sodium dodecyl sulphate was done in accordance with Laemmli [31], using 8% acrylamide gels. The ^{3}H-labelled gels were treated for fluorography in accordance with Bonner & Laskey [9]. ^{14}C-labelled standard proteins were obtained from the Radiochemical Center (Amersham, UK).

RESULTS

Effect of monoclonal antibodies to cell surface antigens on the phorbol ester-induced cell aggregation

The effect of 13 monoclonal antibodies on $P(Bu)_2$-induced cell aggregation was tested. The percentage of antigen-positive cells in the cell preparation is shown in Table I. The mean value of $P(Bu)_2$-induced aggregation was 28.8% of aggregated cells (29.9% in the $P(Bu)_2$-treated sample minus 1.0% in the control (untreated) sample). None of the antibodies except 60.3 exerted inhibition of cell aggregation at concentrations as high as 20 μg/ml (Fig. 1). Slight enhancement of cell–cell binding was observed with antibodies to cytotoxic/suppressor T-cell antigen (T8) and common leukocyte antigen (T200). Antibody 60.3 inhibited intercellular adhesion in a concentration-dependent manner (Fig. 1). Fifty per cent inhibition was obtained with approximately 150 ng/ml. A few cell aggregates (less than 9% of the cells) were observed in control (untreated) samples in the presence of antibodies to cytotoxic/suppressor

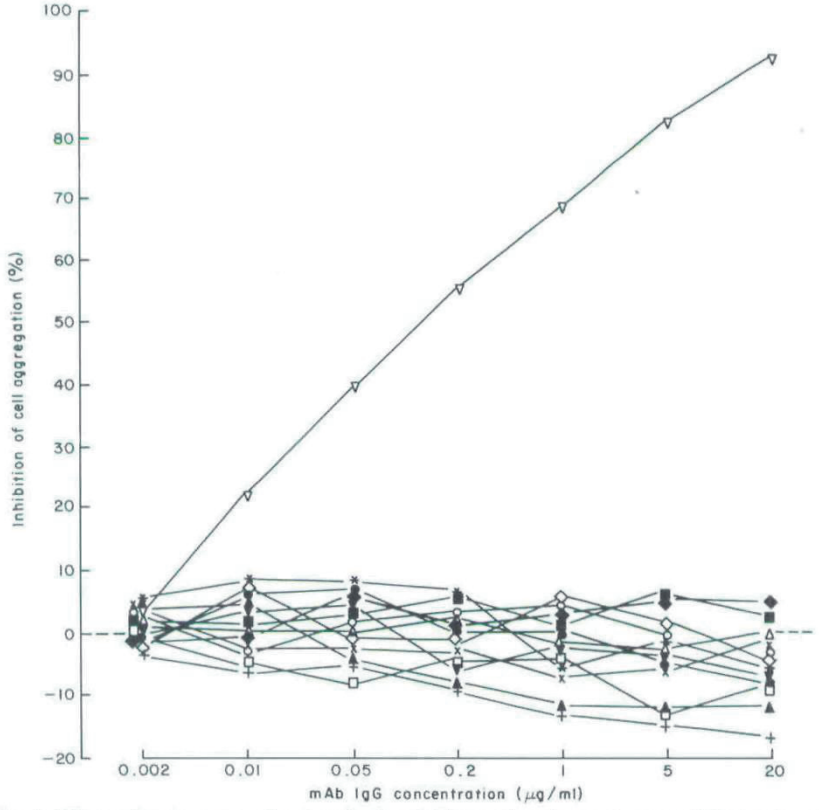

FIG. 1. Effects of various monoclonal antibodies (IgG) to cell surface antigens on $P(Bu)_2$-induced aggregation of mononuclear leukocytes. The following antibodies were used: T 29/32 (▲), TA-1 (▼), OKM1 (△), 60.3 (▽), F 10-44-2 (●), OKT9 (○), NEI-015 (■), anti-Leu 3a (□), anti-Leu 5 (◆), W 6/32 (◇), NEI-039 (+), anti-HLA-DR (×), and NEI-037 (*).

Carl_G_190x270_mm_blokki_FINAL.indd 206 06-Aug-23 1:53:42 PM

T-cell antigen (T8), mature T-cell antigen (T3), Leu 3a (T4), T-cell-associated antigen, and common leukocyte antigen (T200) (data not shown.)

To avoid any possible artefact due to the divalency of the antibody or its Fc portion, Fab′ fragments from antibodies 60.3 and F 10-44-2 were prepared. The antibody activity of these fragments and the lack of Fc portion is shown in Table II. Fab′ fragments prepared from antibody 60.3 but not from antibody F 10-44-2 inhibited the cell aggregation in a concentration-dependent manner (Fig. 2). About 75 ng/ml was needed to inhibit 50% of the intercellular binding. Inhibition of aggregation was observed not only after 20 min of treatment with $P(Bu)_2$ but also after 24 h of incubation with the phorbol ester, when cell aggregates are much larger (Fig. 3).

TABLE II. Determination of antibody activity and presence of Fc portion in papain-digested preparations from antibodies 60.3 and F 10-44-2

Monoclonal antibody	Papain digestion*	Fluorescein-conjugated reagent	Percentage positive cells
60.3	−	Anti-Ig (1:20)†	96
	−	Anti-Fc (γ) (1:20)	95
	+	Anti-Ig (1:20)	95
	+	Anti-Fc (γ) (1:20)	<1
F 10-44-2	−	Anti-Ig (1:20)	95
	−	Anti-Fc (γ) (1:20)	96
	+	Anti-Ig (1:20)	94
	+	Anti-Fc (γ) (1:20)	<1
None		Anti-Ig (1:20)	<1
		Anti-Fc (γ) (1:20)	<1

*Papain digestion was performed as described in Materials and Methods.

†Antiserum dilution in parentheses.

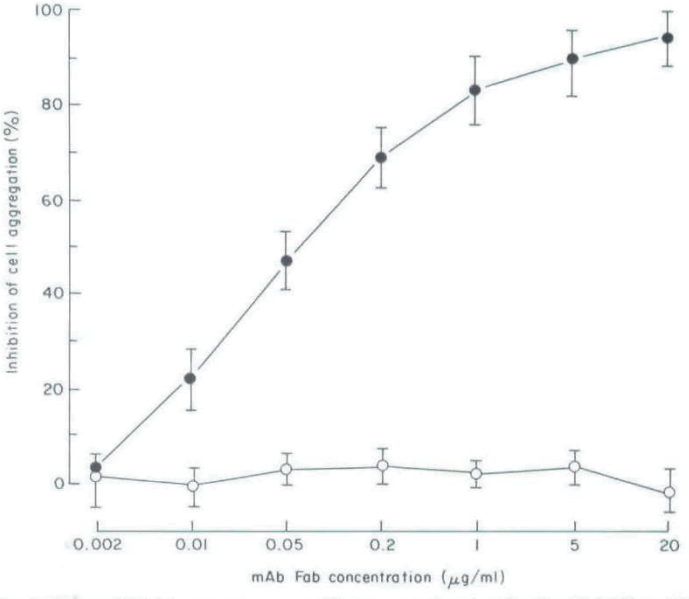

FIG. 2. Effect of Fab′ fragments prepared from monoclonal antibodies 60.3 (●) and F 10-44-2 (○) on $P(Bu)_2$-induced aggregation of mononuclear leukocytes. Mean values and standard deviations of three experiments are shown.

Carl_G_190x270_mm_blokki_FINAL.indd 207 06-Aug-23 1:53:42 PM

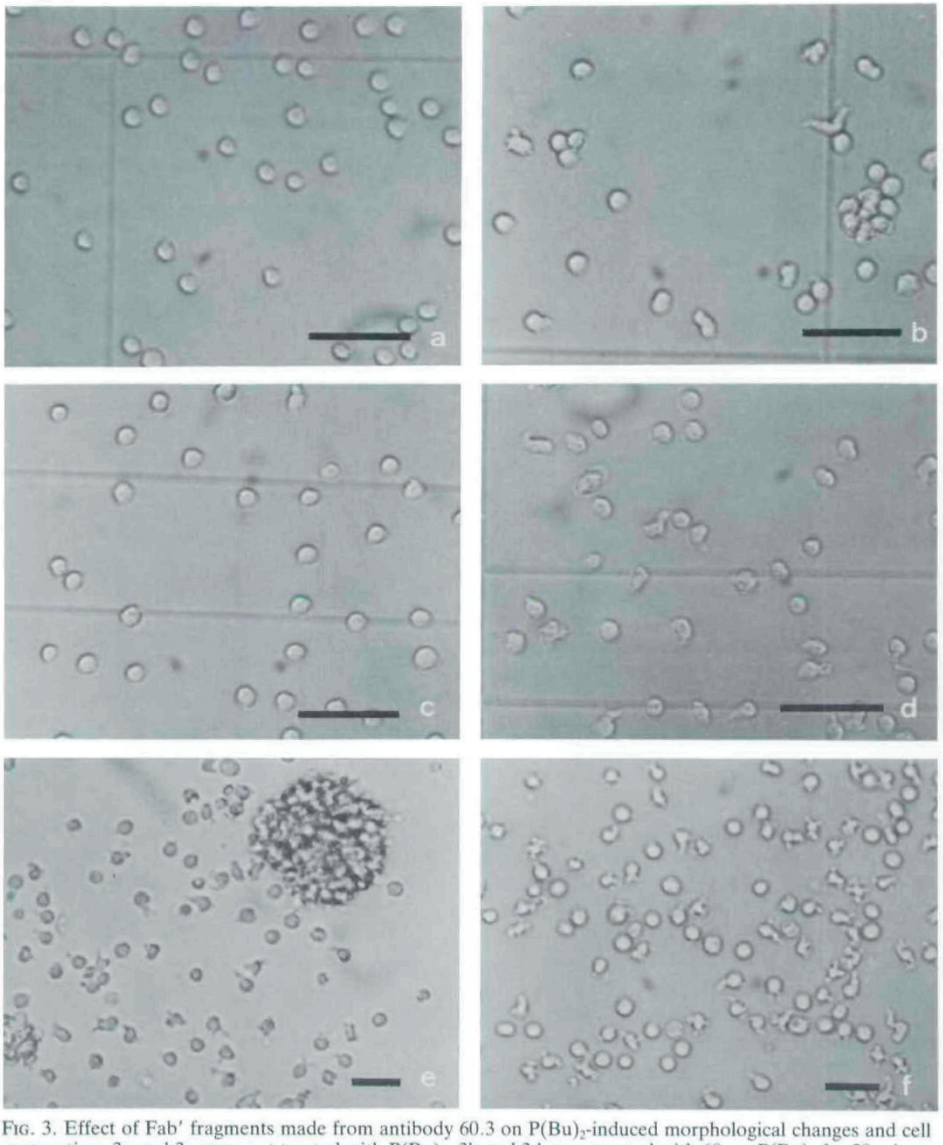

FIG. 3. Effect of Fab′ fragments made from antibody 60.3 on $P(Bu)_2$-induced morphological changes and cell aggregation. 3a and 3c were not treated with $P(Bu)_2$. 3b and 3d were treated with 60 nM $P(Bu)_2$ for 20 min at 37°C. 3c and 3d were preincubated with 20 μg/ml of Fab′ fragments. 3a–d were photographed in a conventional microscope (×190 magnification). Both e and f were treated with $P(Bu)_2$ for 24 h at 37°C, but only f was preincubated with the Fab′ fragments. Samples that were not treated with $P(Bu)_2$ and were incubated at 37°C for 24 h with or without antibody resembled a. 3e and f were photographed in an inverted microscope at ×100 magnification. All samples were continuously rotated at 100 rpm. Scale bar=50 μm.

Carl_G_190x270_mm_blokki_FINAL.indd 208 06-Aug-23 1:53:42 PM

TABLE III. Effect of precoating with antibody 60.3 (Fab' fragments) on $P(Bu)_2$-induced cap formation*

Ligand	Precoating with 60.3†	$P(Bu)_2$ treatment	Percentage capped cells‡
Fluorescein-conjugated Con A	No	−	6.5
		+	58.5
	Yes	−	6.5
		+	54.5
Anti-human leukocyte antibody (T 29/33)+fluorescein-conjugated goat anti-mouse IgG (Fc)	No	−	11.0
		+	49.0
	Yes	−	14.0
		+	46.0

*Cap formation was determined as described in Materials and Methods.
†Twenty micrograms of Fab' fragments were added to 10×10^6 cells before $P(Bu)_2$ treatment.
‡One representative experiment out of three.

Effect of monoclonal antibody 60.3 on stimulation (activation) of the cells by phorbol ester

The induction of morphological changes by phorbol esters, an early sign of stimulation, was not affected by preincubation of the cells with high concentrations of Fab' fragments prepared from antibody 60.3 (Fig. 3). The characteristic uropod formation and ruffled membranes were observed in antibody-coated cells after 20 min or 24 h incubation with $P(Bu)_2$.

Another early sign of phorbol ester-induced stimulation, the enhancement of cap formation [47], was also examined in cells treated with Fab' fragments prepared from antibody 60.3. The lateral mobility and polarization of Con A receptors and common leukocyte antigen (T200) were similar in the absence and presence of the Fab' fragments (Table III).

Immunoprecipitation with antibody 60.3

Surface labelling of the mononuclear leukocytes followed by immunoprecipitation and gel electrophoresis showed under reducing conditions two bands with apparent molecular weights of 90,000 and 160,000 (Fig. 4). A third band with a molecular weight of 130,000 was also detected after longer exposure (faintly seen in Fig. 4F). No detectable differences were observed in these bands when untreated and phorbol ester-treated cells were compared (data not shown). F 10-44-2, an antibody control, precipitated a single band with an apparent molecular weight of 85,000. Labelling of these molecules by ^3H after periodate treatment showed that the polypeptides were sialyated.

DISCUSSION

In solid tissues, cell–cell adhesion is involved in organogenesis and morphogenesis but also in intercellular communication and cell growth and differentiation control [23]. In the immune system monocytes/macrophages and dendritic cells cooperate with lymphocytes, and T-cell subsets (helper, suppressor, and cytotoxic) interact with each other and with B cells. The participation of cell–cell binding in the intercellular communication is poorly understood. Interestingly, the adhesion, also referred to as intercellular adherence, binding, attachment, cohesion, conjugation, and physical contact, is associated with stimulation (activation) of these cells. When single and 'resting' mononuclear leukocytes from immunized donors are incubated with the soluble antigen, the cells interact in aggregates (clusters) [41, 50]. Certain lectins also activate lymphocytes, and the stimulation is accompanied by an increasing tendency of the cells to aggregate [36]. However, molecular bridging between the antigen and the antigen receptor or passive bridging mediated by the lectin between the cells cannot completely explain the cell aggregation.

In contrast to antigens and lectins, phorbol ester does not seem to bind to a cell surface receptor or to cross-link cell surface molecules present on the same cell or on adjacent cells.

Carl_G_190x270_mm_blokki_FINAL.indd 209 06-Aug-23 1:53:42 PM

178 *M. Patarroyo et al.*

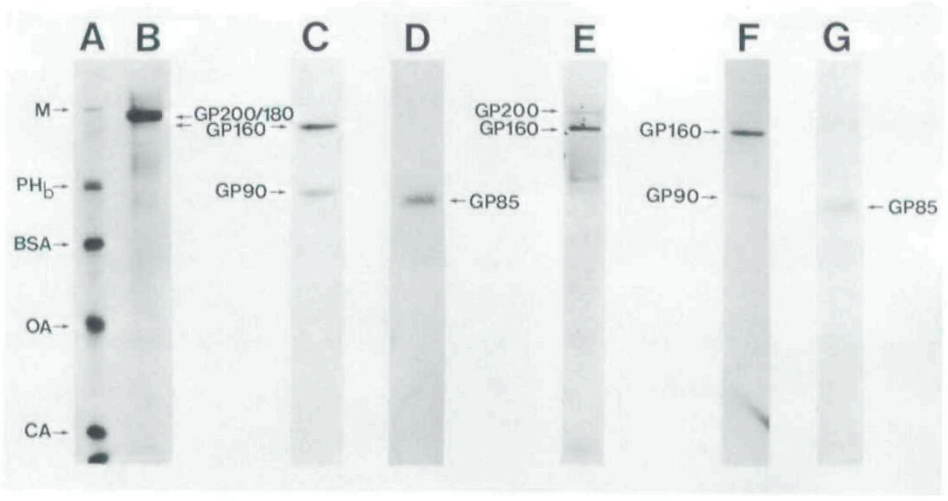

FIG. 4. Polyacrylamide slab gel electrophoresis patterns of ^{125}I- and ^{3}H-labelled surface antigens of mononuclear leukocytes. 4A shows pattern of ^{14}C-labelled standard proteins: M=myosin; PH_b=phophorylase b; BSA=bovine serum albumin; OA=ovalbumin; CA=carbonic anhydrase. 4B–D show ^{125}I-labelled and E–G ^{3}H-labelled cell surface proteins; B, pattern of surface-labelled mononuclear leukocytes; C, pattern obtained by precipitation with antibody 60.3; D, pattern obtained with antibody F 10-44-2; E, pattern of surface-labelled mononuclear leukocytes; F, pattern obtained by precipitation with antibody 60.3; G, pattern obtained with antibody F 10-44-2. GP 200=cell surface glycoprotein with an apparent molecular weight of 200,000, etc.

Specific phorbol ester receptors, identified with $[^{3}H]P(Bu)_2$, have been described in many cell types including lymphocytes [15, 53]. Recently, a phorbol ester receptor was solubilized and purified [2]. Protein kinase activity copurified with the receptor, and all attempts to resolve the enzymatic activity from the receptor were unsuccessful. The isolated receptor required phospholipid and Ca^{2+} for maximal protein kinase activity, a characteristic of protein kinase C [3]. Another report indicated that TPA directly activates protein kinase C, which was isolated from rat brain cytosol [12]. Together, the results strongly suggest that phorbol ester receptor and protein kinase C comprise the same molecular entity. TPA is able to substitute for the endogenous activator of the enzyme, diacylglycerol, which is transiently formed during turnover of phosphatidyl inositol after stimulation of the cell surface. Since phorbol esters are lipophilic, they probably penetrate the plasma membrane easily, and once inside, they bind to protein kinase C. This system, in which the receptor is on the inner surface of the plasma membrane or in the cytosol, is unusual [27] and makes phorbol esters very suitable compounds for studying interactions between cell surfaces such as cell–cell adhesion.

Cell-mediated cytotoxicity, either by cytotoxic T cells or natural killer cells, requires adhesion between effector and target cells [51], and intercellular binding needs surface proteins [22, 48]. Monoclonal antibodies to T4, Leu 2a (T8), sheep erythrocyte receptor, class II antigen, lymphocyte function-associated antigen-1 (LFA-1), LFA-2, and LFA-3 have been reported to inhibit cell conjugate formation [1, 8, 28, 33, 54]. However, identification of cell adhesion molecules in the cell conjugation (either effector to target or similar models) is very difficult because of the complexity of this assay, in which two cell surfaces with many different proteins interact sequentially. Moreover, the target is usually an activated and abnormal cell that has been kept in culture for years. Our results do not support the idea that T4, T8, sheep erythrocyte receptor, or class II antigens are directly involved in intercellular adhesion. LFA-2 and OKT11 appear to recognize the same molecule [29]. However, the possibility that different antibodies recognize different epitopes on the same molecule cannot

Carl_G_190x270_mm_blokki_FINAL.indd 210 06-Aug-23 1:53:42 PM

be excluded. It is more likely that these antigens participate in the earliest interaction between cell surface receptors (recognition) or in activation of the plasma membrane but not directly in cell–cell adhesion. The similarities between LFA-1, a leukocyte surface antigen that involves two polypeptides with apparent molecular weights of 95,000 and 177,000 [59], and the proteins precipitated by antibody 60.3 are remarkable and suggest that the two protein complexes are somehow related. Current studies are aimed to comopare their antigenic structures. The participation of LFA-3 in the phorbol ester-induced adhesion is unknown. Although valuable, the information obtained by other groups using the above monoclonal antibodies is fragmentary, since their studies lacked an assay to analyse exclusively intercellular adhesion.

Because of its divalency IgG might induce cross-linking of cell surface antigens and perturb the plasma membrane. On the other hand, bridging between cells through the Fc portion and Fc receptor might occur and affect the cell aggregation. The inhibitory effect of Fab′ fragments made from antibody 60.3 excluded these possibilities and indicated that the antibody blocks a cell surface structure involved in adhesion. However, this structure might not be involved in adhesion itself but in the stimulation of the cells by phorbol esters. Two early signs of phorbol ester stimulation, morphological changes and enhancement of cap formation, were therefore studied in the presence of the antibody. The lack of effect on these phenomena indicated that $P(Bu)_2$ binds to its receptor and that other structures that might be involved in the stimulation process are not affected by the antibody. The capping studies also excluded the possibility that antibody 60.3 was paralysing the plasma membrane or somehow anchoring surface glycoproteins.

Antibody 60.3 precipitated two major cell surface sialopolypeptides with apparent molecular weights of 90,000 and 160,000 and a minor sialopolypeptide with an apparent molecular weight of 130,000. In contrast, antibody F 10-44-2 precipitated a single sialopolypeptide with an apparent molecular weight of 85,000. Differences in the molecular weights when compared with the ones described in the original publications [6, 14] may be due to technical reasons. Precipitation of three chains by antibody 60.3 might be explained by the presence of the epitope on all three components. However, it is more likely that only one polypeptide carries the epitope and the other two are non-covalently associated. This phenomenon has been observed in various cell surface proteins [52].

As in other cell types, adhesion among mononuclear leukocytes appear to require the participation of ligands, or cell adhesion (binding) molecules, in the formation of cell–cell bonds. Since antibody 60.3 inhibits adhesion but not stimulation of the cells, it is very likely that the 90,000–160,000-dalton protein complex, or at least one of its components, constitutes a ligand in the intercellular binding. However, additional molecular studies, some of them in progress, are required to determine precisely the role of each polypeptide in the phenomenon.

Interestingly, antibody 60.3 reacts with T and B lymphocytes, monocytes, and granulocytes, but not with platelets, erythrocytes, or hepatoma cells [6]. It precipitates almost identical polypeptides from lymphocytes and granulocytes [6, 7] and also inhibits aggregation of the latter cells (Pararroyo *et al.*, to be published). Together, these results indicate that the protein recognized by antibody 60.3 is common to different leukocytes and mediates their intercellular adhesion. As an operational term, we use the name leukocytic cell adhesion molecule (Leu-CAM) for the leukocytic ligand forming the bonds between the cells. Previously described cell adhesion molecules have different molecular weights and tissue distribution [17]. Edelman [16] has postulated that tissues may have only a few adhesion molecules, corresponding in number perhaps to the major classes of cells and tissues, and that the adhesive pattern may arise from local surface modulation. The cell adhesive (binding) phenotype of mononuclear leukocytes induced by phorbol esters may well be the result of a surface modulation originated by phosphorylation of Leu-CAM or associated structures.

Cell–cell adhesion may mediate intercellular communication and cooperation, possibly required for proliferation and maturation control in mononuclear leukocytes. In agreement with this, antibody 60.3 inhibited cell-mediated cytotoxicity and T-cell proliferative response [6]. Consequently, absence of the protein complex precipitated by the antibody in leukocytes was associated with abnormal function of the cells [7].

Carl_G_190x270_mm_blokki_FINAL.indd 211 06-Aug-23 1:53:42 PM

ACKNOWLEDGMENTS

The authors want to thank Prof. Hans Wigzell and Dr Mikael Jondal for valuable suggestions and Dr Magnus Gidlund for assistance with the photomicrographs. Manuel Patarroyo was the recipient of the Nordiskt forskarstipendium from Medicinska Forskningsrådet. This project has been supported by the Swedish Cancer Society, the Karolinska Institute, Cancer föreningen i Stockholm, the Academy of Finland, and National Cancer Institute Grant 2R01 CA 26294-04 (to C. G. Gahmberg).

ADDENDUM

In recent experiments dissociation of the cell surface protein complex allowed the localization of the epitope for antibody 60.3 on the 90-kDa polypeptide.

REFERENCES

1 Argwal, N. & Thomas, D. A role for Ia antigens in thymocyte binding by macrophages. *Cell. Immunol.* **84,** 352, 1984.
2 Ashendel, C., Staller, I. & Boutwell, R. Solubilization, purification, and reconstitution of a phorbol ester receptor from the particulate protein fraction of mouse brain. *Cancer Res.* **43,** 4327, 1983.
3 Ashendel, C., Staller, I. & Boutwell, R. Protein kinase activity associated with a phorbol ester receptor purified from mouse brain. *Cancer Res.* **43,** 4333, 1983.
4 Bell, G.I. Cell–cell adhesion in the immune system. *Immunol. Today* **4,** 237, 1983.
5 Bertolotti, R., Rutishauser, U. & Edelman, G. A cell surface molecule involved in aggregation of embryonic cells. *Proc. natn. Acad. Sci. USA* **77,** 4831, 1980.
6 Beatty, P.G., Ledbetter, J.A., Martin, P.S., Price, T.H. & Hansen, J.A. Definition of a common leukocyte cell-surface antigen (Lp 95-150) associated with diverse cell-mediated immune functions. *J. Immunol.* **131,** 2913, 1983.
7 Beatty, P.G., Ochs, H.D., Harlan, S.M., Price, T.H., Rosen, H., Taylor, R.F., Hansen, J.A. & Klebanoff, S.J. Absence of monoclonal antibody defined protein complex in boy with abnormal leukocyte function. *Lancet* **1,** 535, 1984.
8 Biddison, W.E., Rao, P., Talle, M.A., Goldstein, G. & Shaw, S. Possible involvement of the T4 molecule in T cell recognition of class II HLA antigens. Evidence from studies of CTL-target cell binding. *J. exp. Med.* **159,** 783, 1984.
9 Bonner, W.M. & Laskey, R.A. A film detection method for tritium-labeled proteins and nucleic acids in polyacrylamide gels. *Eur. J. Biochem.* **46,** 83, 1974.
10 Bread, J., Reinherez, E.L., Kung, P.C., Goldstein, G. & Schlossman, S.J. A monoclonal antibody reactive with human peripheral blood monocytes. *J. Immunol.* **124,** 1943, 1980.
11 Böyum, A. Isolation of mononuclear cells and granulocytes from human blood. Isolation of mononuclear cells by one centrifugation and of granulocytes by combining centrifugation and sedimentation. *Scand. J. clin. Lab. Invest.* Suppl. **21,** 77, 1968.
12 Castagna, M., Takai, Y., Mori, T., Kikkawa, U. & Nishizuka, Y. Direct activation of Ca^{++} activated, phospholipid dependent protein kinase by tumor promoting phorbol esters. *J. biol. Chem.* **257,** 7847, 1982.
13 Cherif-Zahar, C., Vaigot, P. & Castagna, M. Tumor promoters enhance cap formation in mouse thymocytes. *Carcinogenesis* **4,** 87, 1983.
14 Dalchau, R., Kirkley, I. & Fabre, J.W. Monoclonal antibody to a human brain-granulocyte–T lymphocyte antigen probably homologous to the W3/13 antigen of the rat. *Eur. J. Immunol.* **10,** 745, 1980.
15 Driedger, P. & Blumberg, P.M. Specific binding of phorbol ester tumor promoters. *Proc. natn. Acad. Sci. USA* **77,** 567, 1980.
16 Edelman, G.M. Surface modulation in cell recognition and cell growth. *Science* **192,** 218, 1976.
17 Edelman, G.M. Cell adhesion molecules: a molecular basis for animal form. *Scient. Amer.* **250,** 80, 1984.
18 Eliasson, L., Kallin, B., Patarroyo, M., Klein, G., Fujiki, H. & Sugimura, H. Induction of the EB viral cycle and aggregation of human blood lymphocytes by the two new classes of tumor promoters: teleocidin, lyngbyatoxin A, aplysiatoxin and debromoaplysiatoxin. *Int. J. Cancer* **31,** 7, 1983.
19 Engleman, E.G., Benike, C.J., Glickman, E. & Evans, R.L. Antibodies to membrane structures that distinguish suppressor/cytotoxic and helper T lymphocyte subpopulations block the mixed leukocyte reaction in man. *J. exp. Med.* **154,** 193, 1981.
20 Gahmberg, C.G. & Andersson, L.C. Selective radioactive labeling of cell surface sialoglycoproteins by periodatetritiated borohydride. *J. biol. Chem.* **252,** 5888, 1977.
21 Gahmberg, C.G. & Andersson, L.C. Leukocyte surface origin of human α_1-acid glycoprotein (orosomucoid). *J. exp. Med.* **148,** 507, 1978.
22 Galili, U., Galili, N., Vanky, F. & Klein, E. Natural species-restricted attachment of human and murine T lymphocytes to various cells. *Proc. natn. Acad. Sci. USA* **75,** 2396, 1978.
23 Glaser, L. From cell adhesion to growth control. Pp. 79–97 in Subtelney, S. (ed.) *The Cell Surface.* Academic Press, New York, 1980.
24 Howard, F.D., Ledbetter, J.A., Wong, J., Bieber, C.P., Stinson, E.B. & Herzenberg, L.A. A human T lymphocyte differentiation marker defined by monoclonal antibodies that block E-rosette formation. *J. Immunol.* **126,** 2117, 1981.

Carl_G_190x270_mm_blokki_FINAL.indd 212 06-Aug-23 1:53:42 PM

25 Hubbard, A.L. & Cohn, Z.A. Enzymatic iodination of the red cell membrane. *J. Cell Biol.* **55,** 390, 1972.

26 Julius, M.H., Simpson, E. & Herzenberg, L.A. A rapid method for the isolation of functional thymus-derived murine lymphocytes. *Eur. J. Immunol.* **3,** 645, 1973.

27 Kolata, G. Clues to cell growth and differentiation. *Science* **220,** 291, 1983.

28 Krensky, A.M., Robbins, E., Springer, T.A. & Burakoff, S.J. LFA-1, LFA-2 and LFA-3 antigens are involved in CTL-target conjugation. *J. Immunol.* **132,** 2180, 1984.

29 Krensky, A.M., Sanchez-Madrid, F., Robbins, E., Nagy, J. A., Springer, T.A. & Burakoff, S.J. The functional significance, distribution and structure of LFA-1, LFA-2 and LFA-3: cell surface antigens associated with CTL-target interactions. *J. Immunol.* **131,** 611, 1983.

30 Kwong, C. & Mueller, G. Influence of tumor promoting phorbol esters on the phosphorylation of membrane proteins in lymphocytes. *Carcinogenesis* **4,** 663, 1983.

31 Laemmli, U.K. Cleavage of structural proteins during the assembly of the head of bacteriophage T4. *Nature, Lond.* **227,** 680, 1970.

32 Lampson, L.A. & Levy, R. Two populations of Ia-like molecules on a human B cell line. *J. Immunol.* **125,** 293, 1980.

33 Landegren, U., Ramstedt, U., Axberg, I., Ullberg, M., Jondal, M. & Wigzell, H. Selective inhibition of human T cell cytotoxicity at levels of target recognition or initiation of lysis by monoclonal OKT3 and Leu-2a antibodies. *J. exp. Med.* **155,** 1579, 1982.

34 LeBien, T.W. & Kersey, J.H. A monoclonal antibody (TA-1) reactive with human T lymphocytes and monocytes. *J. Immunol.* **125,** 2208, 1980.

35 Ledbetter, J.A., Evans, R.L., Lipinski, M., Cunningham-Rudles, C., Good, R.A. & Herzenberg, L.A. Evolutionary conservation of surface molecules that distinguish T lymphocyte helper/inducer and cytotoxic/suppressor subpopulations in mouse and man. *J. exp. Med.* **153,** 310, 1981.

36 Loor, F. Lectin-induced lymphocyte agglutination. An active cellular process? *Exp. Cell Res.* **82,** 415, 1973.

37 Martin, P.J., Hansen, J.A., Siadak, A.W. & Nowinski, R.C. Monoclonal antibodies recognizing normal human T lymphocytes and malignant human B lymphocytes: a comparative study. *J. Immunol.* **127,** 1920, 1981.

38 Mastro, A.M. Phorbol esters: tumor promotion, cell regulation and the immune system. Pp. 263–313 in Mizel, S.B. (ed.) *Lymphokines,* vol. 6. Academic Press, New York, 1982.

39 Moscona, A.A. *The Cell Surface in Development.* Wiley, New York, 1974.

40 Mueller, K. & Gerisch, G. A specific glycoprotein as the target site of adhesion blocking Fab in aggregating dictyostelium cells. *Nature, Lond.* **274,** 445, 1978.

41 Nielsen, M.H., Jensen, J., Braendstrup, O. & Werdelin, O. Macrophage-lymphocyte clusters in the immune response to soluble protein antigen in vitro. II. Ultrastructure of clusters formed during the early response. *J. exp. Med.* **140,** 1260, 1974.

42 Ocklind, C. & Öbrink, B. Intercellular adhesion of rat hepatocytes. Identification of a cell surface glycoprotein involved in the initial adhesion process. *J. biol. Chem.* **257,** 6788, 1982.

43 Omary, M.B., Trowbridge, I.S. & Battifora, H.A. Human homologue of murine T200 glycoprotein. *J. exp. Med.* **152,** 842, 1980.

44 Parham, P., Barnstable, C.J. & Bodmer, W.F. Use of a monoclonal antibody (W6/32) in structural studies of HLA-A, B, C antigens. *J. Immunol.* **123,** 341, 1979.

45 Patarroyo, M., Biberfeld, P., Klein, E. & Klein, G. 12-O-tetradecanoyl-phorbol-13-acetate (TPA) treatment elevates the natural killer (NK) sensitivity of certain human lymphoid lines. *Cell Immunol.* **63,** 237, 1981.

46 Patarroyo, M., Biberfeld, P., Klein, E. & Klein, G. Phorbol 12,13-dibutyrate ($P(Bu)_2$) treated human blood mononuclear cells bind to each other. *Cell. Immunol.* **75,** 144, 1983.

47 Patarroyo, M. & Gahmberg, C.G. Phorbol 12,13-dibutyrate enhances lateral redistribution of membrane glycoproteins in human blood lymphocytes. *Eur. J. Immunol.* **14,** 781, 1984.

48 Patarroyo, M., Jondal, M., Gordon, J. & Klein, E. Characterization of the phorbol 12,13-dibutyrate ($P(Bu)_2$) induced binding between human blood lymphocytes. *Cell. Immunol.* **81,** 373, 1983.

49 Patarroyo, M., Yogeeswaran, G., Biberfeld, P., Klein, E. & Klein, G. Morphological changes, cell aggregation and cell membrane alterations caused by phorbol 12,13-dibutyrate in human blood lymphocytes. *Int. J. Cancer* **30,** 707, 1982.

50 Powell, L.W., Hart, P., Nielsen, M.H. & Werdelin, O. Antigen-dependent physical interaction between human monocytes and T lymphocytes. *Scand. J. Immunol.* **12,** 467, 1980.

51 Roder, J., Kiessling, R., Biberfeld, P. & Andersson, B. Target–effector interaction in the natural killer (NK) cell system. II. The isolation of NK cells and studies on the mechanism of killing. *J. Immunol.* **121,** 2509, 1978.

52 Sanchez-Madrid, F., Nagy, J.A., Robbins, E., Simon, P. & Springer, T.A. A human leukocyte differentiation antigen family with distinct α-subunits and a common β-subunit: the lymphocyte function-associated antigen (LFA-1), the C3bi complement receptor (OKM1/Mac-1) and the p150,95 molecule. *J. exp. Med.* **158,** 1785, 1983.

53 Sando, I., Hilfiker, M., Salomon, D. & Farrar, I. Specific receptors for phorbol esters in lymphoid cell populations: role in enhanced producion of T-cell growth factor. *Proc. natn. Acad. Sci. USA* **78,** 1189, 1981.

54 Schlesinger, M., Levy, J., Laskov, R., Hadar, R., Weinstock, J., Ben-Bassat, H. & Rabinowitz, R. The role of E receptors in the attachment of thymocytes and T lymphocytes to human target cells. *Clin. Immunol. Immunopath.* **29,** 349, 1983.

55 Sutherland, R., Delia, D., Scherder, C., Newman, R., Kemshead, J. & Greaves, M.F. Ubiquitous cell-surface glycoprotein on tumor cells is

Carl_G_190x270_mm_blokki_FINAL.indd 213 06-Aug-23 1:53:42 PM

proliferation associated receptor for transferrin. *Proc. natn. Acad. Sci. USA* **78,** 4515, 1981.
56 Thiery, J., Brackenbury, R., Rutishauser, U. & Edelman, G.M. Adhesion among neural cells of the chick embryo. II. Purification and characterization of a cell adhesion molecule from neural retina. *J. biol. Chem.* **252,** 6841, 1977.
57 Tsien, R.Y., Pozzan, T. & Rink, T.J. T-cell mitogens cause early changes in cytoplasmic free Ca^{++} and membrane potential in lymphocytes. *Nature, Lond.* **295,** 68, 1982.
58 Urushihara, H. & Takeichi, M. Cell–cell adhesion molecule: identification of a glycoprotein relevant to the Ca^{++}-independent aggregation of chinese hamster fibroblasts. *Cell* **20,** 363, 1980.
59 Ware, C.F., Sanchez-Madrid, F., Krensky, A.M., Burakoff, S.J., Strominger, J.L. & Springer, T.A. Human lymphocyte function associated antigen-1 (LFA-1): identification of multiple antigenic epitopes and their relationship to CTL-mediated cytotoxicity. *J. Immunol.* **131,** 1182, 1983.

Received 3 January 1985

Carl_G_190x270_mm_blokki_FINAL.indd 214 06-Aug-23 1:53:42 PM

Scand. J. Immunol. **22,** 619–631, 1985

Identification of a Cell-Surface Glycoprotein Mediating Adhesion in Human Granulocytes

M. PATARROYO, P. G. BEATTY, C. N. SERHAN & C. G. GAHMBERG

Department of Immunology, and Department of Physiological Chemistry, Karolinska Institute, Stockholm, Sweden, Fred Hutchinson Cancer Research Center, University of Washington, Seattle, USA, and Department of Biochemistry, University of Helsinki, Finland

Patarroyo, M., Beatty, P.G., Serhan, C.N. & Gahmberg, C.G. Identification of a Cell-Surface Glycoprotein Mediating Adhesion in Human Granulocytes. *Scand. J. Immunol.* **22,** 619–631, 1985

Previous studies have shown that monoclonal antibody 60.3 reacting with a surface antigen common to human leukocytes inhibits phorbol ester-induced adhesion among blood mononuclear cells and precipitates from these cells three surface polypeptides with apparent molecular weights of 90,000, 130,000 and 160,000. Now we report that the same antibody, either as purified IgG or Fab fragments, also inhibits the extensive adhesion among granulocytes induced by phorbol ester. Inhibition of cell aggregation was not observed with monoclonal antibodies to C3b receptor, common leukocyte antigen T200, C3bi receptor, brain granulocyte–T lymphocyte antigen, IgG Fc receptor, class I transplantation antigen, or a granulocyte-specific antigen. Intercellular adhesion induced by either the chemotactic tripeptide *N*-formylmethionyl-leucyl-phenylalanine (FMLP) or the ionophore A23187 was also inhibited by antibody 60.3. However, this antibody did not affect phorbol ester-induced superoxide (O_2^-) generation or lysozyme release. Two major surface glycopolypeptides with apparent molecular weights of 92,000 and 155,000 were immunoprecipitated from granulocytes. Dissociation of the protein complexes obtained from blood mononuclear cells and granulocytes indicated the presence of the epitope on the 90,000–92,000 molecular-weight components. It is thus concluded that the smallest glycopolypeptides mediate adhesion in human granulocytes and mononuclear leukocytes..

Manuel Patarroyo, Department of Immunology, Karolinska Institute, S-104 01 Stockholm 60, Sweden

Granulocytes are known to play a central role in host defence against pathogenic microorganisms [22] and to mediate tissue injury in various diseases [3, 12]. During acute inflammatory responses, these phagocytic cells leave the blood stream after adhering to vascular endothelial cells, and migrate through the vessel wall to surrounding tissues, where they ingest and kill invading organisms.

Upon stimulation, granulocytes rapidly undergo a variety of physiological responses such as oxidative metabolism, degranulation, and adherence [21]. The adherence response may be manifested as autoaggregation both in vivo [19] and in vitro [21], or by adhesion to cultured endothelium [54] or artificial surfaces including plastic Petri dishes [9] and nylon fibre [31]. Granulocyte aggregation, which can be induced by a variety of both soluble and particulate stimuli such as the chemotactic tripeptide *N*-formyl-methionyl-leucyl-phenylalanine (FMLP), the ionophore A23187, phorbol esters [21], the complement-derived component C5a [10], and leukotriene B_4 (LTB_4) [48], is an energy- and temperature-dependent cell surface-mediated phenomenon which requires extracellular divalent cations [38]. It can occur independently of degranulation [24], and is dissociable from oxidative metabolism [58]. However, the molecular basis of this response is still poorly understood.

In previous studies adhesion among human mononuclear leukocytes (mainly lymphocytes) was analysed by inducing their aggregation with the phorbol esters 12-*O*-tetradecanoyl-phorbol-13-acetate (TPA) and phorbol 12,13-dibutyrate

Carl_G_190x270_mm_blokki_FINAL.indd 215 06-Aug-23 1:53:42 PM

($P(Bu)_2$). Initially, TPA was shown to stimulate aggregation of lymphoblastoid cells and to enhance their adhesion to blood lymphocytes [41]. At nanomolar concentrations $P(Bu)_2$ induces both rapid morphological changes and intercellular adhesion in mononuclear leukocytes [42, 14]. The cell–cell adhesion is an energy- and temperature-dependent process that requires extracellular divalent cations (mainly Mg^{++}). Microfilaments and various cellular enzymes appear to participate, and cell surface proteins, but not protein synthesis, are needed [43, 44], Patarroyo & Jondal. Since passive bridging between the cells by $P(Bu)_2$ itself could be excluded, the results of these studies indicated that phorbol esters induce a cell-adhesive phenotype in certain mononuclear leukocytes, and that cell surface structures such as cell adhesion molecules are involved. We shall use the term leukocytic–cell adhesion molecule (Leu–CAM) to refer to the leukocytic ligand forming the intercellular bonds.

By blocking aggregation of other cell types, antibodies to cell-surface proteins allowed the identification of several cell-adhesion molecules, including neural cell-adhesion molecule (N–CAM) and liver cell-adhesion molecule (L–CAM) [32, 13, 36, 57]. Using a similar approach, a monoclonal antibody (60.3) to a surface antigen expressed on human lymphocytes, monocytes, and granulocytes [4] was found to inhibit phorbol ester-induced aggregation but not stimulation of mononuclear leukocytes [45]. Since the antibody precipitated three surface polypeptides with apparent molecular weights of 90,000, 130,000 and 160,000 it was concluded that this protein complex, or at least one of its components, mediates intercellular adhesion.

The reactivity of antibody 60.3 with granulocytes, but not with erythrocytes, platelets, or hepatoma cells, as well as the similarities between phorbol ester-induced aggregation of mononuclear leukocytes and granulocytes prompted us to test the effects of this antibody on adhesion among granulocytes. In the present study, we report that antibody 60.3 blocks granulocyte aggregation induced by 3 different stimuli but not their activation. Two major surface glycopolypeptides with apparent molecular weights of 92,000 and 155,000 were immunoprecipitated from these cells. Dissociation of the protein complexes from mononuclear leukocytes and granulocytes allowed the localization of the epitope on the smallest components.

MATERIAL AND METHODS

Monoclonal antibodies and other reagents. The antibodies used in the present study are described in Table I. Monoclonal anti-C3bR antibody was obtained from Dakopatts (Copenhagen, Denmark); T29/33 was purchased from Hybritech (San Diego, Calif. USA); OKM1 from Ortho Diagnostic Systems (Raritan, N.J., USA); anti-Leu-11a from Beckton Dickinson (Mechelen, Belgium); W6/32 and MAS 065 from Sera-Lab (London, UK); and NEI-037 from New England Nuclear (Boston, Mass., USA). Monoclonal antibodies 60.3 and F10-44-2 were produced as previously described [4, 11]. All antibodies were dialysed against water for 48 h at 4°C to remove NaN_3. They were then lyophilized and dissolved in phosphate-buffered saline (PBS) to obtain a stock concentration of 400 μg/ml. $P(Bu)_2$ (Sigma, St Louis, Mo., USA) and FMLP (Sigma) were dissolved in dimethylsulphoxide (DMSO), while ionophore A23187 was dissolved in ethanol and stored at −20°C. $P(Bu)_2$, FMLP and A23187 were added to cells to a final concentration of 60, 500, and 500 nM respectively. The final concentration of the solvents was less than 0.1%, which when tested alone did not affect cell aggregation.

Granulocyte preparation. Cell preparations containing 98% granulocytes, as measured by reactivity with a granulocyte-specific monoclonal antibody, from heparinized blood of healthy donors were used (Table I). Approximately 2% of the cells were T lymphocytes and less than 1% were B cells (data not shown). After separation by a discontinuous gradient of Percoll (Pharmacia, Uppsala, Sweden) [20], the cells were resuspended in RMPI 1640 medium (Grand Island Biological Co., Grand Island, USA) containing 0.5% human albumin (Sigma) unless otherwise stated. Cell viability was over 92% in all experiments as measured by trypan blue exclusion.

Measurement of cell aggregation. Aliquots of 0.5 ml of the cell suspension (10^7 cells/ml) in 24-well tissue culture plates (Costar, Cambridge, USA) were rotated in a gyratory shaker (Model G2, New Brunswick Scientific Co., Edison, N.J., USA) at 100 rpm at 37°C. After warming of the cells (10 min, 37°C), either $P(Bu)_2$ (60 nM), FMLP (500 nM), or A23187 (500 nM) was added. To enhance the cell aggregation induced by FMLP and A23187, the cells were pretreated with 0.5 μg/ml cytochalasin B (Sigma, dissolved in DMSO) for 5 min at 37°C [37]. Twenty minutes after adding the stimuli, the cell suspension was briefly inspected in an inverted microscope (Diavert, Leitz, Mainz, FRG) and resuspended by pipetting 5 times before the percentage of aggregated cells was determined in a haemocytometer using a Laborlux K microscope (Leitz, Mainz, FRG) at 400× magnification. The suspension was also inspected before treatment and a control sample was

Carl_G_190x270_mm_blokki_FINAL.indd 216 06-Aug-23 1:53:43 PM

incubated without the stimulus. When FMLP or A23187 were used as stimuli the percentage of aggregated cells (% aggr.) was determined by directly counting the number of cells in aggregates. At least 5×10^2 total cells were counted in each sample. However, $P(Bu)_2$ induced much larger aggregates and the number of participating cells could not be determined accurately by this method. Therefore, $P(Bu)_2$-induced aggregation was measured indirectly by counting the number of single cells in the treated sample in a predetermined area and subtracting this value from the corresponding total number of cells in the untreated sample, both read after 20 min. This method gives an approximate percentage of aggregated cells. The effect of 8 monoclonal antibodies on the $P(Bu)_2$-induced cell aggregation was tested. The cells were incubated with antibody (either IgG or Fab fragments) at concentrations between 50 ng and 20 μg/ml for 20 min at room temperature and for 10 min more at 37°C before being shaken and treated with phorbol ester. Unbound antibodies were also present during $P(Bu)_2$ treatment. The effects of the antibodies (inhibition) are expressed as:

$$\frac{\%P(Bu)_2 \text{ aggr. in control sample} - P(Bu)_2 \text{ aggr. with antibody}}{P(Bu)_2 \text{ aggr. in control sample}} \times 100$$

Usually, $\%P(Bu)_2$-induced aggregation in the control sample was greater than 90%. Each antibody was tested at least twice. The Fab fragments were prepared from the F10-44-2 and 60.3 antibodies by papain digestion as previously described [45].

Indirect immunofluorescence and morphological studies. Cells were stained with the antibodies by indirect immunofluorescence with either fluorescein-conjugated rabbit anti-mouse Ig or goat anti-mouse IgG (Fc) (Nordic Immunology, The Netherlands) as the second step reagent. Incubation with the antibodies was done at room temperature. After staining, the cells were treated with glycerol and observed in a Leitz Fluorescence microscope (Schott, FRG). Cell aggregation and morphological changes were followed in conventional and inverted microscopes at various magnifications. To study the effect of antibody 60.3 the cells were preincubated with 20 μg/ml of its Fab fragments and treated with $P(Bu)_2$ in the presence of antibody excess. Photomicrographs were taken with a Wild microscope camera (Heerbrugg, Switzerland) with a Plus X pan (Kodak, Rochester, USA) film.

Measurements of superoxide generation and lysozyme release. Superoxide generation was measured by superoxide dismutase-inhibitable reduction of ferricytochrome c as previously described [7]. All experiments were performed in duplicate. One-millilitre samples of 5×10^6 granulocytes in PBS containing Ca^{++} and Mg^{++} in 5 ml plastic tubes were treated with cytochalasin B (Sigma) (1 μg/ml) for 5 min at 37°C. Ferricytochrome c (horse heart type III, Sigma) was added to a final concentration of 75 μM, and the reaction mixture was incubated with $P(Bu)_2$ (60 nM) for 5 min at 37°C. Reduction of cytochrome c was measured in supernatants obtained by centrifugation (550 ***g*** for 5 min), employing a Hewlett-Packard 8450A UV/VIS 25 spectrophotometer at 550 nm equipped with a 7470A Platter. Superoxide anion generation is expressed as nmol of cytochrome c reduced per 5×10^6 cells per 5 min.

To measure lysozyme release, 5×10^6 granulocytes in 1 ml of PBS with Ca^{++} and Mg^{++} were preincubated for 5 min at 37°C with cytochalasin B (1 μg/ml). After treating the cells with $P(Bu)_2$ (60 nM) for 5 min at 37°C, the cell supernatants were obtained by centrifugation (550 ***g*** for 5 min) and placed on ice. Duplicate aliquots of supernatants were taken for standard determination of lysozyme using *Micrococcus lysodeikticus* (Sigma) as substrate [30]. Enzyme release is expressed as the percentage of total activity observed in TX-100 (0.1%) disrupted cells. To study the effect of antibody 60.3 on $P(Bu)_2$-induced superoxide generation and lysozyme release, the cells (5×10^6) were preincubated with 10 μg of its Fab fragments for 20 min at room temperature and for 10 min at 37°C before adding other reagents.

Cell surface labelling, dissociation of surface protein complexes, immunoprecipitation, and gel electrophoresis. Cells were surface labelled with ^3H after periodate oxidation [16]. Surface glycoprotein complexes were dissociated by treating the cell lysates with 1% sodium dodecyl sulphate for 15 min at 22°C in granulocytes and for 10 min at 37°C in mononuclear leukocytes. Immunoprecipitation was performed as described previously using rabbit anti-mouse Ig (Dako, Copenhagen, Denmark) in the second step [17]. Polyacrylamide slab gel electrophoresis in the presence of sodium dodecyl sulphate was done according to Laemmli [25] using 8% acrylamide gels. The ^3H-labelled gels were treated for fluorography according to Bonner & Laskey [6]. ^{14}C-labelled standard proteins were obtained from the Radiochemical Centre (Amersham, UK).

RESULTS

Effect of monoclonal antibodies to cell surface antigens on the phorbol ester-induced aggregation of human granulocytes

Phorbol esters are known as potent inducers of granulocyte aggregation [38]. After 20 min treatment under gentle shaking the mean value of $P(Bu)_2$-induced aggregation was 93.2% of aggregated cells compared to a negligible aggregation, less than 1%, in the untreated sample. The effect of 8 monoclonal antibodies on the intercellular adhesion was tested. All antibodies reacted with almost all cells (Table I). None of the antibodies, save 60.3, inhibited cell aggregation at concentrations as high as 20 μg/ml (Fig. 1). Antibody 60.3 inhibited the cell–cell adhesion in a concentration-dependent manner and approximately 2 μg/ml was required to obtain 50% inhibition (Fig. 1). A few cell aggregates

Carl_G_190x270_mm_blokki_FINAL.indd 217 06-Aug-23 1:53:43 PM

TABLE I. List and characteristics of monoclonal antibodies and their reactivity with human granulocytes

Monoclonal antibody	Murine IgG subclass	Cell-surface antigen	Molecular weight of immuno-precipitated proteins (daltons)*	% of antigen-positive cells (mean)†	References
Anti-C3bR	IgG_1	C3b receptor (CR1)‡	205,000	98.5	[15]
T29/33	IgG_{2b}	Common leukocyte antigen T200	200,000	98.5	[39]
OKM1	IgG_{2b}	C3bi receptor (CR3)	165,000/95,000	98.0	[50]
60.3	IgG_{2a}	Common leukocyte surface antigen (Lp 95–150)	95,000/130,000/ 150,000	99.0	[4]
F 10-44-2	IgG_{2a}	Brain granulocyte–T lymphocyte antigen	105,000	99.0	[11]
Anti-Leu-11a	IgG_1	IgG Fc receptor of lymphocytes and granulocytes	50,000–70,000	99.0	[46]
W6/32	IgG_{2a}	HLA-A, B, C shared determinant (class I antigen)	43,000	99.0	[40]
MAS 065	IgG_1	Human granulocyte antigen	Unknown	98.0	[60]
NEI-037	IgG	Mature T cell antigen (T3)	19,000–29,000	2.5	[28]
None	—	—	—	<1	

* Apparent molecular weight under reducing conditions.
† Mean of 2 tests.
‡ Other names given to the immunoprecipitated molecule in parentheses.

(less than 16% of the cells) were observed in samples not exposed to $P(Bu)_2$ but in the presence of 20 μg/ml of antibodies to C3bi receptor, common leukocyte antigen (T 200), granulocyte-specific antigen, IgG Fc receptor, and C3b receptor (data not shown).

Since the divalency of the antibody or its Fc portion might affect the intercellular binding, Fab fragments from antibodies 60.3 and F10-44-2 were prepared. The antibody activity of these fragments and the lack of Fc portion are shown in Table II. Fab fragments prepared from

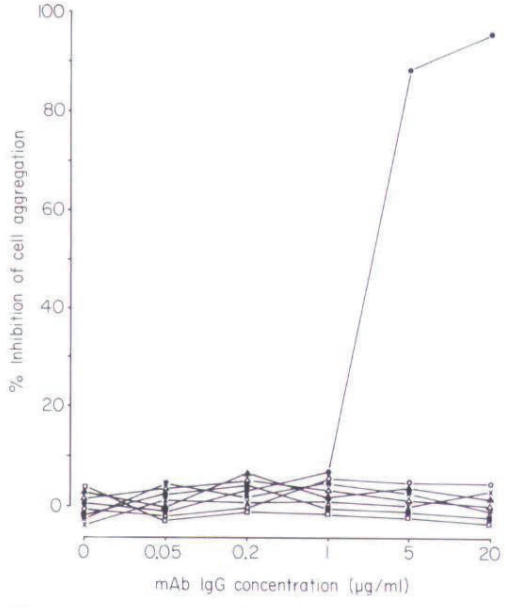

Fig. 1. Effect of various monoclonal antibodies (IgG) to cell surface antigens on $P(Bu)_2$-induced aggregation of granulocytes. The following antibodies were used: Anti-C3bR (□), T29/33 (▲), OKM1 (△), 60.3 (●), F10-44-2 (○), anti-Leu 11a (■), W6/32 (*), and MAS 065 (×).

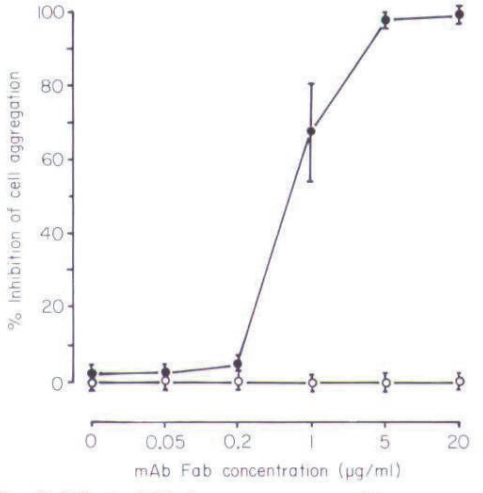

FIG. 2. Effect of Fab fragments prepared from monoclonal antibodies 60.3 (●) and F10-44-2 (○) on $P(Bu)_2$-induced aggregation of granulocytes. Mean values and standard deviations of 3 experiments are shown.

Carl_G_190x270_mm_blokki_FINAL.indd 218 06-Aug-23 1:53:43 PM

TABLE II. Determination of antibody reactivity with human granulocytes and presence of Fc portion in papain-digested preparations from antibodies 60.3 and F 10-44-2

Monoclonal antibody	Papain digestion*	Fluorescent conjugated reagent	Percentage of positive cells‡
60.3	–	Anti-Ig (1:20)†	99.0
		Anti-Fc (γ) (1:20)	99.0
	+	Anti-Ig (1:20)	99.0
		Anti-Fc (γ) (1:20)	<1
F 10-44-2	–	Anti-Ig (1:20)	98.5
		Anti-Fc (γ) (1:20)	98.5
	+	Anti-Ig (1:20)	98.5
		Anti-Fc (γ) (1:20)	<1
None		Anti-Ig (1:20)	<1
		Anti-Fc (γ) (1:20)	<1

* Papain digestion was performed as described in [45].
† Antiserum dilution in parentheses.
‡ Mean of 2 experiments.

antibody 60.3 but not from antibody F10-44-2 inhibited the cell aggregation in a concentration-dependent manner (Fig. 2). Approximately 0.8 μg/ml was needed to block 50% of the intercellular binding. These results were also confirmed by aggregometry with a Payton aggregometer [19], (data not shown). The antibody inhibited not only the formation of large aggregates that contained several thousands of granulocytes, but also the adhesion of the cells to the tissue culture plate surface (Fig. 3 a–h).

Effect of antibody 60.3 (Fab fragments) on granulocyte aggregation induced by FMLP and A23187

The chemotactic tripeptide FMLP and the divalent cation ionophore A23187 are well-known inducers of granulocyte aggregation [21], and their effect is dramatically potentiated by pretreatment of the cells with cytochalasin B [37]. Under these conditions, cell aggregation induced by either FMLP or A23187 was less than that with $P(Bu)_2$ (Table III). Fab fragments from antibody 60.3 also inhibited aggregation induced by FMLP and A23187. It is interesting that while 20 μg/ml of the antibody almost completely inhibited the aggregation induced by either $P(Bu)_2$ or A23187, the same concentration of antibody inhibited 68% of the aggregation induced by FMLP.

Effect of monoclonal antibody 60.3 on phorbol ester-induced superoxide generation and lysozyme release

In addition to cell aggregation phorbol esters induce oxidative metabolism and lysozomal

TABLE III. Effect of antibody 60.3 (Fab fragments) on granulocyte aggregation induced by $P(Bu)_2$, FMLP, and A23187

Stimulus	% cell aggregation (mean±SD),* with antibody 60.3: Absent	Present†	% inhibition of cell aggregation by antibody 60.3
$P(Bu)_2$ (60 nM)	93.3±0.5	1.3±0.5	98.6
FMLP (500 nM)‡	41.0±9.0	13.3±5.4	67.6
A23187 (500 nM)‡	36.7±2.0	1.0±0.8	97.2

* Cell aggregation was determined in a haemocytometer after rotating the cell suspension (10^7 cells/ml) in a giratory shaker (100 rpm) in the presence of the stimulus for 20 min (n=3).
† 20 μg of Fab fragments were added to 10×10^6 cells before the stimulus.
‡ After adding the antibody but before adding the stimulus these samples were incubated with 0.5 μg/ml cytochalasin B for 5 min at 37°C.

Carl_G_190x270_mm_blokki_FINAL.indd 219 06-Aug-23 1:53:43 PM

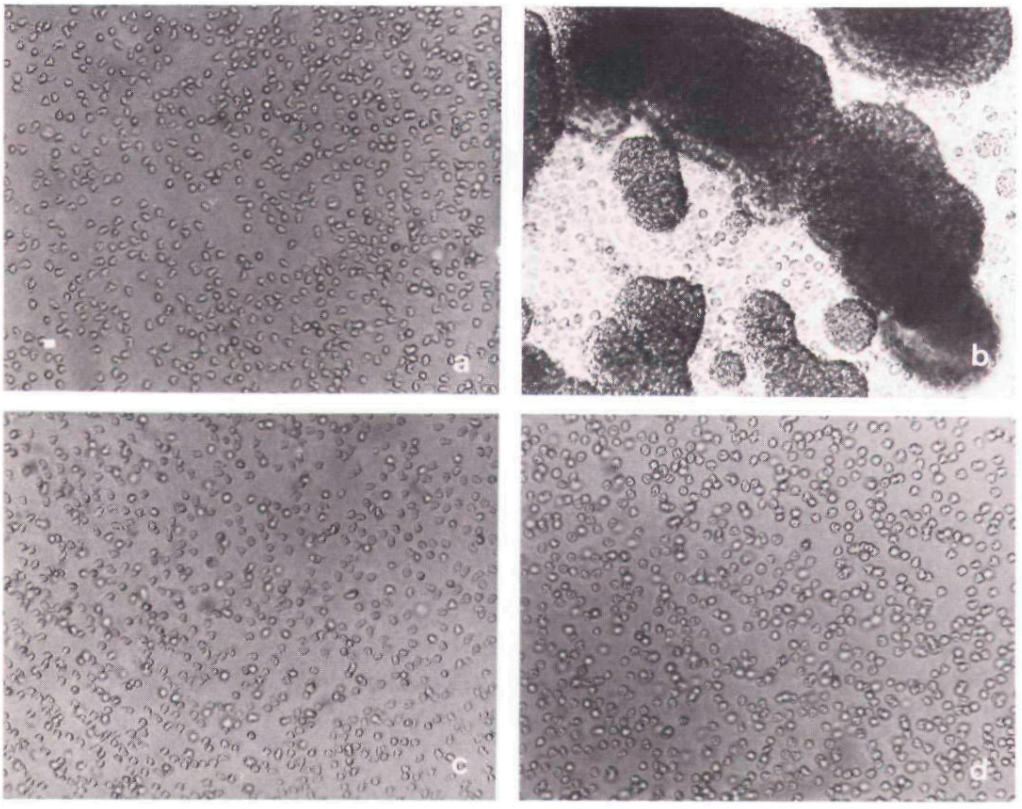

FIG. 3. Light micrographs of the effect of Fab fragments from antibody 60.3 on $P(Bu)_2$-induced cell aggregation, adhesion to the tissue culture plate surface, and morphological changes in granulocytes. a, c, e, g, and i were not treated with $P(Bu)_2$. b, d, f, h, and j were treated with 60 nM $P(Bu)_2$ for 20 min at 37°C. c, d, g, h, and j were preincubated with 20 μg/ml of Fab fragments. a-h and i-j were photographed in an inverted and a conventional microscope, respectively, at 40×(a-d), 320×(e-h), and 1000×(i-j) magnifications. Samples that were preincubated with the antibody but not treated with $P(Bu)_2$ resembled, i. Formation of empty vacuoles as in j were also observed in granulocytes treated with $P(Bu)_2$ alone. All samples were continuously rotated at 100 rpm. Scale bar=40 μm.

TABLE IV. Effect of antibody 60.3 (Fab fragments) on $P(Bu)_2$-induced superoxide (O_2^-) generation and lysozyme release from granulocytes

Addition*	O_2^- (nmol cytochrome c reduced/5×10^6 cells/5 min)†	Lysozyme release (% release)‡
Cells	0.3	0.0
Cells+antibody 60.3§	0.0	4.8
Cells+$P(Bu)_2$¶	26.9	38.9
Cells+antibody 60.3§+$P(Bu)_2$¶	27.5	42.8

* All samples (5×10^6 cells/ml) were treated with 1μg cytochalasin B for 5 min at 37°C before adding $P(Bu)_2$.

† These values represent superoxide dismutase-inhibitable reduction of cytochrome c.

‡ Lysozyme values are expressed as % of detergent (TX-100) disrupted cells.

§ 10 μg of Fab fragments were added to 5×10^6 cells before cytochalasin B and $P(Bu)_2$.

¶ 60 nM $P(Bu)_2$ was added for 5 min at 37°C.

Carl_G_190x270_mm_blokki_FINAL.indd 220 06-Aug-23 1:53:43 PM

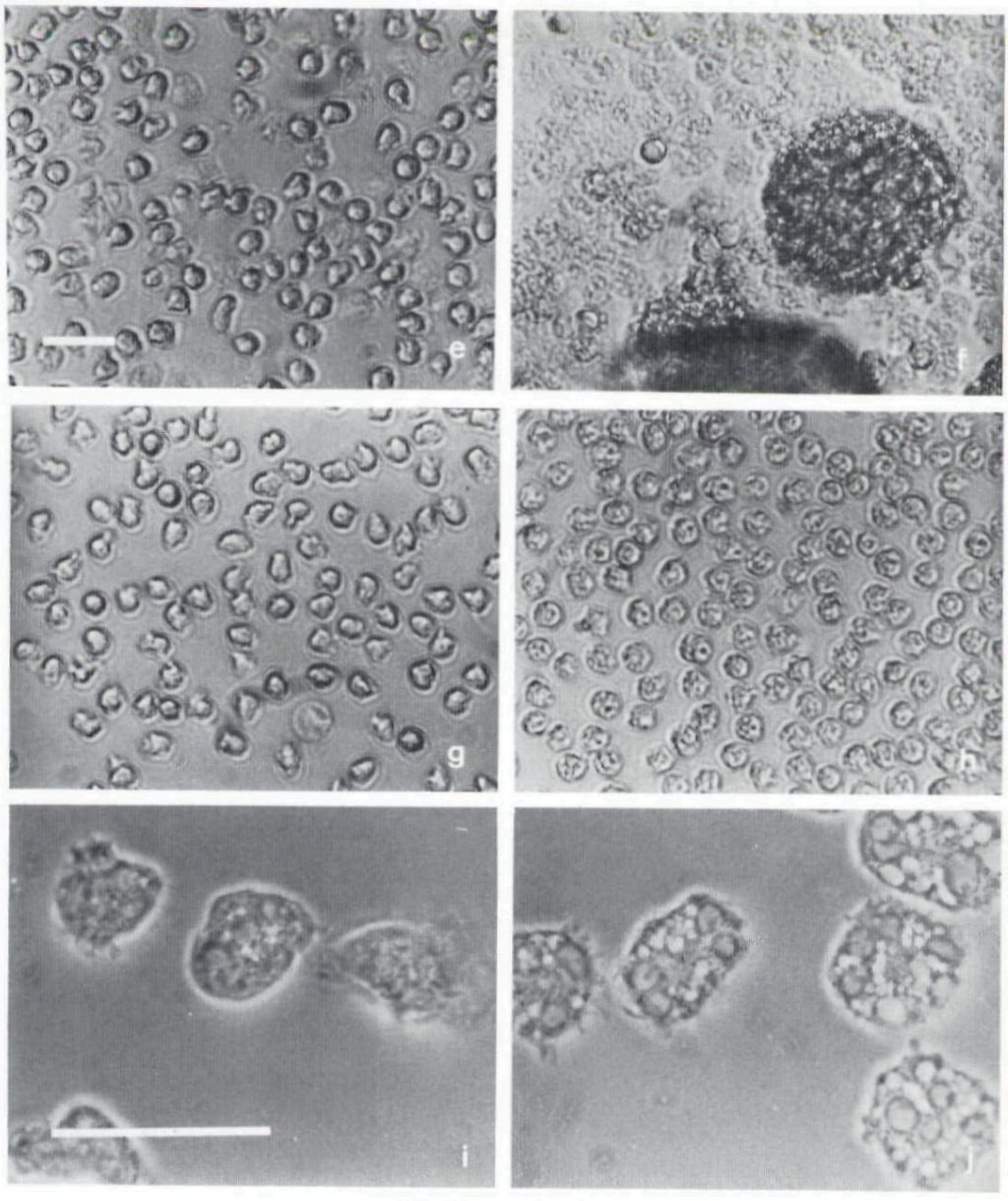

Figure 3 – *continued*

enzyme release in granulocytes [21]. When examined, these 3 responses were affected differently by antibody 60.3. While blocking >97% of cell aggregation, Fab fragments from this antibody did not inhibit superoxide generation or lysozyme release induced by $P(Bu)_2$ (Table IV). A low percentage (4.8%) of lysozyme release was detected in absence of $P(Bu)_2$ when cells were incubated with the antibody alone. Likewise, a morphological sign of phorbol ester stimulation, the formation of empty vacuoles in granulocytes [47], was not affected by the antibody (Fig. 3i, j).

Immunoprecipitation with antibody 60.3

Granulocytes were surface-labelled by ^3H after periodate treatment. Immunoprecipitation

Carl_G_190x270_mm_blokki_FINAL.indd 221 06-Aug-23 1:53:43 PM

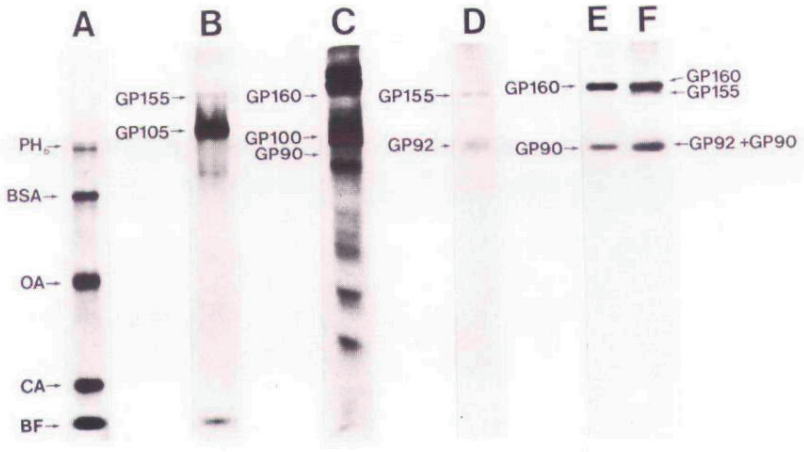

FIG. 4. Polyacrylamide slab gel electrophoresis patterns of ^{3}H-labelled surface antigens of granulocytes and mononuclear leukocytes. A, pattern of ^{14}C-labelled standard proteins: PHb=phosphorylase b, BSA=bovine serum albumin, OA=ovalbumin, CA=carbonic anhydrase, BF=buffer front; B and C, pattern of surface-labelled granulocytes and mononuclear leukocytes, respectively; D and E, pattern obtained by precipitation with antibody 60.3 from granulocytes and mononuclear leukocytes, respectively; F, mixture of immunoprecipitates obtained from granulocytes and mononuclear leukocytes. GP 155=glycoprotein with apparent molecular weight of 155,000, etc.

with antibody 60.3 followed by gel electrophoresis revealed under reducing conditions 2 sialylated polypeptides with apparent molecular weights of 92,000 and 155,000 (Fig. 4D) A third band with an apparent molecular weight of 130,000 was also detected after longer exposure (faintly seen in Fig. 5C). Two major polypeptides with apparent molecular weights of 90,000 and 160,000 were immunoprecipitated from mononuclear leukocytes (Fig. 4E). Co-electrophoresis of the immune precipitates broadened the bands (Fig. 4F). When the protein complexes from mononuclear leukocytes and granulocytes were dissociated by sodium dodecyl sulphate followed by immunoprecipitation, only the 90,000 and 92,000 components were obtained (Fig. 5B and D). No detectable differences were observed in the 2 bands obtained from granulocytes when untreated and phorbol ester-treated cells were compared (data not shown). Under non-reducing conditions the protein complexes exhibited a similar, but not identical, electrophoretical mobility (data not shown) [4].

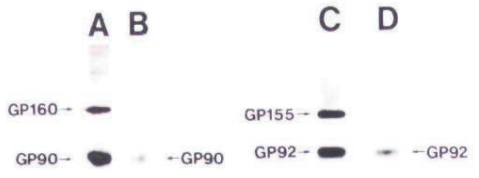

FIG. 5. Polyacrylamide slab gel electrophoresis patterns of immune precipitates obtained with antibody 60.3 from ^{3}H-labelled mononuclear leukocytes and granulocytes after dissociation. A, pattern obtained from mononuclear leukocytes; B, pattern obtained from mononuclear leukocytes after treatment with sodium dodecyl sulphate; C, pattern obtained from granulocytes; D, pattern obtained from granulocytes after treatment with sodium dodecyl sulphate.

DISCUSSION

Adhesion-dependent processes in granulocyte physiology appear to be numerous. In order to leave peripheral circulation, these cells margi-

Carl_G_190x270_mm_blokki_FINAL.indd 222 06-Aug-23 1:53:43 PM

nate and adhere to the vascular endothelium [59]. Thereafter, they enter the tissue by diapedesis and chemotaxis, a process which apparently requires adhesion to surrounding cells and extracellular matrix to provide the necessary traction associated with locomotion. Phagocytosis also appears to require adhesion of the particles to be ingested. In accordance with this, antibody 60.3 was recently shown to inhibit adhesion of granulocytes to bovine endothelium and endotoxin-coated coverslips as well as spreading (anchorage) on the latter substrate. Similarly, their migration in response to FMLP and phagocytosis of zymosan particles was largely inhibited. In contrast, the stimulation of hexose monophosphate shunt and H_2O_2 formation was unaffected by the antibody [5]. In previous studies [4], the same antibody was found to inhibit lymphocyte-mediated cytotoxicity, a process that requires adhesion between effector and target cells [49]. In addition, granulocyte-mediated lysis of virus-infected or tumour cells [29] may also be blocked. Another cell interaction that may be affected by the antibody is attachment of tumour cells to vascular endothelium, a phenomenon involved in metastasis, since this process is enhanced by adhesion of the neoplastic cells to granulocytes [52]. The cell-surface glycoprotein recognized by antibody 60.3, GP 92, may be also involved in the formation of leuko-emboli (granulocyte aggregates), which can block the circulation in capillaries and venules and may finally cause endothelial destruction during acute inflammatory responses [1]. Although nonstimulated human granulocytes preferentially adhere to endothelial cells when compared with fibroblasts or smooth-muscle cells, upon stimulation these cells no longer display the preferential interaction but adhere equally well to different cell types or to artificial substrates such as protein-coated plastic [54]. Thus, destruction of glomerular basement membrane, articular cartilage, and similar structures in certain inflammatory disorders [12, 3] may be mediated by adhesion of activated granulocytes to these protein substrates through GP92.

To analyse cell aggregation in the present study, gentle shaking of the cells was preferred to stirring with magnetic bars, because prolonged stirring has been found to decrease the cell viability by its traumatic effect. Although time-consuming, examination of the samples by light microscopy gives valuable information concerning the size of the aggregates, morphological changes, and adhesion to the plate, events which may not be fully appreciated when studying aggregation by aggregometry alone. After 20 min of treatment with $P(Bu)_2$ and gentle shaking, the cell viability was over 92% in accordance with a previous report, which described no toxic effect within the first hour of treatment as measured by ^{51}Cr release [55]. The cell suspensions contained 0.5% human albumin to reduce the adhesion of non-stimulated cells to surfaces, but $P(Bu)_2$-induced cell aggregation and its inhibition by antibody 60.3 were readily observed in the absence of this protein (data not shown).

After 20 min of $P(Bu)_2$ treatment, only 30% of blood mononuclear cells aggregate [43, 45], while more than 90% of the granulocytes undergo aggregation at this time. Since participation of a passive bridging mediated by phorbol ester in the intercellular adhesion of mononuclear leukocytes has been ruled out [43], and the phorbol ester-induced granulocyte aggregation has been shown to be a response of metabolically active cells [38], it can be similarly assumed that adhesion among granulocytes is due to a cell surface modulation, and mediated by surface structures such cell adhesion molecules (ligands). Thus, a much higher percentage of cells appears to display a cell-adhesive phenotype in the granulocyte preparation. Protein phosphorylation may be responsible for the intercellular adhesion, since protein kinase C constitutes a cellular receptor for phorbol esters [34]. These compounds appear to replace diacylglycerol, which is a physiological activator of the enzyme [35].

Our present results do not support the concept that common leukocyte antigen T200, brain granulocyte–T lymphocyte antigen, class I transplantation antigen, the granulocyte-specific antigen, C3b receptor (CR1), C3bi receptor (CR3) or IgG Fc receptor mediate the $P(Bu)_2$-induced granulocyte aggregation. The 3 latter surface molecules have, however, been reported to be involved in the binding of leukocytes to various particles, mostly erythrocytes, coated with the respective ligands, C3b, C3bi, or IgG [15, 50, 46]. To avoid these factors, our granulocyte preparation did not contain any serum.

The divalency of antibody 60.3 (IgG) and its Fc portion might affect granulocyte aggregation

Carl_G_190x270_mm_blokki_FINAL.indd 223 06-Aug-23 1:53:43 PM

by inducing a membrane perturbation through cross-linking of cell surface antigens or by mediating bridging between cells through the Fc portion and Fc receptor, respectively. The inhibitory effect observed with Fab fragments from the antibody excluded these possibilities and indicated that the antibody blocks a cell surface structure involved in adhesion. It might be argued, as well, that the antibody may block activation (stimulation) of granulocytes by phorbol ester by affecting binding of $P(Bu)_2$ to its putative receptor. However, the lack of inhibition of two other phorbol ester-induced responses in granulocytes, namely superoxide generation and lysozyme release, in the presence of the antibody indicates that phorbol ester binds to its intracellular receptor and that other structures associated with the subsequent activation process are not inhibited. Previous studies have also excluded the possibility that antibody 60.3 might paralyse the plasma membrane or anchorage surface glycoproteins [45]. Interestingly, almost 10 times higher amounts of either IgG or Fab from antibody 60.3 were needed to inhibit 50% of granulocyte aggregation when compared to similar inhibition of mononuclear leukocyte aggregation [45]. This finding suggests a higher number of antigen-binding sites per cell in granulocytes than in the mononuclear leukocytes.

Inhibition of granulocyte aggregation by antibody 60.3 did not occur exclusively when phorbol ester was used as the stimulus, since A23187- and FMLP-induced aggregations were also inhibited. The 3 stimuli activate granulocytes by different mechanisms, although they may have common pathways. While A23187 as an ionophore of divalent cations directly induces an increase in cytosolic free Ca^{++}, and thus bypasses receptor ligand interaction [56], FMLP binds first to its cell surface receptor, a glycoprotein with an apparent molecular weight of 60,000 [33]. The incomplete inhibition of FMLP-induced cell aggregation by antibody 60.3 is puzzling, and suggests the participation of an additional factor mediating the intercellular adhesion. This phenomenon is now being further investigated.

Dissociation of the surface protein complexes from mononuclear leukocytes and granulocytes followed by precipitation with antibody 60.3 indicated that the antibody recognizes the smallest polypeptides (GP90 and GP92) and that the larger components are non-covalently associated. In granulocytes GP 155 may correspond to a surface antigen with apparent molecular weight of 155–165 kDa termed Mol, OKM1, and Mac-1, which is expressed by most granulocytes and monocytes but by few lymphocytes [53, 50]. Less probably, it may constitute the lymphocyte function-associated antigen-1 (LFA-1), a 177,000-molecular weight polypeptide which is strongly expressed by lymphocytes and monocytes but weakly by granulocytes [50]. It was unlikely that antibody 60.3 recognized Mo1 (OKM1 Mac-1) or LFA-1 since its antigen is expressed by practically all lymphocytes [4] and strongly by granulocytes [5]. Interestingly, both Mo1 (OKM1, Mac-1) and LFA-1 as well as a third polypeptide with an apparent molecular weight of 150,000, have been found to be non-covalently associated with a smaller surface polypeptide of 95,000 Da expressed by all leukocytes and referred to as the β subunit of Mo1 (OKM1, Mac-1), LFA-1, and p 150 [50]. The GP90 and GP92 recognized by antibody 60.3 in mononuclear leukocytes and granulocytes, respectively, may be identical to the β subunit of the 3 protein complexes. Studies are being carried out to compare the various antigens. The slight difference in apparent molecular weight of the smallest components precipitated from mononuclear leukocytes and granulocytes may be due to differences in glycosylation. Two recently reported cell-surface antigens involved in granulocyte chemotaxis and detected by monoclonal antibodies NCD-1 [8] and S5-22 [26] differ clearly from GP92 in biochemical characteristics and cellular distribution. The precise role of the cell surface structure recognized by antibody 60.3 in the adhesion process is still unknown. In other cell types, intercellular adhesion is known to require the participation of ligands in the formation of cell–cell bonds [13]. Thus, it is likely that the surface polypeptides of 90,000–92,000 apparent molecular weight constitute ligands in leukocytes. We refer to the leukocytic ligand as Leu-CAM. The apparent lack of specificity of adhesion of activated granulocytes is noteworthy. In agreement with previous reports, phorbol ester-treated granulocytes adhered not only to other granulocytes but also to the tissue culture plate surface (Fig. 3). Since both processes were inhibited by antibody 60.3, it is unlikely that GP92 exerts a major discriminative function.

Carl_G_190x270_mm_blokki_FINAL.indd 224 06-Aug-23 1:53:43 PM

The discovery of an inherited deficiency of the cell-surface structures recognized by antibodies 60.3, OKM1, and anti-LFA-1 in leukocytes from an 8-year-old-boy with severe recurrent bacterial infections also supports the participation of GP92 in adhesion-dependent processes. The granulocytes of the patient did not adhere, or adhered only poorly, to endotoxin-coated coverslips or bovine endothelium, and their migration and phagocytosis were greatly reduced. Interestingly, glucose C-1 oxidation was normal and formate oxidation was raised [5]. A similar clinical syndrome also characterized by progressive periodontitis, delayed wound healing, persistent granulocytosis, and/or delayed umbilical cord separation has been described by other groups [2, 51]. The patients' leukocytes lack, or have very low amounts of, LFA-1, Mo1 (OKM1, Mac1), and p 150 kDa as well as the 95 kDa-associated polypeptide. Their granulocytes have abnormal functions which involve cell adherence such as spreading, aggregation, chemotaxis, and phagocytosis of particles. Interestingly, decreased granulocyte-mediated cytotoxicity of virus-infected cells was found in these patients [2, 23].

Monoclonal antibodies to cell surface antigens mediating leukocyte adhesion not only contribute to our understanding of the molecular basis of this process but may also have therapeutic potential in many inflammatory disorders.

ACKNOWLEDGMENTS

The authors wish to express their gratitude to Drs Jan Palmblad and Robert Szigeti for valuable suggestions concerning the separation of blood granulocytes, and to Dr Magnus Gidlund for assistance with the photomicrographs. Special thanks are due to Professor Hans Wigzell and Ms Inger Lindfors for revising and typing the manuscript, and to Professor John W. Fabre for providing the monoclonal antibody F10-44-2. This project has been supported by the Swedish Cancer Society, the Karolinska Institute, Cancerföreningen i Stockholm, The Academy of Finland,and a National Cancer Institute Grant 5RO1 CA 26294-05 (to C.G.G.).

ADDENDUM

Monoclonal antibody TA-1, which precipitates two surface polypeptides with apparent molecular weights of 170,000 and 95,000 from human leukocytes, labelled faintly most granulocytes, but did not inhibit their aggregation when used at 20 μg/ml [27].

REFERENCES

1 Abell, R.G. & Schenck, H.P. Microscopic observations on the behaviour of living blood vessels of the rabbit during the reaction of anaphylaxis. *J. Immunol.* **34,** 195, 1938.

2 Andersson, D.C., Schmalstieg, F.C., Arnout, M.A., Kohl, S., Tosi, M.F., Dana, N., Buffone, G.J., Hughes, B.J., Brinkely, B.R., Dickey, W.D., Abramson, J.S., Springer, T., Boxer, L.A., Hollers, J.M. & Smith C.W. Abnormalities of polymorphonuclear leukocyte function associated with a heritable deficiency of high molecular weight surface glycoproteins (GP 138): Common relationship to diminished cell adherence. *J. clin. Invest.* **74,** 536, 1984.

3 Barrett, A. The possible role of neutrophil proteinases in damage to articular cartilage. *Agents and Actions* **8,** 11, 1978.

4 Beatty, P.G., Ledbetter, J.A., Martin, P.S., Price, T.H. & Hansen, J.A. Definition of a common leukocyte cell-surface antigen (Lp 95-150) associated with diverse cell-mediated immune functions. *J. Immunol.* **131,** 2913, 1983.

5 Beatty, P.G., Ochs, H.D., Harlan, S.M., Price, T.H., Rosen, H., Taylor, R.F., Hansen, J.A. & Klebanoff, S.J. Absence of monoclonal antibody defined protein complex in boy with abnormal leukocyte function. *Lancet* **i,** 535, 1984.

6 Bonner, W.M. & Laskey, R.A. A film detection method for tritium-labeled proteins and nucleic acids in polyacrylamide gels. *Eur. J. Biochem.* **46,** 83, 1974.

7 Cohen, H.S. & Chovaniec, M.E. Superoxide generation by digitonin-treated guinea pig granulocytes. A basis for continuous assay for monitoring superoxide production and for the study of the activation of the generating system. *J. clin. Invest.* **61,** 1081, 1978.

8 Cottert, T.G. & Henson, P.M. Purification and characterization of an antigen involved in neutrophil chemotaxis and degranulation using a monoclonal antibody. *Eur. J. Immunol.* **14,** 605, 1984.

9 Craddock, P.R., Fehr, J., Dalmasso, A.P., Brigham, K.L. & Jacob, H.S. Hemodialysis leukopenia. Pulmonary vascular leukostasis resulting from complement activation by dialyser cellophane membranes. *J. clin. Invest.* **59,** 879, 1977.

10 Craddock, P.R., Hammerschmidt, D.H., White, J.C., Dalmasso, A.P. & Jacob, H.S. Complement (C5a)-induced granulocyte aggregation in vitro. A possible mechanism of complement-mediated leukostasis and leukopenia. *J. clin. Invest.* **60,** 260, 1977.

11 Dalchau, R., Kirkley, I. & Fabre, J.W. Monoclo-

Carl_G_190x270_mm_blokki_FINAL.indd 225 06-Aug-23 1:53:43 PM

nal antibody to a human brain-granulocyte-T lymphocyte antigen probably homologous to the W3/13 antigen of the rat. *Eur. J. Immunol.* **10,** 745, 1980.

12 Davies, M., Barrett, A.J., Travis, J., Sanders, E. & Coles, G.A. The degradation of human glomerular basement membrane with purified lysosomal proteinases; evidence for the pathogenic role of the polymorphonuclear leukocyte in glomerulonephritis. *Clin. Sci. mol. Med.* **54,** 232, 1978.

13 Edelman, G.M. Cell adhesion molecules: a molecular basis for animal form. *Sci. American* **250,** 80, 1984.

14 Eliasson, L., Kallin, B., Patarroyo, M., Klein, G., Fujiki, H. & Sugimura, H. Induction of the EB cycle and aggregation of human blood lymphocytes by the two new classes of tumor promoters: Teleocidin, lyngbyatoxin A, aplysiatoxin and debromoaplysiatoxin. *Int. J. Cancer* **31,** 7, 1983.

15 Fearon, D.T. Identification of the membrane glycoprotein that is the C3b receptor on the human erythrocyte, polymorphonuclear leukocyte, B lymphocyte and monocyte. *J. exp. Med.* **152,** 20, 1980.

16 Gahmberg, C.G. & Andersson, L.C. Selective radioactive labeling of cell surface sialoglycoproteins by periodate-tritiated borohydride. *J. Biol. Chem.* **252,** 5888, 1977.

17 Gahmberg, C.G. & Andersson, L.C. Leukocyte surface origin of human α 1-acid glycoprotein (orosomucoid) *J. exp. Med.* **148,** 507, 1978.

18 Gerdes, J., Naiem, M., Mason, D.Y. & Stein, H. Human complement (C3b) receptor defined by mouse monoclonal antibody. *Immunol.* **45,** 645, 1982.

19 Hammerschidt, D.E., White, J.G., Craddock, P.R. & Jacob, H.S. Corticosteroids inhibit complement-induced granulocyte aggregation. A possible mechanism for their efficacy in shock states. *J. clin. Invest.* **63,** 798, 1979.

20 Hjorth, R., Jonsson, A.K. & Vretblad, R. A rapid method for purification of human granulocytes using Percoll. A comparison with dextran sedimentation. *J. immunol. Meth.* **43,** 95, 1981.

21 Kaplan, H.B., Edelson, H.S., Friedman, R. & Weissmann, G. The roles of degranulation and superoxide anion generation in neutrophil aggregation. *Biochem. Biophys. Acta* **721,** 55, 1982.

22 Karnovsky, M.L. Biochemical aspects of the function of polymorphonuclear and mononuclear leukocytes. Pp. 25 in Bellanti, J.A. & Dayton, D.H. (eds) *The Phagocytic Cell in Host Resistance,* I. Raven Press, New York, 1975.

23 Kohl, S., Springer, T.A., Sachmalstieg, F.C., Loo, L.S. & Anderson, D.C. Defective natural killer cytotoxicity and polymorphonuclear leukocyte antibody-dependent cellular cytotoxicity in patients with LFA-1/OKM-1 deficiency. *J. Immunol.* **133,** 2972, 1984.

24 Korchak, H.M., Roos, D., Giedd, K.N., Wynkoop, E.M., Vienne, K., Rutherford, L.E., Buyan, J.P., Rich, A.M. & Weissmann, G. Granulocytes without degranulation: Neutrophil function in granule-depleted cytoplasts. *Proc. natn. Acad. Aci.* USA **80,** 4968, 1983.

25 Laemmli, V.K. Cleavage of structural proteins during the assembly of the head of bacteriophage T4. *Nature, Lond.* **227,** 680, 1970.

26 Laskin, D.L. & Rovera, G. Stimulation of human neutrophilic granulocyte chemotaxis by monoclonal antibodies. *J. Immunol.* **134,** 1146, 1985.

27 Le Bien, T.W. & Kersey, J.H. A monoclonal antibody (TA-1) ractive with human T lymphocytes and monocytes. *J. Immunol.* **125,** 2208, 1980.

28 Ledbetter, J.A., Evans, R.L., Lipinski, M., Cunningham-Ruddles, C., Good, R. & Herzenberg, L.A. Evolutionary conservation of surface molecules that distinguish T lymphocyte helper/inducer and cytotoxic/suppressor subpopulations in mouse and man. *J. exp. Med.* **153,** 310, 1981.

29 Lichtenstein, A. & Kahle, J. Anti-tumor effect of inflammatory neutrophiles: Characteristics of in vivo generation and in vitro tumor cell lysis. *Int. J. Cancer* **35,** 121, 1985.

30 Lysozyme assay. *Worthington Enzyme Manual,* Worthington Biochemical Corp., Freehold, N.J. p. 100, 1972.

31 MacGregor, R.R., Macarak, E.J. & Kefalides, N.A. Comparative adherence of granulocytes to endothelial monolayers and nylon fiber. *J. clin. Invest.* **61,** 697, 1978.

32 Mueller, K. & Gerisch, G. A specific glycoprotein as the target site of adhesion blocking Fab in aggregating Dictyostelium cells. *Nature, Lond.* **274,** 445, 1978.

33 Niedel, J.E. Detergent solubilization of the formyl peptide chemotactic receptor. *J. Biol. Chem.* **256,** 9295, 1981.

34 Nishizuka, Y. The role of protein kinase C in cell surface signal transduction and tumor promotion. *Nature, Lond.* **308,** 693, 1984.

35 Nishizuka, Y. Turnover of inositol phospholipid and signal transduction. *Science* **225,** 1365, 1984.

36 Ocklind, C. & Öbrink, B. Intercellular adhesion of rat hepatocytes. Identification of a cell surface glycoprotein involved in the initial adhesion process. *J. Biol. Chem.* **257,** 6788, 1982.

37 O'Flaherty, J.T., Kreutzer, D.L. & Ward, P.A. Effect of cytochalasin B on human neutrophil aggregation. *Exp. Cell. Res.* **120,** 31, 1979.

38 O'Flaherty, J.T., Dechatelet, L.R., McCall, C.E. & Bass, D.A. Neutrophil aggregation: Evidence for a different mechanism of action by phorbol myristate acetate. *Proc. Soc. exp. Biol. Med.* **165,** 225, 1980.

39 Omary, M.B., Trowbridge, I.S. & Battifora, H.A. Human homologue of murine T200 glycoprotein. *J. exp. Med.* **152,** 842, 1980.

40 Parham, P., Barnstable, C.J. & Bodmer, W.F. Use of a monoclonal antibody (W6/32) in structural studies of HLA-A, B, C, antigens. *J. Immunol.* **123,** 341, 1979.

41 Patarroyo, M., Biberfeld, P., Klein, E. & Klein, G. 12-*O*-Tetradecanoyl-phorbol-13-acetate (TPA) treatment elevates the natural killer (NK) sen-

Carl_G_190x270_mm_blokki_FINAL.indd 226 06-Aug-23 1:53:43 PM

sitivity of certain human lymphoid lines. *Cell Immunol.* **63,** 237, 1981.

42 Patarroyo, M., Yogeeswaran, G., Biberfeld, P., Klein, E. & Klein, G. Morphological changes, cell aggregation and cell membrane alterations caused by phorbol 12,13-dibutyrate in human blood lymphocytes. *Int. J. Cancer* **30,** 707, 1982.

43 Patarroyo, M., Biberfeld, P., Klein, E. & Klein, G. Phorbol 12,13-dibutyrate $P(Bu)_2$-treated human blood mononuclear cells bind to each other. *Cell Immunol.* **75,** 144, 1983.

44 Patarroyo, M., Jondal, M., Gordon, J. & Klein, E. Characterization of the phorbol 12,13-dibutyrate $P(Bu)_2$ induced binding between human blood lymphocytes. *Cell Immunol.* **81,** 373, 1983.

45 Patarroyo, M., Beatty, P.G., Fabre, J.W. & Gahmberg, C.G. Identification of a cell surface protein complex mediating phorbol ester-induced adhesion (binding) among human mononuclear leukocytes. *Scand. J. Immunol.* **22,** 171, 1985.

46 Perussio, B., Trinchieri, G., Jackson, A., Warner, N.L., Faust, J., Rumpold, H., Kraft, D. & Lanier, L.L. The Fc receptor for IgG on human natural killer cells: Phenotypic, functional and comparative studies with monoclonal antibodies. *J. Immunol.* **133,** 180, 1984.

47 Repine, J.E., White, J.G., Calwson, C.C. & Holmes, B.M. The influence of phorbol myristate acetate on oxygen consumption by polymorphonuclear leukocytes. *J. Lab. Clin. Med.* **83,** 911, 1974.

48 Ringertz, B., Plamblad, J., Rädmark, O. & Malmsten, C. Leukotriene-induced neutrophil aggregation in vitro. *FEBS Letters* **147,** 180, 1982.

49 Roder, J., Kiessling, R., Biberfeld, P. & Andersson, B. Target–effector interaction in the natural killer (NK) cell system. II. The isolation of NK cells and studies on the mechanisms of killing. *J. Immunol.* **121,** 2509, 1978.

50 Sanchez-Madrid, F., Nagy, J., Robbins, E., Simon, P. & Springer, T.A. A human leukocyte differentiation antigen family with distinct alpha-subunits and a common beta-subunit: The lymphocyte function associated antigen (LFA-1), the C3bi complement receptor (OKM1/Mac-1) and the p 150, 95 molecule. *J. exp. Med.* **158,** 1785, 1983.

51 Springer, T.A., Tompson, W.S., Miller, L.J., Schmalstieg, F.C. & Anderson, P.C.: Inherited deficiency of the Mac-1, LFA-1, p 150, 95 glycoprotein family and its molecular basis. *J. exp. Med.* **160,** 1901, 1984.

52 Starkey, J.R., Liggitt, H.D., Jones, W. & Hosick, H.L. Influence of migratory blood cells on the attachment of tumor cells to vascular endothelium. *Int. J. Cancer* **334,** 535, 1984.

53 Todd, R.F., van Agthoven, A., Schlossman, S.F. & Terhorst, C. Structural analysis of differentiation antigens Mo1 and Mo2 on human monocytes. *Hybridoma* **1,** 329, 1982.

54 Tonnesen, M.G., Smedly, L.A. & Henson, P.M. Neutrophil–endothelial cell interactions. Modulation of neutrophil adhesiveness induced by complement fragments C5a and C5a des arg and formyl-methionyl-leucyl-phenylalanine in vivo. *J. clin. Invest.* **74,** 1581, 1984.

55 Tsan, M-F. & Denison, R.C. Phorbol myristate acetate-induced neutrophil autotoxicity. A comparison with H_2O_2 toxicity. *Inflammation* **4,** 371, 1980.

56 Tsien, R.Y., Pozzan, T. & Rink, T. T-cell mitogens cause early changes in cytoplasmic free Ca^{++} and membrane potential in lymphocytes. *Nature, Lond.* **295,** 68, 1982.

57 Urushihara, H. & Takeichi, M. Cell–cell adhesion molecule: Identification of a glycoprotein relevant to the Ca^{++} independent aggregation of Chinese hamster fibroblasts. *Cell* **20,** 363, 1980.

58 Whitin, J.C. & Cogen, H.J. Dissociation between agregation and superoxide production in human granulocytes. *J. Immunol.* **134,** 1206, 1985.

59 Wilkinson, P.C. & Lackie, J.M. The adhesion, migration and chemotaxis of leukocytes in inflammation. Pp. 48–88 in Movat H. Z. (ed) *Current Topics in Pathology* 68. Springer-Verlag, New York, 1979.

60 Zola, H., McNamara, P., Thomas, M., Smart, I.J. & Bradley, J. The preparation and properties of monoclonal antibodies against human granulocyte membrane antigens. *Br. J. Haematol.* **48,** 481, 1981.

Received 18 April 1985

Carl_G_190x270_mm_blokki_FINAL.indd 227 06-Aug-23 1:53:44 PM

Biochemistry **1991**, *30*, 1561–1571

Structural Study of the Sugar Chains of Human Leukocyte Cell Adhesion Molecules CD11/CD18†

Masahiro Asada,‡ Kiyoshi Furukawa,‡ Carmela Kantor,§ Carl G. Gahmberg,§ and Akira Kobata*,‡

Department of Biochemistry, Institute of Medical Science, University of Tokyo, Minato-ku, Tokyo 108, Japan, and Department of Biochemistry, University of Helsinki, SF-00170 Helsinki, Finland

Received June 8, 1990; Revised Manuscript Received September 4, 1990

ABSTRACT: Leu-CAMs (CD11/CD18) consisting of LFA-1, Mac-1, and p150/95 are leukocyte cell surface glycoproteins that are involved in various leukocyte functions. The asparagine-linked sugar chains were released as oligosaccharides from Leu-CAMs by hydrazinolysis. About 12 mol of sugar chains was released from 1 mol of Leu-CAMs. These sugar chains were converted to radioactive oligosaccharides by reduction with sodium borotritide and separated into neutral and acidic fractions by paper electrophoresis. All of the acidic oligosaccharides were converted to neutral ones by digestion with sialidase, indicating that they are sialyl derivatives. The neutral and sialidase-treated acidic oligosaccharides were fractionated by chromatography on lectin columns followed by Bio-Gel P-4 column chromatography. Structural studies of each oligosaccharide by sequential exo- and endoglycosidase digestion and by methylation analysis revealed that Leu-CAMs contain mainly high mannose type and high molecular weight complex type sugar chains. The latter sugar chains were of bi-, tri-, and tetraantennary complex types with the Galβ1→4(Fucα1→3)GlcNAcβ1→ and/or the Galβ1→3GlcNAcβ1→ groups together with the Galβ1→4GlcNAc group in their outer-chain moieties. In addition to these sugar chains, a small amount of monoantennary complex type and hybrid type sugar chains was found in Leu-CAMs. Furthermore, analysis of the asparagine-linked sugar chains released from the β-subunit of Leu-CAMs by a series of lectin chromatography showed that subunit-specific glycosylation is not observed between the α- and β-subunits of Leu-CAMs.

The leukocyte cell adhesion molecules (Leu-CAMs or CD11/CD18)[1] are members of the integrin superfamily (Hynes, 1987; Kishimoto et al., 1987a; Ruoslahti & Pierschbacher, 1987; Arnaout, 1990). They consist of the lymphocyte function-associated antigen 1 (LFA-1, CD11a/CD18), which is distributed in most leukocytes, the myeloid antigen 1 (Mac-1, CD11b/CD18), and the glycoproteins p150/95 (CD11c/CD18) expressed mainly on the surfaces of macrophages and hairy leukemia cells (Patarroyo et al., 1985a,b; Schwarting et al., 1985; Hogg et al., 1986; Miller et al., 1986). All of these three molecules are composed of α- and β-subunits in which the common β-subunit (CD18) (M_r 95000) is associated noncovalently with a unique α-subunit having a different molecular weights (M_r 180000 for CD11a, M_r 170000 for CD11b, and M_r 150000 for CD11c) (Kurzinger & Springer, 1982; Springer et al., 1987).

Extensive studies on the functions of the CD11a/CD18 molecule revealed that it is involved in numerous adhesion-dependent phenomena, including T cell mediated immune responses. Monoclonal antibodies directed against CD11a/CD18 block the proliferation of antigen-specific helper T cells and cytotoxic T cell mediated cytolysis, antibody-dependent cytotoxity by granulocytes, and natural killer cell activity (Davignon et al., 1981; Krensky et al., 1983; Miedema et al., 1984; Timonen et al., 1988, 1990). In granulocytes and monocytes, a large proportion of CD11b/CD18 and CD11c/CD18 is stored in intracellular compartments and translocated to the cell surfaces upon stimulation of inflammatory mediators, resulting in increased adhesiveness of these cells to endothelial cells (Berger et al., 1984; Todd et al., 1984; Miller et al., 1987).

The oligosaccharide moieties of cell surface glycoproteins appear to be involved in specific cell to cell interactions in many biological systems (Heifetz & Lennarz, 1979; Geltosky et al., 1980; Rutishauser, 1984). Furthermore, carbohydrate groups have been implicated in the recognition processes of lymphocytes (Hart, 1982; Cowing & Chapdelaine, 1983). It has been demonstrated that the structures of the asparagine-(Asn-) linked sugar chains on lymphocyte cell surfaces influence the recognition of Ia antigens by responding T cells in the mixed lymphocyte reaction (Pimlott & Miller, 1986; Powell et al., 1985).

Although Leu-CAMs have been studied extensively because of their involvement in various recognition and/or adhesion phenomena, little is known about their carbohydrate structures. Recently, the genes encoding CD11a/CD18, CD11b/CD18, and CD11c/CD18 molecules have been cloned, and their deduced amino acid sequences showed that there are 12 potential glycosylation sites in CD11a (Larson et al., 1989), 19 in CD11b (Stastre et al., 1986; Arnaout et al., 1988; Corbi et al., 1988), 10 in CD11c, and 6 in CD18 (Corbi et al., 1987; Kishimoto et al., 1987b; Law et al., 1987). However, these consensus sequences in Leu-CAMs are apparently not all glycosylated, as estimated by the decrease in their molecular

† This study was supported in part by a Grant-in-Aid for Scientific Research from the Ministry of Education, Science, and Culture of Japan and by research grants from the Academy of Finland and the Sigrid Juselins Foundation.

* To whom correspondence should be addressed.
‡ University of Tokyo.
§ University of Helsinki.

[1] Abbreviations: CD11/CD18, Leu-CAM, heterocomplex of leukocyte adhesion molecules consisting of specific α-chains and the common β-chain; CD11a/CD18, Leu-CAMa, LFA-1; CD11b/CD18, Leu-CAMb, Mac-1; CD11c/CD18, Leu-CAMc, p150/95; Con A, concanavalin A; AAL, *Aleuria aurantia* lectin; RCA, *Ricinus communis* agglutinin 120. Subscript OT is used to indicate NaB^3H_4-reduced oligosaccharides. All sugars mentioned in this paper have the D-configuration except for fucose, which has the L-configuration.

0006-2960/91/0430-1561$02.50/0 © 1991 American Chemical Society

Carl_G_190x270_mm_blokki_FINAL.indd 228 06-Aug-23 1:53:44 PM

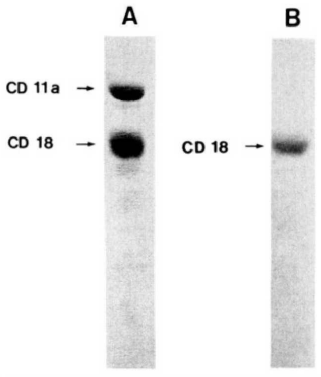

FIGURE 1: SDS–polyacrylamide gel electrophoretogram of purified CD11/CD18 and CD18: (A) pattern of the Leu-CAM complex purified by affinity chromatography; (B) pattern of isolated CD18. The gels were stained with Coomassie Brilliant Blue.

weights on SDS–polyacrylamide gel electrophoresis (SDS–PAGE) after digestion with endoglycosidases (Miller & Springer, 1987; Kantor et al., 1988). In agreement with this, only half of the potential sites in a fibronectin receptor, which is also a member of an integrin family, are reported to be glycosylated (Akiyama & Yamada, 1987). As a first step to elucidate the functional roles of the integrin, an extensive structural study of the sugar chains of Leu-CAMs has been performed in this study.

Experimental Procedures

Purification of Leu-CAMs. Packed human buffy coat cells, which are enriched in T cells, were prepared by Ficoll-Isopaque gradient centrifugation from pooled human blood supplied by Finnish Red Cross Blood Transfusion Service, Helsinki. The cells were homogenized by a Potter-Elvehjem homogenizer in 10 mM phosphate buffer, pH 7.4, containing 0.15 M NaCl, 1% Triton X-100, and 1 mM phenylmethanesulfonyl fluoride. The cell homogenates were centrifuged at 20000*g* for 15 min, and the resultant supernatants were further spun down at 100000*g* for 45 min. Leu-CAMs were purified from the final supernatants, in which solubilized membrane-bound glycoproteins were recovered, by affinity chromatography using a column containing the monoclonal antibody mAb-59 bound to Sepharose 4B. This antibody recognizes the β-subunit common to the three Leu-CAMs. The column was washed with 20 mM glycine–NaOH buffer, pH 9.0, containing 0.1% sodium deoxycholate to remove nonspecifically adsorbed proteins. The bound materials were eluted with 50 mM diethylamine solution, pH 11.5. The eluates were neutralized, dialyzed against distilled water, and lyophilized (Kantor et al., 1988). Leu-CAMs thus prepared contained two major bands migrating with apparent molecular weights of 180000 and 95000 as determined by SDS–PAGE, which is shown in Figure 1. For separation of the β-subunit, preparative SDS–PAGE was used. The isolated protein showed a single band by SDS–PAGE (Figure 1).

Liberation of Asn-Linked Sugar Chains from Leu-CAMs. Leu-CAMs (5 mg) and the isolated β-subunit (approximately 0.1 mg), which were dried thoroughly over P_2O_5 in vacuo, were subjected to hydrazinolysis for 10 h as described previously (Takasaki et al., 1982). After N-acetylation, two-thirds of the liberated oligosaccharide mixture from Leu-CAMs was reduced with NaB^3H_4 to obtain tritium-labeled oligosaccharides for structural analysis, and the remainder was reduced with NaB^2H_4 to obtain deuterium-labeled oligosaccharides for methylation analysis. To facilitate the detection of the deuterium-labeled oligosaccharides, one-ninth of the tritium-labeled oligosaccharides was added. Due to the limited amount of the β-subunit available, the oligosaccharide mixture obtained from this glycoprotein was solely reduced with NaB^3H_4 for structural analysis.

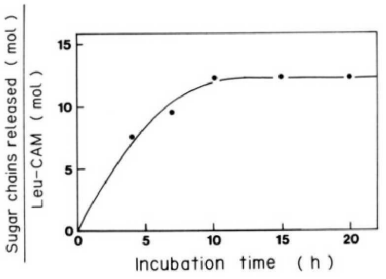

FIGURE 2: Time course of the release of oligosaccharides from Leu-CAMs by hydrazinolysis. The number of sugar chains released from Leu-CAMs was calculated on the basis of the radioactivities incorporated into the oligosaccharides and xylitol and a molecular weight for Leu-CAMs of 275000 as described in the text.

In order to determine the number of Asn-linked sugar chains included in one molecule of glycoprotein sample, a time-course study of the liberation of sugar chains by hydrazinolysis was performed with 100 μg of Leu-CAMs for each incubation time. Xylose was added as an internal standard according to the previously published method (Takasaki et al., 1982). For instance, xylose (25 nmol) was mixed with the released oligosaccharides prior to reduction with NaB^3H_4. The radioactive oligosaccharides and [^{3}H]xylitol were separated by paper chromatography using 1-butanol–ethanol–water (4:1:1 v/v) as a solvent. On the basis of the radioactivities incorporated into xylitol and the oligosaccharide fraction and the molecular weight of Leu-CAMs as 275000, the approximate number of Asn-linked sugar chains liberated from 1 mol of Leu-CAMs was calculated to be 12 mol (Figure 2). This value is consistent with those estimated from the decrease in the molecular weight of CD11a/CD18 and CD11c/CD18 on SDS–PAGE after endoglycosidase treatment (Miller & Springer, 1987; Kantor et al., 1988). The data indicated that about 5–6 Asn-linked sugar chains are included in each subunit.

Analytical Methods. The radioactive oligosaccharides were subjected to high-voltage paper electrophoresis in pyridine–acetate buffer, (3:1:387 pyridine:acetic acid:water), pH 5.4, at 70 V/cm for 90 min. Fractionation of the radioactive oligosaccharides by Bio-Gel P-4 column chromatography was performed as reported by Yamashita et al. (1982). Methylation analysis of oligosaccharides was conducted as described in a previous paper (Furukawa et al., 1989).

Affinity Chromatography of Oligosaccharides on Immobilized Lectin Columns. Lectin column chromatography using immobilized concanavalin A (Con A), *Aleuria aurantia* lectin (AAL), and *Ricinus communis* agglutinin 120 (RCA) was performed as described previously (Ogata et al., 1975; Yamashita et al., 1985; Harada et al., 1987). In brief, the mixture of radioactive oligosaccharides was applied to a Con A–Sepharose column that was equilibrated with 10 mM Tris-HCl buffer, pH 7.4, containing 0.1 M NaCl, 1 mM $MgCl_2$, 1 mM $CaCl_2$, and 1 mM $MnCl_2$. The column was washed with 10 bed volumes of the buffer, and the bound oligosaccharides were eluted with the buffer containing 5 mM methyl α-D-glucopyranoside and then with the buffer containing 100 mM

Carl_G_190x270_mm_blokki_FINAL.indd 229 06-Aug-23 1:53:45 PM

methyl α-D-mannopyranoside. In the case of an AAL–Sepharose column that was equilibrated with 10 mM Tris-HCl buffer, pH 7.4, the column was washed with 10 bed volumes of the buffer, and the bound oligosaccharides were eluted with the buffer containing 1 mM L-fucose. In the case of an RCA–agarose column that was equilibrated with phosphate-buffered saline, pH 7.4, the column was washed with 10 bed volumes of the buffer, and the bound oligosaccharides were eluted with the buffer containing 10 mM lactose.

Chemicals, Enzymes, and Lectins. Con A–Sepharose and RCA–agarose were purchased from Pharmacia Fine Chemical Co., Tokyo, and Hohnen Oil Co., Tokyo, respectively. AAL–Sepharose was kindly supplied by Dr. N. Kochibe, Gunma University. NaB^3H_4 (600 mCi/mmol) was purchased from New England Nuclear (Boston, MA), and NaB^2H_4 was obtained from Nacalai Tesque Co., Kyoto. Streptococcal β-galactosidase and β-*N*-acetylhexosaminidase were purified from culture fluid of *Streptococcus pneumoniae* according to the method of Glasgow et al. (1977). Jack bean β-*N*-acetylhexosaminidase was purified from jack bean meal (Sigma Chemical Co., St. Louis, MO) by the method of Li and Li (1972). β-Galactosidase from *Streptococcus* 6646K, which will be referred to as 6646K β-galactosidase in this paper, and β-mannosidase from snail were kindly supplied by Seikagaku Kogyo Co., Tokyo. *Aspergillus saitoi* α-mannosidases I and II were purified according to the method of Kobata and Amano (1987). Almond emulsin α-fucosidase I was purified according to the method of Kobata (1982). Sialidase from *Arthrobacter ureafaciens* and endo-β-galactosidase from *Escherichia freundii* were purchased from Nacalai Tesque Co., Kyoto, and Seikagaku Kogyo Co., Tokyo, respectively.

Exo- and Endoglycosidase Digestion. Unless otherwise mentioned, oligosaccharides [(3–5) × 10^3 cpm] were incubated with one of the following mixtures at 37 °C for 18h: (1) *Ar. ureafaciens* sialidase (50 milliunits) in 50 μL of 0.5 M acetate buffer (pH 5.0); (2) a mixture of streptococcal β-galactosidase (1 milliunit) and β-*N*-acetylhexosaminidase (4 milliunits) in 80 μL of 0.3 M citrate phosphate buffer (pH 6.0) containing 7.5 μmol of mannose; (3) a mixture of *Streptococcus* 6646K β-galactosidase (5 milliunits) and jack bean β-*N*-acetylhexosaminidase (0.5 units) in 50 μL of 0.3 M citrate phosphate buffer (pH 5.5); (4) *Streptococcus* 6646K β-galactosidase (5 milliunits) in 50 μL of 0.3 M citrate phosphate buffer (pH 6.0); (5) almond emulsin α-fucosidase I (40 microunits) in 50 μL of 0.1 M acetate buffer (pH 5.0); (6) *As. saitoi* α-mannosidase I (0.15 μg) in 30 μL of 0.5 M acetate buffer (pH 5.0); (7) *As. saitoi* α-mannosidase II (20 milliunits) in 50 μL of 0.5 M acetate buffer (pH 5.0); (8) snail β-mannosidase (10 milliunits) in 50 μL of 0.05 M sodium citrate buffer (pH 4.0); (9) jack bean β-*N*-acetylhexosaminidase (0.5 units) in 50 μL of 0.3 M citrate phosphate buffer containing 100 μg of γ-galactonolactone; (10) *E. freundii* endo-β-galactosidase (20 milliunits) in 50 μL of 0.1 M acetate buffer (pH 6.0). One drop of toluene was added to all reaction mixtures to inhibit bacterial growth during incubation. The digestion was terminated by heating the reaction mixture in a boiling water bath for 3 min, and the product was desalted and analyzed by Bio-Gel P-4 column chromatography.

Oligosaccharides. Neu5Acα2→6Galβ1→4GlcNAcβ1→2Manα1→6(Neu5Acα2→6Galβ1→4GlcNAcβ1→2Manα1→3)Manβ1→4GlcNAcβ1→4GlcNAc$_{OT}$ (Neu5Ac$_2$·Gal$_2$·GlcNAc$_2$·Man$_3$·GlcNAc·GlcNAc$_{OT}$) and Neu5Acα2→6Galβ1→4GlcNAcβ1→2Manα1→6 or 3-(Galβ1→4GlcNAcβ1→2Manα1→3 or 6)Manβ1→4GlcNAcβ1→4GlcNAc$_{OT}$ (Neu5Ac·Gal$_2$·GlcNAc$_2$·Man$_3$·GlcNAc·GlcNAc$_{OT}$) were prepared from human transferrin (Spik et al., 1975) by hydrazinolysis, and their desialylated oligosaccharide (Gal$_2$·GlcNAc$_2$·Man$_3$·GlcNAc·GlcNAc$_{OT}$) was prepared by digestion with *Ar. ureafaciens* sialidase. Neu5Acα2→6Galβ1→4GlcNAcβ1→4(Neu5Acα2→6Galβ1→4GlcNacβ1→2)Manα1→3(Neu5Acα2→6Galβ1→4GlcNAcβ1→2Manα1→6)Manβ1→4GlcNAcβ1→4GlcNAc$_{OT}$ (Neu5Ac$_3$·Gal$_3$·GlcNAc$_3$·Man$_3$·GlcNAc·GlcNAc$_{OT}$) and its di- and monosialylated oligosaccharide (Neu5Ac$_2$·Gal$_3$·GlcNAc$_3$·Man$_3$·GlcNAc·GlcNAc$_{OT}$ and Neu5Ac·Gal$_3$·GlcNAc$_3$·Man$_3$·GlcNAc·GlcNAc$_{OT}$) were prepared from fetuin (Takasaki & Kobata, 1986) by hydrazinolysis. Galβ1→4GlcNAcβ1→2Manα1→6(Galβ1→4GlcNAcβ1→2Manα1→3)Manβ1→4GlcNAcβ1→4(Fucα1→6)GlcNAc$_{OT}$(Gal$_2$·GlcNAc$_2$·Man$_3$·GlcNAc·Fuc·GlcNAc$_{OT}$) was prepared from human platelet thrombospondin (Furukawa et al., 1989). Manα1→6(Manα1→3)Manβ1→4GlcNAcβ1→4GlcNAc$_{OT}$ (Man$_3$·GlcNAc·GlcNAc$_{OT}$) and Manα1→6(Manα1→3)Manβ1→4GlcNAcβ1→4(Fucα1→6)GlcNAc$_{OT}$ (Man$_3$·GlcNAc·Fuc·GlcNAc$_{OT}$) were obtained from Gal$_2$·GlcNAc$_2$·Man$_3$·GlcNAc·GlcNAc$_{OT}$ and Gal$_2$·GlcNAc$_2$·Man$_3$·GlcNAc·Fuc·GlcNAc$_{OT}$, respectively, by digestion with a mixture of streptococcal β-galactosidase and β-*N*-acetylhexosaminidase. Manα1→6(Manα1→3)Manα1→6(Manα1→3)Manβ1→4GlcNAcβ1→4GlcNAc$_{OT}$ (Man$_5$·GlcNAc·GlcNAc$_{OT}$) was obtained from bovine pancreatic ribonuclease B (Liang et al., 1980), and Manβ1→4GlcNAcβ1→4GlcNAc$_{OT}$(Man·GlcNAc·GlcNAc$_{OT}$) was prepared from its digest with jack bean α-mannosidase.

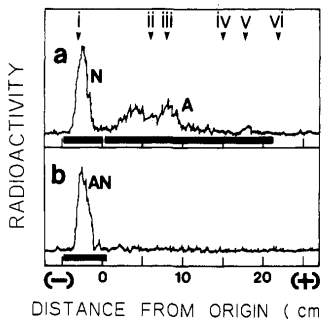

FIGURE 3: Paper electrophoretogram of oligosaccharides released from Leu-CAMs. The radioactive oligosaccharides released from Leu-CAMs by hydrazinolysis followed by reduction with NaB^3H_4 were subjected to paper electrophoresis (a). Fractions N and A were recovered from the paper by elution with water. A part of fraction A was digested with *Ar. ureafaciens* sialidase and analyzed by paper electrophoresis (b). Arrowheads at the top of the figure indicate the migrating positions of authentic oligosaccharides: (i) lactitol; (ii) Neu5Ac·Gal$_3$·GlcNAc$_3$·Man$_3$·GlcNAc·GlcNAc$_{OT}$; (iii) Neu5Ac·Gal$_2$·GlcNAc$_2$·Man$_3$·GlcNAc·GlcNAc$_{OT}$; (iv) Neu5Ac$_2$·Gal$_3$·GlcNAc$_3$·Man$_3$·GlcNAc·GlcNAc$_{OT}$; (v) Neu5Ac$_2$·Gal$_2$·GlcNAc$_2$·Man$_3$·GlcNAc·GlcNAc$_{OT}$; (vi) Neu5Ac$_3$·Gal$_3$·GlcNAc$_3$·Man$_3$·GlcNAc·GlcNAc$_{OT}$.

Results

Fractionation of Oligosaccharides by Paper Electrophoresis. The radioactive oligosaccharides released from Leu-CAMs by hydrazinolysis were subjected to paper electrophoresis and separated into neutral (N) and acidic (A) fractions (Figure 3a). The percent molar ratios of the fractions N and A calculated from their radioactivities were 56% and 44%, respectively. When fraction A was digested exhaustively with

Carl_G_190x270_mm_blokki_FINAL.indd 230 06-Aug-23 1:53:45 PM

Table I: Percent Molar Ratio of Oligosaccharides Fractionated by Serial Immobilized Lectin Column Chromatography

		% molar ratio			
		$\alpha\beta$ complex		β-subunit	
	fractions	N	AN	N	AN
I	Con A^-, AAL^-	5	3	8	9
II	Con A^-, AAL^+	7	26	5	23
III	Con A^+, AAL^-	1	3	2	4
IV	Con A^+, AAL^+	3	10	2	7
V	Con A^{++}, AAL^-	40	2	38	2
VI	Con A^{++}, AAL^+	0	tr[a]	0	tr

[a] Trace, less than 1% of the total oligosaccharides.

Ar. ureafaciens sialidase, all of the acidic oligosaccharides were converted to neutral ones (AN) as shown in Figure 3b. Therefore, most of the acidic nature of the oligosaccharides could be ascribed to their sialic acid residues.

Fractionation of Oligosaccharides in Fractions N and AN by Lectin Chromatography. Oligosaccharides in fractions N and AN were subjected to Con A–Sepharose column chromatography, since Leu-CAMs are reported to contain high mannose type sugar chains (Miller & Springer, 1987). The pass-through fraction (Con A^-), the bound fraction eluted with 5 mM methyl α-D-glucoside (Con A^+), and the fraction eluted with 100 mM methyl α-D-mannoside (Con A^{++}) were obtained. These fractions were applied to an AAL–Sepharose column in order to separate oligosaccharides with and without the Fucα1→6GlcNAc group in their trimannosyl core. The fraction that passed through the column is designated as AAL^- and that bound to the column and eluted with 1 mM L-fucose as AAL^+. The molar ratios of oligosaccharides in each fraction thus separated by the serial lectin column chromatography were calculated on the basis of the radioactivities of the fractions and are summarized in Table I.

Structures of Oligosaccharides in Fractions V and VI. When fraction N-V (Con A^{++}, AAL^-), which contained 40% of the total oligosaccharides, was subjected to Bio-Gel P-4 column chromatography, it was separated into five peaks (Figure 4A). After digestion with *As. saitoi* α-mannosidase I, which cleaves only the Manα1→2Man linkage, about 95% of the oligosaccharides was converted to a radioactive component, the effective size of which was the same as authentic Man_5·GlcNAc·$GlcNAc_{OT}$ (component a in Figure 4B). When component a in Figure 4B was further digested with jack bean α-mannosidase, the product was eluted at the same position as authentic Man·GlcNAc·$GlcNAc_{OT}$ (Figure 4C). That the radioactive product in Figure 4C has the structure Manβ1→GlcNAcβ1→$GlcNAc_{OT}$ was confirmed by sequential digestion with snail β-mannosidase and jack bean β-*N*-acetylhexoaminidase (data not shown). These results indicated that approximately 95% of the oligosaccharides in fraction N-V were a series of high mannose type: (Manα1→2)$_{0\sim4}$·Man_5·GlcNAc·$GlcNAc_{OT}$.

The rest of the oligosaccharides in fraction N-V were resistant to α-mannosidase I digestion and were separated into two radioactive components (b and c in Figure 4B). When component c was digested with streptococcal β-galactosidase, one galactose residue was released (solid line in Figure 4D). When it was further digested with streptococcal β-*N*-acetylhexosaminidase, one *N*-acetylglucosamine residue was released and eluted at the same position as authentic Man_5·GlcNAc·$GlcNAc_{OT}$ (solid line in Figure 4E). That the radioactive solid-line product in Figure 4E has the same structure as Man_5·GlcNAc·$GlcNAc_{OT}$ was further confirmed by the fact that it was converted to Manβ1→4GlcNAcβ1→$4GlcNAc_{OT}$ by jack bean α-mannosidase digestion (solid line in Figure 4F).

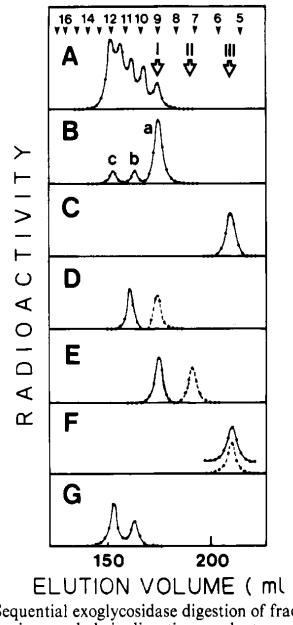

FIGURE 4: Sequential exoglycosidase digestion of fractions N-V and AN-V. Fractions and their digestion products were analyzed by Bio-Gel P-4 column chromatography: (A) fraction N-V; (B) oligosaccharides in panel A digested with *As. saitoi* α-mannosidase I; (C) component a in panel B digested with jack bean α-mannosidase; (D) components b (dotted line) and c (solid line) digested with streptococcal β-galactosidase; (E) solid and dotted lines representing the digestion products of solid- and dotted-line peaks in panel D with streptococcal β-*N*-acetylhexosaminidase, respectively; (F) solid and dotted lines representing the digestion products of solid- and dotted-line peaks in panel E with jack bean α-mannosidase, respectively; (G) fraction AN-V. Arrowheads at the top of the figure indicate the elution positions of glucose oligomers used as internal standards, and the numbers indicate the glucose units. White arrows indicate the elution positions of authentic oligosaccharides: (I) Man_9·GlcNAc·$GlcNAc_{OT}$; (II) Man_5·GlcNAc·$GlcNAc_{OT}$; (III) Man·GlcNAc·$GlcNAc_{OT}$.

These results and Con A binding specificity of the oligosaccharide indicated that component c in Figure 4B has the structure

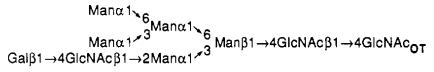

Component b also released one galactose residue by digestion with streptococcal β-galactosidase (dotted line in Figure 4D) and one *N*-acetylglucosamine residue with streptococcal β-*N*-acetylhexosaminidase (dotted line in Figure 4E). The resulting radioactive product was eluted at the same position as authentic Man_3·GlcNAc·$GlcNAc_{OT}$. The dotted-line product in Figure 4E was converted to Man·GlcNAc·$GlcNAc_{OT}$ by digestion with jack bean α-mannosidase (dotted line in Figure 4F). That the dotted line products in Figure 4F have the structure Manβ1→GlcNAcβ1→$GlcNAc_{OT}$ was confirmed by sequential exoglycosidase digestion as described above. The results indicated that component b in Figure 4B is a monoantennary complex type sugar chain with the Galβ1→4GlcNAcβ1→2 group at its outer chain. Since component b was totally resistant to digestion with *As. saitoi* α-mannosidase II, which releases a mannose residue from the Galβ1→4GlcNAcβ1→2Manα1→6(Manα1→3)Man group but not from the Galβ1→4GlcNAcβ1→2Manα1→3-

Carl_G_190x270_mm_blokki_FINAL.indd 231 06-Aug-23 1:53:46 PM

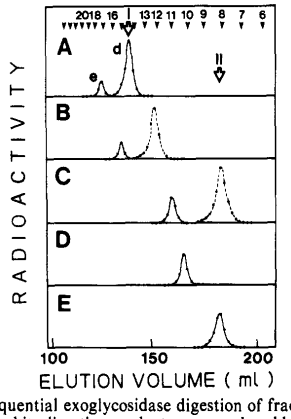

FIGURE 5: Sequential exoglycosidase digestion of fraction AN-IV. The fraction and its digestion products were analyzed by Bio-Gel P-4 column chromatography: (A) fraction AN-IV; (B) dotted and solid lines representing the digestion products of components d and e in panel A with streptococcal β-galactosidase, respectively; (C) dotted and solid lines representing the digestion products of dotted- and solid-line peaks in panel B with streptococcal β-*N*-acetylhexosaminidase; (D) the solid-line peak in panel C digested with streptococcal β-galactosidase; (E) the peak in panel D digested with streptococcal β-*N*-acetylhexosaminidase. Arrowheads at the top of the figure are the same as in Figure 4. White arrows indicate the elution positions of authentic oligosaccharides: (I) Gal_2·$GlcNAc_2$·Man_3·GlcNAc·Fuc·$GlcNAc_{OT}$; (II) Man_3·GlcNAc·Fuc·$GlcNAc_{OT}$.

(Manα1→6)Man group (data not shown), the Galβ1→4GlcNAc group should be attached to the Manα1→3 side. In order to further confirm the structures of components b and c, oligosaccharides in fraction N-V were applied to an RCA–agarose column, which recognizes the terminal galactose residues. About 5% of the oligosaccharides in this fraction was retarded on the column and was separated into two components that were eluted on a Bio-Gel P-4 column at the same positions as those of components b and c in Figure 4B, respectively. Structural studies of these oligosaccharides by sequential glycosidase digestion gave the same series of results as described for components b and c (Figure 4D–F) (data not shown).

The oligosaccharides in fraction AN-V (Con A^{++}, AAL^-) were separated on a Bio-Gel P-4 column into two components whose elution positions were the same as those of components b and c in Figure 4B (Figure 4G). Sequential exoglycosidase digestion of these components gave the same series of results as described already for components b and c in Figure 4B, respectively (data not shown). Therefore, these two components should have the same structures as components b and c. Since fraction AN-VI (Con A^{++}, AAL^+) contained oligosaccharides amounting to less than 1% of the whole oligosaccharide mixture, their structural study was not performed.

Structures of Oligosaccharides in Fractions III and IV. Fraction AN-IV (Con A^+, AAL^+), which included 10% of the total oligosaccharides, was separated into two components with effective sizes of 14.5 and 17.5 glucose units by Bio-Gel P-4 column chromatography (components d and e in Figure 5A). When radioactive components d and e were digested with streptococcal β-galactosidase followed by streptococcal β-*N*-acetylhexosaminidase, two galactose residues (dotted line and solid line in Figure 5B, respectively) and two β-*N*-acetylglucosamine residues (dotted line and solid line in Figure 5C, respectively) were released. The effective size of the dotted-line product in Figure 5C was the same as authentic Man_3·GlcNAc·Fuc·$GlcNAc_{OT}$. That the product has the structure Manα1→6(Manα1→3)Manβ1→4GlcNAcβ1→4(Fucα1→6)$GlcNAc_{OT}$ was confirmed by the method reported previously (Furukawa et al., 1989) (data not shown). These results indicated that component d has the structure Galβ1→4GlcNAcβ1→2Manα1→6(Galβ1→4GlcNAcβ1→2Manα1→3)Manβ1→4GlcNAcβ1→4(Fucα1→6)$GlcNAc_{OT}$.

When the solid-line component in Figure 5C was digested with streptococcal β-galactosidase followed by streptococcal β-*N*-acetylhexosaminidase, one galactose residue (Figure 5D) and one *N*-acetylglucosamine residue (Figure 5E) were released. The radioactive product at this stage was eluted at the same position as authentic Man_3·GlcNAc·Fuc·$GlcNAc_{OT}$. On the basis of the specifities of the enzymes and the lectins, component e was considered to be a biantennary complex type sugar chain with one each of the Galβ1→4GlcNAcβ1→3Galβ1→4GlcNAc and the Galβ1→4GlcNAc outer chains. In order to determine the location of the tetrasaccharide outer chain, the solid-line peak in Figure 5C was digested with *As. saitoi* α-mannosidase II, which releases a mannose residue from the Galβ1→4GlcNAcβ1→2Manα1→6(Manα1→3)Man group but not from the Galβ1→4GlcNAcβ1→2Manα1→3-(Manα1→6)Man group. Since it was totally resistant to the enzyme digestion, the tetrasaccharide outer chain in component e was considered to be attached to the Manα1→3Man arm of the trimannosyl core (data not shown). Oligosaccharides in fraction N-IV (Con A^+, AAL^+) showed the same elution patterns as those of oligosaccharides in fraction AN-IV before and after each digestion with glycosidases.

The elution profiles of oligosaccharides in fraction N-III and AN-III (Con A^+, AAL^-) were also the same as those of oligosaccharides in fraction AN-IV before and after enzyme digestions except that the elution position of each peak was smaller by one glucose unit than the respective peak from fraction AN-IV, reflecting the absence of a fucose residue linked to the trimannosyl core. Therefore, fraction III contains the nonfucosylated forms and fraction IV the fucosylated forms of the oligosaccharides

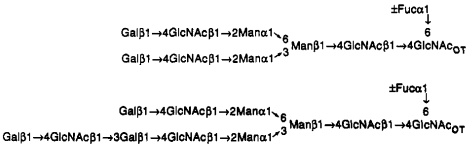

Structures of Oligosaccharides in Fractions I and II. Oligosaccharides in fraction AN-II (Con A^-, AAL^+), which amounted to 26% of the total oligosaccharides, were eluted from a Bio-Gel P-4 column as multiple peaks larger than 15 glucose units (Figure 6A). After digestion with *E. freundii* endo-β-galactosidase, almost all the oligosaccharides were converted to smaller ones, the major peak of which was eluted at 17 glucose units (Figure 6B). The oligosaccharides released by digestion with the endo-β-galactosidase and eluted at smaller than 10 glucose units were recovered and reduced with NaB^3H_4. When these oligosaccharides were subjected to Bio-Gel P-4 column chromatography, they were eluted mainly at 4.5 glucose units with an accompanying small peak at 3.5 glucose units (Figure 6B inset). By digestion with streptococcal β-galactosidase, most of the oligosaccharides eluted at 4.5 glucose units were converted to a radioactive oligosaccharide with mobility of 3.5 glucose units. The oligosaccharide eluted at 3.5 glucose units was further digested with jack bean β-*N*-acetylhexosaminidase, and the radioactive oligosaccharide was eluted at 1.5 glucose units. Analysis of the radioactive product

Carl_G_190x270_mm_blokki_FINAL.indd 232 06-Aug-23 1:53:46 PM

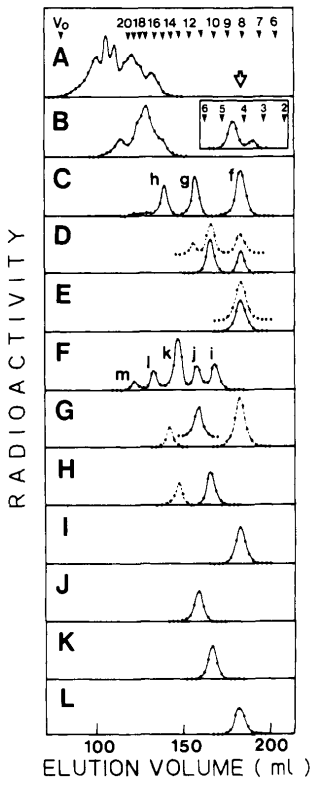

FIGURE 6: Sequential exo- and endoglycosidase digestion of fraction AN-II. The fraction and its digestion products were analyzed by Bio-Gel P-4 column chromatography: (A) fraction AN-II; (B) oligosaccharides in panel A digested with *E. freundii* endo-β-galactosidase; (inset in panel B) the oligosaccharides released by the enzyme digestion reduced with NaB^3H_4 and subjected to Bio-Gel P-4 column chromatography; (C) oligosaccharides in panel A digested with a mixture of 6646K β-galactosidase and jack bean β-*N*-acetylhexosaminidase; (D) solid and dotted lines representing the digestion products of components g and h in panel C treated by one and two cycles of enzyme digestion with almond emulsin α-fucosidase I followed by a mixture of streptococcal β-galactosidase and β-*N*-acetylhexosaminidase, respectively; (E) solid and dotted lines representing the digestion products of the solid-line peak eluted at 10.0 glucose units and the dotted-line peaks eluted at 10.0 and 12.2 glucose units in panel D with jack bean β-*N*-acetylhexosaminidase, respectively; (F) oligosaccharides in panel A treated with two cycles of enzyme digestion first with almond emulsin α-fucosidase I and subsequently with a mixture of streptococcal β-galactosidase and β-*N*-acetylhexosaminidase; (G) dot-dashed line representing each digestion product of components i, j, and k in panel F with jack bean β-*N*-acetylhexosaminidase and solid and dotted lines representing the digestion products of components l and m in panel F with jack bean β-*N*-acetylhexosaminidase, respectively; (H) solid and dotted lines representing the digestion products of solid- and dotted-line peaks in panel G with 6646K β-galactosidase, respectively; (I) solid-line peak in panel H digested with streptococcal β-*N*-acetylhexosaminidase; (J) dotted-line peak in panel H digested with streptococcal β-*N*-acetylhexosaminidase; (K) the peak in panel J digested with streptococcal β-galactosidase; (L) the peak in panel K digested with streptococcal β-*N*-acetylhexosaminidase. Component f in panel C, the solid- and dotted-line peaks eluted at 8.2 glucose units in panel D, the solid- and dotted-line peaks in panel E, the dot-dashed-line peak in panel G, the peak in panel I, and the peak in panel L were shown to have the structure Man_3·GlcNAc·Fuc·$GlcNAc_{OT}$ by sequential enzyme digestion as described in the text. Arrowheads at the top of the figure are the same as in Figure 4. The white arrow indicates the elution position of authentic oligosaccharide Man_3·GlcNAc·Fuc·$GlcNAc_{OT}$.

that is a reducing terminal sugar revealed that it is a galactitol (data not shown). These results indicated that the major and minor oligosaccharides in the Figure 6B inset are Galβ1→4GlcNAcβ1→Gal_{OT} and GlcNAcβ1→Gal_{OT}. Therefore, the majority of oligosaccharides in the Con A$^-$ fraction contain *N*-acetyllactosamine groups in their outer chain moieties.

When oligosaccharides in Figure 6A were digested with a mixture of 6646K β-galactosidase and jack bean β-*N*-acetylhexosaminidase, which removes all Galβ1→GlcNAcβ1→ groups, they were converted to three components (components f, g, and h in Figure 6C). When digested with almond emulsin α-fucosidase I, which cleaves the Fucα1→3GlcNAc and the Fucα1→4GlcNAc linkages, and then digested with a mixture of streptococcal β-galactosidase and β-*N*-acetylhexosaminidase, component g was converted to a mixture of two radioactive oligosaccharides with mobilities of 10.0 and 8.2 glucose units (solid line in Figure 6D). Component h was converted to a mixture of three radioactive oligosaccharides with mobilities of 12.0, 10.0, and 8.2 glucose units when treated with two cycles of the same treatment as above (dotted line in Figure 6D). By digestion with jack bean β-*N*-acetylhexosaminidase, all these oligosaccharides were converted to a single radioactive oligosaccharide eluted at the same position as authentic Man_3·GlcNAc·Fuc·$GlcNAc_{OT}$ (Figure 6E). The results indicated that component g in Figure 6C contains Galβ1→4(Fucα1→3)GlcNAcβ1→2, 4, or 6Manα1→3 or 6Manβ1→4GlcNAcβ1→4(Fucα1→6)-$GlcNAc_{OT}$ and that component h in Figure 5C contains Galβ1→4(Fucα1→3)GlcNAcβ1→2Manα1→6[Galβ1→4-(Fucα1→3)GlcNAcβ1→2Manα1→3]Manβ1→4GlcNAc-β1→4(Fucα1→6)$GlcNAc_{OT}$, Galβ1→4(Fucα1→3)-GlcNAcβ1→2[Galβ1→4(Fucα1→3)GlcNAcβ1→4 or 6]-Manα1→3 or 6(Manα1→6 or 3)Manβ1→4GlcNAcβ1→4-(Fucα1→6)$GlcNAc_{OT}$, Galβ1→4(Fucα1→3)GlcNAcβ1→-4Manα1→3[Galβ1→4(Fucα1→3)GlcNAcβ1→6Manα1→-6]Manβ1→4GlcNAcβ1→4(Fucα1→6)$GlcNAc_{OT}$, or Galβ1→4(Fucα1→3)GlcNAcβ1→3Galβ1→4(Fucα1→3)-GlcNAcβ1→2, 4, or 6Manα1→3 or 6Manβ1→-4GlcNAcβ1→4(Fucα1→6)$GlcNAc_{OT}$. Since the oligosaccharides released by digestion with endo-β-galactosidase were not fucosylated at all, the fucose residue should be attached to the *N*-acetylglucosamine residues that form the branches of the sugar chains, and when the *N*-acetyllactosamine repeat was fucosylated, the repeat should be attached to the fucosylated branch of the sugar chains. In fraction AN-II, Galβ1→GlcNAcβ1→ and its repeating outer chains should be added to these oligosaccharides forming bi-, tri-, and tetraantennary complex type sugar chains.

When fraction AN-II was treated with two cycles of enzyme digestion with almond emulsin α-fucosidase I and then with a mixture of streptococcal β-galactosidase and β-*N*-acetylhexosaminidase, it was converted to a mixture of five oligosaccharides (i–m in Figure 6F). Components, i, j, and k were all converted to a single radioactive product with the same mobility as authentic Man_3·GlcNAc·Fuc·$GlcNAc_{OT}$ by digestion with jack bean β-*N*-acetylhexosaminidase (dot-dashed line in Figure 6G). Therefore, the differences in size of components i, j, and k were ascribed to the different numbers of *N*-acetylglucosamine residues. On the basis of the specificity of streptococcal β-*N*-acetylhexosaminidase, which cleaves the GlcNAcβ1→2Man linkage of the GlcNAcβ1→4-(GlcNAcβ1→2)Man group but not that of the GlcNAcβ1→-6(GlcNAcβ1→2)Man group, components i and j were considered to be derived from triantennary complex type oligosaccharides having the GlcNAcβ1→4(GlcNAcβ1→2)Man group and the GlcNAcβ1→6(GlcNAcβ1→2)Man group, re-

Carl_G_190x270_mm_blokki_FINAL.indd 233 06-Aug-23 1:53:47 PM

Table II: Methylation Analysis of Each Con A Fraction Obtained from a Mixture of Fractions N and AN

partially methylated sugars	molar ratio[a]			
	Con A$^-$	Con A$^-$[b]	Con A$^+$	Con A^{++}
fucitol				
2,3,4-tri-*O*-methyl-1,5-di-*O*-acetyl	1.8	0.8	0.8	tr[c]
galactitol				
2,3,4,6-tetra-*O*-methyl-1,5-di-*O*-acetyl	3.6	3.6	2.0	tr
2,4,6-tri-*O*-methyl-1,3,5-tri-*O*-acetyl	0.5	0.5	tr	
mannitol				
2,3,4,6-tetra-*O*-methyl-1,5-di-*O*-acetyl				1.4
3,4,6-tri-*O*-methyl-1,2,5-tri-*O*-acetyl	0.3	0.3	2.0	1.2
3,6-di-*O*-methyl-1,2,4,5-tetra-*O*-acetyl	0.9	0.9		
3,4-di-*O*-methyl-1,2,5,6-tetra-*O*-acetyl	0.8	0.8		
2,4-di-*O*-methyl-1,3,5,6-tetra-*O*-acetyl	1.0	1.0	1.0	1.0
2-(*N*-methylacetamido)-2-deoxyglucitol				
6-mono-*O*-methyl-1,3,4,5-tetra-*O*-acetyl	1.0			
3,6-di-*O*-methyl-1,4,5-tri-*O*-acetyl	4.0	4.9	3.1	0.5
4,6-di-*O*-methyl-1,3,5-tri-*O*-acetyl	0.2	0.2		
1,3,5,6-tetra-*O*-methyl-4-mono-*O*-acetyl	0.2	0.2	0.2	0.5
1,3,5-tri-*O*-methyl-4,6-di-*O*-acetyl	0.8	0.8	0.8	tr

[a] Numbers in the table were calculated by taking the value of 2,4-di-*O*-methyl-1,3,5,6-tetra-*O*-acetylmannitol as 1.0. [b] After almond emulsin fucosidase I digestion. [c] Trace, less than 0.1.

spectively, and component k was considered to be derived from a tetraantennary complex type oligosaccharide.

When peaks l and m in Figure 6F were digested with jack bean β-*N*-acetylhexosaminidase, three *N*-acetylglucosamine residues were removed and the products were eluted at 11.2 and 14.0 glucose units (solid and dotted lines in Figure 6G, respectively). When the solid- and dotted-line components in Figure 6G were digested with 6646K β-galactosidase, which cleaves the Galβ1→3GlcNAc linkage as well as the Galβ1→4GlcNAc linkage, both components released one galactose residue (solid and dotted lines in Figure 6H, respectively). The resulting solid-line product was converted to the fucosylated trimannosyl core by digestion with sterptococcal β-*N*-acetylhexosaminidase (Figure 6I), and the dotted-line product was also converted to the core by sequential digestion with streptococcal β-*N*-acetylhexosaminidase (Figure 6J), streptococcal β-galactosidase (Figure 6K), and streptococcal β-*N*-acetylhexosaminidase (Figure 6L). The results indicated that component l contains the Galβ1→3GlcNAcβ1→2Manα1→3 or 6Man group and component m contains the Galβ1→3GlcNAcβ1→3Galβ1→4GlcNAcβ1→2Manα1→3 or 6Man group. Since the fucosylated components g and h in Figure 6C were converted to the afucosylated and agalactosylated derivatives (Figure 6D) by one and two cycles of enzyme digestion with almond emulsin α-fucosidase I followed by a mixture of streptococcal β-galactosidase and β-*N*-acetylhexosaminidase, respectively, the fucosylated components were shown to consist of the Galβ1→4GlcNAc group but not the Galβ1→3GlcNAc group. Therefore, the type I group in components l and m in Figure 6F were not fucosylated. Although this type I group in component m should be released upon digestion with endo-β-galactosidase, it was not detected in the oligosaccharides released by the above enzyme treatment, probably due to the lower limitation for detection.

The elution profiles of the oligosaccharides in fraction N-II (Con A$^-$, AAL$^+$) that comprised 7% of the total oligosaccharides were almost identical with those in fraction AN-II. Structural studies of oligosaccharides in this fraction by sequential glycosidase digestion also gave a series of results similar to that described for oligosaccharides in fraction AN-II (data not shown). The elution profiles of oligosaccharides in fraction I (Con A$^-$, AAL$^-$) of fractions N (5%) and AN (3%) were also similar to those of oligosaccharides in fraction II before and after enzyme digestions except that the elution position of each peak was smaller than the respective peak from fraction II by one glucose unit, reflecting the absence of a fucose residue linked to the trimannosyl core. However, in these fractions, the Galβ1→3GlcNAc group could not be detected in a tetraantennary complex type sugar chain, probably due to the lower limitation for detection.

Analysis of the Carbohydrate Structures of the β-Subunit of Leu-CAMs. Radioactive oligosaccharides released from the β-subunit of Leu-CAMs were also analyzed mainly by lectin column chromatography. Due to the limited amount of the glycoprotein sample available, the number of sugar chains attached to the β-subunit was not determined. The percent molar ratio of the oligosaccharides in each fraction obtained by Con A–Sepharose and AAL–Sepharose column chromatography is summarized in Table I.

It became apparent that the percent molar ratio of oligosaccharides in each fraction is almost identical with that of the corresponding fraction obtained from αβ complexes. In addition, the elution profile of the oligosaccharides in each fraction from a Bio-Gel P-4 column was almost identical with that of the oligosaccharides in the corresponding fraction from αβ complexes (data not shown). Because the amount of sample available was limited, methylation analysis of oligosaccharides from the β-subunit could not be performed.

Methylation Analysis of Oligosaccharides. In order to confirm each glycosidic linkage of the carbohydrate structures of Leu-CAMs determined mainly by sequential exoglycosidase digestion, deuterium-labeled fractions N and AN were prepared for methylation analysis. These two fractions were combined and subjected to Con A–Sepharose column chromatography to separate the Con A$^-$, Con A$^+$, and Con A^{++} fractions. After the haptenic monosaccharides used for eluting the bound materials were removed by Bio-Gel P-4 column chromatography, each fraction was subjected to methylation analysis. In the case of the Con A$^-$ fraction, the oligosaccharides before and after almond emulsin α-fucosidase I digestion were also subjected to methylation analysis in order to confirm the structure of the fucosyl-*N*-acetyllactosamine group.

As shown in Table II, the molar ratio of each methylated sugar was calculated by taking the value of 2,4-di-*O*-methyl-1,3,5,6-tetra-*O*-acetylmannitol as 1.0. Comparison of the data for oligosaccharides in fraction Con A$^-$ before and after α-fucosidase I digestion indicated that 40% of the fucose residues is linked at the C-3 position of the *N*-acetylglucosamine residue of the *N*-acetyllactosamine groups, since 6-

Carl_G_190x270_mm_blokki_FINAL.indd 234 06-Aug-23 1:53:48 PM

Table III: Proposed Structures of the Asn-Linked Sugar Chains of Leu-CAMs

proposed structures[a]	molar ratio (%)
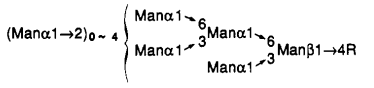	38
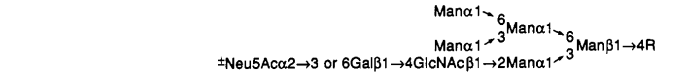	3
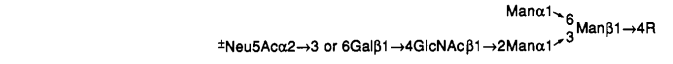	2
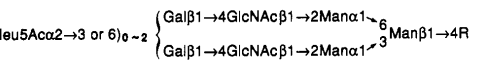	17
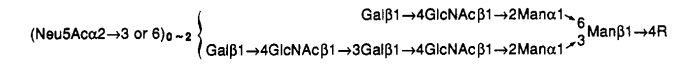	1
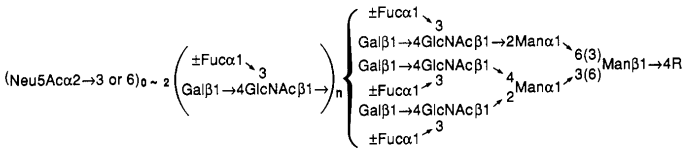	7
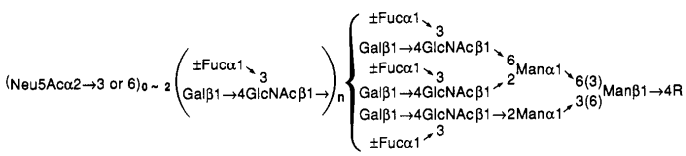	4
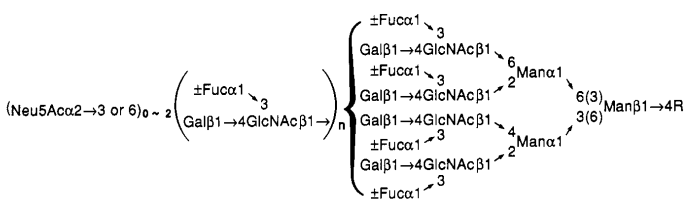	18
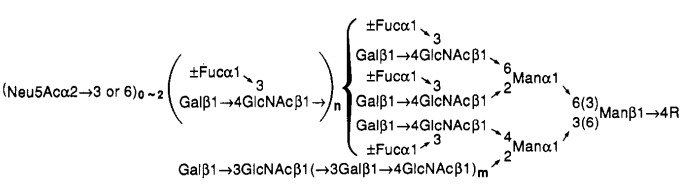	9

[a] R = GlcNAcβ1→4(±Fucα1→6)GlcNAc$_{OT}$ n = 0–4; m = 0–1. The number of fucose residues attached via α1→3 to *N*-acetylglucosamine in the complex-type sugar chains is not more than two.

mono-*O*-methyl-2-(*N*-methylacetamido)-2-deoxyglucitol, which was detected in fraction Con A$^-$, disappeared after the α-fucosidase I digestion. Since 2-(*N*-methylacetamido)-2-deoxyglucitol was detected in a trace amount as a 4,6-di-*O*-methyl derivative in oligosaccharides in fraction Con A$^-$ before and after the enzyme digestion, the presence of the Galβ1→3GlcNAc group in fraction Con A$^-$ is also confirmed by methylation analysis.

Detection of 2,4,6-tri-*O*-methylgalactitol in fraction Con A$^+$ indicated that 3% of the galactose residues of biantennary complex type sugar chains is substituted with an *N*-acetyllactosamine group. The methylation data of fraction Con A^{++} also indicated that oligosaccharides in the fraction are mainly of high mannose type. However, the presence of 2,3,4,6-tetra-*O*-methylgalactitol and 3,6-di-*O*-methyl-2-(*N*-methylacetamido)-2-deoxyglucitol in the same fraction supported the

Carl_G_190x270_mm_blokki_FINAL.indd 235 06-Aug-23 1:53:48 PM

occurrence of monoantennary complex type and hybrid type sugar chains as determined by sequential exoglycosidase digestion (Figure 4).

The proposed oligosaccharide structures of human Leu-CAMs, as determined by sequential exoglycosidase digestion and methylation analysis, are shown in Table III.

Discussion

Since human buffy coat cells are enriched in T cells, the predominant class of molecules present in the Leu-CAMs should be CD11a/CD18. This estimation is also supported by the fact that the α-subunit band corresponding to M_r 180000 was detected by SDS–PAGE analysis of the sample (Figure 1). The CD11a/CD18 molecule is expressed on the surface of virtually all leukocytes and is involved in various functions such as cell adhesions. Monoclonal antibodies against CD11a/CD18 inhibited proliferation of antigen-specific helper T cells and cytolytic functions mediated by cytotoxic T cells and by natural killer cells (Davignon et al., 1981; Krensky et al., 1983; Miedema et al., 1984). Adhesion of leukocytes to endothelial cells, fibroblasts, and keratinocytes at the sites of inflammation is also mediated by the CD11a/CD18 molecule (Dustin & Springer, 1988; Patarroyo et al., 1990). The oligosaccharide moieties of leukocyte cell surface glycoproteins have been implicated in the recognition processes of lymphocytes, including the recognition of Ia molecules by responding T cells in the mixed lymphocyte reaction. Also, homing of lymphocytes to various organs may be due to sugar-binding proteins (Gallatin et al., 1983; Stoolman & Rosen, 1983; Lasky et al., 1989). Little is known, however, about their carbohydrate structures involved in these phenomena.

By use of established methods for structural analysis of oligosaccharides released by hydrazinolysis, structures of the Asn-linked sugar chains of Leu-CAMs have been determined. On the basis of the results presented here, Leu-CAMs were shown to have 12 Asn-linked sugar chains per molecule and their structures are proposed as shown in Table III. The major Asn-linked sugar chains of Leu-CAMs were of high mannose type and bi-, tri-, and tetraantennary complex types. Although the outer chains of biantennary complex type sugar chains contain only the Galβ1→4GlcNAcβ1→ group, those of tri- and tetraantennary sugar chains are enriched with the Galβ1→4(Fucα1→3)GlcNAc group. Small amounts of the Galβ1→3GlcNAcβ1→ and the Galβ1→3GlcNAcβ1→-3Galβ1→4GlcNAc groups are also found in the outer-chain moieties of the tetraantennary sugar chains. These type I structures were not fucosylated as in the case of the Galβ1→-4GlcNAc outer chain from which the type I structure extends. This structural characteristic is quite unique to Leu-CAMs. The fucosylation of the *N*-acetyllactosamine group of tri- and tetraantennary complex type sugar chains is also characteristic to these molecules. Recently, fucosyl-*N*-acetyllactosamine, which is expressed on cell surface glycoconjugates in a stage-specific manner during the development of mouse embryos (Gooi et al., 1985), has been shown to interact homotypically, thus inducing compaction, a tight cellular adhesion (Eggens et al., 1989). Therefore, the fucosyl-*N*-acetyllactosamine residues expressed on Leu-CAMs might be important for initial interaction with ligands such as ICAM-1 and ICAM-2 (Rothlein et al., 1986; Patarroyo et al., 1987; Staunton et al., 1989). The presence of fucosyl-*N*-acetyllactosamine on CD11a/CD18 has previously been demonstrated by using a monoclonal antibody (Spitalnik et al., 1989).

In addition, Leu-CAMs contain a small amount of hybrid type and monoantennary complex type sugar chains. These sugar chains are not widely distributed in mammalian glycoproteins. The latter structure has been found limitedly in chorionic gonadotropin (Endo et al., 1979), urinary ribonuclease (Hitoi et al., 1987), placental β-glucocerebrosidase (Takasaki et al., 1984), and platelet thrombospondin (Furukawa et al., 1989) of human origin.

Comparative study of the oligosaccharides released from $\alpha\beta$ complexes and the β-subunit by lectin chromatography showed that similar series of oligosaccharides were distributed evenly in both α- and β-subunits. The results are consistent with previous reports that the sugar chains of Leu-CAMs were susceptible to endo-β-*N*-acetylglucosaminidases H and F (endo F) and that the reduction of molecular sizes of α- and β-subunits determined by SDS–PAGE after treatment with endo F suggests the presence of 5–6 sugar chains in each subunit (Miller & Springer, 1987; Kantor et al., 1988). The presence of sulfate groups in the sugar chains of the CD11a/CD18 molecule, which was detected by metabolic labeling of mouse T lymphoma EL-4 cells with $^{35}SO_4^{2-}$ (Dahms & Hart, 1985), was not confirmed by the present study. Therefore, the amount of sulfated sugar chains in the Leu-CAMs from peripheral T cells might be very small, even if they occur in CD11a/CD18. Whether hydrazinolysis does release sulfate groups from sugar chains or not was investigated by treatment of radioactive keratan sulfate fragment GlcNAc(6-SO_4)β1→3Gal_{OT} with hydrazine at 100 °C for 10 h. Since the electrophoretic mobility of the sulfated disaccharide was not affected by the treatment, hydrazinolysis does not release sulfate groups from sugar chains. In addition, the carbohydrate structures of the sulfated sugar chains were determined by use of the hydrazine-released oligosaccharides (Yamashita et al., 1983; Edge & Spiro, 1984).

Burkitt lymphoma cells lack or have a low level of the CD11a/CD18 molecule and are not metastatic (Patarroyo et al., 1988; Roossien et al., 1989). Metastatic lymphoma cells were shown to invade monolayers of lymphocytes and fibroblasts. The invasion was totally blocked by anti-CD11a/CD18 antibody. In addition, mutant lymphoma cells, which are deficient in the expression of the CD11a/CD18 molecule on cell surfaces due to the impaired synthesis of either the α- or β-subunit precursor, failed considerably to invade the cell layers. These results strongly suggested the involvement of CD11a/CD18 in the efficient metastasis of certain lymphoma cells. Since the carbohydrate structure of metastasis-associated glycoprotein was determined by the analysis of lectin mutant cell lines, which have lost the metastatic potential but not the tumorigenicity (Stanley, 1984; Dennis et al., 1987), it would be of interest to determine the carbohydrate structures of the CD11a/CD18 molecule isolated from the invasive lymphoma cells.

Acknowledgments

We express our gratitude to Miss Yumiko Kimizuka and Ms. Tamae Takahashi for their excellent secretarial assistance.

References

Akiyama, S. K., & Yamada, K. M. (1987) *J. Biol. Chem. 262*, 17536–17542.

Arnaout, M. A. (1990) *Blood 75*, 1037–1050.

Arnaout, M. A., Gupta, S. K., Pierce, M. W., & Tenen, D. G. (1988) *J. Cell Biol. 106*, 2153–2158.

Beatty, P. G., Ledbetter, J. A., Martin, P. J., Price, T. H., & Hansen, J. A. (1983) *J. Immunol. 131*, 2913–2918.

Berger, M., O'Shea, J., Cross, A. S., Folks, T. M., Chused, T. M., Brown, E. J., & Frank, M. M. (1984) *J. Clin. Invest. 74*, 1566–1571.

Carl_G_190x270_mm_blokki_FINAL.indd 236 06-Aug-23 1:53:49 PM

Corbi, A. L., Miller, L. J., O'Connor, K., Larson, R. S., & Springer, T. A. (1987) *EMBO J. 6*, 4023–4028.

Corbi, A. L., Kishimoto, T. K., Miller, L. J., & Springer, T. A. (1988) *J. Biol. Chem. 263*, 12403–12411.

Cowing, C., & Chapdelaine, J. M. (1983) *Proc. Natl. Acad. Sci. U.S.A. 80*, 6000–6004.

Dahms, N. M., & Hart, G. W. (1985) *J. Immunol. 134*, 3978–3986.

Davignon, D., Martz, E., Reynolds, T., Kurzinger, K., & Springer, T. A. (1981) *J. Immunol. 127*, 590–595.

Dennis, J. W., Laferte, S., Waghorne, C., Breitman, M. L., & Kerbel, R. S. (1987) *Science 236*, 582–585.

Dustin, M. L., & Springer, T. A. (1988) *J. Cell Biol. 107*, 321–331.

Dustin, M. L., Singer, K. H., Tuck, D. T., & Springer, T. A. (1988) *J. Exp. Med. 167*, 1323–1340.

Edge, A. S. B., & Spiro, R. G. (1984) *J. Biol. Chem. 259*, 4710–4713.

Eggens, I., Fenderson, B., Toyokuni, T., Dean, B., Stroud, M., & Hakomori, S. (1989) *J. Biol. Chem. 264*, 9476–9484.

Endo, Y., Yamashita, K., Tachibana, Y., Tojo, S., & Kobata, A. (1979) *J. Biochem. (Tokyo) 85*, 669–679.

Furukawa, K., Roberts, D. D., Endo, T., & Kobata, A. (1989) *Arch. Biochem. Biophys. 270*, 302–312.

Gallatin, W. M., Weissman, I. L., & Butcher, E. C. (1983) *Nature 304*, 30–34.

Geltosky, J. E., Birdwell, C. R., Weseman, J., & Lerner, R. A. (1980) *Cell 21*, 339–345.

Glasgow, L. R., Paulson, J. C., & Hill, R. L. (1977) *J. Biol. Chem. 252*, 8615–8623.

Gooi, H. C., Feizi, T., Kapadia, A., Knowles, B. B., Solter, D., & Evans, M. J. (1985) *Nature 292*, 156–158.

Harada, H., Kamei, M., Tokumoto, Y., Yui, S., Koyama, F., Kochibe, N., Endo, T., & Kobata, A. (1987) *Anal. Biochem. 164*, 374–381.

Hart, G. W. (1982) *J. Biol. Chem. 257*, 151–158.

Heifetz, A., & Lennarz, W. J. (1979) *J. Biol. Chem. 254*, 6119–6127.

Hitoi, A., Yamashita, K., Niwata, Y., Irie, M., Kochibe, N., & Kobata, A. (1987) *J. Biochem. (Tokyo) 101*, 29–41.

Hogg, N., Takacs, L., Palmer, D. G., Selvendran, Y., & Allen, C. (1986) *Eur. J. Immunol. 16*, 240–248.

Hynes, R. O. (1987) *Cell 48*, 549–554.

Kantor, C., Suomalainen-Nevanlinna, H., Patarroyo, M., Osterlund, K., Bergman, T., Jornvall, H., Schroder, J., & Gahmberg, C. G. (1988) *Eur. J. Biochem. 170*, 653–659.

Kishimoto, T. K., Miller, L. J., & Springer, T. A. (1987a) in *Leukocyte Typing III* (McMichael, A. Ed.) pp 896–898, Springer-Verlag, New York, NY.

Kishimoto, T. K., O'Connor, K., Lee, A., Roberts, T. M., & Springer, T. A. (1987b) *Cell 48*, 681–690.

Kobata, A. (1982) *Methods Enzymol. 83*, 625–631.

Kobata, A., & Amano, J. (1987) *Methods Enzymol. 138*, 779–785.

Krensky, A. M., Sanchez-Madrid, F., Robbins, E., Nagy, J. A., Springer, T. A., & Burakoff, S. J. (1983) *J. Immunol. 131*, 611–616.

Kurzinger, K., & Springer, T. A. (1982) *J. Biol. Chem. 257*, 12412–12418.

Larson, R. S., Corbi, A. L., Berman, L., & Springer, T. A. (1989) *J. Cell Biol. 108*, 703–712.

Lasky, L. A., Singer, M. A., Yednock, T. A., Dowbenco, D., Fennie, C., Rodriguez, H., Nguyen, T., Stachel, S., & Rosen, S. D. (1989) *Cell 56*, 1045–1055.

Law, S. K. A., Gagnon, J., Hildreth, J. E. K., Wells, C. E., Willis, A. C., & Wong, A. J. (1987) *EMBO J. 6*, 915–919.

Li, Y.-T., & Li, S.-C. (1972) *Methods Enzymol. 28*, 702–713.

Liang, C.-J., Yamashita, K., & Kobata, A. (1980) *J. Biochem. (Tokyo) 88*, 51–58.

Miedema, F., Tetteroo, P. A. T., Hesselink, W. G., Werner, G., Spits, H., & Melief, C. J. M. (1984) *Eur. J. Immunol. 14*, 518–523.

Miller, L. J., & Springer, T. A. (1987) *J. Immunol. 139*, 842–847.

Miller, L. J., Schwarting, R., & Springer, T. A. (1986) *J. Immunol. 137*, 2891–2900.

Miller, L. J., Bainton, D. F., Borregaard, N., & Springer, T. A. (1987) *J. Clin. Invest. 80*, 535–544.

Ogata, S., Muramatsu, T., & Kobata, A. (1975) *J. Biochem. (Tokyo) 78*, 687–696.

Patarroyo, M., Beatty, P. G., Fabre, J. W., & Gahmberg, C. G. (1985a) *Scand. J. Immunol. 22*, 171–182.

Patarroyo, M., Beatty, P. G., Serhan, C. N., & Gahmberg, C. G. (1985b) *Scand. J. Immunol. 22*, 619–631.

Patarroyo, M., Clark, E. A., Prieto, J., Kantor, C., & Gahmberg, C. G. (1987) *FEBS Lett. 210*, 127–131.

Patarroyo, M., Prieto, J., Ernberg, I., & Gahmberg, C. G. (1988) *Int. J. Cancer 41*, 901–907.

Patarroyo, M., Prieto, J., Rincon, J., Timonen, T., Lundberg, C., Lindbom, L., Asjo, B., & Gahmberg, C. G. (1990) *Immunol. Rev. 114*, 67–108.

Pimlott, N. J. G., & Miller, R. G. (1986) *J. Immunol. 136*, 6–11.

Powell, L. D., Bause, E., Legler, G., Molyneux, R. J., & Hart, G. W. (1985) *J. Immunol. 135*, 714–724.

Roossien, F. F., de Rijk, D., Bikker, A., & Roos, E. (1989) *J. Cell Biol. 108*, 1979–1985.

Rothlein, R., Dustin, M. L., Marlin, S. D., & Springer, T. A. (1986) *J. Immunol. 137*, 1270–1274.

Ruoslahti, E., & Pierschbacher, M. D. (1987) *Science 238*, 491–497.

Rutishauser, U. (1984) *Nature 310*, 549–554.

Schwarting, R., Stein, H., & Wang, C. Y. (1985) *Blood 65*, 974–983.

Spik, G., Bayard, B., Fournet, B., Strecker, G., Bonquelet, S., & Montreuil, J. (1975) *FEBS Lett. 50*, 296–299.

Spitalnik, P. F., Spitalnik, S. L., Danley, J. M., Lopez, A. F., Vadas, M. A., Civin, C. I., & Ginsburg, V. (1989) *Arch. Biochem. Biophys. 271*, 168–176.

Springer, T. A., Dustin, M. L., Kishimoto, T. K., & Marlin, S. D. (1987) *Annu. Rev. Immunol. 5*, 223–252.

Stanley, P. (1984) *Annu. Rev. Genet. 18*, 525–552.

Stastre, L., Kishimoto, T. K., Gee, C., Roberts, T., & Springer, T. A. (1986) *J. Immunol. 137*, 1060–1065.

Staunton, D. E., Dustin, M. L., & Springer, T. A. (1989) *Nature 339*, 61–64.

Stoolman, L. M., & Rosen, S. D. (1983) *J. Cell Biol. 96*, 722–729.

Takasaki, S., & Kobata, A. (1986) *Biochemistry 25*, 5709–5715.

Takasaki, S., Mizuochi, T., & Kobata, A. (1982) *Methods Enzymol. 83*, 263–268.

Carl_G_190x270_mm_blokki_FINAL.indd 237 06-Aug-23 1:53:49 PM

Takasaki, S., Murray, G. J., Furbish, F. S., Brady, R. O., Barranger, J. A., & Kobata, A. (1984) *J. Biol. Chem. 259*, 10112–10117.
Timonen, T., Patarroyo, M., & Gahmberg, C. G. (1988) *J. Immunol. 191*, 1041–1046.
Timonen, T., Gahmberg, C. G., & Patarroyo, M. (1990) *Int. J. Cancer* (in press).
Todd, R. F., III, Arnaout, M. A., Rosin, R. E., Crowley, C. A., Peters, W. A., & Babior, B. M. (1984) *J. Clin. Invest. 74*, 1280–1290.
Yamashita, K., Mizuochi, T., & Kobata, A. (1982) *Methods Enzymol. 83*, 105–126.
Yamashita, K., Ueda, I., & Kobata, A. (1983) *J. Biol. Chem. 258*, 14144–14147.
Yamashita, K., Kochibe, N., Ohkura, T., Ueda, I., & Kobata, A. (1985) *J. Biol. Chem. 260*, 4688–4693.

Carl_G_190x270_mm_blokki_FINAL.indd 238 06-Aug-23 1:53:50 PM

Glycobiology Vol. 3 no. 2 pp. 131–136, 1993

The vascular E-selectin binds to the leukocyte integrins CD11/CD18

Pekka Kotovuori[1], Eveliina Tontti[1], Rod Pigott[2], Maura Shepherd[2], Makoto Kiso[3], Akira Hasegawa[3], Risto Renkonen[4], Pekka Nortamo[1], Dario C.Altieri[5] and Carl G.Gahmberg[1,6]

[1]Department of Biochemistry, University of Helsinki, Unioninkatu 35, SF-00170 Helsinki, Finland, [2]British Bio-Technology Ltd, Oxford, UK, [3]Department of Applied Bioorganic Chemistry, Gifu University, Gifu, Japan, [4]Department of Bacteriology and Immunology, University of Helsinki, Helsinki, Finland and [5]Scripps Research Institute, La Jolla, CA, USA

[6]To whom correspondence should be addressed

Leukocyte adhesion involves at least three molecular families of adhesion proteins: the leukocyte integrins CD11/CD18, the intercellular adhesion molecules (ICAMs) and the carbohydrate-binding L-, E- and P-selectins. The intercellular adhesion molecules are well-known ligands for the CD11/CD18 integrins. We now show that E-selectin specifically binds to the sialyl Le^x carbohydrate epitopes of leukocyte integrins. Thus, the different families of leukocyte adhesion molecules form an integrated adhesion network.

Key words: adhesion/integrins/leukocyte/selectin

Introduction

Leukocyte adhesion is a complex process requiring several types of adhesion molecules. The leukocyte-specific integrins CD11a/CD18 (LFA-1), CD11b/CD18 (CR3,Mac-1) and CD11c/CD18 (p150/95) are pivotal in adhesion (Arnaout, 1990; Patarroyo *et al.*, 1990; Springer, 1990; Hynes, 1992). These integrins are heterodimeric type 1 membrane glycoproteins present in different proportions on all leukocytes. The integrins require activation to a high-affinity state to be able to bind their ligands. Among the most effective activators are various phorbol esters (Patarroyo *et al.*, 1985a,b; Rothlein and Springer, 1986; Wright and Meyer, 1986), indicating a role for protein kinase C.

Three cellular ligands for CD11/CD18 have been described: the intercellular adhesion molecules ICAM-1 (CD54) (Rothlein *et al.*, 1986; Patarroyo *et al.*, 1987; Hogg, 1991), ICAM-2 (Staunton *et al.*, 1989; de Fougerolles *et al.*, 1991; Gahmberg *et al.*, 1991) and ICAM-3 (de Fougerolles and Springer, 1992). These belong to the immunoglobulin superfamily of cell surface proteins, ICAM-1 containing five immunoglobulin domains (Simmons *et al.*, 1988; Staunton *et al.*, 1988) and ICAM-2 two (Staunton *et al.*, 1989). The amino acid sequence of ICAM-3 is not yet known. ICAM-1 is basally expressed, but strongly upregulated on endothelial cells by various cytokines (Rothlein *et al.*, 1988). ICAM-2 is found predominantly on endothelial cells. In most tissues it is stably expressed (de Fougerolles *et al.*, 1991; Nortamo *et al.*, 1991a,b), but the expression is enhanced in endothelium in lymph nodes with malignant lymphomas (Renkonen *et al.*, 1992).

Three members of the selectin family (Bevilacqua *et al.*, 1991) of adhesion lectins are currently known. L-Selectin (LECAM-1, Leu8) is found on leukocytes, and is important in homing of circulating cells and in adhesion to activated endothelium (Gallatin *et al.*, 1983). Surface expression of P-selectin (PADGEM, GMP140, CD62) and E-selectin (ELAM-1) (Bevilacqua *et al.*, 1989; Larsen *et al.*, 1989) is inducible on endothelial cells. Upon activation, P-selectin is translocated in minutes from intracellular Weibel–Palade bodies to the endothelial cell surface. Expression of E-selectin requires protein synthesis and is maximal at 4 h *in vitro*.

Both E- and P-selectin recognize the carbohydrate sialyl Le^x (Phillips *et al.*, 1990; Walz *et al.*, 1990; Polley *et al.*, 1991; Tiemeyer *et al.*, 1991; Zhou *et al.*, 1991). The positional isomer sialyl Le^a may also act as a ligand (Berg *et al.*, 1991; Takada *et al.*, 1991; Majuri *et al.*, 1992). Recent experiments have shown that the selectins slow down the movement of PMNs or induce 'rolling' of the cells over the endothelial cell surface (Lawrence and Springer, 1991; Ley *et al.*, 1991; von Andrian *et al.*, 1991). During this process, the leukocyte integrins are activated, and become able to bind to ICAM-1 and ICAM-2 on endothelial cells.

The mechanism(s) of activation of leukocyte adhesion remains poorly understood, but recent work has shown that E-selectin is able to activate PMN CD11b/CD18-dependent functions, resulting in increased chemotaxis and binding of C3bi-coated erythrocytes (Butcher, 1991; Kuijpers *et al.*, 1991; Lo *et al.*, 1991).

We now show that E-selectin binds to CD11a/CD18 and CD11b/CD18. These interactions may be important in the activation of integrins in living cells, leading to firm adhesion of granulocytes to endothelium. It also means that the three major families of adhesion proteins may cooperate to generate physiologically useful adhesion.

Results

Recombinant soluble E-selectin binds to purified CD11/CD18

Leukocyte integrins were purified from human blood buffy coat cells essentially as described previously, using monoclonal antibodies and affinity chromatography. Figure 1 shows a Coomassie blue-stained gel of the CD11/CD18 preparations. The CD11b polypeptide was poorly stained. CD11/CD18 (mixture of CD11a/CD18, CD11b/CD18 and CD11c/CD18) was coated on plastic plates using a ^{125}I-labelled preparation to estimate the efficiency of coupling. Using 2.5 μg of the integrins, ~0.3 μg of protein was coupled/well (not shown). Using purified CD11a/CD18 and CD11b/CD18, we found that both heterodimers were active in binding (Figure 2A). The binding was inhibited by the sialyl Le^x oligosaccharide in a dose-dependent manner, whereas the control blood group B-active pentasaccharide had no effect (Figure 2B). Seventy per cent of the binding was inhibited using 5 μg of non-radioactive

© Oxford University Press

Carl_G_190x270_mm_blokki_FINAL.indd 239 06-Aug-23 1:53:50 PM

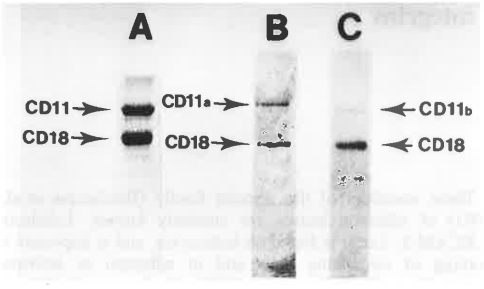

Fig. 1. PAGE of purified CD11/CD18 mixture (**A**), CD11a/CD18 (**B**) and CD11b/CD18 (C). The purified heterodimers were run on 8% acrylamide slab gels and visualized after staining with Coomassie blue. The positions of the polypeptides are indicated.

E-selectin (Figure 2C). The anti-E-selectin antibody 1.2B6 inhibited binding by ~40% (Figure 2C) and the anti-sialyl Le^x antibody by ~70%, as did the sialyl Le^x oligosaccharide (Figure 2C). The anti-E-selectin antibody BBIG-E1 showed no inhibition (not shown). EDTA inhibited binding to 90%.

E-Selectin-transfected COS cells bind to CD11a/CD18

To obtain further evidence that E-selectin binds to CD11/CD18, we transfected COS-1 cells with an E-selectin expression vector and assayed for the binding of cells to CD11a/CD18 coupled to plastic. CD11b/CD18-containing preparations were not used because COS cells contain substantial endogenous CD11b/CD18 binding activity. Figure 3A shows that transfected COS cells specifically bound to CD11a/CD18. The binding was partially inhibited by the BBIG-E1 and 1.2B6 anti-E-selectin antibodies (results for 1.2B6 not shown), and also by the sialyl Le^x oligosaccharide (Figure 3B). The difference in binding of E-selectin-transfected and mock-transfected cells to CD11a/CD18-coated plates was highly significant (** $P < 0.01$, *** $P < 0.001$). The background binding of COS cells to CD11/CD18 may be due to ICAM-like molecules or other ligands for CD11/CD18 present in untransfected cells.

Discussion

Recently, several groups reported that the ligands for E-selectin are sialyl Le^x- and sialyl Le^a-containing oligosaccharides (Phillips *et al.*, 1990; Walz *et al.*, 1990; Polley *et al.*, 1991; Tiemeyer *et al.*, 1991; Zhou *et al.*, 1991). Furthermore, Picker *et al.* (1991) found that PMN L-selectin itself contains sialyl Le^x, and is able to present it to E- and P-selectins. Other PMN glycoproteins binding to these selectins have not been reported, although there is evidence for their existence (Picker *et al.*, 1991).

The carbohydrate structures of the leukocyte integrins, isolated from blood buffy coat cells, were recently determined (Asada *et al.*, 1991). The oligosaccharides are all N-linked and a large proportion of them contain a repeating galactose β1-4 (fucose α1-3) *N*-acetylglucosamine β1-3 unit with terminal sialic acid, i.e. the sialyl Le^x structure. This finding suggested that the leukocyte integrins themselves could act as ligands for vascular selectins.

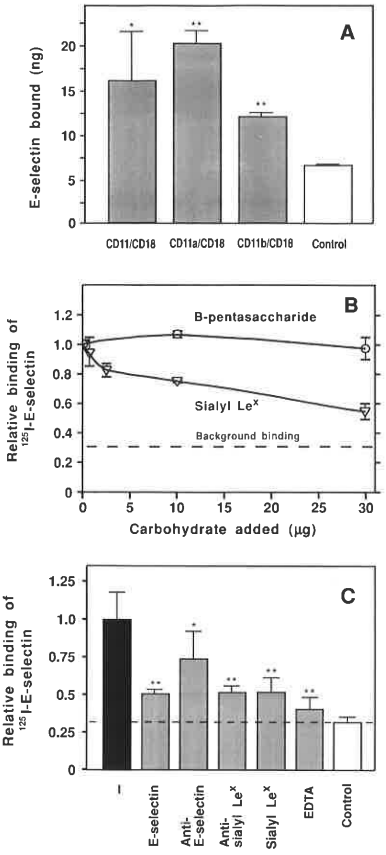

Fig. 2. Binding of soluble E-selectin to purified CD11/CD18 integrins, and its inhibition by oligosaccharides and antibodies. (**A**) Binding of E-selectin to plates coated with 2.5 μg purified mixture of CD11/CD18, CD11a/CD18 and CD11b/CD18. The difference in binding was significant as compared to control (*$P < 0.1$, ** $P < 0.01$). (**B**) Binding of E-selectin to plates coated with 2.5 μg CD11/CD18 mixture in the presence of the indicated amounts of sialyl Le^x oligosaccharide or control blood group B-active oligosaccharide. The background binding is shown by the dashed line. (**C**) Binding of E-selectin to plates coated with 2.5 μg CD11/CD18 in 0.05 ml binding buffer only, or in the presence of 5 μg E-selectin, 10 μg of the anti-selectin antibody 1.2B6, 10 μg of the anti-sialyl Le^x antibody, 30 μg of sialyl Le^x oligosaccharide or 2.5 mM EDTA. The control plates were coated with BSA only. The background is indicated by the dashed line. The differences in binding between the E-selectin in the absence or presence of inhibitors were significant (*$P < 0.1$, **$P < 0.01$).

We have demonstrated that this is indeed the case. Both isolated CD11a/CD18 and CD11b/CD18 were able to bind specifically recombinant, soluble E-selectin. These integrins must mainly derive from PMNs, a major cellular component of the buffy coat cells used for isolation of the integrins. Most lymphocytes do not contain the sialyl Le^x structure (Picker *et al.*, 1991).

In addition, we have shown that COS cells transfected with an E-selectin expression vector specifically bound to

Carl_G_190x270_mm_blokki_FINAL.indd 240 06-Aug-23 1:53:50 PM

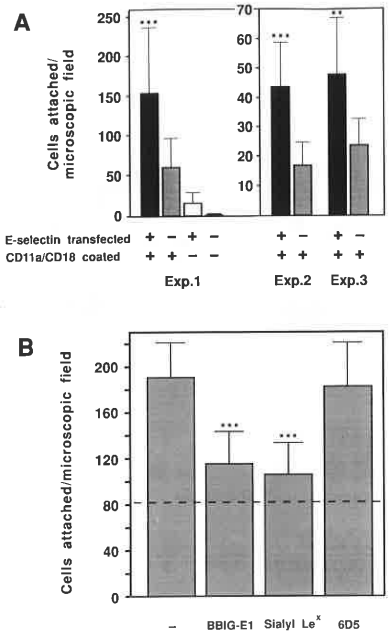

Fig. 3. Binding of E-selectin-transfected and mock-transfected COS-1 cells to purified CD11a/CD18. Ten micrograms of CD11a/CD18 in 1 ml were used for coating to 35 mm Petri dishes and bound COS cells counted. (**A**) Results from three independent experiments are shown. (**B**) Effects of anti-E-selectin antibody BBIG-E1 (50 μg/ml) , sialyl Le^x oligosaccharide (0.2 mg in 1 ml medium) and 50 μg/ml ICAM-2 control antibody (6D5). The background binding of mock-transfected cells to CD11/CD18-coated plates in (**B**) is shown by the dashed line.

CD11a/CD18 coated to plastic. The CD11/CD18–E-selectin interactions were efficiently inhibited by oligosaccharides containing the sialyl Le^x structure, whereas a control oligosaccharide had no effect. An antibody specific for sialyl Le^x was also effective in inhibition. The two anti-E-selectin antibodies differed in inhibition of binding of E-selectin. Only the 1.2B6 antibody inhibited the binding of soluble E-selectin to CD11/CD18, whereas both were inhibitory at the cellular level. Antibodies to CD11/CD18 did not show clear inhibition, probably because they were unable to cover the ~12 oligosaccharides found per CD11/CD18 heterodimer (Asada *et al.*, 1991) (not shown). The selectins need Ca^{2+} for activity and, as expected, EDTA inhibited binding.

It is quite possible that several other leukocyte surface glycoconjugates contain the sialyl Le^x epitope (Fukuda *et al.*, 1985), but its presence in CD11/CD18 integrins may be physiologically important, as discussed below.

Our current view of PMN binding to endothelium may be summarized as outlined in Figure 4 [adapted from Lo *et al.* (1991)]: inflammatory cytokines rapidly induce the expression of P-selectin on endothelial cells by its translocation from intracellular granules. In ~2 h, E-selectin appears on the endothelial cell surface. These selectins interact with circulating PMNs, resulting in the 'rolling' phenomenon (Lawrence and Springer, 1991; von Andrian *et al.*, 1991). During this process, the PMNs are brought near to the membrane of endothelial cells, which is necessary for efficient activation by receptor-ligand-mediated contact. Only after activation and a decrease in the rate of passage of PMNs over the endothelium do CD11/CD18–ICAM interactions become possible (Lawrence and Springer, 1991).

E-Selectin is able to activate PMN adhesion (Kuijpers *et al.*, 1991; Lo *et al.*, 1991), possibly through the binding to CD11/CD18 molecules. P-Selectin also binds to sialyl Le^x and may also be activating. Activated PMNs would then bind to the endothelium through CD11/CD18 interactions with ICAM-2 and ICAM-1, leading to migration into inflamed tissues (Stoolman, 1989; Osborn, 1990). Furthermore, the selectin–CD11/CD18 interactions could strengthen the attachment of leukocytes to endothelial cells at this stage.

Leukocytes from patients with leukocyte adhesion deficiency, which lack the CD11/CD18 integrins, are able to roll on the endothelial cell surface. The rolling may be mediated through various leukocyte glycoconjugates expressing the sialyl Le^x/sialyl Le^a epitopes, but obviously the activation of the integrins cannot take place and the cells cannot, therefore, penetrate the endothelial cell layer.

In spite of intensive studies, the mechanism(s) of integrin activation has remained unclear. Phorbol esters, which efficiently induce leukocyte adhesion, activate protein kinase C (Nishizuka, 1984). Several studies have shown that CD11 is constitutively phosphorylated and upon activation the CD18 β-chain is phosphorylated mainly on serine residues (Hara and Fu, 1986; Chatila *et al.*, 1989; Buyon *et al.*, 1990). An excellent correlation between CD18 phosphorylation and leukocyte adhesion was recently observed (Valmu *et al.*, 1991). However, deletion of acceptor serines in the cytoplasmic portion of CD18 did not abolish adhesion, whereas threonine deletion did (Hibbs *et al.*, 1991).

Wright's group recently described an interesting fatty acid-like molecule (integrin modulating factor) isolated from phorbol ester-stimulated leukocytes, which was able to induce a transient adhesion (Hermanowski-Vosatka *et al.*, 1992). This may be an important physiologic activator.

As an alternative to activation signals originating from the inside of the cells, agents interacting directly with the external portions of the leukocyte integrins could be important. Divalent cations are needed for leukocyte adhesion and the CD11 polypeptides contain three cation-binding motifs in their external parts. Ca^{2+} has been shown to bind to CD11a (Gahmberg *et al.*, 1988). Mg^{2+} is known to be important and most probably it also binds here. Dransfield *et al.* (1992) have shown, using a monoclonal antibody, that Mg^{2+} induces a conformational change in CD11a/CD18. van Kooyk *et al.* (1991) have shown that the monoclonal CD11a/CD18 antibody NKI-L16 induces CD11/CD18 activation in the presence of Ca^{2+}. In addition, extracellular Mn^{2+} ions are able to activate CD11b/CD18 by increasing its affinity for ligands (Altieri, 1991). Furthermore, Keizer *et al.* (1988) have described an anti-CD11a antibody which was able to activate CD11a/CD18-dependent adhesion, and Robinson *et al.* (1992) a CD18-reactive antibody which induced activation of both CD11a/CD18 and CD11b/CD18.

Because E-selectin can activate CD11/CD18 and we have shown that it binds to the integrins, we favour the hypothesis that activation in same cases can occur directly through selectin–integrin interactions. Importantly, this mechanism would bring together the three major groups of leukocyte

Carl_G_190x270_mm_blokki_FINAL.indd 241 06-Aug-23 1:53:50 PM

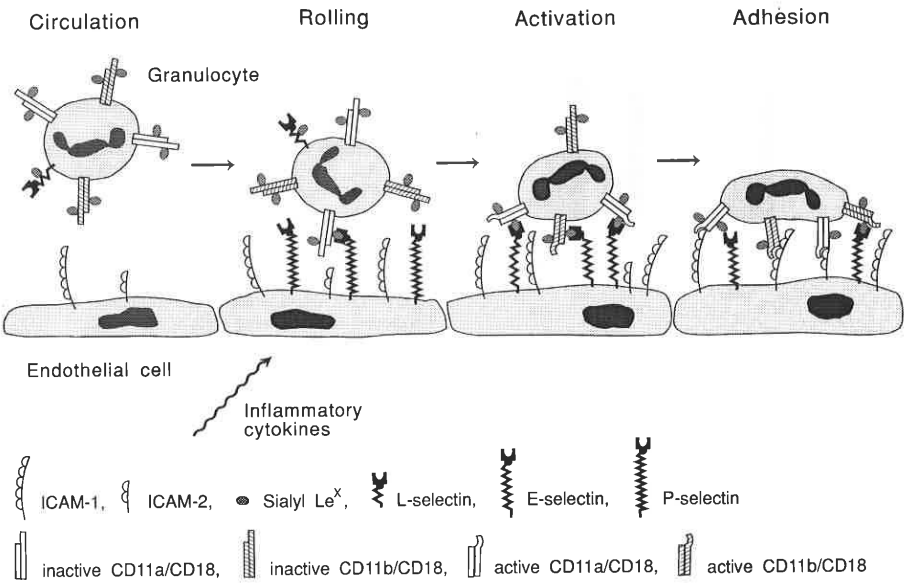

Fig. 4. A model for granulocyte binding to endothelial cells. Circulating PMNs express inactive CD11/CD18 complexes and L-selectin. The unstimulated endothelial cell expresses ICAM-2 and relatively small amounts of ICAM-1. The release of inflammatory cytokines induces the expression of E- and P-selectins, and increases that of ICAM-1. The selectins are able to bind to the leukocyte integrins and activate them, probably by the induction of a conformational change. The activated integrins subsequently bind to the ICAM-molecules on the endothelial cell and firm attachment occurs.

adhesion molecules, selectins, integrins and some members of the immunoglobulin supergene family, with the integrins playing a pivotal role.

Materials and methods

Isolation of CD11/CD18 integrins

A mixture of leukocyte integrins was isolated from normal human buffy coats by affinity chromatography using the anti-CD18 antibody 7E4 (Nortamo *et al.*, 1988), as described in detail previously (Kantor *et al.*, 1988). CD11a/CD18 was isolated in a similar way using the CD11a-specific antibody E83 [Dr V.Bazil, see Nortamo *et al.* (1991)], and CD11b/CD18 using the CD11b-specific antibody 3F5 (P.Nortamo, unpublished). Their purity was checked by PAGE in the presence of SDS (Laemmli, 1970).

Binding of recombinant E-selectin to immobilized CD11/CD18 integrins

A soluble E-selectin construct was made as described previously (Pigott *et al.*, 1991) and the protein expressed in Chinese hamster ovary (CHO) cells. E-Selectin was isolated using the BBIG-E1 antibody by affinity chromatography. The E-selectin was >97% pure, as determined by N-terminal sequence analysis. Ten micrograms of CD11/CD18 were labelled with ^{125}I (The Radiochemical Centre, Amersham) using the chloramine T method (Greenwood *et al.*, 1963) and this preparation was used to estimate the efficiency of coating to plastic. Two and a half micrograms of integrins were used for subsequent coating in 0.05 ml of 25 mM Tris (pH 8.0)–0.15 M NaCl–2 mM $MgCl_2$–0.1% octylglucoside overnight at +4°C to Nunc-Immuno plates (Roskilde, Denmark), which resulted in binding of ~0.3 μg of integrins. The plates were subsequently saturated by coating with 1% bovine serum albumin (BSA) for 3 h at room temperature. Binding of E-selectin was determined using ^{125}I-labelled preparations, which were incubated for 1 h at room temperature with CD11/CD18-coated plates in 0.05 ml of binding buffer consisting of phosphate-buffered saline (PBS) (pH 7.3)–1.5 mM $MgCl_2$–1.5 mM $CaCl_2$–0.4% BSA in the absence or presence of competing reagents. After incubation, the plates were washed three times in binding buffer and the associated radioactivity counted. When indicated, EDTA was used at a concentration of 2.5 mM in PBS without divalent cations. The sialyl Le^x active pentasaccharide sialyl α2-3 galactose β1-4 (fucose α1-3) *N*-acetyl-glucosamine β1-3 galactose was synthesized as described previously (Kameyama *et al.*, 1991). A blood group B-active pentasaccharide was obtained from BioCarb, Lund, Sweden. The 1.2B6 anti-E-selectin antibody (Wellicome *et al.*, 1990) and the anti-sialyl Le^x antibody (Fukushima *et al.*, 1984) have been described previously. The anti-E- selectin antibody BBIG-E1 was produced by British Bio-Technology Ltd. The anti-ICAM-2 6D5 antibody used as a control has been described previously (Nortamo *et al.*, 1991).

Cellular binding assays

COS-1 cells were purchased from the American Type Culture Collection and used at a passage number <20. They were transfected with E-selectin in the CDM8 vector (British Biotechnology Products), by the dextran sulphate procedure. Routinely, >20% of the cells were transfected, as shown by immunofluorescence using anti-E-selectin antibody. Control cells were mock-transfected. Petri dishes (Greiner GmbH, Kremsmünster, Austria) were coated with 10 μg of CD11a/CD18 in 1 ml of coating buffer as described above. Binding was performed using Dulbecco's modified Eagle's medium (MEM), 50 mM Hepes (pH 7.4)–2 mM $MgCl_2$–2 mM $CaCl_2$–5% fetal calf serum (FCS) for 1 h at room temperature. After incubation, the plates were washed three times in the same buffer and the attached cells counted.

Acknowledgements

This study was supported by the Academy of Finland, the Finnish Cancer Society and the Sigrid Jusélius Stiftelse. We thank Yvonne Heinilä for expert secretarial assistance. We thank the following individuals for monoclonal antibodies: D.O.Haskard (E-selectin), P.I.Terasaki (anti-sialyl Le^x) and V.Bazil (CD11a).

Abbreviations

BSA, bovine serum albumin; CD11a/CD18 = LFA-1; CD11b/CD18 = CR3, Mac-1; CD11c/CD18 = p150/95; CHO, Chinese hamster ovary; E-selectin = ELAM-1; FCS, fetal calf serum; ICAM-1, intercellular adhesion molecule-1

Carl_G_190x270_mm_blokki_FINAL.indd 242 06-Aug-23 1:53:50 PM

(CD54); ICAM-2, intercellular adhesion molecule-2; ICAM-3, intercellular adhesion molecule-3; L-selectin = LECAM-1, Leu8; MEM, modified Eagle's medium; P-selectin = PADGEM, GMP140, CD62; PBS, phosphate-buffered saline.

References

Altieri,D.C. (1991) Occupancy of CD11b/CD18 (Mac-1) divalent ion binding site(s) induces leukocyte adhesion. *J. Immunol.*, **147**, 1891–1898.

Arnaout,M.A. (1990) Structure and function of the leukocyte adhesion molecules CD11/CD18. *Blood*, **75**, 1037–1050.

Asada,M., Furukawa,K., Kantor,C., Gahmberg,C.G. and Kobata,A. (1991) Structural study of the sugar chains of human leukocyte cell adhesion molecules CD11/CD18. *Biochemistry*, **30**, 1561–1571.

Berg,E.L., Robinson,M.K., Mansson,O., Butcher,E.C. and Magnani,J.C. (1991) A carbohydrate domain common to both sialyl Le^a and sialyl Le^x is recognized by the endothelial cell leukocyte adhesion molecule ELAM-1. *J. Biol. Chem.*, **266**, 14869–14872.

Bevilacqua,M.P., Stengelin,S., Gimbrone,M.A.,Jr and Seed,B. (1989) Endothelial leukocyte adhesion molecule 1: an inducible receptor for neutrophils related to complement regulatory proteins and lectins. *Science*, **243**, 1160–1165.

Bevilacqua,M., Butcher,E., Furie,B., Furie,B., Gallatin,M., Gimbrone,M., Harlan,J., Kishimoto,K., Lasky,L., McEver,R., Paulson,J., Rosen,S., Seed,B., Siegelman,M., Springer,T., Stoolman,L., Tedder,T., Varki,A., Weissman,I. and Zimmerman,G. (1991) Selectins: a family of adhesion receptors. *Cell*, **67**, 233.

Butcher,E.C. (1991) Leukocyte–endothelial cell recognition: Three (or more) steps to specificity and diversity. *Cell*, **67**, 1033–1036.

Buyon,J.P., Slade,S.G., Reibman,J., Abramson,S.B., Philips,M.R., Weissmann,G. and Winchester,R. (1990) Constitutive and induced phosphorylation of the α- and β-chains of the CD11/CD18 leukocyte integrin family. *J. Immunol.*, **144**, 191–197.

Chatila,T.A., Geha,R.S. and Arnaout,M.A. (1989) Constitution and stimulus-induced phosphorylation of CD11/CD18 leukocyte adhesion molecules. *J. Cell Biol.*, **109**, 3435–3444.

de Fougerolles,A.R. and Springer,T.A. (1992) Intercellular adhesion molecule 3, a third adhesion counter-receptor for lymphocyte function-associated molecule 1 on resting lymphocytes. *J. Exp. Med.*, **175**, 185–190.

de Fougerolles,A.D., Stacker,S.A., Schwarting,R. and Springer,T.A. (1991) Characterization of ICAM-2 and evidence for a third counter-receptor for LFA-1. *J. Exp. Med.*, **174**, 253–267.

Dransfield,I., Cabañas,C., Craig,A. and Hogg,N. (1992) Divalent cation regulation of the function of the leukocyte integrin LFA-1. *J. Cell Biol.*, **116**, 219–226.

Fukuda,M., Bother,B., Ramsamooj,P., Dell,A., Tiller,P.R., Varki,A. and Klock,J.C. (1985) Structures of sialylated fucosyl polylactosaminoglycans isolated from chronic myelogenous leukemia cells. *J. Biol. Chem.*, **260**, 12957–12967.

Fukushima,K., Hirota,M., Terasaki,P.I., Wakisaka,A., Togashi,H., Chia,D., Suyama,N., Fukushi,Y., Nudelman,E. and Hakomori,S. (1984) Characterization of sialosylated LewisX as a new tumor-associated antigen. *Cancer Res.*, **44**, 5279–5285.

Gahmberg,C.G., Kantor,C., Nortamo,P., Kotovuori,P., Prieto,J. and Patarroyo,M. (1988) The human leukocyte adhesion molecules CD11a-c/CD18 and ICAM-1. In Lernmark,Å., Dyrberg,T., Terenius,L. and Hökfelt,B. (eds), *Molecular Mimicry in Health and Disease*. Excerpta Medica, International Congress Series 823, Elsevier Science Publishers B.V., Amsterdam, The Netherlands, pp. 105–121.

Gahmberg,C.G., Nortamo,P., Zimmermann,D. and Ruoslahti,E. (1991) The human leukocyte adhesion ligand, intercellular-adhesion molecule 2. Expression and characterization of the protein. *Eur. J. Biochem.*, **195**, 177–182.

Gallatin,W.M., Weissman,I.L. and Butcher,E.C. (1983) A cell surface molecule involved in organ-specific homing of lymphocytes. *Nature*, **303**, 30–34.

Greenwood,F.C., Hunter,W.M. and Gloves,J.S. (1963) The preparation of ^{131}I-labeled human growth hormone of high specific radioactivity. *Biochem. J.*, **89**, 114–123.

Hara,T. and Fu,S.M. (1986) Phosphorylation of α, β subunits of 180/100-Kd polypeptides (LFA-1) and related antigens. In Reinherz,E.L., Haynes,B.F., Nadler,L.M. and Bernstein,I.D. (eds), *Leukocyte Typing II*. Springer-Verlag, New York, Vol. **3**, pp. 77–84.

Hermanowski-Vosatka,A., Van Strijp,J.A.G., Swiggard,W.J. and Wright,S.D. (1992) Integrin modulating factor-1: A lipid that alters the function of leukocyte integrins. *Cell*, **68**, 341–352.

Hibbs,M.L., Jakes,S., Stacker,S.A., Wallace,R.W. and Springer,T.A. (1991) The cytoplasmic domain of the integrin lymphocyte function-associated antigen 1 β subunit: sites required for binding to intercellular adhesion molecule 1 and the phorbol ester-stimulated phosphorylation site. *J. Exp. Med.*, **174**, 1227–1238.

Hogg,N. (1991) Structure and function of intercellular adhesion molecule-1. In Hogg,N. (ed.), *Chemical Immunology. Integrins and ICAM-1 in Immune Responses*. S.Karger AG, Basel, Switzerland, pp. 99–115.

Hynes,R.O. (1992) Integrins: versatility, modulation, and signaling in cell adhesion. *Cell*, **69**, 11–25.

Kameyama,A., Ishida,H., Kiso,M. and Hasegawa,A. (1991) Synthetic studies on sialoglycoconjugates 27: synthesis of sialyl-a(2-6)-Lewis X. *J. Carbohydr. Chem.*, **10**, 729–738.

Kantor,C., Suomalainen-Nevanlinna,H., Patarroyo,M., Österlund,K., Bergman,T., Jörnvall,H., Schröder,J. and Gahmberg,C.G. (1988) Purification in large scale and characterization of the human leukocyte adhesion glycoproteins GP90 (CD18). *Eur. J. Biochem.*, **170**, 653–659.

Keizer,G.D., Visser,W., Vliem,M. and Figdor,C.G. (1988) A monoclonal antibody (NKI-L16) directed against a unique epitope on the α-chain of human leukocyte function-associated antigen 1 induces homotypic cell–cell interactions. *J. Immunol.*, **140**, 1393–1400.

Kuijpers,T.W., Hakkert,B.C., Hoogerwerf,M., Leeuwenberg,J.F.M. and Roos,D. (1991) Role of endothelial leukocyte adhesion molecule-1 and platelet-activating factor in neutrophil adherence to IL-1-prestimulated endothelial cells. *J. Immunol.*, **147**, 1369–1376.

Laemmli,U.K. (1970) Cleavage of structural proteins during the assembly of the head of bacteriophage T4. *Nature*, **227**, 680–685.

Larsen,E., Celi,A., Gilbert,G.E., Furie,B.C., Erban,J.K., Bonfanti,R., Wagner,D.D. and Furie,B. (1989) PADGEM protein: a receptor that mediates the interaction of activated platelets with neutrophils and monocytes. *Cell*, **59**, 305–312.

Lawrence,M.B. and Springer,T.A. (1991) Leukocytes roll on a selectin at physiologic flow rates: Distinction from and prerequisite for adhesion through integrins. *Cell*, **65**, 859–873.

Ley,K., Gaehtgens,P., Fennie,C., Singer,M.S., Lasky,L.A. and Rosen,S.D. (1991) Lectin-like cell adhesion molecule 1 mediates leukocyte rolling in mesenteric venules *in vivo*. *Blood*, **77**, 2553–2555.

Lo,S.K., Lee,S., Ramos,R.A., Lobb,R., Rosa,M., Chi-Rosso,G. and Wright,S.D. (1991) Endothelial–leukocyte adhesion molecule 1 stimulates the adhesive activity of leukocyte integrin CR3 (CD11b/CD18, Mac-1, $\alpha m\beta 2$) on human neutrophils. *J. Exp. Med.*, **173**, 1493–1500.

Majuri,M.-L., Mattila,P. and Renkonen,R. (1992) Recombinant E-selectin-protein mediates tumor cell adhesion via sialyl-Le^a and sialyl-Le^x. *Biochem. Biophys. Res. Commun.*, **182**, 1376–1382.

Nishizuka,Y. (1984) The role of protein kinase C in cell surface signal transduction and tumor promotion. *Nature*, **308**, 693–698.

Nortamo,P., Patarroyo,M., Kantor,C., Suopanki,J. and Gahmberg,C.G. (1988) Immunological mapping of the human leukocyte adhesion glycoprotein GP90 (CD18) by monoclonal antibodies. *Scand. J. Immunol.*, **28**, 537–546.

Nortamo,P., Li,R., Renkonen,R., Timonen,T., Prieto,J., Patarroyo,M. and Gahmberg,C.G. (1991a) The expression of human intercellular adhesion molecule-2 is refractory to inflammatory cytokines. *Eur. J. Immunol.*, **21**, 2629–2632.

Nortamo,P., Salcedo,R., Timonen,T., Patarroyo,M. and Gahmberg,C.G. (1991b) A monoclonal antibody to the human leukocyte adhesion molecule intercellular adhesion molecule-2. Cellular distribution and molecular characterization of the antigen. *J. Immunol.*, **146**, 2530–2535.

Osborn,L. (1990) Leukocyte adhesion to endothelium in inflammation. *Cell*, **62**, 3–6.

Patarroyo,M., Beatty,P.G., Fabre,J.W. and Gahmberg,C.G. (1985a) Identification of a cell surface protein complex mediating phorbol ester-induced adhesion (binding) among human mononuclear leukocytes. *Scand. J. Immunol.*, **22**, 171–182.

Patarroyo,M., Beatty,P.G., Serhan,C.N. and Gahmberg,C.G. (1985b) Identification of a cell surface glycoprotein mediating adhesion in human granulocytes. *Scand. J. Immunol.*, **22**, 619–631.

Patarroyo,M., Clark,E.A., Prieto,J., Kantor,C. and Gahmberg,C.G. (1987) Identification of a novel adhesion molecule in human leukocytes by monoclonal antibody LB-2. *FEBS Lett.*, **210**, 127–131.

Patarroyo,M., Prieto,J., Rincon,J., Timonen,T., Lundberg,C., Lindbom,L., Åsjö,B. and Gahmberg,C.G. (1990) Leukocyte-cell adhesion: A molecular process fundamental in leukocyte physiology. *Immunol. Rev.*, **114**, 67–108.

Phillips,M.L., Nudelman,E., Gaeta,F.C.A., Perez,M., Singhal,A.K., Hakomori,S. and Paulson,J.C. (1990) ELAM-1 mediates cell adhesion by recognition of a carbohydrate ligand, sialyl-LeX. *Science*, **250**, 1130–1132.

Carl_G_190x270_mm_blokki_FINAL.indd 243 06-Aug-23 1:53:50 PM

Picker,L.J., Warnock,R.A., Burns,A.R., Doerschuk,C.M., Berg,E.L. and Butcher,E.C. (1991) The neutrophil selectin LECAM-1 presents carbohydrate ligands to the vascular selectins ELAM-1 and GMP-140. *Cell*, **66**, 921–933.

Pigott,R., Needham,L.A., Edwards,R.M., Walker,C. and Power,C. (1991) Structural and functional studies of the endothelial activation antigen endothelial leukocyte adhesion molecule-1 using a panel of monoclonal antibodies. *J. Immunol.*, **147**, 130–135.

Polley,M.J., Phillips,M.L., Wayner,E., Nudelman,E., Singhal,A.K., Hakomori,S. and Paulson,J.C. (1991) CD62 and endothelial cell–leukocyte adhesion molecule 1 (ELAM-1) recognize the same carbohydrate ligand, sialyl-Lewis x. *Proc. Natl. Acad. Sci. USA*, **88**, 6224–6228.

Renkonen,R., Paavonen,T., Nortamo,P. and Gahmberg,C.G. (1992) Regulation of the expression of endothelial adhesion molecules *in vivo*. Increased expression of ICAM-2 in lymphoid malignancies. *Am. J. Pathol.*, **140**, 763–767.

Robinson,M.K., Andrew,D., Rosen,H., Brown,D., Ortlepp,S., Stephens,P. and Butcher,E.C. (1992) Antibody against the Leu-CAM β-chain (CD18) promotes both LFA-1- and CD3-dependent adhesion events. *J. Immunol.*, **148**, 1080–1085.

Rothlein,R. and Springer,T.A. (1986) The requirement for lymphocyte function-associated antigen 1 in homotypic leukocyte adhesion stimulated by phorbol ester. *J. Exp. Med.*, **163**, 1132–1149.

Rothlein,R., Dustin,M.L., Marlin,S.D. and Springer,T.A. (1986) A human intercellular adhesion molecule (ICAM-1) distinct from LFA-1. *J. Immunol.*, **137**, 1270–1274.

Rothlein,R., Czajkowski,M., O'Neill,M.M., Marlin,S.D., Mainolfi,E. and Merluzzi,V.J. (1988) Induction of intercellular adhesion molecule 1 on primary and continuous cell lines by proinflammatory cytokines. *J. Immunol.*, **141**, 1665–1669.

Simmons,D., Makgoba,M.W. and Seed,B. (1988) ICAM, an adhesion ligand of LFA-1, is homologous to the neural cell adhesion molecule NCAM. *Nature*, **331**, 624–627.

Springer,T.A. (1990) Adhesion receptors of the immune system. *Nature*, **346**, 425–434.

Staunton,D.E., Marlin,S.D., Stratowa,C., Dustin,M.L. and Springer,T.A. (1988) Primary structure of ICAM-1 demonstrates interaction between members of the immunoglobulin and integrin supergene families. *Cell*, **52**, 925–933.

Staunton,D.E., Dustin,M.L. and Springer,T.A. (1989) Functional cloning of ICAM-2, a cell adhesion ligand for LFA-1 homologous to ICAM-1. *Nature*, **339**, 61–64.

Stoolman,L.M. (1989) Adhesion molecules controlling lymphocyte migration. *Cell*, **56**, 907–910.

Takada,A., Ohmori,K., Takahashi,N., Tsuyuoka,K., Yago,A., Zenita,K., Hasegawa,A. and Kannagi,R. (1991) Adhesion of human cancer cells to vascular endothelium mediated by a carbohydrate antigen, sialyl Lewis^a. *Biochem. Biophys. Res. Commun.*, **179**, 713–719.

Tiemeyer,M., Swiedler,S.J., Ishihara,M., Moreland,M., Schweingruber,H., Hirtzer,P. and Brandley,B.K. (1991) Carbohydrate ligands for endothelial-leukocyte adhesion molecule 1. *Proc. Natl. Acad. Sci. USA*, **88**, 1138–1142.

Valmu,L., Autero,M., Siljander,P., Patarroyo,M. and Gahmberg,C.G. (1991) Phosphorylation of the β-subunit of CD11/CD18 integrins by protein kinase c correlates with leukocyte adhesion. *Eur. J. Immunol.*, **21**, 2857–2862.

von Andrian,U.H., Chambers,J.D., McEvoy,L.M., Bargatze,R.F., Arfors,K.-D. and Butcher,E.C. (1991) Two-step model of leukocyte–endothelial cell interaction in inflammation: Distinct roles for LECAM-1 and the leukocyte β2 integrins *in vivo*. *Proc. Natl. Acad. Sci. USA*, **88**, 7538–7542.

van Kooyk,Y., Weder,P., Hogervorst,F., Verhoeven,A.J., van Seventer,G., te Velde,A.A., Borst,J., Keizer,G.D. and Figdor,G. (1991) Activation of LFA-1 through a Ca^{2+}-dependent epitope stimulates lymphocyte adhesion. *J. Cell Biol.*, **112**, 345–354.

Walz,G., Aruffo,A., Kolanus,W., Bevilacqua,M. and Seed,B. (1990) Recognition by ELAM-1 of the sialyl-LeX determinant on myeloid and tumor cells. *Science*, **250**, 1132–1135.

Wellicome,S.M., Thornhill,M.H., Pitzalis,C., Thomas,D.S., Lanchbury, J.S.S., Panayi,G.S. and Haskard,D.O. (1990) A monoclonal antibody that detects a novel antigen on endothelial cells that is induced by tumor necrosis factor, IL-1, or lipopolysaccharide. *J. Immunol.*, **144**, 2558–2565.

Wright,S.D. and Meyer,B.D. (1986) Phorbol esters cause sequential activation and deactivation of complement receptors on polymorphonuclear leukocytes. *J. Immunol.*, **136**, 1759–1769.

Zhou,Q., Moore,K.L., Smith,D.F., Varki,A., McEver,R.P. and Cummings,R.D. (1991) The selectin GMP-140 binds to sialylated, fucosylated lactosaminoglycans on both myeloid and nonmyeloid cells. *J. Cell Biol.*, **115**, 557–564.

Received on November 6, 1992; accepted on December 7, 1992

Carl_G_190x270_mm_blokki_FINAL.indd 244 06-Aug-23 1:53:50 PM

Carl_G_190x270_mm_blokki_FINAL.indd 245 06-Aug-23 1:53:50 PM

Carl_G_190x270_mm_blokki_FINAL.indd 246 06-Aug-23 1:53:50 PM

Part IV

THE INTERCELLULAR ADHESION MOLECULES -1 TO -5

Carl_G_190x270_mm_blokki_FINAL.indd 247 06-Aug-23 1:53:50 PM

Introduction

Fibronectin became a "classical" integrin ligand, and the RGD recognition sequence is present in several additional proteins such as vitronectin and fibrinogen. The integrins αVβ3, αVβ5, αVβ6, αVβ8, α4β1, α5β1 and αIIbβ3 bind RGD containing ligands. In contrast, the leukocyte β2-integrins bind to the intercellular adhesion molecules (ICAM), and use larger recognition sequences. In fact, the ICAMs do not contain RGD sequences.

ICAM-1 was the first β2 integrin ligand identified, independently by T.A. Springer´s and our groups. We used stimulation of lymphocytes with phorbol esters, and tested for inhibition of aggregation with monoclonal antibodies. The antigen recognized was immune precipitated and identified using SDS gel electrophoresis. ICAM-1 is expressed on leukocytes, endothelial cells and many other types of cells, and it is induced by cytokines, and other stimulatory molecules. ICAM-1 is an immunoglobulin superfamily protein, containing five immunoglobulin domains. The ICAM family consists of five members. ICAM-1 and ICAM-3 contain five immunoglobulin domains, ICAM-2 and ICAM-4, two domains, whereas ICAM-5 has nine immunoglobulin domains. ICAM-2 is expressed on leukocytes and endothelial cells, and it is not easily up-regulated by cytokines. ICAM-3 is expressed on leukocytes and it may be important in signal transduction. Endothelial cells in lymphomas show a strong ICAM-3 expression. ICAM-4 is present in erythrocytes, and ICAM-5, originally named telencephalin, is the most complex one, and it is expressed in dendrites of central neurons. Our group has worked a lot on all ICAMs, and named ICAM-4 and ICAM-5 (Paper 30).

Comments on Papers 30 to 42

RGD peptides did not inhibit the phorbol ester induced adhesion of leukocytes, and therefore we looked for β2 integrin ligand molecules expressed in leukocytes. Using the LB2 antibody (1), which prevented adhesion, we identified a surface glycoprotein with an apparent molecular weight of 84000 (Paper 31). Independently, Rothlein et al. (2) discovered the same molecule, and named it intercellular adhesion molecule-1 (ICAM-1). ICAM-1 is expressed in different leukocytes, but also in several tissues, and it is often up-regulated during inflammation. Among others, human large granular lymphocytes express the CD11a-c/CD18 integrins and ICAM-1 (3).

Later Staunton et al. (4) transfected COS cells with an endothelial cell cDNA library, and cloned a cDNA related to ICAM-1, and named it ICAM-2. We synthesized the ICAM-2 cDNA using PCR, expressed it in bacteria and made an ICAM-2 antiserum. This enabled the identification of the cellular protein as a 55000 molecular weight glycoprotein (5). Later we made a monoclonal antibody to ICAM-2 (6). The expression of ICAM-2 turned out to

Carl_G_190x270_mm_blokki_FINAL.indd 248 06-Aug-23 1:53:50 PM

be refractory to several tested cytokines (7), but its expression was increased in lymphoid malignancies (8).

Our ICAM-2 monoclonal antibody (6D5) inhibited ICAM-2 dependent adhesion, and it bound to the first immunoglobulin domain in ICAM-2. This finding indicated that the LFA-1 adhesion site is in this domain. We then compared the sequences in the first domains of ICAM-2 and ICAM-1, and synthesized a peptide covering the sequence 21-42 of ICAM-2. The peptide efficiently inhibited the binding of endothelial cells to LFA-1 (Paper 32). Importantly, low levels of the peptide stimulated leukocyte adhesion and natural killing cell activity (9) (Paper 33). The peptide also bound to CD11b/CD18 (Mac-1, αMβ2), but not to CD11c/CD18 (αXβ2). The peptide strongly stimulated the CD11b/CD18 dependent aggregation of the monocytic cell lines U937 and THP-1 (Paper 34). How can we explain that low levels of the peptide are stimulatory, whereas higher amounts are inhibitory? New results show that β2 integrins are bound to ICAMs in *cis* in resting neutrophils (10,11). Probably, the affinity of the closed integrin in *cis* binding is lower than its binding in *trans* to ICAMs in neighbouring cells. In leukocyte adhesion to other cells, the integrins are in open, high affinity conformation. High concentrations of the peptide or soluble ICAM-2-Fc inhibited adhesion, which must be due to competitive inhibition (Paper 35).

Using a phage display library we identified a short β2-integrin binding peptide, LLG (Paper 36). This sequence is located in the first Ig-domain of ICAM-1, and it is within the synthetic ICAM-2 peptide. The LLG sequence is also present in von Willebrand factor. The LLG peptide efficiently inhibited leukocyte adhesion.

ICAM-3 is a major ICAM on resting leukocytes (12,13), and it is involved in the initiation of the immune response (14). ICAM-3 acts as receptor for DC-SIGN, and it is a stimulatory molecule in immune responses (15). We isolated the molecule, and were involved in the structural analysis of its N-glycosidic oligosaccharides (16). ICAM-3 to expresses Lewis X, and the oligosaccharides acted as ligands for DC-SIGN (17).

ICAM-4 has an interesting history. The red cell LW blood group antigen was somehow associated with the Rh blood group antigens, but cloning and sequencing of LW, showed homology with the ICAM molecules (18). In collaboration with J.-P. Cartron´s group, we then isolated the protein and showed that it binds to LFA-1 and Mac-1 on different leukocytes. We named it ICAM-4 (Paper 37). Subsequent studies showed that the binding site on ICAM-4 for LFA-1 is on the first Ig domain, whereas both Ig domains are involved in Mac-1 binding. Mutational analysis showed that the binding sites on ICAM-4 for LFA-1 and Mac-1 overlap, but are distinct (19). Further work then showed that ICAM-4 binds to the I domains of the LFA-1 and Mac-1 integrins (20).

CD11c/CD18 (αXβ2) is strongly expressed on macrophages, and it is thought to be important in the uptake of senescent red cells from the circulation. We showed that ICAM-4 binds to CD11c/CD18, and erythrophagocytosis was efficiently inhibited by ICAM-4 and β2 integrin antibodies (Paper 38).

A neuronal membrane protein, named telencephalin, was first identified by use of a monoclonal antibody (21), and when cloned it was found to show high homology to the ICAM molecules (22). Together with K. Mori´s group, we then showed that it binds to LFA-1 (Paper 39). Accordingly, we renamed it ICAM-5. In addition to LFA-1 binding, it showed homophilic binding with Ig domain-1 binding to Ig domains 4-5 (Paper 40). ICAM-5 stimulated dendritic outgrowth and arborisation. We showed that T lymphocytes bind to domain-1 of ICAM-5, and monoclonal antibodies, which blocked the binding, bound to domain-1.

Carl_G_190x270_mm_blokki_FINAL.indd 249 06-Aug-23 1:53:50 PM

Human T cells adhered to rat hippocampal neurons, and an ICAM-5 monoclonal antibody to the human molecule blocked the interaction (23). Later we showed that a soluble form of ICAM-5 was released into the cerebrospinal fluid during encephalitis (24). The molecular weight of the released fragment, indicated that the cleavage took place close to the membrane. After the biochemical characterization of ICAM-5, and its interactions, we studied its role in neuron functions. When rat hippocampal neurons were treated with N-methyl-D-aspartic acid (NMDA) or α-amino-3-hydroxy-5-methylisoxazole-propionic acid (AMPA) ICAM-5 was cleaved, and the cleavage was blocked by metalloprotease-2 and -9 inhibitors. Interestingly, the treatment promoted dendritic spine development (Paper 41). Metalloprotease deficient mice showed more intact ICAM-5 than the wild type mice. Furthermore, soluble ICAM-5 promoted elongation of dendritic filopodia in wild-type neurons, but not in neurons of ICAM-5 deficient mice. Soluble ICAM-5 suppressed T cell activation, and it may act as an anti-inflammatory molecule (25). Structural studies showed that when ICAM-5 bound to the I domain of LFA-1, there was an unusual allosteric mobility of the C-terminal helix in the I domain (26). The homophilic ICAM-5 binding, was studied by structural analysis (27). Further work showed that ICAM-5 determined spine maturation by regulating the interaction of NMDA receptor binding to α-actinin (28). Altogether, the studies on ICAM-5 were rewarding, coupling immunology to neuroscience.

The soluble Del-1 (Development endothelial locus-1) protein is secreted from endothelial cells and associates with the cells (29). It is deposited on endothelial cells mainly in the brain and lung. In collaboration with T. Chavakis´ group we found that it acts as an endogenous inhibitor of leukocyte adhesion (Paper 42). It binds to LFA-1, and competes with leukocyte binding to ICAMs on endothelial cells. Endothelial cell deficiency of Del-1 increased neutrophil accumulation in lung inflammation in mice. Del-1 inhibited Mac-1 dependent phagocytosis (30). Del-1 was the first endogenous integrin inhibitor described.

References

1. Clark, E.A., Ledbetter, J.A., Holly, R.C., Dinndorf, P.A. and Shu, G. (1986) Polypeptides on human B lymphocytes associated with cell activation. *Hum. Immunol*. **16**, 100-113.
2. Rothlein, R., Dustin, M.L., Marlin, S.D. and Springer, T.A. (1986) A human intercellular adhesion molecule (ICAM-1) distinct from LFA-1. *J. Immunol*. **137**, 1270-1274.
3. Timonen, T., Patarroyo, M. and Gahmberg, C.G. (1988) CD11a-c/CD18 and GP84 (LB-2) adhesion molecules on human large granular lymphocytes and their participation in natural killing. *J. Immunol*. **141**, 1041-1046.
4. Staunton, D.E., Dustin, M.L. and Springer, T.A. (1989) Functional cloning of ICAM-2, a cell adhesion ligand for LFA-1 homologous to ICAM-1. *Nature* **339**, 61-64.
5. Gahmberg, C.G., Nortamo, P., Zimmermann, D. and Ruoslahti, E. (1991) The human leukocyte adhesion ligand, intercellular-adhesion molecule 2. Expression and characterization of the protein. *Eur. J. Biochem*. **195**, 177-182.
6. Nortamo, P., Salcedo, R., Timonen, T., Patarroyo, M. and Gahmberg, C.G. (1991) A monoclonal antibody to the human leukocyte adhesion molecule ICAM-2. Cellular distribution and molecular characterization of the antigen. *J. Immunol*. **146**, 2530-2535.

Carl_G_190x270_mm_blokki_FINAL.indd 250 06-Aug-23 1:53:50 PM

7. Nortamo, P., Li, R., Renkonen, R., Timonen, T., Prieto, J., Patarroyo, M. and Gahmberg, C.G. (1991) The expression of human intercellular adhesion molecule-2 is refractory to inflammatory cytokines. *Eur. J. Immunol*. **21**, 2629-2632.
8. Renkonen, R., Paavonen, T., Nortamo, P. and Gahmberg, C.G. (1992) Expression of endothelial adhesion molecules in vivo. Increased endothelial ICAM-2 expression in lymphoid malignancies. *Am. J. Pathol*. **140**, 763-767.
9. Somersalo, K., Carpén, O., Saksela, E., Gahmberg, C.G., Nortamo, P. and Timonen, T. (1995) Activation of natural killer cell migration by leukocyte integrin-binding peptide from intercellular adhesion molecule-2 (ICAM-2). *J. Biol. Chem*. **270**, 8629-8636.
10. Fan, Z., McArdle, S., Marki, A., Mikulski, Z., Gutierrez, E., Engelhardt, B., Deutsch, U., Ginsberg, M., Groisman, A. and Ley, K. (2016) Neutrophil recruitment limited by high-affinity bent β2 integrin binding ligand in *cis. Nature Commun*. **7**, 12658.
11. Fan, Z., Kiosses, W.B., Sun, H., Orecchioni, M., Ghosheh, Y., Zajonc, D.M., Arnaout, M.A., Gutierrez, E., Groisman, A., Ginsberg, M.H. and Ley, K. (2019) High-affinity bent β2-integrin molecules in arresting neutrophils face each other through binding to ICAMs in *cis. Cell Rep*. **26**, 119-130.
12. Vazeux, R., Hoffman, P.A., Tomita, J.K., Dickinson, E.S., Jasman, R.L., St. John, T. and Gallatin, W.M. (1992) Cloning and characterization of a new intercellular adhesion molecule ICAM-R. *Nature* **360**, 485-488.
13. Fawcett, J., Holness, C.L.L., Needham, L.A., Turley, H., Gatter, K.C., Mason, D.Y. and Simmons, D.L. (1992) Molecular cloning of ICAM-3, a third ligand for LFA-1, constitutively expressed on resting leukocytes. *Nature* **360**, 481-484.
14. de Fougerolles, A.R., Qin, X. and Springer, T.A. (1994) Characterization of the function of intercellular adhesion molecule (ICAM)-3 and comparison with ICAM-1 and ICAM-2 in immune response. *J. Exp. Med*. **179**, 619-629.
15. Geijtenbeek, T.B.H., Torensma, R., van Vliet, S.J., van Duijnhoven, G.C.F., Adema, G.J., van Kooyk, Y. and Figdor, C.G. (2000) Identification of DC-SIGN, a novel dendritic cell-specific ICAM-3 receptor that supports primary immune responses. *Cell* **100**, 575-585.
16. Funatsu, O., Sato, T., Kotovuori, P., Gahmberg, C.G., Ikekita, M. and Furukawa, K. (2001) Structural study of N-linked oligosaccharides of human intercellular adhesion molecule-3 (CD50). *Eur. J. Biochem*. **268**, 1020-1029.
17. Bogoevska, V., Nollau, P., Lucka, L., Grunow, D., Klampe, B., Uotila, L.M., Samsen, A., Gahmberg, C.G. and Wagener, C. (2007) DC-SIGN binds ICAM-3 isolated from peripheral human leukocytes through Lewis x residues. *Glycobiology* **17**, 324-333.
18. Bailly, P., Hermand, P., Callebaut, I., Sonneborn, H.H., Khamlichi, S., Mornon, J.-P. and Cartron, J.-P. (1994) The LW blood group glycoprotein is homologous to intercellular adhesion molecules. *Proc. Natl. Acad. Sci. USA*. **91**, 5306-53010.
19. Hermand, P., Huet, M., Callebaud, I., Gane, P., Ihanus, E., Gahmberg, C.G., Cartron, J.-P. and Bailly, P. (2000) Binding sites of leukocyte β2 integrins (LFA-1, Mac-1) on the human ICAM-4/LW blood group protein. *J. Biol. Chem*. **275**, 26002-26010.
20. Ihanus, E., Uotila, L., Toivanen, A., Stefanidakis, M., Bailly, P., Cartron, J.-P. and Gahmberg, C.G. (2003) Characterization of ICAM-4 binding to the I domains of the CD11a/CD18 and CD11b/CD18 leukocyte integrins. *Eur. J. Biochem*. **270**, 1710-1723.
21. Mori, K., Fujita, C., Watanabe, Y., Obata, K. and Hayaishi, O. (1987) Telencephalon-specific antigen identified by monoclonal antibody. *Proc. Natl. Acad. Sci. USA*. **84**, 3921-3925.

Carl_G_190x270_mm_blokki_FINAL.indd 251 06-Aug-23 1:53:50 PM

22. Yoshihara, Y., Oka, S., Nemoto, Y., Watanabe, Y., Nagata, S., Kagamiyama, H. and Mori, K. (1984) An ICAM-related neuronal glycoprotein, telencaphalin, with brain segment-specific expression. *Neuron* **12**, 541-553.
23. Tian, L., Kilgannon, P., Yoshihara, Y., Mori, K., Gallatin, W.M., Carpén, O. and Gahmberg, C.G. (2000) Binding of T lymphocytes to hippocampal neurons through ICAM-5 (telencephalin) and characterization of its interaction with the leukocyte integrin CD11a/CD18. *Eur. J. Immunol*. **30**, 810-818.
24. Lindsberg, P.J., Launes, J., Tian, L., Mikola, H., Subramanian, V., Sirén, J., Hokkanen, L., Hyypiä, T., Carpén, O. and Gahmberg, C.G. (2002) Release of soluble ICAM-5, a neuronal adhesion molecule, in acute encephalitis. *Neurology* **58**, 446-451.
25. Tian, L., Lappalainen, J., Autero, M., Hänninen, S., Rauvala, H. and Gahmberg, C.G. (2008). Shedded neuronal ICAM-5 suppresses T cell activation. *Blood* **111**, 3615-3625.
26. Zhang, H., Casasnovas, J.M., Jin, M., Liu, J., Gahmberg, C.G., Springer, T.A. and Wang, J. (2008) An unusual allosteric mobility of the C-terminal helix of a high-affinity αL integrin I domain variant bound to ICAM-5. *Mol. Cell* **31**, 432-437.
27. Recacha, R., Jiménez, D., Tian, L., Barredo, R., Gahmberg, C.G. and Casasnovas, J.M. (2014) Crystal structures of an ICAM-5 ectodomain fragment show electrostatic-based homophilic adhesions. *Acta Cryst. Sect. D*. **70**, 1934-1943.
28. Ning, L., Paetau, S., Nyman-Huttunen, H., Tian, L. and Gahmberg, C.G. (2014) ICAM-5 affects spine maturation by regulation of NMDA receptor binding to α-actinin. *Biol. Open* **4**, 125-136.
29. Hidai, C., Kawana, M., Kitano, H. and Kokubun, S. (2007) Discoidin domain of Del1 protein contributes to its deposition in the extracellular matrix. *Cell Tissue Res*. **330**, 83-95.
30. Mitroulis, I., Kang, Y.-Y., Gahmberg, C.G., Siegert, G., Hajishengallis, T.C., Chavakis, T. and Choi, E.-Y. (2014) Developmental endothelial locus-1 attenuates complement-dependent phagocytosis through inhibition of Mac-1 integrin. *J. Thromb. Haem*. **111**, 1004-1006.

Carl_G_190x270_mm_blokki_FINAL.indd 252 06-Aug-23 1:53:50 PM

643

Leukocyte adhesion: CD11/CD18 integrins and intercellular adhesion molecules

Carl G Gahmberg

Leukocyte integrins and intercellular adhesion molecules play pivotal roles in leukocyte adhesion to target cells and extracellular matrices. Recently, novel intercellular adhesion molecules have been identified, and much information has been obtained on the structures and binding sites of leukocyte integrins and of intercellular adhesion molecules. Furthermore, much progress has been made in the study of integrin activation and the role of leukocyte adhesion molecules in disease.

Addresses
Department of Biosciences, Division of Biochemistry, PO Box 56, Viikinkaari 5, University of Helsinki, FIN-00014, Finland; e-mail: Carl.Gahmberg@Helsinki.Fi

Current Opinion in Cell Biology 1997, 9:643–650

http://biomednet.com/elecref/0955067400900643

© Current Biology Ltd ISSN 0955-0674

Abbreviations

I	intervening
ICAM	intercellular adhesion molecule
mAb	monoclonal antibody
MIDAS	metal ion dependent activation site
VCAM-1	vascular cell adhesion molecule-1
VLA	very late antigen

Introduction

Most leukocytes circulate in the body and home to various tissues, where they exert a number of functions. In order to function they must adhere to other cells and sometimes to the extracellular matrix. For this purpose, they utilize members of three major groups of adhesion molecules, namely, integrins, members of the immunoglobulin superfamily, and carbohydrate-binding selectins. Several reviews (e.g. [1]) have been published on selectins and these molecules will not be dealt with here. Instead, I will concentrate on the leukocyte-specific integrins (CD11/CD18) and their ligands, the intercellular adhesion molecules (ICAMs).

There is an enormous amount of research going on in the field of leukocyte adhesion. There are several reasons for this. Leukocytes have for a long time been extensively studied by immunologists and other researchers, and early on much was known about their surface antigens, relation to disease, and functions *et cetera*. With the development of monoclonal antibodies, which enable the identification and isolation of individual leukocyte cell surface molecules, and with the advances in molecular gene cloning and expression techniques, the research basis of the field has become more molecular, resulting in rapid progress in the understanding of leukocyte functions. Much of the information obtained from leukocyte work has been applied to other areas of molecular cell biology.

Leukocyte adhesion is of pivotal functional importance. This importance is most obvious from the disease known as leukocyte adhesion deficiency. Here, the ability of leukocytes to adhere to other cells or tissues is defective because of integrin mutations, and the result is a life-threatening condition. On the other hand, enhanced adhesion may also be deleterious. Therefore, leukocyte adhesion must be strictly regulated. It is evident that by interfering with adhesion it could be possible to treat a number of major diseases affecting mankind. Therefore, most major drug companies are heavily involved in the field. All this activity has resulted in a large number of papers published on leukocyte adhesion and only a few can be dealt with in this review. Several general reviews on leukocyte adhesion have appeared relatively recently and readers interested in the topic are referred to these [2–7].

Several questions relating to leukocyte adhesion currently need answering. In my view, among the most important are the following: first, how is integrin activity regulated? Second, are the different ICAMs redundant or do they have specific functions of their own? Third, where in integrins and ICAMs are binding sites found and what are these binding sites like? Fourth, can we develop reagents that affect cell adhesion for eventual use in clinical medicine? Substantial progress has occurred in these areas during 1996 and until the writing of this review (May 1997), and this progress forms the subject of this review. Throughout the review, I use CD18 to refer to the integrin β_2 polypeptide, CD11a to refer to the integrin α_L polypeptide, and CD11b to refer to the integrin α_M polypeptide. Thus, CD11a/CD18 is integrin $\alpha_L\beta_2$.

Activation of integrins

It is becoming increasingly apparent that integrins (see Figure 1) can be activated by a variety of agents, and there are at least two major pathways of activation. When leukocyte adhesion is activated it can occur by increasing the affinity of individual integrin molecules for their ligands or by increasing the avidity of adhesion. In the former case it is probable that conformational changes occur in the integrins, whereas increased avidity may result from an increase in number or clustering of integrins in the plane of the membrane, thus increasing adhesion by means of a high local concentration of the molecules [6].

Carl_G_190x270_mm_blokki_FINAL.indd 253 06-Aug-23 1:53:50 PM

Figure 1

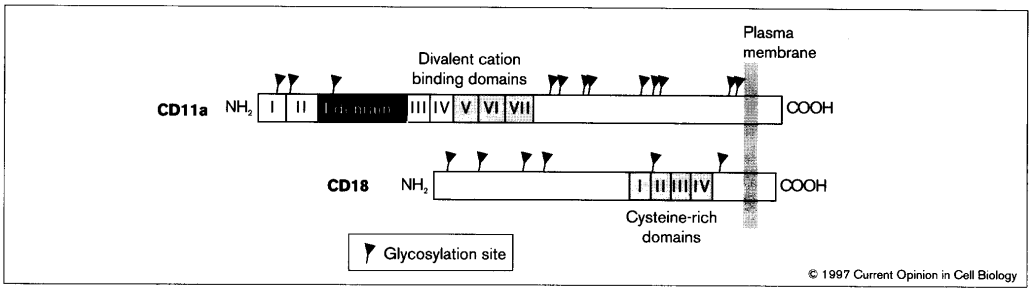

Schematic diagram of the integrin CD11a/CD18. Note the presence of the I domain, the glycosylation sites and the metal-binding (divalent cation binding) repeats. Shaded domains in CD11a represent divalent cation binding domains and in CD18 represent cysteine-rich domains. The Roman numbers in CD11a refer to repeated domains. The Roman numbers in CD18 denote distinct cysteine-rich domains. NH_2, amino terminus; COOH, carboxyl terminus. The amino termini are extracellular.

Activation by redistribution in the plane of the membrane

For more than 15 years it has been known that phorbol esters are potent activators of leukocyte adhesion. Hogg and co-workers [8,9•] have now convincingly shown that activation of adhesion by these agents takes place by clustering of CD11a/CD18 integrin molecules at the cell surface, without any increase in integrin affinity. Mg^{2+} and Mn^{2+} are also efficient activators of adhesion and it has been shown that Mg^{2+} treatment increases the expression of the CD11a/CD18 activation epitope that is recognized by monoclonal antibody (mAb)24, indicating the occurrence of a conformational change in CD11a/CD18 [9•].

An important result was obtained by Helander *et al.* [10••] who were studying cytotoxicity of natural killer cells towards murine thymoma cell lines. The parent BW5147 thymoma cell line was relatively resistant to killing, whereas a hybrid cell line containing human chromosome 6 was much more sensitive. The killing was efficiently inhibited by an anti-mouse-ICAM-2 antibody, which shows that ICAM-2 formed the major killer cell target. But, surprisingly, there was no difference in the amount of murine ICAM-2 on resistant and sensitive cells. In the sensitive line, however, ICAM-2 was concentrated into uropods, resulting in a high local concentration of the ligand. But why then was the hybrid cell making uropods? Immunochemical studies showed that the cytoskeletal protein ezrin, which is encoded by a gene on human chromosome 6, co-localized with ICAM-2. Further proof for the pivotal role of ezrin was obtained when its cDNA was transfected into BW5147 cells. This resulted in uropod formation and concentration of ICAM-2 into these structures, leading to increased natural killer cell killing. Del Pozo *et al.* [11] have shown that uropods are functionally important, because through these structures additional leukocytes are recruited to adhesion sites by using CD11a/CD18, ICAM-1 and ICAM-3.

Recent work has shown that ICAM-2 also binds to α-actinin and, more specifically, that it does this through the VRAAWRRL (single-letter code for amino acids) sequence located at about the middle of the cytoplasmic portion of ICAM-2 [12]. This sequence, being basic, resembles the binding site in ICAM-1 for α-actinin, but in ICAM-1 the sequence is located more closely to the membrane. The significance of this binding may be that integrin binding activity may require a link to the cytoskeleton. Holland and Owens [13•] found that ICAM-1 can act as a signaling molecule in a B cell lymphoma line. Rapid tyrosine phosphorylation on several proteins was observed after cross-linking of ICAM-1, and the kinase Lyn was activated. Furthermore, this treatment resulted in activation of Raf-1 and mitogen-activated protein kinases.

Activation from the outside

Previous work has convincingly shown that ICAMs, and in particular a peptide from the first domain of ICAM-2, strongly activate leukocyte integrins [14]. Using activating monoclonal antibodies to the CD11a polypeptide, binding to ICAM-1 but not to ICAM-3 was enhanced [12,15•]. On the other hand, activating antibodies specific to integrin β_2 activated binding to both ligands. These findings strengthen the view that CD11a/CD18 can exist in different states of activation. Importantly, when CD11a/CD18-transfected K562 erythroleukemic cells were activated with ICAM-1Fc, the binding to ICAM-3Fc was enhanced. These and previous results [6] show that ICAMs should not be considered to be passive integrin ligands, and that they themselves may regulate integrin activity.

The intervening (I) domain in CD11 α chains is considered to be an important binding region for ICAMs and soluble ligands. The I domains from CD11b and CD11a have been crystallized and their three-dimensional structures determined [6]. They are composed of seven

Carl_G_190x270_mm_blokki_FINAL.indd 254 06-Aug-23 1:53:50 PM

α helices and five β sheets with an Mg^{2+} coordinated in a MIDAS (metal ion dependent activation site) motif [6]. Mutations of two short loops in the CD11b I domain (loop sequences are E_{162}QLKKSKTL and Q_{190}NNPNPRS; the single-letter amino acid code is used, and subscripted numbers refer to positions of the first amino acids of the sequence in the protein) yielded constitutively active domains [16•]. Interestingly, like the wild-type I domain the latter mutant could be activated by the mAb KIM185 to become a super I domain, but the former mutant could not. These results indicate that these regions possess important regulatory functions, which can be affected by ligands.

Chemokines are known to activate leukocyte adhesion, and they are evidently important physiological activators. The MCP-1 (monocyte chemotactic protein-1), RANTES (regulated on activation, normal T cell expressed and secreted), and MIP-1 (macrophage inhibitory protein-1) chemokines efficiently activated the β_1 integrins VLA (very late antigen)-4 and VLA-5 in T cells, resulting in enhanced binding to fibronectin [17]. There was no increased binding to ICAM-1. Using eosinophils, RANTES and MCP-3 rapidly but transiently activated VLA-4 whereas phorbol esters induced a long-lasting effect [18]. However, the binding of the chemokine-activated cells to ICAM-1 by CD11b/CD18 was prolonged. Thus, the same chemokine can differentially activate β_1 and β_2 integrins on a certain cell. These findings further support the proposal that the activity of different integrins may be regulated by different mechanisms.

Cytohesin-1, an intracellular adaptor molecule

Kolanus *et al.* [19••] have described a potentially important integrin regulatory molecule, cytohesin-1. Cytohesin-1 protein contains a pleckstrin homology domain. This protein was shown to bind to CD18 and activated CD11/CD18 integrins to allow them to bind to ICAM-1. But when the isolated pleckstrin domain was overexpressed, adhesion of T cells was inhibited. How this protein really works is not known. Possibly, cytohesin-1 could act as an adaptor molecule which, together with other molecules or through post-translational modifications of itself or other molecules, could regulate the interaction between integrins and the cytoskeleton.

Certainly, during the coming years we will continue to witness much more research into the regulation of leukocyte adhesion by integrin activation. Useful reagents affecting adhesion will be developed. These reagents could, for example, interfere with various phosphorylation reactions or with the function of the cytoskeleton, or could directly affect the target-binding sites at the cell surface. Work along these lines is going on in a number of laboratories whose members are using a variety of different techniques. Already enough information has accumulated to show that it will be possible to develop suitable reagents affecting integrin activation.

More and more ICAMs

The first ICAM molecule to be discovered, ICAM-1 (CD54), was described in 1986–1987. ICAM-1 is still the most extensively studied molecule in the ICAM family (see Figure 2), and is perhaps the most important of them (it is the most widely distributed and its expression appears to be strictly regulated). The gene encoding ICAM-2 (CD102) was cloned in 1989, and the protein was characterized in 1991 (reviewed in [6]). It may have a major function in the stimulation of leukocyte adhesion [14]. ICAM-3 (CD50) had been found earlier, but only much later when its cDNA was cloned was it identified as an ICAM molecule (see [6]). It may be important in signal transduction and in the immune response.

ICAM-1 is the most widely distributed ICAM, but like it ICAM-2 and ICAM-3 are not restricted to leukocytes. ICAM-2 also occurs on endothelial cells and the expression of both ICAM-2 and ICAM-3 is induced in endothelial cells in lymphomas [6]. It has now been shown that both ICAM-2 and ICAM-3 are strongly expressed on B chronic lymphatic leukemia cells [20]. Patey *et al.* [21] carefully compared the expression of ICAM-3 in endothelial cells of tumors and inflamed areas. In contrast to E-selectin and vascular cell adhesion molecule-1 (VCAM-1) expression, ICAM-3 expression did not increase during inflammation and increased only in tumor endothelium. The reason for the tumor-induced expression of ICAM-2 and ICAM-3 is not known, but possibly the tumor cells secrete stimulatory factors, which act on the surrounding endothelium.

In contrast to these, ICAM-4, characterized as the Landsteiner–Wiener antigen in 1994 and shown to act as an ICAM molecule in 1995 [22], is restricted to erythrocytes and erythroid precursors. Its function is not known. The cDNA encoding telencephalin, which was first recognized as a neuron-specific molecule expressed in the telencephalon of several mammals, was cloned in 1994, and telencephalin showed high homology with the then known ICAMs [23]. Early this year the cDNA encoding this molecule, now called ICAM-5, was cloned from humans [24•]; ICAM-5 was shown to bind to the CD11a/CD18 integrin [24•,25•]. It is strongly expressed in the grey matter of the telencephalon, but is lacking from cerebellum and pons. What it does in the brain remains an enigma. The microglia cells could probably bind to this molecule, but is that the only purpose of this molecule? Perhaps it has other functions, not directly related to leukocyte adhesion.

In leukocytes ICAM-1, ICAM-2 and ICAM-3 are partially redundant. Why? ICAM-1 is known to be easily inducible, whereas ICAM-2 and ICAM-3 are more stably expressed. ICAM-1 is perhaps the most important binding molecule

Carl_G_190x270_mm_blokki_FINAL.indd 255 06-Aug-23 1:53:50 PM

Figure 2

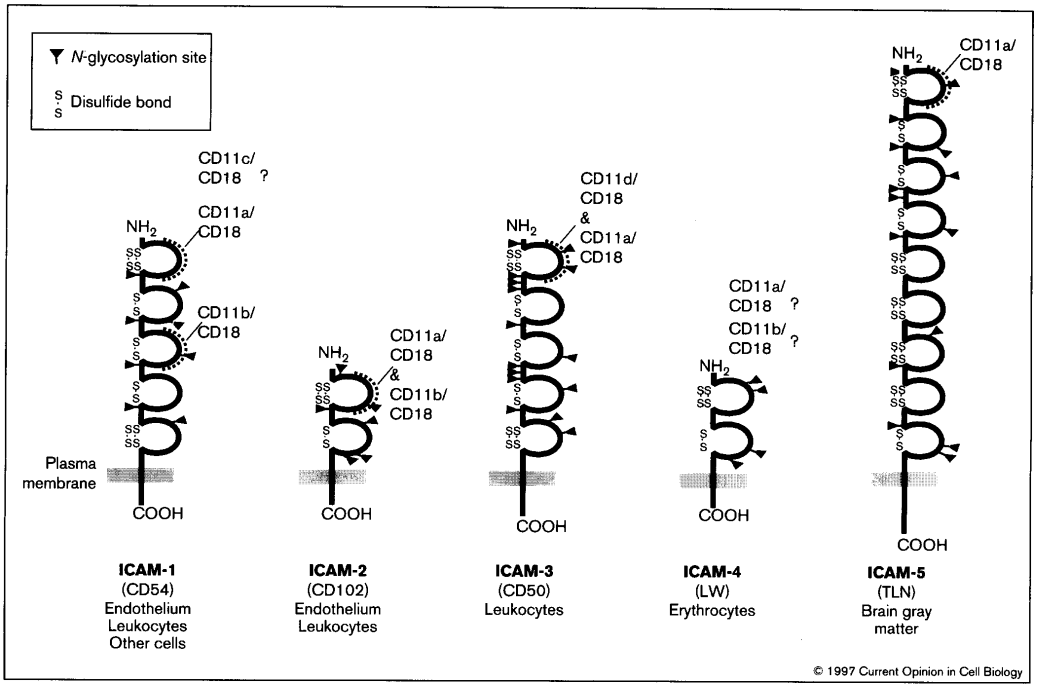

The five presently known ICAM molecules are shown schematically. The binding regions for integrins (CD11a, CD11b, CD11c, CD11d, and CD18) have been highlighted with small squares, and the potential *N*-glycosylation sites are shown. Question marks indicate that the integrin-binding sites in the ICAM molecules are not known. Alternative names for the ICAMs are shown in parentheses at the bottom of the figure and locations of the ICAMs are also shown at the bottom of the figure. NH_2, amino terminus; COOH, carboxyl terminus; LW, Landsteiner–Wiener antigen; TLN, telencephalin.

of these, whereas the others have some other functions in integrin stimulation and signal transduction. However, they certainly partially substitute for each other. This may be the reason that no disease has been described in which ICAMs are lacking or defective.

Structure and adhesion sites of ICAMs and integrins

Previous work has established that the first domain in ICAM-1 and ICAM-2 is the most important in binding to CD11a/CD18 [6]. The same domain in ICAM-2 also binds to CD11b/CD18. In ICAM-1, domain 3 binds to CD11b/CD18.

ICAM-1 binds not only to leukocyte integrins but also to fibrinogen and to *Plasmodium falciparum* infected red cells [6]. The fibrinogen binding may be an important means of recruiting inflammatory cells to injured organs. The first domain of ICAM-1 is responsible for fibrinogen binding as shown by Duperray *et al.* [26•] using different anti-ICAM-1 mAbs. Two antibodies that blocked fibrinogen binding also blocked binding to *Plasmodium falciparum* infected erythrocytes. They had no effect on CD11a/CD18 binding. Using a synthetic peptide approach, D'Souza *et al.* [27•] were able to show that amino acids 8–21 within the first domain of ICAM-1 were responsible for binding to fibrinogen. These amino acids correspond to the amino-terminal sequence of the ICAM-2 peptide P1, which efficiently binds to leukocyte integrins [6,14].

It was shown in 1995 that domain 1 of ICAM-3 is responsible for its binding to CD11a/CD18 [28], but a further detailed study has now been made [29]. In this study, the deletion of ICAM-3 domains, epitope mapping using mAbs, and mutational analysis were used to analyze the binding of domain 1 of ICAM-3 to CD11a/CD18. Largely, the results resemble those obtained with ICAM-1, in that they show that the corresponding amino acids in the two proteins have similar functions.

The crystal structure of the external portion of ICAM-2 has just been reported [30••], and this information can be used to predict the corresponding structures of other ICAMs. The ICAM-2 first domain has a compact structure

composed of 85 amino acids. The amino-terminal amino acid is lysine and the protein is three amino acids shorter than predicted from the cDNA sequence. The two external domains are bended in relation to each other at a 35° angle. The predicted binding region for integrins is remarkably flat, and quite different from the model structure of VCAM-1, where the acidic residue (Asp40) corresponding to Glu37 in ICAM-2 protrudes from the CD loop (see [6]). The structure in fact much resembles the earlier predicted structure [31]. Interestingly, the three *N*-linked oligosaccharides in the second domain may form a tripod-like skirt around the proximal part of the second domain; this skirt could facilitate an orientation perpendicular to the membrane. Due to the kink between domains 1 and 2, the binding site may present itself more efficiently to the integrins.

The binding sites in CD11a/CD18 for ICAM-1, ICAM-2 and ICAM-3 seem to be partially different. Murine CD11a/CD18 does not bind to human ICAM-1, whereas it does bind to human ICAM-2 and ICAM-3 [32,33]. Van Kooyk *et al.* [34] identified an Ile–Lys–Gly–Asn motif in the amino-terminal part of the CD11a I domain, a peptide from which inhibited ICAM-3 binding. Likewise, antibodies that blocked CD11a/CD18 binding to ICAM-3 were found to bind to a specific part of CD11a [35]. These antibodies did not block binding to ICAM-1.

It has long been thought that the CD18 polypeptide also contains a domain similar to the I domain found in CD11 α chains. By mutational analysis, CD18 residues Asp134, Ser136, Asp232 and Glu235 were shown to be involved in binding to ICAM-1 [36]. These residues are most probably involved in forming a β_2 MIDAS structure analogous to that of the CD11b I domain.

The structures of the CD11b and CD11a I domains were elucidated in 1995 (reviewed in [6]). They have a classical Rossmann dinucleotide-binding fold that is formed by six β strands surrounded by seven α helices. Springer [37•] has now proposed that the CD11a polypeptide has a β-propeller structure that is related to that of a G protein β subunit. This propeller is formed by seven β sheets, each formed by four antiparallel β strands; four antiparallel β strands form the legs of a W. The sheets are twisted in a propellerwise shape and the I domain is predicted to insert itself between the fourth β strand of W2 and the first β strand of W3 on the top of the β propeller. It is notable that the I domains show homology to α subunits of G proteins and it is possible that the interactions between the I domains and the β propellers are similar to those of the α and β subunits in G proteins. Although the model that the CD11a polypeptide has a β-propeller structure is speculative, it definitely contains several appealing and stimulating characteristics.

Using mAbs to different regions of the CD18 and CD11a polypeptides, information was obtained on the folding of the chains during biosynthesis [38•,39]. Antibodies to the conserved region in CD18 (residues 102–344), which is predicted to have an I domain like structure, did not react with the precursor that had not yet become associated with the α chain. On the other hand, antibodies reacting with epitopes before or after the I domain like region reacted well with the precursor forms. When the CD11a polypeptide was studied, the I domain was found to fold before association with CD18, whereas the proposed β-propeller domain folded upon association with CD18.

Adhesion molecules *in vivo* and in medical applications

The medical importance of leukocyte integrins is most evident from the clinical condition known as leukocyte adhesion deficiency type I (LADI), in which a mutation is found in the common CD18 polypeptide. LADI is characterized by a number of leukocyte defects (see [6] for further information and literature). All leukocyte β_2 integrins are absent or greatly reduced. The affected patients often die at a young age.

By gene targeting and other techniques, it is now possible, using animal models, to more precisely study the functions of individual integrins. Furthermore, the living conditions of animals can be strictly controlled enabling detailed studies.

When CD18-deficient 129/Sv mice were backcrossed into the PL/J mouse strain, the homozygotes developed a skin condition resembling psoriasis [40•]. The epidermis showed hyperplasia and lymphocyte exocytosis from the bloodstream, and the animals suffered from hair loss, erythema and the development of scales and crusts. Obviously, as the CD18-deficient 129/Sv mice showed none of these defects, some gene in addition to the CD18 deficiency determines susceptibility to this disorder. This must mean that this presently unknown gene product in some way interacts with leukocyte integrins, resulting in the condition.

A surprising finding was made in the study of CD11b/CD18-deficient mice. Chemoattractant-induced neutrophil adhesion to endothelium was reduced as expected, whereas thioglycollate-induced neutrophil accumulation was increased in the peritoneal cavity [41•]. The extravasated cells exhibited a delay in apoptosis as compared with normal cells. When normal neutrophils were incubated with opsonized particles apoptosis occurred, but this was inhibited with anti-CD11b/CD18 antibodies. These findings indicate that CD11b/CD18 normally functions in programmed cell death of neutrophils.

The novel leukocyte integrin CD11d/CD18 [42] was found to be constitutively expressed, together with CD11b/CD18, by synovial macrophages [43]. In rheumatoid arthritis the expression of CD11d/CD18 strongly increased as did expression of its ligand, ICAM-3 [42].

Carl_G_190x270_mm_blokki_FINAL.indd 257 06-Aug-23 1:53:50 PM

Therefore, reagents targeting this integrin could be potentially important in therapeutic applications.

A common complication of reduced blood flow to various organs followed by necrotic tissue damage is the reperfusion syndrome. Here, leukocytes, especially neutrophils, accumulate in the diseased tissue, leading to tissue destruction. Because adhesion molecules are responsible for the attachment of leukocytes and often also for subsequent events, inhibition of accumulation of inflammatory cells should alleviate the complications. Some examples of inhibition of accumulation using adhesion molecule deficient mice have now been published. Thus, ICAM-1-deficient mice were relatively protected against complications of cerebral ischemia after occlusion of the middle cerebral artery [44]. Interestingly, the blood flow to the cerebrum was increased 3.5-fold in the ICAM-1-deficient animals. In a similar way, ICAM-1-deficient mice were protected against injury after renal ischemia [45]. An efficient inhibition of early myocardial reperfusion injury was achieved with CD18 antibodies [46], further emphasizing the potential use of anti-adhesive therapy in the reperfusion syndrome.

Concluding remarks

Activation and downregulation of leukocyte adhesion are still relatively poorly understood, and certainly detailed information about these events is essential for the development of useful drugs, which may, for example, be used in the treatment of reperfusion syndrome, rheumatoid arthritis, and various other inflammatory conditions. On the other hand, much is already known about the binding sites in integrins for ICAMs and other molecules and, reciprocally, about the integrin-recognition sites in the ICAMs. This information, combined with increasing amounts of structural data, should result in the development of new useful agents affecting the binding events. The recent description of novel ICAMs and the fourth CD11/CD18 integrin (CD11d/CD18) [42] may indicate that we do not yet have a complete list of leukocyte integrins and of ICAMs. A large amount of work is needed to elucidate the possible functions and relevance of these molecules in disease.

Clinical applications of results obtained from leukocyte adhesion research have, however, been disappointingly slow to emerge. This is not particularly unexpected because drug development always takes time. However, leukocyte adhesion is so complex that an enormous amount of basic research remains to be done. I have not dealt in this review with selectins and their carbohydrate ligands, but a combination of reagents interfering with the different steps in adhesion [47•] may be the most useful approach to treating life-threatening acute situations. On the other hand, in most clinical applications we only want to affect highly specific functions and molecules, without eliciting many side effects, and here we still have a long way to go.

Acknowledgements

I thank Yvonne Heinilä for secretarial assistance and Pekka Kotovuori for drawing the figures. The original research reported from the author's laboratory was supported by the Academy of Finland, the Sigrid Jusélius Foundation and the Finnish Cancer Society.

References and recommended reading

Papers of particular interest, published within the annual period of review, have been highlighted as:

- • of special interest
- •• of outstanding interest

1. Kansas GS: **Selectins and their ligands: current concepts and controversies.** *Blood* 1996, **88**:3259-3287.

2. Carlos TM, Harlan JM: **Leukocyte-endothelial adhesion molecules.** *Blood* 1994, **84**:2068-2101.

3. Diamond MS, Springer TA: **The dynamic regulation of integrin adhesiveness.** *Curr Biol* 1994, **4**:506-517.

4. Stewart M, Thiel M, Hogg N: **Leukocyte integrins.** *Curr Opin Cell Biol* 1995, **7**:690-696.

5. Humphries MJ: **Integrin activation: the link between ligand binding and signal transduction.** *Curr Opin Cell Biol* 1996, **8**:632-640.

6. Gahmberg CG, Tolvanen M, Kotovuori P: **Leukocyte adhesion. Structure and function of human leukocyte β2-integrins and their cellular ligands.** *Eur J Biochem* 1997, **245**:215-232.

7. Dunon D, Piali L, Imhof BA: **To stick or not to stick: the new leukocyte homing paradigm.** *Curr Opin Cell Biol* 1996, **8**:714-723.

8. Stewart M, Hogg N: **Regulation of leukocyte integrin function: affinity vs. avidity.** *J Cell Biochem* 1996, **61**:554-561.

9. • Stewart MP, Cabañas C, Hogg N: **T cell adhesion to intercellular adhesion molecule-1 (ICAM-1) is controlled by cell spreading and the activation of integrin LFA-1.** *J Immunol* 1996, **156**:1810-1817.
The authors show that leukocyte adhesion can occur by an increase in integrin affinity induced by Mg^{2+} or by an increased avidity as seen after activation with phorbol esters.

10. •• Helander TS, Carpén O, Turunen O, Kovanen PE, Vaheri A, Timonen T: **ICAM-2 redistributed by ezrin as a target for killer cells.** *Nature* 1996, **382**:265-268.
It is shown that the cytoskeletal protein ezrin is able to induce the formation of uropods on target cells and brings the integrin ligand ICAM-2 to these structures. This increases the susceptibility of target cells to cytotoxicity.

11. Del Pozo MA, Cabañas C, Montoya MC, Ager A, Sánchez-Mateos P, Sánzes-Madrid F: **ICAMs redistributed by chemokines to cellular uropods as a mechanism for recruitment of T lymphocytes.** *J Cell Biol* 1997, **137**:493-508.

12. Heiska L, Kantor C, Parr T, Critchley DR, Vilja P, Gahmberg CG, Carpén O: **Binding of the cytoplasmic domain of intercellular adhesion molecule-2 (ICAM-2) to α-actinin.** *J Biol Chem* 1996, **271**:26214-26219.

13. • Holland J, Owens T: **Signaling through intercellular adhesion molecule 1 (ICAM-1) in a B cell lymphoma line.** *J Biol Chem* 1997, **272**:9108-9112.
Cross-linking of ICAM-1 resulted in increased tyrosine phosphorylation of many unidentified proteins and activation of serine–threonine kinases.

14. Li R, Xie J, Kantor C, Koistinen V, Altieri DC, Nortamo P, Gahmberg CG: **A peptide derived from the intercellular adhesion molecule-2 regulates the avidity of the leukocyte integrins CD11b/CD18 and CD11c/CD18.** *J Cell Biol* 1995, **129**:1143-1153.

15. Buckley CD, Ferguson ED, Littler AJ, Bossy D, Simmons DL:
• **Role of ligands in the activation of LFA-1.** *Eur J Immunol* 1997, **27**:957-962.
Evidence was obtained that CD11a/CD18 can exist in at least two different states of activation.

16. Zhang L, Plow EF: **A discrete site modulates activation of I**
• **domains.** *J Biol Chem* 1996, **271**:29953-29957.
The authors of this paper used mutational analysis to demonstrate that two loops from the CD11b/CD18 integrin I domain can regulate integrin activity. The work suggests that binding of ligand could alter I domain structure, resulting in integrin activation.

17. Carr MW, Alon R, Springer TA: **The C-C chemokine MCP-1 differentially modulates the avidity of β1 and β2 integrins on T lymphocytes.** *Immunity* 1996, **4**:179-187.

18. Weber C, Kitayama J, Springer TA: **Differential regulation of β1 and β2 integrin avidity by chemoattractants in eosinophils.** *Proc Natl Acad Sci USA* 1996, **93**:10939-10944.

19. Kolanus W, Nagel W, Schiller B, Zeitlmann L, Godar S,
•• Stodinger H, Seed B: **αLβ2 integrin/LPA-1 binding to ICAM-1 induced by cytohesin-1, a cytoplasmic regulatory molecule.** *Cell* 1996, **86**:233-242.
The cytoplasmic protein cytohesin-1 is described in this paper. Cytohesin-1 activates leukocyte integrins from the inside of the cell. If the pleckstrin homology domain alone of cytohesin-1 was overexpressed, adhesion was inhibited, probably by competitive inhibition.

20. Molica S, Dattilo A, Mannella A, Levato D: **Intercellular adhesion molecules (ICAMs) 2 and 3 are frequently expressed in B cell chronic lymphocytic leukemia.** *Leukemia* 1996, **10**:907-908.

21. Patey N, Vazeux R, Canioni D, Potter T, Gallatin WM, Brousse N: **Intercellular adhesion molecule-3 on endothelial cells. Expression in tumors but not in inflammatory responses.** *Am J Pathol* 1996, **148**:465-472.

22. Bailly P, Tontti E, Hermand P, Cartron J-P, Gahmberg CG: **The red cell LW blood group protein is an intercellular adhesion molecule which binds to CD11/CD18 leukocyte integrins.** *Eur J Immunol* 1995, **25**:3316-3320.

23. Yoshihara Y, Oka S, Nemoto Y, Watanabe Y, Nagata S, Kagamiyama H, Mori K: **An ICAM-related neurone glycoprotein, telencephalin, with brain segment-specific expression.** *Neuron* 1994, **12**:541-553.

24. Mizuno T, Yoshihara Y, Inazawa J, Kagamiyama H, Mori K:
• **cDNA cloning and chromosomal localization of the human telencephalin and its distinctive interaction with lymhocyte function-associated antigen-1.** *J Biol Chem* 1997, **272**:1156-1163.
Describes the cloning of the cDNA encoding human telencephalin and its localization to chromosome 19p13.2, the chromosomal region where the genes for ICAM-1, ICAM-3 and ICAM-4 are also located.

25. Tian L, Yoshihara Y, Mizuno T, Mori K, Gahmberg CG: **The**
• **neuronal glycoprotein telenchephalin is a cellular ligand for the CD11a/CD18 leukocyte integrin.** *J Immunol* 1997, **158**:928-936.
The binding of telencephalin to CD11a/CD18 was demonstrated. Telencephalin is the first brain-specific ICAM molecule, and intriguing questions are raised about its possible functions.

26. Duperray A, Languino LR, Plescia J, McDowall A, Hogg N,
• Craig AG, Berendt AR, Altieri DC: **Molecular identification of a novel fibrinogen binding site on the first domain of ICAM-1 regulating leukocyte-endothelium bridging.** *J Biol Chem* 1997, **272**:435-441.
These authors characterized the binding of fibrinogen to ICAM-1 by using monoclonal antibodies. This binding may be important in wound healing and perhaps in the development of atherosclerotic plaques.

27. D'Souza SE, Byers-Ward VJ, Gardiner EE, Wang H, Sung S-
• S: **Identification of an active sequence within the first immunoglobulin domain of intercellular cell adhesion molecule-1 (ICAM-1) that interacts with fibrinogen.** *J Biol Chem* 1996, **271**:24270-24277.
Here the binding sites for fibrinogen in ICAM-1 were mapped in detail using blocking peptides and antibodies.

28. Holness CL, Bates PA, Littler AJ, Buckley CD, McDowall A, Bossy D, Hogg N, Simmons DL: **Analysis of the binding site on intercellular adhesion molecule 3 for the leukocyte integrin lymphocyte function-associated 1.** *J Biol Chem* 1995, **270**:877-884.

29. Klickstein LB, York MR, de Fougerolles AR, Singer TA: **Localization of the binding site on intercellular adhesion molecule-3 (ICAM-3) for lymphocyte function-associated antigen 1 (LFA-1).** *J Biol Chem* 1996, **271**:23920-23927.

30. Casasnovas JM, Springer TA, Liu J-H, Harrison SC, Wang J-
•• H: **Crystal structure of ICAM-2 reveals a distinctive integrin recognition surface.** *Nature* 1997, **387**:312-315.
Here, for the first time, the three-dimensional structure of the external part of an ICAM molecule is described. The binding region for integrins is rather flat and this region lacks the protruding loop seen in VCAM-1; this region is probably important for binding. In contrast to the first domains of ICAM-2 and VCAM-1 which are rather different, probably reflecting different functions, the second domains are quite similar.

31. Li R, Nortamo P, Valmu L, Tolvanen M, Kantor C, Gahmberg CG: **A peptide from ICAM-2 binds to the leukocyte integrin CD11a/CD18 and inhibits endothelial cell adhesion.** *J Biol Chem* 1993, **268**:17513-17518.

32. Lub M, van Kooyk Y, Figdor CG: **Competition between lymphocyte function-associated antigen 1 (CD11a/CD18) and Mac-1 (CD11b/CD18) for binding to intercellular adhesion molecule-1 (CD54).** *J Leukoc Biol* 1996, **59**:648-655.

33. Driessens MHE, van Hulten P, Zuurbier A, La Rivière G, Roos E: **Inhibition and stimulation of LFA-1 and Mac-1 functions by antibodies against murine CD18. Evidence that the LFA-1 binding sites for ICAM-1, -2, and -3 are distinct.** *J Leukoc Biol* 1996, **60**:758-765.

34. Van Kooyk Y, Binnerts ME, Edwards CP, Champe M, Berman PW, Figdor CG, Bodary SC: **Critical amino acids in the lymphocyte function-associated antigen-1 I domain mediate intercellular adhesion molecule 3 binding and immune function.** *J Exp Med* 1996, **183**:1247-1252.

35. Binnerts ME, van Kooyk Y, Edwards CP, Champe M, Presta L, Bodary SC, Figdor CG, Berman PW: **Antibodies that selectively inhibit leukocyte function-associated antigen 1 binding to intercellular adhesion molecule-3 recognize a unique epitope within the CD11a I-domain.** *J Biol Chem* 1996, **271**:9962-9968.

36. Goodman TG, Bajt ML: **Identifying the putative metal ion-dependent adhesion site in the β2 (CD18) subunit required for αLβ2 and αMβ2 ligand interactions.** *J Biol Chem* 1996, **271**:23729-23736.

37. Springer TA: **Folding of the N-terminal, ligand-binding region of**
• **integrin α-subunits into a β-propeller domain.** *Proc Natl Acad Sci USA* 1997, **94**:65-72.
The proposal is made that the amino-terminal part of an integrin α subunit forms a β-propeller-like structure, which may resemble G proteins. Although still hypothetical, this proposal is interesting and certainly stimulates research on this topic.

38. Huang C, Lu C, Springer TA: **Folding of the conserved domain**
• **but not of flanking regions in the integrin β2 subunit requires association with the α subunit.** *Proc Natl Acad Sci USA* 1997, **94**:3156-3161.
In this paper and [39], monoclonal antibodies were used to probe the folding of CD18 and CD11a polypeptides during integrin biosynthesis.

39. Huang C, Springer TA: **Folding of the β-propeller domain of the integrin αL subunit is independent of the I domain and dependent on the β2 subunit.** *Proc Natl Acad Sci USA* 1997, **94**:3162-3167.

40. Bullard DC, Scharffetter-Kochanek K, McArthur MJ, Chosay JG,
• McBride ME, Montgomery CA, Beaudet AL: **A polygenic mouse model of psoriasiform skin disease in CD18-deficient mice.** *Proc Natl Acad Sci USA* 1996, **93**:2116-2121.
Homozygous 129/Sv mice lacking the CD18 gene showed, as expected, a number of defects in leukocyte functions. However, when mice of this strain were backcrossed into the PL/J strain, the next generation mice developed a psoriasis-like skin disease. The finding shows the importance of

Carl_G_190x270_mm_blokki_FINAL.indd 259 06-Aug-23 1:53:50 PM

CD11/CD18 integrins but also that other gene products are involved in the development of this skin disease.

41. • Coxon A, Rieu P, Barkalow FJ, Askari S, Sharpe AH, von Andrian UH, Arnaout MA, Mayadas TN: **A novel role for the β2 integrin CD11b/CD18 in neutrophil apoptosis: a homeostatic mechanism in inflammation.** *Immunity* 1996, **5**:653-666.
This paper describes results that indicate an important role of CD11b/CD18 in apoptosis.

42. Van der Vieren M, Le Trong H, Wood CL, Moore PF, St John T, Staunton DE, Gallatin WM: **A novel leukointegrin, αdβ2, binds preferentially to ICAM-3.** *Immunity* 1995, **3**:683-690.

43. El-Gabalawy H, Canvin J, Ma GM, Van der Vieren M, Hoffman P, Gallatin M, Wilkins JA: **Synovial distribution of αd/CD18, a novel leukointegrin.** *Arthritis Rheum* 1996, **39**:1913-1921.

44. Connolly ES Jr, Winfree CJ, Springer TA, Naka Y, Liao H, Yan SD, Stern DM, Solomon RA, Gutierrez-Ramos J-C, Pinsky DJ: **Cerebral protection in homozygous null ICAM-1 mice after middle cerebral artery occlusion.** *J Clin Invest* 1996, **97**:209-216.

45. Kelly KJ, Williams WW Jr, Colvin RB, Meehan SM, Springer TA, Gutiérraz-Ramos J-C, Bonventre JV: **Intercellular adhesion molecule-1-deficient mice are protected against ischemic renal injury.** *J Clin Invest* 1996, **97**:1056-1063.

46. McDonagh PF, Wilson DS, Iwamura H, Smith CW, Williams SK, Copeland JG: **CD18 antibody treatment limits early myocardial reperfusion injury after initial leukocyte deposition.** *J Surg Res* 1996, **64**:139-149.

47. • Ginsberg MH, Ruggeri ZM, Varki AP: **Cell adhesion in vascular biology: series introduction.** *J Clin Invest* 1996, **98**:1505.
Since October 1996 this journal has published a number of important reviews on leukocyte adhesion. The reader is strongly advised to read these articles.

Volume 210, number 2, 127–131 FEB 04339 January 1987

Identification of a novel adhesion molecule in human leukocytes by monoclonal antibody LB-2

Manuel Patarroyo, Edward A. Clark*, Jacqueline Prieto, Carmela Kantor+ and Carl G. Gahmberg+

*Department of Immunology, Karolinska Institute, S-104 01, Stockholm 60, Sweden, *Department of Microbiology, University of Washington, Seattle, WA 98195, USA* and *+Department of Biochemistry, University of Helsinki, 00170 Helsinki 17, Finland*

Received 30 October 1986; revised version received 11 November 1986

Monoclonal antibody LB-2 to a surface antigen on human B cells, lymphoblast, monocytes and vascular endothelial cells largely inhibited adhesion among Epstein Barr virus-immortalized normal B cells (EBV-B) and concanavalin A-stimulated blood mononuclear cells (Con A-BMC) before and after phorbol ester treatment. The antibody inhibited to a lesser extent phorbol ester-induced aggregation of monocytes, U937 cells and fresh BMC and had virtually no inhibitory effect on the adhesion among enriched T cells and granulocytes. A surface glycoprotein band of 84 kDa was obtained from EBV-B cells by immunoprecipitation and gel electrophoresis. Immunological and biochemical studies clearly distinguished this molecule from gp90 and associated glycoproteins which also mediate leukocyte adhesion.

LB-2 antibody; Leukocyte antigen; Adhesion molecule

1. INTRODUCTION

Mononuclear leukocytes interact with each other and with vascular endothelium to generate immune and inflammatory responses. Some of these interactions are known to require cell-cell adhesion [1,2].

Phorbol esters, such as tetradecanoyl phorbol acetate (TPA) and phorbol dibutyrate ($P(Bu)_2$), induce and enhance leukocyte adhesion and aggregation [3]. The intercellular binding is an energy- and temperature-dependent process that requires cell surface structures. Some of these adhesion molecules appear to constitute ligands forming adhesive cell–cell bonds referred to as CAMs (cell-adhesion molecules) [4].

Monoclonal antibody 60.3 to a leukocyte common antigen [5] almost completely inhibits phorbol ester-induced adhesion among blood mononuclear cells (BMC), granulocytes and EBV-immortalized normal B cells (EBV-B) [6–8]. This antibody binds to gp90, a leukocyte surface glycoprotein which is non-covalently associated to gp160, gp155 and gp130 [4,9].

Another antigen weakly expressed on 'resting' B cells and monocytes but strongly displayed on activated B cells and T cells is recognized by monoclonal antibody LB-2, previously named BB-2 [10,11]. Here, this antibody allowed the identification of a novel adhesion molecule in EBV-B cells and concanavalin A (Con A)-stimulated blood mononuclear cells and was also found to react with vascular endothelial cells.

Correspondence address: C.G. Gahmberg, Dept of Biochemistry, University of Helsinki, 00170 Helsinki 17, Finland

2. MATERIALS AND METHODS

2.1. *Cells*

Unless otherwise stated the lymphoblastoid cell

Published by Elsevier Science Publishers B.V. (Biomedical Division)
00145793/87/$3.50 © 1987 Federation of European Biochemical Societies

Carl_G_190x270_mm_blokki_FINAL.indd 261 06-Aug-23 1:53:50 PM

line PSB-1 was used as source of EBV-B cells. Other cell lines used in this study have been described in [11]. The SKW-3 cell line, derived from a T cell leukemia, was kindly provided by Professor Hans Wigzell. Blood mononuclear cells, a T cell-enriched population, and granulocytes were separated as in [6,7]. Monocytes were obtained from blood mononuclear cells by adherence to plastic dishes and this cell preparation contained 99% OKM1 positive cells and less than 2% T cells (T3 positive). Activated blood mononuclear cells were obtained by incubation with Con A (Sigma, St. Louis, MO) at 5 μg/ml for 3 days. Before use, these cells were extensively washed with 100 mM α-methyl-D-mannoside (Sigma) to remove any residual lectin. Vascular endothelial cells were prepared from human umbilical veins and cultured as in [12].

2.2. *Monoclonal antibodies*

Antibodies LB-2 (previously named BB-2) and 60.3 were produced as previously reported [5,10,11]. Antibody W6/32 to class I transplantation antigen was purchased from Sera-Lab (London, England). The three antibodies are murine IgG_{2a} and were used as ascites (LB-2 and W6/32, Ig content $\geqslant$ 2 mg/ml) or purified Ig (60.3). OKM1 and anti-T3 antibodies were obtained from Ortho Diagnostic Systems (Raritan, NJ) and New England Nuclear (Boston, MA), respectively. Indirect immunofluorescence studies were performed as in [8].

2.3. *Measurement of cell aggregation*

After extensive washing, cells were resuspended at 5×10^6 (cell lines) or 10×10^6 (fresh blood cells) cells/ml in RPMI 1640 medium (Grand Island, NY) with 0.5% human albumin (KabiVitrum, Stockholm). Cell suspensions were spun at 100 rpm at 37°C and treated with 60 nM $P(Bu)_2$ (Sigma) for 20 min. Cell aggregation and the effect of antibodies (at approx. 20 μg/ml, unless otherwise stated) were measured microscopically as reported [6–8].

2.4. *Cell surface labelling, immunoprecipitation and gel electrophoresis*

EBV-B cells were surface-labelled with ^3H after periodate oxidation and NaB^3H_4 reduction [13]. Immunoprecipitation was performed using rabbit anti-mouse IgG (Dakopatts, Copenhagen) in the second step [14]. Polyacrylamide slab gel electrophoresis in the presence of SDS was done according to Laemmli [15] using 8% acrylamide gels. The ^3H-labelled gels were treated for fluorography according to Bonner and Laskey [16]. ^{14}C-labelled standard proteins were obtained from the Radiochemical Centre (Amersham, England).

3. RESULTS

Antibody LB-2 inhibited phorbol ester-enhanced aggregation of EBV-B cell (72%) in a concentration-dependent manner (fig.1). At 20 μg/ml, the antibody blocked the cell aggregation in more than 70%. Half inhibition was obtained with approx. 50 ng/ml. The spontaneous cell aggregation (22%) was also largely blocked by both antibodies while the characteristic phorbol ester-induced morphological changes [8] were not affected (not shown). Antibody LB-2 inhibited intercellular adhesion in EBV-B cells from four different lines which had been passaged in vitro for a few months up to several years (not shown). In contrast, antibody W6/32 as well as many other antibodies to cell-surface antigens did not inhibit cell-cell binding [4,8]. Antibody LB-2 also inhibited to a large extent phorbol ester-enhanced adhesion among lectin-activated blood mononuclear cells while a minor inhibitory effect was obtained when monocytes, U937 cells or fresh

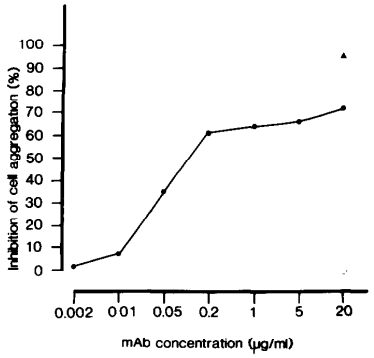

Fig.1. Effect of monoclonal antibodies LB-2 (●), 60.3 (▲) and W6/32 (○) on phorbol ester-enhanced aggregation of EBV-B cells.

Carl_G_190x270_mm_blokki_FINAL.indd 262 06-Aug-23 1:53:51 PM

Table 1

Effect of monoclonal antibodies LB-2, 60.3 and W6/32 on phorbol ester-induced adhesion among different leukocytes

Leukocyte[a]	Per cent cell aggregation[b]	Per cent inhibition of cell aggregation by monoclonal antibodies[c]		
		LB-2	60.3	W6/32
EBV-B cells	67	72[d]	92	−4
Con A-blood mononuclear cells	60	73	90	−5
Monocytes	72	32	98	1
U937 cells	24	23	97	−15
Blood mononuclear cells	58	13	74	−3
Enriched T cells	31	3	89	−5
Granulocytes	90	0	82	0

[a] All cells were resuspended in RPMI 1640 medium with 0.5% human albumin at 5×10^6 (cell lines) or 10×10^6 (fresh blood cells) per ml

[b] Leukocyte aggregation was measured by counting aggregated or single cells after 20 min treatment with 60 nM $P(Bu)_2$ and rotation at 100 rpm at 37°C

[c] Approx. 20 μg/ml of antibodies was added to the cells before phorbol ester treatment

[d] Mean of at least two experiments

Table 2

Reactivity of monoclonal antibodies LB-2 and 60.3 with different cell types

Cells (type)	Immunofluorescence reactivity	
	LB-2	60.3
Blood mononuclear cells	42 ±/+	95 + +/+ + +
Enriched T cells	23 ±	98 + +/+ + +
Monocytes	90 +	98 + +/+ + +
Con A-blood mononuclear cells	64 ±/+ + +	99 + +/+ + +
Granulocytes	13 ±	99 + +/+ + +
Erythrocytes	0	0
Vascular endothelial cells	99 + +/+ + +	0
PSB-1 (EBV-B)	80 +/+ + +	90 +/+ + +
Raji (Burkitt's lymphoma-B)	96 +/+ + +	41 ±
Molt-4 (T leukemia)	97 ±, 3 + + +	96 +, 3 + + +
SKW-3 (T leukemia)	82 ±, 18 + +	98 + +/+ + +
U937 (histiocytic lymphoma)	98 +/+ +	70 +/+ +
K562 (erythroleukemia)	85 + +	60 ±

Percentage of positive cells and labelling intensity were measured in a fluorescence microscope: (±) very weak, (+) weak, (+ +) intermediate and (+ + +) strong

Carl_G_190x270_mm_blokki_FINAL.indd 263 06-Aug-23 1:53:51 PM

blood mononuclear cells were used (table 1). In contrast to antibody 60.3, no significant effect was observed with the antibody on enriched T cells and granulocytes.

As reported in [10,11], antibody LB-2 reacted weakly with some blood cells, particularly monocytes, while T cells, granulocytes and erythrocytes were virtually negative (table 2). After a 3 day stimulation of blood mononuclear cells with Con A, labelling with the antibody was stronger in a larger number of cells. The reactivity of the antibody with cells from T, B, myelomonocytic and erythroid lineages was confirmed and in addition, the antibody was found to react strongly with cultured vascular endothelial cells and to have a different specificity from antibody 60.3 (table 2).

Under reducing conditions, a surface glycoprotein band of 84 kDa was obtained from EBV-B cells by immunoprecipitation with antibody LB-2 and gel electrophoresis (fig.2C), while an apparent molecular mass of 77 kDa was observed under non-reducing conditions (fig.2F). Some labelled material remained on the top of the gel indicating aggregation. This may occur between the gp84 molecules or between these and other molecules like the monoclonal antibody present in the immune precipitate. Antibody 60.3 precipitated two major surface glycoproteins with apparent molecular masses of 90 and 160 kDa from the same cells (fig.2D), as previously reported [8].

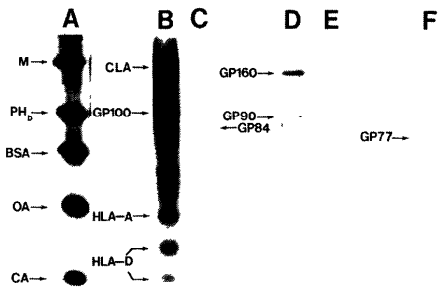

Fig.2. Polyacrylamide slab gel electrophoresis patterns of ^{3}H-labelled EBV-B cells. (A) ^{14}C-labelled standard proteins: M, myosin; PH_b, phosphorylase *b*; BSA, bovine serum albumin; OA, ovalbumin; CA, carbonic anhydrase; (B) pattern of surface-labelled EBV-B cells: CLA, common leukocyte antigen; GP100, major sialoglycoprotein; HLA-A, class I transplantation antigen heavy chain; HLA-D, class II transplantation antigen; (C) pattern obtained by precipitation with antibody LB-2 under reducing conditions: GP84, glycoprotein with apparent molecular mass of 84 kDa; (D) pattern obtained by precipitation with antibody 60.3 under reducing conditions; (E) pattern with no monoclonal antibody; (F) pattern obtained by precipitation with antibody LB-2 and run under nonreducing conditions.

4. DISCUSSION

The inhibitory effect of antibody LB-2 on cell aggregation induced or enhanced by phorbol esters indicates the participation of gp84 in the intercellular adhesion. We have previously tested several hundred different monoclonal antibodies directed against human leukocyte surface glycoproteins, and with one exception (antibody 60.3), no antibody inhibited cell adhesion. Fab fragments from 60.3 inhibited adhesion as well. Since the LB-2 antibody does not affect induction of morphological changes, this surface molecule is apparently not involved in stimulation of the cells by these compounds. Thus, it seems probable that gp84 is directly involved in the intercellular binding and it may constitute an adhesive ligand or CAM. It is also likely that gp84 interacts with a previously described adhesion molecule [6–8]. Interestingly, inhibition of cell aggregation by antibody LB-2 was less than that shown by antibody 60.3 and never complete, suggesting the participation of additional adhesion molecules. When tables 1 and 2 are compared, the inhibitory effect of antibody LB-2 on cell aggregation correlates well with the expression of its antigen on the cells. Since the antigen expression increases after stimulation of the cells with lectins or EBV, gp84 seems to mediate adhesion mainly in 'activated' mononuclear leukocytes. Moreover, the strong reactivity of the antibody with vascular endothelial cells suggests that the antigen constitutes an adhesion molecule also in these cells.

In contrast to antibody LB-2, antibody 60.3 inhibits adhesion among all types of leukocytes tested thus far. The latter antibody recognizes gp90, which is separately and non-covalently associated to gp160, gp155 and gp130 identified by monoclonal antibodies anti TA-1/LFA-1, OKM1

Carl_G_190x270_mm_blokki_FINAL.indd 264 06-Aug-23 1:53:51 PM

and anti-LeuM5, respectively [4,17]. All members of this protein complex are distinct from gp84 in both structure and cell distribution. In addition, the genes coding for gp90 and gp84 have been assigned to chromosome 21 and 19, respectively [9,18].

Slight changes in the electrophoretic mobility of the sialoglycoprotein recognized by antibody LB-2 suggest the presence of intra-chain disulfide bonds. The small difference in molecular mass from that described in the original publications, p76 [10,11], may be due to technical reasons.

Interestingly, cells which react with antibody LB-2, namely monocytes, B lymphoblast, U937, K562 and endothelial cells, are known to exert an 'accessory function' in T cell proliferation induced by lectins [19–21]. gp84 may mediate adhesion in this cell–cell interaction as well as in antigen presentation by the former cells. Moreover, adhesion of endothelial cells to lymphocytes may allow recirculation and localization of the latter cells in different lymphoid organs [2].

Recently, monoclonal antibody RR1/1 was reported to define a novel cell surface molecule involved in phorbol ester-induced aggregation of EBV-B cells [22]. Although the structure and cell distribution of this molecule are similar to those of gp84, only an extensive and parallel comparison of the two antigens will determine their relationship.

Adhesion of mononuclear leukocytes to each other and to vascular endothelial cells may allow proliferation and differentiation of the former cells and control of EBV-B cells in vivo [6,8]. On the other hand, abnormal adhesion may contribute to the development of leukemia and lymphoma.

ACKNOWLEDGEMENTS

The authors thank Dr P.G. Beatty for providing antibody 60.3. This project was supported by the Karolinska Institute, the Swedish Cancer Society, the Academy of Finland, The Sigrid Jusélius Foundation, a National Cancer Institute grant 5R01 CA 26294-06 (to C.G.G.) and a National Institute of Health grant RR00166 (to E.A.C.).

REFERENCES

[1] Bell, G.I. (1983) Immunol. Today 4, 237–240.
[2] Harlan, J.M. (1985) Blood 65, 513–525.
[3] Patarroyo, M. (1982) PhD Thesis, Karolinska Institute, Stockholm.
[4] Patarroyo, M. and Ansotegui, I.J. (1987) in: Leukocytes Typing III (McMichael, A. ed.) Oxford University Press, Oxford, in press.
[5] Beatty, P.G., Ledbetter, J.A., Martin, P.S., Price, T.H. and Hansen, J.A. (1983) J. Immunol. 131, 2913–2918.
[6] Patarroyo, M., Beatty, P.G., Fabre, J.W. and Gahmberg, C.G. (1985) Scand. J. Immunol. 22, 171–182.
[7] Patarroyo, M., Beatty, P.G., Serham, C.N. and Gahmberg, C.G. (1985) Scand. J. Immunol. 22, 619–631.
[8] Patarroyo, M., Beatty, P.G., Nilsson, K. and Gahmberg, C.G. (1986) Int. J. Cancer 38, 359–547.
[9] Suomalainen, H.A., Gahmberg, C.G., Patarroyo, M., Beatty, P.G. and Schröder, J. (1986) Somat. Cell. Mol. Genet. 12, 297–302.
[10] Clark, E.A. and Yokochi, T. (1984) in: Leukocyte Typing I (Bernard, A. et al. eds) pp.339–346, Springer, Berlin.
[11] Clark, E.A., Ledbetter, J.A., Holly, R.C., Dinndorf, P.A. and Shu, G. (1986) Human Immunol. 16, 100–113.
[12] Jaffe, E.A., Nachman, R.L., Becker, C.G. and Minick, C.R. (1973) J. Clin. Invest. 52, 2745–2756.
[13] Gahmberg, C.D. and Andersson, L.C. (1977) J. Biol. Chem. 252, 5888–5894.
[14] Gahmberg, C.G. and Andersson, L.C. (1978) J. Exp. Med. 148, 507–521.
[15] Laemmli, U.K. (1970) Nature 227, 680–685.
[16] Bonner, W.M. and Laskey, R.A. (1974) Eur. J. Biochem. 46, 83–88.
[17] Springer, T.A. and Andersson, D.C. (1986) in: Leukocyte Typing II (Reinherz, E.L. et al. eds) vol.3, pp.55–68, Springer, New York.
[18] Katz, F.E., Parkar, M., Stanley, K., Murray, L.J., Clark, E.A. and Greaves, M.F. (1985) Eur. J. Immunol. 15, 103–106.
[19] Arnold, A., Lipkowitz, S., Suthanthiran, M., Novogrodsky, A. and Stenzel, K.H. (1985) J. Immunol. 134, 3876–3881.
[20] Wakasugi, H., Harel, A., Dokhelar, M.C., Fradelizi, D. and Tursz, T. (1983) Proc. Natl. Acad. Sci. USA 80, 6028–6031.
[21] Hirschberg, H., Braathen, L.R. and Thorsby, E. (1982) Immunol. Rev. 66, 57–77.
[22] Rothlein, R., Dustin, M.L., Marlin, S.D. and Springer, T.A. (1986) J. Immunol. 137, 1270–1274.

Carl_G_190x270_mm_blokki_FINAL.indd 265 06-Aug-23 1:53:51 PM

THE JOURNAL OF BIOLOGICAL CHEMISTRY
Vol. 268, No. 23, Issue of August 15, pp. 17513–17518, 1993
Printed in U.S.A.
© 1993 by The American Society for Biochemistry and Molecular Biology, Inc.

A Peptide from ICAM-2 Binds to the Leukocyte Integrin CD11a/CD18 and Inhibits Endothelial Cell Adhesion*

(Received for publication, October 5, 1992, and in revised form, April 6, 1993)

Rui Li, Pekka Nortamo, Leena Valmu, Martti Tolvanen, Jarkko Huuskonen, Carmela Kantor, and Carl G. Gahmberg‡

From the Department of Biochemistry, University of Helsinki, SF-00170 Helsinki, Finland

Numerous leukocyte functions depend on adhesive intercellular interactions. The leukocyte-specific integrins CD11a/CD18 (lymphocyte function-associated antigen-1 (LFA-1)) and CD11b/CD18 (complement type 3 receptor (Mac-1)), which bind to the intercellular adhesion molecules ICAM-1 and ICAM-2, play a key role in adhesion. Little is known about the binding in molecular detail. We have now defined a peptide region from the first immunoglobulin domain of ICAM-2 that is specifically involved in binding to CD11a/CD18. A synthetic peptide from this part of ICAM-2, covering residues 21–42, bound to purified CD11a/CD18 and inhibited the adhesion of endothelial cells to this integrin. It also inhibited the binding of B lymphoblastoid cells to endothelial cells. Leukocytes bound to the peptide coated on plastic. Several shorter peptides from the same region showed less or no activity.

The CD11/CD18[1] leukocyte integrins, which bind to ICAMs present on leukocytes and various other cells, are of critical importance in leukocyte adhesion (1–4). The ICAM polypeptides belong to the immunoglobulin superfamily of adhesion ligands (5). ICAM-1 (CD54) contains five immunoglobulin domains (6, 7), but ICAM-2 contains only two, which show the highest homology to the two NH_2-terminal domains of ICAM-1 (8). ICAM-1 is widely distributed, and its expression can be up-regulated by various cytokines. It acts as a receptor for the malaria parasite *Plasmodium falciparum* (9) and for rhinoviruses (10, 11), and soluble ICAM-1 may become useful in the treatment of asthma and rhinovirus infections (12, 13). ICAM-1 binds to both CD11a/CD18 and CD11b/CD18.

Much less is known about ICAM-2. In contrast to ICAM-1, ICAM-2 binds only to CD11a/CD18 and not to CD11b/CD18 nor to rhinovirus. It was originally cloned by a functional adhesion assay using COS cells transfected with an endothelial cell expression library (8). We synthesized the ICAM-2 cDNA by the polymerase chain reaction, expressed the protein in *Escherichia coli* as a fusion protein, and first made a polyclonal antiserum (14). Later, a monoclonal antibody, 6D5, that inhibited ICAM-2-dependent cell adhesion was obtained (15). The ICAM-2 protein has an apparent molecular weight of 55,000 and is evidently heavily *N*-glycosylated. The 6D5 antibody was shown to react with the first immunoglobulin domain in ICAM-2.

In contrast to ICAM-1, ICAM-2 seems to be constitutively expressed in most cells and tissues examined (16, 17). We recently showed, however, that *in vivo* the reactivity of monoclonal antibody 6D5 with endothelium in malignant lymph nodes was higher than in nonmalignant ones (18). Damle *et al.* (19) demonstrated that ICAM-2 has a costimulatory effect during the activation of human T cells.

Obviously, it would be important to identify the binding site(s) on ICAMs in order to be able to develop reagents that could interfere with leukocyte adhesion. Several integrins bind to the arginine/glycine/aspartic acid (RGD) sequence (20) present in various proteins like fibronectin, fibrinogen, and snake venom proteins, but other recognition sequences have also been defined (21). These sequences are not found in human ICAM-1 or ICAM-2 and are therefore excluded as binding sites.

To get information on which amino acid residues in ICAMs are important for binding to CD11a/CD18, Staunton *et al.* (22) and Berendt *et al.* (23) made mutations in ICAM-1 and assayed for the binding of transfected COS cells to CD11a/CD18. The most obvious effects on CD11a/CD18 binding were seen by introducing mutations in the first domain.

The human ICAM-2 and ICAM-1 NH_2-terminal immunoglobulin domains are 35% identical and are related to murine ICAM-1 (24), which also binds to human CD11a/CD18. Similar motifs in the CD11a/CD18 binding regions of all three ICAMs are therefore expected. Fig. 1 shows an alignment of the amino acid sequences from the first domains of human ICAM-2, human ICAM-1, and mouse ICAM-1, which show the highest homology. In the present study we have defined a peptide from this part of the first domain of ICAM-2 (Fig. 1, *P1*) that specifically binds to CD11a/CD18.

EXPERIMENTAL PROCEDURES

Cell Lines and Cell Culture—The cell line Eahy926 is a hybrid between vascular endothelial and carcinoma cells and expresses endothelial cell markers (25). It was cultured in Dulbecco's hypoxanthine/aminopterin/thymidine medium containing 10% fetal calf serum. Eahy926 was induced to express ICAMs by incubating the cells with 10 ng/ml TNF-α (Boehringer Mannheim) overnight (16). The Epstein-Barr virus-transformed B cell line NAD-20 was maintained in RPMI 1640 medium containing 20% fetal calf serum.

Antibodies—The monoclonal antibodies 7E4 (anti-CD18) (26), LB-2 (anti-ICAM-1) (27), 6D5 (anti-ICAM-2) (15), IC 2/2 (anti-ICAM-2) (17), TS2/4 (anti-CD11a) (28), and the irrelevant antibody 84–3C1 (anti-CD43) (29) have been described. Mouse IgG (Dakopatts A/

* This work was supported by the Academy of Finland, the Sigrid Jusélius Stiftelse, the Finnish Cancer Society, and the Magnus Ehrnrooth Foundation. The costs of publication of this article were defrayed in part by the payment of page charges. This article must therefore be hereby marked "*advertisement*" in accordance with 18 U.S.C. Section 1734 solely to indicate this fact.

‡ To whom correspondence should be addressed: Dept. of Biochemistry, University of Helsinki, Unioninkatu 35, SF-00170 Helsinki, Finland. Tel.: 358-0-1917773; Fax: 358-0-1917769.

[1] The abbreviations used are: CD, cluster of differentiation antigen; CD11a/CD18, lymphocyte function-associated antigen-1 (LFA-1); CD11b/CD18, complement type 3 receptor (Mac-1); ICAM-1, intercellular adhesion molecule-1; ICAM-2, intercellular adhesion molecule-2; BSA, bovine serum albumin; TNF-α, tumor necrosis factor-α; P1–P8, peptides 1–8; CHO, Chinese hamster ovary.

This is an Open Access article under the CC BY license.

Carl_G_190x270_mm_blokki_FINAL.indd 266 06-Aug-23 1:53:51 PM

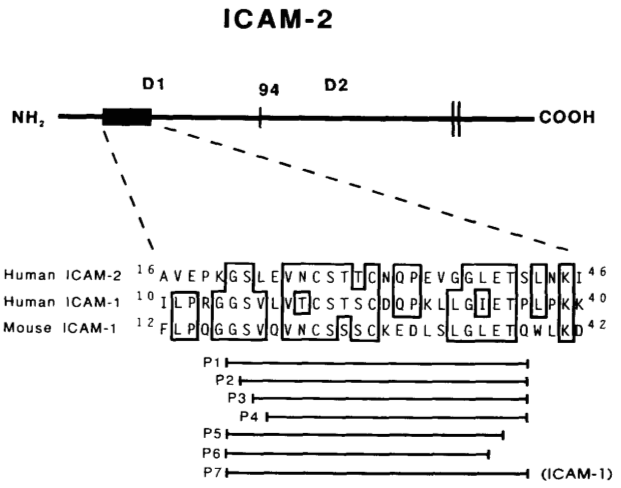

FIG. 1. **Alignment of homologous sequences from the first immunoglobulin domains in human and mouse ICAMs.** The sequences corresponding to the *ICAM-2* peptides *P1–P6* and the *ICAM-1* peptide *P7* are indicated. The boundary between the two immunoglobulin domains (*D1* and *D2*) is shown.

S, Denmark) was used as a negative control.

Synthetic Peptides—Synthetic peptides were prepared by solid phase synthesis on an Applied Biosystems model 430A peptide synthesizer, using *t*-butoxycarbonyl chemistry. Peptides were reduced with dithiothreitol for 2 h at room temperature and purified by high pressure liquid chromatography to >98% purity, using a C18 μBondapak column with a linear gradient of 0–70% acetonitrile in 0.1% trifluoroacetic acid. Their structures were confirmed by amino acid analysis and plasma desorption mass spectrometry. A 22-amino acid peptide (residues 21–42, P1) from the first domain of ICAM-2 (Fig. 1), its subpeptides, one amino acid less at a time from the NH_2 terminus (P2–P4), and 2 or 3 residues shorter from the COOH terminus (P5, P6), the corresponding peptide from human ICAM-1 (P7), and a control peptide (P8) containing the same amino acids as P1 were synthesized. P8 contains the 2 conserved cysteine residues in the right positions, but the rest of the amino acids are in random order (EVGTGSCNLECVSTNPLSGTEQ). A COOH-terminal tyrosine was added to all peptides to enable ^{125}I labeling. All peptides were soluble at the concentrations tested.

Binding of ^{125}I-Labeled P1 Peptide to Purified CD11a/CD18—CD11a/CD18 was purified from human buffy coat cell lysates by immunoaffinity chromatography on TS2/4 monoclonal antibody-Sepharose and eluted at pH 11.5 in the presence of 2 mM $MgCl_2$ and 1% octyl glucoside (30). Its purity was checked by polyacrylamide gel electrophoresis in the presence of SDS (31). The detergent-solubilized protein was diluted with 25 mM Tris, pH 8.0, 150 mM NaCl, and 2 mM $MgCl_2$, and attached to enzyme-linked immunosorbent assay plates (Nunc, Roskilde, Denmark) (5 μg in 50 μl/well) by overnight incubation at 4 °C. The wells were blocked with 1% BSA for 1 h at room temperature. Ten ng of ^{125}I-labeled P1, labeled by the chloramine-T method (32), was added to each well in 50 μl of 0.15 M NaCl, 0.01 M sodium phosphate, pH 7.4 (phosphate-buffered saline), 2 mM $MgCl_2$, 0.5% BSA, and 0.02% NaN_3 with or without nonradioactive peptides and incubated at 37 °C for 1 h. After washing, the attached ^{125}I-labeled P1 was solubilized with 1% SDS and counted.

Binding of Endothelial Cells to Purified CD11a/CD18—Purified CD11a/CD18 (50 μg in 1 ml/plate) was coated on 3.5-cm bacteriological dishes (Greiner GmbH, Kremsmünster, Austria), and the plates were saturated with 1% BSA as described above. The control plates were treated with BSA only. TNF-α-stimulated Eahy926 cells were removed from the tissue culture flasks with 5 mM EDTA in phosphate-buffered saline, washed, and resuspended in hypoxanthine/aminopterin/thymidine medium, 40 mM HEPES, pH 7.2, 2 mM $MgCl_2$, and 5% fetal calf serum. Cells (7×10^5) in 1 ml were added to each plate in the presence of peptides as indicated and incubated for 1 h at room temperature. Unbound cells were removed by washing three times with the same medium. The binding was quantitated by counting bound cells/2.5-mm^2 microscopic field. Fifteen fields at the periphery of the plates were screened by using a × 100 magnification.

Binding of NAD-20 Cells to Peptide-coated Plates—Peptides P1, P7, and P8 were covalently attached to Costar's amine surface plates (Costar Europe Ltd., Badhoevedorp, The Netherlands) by incubating 10 μg of peptide with 0.4 mg of 1-ethyl-3-(3-dimethylaminopropyl)-carbodiimide hydrochloride (Pierce Europe BV, Oud-Beijerland, The Netherlands) in 100 μl of dilute HCl, pH 4.0, in each well for 2 h at 22 °C. The wells were then saturated with 1% nonfat dry milk solution by incubating for 1 h at room temperature. The amount of peptide attached was about 5 ng/well for each peptide as determined with ^{125}I-labeled peptides. NAD-20 cells (8×10^4) in 100 μl of RPMI 1640, 40 mM HEPES, pH 7.2, 2 mM $MgCl_2$, and 5% fetal calf serum were incubated for 1 h at 22 °C in the presence of 5 μg of LB-2 antibody to avoid spontaneous intercellular aggregation. After being washed three times, the bound cells in each microscopic field were counted. Four fields were evaluated for each well as described above.

Inhibition of Binding of NAD-20 Cells to Endothelial Cells and ICAM-2-transfected CHO Cells—Eahy926 cells were cultured in 3.5-cm tissue culture plates (Costar, Cambridge, MA) in the absence or presence of 10 ng/ml TNF-α. CHO cells were stably transfected with ICAM-2 in the CDM8 vector (14) by using co-transfection with a pCDM8-neo vector (obtained from Dr. J. Ylänne). After G-418 selection, positive clones were isolated and confirmed by DNA sequencing. The cells were grown on the same plates as above. After overnight incubation, 6.5×10^5 NAD-20 cells labeled with 6-carboxyfluorescein diacetate (Sigma) were added to the dishes in the absence or presence of peptides or antibodies. After incubation for 1 h at room temperature, free cells were removed by washing three times, and the bound cells were counted by using a fluorescence microscope, 8 fields for each dish.

Computer Modeling of Domain 1 of ICAM-2—A model of the amino acid residues 1–90 of ICAM-2 was built by homology modeling. InsightII molecular graphics and model building program (Biosym Technologies, Inc., San Diego, CA), version 2.1.2, was used on a Silicon Graphics Iris 4D/380 VGX work station. The β strands and disulfide bonds in ICAM-2 were assigned based on conserved residues in immunoglobulin C2-type domains (5). The model structures that served as templates were crystal structures of several immunoglobulins: CD4 (33, 34) and CD8-α (35), taken from the Brookhaven Protein Data Bank (Ref. 36; entries 1cd4, 2cd4, and a preliminary entry 1cd8); crystal structure of CD2 (37); and a previous model of ICAM-1 (38), kindly sent by the respective authors.

After initial building, all loop structures were energy minimized, based on molecular mechanics calculations, while holding the strands fixed. Finally, the whole domain was relaxed. No molecular dynamics has been performed on this model.

RESULTS

Binding of Peptides to CD11a/CD18—The purified CD11/CD18 preparation was studied by polyacrylamide gel electrophoresis in the presence of SDS. It contained the expected

Carl_G_190x270_mm_blokki_FINAL.indd 267 06-Aug-23 1:53:51 PM

CD11a and CD18 polypeptides, and no major impurities were observed (Fig. 2). About 10% of the ICAM-2-derived peptide P1 bound to purified CD11a/CD18 coated on plastic, and the binding of ^{125}I-labeled P1 was specifically and almost totally inhibited by unlabeled P1 (Fig. 3*A*). Using ^{125}I-labeled P1, the effects of other peptides on the binding to CD11a/CD18 were determined. The peptide P2, lacking the NH_2-terminal glycine of P1, was much less efficient than P1, and P3, lacking the next serine, was even less active. Peptide P5, lacking the two COOH-terminal amino acids of P1, was only partially active, and P6, lacking Glu-40, was even less active. The ICAM-1 peptide P7 blocked the binding to a similar extent as P6. Peptides P4 and P8 were not inhibitory (Fig. 3*B*). The binding of ^{125}I-labeled P1 was inhibited in a concentration-dependent manner by nonradioactive P1, less by P7, and not at all by the control peptide P8 (Fig. 3*C*). A 50% inhibition was obtained at about 5 μM P1 peptide. The results suggest that both the NH_2 terminus and the COOH terminus of P1 are essential for activity.

Inhibition of Endothelial Cell Binding to CD11a/CD18 by Peptides—Peptide P1 efficiently inhibited the binding of TNF-α-induced Eahy926 cells to purified CD11a/CD18 (Fig. 4 *A*). It blocked the binding of uninduced cells to 90% (not shown). The ICAM-1-derived peptide P7 showed a smaller inhibition. The binding was efficiently blocked by the CD18 antibody 7E4. The inhibition was concentration-dependent as shown in Fig. 4*B*. A 50% inhibition was obtained at about 18 μM (43 μg/ml) of peptide P1. The control peptide P8 had no effect. In order to elucidate the relative contribution of ICAM-1 and ICAM-2, the binding was tested in the presence of ICAM antibodies (Fig. 4*C*). The anti-ICAM-1 antibody LB-2 efficiently blocked binding, whereas the anti-ICAM-2 antibody 6D5 had only a marginal effect. The background binding in this experiment was higher than that shown in Fig. 4, *A* and *B*, due to another preparation of CD11a/CD18.

Binding of Leukocytes to Peptides Coated on Plastic—NAD-20 B lymphocytes bound efficiently to peptide P1 but not to the control peptide coated on plastic (Fig. 5). The binding was not blocked by the monoclonal antibody 7E4.

Inhibition of Binding of NAD-20 Cells to Endothelial Cells and ICAM-2-transfected CHO Cells—Uninduced endothelial cells showed some binding of NAD-20 cells, but a much stronger binding was observed after treatment of endothelial cells with TNF-α (Fig. 6). P1 partially inhibited the binding,

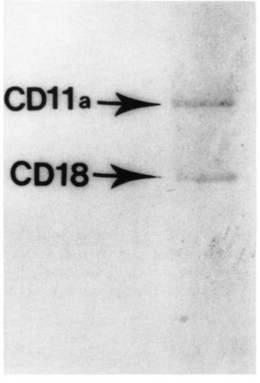

FIG. 2. **Polyacrylamide gel of purified CD11a/CD18.** Purified CD11a/CD18 was run on an 8% polyacrylamide gel in the presence of SDS and stained with Coomassie Blue.

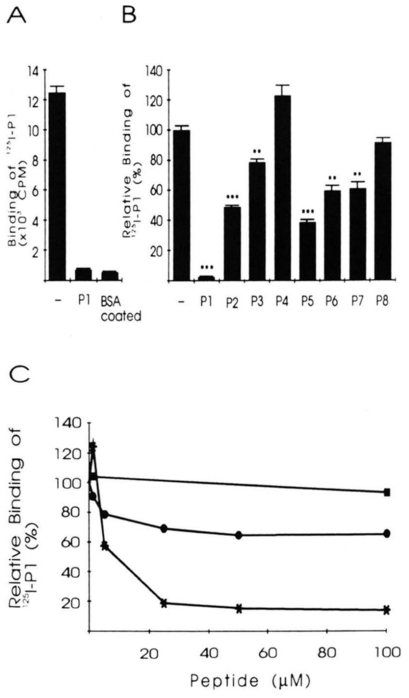

FIG. 3. **Binding of ^{125}I-labeled P1 peptide to purified CD11a/CD18 in the absence or presence of competing peptides.** Ten ng of ^{125}I-labeled P1 was incubated in CD11a/CD18-coated wells together with 100 μM different nonradioactive peptides (*A*, *B*) and indicated concentrations of nonradioactive P1 (*), P7 (●), and P8 (■) peptides (*C*). The differences in binding in the absence of competing peptides and in their presence were significant. **, $p < 0.01$; ***, $p < 0.001$. The standard deviations in *panel C* were less than 12%.

but not the control peptide P8. The CD18 antibody 7E4 also clearly blocked the binding as did the anti-ICAM-1 antibody LB-2 (Fig. 6). NAD-20 cells bound strongly to ICAM-2-transfected CHO cells grown on plastic. The binding was partially inhibited by P1 but most strongly inhibited by 7E4 (Fig. 7).

Model of the First Immunoglobulin-like Domain of ICAM-2—The molecular model of the first immunoglobulin-like domain of ICAM-2 (Fig. 8) shows resemblance to those of ICAM-1 (23, 38). The main difference to these models is the stretch from strand *C* to strand *E* (residues 40–60), being modeled closely after the second domain of rat CD2 (37). In addition, another difference from the ICAM-1 model of Giranda *et al.* (38) is a larger loop (residues 16–22) between the β strands *A* and *B*.

The peptide P1, indicated in *dark shading* in Fig. 8, is largely deeply embedded in the structure, which can be seen more clearly in a space-filling model (not shown). The exposed parts are in the amino- and carboxyl-terminal ends of the peptide and in the loop between strands *B* and *C* (around Asn-32). The residues most critical for peptide binding to CD11a/CD18 (Gly-21 and residues 40–42) are shown in *black*.

DISCUSSION

The external part of ICAM-2 is relatively simple, containing only two immunoglobulin domains. Therefore, this protein

Carl_G_190x270_mm_blokki_FINAL.indd 268 06-Aug-23 1:53:51 PM

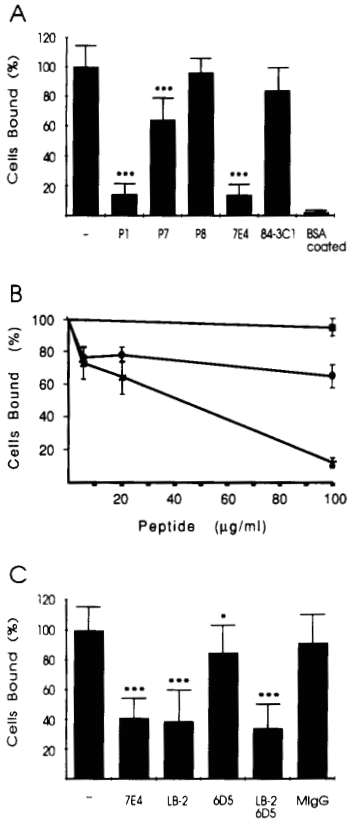

FIG. 4. **Inhibition of endothelial cell binding to purified CD11a/CD18 by peptides and antibodies.** One hundred μg of ICAM-2 and ICAM-1 peptides P1 and P7, control peptide P8, and monoclonal antibodies 7E4 (CD18, *A* and *C*), and *84-3C1* (CD43, *A*), *LB-2* (ICAM-1, *C*), *6D5* (ICAM-2, *C*), and indicated concentrations of P1 (*), P7 (●), and P8 (■, *B*) were used to block the adhesion of Eahy926 cells to purified CD11a/CD18. In *C* a different preparation of CD11a/CD18 was used. The cells bound as percentage of maximum is given. The effects of peptides were significant. ***, = $p < 0.001$; *, = $p < 0.05$; *MIgG*, mouse immunoglobulin G.

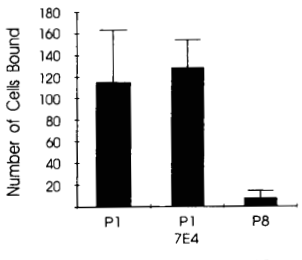

FIG. 5. **Binding of NAD-20 cells to peptide-coated plates.** The binding of NAD-20 cells to P1 was significantly higher than to the control peptide P8 ($p < 0.01$). The monoclonal antibody 7E4 had no effect on the adhesion of cells to P1. The number of cells bound/microscopic field is given.

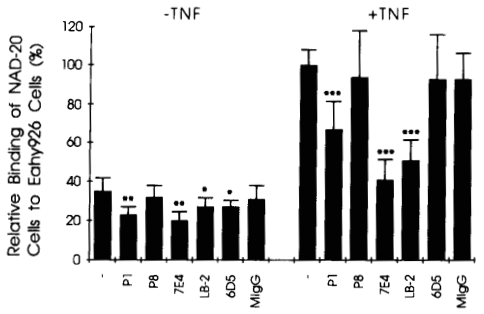

FIG. 6. **Binding of NAD-20 cells to Eahy926 cells in the absence or presence of peptides and antibodies.** Peptides *P1* and *P8* or antibodies *7E4*, *LB2*, and *6D5* (100 μg/ml) were used to block the adhesion of NAD-20 cells to Eahy926 cells. The results are given as percent of cells bound to TNF-α-induced Eahy926 cells in the absence of peptides or antibodies. *MIgG*, mouse immunoglobulin G.

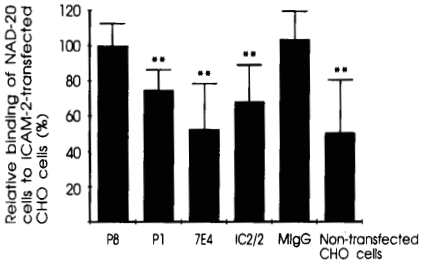

FIG. 7. **Binding of NAD-20 cells to ICAM-2-transfected and non-transfected CHO cells.** Peptides *P1* and *P8* or antibodies *7E4* and *IC 2/2* (100 μg/ml, except IC 2/2, which was used at 2.5 μg/ml) were used to block adhesion. The results are given as percent of cells bound in the presence of control peptide P8. *MIgG*, mouse immunoglobulin G.

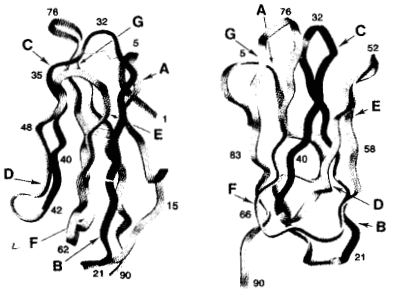

FIG. 8. **Two views of the peptide backbone of the model of the first domain of ICAM-2, rotated approximately 90° to the right around the vertical axis.** *Letters* indicate the approximate starting positions of each β-strand. The position of P1 (21–42) is shown in *dark gray* and *black*. The residues most critical for binding are drawn in *black*.

offers some advantages as a model protein as compared with ICAM-1. Earlier work indicated that domains 1 in ICAM-1 and ICAM-2 are most important in binding to CD11a/CD18 (15, 22, 23, 39). Since not only human ICAM-1 and ICAM-2 but also murine ICAM-1 (24) binds to human CD11a/CD18,

we assumed that the binding regions in the first immunoglobulin domains must be closely similar.

We have defined a peptide P1, which shows several interesting characteristics. It spans the whole *B* and *C* strands in the first domain of ICAM-2 (Fig. 8), but it is the NH_2- and COOH-terminal parts that are most exposed in the model. Staunton *et al.* and Diamond *et al.* (22, 39) and Berendt *et al.* (23) identified by mutational analysis a few critical regions, located in predicted β-turns in the ICAM-1 molecule. The most dramatic reduction in binding to CD11a/CD18 occurred when Glu-34 was mutated to alanine. This change, which corresponds to Glu-40 in ICAM-2 near the COOH terminus of P1 (Fig. 1), completely abolished binding activity (22). In line with this finding, our ICAM-2 peptide P6, which ended at Leu-39, had little activity and clearly less than P5, which contains Glu-40. Peptide P2, lacking the NH_2-terminal glycine of P1, was much less active than P1 in binding to CD11a/CD18, and deletion of the serine further lowered the activity. Therefore, it is evident that both the NH_2- and COOH-terminal amino acids in P1 are important for its activity, even though they are located on opposite faces of the domain in our model.

The peptide P1 does not seem to form any intrapeptide contacts in the complete domain, which is best seen in the view of the model at the *left* in Fig. 8. Accordingly, we predict that P1 has a flexible and poorly defined structure in solution. Surprisingly, when the P1 peptide was elongated with a lysine at its NH_2 terminus, which is found in the natural sequence of ICAM-2, the peptide had no activity (data not shown). The lysine may fix the conformation of the peptide by forming a salt bridge to one of the three glutamic acids in the peptide.

P1 coated on plastic efficiently bound leukocytes, but the CD18 antibody 7E4, which efficiently blocks CD11/CD18-dependent adhesion (26), had no effect. The 7E4 antibody also could not prevent the binding of ^{125}I-labeled P1 to purified CD11a/CD18 (not shown). The results show that the peptide is able to bind to the CD11a/CD18 well in the presence of antibody, whereas the ICAMs cannot. This is probably due to less steric hindrance for the smaller peptide as compared with the natural ligands.

The binding of endothelial cells to CD11a/CD18 was efficiently inhibited by the P1 peptide. Induced Eahy926 endothelial cells contain more ICAM-1 than ICAM-2 (16), and ICAM-1 is more important here than ICAM-2 (Fig. 4*C*), and therefore the effect of P1 must partially be due to interference with the binding of ICAM-1 to CD11a/CD18. We assume that ICAM-2 and ICAM-1 bind to the same or closely spaced sites in CD11a/CD18.

P1 partially blocked the binding of NAD-20 cells to endothelial cells and to ICAM-2-transfected CHO cells, but it was not able to block the spontaneous or induced homotypic aggregation of NAD-20 cells (not shown). Antibodies to CD11a block most of this aggregation as do anti-ICAM-1 antibodies (4). Evidently leukocyte-leukocyte adhesion is more complex, and its elucidation needs further work.

The ICAM-1 peptide P7 showed less activity in all test systems, and binding of ^{125}I-labeled P7 to CD11a/CD18 was difficult to measure, amounting to <10% of P1 binding (data not shown). Evidently P7 binds to the same or a closely spaced region in CD11a/CD18 as P1, but the affinity is lower. Possibly small adjustments in the peptide sequence could greatly influence its activity as is the case for P1.

Seth *et al.* (40) recently described an ICAM-2 peptide from the second Ig domain, which when coated on plastic was able to bind B lymphoblastoid cells. Some inhibition of binding was obtained both with CD18 and very late antigen-4 antibodies. Fecondo *et al.* (41) made a peptide from the fourth domain of ICAM-1, which was claimed to inhibit T cell cytotoxicity toward K562 cells and the spontaneous aggregation of Raji Burkitt's lymphoma B cells. These findings are difficult to reconcile with our work and that of Staunton *et al.* (22), who showed that domains D3–D5 in ICAM-1 can be deleted without loss of CD11a/CD18 binding activity. On the other hand, Ross *et al.* (42) found that peptides from ICAM-1, spanning residues 1–20, 26–50, and 132–146 partially inhibited the binding of Molt-4 lymphoblastic cells to endothelial cells. The first two peptides partially overlap with the peptide P7. These results are somewhat difficult to judge because of the complex situation when working with intact cells. The most efficient peptide inhibited 29% of the binding, but the contribution of ICAM-1 in the adhesion assay was estimated to be only 35%. Evidently, several regions in ICAM-1 show some binding activity.

It will be important to study which leukocyte functions can be modified by the peptides and whether they can be used to determine the binding site(s) on CD11a/CD18 as has recently been done for the platelet IIb/IIIa integrin (43, 44).

Acknowledgments—The skillful technical assistance of Ella Jääskeläinen, Leena Kuoppasalmi, and Kaija Antila is acknowledged, and we thank Yvonne Heinilä for secretarial help. We thank Drs. E. A. Clark, T. A. Springer, and J. Vives for antibodies; Drs. E. Y. Jones and M. S. Chapman for protein structure coordinates; and Dr. J. Ylänne for the pCDM8-neo vector.

REFERENCES

1. Springer, T. A. (1990) *Nature* **346,** 425–434
2. Hogg, N. (1991) in *Chemical Immunology: Integrins and ICAM-1 in Immune Responses* (Hogg, N., ed) pp. 99–115, S. Karger AG, Basel, Switzerland
3. Arnaout, M. A. (1990) *Blood* **75,** 1037–1050
4. Patarroyo, M., Prieto, J., Rincon, J., Timonen, T., Lundberg, C., Lindbom, L., Asjö, B., and Gahmberg, C. G. (1990) *Immunol. Rev.* **114,** 67–108
5. Williams, A. F., and Barclay, A. N. (1988) *Annu. Rev. Immunol.* **6,** 381–405
6. Simmons, D., Makgoba, M. W., and Seed, B. (1988) *Nature* **331,** 624–627
7. Staunton, D. E., Marlin, S. D., Stratowa, C., Dustin, M. L., and Springer, T. A. (1988) *Cell* **52,** 925–933
8. Staunton, D. E., Dustin, M. L., and Springer, T. A. (1989) *Nature* **339,** 61–64
9. Berendt, A. R., Simmons, D. L., Tansey, J., Newbold, C. I., and Marsh, K. (1989) *Nature* **341,** 57–59
10. Greve, J. M., Davis, G., Meyer, A. M., Forte, C. P., Yost, S. C., Marlor, C. W., Kamarck, M. E., and McClelland, A. (1989) *Cell* **56,** 839–847
11. Staunton, D. E., Merluzzi, V. J., Rothlein, R., Barton, R., Marlin, S. D., and Springer, T. A. (1989) *Cell* **56,** 849–853
12. Wegner, C. D., Gundel, R. H., Reilly, P., Haynes, N., Letts, L. G., and Rothlein, R. (1990) *Science* **247,** 456–459
13. Marlin, S. D., Staunton, D. E., Springer, T. A., Stratowa, C., Sommerguber, W., and Merluzzi, V. J. (1990) *Nature* **344,** 70–72
14. Gahmberg, C. G., Nortamo, P., Zimmermann, D., and Ruoslahti, E. (1991) *Eur. J. Biochem.* **195,** 177–182
15. Nortamo, P., Salcedo, R., Timonen, T., Patarroyo, M., and Gahmberg, C. G. (1991) *J. Immunol.* **146,** 2530–2535
16. Nortamo, P., Li, R., Renkonen, R., Timonen, T., Prieto, J., Patarroyo, M., and Gahmberg, C. G. (1991) *Eur. J. Immunol.* **21,** 2629–2632
17. de Fougerolles, A. D., Stacker, S. A., Schwarting, R., and Springer, T. A. (1991) *J. Exp. Med.* **174,** 253–267
18. Renkonen, R., Paavonen, T., Nortamo, P., and Gahmberg, C. G. (1992) *Am. J. Pathol.* **140,** 763–767
19. Damle, N. K., Klussman, K., and Aruffo, A. (1992) *J. Immunol.* **148,** 665–671
20. Ruoslahti, E., and Pierschbacher, M. D. (1987) *Science* **238,** 491–497
21. Yamada, K. M. (1991) *J. Biol. Chem.* **266,** 12809–12812
22. Staunton, D. E., Dustin, M. L., Erickson, H. P., and Springer, T. A. (1990) *Cell* **61,** 243–254
23. Berendt, A. R., McDowall, A., Craig, A. G., Bates, P. A., Sternberg, M. J. E., Marsh, K., Newbold, C. I., and Hogg, N. (1992) *Cell* **68,** 71–81
24. Horley, K. J., Carpenito, C., Baker, B., and Takei, F. (1989) *EMBO J.* **8,** 2889–2896
25. Edgell, C.-J. S., McDonald, C. C., and Graham, J. B. (1983) *Proc. Natl. Acad. Sci. U. S. A.* **80,** 3734–3737
26. Nortamo, P., Patarroyo, M., Kantor, C., Suopanki, J., and Gahmberg, C. G. (1988) *Scand. J. Immunol.* **28,** 537–546
27. Clark, E. A., Ledbetter, J. A., Holly, R. C., Dinndorf, P. A., and Shu, G. (1986) *Hum. Immunol.* **16,** 100–113
28. Sánchez-Madrid, F., Krensky, A. M., Ware, C. F., Robbins, E., Strominger, J. L., Burakoff, S. F., and Springer, T. A. (1982) *Proc. Natl. Acad. Sci. U. S. A.* **79,** 7489–7493
29. Borche, L., Lozano, F., Vilella, R., and Vives, J. (1987) *Eur. J. Immunol.* **17,** 1523–1526
30. Dustin, M. L., and Springer, T. A. (1989) *Nature* **341,** 619–624
31. Laemmli, U. K. (1970) *Nature* **227,** 680–685

Carl_G_190x270_mm_blokki_FINAL.indd 270 06-Aug-23 1:53:51 PM

32. Greenwood, F. C., Hunter, W. M., and Gloves, J. S. (1963) *Biochem. J.* **89,** 114–123
33. Wang, J., Yan, Y., Garrett, T. P. J., Liu, J., Rodgers, D. W., Garlick, R. L., Tarr, G. E., Husain, Y., Reinherz, E. L., and Harrison, S. C. (1990) *Nature* **348,** 411–418
34. Ryu, S.-E., Kwong, P. D., Trunch, A., Porter, T. G., Arthos, J., Rosenberg, M., Dai, X., Xuong, N. H., Axel, R., Sweet, R. W., and Hendrickson, W. A. (1990) *Nature* **348,** 419–425
35. Leahy, D. J., Axel, R., and Hendrickson, W. A. (1992) *Cell* **68,** 1145–1162
36. Abola, E. E., Bernstein, F. C., Bryant, S. H., Koetzle, T. F., and Weng, J. (1987) in *Crystallographic Databases: Information Content, Software Systems, Scientific Applications* (Allen, F. H., Bergerhoff, G., and Sievers, R., eds) pp. 107–132, Data Commission of the International Union of Crystallography, Bonn
37. Jones, E. Y., Davis, S. J., Williams, A. F., Harlos, K., and Stuart, D. I. (1992) *Nature* **360,** 232–239
38. Giranda, V. L., Chapman, M. S., and Rossmann, M. G. (1990) *Proteins Struct. Funct. Genet.* **7,** 227–233
39. Diamond, M. S., Staunton, D. E., Marlin, S. D., and Springer, T. A. (1991) *Cell* **65,** 961–971
40. Seth, R., Salcedo, R., Patarroyo, M., and Makgoba, M. W. (1991) *FEBS Lett.* **282,** 193–196
41. Fecondo, J. V., Kent, S. B. H., and Boyd, A. W. (1991) *Proc. Natl. Acad. Sci. U. S. A.* **88,** 2879–2882
42. Ross, L., Hassman, F., and Molony, L. (1992) *J. Biol. Chem.* **267,** 8537–8543
43. D'Souza, S. E., Ginsberg, M. H., Burke, T. A., and Plow, E. F. (1990) *J. Biol. Chem.* **265,** 3440–3446
44. D'Souza, S. E., Ginsberg, M. H., Matsueda, G. R., and Plow, E. F. (1991) *Nature* **350,** 66–68

Carl_G_190x270_mm_blokki_FINAL.indd 271 06-Aug-23 1:53:51 PM

Communication

THE JOURNAL OF BIOLOGICAL CHEMISTRY
Vol. 268, No. 29, Issue of October 15, pp. 21474–21477, 1993
© 1993 by The American Society for Biochemistry and Molecular Biology, Inc.
Printed in U.S.A.

A Leukocyte Integrin Binding Peptide from Intercellular Adhesion Molecule-2 Stimulates T Cell Adhesion and Natural Killer Cell Activity*

(Received for publication, July 20, 1993)

Rui Li‡, Pekka Nortamo‡, Carmela Kantor‡, Panu Kovanen§, Tuomo Timonen§, and Carl G. Gahmberg‡¶

From the Departments of ‡Biochemistry and §Pathology, University of Helsinki, 00014 Helsinki, Finland

Adhesion is of pivotal importance for a number of leukocyte functions. Little is known about the binding between leukocyte integrins and the intercellular adhesion molecules (ICAMs). Normally integrins are nonadhesive, and require a stimulus to become active. We have now identified a peptide from ICAM-2, which binds to leukocyte integrins and activates adhesion. Furthermore, the peptide strongly increased the binding and cytotoxicity of natural killer cells. These findings show that adhesion-dependent leukocyte functions can be activated by ligand-derived peptides, and therefore provide evidence that the avidity of leukocyte integrins is up-regulated by integrin-ligand interactions.

Many leukocyte functions depend on the ability of the cells to specifically adhere to other leukocytes or to various target cells. The binding involves several adhesion molecules, among the most important of which are the heterodimeric leukocyte integrins, consisting of three specific α-chains (CD11a,[1] CD11b, and CD11c) and a common β_2-chain (CD18) (1–3). The biological significance of the leukocyte integrins is exemplified by the leukocyte adhesion deficiency syndrome, in which mutations in CD18 give rise to diminished leukocyte binding, resulting in immunological disorders and repeated infections (4, 5).

The predominant lymphocyte integrin CD11a/CD18 binds to the intercellular adhesion molecules ICAM-1 (CD54) (6, 7), ICAM-2 (8, 9) and ICAM-3 (10–12), all of which are members of the immunoglobulin superfamily (13). ICAM-1 has been studied extensively, and mutational analysis indicates that the site recognized by CD11a/CD18 is located in the first immunoglobulin domain (14, 15).

The leukocyte integrins need to be activated in order to become adhesive. Despite of extensive studies, the mechanism(s) of activation is not understood. Early work showed that phorbol esters can induce the adhesive phenotype, without an increase in the amount of surface located integrins (16, 17). This suggested that signaling receptors, circumvented by phorbol esters through direct activation of protein kinase C, may somehow induce a change in the integrins. This interpretation was substantiated by the finding that ligation of the T cell receptor induces an increased adhesion through CD11a/CD18 (18).

In addition to the cross-talk of a signaling receptor and integrins, the adhesive state of CD11a/CD18 has also been induced by certain monoclonal anti-CD11a antibodies, suggesting that integrin activation may also occur through direct ligand binding from the outside of the cell (19, 20). However, there exists no direct evidence in support of the activating role of ligands in adhesion, although ICAM-1 and ICAM-2 have been shown to be co-stimulatory in T cell proliferation (21, 22).

We have studied ICAM-2 extensively as a relatively simple model ligand of CD11a/CD18, and we recently identified a 22-residue peptide from the first immunoglobulin domain of ICAM-2, which spans the B and C β-strands and specifically binds to purified CD11a/CD18 (23). It also inhibits the binding of endothelial cells to CD11a/CD18-coated plastic. We now report that the same peptide, when added to leukocyte cultures, is able to strongly activate leukocyte adhesion. The increased adhesion was also reflected in a remarkably augmented natural killer activity against leukemic target cells.

EXPERIMENTAL PROCEDURES

Isolation of Cells—Human T cells were isolated from buffy coats using the Ficoll-Paque (Pharmacia, Uppsala, Sweden) technique and employing a nylon wool column. The purity was >90%. After overnight culture in RPMI 1640 culture medium (Life Technologies, Inc.) containing 10% fetal calf serum (Flow Laboratories), the cells were washed and resuspended in binding medium (RPMI 1640, 40 mM HEPES, 2 mM $MgCl_2$, 5% fetal calf serum). Natural killer cells were purified from Ficoll-Isopaque-centrifuged and nylon wool-filtered peripheral blood lymphocytes by centrifugation on discontinuous Percoll density gradients (24). T lymphocytes were depleted with paramagnetic beads (Dynal, Oslo, Norway) from the low density fractions using OKT3 monoclonal antibodies (Ortho Pharmaceuticals, Raritan, NJ).

Peptide Synthesis—Peptides were prepared by solid phase synthesis on an Applied Biosystems model 430A peptide synthesizer, using *t*-butoxycarbonyl chemistry. The structures were confirmed by amino acid analysis and plasma desorption mass spectrometry (23).

Antibodies—The monoclonal antibodies used were 7E4 (CD18) (25), TS1/22 (CD11a) (26), 60.1 (CD11b) (27), B-H19 (ICAM-1),[2] 6D5 (ICAM-2) (8), IOP49d (VLA-4α) (Immunotech S.A., France), and mouse IgG (negative control) (Dakopatts A/S, Glostrup, Denmark).

Chemicals—4β-Phorbol 12,13-dibutyrate (PDBu), cytochalasin B, staurosporine, and okadaic acid used were from Sigma; dibutyryl cAMP was from Boehringer GmbH (Mannheim, Germany).

T Cell Aggregation Assay—T cells (2×10^5) in 100 μl of binding medium/well of microtiter plates (Dynatech Laboratories, Alexandria, VA) were incubated with PDBu and peptides P1 and P8 at 37 °C. The free cells of four randomly chosen areas/well were counted. Percent aggregation was calculated by the following equation: percent aggregation = 100 × (1 − (no. of free cells)/(total no. of cells)). For inhibition of P1-induced T cell aggregation, T cells were preincubated with different monoclonal antibodies or different kinds of inhibitors for 10 min at room temperature before treated with peptide P1.

* These studies were supported by the Academy of Finland, the Finnish Cancer Society, the Sigrid Jusélius Foundation, and the Magnus Ehrnrooth Foundation. The costs of publication of this article were defrayed in part by the payment of page charges. This article must therefore be hereby marked "*advertisement*" in accordance with 18 U.S.C. Section 1734 solely to indicate this fact.

¶ To whom correspondence should be addressed: Dept. of Biochemistry, P. O. Box 5 (Unioninkatu 35), University of Helsinki, 00014 Helsinki, Finland. Tel.: 358-0-1917773; Fax: 358-0-1917769.

[1] The abbreviations used are: CD, cluster of differentiation antigen; CD11/CD18, leukocyte integrins; CD11a/CD18, LFA-1; CD11b/CD18, Mac-1; CD11c/CD18, p150/95; ICAM, intercellular adhesion molecule; NK, natural killer; PDBu, 4β-phorbol 12,13-dibutyrate.

[2] R. Li, P. Nortamo, C. Kantor, P. Kovanen, T. Timonen, and C. G. Gahmberg, unpublished data.

This is an Open Access article under the CC BY license.

Carl_G_190x270_mm_blokki_FINAL.indd 272 06-Aug-23 1:53:51 PM

Natural Killer Cell Binding and Cytotoxicity—NK cells were preincubated with 100 μg/ml peptides in RPMI 1640 medium complemented with 0.5% bovine serum albumin (Finnish Red Cross Blood Transfusion Service) in standard cell culture conditions for various periods before being tested for cytotoxicity against K562 target cells in a 4-h ^{51}Cr assay at a 10:1 effector target cell ratio. The binding capacity to target cells was tested at a 1:2 ratio after centrifugation for 8 min at 120 × *g*. The binding is expressed as percentage of binding cells from the total amount of lymphocytes. At least 300 cells were counted in each combination.

RESULTS AND DISCUSSION

Several ICAM-2 peptides were initially synthesized and tested for the ability to bind to purified CD11a/CD18 (23). Only the P1 peptide (see Table I for sequence) showed strong and specific binding (23). When this peptide was added to a suspension of blood T cells, aggregation of lymphocytes occurred by 30 min and continued to increase, and the cells remained in clusters (Fig. 1*A*). 8.4 μM P1 induced a substantial aggregation (Fig. 1*B*). The control peptide (P8), with the same composition as P1, but with the rest of the amino acids in random order except for the 2 cysteines, showed no activity (Fig. 1, *A*, *B*, and *Dd*; Table I). The aggregation of T cells was largely CD11a/CD18-ICAM-1-dependent, as shown by using antibodies to CD18, CD11a, and ICAM-1 (Fig. 1*C*). We have also found that T cells after activation with P1, followed by washing, showed an increased binding to purified recombinant ICAM-1 coated on plastic, and this binding was completely inhibited by CD18 antibody (results not shown). In fact, the inhibition by antibodies was more efficient than is evident from Fig. 1*C*, because the remaining aggregates were small and loose (Fig. 1*Dc*). The inability to completely block aggregation by the antibodies could be due to the fact that additional, presently unknown, adhesion molecules are also activated by P1. Shortening of P1 by removal of the NH_2-terminal glycine resulted in an inactive peptide, and the removal of amino acids from the COOH-end diminished the activity (Table I). The P7 peptide, made from the homologous region of ICAM-1, showed no activity. In addition, it does not efficiently bind to CD11a/CD18 (23).

An important issue is whether the adhesion of T cells induced by P1 is due to integrin activation or merely a bridging effect. It is known that CD11/CD18-dependent adhesion does not take place at 4 °C and requires energy, an intact cytoskeleton, and divalent cations (1–3, 18). Fig. 2 shows indeed that no P1-induced aggregation took place at low temperature and that it was blocked by sodium azide and deoxyglucose, partially by EDTA, as well as by cytochalasin B. Interestingly, dibutyryl cAMP also significantly inhibited the P1-induced aggregation.

Staurosporine, an inhibitor of protein kinase C, blocked the phorbol ester-induced T cell aggregation (Fig. 3*A*), but not that induced by the P1 peptide. In contrast, the phosphatase inhibitor okadaic acid blocked both P1- and phorbol ester-induced aggregations (Fig. 3*B*), similar to that reported for B cells (28).

The binding of NK cells to K562 leukemic cells was remarkably increased by the pretreatment of effector cells with P1 (Fig. 4*A*), and this resulted in enhanced cytotoxicity, detectable after 2 h of preincubation (Fig. 4*B*).

TABLE I
Aggregation of T cells induced by different ICAM peptides

T cells were incubated with 42 μM peptides. Aggregation was scored after a 2-h incubation at 37 °C.

Peptide	Sequence	Aggregation ± S.D.
		%
P1 (ICAM-2)	GSLEVNCSTTCNQPEVGGLETS	71 ± 3
P2 (ICAM-2)	SL----------LETS	2 ± 2
P5 (ICAM-2)	GSL----------LE	45 ± 4
P6 (ICAM-2)	GSL----------L	20 ± 6
P7 (ICAM-1)	GSVLVTCSTSCDQPKLLGIETP	0
P8 (control)	EVGTGSCNLECVSTNPLSGTEQ	0

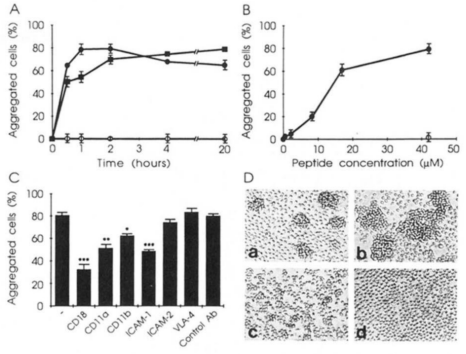

FIG. 1. **T cell adhesion induced by phorbol ester and the ICAM-2 peptide P1.** 2 × 10^5 T cells/100 μl/well were incubated with 42 μM peptide P1 (●), control peptide P8 (○), or 60 nM PDBu (■) for indicated time periods at 37 °C (*A*) or with different amounts of P1 (*B*), or pretreated with 10 μg of monoclonal antibodies to: CD18 (7E4), CD11a (TS 1/22), CD11b (4 μg of 60.1), ICAM-1 (B-H19), ICAM-2 (6D5), VLA-4α (IOP49d), and mouse control IgG before adding 42 μM P1 (*C*). *Da*, microscopic field of cells treated with PDBu (original magnification, × 200); *Db*, cells treated with P1; *Dc*, cells treated with P1 and antibody to CD18; *Dd*, cells treated with P8. After a 2-h incubation, the aggregations in *panels B* and *C* were evaluated and the pictures in *D* taken. The standard deviations are given. *, $p < 0.05$; **, $p < 0.01$; ***, $p < 0.001$.

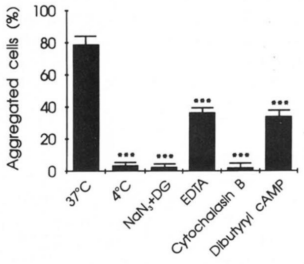

FIG. 2. **Inhibition of P1-induced T cell aggregation.** T cells were kept at 4 °C or pretreated with 0.2% NaN_3 and 50 mM 2-deoxyglucose (*DG*), 5 mM EDTA, 20 μM cytochalasin B, or 2 mM dibutyryl cAMP before the addition of 42 μM P1. Aggregations were determined after a 2-h incubation at 37 °C, with the exception of the experiment marked 4 °C. Sodium butyrate (2 mM) had no effect on the aggregation (not shown).

Our results support the hypothesis that the activation of cellular adhesion induced by P1 involves intracellular signaling mechanisms. It is different from that induced by phorbol esters in being protein kinase C-independent. The inhibition of P1-induced aggregation by okadaic acid indicates, however, that phosphorylation is somehow involved, and the fact that cAMP partially blocked the aggregation indicates a role for protein kinase A. This is similar to the finding of Dustin and Springer (18), who showed that triggering of the T cell receptor resulted in CD11a/CD18-ICAM-1-dependent adhesion, which was partially inhibited by treatment with cAMP.

Several groups have shown that the α-chains of CD11/CD18 are constitutively phosphorylated; upon activation by phorbol esters, the β-chain becomes phosphorylated (29–31). However, mutational analysis of CD18 has shown that the predominant phosphorylation site at Ser-756 is not needed for adhesion (32).

Carl_G_190x270_mm_blokki_FINAL.indd 273 06-Aug-23 1:53:51 PM

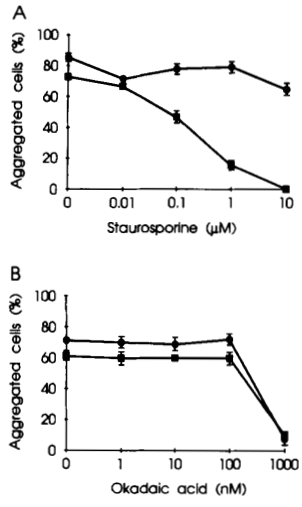

FIG. 3. **Effects of staurosporine and okadaic acid on P1 and phorbol ester-induced T cell aggregation.** 2×10^5 of T cells were pretreated in 100 μl of binding medium with indicated amounts of staurosporine (*A*) or okadaic acid (*B*) before adding 42 μM P1 (●) or 60 nM PDBu (■). Aggregation was evaluated after a 2-h incubation at 37 °C.

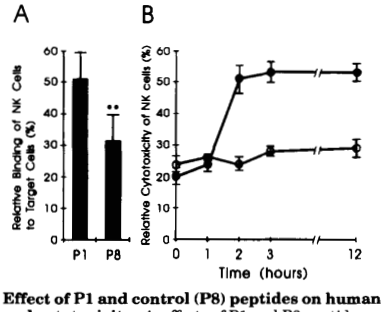

FIG. 4. **Effect of P1 and control (P8) peptides on human NK cell binding and cytotoxicity.**. *A*, effects of P1 and P8 peptides on NK cell binding to K562 target cells. Purified NK cells were pretreated for 12 h with 42 μM peptides and subsequently tested for binding capacity to K562 cells. Mean ± standard deviation from three experiments is shown. *B*, kinetics of NK activation by peptides. Enriched NK cells were preincubated with 42 μM P1 (●) and P8 (○) peptide before being tested for cytotoxicity against K562 cells. Mean ± S.D. of three separate experiments is shown.

It is therefore possible that either minor phosphorylation sites of CD18 or dephosphorylation of a separate integrin activating factor are important (28, 33). No change in the phosphorylation of CD11/CD18 by P1 was observed (results not shown).

The increase in the adhesion induced by P1 bears some resemblance to the activation of the platelet integrin gpIIb/IIIa by arginine-glycine-aspartic acid-containing peptides, resulting in an increased binding of platelets to fibrinogen (34–37).

NK activity is highly dependent on the CD11/CD18-ICAM pathway, as shown by the inhibition of cell binding, cytotoxicity, and migration by antibodies against these polypeptides (38–40). However, mere clustering of NK cells with their targets does not lead to increased cytotoxicity (24). Therefore, our results suggest that P1 directly activates NK cells. There are two possible, not mutually exclusive explanations for the activation. First, leukocyte integrins and putative NK cell triggering receptors could exert cross-talk in NK activity by adhesion through integrins, which would increase recognition through NK cell receptors and vice versa. This would be analogous to T cell activation (18). Second, the integrin itself may be a triggering NK cell receptor.

The activating effect of P1 is not restricted to T cells and NK cells, since the homotypic adhesion of Burkitt lymphoma and Epstein-Barr virus-transformed lymphoblastoid cell lines was activated by P1 mainly in a CD11/CD18-dependent manner. This also occurred when the peptide was covalently coupled to plastic, supporting the interpretation that the increased cell aggregation caused by the peptide is due to an effect on the cell surface (data not shown). P1 inhibits endothelial cell binding to purified CD11a/CD18, evidently by competitive inhibition (23). Presently, we do not know why the binding of lymphoblastoid B cells to endothelial cells and to ICAM-2-transfected COS-cells is inhibited (23).

To conclude, our results show that leukocyte integrin mediated adhesion can be up-regulated by a peptide derived from the integrin ligand ICAM-2 and that this results in increased leukocyte aggregation and greatly enhanced NK cell activity. The possibility of being able to increase the activity of NK cells has important implications in treatment of malignant disease.

Acknowledgments—We thank Yvonne Heinilä for expert secretarial assistance and Ella Jääskeläinen and Leena Kuoppasalmi for technical assistance.

REFERENCES

1. Springer, T. A. (1990) *Nature* **346,** 425–434
2. Arnaout, M. A. (1990) *Blood* **75,** 1037–1050
3. Patarroyo, M., Prieto, J., Rincon, J., Timonen, T., Lundberg, C., Lindbom, L., Åsjö, B., and Gahmberg, C. G. (1990) *Immunol. Rev.* **114,** 67–108
4. Arnaout, M. A. (1990) *Immunol. Rev.* **114,** 145–180
5. Anderson, D. C., and Springer, T. A. (1987) *Annu. Rev. Med.* **38,** 175–194
6. Rothlein, R., Dustin, M. L., Marlin, S. D., and Springer, T. A. (1986) *J. Immunol.* **137,** 1270–1274
7. Patarroyo, M., Clark, E. A., Prieto, J., Kantor, C., and Gahmberg, C. G. (1987) *FEBS Lett.* **210,** 127–131
8. Nortamo, P., Salcedo, R., Timonen, T., Patarroyo, M., and Gahmberg, C. G. (1991) *J. Immunol.* **146,** 2530–2535
9. de Fougerolles, A. D., Stacker, S. A., Schwarting, R., and Springer, T. A. (1991) *J. Exp. Med.* **174,** 253–267
10. de Fougerolles, A. R., and Springer, T. A. (1992) *J. Exp. Med.* **175,** 185–190
11. Vazeux, R., Hoffman, P. A., Tomita, J. K., Dickinson, E. S., Jasman, R. L., St. John, T., and Gallatin, W. M. (1992) *Nature* **360,** 485–488
12. Fawcett, J., Holness, C. L. L., Needham, L. A., Turley, H., Gatter, K. C., Mason, D. Y., and Simmons, D. L. (1992) *Nature* **360,** 481–484
13. Williams, A. F., and Barclay, A. N. (1988) *Annu. Rev. Immunol.* **6,** 381–405
14. Staunton, D. E., Dustin, M. L., Erickson, H. P., and Springer, T. A. (1990) *Cell* **61,** 243–254
15. Berendt, A. R., McDowall, A., Craig, A. G., Bates, P. A., Sternberg, M. J. E., Marsh, K., Newbold, C. I., and Hogg, N. (1992) *Cell* **68,** 71–81
16. Patarroyo, M., Beatty, P. G., Fabre, J. W., and Gahmberg, C. G. (1985) *Scand. J. Immunol.* **22,** 171–182
17. Rothlein, R., and Springer, T. A. (1986) *J. Exp. Med.* **163,** 1132–1149
18. Dustin, M. L., and Springer, T. A. (1989) *Nature* **341,** 619–624
19. Koopman, G., de Graaff, M., Huysmans, A. C. L. M., Meijer, C. J. L. M., and Pals, S. T. (1992) *Eur. J. Immunol.* **22,** 1851–1856
20. Landis, R. C., Bennett, R. I., and Hogg, N. (1993) *J. Cell Biol.* **120,** 1519–1527
21. van Seventer, G. A., Shimizu, Y., Horgan, K. J., and Shaw, S. (1990) *J. Immunol.* **144,** 4579–4586
22. Damle, N. K., Klussman, K., and Aruffo, A. (1992) *J. Immunol.* **148,** 665–671
23. Li, R., Nortamo, P., Valmu, L., Tolvanen, M., Huuskonen, J., Kantor, C., and Gahmberg, C. G. (1993) *J. Biol. Chem.* **268,** 17513–17518
24. Timonen, T., Ortaldo, J. R., and Herberman, R. B. (1981) *J. Exp. Med.* **153,** 569–582
25. Nortamo, P., Patarroyo, M., Kontor, C., Suopanki, J., and Gahmberg, C. G. (1988) *Scand. J. Immunol.* **28,** 537–546
26. Sanchez-Madrid, F., Krensky, A. M., Ware, C. F., Robbins, E., Strominger, J. L., Burakoff, S. J., and Springer, T. A. (1982) *Proc. Natl. Acad. Sci. U. S. A.* **79,** 7489–7493
27. Wallis, W. J., Hickstein, D. D., Schwartz, B. R., June, C. H., Ochs, H. D., Beatty, P. G., Klebanoff, S. J., and Harlan, J. M. (1986) *Blood* **67,** 1007–1013
28. Hedman, H., and Lundgren, E. (1992) *J. Immunol.* **149,** 2295–2299
29. Chatila, T. A., Geha, R. S., and Arnaout, M. A. (1989) *J. Cell Biol.* **109,** 3435–3444

Carl_G_190x270_mm_blokki_FINAL.indd 274 06-Aug-23 1:53:51 PM

30. Buyon, J. P., Slade, S. G., Reibman, J., Abramson, S. B., Philips, M. R., Weissmann, G., and Winchester, R. (1990) *J. Immunol.* **144,** 191–197
31. Valmu, L., Autero, M., Siljander, P., Patarroyo, M., and Gahmberg, C. G. (1991) *Eur. J. Immunol.* **21,** 2857–2862
32. Hibbs, M. L., Jakes, S., Stacker, S. A., Wallace, R. W., and Springer, T. A. (1991) *J. Exp. Med.* **174,** 1227–1238
33. Hermanowski-Vosatka, A., Van Strijp, J. A. G., Swiggard, W. J., and Wright, S. D. (1992) *Cell* **68,** 341–352
34. Ruoslahti, E., and Pierschbacher, M. D. (1986) *Cell* **44,** 517–518
35. Ruoslahti, E., and Pierschbacher, M. D. (1987) *Science* **238,** 491–497
36. Ginsberg, M., Pierschbacher, M. D., Ruoslahti, E., Marguerie, G., and Plow, E. (1985) *J. Biol. Chem.* **260,** 3931–3936
37. Du, X., Plow, E. F., Frelinger, A., III, O'Toole, T., Loftus, J. C., and Ginsberg, M. H. (1991) *Cell* **65,** 409–416
38. Timonen, T., Patarroyo, M., and Gahmberg, C. G. (1988) *J. Immunol.* **141,** 1041–1046
39. Timonen, T., Gahmberg, C. G., and Patarroyo, M. (1990) *Int. J. Cancer* **46,** 1035–1040
40. Jääskeläinen, J., Mäenpää, A., Patarroyo, M., Gahmberg, C. G., Somersalo, K., Tarkkanen, J., Kallio, M., and Timonen, T. (1992) *J. Immunol.* **149,** 260–268

Carl_G_190x270_mm_blokki_FINAL.indd 275 06-Aug-23 1:53:51 PM

A Peptide Derived from the Intercellular Adhesion Molecule-2 Regulates the Avidity of the Leukocyte Integrins CD11b/CD18 and CD11c/CD18

Rui Li,* Jinglin Xie,* Carmela Kantor,* Vesa Koistinen,‡ Dario C. Altieri,§ Pekka Nortamo,* and Carl G. Gahmberg*

*Department of Biochemistry, 00014 University of Helsinki, Helsinki, Finland; ‡Finnish Red Cross Blood Transfusion Service, Helsinki, Finland; §Department of Immunology, The Scripps Research Institute, La Jolla, California 92037

Abstract. β_2 integrin (CD11a,b,c/CD18)-mediated cell adhesion is required for many leukocyte functions. Under normal circumstances, the integrins are nonadhesive, and become adhesive for their cell surface ligands, the intercellular adhesion molecules (ICAMs), or soluble ligands such as fibrinogen and iC3b, when leukocytes are activated. Recently, we defined a peptide derived from ICAM-2, which specifically binds to purified CD11a/CD18. Furthermore, this peptide strongly induces T cell aggregation mainly mediated by CD11a/CD18-ICAM-1 interaction, and natural killer cell cytotoxicity. In the present study, we show that the same ICAM-2 peptide also avidly binds to purified CD11b/CD18, but not to CD11c/CD18. This binding can be blocked by the CD11b antibody OKM10. The peptide strongly stimulates CD11b/CD18-ICAM-1–mediated cell aggregations of the monocytic cell lines THP-1 and U937. The aggregations are energy and divalent cation-dependent. The ICAM-2 peptide also induces CD11b/CD18 and CD11c/CD18-mediated binding of THP-1 cells to fibrinogen and iC3b coated on plastic. These findings indicate that in addition to induction of CD11a/CD18-mediated cell adhesion, the ICAM-2 peptide may also serve as a "trigger" for high avidity ligand binding of other β_2 integrins.

THE leukocyte-specific β_2 integrins (CD11/CD18),[1] consist of three high mol wt heterodimers with specific α chains (CD11a,b,c) and a common β chain (CD18), and play a prominent role in mediating diverse cell adhesions required for many leukocyte functions (Springer, 1990; Arnaout, 1990; Patarroyo et al., 1990).

CD11a/CD18 lymphocyte function-associated antigen-1 (LFA-1), which is mainly found on mononuclear leukocytes, probably binds to the NH_2-terminal immunoglobulin domains of the intercellular adhesion molecules (ICAM)-1 (CD54) (Rothlein et al., 1986; Patarroyo et al., 1987; Staunton et al., 1990; Berendt et al., 1992), ICAM-2 (CD102) (Staunton et al., 1989; Nortamo et al., 1991*b*; de Fougerolles et al., 1991), and ICAM-3 (CD50) (de Fougerolles et al., 1992; Vazeux et al., 1992; Fawcett et al., 1992; Juan et al., 1993), members of the immunoglobulin superfamily. CD11b/CD18 (Mac-1), which is expressed primarily on cells of the myelo-monocytic lineage, binds to ICAM-1 through the third immunoglobulin domain (Diamond et al., 1991). In addition, CD11b/CD18 also binds to several soluble ligands including the complement fragment iC3b (Beller et al., 1982; Wright et al., 1983), fibrinogen (Wright et al., 1988; Altieri et al., 1988), and factor X (Altieri and Edgington, 1988*a*), which become insolubilized during activation of the complement and clotting cascades. CD11c/CD18 (p150,95) is enriched on macrophages. The ligands for CD11c/CD18 are poorly characterized. It has been shown that CD11c/CD18 binds to iC3b (Micklem and Sim, 1985; Myones et al., 1988), and recent reports suggest that it also binds to fibrinogen (Loike et al., 1991; Postigo et al., 1991), and at least to one counter-receptor on the surface of endothelial cells (Stacker and Springer, 1991).

The leukocyte integrins need to be activated in order to become adhesive. The molecular mechanisms involved in the activation of CD11/CD18 are incompletely understood. Quantitative as well as qualitative changes occur in these receptors after cell activation. Phorbol ester treatment (Patarroyo et al., 1985; Rothlein and Springer, 1986), or cross-linking the T cell receptor on lymphocytes (Dustin and Springer, 1989) induces a high avidity state of CD11a/CD18

Please address all correspondence to Dr. Carl G. Gahmberg, Department of Biochemistry, P.O. Box 5 (Unioninkatu 35), 00014 University of Helsinki, Helsinki, Finland. Tel: 358 0 1917773. Fax: 358 0 1917769.

1. *Abbreviations used in this paper*: BSA, bovine serum albumin; CD11/CD18, leukocyte-specific β_2 integrins; CD11a/CD18 (LFA-1), lymphocyte function-association antigen-1; ICAM, intercellular adhesion molecule.

© The Rockefeller University Press, 0021-9525/95/05/1143/11 $2.00

Carl_G_190x270_mm_blokki_FINAL.indd 276 06-Aug-23 1:53:51 PM

for ICAM-1, without any substantial increase in lymphocyte surface expression of this integrin. CD11a/CD18 can also be activated by monoclonal antibodies reacting with a variety of leukocyte cell surface glycoproteins (van Kooyk et al., 1989; Koopman et al., 1990; Kansas and Tedder, 1991), evidently through "inside-out" signaling. In addition, certain monoclonal antibodies against the α chain of CD11a/CD18 has been shown to be able to induce CD11a/CD18-dependent homotypic T cell adhesion (Koopman et al., 1992; Landis et al., 1993), indicating that integrin activation could also be induced by direct ligand binding from the outside of the cells.

Unlike CD11a/CD18, the amount of cell surface CD11b/CD18 and CD11c/CD18 on granulocytes and monocytes can be rapidly upregulated by translocation of these two receptors from an intracellular pool to the cell surface in response to cell activation (Miller et al., 1987; Bainton et al., 1987). However, the change in CD11b/CD18 surface expression that occurs after stimulation does not parallel the kinetics or magnitude of cell adhesion (Buyon et al., 1988; Lo et al., 1989). Thus, CD11b/CD18 is hypothesized to undergo additional qualitative conformational changes that facilitate adhesion (Buyon et al., 1988; Lo et al., 1989; Philips et al., 1988; Vedder and Harlan, 1988). The phorbol ester and adenine nucleotide ADP-induced functional modulation of CD11b/CD18 appears to involve allosteric or qualitative remodeling of the receptor characterized by the formation of activation-dependent neoantigenic epitopes (Diamond and Springer, 1993; Altieri and Edgington, 1988*b*). Alternatively, the enhanced avidity of CD11b/CD18 could be due to a signal to cluster the receptors in the plane of the membrane (Detmers et al., 1987).

Recent work has demonstrated that ICAM-1, ICAM-2, and ICAM-3 provide important costimulatory signals via their adhesive interactions with the CD11a/CD18 complex during the CD3/TCR-mediated activation of resting T cells (van Seventer et al., 1990; Damle et al., 1992; Hernàndez-Caselles et al., 1993). Furthermore, ICAM-1 has been shown to be able to induce the high affinity state of CD11a/CD18 characterized by expression of the mAb 24 epitope (Cabanas and Hogg, 1993), which has been thought to be a "reporter" of the activated state of CD11a/CD18 (Dransfield et al., 1990). However, there is no direct evidence for inducing a high avidity state of leukocyte integrins by direct ligand binding.

ICAM-2 is the second ligand found for CD11a/CD18 (Staunton et al., 1989). The external portion of this molecule consists of two immunoglobulin domains, which have 34% identity in amino acid sequences with the two NH_2-terminal domains of ICAM-1 and ICAM-3. To identify the binding site(s) in ICAM-2 for CD11a/CD18, we recently synthesized several peptides from the first immunoglobulin domain of ICAM-2, and characterized a 22-amino acid long peptide, P1, which specifically binds to CD11a/CD18 (Li et al., 1993*b*). Furthermore, the peptide strongly stimulates blood T cell aggregation mainly mediated by CD11a/CD18-ICAM-1 interaction, and natural killer cell cytotoxicity (Li et al., 1993*a*). In the present study, we report that the ICAM-2 peptide also binds to purified CD11b/CD18, but not to CD11c/CD18. The peptide strongly induces CD11b/CD18-ICAM-1-mediated homotypic cell adhesion of monocytic cell lines, and CD11b/CD18 and CD11c/CD18-mediated binding of leukocytes to fibrinogen and iC3b.

Materials and Methods

Cell Culture

The endothelial cell line Eahy926 was cultured in DMEM (Sigma Chem. Co., St. Louis, MO) containing hypoxanthine/aminopterin/thymidine, and 10% of FCS (Flow Laboratories, Irvine, Scotland). Eahy926 cells were stimulated by incubating them with 10 ng/ml of TNF-α (Boehringer Mannheim, Mannheim, Germany) overnight (Nortamo et al., 1991*a*). The monocytic cell line THP-1 (American Type Culture Collection, Rockville, MD) (Tsuchiya et al., 1980) was maintained in continuous culture in RPMI 1640 medium (GIBCO BRL, Gaithersburg, MD) containing 10% FCS, 2 mM L-glutamine (Biological Industries, Kibbutz Bet Haemek, Israel), 10 mM Hepes, and 50 μM 2-mercaptoethanol (Fluka Chemie AG, Switzerland). The monocytic cell line U937 (Sundström and Nilsson, 1976) was cultured in RPMI 1640 supplemented with 10% FCS, 100 u/ml of penicillin, 100 μg/ml of streptomycin and 2 mM of L-glutamine.

Peptide Synthesis

Peptides were synthesized on a model 430A peptide synthesizer, using Fmoc-chemistry (Applied Biosystems, Inc., Foster City, CA). The structures were confirmed by FAB-mass spectrometric analysis (JEOL SX-102). The sequence of the ICAM-2 peptide P1 is GSLEVNCSTTCNQPEVGGLETS. The amino acids of the control peptide P8 are the same as those of P1, but in random order, except that the two conserved cysteine residues are in the right positions (Li et al., 1993*b*). After synthesis, the P1 and P8 peptides were reduced with dithiothreitol (1:1.5 by wt/wt, in 0.1 M $NaHCO_3$, pH 8.0) for 1.5 h at room temperature, and purified by high pressure liquid chromatography, using a reverse phase column (Waters C_{18}). A COOH-terminal tyrosine was added to the peptides to enable ^{125}I-labeling (Li et al., 1993*b*).

Monoclonal Antibodies

A panel of monoclonal antibodies that bind to immunochemically and functionally distinct epitopes on the leukocyte integrins CD11a,b,c/CD18 was used. The monoclonal antibody 7E4 (Nortamo et al., 1988) reacts with the common β chain of the three leukocyte integrins. Antibody TS1/22 (Sànchez-Madrid et al., 1982) recognizes an epitope on the α subunit of CD11a/CD18. Monoclonal antibodies OKM1, OKM10 (Wright et al., 1983), LM2/1 (Miller et al., 1986), and 60.1 (Wallis et al., 1986) are specific for spatially separate epitopes localized on the α chain of CD11b/CD18. Antibodies 3.9 (Myones et al., 1988) and 2E1 (from the 5th International Workshop on Human Leukocyte Differentiation Antigens) react with different epitopes on the α subunit of CD11c/CD18. Antibody LM609 recognizes an epitope on the α chain of the vitronectin receptor ($\alpha_v\beta_3$) and the recognition requires association of the α and β subunits (Cheresh and Spiro, 1987). The ICAM antibodies were LB-2 (ICAM-1) (Clark et al., 1986), B-T1 (ICAM-2) (Diaclone, Besancon Cedex, France) and CG106 (ICAM-3) (Cordell et al., 1994). A mouse IgG1 negative control was from Dakopatts A/S, Denmark.

Chemicals

ADP, 2-deoxy-D-glucose (DG) and cytochalasin B used were from Sigma Chem. Co., dibutyryl cAMP from Boehringer GmbH.

Purification of the Complement Fragment iC3b

The complement protein C3 was isolated from human plasma as described (Koistinen et al., 1989), dissolved in 0.01 M Na-5,5'-diethylbarbiturate, 0.15 M NaCl, 0.02% NaN_3, pH 7.3, and converted to C3b by incubating with 0.5% (wt/wt) trypsin (Sigma) for 5 min at room temperature, followed by addition of 1.5% (wt/wt) soybean trypsin inhibitor. C3b was converted to iC3b by incubating with 0.15 mg/ml factor H and 0.012 mg/ml factor I for 1 h at 37°C. iC3b was isolated from the mixture on a Mono Q column by eluting with a 0.05–0.4 M NaCl gradient in 0.01 M phosphate, 5 mM EDTA, pH 7.5.

Binding of ^{125}I-labeled P1 Peptide to Purified CD11b/CD18 and CD11c/CD18

CD11b/CD18 and CD11c/CD18 were purified from human buffy coat cell

Carl_G_190x270_mm_blokki_FINAL.indd 277 06-Aug-23 1:53:51 PM

lysates by affinity chromatography on monoclonal antibody LM2/1-Sepharose CL 4B and 3.9-Sepharose CL 4B, respectively, and eluted at pH 11.5 in the presence of 2 mM $MgCl_2$ and 1% *n*-octyl glucoside (Dustin and Springer, 1989). The purity of the proteins were checked by polyacrylamide gel electrophoresis (PAGE) in the presence of SDS (Laemmli, 1970). The heterodimeric forms of the purified integrins were examined by running the preparations once again through the same affinity columns and checking the eluates by SDS-PAGE. The proteins were diluted 1:10 with 25 mM Tris, pH 8.0, 150 mM NaCl and 2 mM $MgCl_2$, and attached to flat-bottomed, 96-well microtiter plates (Dynatech Laboratories, VA) by overnight incubation at 4°C. The wells were blocked with 1% BSA for 1 h at room temperature. 12 pmol of ^{125}I-labeled Pl, labeled by using the chloramine-T method (Greenwood et al., 1963), was added to each well in 40 μl of 0.15 M NaCl, 0.01 M sodium phosphate, pH 7.4 (PBS), containing 2 mM $MgCl_2$, 0.5% BSA and 0.02% NaN_3 with or without nonradioactive peptides, monoclonal antibodies, or some soluble ligands for CD11b/CD18, and incubated for 1 h at 37°C. After washing the wells for three times with the binding buffer, the attached ^{125}I-labeled Pl was solubilized with 1% SDS and counted. Saturation binding of peptide Pl to purified CD11b/CD18 was analyzed in dose response experiments in which increasing amounts of nonradioactive Pl were incubated in CD11b/CD18-coated wells together with 12 pmol of ^{125}I-labeled Pl. Nonspecific binding was defined as the amount of ^{125}I-Pl bound to CD11b/CD18 in the presence of a 100-fold excess of unlabeled Pl, and was substracted from the total to calculate specific binding.

Binding of Endothelial Cells to Purified CD11c/CD18

Purified CD11c/CD18 was diluted 1:10 and coated on flat-bottomed, 96-well microtiter plates, and the plates were saturated with 1% BSA as described above. The control plates were treated with BSA only. TNF-α-stimulated Eahy926 cells were removed from the tissue culture flasks with 5 mM EDTA in PBS, washed, and resuspended in DMEM, 40 mM Hepes, pH 7.2, 2 mM $MgCl_2$ and 5% FCS. Cells (5×10^4) in 50 μl were added to each well in the absence or presence of 50 μg/ml of mAb 3.9 or control antibody MIgG, and incubated for 1 h at 37°C. Unbound cells were removed by gentle washing. The binding was quantitated by counting bound cells using 200× magnification of four randomly chosen fields from each well.

Aggregation Assays

Cells were washed with RPMI 1640 medium containing 40 mM Hepes, 2 mM $MgCl_2$ and 2 mM $CaCl_2$ and resuspended to a concentration of 10^6 cells/ml. Aliquots of 100 μl were added to each well of flat-bottomed, 96-well microtiter plates in the absence or presence of peptides, and incubated at 37°C for appropriate time periods. For inhibition of the ICAM-2 peptide Pl-induced cell aggregation, cells were preincubated with different monoclonal antibodies or inhibitors for 15 min at room temperature before being treated with the peptide. For quantitative measurement of cell aggregation, the free cells of four randomly chosen areas (2.5 mm^2) per well were counted. The amount of aggregated cells was expressed as: percent aggregation = 100 × [1-(number of free cells)/(total number of cells)].

Flow Cytometry Studies

THP-1 and U937 cells were washed and resuspended in PBS, and treated with preimmune rabbit immunoglobulin to block the Fc receptors on the cells. Aliquots of 100 μl of cell suspensions (10^6 cells) were incubated with 25 μg/ml of different mAbs for 30 min at 0°C. The cells were washed and incubated with FITC-conjugated rabbit-anti-mouse $F(ab')_2$ (Dako, Copenhagen, Denmark) for 30 min on ice. After washing, the cells were fixed with 1% paraformaldehyde in PBS, and 5×10^3 cells were analyzed immediately with a Becton-Dickinson (Immunocytometry System, San Jose, CA) FACScan flow cytometer.

Binding of THP-1 Cells to Fibrinogen or iC3b Coated on Plastic

96-well microtiter plates were coated with purified fibrinogen (30 μg/ml in PBS), iC3b (2 μg/ml in PBS), or C3b (2 μg/ml in PBS) for 16 h at 4°C. At the end of incubation, the wells were blocked with 1% BSA in PBS for 2 h at room temperature. 100-μl aliquots of ADP or ICAM-2 peptide-stimulated THP-1 cells at 2×10^6/ml in RPMI 1640 medium supplemented with 40 mM Hepes, 2 mM $MgCl_2$, 2 mM $CaCl_2$ were added to each well, and incubated for 30 min at room temperature. For blocking experiments, the peptide-stimulated cells were pretreated with different mAbs for 10 min at 22°C before being added to fibrinogen, iC3b-, or C3b-coated wells. Nonadherent cells were removed by three washes with the binding medium. The binding was quantitated by scoring the number of attached cells with 200× magnification of four randomly chosen fields from each well.

Results

Binding of ICAM-2 Peptide to CD11b/CD18

The purified CD11b/CD18 and CD11c/CD18 preparations were checked by polyacrylamide gel electrophoresis in the presence of SDS. The preparations contained the expected CD11b, CD11c, and CD18 polypeptides, and no major impurities were observed (Fig. 1 *A*, *a* and *b*). Most of the purified integrins was in functional intact heterodimeric forms as examined by running the preparations through the affinity columns once again, and checking the eluates by SDS-PAGE (Fig. 1 *A*, *c* and *d*). The ^{125}I-labeled ICAM-2 peptide Pl bound to purified CD11b/CD18 coated on plastic, while little binding was observed to the purified CD11c/CD18 or BSA. The binding of ^{125}I-labeled Pl to CD11b/CD18 was specifically and almost totally inhibited by unlabeled Pl (Fig. 2 *A*). The control peptide P8 had no effect. The purified CD11c/CD18 was in active form as shown by the fact that Eahy926 cells bound to CD11c/CD18 coated on plastic, and the binding was blocked by the CD11c antibody 3.9 (Fig. 2 *B*). The binding of ^{125}I-labeled Pl to CD11b/CD18 was saturable (Fig. 3 *A*), and efficiently blocked by the anti-CD11b mAb

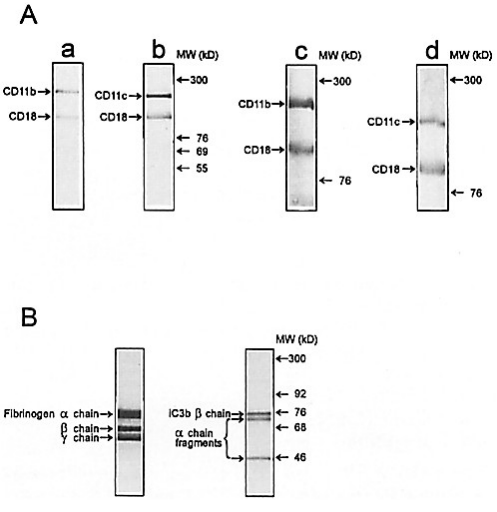

Figure 1. Polyacrylamide gels of purified CD11b/CD18, CD11c/CD18, fibrinogen, and iC3b. Purified CD11b/CD18 (*A a*) and CD11c/CD18 (*A b*) were run on 8% poyacrylamide gels in the presence of SDS and stained with Coomassie blue. The heterodimeric forms of CD11b/CD18 (*A c*) and CD11c/CD18 (*A d*) were checked on 6% polyacrylamide gels. The positions of the molecular weight markers are indicated to the right. *B* shows the purified fibrinogen and iC3b preparations.

Carl_G_190x270_mm_blokki_FINAL.indd 278 06-Aug-23 1:53:51 PM

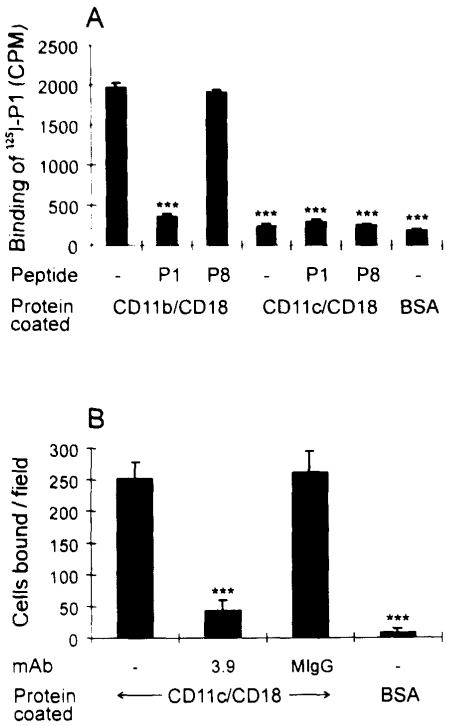

Figure 2. Binding of ^{125}I-labeled P1 peptide to purified CD11b/CD18 and CD11c/CD18, and binding of Eahy926 cells to CD11c/CD18. 12 pmol of ^{125}I-labeled P1 was incubated in CD11b/CD18 or CD11c/CD18-coated wells in the absence or presence of 100 μM of nonradioactive P1 or P8 peptides (*A*). 50 μg/ml of mAb 3.9 and control antibody MIgG was used to block the adhesion of Eahy926 cells to CD11c/CD18 coated on plastic (*B*). The standard deviations are shown. The inhibitory effects of competing peptide P1 and mAb 3.9 were significant. ***, $p < 0.001$.

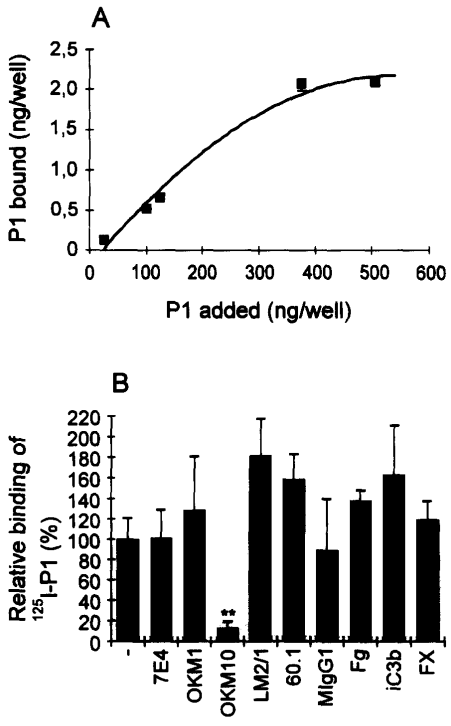

Figure 3. Saturation curve of the binding of ^{125}I-labeled P1 to purified CD11b/CD18, and inhibition of the interaction with monoclonal antibodies. 12 pmol of ^{125}I-P1 was incubated in CD11b/CD18-coated wells in the presence of increasing amounts of unlabeled P1 (*A*), or 50 μg/ml of monoclonal antibodies to CD18 (7E4), CD11b (OKM1, OKM10, LM2/1, and 60.1), and control antibody MIgG1, or 50 μg/ml of fibrinogen (*Fg*), iC3b, or factor X (*FX*) (*B*). The inhibitory effect of mAb OKM10 was significant. **, $p < 0.01$.

OKM10, but not by the other CD11b antibodies OKM1, LM2/1, or 60.1, nor by the anti-CD18 mAb 7E4. The soluble CD11b/ CD18 ligands fibrinogen, iC3b, and factor X were not inhibitory (Fig. 3 *B*).

ICAM-2 Peptide P1-induced CD11b/CD18-ICAM-1–dependent Cell Aggregation

The kinetics of THP-1 and U937 cell aggregation induced by the peptide P1 was similar (Fig. 4 *A* and Fig. 5 *A*). After 0.5–1 h incubation with P1, the cells clearly aggregated as compared to cells treated with the control peptide P8, or cells left without any treatment. Maximal aggregation was observed after 3–4 h incubation, and the cells remained in clusters during the experiments. Peptide P1 induced cell aggregation in a concentration-dependent manner, and a 50% aggregation was obtained with ~30 or 40 μM of P1 for THP-1 or U937 cells, respectively (Fig. 4 *B* and Fig. 5 *B*). The expression of leukocyte adhesion molecules on THP-1 and U937 cells was studied by flow cytometry. CD18, CD11b, CD11c, ICAM-1, ICAM-2, and ICAM-3 were well expressed on both THP-1 and U937 cells, while little expression of CD11a was found (Fig. 6). Monoclonal antibodies against CD18 and ICAM-1 efficiently blocked the homotypic adhesion of both THP-1 and U937 cells, whereas the anti-CD11b antibodies OKM1, LM2/1, and 60.1 (for U937) blocked to a smaller, but significant extent (Fig. 4 *C* and Fig. 5 *C*). The CD11b antibody OKM10 and antibodies against CD11a, CD11c, ICAM-2, and ICAM-3 did not inhibit the aggregation.

Temperature, Energy, Microfilament, and Divalent Cation Requirements for ICAM-2 Peptide P1-induced Cell Aggregation

No P1-stimulated homotypic adhesion of THP-1 and U937 cells was detected at 4°C (Fig. 7, *A* and *B*). The aggregation was partially blocked by NaN_3, but completely inhibited by using NaN_3 in combination with 2-deoxy-D-glucose. Cytochalasin B, which prevents the formation of microfilaments, partially inhibited the aggregation, and EDTA blocked effi-

Carl_G_190x270_mm_blokki_FINAL.indd 279 06-Aug-23 1:53:51 PM

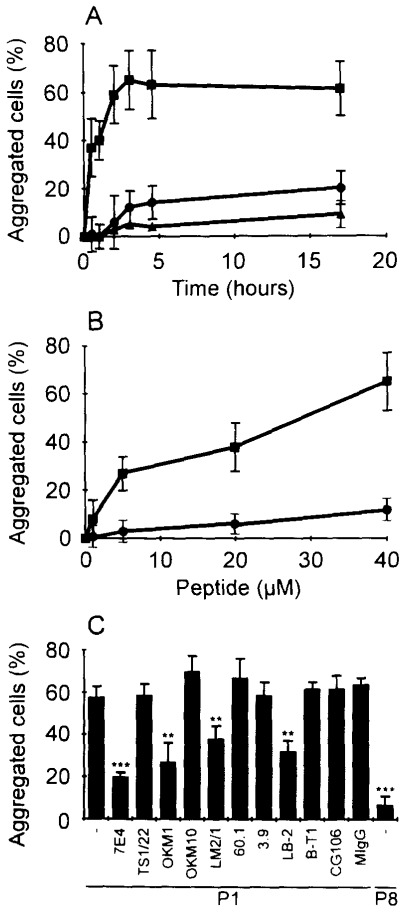

Figure 4. Peptide P1-induced THP-1 cell aggregation. (*A*) THP-1 cells were treated with 40 μM of peptides P1 (■) or P8 (●), or left without any treatment (▲), for indicated time periods. (*B*) The cells were treated with different amounts of P1 or P8. (*C*) 50 μg/ml of mAbs 7E4 (CD18), TS1/22 (CD11a), OKM1 (CD11b), OKM10 (CD11b), LM2/1 (CD11b), 60.1 (CD11b), 3.9 (CD11c), LB-2 (ICAM-1), B-T1 (ICAM-2), CG106 (ICAM-3), and MIgG1 control atnibody were used in the blocking assays. The cell aggregations in *B* and *C* were evaluated after a 3-h incubation. The standard deviations and statistic significances are shown.

ciently. Treatment of cells with dibutyryl cAMP, a cell-permeable cAMP analogue, slightly blocked the homotypic cell adhesion of THP-1 cells, but had no effect on U937 cells.

ICAM-2 Peptide P1-induced Adhesion of THP-1 Cells to Fibrinogen

The purified fibrinogen was checked by polyacrylamide gel electrophoresis in the presence of SDS and found to be essentially pure (Fig. 1 *B*). THP-1 cells stimulated with the peptide P1 bound much more efficiently to fibrinogen coated on plastic (Fig. 8, *A*, *B*, and *C a*) than cells pretreated with the control peptide P8 (Fig. 8, *A*, *B*, and *C b*) or cells left without any treatment (Fig. 8, *A* and *B*). ADP treatment also increased the binding of THP-1 cells to fibrinogen, but to a smaller extent (Fig. 8 *A*). 1 μM of P1 induced a substantial binding of THP-1 cells to fibrinogen, and the adhesion increased with increasing amounts of the P1 peptide (Fig. 8 *B*). The P1-induced adhesion of THP-1 cells to fibrinogen was efficiently blocked by monoclonal antibodies to CD18 (7E4) and CD11b (OKM10), partially blocked by the CD11c antibodies 3.9 and 2E1, and totally inhibited when antibodies OKM10 and 3.9 were used together (Fig. 9). The epitopes on CD11b/CD18 recognized by the monoclonal antibodies OKM1, OKM10, LM2/1, and 60.1 were expressed at similar levels on THP-1 cells (Fig. 6, data not shown). However, with the exception of OKM10, the other CD11b antibodies OKM1, LM2/1, and 60.1 did not block the binding. Another integrin receptor for fibrinogen, $\alpha_v\beta_3$, is also expressed on THP-1 cells (data not shown), but the antibody LM609 reacting with this receptor was not inhibitory. The antibody to CD11a (TS1/22), and the control antibody had no effect. EDTA abolished the adhesion completely.

ICAM-2 Peptide P1-induced Adhesion of THP-1 Cells to Complement Fragment iC3b

The purified iC3b preparation was checked by polyacrylamide gel electrophoresis in the presence of SDS. It contained the β chain and the typical α chain fragments, and no major impurities were observed (Fig. 1 *B*). Nonstimulated THP-1 cells bound to iC3b coated on plastic, but ADP and P1 peptide increased the binding to a small but significant extent, whereas the control peptide P8 had no effect (Fig. 10 *A*). The binding was efficiently inhibited by mAb 7E4, partially by OKM10 and 3.9, and an additive effect was observed when OKM10 and 3.9 were used together (Fig. 10 *B*). Antibodies TS1/22, OKM1, LM2/1, and 60.1 were not inhibitory, whereas EDTA blocked the interaction. Little binding occurred to C3b.

Discussion

CD11b/CD18 is the predominant myeloid cell integrin (Springer, 1990; Arnaout, 1990; Patarroyo et al., 1990). It is involved in cell–cell interactions, and has been shown to bind to the third immunoglobulin domain of ICAM-1 (Diamond et al., 1991). Furthermore, it binds to several soluble proteins like fibrinogen (Wright et al., 1988; Altieri et al., 1988), iC3b (Beller et al., 1982; Wright et al., 1983), and factor X (Altieri and Edgington, 1988*a*), and to various complex carbohydrates (Ross et al., 1985; Wright and Jong, 1986). The binding specificity of CD11c/CD18, which is mainly found on macrophages, is less understood, but it binds to fibrinogen (Loike et al., 1991; Postigo et al., 1991), iC3b (Micklem et al., 1985; Myones et al., 1988), and a counter-receptor on the surface of endothelial cells (Stacker and Springer, 1991), which was confirmed in the present work.

Obviously, it is important to define the leukocyte integrin ligands in detail, determine the binding sites, and establish the mode of activation. ICAM-2 is a relatively simple integrin ligand, and therefore we thought that it should be an ex-

Carl_G_190x270_mm_blokki_FINAL.indd 280 06-Aug-23 1:53:51 PM

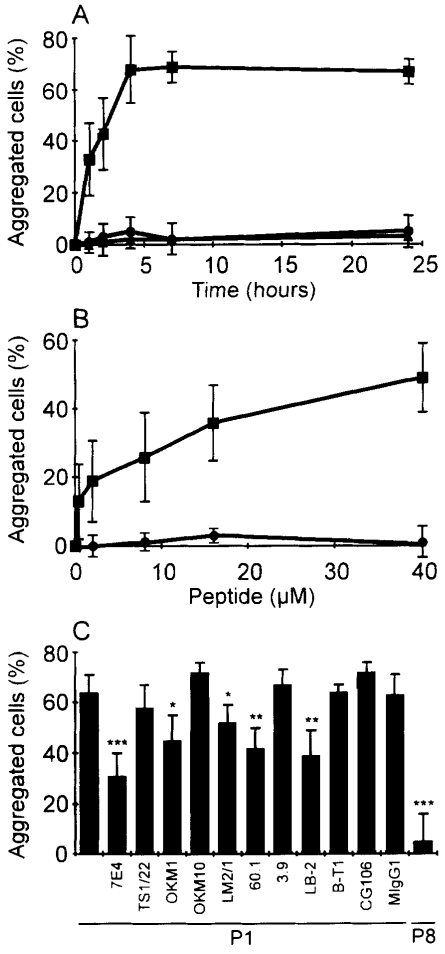

Figure 5. Peptide P1-induced U937 cell aggregation. (*A*) U937 cells were treated with 40 μM of peptides P1 (■) or P8 (●), or left without any treatment (▲), for indicated time periods. (*B*) The cells were treated with different amounts of P1 or P8. (*C*) The antibody blocking assays were performed as shown in Fig. 4. The aggregations of cells in *B* and *C* were evaluated after a 4-h incubation. The standard deviations are shown. *, $p < 0.05$; **, $p < 0.01$; ***, $p < 0.001$.

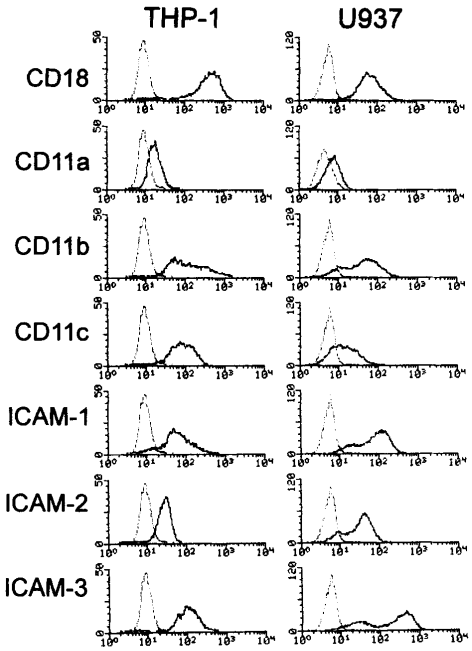

Figure 6. Expression of CD11/CD18 integrins and ICAMs on the monocytic cell lines THP-1 and U937. The monoclonal antibodies 7E4 (CD18), TS1/22 (CD11a), OKM10 (CD11b), 3.9 (CD11c), LB-2 (ICAM-1), B-T1 (ICAM-2), CG106 (ICAM-3) (*dark lines*), and mouse IgG1 (*control*) (*gray lines*) were used. The expression of the epitopes recognized by the CD11b antibodies OKM1, LM2/1, and 60.1 was similar to that of the OKM10 epitope (data not shown).

cellent model for detailed studies on integrin-ligand interactions.

We previously showed that the 22-amino acid residue peptide P1, derived from the first immunoglobulin domain of ICAM-2, specifically binds to CD11a/CD18 (Li et al., 1993*b*). However, we did not find any CD11a antibody that blocked the interaction. The P1 peptide inhibits the binding of endothelial cells to purified CD11a/CD18, and the binding of lymphoblastoid cells to endothelial cells (Li et al., 1993*b*). In the present study, we show that the same peptide also specifically binds to purified CD11b/CD18, but not to CD11c/CD18. The anti-CD11b mAb, OKM10, which recognizes a discontinuous epitope that requires the presence of both the NH_2-terminal and divalent cation-binding regions (Diamond et al., 1993), efficiently blocked this interaction. The results suggest that the epitope recognized by mAb OKM10 on the α chain is in the vicinity of the binding site for the P1 peptide. However, the soluble ligands for CD11b/CD18 fibrinogen, iC3b, and factor X, were not able to interfere with this interaction, indicating that different regions on CD11b/CD18 are involved in binding of P1 and these ligands. The binding of the ICAM-2 derived peptide to CD11b/CD18 raises the interesting possibility that ICAM-2 could bind to this integrin. It has been shown that there exists a second CD11b/CD18 ligand on vascular endothelium, besides ICAM-1 (Carlos and Harlan, 1994). Our preliminary results indicate that ICAM-2 binds to CD11b/CD18 (Xie, J., R. Li, P. Kotou, C. Kantor, C. Vermot-Desroches, J. Wijdenes, M. A. Arnaout, P. Natamo, and C. G. Gahmberg, manuscript in preparation).

The peptide P1 is relatively hydrophobic, and most part of it is probably buried in the first domain of ICAM-2, except that both of its NH_2- and COOH-terminals seem to be exposed (Li et al., 1993*b*). It is essential that the peptide is in reduced form. We have found that when preserved without the presence of reducing agents, the peptide was easily oxi-

Carl_G_190x270_mm_blokki_FINAL.indd 281 06-Aug-23 1:53:51 PM

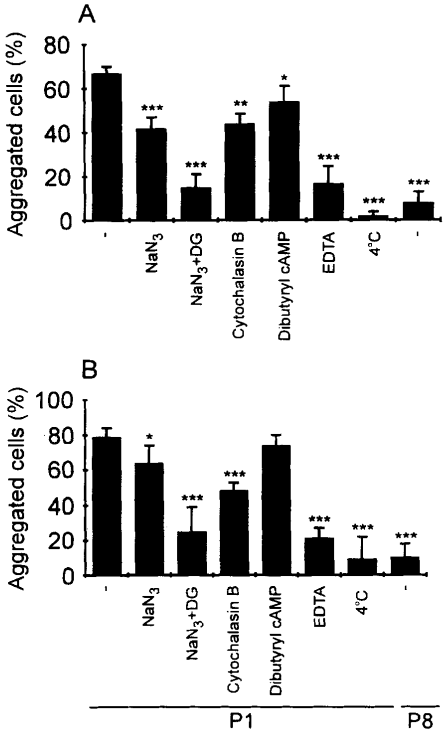

Figure 7. Inhibition of peptide P1-induced THP-1 and U-937 cell aggregations. THP-1 (*A*) and U937 (*B*) cells were kept at 4°C or pretreated with 0.2% of NaN_3, 0.2% NaN_3 and 50 mM 2-deoxy-D-glucose, 20 μM cytochalasin B, 2 mM dibutyryl cAMP or 5 mM EDTA for 15 min at room temperature, before the addition of 40 μM of P1 peptide. The aggregations were determined after 3-h or 4-h incubations for THP-1 and U937, respectively, at 37°C, with the exception of the assay marked 4°C.

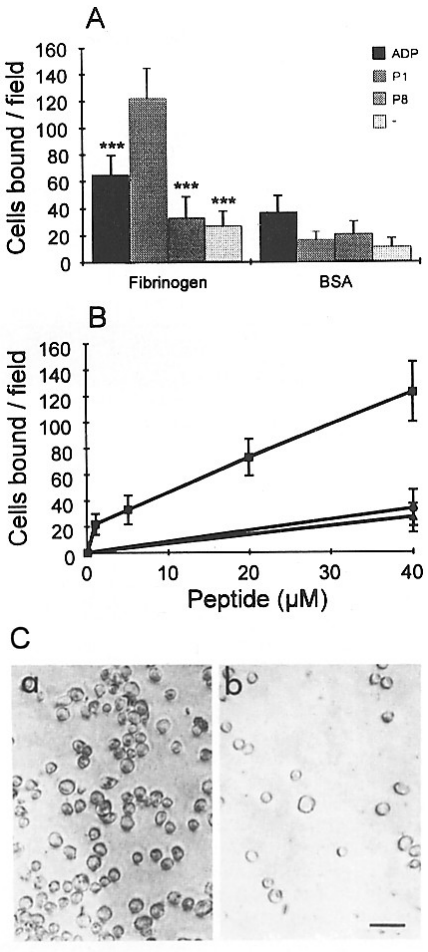

Figure 8. Peptide P1-induced adhesion of THP-1 cells to fibrinogen coated on plastic. (*A*) THP-1 cells were preincubated with 40 μM of peptides P1 or P8 for 2 h at 37°C, washed, and resuspended by pipetting, before being added to fibrinogen or BSA-coated wells. 10 μM of ADP was added at the same time when the cell suspension was added to the wells. (*B*) THP-1 cells were stimulated with different concentrations of P1 (■) or P8 (●), or left without any treatment (▲), before being added to fibrinogen-coated wells. (*C*) Binding of peptide P1 (*C a*) or P8 (*C b*)-stimulated THP-1 cells to immobilized fibrinogen. The photomicrographs were taken after the nonadherent cells had been removed by washing three times. A 200× magnification was used. The bar indicates 50 μm.

dized and lost activity. On the other hand, alkylated peptide did not work either (data not shown). Therefore, the two cysteines in the peptide seem to be essential for its activity.

Recently, we found that the ICAM-2 peptide strongly induces blood T cell aggregation, which is mainly mediated by CD11a/CD18-ICAM-1 interaction, and an increase in the binding and cytotoxicity of natural killer cells (Li et al., 1993*a*). Here we show that the stimulatory effect is not restricted to T lymphocytes and natural killer cells. Myelomonocytic THP-1 and U937 cells became aggregated after treatment with the P1 peptide. Blood neutrophils were also strongly aggregated by P1 stimulation (data not shown). Unlike T lymphocytes, on which CD11a/CD18 is the main leukocyte integrin expressed, CD11b/CD18 and CD11c/CD18 are well expressed on THP-1 and U937 cells, while there is little expression of CD11a/CD18. The THP-1 and U937 cell aggregations were efficiently blocked by CD18 and ICAM-1 antibodies. The CD11b antibodies OKM1, LM2/1, and 60.1 (for U937) blocked to a smaller, but significant extent, while CD11a and CD11c antibodies had no effect. These results indicate that CD11b/CD18 becomes activated, and mediates the cell aggregation by interacting with ICAM-1. Since the CD11b antibody OKM10, which blocked the binding of P1 peptide to purified CD11b/CD18, did not inhibit the THP-1 and U937 cell aggregation, it is probable that CD11b/CD18 is activated by signals resulting from the interaction of P1 with the small amount of CD11a/CD18 expressed on the

Carl_G_190x270_mm_blokki_FINAL.indd 282 06-Aug-23 1:53:51 PM

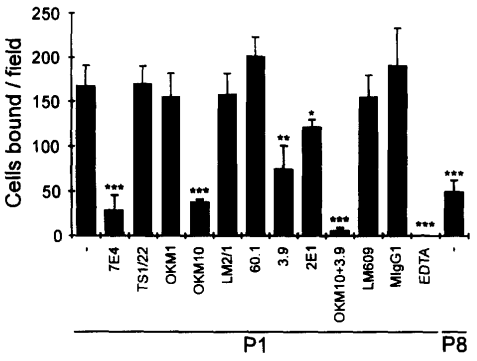

Figure 9. Inhibition of peptide P1-induced adhesion of THP-1 cells to immobilized fibrinogen by monoclonal antibodies and EDTA. Aliquots of P1-stimulated THP-1 cells were separately pretreated with 50 μg/ml of mAbs against CD18 (7E4), CD11a (TS1/22), CD11b (OKM1, OKM10, LM2/1, and 60.1), CD11c (3.9, 2E1), $\alpha_v\beta_3$ (LM609) and control MIgG1, before being added to fibrinogen-coated wells. 5 mM EDTA was used. The effect of P1 is significant as indicated.

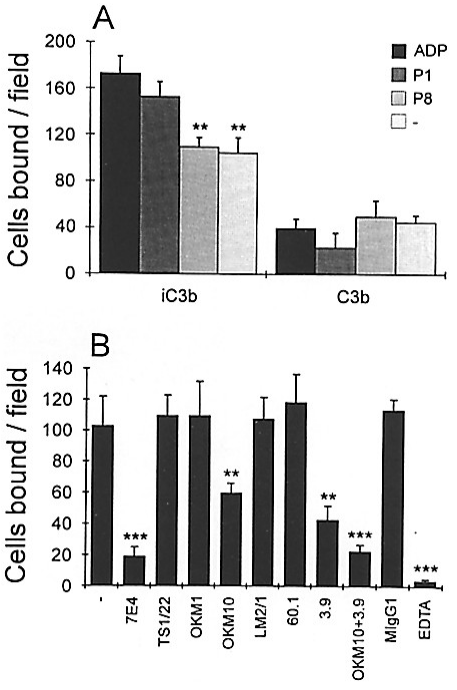

Figure 10. Peptide P1-induced adhesion of THP-1 cells to iC3b or C3b coated on plastic. (*A*) THP-1 cells were preincubated with 40 μM of peptides P1 or P8 for 2 h at 37°C, washed, resuspended by pipetting, and added to iC3b- or C3b-coated wells. 10 μM of ADP was added at the same time when the cell suspension was added to the wells. (*B*) Aliquots of P1-stimulated THP-1 cells were separately pretreated with 50 μg/ml of mAbs against CD18 (7E4), CD11a (TS1/22), CD11b (OKM1, OKM10, LM2/1, and 60.1), CD11c (3.9), and control MIgG1, before being added to iC3b-coated wells. 5 mM EDTA was used.

cells. Alternatively, during the incubation of the cells at 37°C, the OKM10-engaged CD11b/CD18 molecules are no longer available on the cell surface, because of the rapid internalization of occupied CD11b/CD18 (Rab et al., 1993). It has been shown that translocation of neutrophil CD11b/CD18 complex to the cell surface can be induced at 37°C (Todd et al., 1984). We think that a minor possibility could be that these OKM10-free CD11b/CD18 derived from the intracellular pool bound P1 and became activated.

Peptide P1-induced homotypic adhesion of THP-1 and U937 cells does not happen at 4°C, and requires energy, intact microfilaments, and divalent cations. However, cytochalasin B, which prevents the formation of microfilaments, could not totally block the aggregation; and CD18 antibody 7E4 was not able to completely inhibit the aggregation either. These findings suggested that besides β_2 integrins, some other integrins or adhesion systems were also activated.

We previously reported that cross-linking of CD11b/CD18 on neutrophils with monoclonal antibodies causes a rise in cytosolic free Ca^{2+}, which is functionally coupled to a transient activation state of CD11b/CD18 (Altieri et al., 1992). In addition, engagement of the divalent ion binding site(s) on CD11b/CD18 induces the expression of activation-dependent neoantigenic epitopes on CD11b/CD18 and leukocyte adhesion (Altieri, 1991). Furthermore, binding of eosinophils to endothelial cells causes a considerable upregulation of CD11b and an increased capacity to generate an oxidative burst (Walker et al., 1993). It is possible that binding of P1 to CD11b/CD18 has a similar effect as CD11b-specific activating antibodies. The complexity of integrin-activating antibodies is illustrated by the opposite effects of CD11a and CD18 antibodies on T cell activation (van Noesel et al., 1988). In the presence of CD18 antibodies, CD11a antibodies increased T cell proliferation, whereas CD18 antibodies were inhibitory. These findings indicate that integrin-ligand binding may have different effects on integrin functions depending on the site of interaction.

Although several stimuli such as phorbol esters, the peptide formyl-methionyl-leucyl-phenylalanine and complement fragment C5a, can increase the cell surface expression of CD11b/CD18 (Lo et al., 1989; Detmers et al., 1990; Diamond and Springer, 1993), no detectable increase in CD11b/CD18 expression on granulocytes and THP-1 cells was observed after treatment with P1 (data not shown). Phorbol ester or ADP-induced high avidity state of CD11b/CD18 is characterized by the formation of activation-dependent neoantigenic epitopes recognized by the α chain antibodies CBRM1/5 (Diamond and Springer, 1993) or 7E3 (Altieri and Edgington, 1988*b*). However, the P1 peptide-stimulated functional modulation of CD11b/CD18 was not accompanied by an increased expression of these epitopes (data not shown). Recent work has shown by using CD18 antibodies, that the peptide P1 was able to induce the aggregation of the β_2 integrins in the plane of cell membrane on natural killer cells (Somersalo et al., 1995), which is supposed to be

Carl_G_190x270_mm_blokki_FINAL.indd 283 06-Aug-23 1:53:52 PM

tightly correlated with high ligand-binding capacity of CD11b/CD18 (Detmers et al., 1987).

The adhesion of THP-1 cells to fibrinogen and iC3b, was increased by stimulating the cells with peptide P1. The interactions were efficiently blocked by CD18, CD11b, and CD11c antibodies, and an additive effect was observed when CD11b and CD11c antibodies were used together. The P1-stimulated adhesion of THP-1 cells to immobilized fibrinogen and iC3b was blocked by the antibody OKM10, which was found previously to be able to block the interactions between leukocytes and immobilized fibrinogen and iC3b (Wright et al., 1983, 1988; Anderson et al., 1986). On the other hand, some reports have shown that OKM1, rather than OKM10, inhibits the interaction between the leukocytes and soluble fibrinogen (Altieri et al., 1988, 1990). It has been found that conformational changes occur in fibrinogen when the protein is adsorbed onto a plastic surface (Ugarova et al., 1993). This could be the reason for the fact that soluble fibrinogen did not inhibit the interaction between P1 and CD11b/CD18, in which the OKM10 epitope was involved. The background binding of resting THP-1 cells to iC3b coated on plastic was quite high, because iC3b constitutes a ligand for nonactivated CD11b/CD18 (Ross and Vetvicka, 1993).

Taken together, our results are compatible with a model in which the ICAM-2–derived peptide P1 binds to the leukocyte integrins CD11a/CD18 (Li et al., 1993*b*) and CD11b/CD18, but not to CD11c/CD18. These interactions induce high avidity states of CD11a/CD18 on T lymphocytes (Li et al., 1993*a*), and CD11b/CD18 and CD11c/CD18 on monocytic cells for their ligands (Fig. 11). Evidently, the activation of CD11b/CD18 and CD11c/CD18 involves both outside-in and inside-out signals, but it is not clear yet whether the signals come from the interaction of P1 peptide with CD11a/CD18, or with CD11b/CD18, or with both. The detailed mechanisms involved in the signaling remain poorly understood.

We tested the ability of peptide P1 to induce the binding of CD11b/CD18 transfected CHO cells to fibrinogen. The CD11b and CD18 are in the expression vector πH3M (Dana et al., 1991), and was obtained from Dr. M. A. Arnaout. Approximately 20–30% of the transfected cells expressed CD11b/CD18 as determined by FACScan analysis. The CD11b/CD18 transfected cells bound to fibrinogen, but no additional activation by P1 was observed (data not shown). Phorbol esters were not either capable of activating the transfected cells. These findings show that the CD11b/CD18 is active in the transfected cells, but further activation is difficult to achieve. Evidently, CHO cells lack the activation system found in leukocytes.

Recent studies have provided evidence of how fibrinogen participates in inflammatory responses and host defense. Fibrinogen is involved in the regulation of leukocyte adhesion to vascular endothelium by interacting with both CD11b/CD18 on leukocytes and ICAM-1 on endothelium (Altieri et al., 1993; Languino et al., 1993). The finding that P1 stimulates the binding of leukocytes to fibrinogen raises the intriguing possibility that ICAM-2, which is constitutively expressed on most endothelia (Nortamo et al., 1991*a*; de Fougerolles et al., 1991), could have an important regulatory role in leukocyte binding during physiological conditions.

Besides the proposed triggering role for ICAM-2 peptide P1 in ligand binding to integrin, it is obvious that this peptide also contributes to the adhesive interaction itself. This is based on the capacity of P1 to bind to purified CD11a/CD18 and CD11b/CD18, as well as the capacity of this peptide to inhibit the adhesion of endothelial cells to purified CD11a/CD18. Furthermore, it partially blocks the binding of B lymphoblastoid cells to endothelial cells (Li et al., 1993*b*). The ability of P1, on one hand, to inhibit the binding of ICAM-2 containing nonleukocytic cells to CD11a/CD18, but on the other hand, to activate leukocyte binding, is incompletely understood. The main reason may be that as shown here, the three CD11/CD18 cellular integrins become activated by P1, and they bind to several ligands at different binding sites. Therefore, blocking of activated cell-bound integrins is more difficult than interference with the binding of single purified integrin to its ligands.

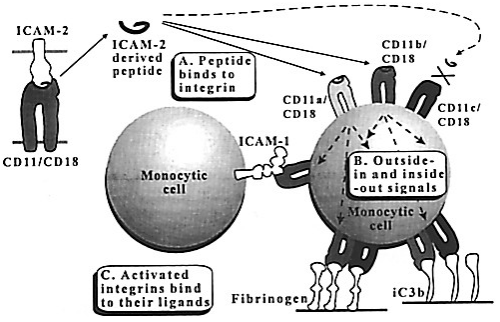

Figure 11. Hypothetical model to explain the ability of the ICAM-2-derived peptide P1 to regulate the avidity of leukocyte integrins. Peptide P1 binds to CD11a/CD18 and CD11b/CD18, but not to CD11c/CD18. The binding induces outside-in and inside-out signals, by which CD11a/CD18 (Li et al., 1993*a*), CD11b/CD18, and CD11c/CD18 are activated to bind to their ligands.

An explanation for the high avidity ligand binding triggered by peptide P1 could be that additional ligand-binding sites are generated in the integrin, as proposed for the activation of the platelet integrin gpIIb/IIIa by arginine-glycine-aspartic acid (RGD)-containing peptides (Ruoslahti and Pierschbacher, 1986, 1987; Du et al., 1991). However, unlike the RGD-containing peptide-induced high affinity state of gpIIb/IIIa, which appears to be due to a direct conformational change in the receptor itself (Du et al., 1991), the P1-induced activation of β_2 integrins seems to involve signal transduction events (Li et al., 1993*a*), although a direct effect on CD11/CD18 integrins cannot be excluded.

Our results show that the high avidity state of leukocyte integrins for different ligands can be induced by interaction between the integrins and the ICAM-2-derived P1 peptide. This indicates the possibility of induction of active forms of leukocyte integrins through interaction with agonistic ligands. Such regulatory reagents could be useful in therapeutical maneuvers in the future.

We thank Veronica Ehrnrooth and Yvonne Heinilä for expert secretarial assistance, Leena Kuoppasalmi for technical assistance, Dr. T. A. Springer

Carl_G_190x270_mm_blokki_FINAL.indd 284 06-Aug-23 1:53:52 PM

for the CD11a antibody TS1/22, Dr. N. Hogg for the CD11c antibody 3.9, Dr. C. Vermot-Desroches for the ICAM-2 antibody B-T1, Dr. D. L. Simmons for the ICAM-3 antibody CG106,, Dr. Jari Ylänne for the $\alpha_v\beta_3$ antibody LM609 and purified fibrinogen, and Dr. M. A. Arnaout for the CD11b and CD18 containing expression vectors.

This study was supported by the Academy of Finland, the Finnish Cancer Society, the Sigrid Jusélius Foundation, University of Helsinki, the Magnus Ehrnroorth Foundation, the Centre for International Mobility (CIMO) Foundation, and grants ROI HL-43773 and HL-51372 from the National Institutes of Health.

Received for publication 28 June 1994 and in revised form 26 January 1995.

References

Altieri, D. C. 1991. Occupancy of CD11b/CD18 (Mac-1) divalent ion binding site(s) induces leukocyte adhesion. *J. Immunol.* 147:1891–1898.

Altieri, D. C., and T. S. Edgington. 1988*a*. The saturable high affinity association of factor X to ADP-stimulated monocytes defines a novel function of the Mac-1 receptor. *J. Biol. Chem.* 263:7007–7015.

Altieri, D. C., and T. S. Edgington. 1988*b*. A monoclonal antibody reacting with distinct adhesion molecules defines a transition in the functional state of the receptor CD11b/CD18 (Mac-1). *J. Immunol.* 141:2656–2660.

Altieri, D. C., R. Bader, P. M. Mannucci, and T. S. Edgington. 1988. Oligospecificity of the cellular adhesion receptor Mac-1 encompasses an inducible recognition specificity for fibrinogen. *J. Cell Biol.* 107:1893–1900.

Altieri, D. C., F. R. Agbanyo, J. Plescia, M. H. Ginsberg, T. S. Edgington, and E. F. Plow. 1990. A unique recognition site mediates the interaction of fibrinogen with the leukocyte integrin Mac-1 (CD11b/CD18). *J. Biol. Chem.* 265:12119–12122.

Altieri, D. C., J. Plescia, and E. F. Plow. 1993. The structural motif glycine 190-valine 202 of the fibrinogen gamma chain interacts with CD11b/CD18 integrin ($\alpha_m\beta_2$, Mac-1) and promotes leukocyte adhesion. *J. Biol. Chem.* 268:1847–1853.

Altieri, D. C., S. J. Stamnes, and C. G. Gahmberg. 1992. Regulated Ca^{2+} signaling through leukocyte CD11b/CD18 integrin. *Biochem. J.* 288:465–473.

Anderson, D. C., L. J. Miller, F. C. Schmalstieg, R. Rothlein, and T. A. Springer. 1986. Contributions of the Mac-1 glycoprotein family to adherence-dependent granulocyte functions: structure-function assessments employing subunit-specific monoclonal antibodies. *J. Immunol.* 137:15–27.

Arnaout, M. A. 1990. Structure and function of the leukocyte adhesion molecules CD11/CD18. *Blood.* 75:1037–1050.

Bainton, D. F., L. J. Miller, T. K. Kishimoto, and T. A. Springer. 1987. Leukocyte adhesion receptors are stored in peroxidase-negative granules of human neutrophils. *J. Exp. Med.* 166:1641–1653.

Beller, D. I., T. A. Springer, and R. D. Schreiber. 1982. Anti-Mac-1 selectively inhibits the mouse and human type three complement receptor. *J. Exp. Med.* 156:1000–1009.

Berendt, A. R., A. McDowall, A. G. Craig, P. A. Bates, M. J. E. Sternberg, K. Marsh, C. I. Newbold, and N. Hogg. 1992. The binding site on ICAM-1 for plasmodium falciparum-infected erythrocytes overlaps, but is distinct from, the LFA-1-binding site. *Cell.* 68:71–81.

Buyon, J. P., S. B. Abramson, M. R. Philips, S. G. Slades, G. D. Ross, G. Weissman, and R. J. Winchester. 1988. Dissociation between increased surface expression of gp165/95 and homotypic neutrophil aggregation. *J. Immunol.* 140:3156–3160.

Cabanas, C., and N. Hogg. 1993. Ligand intercellular adhesion molecule 1 has a necessary role in activation of integrin lymphocyte function-associated molecule 1. *Proc. Natl. Acad. Sci. USA.* 90:5838–5842.

Carlos, T. M., and J. M. Harlan. 1994. Leukocyte-endothelial adhesion molecules. *Blood.* 84:2068–2101.

Cheresh, D. A., and R. C. Spiro. 1987. Biosynthetic and functional properties of an Arg-Gly-Asp-directed receptor involved in human melanoma cell attachment to vitronectin, fibrinogen, and von Willebrand factor. *J. Biol. Chem.* 262:17703–17711.

Clark, E. A., J. A. Ledbetter, R. C. Holly, P. A. Dinndorf, and G. Shu. 1986. Polypeptides on human B lymphocytes associated with cell activation. *Hum. Immunol.* 16:100–113.

Cordell, J. L., K. Pulford, H. Turley M. Jones K. Micklem, I. A. Doussis, X. Tyler, K. Mayne, K. C. Gatter, and D. Y. Mason. 1994. Cellular distribution of human leukocyte adhesion molecule ICAM-3. *J. Clin. Pathol.* 47:143–147.

Damle, N. K., K. Klussman, and A. Aruffo. 1992. Intercellular adhesion molecule-2, a second counter-receptor for CD11a/CD18 (leukocyte function-associated antigen-1), provides a costimulatory signal for T-cell receptor-initiated activation of human T cells. *J. Immunol.* 148:665–671.

Dana, N., D. M. Fathallah, and M. A. Arnaout. 1991. Expression of a soluble and functional form of the human β_2 integrin CD11b/CD18. *Proc. Natl. Acad. Sci. USA.* 88:3106–3110.

Detmers, P. A., S. K. Lo, E. Olsen-Egbert, A. Walz, M. Baggiolini, and Z. A. Cohn. 1990. Neutrophil-activating protein 1/interleukin 8 stimulates the binding activity of the leukocyte adhesion receptor CD11b/CD18 on human neutrophils. *J. Exp. Med.* 171:1155–1162.

Detmers, P. A., S. D. Wright, E. Olsen, B. Kimball, and Z. A. Cohn. 1987. Aggregation of complement receptors on human neutrophils in the absence of ligand. *J. Cell Biol.* 105:1137–1145.

Diamond, M. S., and T. S. Springer. 1993. A subpopulation of Mac-1 (CD11b/CD18) molecules mediates neutrophil adhesion to ICAM-1 and fibrinogen. *J. Cell Biol.* 120:545–556.

Diamond M. S., D. E. Staunton, S. D. Marlin, and T. A. Springer. 1991. Binding of the integrin Mac-1 (CD11b/CD18) to the third immunoglobulin-like domain of ICAM-1 (CD54) and its regulation by glycosylation. *Cell.* 65:961–971.

Diamond, M. S., J. Garcia-Aguilar, J. K. Bickford A. L. Corbi, and T. A. Springer. 1993. The I domain is a major recognition site on the leukocyte integrin Mac-1 (CD11b/CD18) for four distinct adhesion ligands. *J. Cell Biol.* 120:1031–1043.

Dransfield, I., A.-M. Buckle, and N. Hogg. 1990. Early events of the immune response mediated by leukocyte integrins. *Immunol. Rev.* 114:29–44.

Du, X., E. F. Plow, A. Frelinger III, T. O'Toole, J. C. Loftus, and M. H. Ginsberg. 1991. Ligands "activate" integrin $\alpha_{IIb}\beta_3$ (platelet GPIIb-IIIa). *Cell.* 65:409–416.

Dustin, M. L., and T. A. Springer. 1989. T-cell receptor cross-linking transiently stimulates adhesiveness through LFA-1. *Nature (Lond.).* 341: 619–624.

Fawcett, J., C. L. L. Holness, L. A. Needham, H. Turley, K. C. Gater, D. Y. Mason, and D. L. Simmons. 1992. Molecular cloning of ICAM-3, a third ligand for LFA-1, constitutively expressed on resting leukocytes. *Nature (Lond.).* 360:481–484.

de Fougerolles, A. R., and T. A. Springer. 1992. Intercellular adhesion molecule 3, a third adhesion counter-receptor for lymphocyte function-associated molecule 1 on resting lymphocytes. *J. Exp. Med.* 175:185–190.

de Fougerolles, A. D., S. A. Stacker, R. Schwarting, and T. A. Springer. 1991. Characterization of ICAM-2 and evidence for a third counter-receptor for LFA-1. *J. Exp. Med.* 174:253–267.

Greenwood, F. C., W. M. Hunter, and J. S. Gloves. 1963. The preparation of ^{131}I-labeled human growth hormone of high specific radioactivity. *Biochem. J.* 89:114–123.

Hernàndez-Caselles, T., G. Rubio, M. R. Campanero, M. A. de Pozo, M. Muro, F. Sànchez-Madrid, and P. Aparicio. 1993. ICAM-3, the third LFA-1 counter-receptor, is a costimulatory molecule for both resting and activated T lymphocytes. *Eur. J. Immunol.* 23:2799–2806.

Juan, M., R. Vilella, J. Mila, J. Yagüe, A. Miralles, K. S. Campbell, R. J. Friedrich, J. Cambier, J. Vives, A. R. de Fougerolles, et al. 1993. CDw50 and ICAM-3: two names for the same molecule. *Eur. J. Immunol.* 23:1508–1512.

Kansas, G. S., and T. F. Tedder. 1991. Transmembrane signals generated through MHC class II, CD19, CD20, CD39, and CD40 antigens induce LFA-1-dependent and independent adhesion in human B cells through a tyrosine kinase-dependent pathway. *J. Immunol.* 147:4094–4102.

Koistinen, V., S. Wessberg, and J. Leikola. 1989. Common binding region of complement factors B, H and CR1 on C3b revealed by monoclonal anti-C3d. *Complement Inflamm.* 6:270–280.

Koopman, G., M. de Graaff, A. C. L. M. Huysmans, C. J. L. M. Meijer, and S. T. Pals. 1992. Induction of homotypic T cell adhesion by triggering of leukocyte function-associated antigen-1α (CD11a): differential effects on resting and activated T cells. *Eur. J. Immunol.* 22:1851–1856.

Koopman, G., Y. van Kooyk, M. de Graaff, C. J. L. M. Meyer, C. G. Figdor, and S. T. Pals. 1990. Triggering of the CD44 antigen on T lymphocytes promotes T cell adhesion through the LFA-1 pathway. *J. Immunol.* 145: 3589–3593.

van Kooyk, Y., P. van de Wiel-van Kemenade, P. Weder, T. W. Kuijpers, and C. G. Figdor. 1989. Enhancement of LFA-1-mediated cell adhesion by triggering through CD2 or CD3 on T lymphocytes. *Nature (Lond.).* 342: 811–813.

Laemmli, U. K. 1970. Cleavage of structural proteins during assembly of the head of bacteriophage T4. *Nature (Lond.).* 227:680–685.

Landis, R. C., R. I. Bennett, and N. Hogg. 1993. A novel LFA-1 activation epitope maps to the I domain. *J. Cell Biol.* 120:1519–1527.

Languino, L. R., J. Plescia, A. Duperray, A. A. Brian, E. F. Plow, J. W. Geltosky, and D. C. Altieri. 1993. Fibrinogen mediates leukocyte adhesion to vascular endothelium through an ICAM-1-dependent pathway. *Cell.* 73: 1423–1434.

Li, R., P. Nortamo, C. Kantor, P. Kovanen, T. Timonen, and C. G. Gahmberg. 1993*a*. A leukocyte integrin binding peptide from intercellular adhesion molecule-2 stimulates T cell adhesion and natural killer cell activity. *J. Biol. Chem.* 268:21474–21477.

Li, R., P. Nortamo L. Valmu, M. Tolvanen, C. Kantor, and C. G. Gahmberg. 1993*b*. A peptide from ICAM-2 binds to the leukocyte integrin CD11a/CD18 and inhibits endothelial cell adhesion. *J. Biol. Chem.* 268:17513–17518.

Lo, S. K., P. A. Detmers, S. M. Levin, and S. D. Wright. 1989. Transient adhesion of neutrophils to endothelium. *J. Exp. Med.* 169:1779–1793.

Loike, J. D., B. Sodeik, L. Cao, S. Leucona, J. I. Weitz, P. A. Detmers, S. D. Wright, and S. C. Silverstein. 1991. CD11c/CD18 on neutrophils recognizes a domain at the N terminus of the Aα chain of fibrinogen. *Proc. Natl. Acad. Sci. USA.* 88:1044–1048.

Carl_G_190x270_mm_blokki_FINAL.indd 285 06-Aug-23 1:53:52 PM

Micklem, K. J., and R. B. Sim. 1985. Isolation of complement-fragment-iC3b-binding proteins by affinity chromatography. The identification of p150,95 as an iC3b-binding protein. *Biochem. J.* 231:233–236.

Miller, L. J., D. F. Bainton, N. Booregaard, and T. A. Springer. 1987. Stimulated mobilization of monocyte Mac-1 and p150,95 adhesion proteins from an intracellular vesicular compartment to the cell surface. *J. Clin. Invest.* 80:535–544.

Miller, L. J., R. Schwarting, and T. A. Springer. 1986. Regulated expression of the Mac-1, LFA-1, p150,95 glycoprotein family during leukocyte differentiation. *J. Immunol.* 137:2891–2900.

Myones, B. L., J. G. Daizell, N. Hogg, and G. D. Ross. 1988. Neutrophil and monocyte cell surface p150,95 has iC3b-receptor (CR4) activity resembling CR3. *J. Clin. Invest.* 82:640–651.

van Noesel, C., F. Miedema, M. Brouwer, M. A. de Rie, L. A. Aarden, and R. A. W. van Lier. 1988. Regulatory properties of LFA-1 α and β chains in human T-lymphocyte activation. *Nature (Lond.).* 333:850–852.

Nortamo, P., M. Patarroyo, C. Kantor, J. Suopanki, and C. G. Gahmberg. 1988. Immunological mapping of the human leukocyte adhesion glycoprotein GP90 (CD18) by monoclonal antibodies. *Scand. J. Immunol.* 28:537–546.

Nortamo, P., R. Li, R. Renkonen, T. Timonen, J. Prieto, M. Pataroyo, and C. G. Gahmberg. 1991*a*. The expression of human intercellular adhesion molecule-2 is refractory to inflammatory cytokines. *Eur. J. Immunol.* 21: 2629–2632.

Nortamo P., R. Salcedo, T. Timonen, M. Patarroyo, and C. G. Gahmberg. 1991*b*. A monoclonal antibody to the human leukocyte adhesion molecule intercellular adhesion molecule-2. Cellular distribution and molecular characterization of the antigen. *J. Immunol.* 146:2530–2535.

Patarroyo, M., P. G. Beatty, J. W. Fabre, and C. G. Gahmberg. 1985. Identification of a cell surface protein complex mediating phorbol ester-induced adhesion (binding) among human mononuclear leukocytes. *Scand. J. Immunol.* 22:171–182.

Patarroyo, M., E. A. Clark, J. Prieto, C. Kantor, and C. G. Gahmberg. 1987. Identification of a novel adhesion molecule in human leukocytes by monoclonal antibody LB-2. *FEBS (Fed. Eur. Biochem. Soc.) Lett.* 210:127–131.

Patarroyo, M., J. Prieto, J. Rincon, T. Timonen, C. Lundberg, L. Lindbom, B. Åsjö, and C. G. Gahmberg. 1990. Leukocyte-cell adhesion: a molecular process fundamental in leukocyte physiology. *Immunol. Rev.* 114:67–108.

Philips, M. R., J. P. Buyon, R. Winchester, G. Weissman, and S. B. Abramson. 1988. Up regulation of the iC3b receptor (CR3) is neither necessary nor sufficient to promote neutrophil aggregation. *J. Clin Invest.* 82:495–501.

Postigo, A. A., A. L. Corbí, F. Sánchez-Madrid, and M. O. de Landázuri. 1991. Regulated expression and function of CD11c/CD18 integrin on human B lymphocytes. Relation between attachment to fibrinogen and triggering of proliferation through CD11c/CD18. *J. Exp. Med.* 174:1313–1322.

Rabb, H., M. Michishita, C. P. Sharma, D. Brown, and M. A. Arnaout. 1993. Cytoplasmic tails of human complement receptor type 3 (CR3, CD11b/CD18) regulate ligand avidity and the internalization of occupied receptor. *J. Immunol.* 151:990–1002.

Ross, G. D., J. A. Cain, and P. J. Lachmann. 1985. Membrane complement receptor type 3 has lectin-like properties analogous to bovine conglutinin and functions as a receptor for zymosan and rabbit erythrocytes as well as a receptor for iC3b. *J. Immunol.* 134:3307–3315.

Ross, G. D., and V. Vetvicka. 1993. CR3 (CD11b, CD18): a phagocyte and NK cell membrane receptor with multiple ligand specificities and functions. *Clin. Exp. Immunol.* 92:181–184.

Rothlein, R., and T. A. Springer. 1986. The requirement for lymphocyte function-associated antigen 1 in homotypic leukocyte adhesion stimulated by phorbol ester. *J. Exp. Med.* 163:1132–1149.

Rothlein, R., M. L. Dustin, S. D. Marlin, and T. A. Springer. 1986. A human intercellular adhesion molecule (ICAM-1) distinct from LFA-1. *J. Immunol.* 137:1270–1274.

Ruoslahti, E., and M. D. Pierschbacher. 1987. New perspectives in cell adhesion: RGD and integrins. *Science (Wash. DC).* 238:491–497.

Ruoslahti, E., and M. D. Pierschbacher. 1986. Arg-Gly-Asp: a versatile cell recognition signal. *Cell.* 44:517–518.

Sánchez-Madrid, F., A. M. Krensky, C. F. Ware, E. Robbins, J. L. Strominger, S. F. Burakoff, and T. A. Springer. 1982. Three distinct antigens associated with human T-lymphocyte-mediated cytolysis: LFA-1, LFA-2, and LFA-3. *Proc. Natl. Acad. Sci. USA.* 79:7489–7493.

van Seventer, G. A., Y. Shimizu, K. J. Horgan, and S. Shaw. 1990. The LFA-1 ligand ICAM-1 provides an important costimulatory signal for T cell receptor-mediated activation of resting T cell. *J. Immunol.* 144:4579–4586.

Somersalo, K., O. Carpén, E. Saksela, C. G. Gahmberg, P. Nortamo, and T. Timonen. 1995. Activation of NK cell migration by leukocyte integrin binding peptide from ICAM-2. *J. Biol. Chem.* In press.

Springer, T. A. 1990. Adhesion receptors of the immune system. *Nature (Lond.).* 346:425–434.

Stacker, S. A., and T. A. Springer. 1991. Leukocyte integrin p150,95 (CD11c/CD18) functions as an adhesion molecule binding to a counter-receptor on simulated endothelium. *J. Immunol.* 146:648–655.

Staunton, D. E., M. L. Dustin, and T. A. Springer. 1989. Functional cloning of ICAM-2, a cell adhesion ligand for LFA-1 homologous to ICAM-1. *Nature (Lond.).* 339:61–64.

Staunton, D. E., M. L. Dustin, H. P. Erickson, and T. A. Springer. 1990. The arrangement of the immunoglobulin-like domains of ICAM-1 and the binding sites for LFA-1 and rhinovirus. *Cell.* 61:243–254.

Sundström, C., and K. Nilsson. 1976. Establishment and characterization of a human histiocytic lymphoma cell line (U937). *Int. J. Cancer.* 17:565–577.

Todd, R. F., M. A. Arnaout, R. E. Rosin, C. A. Crowley, W. A. Peters, and B. M. Babior. 1984 Subcellular localization of the large subunit of Mol (Mol alpha; formerly gp110), a surface glycoprotein associated with neutrophil adhesion. *J. Clin. Invest.* 74:1280–1290.

Tsuchiya, S., M. Yamabe, Y. Yamaguchi, Y. Kobayashi, T. Konno, and K. Tada. 1980. Establishment and characterization of a human acute monocytic leukemia cell line (THP-1). *Int. J. Cancer.* 26:171–176.

Ugarova, T. P., A. Z. Budzynski, S. J. Shattil, Z. M. Ruggeri, M. H. Ginsberg, and E. F. Plow. 1993. Conformational changes in fibrinogen elicited by its interaction with platelet membrane glycoprotein GPIIb-IIIa. *J. Biol. Chem.* 268:21080–21087.

Vazeux, R., P. A. Hoffman, J. K. Tomita, E. S. Dickinson, R. L. Jasman, T. St. John, and W. M. Gallatin. 1992. Cloning and characterization of a new intercellular adhesion molecule ICAM-R. *Nature (Lond.).* 360:485–488.

Vedder, N. B., and J. M. Harlan. 1988. Increased surface expression of Cd11b/CD18 (Mac-1) is not required for stimulated neutrophil adherence to cultured endothelium. *J. Clin. Invest.* 81:676–682.

Walker, C., S. Rihs, R. K. Braun, S. Betz, and P. L. B. Bruijnzeel. 1993. Increased expression of CD11b and functional changes in eosinophils after migration across endothelial cell monolayers. *J. Immunol.* 150:4061–4071.

Wallis, W. J., D. D. Hickstein, B. R. Schwartz, C. H. June, H. D. Ochs, P. G. Beatty, S. J. Klebanoff, and J. M. Harlan. 1986. Monoclonal antibody-defined functional epitopes on the adhesion-promoting glycoprotein complex (CDw18) of human neutrophils. *Blood.* 67:1007–1013.

Wright, S. D., and M. T. C. Jong. 1986. Adhesion-promoting receptors on human macrophages recognize *Eschericia coli* by binding to lipopolysaccharide. *J. Exp. Med.* 164:1876–1888.

Wright, S. D., P. E. Rao, W. C. Van Voorhis, L. S. Craigmyle, K. Iida, M. A. Talle, E. F. Westberg, G. Goldstein, and S. C. Silverstein. 1983. Identification of the C3bi receptor of human monocytes and macrophages by using monoclonal antibodies. *Proc. Natl. Acad. Sci. USA.* 80:5699–5703.

Wright, S. D., J. I. Weitz, A. J. Huang, S. M. Levin, S. C. Silverstein, and J. D. Loike. 1988. Complement receptor type 3 (CD11b/CD18) of human polymorphonuclear leukocytes recognizes fibrinogen. *Proc. Natl. Acad. Sci. USA.* 85:7734–7738.

Carl_G_190x270_mm_blokki_FINAL.indd 286 06-Aug-23 1:53:52 PM

The Journal of Immunology
RESEARCH ARTICLE | JUNE 01 1999

ICAM-2 and a Peptide from Its Binding Domain Are Efficient Activators of Leukocyte Adhesion and Integrin Affinity[1]

Annika Kotovuori, Tiina Pessa-Morikawa, Pekka Kotovuori, Pekka Nortamo, and Carl G. Gahmberg[2]

Cell adhesion mediated by the CD11/CD18 integrins and their ligands, the ICAMs, is required for many leukocyte functions. In resting cells the integrins are nonadhesive, but when activated they become adhesive for their ligands. Previous findings have shown that a peptide derived from the first Ig domain of ICAM-2 (P1) binds to LFA-1 (CD11a/CD18) and Mac-1 (CD11b/CD18) and activates leukocyte aggregation. Because its mechanism of action has remained poorly understood, we have now studied the peptide-induced ligand binding in detail. Here we show that P1 was able to induce CD11/CD18-dependent adhesion of human T lymphocytes to immobilized, purified ICAM-1, -2, and -3. The optimal peptide concentration was 150 μg/ml, whereas concentrations higher than 400 μg/ml did not have any stimulatory effect. The increase in adhesion was detectable within 10 min of treatment with the peptide; it was dependent on energy, divalent cations, temperature, and an intact cytoskeleton but was unaffected by protein kinase C and protein tyrosine kinase inhibitors. Peptide treatment resulted in strong stimulation of the binding of soluble, recombinant ICAMs to T lymphocytes, showing that the integrin affinity toward its ligands was increased. Importantly, soluble ICAM-2Fc was also able to induce T lymphocyte adhesion to purified ICAM-1, -2, and -3, and it was a more potent stimulatory molecule than ICAM-1Fc or ICAM-3Fc. ***The Journal of Immunology,*** **1999, 162: 6613–6620.**

The leukocyte-specific β_2 integrins (CD11/CD18) consist of four heterodimeric glycoproteins with specific α-chains (CD11a, -b, -c, -d) and a common β_2-chain (CD18). They play an essential role in mediating diverse cell-cell interactions required for many leukocyte functions, such as the production of Ig, phagocytosis and chemotaxis, cytotoxicity of T lymphocytes and NK cells, and leukocyte extravasation through capillary endothelium (1–5).

CD11a/CD18 (LFA-1, α_L/β_2)[3] is expressed on all leukocytes. CD11b/CD18 (Mac-1, α_M/β_2) is mainly expressed on cells of the myeloid lineage, whereas CD11c/CD18 (p150/95, α_X/β_2) is considered a good marker for mononuclear phagocytes. The most recently found member of the β_2 integrin family, CD11d/CD18 (α_d/β_2), is expressed on myelomonocytic cell lines and subsets of peripheral blood leukocytes. CD11d is more closely related to CD11b and CD11c than to CD11a (6).

A 200-residue I (inserted) domain has been identified at a similar location in the α subunits of the β_2 integrins. The leukocyte integrins mediate adhesive functions through this domain. The I domains contain no cysteine residues or *N*-linked glycosylation sites, but cysteines are usually found at their boundaries. These two features may allow accessibility to ligands and flexibility to adopt variable conformations (7).

The β_2 integrins mediate cell adhesion through binding to the ICAMs. At present, five human ICAM molecules have been described, namely ICAM-1 (CD54), ICAM-2 (CD102), ICAM-3 (CD50), ICAM-4 (LW blood group Ag), and ICAM-5 (telencephalin) (see Ref. 5). ICAM-1 consists of five Ig-like domains, is found on the surface of leukocytes and various other cells, and can be up-regulated by numerous proinflammatory cytokines (1, 5, 8). ICAM-2 has two Ig-like domains; it is expressed on endothelial cells, various leukocytes, and platelets (9); and it is refractory to commonly used proinflammatory cytokines (10, 11). ICAM-3 is composed of five Ig-like domains, and it is present at high levels on resting lymphocytes, monocytes, and granulocytes. It is the only ICAM significantly expressed on neutrophils (12). ICAM-4 is RBC specific (13), and ICAM-5 is confined to the brain (14–15). The ICAMs may also exist in soluble forms in human plasma, which may result from postactivation proteolytic mechanisms at the cell surface of various cells (16–18).

CD11a/CD18 is able to bind all five ICAM-molecules. The NH_2-terminal domains of ICAM-1, ICAM-2, and ICAM-3 are evidently most important for binding (11, 19–25). CD11b/CD18 binds ICAM-1, ICAM-2, and ICAM-4. The third Ig-like domain in ICAM-1 (26) and the first NH_2-terminal domain in ICAM-2 seem to be important for CD11b/CD18 binding (22). CD11b also binds to several soluble ligands including the complement fragment iC3b, fibrinogen, and factor X (27–28). CD11c/CD18 binds ICAM-1, but also to iC3b and fibrinogen. CD11d/CD18 exhibits preferential recognition of ICAM-3 (6).

Integrins alternate between states of low and high affinity and avidity for their ligands. The mechanisms underlying the transitions between the different states are still incompletely known. Integrins can be activated in a variety of ways. Activation through the TCR complex (29, 30) or directly by the protein kinase C (PKC)-activating phorbol esters (31, 32) occurs through inside out

Department of Biosciences, Division of Biochemistry, University of Helsinki, Helsinki, Finland

Received for publication September 28, 1998. Accepted for publication March 11, 1999.

The costs of publication of this article were defrayed in part by the payment of page charges. This article must therefore be hereby marked *advertisement* in accordance with 18 U.S.C. Section 1734 solely to indicate this fact.

[1] The work was supported by the Academy of Finland, the Sigrid Jusélius Foundation, the Magnus Ehrnrooth Foundation, the Ella and Georg Ehrnrooth Foundation, and the Finnish Cancer Society.

[2] Address correspondence and reprint requests to Dr. Carl G. Gahmberg, Department of Biosciences, Division of Biochemistry, P. O. Box 56 (Viikinkaari 5), FIN-00014 University of Helsinki, Helsinki, Finland. E-mail address: carl.gahmberg@helsinki.fi

[3] Abbreviations used in this paper: CD11a/CD18, LFA-1; $\alpha_L\beta_2$ CD11b/CD18, Mac-1; $\alpha_M\beta_2$ CD11c/CD18, p150/95; $\alpha_X\beta_2$ CD11d/CD18, $\alpha_d\beta_2$; NCAM, neural cell adhesion molecule; P1, synthetic peptide corresponding to amino acids 21–42 from human ICAM-2; P8, scrambled control peptide; PdBu, phorbol dibutyrate; PKC, protein kinase C; sICAM-1, soluble ICAM-1.

Copyright © 1999 by The American Association of Immunologists

0022-1767/99/$02.00

Carl_G_190x270_mm_blokki_FINAL.indd 287 06-Aug-23 1:53:52 PM

signaling. CD11/CD18 activation can also be induced by specific mAbs against a number of other cell surface molecules like CD2 (29), CD43 (33), and CD44 (34, 35). The cellular signaling events leading to integrin activation in each case may be at least partially different. Some reagents, like the divalent cations Mg^{2+} and Mn^{2+}, and some integrin-binding mAbs, such as MEM83 (36), KIM127, and KIM185 (37–39), may induce integrin activation without the need of intracellular signaling.

We have earlier described a synthetic 22-amino acid peptide (P1) corresponding to a sequence from the first Ig domain of ICAM-2 that is able to bind to CD11a/CD18 and CD11b/CD18 and stimulate the aggregation of various leukocytes. Furthermore, it also stimulates the migration and cytotoxicity of NK cells (40–42). Its mechanism of action has, however, remained elusive. Here we have studied in more detail how the P1 peptide acts. The results show that it stimulates CD11/CD18-dependent adhesion of T lymphocytes to purified immobilized ICAM-1, -2, and -3 with the optimal concentration of 150 μg/ml for activation. P1 induced increased integrin affinity for ICAMs, as shown by an increased binding of soluble forms of ICAMs to T lymphocytes. Like P1, purified ICAM-1, ICAM-2, and ICAM-3 were all able to stimulate the T lymphocyte adhesion to immobilized ligands, but ICAM-2 was found to be the most efficient stimulatory ICAM.

Materials and Methods

Antibodies

mAb 7E4 against the CD18 subunit of CD11/CD18 has been described previously (43). mAb OKT3, which reacts with CD3, was used in the form of ascites fluid (Clone CRL 8001; American Type Culture Collection, Rockville, MD).

Isolation of T lymphocytes

Human T lymphocytes were isolated from buffy coats obtained from the Finnish Red Cross Blood Transfusion Service as described (44). Cells were suspended to a density of 10^6 cells/ml in RPMI 1640 medium supplemented with 10% FCS, L-glutamine, and antibiotics and kept in culture overnight at 37°C.

Isolation and expression of leukocyte adhesion molecules

Cellular ICAM-2 and CD11a/CD18 were isolated from human buffy coat cell lysates from 200 U of blood as previously described (22, 45).

The ICAM-1Fc, ICAM-2Fc, ICAM-3Fc, and NCAMFc (neural cell adhesion molecule fused to the Fc portion of IgG) fusion proteins were produced by transient transfection of COS-1 cells and isolated from the culture supernatants by protein A-Sepharose affinity chromatography as described (46). Their purities were checked by SDS-PAGE (47). The ICAM-1Fc, ICAM-2Fc, ICAM-3Fc, and NCAMFc cDNA vectors were kindly provided by D. L. Simmons. Soluble ICAM-1 (sICAM-1) and ICAM-3 consisting of the extracellular parts of the molecules were obtained from Dr. W. M. Gallatin (ICOS, Bothell, WA). ICAM-1Fc fusion protein for competition assay was produced using the CHO K-1 cell line (48) and purified from the cell culture supernatant by protein A-Sepharose affinity chromatography.

Peptides

The ICAM-2-derived peptide P1 (GSLEVNCSTTCNQPEVGGLETSY) and the scrambled control peptide P8 (EVGTGSCNLECVSTNPLSGTEQY) were synthesized by fluorenylmethoxycarbonyl chemistry as described (22, 40), and their structures were verified by mass analysis.

Adhesion experiments

Purified ICAM-1, ICAM-2, ICAM-3, or CD11a/CD18 were coated (0.3 μg/well) on flat-bottom 96-well microtiter plates by overnight incubation at 4°C. For coating, ICAM molecules lacking the Fc portions were used. The wells were blocked with 1% BSA for 90 min at 20°C. Aliquots (50 μl) of T lymphocytes (5×10^5 cells) suspended in binding medium (RPMI 1640, 40 mM HEPES, 2 mM $MgCl_2$, 5% FCS) were added to each well and treated with the peptides, PdBu (Sigma Chemical, St. Louis, MO), OKT3, or ICAM/NCAM Fc fusion proteins. Pretreatments with NaN_3 and deoxyA (Calbiochem) were for 30 min, and for those for bisindolylmaleimide I (Calbiochem, La Jolla, CA) were for 90 min before the addition of peptides. After incubation for 1 h at 20°C, unbound cells were removed by gentle washing. The binding was quantitated by counting bound cells in four randomly chosen fields from each well using ×200 magnification. The results are expressed as mean ± SD.

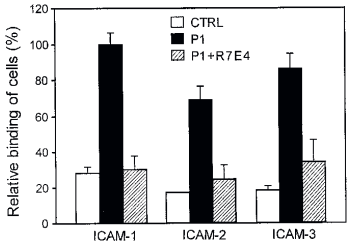

FIGURE 1. Adhesion of T lymphocytes to purified ICAM-1, -2, and -3 induced by P1 peptide. T lymphocytes were incubated with 150 μg/ml P1 in the presence or absence of 40 μg/ml anti-CD18 (R7E4) in ICAM-1-coated microwells at 20°C for 1 h, and the number of bound cells was counted. The results are given as percentage of cells bound to ICAM-1. The white bars represent untreated cells. P8-treated cells gave results similar to those of untreated cells (CTRL). The background binding to BSA was 5–10%. The experiment was repeated three times with similar results.

Competitive binding assay

Purified CD11a/CD18 was coated on flat-bottom 96-well microtiter plate by overnight incubation at 4°C. The wells were blocked with 2% BSA for 30 min at 37°C. ICAM-1Fc (0.33 μM), 50 μl in PBS/2 mM $MgCl_2$, was then added to the wells in duplicate in the presence or absence of the peptides or DTT (Sigma). After incubation for 1 h at 20°C, the wells were washed, and 50 μl of rabbit anti-mouse Ig alkaline phosphatase conjugate (Dako, Copenhagen, Denmark) diluted 1:2000 in 1% BSA/PBS/2 mM $MgCl_2$ were added to each well and incubated for 30 min at 37°C. After washing, 50 μl of *p*-nitrophenyl phosphate (1 mg/ml) (Sigma) in 50 mM diethylamine (Fluka Chemie AG, Buchs, Switzerland), pH 10, 0.5 mM $MgCl_2$ were added to each well, and the plates were incubated at 37°C for 45 min. The absorbance was then measured using a Titertek Multiskan plate reader (Eflab Oy, Helsinki, Finland) at 405 nm.

Binding of soluble ligands

T lymphocytes were washed three times with 20 mM HEPES, 140 mM NaCl, and 2 mg/ml glucose, pH 7.4. Cells (5×10^5) were incubated in 25 μl of this buffer supplemented with indicated $MgCl_2$ concentrations in the presence or absence of stimulators and 400 μg/ml of ligand protein at 37°C for 60 min. After removal of the unbound ligand by washing with PBS, the cells were incubated with 10 μg/ml FITC-conjugated anti-human IgG-Fc specific Abs (Jackson Immunoresearch Laboratories, West Grove, PA) on ice for 20 min, washed, and analyzed with a Becton Dickinson FACScan flow cytometer (Immunocytometry System, Mountain View, CA) (49). In a similar way, the binding of mAb 24 was studied, using FITC-conjugated rabbit anti-mouse $F(ab')_2$ (Dako) as a secondary Ab.

Results

P1 induced CD11/CD18-dependent adhesion of T lymphocytes to immobilized ICAM-1, -2, and -3

It was earlier shown that peptide P1 induced the aggregation of various leukocytes (22, 40, 41). We have now studied the mechanism of P1-induced adhesion in more detail. Treatment of human T lymphocytes with P1 stimulated adhesion of the cells to purified, immobilized ICAM-1, -2, and -3, and most efficiently to ICAM-1 (Fig. 1). The adhesion was CD11/CD18 dependent as shown by inhibition of the adhesion with the blocking mAb 7E4.

We further studied the kinetics of the peptide induced activation. As can be seen in Fig. 2, the effect of the peptide on the adhesion to ICAM-1 was detectable after a 10-min treatment, and it reached

Carl_G_190x270_mm_blokki_FINAL.indd 288 06-Aug-23 1:53:53 PM

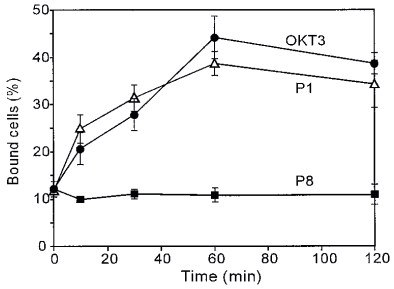

FIGURE 2. Kinetics of T lymphocyte adhesion to ICAM-1. T lymphocytes were treated with 150 μg/ml P1 or P8 or 1:200 diluted OKT3 mAb ascites for the indicated times at 20°C, and the cells bound to ICAM-1 were counted.

similar kinetics. The scrambled control peptide P8 had no effect. Similar kinetics was observed when ICAM-2 or -3 were coated (not shown).

The effect of P1 is dependent on peptide concentration

The effect of different P1 or P8 concentrations on the adhesion of T lymphocytes to purified ICAM-1 (Fig. 3*A*), ICAM-2 (Fig. 3*B*), and ICAM-3 (Fig. 3*C*) was studied. In Fig. 3, it can be seen that low P1 concentrations were stimulating and that the optimal stimulatory P1 concentration was ~150 μg/ml. Importantly, concentrations of 400 μg/ml or above did not stimulate adhesion. The P1-induced T lymphocyte activation showed a similar dependence on peptide concentrations with ICAM-1, -2, and -3. The control peptide P8 had no effect.

P1-induced adhesion is dependent on temperature, divalent cations, metabolic energy, and intact actin cytoskeleton but insensitive to inhibitors of protein kinase C and protein tyrosine kinases

Fig. 4A shows that the P1-induced binding of T lymphocytes to coated ICAM-1 did not take place at low temperature and that it was blocked by pretreatment of the cells with sodium azide and deoxyglucose or with EDTA. Similar results were obtained with immobilized ICAM-2 or -3 (not shown).

Pretreatment of T lymphocytes with cytochalasin D, which inhibits actin polymerization, inhibited the P1- and PdBu-induced adhesion of the cells to ICAM-1 (Fig. 4*B*). The inhibitory effect could be seen when the cytochalasin D concentration was 1 μM, but when used at concentrations of 5 μM and above, the effect was stronger.

Preincubation of T lymphocytes with increasing concentrations of the PKC inhibitor bisindolylmaleimide I (Fig. 5*A*) or the protein tyrosine kinase inhibitor herbimycin A (Fig. 5*B*) did not inhibit the P1-induced adhesion of the cells to ICAM-1. As expected, the PdBu-induced adhesion was efficiently inhibited by bisindolylmaleimide I.

P1 induced binding of sICAM-1Fc, ICAM-2Fc, and ICAM-3Fc to T lymphocytes

To be able to study changes in integrin affinity, we wanted to measure the effect of peptide treatment on the binding of soluble integrin ligands to T lymphocytes. For this purpose, sICAM-1Fc, ICAM-2Fc, ICAM-3Fc, and NCAMFc fusion proteins were produced by transient transfection in COS cells and purified by affinity chromatography. The preparations contained the expected pro-

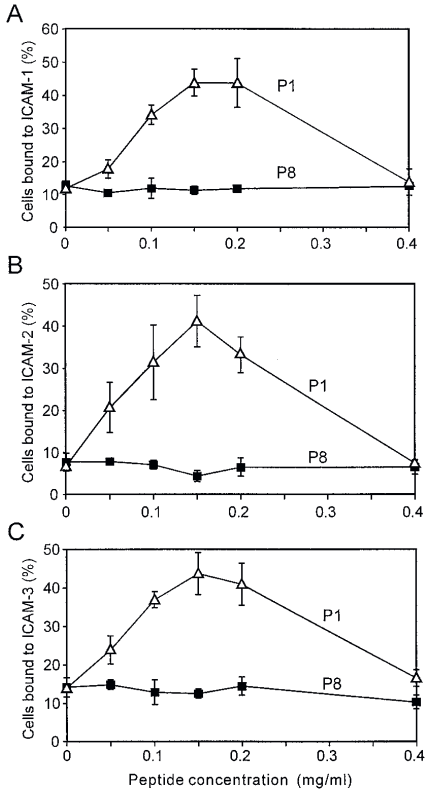

FIGURE 3. Effect of different peptide concentrations on the binding of T lymphocytes to purified ICAM-1 (*A*), ICAM-2 (*B*), and ICAM-3 (*C*). T lymphocytes were activated with indicated peptide concentrations for 1 h, and the cells bound to the coated proteins were counted.

The binding of soluble Fc fusion proteins to T lymphocytes was studied by flow cytometry using a FITC-conjugated anti-Fc mAb to trace the Fc portions of the bound proteins. Fig. 7*A* shows that the P1 peptide stimulated the binding of sICAM-1Fc to T lymphocytes, whereas the control peptide P8 or PdBu had no effect. No increase in binding of the control protein, NCAMFc, to the cells was observed (Fig. 7*B*). The binding of sICAM-2Fc and ICAM-3Fc to the cells was also increased after peptide treatment (Fig. 7*C*).

It has been shown that Mg^{2+}/EGTA treatment of T lymphocytes induces significant binding of sICAM-1 by the same method (49), and this treatment was also used here as a positive control. According to our results, P1 is at least as efficient a stimulator of sICAM-1 binding as 10 mM Mg^{2+}/1 mM EGTA, and in some experiments it turned out to be even more effective (results not shown). The results also suggest that the effect of P1 is clearly less dependent on the Mg^{2+} concentration. P1 worked very efficiently when the Mg^{2+} concentration was as low as 1 mM.

The ability of P1 to induce the expression of the CD11a/CD18 activation reporter epitope recognized by mAb 24 was also tested by flow cytometry using T lymphocytes. In these experiments, 10 mM Mg^{2+}/1 mM EGTA treatment was used as a positive control

Carl_G_190x270_mm_blokki_FINAL.indd 289 06-Aug-23 1:53:54 PM

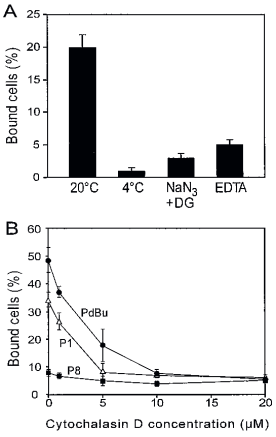

FIGURE 4. Inhibition of induced adhesion of T lymphocytes to immobilized ICAM-1. T lymphocytes were kept at 4°C or pretreated with 0.2% NaN_3 and 50 mM 2-deoxyglucose (DG) or 5 mM EDTA before the addition of 150 μg/ml P1 (*A*). In *B* the cells were pretreated with 0, 1, 5, 10, or 20 μM cytochalasin D before the addition of 150 μg/ml P1 or P8 or 60 nM PdBu. The cells bound to ICAM-1 were counted after a 1-h incubation.

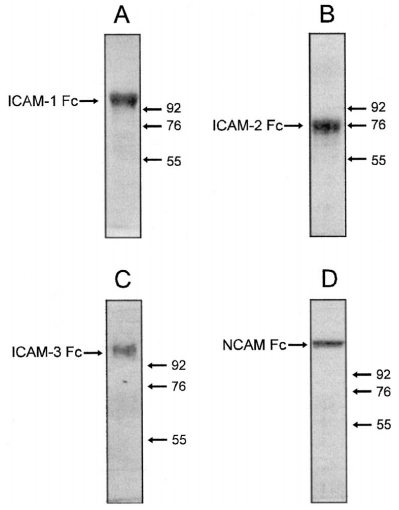

FIGURE 6. Polyacrylamide gels of purified ICAM-1Fc (*A*), ICAM-2Fc (*B*), ICAM-3Fc (*C*), and NCAMFc (*D*). Proteins were run on 8% polyacrylamide gels in the presence of SDS and stained with Coomassie blue. The positions of the m.w. markers are indicated.

whereas the effect of Mg^{2+}/EGTA was obvious. The median fluorescence intensities were 10.8, 31.6, 8.1, and 7.6 using 0 mM Mg^{2+}, 10 mM Mg^{2+}/1 mM EGTA, 10 mM Mg^{2+}/150 μg/ml P1, and 10 mM Mg^{2+}/150 μg/ml P8 as stimulators, respectively. The experiments have been repeated with similar results.

When the binding of sICAM-1 to purified CD11a/CD18 integrin coated on plastic was studied, no inhibition was observed in the presence of P1 up to a concentration of 4.1 μM (10 μg/ml) (Table I). Higher concentrations were inhibitory, but P8 and DTT showed a similar effect. The results indicate that at higher concentrations the sulfhydryl groups become inhibitory.

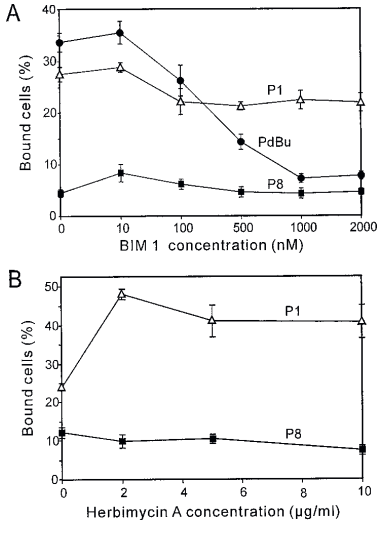

FIGURE 5. Effect of bisindolylmaleimide 1 (BIM 1) and herbimycin A on the P1-, P8-, or PdBu-induced T lymphocyte adhesion to immobilized ICAM-1. The cells were pretreated with the indicated concentrations of bisindolylmaleimide 1 (*A*) or herbimycin A (*B*) at 37°C for 30 min before addition of the activating agents. The bound cells were counted after 1 h of

sICAM-2Fc stimulates T lymphocyte adhesion to immobilized ICAM-1, -2, and -3

It was of interest to see whether also the ICAM-2 protein was able to stimulate adhesion. Fig. 8 shows that treatment of T lymphocytes with sICAM-2Fc (0.27–0.67 μM) stimulated the adhesion of the cells to purified, immobilized ICAM-1 (Fig. 8*A*), ICAM-2 (Fig. 8*B*), and ICAM-3 (Fig. 8*C*). The percentage of bound cells after ICAM-2Fc stimulation was usually a little higher when ICAM-1 was coated compared with ICAM-2 or ICAM-3. NCAMFc had no significant effect on adhesion.

The percentages of bound cells after activation of the cells with 62 μM P1 in the experiment shown in Fig. 6 were 39%, 27%, and 33% for *A*, *B*, and *C*, respectively.

ICAM-2Fc is a more potent stimulator of T lymphocyte binding than ICAM-1Fc or ICAM-3Fc

When the abilities of the different ICAMFcs to induce adhesion of T lymphocytes to purified ICAM-1 were compared, ICAM-2Fc appeared to be the most potent activator. ICAM-3Fc showed some activating effect while ICAM-1Fc had almost no activity (Fig. 9*A*). Because of the possibility that the binding of the cells to immobilized ICAM-1 could be preferentially inhibited by sICAM-1Fc, we also tested the effect of the different sICAMs on binding of T lymphocytes to coated ICAM-2 (Fig. 9*B*). The results show that the stimulation by ICAM-2Fc also in this case was stronger than that by ICAM-1Fc or ICAM-3Fc.

Discussion

It is known that changes in integrin binding activity may occur

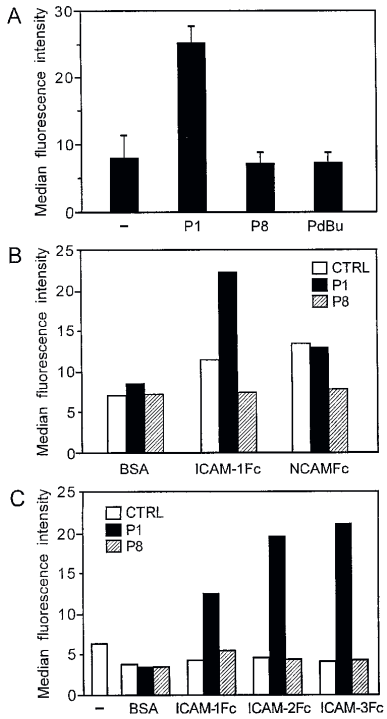

FIGURE 7. Binding of soluble ligands to T lymphocytes after treatment with peptide or PdBu. T lymphocytes were incubated with 150 μg/ml P1 or P8 or with 60 nM PdBu in the presence of 400 μg/ml ICAM-1Fc, and the binding was determined by flow cytometry. The $MgCl_2$ concentration used was 2 mM. The results are expressed as median fluorescence intensity. *A*, Mean and SD of six independent experiments. In *B* the cells were incubated without (control (CTRL) bars) or with 150 μg/ml P1 or P8 in the presence of 400 μg/ml BSA, ICAM-1Fc, or NCAM-Fc. The results represent means of median fluorescence intensities from two experiments. In *C* the binding of ICAM-1Fc, ICAM-2Fc, and ICAM-3Fc at 1.9 μM is shown.

in the affinity of the integrins for ligand probably due to conformational changes. On the other hand, integrin clustering, multimerization, or redistribution in the plane of the membrane, such as that seen after phorbol ester treatment, also affects the ligand-binding ability by increasing integrin avidity (5, 50–52).

Table I. *Inhibition of ICAM-1Fc binding to purified CD11a/CD18*

Concentration of Competing Agent (μM)	OD_{405}[a]		
	P1	P8	DTT
0	0.332	0.332	0.332
0.8	0.347	0.397	0.373
2.1	0.344	0.364	0.328
4.1	0.351	0.378	0.310
10.4	0.299	0.275	—
20.7	0.248	0.249	0.290
31.3	0.198	0.170	—
62.5	0.120	0.179	0.091

[a] Mean of duplicate values; —, not tested.

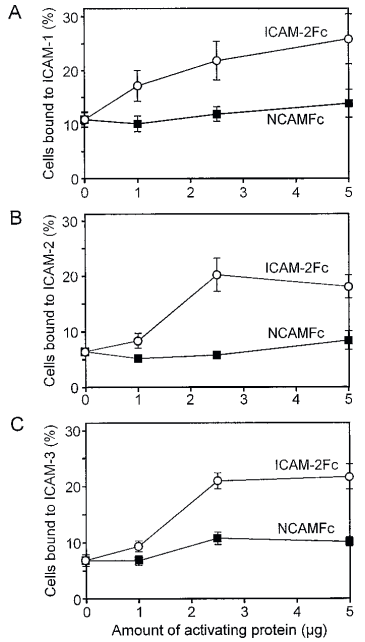

FIGURE 8. T lymphocyte adhesion to purified ICAM-1 (*A*), ICAM-2 (*B*), and ICAM-3 (*C*) induced by sICAM-2Fc and NCAMFc. T lymphocytes were treated with indicated amounts of ICAM-2Fc or NCAMFc for 1 h at 20°C, and the bound cells were counted.

Several different types of external ligands are known, which induce increased integrin activity, but despite much effort their mechanisms of action have remained poorly understood (5, 53). As a model compound, we have used a 22-amino acid peptide, P1, derived from the first Ig-like domain of ICAM-2, which binds to CD11a/CD18 and CD11b/CD18 and stimulates the aggregation of various leukocytes, and among other things increases the migration and cytotoxicity of NK cells (22, 40–42).

In our earlier reports, the P1-induced integrin activation was monitored at the cellular level by increased aggregation of various leukocytes, and this interaction was shown to be largely CD11a/CD18-ICAM-1 dependent, as shown by using Abs to CD11a, CD18, and ICAM-1. Abs to ICAM-2 and ICAM-3 did not block the aggregation (22, 41). Now we have studied the P1-induced leukocyte integrin activation in more detail. Because of the complexicity when studying cell-cell interaction, we have used purified ICAMs. P1 induced T lymphocyte adhesion to all three plastic-coated ICAMs, and the interactions were CD11/CD18 dependent since the binding could be blocked with the CD18 mAb. The amounts of bound cells were usually higher when ICAM-1 was coated as compared with ICAM-2 and -3. Interestingly, activating Abs against CD11a, such as MEM83 and NKI-L16, are incapable of inducing the CD11a/CD18-mediated adhesion of cells to all three ICAMs (54). The Ab MEM83 stimulated the binding of T lymphocytes to L cells expressing ICAM-1, while inhibiting the interaction of CD11a/CD18 with cells expressing ICAM-2 and -3. The Ab NKI-L16 selectively induced adhesion to ICAM-1 and -2, but not to ICAM-3. On the other hand, PdBu was able to enhance the adhesion of T lymphocytes to all immobilized ICAMs (35). The differential effects of the activating Abs may be due to the

Carl_G_190x270_mm_blokki_FINAL.indd 291 06-Aug-23 1:53:55 PM

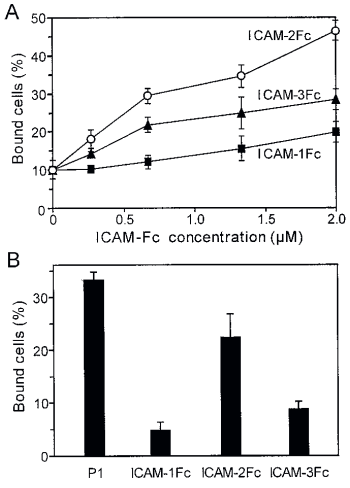

FIGURE 9. T lymphocyte adhesion to purified ICAM-1 and ICAM-2 induced by sICAM-1Fc, ICAM-2Fc, and ICAM-3Fc. *A*, T lymphocytes were treated with indicated concentrations of sICAMFc for 1 h at 20°C, and the cells bound to immobilized ICAM-1 were counted. In *B* the wells were coated with ICAM-2, and the cells stimulated with P1 (62 μM), ICAM-1Fc (1.4 μM), ICAM-2Fc (1.3 μM), or ICAM-3Fc (1.4 μM).

presence of different binding sites for ICAMs in the integrins (54). On the other hand, Woska et al. (55) have compared the binding of sICAM-1 and sICAM-3 with that of CD11a/CD18, and their data demonstrate that these two ICAMs share a common or an overlapping binding site on CD11a/CD18. Instead they found that the affinity of the sICAM-3/CD11a/CD18 interaction is 9–10 times weaker than the sICAM-1/CD11a/CD18 interaction. Therefore, the apparent differences in the binding sites for ICAMs in the integrins found in some reports could be attributed to these different affinities of ICAMs for β_2 integrins.

The P1 induced adhesion was dependent on temperature, energy, divalent cations, and an intact cytoskeleton, as it did not take place at low temperature, and it was blocked by a combination of sodium azide and deoxyglucose, by EDTA, and by the actin cytoskeleton disrupting agent cytochalasin D. Even though the adhesion requires a functional cytoskeleton, the P1 induced CD11/CD18 activation itself may not still need it. The P1 induced adhesion was insensitive to inhibitors of PKC and protein tyrosine kinases, suggesting that signaling events involving protein phosphorylation by these kinases are not required for activation of adhesion by the peptide. Petruzzelli et al. (56) have compared two mechanisms of activation of CD11a/CD18, namely inside out signaling by PMA and direct activation by the β2 Ab CBR LFA-1/2. Interestingly, and similarly to our findings with P1, they found that the activation of CD11a/CD18 by the mAb, in contrast to inside out signaling mechanisms, does not require PKC activation or protein phosphatase 2A activity, but it still requires cellular energy.

Intracellular calcium fluxes are apparently not involved in P1 induced activation either, as P1 did not increase the cytoplasmic free calcium concentration in Jurkat cells (results not shown). These results do not rule out the possibility that some signals are generated after P1 treatment. In fact, it has been shown that when increasing the migration and cytotoxicity of NK cells, P1 also increases the tyrosine phosphorylation of 150- and 35-kDa proteins

Importantly, leukocyte adhesion to ligands is critically dependent on the concentration of P1. Lower peptide concentrations (50–150 μg/ml) were stimulating, whereas high P1 concentrations (400 μg/ml and over) did not stimulate. It is possible that at lower P1 concentrations the peptide activates integrins by binding to stimulatory sites but that at higher concentrations it inhibits ICAM binding. Inhibition by sulfhydryl groups may also become important at higher concentrations, which is clearly seen in vitro (Table I). The concentration dependence could also explain why P1 inhibited the binding of endothelial cells to purified CD11a/CD18 integrin (22), when it on the other hand very efficiently stimulated the leukocyte adhesion to immobilized ICAMs. To block endothelial cell binding to plastic-coated integrins, 100 μg/ml P1 were needed. Evidently, this amount of peptide is enough to block the adhesion sites on the immobilized integrins, whereas higher concentrations are clearly needed for blocking the stimulatory effect of cellular integrins. Most probably, P1 cannot stimulate the activity of purified integrins, but additional cellular factors are needed.

The binding of sICAMs to T lymphocytes was strongly stimulated by P1. The effect of P1 resembles that obtained with Mg^{2+}/EGTA or Mn^{2+} treatment, which increases the affinity of integrins for sICAM-1 (57). P1 is clearly able to induce a high affinity state of the integrin, but in contrast to the Mg^{2+}/EGTA treatment it did not have the ability to induce the β_2 integrin LIBS (ligand-induced binding site) epitopes on T lymphocytes detected by mAb 24 or NKI-L16 (results not shown). These results indicate that P1 induces a different activation state than the other treatments.

The efficient activation of integrins by P1 made us consider whether ICAM-2 itself showed similar activity. We therefore produced the ICAM-2Fc fusion protein where the two extracellular Ig domains of ICAM-2 were fused with the Fc part of human IgG1. When these proteins were tested in the adhesion assays, we found that like P1, ICAM-2Fc was able to induce T lymphocyte adhesion to immobilized ICAM-1, -2, and -3. The control protein NCAMFc had a negligible effect. As often seen with proteins vs peptides, the ICAM-2Fc concentrations needed (0.27 to 2 μM) were much lower than the optimal P1 concentration (62 μM). When comparing the abilities of sICAMs to induce the adhesion of T lymphocytes to immobilized ICAM-1, we found that ICAM-2Fc was the most potent activator. ICAM-3Fc also had some activating effect on the T lymphocytes, whereas ICAM-1Fc showed almost no effect.

Because sICAM-2Fc has the ability to stimulate lymphocyte binding to ICAMs, it could be expected that immobilized ICAM-2 stimulates lymphocyte adhesion to itself in these adhesion experiments. This appears, however, not to be the case because the background binding of unstimulated cells to immobilized ICAM-1, -2 -and 3 (Fig. 8) and BSA (not shown) was almost the same. ICAM-2 is strongly expressed on endothelial cells and on lymphocytes (10, 11), and these results with sICAMFc proteins suggest that under some conditions ICAM-2 and specifically its P1 region could act as a stimulatory molecule, e.g., during leukocyte rolling on endothelium. Additional activity signals are evidently needed such as those provided by selectins or chemokines. ICAMs have been found as soluble molecules in plasma (16–18), and these could be physiologically important and not just shed inactive degradation products.

The ligand-induced adhesion by P1 is clearly different from that induced by inside out signaling stimulated by phorbol esters or by engagement of the CD3. Phorbol esters act through the activation of PKC, and these compounds as well as stimulation through the TCR induce serine and threonine phosphorylation in CD18 (44) and clustering of leukocyte integrins (58, 59). This is in contrast to

Carl_G_190x270_mm_blokki_FINAL.indd 292 06-Aug-23 1:53:56 PM

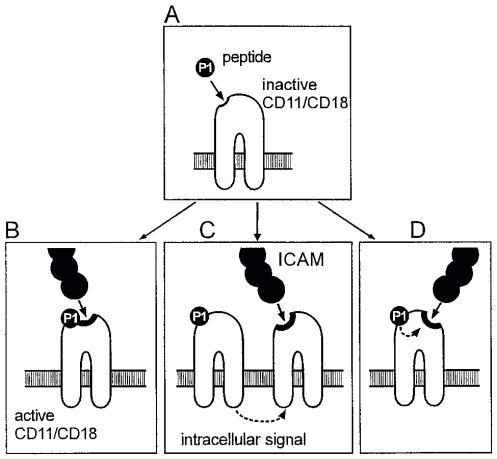

FIGURE 10. Three possible mechanisms for the P1-induced activation of CD11/CD18. After binding of the peptide to CD11/CD18 at a partially overlapping site, a conformational change may take place in the integrins, resulting in high affinity of the binding site for ICAMs (*B*). Another possibility is that intracellular signals are generated, and other integrins become activated by inside out signaling (*C*). The third major possibility is that P1 binding activates a separate binding site for ICAMs (*D*).

CD18 phosphorylation has been observed (22, 40). We could confirm the result of Hogg and coworkers that treatment with PdBu did not affect the affinity for ICAM-1 (49).

Three possible mechanisms of P1-induced CD11/CD18 activation are presented in Fig. 10. P1 binds to inactive CD11a/CD18 or CD11b/CD18 on leukocytes possibly in a slightly different position than ICAM-1 (Fig. 10*A*). In Fig. 10*B*, P1 binding induces a conformational change in the integrin resulting in a high affinity form of CD11/CD18. This change may persist after dissociation of the peptide. Alternatively, P1 generates intracellular signals, and this results in the activation of other integrins on the same cell by inside out signaling (Fig. 10*C*). In Fig. 10*D*, P1 and ICAMs bind to different sites on the CD11/CD18, and the binding of P1 induces a conformational change in the integrins resulting in a high affinity state of CD11/CD18 for ICAMs.

Our results suggest that intracellular signals are not necessarily needed for the binding of ICAM to P1-activated CD11/CD18. However, the interaction of integrins and ICAMs certainly generates intracellular signals which in turn result in, e.g., cell spreading and migration through endothelium or to the activation of molecules that are not directly bound by P1 such as CD11c/CD18 (42).

This finding that a peptide derived from ICAM-2 can stimulate integrin function resembles earlier findings using RGD peptides. RGD peptide binding leads to changes in $\alpha_{IIb}\beta_3$, which are associated with acquisition of high affinity fibrinogen binding function and subsequent platelet aggregation. No signal transduction event has been found, but rather the activation appears to be due to a conformational change in the receptor itself. Therefore, in addition to being recognized by the integrin, the RGD sequence serves as a trigger for high affinity ligand binding (60).

Acknowledgments

We thank Aili Grundström and Leena Kuoppasalmi for technical assistance, Yvonne Heinilä for secretarial work, and Drs. D. L. Simmons and W. M. Gallatin for providing vectors and proteins.

References

1. Springer, T. A. 1990. Adhesion receptors of the immune system. *Nature 346:425.*
2. Arnaout, M. A. 1990. Structure and function of the leukocyte adhesion molecules CD11/CD18. *Blood 75:1037.*
3. Patarroyo, M., J. Prieto, J. Rincon, T. Timonen, C. Lundberg, L. Lindbom, B. Åsjö, and C. G. Gahmberg. 1990. Leukocyte-cell adhesion: a molecular process fundamental in leukocyte physiology. *Immunol. Rev. 114:67.*
4. Carlos, T. M., and J. M. Harlan. 1994. Leukocyte-endothelial adhesion molecules. *Blood 84:2068.*
5. Gahmberg, C. G., M. Tolvanen, and P. Kotovuori. 1997. Leukocyte adhesion: structure and function of human leukocyte β_2-integrins and their cellular ligands. *Eur. J. Biochem. 245:215.*
6. Van der Vieren, M., H. Le Trong, C. L. Wood, P. F. Moore, T. St. John, D. E. Staunton, and W. M. Gallatin. 1995. A novel leukointegrin, $\alpha_d\beta_2$, binds preferentially to ICAM-3. *Immunity 3:683.*
7. Corbi, A. L. 1996. *Leukocyte Integrins: Structure, Expression and Function.* R. G. Landes Company, Austin, TX.
8. Hogg, N., P. A. Bates, and J. Harvey. 1991. Structure and function of intercellular adhesion molecule-1. In *Chemical Immunology. Integrins and ICAM-1 in Immune Responses,* N. Hogg, ed. S. Karger AG, Basel, p. 99.
9. Diacovo, T. G., A. R. De Fougerolles, D. F. Bainton, and T. A. Springer. 1994. A functional integrin ligand on the surface of platelets: intercellular adhesion molecule-2. *J. Clin. Invest. 94:1243.*
10. Nortamo, P., R. Li, R. Renkonen, T. Timonen, J. Prieto, M. Patarroyo, and C. G. Gahmberg. 1991. The expression of human intercellular adhesion molecule-2 is refractory to inflammatory cytokines. *Eur. J. Immunol. 21:2629.*
11. de Fougerolles, A. D., S. A. Stacker, R. Schwarting, and T. A. Springer. 1991. Characterization of ICAM-2 and evidence for a third counter-receptor for LFA-1. *J. Exp. Med. 174:253.*
12. de Fougerolles, A. R., and T. A. Springer. 1992. Intercellular adhesion molecule 3, a third adhesion counter-receptor for lymphocyte function-associated molecule 1 on resting lymphocytes. *J. Exp. Med. 175:185.*
13. Bailly, P., E. Tontti, P. Hermand, J.-P. Cartron, and C. G. Gahmberg. 1995. The red cell LW blood group protein is an intercellular adhesion molecule which binds to CD11/CD18 leukocyte integrins. *Eur. J. Immunol. 25:3316.*
14. Tian, L., Y. Yoshihara, T. Mizuno, K. Mori, and C. G. Gahmberg. 1997. The neuronal glycoprotein telencephalin is a cellular ligand for the CD11a/CD18 leukocyte integrin. *J. Immunol. 158:928.*
15. Mizuno, T., Y. Yoshihara, J. Inazawa, H. Kagamiyama, and K. Mori. 1997. cDNA cloning and chromosomal localization of the human telencephalin and its distinctive interaction with lymphocyte function-associated antigen-1. *J. Biol. Chem. 272:1156.*
16. Rothlein, R., E. A. Mainolfi, M. Czajkowski, and S. D. Marlin. 1991. A form of circulating ICAM-1 in human serum. *J. Immunol. 147:3788.*
17. Pozo del, M. A., R. Pulido, C. Muños, V. Alvarez, A. Humbría, M. R. Campanero, and F. Sánchez-Madrid. 1994. Regulation of ICAM-3 (CD50) membrane expression on human neutrophils through a proteolytic shedding mechanism. *Eur. J. Immunol. 24:2586.*
18. Pino-Otín, M., O. Viñas, M. A. de la Fuente, M. Juan, J. Font, M. Torradeflot, L. Pallarés, F. Lozano, J. Alberola-Ila, J. Martorell, J. Yague, J. Vives, and A. Gaya. 1995. Existence of a soluble form of CD50 (intercellular adhesion molecule-3) produced upon human lymphocyte activation. *J. Immunol. 154:3015.*
19. Staunton, D. E., M. L. Dustin, H. P. Erickson, and T. A. Springer. 1990. The arrangement of the immunoglobulin-like domains of ICAM-1 and the binding sites for LFA-1 and rhinovirus. *Cell 61:243.*
20. Ross, L., F. Hassman, and L. Molony. 1992. Inhibition of Molt-4-endothelial adherence by synthetic peptides from the sequence of ICAM-1. *J. Biol. Chem. 267:8537.*
21. Staunton, D. E., M. L. Dustin, and T. A. Springer. 1989. Functional cloning of ICAM-2, a cell adhesion ligand for LFA-1 homologous to ICAM-1. *Nature 339:61.*
22. Li, R., P. Nortamo, L. Valmu, M. Tolvanen, C. Kantor, and C. G. Gahmberg. 1993. A peptide from ICAM-2 binds to the leukocyte integrin CD11a/CD18 and inhibits endothelial cell adhesion. *J. Biol. Chem. 268:17513.*
23. Vazeux, R., P. A. Hoffman, J. K. Tomita, E. S. Dickinson, R. L. Jasman, T. St. John, and W. M. Gallatin. 1992. Cloning and characterization of a new intercellular adhesion molecule ICAM-R. *Nature 360:485.*
24. Fawcett, J., C. L. L. Holness, L. A. Needham, H. Turley, K. C. Gatter, D. Y. Mason, and D. L. Simmons. 1992. Molecular cloning of ICAM-3, a third ligand for LFA-1, constitutively expressed on resting leukocytes. *Nature 360: 481.*
25. Juan, M., R. Vilella, J. Mila, J. Yagüe, A. Miralles, K. S. Campbell, R. J. Friedrich, J. Cambier, J. Vives, A. R. de Fougerolles, and T. A. Springer. 1993. CDw50 and ICAM-3: two names for the same molecule. *Eur. J. Immunol. 23:1508.*
26. Diamond, M. S., D. E. Staunton, S. D. Marlin, and T. A. Springer. 1991. Binding of the integrin Mac-1 (CD11b/CD18) to the third immunoglobulin-like domain of ICAM-1 (CD54) and its regulation by glycosylation. *Cell 65:961.*
27. Altieri, D. C., R. Bader, P. M. Mannucci, and T. S. Edgington. 1988. Oligospecificity of the cellular adhesion receptor MAC-1 encompasses an inducible recognition specificity for fibrinogen. *J. Cell. Biol. 107:1893.*
28. Altieri, D. C., and T. S. Edgington. 1988. The saturable high affinity association of factor X to ADP-stimulated monocytes defines a novel function of the Mac-1 receptor. *J. Biol. Chem. 263:7007.*
29. Dustin, M. L., and T. A. Springer. 1989. T-cell receptor cross-linking transiently stimulates adhesiveness through LFA-1. *Nature 341:619.*

30. van Kooyk, Y., P. van de Wiel, P. van de Kemenade, P. Weder, T. W. Kuijpers, and C. G. Figdor. 1989. Enhancement of LFA-1-mediated cell adhesion by triggering through CD2 or CD3 on T lymphocytes. *Nature 342:811.*
31. Patarroyo, M., P. G. Beatty, J. W., Fabre, and C. G. Gahmberg. 1985. Identification of a cell surface protein complex mediating phorbol ester-induced adhesion (binding) among human mononuclear leukocytes. *Scand. J. Immunol. 22: 171.*
32. Rothlein, R., and T. A. Springer. 1986. The requirement for lymphocyte function-associated antigen 1 in homotypic leukocyte adhesion stimulated by phorbol ester. *J. Exp. Med. 163:1132.*
33. Axelsson, B., R. Youseffi-Etemad, S. Hammarström, and P. Perlmann. 1988. Induction of aggregation and enhancement of proliferation and IL-2 secretion in human T cells by antibodies to CD43. *J. Immunol. 141:2912.*
34. Koopman, G., Y. van Kooyk, M. de Graaff, C. J. L. M. Meyer, C. G. Figdor, and S. T. Pals. 1990. Triggering of the CD44 antigen on T lymphocytes promotes T cell adhesion through the LFA-1 pathway. *J. Immunol. 145:3589.*
35. Vermot-Desroches, C., J. Wijdenes, L. Valmu, C. Roy, R. Pigott, P. Nortamo, and C. G. Gahmberg. 1995. A CD44 monoclonal antibody differentially regulates CD11a/CD18 binding to intercellular adhesion molecules CD54, CD102 and CD50. *Eur. J. Immunol. 25:2460.*
36. Landis, R. C., R. I. Bennett, and N. Hogg. 1993. A novel LFA-1 activation epitope maps to the I domain. *J. Cell Biol. 120:1519.*
37. Robinson, M. K., D. Andrew, H. Rosen, D. Brown, S. Ortlepp, P. Stephens, and E. C. Butcher. 1992. Antibody against the Leu-CAM β-chain (CD18) promotes both LFA-1- and CD3-dependent adhesion events. *J. Immunol. 148:1080.*
38. Andrew, D., A. Shock, E. Ball, S. Ortlepp, J. Bell, and M. Robinson. 1993. KIM185, a monoclonal antibody to CD18 which induces a change in the conformation of CD18 and promotes both LFA-1- and CR3-dependent adhesion. *Eur. J. Immunol. 23:2217.*
39. Ortlepp, S., P. E. Stephens, N. Hogg, C. G. Figdor, and M. K. Robinson. 1995. Antibodies that activate β_2 integrins can generate different ligand binding states. *Eur. J. Immunol. 25:637.*
40. Li, R., P. Nortamo, C. Kantor, P. Kovanen, T. Timonen, and C. G. Gahmberg. 1993. A leukocyte integrin binding peptide from intercellular adhesion molecule-2 stimulates T cell adhesion and natural killer cell activity. *J. Biol. Chem. 268:21474.*
41. Li, R., J. Xie, C. Kantor, V. Koistinen, D. C. Altieri, P. Nortamo, and C. G. Gahmberg. 1995. A peptide derived from the intercellular adhesion molecule-2 regulates the avidity of the leukocyte integrins CD11b/CD18 and CD11c/CD18. *J. Cell Biol. 129:1143.*
42. Somersalo, K., O. Carpén, E. Saksela, C. G. Gahmberg, P. Nortamo, and T. Timonen. 1995. Activation of natural killer cell migration by leukocyte integrin-binding peptide from intercellular adhesion molecule-2 (ICAM-2). *J. Biol. Chem. 270:8629.*
43. Nortamo, P., M. Patarroyo, C. Kantor, J. Suopanki, and C. G. Gahmberg. 1988. Immunological mapping of the human leukocyte adhesion glycoprotein GP90 (CD18) by monoclonal antibodies. *Scand. J. Immunol. 28:537.*
44. Valmu, L., and C. G. Gahmberg. 1995. Treatment with okadaic acid reveals strong threonine phosphorylation of CD18 after activation of CD11/CD18 leukocyte integrins with phorbol esters or CD3 antibodies. *J. Immunol. 155:1175.*
45. Xie, J., R. Li, P. Kotovuori, C. Vermot-Desroches, J. Wijdenes, M. A. Arnaout, P. Nortamo, and C. G. Gahmberg. 1995. Intercellular adhesion molecule-2 (CD102) binds to the leukocyte integrin CD11b/CD18 through the A domain. *J. Immunol. 155:3619.*
46. Simmons, D. L. 1993. Cloning cell surface molecules by transient expression in mammalian cells. In *Cellular Interaction in Development*, D. Hartley, ed. Oxford University Press, Oxford, p. 93.
47. Laemmli, U. K. 1970. Cleavage of structural proteins during the assembly of the head of bacteriophage T4. *Nature 227:680.*
48. Hedman, H., H. Brändén, and E. Lundgren. 1992. Physical separation of ICAM-1 binding cells. *J. Immunol. Methods 146:203.*
49. Stewart, M. P., C. Cabañas, and N. Hogg. 1996. T cell adhesion to intercellular adhesion molecule-1 (ICAM-1) is controlled by cell spreading and the activation of integrin LFA-1. *J. Immunol. 156:1810.*
50. Detmers, P. A., S. D. Wright, E. Olsen, B. Kimball, and Z. A. Cohn. 1987. Aggregation of complement receptors on human neutrophils in the absence of ligand. *J. Cell Biol. 105:1137.*
51. Ross, G. D., W. Reed, J. G. Dalzell, S. E. Becker, and N. Hogg. 1992. Macrophage cytoskeleton association with CR3 and CR4 regulates receptor mobility and phagocytosis of iC3b-opsonized erythrocytes. *J. Leukocyte Biol. 51:109.*
52. Helander, T. S., O. Carpén, O. Turunen, P. E. Kovanen, A. Vaheri, and T. Timonen. 1996. ICAM-2 redistributed by ezrin as a target for killer cells. *Nature 382:265.*
53. Dedhar, S. and G. E. Hannigan. 1996. Integrin cytoplasmic interactions and bidirectional transmembrane signalling. *Curr. Opin. Cell Biol. 8:657.*
54. Binnerts, M. E., Y. van Kooyk, D. L. Simmons, and C. G. Figdor. 1994. Distinct binding of T lymphocytes to ICAM-1, -2 or -3 upon activation of LFA-1. *Eur. J. Immunol. 24:2155.*
55. Woska, J. R., Jr., M. M. Morelock, D. D. Jeanfavre, G. O. Caviness, B.-J. Bormann, and R. Rothlein. 1998. Molecular comparison of soluble intercellular adhesion molecule (sICAM)-1 and sICAM-3 binding to lymphocyte function-associated antigen-1. *J. Biol. Chem. 273:4725.*
56. Petruzzelli, L., L. Maduzia, and T. A. Springer. 1998. Differential requirements for LFA-1 binding to ICAM-1 and LFA-1-mediated cell aggregation. *J. Immunol. 160:4208.*
57. Dransfield, I., C. Cabañas, A. Craig, and N. Hogg. 1992. Divalent cation regulation of the function of the leukocyte integrin LFA-1. *J. Cell Biol. 116:219.*
58. Lub, M., Y. van Kooyk, and C. G. Figdor. 1995. Ins and outs of LFA-1. *Immunol. Today 16:479.*
59. Kucik, D. F., M. L. Dustin, J. M. Miller, and E. J. Brown. 1996. Adhesion-activating phorbol ester increases the mobility of leukocyte integrin LFA-1 in cultured lymphocytes. *J. Clin. Invest. 97:2139.*
60. Du, X., E. F. Plow, A. Frelinger III, T. O'Toole, J. C. Loftus, and M. H. Ginsberg. 1991. Ligands "activate" integrin $\alpha_{IIb}\beta_3$ (platelet GPIIb-IIIa). *Cell 65:409.*

Carl_G_190x270_mm_blokki_FINAL.indd 294 06-Aug-23 1:53:57 PM

Inhibition of β_2 Integrin–mediated Leukocyte Cell Adhesion by Leucine–Leucine–Glycine Motif–containing Peptides

Erkki Koivunen,* Tanja-Maria Ranta,* Arto Annila,‡ Seija Taube,* Asko Uppala,* Marjukka Jokinen,* Gijsbert van Willigen,* Eveliina Ihanus,* and Carl G. Gahmberg*

*Department of Biosciences, Division of Biochemistry, and ‡VTT Biotechnology, University of Helsinki, FIN-00014 Helsinki, Finland

Abstract. Many integrins mediate cell attachment to the extracellular matrix by recognizing short tripeptide sequences such as arginine–glycine–aspartic acid and leucine–aspartate–valine. Using phage display, we have now found that the leukocyte-specific β_2 integrins bind sequences containing a leucine–leucine–glycine (LLG) tripeptide motif. An LLG motif is present on intercellular adhesion molecule (ICAM)-1, the major β_2 integrin ligand, but also on several matrix proteins, including von Willebrand factor. We developed a novel β_2 integrin antagonist peptide CPCFLLGCC (called LLG-C4), the structure of which was determined by nuclear magnetic resonance. The LLG-C4 peptide inhibited leukocyte adhesion to ICAM-1, and, interestingly, also to von Willebrand factor. When immobilized on plastic, the LLG-C4 sequence supported the β_2 integrin–mediated leukocyte adhesion, but not β_1 or β_3 integrin–mediated cell adhesion. These results suggest that LLG sequences exposed on ICAM-1 and on von Willebrand factor at sites of vascular injury play a role in the binding of leukocytes, and LLG-C4 and peptidomimetics derived from it could provide a therapeutic approach to inflammatory reactions.

Key words: cell adhesion • extracellular matrix • leukocyte • phage display • peptides

Introduction

The migration of leukocytes through the body and the various lymphoid organs is an essential element of the immune system. While circulating in blood or lymphatic vessels, leukocytes are in a resting and low adhesive state. However, when leukocytes are stimulated by signals from the immune system, such as exposure to an immune complex or a chemokine gradient, their integrin adhesion receptors become activated (Hemler, 1990; Hynes, 1992; Springer, 1994; Gahmberg et al., 1997). The activation of the integrins is essential for the many leukocyte functions. Such functions are, for example, binding to antigen-presenting cells, recirculation through lymph nodes, and migration out of the vasculature and through the extracellular matrix to sites of inflammation. The integrin activation needs to be tightly regulated as inappropriate leukocyte adhesion leads to injury of normal tissues.

Leukocytes express a specific subset of the integrin family, the β_2 integrins, of which four members are known. They have a common β_2 chain (CD18), but different α subunits (α_L or CD11a, α_M or CD11b, α_X or CD11c, α_D or CD11d) (Gahmberg et al., 1997). The α subunits contain a conserved 200-residue A or I domain, which is essential for binding of most ligands. The crystal structures of I domains from the α_L and α_M subunits indicate the presence of a cation binding site called the metal-dependent adhesion site (Lee et al., 1995; Qu and Leahy, 1995). Amino acid substitutions in this site abrogate ligand binding (Huang and Springer, 1995; Kamata et al., 1995).

The major ligands of these integrins, the intercellular adhesion molecules (ICAMs),[1] belong to the Ig superfamily, and five ICAMs with slightly different binding specificities have been described (Simmons et al., 1988; Staunton et al., 1989; Fawcett et al., 1992; Bailly et al., 1995; Tian et al., 1997). The expression of ICAM-1 on endothelial cells is subject to stimulation by inflammatory cytokines, which enhances the β_2 integrin–mediated adhesion of leukocytes on endothelial cells (Springer, 1994; Gahmberg et al., 1997). In addition to the ICAMs, fibrinogen (Languino et al., 1993) and the iC3b complement protein (Ueda et al., 1994; Kamata et al., 1995) are known ligands of the β_2 integrins, particularly of $\alpha_M\beta_2$ (Mac-1).

Address correspondence to Erkki Koivunen, Department of Biosciences, Division of Biochemistry, University of Helsinki, Viikinkaari 5, FIN-00014 Helsinki, Finland. Tel.: (358) 9-191-59023. Fax: (358) 9-191-59068. E-mail: erkki.koivunen@helsinki.fi

[1]*Abbreviations used in this paper:* GST, glutathione *S*-transferase; ICAM, intercellular adhesion molecule; LLG, leucine–leucine–glycine; NMR, nuclear magnetic resonance; nOe, nuclear Overhauser enhancement; RGD, arginine–glycine–aspartic acid; TNF, tumor necrosis factor.

© The Rockefeller University Press, 0021-9525/2001/05/905/11 $5.00
The Journal of Cell Biology, Volume 153, Number 5, May 28, 2001 905–915
http://www.jcb.org/cgi/content/full/153/5/905

Carl_G_190x270_mm_blokki_FINAL.indd 295 06-Aug-23 1:53:58 PM

Because of the importance of the β_2 integrins for leukocyte function, antagonists of them are potential antiinflammatory agents. Antibodies to β_2 integrins or ICAMs have a therapeutic effect in animal models of immune system disorders (Clark et al., 1991; Kavanaugh et al., 1994; Miyamoto et al., 1999). Agents targeting the β_2 integrins could also be valuable in the development of therapeutic strategies to human leukemias (Lalancette et al., 2000). However, only a few small molecule antagonists of the β_2 integrins have been described so far (Kallen et al., 1999; Kelly et al., 1999). Lack of such compounds has prevented the detailed examination of the role of each member of the β_2 integrin family in leukemia dissemination as well in inflammatory diseases. In particular, it would be desirable to design compounds that distinguish between the inactive and active state of an integrin. Modeling of such small molecule inhibitors has been hampered by the large size of the peptide ligands developed so far. Linear peptides are often without a well-defined structure when free in solution. Among the few β_2 integrin ligands discovered is the 22–amino acid–long peptide known as P1, which was derived from ICAM-2 (Li et al., 1993). This peptide retains the leukocyte integrin–activating effect that is typical for ICAM-2 (Li et al., 1995; Kotovuori et al., 1999). Complementarity-determining regions of anti-β_2 integrin antibodies have been another source of ligand peptides (Feng et al., 1998).

To develop smaller peptide ligand-leads to the β_2 integrins, we have screened random peptide libraries displayed on filamentous phage. The phage display technique has previously yielded selective peptide ligands to the integrin species $\alpha_5\beta_1$ (Koivunen et al., 1994), $\alpha_V\beta_3/\beta_5$ (Koivunen et al., 1995), and $\alpha_V\beta_6$ (Kraft et al., 1999). Phage library screenings have confirmed the earlier findings that the tripeptide sequence arginine–glycine–aspartic acid (RGD) is a common recognition sequence of a subset of integrins (Pierschbacher and Ruoslahti, 1984). The leukocyte integrins $\alpha_4\beta_1$ and $\alpha_4\beta_7$ are known to have a specificity for peptides containing another type of tripeptide sequence, leucine–aspartate–valine (Komoriya et al., 1991). We have now found that the $\alpha_M\beta_2$ integrin also shares the ability to recognize a motif comprising three amino acids, thus showing a functional similarity to other integrins. The tripeptide favored by $\alpha_M\beta_2$ turned out to be a previously unknown adhesion motif, leucine–leucine–glycine (LLG). Interestingly, such sequences are present on several adhesion proteins, such as ICAM-1 and von Willebrand factor. We developed a nonapeptide ligand LLG-C4, which has a compact disulfide-restrained structure as determined by nuclear magnetic resonance (NMR). This biscyclic peptide is a potent inhibitor of leukocyte cell adhesion and migration, and is a novel lead compound for development of antiinflammatory agents.

Materials and Methods

Monoclonal Antibodies

Antibodies against the integrin β_2 subunit were 7E4, 11D3, 3F9, 2E7, 1D10, and 2F3 (Nortamo et al., 1988). The anti-α_L subunit antibodies were TS2/4 and MEM-83 (Monosan). The antibodies OKM1, OKM10, and MEM-170 were used against the anti-α_M subunit, and the antibody 3.9 was used against the α_X subunit (Li et al., 1993, 1995). The $\alpha_{IIb}\beta_3$ integrin antibody P2 was purchased from Immunotech, and the $\alpha_V\beta_3$ integrin antibody LM609 and the β_1 subunit antibody 6S6 were from Chemicon.

Peptide Synthesis

Peptide synthesis was carried out using Fmoc chemistry (model 433A; Applied Biosystems). Disulfides were formed by oxidation in 10 mM ammonium bicarbonate buffer, pH 9, overnight. Peptides were then purified by HPLC on an acetonitrile gradient. Generation of disulfides was confirmed by mass spectrometry analysis. The C(1-8;3-9) and C(1-9;3-8) peptides with the guided disulfide bridges were custom-made by Anaspec. The ACDCRGDCFCG (RGD-4C) peptide (Koivunen et al., 1995) was obtained from Dr. E. Ruoslahti (The Burnham Institute, San Diego, CA).

Phage Display

The $\alpha_M\beta_2$ integrin was purified by antibody affinity chromatography from buffy coats obtained from the Finnish Red Cross blood transfusion service (Li et al., 1995). Integrin was diluted in TBS/1 mM $MnCl_2$ and coated onto microtiter wells using 1 μg/well for the first biopanning and 100, 10, and 1 ng for subsequent pannings. Biopanning was performed using CX_7C and CX_9C phage libraries essentially as described (Koivunen et al., 1994). For construction of the libraries, the single-stranded DNA encoding degenerate sequences was converted into a double-stranded form using 5 cycles of PCR with only the reverse primer, followed by 11 cycles in the presence of both the reverse and forward primers. 6 μg of the double-stranded oligonucleotide was purified using a PCR purification kit (QIAGEN) and ligated with 42 μg of the Fuse5 phage vector. The number of recombinants in the libraries was $>10^9$. Phage binding, elution, and subsequent amplification in *Escherichia coli* were repeated five times, and after each panning bacterial colonies were picked up and stored in a 10-μl vol of TBS in microtiter wells at −20°C. For direct colony sequencing, a 1-μl aliquot of the thawed samples was subjected to PCR with 10 pmol each of the forward primer 5′-TAATACGACTCACTATAGGGCAAGCTGATAAACCGATACAATT-3′ and the reverse primer 5′-CCCTCATAGTTAGCGTAACGATCT-3′. The PCR conditions were 92°C for 30 s, 60°C for 30 s, and 72°C for 60 s, and the cycle number was 35. A 1-μl aliquot of the PCR reaction was taken for sequencing using 15 pmol of either one of the primers and analyzed on an ABI 310 apparatus (PE Biosystems).

Preparation of Glutathione S-transferase and Fc Fusion Proteins

The nucleotide sequence coding for LLG-C4 was PCR amplified from phage DNA with the primers containing a BamHI 5′-AGGCTCGAGGATCCTCGGCCGACGGGGCT-3′ and an EcoRI site 5′-AGGTCTAGAATTCGCCCCAGCGGCCCC-3′. The PCR product was purified on an agarose gel, digested with the two restriction enzymes, and ligated into the PGEX-2TK vector (Amersham Pharmacia Biotech). Recombinants expressing LLG-C4-Glutathione S-transferase (GST) were verified by DNA sequencing. LLG-C4-GST was produced in *E. coli* strain BL 21 and purified by glutathione affinity chromatography followed by dialysis. ICAM-1-Fc fusion protein containing the five ICAM-1 Ig domains was produced in CHO cells and purified by protein A affinity chromatography (Hedman et al., 1992) α_M I domain was expressed as a GST fusion protein in *E. coli* and purified by affinity chromatography on glutathione-coupled beads followed by cleavage with thrombin to release the recombinant I domain (Ueda et al., 1994).

Integrin Binding Assays

Integrins were immunocaptured on microtiter wells that were coated with nonspecific IgG or the subunit antibodies OKM1, MEM170, TS2/4, 2E7, or 7E4. A 200-μl aliquot of the buffy coat lysate in 1% octylglucoside/1 mM $MnCl_2$/TBS was allowed to incubate for 2 h at 4°C. The wells were then washed five times with the octylglucoside-containing buffer. LLG-C4-GST or GST (10 μg/ml) was incubated in the integrin-coated or the α_M I domain–coated wells in 25 mM octylglucoside/TBS/1 mM $MnCl_2$ for 1 h. After washing of the wells, the bound GST was determined with anti-GST antibodies (Amersham Pharmacia Biotech), which were labeled with an Eu^{3+} chelate according to the instructions of the manufacturer (Wallac). The Eu^{3+} fluorescence was measured with a fluorometer (1230 Arcus; Wallac).

Cell Culture

The leukocytic cell lines THP-1, Jurkat, U-937, and K562 were maintained as described (Li et al., 1995). The nonleukocytic cell lines Eahy926, HT1080, KS6717, and SKOV-3 were as described previously (Koivunen et al., 1999). T cells were isolated from blood buffy coats by Ficoll-Hypaque

Carl_G_190x270_mm_blokki_FINAL.indd 296 06-Aug-23 1:53:59 PM

centrifugation, followed by passage through nylon wool columns (Valmu and Gahmberg, 1995). Wild-type mouse L929 cells and the $\alpha_X\beta_2$ integrin–transfected L cell line were obtained from Dr. Y. van Kooyk (University Hospital, Nijmegen, Netherlands).

Cell Adhesion

Fibrinogen (Calbiochem), fibronectin (Boehringer), von Willebrand factor (Calbiochem), GST fusion proteins, Fc fusion proteins, or synthetic peptides were coated on microtiter wells at a concentration of 2 μg in 50 μl TBS unless otherwise indicated. The wild-type and A2 domain–deleted recombinant von Willebrand factors (Lankhof et al., 1997) and a capturing anti-von Willebrand factor antibody D′-D3 used for coating were provided by Drs. J.J. Sixma and Ph.G. de Groot (University Medical Center, Utrecht, Netherlands). To prepare polymerized peptides, glutaraldehyde (Merck) was added at a final concentration of 0.25%. The wells were saturated with 5% BSA and then washed five times with PBS. Before adhesion assays, cells were treated with 50 nM 4β-phorbol 12,13-dibutyrate (Sigma-Aldrich) or with 200 μM P1 peptide (Kotovuori et al., 1999) in serum-free medium for 30 min at room temperature to activate the integrins. Alternatively, cells were stimulated for 60 min at 37°C with the phorbol ester (50 nM) and the C(1-8;3-9) and RGD-4C peptides, each at a 2.5 μM concentration, after which the peptides were removed by washing with PBS/2.5 mM EDTA. Cells (100,000 per well) were incubated in the microtiter wells for 60 min at 37°C in the absence or presence of competing peptides, antibodies, or EDTA. Unbound cells were removed by gently washing with PBS and pressing the plate against paper towels. The bound cells were determined by an assay measuring cellular phosphatase activity (Li et al., 1995). Alternatively, the attached cells were stained with Crystal Violet (Sigma-Aldrich) essentially as described (Mould et al., 1995). To study T cell binding to an endothelial cell monolayer, Eahy926 endothelial cells were plated on microtiter plates at a density of 5×10^4 cells per well and grown for 3 d. To stimulate the production of ICAM-1, the cells were further grown for 16 h in the presence of tumor necrosis factor (TNF)-α (10 ng/ml; Roche). T cells (1.5×10^5 per well) were allowed to bind to Eahy926 cells for 30 min at 4°C, and then 15 min at 37°C. The unbound T cells were removed by immersing the microtiter plate upside down in PBS. The bound cells were determined by the phosphatase assay.

Cell Migration

Cell migration was studied using 8-μm pore size Transwell filters (Costar). Both the upper and lower filter surfaces were coated with fibrinogen, LLG-C4-GST, or GST at a concentration of 40 μg/ml. Free binding sites were blocked with 5% BSA. THP-1 cells (5×10^4 in 100 μl) were plated on the upper compartment in 10% serum-containing medium in the absence or presence of C(1-8;3-9) or C(1-9;3-8) (200 μM). The lower compartment was filled with 750 μl of the same medium. After a culture for 18 h at 37°C, the filters were immersed in methanol for 15 min, in water for 10 s, and in 0.1% toluidine blue (Sigma-Aldrich) for 5 min. The filters were then washed three to five times with water until cell staining was clear. Cells were removed from the upper surface of the filter with a cotton swab, and cells migrated on the lower surface were counted microscopically. A Student's *t* test was used for statistical analysis.

NMR Analysis of Peptides

For NMR structure determination, the C(1-8;3-9) peptide was dissolved in DMSO/H_2O (90/10) and C(1-9;3-8) in H_2O at the concentrations of 1–3 mM. Two-dimensional spectra, acquired with spectrometers operating at 600- and 800-MHz ^1H frequency, allowed us to identify 114 nuclear Overhauser enhancements (nOes) for C(1-8;3-9) and 85 for C(1-9;3-8) peptide. 40 structures with no restraint violations above 0.2 Å were selected from families of 200 structures generated by simulated annealing (DYANA program; Güntert et al., 1997).

Results

The LLG Peptide Motif Binds to a β_2 Integrin

We used the CX_7C and CX_9C phage libraries to search for peptide ligands to purified $\alpha_M\beta_2$ integrin. After the fifth round of selection, the CX_7C library gave a 600-fold enrichment and CX_9C a 1,000-fold enrichment of phage bound to the integrin in comparison to background. Sequencing of the bound phage revealed altogether only seven different sequences, indicating selection of specific peptides by the integrin (Table I). Four of them contained the LLG tripeptide motif. The two sequences most strongly enriched were CPCFLLGCC (LLG-C4) and CWKLLGSEEEC, and these were the only clones remaining after searching for high affinity binders by using low integrin-coating concentrations. Screening protein databases indicated that the LLG tripeptide sequence is present on several adhesion proteins. Most interestingly, it is located on the first Ig domain of ICAM-1, just preceding the Glu-34 residue, which is critical for ICAM-1 binding to the $\alpha_L\beta_2$ integrin (Staunton et al., 1990; Stanley and Hogg, 1998). The CWKLLGSEEEC peptide showed the highest similarity, five out of six consecutive residues being identical to the ICAM-1 sequence (Table I). The LLG tripeptide sequence is also contained in domains A2 and D3 of von Willebrand factor. These LLG-containing sequences, except that of ICAM-1, have not been reported previously to contain potential cell attachment sites.

We focused our studies on the LLG-C4 nonapeptide because it showed higher affinity to $\alpha_M\beta_2$ in phage-binding experiments in comparison to the other clones (data not shown). Due to the presence of four cysteine residues, the peptide appeared to be structurally constrained by two disulfide bonds. We first examined whether an integrin-binding peptide could be obtained by bacterial expression of LLG-C4 tethered to GST. The LLG-C4-GST fusion protein, but not GST alone, had a potent activity and bound to the $\alpha_M\beta_2$ integrin in a divalent cation–sensitive manner like a typical integrin ligand. The cation chelator EDTA inhibited the binding of LLG-C4-GST to the integrin, which was immunocaptured on microtiter wells with the α_M subunit antibodies MEM170 or OKM1 (Fig. 1 A). Similar EDTA-inhibitable binding of LLG-C4-GST was detected with the $\alpha_L\beta_2$ integrin, which was captured with the TS2/4 antibody. Surprisingly, EDTA only partially inhibited LLG-C4-GST binding when the β_2 subunit antibody 2E7 was used. We have found this antibody to stimulate leukocyte adhesion to various matrix proteins. LLG-C4-GST binding did not differ from GST control and was not inhibitable by EDTA, when a nonspecific IgG was used for immunocapture (not shown).

We next studied whether the peptide can directly interact with the I domain of the $\alpha_M\beta_2$ integrin, the known ligand binding site. LLG-C4-GST, examined at the concentrations of 0.01–100 μg/ml, showed a concentration-dependent binding to the isolated I domain of the α_M subunit (Fig. 1 B). GST at the same concentrations did not bind. The ability of the I domain to bind LLG-C4-GST was dependent on the Mn^{2+} cations added to the binding medium, and chelating Mn^{2+} with EDTA blocked the binding (Fig. 1 C). Initially, we encountered difficulties in chemical synthesis of an active and water-soluble LLG-C4 peptide, apparently because mixed disulfides easily formed during air oxidation. One LLG-C4 (1) preparation was highly active and blocked the ability of the I domain to bind the LLG-C4-GST (Fig. 1 C). The same peptide was also active in cell culture experiments. Another preparation, LLG-C4 (2), was inactive apparently due to disad-

Carl_G_190x270_mm_blokki_FINAL.indd 297 06-Aug-23 1:53:59 PM

Table I. Seven Phage Sequences Bound to the $\alpha_M\beta_2$ Integrin (Mac-1) and their Alignment with LLG-containing Sequences Present in Cell Adhesion Proteins

	CPCFLLGCC	(15)
	CWKLLGSEEEC	(15)
	CWHKDLLGC	(4)
	CWSMELLGC	
	CPPDLFWYC	(4)
	CPEDLYFFC	(3)
	CPEDFIFFC	
ICAM-1	CDQPKLLGIETPL	
von Willebrand factor A2	TVGPGLLGVSTLG	
von Willebrand factor D3	GRYIILLGKALSV	
Type I collagen-α2	PGPQGLLGAPGIL	
Type IV collagen-α4	PGPPGLLGRPGEA	

The amino acids that are identical to the phage peptides are shown in bold. The ICAM-1 sequence is from the first Ig domain (Simmons et al., 1988). The von Willebrand factor sequences are from A2 and D3 domains (Lynch et al., 1985) and the type I and IV collagen sequences are from α chains (De Wet et al., 1987; Leinonen et al., 1994). The number of isolated nucleotide sequences encoding each peptide is indicated in parentheses.

vantageous disulfide bonding and did not inhibit LLG-C4-GST binding to the I domain.

Immobilized LLG-C4 Nonapeptide Selectively Supports β2 Integrin–mediated Cell Adhesion

We examined the integrin-binding specificity of LLG-C4 in cell adhesion assays. Phorbol ester–activated THP-1 monocytic cells efficiently bound to LLG-C4-GST, but not to GST or peptide-GST controls (CLRSGRGC-GST, CPPWWSQC-GST) coated on microtiter wells (Fig. 2 A). EDTA at a concentration of 2.5 mM abolished the binding. Screening with a panel of antiintegrin antibodies indicated that the cell adhesion on LLG-C4-GST was completely inhibited by the blocking antibody to the β_2 chain, 7E4 (Fig. 2 B). Antibodies to the β_1 (6S6) and β_3 integrins (LM609, P2) had no effect. Partial inhibition was obtained with the β_2 chain antibodies 11D3 and 3F9. The order of the potency of the three β_2 antibodies is the same as that obtained previously in other assays (Nortamo et al., 1988). We also studied the β_2 chain antibodies 2E7, 1D10, and 2F3 that activate the β_2 integrin–mediated cell adhesion. In accordance, each of these antibodies stimulated THP-1 adhesion on LLG-C4-GST (data not shown).

Studies with antibodies against the integrin α subunits showed that the α_X subunit antibody 3.9 effectively inhibited the THP-1 adhesion to LLG-C4-GST. The α_M subunit antibodies OKM10, MEM170, and 60.1 were weakly inhibitory, whereas the α_L-directed antibodies TS1/22 and TS2/4 had hardly any effect. Furthermore, we found that the α_X antibody 3.9 and the α_M antibody OKM10 had a synergistic effect when added together, causing a complete inhibition of the cell adhesion.

THP-1 cells similarly bound strongly to the synthetic air-oxidized LLG-C4 nonapeptide coated on plastic, and the antibodies against the $\alpha_M\beta_2$ and $\alpha_X\beta_2$ integrins (3.9, OKM10, and 7E4) prevented the binding (data not shown). To determine the arrangement of the disulfide bonds in the active form of LLG-C4, we prepared synthetic peptides with different disulfide configurations. The most active peptide, C(1-8;3-9), was obtained by directing one disulfide

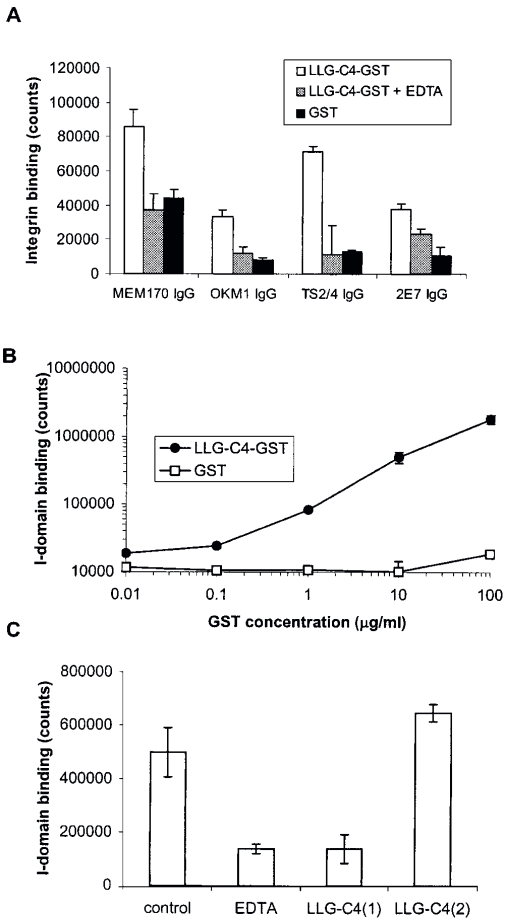

Figure 1. Divalent cation–dependent binding of LLG-C4 nonapeptide to leukocyte β_2 integrin and its I domain. (A) Integrin from a blood cell lysate was immunocaptured on microtiter wells using the α_M subunit antibody MEM170 or OKM1, the α_X subunit antibody TS2/4, or the β_2 subunit antibody 2E7. Purified LLG-C4-GST or GST control (2 μg/well) was allowed to bind for 60 min in the absence or presence of EDTA. The bound GST protein was determined by using anti-GST antibodies. The results show the means ± SD from triplicate wells. The experiment was repeated three times with similar results. (B) LLG-C4-GST or GST was incubated in microtiter wells coated with purified α_M subunit I domain. The concentrations of GST proteins were as indicated. The bound GST was determined with anti-GST antibodies. The results are means ± SD from triplicate wells. The results were similar in two other experiments. (C) LLG-C4-GST (10 μg/ml) was incubated in I domain–coated wells in the absence or presence of EDTA (2.5 mM), the LLG-C4 (1) peptide (100 μM), or the inactive LLG-C4(2) peptide (100 μM). The binding was determined with anti-GST antibodies. The results are the means ± SD from triplicate wells.

Carl_G_190x270_mm_blokki_FINAL.indd 298 06-Aug-23 1:54:00 PM

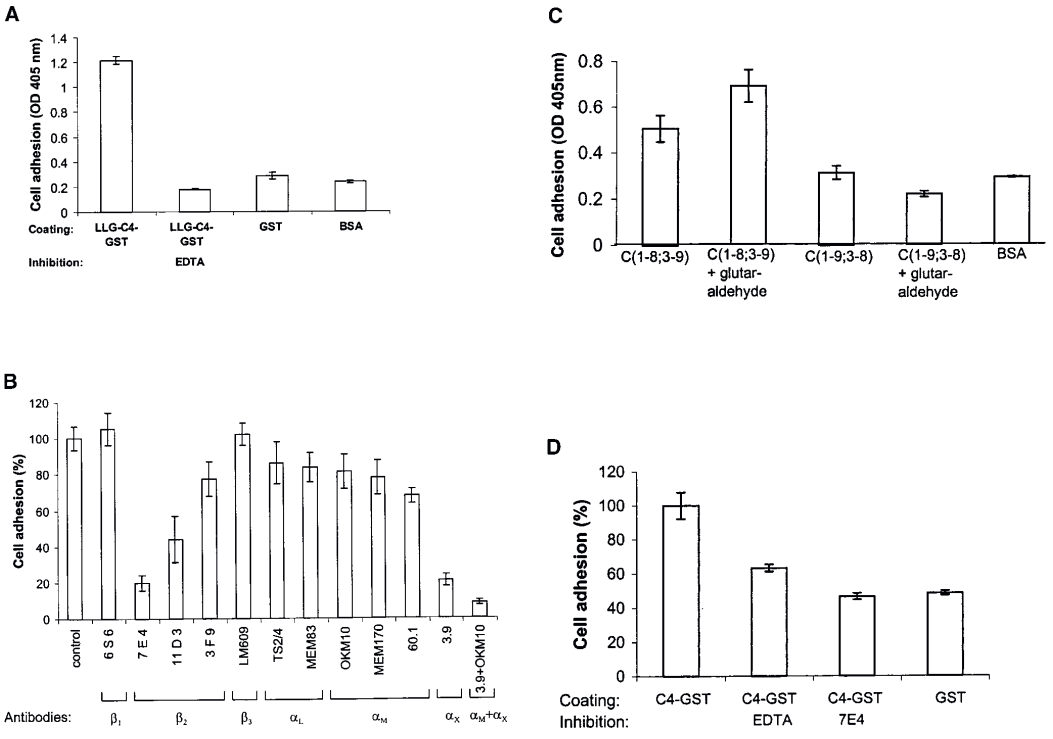

Figure 2. Immobilized LLG-C4 supports β_2 integrin–directed cell adhesion. (A) Phorbol ester–activated THP-1 cells were allowed to bind for 60 min to microtiter wells coated with LLG-C4-GST, GST, or albumin. EDTA was included at a 2.5-mM concentration. The bound cells were determined by the assay measuring cellular phosphatase activity as described in Materials and Methods. The data are the means ± SD from triplicate wells. Similar results were obtained in six other experiments. (B) THP-1 cells were mixed with each antibody against the β_1, β_2, β_3, α_X, α_M, or α_L integrin subunit as indicated. An aliquot of cells was then transferred to wells coated with LLG-C4-GST and incubated for 60 min. The bound cells were determined by the phosphatase assay. The results are the mean percentage of adhesion ± SD of two to four independent experiments, each done in triplicate wells. (C) The C(1-8;3-9) and C(1-9;3-8) peptides were coated on microtiter wells in the absence or presence of glutaraldehyde. THP-1 cells (10^5 per well) were allowed to bind for 60 min and the bound cells were determined. The results show the mean ± SD of triplicate wells. The experiment was repeated twice. (D) The $\alpha_X\beta_2$ integrin–transfected L cells were allowed to bind to LLG-G4-GST or GST. The 7E4 antibody and EDTA were used as competitors. The results, mean percentage of adhesion ± SD, are representative of three experiments conducted in triplicate wells. The difference in the binding to LLG-C4-GST versus GST is statistically significant ($P = 0.016$).

bond between the C1 and C8 cysteines and a second one between the C3 and C9 cysteines. Cells bound to the C(1-8;3-9) disulfide–containing peptide but failed to bind to the conformer with C(1-9;3-8) disulfides (Fig. 2 C). Cross-linking of the C(1-8;3-9) peptide with glutaraldehyde further enhanced cell binding, apparently due to better coating of the multimeric peptide. C(1-9;3-8) was inactive even after the cross-linking. In general, the C(1-8;3-9) peptide specifically supported the binding of β_2 integrin–expressing cells lines such β_2 integrin–transfected L cells and the leukocytic cell lines THP-1, U-937, and Jurkat. The binding of $\alpha_X\beta_2$-transfected L cells to LLG-C4-GST was inhibited by EDTA and the β_2 integrin–blocking antibody 7E4 (Fig. 2 D). Nonleukocytic cell lines L929, K562, SKOV-3, KS6717, and Eahy96, which do not express β_2 integrins, showed no binding to the peptide or LLG-C4-GST, whether the cells were pretreated with phorbol ester or not (data not shown).

LLG-C4 Nonapeptide Specifically Blocks β_2 Integrin–mediated Adhesion of Leukocytes

We examined the ability of LLG-containing peptides to block leukocyte binding to adhesion proteins containing or lacking an LLG tripeptide sequence. THP-1 cell adhesion on LLG-C4-GST was inhibited by the C(1-8;3-9) peptide with an IC_{50} of 20 μM (Fig. 3 A**)**. The other conformer, C(1-9;3-8), was 20-fold less active than C(1-8;3-9). To study whether the LLG tripeptide sequence is sufficient for recognition by the β_2 integrins, we prepared the minimal cyclic CLLGC peptide. In a control peptide the leucines were replaced by alanines. THP-1 cell adhesion experiments using the LLG-C4-GST substratum indicated that CAAGC was only a weak competitor of cell adhesion, whereas CLLGC readily inhibited cell adhesion at concentrations of ≥1 mM, indicating a specific recognition of the LLG motif by the β_2 integrins (Fig. 3 B).

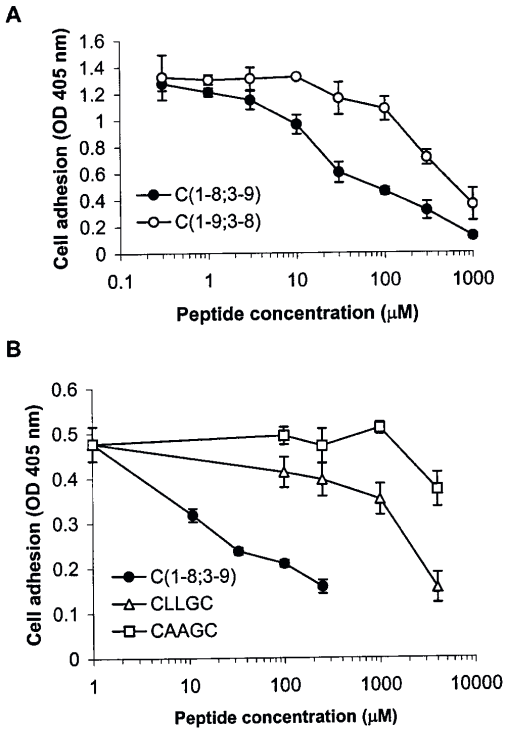

Figure 3. Effect of guided disulfide bridges on activity of LLG-C4. (A) THP-1 cells were mixed in suspension with peptides containing the C(1-8;3-9) or C(1-9;3-8) disulfides. The final peptide concentrations are indicated. Cells were then incubated for 60 min in microtiter wells coated with LLG-C4-GST. The bound cells were quantitated by the phosphatase assay. The results represent the mean ± SD of triplicate wells with similar results obtained in two other experiments. (B) THP-1 cell binding to LLG-C4-GST was examined in the presence of C(1-8;3-9), CLLGC, or CAAGC. The bound cells were determined by the phosphatase assay. The data show the means ± SD from triplicate wells and were similar in two other experiments.

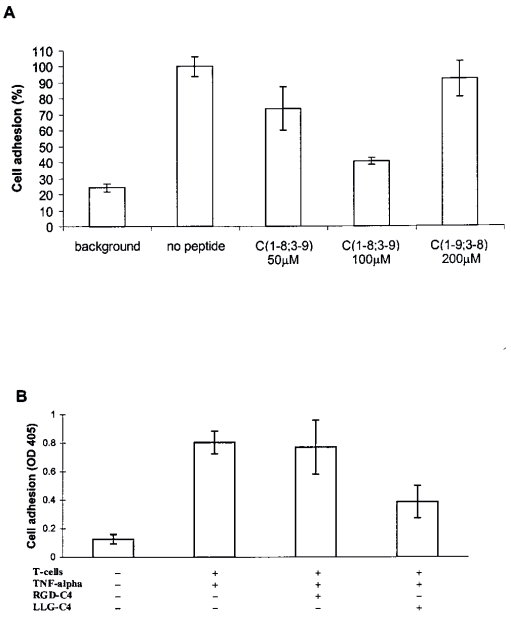

Figure 4. Inhibition of leukocyte cell adhesion to ICAM-1 by LLG-C4. (A) Jurkat cells were allowed to attach to immobilized ICAM-1-Fc in microtiter wells in the absence or presence of the LLG-C4 peptides. After a 45-min incubation, the unbound cells were removed by immersing the microtiter plate upside down on a decanter containing PBS. The attached cells were stained with Crystal Violet. The results show the percentage of cell adhesion ± SD derived from two experiments, each with triplicate or quadruplicate wells. (B) T cells were allowed to bind to TNF-α–stimulated EaHy926 endothelial cell monolayers that were grown on microtiter wells. LLG-C4 or RGD-4C was included at a concentration of 50 μM. After a 45-min incubation, the unbound cells were removed by immersing the microtiter plate in a PBS solution, and the bound T cells were determined by the phosphatase assay. The data are the mean ± SD of triplicate wells.

We next examined the ability of LLG-containing peptides to inhibit the $\alpha_L\beta_2$ integrin–mediated binding of Jurkat cells to ICAM-1-Fc recombinant protein, which contains the LLG sequence of the first Ig domain. ICAM-1-Fc was directly coated on microtiter wells or captured via protein A. In both cases we found concentration-dependent inhibition by C(1-8;3-9) on Jurkat cell adhesion and the IC_{50} was ~80 μM (Fig. 4 A). The C(1-9;3-8) conformer was severalfold less active and had hardly any effect. C(1-8;3-9) similarly inhibited the binding of freshly isolated T cells to cultured endothelial cells which were stimulated to express ICAM-1 by treatment with TNF-α (Fig. 4 B). T cells did not bind to unstimulated endothelial cells. As a control, the RGD-C4 peptide had no effect on T cell binding to endothelial ICAM-1.

As von Willebrand factor contains LLG peptide motifs, we were interested in the capability of the protein to function as a substratum for leukocytes. We found that phorbol ester–activated THP-1 cells strongly bound. The β_2 integrin antibody 7E4 blocked the THP-1 cell binding to von Willebrand factor (Fig. 5 A) and was nearly as efficient an inhibitor as the cation chelator EDTA (data not shown). The β_3 integrin antibodies LM609 and P2 were without effect. C(1-8;3-9) was a potent inhibitor of THP-1 cell binding to von Willebrand factor. The peptide inhibited with an IC_{50} of ~20 μM (Fig. 5 B**)**. In addition, CLLGC but not CAAGC inhibited at a 500 μM concentration (data not shown). Similar C(1-8;3-9) peptide–mediated inhibition was observed on Jurkat cell binding to von Willebrand factor (not shown). Importantly, THP-1 showed weaker binding (35% of wild-type) to a mutated von Willebrand factor, from which the A2 domain, including the LLG sequence, was deleted (Fig. 5 C). Furthermore, THP-1 adhesion to the A2-deleted von Willebrand factor was not blocked by C(1-8;3-9), but by the RGD-4C peptide. To further study the specificity of the LLG peptides, we examined THP-1

Carl_G_190x270_mm_blokki_FINAL.indd 300 06-Aug-23 1:54:00 PM

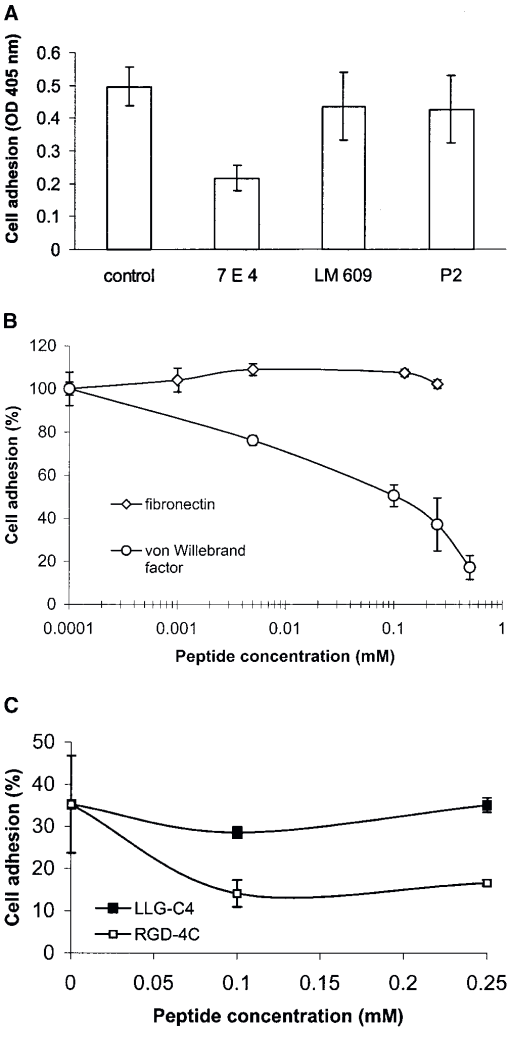

Figure 5. THP-1 cell adhesion to von Willebrand factor is inhibited by the LLG-C4 peptide. (A) THP-1 cell binding to von Willebrand factor was examined in the presence of antibodies against the β_2 (7E4), $\alpha_V\beta_3$ (LM609), or $\alpha_{IIb}\beta_3$ (P2) integrins. After a 60-min incubation in von Willebrand factor–coated wells, the bound cells were determined. The data are the mean ± SD of triplicate wells. The experiment was repeated three times. (B) THP-1 cell binding to wild-type von Willebrand factor or fibronectin in the presence of the indicated concentrations of C(1-8;3-9). (C) Binding of THP-1 cells to domain A2–deleted von Willebrand factor. The binding to wild-type von Willebrand factor was given as 100%. C(1-8;3-9) or RGD-4C was included as competitor at the concentrations described. The bound cells were determined by the phosphatase assay. The data are the mean ± SD of triplicate wells and were similar in two other experiments.

adhesion to fibronectin, a known ligand of several β_1 and β_3 integrins. C(1-8;3-9) showed no significant inhibition of fibronectin binding by THP-1 cells. C(1-8;3-9) also had no effect on binding of nonleukocytic cell lines such as HT1080 on fibronectin or fibrinogen (data not shown).

Finally, we examined THP-1 adhesion to fibrinogen, which is predominantly mediated via the $\alpha_M\beta_2$ and $\alpha_X\beta_2$ integrins (Li et al., 1995). C(1-8;3-9) readily inhibited the binding, whereas C(1-9;3-8) did not (Fig. 6 A). Similar results were obtained with U937 cells, which also express the $\alpha_M\beta_2$ and $\alpha_X\beta_2$ integrins (data not shown). As RGD-directed integrins can also mediate cell attachment on fibrinogen, we compared C(1-8;3-9) to the RGD-4C peptide, the selective ligand of $\alpha_V\beta_3/\beta_5$ integrins. We prestimulated THP-1 cells with low concentrations of C(1-8;3-9) and RGD-4C to fully activate both the β_2 and RGD-dependent integrins. After the peptide prestimulation, RGD-4C inhibited THP-1 cell adhesion on fibrinogen more effectively than C(1-8;3-9) (Fig. 6 B). To study whether C(1-8;3-9) and RGD-4C target different integrins, the peptides were given together to cells. The effects of C(1-8;3-9) and RGD-4C were additive and the peptide combination blocked cell adhesion efficiently.

As a model of monocyte rolling and extravasation, we examined in vitro migration of THP-1 cells on fibrinogen immobilized on Transwell filters. Cells effectively migrated in the presence of 10% serum. C(1-8;3-9) at a concentration of 200 μM completely abolished the ability of the cells to traverse the filter and bind to its lower surface (Fig. 6 C; $P = 0.005$, $n = 6$). The C(1-9;3-8) conformer was less active than C(1-8;3-9) and inhibited only partially ($P = 0.01$, $n = 6$). The activity difference between C(1-8;3-9) and C(1-9;3-8) was significant ($P = 0.003$). In a reverse strategy, when the filter was coated with LLG-C4, cell migration was strongly enhanced. Approximately 10-fold more cells migrated on the LLG-C4-GST substratum than on control GST substratum (Fig. 6 D). Cell migration on LLG-C4-GST was also more efficient when compared with fibronectin and fibrinogen coatings. C(1-8;3-9) at the 200 μM concentration completely suppressed the cell migration on LLG-C4-GST ($P = 0.0026$, $n = 6$; data not shown).

NMR Structures of Nonapeptide Conformers

We analyzed the C(1-8;3-9) and C(1-9;3-8) peptides by NMR spectroscopy to determine whether there are differences in peptide conformations due to the directed arrangement of the disulfide bonds. The structure determinations resulted in well-defined backbone conformations. The root mean square of deviation of the main chain atoms was 0.4 ± 0.2 Å for C(1-8;3-9) and 0.3 ± 0.2 Å for C(1-9;3-8) calculated from ensembles of 40 structures. For both peptides, all main chain dihedrals ϕ and ψ are in the favorable and allowed regions of Ramachandran plot. There are only a few nOes to define the side chain orientation, and therefore the side chain dihedrals of F4, L5, and L6, in particular, are dispersed (Fig. 7 A).

The pairing of the disulfides in the two ways influenced the structure of the nonapeptide considerably. The "crossing arrangement of disulfides" of C(1-8;3-9) constrains the overall structure tighter than the "parallel arrangement of disulfides" of C(1-9;3-8). This is reflected by the larger

Carl_G_190x270_mm_blokki_FINAL.indd 301 06-Aug-23 1:54:01 PM

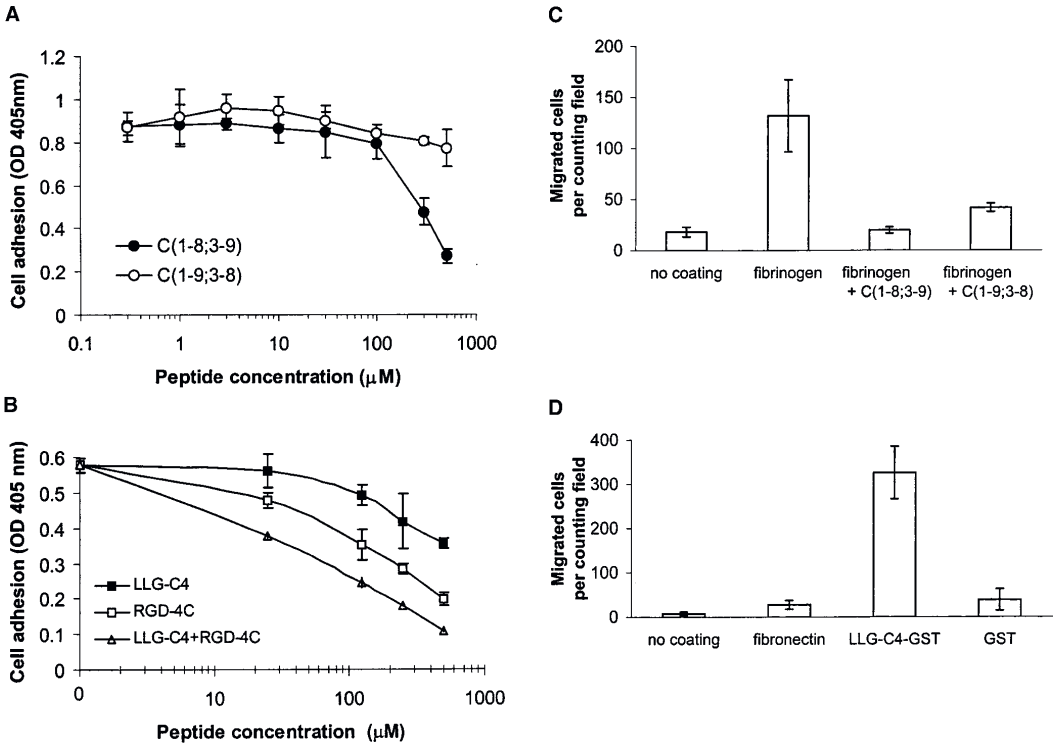

Figure 6. Synthetic LLG-C4 peptide prevents adhesion and migration of THP-1 cells on fibrinogen substratum. (A) Phorbol ester–activated THP-1 cells were administered together with C(1-8;3-9) or C(1-9;3-8), or in the absence of peptides, in microtiter wells coated with fibrinogen. After a 60-min incubation the bound cells were determined by the phosphatase assay. The results are the mean ± SD of triplicate wells and were similar in two other experiments. (B) To activate integrins, THP-1 were stimulated both with phorbol ester (50 nM) and the RGD-4C and C(1-8;3-9) peptides (each 2.5 μM) for 1 h. After washing, the cells were allowed to bind to fibrinogen-coated wells in the presence of C(1-8;3-9) or RGD-4C or both peptides at the concentrations indicated. After a 30-min incubation the bound cells were determined. The results are the mean ± SD of triplicate wells and were similar in two other experiments. At some data points the SD values are too small to be seen. (C) Transwell filters were coated both on the upper and lower surface with fibrinogen, or left uncoated, and then saturated with BSA. THP-1 cells were plated on the upper surface of the filter in the presence of 10% serum-containing medium. The concentrations of C(1-8;3-9) and C(1-9;3-8) were 200 μM. After an 18-h culture, the cells migrated underneath the filter were determined. The cells were fixed, stained, and counted under a microscope. The results show means ± SD of at least three experiments. (D) Both sides of the Transwell filters were coated with LLG-C4-GST, GST, fibrinogen, or BSA. A total of 5×10^4 THP-1 cells were administered per filter in 10% serum-containing medium and cultured for 18 h. The number of cells migrated to the lower surface of filter was counted microscopically. The results show means ± SD of at least three experiments.

number of nOes observed for C(1-8;3-9) (114) than for C(1-9;3-8) (85). There is no bias towards shorter distance restraints in C(1-8;3-9) compared with those of C(1-9;3-8). As a result of the different disulfide configurations, there are interresidue nOes found exclusively in one of the structures, 37 in C(1-8;3-9) and 20 in C(1-9;3-8). The crossing arrangement of disulfides in C(1-8;3-9) is topologically more complicated than the parallel bridging in C(1-9;3-8). In the short nonapeptide the adjacent disulfides with large van der Waals radii of sulphur atoms give rise to numerous steric restraints. The residue P2 also limits conformational freedom, whereas G7 contributes to it. The impact of mere topology on the steric restraints is apparent from the representative structures (Fig. 7 B). C(1-8;3-9) is more compact than C(1-9;3-8). Furthermore, there is a continuous hydrophobic surface patch composed of aliphatic groups of P2, F4, and L5 in the C(1-8;3-9) peptide. Overall, the disulfide bridges and the F4-L6 strand are buckled in C(1-8;3-9), whereas in C(1-9;3-8) they are extended. This likely accounts for the poorer water solubility of C(1-8;3-9) and may contribute to its higher activity.

Discussion

We have developed highly specific peptide antagonists of the leukocyte β_2 integrins using phage display. The most active antagonist, LLG-C4, is a biscyclic nonapeptide that is structurally restrained by two disulfide bonds and con-

Carl_G_190x270_mm_blokki_FINAL.indd 302 06-Aug-23 1:54:01 PM

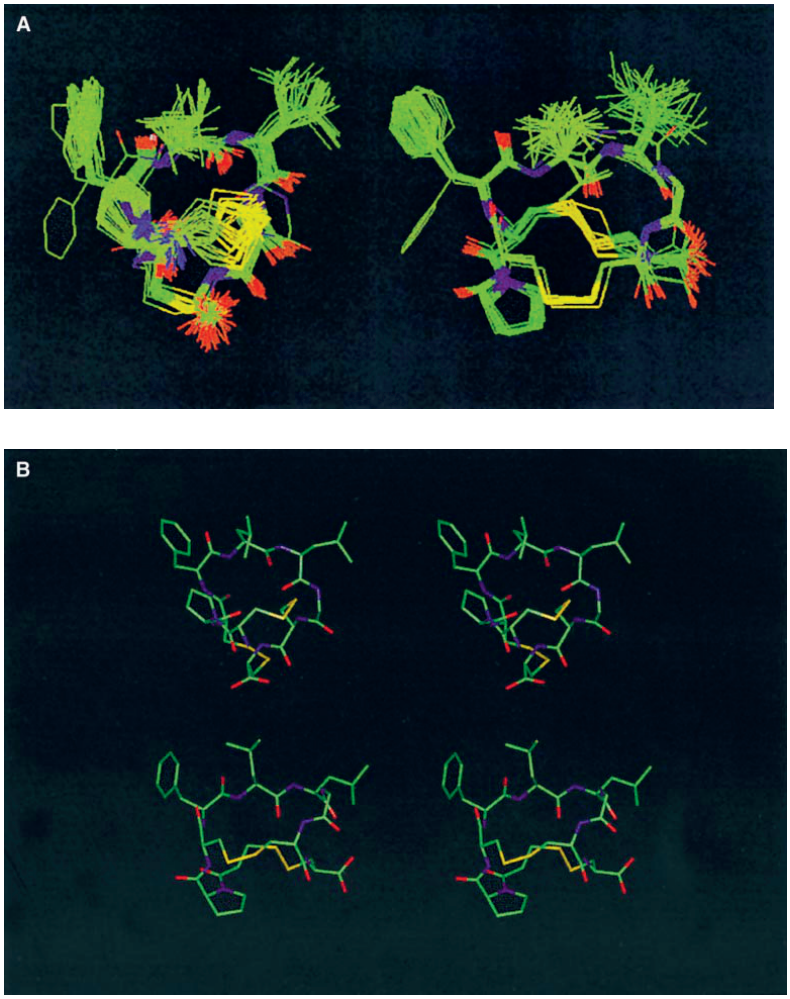

Figure 7. Comparison of structures of cyclic LLG-C4 peptide conformers by NMR. (A) Families of 40 conformations of C(1-8;3-9) (left) and C(1-9;3-8) (right) are shown. The heavy atoms of the disulfide-closed backbones are superimposed in each family and then the two families are translated apart for viewing. (B) Stereo views of representative solution structures C(1-8;3-9) (top) and C(1-9;3-8) (bottom) are shown. For this presentation the two structures were initially superimposed on the main chain atoms of F4, L5, and L6, and then translated apart for viewing. In the C(1-8;3-9) peptide C1 pairs with C8 above and C3 with C9 below the cyclic structure. Likewise, in the C(1-9;3-8) peptide C1 pairs with C9 above and C3 with C8 below the ring.

tains a novel LLG tripeptide adhesion motif. The LLG-C4 peptide specifically blocked the β_2 integrin–mediated leukocyte adhesion and inhibited leukocyte binding to their major ligand ICAM-1. Furthermore, like a typical integrin ligand, the peptide supported cell adhesion when immobilized on plastic and bound leukocytic cell lines, but not cells lacking β_2 integrins. The effectiveness and leukocyte specificity of the peptide are explained by its ability to interact with the I domain, which is a known active site in the leukocyte integrins. Interestingly, not only ICAM-1 but also several other adhesion proteins, including von Willebrand factor, contain the consensus PP/XXLLG sequence identified by phage display.

The activity of the LLG-C4 nonapeptide was strictly dependent on the correct formation of two disulfide bridges. There was a 20-fold difference in the activities of two bicyclic conformers that differed only in the configuration of the disulfide bridges. The more active peptide had a very compact structure due to a "crossing" arrangement of the disulfide bonds as shown by NMR. Interestingly, the leucine side chains protrude from the cyclic structure like antennae, suggesting that they can directly interact with the integrin. The small glycine residue may adjust a correct distance between the leucine side chains. The biscyclic RGD-4C peptide can also exist in two different isomers, depending on internal disulfide bonding, and the two structures have clearly different integrin-binding activities (Assa-Munt et al., 2001).

LLG-C4-GST is a highly efficient adhesion substratum for phorbol ester–activated THP-1 leukemia cells. We also detected cell binding to the immobilized nonapeptide, but the overall binding was weaker, apparently because the short peptide coats less efficiently on microtiter plates. We were not able to detect a similar strong binding of the $\alpha_X\beta_2$

Carl_G_190x270_mm_blokki_FINAL.indd 303 06-Aug-23 1:54:01 PM

integrin–transfected L cells to LLG-C4-GST as with THP-1. This is likely due to the fact that the integrin expression was limited only to a subset of L cells as determined by FACS® analysis.

Immunocapture experiments with different β_2 integrin antibodies showed that LLG-C4 is able to bind to each of the three integrin species, $\alpha_L\beta_2$, $\alpha_M\beta_2$, and $\alpha_X\beta_2$. EDTA inhibition showed that the binding of LLG-C4 to the integrins as well as to purified I domain is cation dependent. However, one of the antibodies used for integrin immunocapture gave an exceptional result in that EDTA could not completely inhibit the binding of LLG-C4-GST fusion protein. This antibody, 2E7, which recognizes the common β_2 subunit, shows an integrin-activating effect in cell culture and stimulates leukocyte cell adhesion to LLG-C4-GST and various matrix proteins. Thus, it is possible that this antibody changes the conformation of integrin, resulting in stronger binding. The antibody may expose secondary binding sites for ligands in integrins, and GST protein itself may then contribute to the cation-independent binding.

Previous studies have indicated that synthetic peptides spanning the LLG region of ICAM-1 (Ross et al., 1992; Li et al., 1993) or the corresponding region of ICAM-2 (Li et al., 1993) support leukocyte cell adhesion when the peptides are immobilized on plastic. In soluble forms, the peptides block binding of leukocytic cells to ICAM-1 expressed on an endothelial cell monolayer (Ross et al., 1992; Li et al., 1995). The LLG-C4 nonapeptide is significantly smaller than the peptide ligands described previously for the β_2 integrins, and showed high activity, though lacking a negatively charged amino acid residue such as glutamate. Also, the pentapeptide CLLGC inhibited cell adhesion. Thus, β_2 integrin–targeting ligands can be constructed based on the noncharged LLG motif. This is in accordance with the crystal structures and structural models of the first Ig domain of ICAM-1, where the LLG sequence is seen as part of a short β strand apparently capable of directly contacting with an integrin I domain (Bella et al., 1998; Casasnovas et al., 1998). Alanine-scanning mutagenesis studies of individual amino acids within the first Ig domain of ICAM-1 have shown that the LLG region is important for the integrin binding of ICAM-1. Mutation of one of the leucine's residues decreases ICAM-1 binding activity partially and mutation of the glycine completely (Fisher et al., 1997). Because of the inactivity of the glycine-mutated ICAM-1, it has been suggested that the glycine residue does not play a structural role, but rather directly interacts with the integrin (Fisher et al., 1997). Mutations of the corresponding valine and glycine amino acids to alanines in ICAM-2 also give proteins with impaired integrin-binding activity (Casasnovas et al., 1999). Mutation of leucine to alanine can be considered a conservative substitution, which could explain the only marginal, though significant, decrease in the activities this substitution causes in ICAM-1 and the synthetic peptides.

von Willebrand factor contains two LLG sequences, but an ability of these sequences to interact with integrins has not been reported. von Willebrand factor is a multifunctional adhesive ligand binding several proteins, and it prevents bleeding during vascular injury by mediating platelet adhesion to exposed subendothelium (Savage et al., 1998). It contains two RGD sequences, at least one of which is important in binding the platelet integrin $\alpha_{IIb}\beta_3$ (Weiss et al., 1993; Savage et al., 1996). We found that phorbol ester–activated leukocytic cells can bind to von Willebrand factor in an RGD-independent manner. Under these circumstances, leukocyte binding to wild-type von Willebrand factor was inhibited by the β_2 integrin–targeting LLG peptides and by the β_2 integrin–blocking antibody 7E4, but not by antibodies against the β_3 integrins. When the whole A2 domain of von Willebrand factor, including the LLG motif, was deleted, leukocytic cells showed much weaker binding and the LLG-C4 peptide was not inhibitory. It is notable that, besides the LLG sequences, von Willebrand factor contains I domains (Colombatti et al., 1993; Perkins et al., 1994) similar to those present in the α subunits of the β_2 integrins (Li et al., 1995; Qu and Leahy, 1995). Thus, it is possible that there are intra- or intermolecular interactions between the LLG sequences and adjacent I domains, affecting the folding of the protein. If such interactions occur, they could in part explain the inactivity of the plasma form of von Willebrand factor. Our results suggest that leukocytes can bind to the immobilized form of von Willebrand factor, such as that present in vascular subendothelium or other surfaces, and these interactions could play a role in the initial phases of inflammation.

As the β_2 integrins exist in an inactive state and become activated only after physiologic stimuli, such as by chemokines or through contact with antigen-presenting cells, it would be desirable to develop compounds binding preferentially to cells bearing the activated integrins. We found that LLG-C4 exhibits such properties and reacts with cells after integrin activation. Furthermore, LLG-C4 is a promising β_2 integrin–targeting agent, as the sequence can specifically direct phage binding to β_2 integrin–expressing cell lines, and low concentrations of the soluble peptide inhibit the binding (Koivunen, E., R. Pasqualini, and W. Arap, manuscript in preparation). Finally, the presence of LLG sequences in von Willebrand factor suggests a novel function for the protein in mediating not only platelet but also leukocyte adhesion.

We thank Minna Ekström, Marja Pietilä, Sanna Pesonen, and Kari Kaitila for technical assistance.

This work was supported by the Academy of Finland, the Finnish Cancer Society, the Sigrid Juselius Foundation, the Finnish Cultural Fund, and the Technology Development Centre of Finland. G. van Willigen was supported by the Netherlands Organization for Scientific Research (grant R91-266), the Catharijne Foundation, and the Dirk-Zwager Assink Foundation.

Submitted: 1 September 2000
Revised: 26 March 2001
Accepted: 11 April 2001

References

Assa-Munt, N., X. Jia, P. Laakkonen, and E. Ruoslahti. 2001. Solution structures and integrin binding activities of an RGD peptide with two isomers. *Biochemistry*. 40:2373–2378.

Bailly, P., E. Tontti, P. Hermand, J.-P. Carton, and C.G. Gahmberg. 1995. The red cell LW blood group protein is an intercellular adhesion molecule which binds to CD11/CD18 leukocyte integrins. *Eur. J. Immunol*. 25:3316–3320.

Bella, J., P.R. Kolatkar, C.W. Marlor, J.M. Greve, and M.G. Rossmann. 1998. The structure of the two amino-terminal domains of human ICAM-1 suggests how it functions as a rhinovirus receptor and as an LFA-1 integrin ligand. *Proc. Natl. Acad. Sci. USA*. 95:4140–4145.

Casasnovas, J.M., T. Stehle, J. Liu, J. Wang, and T.A. Springer. 1998. A dimeric crystal structure for the N-terminal two domains of intercellular adhesion molecule-1. *Proc. Natl. Acad. Sci. USA*. 95:4134–4139.

Casasnovas, J.M., C. Pieroni, and T.A. Springer. 1999. Lymphocyte function-

associated antigen-1 binding residues in intercellular adhesion molecule-2 (ICAM-2) and the integrin binding surface in the ICAM subfamily. *Proc. Natl. Acad. Sci. USA*. 96:3017–3022.

Clark, W.M., K.P. Madden, R. Rothlein, and J.A. Zivin. 1991. Reduction of central nervous system ischemic injury in rabbits using leukocyte adhesion antibody treatment. *Stroke.* 22:877–883.

Colombatti, A., P. Bonaldo, and R. Doliana. 1993. Type A modules: interacting domains found in several non-fibrillar collagens and in other extracellular matrix proteins. *Matrix.* 13:297–306.

De Wet, W., M.P. Bernard, V. Benson-Chanda, M.-L. Chu, L. Dickson, D. Weil, and F. Ramirez. 1987. Organization of the human pro-alpha 2(I) collagen gene. *J. Biol. Chem*. 262:16032–16036.

Fawcett, J., C.L.L. Holness, L.A. Needham, H. Turley, K.C. Gatter, D.Y. Mason, and D.L. Simmons. 1992. Molecular cloning of ICAM-3, a third ligand for LFA-1, constitutively expressed on resting leukocytes. *Nature.* 360:481–484.

Feng, Y., D. Chung, L. Garrard, G. McEnroe, D. Lim, J. Scardina, K. McFadden, A. Guzzetta, A. Lam, J. Abraham, D. Liu, and G. Endemann. 1998. Peptides derived from the complementary-determining regions of anti-Mac-1 antibodies block intercellular adhesion molecule-1 interaction with Mac-1. *J. Biol. Chem*. 273:5625–5630.

Fisher, K.L., J. Lu, L. Riddle, K.J. Kim, L.G. Presta, and S.C. Bodary. 1997. Identification of the binding site in intercellular adhesion molecule 1 for its receptor, leukocyte function-associated antigen 1. *Mol. Biol. Cell*. 8:501–515.

Gahmberg, C.G., M. Tolvanen, and P. Kotovuori. 1997. Leukocyte adhesion. Structure and function of human leukocyte integrins and their cellular ligands. *Eur. J. Biochem*. 245:215–232.

Güntert, P., C. Mumenthaler, and K. Wüthrich. 1997. Torsion angle dynamics for NMR structure calculation with the new program DYANA. *J. Mol. Biol*. 273:283–298.

Hedman, H., B. Brändén, and E. Lundgren. 1992. Physical separation of ICAM-1 binding cells. *J. Immunol. Methods.* 146:203–211.

Hemler, M.E. 1990. VLA proteins in the integrin family: structures, functions, and their role on leukocytes. *Annu. Rev. Immunol*. 8:365–400.

Huang, C., and T.A. Springer. 1995. A binding interface on the I domain of lymphocyte function-associated antigen-1 (LFA-1) required for specific interaction with intercellular adhesion molecule-1 (ICAM-1). *J. Biol. Chem*. 270:19008–19016.

Hynes, R.O. 1992. Integrins: versatility, modulation, and signalling in cell adhesion. *Cell.* 69:11–25.

Kallen, J., K. Welzenbach, P. Ramage, D. Geyl, R. Kriwacki, G. Legge, S. Cottens, G. Weitz-Schmidt, and U. Hommel. 1999. Structural basis for LFA-1 inhibition upon lovastatin binding to the CD11a I-domain. *J. Mol. Biol*. 292: 1–9.

Kamata, T., R. Wright, and Y. Takada. 1995. Critical threonine and aspartic acid residues within the I domains of β_2 integrins for interactions of intercellular adhesion molecule-1 (ICAM-1) and C3bi. *J. Biol. Chem*. 270:12531–12535.

Kavanaugh, A.F., L.S. Davis, L.A. Nichols, S.H. Norris, R. Rothlein, L.A. Scharschmidt, and P.E. Lipsky. 1994. Treatment of refractory rheumatoid arthritis with a monoclonal antibody to intercellular adhesion molecule 1. *Arthritis Rheum*. 37:992–999.

Kelly, T.A., D.D. Jeanfavre, D.W. McNeil, J.R. Woska, Jr., P.L. Reilly, E.A. Mainolfi, K.M. Kishimoto, G.H. Nabozny, R. Zinter, B.-J. Bormann, and R. Rothlein. 1999. A small molecule antagonist of LFA-1-mediated cell adhesion. *J. Immunol*. 163:5173–5177.

Koivunen, E., B. Wang, and E. Ruoslahti. 1994. Isolation of a highly specific ligand for the $\alpha_5\beta_1$ integrin from a phage display library. *J. Cell Biol*. 124: 373–380.

Koivunen, E., B. Wang, and E. Ruoslahti. 1995. Phage libraries displaying cyclic peptides with different ring sizes: ligand specificities of the RGD-directed integrins. *Biotechnology*. 13:265–270.

Koivunen, E., W. Arap, H. Valtanen, A. Rainisalo, O.P. Medina, P. Heikkilä, C. Kantor, C.G. Gahmberg, T. Salo, Y.T. Konttinen, et al. 1999. Tumor targeting with a selective gelatinase inhibitor. *Nat. Biotechnol*. 17:768–774.

Komoriya, A., L.J. Green, M. Mervic, S.S. Yamada, K.M. Yamada, and M.J. Humphries. 1991. The minimal essential sequence for a major cell type-specific adhesion site (CS1) within the alternatively spliced type III connecting segment domain of fibronectin is leucine-aspartic acid-valine. *J. Biol. Chem*. 266:15075–15079.

Kotovuori, A., T. Pessa-Morikawa, P. Kotovuori, P. Nortamo, and C.G. Gahmberg. 1999. ICAM-2 and a peptide from its binding domain are efficient activators of leukocyte adhesion and integrin affinity. *J. Immunol*. 162:6613–6620.

Kraft, S., B. Diefenbach, R. Mehta, A. Jonczyk, G.A. Luckenbach, and S.L. Goodman. 1999. Definition of an unexpected ligand recognition motif for $\alpha_V\beta_6$ integrin. *J. Biol. Chem*. 274:1979–1985.

Lalancette, M., F. Aoudjit, E.F. Potworowski, and Y. St-Pierre. 2000. Resistance of ICAM-1-deficient mice to metastasis overcome by increased aggressiveness of lymphoma cells. *Blood*. 95:314–319.

Languino, L.R., J. Plescia, A. Duperray, A.A. Brain, E.F. Plow, J.E. Geltosky, and D.C. Altieri. 1993. Fibrinogen mediates leukocyte adhesion to vascular endothelium through an ICAM-1-dependent pathway. *Cell.* 73:1423–1434.

Lankhof, H., C. Damas, M.E. Schiphorst, M.J. Ijsseldijk, M. Bracke, M. Furlan, H.M. Tsai, P.G. de Groot, J.J. Sixma, and T. Vink. 1997. von Willebrand factor without the A2 domain is resistant to proteolysis. *Thromb. Haemost.* 77: 1008–1013.

Lee, J.O., P. Rieu, M.A. Arnaout, and R. Liddington. 1995. Crystal structure of the A domain from the α-subunit of integrin CR3 (CD11b/CD18). *Cell.* 80: 631–638.

Leinonen, A., M. Mariyama, T. Mochizuki, K. Tryggvason, and S.T. Reeders. 1994. Complete primary structure of the human type IV collagen alpha 4(IV) chain. Comparison with structure and expression of the other alpha (IV) chains. *J. Biol. Chem*. 269:26172–26177.

Li, R., P. Nortamo, L. Valmu, M. Tolvanen, J. Huuskonen, C. Kantor, and C.G. Gahmberg. 1993. A peptide from ICAM-2 binds to the leukocyte integrin CD11a/CD18 and inhibits endothelial cell adhesion. *J. Biol. Chem*. 268: 17513–17518.

Li, R., J. Xie, C. Kantor, V. Koistinen, D.C. Altieri, P. Nortamo, and C.G. Gahmberg. 1995. A peptide derived from the intercellular adhesion molecule-2 regulates the avidity of the leukocyte integrins CD11b/CD18 and CD11c/CD18. *J. Cell Biol*. 129:1143–1153.

Lynch, D.C., T.S. Zimmerman, C.J. Collins, M. Brown, M.J. Morin, E.H. Ling, and D.M. Livingston. 1985. Molecular cloning of cDNA for human von Willebrand factor: authentication by a new method. *Cell.* 41:49–56.

Miyamoto, K., S. Khosrof, S.-E. Bursell, R. Rohan, T. Murata, A.C. Clermont, L.P. Aiello, Y. Ogura, and A.P. Adamis. 1999. Prevention of leukostasis and vascular leakage in streptozotocin-induced diabetic retinopathy via intercellular adhesion molecule-1 inhibition. *Proc. Natl. Acad. Sci. USA*. 96:10836–10841.

Mould, A.P., S.K. Akiyama, and M.J. Humphries. 1995. Regulation of integrin $\alpha_5\beta_1$–fibronectin interactions by divalent cations. Evidence for distinct classes of binding sites for Mn^{2+}, Mg^{2+}, and Ca^{2+}. *J. Biol. Chem.* 270:26270–26277.

Nortamo, P., M. Patarroyo, C. Kantor, J. Suopanki, and C.G. Gahmberg. 1988. Immunological mapping of the human leukocyte adhesion glycoprotein gp90 (CD18) by monoclonal antibodies. *Scand. J. Immunol*. 28:537–546.

Perkins, S.J., K.F. Smith, S.C. Williams, P.I. Haris, D. Chapman, and R.B. Sim. 1994. The secondary structure of the von Willebrand factor type A-domain in factor B of human complement by Fourier transform infrared spectroscopy: its occurrence in collagen types VI, VII, XII and XIV, the integrins and other proteins by averaged structure predictions. *J. Mol. Biol.* 238:104–119.

Pierschbacher, M.D., and E. Ruoslahti. 1984. The cell attachment activity of fibronectin can be duplicated by small fragments of the molecule. *Nature.* 309: 30–33.

Qu, A., and D.J. Leahy. 1995. Crystal structure of the I-domain from the CD11a/CD18 (LFA-1, $\alpha_L\beta_2$) integrin. *Proc. Natl. Acad. Sci. USA*. 92:10277–10281.

Ross, L., F. Hassman, and L. Molony. 1992. Inhibition of Molt-4-endothelial adherence by synthetic peptides from the sequence of ICAM-1. *J. Biol. Chem*. 267:8537–8543.

Savage, B., E. Saldivar, and Z.M. Ruggeri. 1996. Initiation of platelet adhesion by arrest onto fibrinogen or translocation on von Willebrand factor. *Cell.* 84: 289–297.

Savage, B., F. Almus-Jacobs, and Z.M. Ruggeri. 1998. Specific synergy of multiple substrate-receptor interactions in platelet thrombus formation under flow. *Cell.* 94:657–666.

Simmons, D., M.W. Makgoba, and B. Seed. 1988. ICAM, an adhesion ligand of LFA-1, is homologous to the neural cell adhesion molecule NCAM. *Nature.* 331:624–627.

Springer, T.A. 1994. Traffic signals for lymphocyte recirculation and leukocyte emigration: the multistep paradigm. *Cell.* 76:301–314.

Stanley, P., and N. Hogg. 1998. The I domain of integrin LFA-1 interacts with ICAM-1 domain 1 at residue Glu-34 but not Gln-73. *J. Biol. Chem*. 273: 3358–3362.

Staunton, D.E., M.L. Dustin, H.P. Erickson, and T.A. Springer. 1989. Functional cloning of ICAM-2, a cell adhesion ligand for LFA-1 homologous ICAM-1. *Nature.* 339:61–64.

Staunton, D.E., M.L. Dustin, H.P. Erickson, and T.A. Springer. 1990. The arrangement of the immunoglobulin-like domains of ICAM-1 and the binding sites for LFA-1 and rhinovirus. *Cell*. 61:243–254.

Tian, L., Y. Yoshihara, T. Mizuno, K. Mori, and C.G. Gahmberg. 1997. The neuronal glycoprotein telencephalin is a cellular ligand for the CD11a/CD18 integrin. *J. Immunol*. 158:928–936.

Ueda, T., P. Rieu, J. Brayer, and M.A. Arnaout. 1994. Identification of the complement iC3b binding site in the β_2 integrin CR3 (CD11b/CD18). *Proc. Natl. Acad. Sci. USA*. 91:10680–10684.

Valmu, L., and C.G. Gahmberg. 1995. Treatment with ockadaic acid reveals strong threonine phosphorylation of CD18 after activation of CD11/CD18 leukocyte integrins with phorbol esters or CD3 antibodies. *J. Immunol*. 155: 1175–1183.

Weiss, H.J., T. Hoffman, A. Yoshioka, and Z.M. Ruggeri. 1993. Evidence that the $Arg^{1744}Gly^{1745}Asp^{1746}$ sequence in the GPIIb-IIIa-binding domain of von Willebrand factor is involved in platelet adhesion and thrombus formation on subendothelium. *J. Lab. Clin. Med.* 122:324–332.

Carl_G_190x270_mm_blokki_FINAL.indd 305 06-Aug-23 1:54:02 PM

Pascal Bailly[1], Eveliina Tontti[2], Patricia Hermand[1], Jean-Pierre Cartron[1] and Carl G. Gahmberg[2]

[1] INSERM U76, Institut National de Transfusion Sanguine, Paris, France
[2] Department of Biosciences, Division of Biochemistry, University of Helsinki, Helsinki, Finland

The red cell LW blood group protein is an intercellular adhesion molecule which binds to CD11/CD18 leukocyte integrins

Leukocyte adhesion involves the leukocyte-specific integrins CD11a/CD18, CD11b/CD18 and CD11c/CD18, which bind to intercellular adhesion molecules (ICAM). Three ICAM have been described, and are expressed on leukocytes and various other cells, but are absent from red cells. Here, we show that the red cell Landsteiner-Wiener (LW) blood group glycoprotein is an ICAM which binds to the leukocyte-specific integrins. This finding has important implications in red cell physiology.

1 Introduction

Leukocyte adhesion is of fundamental functional importance. Members of three molecular families of adhesion proteins are involved in leukocyte-leukocyte interactions and leukocyte-target cell binding: integrins, members of the immunoglobulin superfamily, and carbohydrate binding selectins [1–3]. After activation, the leukocyte-specific integrins CD11a/CD18 (LFA-1), CD11b/CD18 (Mac-1), and possibly CD11c/CD18 (p150/95) bind to intercellular adhesion molecules (ICAM). ICAM-1 (CD54) was the first intercellular adhesion molecule described [4–7]. It contains five immunoglobulin domains, and is found in relatively low amounts on resting leukocytes and various other cells like endothelial cells. It is rapidly up-regulated by various cytokines [1]. ICAM-2 (CD102) has two immunoglobulin domains, and is expressed on leukocytes and endothelial cells [8, 9]. ICAM-3 (CD50) also has five immunoglobulin domains, and is enriched on lymphocytes, but is absent from endothelial cells [10, 11].

The LW (Landsteiner-Wiener) blood group was initially confused with the Rh (Rhesus) blood group [12]. These blood groups show an interesting phenotypic relationship, since the level of LW antigen expression is greater in $Rh(D)^+$ than in $Rh(D)^-$ cells, and extremely rare red cells deficient in Rh-antigens (Rh^{null} cells) also lack the LW antigens. The Rh antigens are carried by a family of hydrophobic membrane proteins of 30–32 kDa and are exceptional among cell surface proteins in that they lack carbohydrate [13]. The LW antigens reside on a 42 kDa glycoprotein, which requires intramolecular disulfide bonds and the presence of divalent cations, notably Mg^{2+}, for antigenic reactivity [14, 15]. Recently, the LW blood group protein was immunopurified, partially sequenced and cloned [16, 17]. It is a 271-amino-acid polypeptide including a 30-amino-acid signal peptide, four potential N-glycosylation sites, a single transmembrane domain and a short cytoplasmic segment. No structural homology between the Rh and LW sequences was found, and the structural genes are located on different chromosomes (1p36 and 19p13, respectively). Most remarkably, the LW protein showed significant sequence homology to ICAM molecules. It contains two immunoglobulin domains, and the first domain is 30 % identical to the first domains of ICAM-1, ICAM-2 and ICAM-3.

The sequence homology of the LW protein with the ICAM led us consider the possibility that it could act as an intercellular adhesion molecule. We therefore purified the LW protein from red cells and have indeed found that various leukocytes bind to the isolated protein in a CD11/CD18-dependent manner. Furthermore, red cells bind to immobilized CD11a/CD18 and CD11b/CD18 integrins. Thus the LW protein is a novel red cell ICAM molecule, which we accordingly designate ICAM-4.

2 Materials and methods

2.1 Purification of the LW protein and the CD11a/CD18 and CD11b/CD18 integrins

The LW protein was isolated from human red cell membranes using the BS46 anti-LW mAb as described [16]. The leukocyte integrins were purified from human buffy-coat cells using the mAb TS1/22 for CD11a/CD18 and LM2/1 for CD11b/CD18, as described [18]. The purities of the isolated proteins were evaluated by SDS-PAGE [19].

2.2 Cells and cell lines

Blood T cells, B cells and NK cells were isolated from fresh blood buffy coats using negative selection and magnetic beads. Their purities were determined using leukocyte markers and a fluorescence-activated cell sorter (Becton Dickinson, San Jose, CA). The purities of the T cell preparations were 91–99 %, that of the B cell preparation > 97 %, and those of the NK cell preparations 88–94 %. Red cells were obtained from normal volunteers using

[I 14413]

Correspondence: Carl G. Gahmberg, Department of Biosciences, Division of Biochemistry, P.O.Box 56, Viikinkaari 5, FIN-00014 University of Helsinki, Finland (Fax: +358-0-70859068)

Abbreviations: ICAM: Intercellular adhesion molecule **LFA-1:** Leukocyte function-associated antigen **LW:** Landsteiner-Wiener blood group antigen

Key words: ICAM / LW / Adhesion / Leukocyte

0014-2980/95/1212-3316$10.00 + .25/0

© VCH Verlagsgesellschaft mbH, D-69451 Weinheim, 1995

Carl_G_190x270_mm_blokki_FINAL.indd 306 06-Aug-23 1:54:03 PM

Eur. J. Immunol. 1995. *25:* 3316–3320

heparin as an anticoagulant. The monocytic cell line THP-1, an EBV-transformed normal B lymphoblastoid cell line NAD-20 and a B lymphoblastoid line established from a patient with leukocyte adhesion deficiency (LAD) were grown in RPMI 1640 with 10% FCS [18]. The cell line from the patient contained less than 1% of the normal amount of CD11/CD18 integrins, and was obtained from Dr. Carl Figdor, Amsterdam.

2.3 Binding assays

Indicated amounts of the purified LW protein, leukocyte integrins or the control proteins ICAM-3 (CD50) and glycophorin A (Sigma, St. Louis, MO) were coated on plastic 96-well plates (Nunc, Roskilde, Denmark) in 25 mM Tris pH 8.0, 150 mM NaCl, 2 mM $MgCl_2$ at 4°C overnight, and saturated with 1% BSA by coating for an additional 2 h at room temperature. The ICAM-3 protein was purified from human buffy coats by affinity chromatography using the TP1/24 mAb [20]. It was >95% pure when checked by SDS-PAGE. After washing with RPMI-1640 containing 40 mM Hepes, 2 mM $MgCl_2$ and 5% FCS (binding buffer) mAb were added as indicated at final concentrations of 50 μg/ml, followed by the addition of leukocytes or red cells in a total volume of 100 μl. After incubation for 1 h at room temperature for leukocytes and 37°C for red cells, the plates were carefully washed in binding buffer, and the attached cells counted. The monoclonal antibodies were 7E4 (anti-CD18) [21], TS1/22 or TS2/4 (anti-CD11a) [22], LM 2/1 (anti-CD11b) [23] and 3.9 (anti-CD11c) [24]. The control antibody was an antibody to Rh(D) (clone F5, IgG1).

3 Results and discussion

The purified LW protein migrated as a 42-kDa band detected by silver staining on SDS polyacrylamide gels and the preparation did not contain any major impurities (Fig. 1A, insert). Cells of various leukocytic lines readily bound to the immobilized protein in a concentration-dependent manner. The monocytic line THP-1 and the EBV-transformed B lymphoblastoid line NAD-20 showed LW-dependent binding (Fig. 1A), whereas no binding was observed with EBV-transformed cells established from the patient with leukocyte adhesion deficiency lacking CD11/CD18 integrins [1, 2]. Fig. 1B shows that B lymphocytes and NK cells bound well, whereas a lower binding was obtained with T cells and THP-1 cells. The binding of leukocytes to the LW protein was clearly integrin-dependent (Fig. 2). The 7E4 CD18 antibody efficiently blocked binding of all leukocytes studied (Fig. 2A–D). The CD11a antibody efficiently blocked binding of T cells (Fig. 2B), whereas B cells (Fig. 2A) and NK cells (Fig. 2C) seemed to utilize all three leukocyte integrins. Efficient blocking of THP-1 cells was obtained with the CD11c mAb 3.9 (Fig. 2D). The antibody effects largely reflect the expression of the various CD11/CD18 integrins on the leukocytes. The BS46 antibody inhibitions were not significant (not shown), suggesting that this monoclonal antibody does not efficiently recognize the LW protein coated on plastic.

We then purified CD11a/CD18 and CD11b/CD18 integrins, attached them to plastic, and studied the binding of red cells to these receptors. The integrin preparations were

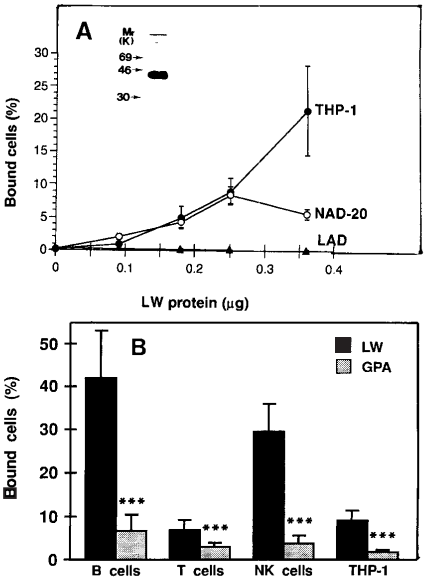

Figure 1. Binding of leukocytes to isolated LW protein. (A) The LW protein was isolated from human red cell membranes, and an aliquot of the preparation was analyzed by SDS-10% PAGE and silver stained. The insert shows a single protein band. The purified protein was coated on plastic, and the binding of leukocytes studied. ●–●, binding of THP-1 cells; ○–○, binding of NAD-20 cells; ▲–▲ binding of lymphoblastoid cells from the patient with leukocyte adhesion deficiency. (B) Percent binding of added B, T, NK, and TNP-1 cells to 0.25 μg LW protein or glycophorin A (GPA) coated on plastic. *** $p < 0.001$.

>95% pure (Fig. 3). Red cells readily bound to CD11a/CD18 in a concentration-dependent manner (Fig. 4A). Little binding occurred to the control protein ICAM-3. The binding to isolated CD11a/CD18 was only partially blocked by specific antibodies or EDTA (Fig. 4B), indicating additional interactions. Red cells also bound to isolated CD11b/CD18 in a concentration dependent manner (Fig. 4C), and the binding was efficiently blocked by relevant antibodies or EDTA down to background levels (Fig. 4D). No blocking was obtained with the CD11a-specific antibody TS2/4.

We also purified CD11c/CD18 using antibody 3.9 [25], and attached it to plastic. No specific binding of red cells was observed. This could be due to the relatively low affinity of purified CD11c/CD18 for LW, in combination with the low number of LW polypeptides/red cell (≈4400) [14]. All the experiments have been performed at least four independent times with similar results.

In ICAM-2, the first immunoglobulin domain is important for integrin binding [9, 18], and the first domain is also involved in binding of ICAM-1 to CD11a/CD18 [26]. On the other hand, there is evidence that the third Ig domain of ICAM-1 is important in binding to CD11b/CD18 [27]. The first Ig domain of the LW protein shows the highest degree of sequence similarity to the first domains of the

Carl_G_190x270_mm_blokki_FINAL.indd 307 06-Aug-23 1:54:03 PM

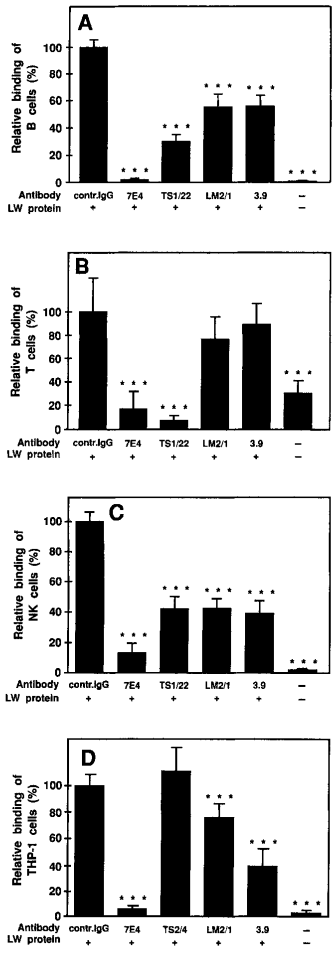

Figure 2. Inhibition of leukocyte binding to isolated LW protein using monoclonal antibodies. The purified LW protein was coupled to plastic using 0.25 μg/well. Leukocytes were added in the presence of the indicated antibodies in binding medium, and incubated at room temperature for 1 h. After washing three times, the attached cells were counted. (A) binding of B lymphocytes; (B) binding of T lymphocytes; (C) binding of NK cells; (D) binding of THP-1 cells. *** $p < 0.001$.

other ICAM, whereas the second domain has a lower sequence identity (26–27%). We do not know which domain in the LW protein is essential for binding, but the inhibition of red cell adhesion to both CD11a/CD18 and CD11b/CD18 by the BS46 antibody indicates that the binding sites are identical or closely spaced.

Mature red cells do not express ICAM-1, -2, or -3, and no inhibition of binding to leukocyte integrins was observed using blocking ICAM-1, -2 or -3 antibodies (not shown). Interestingly, the binding of red cells to isolated CD11a/CD18 was only partially inhibited by the various antibodies. This finding indicated that there is a separate site(s) on CD11a/CD18 which is used by an unidentified red cell ligand.

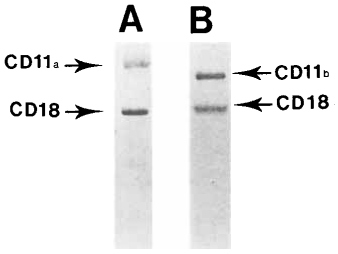

Figure 3. SDS-PAGE analysis of purified CD11a/CD18 (A) and CD11b/CD18 (B) integrins. Aliquots of 5 μg of each preparation were electrophoresed and stained using Coomassie Brilliant Blue.

Erythrocytes express the LFA-3 (CD58) adhesion molecule which binds to leukocyte CD2. Like LW, both CD2 and CD58 have two immunoglobulin domains. CD58 is involved in rosette formation between leukocytes and red cells, and may be important in the immune response. The functional and biological properties of the red cell ICAM molecule are unknown. Rh^{null} cells lack all Rh antigens and exhibit morphological and functional abnormalities that may be responsible for the chronic hemolytic anemia seen in these individuals [12]. Importantly, they lack LW antigens as well as other membrane proteins. It is thought that the Rh proteins are assembled within the membrane as a complex with genetically unrelated proteins, including LW, which are kept together by non-covalent bonds [12]. The lack of LW expression in Rh^{null} cells could mean that these gene products must be associated to be transported to the cell surface. Thus, erythroid expression could be regulated by any of these antigens. LW blood group antigens are also most unusual in that they appear to be very sensitive to changes in immune status. Thus, a loss of LW antigens together with transient LW antibody production has been associated with pregnancy and other immunologically altered states (Hodgkin's disease, autoimmune thrombocytopenic purpura) [28]. A reduced expression of LW antigens has been noticed also in congenital dyserythropoietic anemia [29].

Relatively little is known about how the number of red cells in circulation is regulated. A steady state is maintained by regulated synthesis in the bone marrow and removal through the reticuloendothelial system. The finding that human red cells contain a specific ICAM which is able to bind to all leukocyte integrins indicates that it is functionally important, and possibly involved in red cell turnover. Most probably, spleen macrophages contain CD11/CD18 integrins, and these could bind senescent red cells through the LW protein. Sadahira et al. [30] recently showed that the very late antigen-4-(VLA-4)-vascular cell adhesion molecule-1 (VCAM-1) interaction is important in the formation of erythroblastic islands in the bone marrow. However, erythroblast adhesion was only partially due to VLA-4-VCAM-1, and additional interactions were found to exist. Our preliminary results show strong expression of LW on immature red cells: this could be functionally important.

Carl_G_190x270_mm_blokki_FINAL.indd 308 06-Aug-23 1:54:03 PM

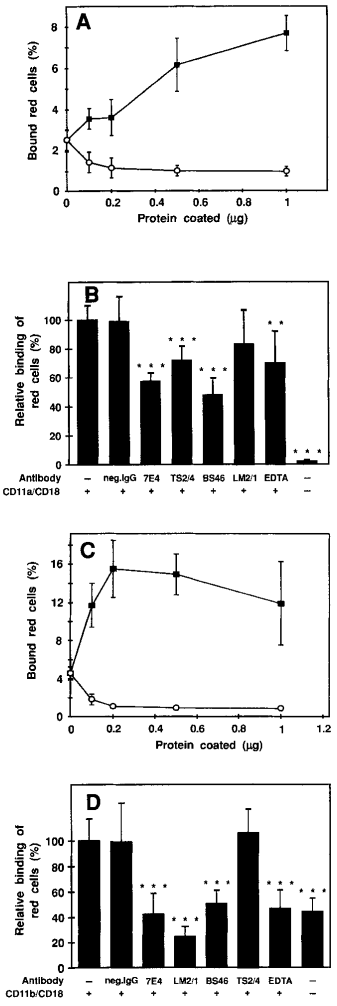

Figure 4. Binding of red cells to purified CD11a/CD18 and CD11b/CD18 integrins. In (A) the indicated amounts of CD11a/CD18 (■) or ICAM-3 (○) were coated in each well. (B) shows the effect of control IgG (neg. IgG) 7E4 (CD18), TS2/4 (CD11a), BS46 (LW) and LM2/1 (CD11b) mAb and EDTA (5 mM) on binding of red cells to 1 μg immobilized CD11a/CD18. In (C), wells were coated with the indicated amounts of CD11b/CD18 (■) or ICAM-3 (○), and in (D), the effect of antibodies and EDTA on binding of red cells to 1 μg immobilized CD11b/CD18 was studied. After incubation, the plates were carefully washed, and the bound cells counted. *** $p < 0.001$, ** $p < 0.01$.

Whether LW, like ICAM-1, may also act as a receptor for pathogens such as rhinoviruses [31, 32] or as a cytoadhesion receptor for *Plasmodium falciparum*-infected erythrocytes [33] is still unknown. ICAM-1 has been implicated as an attachment site to human venular endothelium in the primary step leading to complications in cerebral malaria [33, 34]. In the rosetting phenomenon, uninfected erythrocytes are attached around a central infected erythrocyte containing a mature asexual malaria parasite [35]. It is possible that adhesion between *Plasmodium falciparum*-infected and uninfected red cells is mediated by LW. Experiments along these lines are now amenable for study.

4 Concluding remarks

The red cell LW protein was shown to be an intercellular adhesion molecule, which we designate ICAM-4. It binds to the leukocyte CD11a/CD18 and CD11b/CD18 integrins and possibly to CD11c/CD18, and may be involved in the regulation of red cell turnover.

We thank P. Gane (Paris) for technical assistance, Veronica Ehrnrooth and Yvonne Heinilä for secretarial assistance, Dr. H. H. Sonneborn (Biotest, Offenbach, Germany) for the BS46 antibody, Dr. F. Sánchez-Madrid for the TP1/24 antibody, and Dr. C. Figdor (Amsterdam, The Netherlands) for the gift of the LAD lymphoblastoid cell line. These studies were supported by INSERM, the Caisse National d'Assurances Maladies des Travailleurs Salariés, The Academy of Finland, the Sigrid Jusélius Foundation and the Finnish Cancer Society.

Received May 10, 1995; in final revised form September 28, 1995; accepted October 6, 1995.

5 References

1 Springer, T. A., *Nature* 1990. *346:* 425.
2 Arnaout, M. A., *Blood* 1990. *75:* 1037.
3 Patarroyo, M., Prieto, J., Rincon, J., Timonen, T., Lundberg, C., Lindbom, C., Åsjö, B. and Gahmberg, C. G., *Immunol. Rev.* 1990. *114:* 67.
4 Rothlein, R., Dustin, M. L., Marlin, S. D. and Springer, T. A., *J. Immunol.* 1986. *137:* 1270.
5 Patarroyo, M., Clark, E. A., Prieto, J., Kantor, C. and Gahmberg, C. G., *FEBS Lett.* 1987. *210:* 127.
6 Simmons, D., Makgoba, M. W. and Seed, B., *Nature* 1988. *331:* 624.
7 Hogg, N., in Hogg, N. (Ed.), *Chemical Immunology. Integrins & ICAM-1 in Immune Responses,* S. Karger AG, Basel 1991, p. 99.
8 Staunton, D. E., Dustin, M. L. and Springer, T. A., *Nature* 1989. *339:* 61.
9 Nortamo, P., Salcedo, R., Timonen, T., Patarroyo, M. and Gahmberg, C. G., *J. Immunol.* 1991. *146:* 2530.
10 Fawcett, J., Holness, C. L. L., Needham, L. A., Turley, H., Gatter, K. C., Mason, D. Y. and Simmons, D. L., *Nature* 1992. *360:* 481.
11 Vazeux, R., Hoffman, P. A., Tomita, J. K., Dickinson, E. S., Jasman, R. L., St. John, T. and Gallatin, W. M., *Nature* 1992. *360:* 485.
12 Cartron, J.-P. and Agre, P. C., *Semin. Hematol.* 1993. *30:* 193.
13 Gahmberg, C. G., *EMBO J.* 1983. *2:* 223.
14 Mallison, G., Martin, P. G., Anstee, D. J., Tanner, M. J. A., Merry, A. H., Tills, D. and Sonneborn, H. H., *Biochem. J.* 1986. *234:* 649.
15 Bloy, C., Hermand, P., Blanchard, D., Cherif-Zahar, B., Goossens, D. and Cartron, J.-P., *J. Biol. Chem.* 1990. *265:* 21482.
16 Bailly, P., Hermand, P., Callebaut, I., Sonneborn, H. H., Khamlichi, S., Mornon, J.-P. and Cartron, J.-P., *Proc. Natl. Acad. Sci. USA* 1994. *91:* 5306.
17 Herman, P., Gane, P., Mattei, M. G., Sistonen, P., Cartron, J.-P. and Bailly, P., *Blood,* 1995. *86:* 1590.

Carl_G_190x270_mm_blokki_FINAL.indd 309 06-Aug-23 1:54:03 PM

18 Li, R., Nortamo, P., Valmu, L., Tolvanen, M., Huuskonen, J., Kantor, C. and Gahmberg, C. G., *J. Biol. Chem.* 1993. *268:* 17513.
19 Laemmli, U. K., *Nature* 1970. *227:* 680.
20 Campanero, M. R., Sánchez-Mateos, P., del Pozp, M. A. and Sánchez-Madrid, F., *J. Cell. Biol.* 1994. *127:* 867.
21 Nortamo, P., Patarroyo, M., Kantor, C., Suopanki, J. and Gahmberg, C. G., *Scand. J. Immunol.* 1988. *28:* 537.
22 Sánchez-Madrid, F., Krensky, A. M., Ware, C. F., Robbins, E., Strominger, J. L., Burakoff, S. F. and Springer, T. A., *Proc. Natl. Acad. Sci. USA* 1982. *79:* 7489.
23 Miller, L. J., Schwarting, R. and Springer, T. A., *J. Immunol.* 1986. *137:* 2891.
24 Myones, B. L., Daizell, J. G., Hogg, N. and Ross, G. D. J., *Clin. Invest.* 1988. *82:* 640.
25 Li, R., Xie, J., Kantor, C., Koistinen, V., Altieri, D. C., Nortamo, P. and Gahmberg, C. G., *J. Cell Biol.* 1995. *129:* 1143.
26 Staunton, D. E., Dustin, M. L., Erickson, H. P. and Springer, T. A., *Cell* 1990. *61:* 243.
27 Diamond, M. S., Staunton, D. E., Marlin, S. D. and Springer, T. A., *Cell* 1991. *65:* 961.
28 Storry, J. R., *Immunohematology* 1992. *8:* 87.
29 Parsons, S. F., Jones, J., Anstee, D. J., Judson, P. A., Gardner, B., Wiener, E., Poole, J., Illum, N. and Wickramasinghe, S. N., *Blood* 1994. *83:* 860.
30 Sadahir, Y., Yoshino, T. and Monobe, Y., *J. Exp. Med.* 1995. *181:* 411.
31 Greve, J. M., Davis, G., Meyer, A. M., Forte, C. P., Yost, C. S., Marlor, C. W., Kamarck, M. E. and McClelland, A., *Cell* 1989. *56:* 839.
32 Ockenhouse, C. F., Betageri, R., Springer, T. A. and Staunton, D. E., *Cell* 1992. *68:* 63.
33 Ockenhouse, C. F., Ho, M., Tandon, N. N., Van Seventer, G. A., Shaw, S., White, N. J., Jamieson, G. A., Chulay, J. D. and Webster, H. K., *J. Inf. Dis.* 1991. *164:* 163.
34 Berendt, A. R., McDowall, A., Craig, A. G., Bates, P. A., Sternberg, M. J. E., Marsh, K., Newbold, C. I. and Hogg, N., *Cell* 1992. *68:* 71.
35 Handunnetti, S. M., Gilladoga, A. D. and Howard, R. J., in *Cellular and Molecular Biology of Normal and Abnormal Erythroid Membranes,* Alan R. Liss, New York 1990, p. 249.

RED CELLS

Red-cell ICAM-4 is a ligand for the monocyte/macrophage integrin CD11c/CD18: characterization of the binding sites on ICAM-4

Eveliina Ihanus,[1] Liisa M. Uotila,[1] Anne Toivanen,[1] Minna Varis,[1] and Carl G. Gahmberg[1]

[1]Faculty of Biosciences, Division of Biochemistry, University of Helsinki, Finland

Intercellular adhesion molecule 4 (ICAM-4) is a unique member of the ICAM family because of its specific expression on erythroid cells and ability to interact with several types of integrins expressed on blood and endothelial cells. The first reported receptors for ICAM-4 were CD11a/CD18 and CD11b/CD18. In contrast to these 2, the cellular ligands and the functional role of the third β_2 integrin, CD11c/CD18, have not been well defined. Here, we show that ICAM-4 functions as a ligand for the monocyte/macrophage-specific CD11c/CD18. Deletion of the individual immunoglobulin domains of ICAM-4 demonstrated that both its domains contain binding sites for CD11c/CD18. Analysis of a panel of ICAM-4 point mutants identified residues that affected binding to the integrin. By molecular modeling the important residues were predicted to cluster in 2 distinct but spatially close regions of the first domain with an extension to the second domain spatially distant from the other residues. We also identified 2 peptides derived from sequences of ICAM-4 that are capable of modulating the binding to CD11c/CD18. CD11c/CD18 is expressed on macrophages in spleen and bone marrow. Inhibition of erythrophagocytosis by anti–ICAM-4 and anti-integrin antibodies suggests a role for these interactions in removal of senescent red cells. (Blood. 2007;109:802-810)

© 2007 by The American Society of Hematology

Introduction

In general, the major roles of the red blood cells, such as the transport of oxygen and carbon dioxide throughout the body, have not been thought to require adhesion of these cells.[1] However, recently it has been demonstrated that erythrocytes express on their surface proteins known to provide adhesive functions. Many of these adhesion proteins belong to the immunoglobulin superfamily of proteins. These molecules may participate in normal red-cell physiology by mediating cellular interactions during their life cycle as well as the pathology of human diseases. In bone marrow, erythroblasts surround central macrophages, forming erythroblastic islands where cell-adhesion events play critical roles in regulating erythropoiesis. A physiologic interaction between red cells and leukocytes, platelets, and endothelial cells can also occur during normal hemostatic conditions (clot formation), pathologic occlusive conditions, and inflammation. Finally, the interaction of senescent red cells with splenic macrophages is important for red-cell clearance.[1-7]

ICAM-4 is a glycoprotein expressed on red blood cells and erythroid precursor cells concurrently with glycophorin A and Rh glycoproteins.[8-10] The protein was originally described as the LW blood group antigen (Landsteiner-Wiener), but elucidation of its primary structure revealed significant similarity to the intercellular adhesion molecules (ICAMs). It is a 42-kDa glycoprotein composed of 2 immunoglobulin-like domains, a transmembrane part, and a short cytoplasmic tail.[11] The primary cellular counterreceptors for the ICAMs are the leukocyte-specific β_2 integrins, which consist of 4 heterodimeric glycoproteins with specific α chains (CD11a, CD11b, CD11c, CD11d) and a common β_2 chain (CD18).[12-15] However, ICAM-4 is an unusual ICAM in that it has recently been found to interact with several types of integrins expressed on blood and endothelial cells. Like all other members of the ICAM family,[16-20] ICAM-4 binds to the CD11a/CD18 (LFA-1, $\alpha_L\beta_2$) integrin expressed on leukocytes.[21] ICAM-4 also interacts with the granulocyte/monocyte-enriched β_2 integrin CD11b/CD18 (Mac-1, $\alpha_M\beta_2$),[21] as do ICAM-1 and ICAM-2.[22,23] In addition to β_2 integrins, ICAM-4 has been shown to bind to α_v integrins ($\alpha_v\beta_1$, $\alpha_v\beta_3$, and $\alpha_v\beta_5$) on nonhemopoietic cells, $\alpha_4\beta_1$ on hemopoietic cells, and $\alpha_{IIb}\beta_3$ on platelets.[24-27]

Using mutational analysis, we have previously mapped the binding sites on ICAM-4 for the CD11a/CD18 and CD11b/CD18 integrins.[28] The binding site for CD11a/CD18 was shown to be confined to the first Ig-like domain of ICAM-4, whereas both Ig domains are involved in CD11b/CD18 binding. Unlike the other ICAMs, ICAM-4 does not contain the conserved functionally important glutamate residue in the first domain, which is replaced by an arginine-52 residue. Mutation of arginine-52 back to glutamate did not affect CD11a/CD18 binding and even reduced the interaction with CD11b/CD18. Despite the lack of the conserved glutamate residue in ICAM-4, we have demonstrated that the CD11a and CD11b I domains contain an ICAM-4–binding region.[29] These data suggest that the β_2 integrin–binding motifs of ICAM-4 differ from those of other ICAMs.

We and others have previously suggested that ICAM-4 could mediate red-cell interactions with macrophages.[4,21] These interactions are evidently important during the life span of red cells from erythropoiesis to erythrocyte senescence. CD11c/CD18 is the major β_2 integrin on monocytes/macrophages[30]; therefore, we thought that it is important to study its binding characteristics. Whereas many ligands have been described for the CD11b/CD18 integrin,[23,31-34] much less is known about CD11c/CD18. In this

Submitted April 5, 2006; accepted August 17, 2006. Prepublished online as *Blood* First Edition Paper, September 19, 2006; DOI 10.1182/blood-2006-04-014878.

The online version of this article contains a data supplement.

The publication costs of this article were defrayed in part by page charge payment. Therefore, and solely to indicate this fact, this article is hereby marked "advertisement" in accordance with 18 USC section 1734.

© 2007 by The American Society of Hematology

Carl_G_190x270_mm_blokki_FINAL.indd 311 06-Aug-23 1:54:03 PM

report we show that ICAM-4 directly binds to the I domain of CD11c/CD18 and mediates erythrophagocytosis. Furthermore, using ICAM-4 mutants as well as synthetic peptides of ICAM-4, we have identified critical sites on ICAM-4 required for its interaction with CD11c/CD18.

Materials and methods

Antibodies

The monoclonal antibodies (mAbs) used in this study were as follows. The 7E4 and 2E7 mAbs react with the β_2 chain,[35] TS1/22 (ATCC, Rockville, MD) recognize the α chain of CD11a/CD18, and MEM170 is specific for the I domain of CD11b/CD18.[36] The anti-CD11c mAbs used included CBRp150/4G1 and 3.9[37,38] which were provided by Dr T. Springer (Harvard Medical School, Boston, MA) and Dr N. Hogg (Cancer Research UK, London, United Kingdom), respectively, Bly6 (BD PharMingen, San Diego, CA), BU15 (Serotec, Oxford, United Kingdom), and BL4H4 (Monosan, Hameenlinna, Finland). The mAbs against the first domain of ICAM-4 (BS46 and BS56) were from Dr H. Sonneborn (Biotest, Dreieich, Germany).[28,39] The mAbs 4C8 and 1A1 against ICAM-4 were from Dr J.-P. Cartron (Institut National de Transfusion Sanguine, Paris, France). A mouse IgG_1-negative control was purchased from Chemicon (Boronia, Australia) and a human IgG_1 used as a control was from Sigma (St Louis, MO). FITC-conjugated rabbit anti–mouse $F(ab')_2$ (Dakopatts a/s, Copenhagen, Denmark) was used for the flow cytometry studies (fluorescence-activated cell sorting; FACS).

Purification of CD18 integrins and soluble recombinant Fc proteins

CD11a/CD18, CD11b/CD18, and CD11c/CD18 integrins were purified from human blood as described previously (Figure S1, available on the *Blood* website; see the Supplemental Figure link at the top of the online article).[37,40] cDNA clones encoding the extracellular domains (residues 1-208) of native or mutagenized ICAM-4 and deletion mutants of ICAM-4 containing domain 1 (residues 1-101) or domain 2 (residues 102-208) in the pIg vector were used to produce soluble Fc-fusion proteins in COS-1 cells.[28] The wild-type and Ile314Gly mutant CD11c I domains were expressed and purified as described.[41]

Cells and cell lines

Approval was obtained from the Division of Biochemistry, University of Helsinki institutional review board for these studies. Informed consent was obtained in accordance with the Declaration of Helsinki.

Blood samples from common LW and Rh phenotypes (ICAM-4–positive red cells) were obtained from healthy volunteers using heparin as an anticoagulant.

The wild-type and L929 cells expressing ICAM-1, ICAM-2, or ICAM-4 have been previously described.[29] All the transfectants were grown in IMDM medium supplemented with 1 mg/mL G418, 10% FBS, 100 U/mL penicillin, and 100 μg/mL streptomycin. The CD11c/CD18-transfected L929 cell line was provided by Dr Y. van Kooyk (Vrije Universiteit Medical Center, Amsterdam, The Netherlands) and purified by sorting with a FACStar Sorter (Becton Dickinson, Immunocytometry Systems, San Jose, CA), and the G418-resistant cell populations were analyzed with a Becton Dickinson (Immunocytometry Systems) FACScan flow cytometer. For FACS analysis macrophages were pretreated with 3% BSA and 20% rabbit serum, and the stainings were performed in the presence of 1% BSA, 3% rabbit serum. The COS-1 (ATCC, Manassas, VA) cells were grown in DMEM.

Adhesion assays

Cell adhesion assays were performed as described previously.[28,29]

For cell-adhesion assays of transfected and wild-type L929 cells 2 mM $MnCl_2$ was added to the buffers. The biotinylated peptides were immobilized to streptavidin plates (Immobilizer Streptavidin Plate; Nunc, Kamstrup, Denmark) in 25 mM Tris, pH 8.0, 150 mM NaCl, 2 mM $MgCl_2$, 2 mM $CaCl_2$, 2 mM $MnCl_2$ for 1 hour at room temperature or by overnight incubation at 4°C.

For the binding study with or without divalent cations, the adhesion assays were performed with buffers containing 5 mM EDTA, 5 mM EGTA and 2 mM $MgCl_2$, 2 mM $MgCl_2$ and 2 mM $CaCl_2$, or 2 mM $MnCl_2$.

Solid-phase ELISA assay

Ninety-six–well plates (Greiner, Solingen, Germany) were coated at 4°C with indicated amounts of CD11c/CD18 in assay buffer (25 mM Tris-HCl, pH 7.4, 150 mM NaCl, 2 mM $CaCl_2$, 2 mM $MgCl_2$, 2 mM $MnCl_2$). After blocking nonspecific sites with 1% HSA for 1 hour at room temperature (RT) the wells were washed 3 times with assay buffer. The recombinant ICAM-Fc proteins (25 μg/well) were then added to the wells and incubated for 2 hours at RT. The wells were washed prior to the addition of a peroxidase-conjugated anti–human Fc mAb (1:1000 dilution; Amersham Biosciences, Freiburg, Germany) to the wells. After a 1-hour incubation at 37°C, the plates were washed, and the bound proteins were detected with 100 μL/well 0.5 mg/mL *o*-phenylenediamine dihydrochloride added for 10 minutes, stopped by the addition of 50 μL 12.5% H_2SO_4, and read in an enzyme-linked immunoabsorbent assay (ELISA) reader. For inhibition experiments, the recombinant soluble Fc fusion proteins or protein-coated wells were pretreated with different mAbs (50 μg/mL).

Synthetic peptides

Peptides synthesized as spots on derivatized cellulose membranes. The protein sequence of the extracellular part of ICAM-4 was synthesized as 56 membrane-bound peptides 15 amino acids long (SPOTs) with a 3–amino acid overlap using Abimed Auto-Spot robot ASP 222 (with F-moc chemistry; Abimed, Langensfeld, Germany).

Soluble peptides. ICAM-4 sequence-derived peptides were synthesized by solid-phase synthesis using F-moc chemistry in an Applied Biosystems (Weiterstadt, Germany) model 433A automatic peptide synthesizer and purified by reverse-phase chromatography. The sequences of the peptides were confirmed by MALDI-TOF mass analysis.

The following peptides were synthesized: a 13–amino acid peptide derived from the Ig-like domain 1 of ICAM-4 (residues 44-56 of ICAM-4 = P-D1; sequence, PQPQNSSLRTPLR), a 13–amino acid peptide derived from the Ig-like domain 2 of ICAM-4 (residues 161-173 of ICAM-4 = P-D2; sequence, VTLTYEFAAGPRD). Biotinylated versions of the same peptides were also synthesized to enable possible detection and immobilization. For the inhibition studies a control peptide (Pcontr1) of 10 residues with the sequence of ELSGRLPWLY was used, as well as a biotinylated control peptide derived from the cytoplasmic part of ICAM-5 (Pcontr2; sequence, GGGKKGEY).

Peptide-binding assays

For interaction studies, the PepSpot membrane containing the ICAM-4–derived peptides was blocked o/n at RT with TBST (Tris-buffered saline, pH 8.0, 0.05% Tween 20) containing 2.5% dried milk, 1.5% BSA, and 5% sucrose. The membrane was washed 3 times with Tris-buffered saline and incubated for 1.5 hours at 37°C with purified CD11c/CD18 integrin at a concentration of 5 μg/mL in blocking buffer diluted 3:1 with TBST in the presence of 1 mM $CaCl_2$, 1 mM $MgCl_2$, and 1 mM $MnCl_2$. After washes the bound integrin was visualized on X-ray film according to the protocol of enhanced chemiluminescence (ECL) Western blotting (Amersham Biosciences) using the CD11c/CD18 mAb CBRp150/4G1 (1 μg/mL) and peroxidase-conjugated rabbit antimouse antibody (1:5000 dilution).

Erythrophagocytosis assay

Human buffy coat cells separated by Ficoll-Hypaque centrifugation were placed in 12-well culture dishes (Greiner) at 3.5 million cells/well. The adhered monocytes were differentiated to macrophages as described.[42] The phagocytosis experiments were adapted from the method of Bratosin et al.[43] First, the macrophage Fc receptors were blocked with heat-inactivated bovine serum for 10 minutes. Monoclonal anti–ICAM-4 or anti-integrin

antibodies (40 μg/mL) were incubated with macrophages for 20 minutes before adding 15×10^6 PKH-26–labeled (cell linker kit; Sigma) red cells. After 2 hours of incubation at 37°C, macrophages were washed 3 times with RPMI 1640 medium. Noninternalized red cells were lysed with hypotonic buffer, and macrophages were detached with lidocaine solution. Cells were fixed with 70% ethanol and analyzed by flow cytometry. The results were presented as relative (%) phagocytosis derived from mean values of the data. Experiments were repeated 3 times in duplicates.

Modeling of ICAM-4

The ICAM-4[11] (SWISS-PROT accession no. Q14773) model was built on the structure of ICAM-2[44] (Protein Data Base code 1ZXQ). Twenty models were made using the modeling program MODELLER (A. Sali, Department of Pharmaceutical Sciences, University of California–San Francisco).[45] Each model was analyzed first at the overall structural level at which the models with the highest objective functions were discarded. The objective function describes the degree of fit of the model to the input structural data used in its construction, derived by the program MODELLER.[45] Then the orientation of the amino acids in the models were analyzed one amino acid at a time, giving higher values to those amino acids that have been shown to be involved in ligand binding.[28] In the final model most of the orientations of the amino acids were shared with the template structure. The objective function was near the average of the objective functions of all models. The detailed structural analysis of the ICAM-4 models was made using the Bodil Molecular Modeling Environment (M. S. Johnson, Structural Bioinformatics, Åbo Akademi University, Åbo, Finland).[46] The ICAM-4 model was also validated with PROCHECK (J. M. Thornton, European Bioinformatics Institute, Cambridge, United Kingdom).[47] Figure 7A and 7B were made using the program MOLSCRIPT[48] (P. E. Kraulis, Stockholm University, Sweden) and Raster3D (D. J. Bacon and E. A. Merritt, Department of Biochemistry, University of Washington, Seattle).[49,50]

Results

Red cells and ICAM transfectants adhere to purified CD11c/CD18 integrin

In SDS–polyacrylamide gel electrophoresis (PAGE) analysis of the purified CD11a/CD18, CD11b/CD18, CD11c/CD18, and the wild-type and mutant CD11c I domain preparations no major impurities were observed (Figure S1). Both the purified integrins and the recombinant I domains were tested for correct folding by ELISA using several anti-integrin antibodies. Red cells readily bound to coated CD11c/CD18 as well as to the other 2 CD18 integrins (Figure 1A). The binding to CD11c/CD18 was efficiently inhibited by monoclonal antibodies to ICAM-4 and CD11c/CD18 (Figure 1B). However, the adhesion was not completely blocked by the CD11c and ICAM-4 mAbs. There may exist other red-cell receptors for CD11c/CD18, and the purified immobilized CD11c/CD18 may not be recognized by the 3.9 antibody with equal efficiency as cellular integrins. Using purified CD11c/CD18, we also studied the adhesion of ICAM transfectants[29] to coated CD11c/CD18 (Figure 1C). Their ICAM expression was ascertained by FACS analysis (Table 1). All the ICAM transfectants adhered to the coated integrin with similar efficiency (approximately 20% of the total added cells). Because the expression levels of ICAM-4 and ICAM-2 in L-cell transfectants were about 70% lower than ICAM-1 transfectants,[29] these results suggest that ICAM-4 might be an even more potent ligand for CD11c/CD18 than ICAM-1. To a certain extent (10%-20%) the binding efficiencies to ICAMs varied between different preparations of CD11/CD18 integrins. However, the same preparations were used in all experiments reported here. The mAbs to CD11c/CD18 and ICAM-4 clearly inhibited the binding of ICAM-4 L cells to coated CD11c/CD18 integrin (Figure 1D). The ICAM-4 transfectants also bound to purified CD11c I domains, and the level of binding was similar both in the wild-type and the active Ile314Gly mutants[41] (not shown).

Soluble ICAM-4 binds to purified CD11c/CD18

Further proof for the specific binding of ICAM-4 to the CD11c/CD18 integrin was obtained using a cell-free assay (Figure 2). By performing solid-phase ELISA assays with recombinant soluble ICAM-4Fc, we showed that ICAM-4 bound to coated purified CD11a/CD18, CD11b/CD18, and CD11c/CD18 in a dose-dependent fashion (Figure 2A). High amounts of coated integrin resulted in decreased binding possibly because of steric hindrance. Similar effects have been seen before.[29] We also found that both

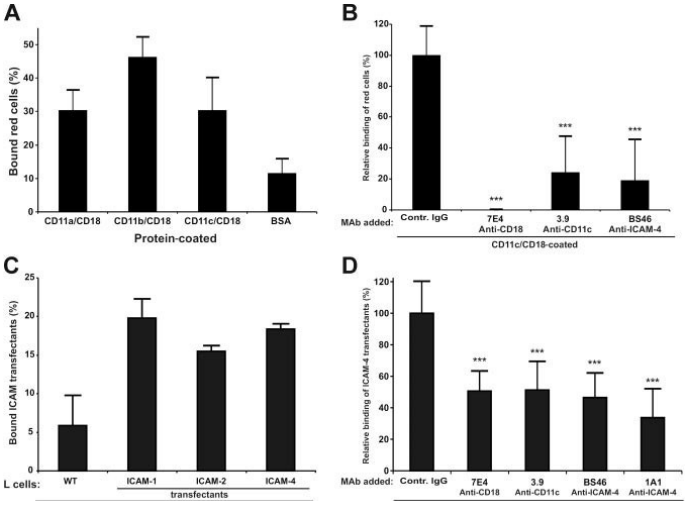

Figure 1. Adhesion of red cells and ICAM-4 transfectants to CD11c/CD18 is mediated by ICAM-4. Adhesion assays were as described in "Materials and methods." (A) The binding of erythrocytes to 1 μg coated β_2 integrins; (B) the inhibitory effect of anti–ICAM-4 (BS46), anti-CD18 (7E4), and anti-CD11c (3.9) monoclonal antibodies on the adhesion of red cells to purified CD11c/CD18. (C) Wells were coated with 1 μg purified CD11c/CD18, and the adhesion of parental L cells and different ICAM L-cell transfectants was measured. (D) The effect of antibodies on binding of ICAM-4 L-cell transfectants to 1 μg coated CD11c/CD18 was studied. The data in panels A and C are presented as a percentage of attached cells (amount of bound cells divided by input of cells). The results in panels B and D are expressed as a relative percentage of bound cells, where 100% is calculated from the total number of cells bound to the CD11c/CD18 in the absence of pretreatment with MAbs. The significance was determined by unpaired Student *t* test. Controls included unrelated mouse IgG antibody and wells with coated control protein (GPA) or without coated protein (BSA only). Background binding of cells to GPA or BSA was subtracted. The experiments were repeated 3 times with similar results. Data are expressed as mean ±

Table 1. Antigen profiles of the L cells and macrophages determined by flow cytometry

Antigen	Wt L cells	ICAM-1 L cells	ICAM-2 L cells	ICAM-4 L cells	CD11c L cells	Macrophages
Isotype control Ig	2.3 ± 0.2	3.2 ± 1.1	3.2 ± 0.7	3.4 ± 0.5	4.0 ± 0.9	11.7 ± 4.9
ICAM-1	3.4 ± 1.3	98.6 ± 12.1	6.3 ± 9.9	4.2 ± 0.3	—	—
ICAM-2	2.7 ± 0.4	3.4 ± 1.4	25.7 ± 0.7	3.4 ± 0.4	—	—
ICAM-4	2.7 ± 0.5	4.4 ± 1.7	3.0 ± 0.7	29.0 ± 3.8	—	—
CD11a	2.1 ± 0.1	—	—	—	5.2 ± 1.9	69.5 ± 35.5
CD11b	2.3 ± 0.1	—	—	—	3.9 ± 1.1	95.6 ± 19.5
CD11c	2.1 ± 0.1	—	—	—	35.9 ± 14.8	74.9 ± 34.8
CD18	2.4 ± 0.3	—	—	—	28.2 ± 15.6	78.9 ± 56.8

The values given are the mean fluorescence intensities ± SEM of 3 flow cytometric experiments. Cultured macrophages were from different healthy donors.
— indicates not applicable.

CD11c/CD18-specific mAbs (3.9 and BU15) and anti-CD18 antibody 7E4 partially but significantly inhibited the binding, whereas the 1A1 (anti–ICAM-4) blocked more efficiently (Figure 2B).

Integrin transfectants adhere to ICAM-4

The surface expression of β_2 integrins on CD11c/CD18 transfectants was studied by FACS (Table 1). As shown in Figure 3A the coated chimeric ICAM-4Fc protein supported the adhesion of CD11c/CD18 transfectants. Some background binding of untransfected L cells was observed, indicating additional interactions. To check the specificity of the interaction, we studied the effects of mAbs on the adhesion of transfectants to ICAM-4Fc (Figure 3B). Monoclonal antibodies against either the α or β chain inhibited the binding of CD11c/CD18 transfectants approximately by 50% to 85%, whereas the anti–ICAM-4 mAbs blocked the binding efficiently down to background levels. To obtain further evidence of specificity, we investigated the divalent cation requirements of the CD11c/CD18 transfectant binding to ICAM-4Fc (Figure 3C). In the absence of cations, the adhesion was efficiently but not totally abolished. As can be seen in Figure 3C, $MgCl_2$ alone or in combination with $CaCl_2$ was not sufficient to support the maximal binding of CD11c/CD18 L cells to ICAM-4Fc. Indeed, the presence of Mn^{2+} seems to be required for high-affinity binding of CD11c/CD18 transfectants to ICAM-4. Interestingly, the binding was efficiently inhibited by the soluble active mutant of CD11c I domain (Figure 3D).

CD11c/CD18 integrin binding sites on ICAM-4

To establish which ICAM-4 Ig domains contain CD11c/CD18 binding sites, ICAM-4 deletion mutants lacking either domain D1 or D2 were tested in cell-adhesion assays (Figure 4A). Neither domain alone was sufficient for the maximal binding of CD11c/CD18 transfectants. However, both domain deletion mutants retained partial binding capacity. As expected, the anti–ICAM-4 mAb, 1A1, the epitopes of which reside within domain D1, affected only the binding to the wild-type ICAM-4Fc and the deletion mutant carrying domain D1. The I domain–specific anti-CD11c mAb, 3.9, inhibited CD11c/CD18 transfectant binding partially to wild-type ICAM-4 and only slightly to the mutant lacking D1. Instead, the adhesion to the mutant lacking domain D2 was almost totally abolished by 3.9.

To define the binding sites of CD11c/CD18 in ICAM-4 in more detail, we tested 32 ICAM-4Fc mutant proteins.[28] The residues targeted for mutation were all expected to be surface exposed, being able to participate in molecular interactions with counter-receptors. The mutant proteins were tested for correct folding by ELISA with the anti–ICAM-4 mAb, 1A1. This mAb also reacted with the Trp19Ala mutant not recognized by the BS mAbs in our previous report, indicating partially correct folding.

As shown in Figure 4B, 4 single point mutations caused a reduction in cell adhesion by 38% or greater. However, when the control binding (29%) is taken into account, the adhesion was reduced by 54% or greater. Three of these are located within domain D1 on the A strand at position Trp19, on the C strand at position Arg52, and in the E to F loop at position Trp77. One of these 4 mutations localized to D2, on the strand E at position Glu166. The Arg52Ala mutation almost completely eliminated binding. In addition to these 4 ICAM-4 mutants, the adhesion to mutants at positions Thr91, Trp93, and Arg 97 reduced adhesion by 25% to 30% (background not subtracted). When the Arg residues at positions 52 and 97 were mutated to opposite charge (Glu), the

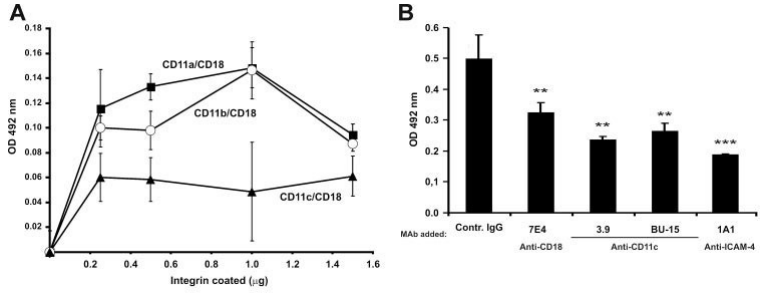

Figure 2. Soluble ICAM-4Fc binds specifically to immobilized purified CD11c/CD18 in a solid-phase assay. (A) Dose-dependent binding of recombinant ICAM-4Fc to coated integrins. ICAM-4Fc + CD11a/CD18 (■), ICAM-4Fc + CD11b/CD18 (○), ICAM-4Fc + CD11c/CD18 (▲). Background binding of control protein (human IgG_1) was subtracted. (B) The effect of monoclonal antibodies on binding of soluble ICAM-4Fc to 0.4 μg coated CD11c/CD18 in a solid-phase assay is shown. The ICAM-4Fc binding to CD11c/CD18 was examined in the presence of mAbs (50 μg/mL) against the ICAM-4 (1A1), CD18 (7E4), and CD11c (3.9, BU15). Data shown are from 1 representative experiment of 3. Standard deviations and statistical significances are shown; $^{***}P < .005$, $^{**}P < .05$. The significances were determined by unpaired Student *t* test.

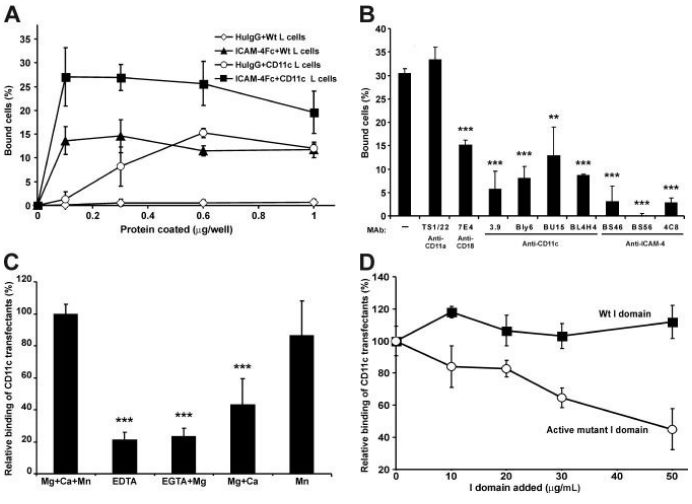

Figure 3. CD11c/CD18 transfectants show specific cation-dependent binding to coated ICAM-4Fc. (A) The adhesion of parental L cells and CD11c/CD18 transfectants to ICAM-4Fc and human IgG proteins coated on plastic wells. CD11c/CD18 L cells + ICAM-4Fc (■), parental L cells + ICAM-4Fc (▲), CD11c/CD18 L cells + human IgG (○), parental L cells + human IgG (◇). (B) The effects of anti–ICAM-4, anti-CD18, and anti-CD11c mAbs on adhesion of CD11c/CD18 transfectants to 0.5 μg purified ICAM-4Fc fusion protein. Controls included wells with binding of wild-type L cells (not shown) and the effect of control antibody (anti-CD11a mAb). (C) The binding of transfectants to ICAM-4Fc in the absence or presence of divalent cations. (D) The binding of CD11c/CD18 transfectants to coated ICAM-4Fc in the presence of indicated concentrations of soluble wild-type CD11c I domain (■) and the active mutant I domain (○). In panels A and B the results are shown as the percentage of input cells bound ± SD. In panels C and D the results are expressed as a relative percentage of bound cells, where 100% is given as the number of cells bound to the ICAM-4Fc in the presence of divalent cations (C) or in the absence of soluble I domain (D). Background binding of cells to HSA was subtracted. The experiments were repeated 3 to 5 times with similar results. Standard deviations and statistical significances are shown; $***P < .001$, $**P < .01$.

effect on cell adhesion was weaker than observed with substitution by an apolar amino acid (Ala), indicating that charge is needed at these positions. Furthermore, replacement of Trp at position 77 by Phe caused a severe reduction of CD11c/CD18 L-cell adhesion, whereas substitution by Ala had a minor effect. However, for the double mutants Arg52Glu/Thr91Gln and Trp77Ala/Glu151Ala a 40% and 30% reduction in cell adhesion was noted, respectively, confirming the importance of ICAM-4 residues Arg52, Thr91, and Trp77 in CD11c/CD18 binding. According to these data, of the 7 residues critical for ICAM-4 interaction with CD11c/CD18 integrin, 6 are spatially close, spanning the interface between the ABED and CFG faces of domain D1 with an extension of one important residue far from the others in the domain D2 (Figure 5A).

ICAM-4–derived peptides interact with CD11c/CD18 and inhibit cell adhesion

Using a PepSpot assay, we were able to identify 2 peptide regions derived from ICAM-4 which selectively bound to soluble purified CD11c/CD18 integrin. CD11c/CD18 reacted with 5 overlapping peptides spanning the ICAM-4 sequence of amino acids 39 to 65 located in domain D1 and with 3 peptides spanning the sequence of amino acids 159 to 179 located in domain D2 (Figure 6). Consistent with the mutation results the peptide region from domain D1 includes the important Arg52 (see Figure 4). Furthermore, the only critical amino acid mutation localized to D2 at position Glu166 was included in the selected peptide sequences from D2. According to these results, 2 peptides were chosen for further analysis in cell-adhesion assays: P-D1 (PQPQNSSLR**T**PLR) covering the C strand and parts of the loops at both ends of the C strand in the domain 1 and P-D2 (VTLTY**E**FAAGPRD) derived from the domain 2 and covering the E strand and part of the loop connecting the E strand to F strand (Figure 5B). Two available control peptides, Pcontr1 (ELSGRLPWLY) and Pcontr2 (biotinylated GGGKKGEY), were used in the cell-adhesion assays, but in the PepSpot assays the negative and flanking peptides also acted as controls.

The immobilized P-D2 peptide supported binding of CD11c/CD18 transfectants efficiently, whereas the P-D1 peptide supported

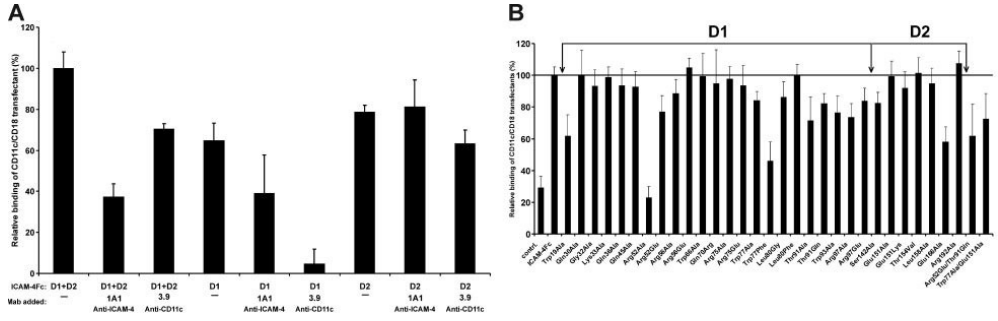

Figure 4. Effects of domain deletion mutations and amino acid substitutions on ICAM-4 binding to CD11c/CD18 transfectants. Adhesion of CD11c/CD18-expressing L cells to plastic-coated native and mutated ICAM-4Fc (0.5 μg/well). Results are shown as the percentage of CD11c/CD18 transfectant-cell binding relative to native ICAM-4Fc (100%). (A) The binding of CD11c/CD18 transfectants to ICAM-4 domain deletion mutants in the absence or the presence of mAbs 1A1 (anti–ICAM-4) or 3.9 (anti-CD11c). Controls included wells with binding of wild-type L cells and the effect of control antibody (not shown). Background binding of cells to HSA was subtracted. Panel B shows the adhesion of CD11c/CD18 transfectants to a panel of ICAM-4 mutants. The mean ± SD from 3 experiments is shown.

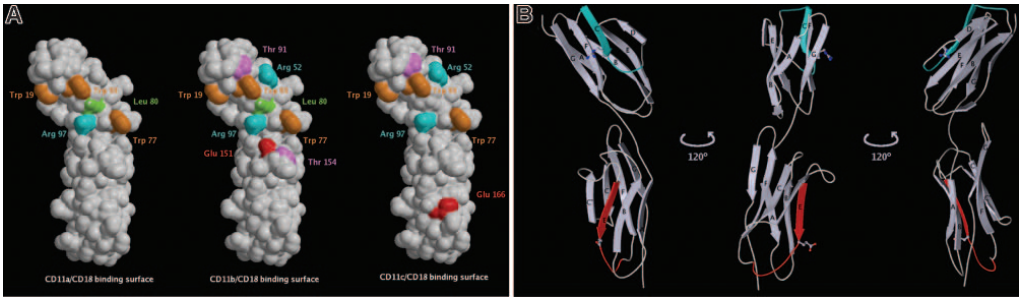

Figure 5. Critical residues of ICAM-4 involved in interaction with β_2 integrins and location of ICAM-4 peptides that mediate adhesion to CD11c/CD18 integrin. (A) Three-dimensional representation of an ICAM-4 model constructed on the basis of ICAM-2 structure. Amino acids are designated by 3-letter codes and residue numbers. The solvent-accessible surfaces of ICAM-4 residues that when mutated cause a decrease in adhesion to CD11a/CD18 (left), CD11b/CD18 (middle), and CD11c/CD18 (right) are colored (Trp, orange; Arg, cyan; Leu, green; Thr, magenta; Glu, red). (B) A ribbon diagram of ICAM-4 displayed in 3 orientations 120 degrees to one another. The strands of the antiparallel β sheets are labeled by capital letters. The locations of the ICAM-4 peptides are colored: P-D1 (PQPQNSSLRTPLR), residues 44 to 56 (cyan); P-D2 (VTLTYEFAAGPRD), residues 161 to 173 (red). Side chains of the 2 peptide residues found to be involved in CD11c/CD18 binding by mutagenesis studies are shown as ball and stick.

adhesion only weakly. The binding profiles of the 2 peptides were clearly different as well (Figure 6B). Both peptides inhibited the interaction between ICAM-4 and CD11c/CD18. However, the P-D2 peptide was a significantly more effective blocker of the CD11c/CD18 L-cell binding. Figure 6C shows that the inhibition of CD11c/CD18 transfectant adhesion to ICAM-4Fc by the P-D2 peptide was concentration dependent, and 65% inhibition was obtained with a peptide concentration of 500 μM. The P-D1 peptide was less active. The blocking activity was reduced with higher P-D1 amounts. When the peptides were tested together, there was an additional inhibition of binding.

Erythrophagocytosis is mediated by ICAM-4/β_2 integrin interaction

To find a possible physiologic role of the ICAM-4/β_2 integrin interaction we studied erythrophagocytosis. The expression of β_2 integrins on cultured, monocyte-derived macrophages was verified by FACS (Table 1). The uptake of PKH-26–labeled red cells by human macrophages was effectively inhibited by antibodies against ICAM-4 and β_2 integrins. Figure 7 shows that these mAbs reduced the phagocytosis of red cells by 50% or more. Greater than 60% inhibition was obtained in the presence of the 3.9 CD11c mAb.

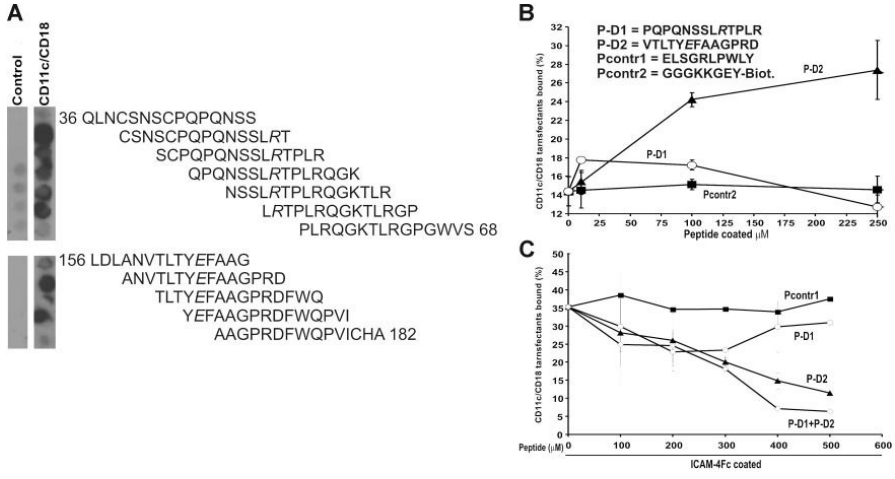

Figure 6. CD11c/CD18 binds selectively to peptides derived from the ICAM-4 sequence. (A) A total of 56 overlapping synthetic peptides 15 amino acid-long that corresponded to the protein sequence of the extracellular part of ICAM-4 were synthesized as immobilized spots on a cellulose membrane. The reactivities of the peptides with purified CD11c/CD18 integrin were tested. The CD11c/CD18 mAb CBRp150/4G and peroxidase-conjugated rabbit antimouse antibody were used to detect bound CD11c/CD18 integrin. The figure shows the reactivity of the overlapping peptides selected with the soluble CD11c/CD18 integrin. Negative control was carried out in the absence of the integrin. According to these results 2 peptides were chosen for solid-phase synthesis: P-D1 derived from the ICAM-4 Ig-like domain 1 and P-D2 derived from the domain 2. Both of the peptides included an amino acid shown to be involved in adhesion to CD11c/CD18 according to our mutational studies (see Figure 4). (B) The adhesion of the CD11c/CD18 transfectants to biotinylated versions of the selected ICAM-4 peptides and a control peptide (Pcontr2) captured by streptavidin microplates. Indicated amounts of the peptides were coated per well, and the cell adhesion was performed as described in "Materials and methods." Sequences of the synthesized ICAM-4–derived peptides and the peptides used as control are listed in the figure. (C) The effects of the defined ICAM-4 peptides and the control peptide on adhesion of the CD11c/CD18 transfectants to coated ICAM-4Fc are shown. The cells were pretreated or not with the control peptide (Pcontr1), P-D1, P-D2 or the P-D1 and P-D2 peptides together at different final concentrations. A representative binding experiment with results expressed as the percentage of input cells bound are shown. Control peptides (■), P-D2 (▲), P-D1 (○), P-D1 + P-D2 (◇).

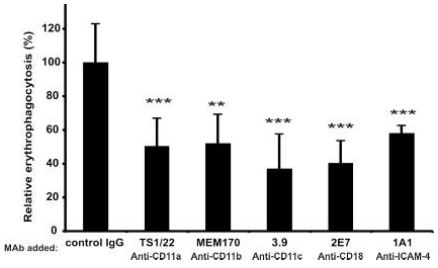

Figure 7. Phagocytosis of red cells by macrophages is inhibited by β_2 integrin and ICAM-4 antibodies. (A) Effect of mAbs against the CD11a (TS1/22), CD11b (MEM170), CD11c (3.9), CD18 (2E7), and ICAM-4 (1A1) on erythrophagocytosis. The results are presented as relative phagocytosis derived from mean values of the data; $^{***}P < .001$, $^{**}P < .01$.

Discussion

ICAM-4 is remarkable because of its ability to bind several members of integrin subclasses. These include the α_v integrins ($\alpha_v\beta_1$, $\alpha_v\beta_3$, and $\alpha_v\beta_5$), $\alpha_4\beta_1$ and $\alpha_{IIb}\beta_3$,[24-26] in addition to CD11a/CD18 and CD11b/CD18.[21] The binding sites for all the ICAM-4 receptor integrins, except for CD11a/CD18, comprise residues on both Ig-like domains of ICAM-4. The regions of ICAM-4 identified as β_2 and β_3 integrin interaction sites appear clearly distinct, although they all share W77. The ICAM-4 amino acids predicted to be critical for binding to $\alpha_v\beta_1$ and $\alpha_v\beta_5$ are located in close proximity to those needed for β_2 integrin interaction. However, R97 is the only residue that is shared between the 2 sites.[25,26,28,51] The ability of ICAM-4 to interact selectively with several different integrin receptors suggests multiple functions for ICAM-4 in red-cell physiology and pathology.[27]

The CD11c/CD18 ($\alpha_x\beta_2$) integrin is most homologous to the CD11b/CD18 and CD11d/CD18 integrins with 60% to 66% amino acid identity, whereas it is only 37% identical to CD11a/CD18.[52-54] CD11c/CD18 plays an important role in phagocytosis, chemotaxis, and regulation of the immune response.[12,13] Little is known about the cellular ligands of CD11c/CD18, but the ligands appear to overlap in part with those of CD11b/CD18. In addition to several soluble and matrix ligands, the only reported cellular ligands for CD11c/CD18 are ICAM-1[37,55] and Thy-1.[56] A recent study shows that the binding site of CD11c/CD18 on ICAM-1 resides on domain D4,[57] and another report suggested that negatively charged residues in structurally decayed proteins serve as a pattern recognition motif for CD11c/CD18.[58] Preliminary experiments indicated that CD11c/CD18 in THP-1 cells binds to purified ICAM-4, but we failed to see binding to red cells.[21] This could be due to low affinity of CD11c/CD18, but now we have used an antibody, which allows purification in a functionally active form.[37]

In this study we have convincingly demonstrated that red-cell ICAM-4 binds to CD11c/CD18: (1) red cells and ICAM-4 L-cell transfectants adhered to immobilized purified CD11c/CD18; (2) the specificity was confirmed by the ability of antibodies against CD11c/CD18 and ICAM-4 to block the adhesion;, (3) with purified CD11c/CD18 and ICAM-4 a direct binding was observed; (4) adhesion of the CD11c/CD18 transfectants to recombinant-coated ICAM-4Fc was inhibited by soluble I domain, the antibodies against ICAM-4, and the α and β subunits of the CD11c/CD18; (5) ICAM-4 deletion mutants lacking either domain D1 or D2 showed lower binding to CD11c/CD18; (6) the panel of point mutants studied resulted in the identification of 7 residues of ICAM-4 important for binding to CD11c/CD18. ICAM-4 residues in domain D1 (Trp19, Arg52, Trp77, Thr91, Trp93, and Arg97) have previously been shown to be involved in binding to CD11b/CD18 as well.

Figure 5 shows a model of the external part of the ICAM-4 molecule, with critical amino acids marked defining distinct but overlapping β_2 integrin binding footprints on ICAM-4. As expected, our model is consistent with the one published by Hermand et al[28] because these both have the same template structure. Furthermore, the amino acids that were reported to reside on the surface of the protein[51] are on the surface in our model as well. D1 residues showing the greatest specific effect on CD11c/CD18 binding, and which may be central in the binding site, are Arg52 at the bottom of strand C, Trp19 at the top of strand A, and Trp77 on the E to F loop. Trp19, Arg52, Thr91, and Trp93 lie approximately in the middle of domain D1.

Previous and current results show that both Ig-like domains of ICAM-4 are involved in binding to CD11b/CD18 and CD11c/CD18. However, the vital ICAM-4 residues in domain D2 mediating adhesion to the 2 integrins are different. Mutation of Glu166 at the bottom of strand E in D2 reduced binding to CD11c/CD18, whereas the recognition site for CD11b/CD18 is located in the C′ to E loop of D2 far from the CD11c/CD18 binding site. The model of ICAM-4 shows that the location of the Glu166 is spatially distant from the rest of the integrin-binding footprint. This could indicate that the integrin molecules interact with a large surface area of the ICAM-4 molecule. It is interesting to note that in all other ICAMs there is a glutamic acid residue in the first domains, which are needed for adhesion, but in ICAM-4 this is replaced by Arg52. Glu166 may substitute for this. The binding of the CD11b/CD18 and CD11c/CD18 integrins to additional sites present on domain D2 of ICAM-4 is consistent with the stronger binding to ICAM-4 observed for these 2 β_2 integrins as compared with CD11a/CD18. The I domain–specific anti-CD11c mAb, 3.9, efficiently blocked the binding to the D2 deletion mutant but only slightly to the D1 deletion mutant. These data suggest that the I domain mainly binds to the D1 of ICAM-4, but they also indicate that multiple regions of the CD11c/CD18 could be involved in the interaction with ICAM-4.

Our results with synthetic peptides provided additional support for the role of ICAM-4 residues identified by site-directed mutagenesis. Using PepSpot analysis, we found 2 peptides derived from ICAM-4 reacting with CD11c/CD18. Both peptides included amino acids (Arg52 in D1 and Glu166 in D2) shown to be needed for CD11c/CD18 binding. The peptide binding and inhibition data are consistent with those of our mutational results and support the finding that both ICAM-4 domains are involved in binding to CD11c/CD18. The 2 peptides and the critical residues are exposed at the surface of the ICAM-4 molecule being available for interactions (Figure 5).

The role of ICAM-4 in red-cell physiology has remained poorly understood. CD11c/CD18 is expressed on macrophages[30] (Table 1), and we report here that erythrophagocytosis was prevented by the inhibition of ICAM-4-β_2 integrin binding, indicating that this interaction may be important in removal of erythrocytes from the circulation by splenic macrophages. Interestingly, in a recent report erythroblastic island formation was shown to decrease in ICAM-4–null mice, and the interactions between erythroblast ICAM-4 and macrophage α_v integrin were reported to be critical for island

Carl_G_190x270_mm_blokki_FINAL.indd 317 06-Aug-23 1:54:06 PM

integrity.[59] Thus, ICAM-4 seems to be important for red-cell development and turnover. Furthermore, secreted isoforms of ICAM-4 may be important regulators of these molecular interactions.[11,60]

Although it has been commonly accepted that normal red cells are fairly nonadhesive during coagulation and thrombosis, increasing evidence shows that red cells are in fact able to form adhesive interactions during these physiologic processes. The ICAM-4/integrin interactions could be important during hemostasis where, in the developing thrombus, erythrocytes interact with activated neutrophils and monocytes. This possibility is supported by the fact that under low flow conditions adhesion of red cells to activated neutrophils involves interaction of ICAM-4 with CD11b/CD18.[61] The finding that ICAM-4 binds to the platelet integrin $\alpha_{IIb}\beta_3$ indicates that this interaction may be involved in platelet-erythrocyte aggregate formation during coagulation.[26] Interestingly, recent data indicate that during the pathogenesis of sickle red-cell vasoocclusion, adherent leukocytes bind not only to the inflamed endothelium but also to the erythrocytes.[62] Furthermore, a recent report shows that activated ICAM-4 mediates binding of the sickle red cells to endothelial $\alpha_v\beta_3$ integrin.[63] These findings indicate that drugs targeting ICAM-4-integrin interactions would be of great therapeutic value. Our results with synthetic peptides suggest that modulation of these interactions is possible.

Acknowledgments

We thank T.A. Springer for the CD11c I domain constructs, Cami Kantor-Aaltonen for synthetic peptides, and Jussi Hepojoki for PepSpot preparations. We also thank them for their generous help and valuable comments on peptides. We thank Leena Kuoppasalmi and Maria Aatonen for expert technical support and Yvonne Heinilä for secretarial assistance.

This work was supported by the University of Helsinki, the Academy of Finland, the Sigrid Jusélius Foundation, the Magnus Ehrnrooth Foundation, and the Finnish Cancer Society.

Authorship

Contribution: E.I., L.M.U., and A.T. did the experimental work and planned several experiments; E.I. wrote the first version of the manuscript; M.V. made the structural model; and C.G.G. planned much of the work and obtained most of the financial support.

Conflict-of-interest disclosure: The authors declare no competing financial interests.

Correspondence: Carl G. Gahmberg, Faculty of Biosciences, Division of Biochemistry, PO Box 56, Viikinkaari 5, University of Helsinki 00014, Finland; e-mail: Carl.Gahmberg@helsinki.fi.

References

1. Telen MJ. Red blood cell surface adhesion molecules: their possible roles in normal human physiology and disease. Semin Hematol. 2000; 37:130-142.
2. Daniels G. Functional aspects of red cell antigens. Blood Rev. 1999;13:14-35.
3. Cartron JP, Colin Y. Structural and functional diversity of blood group antigens. Transfus Clin Biol. 2001;8:163-199.
4. Parsons SF, Spring FA, Chasis JA, Anstee DJ. Erythroid cell adhesion moleculles Lutheran and LW in health and disease. Bailliers Best Pract Res Clin Haematol. 1999;12:729-745.
5. Stuart MJ, Nagel RL. Sickle-cell disease. Lancet. 2004;364:1343-1360.
6. Andrews DA, Low PS. Role of red blood cells in thrombosis. Curr Opin Hematol. 1999;6:76.
7. Barker JE, Wandersee NJ. Thrombosis in heritable hemolytic disorders. Curr Opin Hematol. 1999;6:71-75.
8. Gahmberg CG, Jokinen M, Andersson LC. Expression of the major sialoglycoprotein (glycophorin) on erythroid cells in human bone marrow. Blood. 1978;52:379-387.
9. Bony V, Gane P, Bailly P, Cartron J-P. Time-course expression of polypeptides carrying blood group antigens during human erythroid differentiation. Br J Haematol. 1999;107:263-274.
10. Southcott MJG, Tanner MJA, Anstee DJ. The expression of human blood group antigens during erythropoiesis in a cell culture system. Blood. 1999;93:4425-4435.
11. Bailly P, Hermand P, Callebaut I, et al. The LW blood group glycoprotein is homologous to intercellular adhesion molecules. Proc Natl Acad Sci U S A. 1994;91:5306-5310.
12. Springer TA. Adhesion receptors of the immune system. Nature. 1990;346:425-434.
13. Gahmberg CG, Tolvanen M, Kotovuori P. Leukocyte adhesion. Structure and function of human leukocyte β2-integrins and their cellular ligands. Eur J Biochem. 1997;245:215-232.
14. Gahmberg CG. Leukocyte adhesion. CD11/CD18 integrins and intercellular adhesion molecules. Curr Opin Cell Biol. 1997;9:643-650.
15. Hayflick JS, Kilgannon P, Gallatin WM. The intercellular adhesion molecule (ICAM) family of proteins. New members and novel functions. Immunol Res. 1998;17:313-327.
16. Marlin SD, Springer TA. Purified intercellular adhesion molecule-1 (ICAM-1) is a ligand for lymphocyte function-associated antigen 1 (LFA-1). Cell. 1987;51:813-819.
17. Patarroyo M, Clark EA, Prieto J, Kantor C, Gahmberg CG. Identification of a novel adhesion molecule in human leukocytes by monoclonal antibody LB-2. FEBS Lett. 1987;210:127-131.
18. Staunton DE, Dustin ML, Springer TA. Functional cloning of ICAM-2, a cell adhesion ligand for LFA-1 homologous to ICAM-1. Nature. 1989;339: 61-64.
19. Fawcett J, Holness CLL, Needham LA, et al. Molecular cloning of ICAM-3, a third ligand for LFA-1, constitutively expressed on resting leukocytes. Nature. 1992;360:481-484.
20. Tian L, Yoshihara Y, Mizuno T, Mori K, Gahmberg CG. The neuronal glycoprotein telenchephalin is a cellular ligand for the CD11a/CD18 leukocyte integrin. J Immunol. 1997;158:928-936.
21. Bailly P, Tontti E, Hermand P, Cartron J-P, Gahmberg CG. The red cell LW blood group protein is an intercellular adhesion molecule which binds to CD11/CD18 leukocyte integrins. Eur J Immunol. 1995;25:3316-3320.
22. Diamond MS, Staunton DE, de Fougerolles AR, et al. ICAM-1 (CD54): a counter-receptor for Mac-1 (CD11b/CD18). J Cell Biol. 1990;111: 3129-3139.
23. Xie J, Li R, Kotovuori P, et al. Intercellular adhesion molecule-2 (CD102) binds to the leukocyte integrin CD11b/CD18 through the A domain. J Immunol. 1995;155:3619-3628.
24. Spring FA, Parsons SF, Ortlepp S, et al. Intercellular adhesion molecule-4 binds $\alpha_4\beta_1$ and α_v-family integrins through novel integrin-binding mechanisms. Blood. 2001;98:458-466.
25. Hermand P, Gane P, Callebaut I, Kieffer N, Cartron J-P, Bailly P. Integrin receptor specificity for human red cell ICAM-4 ligand. Eur J Biochem. 2004;271:3729-3740.
26. Hermand P, Gane P, Huet M, et al. Red cell ICAM-4 is a novel ligand for platelet-activated $\alpha_{IIb}\beta_3$ integrin. J Biol Chem. 2003;278:4892-4898.
27. Gahmberg CG. Cell adhesion: a partner for many. Blood. 2004;103:1183.
28. Hermand P, Huet M, Callebaut I, et al. Binding sites of leukocyte β2 integrins (LFA-1, Mac-1) on the human ICAM-4/LW blood group protein. J Biol Chem. 2000;275:26002-26010.
29. Ihanus E, Uotila L, Toivanen A, et al. Characterization of ICAM-4 binding to the I domains of the CD11a/CD18 and CD11b/CD18 leukocyte integrins. Eur J Biochem. 2003;270:1710-1723.
30. Ammon C, Meyer SP, Schwarzfischer L, Krause SW, Andreesen R, Kreutz M. Comparative analysis of integrin expression on monocyte-derived macrophages and monocyte-derived dendritic cells. Immunology. 2000;100:364-369.
31. Micklem KJ, Sim RB. Isolation of complement-fragment-iC3b-binding proteins by affinity chromatography. The identification of p150,95 as an iC3b-binding protein. Biochem J. 1985;231:233-236.
32. Altieri DC, Agbanyo FR, Plescia J, Ginsberg MH, Edgington TS, Plow EF. A unique recognition site mediates the interaction of fibronogen with the leukocyte integrin Mac-1 (CD11b/CD18). J Biol Chem. 1990;265:12119-12122.
33. Diamond MS, Alon R, Parkos CA, Quinn MT, Springer TA. Heparin is an adhesive ligand for the leukocyte integrin Mac-1 (CD11b/CD18). J Cell Biol. 1995;130:1473-1482.
34. Santoso S, Sachs UJH, Kroll H, et al. The junctional adhesion molecule 3 (JAM-3) on human platelets is a counterreceptor for the leukocyte integrin Mac-1. J Exp Med. 2002;196:679-691.
35. Nortamo P, Patarroyo M, Kantor C, Suopanki J, Gahmberg CG. Immunological mapping of the human leukocyte adhesion glycoprotein GP90 (CD18) by monoclonal antibodies. Scand J Immunol. 1988;28:537-546.

36. Zhou L, Lee DHS, Plescia J, Lau JY, Altieri DC. Differential ligand binding specificities of recombinant CD11b/CD18 integrin-I-domain. J Biol Chem. 1994;269:17075-17079.
37. Stacker SA, Springer TA. Leukocyte integrin P150,95 (CD11c/CD18) functions as an adhesion molecule binding to a counter-receptor on stimulated endothelium. J Immunol. 1991;146:648-655.
38. Myones BL, Daizell JG, Hogg N, Ross GD. Neutrophil and monocyte cell surface p150,95 has iC3b-receptor (CR4) activity resembling CR3. J Clin Invest. 1988;82:640-651.
39. Sonneborn HH, Uthemann H, Tills D, Lomas CG, Shaw MA, Tippett P. Monoclonal anti-LWab. Biotest Bull. 1984;2:145-148.
40. Li R, Nortamo P, Valmu L, Tolvanen M, Kantor C, Gahmberg CG. A peptide from ICAM-2 binds to the leukocyte integrin CD11a/CD18 and inhibits endothelial cell adhesion. J Biol Chem. 1993;268:17513-17518.
41. Vorup-Jensen T, Ostermeier C, Shimaoka M, Hommel U, Springer TA. Structure and allosteric regulation of the αXβ2 integrin I domain. Proc Natl Acad Sci U S A. 2003;100:1873-1878.
42. Saren P, Welgus HG, Kovanen P. TNF-alfa and IL-1beta selectively induce expression of 92-kDa gelatinase by human macrophages. J Immnol. 1996;157:4159-4165.
43. Bratosin D, Estaquier J, Ameisen JC, Aminoff D, Montreuil J. Flow cytometric approach to the study of erythrophagocytosis: evidence for an alternative immunoglobulin-independent pathway in agammaglobulinemic mice. J Immunol Methods. 2002;265:133-143.
44. Casasnovas JM, Springer TA, Liu J-h, Harrison SC, Wang J-H. Crystal structure of ICAM-2 reveals a distinctive integrin recognition surface. Nature. 1997;387:312-315.
45. Sali A, Blundell TL. Comparative protein modelling by satisfaction of spatial restraints. J Mol Biol. 1993;234:779-815.
46. Lehtonen JV, Still DJ, Rantanen VV, et al. BODIL: a molecular modelling environment for structure-function analysis and drug design. J Comput Aided Mol Des. 2004;18:401-419.
47. Laskowski RA, MacArthur MW, Moss DS, Thornton JM. PROCHECK: a program to check the stereochemical quality of protein structures. J Appl Cryst. 1993;26:283-291.
48. Kraulis PJ. MOLSCRIPT: a program to produce both detailed and schematic plots of protein structures. J Appl Cryst. 1991;24:946-950.
49. Bacon D, Anderson WF. A fast algorithm for rendering space-filling molecule pictures. J Molec Graphics. 1988;6:219-220.
50. Merritt EA, Murphy MEP. Raster3D version 2.0. A program for photorealistic molecular graphics. Acta Cryst. 1994;D50:869-873.
51. Mankelow TJ, Spring FA, Parsons SF, et al. Identification of critical amino-acid residues on the erythroid intercellular adhesion molecule-4 (ICAM-4) mediating adhesion to α_v integrins. Blood. 2004;103:1503-1508.
52. Corbi AL, Miller LJ, O'Connor K, Larson RS, Springer TA. cDNA cloning and complete primary structure of the alpha subunit of a leukocyte adhesion glycoprotein, p150,95. EMBO J. 1987;6:4023-4028.
53. Miller LJ, Wiebe M, Springer TA. Purification and alpha subunit N-terminal sequences of human Mac-1 and p150,95 leukocyte adhesion proteins. J Immunol. 1987;138:2381.
54. Larson RS, Corbi AL, Berman L, Springer T. Primary structure of the leukocyte function-associated molecule-1 alpha subunit: an integrin with an embedded domain defining a protein superfamily. J Cell Biol. 1989;108:703-712.
55. Diamond MS, Garcia-Aguilar J, Bickford JK, Corbi AL, Springer TA. The I domain is a major recognition site on the leukocyte integrin Mac-1 (CD11b/CD18) for four distinct adhesion ligands. J Cell Biol. 1993;120:1031-1043.
56. Choi J, Leyton L, Nham S-U. Characterization of alphaX I-domain binding to thy-1. Biochem Biophys Res Commun. 2005;331:557-561.
57. Frick C, Odrmatt A, Zen K, et al. Interaction of ICAM-1 with β_2-integrin CD11c/CD18: characterization of a peptide ligand that mimics a putative binding site on domain D4 of ICAM-1. Eur J Biochem. 2005;35:3610-3621.
58. Vorup-Jensen T, Carman CV, Shimaoka M, Schuck P, Svitel J, Springer TA. Exposure of acidic residues as a danger signal for recognition of fibrinogen and other macromolecules by integrin $\alpha_x\beta_2$. Proc Natl Acad Sci U S A. 2005;102:1614-1619.
59. Lee G, Lo A, Short SA, et al. Targeted gene deletion demonstrates that cell adhesion molecule ICAM-4 is critical for erythroblastic island formation. Blood. 2006;108:2064-2071.
60. Lee G, Spring FA, Parsons SF, et al. Novel secreted isoform of adhesion molecule ICAM-4: potential regulator of membrane-associated ICAM-4 interactions. Blood. 2003;101:1790-1797.
61. Goel MS, Diamond SL. Adhesion of normal erythrocytes at depressed venous shear rates to activated neutrophils, activated platelets, and fibrin polymerized from plasma. Blood. 2002;100:3797-3803.
62. Turhan A, Weiss LA, Mohandas N, Coller BS, Frenette PS. Primary role for adherent leukocytes in sickle cell vascular occlusion: a new paradigm. Proc Natl Acad Sci U S A. 2002;99:3047-3051.
63. Zennadi R, Hines PC, De Castro LM, Cartron J-P, Parise LV, Telen MJ. Epinephrine acts through erythroid signaling pathways to activate sickle cell adhesion to endothelium via LW-αvβ3 interactions. Blood. 2004;104:3774-3781.

The Journal of Immunology
RESEARCH ARTICLE | JANUARY 15 1997

The Neuronal Glycoprotein Telencephalin Is a Cellular Ligand for the CD11a/CD18 Leukocyte Integrin[1]

Li Tian,* Yoshihiro Yoshihara,[†‡] Takeo Mizuno,[†‡] Kensaku Mori,[†§] and Carl G. Gahmberg[2]*

Many leukocyte functions depend on interactions between the leukocyte-specific β_2 integrins CD11/CD18 and their ligands, the intercellular adhesion molecules (ICAMs). Telencephalin (TLN) is a novel member of the Ig superfamily expressed in the central nervous system. The NH_2-terminal five Ig-like domains of TLN show the highest homology with the Ig domains of ICAM-1, ICAM-2, ICAM-3, and LW (ICAM-4), the known cellular ligands for CD11a/CD18. Here, we demonstrate that TLN interacts with CD11a/CD18. Peripheral blood T cells, Jurkat T cells, and B lymphoblastoid cells bound to immunopurified recombinant human TLN proteins. This adhesion was through CD11a/CD18 and was significantly inhibited by an Ab to CD11a/CD18. Reciprocally, TLN-transfected L cells also bound to purified CD11a/CD18. Recombinant TLN proteins comprising either the first five Ig domains (TLN(1–5)) or the entire extracellular portion (TLN(1–9)) showed binding to CD11a/CD18. We conclude that TLN is a novel neuronal cell adhesion molecule that may be important in integrin-mediated cell-cell interactions in the central nervous system, and that the CD11a/CD18-dependent recognition site of human TLN is located within the NH_2-terminal five domains of this molecule. ***The Journal of Immunology,*** **1997, 158: 928–936.**

Many leukocyte functions depend on cell adhesion. On leukocytes, integrins are involved in cell-cell and cell-extracellular matrix interactions and play a role in physiologic processes, such as the regulation of lymphocytic responses to antigenic stimulation, the recirculation into lymphoid tissues, or the extravasation at sites of inflammation (1–6). The β_2 integrins CD11a/CD18 ($\alpha_L\beta_2$, LFA-1),[3] CD11b/CD18 ($\alpha_M\beta_2$, Mac-1), CD11c/CD18 ($\alpha_X\beta_2$, p150, 95), $\alpha_d\beta_2$, and the integrins of the VLA family participate in distinct mechanisms of leukocyte-endothelium and leukocyte-leukocyte binding.

CD11a/CD18, which is mainly found on mononuclear leukocytes, binds to the NH_2-terminal Ig domain of ICAM-1 (CD54) (7–10) and ICAM-2 (CD102) on the surface of stimulated or unstimulated endothelial cells and leukocytes (11–15), to ICAM-3 (CD50) on lymphocytes (16–20), and to LW (ICAM-4) on RBC (21). CD11b/CD18, which is expressed primarily on cells of the myelo-monocytic lineage, binds to ICAM-1 (22, 23), ICAM-2 (24), and several soluble ligands, including the complement fragment iC3b, and fibrinogen (25–29). The cellular ligand for CD11c/CD18 may also be ICAM-1 (30). The novel $\alpha_d\beta_2$ integrin preferentially binds to ICAM-3 (31).

Although considerable progress has been made in defining the basic mechanisms associated with the functions of leukocytes, issues concerning the specific interactions between the immune system and the central nervous system (CNS) have been poorly addressed. In recent years, immunohistochemical studies of CNS have defined an increased expression of ICAM-1 and VCAM-1 by a number of cell types, such as microvascular endothelial cells and glial cells in human brain, as well as in several animal models of infectious CNS disorders and immune-related diseases, such as multiple sclerosis (32–36). Additionally, it has been suggested that microglia are capable of expressing a variety of immunologically relevant proteins, such as class I and II MHC proteins, β_2 integrins, and VLA-4 upon cytokine stimulation (35, 36).

TLN was first identified as a 130-kDa type I integral membrane glycoprotein expressed by subsets of neurons, but not by glial cells, exclusively within the telencephalon of mammalian brains (37–40). In neurons, it is localized to the soma and dendritic membranes, but not to the axonal membranes. TLN comprises a characteristic extracellular region with nine Ig domains, a single transmembrane region, and a COOH-terminal cytoplasmic tail. The NH_2-terminal Ig domain of TLN contains four cysteine residues that are capable of forming two intradomain disulfide bridges. Similarly spaced cysteine residues in the NH_2-terminal Ig domains are seen in other members of the Ig superfamily (41), such as ICAM-1 (42, 43), ICAM-2 (12), ICAM-3 (16, 17), and LW (44). TLN is most closely related to ICAM-1 and -3. The total amino acid identity is 50% with ICAM-1 and 55% with ICAM-3 (domains I–V). These data indicate that TLN could function as an intercellular adhesion molecule within the CNS.

In the present study, we have used purified recombinant human TLN-Fc proteins to examine whether they can interact with leukocytes. We found that various leukocytes bound to the isolated proteins in a CD11a/CD18-dependent manner. Furthermore, TLN-transfected L cells bound specifically to immobilized CD11a/CD18. Therefore, we propose a novel mechanism underlying cell-cell interactions between TLN-expressing telencephalic neurons and CD11a/CD18-expressing cells within the CNS.

*Department of Biosciences, Division of Biochemistry, University of Helsinki, Helsinki, Finland; [†]Department of Neuroscience, Osaka Bioscience Institute, Suita, Japan; [‡]Department of Biochemistry, Osaka Medical College, Takatsuki, Osaka, Japan; and [§]Laboratory for Neuronal Recognition Molecules, Frontier Research Program, RIKEN, Wako, Saitama, Japan

Received for publication June 10, 1996. Accepted for publication October 18, 1996.

The costs of publication of this article were defrayed in part by the payment of page charges. This article must therefore be hereby marked *advertisement* in accordance with 18 U.S.C. Section 1734 solely to indicate this fact.

[1] This work was supported by the University of Helsinki, the Academy of Finland, the Sigrid Jusélius Foundation, and the Finnish Cancer Society.

[2] Address correspondence and reprint requests to Dr. Carl G. Gahmberg, Department of Biosciences, Division of Biochemistry, University of Helsinki, P.O. Box 56, Viikinkaari 5, FIN-00014 Helsinki, Finland.

[3] Abbreviations used in this paper: CD11a/CD18 = $\alpha_L\beta_2$ = LFA-1 (leukocyte function-associated antigen 1); CD11/CD18, leukocyte β_2 integrins; CD11b/CD18 = $\alpha_M\beta_2$ = Mac-1; CD11c/CD18 = $\alpha_X\beta_2$ = p150/95; VLA, very late antigen; ICAM, intercellular adhesion molecule; CNS, central nervous system; VCAM-1, vascular cell adhesion molecule 1; TLN, telencephalin; PDBu, 4β-phorbol 12,13-dibutyrate; LAD, leukocyte adhesion deficiency; TLN(1–5)-Fc, telencephalin containing the first five Ig domains fused to Fc; TLN(1–9)-Fc, telencephalin containing the nine Ig domains fused to Fc; ANOVA, analysis of variance; LW, Landsteiner-Wiener Antigen (ICAM-U).

Copyright © 1997 by The American Association of Immunologists

0022-1767/97/$02.00

Carl_G_190x270_mm_blokki_FINAL.indd 320 06-Aug-23 1:54:07 PM

Materials and Methods

Reagents

4β-Phorbol 12,13-dibutyrate (PDBu) and phosphatase substrate were purchased from Sigma Chemical Co. (St. Louis, MO). Anti-human IgG alkaline phosphatase-conjugated Ab and nitro blue tetrazolium/5-bromo-4-chloro-3-indolyl-phosphate substrate were obtained from Promega (Madison, WI). Sodium metaperiodate was purchased from Merck AG (Darmstadt, Germany). Tritiated sodium borohydride (8.2 Ci/mmol) was obtained from the Radiochemical Center Ltd. (Amersham, U.K.). Human IgG was purchased from Dako Corp. (Carpenteria, CA).

Antibodies

Integrin-specific mAbs used in these studies include 7E4, TS2/4, G43-25B, MEM83, LM2/1, 3.9, HP2/1, and LM609. The blocking Ab 7E4 (45) reacts with the common β_2-chain of the leukocyte integrins. TS2/4 (46) and G43-25B (PharMingen, San Diego, CA) recognize the α-chain of CD11a/CD18. MEM83 is a stimulating mAb against the α-chain of CD11a/CD18 (47). The blocking Abs LM2/1 (48) and 3.9 (49) are specific for the I domain of the α-subunit of CD11b/CD18 and CD11c/CD18, respectively. HP2/1 is a monoclonal inhibiting Ab to VLA-4α (CD 49d) (50). LM609 recognizes the α-chain of vitronectin receptor $\alpha_v\beta_3$ (CD51/CD61) and inhibits the binding in a complex-dependent manner (51). The monoclonal blocking Ab LB-2 (52) reacts with the first domain of ICAM-1. All Abs are IgG1 except G43–25B, which is IgG2b. A mouse IgG1-negative control was purchased from Silenus (Hawthorn, Australia), and a IgG2b-negative control was obtained from Medix Biochemica (Helsinki, Finland).

All the mAbs except HP2/1 and LM609 were used as purified IgG. They were used either at 50 μg/ml for the inhibition assays or at 20 μg/ml for the immunochemical staining. HP2/1 and LM609 were obtained as ascites, they were used at 1/100 and 1/1000 dilutions, respectively, for both the inhibition assays and the immunochemical staining. Rabbit antisera were produced using the COOH-terminal peptide (17 residues) of mouse TLN or human TLN recombinant TLN-Fc proteins as immunogens.

Peptide synthesis

Peptides were synthesized on an Applied Biosystems model 430A peptide synthesizer (Foster City, CA), using F-moc chemistry. The structures were confirmed by fast atom bombardment-mass spectrometric analysis (JEOL SX-102, Peabody, MA). The sequence of the ICAM-2 peptide P1 is GSLEVNCSTTCNQPEVGGLETS. The amino acids of the control peptide P8 are the same as those of P1, but in random order, except that the two conserved cysteine residues are in the correct positions (11). After synthesis, the P1 and P8 peptides were reduced with DTT (1/1.5. w/w, in 0.1 M $NaHCO_3$, pH 8.0) for 1.5 h at room temperature, and purified by HPLC using a reverse phase column (C_{18}, Waters Associates, Milford, MA).

Cell culture

Human T cells were isolated from fresh blood buffy coats using the Ficoll-Hypaque (Pharmacia, Uppsala, Sweden) technique and employing a nylon wool column. The purity was >90%. The acute human T leukemia cell line Jurkat (American Type Culture Collection (ATCC), Rockville, MD) (53) was maintained in RPMI 1640 medium (Life Technologies, Grand Island, NY) with 10% FCS (Flow Laboratories, Irvine, Scotland). The EBV-transformed normal human B lymphoblastoid cell line NAD-20 and the B lymphoblastoid cell line established from a patient with leukocyte adhesion deficiency (LAD) (54) were maintained in RPMI 1640 medium with 10% FCS (Biological Industries, Kibbutz Bet Haemek, Israel). The SV40-transformed African green monkey kidney cell line COS-1 (ATCC) was grown in DMEM with 10% FCS. The mouse fibroblast cells L929 were grown in Iscove's modified Eagle's medium (Hyclone, Logan, UT) with 10% FCS.

Purification of ICAM-1-Fc and TLN-Fc recombinant proteins

Recombinant soluble Fc-chimeric proteins were produced essentially as previously described (55). Briefly, a ICAM-1-Fc vector was constructed with the human ICAM-1 cDNA encoding the extracellular region (the NH_2-terminal signal peptide and the five Ig-like domains) fused to the human IgG1 sequence coding for the hinge, CH2, and CH3 domains of human IgG1 (56). The human TLN-Fc recombinant proteins, which contain either the five (TLN(1–5)) or nine (TLN(1–9)) NH_2-terminal Ig domains, were constructed in a similar way. The sequence of the human TLN will be published separately (T. Mizuno et al., manuscript in preparation). The fused cDNAs were then subcloned into the mammalian expression vector pEF-BOS (57). The plasmids were transiently transfected into COS-1 cells by the DEAE-dextran method (Pharmacia). ICAM-1-Fc, TLN(1–5)-Fc, and TLN(1–9)-Fc were purified from culture medium by protein A-Sepharose CL-4B chromatography (Pharmacia; Fig. 1, *A* and *B*).

Purification of integrins

CD11a/CD18, CD11b/CD18, and CD11c/CD18 were purified from human blood buffy coat cell lysates, obtained from 250 blood units, by adsorption to the Abs TS2/4 (anti-CD11a), MEM170 (anti-CD11b), and 3.9 (anti-CD11c) linked to protein A-Sepharose CL 4B, and eluted at pH 11.5 in the presence of 2 mM $MgCl_2$ and 1% *n*-octyl glucoside as described previously (58). The purity of the proteins was >90% when studied by 8% SDS-PAGE.

Establishment of TLN- and ICAM-1-transfected L cell lines

Plasmids containing either the full-length TLN cDNA or the full-length ICAM-1 cDNA subcloned into the mammalian expression vector pEF-BOS were cotransfected with pCDM8-neo stuffer into L929 mouse fibroblast cells according to standard procedures using the Lipofectamine reagent kit (Life Technologies, Gaithersburg, MD). Stable transfectants were selected in medium containing 0.5 mg/ml G418. Cells were screened for TLN or ICAM-1 expression by FACS analysis using a rabbit antiserum against the extracellular region of human TLN or an Ab to ICAM-1 (LB-2), respectively. The cell lines with the strongest expressions of TLN or ICAM-1 were chosen for functional studies.

Immunoblotting and immunoprecipitation

Samples of ICAM-1-Fc, TLN(1–5)-Fc, and TLN(1–9)-Fc purified proteins were prepared as described above. Following SDS-PAGE and blotting to nitrocellulose membranes, the membranes were blocked with 5% dry milk in 10 mM Tris/0.15 M NaCl, pH 7.4. After washing, the membranes were incubated with a 1/7500 dilution of alkaline phosphatase-conjugated anti-human IgG (Promega) in 1% BSA/10 mM Tris/0.15 M NaCl/1% Tween. After washing, the membranes were developed with the phosphatase substrate buffer according to the manufacturer's instructions.

Immunoprecipitations were performed after surface-labeling using the periodate-tritiated borohydride method (59). Briefly, detached, washed 50×10^6 L cells were suspended in 1 ml of PBS (0.15 M NaCl and 0.01 M sodium phosphate), pH 7.4, and incubated with 20 μl of 0.1 M sodium metaperiodate for 10 min on ice. After washing, the cells were resuspended in 0.5 ml of PBS, pH 8.0, and labeled with 0.5 mCi of tritiated sodium borohydride for 30 min at room temperature. After washing, the ^{3}H-labeled cells were lysed with 1% Triton X-100 and centrifuged at $3000 \times g$ for 5 min. The supernatants were collected and used for immunoprecipitation. The immune complexes were eluted from the *Staphylococcus aureus* cells by 1% SDS and applied to 8% SDS-PAGE. The gels were fixed, dried, and exposed using Kodak film (X-OMAT AR 5, Eastman Kodak, Rochester, NY). The anti-mouse TLN specifically recognized human TLN (Fig. 1*Cf*), but not human ICAM-1 (Fig. 1*Cc*), while LB-2 selectively recognized human ICAM-1 (Fig. 1*Cb*). The molecular mass of human TLN and ICAM-1 are 150 and 90 kDa, respectively. The minor band in Cf is probably a degradation product (Fig. 1*C*).

FACS analysis

Jurkat, NAD-20, LAD, TLN-transfected, and ICAM-1-transfected L cells were washed and resuspended in 0.1% BSA in PBS, pH 7.4. Aliquots of 1×10^6 cells were incubated with 20 μg/ml of different mAbs (except that TLN-$^+$ L transfectants were incubated with a 1/500 diluted rabbit antiserum against the extracellular region of human TLN) for 30 min on ice. After washing, the cells were incubated with FITC-conjugated rabbit anti-mouse $F(ab')_2$ (Dakopatts a/s, Copenhagen, Denmark) or with FITC-conjugated goat anti-rabbit IgG (Jackson ImmunoResearch Laboratories, Inc., West Grove, PA) for 30 min on ice. After washing, 1×10^4 cells were analyzed immediately with a Becton Dickinson (Immunocytometry Systems, San Jose, CA) FACScan flow cytometer.

Cell adhesion assay

The indicated amounts of purified ICAM-1-Fc, TLN(1–5)-Fc, TLN(1–9)-Fc, and human IgG; leukocyte integrins; or BSA were attached to flat-bottom 96-well microtiter plates (Nunc, Roskilde, Denmark) in PBS-2 mM $MgCl_2$ by incubation overnight at 4°C. The wells were blocked with 1% BSA for 2 h at room temperature. Resting; 60 nM PDBu- or 62 μM P1/P8 peptide-stimulated T cells (5×10^5/well); PDBu-stimulated Jurkat, NAD-20, or LAD cells (2×10^5/well); and ICAM-1- or TLN-transfected L cells (7×10^4/well) in RPMI 1640 supplemented with 40 mM HEPES, pH 7.4, 2 mM $MgCl_2$, and 5% FCS were added to the wells and incubated for 60 min at room temperature. In the case of experiments using $MnCl_2$, the

Carl_G_190x270_mm_blokki_FINAL.indd 321 06-Aug-23 1:54:07 PM

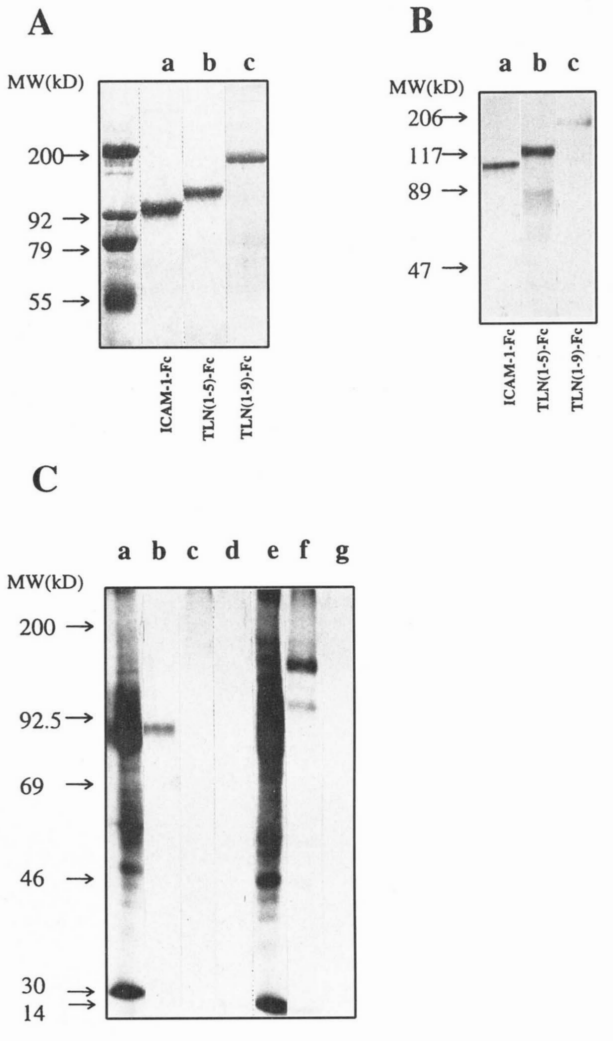

FIGURE 1. *A,* SDS-PAGE analysis of purified ICAM-1-Fc, TLN(1–5)-Fc, and TLN(1–9)-Fc proteins. Eight micrograms of the proteins was run on SDS-PAGE and subjected to Coomassie blue staining. The migration positions of the M_r standards are indicated on the *left.* The M_r deduced from electrophoretic mobilities are: ICAM-1-Fc, 105 kDa (Aa); TLN(1–5)-Fc, 115 kDa (Ab); and TLN(1–9)-Fc, 170 kDa (Ac). *B,* Western blot analysis of recombinant ICAM-1-Fc (Ba), TLN(1–5)-Fc (Bb), and TLN(1–9)-Fc (Bc) proteins. Two micrograms of protein was analyzed. The rabbit anti-mouse TLN Ag was used in Bb and Bc. The migration positions of M_r standards are indicated on the *left.* *C,* Eight percent SDS-PAGE analysis of immunoprecipitated human ICAM-1 and TLN. ICAM-1-transfected L cell lysates (Ca) were immunoprecipitated with 5 μg of mAb against ICAM-1 (LB-2) (Cb), polyclonal Ab against the cytoplasmic part of mouse TLN (Cc), or control mouse IgG1 (Cd). TLN-transfected L cell lysates (Ce) were immunoprecipitated with 5 μg of polyclonal Ab against the cytoplasmic part of TLN (Cf) or normal mouse IgG1 (Cg). The positions of M_r standards are indicated on the *left.*

binding solution was 137 mM NaCl and 2 mM $MnCl_2$. For blocking experiments, the cells or protein-coated wells were pretreated with different mAbs or inhibitors for 30 min at 4°C before starting the adhesion. Nonadherent cells were removed by gentle washing with PBS/2 mM $MgCl_2$. After washing, the bound cells were lysed in 100 μl/well phosphatase substrate-containing lysis buffer (1% Triton X-100 and 50 mM sodium acetate, pH 5.0) and incubated at 37°C for 30 min, the reaction was stopped by adding 50 μl/well of 1 M NaOH, and the absorbance at 405 nm was measured. The percentage of bound cells was calculated as:

$$\% \text{ bound cells} = \frac{A_{405} \text{ bound cells/well}}{A_{405} \text{ total amount of cells/well}} \times 100.$$

Statistical analysis

Statistical analysis was performed using analysis of variance (ANOVA) for multiple comparisons as indicated.

Results

Binding of leukocytes to purified recombinant human TLN(1–5)-Fc, TLN(1–9)-Fc, and ICAM-1-Fc proteins

The expression patterns of integrins on Jurkat, NAD-20, LAD, and T cells were studied by flow cytometry. On Jurkat cells, CD11a, CD18, and CD49d (VLA-4α) were well expressed, with lesser expression of CD11b and CD51/CD61 ($\alpha_v\beta_3$); no expression of CD11c was found (Fig. 2). NAD-20 cells showed a strong expression of CD11a/CD18 and a low expression of CD11b/CD18 (Fig. 2). The LAD cells showed no expression of CD11a/CD18. All the cell lines contained CD49d (VLA-4α), whereas CD51/CD61 ($\alpha_v\beta_3$) was mainly expressed on the Jurkat cells (Fig. 2). The T cells showed a strong expression of CD11a, some CD11b, and little CD11c.

Carl_G_190x270_mm_blokki_FINAL.indd 322 06-Aug-23 1:54:08 PM

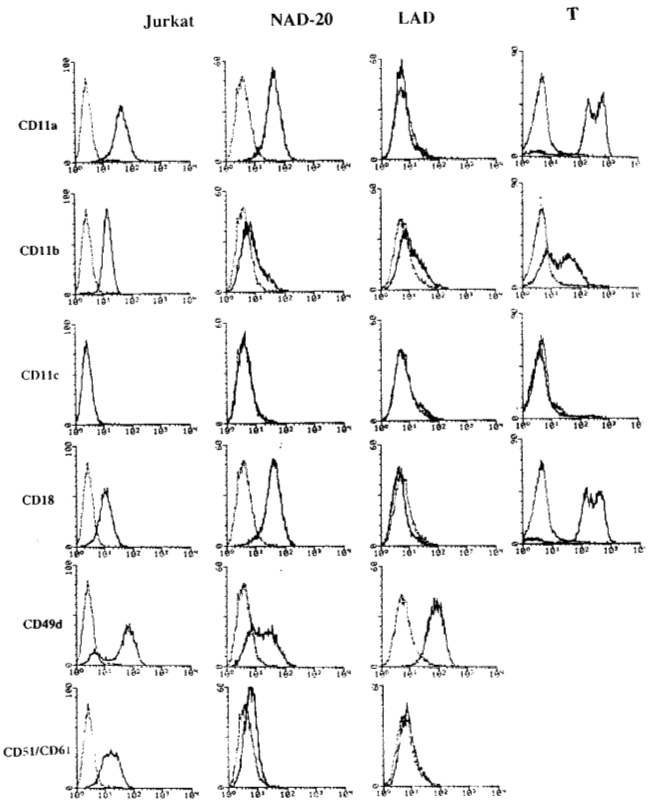

FIGURE 2. Integrin expression patterns of Jurkat, NAD-20, LAD cell lines, and T cells. Cells were stained with the mAbs mouse IgG1 (control; gray lines), TS2/4 (CD11a), MEM170 (CD11b), 3.9 (CD11c), 7E4 (CD18), HP2/1 (CD49d), and LM609 (CD51/CD61; dark lines).

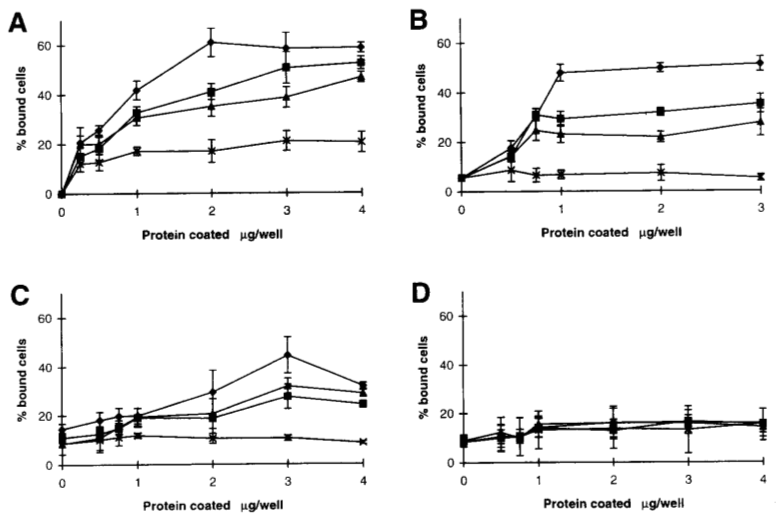

FIGURE 3. Binding of T cells (*A*), Jurkat cells (*B*), NAD-20 cells (*C*), and LAD cells (*D*) to the indicated amounts of purified ICAM-1-Fc (♦), TLN(1–5)-Fc (■), TLN(1–9)-Fc (●), and human IgG (X). Cells were added to wells precoated with the indicated amounts of recombinant proteins and incubated for 60 min at room temperature. T cells and Jurkat cells were stimulated with PDBu at a final concentration of 60 nM during the incubation periods. Data are expressed as the mean ± SD. At least three independent experiments were performed with similar results.

Carl_G_190x270_mm_blokki_FINAL.indd 323 06-Aug-23 1:54:08 PM

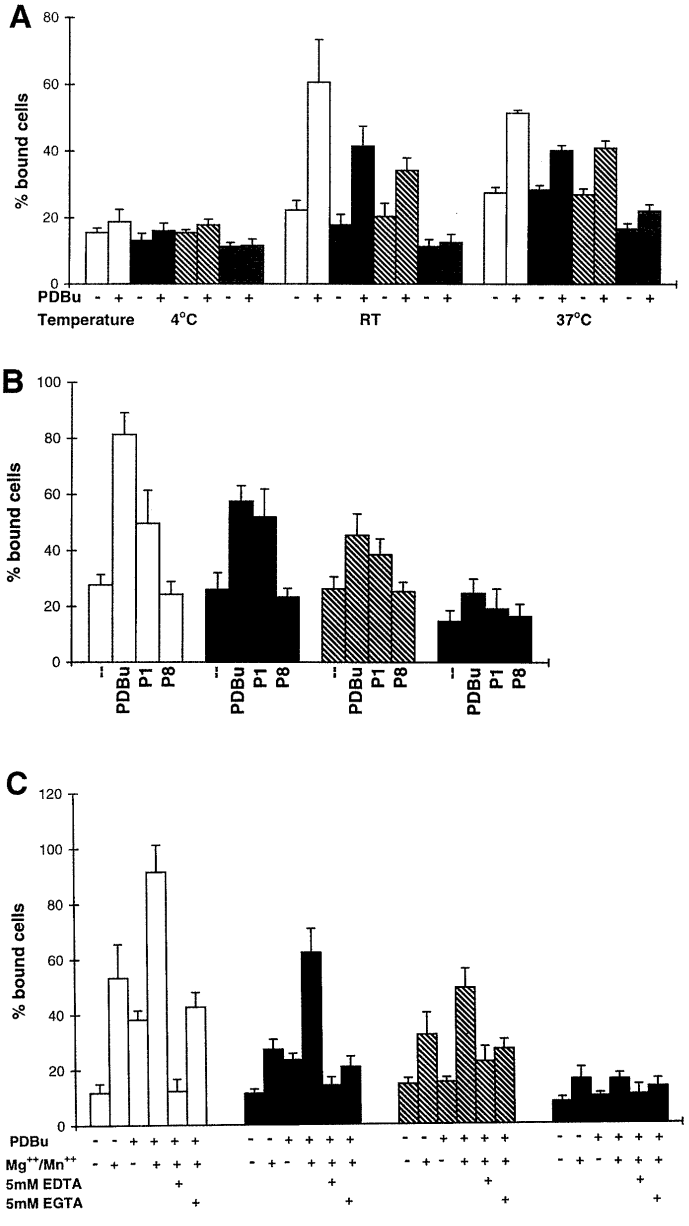

FIGURE 4. Characteristics of T cell adhesion to ICAM-1-Fc (white bars), TLN(1–5)-Fc (black bars), TLN(1–9)-Fc (hatched bars), and human IgG (gray bars). Two micrograms of the individual proteins was coated per well. *A*, T cells were added to the wells and incubated for 60 min at 4°C, room temperature (RT), or 37°C with or without stimulation by 60 nM PDBu. *B*, T cells were incubated at room temperature for 60 min with or without stimulation by 60 nM PDBu, the P1 peptide, or the P8 control peptide. *C*, Resting or PDBu-stimulated T cells were incubated at room temperature for 60 min with or without 2 mM $MgCl_2$-2 mM $MnCl_2$ in the binding medium. When indicated T cells were pretreated with EDTA or EGTA at a final concentration of 5 mM, before activation with PDBu. Data are expressed as the mean ± SD. Three independent experiments with similar results were performed.

PDBu-activated T cells and Jurkat cells bound to purified TLN(1–5)-Fc and TLN(1–9)-Fc proteins coated on plastic as well as to purified ICAM-1-Fc in a dose-dependent manner (Fig. 3, *A* and *B*). The significance of binding was calculated by two-way or three-way ANOVA for the results shown in Figures 3, 4, and 6, whereas one way-ANOVA was used in Figures 5 and 7. The binding to TLN-Fc and ICAM-1-Fc was considerably higher than the background binding to human IgG ($p < 0.001$), indicating that the interactions of the cells with the fusion proteins were due to TLN and ICAM-1, but not to the Fc portions. Also, NAD-20 cells bound to purified TLN-Fc and ICAM-1-Fc in a dose-dependent fashion ($p < 0.001$), while no significant binding of LAD cells to either ICAM-1-Fc or TLN-Fc was found (Fig. 3, *C* and *D*).

Characteristics of T cell adhesion to purified TLN and ICAM-1 proteins

Figure 4*A* shows that the binding of T cells to both TLN-Fc and ICAM-1-Fc was much lower at 4°C than at room temperature or

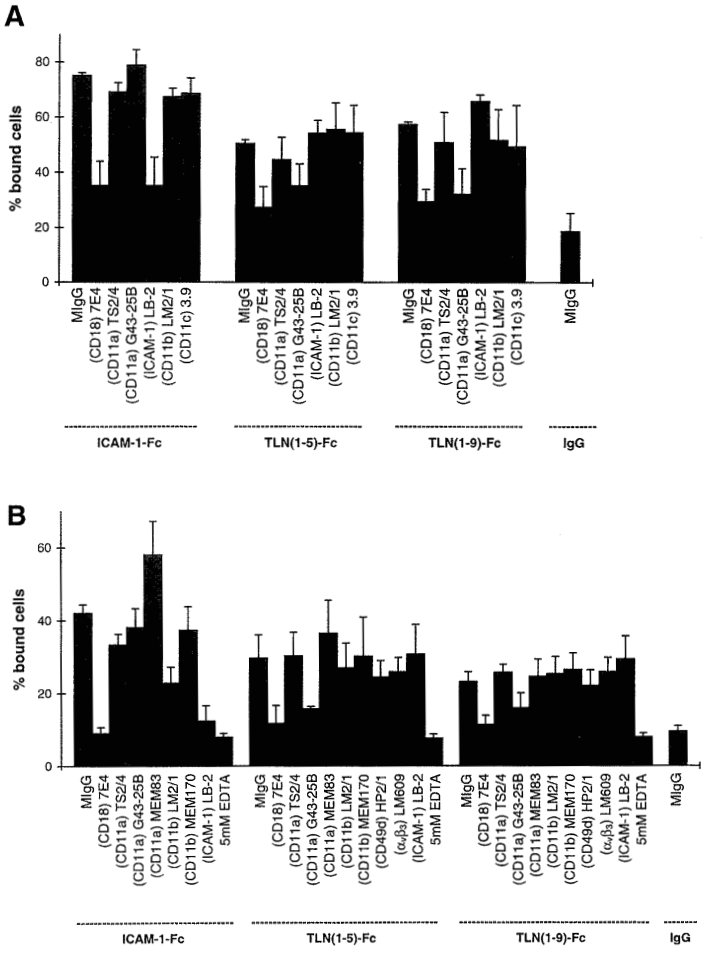

FIGURE 5. Effects of mAbs and EDTA on the binding of T cells and Jurkat cells to immobilized ICAM-1-Fc, TLN(1–5)-Fc, and TLN(1–9)-Fc. Aliquots of T cells (*A*) or Jurkat cells (*B*) were separately pretreated with 50 μg/ml of mAbs against CD18 (7E4), CD11a (TS2/4, G43–25B, MEM83), CD11b (LM2/1, MEM170), CD11c (3.9), ICAM-1 (LB-2), control $MIgG_1$, 1/100 diluted ascites containing (HP2/1), CD49d (HP2/1), 1/1000 diluted ascites containing mAb (LM609) to CD51/CD61, or 5 mM EDTA before adding the cells to the wells. Data are expressed as the mean ± SD. At least three independent experiments were performed with similar results. A control IgG2b Ab was also used, and it behaved similarly to IgG1.

37°C, and that PDBu greatly induced the binding of T cells to TLN-Fc, although to a lesser extent than to ICAM-1-Fc ($p < 0.001$ at room temperature and 37°C). Both EDTA and EGTA inhibited the binding of T cells to TLN and ICAM-1 ($p < 0.001$; Fig. 4*C*). In addition, the presence of 2 mM $MnCl_2$-$MgCl_2$ greatly stimulated the interaction of T cells with TLN and ICAM-1 ($p < 0.001$; Fig. 4*C*).

Interestingly, the 22-amino acid ICAM-2 peptide P1 activated the binding of T cells to both ICAM-1 and TLN, although not as efficiently as PDBu ($p < 0.001$; Fig. 4*B*). The control peptide P8 had no effect.

Effects of mAbs on the adhesion of T cells and Jurkat cells to purified TLN(1–5)-Fc, TLN(1–9)-Fc, and ICAM-1-Fc

To show that the binding of leukocytes to TLN involves β_2 integrins, a panel of different mAbs was tested for adhesion-inhibiting activity (Fig. 5). The mAb against CD18 (7E4) efficiently blocked the binding of T cells ($p < 0.001$; Fig. 5*A*) and Jurkat cells ($p < 0.001$; Fig. 5*B*) to both TLN(1–5)-Fc and TLN(1–9)-Fc. More importantly, a mAb against CD11a (TS2/4) partially, but significantly ($p < 0.001$), inhibited the adhesion of Jurkat cells to ICAM-1, but not to TLN. On the other hand, the CD11a mAb G43–25B efficiently inhibited the binding of both T cells and Jurkat cells to TLN ($p < 0.001$), but not to ICAM-1. Interestingly, the stimulating mAb MEM83 recognizing the I domain of CD11a (49) significantly ($p < 0.001$) enhanced the binding of Jurkat cells to ICAM-1-Fc, while it had no effect on TLN-Fc. Of the two mAbs against CD11b, LM2/1, but not MEM170, significantly blocked the adhesion of Jurkat cells to ICAM-1-Fc ($p < 0.001$), while neither had any effect on the binding of Jurkat cells to TLN-Fc. The adhesion of T cells and Jurkat cells was not affected by the CD11c mAb 3.9. In addition, the mAb LB-2 against ICAM-1 completely blocked

Carl_G_190x270_mm_blokki_FINAL.indd 325 06-Aug-23 1:54:08 PM

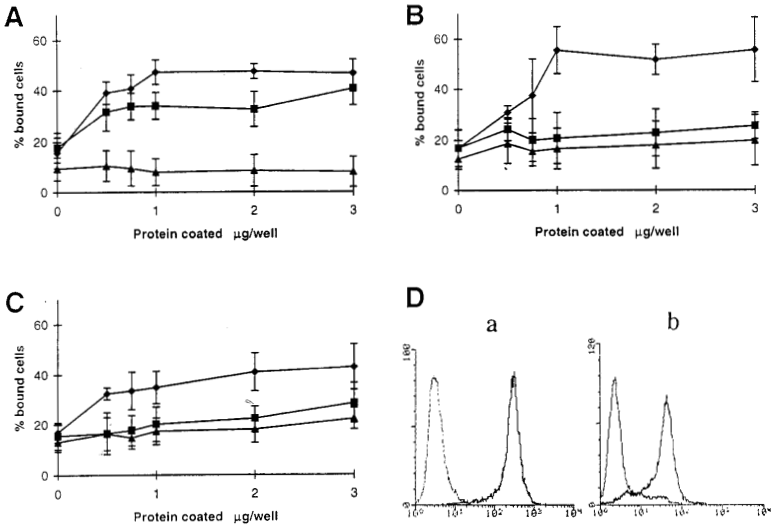

FIGURE 6. Adhesion of ICAM-1-transfected L cells (♦), TLN-transfected L cells (■), or wild-type L cells (●) to purified β_2 integrins. Cells were added to wells precoated with the indicated amounts of CD11a/CD18 (*A*), CD11b/CD18 (*B*), or CD11c/CD18 (*C*) and incubated for 40 min at 37°C. The expression of ICAM-1 (*Da*; dark line) or TLN (*Db*; dark line) on transfected L cells was checked by FACS analysis and compared with that of wild-type L cells (gray lines). Here the rabbit anti-recombinant TLN antisera were used. Data are expressed as the mean ± SD. At least three independent experiments were performed with similar results.

the adhesion of Jurkat cells to ICAM-1-Fc ($p < 0.001$), but not to TLN.

Because Jurkat cells also express other integrins, such as CD49/CD29 (VLA-4) and CD51/CD61 ($\alpha_v\beta_3$; Fig. 2), we tested mAb HP2/1, which inhibits the binding of VLA-4 to its counter-receptor, VCAM-1 (50), and mAb LM609, which blocks the interaction of $\alpha_v\beta_3$ with vitronectin (51). Neither HP2/1 nor LM609 inhibited the binding of Jurkat cells to TLN (Fig. 5*B*).

Binding of TLN-transfected L cells to purified CD11a/CD18, CD11b/CD18, and CD11c/CD18

Further proof for the interaction of CD11a/CD18 with TLN was obtained by establishing stable mouse L cell transfectants expressing high levels of TLN (Fig. 6*Db*). Using purified CD11a/CD18, CD11b/CD18, and CD11c/CD18, we studied the binding of TLN- or ICAM-1-transfected L cells to the integrins coated on plastic. Both TLN$^+$ and ICAM-1$^+$ L transfectants, but not wild-type L cells bound strongly to purified CD11a/CD18 in a dose-dependent manner ($p < 0.001$; Fig. 6*A*). About 50 and 35% of the total added ICAM-1- and TLN-transfected L cells adhered to CD11a/CD18, respectively, while only about 5% of the total added wild-type L cells did so. Whereas the ICAM-1 transfectants clearly adhered to purified CD11b/CD18 and CD11c/CD18 ($p < 0.001$), low or no binding to CD11b/CD18 and CD11c/CD18 was observed with TLN-transfected L cells (Fig. 6, *B* and *C*).

We next investigated the effects of different mAbs on the interaction of TLN-transfected L cells with CD11a/CD18 (Fig. 7). The binding of both ICAM-1- and TLN-transfected L cells was completely blocked by mAb 7E4. Of the three mAbs against CD11a, G43–25B completely and selectively blocked the adhesion of TLN-transfected L cells ($p < 0.001$), but not to ICAM-1-transfected L cells, while the other two mAbs (TS2/4 and MEM83) had

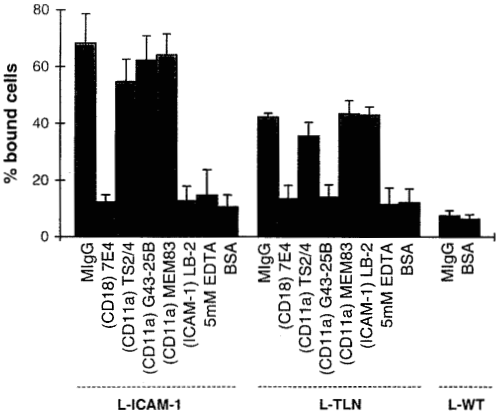

FIGURE 7. Effects of mAbs and EDTA on the adhesion of ICAM-1-transfected L cells and TLN-transfected L cells to immobilized CD11a/CD18. Aliquots of ICAM-1-L cell transfectants, TLN-L cell transfectants, or protein-coated wells were separately pretreated with 50 µg/ml of mAbs against ICAM-1, CD18, and CD11a (TS2/4, G43–25B, MEM83) or with 5 mM EDTA before adding the cells to CD11a/CD18-coated wells. Data are expressed as the mean ± SD. At least three independent experiments were performed with similar results.

no effect on either ICAM-1$^+$ or TLN-$^+$ L transfectants. The mAb against ICAM-1 Ab totally inhibited the binding of ICAM-1-transfected, but not TLN-transfected, L cells to CD11a/CD18. In addition, the binding of CD11a/CD18 to both L transfectants was almost completely abrogated by 5 mM EDTA.

Carl_G_190x270_mm_blokki_FINAL.indd 326 06-Aug-23 1:54:08 PM

Discussion

Here we have shown that TLN is a ligand for CD11a/CD18 by demonstrating that purified TLN-Fc fusion protein mediates leukocyte adhesion dependent on CD11a/CD18, and reciprocally, that purified CD11a/CD18 mediates cell adhesion dependent on TLN. However, the binding of TLN is different from that of ICAM-1. The CD11a mAb G43–25B was able to completely block binding of TLN-transfected L cells to substrates coated with CD11a/CD18, whereas it was ineffective in blocking the binding of ICAM-1-transfected L cells to CD11a/CD18. In addition, the mAb TS2/4, which blocks CD11a/CD18-ICAM-1 interaction, did not inhibit the binding of CD11a/CD18 to TLN. Furthermore, the mAb MEM83 enhanced the interaction of CD11a/CD18 with ICAM-1, but had no effect on CD11a/CD18-TLN binding.

We also demonstrated that leukocyte adhesion to purified TLN is temperature dependent, needs divalent cations, and can be increased by stimulation. These characteristics are typical of integrin binding to their ligands. Addition of Mg^{2+}-Mn^{2+} or PDBu substantially enhanced the binding of leukocytes to purified TLN. No detectable increase in CD11a/CD18 expression on leukocytes was observed after these treatments (data not shown), indicating that TLN recognizes a high avidity state of CD11a/CD18. Interestingly, the ICAM-2 peptide increased leukocyte binding to TLN. We have previously shown that P1 binds to CD11a/CD18 and CD11b/CD18, and increases integrin activity (58). How the peptide works is not yet known. These findings show that different binding and activation sites exist in CD11a/CD18 for ICAM-1 and TLN. The ability of TLN(1–5) to bind to CD11a/CD18 shows that the integrin binding site is somewhere in the first five Ig domains.

The tissue distribution of TLN is unique among ICAMs, in that only the telencephalic regions (the cerebral neocortex, olfactory cortex, hippocampus, striatum, amygdala, septum, and olfactory bulb) of the CNS express this molecule, and it is present on neurons and absent from glial cells (39). Although TLN mRNA was not detected in adult rabbit peripheral tissues (39), the possibility of stage-specific expression of TLN during development has not been ruled out.

Our present data indicate that TLN might be involved in the interactions between the immune system and the CNS. Mounting evidence has suggested the involvement of cell adhesion molecules, such as ICAM-1 and VCAM-1, and their counter-receptors in the process of many CNS disorders, ranging from infectious diseases to autoimmune diseases, and Alzheimer's disease (32, 34, 35, 60, 61). Most of these studies have referred to an important role of microglia, the resident macrophages of the CNS parenchyma. When activated, microglia undergo morphologic changes, up-regulate surface Ags, including β_2 integrins, and exhibit features indicative of phagocytic activities (62). It has been reported that the expression of CD11a/CD18 is markedly increased on microglia when they are activated, for example, by facial nerve transection (63). CD11a/CD18 could be important in the regulation of direct cell-cell interaction between activated microglia and injured neurons (63). TLN might be a neuronal target for activated microglia or infiltrating monocytes that participate in a local inflammatory cascade that promotes tissue damage during pathologic processes.

In conclusion, we have found a novel ligand for CD11a/CD18 that is located in the telencephalon of the mammalian brain. It will be important to study the functional meaning of this interaction.

Acknowledgments

We thank Drs. Jari Ylänne, Pekka Nortamo, and Juni Palmgren for valuable comments and generous help, Leena Kuoppasalmi for excellent technical assistance, and Yvonne Heinilä for secretarial work.

References

1. Springer, T. A. 1990. Adhesion receptors of the immune system. *Nature 346:425.*
2. Patarroyo, M., J. Prieto, J. Rincon, T. Timonen, C. Lundberg, L. Lindbom, B. Åsjö, and C. G. Gahmberg. 1990. Leukocyte-cell adhesion: a molecular process fundamental in leukocyte physiology. *Immunol. Rev. 114:67.*
3. Arnaout, M. A. 1990. Structure and function of the leukocyte adhesion molecules CD11/CD18. *Blood 75:1037.*
4. Hynes, R. O. 1992. Integrins: versatility, modulation, and signalling in cell adhesion. *Cell 69:11.*
5. Butcher, E. C. 1991. Leukocyte-endothelial cell recognition: three (or more) steps to specificity and diversity. *Cell 67:1033.*
6. Carlos, T. M., and J. M. Harlan. 1994. Leukocyte-endothelial adhesion molecules. *Blood 84:2068.*
7. Rothlein, R., M. L. Dustin, S. D. Marlin, and T. A. Springer. 1986. A human intercellular adhesion molecule (ICAM-1) distinct from LFA-1. *J. Immunol. 137: 1270.*
8. Marlin, S. D., and T. A. Springer. 1987. Purified intercellular adhesion molecule-1 (ICAM-1) is a ligand for lymphocyte function-associated antigen-1 (LFA-1). *Cell 51:813.*
9. Staunton, D. E., M. L. Dustin, H. P. Erickson, and T. A. Springer. 1990. The arrangement of the immunoglobulin-like domains of ICAM-1 and the binding sites for LFA-1 and rhinovirus. *Cell 61:243.*
10. Berendt, A. R., A. McDowall, A. G. Craig, P. A. Bates, M. J. E. Sternberg, K. Marsh, C. I. Newbold, and N. Hogg. 1992. The binding site on ICAM-1 for *Plasmodium falciparum*-infected erythrocytes overlaps, but is distinct from, the LFA-1 binding site. *Cell 68:71.*
11. Li, R., P. Nortamo, L. Valmu, M. Tolvanen, C. Kantor, and C. G. Gahmberg. 1993. A peptide from ICAM-2 binds to the leukocyte integrin CD11a/CD18 and inhibits endothelial cell adhesion. *J. Biol. Chem. 268:17513.*
12. Staunton, D. E., M. L. Dustin, and T. A. Springer. 1989. Functional cloning of ICAM-2, a cell adhesion ligand for LFA-1 homologous to ICAM-1. *Nature 339: 61.*
13. Nortamo, P., R. Salcedo, T. Timonen, M. Patarroyo, and C. G. Gahmberg. 1991. A monoclonal antibody to the human leukocyte adhesion molecule intercellular adhesion molecule-2: cellular distribution and molecular characterization of the antigen. *J. Immunol. 146:2530.*
14. Gahmberg, C. G., P. Nortamo, D. Zimmerman, and E. Ruoslahti. 1991. The human leukocyte adhesion ligand, intercellular-adhesion molecule 2: expression and characterization of the protein. *Eur. J. Biochem. 195:177.*
15. de Fougerolles, A. D., S. A. Stacker, R. Schwarting, and T. A. Springer. 1991. Characterization of ICAM-2 and evidence for a third counter-receptor for LFA-1. *J. Exp. Med. 174:253.*
16. de Fougerolles, A. D., and T. A. Springer. 1992. Intercellular adhesion molecule-3, a third adhesion counter-receptor for lymphocyte function-associated molecule 1 on resting lymphocytes. *J. Exp. Med. 175:185.*
17. Vazeux, R., P. A. Hoffman, J. K. Tomita, E. S. Dickinson, R. L. Jasman, T. St. John, and W. M. Gallatin. 1992. Cloning and characterization of a new intercellular adhesion molecule ICAM-R. *Nature 360:485.*
18. Fawcett, J., C. L. Holness, L. A. Needham, H. Turley, K. C. Gatter, D. Y. Mason, and D. L. Simmons. 1992. Molecular cloning of ICAM-3, a third ligand for LFA-1, constitutively expressed on resting leukocytes. *Nature 360:481.*
19. Juan, M., R. Vilella, J. Mila, J. Yagüe, A. Miralles, K. S. Campbell, R. J. Friedrich, J. Cambier, J. Vives, A. R. de Fougerolles, and T. A. Springer. 1993. Cdw50 and ICAM-3: Two names for the same molecule. *Eur. J. Immunol. 23: 1508.*
20. Holness, C. L., P. A. Bates, A. J. Littler, C. D. Buckley, A. Mcdowall, D. Bossy, N. Hogg, and D. L. Simmons. 1995. Analysis of the binding site on intercellular adhesion molecule 3 for the leukocyte integrin lymphocyte function-associated antigen 1. *J. Biol. Chem. 270:877.*
21. Bailly, P., E. Tontti, P. Hermand, J.-P. Carton, and C. G. Gahmberg. 1995. The red cell LW blood group protein is an intercellular adhesion molecule which binds to CD11/CD18 leukocyte integrins. *Eur. J. Immunol. 25:3316.*
22. Diamond, M. S., D. E. Staunton, A. R. de Fougerolles, S. A. Stacker, J. Garcia-Aguilar, M. L. Hibbs, and T. A. Springer. 1990. ICAM-1 (CD54): a counter-receptor for Mac-1 (CD11b/CD18). *J. Cell Biol. 111:3129.*
23. Diamond, M. S., D. E. Staunton, S. D. Marlin, and T. A. Springer. 1991. Binding of the integrin Mac-1 (CD11b/CD18) to the third immunoglobulin-like domain of ICAM-1 (CD54) and its regulation by glycosylation. *Cell 65:961.*
24. Xie, J., R. Li, P. Kotovuori, C. Vermot-Desroches, J. Wijdenes, M. A. Arnaout, P. Nortamo, and C. G. Gahmberg. 1995. Intercellular adhesion molecule-2 (CD102) binds to the leukocyte integrin CD11b/CD18 through the A domain. *J. Immunol. 155:3619.*
25. Beller, D. I., T. A. Springer, and R. D. Schreiber. 1982. Anti-Mac-1 selectively inhibits the mouse and human type three complement receptor. *J. Exp. Med. 156:1000.*
26. Wright, S. D., P. E. Rao, W. C. Van Voorhis, L. S. Craigmyle, K. Iida, M. A. Talle, E. F. Westberg, G. Goldstein, and S. C. Silverstein. 1983. Identification of the C3bi receptor of human monocytes and macrophages by using monoclonal antibodies. *Proc. Natl. Acad. Sci. USA 80:5699.*
27. Wright, S. D., J. I. Weitz, A. J. Huang, S. M. Levin, S. C. Silverstein, and J. D. Loike. 1988. Complement receptor type 3 (CD11b/CD18) of human polymorphonuclear leukocytes recognizes fibrinogen. *Proc. Natl. Acad. Sci. USA 85: 7734.*
28. Altieri, D. C., and T. S. Edgington. 1988. The saturable high affinity association of factor X to ADP-stimulated monocytes defines a novel function of the Mac-1 receptor. *J. Biol. Chem. 263:7007.*

Carl_G_190x270_mm_blokki_FINAL.indd 327 06-Aug-23 1:54:08 PM

29. Altieri, D. C., R. Bader, P. M. Mannucci, and T. S. Edgington. 1988. Oligospecificity of the cellular adhesion receptor Mac-1 encompasses an inducible recognition specificity for fibrinogen. *J. Cell Biol. 107:1893.*
30. Blackford, J., H. W. Reid, D. J. C. Pappin, F. S. Bowers, and J. M. Wilkinson. 1996. A monoclonal antibody, 3/22, to rabbit CD11c which induces homotypic T cell aggregation: evidence that ICAM-1 is a ligand for CD11c/CD18. *Eur. J. Immunol. 26:525.*
31. Van der Vieren, M., H. L. Trong, C. L. Wood, P. F. Moore, T. St. John, D. E. Staunton, and W. M. Gallatin. 1995. A novel leukointegrin, $\alpha_d\beta_2$, binds preferentially to ICAM-3. *Immunity 3:683.*
32. Sobel, R. A., M. E. Mitchell, and G. Fondren. 1990. Intercellular adhesion molecule-1 (ICAM-1) in cellular immune reactions in the human central nervous system. *Am. J. Pathol. 136:1309.*
33. Cannella, B., A. H. Cross, and C. S. Raine. 1991. Adhesion-related molecules in the central nervous system: up-regulation correlates with inflammatory cell influx during relapsing experimental autoimmune encephalomyelitis. *Lab. Invest. 65: 23.*
34. Greenwood, J., Y. Wang, and V. L. Calder. 1995. Lymphocyte adhesion and transendothelial migration in the central nervous system: the role of LFA-1, ICAM-1, VLA-4 and VCAM-1. *Immunology 86:408.*
35. Deckert-Schlüter, M., D. Schlüter, H. Hof, O. D. Wiestler, and H. Lassmann. 1994. Differential expression of ICAM-1, VCAM-1 and their ligands LFA-1, Mac-1, CD43, VLA-4, and MHC class II antigens in murine toxoplasma encephalitis: a light microscopic and ultrastructural immunohistochemical study. *J. Neuropathol. Exp. Neurol. 53:457.*
36. McGeer, P. L., T. Kawamata, D. G. Walker, H. Akiyama, I. Tooyama, and E. McGeer. 1993. Microglia in degenerative neurological disease. *Glia 7:84.*
37. Mori, K., C. Fujita, Y. Watanabe, K. Obata, and O. Hayaishi. 1987. Telencephalon-specific antigen identified by monoclonal antibody. *Proc. Natl. Acad. Sci. USA 84:3921.*
38. Oka, S., K. Mori, and Y. Watanabe. 1990. Mammalian telencephalic neurons express a segment-specific membrane glycoprotein, telencephalin. *Neuroscience 35:93.*
39. Yoshihara, Y., S. Oka, Y. Nemoto, Y. Watanabe, S. Nagata, H. Kagamiyama, and K. Mori. 1994. An ICAM-related neuronal glycoprotein, telencephalin, with brain segment-specific expression. *Neuron 12:541.*
40. Yoshihara, Y., and K. Mori. 1994. Telencephalin: a neuronal area code molecule? *Neurosci. Res. 21: 119.*
41. Williams, A. F., and A. N. Barclay. 1988. The immunoglobulin superfamily-domains for cell surface recognition. *Annu. Rev. Immunol. 6:381.*
42. Simmons, D. L., M. W. Makgova, and B. Seed. 1988. ICAM, an adhesion ligand of LFA-1, is homologous to the neural cell adhesion molecule NCAM. *Nature 331:624.*
43. Staunton, D. E., S. D. Marlin, C. Stratowa, M. L. Dustin, and T. A. Springer. 1988. Primary structure of intercellular adhesion molecule 1 (ICAM-1) demonstrates interaction between members of the immunoglobulin and integrin supergene families. *Cell 52:925.*
44. Bailly, P., P. Hermand, I. Callebaut, H. H. Sonneborn, S. Khamlichi, J. P. Mornon, and J. P. Cartron. 1994. The LW blood group glycoprotein is homologous to intercellular adhesion molecules. *Proc. Natl. Acad. Sci. USA 91:5306.*
45. Nortamo, P., M. Patarroyo, C. Kantor, J. Suopanki, and C. G. Gahmberg. 1988. Immunological mapping of the human leukocyte adhesion glycoprotein GP90 (CD18) by monoclonal antibodies. *Scand. J. Immunol. 28:537.*
46. Sánchez-Madrid, F., A. M. Krensky, C. F. Ware, E. Robbins, J. L. Strominger, S. F. Burakoff, and T. A. Springer. 1982. Three distinct antigens associated with human T-lymphocyte-mediated cytolysis: LFA-1, LFA-2, and LFA-3. *Proc. Natl. Acad. Sci. USA 79:7489.*
47. Landis, R. C., R. I. Bennett, and N. J. Hogg. 1993. A novel LFA-1 action epitope maps to the I domain. *J. Cell Biol. 120:1519.*
48. Miller, L. J., R. Schwarting, and T. A. Springer. 1986. Regulated expression of the Mac-1, LFA-1, p150,95 glycoprotein family during leukocyte differentiation. *J. Immunol. 137:2891.*
49. Hogg, N., L. Takacs, D. B. Palmer, Y. Selvendran, and C. Allen. 1986. The p150,95 molecule is a marker of human mononuclear phagocytes: comparison with expression of class II molecules. *Eur. J. Immunol. 16:240.*
50. Pulido, R., M. J. Elices, M. R. Campanero, L. Osborn, S. Schiffer, A. Garcia-Pardo, R. Lobb, M. E. Hemler, and F. Sánchez-Madrid. 1991. Functional evidence for three distinct and independently inhibitable adhesion activities mediated by the human integrin VLA-4. Correlation with distinct alpha 4 epitopes. *J. Biol. Chem. 266:10241.*
51. Cheresh, D. A., and R. C. Spiro. 1987. Biosynthetic and functional properties of an Arg-Gly-Asp-directed receptor involved in human melanoma cell attachment to vitronectin, fibrinogen and von Willebrand factor. *J. Biol. Chem. 262:17703.*
52. Clark, E. A., J. A. Ledbetter, R. C. Holly, P. A. Dinndorf, and G. Shu. 1986. Polypeptides on human B lymphocytes associated with cell activation. *Hum. Immunol. 16:100.*
53. Weiss, A., R. L. Wiskocil, and J. D. Stobo. 1984. The role of T3 surface molecules in the activation of human T cells: a two-stimulus requirement for IL2 production reflects events occurring at a pretranslational level. *J. Immunol. 133: 123.*
54. Arnaout, M. A. 1990. Leukocyte adhesion molecules deficiency: its structural basis, pathophysiology and implications for modulating the inflammatory response. *Immunol. Rev. 114:145.*
55. Simmons, D. L. 1993. Cloning cell surface molecules by transient expression in mammalian cells. In *Cellular Interactions in Development: A Practical Approach.* D. A. Hartley, ed. IRL Press, Oxford, p. 93.
56. Nishimura, Y., M. Yokoyama, K. Araki, R. Ueda, A. Kudo, and T. Watanabe. 1987. Recombinant human-mouse chimeric monoclonal antibody specific for common acute lymphocytic leukaemia. *Cancer Res. 47:999.*
57. Mizushima, S., and S. Nagata. 1990. pEF-BOS, a powerful mammalian expression vector. *Nucleic Acids Res. 18:5322.*
58. Li, R., J. Xie, C. Kantor, V. Koistinen, D. C. Altieri, P. Nortamo, and C. G. Gahmberg. 1995. A peptide from the intercellular adhesion molecule-2 regulates the avidity of the leukocyte integrins CD11b/CD18 and CD11c/CD18. *J. Cell. Biol. 129:1143.*
59. Gahmberg, C. G., and L. C. Andersson. 1977. Selective radioactive labelling of cell surface sialoglycoproteins by periodate-tritiated borohydride. *J. Biol. Chem. 252:5888.*
60. Shrikant, P., E. Weber, L. P. Tang, and E. N. Benveniste. 1995. Intercellular adhesion molecule-1 gene expression by glial cells. *J. Immunol. 155:1489.*
61. Akiyama, H., and P. L. McGeer. 1990. Brain microglia constitutively express β_2 integrins. *J. Neuroimmunol. 30:81.*
62. Gehrmann, J., Y. Matsumoto, and G. W. Kreutzberg. 1995. Microglia: intrinsic immunoeffector cell of the brain. *Brain Res. Rev. 20:269.*
63. Moneta, M. E., J. Gehrmann, R. Topper, R. B. Banati, and K. W. Kreutzberg. 1993. Cell adhesion molecule expression in the regenerating rat facial nucleus. *J. Neuroimmunol. 45:203.*

Carl_G_190x270_mm_blokki_FINAL.indd 328 06-Aug-23 1:54:08 PM

Intercellular Adhesion Molecule-5 Induces Dendritic Outgrowth by Homophilic Adhesion

Li Tian,* Henrietta Nyman,* Patrick Kilgannon,‡ Yoshihiro Yoshihara,§ Kensaku Mori,‖ Leif C. Andersson,¶ Sami Kaukinen,* Heikki Rauvala,** W. Michael Gallatin,‡ and Carl G. Gahmberg***

*Department of Biosciences, Division of Biochemistry, Viikinkaari 5, University of Helsinki, Helsinki 00014, Finland; ‡ICOS Corporation, Bothell, Washington 98021; §Laboratory for Neurobiology of Synapse, Brain Science Institute, The Institute of Physical and Chemical Research (RIKEN), Wako-City, Saitama 351, Japan; ‖Laboratory for Neuronal Recognition Molecules, Brain Science Institute, RIKEN, Wako-City, Saitama 351, Japan; ¶Haartman Institute, Department of Pathology, University of Helsinki, Helsinki 00014, Finland; and **Laboratory of Molecular Neurobiology, Institute of Biotechnology, University of Helsinki, Helsinki 00014, Finland

Abstract. Intercellular adhesion molecule-5 (ICAM-5) is a dendritically polarized membrane glycoprotein in telencephalic neurons, which shows heterophilic binding to leukocyte β_2-integrins. Here, we show that the human ICAM-5 protein interacts in a homophilic manner through the binding of the immunoglobulin domain 1 to domains 4–5. Surface coated ICAM-5-Fc promoted dendritic outgrowth and arborization of ICAM-5–expressing hippocampal neurons. During dendritogenesis in developing rat brain, ICAM-5 was in monomer form, whereas in mature neurons it migrated as a high molecular weight complex. The findings indicate that its homophilic binding activity was regulated by nonmonomer/monomer transition. Thus, ICAM-5 displays two types of adhesion activity, homophilic binding between neurons and heterophilic binding between neurons and leukocytes.

Key words: leukocyte • integrin • adhesion • dendrite • neuron

Introduction

Neuron–neuron contact mediated by adhesion molecules is an important way to influence brain architecture (Hynes and Lander, 1992; Goodman and Shatz, 1993; Walsh and Doherty, 1997). Since neurons are polarized, extending an axon and dendrites from the soma (Craig and Banker, 1994), neural cell adhesion molecules can be divided into axon-associated cell adhesion molecules (AxCAMs)[1] and dendrite-associated cell adhesion molecules (DenCAMs; Yoshihara et al., 1994; Brümmendorf and Rathjen, 1996). Whereas a great deal is known about the roles of AxCAMs in axonal elongation, fasciculation, and guidance by mechanisms involving transmembrane signaling pathways (Sonderegger and Rathjen, 1992; Walsh and Doherty, 1997), little is known about DenCAMs. However, DenCAMs are supposed to guide the formation of dendritic fasciculation and arborization, and to function as counter-receptors for AxCAMs in synaptogenesis.

Intercellular adhesion molecule-5 (ICAM-5; telencephalin; Yoshihara et al., 1994; Mizuno et al., 1997) is a cell surface glycoprotein that belongs to the immunoglobulin superfamily and shares 38–55% amino acid identity with the other ICAMs, which play important roles as adhesion molecules in the hematopoietic system (Springer, 1994; Gahmberg, 1997; Hayflick et al., 1998). Many cell surface proteins involved in cell adhesion belong to the immunoglobulin superfamily. Such proteins contain a variable number of immunoglobulin domains, which are ~100 amino acids long and form two β-sheets. Human ICAM-5 consists of nine extracellular immunoglobulin domains with a total of 832 amino acids, a 28-amino acid transmembrane segment, and a 64-amino acid cytoplasmic domain. Like other ICAMs, it binds to the leukocyte integrin CD11a/CD18 (Mizuno et al., 1997; Tian et al., 1997) and it may be an important regulator of the immune response in the central nervous system.

ICAM-5 has several features that make it a candidate

Address correspondence to Carl G. Gahmberg, Department of Biosciences, Division of Biochemistry, Viikinkaari 5, University of Helsinki, Helsinki 00014, Finland. Tel.: 358-9-19159028. Fax: 358-9-19159068. E-mail: carl.gahmberg@helsinki.fi

[1]*Abbreviations used in this paper:* AxCAM, axon-associated cell adhesion molecule; D, immunoglobulin domain; DenCAM, dendrite-associated cell adhesion molecule; E19, embryonic day 19; ICAM, intercellular adhesion molecule; MAP-2, microtubule-associated protein-2; P, postnatal day; WT, wild-type.

© The Rockefeller University Press, 0021-9525/2000/07/243/10 $5.00

Carl_G_190x270_mm_blokki_FINAL.indd 329 06-Aug-23 1:54:08 PM

for a DenCAM. Firstly, it is localized to cell somata and dendrites of neurons, and neurons expressing ICAM-5 have more extensive dendritic branches than neurons without ICAM-5 (Benson et al., 1998). Secondly, it is expressed only in the telencephalon, the most rostral segment of the brain, and not in the caudal segments (Yoshihara and Mori, 1994). Thirdly, the onset of its expression temporally parallels the onset of dendritic elongation and synaptogenesis during the postnatal period. These facts together support the hypothesis that ICAM-5 may provide a brain segment-specific cue for synaptogenesis or dendrite–dendrite interactions in the telencephalon. Indeed, earlier studies have shown that ICAM-5 promotes embryonic hippocampal neurite outgrowth (Tamada et al., 1998) and is involved in hippocampal long-term potentiation (Sakurai et al., 1998). However, the molecular basis has remained poorly understood.

Here, we attempted to address this issue by studying purified recombinant human ICAM-5 proteins, ICAM-5 transfected into a human neural crest derived cell line (Paju), and ICAM-5 in developing rat brain. We found that ICAM-5 induced neurite outgrowth of Paju cells and rat hippocampal neurons through homophilic interaction, and it also promoted the dendritic arborization of hippocampal neurons through homophilic binding. The adhesive domains in ICAM-5 were mapped, and we propose that the homophilic activity of ICAM-5 is regulated by a monomer/nonmonomer transition.

Materials and Methods

Cell Culture and Immunocytostaining

Wild-type Paju cells (Paju-WT) are a human neural crest-derived cell line, which was cultured in RPMI 1640 and 10% FCS (BioWhittaker) on glass coverslips. Paju-ICAM-5 was obtained by transfection of Paju-WT with the human ICAM-5 in the vector pEF-BOS (Tian et al., 1997; Tamada et al., 1998) and was cultured as above, but in the presence of 0.5 mg/ml G418 (Sigma-Aldrich). For mAb blocking assay, Paju-ICAM-5 cells were cultured in the presence of 100 μg/ml mAbs to ICAM-5 for 3 d. The antibodies were made by immunizing mice with purified ICAM-5-Fc and antibody-producing clones identified by flow cytometry analysis. Control cells were stained with 10 μg/ml mAb TL-3 after culture.

After methanol fixation, the cells were stained with FITC-conjugated rabbit anti–mouse antiserum (Jackson ImmunoResearch Laboratories). Cells were observed by immunofluorescence microscopy (Olympus Provis 70) at 400×.

Production of Recombinant Proteins

Truncated ICAM-5 extracellular domains were cloned by PCR from human ICAM-5 cDNA, sequenced, and inserted into the pEF-Fc (Tian et al., 1997; Tamada et al., 1998) expression vector. The recombinant proteins were purified from transiently transfected COS-1 (American Type Culture Collection) cells using protein A–Sepharose CL 4B (Amersham Pharmacia Biotech) and their purities checked by Western blotting using HRP-conjugated anti-human Ig (Amersham Pharmacia Biotech). Soluble ICAM-5 immunoglobulin domain 1–9 (D1–9) without Fc was purified from a baculovirus-expression system (Bac-to-bac system; GIBCO BRL).

Flow Cytometry and ELISA

10^6 Paju-WT and Paju-ICAM-5 cells were first incubated with 100 μg/ml recombinant ICAM-5-Fc, ICAM-1-Fc, and NCAM-Fc proteins, followed by FITC-conjugated anti-human IgG (Dako) at room temperature for 30 min. After washings, samples were analyzed with FACScan and CellQuest software (Becton Dickinson). The mean fluorescent value of Paju-ICAM-5 was subtracted with that of Paju-WT for each recombinant protein. For ELISA, 5 μg/ml recombinant proteins were coated on microtiter plates, blocked with BSA (Sigma-Aldrich), and then incubated first with biotinylated domains 1–2 Fc (D1–2-Fc; Pierce) of ICAM-5, and then with HRP-conjugated streptavidin (Pierce Chemical Co.) at 37°C for 1 h, and the color measured at 492 nm. For mAb blocking assay, 5 μg/ml ICAM-5 D1–9 was coated and preincubated with anti–ICAM-5 mAbs at room temperature for 30 min, followed by the steps mentioned above.

Native PAGE and Western Blotting

Brains of embryonic (embryonic day 19, E19), newborn (postnatal day 1–10, P1-10), and adult rats were homogenized in 10 mM Tris, 1 mM EDTA, 10 mM Chaps, 300 mM NaCl, and 1 mM PMSF. Paju-ICAM-5 cells were treated with 5 μM cytochalasin D (Calbiochem-Novabiochem) or 0.5 mg/ml ICAM-5 D1–2-Fc protein for 8 or 4 h, respectively, and were then lysed with the same buffer. Brain homogenates or cell lysates were run on native PAGE with PhastGel 4-15 (Amersham Pharmacia Biotech) and blotted onto nitrocellulose membranes. ICAM-5 protein was detected by a polyclonal antibody against the cytoplasmic part of mouse ICAM-5 (Tian et al., 1997).

Neurite Outgrowth Assay

0.5 μg of D1–2-Fc or D1–9-Fc of ICAM-5 and ICAM-1-Fc proteins were coated in drops on coverslips in 24-well plates. After blocking, the coverslips with BSA, 10^4/well Paju-WT and Paju-ICAM-5 cells were seeded and cultured for 30–36 h. For mAb inhibition assay, 50 μg/ml mAb 179B was incubated with Paju-WT and Paju–ICAM-5 cells. Cells were observed under phase-contrast microscope (Olympus Provis 70) at 400×. The length of the neurites was measured as the distance between the soma and the tip of the neurite counted in three random fields.

Hippocampus and cerebellum were dissected from 19-d-old rat embryos and treated with 0.5 mg/ml papain for 10 min (Worthington Biochemical Corp.) in HBSS (GIBCO BRL). After washing in HBSS, neurons suspended in Neurobasal medium (GIBCO BRL), 2% B27 supplement (GIBCO BRL), 25 μM L-glutamic acid (Sigma-Aldrich), and 1% L-glutamine (GIBCO BRL) were seeded at 10^4/well density in 8-chamber slides (Nunc) coated with laminin (50 μg/ml; Sigma-Aldrich), HB-GAM (Rauvala and Peng, 1997; 50 μg/ml), poly-DL-ornithine (100 μg/ml; Sigma-Aldrich), or ICAM-5 recombinant proteins (100 μg/ml). For inhibition assay, 100 μg/ml of each antibody or recombinant protein was added to the culture medium. Neurons were cultured for 48 or 72 h, and were then fixed with 4% paraformaldehyde for 25 min. After permeabilization with 0.2% Triton X-100 for 10 min, the neurons were visualized with the dendritic marker, antimicrotubule associated protein-2 (anti–MAP-2) mAb (Boehringer), the axonal marker antitau mAb (Boehringer), or rabbit anticytoplasmic mouse ICAM-5 antiserum for 1 h at room temperature (Benson et al., 1998), followed by incubation with TRITC-conjugated goat anti–rabbit and FITC-conjugated goat anti–mouse antibodies (Jackson ImmunoResearch Laboratories, Inc.). The proportion of neurite-bearing cells (processes longer than 1 diam of the cell body) was counted in four random fields using a fluorescence microscope (Olympus Provis 70) at 400×.

Statistical Analysis

For all the quantitations, statistical analysis of variance (ANOVA) was used to compare the different groups in each experiment.

Results

Expression of ICAM-5 in Transfected Neural Crest Cells

To study neuronal functions of ICAM-5, we used the human neural crest-derived cell line, Paju (Zhang et al., 1996). This cell line does not constitutively express ICAM-5, and therefore we transfected it with human ICAM-5. When we stained the Paju-ICAM-5 cells with mAbs against ICAM-5, we observed that ICAM-5 did not distribute evenly on the membrane. It showed a bimodal distribution to the uropods of Paju-ICAM-5 cells and to

Carl_G_190x270_mm_blokki_FINAL.indd 330 06-Aug-23 1:54:08 PM

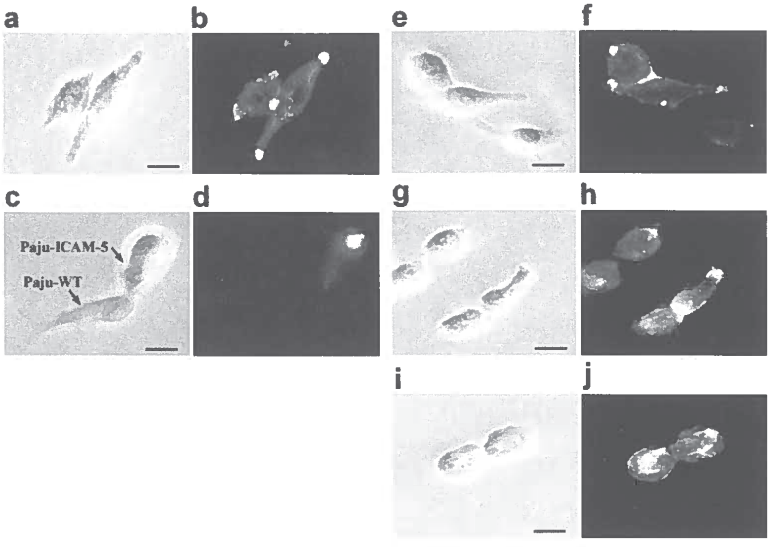

Figure 1. Colocalization of ICAM-5 at cell–cell contact sites in Paju neuronal cells. Human ICAM-5 transfected into Paju cells was expressed at cell–cell contact sites and the uropods of Paju-ICAM-5 cells (a and b), but not in Paju-WT/Paju-ICAM-5 contact regions (c and d). When Paju-ICAM-5 cells were cultured in the presence of the antiadhesive-ICAM-5 mAbs, like TL-3 (i and j), the localization of ICAM-5 at contact sites was diminished as compared with treatment with control mAb (antiglycophorin A; e and f) or the mAb TL-1 treatment (g and h), which does not affect adhesion. a, c, e, g, and i, Phase-contrast photographs; b, d, f, h, and j, immunofluorographs. Bars, 20 μm.

cell–cell contact sites (Fig. 1, a and b). When Paju-WT cells were cocultivated with Paju-ICAM-5 cells, localization of ICAM-5 to cell–cell contact sites was no longer observed, although the uropodal expression remained (Fig. 1, c and d; Table I). When Paju-ICAM-5 cells were cultured in the presence of anti–ICAM-5 mAbs, we found that mAbs that do not inhibit leukocyte integrin-ICAM-5 adhesion, like TL-1 (Fig. 1, g and h) and 179K, did not influence ICAM-5 colocalization much, whereas antileukocyte-adhesive mAbs, like TL-3 (Fig. 1, i and j) and 179B, blocked the colocalization at cell–cell contact sites. With control antibody, ICAM-5 remained at sites of cell contact (Fig. 1 e and f; Table I).

Homophilic Binding of Recombinant ICAM-5 Fragments

Since these findings suggested that ICAM-5 can bind in a homophilic manner, we studied this possibility in more detail by constructing a series of extracellular domain de-

Table I. ICAM-5 Localization at Cell–Cell Contact Sites in the Paju Neuronal Crest Cell Line

mAb treatment	Paju-WT/Paju-ICAM-5	Paju-ICAM-5/Paju-ICAM-5
	% (*n*)	% (*n*)
None	5.7 (35)	91.2 (35)
TL-1 (not antiadhesive)		88.2 (34)
TL-3 (antiadhesive)		14.3 (35)
179B (antiadhesive)		8.6 (35)
179K (not antiadhesive)		90.9 (33)

Data are presented as the percentage of cell–cell contact sites with ICAM-5 localized at the sites. The concentration of each mAb was 100 μg/ml.

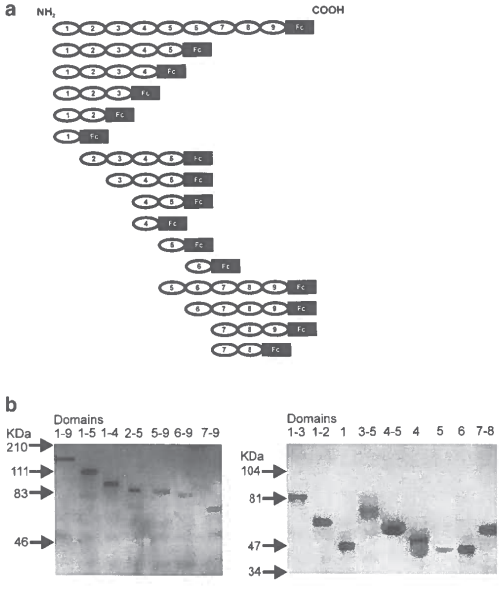

Figure 2. ICAM-5 recombinant molecules. a, A schematic representation of the ICAM-5 constructs used. The domains are numbered from the NH_2-terminal. Fc, Immunoglobulin Fc domain. b, Western blot of purified ICAM-5 proteins. The positions of the molecular weight markers are shown to the left. The left-hand gel was made using 8% acrylamide and the right-hand gel was made using 10% acrylamide.

Carl_G_190x270_mm_blokki_FINAL.indd 331 06-Aug-23 1:54:08 PM

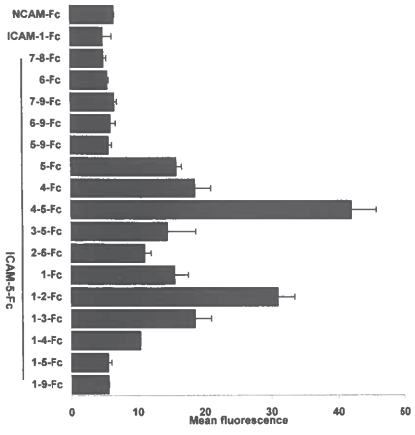

Figure 3. ICAM-5 binds in a homophilic manner. Paju-WT and Paju-ICAM-5 cells were stained with truncated ICAM-5-Fc proteins and analyzed by flow cytometry. The values obtained with Paju-WT were subtracted from the Paju-ICAM-5 values. Note that D1–2-Fc and D4–5-Fc of ICAM-5 gave especially strong binding to Paju-ICAM-5 cells, as compared with the other proteins.

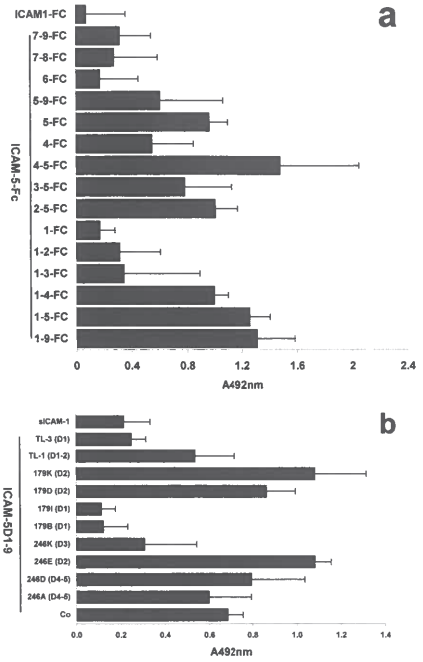

Figure 4. Homophilic binding of ICAM-5 D1–2-Fc to different ICAM-5-Fc constructs. When the binding of biotinylated D1–2-Fc of ICAM-5 to immobilized truncated ICAM-5-Fc proteins was studied, direct binding was observed between D1–2 and D4–5 containing proteins (a). The ICAM-5 mAbs 179B, 179I, and TL-3 (all recognizing domain 1) blocked the binding of D1–2-Fc to immobilized D1–9 of ICAM-5 (b). The Ig-domains of ICAM-5, which are recognized by the respective antibodies are shown in parentheses. Co, Control mouse IgG. SDs are shown.

letion constructs of ICAM-5 (Fig. 2). These truncated ICAM-5 proteins were linked at their COOH terminals to the Fc portion of human IgG_1. The purity of the recombinant proteins was at least 90% (Fig. 2 b). After isolation, these constructs were incubated with Paju-WT and Paju-ICAM-5 cells, and the binding was analyzed by flow cytometry. Whereas recombinant proteins containing domains 1–9, 1–5, 5–9, 6–9, 7–9, 6, and 7–8 ICAM-5-Fc proteins, as well as ICAM-1-Fc and NCAM-Fc proteins showed little binding to Paju-ICAM-5, truncated proteins containing domains 1–4, 1–3, 1–2, 1, 2–5, 3–5, 4–5, 4, and 5 showed significant binding, especially the domains 1–2 and 4–5 constructs (Fig. 3). The results indicated that the homophilic interactions mainly involve the first five domains of ICAM-5, and the reason for the low binding of domains 1–9-Fc and domains 1–5-Fc proteins might be that these proteins were inhibited by intramolecular association.

Further support for homophilic interaction was obtained when we coated truncated, isolated ICAM-5-Fc proteins on plastic, and detected that biotinylated D1–2-Fc bound especially well to various constructs containing domains 4–5 (Fig. 4 a). We further studied the effects of anti–ICAM-5 mAbs on the interaction of D1–2 with immobilized D1–9 (without Fc), and observed that mAbs TL-3, 179B, and 179I (recognizing D1) almost completely blocked the binding, whereas mAbs 179K, 179D, and 246E (recognizing D2) were inactive or even increased binding (Fig. 4 b). These data indicate that the homophilic interaction takes place mainly through the binding of the NH_2-terminal domain 1 to domains 4–5. The homophilic binding of ICAM-5 was Ca^{2+}-independent, and EDTA treatment had no effect (not shown).

High Molecular Weight Form of ICAM-5

Earlier studies have failed to detect any aggregation of ICAM-5–transfected mouse fibroblasts (Yoshihara et al., 1994). This is now understandable in light of our findings that the complete external part of ICAM-5 does not bind to transfected cells. The rabbit ICAM-5 molecule has been proposed to exist as a tetramer (Oka et al., 1990), and therefore we thought that it would be important to study ICAM-5 during development. Fig. 5 a shows that during the first postnatal week of development of the central nervous system in the rat, the molecule existed as a monomer (Fig. 5 a) and at the tenth day of postnatal development a high molecular weight form corresponding in molecular weight to a tetramer began to appear (Fig. 5 a). In the brain of adult rats, almost all ICAM-5 molecules migrated as the high molecular weight form (Fig. 5 a). Also, in transfected Paju-ICAM-5 cells, ICAM-5 mainly existed as nonmonomers (Fig. 5 b). Disruption of the actin cytoskeleton in Paju-ICAM-5 cells by cytochalasin D (Fig. 5 b)

Carl_G_190x270_mm_blokki_FINAL.indd 332 06-Aug-23 1:54:08 PM

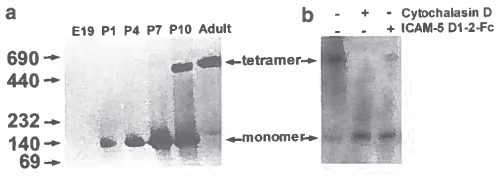

Figure 5. Membrane-bound ICAM-5 undergoes monomer/nonmonomer transition in rat brain (a) and Paju-ICAM-5 cells (b). Brain homogenates or Paju-ICAM-5 cell lysates with or without indicated pretreatments were run on PhastGel 4-15 under native conditions, and were then blotted with a polyclonal antibody against the cytoplasmic part of ICAM-5. In rat brain, ICAM-5 was not expressed at E19, but present after birth. At postnatal 1 (P1), 4 (P4), and 7 (P7) days, ICAM-5 mainly existed as monomers of 140 kD, while it partially changed to nonmonomers (which could be tetramers) of 550 kD at P10. Brains from adult rats contained only nonmonomers. In Paju-ICAM-5 cells (b), ICAM-5 existed mainly as nonmonomers, with a minor monomer component. If the cells were pretreated with 5 μM cytochalasin D or 0.5 mg/ml ICAM-5 D1–2-Fc protein, most of membrane-bound ICAM-5 was brought into monomers.

brought most of ICAM-5 into the monomer form. Incubation of Paju-ICAM-5 cells with the ICAM-5 D1–2-Fc protein (Fig. 5 b) also resulted in monomers.

ICAM-5 Homophilic Interaction Promotes Neurite Outgrowth from Paju Cells and Is Involved in Dendritogenesis and Arborization of Rat Hippocampal Neurons

When we coated ICAM-5 D1–9-Fc on plastic, and then seeded Paju-WT or Paju-ICAM-5 cells, we observed neurites extending from Paju-ICAM-5 cells (Fig. 6 b), but not from Paju-WT cells (Fig. 6 a). When coated on ICAM-5 D1–2, the effect was more pronounced (Fig. 6 d). In the presence of mAb 179B, the neurite extension from Paju-ICAM-5 cells was inhibited (Fig. 6 f). We found significantly less neurites from either type of cells on ICAM-1-Fc coated surfaces (Fig. 6, g and h; Table II).

We then tested if ICAM-5 is involved in the dendritic outgrowth using ICAM-5–expressing rat hippocampal neurons and rat cerebellar neurons, which do not express ICAM-5. By staining the neurons with the dendritic marker, MAP-2, and the axonal marker, tau (Fig. 7), we found that rat hippocampal neurons were induced for dendritic outgrowth on surfaces coated with ICAM-5 D1–9-Fc, D1–2-Fc, laminin, heparin-binding growth-associated molecule (HB-GAM), or poly-DL-ornithine (Fig. 7 a), but not on ICAM-1-Fc. Interestingly, the morphology of dendrites induced by the different molecules was different from one another; the most dramatic difference was seen on ICAM-5 coated surfaces (Fig. 7, a and b), which induced a network of dendritic arbors. When we calculated the number of major dendritic branches extending from the cell soma, there was no significant difference in neurite induction by these molecules (with exception of ICAM-1; $P > 0.01$). Fig. 7 b, left, shows double staining of MAP-2 (green) and ICAM-5 (red). Coexpression of MAP-2 and ICAM-5 was seen (yellow), indicating that ICAM-5 is

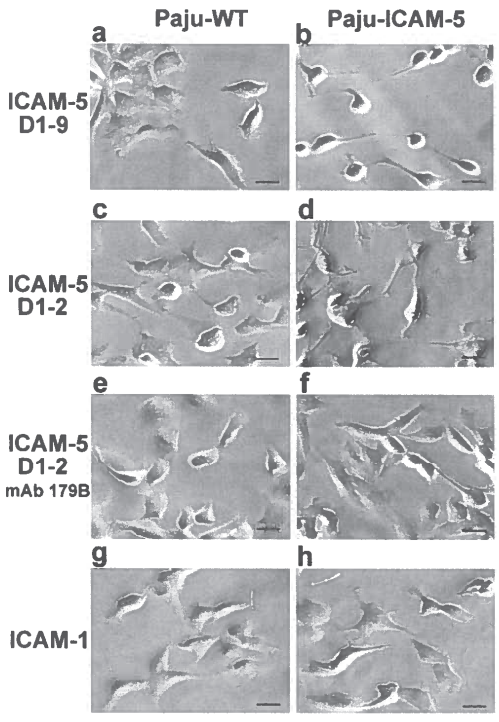

Figure 6. Paju-ICAM-5 cells induced for neurite outgrowth by ICAM-5. When Paju-WT and Paju-ICAM-5 cells were seeded on immobilized ICAM-5 D1–9-Fc or D1–2-Fc proteins, neurite outgrowth was clearly seen with Paju-ICAM-5 cells, but not with Paju-WT cells. mAb 179B inhibited neurite outgrowth of Paju-ICAM-5 cells, but had no effect on Paju-WT cells. Neither Paju-ICAM-5 nor Paju-WT cells developed neurites on ICAM-1-Fc protein. Bars, 20 μm.

largely dendrite-associated. Fig. 7 b, right, shows that ICAM-5 (red) is strongly stained on neurons grown on ICAM-5 and little tau staining (green) was seen. In contrast, when cells were coated on laminin, tau staining was evident. Furthermore, the axonal arbors were more complex on laminin than on ICAM-5 (Fig. 7 b, right), while the dendritic arbors were more extensive on ICAM-5 than on laminin (Fig. 7 b, left). In comparison to hippocampal neu-

Table II. Neurite Outgrowth of Paju Cells

Substrate	Length of neurites	
	Paju-WT	Paju-ICAM-5
	μm (n)	μm (n)
ICAM-1-Fc	4 ± 2 (70)	3 ± 2 (68)
ICAM-5 D1–2-Fc	4 ± 1 (75)	43 ± 10 (72)
ICAM-5 D1–2-Fc + mAb 179B	6 ± 3 (66)	12 ± 3 (65)

Each substrate was coated at a concentration of 10 μg/ml. mAb 179B was used at 50 μg/ml. Length of neurites is shown in micrometers, mean ± SD.

Carl_G_190x270_mm_blokki_FINAL.indd 333 06-Aug-23 1:54:08 PM

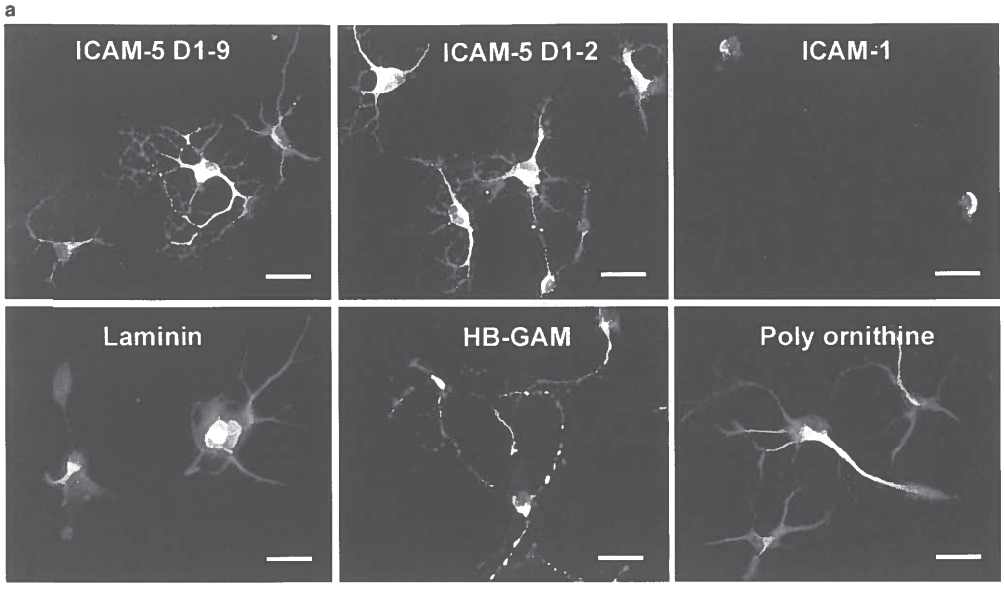

Figure 7 (continues on facing page).

rons, the cerebellar neurons, which do not express ICAM-5, showed significantly less capability of dendritic outgrowth on ICAM-5 coated surfaces than on the surfaces coated with the other molecules (Fig. 7 c). Table III shows a quantitation of the ICAM-5–induced dendrite outgrowth.

To block the function of endogenous ICAM-5 expressed on hippocampal neurons, we coated them with ICAM-5 D1–2-Fc and then incubated the hippocampal neurons with antibodies and ICAMs in the medium. We found that an antiserum against rat ICAM-5 (pAb 1000J) significantly inhibited dendritic outgrowth, as compared with a control serum (Fig. 8 a). Soluble ICAM-5 D1–2-Fc, but not ICAM-1-Fc, also showed a significant blocking effect. The effect of these proteins was quantitated and shown in Fig. 8 b.

Table III. Quantitation of Rat Hippocampal Neurons Expressing Axons or Dendrites

	Percentage of neurons with	
Coated protein	Axons	Dendrites
	%	%
Laminin	72 ± 8.0	20 ± 9.2
ICAM-5 D1–2	7.5 ± 2.5	63 ± 6.5
ICAM-5 D1–9	6.5 ± 3.8	52 ± 8.2

80 neurons were studied for each protein. 50 μg/ml of laminin and 100 μg/ml of ICAM-5 was used for coating. The cells were grown for 72 h. Axons were identified by antitau staining and dendrites were identified by double-staining with anti–ICAM-5 and MAP-2.

Discussion

Neurons are known for their elaborate subcellular structures that enable the transmission of signals from one cell to another. To be meaningful, they must make precise connections with their respective target cells (Goodman and Shatz, 1993). This developmental process includes axonal and dendritic elongation, axonal guidance, and adhesive interactions between axonal growth cones and soma-dendritic membranes of target neurons that give rise to the formation of synaptic connections. Although much is known about axonal elongation and guidance (Tessier-Lavigne and Goodman, 1996; Cook et al., 1998), little is known about dendritic development and how dendrites participate in synaptic interaction.

A number of factors are known to be involved in axonal guidance, including diffusible or surface-bound growth-promoting molecules and various adhesion molecules (Jessell, 1988), such as cadherins (Takeichi, 1991; Tamura et al., 1998), integrins (Hynes, 1992), and immunoglobulin superfamily molecules (Sonderegger and Rathjen, 1992; Goodman and Shatz, 1993). In contrast, only ICAM-5 has been shown to have a restricted expression to soma-dendritic membranes of telencephalic neurons (Yoshihara et al., 1994; Benson et al., 1998). The immunofluorescence studies show that ICAM-5 had a similar distribution as the dendritic marker MAP-2. MAP-2 evidently also stained some axons (Fig. 7 b), probably due to the fact that the neurons at this stage are not absolutely polarized. In contrast, axon staining with antitau showed a different distribution and little overlap was seen in cells grown on

Carl_G_190x270_mm_blokki_FINAL.indd 334 06-Aug-23 1:54:08 PM

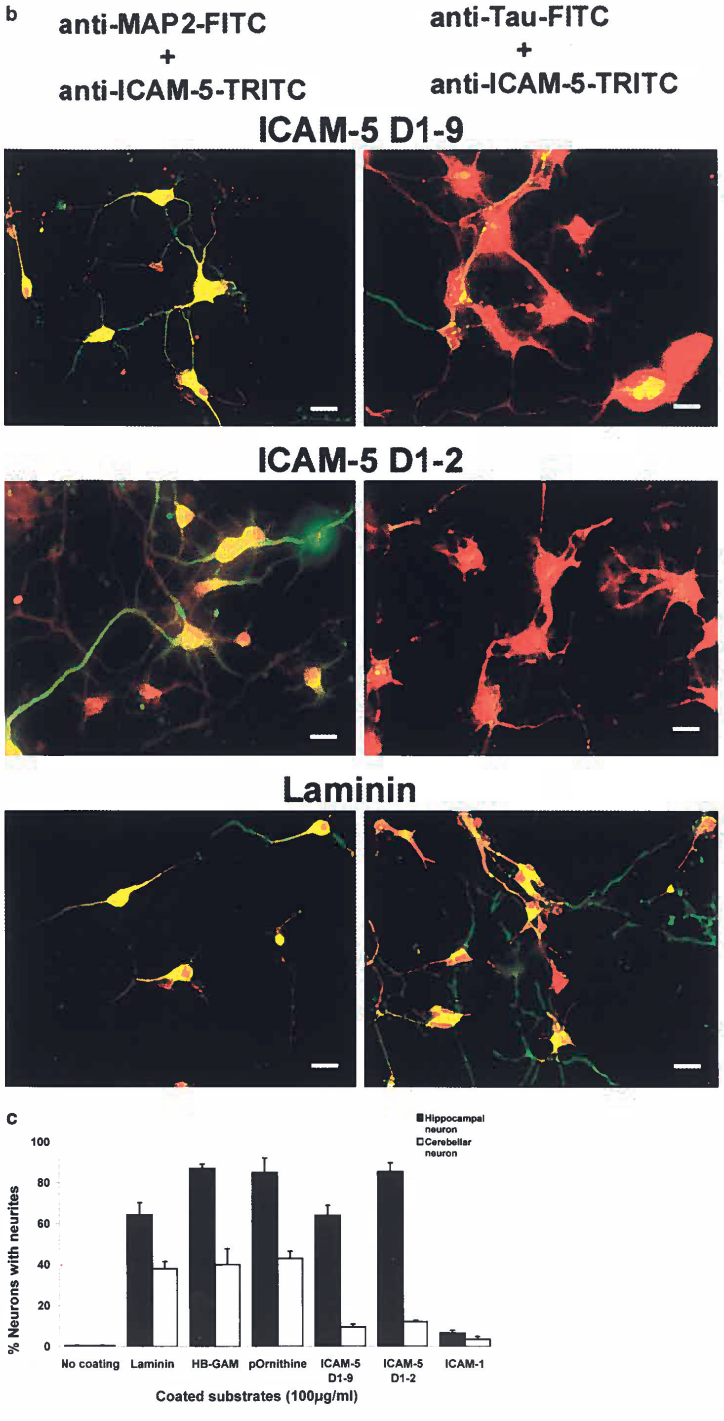

Figure 7. ICAM-5 promotes dendritic outgrowth from rat hippocampal neurons. Rat E19 hippocampal or cerebellar neurons were cultured on different substrate coated surfaces for 48 (a) and 72 h (b), and were then visualized by staining with the dendritic marker, MAP-2 (a and b), and axonal marker, tau (b) together with anti–ICAM-5 polyclonal antibody. The proportion of neurons with neurites was quantitated (c). All photographs were taken at 400×. Bars, 20 µm. In a, neurites from hippocampal neurons were induced on ICAM-5 D1–9, ICAM-5 D1–2, laminin, HB-GAM, or poly-DL-ornithine coated surfaces, but not on ICAM-1 coated plates. Note the more elaborate network of neurites induced by ICAM-5 than on laminin, HB-GAM, or poly-DL-ornithine. b, Shows double-staining of the dendritic marker MAP-2 with FITC-labeled antibody (green, left) and ICAM-5 with TRITC-labeled antibody (red). On the right, the expression of the axonal marker tau has been studied using FITC-labeled antibody and ICAM-5 has been stained with TRITC. The yellow staining in the left shows that MAP-2 and ICAM-5 are largely co-expressed, whereas it is evident from the right that ICAM-5 and axons have a different distribution. The results show that laminin promoted the development of an axonal network much better than ICAM-5, whereas ICAM-5 promoted dendritic outgrowth. c, Shows that ICAM-5 D1–2 and D1–9 induced similar amounts of neurite-containing hippocampal neurons (black bars) as the other substrates, except for ICAM-1, which had almost no neurite-promoting effect. Cerebellar neurons (white bars) showed less neurite outgrowth than hippocampal neurons, especially on ICAM-5 coated surfaces. In all cases, 100 neurons were examined. SDs are shown.

Carl_G_190x270_mm_blokki_FINAL.indd 335 06-Aug-23 1:54:08 PM

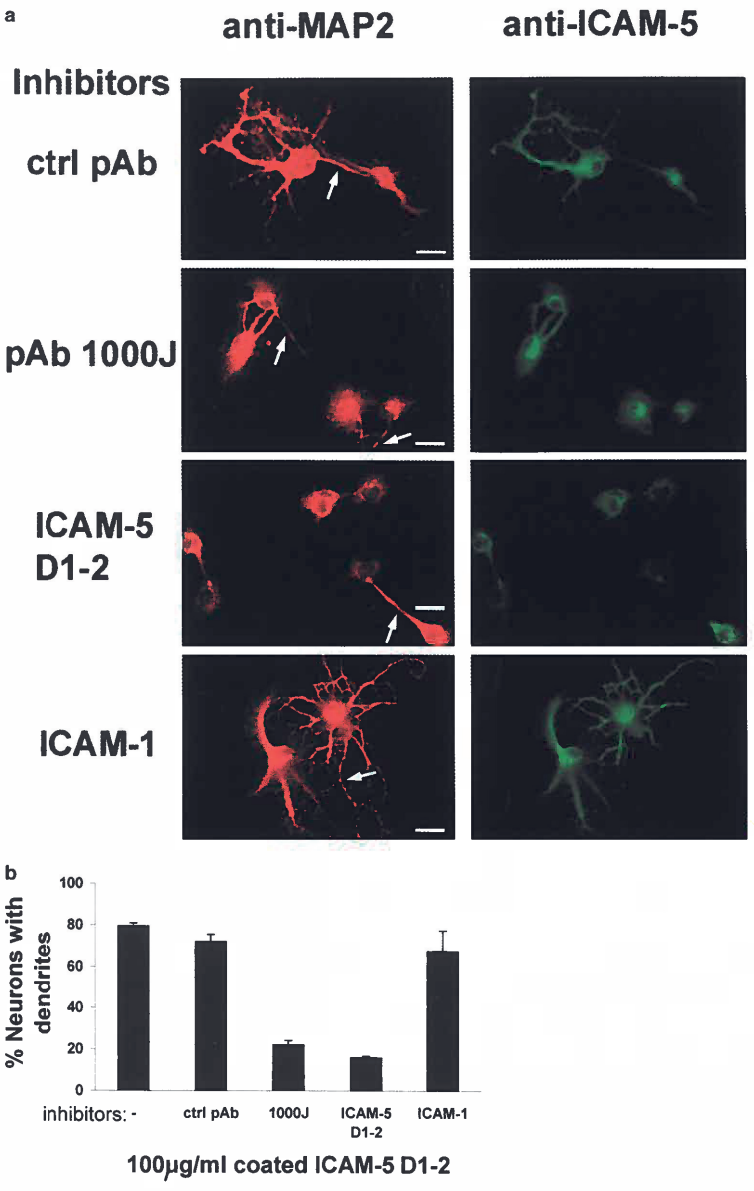

Figure 8. Inhibition of dendritic outgrowth from hippocampal neurons by anti–ICAM-5 antiserum or soluble ICAM-5 D1–2 or ICAM-1. a, Rat E19 hippocampal neurons were cultured on ICAM-5 D1–2 coated surfaces for 48 h. The neurons were stained by anti–MAP-2 (red) and anti–ICAM-5 (green). The polyclonal antibody against rat ICAM-5, 1000J (100 μg/ml), significantly inhibited dendrite outgrowth, compared with the control polyclonal serum (ctrl pAb). A similar inhibitory effect was seen with soluble ICAM-5 D1–2 (100 μg/ml), but not with ICAM-1. Arrows indicate neurites that may be axons stained by anti–MAP-2, but not by anti–ICAM-5. Bars, 20 μm. In b, the number of dendrite-bearing hippocampal neurons subjected to different treatments was counted. 100 neurons in each case were examined.

ICAM-5. When coated on laminin, a number of tau$^+$ neurites were seen. The stainings indicate that ICAM-5 promotes the expression of dendritic proteins, such as MAP-2, much better than laminin, whereas laminin promotes the expression of axonal proteins such as tau.

Although the function of ICAM-5 as a brain-specific leukocyte-binding protein is well established (Mizuno et al., 1997; Tian et al., 1997), its strong and specific expression in the telencephalon, especially in the cerebrum and hippocampus, indicated that it may possess other functions. Here, we describe that ICAM-5 induces dendritic extension and branching through homophilic adhesion, the effect of which is dramatically different from that of laminin (Höpker et al., 1999) or HG-GAM (Rauvala and

Carl_G_190x270_mm_blokki_FINAL.indd 336 06-Aug-23 1:54:08 PM

Peng, 1997), which are known to mainly promote axonal outgrowth, and that this activity can be blocked by mAbs against ICAM-5.

The first indication of homophilic binding was obtained when we observed that ICAM-5 transfected in Paju cells was enriched at the cell–cell contact sites. However, when we made the entire external part of ICAM-5 by recombinant methods, it did not show homophilic binding. This issue was then studied by making truncated shorter constructs of the molecule. We then found that the binding activity was mediated by homophilic binding of the NH_2-terminal domain 1 to domains 4–5. Constructs containing domains 1–2 were more efficient in binding than the single first domain. The finding that mAbs reacting with domain 2 did not inhibit binding further indicates that domain 2 is not directly involved in binding. In fact, some antibodies to D2 enhanced binding, which could be due to conformational changes in D1. The reason for the inability of the isolated D1–9 construct to mediate binding could be its strong tendency to form higher aggregates, possibly tetramers in vitro.

When we performed an analysis of the calculated pI values of the ICAM-5 extracellular domains, we found that in all species of cloned ICAM-5, the pI values of domains 1–2 were ~11.3, whereas those of domains 4–5 were ~4.3, suggesting that the homophilic interaction of D1 with D4–5 could be at least partially mediated by electrostatic interactions between the respective domains. This characteristic of highly oppositely charged domains in ICAM-5 is unique among the ICAMs. This may be the reason that ICAM-1 did not show any homophilic binding. Nor did ICAM-1 bind ICAM-5, which shows that the binding is highly specific.

Earlier studies on neural adhesion molecules have shown that the homophilic binding of the neuronal cell adhesion molecule (NCAM) involves all of the five Ig domains (Ranheim et al., 1996), whereas in the case of L1 and cadherin, only Ig domain 2 in L1 (Zhao and Siu, 1995) and domain 1 in cadherin (Tamura et al., 1998) are involved. The complex phenomena of homophilic binding of different cell adhesion molecules must underlie their different functions, not only in adhesion, but also in possible signaling events (Brümmendorf and Rathjen, 1996).

Multimerization of cell surface molecules is commonly believed to enhance the binding to their ligands/receptors through an increase in avidity. Such examples are the homodimerization of cadherin (Tamura et al., 1998) and ICAM-1 (Miller et al., 1998), and the heterodimerization of NgCAM and axonin-1 (Kunz et al., 1998). The behavior of ICAM-5 is different from that of the other studied Ig domain-containing adhesion proteins.

We think that the inability of the ICAM-5 high molecular weight form to adhere is due to the fact that the homophilic binding of ICAM-5 requires a deeper accessibility of two opposite polypeptides. Furthermore, the studies with the truncated ICAM-5 molecules show that intramolecular associations may exist. The short constructs, like D1–2, can bind because they have their binding domains accessible, whereas longer constructs, like D1–5, are inactive because of interpolypeptide association between D1 and D4–5.

High local concentrations of ICAM-5 may promote high molecular weight complex formation as seen in Paju cells where the uropods are especially rich in the protein. The nonmonomer state must not, however, be permanent in vivo because when Paju-ICAM-5 cells were incubated with truncated ICAM-5 fusion proteins containing the two NH_2-terminal domains, the ICAM-5 molecules cells were brought into monomers. How this phenomenon is regulated in vivo remains unknown. When Paju-ICAM-5 cells were treated with cytochalasin D, ICAM-5 completely switched into monomers. These facts indicate a linkage of ICAM-5 with cytoskeletal proteins, as with other ICAM molecules (Carpén et al., 1992; Heiska et al., 1996). ICAM-5 was previously observed to concentrate in dendritic growth cones and filopodia in hippocampal neurons (Benson et al., 1998). Experiments with cytochalasins to disrupt actin filaments within axonal growth cones have shown that the actin cytoskeleton is necessary for correct pathfinding in vivo (Forscher and Smith, 1988; Sheetz et al., 1992; Chien et al., 1993), and for directed neurite outgrowth in vitro (Smith, 1988; Sheetz et al., 1992). The binding of adhesion molecules on the surface of cells may mediate changes in the cytoskeletal scaffold, thereby resulting in stabilized adhesion or forward growth (Lin et al., 1994). The dynamic change of adhesiveness between monomers and nonmonomers of ICAM-5, which may be regulated by the cytoskeleton, offers an interesting possibility of regulation of dendritic outgrowth.

Regulation of ICAM-5 binding by nonmonomer/monomer transition could also be a means of influencing leukocyte integrin–ICAM-5 interaction. We have found that CD11a/CD18 binds to the first Ig domain of ICAM-5 (Tian et al., 2000), and some mAbs that blocked the ICAM-5-integrin interaction also blocked the ICAM-5 homophilic binding, so the binding sites for these two activities are partially overlapping.

It has been known that dendritogenesis and synaptogenesis take place during the early postnatal period (Goodman and Shatz, 1993; Craig and Banker, 1994). Therefore, we studied ICAM-5 during this time in rats where brain development has been extensively studied (Craig and Banker, 1994). Interestingly, during the first postnatal week, ICAM-5 mainly existed as monomers, whereas at postnatal days 7–10, it gradually changed into nonmonomers. Whether the nonmonomer form is a tetramer or a complex of ICAM-5 with other proteins is not known. This transition coincides with dendritogenesis in the early postnatal period of the rodent central nervous system. Obviously, it is important that when neurons extend branches of dendrites they also need signals for distinguishing axonal growth cones from dendritic ones so that the correct synapses are formed. At an early stage of dendritogenesis, ICAM-5 monomers could promote dendritic elongation and arborization through homophilic interaction. When neurons become developmentally more mature, ICAM-5 mainly exists as nonmonomers, whereby it does not promote dendrite–dendrite/soma interactions. It is possible that promotion of dendrite–dendrite adhesion by monomeric ICAM-5 does not promote branching, and conversely, that the nonmonomeric form could induce more branching.

We are grateful to Dr. Urmas Arumäe for help with hippocampal neu-

Carl_G_190x270_mm_blokki_FINAL.indd 337 06-Aug-23 1:54:08 PM

ronal cultures. We thank Outi Nikkilä and Leena Kuoppasalmi for technical assistance and Yvonne Heinilä for secretarial help.

This study was supported by the Academy of Finland, the Sigrid Jusélius Foundation, and the Finnish Cancer Society.

Submitted: 29 November 1999
Revised: 23 May 2000
Accepted: 25 May 2000

References

Benson, D.L., Y. Yoshihara, and K. Mori. 1998. Polarized distribution and cell type-specific localization of telencephalin, an intercellular adhesion molecule. *J. Neurosci. Res.* 52:43–53.

Brümmendorf, T., and F.G. Rathjen. 1996. Structure/function relationships of axon-associated adhesion receptors of the immunoglobulin superfamily. *Curr. Opin. Neurobiol.* 6:584–593.

Carpén, O., P. Pallai, D.E. Staunton, and T.A. Springer. 1992. Association of intercellular adhesion molecule-1 (ICAM-1) with actin-containing cytoskeleton and α-actinin. *J. Cell Biol.* 118:1223–1234.

Chien, C.B., D.E. Rosenthal, W.A. Harris, and C.E. Holt. 1993. Navigational errors made by growth cones without filopodia in the embryonic *Xenopus* brain. *Neuron.* 11:237–251.

Cook, G., D. Tannahill, and R. Keynes. 1998. Axon guidance to and from choice points. *Curr. Opin. Neurobiol.* 8:64–72.

Craig, A.M., and G. Banker. 1994. Neuronal polarity. *Annu. Rev. Neurosci.* 17: 267–310.

Forscher, P., and S.J. Smith. 1988. Actions of cytochalasins on the organization of actin filaments and microtubules in a neuronal growth cone. *J. Cell Biol.* 107:1505–1516.

Gahmberg, C.G. 1997. Leukocyte adhesion: CD11/CD18 integrins and intercellular adhesion molecules. *Curr. Opin. Cell Biol.* 9:643–650.

Goodman, C.S., and C.J. Shatz. 1993. Developmental mechanisms that generate precise patterns of neuronal connectivity. *Cell.* 72:77–98.

Hayflick, J.S., P. Kilgannon, and W.M. Gallatin. 1998. The intercellular adhesion molecule (ICAM) family of proteins. New members and novel functions. *Immunol. Res.* 17:313–327.

Heiska, L., C. Kantor, T. Parr, D.R. Critchley, P. Vilja, C.G. Gahmberg, and O. Carpén. 1996. Binding of the cytoplasmic domain of intercellular adhesion molecule-2 (ICAM-2) to α-actinin. *J. Biol. Chem.* 271:26214–26219.

Höpker, V.H., D. Shewan, M. Tessier-Lavigne, M.M. Poo, and C. Holt. 1999. Growth-cone attraction to netrin-1 is converted to repulsion by laminin-1. *Nature.* 401:69–73.

Hynes, R.O. 1992. Integrins: versatility, modulation, and signaling in cell adhesion. *Cell.* 69:11–25.

Hynes, R.O., and A.D. Lander. 1992. Contact and adhesive specificities in the associations, migrations, and targeting of cells and axons. *Cell.* 68:303–322.

Jessell, T.M. 1988. Adhesion molecules and the hierarchy of neural development. *Neuron.* 1:3–13.

Kunz, S., M. Spirig, C. Ginsburg, A. Buchstaller, P. Berger, R. Lanz, C. Rader, L. Vogt, B. Kunz, and P. Sondereger. 1998. Neurite fasciculation mediated by complexes of axonin-1 and Ng cell adhesion molecule. *J. Cell Biol.* 143: 1673–1690.

Lin, C.H., P. Lamoureux, R.E. Buxbaum, and P. Forscher. 1994. Cytoskeletal reorganization underlying growth cone motility. *Curr. Opin. Neurobiol.* 4:640–647.

Miller, J., R. Knorr, M. Ferrone, R. Houdei, C.P. Carron, and M.L. Dustin. 1998. Intercellular adhesion molecule-1 dimerization and its consequences for adhesion mediated by lymphocyte function associated-1. *J. Exp. Med.* 182:1231–1241.

Mizuno, T., Y. Yoshihara, J. Inazawa, H. Kagamiyama, and K. Mori. 1997. cDNA cloning and chromosomal localization of the human telencephalin and its distinctive interaction with lymphocyte function-associated antigen-1. *J. Biol. Chem.* 272:1156–1163.

Oka, S., K. Mori, and Y. Watanabe. 1990. Mammalian telencephalic neurons express a segment-specific membrane glyprotein, telencephalin. *Neurosci.* 35:93–103.

Ranheim, T.S., G.M. Edelman, and B.A. Cunningham. 1996. Homophilic adhesion mediated by the neural cell adhesion molecule involves multiple immunoglobulin domains. *Proc. Natl. Acad. Sci.* 93:4071–4075.

Rauvala, H., and H.B. Peng. 1997. HB-GAM (heparin-binding growth-associated molecule) and heparin type glycans in the development and plasticity of neuron-target contacts. *Progress Neurobiol.* 52:127–144.

Sakurai, E., T. Hashikawa, Y. Yoshihara, S. Kaneko, M. Satoh, and K. Mori. 1998. Involvement of dendritic adhesion molecule telencephalin in hippocampal long-term potentiation. *Neuroreport.* 9:881–886.

Sheetz, M.P., D.B. Wayne, and A.L. Pearlman. 1992. Extension of filopodia by motor-dependent actin assembly. *Cell. Motil. Cytoskel.* 22:160–169.

Smith, S.J. 1988. Neuronal cytomechanics: the actin-based motility of growth cones. *Science.* 242:708–715.

Sonderegger, P., and F.G. Rathjen. 1992. Regulation of axonal growth in the vertebrate nervous system by interactions between glycoproteins belonging to two subgroups of the immunoglobulin superfamily. *J. Cell Biol.* 119:1387–1394.

Springer, T.A. 1994. Traffic signals for lymphocyte recirculation and leukocyte emigration: the multistep paradigm. *Cell.* 76:301–314.

Takeichi, M. 1991. Cadherin cell adhesion receptors as a morphogenetic regulator. *Science.* 251:1451–1455.

Tamada, A., Y. Yoshihara, and K. Mori. 1998. Dendrite-associated cell adhesion molecule, telencephalin, promotes neurite outgrowth in mouse embryo. *Neurosci. Lett.* 240:163–166.

Tamura, K., W.S. Shan, W.A. Hendrickson, D.R. Colman, and L. Shapiro. 1998. Structure–function analysis of cell adhesion by neural (N^-) cadherin. *Neuron.* 20:1153–1163.

Tessier-Lavigne, M., and C.S. Goodman. 1996. The molecular biology of axon guidance. *Science.* 274:1123–1133.

Tian, L., Y. Yoshihara, T. Mizuno, K. Mori, and C.G. Gahmberg. 1997. The neuronal glycoprotein telencephalin is a cellular ligand for the CD11a/CD18 leukocyte integrin. *J. Immunol.* 158:928–936.

Tian, L., P. Kilgannon, Y. Yoshihara, K. Mori, W.M. Gallatin, O. Carpén, and C.G. Gahmberg. 2000. Binding of T lymphocytes to hippocampal neurons through ICAM-5 (telencephalin) and characterization of its interaction with the leukocyte integrin CD11a/CD18. *Eur. J. Immunol.* 30:810–818.

Walsh, F.S., and P. Doherty. 1997. Neural cell adhesion molecules of the immunoglobulin superfamily: role in axon growth and guidance. *Annu. Rev. Cell Dev. Biol.* 13:425–456.

Yoshihara, Y., and K. Mori. 1994. Telencephalin: a neuronal area code molecule? *Neurosci. Res.* 21:119–124.

Yoshihara, Y., S. Oka, Y. Nemoto, Y. Watanabe, S. Nagata, H. Kagamiyama, and K. Mori. 1994. An ICAM-related neuronal glycoprotein, telencephalin, with brain segment-specific expression. *Neuron.* 12:541–553.

Zhang, K.Z., J.A. Westberg, E. Hölttä, and L.C. Andersson. 1996. BCL2 regulates neural differentiation. *Proc. Natl. Acad. Sci.* 93:4504–4508.

Zhao, X., and C.H. Siu. 1995. Colocalization of the homophilic binding site and the neuritogenic activity of the cell adhesion molecule L1 to its second Ig-like domain. *J. Biol. Chem.* 270:29413–29421.

Carl_G_190x270_mm_blokki_FINAL.indd 338 06-Aug-23 1:54:08 PM

JCB: ARTICLE

THE JOURNAL OF CELL BIOLOGY

Activation of NMDA receptors promotes dendritic spine development through MMP-mediated ICAM-5 cleavage

Li Tian,[1] Michael Stefanidakis,[1] Lin Ning,[1] Philippe Van Lint,[3] Henrietta Nyman-Huttunen,[1] Claude Libert,[3] Shigeyoshi Itohara,[4] Masayoshi Mishina,[5] Heikki Rauvala,[2] and Carl G. Gahmberg[1]

[1]Division of Biochemistry, Department of Biological and Environmental Sciences, Faculty of Biosciences, and [2]Neuroscience Center, University of Helsinki, FIN-00014 Helsinki, Finland
[3]Department for Molecular Biomedical Research, Flanders Interuniversity Institute for Biotechnology and Ghent University, B-9052 Ghent (Zwijnaarde), Belgium
[4]Laboratory of Behavioral Genetics, Institute of Physical and Chemical Research, Brain Science Institute, Wako, 351-0198, Japan
[5]Department of Molecular Neurobiology and Pharmacology, Graduate School of Medicine, University of Tokyo, Bunkyo-ku, Tokyo, 113-0033, Japan

Matrix metalloproteinase (MMP)-2 and -9 are pivotal in remodeling many tissues. However, their functions and candidate substrates for brain development are poorly characterized. Intercellular adhesion molecule-5 (ICAM-5; Telencephalin) is a neuronal adhesion molecule that regulates dendritic elongation and spine maturation. We find that ICAM-5 is cleaved from hippocampal neurons when the cells are treated with *N*-methyl-D-aspartic acid (NMDA) or α-amino-3-hydroxy-5-methylisoxazole-propionic acid (AMPA). The cleavage is blocked by MMP-2 and -9 inhibitors and small interfering RNAs. Newborn MMP-2– and MMP-9–deficient mice brains contain more full-length ICAM-5 than wild-type mice. NMDA receptor activation disrupts the actin cytoskeletal association of ICAM-5, which promotes its cleavage. ICAM-5 is mainly located in dendritic filopodia and immature thin spines. MMP inhibitors block the NMDA-induced cleavage of ICAM-5 more efficiently in dendritic shafts than in thin spines. ICAM-5 deficiency causes retraction of thin spine heads in response to NMDA stimulation. Soluble ICAM-5 promotes elongation of dendritic filopodia from wild-type neurons, but not from ICAM-5–deficient neurons. Thus, MMPs are important for ICAM-5–mediated dendritic spine development.

Introduction

Dendritic spines are small, actin-rich protrusions scattered along dendrites, and they carry the postsynaptic components of >90% of excitatory synapses. Despite of being tiny in size, spines are highly dynamic structures that continuously undergo changes in shape and size over time (Hering and Sheng, 2001; Yuste and Bonhoeffer, 2004). A multitude of molecules has been implicated in dendritic spine development and remodeling. Among these, the neurotransmitter receptors, especially *N*-methyl-D-aspartic acid (NMDA) receptor (NR) and α-amino-3-hydroxy-5-methylisoxazole-propionic acid (AMPA) receptor (GluR), which are well-known inducers of spine formation, regulate spine maturation and stabilization via calcium-dependent regulation of filamentous actin turnover (Matus, 2000; Oertner and Matus, 2005). Besides, other cell surface molecules also influence spine properties in response to external signals by mediating cell adhesion and regulating the networks of interconnected signaling pathways, which converge to regulate actin dynamics in spines (Ethell and Pasquale, 2005; Tada and Sheng, 2006).

Cell adhesion molecules (CAMs) and ECM molecules are instrumental in providing physical connections and generating cellular signaling events. Importantly, several recent studies have suggested the involvement of CAMs and ECMs in dendritic spine remodeling (Ethell and Pasquale, 2005) and synaptic plasticity (Washbourne et al., 2004; Gerrow and El-Husseini, 2006). These include N-cadherin (Togashi et al., 2002), syndecan-2

M. Stefanidakis and L. Ning contributed equally to this paper.

Correspondence to Li Tian: li.tian@helsinki.fi

M. Stefanidakis's present address is Department of Pathology, Harvard Medical School, Brigham and Women's Hospital, Center for Excellence in Vascular Biology, Boston, MA 02115.

Abbreviations used in this paper: AMPA, α-amino-3-hydroxy-5-methylisoxazole-propionic acid; CAM, cell adhesion molecule; CTF, C-terminal fragment; DIV, day in vitro; DNQX, 6,7,-dinitroquinoxaline-2,3 (1H,4H)-dione; ICAM, intercellular adhesion molecule; LTP, long-term potentiation; MALDI-TOF, matrix-assisted laser desorption/ionization–time of flight; MAP, microtubule-associated protein; MMP, matrix metalloproteinase; NMDA, *N*-methyl-D-aspartic acid; NR, NMDA receptor; NTF, N-terminal fragment; PSD, postsynaptic density; sICAM-5, soluble ICAM-5; WT, wild type.

The online version of this article contains supplemental material.

© The Rockefeller University Press $15.00
The Journal of Cell Biology, Vol. 178, No. 4, August 13, 2007 687–700
http://www.jcb.org/cgi/doi/10.1083/jcb.200612097

Carl_G_190x270_mm_blokki_FINAL.indd 339 06-Aug-23 1:54:09 PM

(Ethell et al., 2001), neural CAM (Dityatev et al., 2004), integrins (Shi and Ethell, 2006), laminins (Oray et al., 2004), and reelin (Liu et al., 2001).

Intercellular adhesion molecule-5 (ICAM-5; Telencephalin) belongs to the Ig superfamily (Yoshihara et al., 1994; Gahmberg et al., 1998). It is specifically expressed in the postnatal excitatory neuronal cell bodies, dendritic shafts, and dendritic filopodia of the telencephalon (Benson et al., 1998; Mitsui et al., 2005). The expression of ICAM-5 temporally parallels dendritogenesis and synaptogenesis (Yoshihara et al., 1994). In agreement, ICAM-5 has been shown to promote dendritic elongation and branching of hippocampal neurons in vitro (Tian et al., 2000). ICAM-5–deficient mice exhibited decreased density of dendritic filopodia, accelerated maturation of dendritic spines (Matsuno et al., 2006), and changes in long-term potentiation (LTP) in the hippocampus (Nakamura et al., 2001).

Soluble ICAM-5 (sICAM-5) has been detected in physiological fluids under several pathological conditions (Guo et al., 2000; Lindsberg et al., 2002; Borusiak et al., 2005). However, the nature of candidate proteinases and the physiological meaning of the proteolytic cleavage of membrane-bound ICAM-5 have remained unknown.

Matrix metalloproteinases (MMPs) form a large family of mostly secreted, zinc-dependent endopeptidases, which are important for the regulation of cellular behavior through proteolytic cleavage of ECMs and cell surface proteins (Malemud, 2006). Although a large body of data has connected MMPs to brain injury and pathology, accumulating evidence has extended their roles into the normal physiological functions of the brain (Dzwonek et al., 2004; Luo, 2005; Ethell and Ethell, 2007).

Among MMPs, MMP-2 and -9 are most abundantly expressed in the developing brain. MMP-2 is found mainly in astrocytes, whereas MMP-9 is highly expressed in neuronal cell bodies and dendrites (Szklarczyk et al., 2002; Ayoub et al., 2005). The expression and activity of MMP-9 have been shown to depend on NR activation and LTP (Meighan et al., 2006; Nagy et al., 2006). Growing data also suggest the association of MMP-9 (Meighan et al., 2006; Nagy et al., 2006) and other ECM-degrading enzymes (Oray et al., 2004; Bilousova et al., 2006; Monea et al., 2006) with dendritic spine remodeling, synaptic plasticity, learning, and memory formation. Although several ECMs and cell surface proteins, which play important roles in the aforementioned functions, have been identified as MMP substrates, the target molecules for MMP-2 or -9 in the brain have remained largely elusive.

In the present study, we examined the possibility of ICAM-5 acting as a substrate for MMP-2 or -9, using a variety of experimental approaches, and investigated the role of MMP-mediated ICAM-5 proteolytic cleavage in the regulation of dendritic spine development.

Results

NMDA and AMPA promote cleavage of ICAM-5 from hippocampal neurons

Because sICAM-5 has been detected under various pathological conditions, we studied whether ICAM-5 cleavage takes place during physiological neuronal maturation. For this purpose, we examined the release of sICAM-5 from cultured hippocampal neurons at different developmental stages in vitro (3–21 d in vitro [DIV]). The expression of full-length ICAM-5 of 130 kD was low in the 3-DIV hippocampal neurons, but starting from 7 DIV, when dendrites extensively develop in hippocampal neurons, the expression of full-length ICAM-5 dramatically increased and reached a plateau thereafter (Fig. 1, A and B, right). In comparison with this, sICAM-5 of 85–110 kD was most strongly released at 14–21 DIV (Fig. 1, A and B, left), which parallels the period of dendritic spine maturation and synaptic formation. This indicates that the cleavage of membrane-bound ICAM-5 may play an important role during spine maturation.

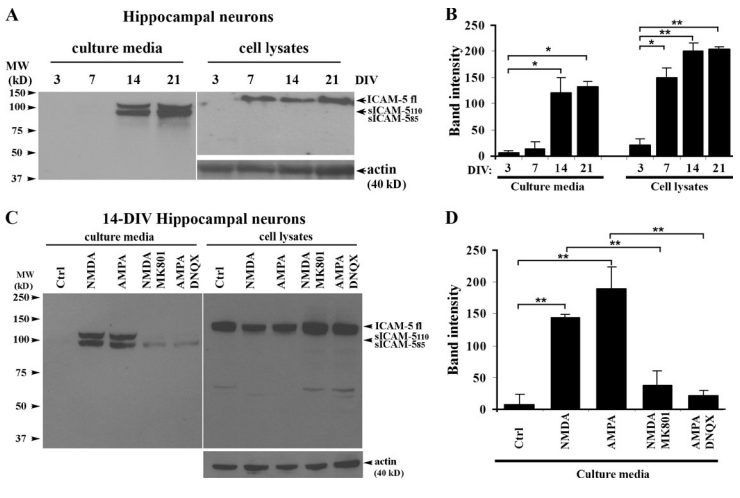

Figure 1. **Cleavage of ICAM-5 from hippocampal neurons is promoted by NMDA and AMPA.** (A) Cell lysates and culture media from rat primary hippocampal neurons of different developmental stages (3–21 DIV) were collected separately, and ICAM-5 was detected by polyclonal antibodies against the ICAM-5 cytoplasmic tail (ICAM-5cp) or ectodomains (1000J), respectively. sICAM-5 of 85- and 110-kD fragments were released into the media and reached a maximum at 14–21 DIV, whereas the expression of full-length ICAM-5 of 130 kD in neurons started to increase from 7 DIV onward. (B) Quantitative analysis of band intensities. (C) In 14-DIV hippocampal neurons, 5 μM NMDA or AMPA treatment caused a significant release of the sICAM-5 fragments with a concomitant reduction of the membrane-bound ICAM-5-fl level, which was inhibited by 20 μM of their respective antagonists, MK801 or DNQX. Half of each medium sample was applied to SDS-PAGE gel for analysis. (D) Quantitative analysis of band intensities of the sICAM-5_{110} from the culture media. Error bars indicate mean ± SD. *, $P < 0.05$; **, $P < 0.01$.

The NRs and GluRs are key regulators of spine formation and maturation. Therefore, we tested the effects of NMDA and AMPA on ICAM-5 cleavage from hippocampal neurons. In 14-DIV hippocampal neurons, 5 μM NMDA or AMPA treatment caused significant release of the sICAM-5 fragments of 110 and 80–85 kD, with concomitant reduction of the membrane-bound ICAM-5 (Fig. 1, C and D). Moreover, the cleavage of ICAM-5 was inhibited by the NMDA antagonist MK801 and the non-NMDA antagonist DNQX (6,7,-dinitroquinoxaline-2,3[1H,4H]-dione; Fig. 1, C and D).

MMP-2 and -9 cleave the membrane-bound ICAM-5

To further investigate the mechanism of ICAM-5 proteolytic cleavage, we used various chemical or peptide inhibitors of MMPs. As shown in Fig. 2, ICAM-5 cleavage was almost completely inhibited by the broad-spectrum MMP inhibitor GM6001, but not by its negative control. A variety of MMP-2 and -9 inhibitors also partially or completely blocked the cleavage (Fig. 2, A and B). These data provide the first evidence that MMP-2 and -9, especially when activated by

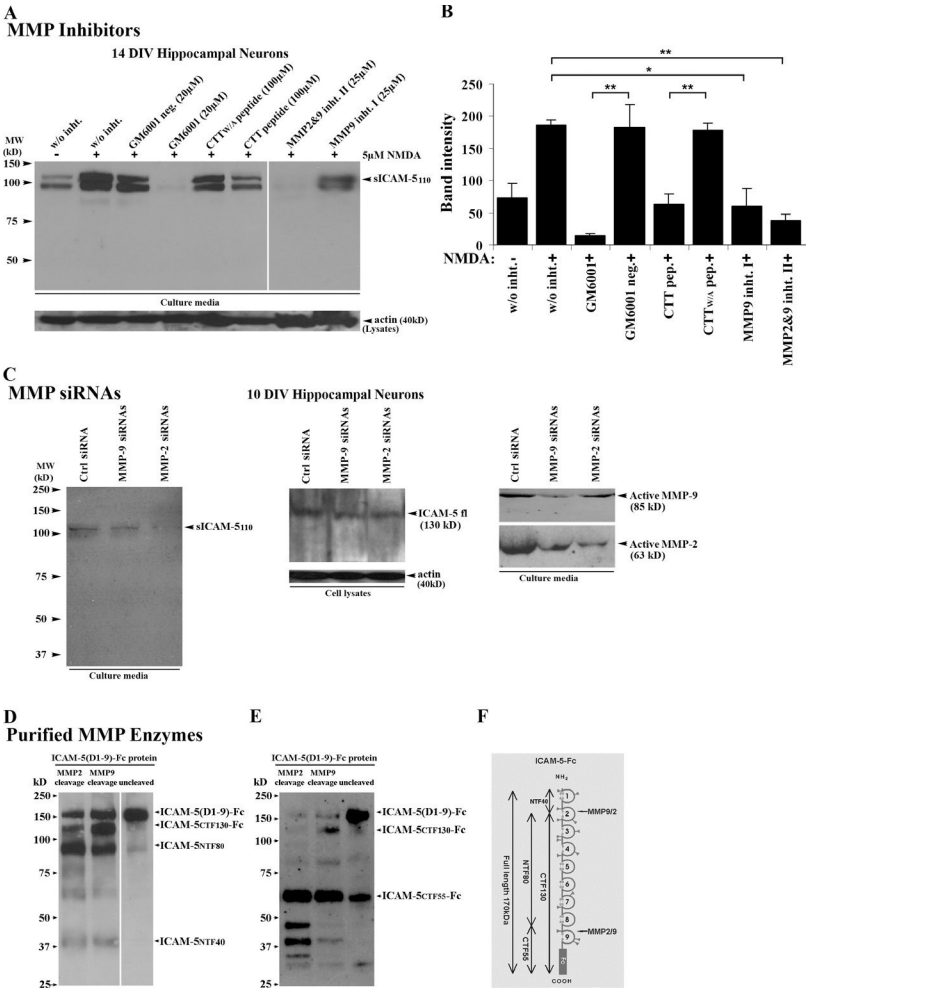

Figure 2. **Cleavage of ICAM-5 is mediated by MMP-2 and -9.** (A) 14-DIV neurons were left untreated or treated with NMDA in the presence of MMP inhibitors. The NMDA-induced cleavage of ICAM-5 was blocked by MMP-2 and -9 inhibitors, as compared with the negative controls. Actin in cell lysates was used to quantitate the amount of cells from which the culture media were collected. (B) Quantitative analysis of A. Error bars indicate mean ± SD. *, $P < 0.05$; **, $P < 0.01$. (C) The siRNAs for rat MMP-2 and -9 transfected into the 9-DIV neurons efficiently blocked the ICAM-5 cleavage. Incubation of recombinant mouse ICAM-5 D1-9-Fc protein with active MMP-2 or -9 enzyme resulted in cleavage of the recombinant protein into multiple fragments, as detected by anti–ICAM-5 (D) or anti-Fc antibody (E). Interestingly, the two MMPs seemed to prefer different cleavage sites, although both cleave ICAM-5 in a similar way, as depicted in F. The indicated cleaved fragments (CTF130, NTF80, and NTF40) were analyzed by mass spectrometry peptide mapping.

Carl_G_190x270_mm_blokki_FINAL.indd 341 06-Aug-23 1:54:10 PM

NMDA, are mainly responsible for the proteolytic cleavage of ICAM-5.

Because the expression and activity of MMP-9 have been shown to be up-regulated in response to stimuli that induce NR activation and LTP (Meighan et al., 2006; Nagy et al., 2006), we tested the conditioned culture media from treated hippocampal neurons and found increased levels of both active MMP-2 and -9 upon NMDA stimulation (Fig. S1, available at http://www.jcb.org/cgi/content/full/jcb.200612097/DC1). We then used the RNA interference technique to temporarily decrease the expression of MMP-2 or -9 in hippocampal neurons (Fig. 2 C). After transfection into neurons, the MMP-2 and -9 siRNAs substantially decreased the protein levels of MMP-2 and -9, respectively (Fig. 2 C, right), with the concomitant inhibition of ICAM-5 cleavage from the transfected neurons (Fig. 2 C, left).

We further incubated the recombinant mouse ICAM-5 D1-9-Fc protein with activated MMP-2 or -9 and studied the cleavage using anti–ICAM-5 polyclonal antibody 1000J (Fig. 2 D) or anti-Fc polyclonal antibody (Fig. 2 E) in Western blots. The cleaved proteins were then analyzed by matrix-assisted laser desorption/ionization–time of flight (MALDI-TOF) peptide mass mapping to identify the individual fragments (C-terminal fragment [CTF] 130-Fc, N-terminal fragment [NTF] 80–85, and NTF40; Fig. S2, available at http://www.jcb.org/cgi/content/full/jcb.200612097/DC1). We found that both MMP-2 and -9 cut at similar sites in the second and ninth ectodomains of ICAM-5, as depicted in Fig. 2 F. Interestingly, they seemed to show selectivity for the cleavage sites, as shown by the intensities of the fragments they produced. The minor bands detected within 30–75 kD in Fig. 2 (D and E) may be caused by protein degradation.

Dissociation of ICAM-5 from the cytoskeleton promotes its cleavage

Because the NRs and GluRs are known to regulate actin dynamics, we examined whether the NR-promoted cleavage of ICAM-5 is dependent on its anchorage to actin filaments. Interestingly, we found that cytochalasin D and latrunculin A, which prevent actin polymerization by capping the barbed end of actin filaments and monomeric actin, respectively, significantly increased the cleavage of ICAM-5 (Fig. 3, A and B). This indicates that the association between ICAM-5 and actin filaments may affect the MMP-mediated proteolytic cleavage. Furthermore, we found that treatment of hippocampal neurons with 20 μM NMDA for 1 h resulted in a considerable release of ICAM-5 from the cytoskeletal fraction into the soluble fraction of neuronal lysates (Fig. 3, C and D). These findings strongly support the hypothesis that dissociation of ICAM-5 from the actin cytoskeleton promotes its cleavage.

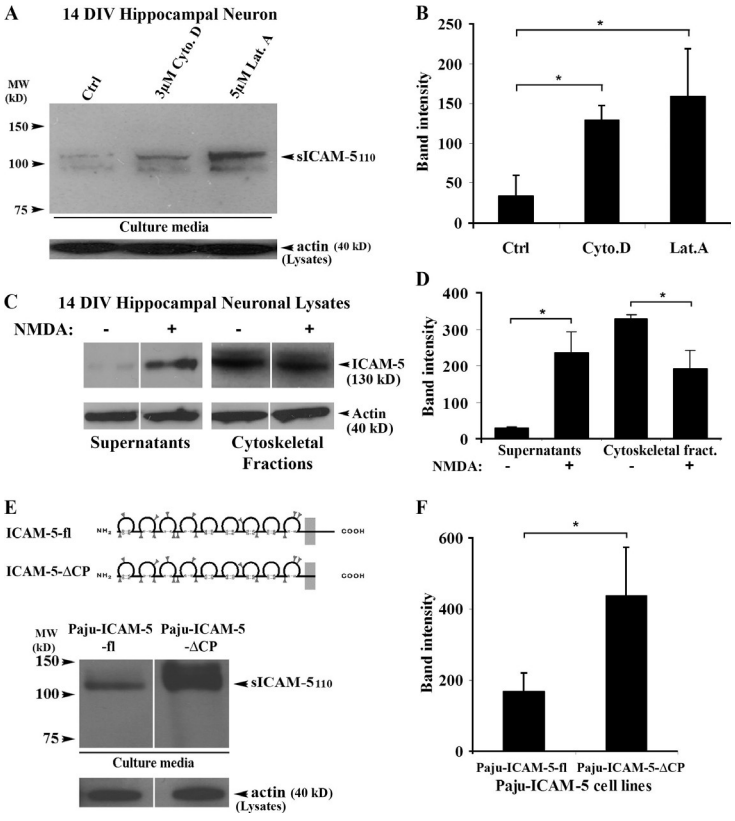

Figure 3. **Dissociation of ICAM-5 from the actin cytoskeleton promotes its cleavage.** 14-DIV neurons were left untreated or treated with cytochalasin D or latrunculin A. The results from Western blotting (A) and quantitative analysis of the band intensities (B) showed that both cytochalasin D and latrunculin A strongly increased the cleavage of ICAM-5. Furthermore, 14-DIV neurons were treated with 20 μM NMDA for 60 min before being lysed, and the lysates were then separated by ultracentrifugation into soluble fractions, which contain dissolved membrane proteins and soluble cytosolic proteins, and cytoskeletal fractions, which contain the majority of actin filaments. Detection of ICAM-5 and actin showed dissociation of ICAM-5 from the actin cytoskeleton after NMDA treatment (C). (D) ICAM-5 levels in the soluble and cytoskeletal fractions were quantified. Moreover, the transfected neural crest cell lines, Paju-ICAM-5-fl and Paju-ICAM-5-ΔCP, which expressed full-length or cytoplasmic tail-truncated ICAM-5, respectively, were analyzed (E and F). Schematic drawings of the two ICAM-5 constructs are shown. Paju-ICAM-5-ΔCP cells released a considerably larger amount of the sICAM-5 than Paju-ICAM-5-fl cells (E and F). Quantitation of actin was done as described in Fig. 2 A. Error bars indicate mean ± SD. *, $P < 0.05$.

To further study this phenomenon, we compared Paju-ICAM-5-fl and Paju-ICAM-5-ΔCP cell lines, which express the full-length ICAM-5 or the truncated ICAM-5 without the cytoplasmic domain (Fig. 3 E), respectively. We have shown that truncation of the cytoplasmic tail of ICAM-5 results in a more diffuse distribution of the molecule on the plasma membrane and reduced colocalization with the subcortical actin filaments (Nyman-Huttunen et al., 2006). The cell surface expression level of ICAM-5 on both cell lines was comparable (Fig. S3, available at http://www.jcb.org/cgi/content/full/jcb.200612097/DC1). Compared with Paju-ICAM-5-fl, Paju-ICAM-5-ΔCP cells showed a considerable increase of ICAM-5 cleavage (Fig. 3, E and F).

Abnormal ICAM-5 expression during early postnatal development of MMP-2– and MMP-9–deficient mice

To further clarify the involvement of MMP-2 and -9 on ICAM-5 cleavage, we studied the expression of ICAM-5 in MMP-deficient mice at different postnatal developmental stages (from postnatal 1 d to 10 wk). ICAM-5 expression was increased in all MMP-deficient mice after birth, whereas L1CAM showed a decreased expression (Fig. 4, A and C). Moreover, it is noteworthy that, compared with the wild-type (WT) mice, the MMP-$2^{-/-}$ and MMP-$9^{-/-}$ deficient mice contained significantly more full-length ICAM-5 at the early postnatal stage (postnatal day 1). However, the MMP-$2^{-/-}$/MMP-$9^{-/-}$ double-deficient mice expressed lower levels of ICAM-5 (Fig. 4, A and C). The changes in the MMP-$2^{-/-}$, MMP-$9^{-/-}$, and MMP-$2^{-/-}$/MMP-$9^{-/-}$ double-deficient mice tended to disappear after 1 wk postnatally, except in the MMP-$2^{-/-}$/MMP-$9^{-/-}$ double-deficient mice, where ICAM-5 expression still remained slightly but significantly lower than in the WT mice (Fig. 4, A and C). Studies on the enzymatic activities of MMP-2 and -9 by gelatinase zymography verified the identity of the respective deficient mice (Fig. 4 B) and indicated that the activity of MMP-2 in both the MMP-$9^{-/-}$ deficient mice and the WT mice decreased during the postnatal development. However, there seemed to be some compensating up-regulation of the proMMP-9 level in the adult MMP-$2^{-/-}$

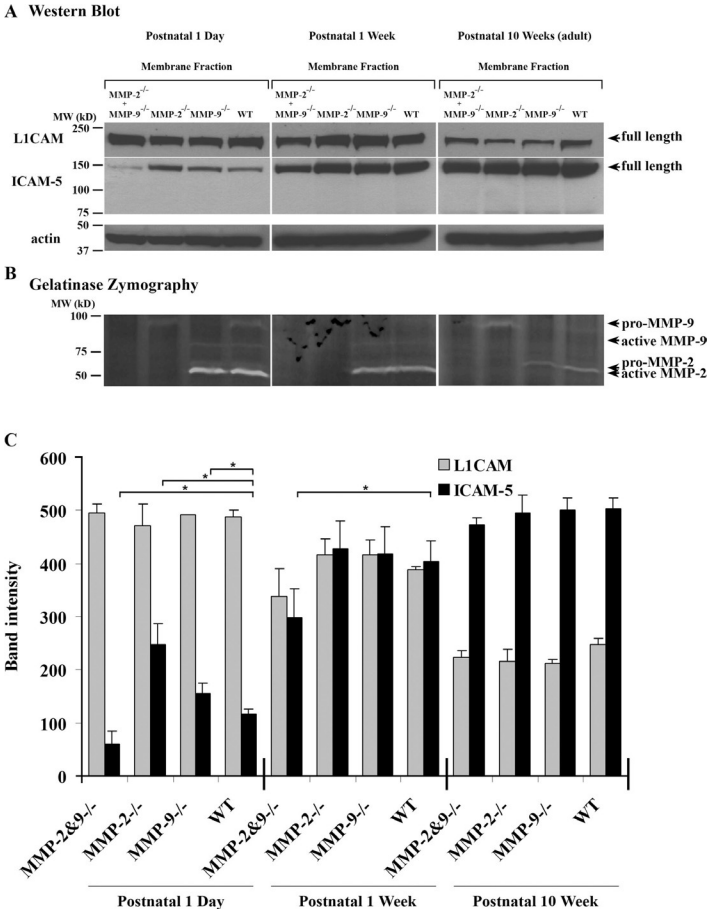

Figure 4. **ICAM-5 expression is abnormal during early postnatal development of MMP-2– and MMP-9–deficient mice.** The forebrains from postnatal (1 d to 10 wk) MMP-deficient and WT mice were homogenized, and the membrane fractions were obtained by ultracentrifugation. The results from Western blotting (A) and quantitative analysis of the band intensities (C) both showed that in postnatal 1-d mice, the expression levels of ICAM-5 were significantly higher in MMP-$2^{-/-}$ and MMP-$9^{-/-}$ mice than in WT mice, whereas in MMP-$2^{-/-}$/MMP-$9^{-/-}$ double-deficient mice, the expression was lower (A and C, left). Error bars indicate mean ± SD. *, $P < 0.05$. After the first postnatal week, ICAM-5 expression was increased in all mice, and the difference was not as obvious as before, although a considerably lower amount was still detected in the double-deficient mice (A and C, middle and right). In comparison, the expression of L1CAM gradually decreased during the postnatal period, and little difference between the deficient and WT mice was observed. *, $P < 0.05$. (B) Gelatinase zymography confirmed the identity of each type of mice and showed that the activity of MMP-2 considerably decreased during the postnatal development of the brain.

Carl_G_190x270_mm_blokki_FINAL.indd 343 06-Aug-23 1:54:10 PM

deficient mice, which was not obvious in the younger mice (Fig. 4 B, right). Similar findings have been reported (Esparza et al., 2004).

Our histological analysis of the brains of MMP-2– and MMP-9–deficient mice showed that both, especially the MMP-2–deficient mice, had abnormal cerebral cortical and hippocampal structures. The cortical layers 2–3 seemed to have increased number of cells (Fig. S4, available at http://www.jcb.org/cgi/content/full/jcb.200612097/DC1). Similar findings have been reported in the cerebellar cortex of MMP-9–deficient mice, which showed an abnormal accumulation of granular precursors in the external granular layer (Vaillant et al., 2003). We believe that the increased level of ICAM-5 in MMP-2–deficient mice is not due to the increased number of neurons in the cortex, because we carefully controlled the protein load per sample and monitored the amount of loaded actin during Western blotting.

ICAM-5 is enriched in filopodia and thin spines but not in mature mushroom spines

Dendritic spines occur in a range of sizes and in a variety of shapes, commonly classified as thin, stubby, and mushroom (Hering and Sheng, 2001; Yuste and Bonhoeffer, 2004). There is a strong correlation between the size of the spine head and the strength of the synapse, presumably related to the higher levels of GluRs in larger spines (Kasai et al., 2003). There is also evidence that the smaller weaker spines preferentially undergo LTP, whereas larger spines are more stable and show less plasticity (Matsuzaki et al., 2004). Such observations have led to the view that thin spines represent "plasticity spines" and large mushrooms "memory" spines (Kasai et al., 2003).

ICAM-5 was earlier found to be mainly expressed in dendritic filopodia, and its expression inversely correlated with synapse maturation (Matsuno et al., 2006). To further clarify whether ICAM-5 is distinctively expressed in spines at different maturation stages, we studied the dendritic protrusions of 10–17-DIV hippocampal neurons. Such neurons contain various dendritic protrusions, including filopodia, small-head thin spines, and large-head mushroom spines. The dendritic fine structures were visualized by transfection of the EGFP into the 12-DIV neurons. The overlapping of immunostained ICAM-5 with EGFP was measured by calculation of the Pearson's colocalization efficiency (Fig. 5). Our result showed that ICAM-5 was more abundantly expressed in filopodia (Fig. 5 A, arrow) and thin spines (Fig. 5 A, arrowheads) but much less in the mushroom spines (Fig. 5 A, asterisks), particularly when the heads of the two different types of spines were compared (Fig. 5 A). These data suggest that ICAM-5 may play a more active role in the "plastic" thin spines than in the more "stable" mushroom spines.

Activation of the NRs decreases the colocalization of ICAM-5 with F-actin

Because we found that activation of the NRs led to dissociation of membrane-bound ICAM-5 from the actin cytoskeleton, it became important to study ICAM-5 and F-actin distributions in neurons upon activation of NRs. We treated the 10-DIV hippocampal neurons with 5 μM NMDA and triple stained the neurons for the ICAM-5 cytoplasmic tail, the F-actin, and the postsynaptic density (PSD) 95 protein (Fig. 6 A). Treatment of hippocampal neurons with NMDA resulted in reduced colocalization of ICAM-5 with F-actin not only along dendritic shafts (Fig. 6, A and B) but also in thin and mushroom spines (Fig. 6 A, arrowheads and asterisks, respectively). The reduced colocalization of ICAM-5 with F-actin was partially counteracted by pretreatment of neurons with the NR antagonist MK801 (Fig. 6, A and B). NMDA treatment led to a significantly increased amount of mushroom spines (Fig. 6 C).

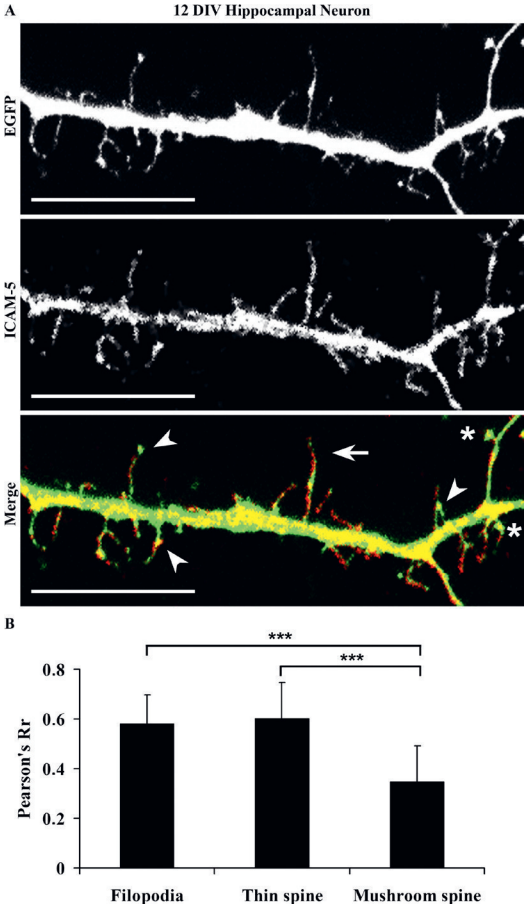

Figure 5. **ICAM-5 is enriched in thin spines rather than in mushroom spines.** (A) 12-DIV hippocampal neurons were transfected with EGFP and immunostained with anti–ICAM-5cp polyclonal antibody. ICAM-5 was strongly expressed in dendritic shafts. In the protrusions along the shaft, ICAM-5 was clearly located in filopodia (arrow) and thin spines (arrowheads), but much less in mushroom spines (asterisks), especially when the heads of the two different types of spines were compared (A). The colocalization of ICAM-5 with EGFP in different protrusions was analyzed and represented by Pearson's coefficiency (Rr). Mushroom spines gave the least colocalization degree, whereas thin spines and filopodia gave higher values (B). Error bars indicate mean ± SD. ***, $P < 0.001$. Bars, 10 μm.

The NR-induced cleavage of ICAM-5 is blocked by MMP inhibitors along dendritic shafts but not in thin spines

Because we found that NMDA and AMPA reduced anchorage of ICAM-5 to the actin cytoskeleton and promoted its cleavage through MMP-2 and -9, these facts could be the reasons for the exclusion of ICAM-5 from maturating spines. Therefore, it was important to study whether the ICAM-5 cleavage from spines, as a result of activation of the NRs, could be blocked by MMP inhibitors. For this purpose, we studied the EGFP-transfected 17-DIV hippocampal neurons that were treated with 5 μM NMDA and various MMP inhibitors (Fig. 7 A). To measure the effects of MMP inhibitors more accurately, ICAM-5 was visualized by immunostaining with a mAb that recognizes its extracellular region. We found that NMDA reduced the localization of ICAM-5 in both the dendritic shafts and thin spines in 17-DIV neurons (Fig. 7 A), similar to what was observed in younger neurons (Fig. 6). Blocking the NRs with MK801 clearly recovered the localization of ICAM-5 in both shafts and thin spines. When various MMP inhibitors, including the general inhibitor GM6001, the MMP-2/9–specific peptide inhibitor CTT, and the inhibitor II, were applied together with NMDA, most ICAM-5 along dendritic shafts was recovered (Fig. 7 A). However, the recovery of ICAM-5 in thin spines, especially in spine heads, was much less efficient by inhibition of MMPs, as compared with the NR antagonist MK801 (Fig. 7, A and B). This may be due to the fact that ICAM-5 was more vulnerable for MMPs in spine heads, which contain highly motile and dynamic actin filaments, as compared with the shafts that contain a more stable actin cytoskeleton. We further found that pretreatment with the MMP-2/9 inhibitor II significantly decreased the number of spines induced by NMDA (Fig. 7 C).

WT and ICAM-5–deficient neurons respond differently to NMDA stimulation

To further study the function of ICAM-5 in thin spines, we compared the response of WT and ICAM-5$^{-/-}$ hippocampal neurons to NMDA stimulation. The EGFP-transfected 17-DIV fixed neurons were first immunostained for ICAM-5 and PSD95. ICAM-5 immunostaining verified the identity of ICAM-5$^{-/-}$ neurons (Fig. 8 A). In addition, the size of mushroom spines in ICAM-5$^{-/-}$ neurons seemed to be larger than those in WT neurons,

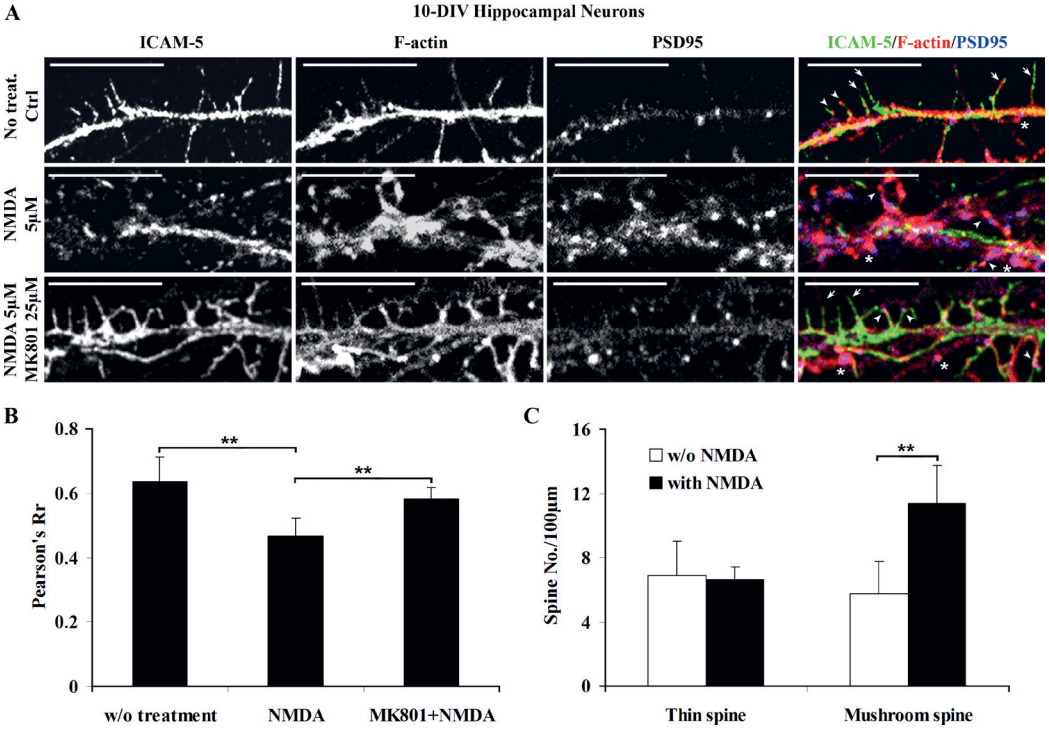

Figure 6. **NMDA decreases the colocalization of ICAM-5 with F-actin in spines.** (A) 10-DIV hippocampal neurons were left untreated or treated for 6 h with 5 μM NMDA, with or without a 1-h pretreatment with the NR antagonist MK801. The neurons were then triple stained for ICAM-5 (green), F-actin (red), and PSD95 (blue). ICAM-5 colocalized with F-actin in dendritic filopodia (arrows) and thin spines (arrowheads), but much less in mushroom spines (asterisks). (B) The degree of colocalization between ICAM-5 and F-actin was analyzed after the above treatments. Note that NMDA significantly decreased the colocalization of ICAM-5 with F-actin, which was partially counteracted by MK801. (C) The effects of NMDA on formation of thin and mushroom spines were quantified. Error bars indicate mean ± SD. **, $P < 0.01$. Bars, 10 μm.

Carl_G_190x270_mm_blokki_FINAL.indd 345 06-Aug-23 1:54:12 PM

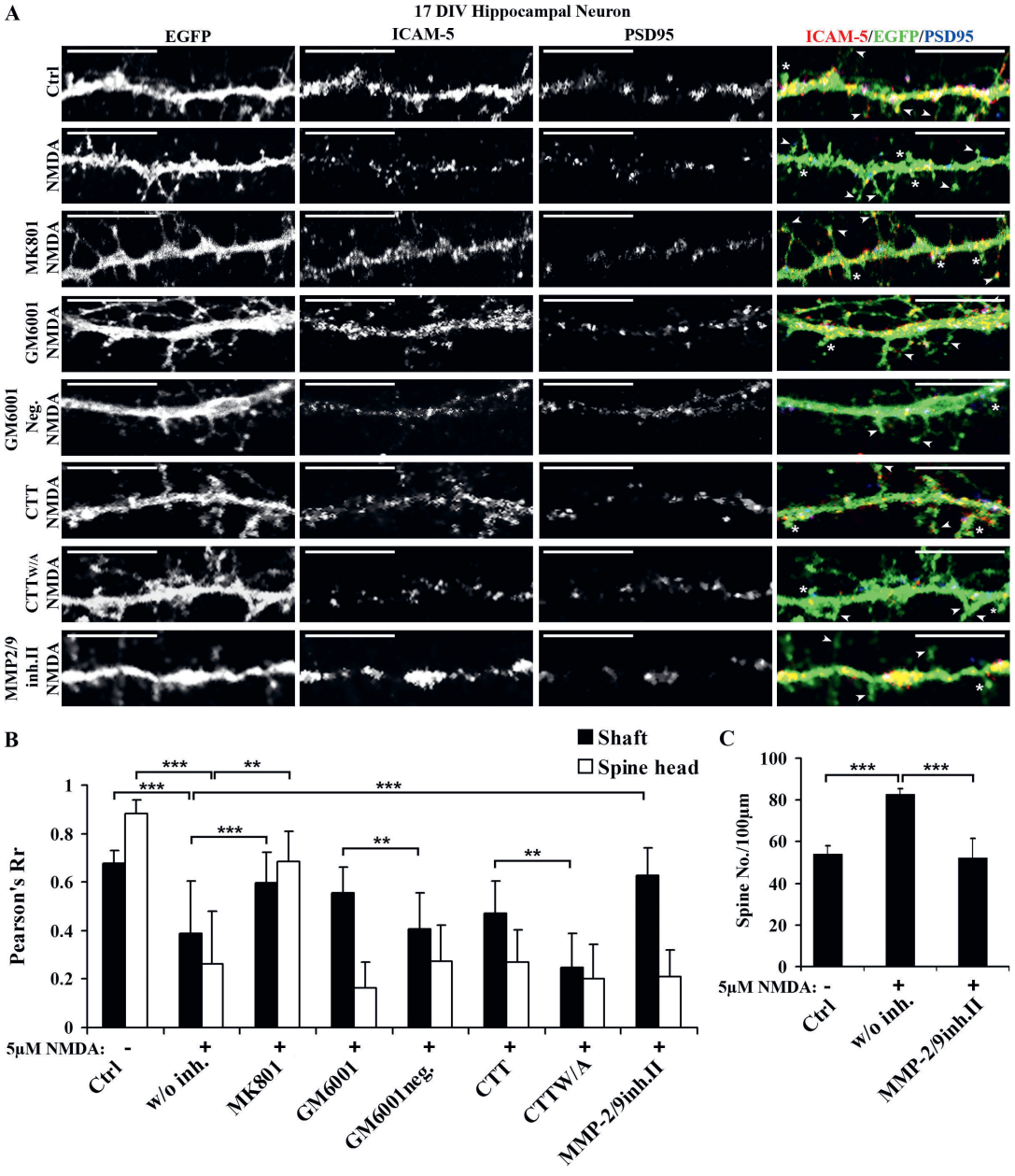

Figure 7. **MMP inhibitors prevent the NMDA-induced ICAM-5 cleavage in dendritic shafts but not in spines.** (A) 17-DIV hippocampal neurons were transfected with EGFP and either left untreated or treated for 6 h with 5 μM NMDA, with or without a 1-h pretreatment with 20 μM MK801 or MMP inhibitors. The neurons were then double stained for ICAM-5 by a mAb against the ectodomains of rat ICAM-5 (red) and PSD95 (blue). (B) The colocalization of ICAM-5 with EGFP in dendritic shafts or thin spine heads was measured. The localization of ICAM-5 in both dendritic shafts and thin spine heads (A, arrowheads) were significantly reduced by NMDA, which was efficiently counteracted by MK801. The MMP broad-spectrum inhibitor GM6001, in comparson to its negative control compound, significantly blocked the NMDA-induced reduction of ICAM-5 localization in dendritic shafts. Similar effects were found with the MMP-2/9–specific inhibitors, CTT peptide, and MMP-2/9 inhibitor II. However, none of the MMP inhibitors gave substantial recovery of ICAM-5 in thin spine heads. Furthermore, MMP-2/9 inhibitor II significantly blocked the NMDA-induced formation of spines (C). The experiment was repeated three times with similar results. Error bars indicate mean ± SD. **, $P < 0.01$; ***, $P < 0.001$. Bars, 10 μm.

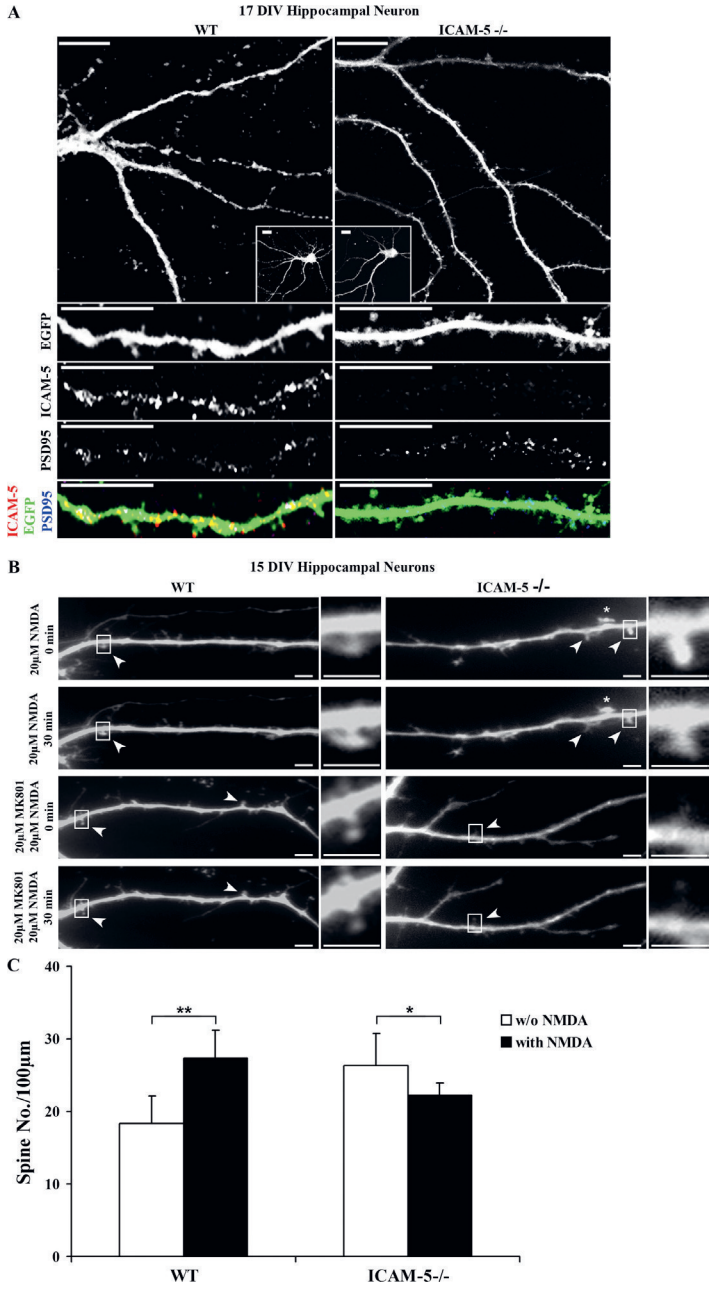

Figure 8. **ICAM-5 deficiency results in retraction of spine heads in response to NMDA stimulation.** (A) The responses of WT and ICAM-5$^{-/-}$ hippocampal neurons to NMDA stimulation were compared. To verify the identity of ICAM-5–deficient neurons, the EGFP-transfected 17-DIV fixed neurons of the two types were immunostained for ICAM-5 and PSD95. The size of mushroom spines in ICAM-5$^{-/-}$ neurons seemed to be larger than those in WT neurons. (B) The 15-DIV EGFP-transfected neurons were then monitored with a time-lapse fluorescence microscope. The neurons were treated by 20 μM NMDA for 1 h with or without a 1-h pretreatment with 20 μM MK801 and recorded during the 1-h period of NMDA stimulation. Thin spines of WT neurons showed increased growth of spine heads in response to NMDA stimulation within 1 h. In contrast, spine heads in ICAM-5$^{-/-}$ neurons seemed to be retracted during the 1-h treatment of NMDA (B, arrowheads). Intriguingly, mushroom spines in ICAM-5$^{-/-}$ neurons respond positively toward NMDA stimulation, with increased size of spine heads (B, asterisks). (C) Spine numbers were increased in WT neurons but not in ICAM-5$^{-/-}$ neurons after treatment with 5 μM NMDA for 8 h. The experiment was repeated three times with similar results. Error bars indicate mean ± SD. *, $P < 0.05$; **, $P < 0.01$. Bars, 3 μm.

which was similar to an earlier report (Matsuno et al., 2006). To monitor the growth of thin spines in these neurons, we studied the 15-DIV EGFP-transfected neurons with a time-lapse fluorescence microscope. The neurons were treated with 20 μM NMDA for 1 h with or without a 1-h pretreatment with MK801, and monitored for 1 h. We found that thin spines in WT neurons showed increased growth of spine heads in response to NMDA stimulation. In contrast, spine heads in ICAM-5$^{-/-}$ neurons seemed to be retracting (Fig. 8 B, arrowheads). Spine numbers were increased in WT neurons, but not in ICAM-5$^{-/-}$ neurons

Carl_G_190x270_mm_blokki_FINAL.indd 347 06-Aug-23 1:54:13 PM

after treatment with 5 μM NMDA for 8 h (Fig. 8 C). These data indicate that ICAM-5 is important for the motility of thin spines. Interestingly, we also found that mushroom spines in ICAM-5$^{-/-}$ neurons respond positively toward NMDA stimulation, with increased size of spine heads (Fig. 8 B, asterisks).

sICAM-5 promotes dendritic filopodia elongation

To study functions of the sICAM-5, we cultured the EGFP-transfected 9-DIV WT and ICAM-5$^{-/-}$ neurons in the presence of 10 μg/ml recombinant sICAM-5 D1-4-Fc protein for 3 d. The neurons were then immunostained for ICAM-5 and microtubule-associated protein-2 (MAP-2; Fig. 9 A). sICAM-5 D1-4-Fc protein induced a significantly higher number of filopodia from the WT neurons, compared with the ICAM-5$^{-/-}$ neurons (Fig. 9, B and C). The filopodial length of WT neurons also significantly increased in the presence of sICAM-5 D1-4-Fc protein, as compared with the ICAM-5$^{-/-}$ neurons (Fig. 9 D).

Discussion

ICAM-5 has been shown to be gradually excluded from mature synapses, but the mechanism was not elucidated (Matsuno et al., 2006). Here, we show that activation of the NRs induced cleavage of ICAM-5 (Fig. 1), which evidently is mediated by active MMP-2 and -9 (Fig. 2). The association of ICAM-5 with the actin cytoskeleton was decreased in dendritic spines in response to activation of the NRs, which affected the ICAM-5 cleavage (Figs. 3 and 6). ICAM-5 deficiency led to the retraction of spine heads and a decreased number of spines in response to NMDA stimulation (Fig. 8). sICAM-5 protein increased the number and length of filopodia in WT neurons but not in ICAM-5–deficient neurons (Fig. 9).

Combining these data with the earlier findings on ICAM-5 (Tian et al., 2000; Matsuno et al., 2006; Nyman-Huttunen et al., 2006), we present a schematic model depicting the NR-mediated spine development in which ICAM-5 is involved (Fig. 10). NMDA or AMPA stimulation causes increased MMP-2 and -9 activities in neurons and neighboring glial cells (not depicted), resulting in cleavage of the ectodomains of ICAM-5 from immature nascent spines. The reduced membrane level of ICAM-5 may facilitate local membrane and cytoskeleton reorganization, and thereby morphological remodeling of dendritic spines.

We have shown that ICAM-5 promotes dendritic elongation through homophilic interaction (Tian et al., 2000). Our current data further indicate that the increased number and length of filopodia from WT neurons is mediated by the homophilic interaction of sICAM-5 D1-4-Fc protein with membrane-bound

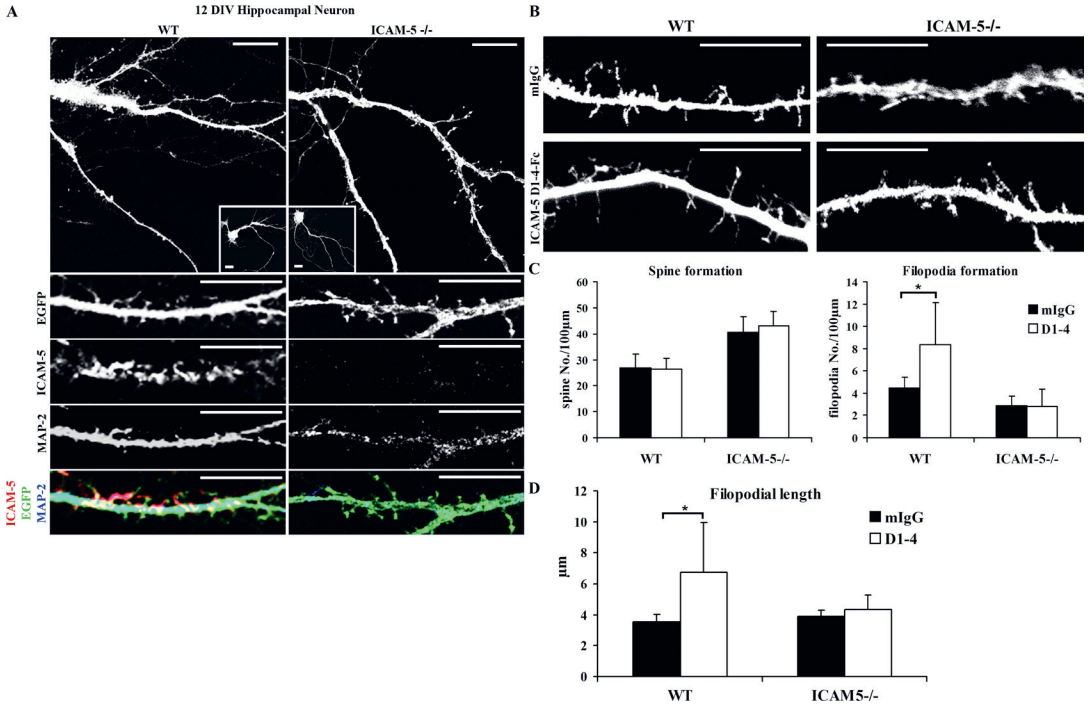

Figure 9. **sICAM-5 promotes dendritic filopodia elongation.** 9-DIV EGFP-transfected WT and ICAM-5$^{-/-}$ hippocampal neurons were incubated with 10 μg/ml soluble recombinant ICAM-5 D1-4-Fc protein or control mIgG for 72 h. The neurons were then double stained for ICAM-5 (A, red) and MAP-2 (A, blue). Compared with mIgG control protein, sICAM-5 D1-4-Fc protein induced significantly more filopodia from WT neurons, but not from ICAM-5$^{-/-}$ neurons (B and C). The filopodial length of WT neurons, but not ICAM-5$^{-/-}$ neurons, also significantly increased in the presence of sICAM-5 D1-4-Fc protein (D). The experiment was repeated three times with similar results. Error bars indicate mean ± SD. *, $P < 0.05$. Bar, 10 μm.

ICAM-5. These data extend our knowledge on functions of ICAM-5 in the context of the NR-regulated dendritic development. Indeed, blocking the ionotropic glutamate receptors has been demonstrated to result in an ∼35% decrease in the density and turnover of shaft filopodia, whereas focal glutamate application leads to a 75% increase in the length of shaft filopodia (Portera-Cailliau et al., 2003).

ICAM-5 has been postulated to be a negative regulator of filopodia-to-spine transition (Matsuno et al., 2006). In this sense, the promoted cleavage by NRs implies an important mechanism for a transformation of immature spines toward maturation. Moreover, the cooperative performance of ICAM-5 together with the NRs and MMPs may fine-tune the process of spine remodeling. The phenomenon that thin spines in ICAM-5$^{-/-}$ neurons retracted in response to NMDA treatment (Fig. 8) seems to be contradictory to the fact that ICAM-5$^{-/-}$ neurons have eventually larger mature spines (Matsuno et al., 2006). As the expression of ICAM-5 is the lowest in mature spines, we suspect that the eventual increase in size of mature spine heads is either not directly ICAM-5 related or resulted from secondary effects of ICAM-5 deficiency, which needs further clarification.

We provide several lines of evidence that MMP-2 and -9 are responsible for the proteolytic processing of ICAM-5, leading to the production of the sICAM-5. First of all, we detected a steady-state cleavage of ICAM-5 from the cultured primary neurons, which was increased by NMDA or AMPA stimulation (Fig. 1). As earlier shown, MMP-9 gene expression is upregulated in response to extracellular stimuli, like growth factors, cytokines, and neurotransmitters, whereas there is lack of transcriptional regulation of MMP-2 expression (Chakraborti et al., 2003; Meighan et al., 2006; Nagy et al., 2006). These facts suggest that MMP-2 is involved in the basal processing of ICAM-5 and MMP-9 in the activity-dependent cleavage of ICAM-5. In addition, NMDA-induced ICAM-5 cleavage was efficiently prevented by various MMP-2 and -9 inhibitors and siRNAs (Fig. 2). Abnormally high expression levels of ICAM-5 were found in the newborn MMP-2– or MMP-9–deficient mice (Fig. 4 A), supporting the finding of involvement of MMP-2 and -9 in ICAM-5 proteolytic processing.

Interestingly, the difference in ICAM-5 expression between the MMP-2– or MMP-9–deficient mice and the WT mice gradually disappeared during postnatal brain development (Fig. 4 A), which may partially be due to the decrease of MMP-2 enzymatic activity (Fig. 4 B) with the simultaneous increase of ICAM-5 expression during the later postnatal period. In contrast to ICAM-5, another important CAM, L1CAM, did not show changes in the expression levels in the MMP-2– or MMP-9–deficient mice as compared with the WT mice. Furthermore, L1CAM showed a gradual decrease in expression during the postnatal period (Fig. 4 A), indicating a shift of roles between the two molecules during brain maturation.

An earlier report on MMP-2–deficient mice has shown that MMP-9 activity is up-regulated (Esparza et al., 2004). Here, we found a similar phenomenon in the brains of adult MMP-2–deficient mice (Fig. 4 B). The expression of ICAM-5 in the MMP double-deficient mice was reduced during the early postnatal period (Fig. 4 A), which may be due to compensating effects of other proteases. Another possibility could be that protein synthesis is deficient in these mice because of developmental defects.

We found that the cytoskeletal anchorage of membrane-bound ICAM-5 was critical for controlling its proteolytic cleavage by MMPs. Disruption of actin filaments by cytochalasin D or latrunculin A, or deletion of the cytoplasmic tail of ICAM-5, significantly promoted its cleavage. Activation of the NRs resulted in dissociation of ICAM-5 from the actin cytoskeleton. The actin cytoskeleton determines the shape, motility, and stability of dendritic spines and provides the substrates for the Rho family small GTPases, which are the key regulators of actin polymerization and spine motility (Scott and Luo, 2001; Calabrese et al., 2006). The NRs and GluRs have been shown to promote

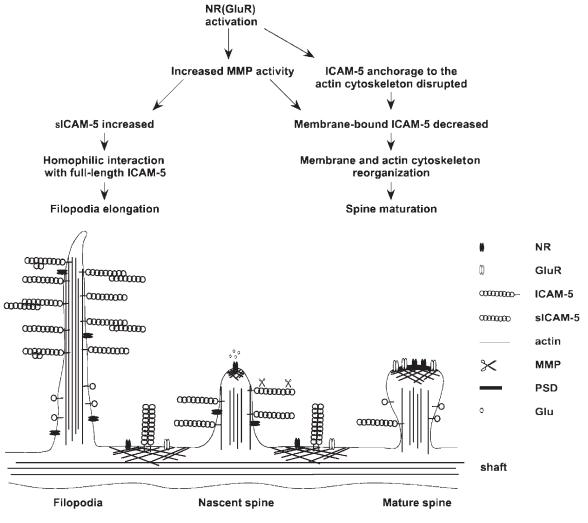

Figure 10. **Schematic model of ICAM-5 involvement in spine maturation and filopodia elongation through activation of glutamate receptors.** The activation of NRs or GluRs in neurons induces increased MMP-2 and -9 activities, which cleave the ectodomains of ICAM-5 from nascent spines, and results in dissociation of ICAM-5 from the actin cytoskeleton. The remaining CTF of ICAM-5 may compete and disrupt the anchorage of full-length ICAM-5 to the actin cytoskeleton, which further promotes its cleavage from spines by MMPs. Reduced membrane levels of ICAM-5 may facilitate local membrane and cytoskeleton reorganization, which induces the maturation of dendritic spines. Concomitantly, the sICAM-5 fragments produced by MMPs can bind in homophilic manner to the full-length ICAM-5 in the neighborhood filopodia and promote their elongation.

Carl_G_190x270_mm_blokki_FINAL.indd 349 06-Aug-23 1:54:14 PM

formation and stabilization of dendritic spines, respectively, by inhibiting the actin-based protrusive activity from the spine heads (Fischer et al., 2000) and increasing the turnover time of dynamic actin in spines (Star et al., 2002). Inhibition of actin motility caused spines to round up so that spine morphology became more stable and regular (Fischer et al., 2000). These facts indicate that the cytoplasmic part of ICAM-5 participates in the NR-dependent morphological change of spines by exerting a regulatory role on MMP-mediated ICAM-5 cleavage.

We have shown that ICAM-5 associates with the actin filaments via α-actinin and promotes neuritic outgrowth (Nyman-Huttunen et al., 2006). The NR subunit (NR2B) has been shown to interact with α-actinin (Wyszynski et al., 1997; Husi et al., 2000). α-Actinin has been implicated in the regulation of spine morphology (Nakagawa et al., 2004). Therefore, it is plausible that the NR may directly compete with ICAM-5 for interaction with actin filaments (Fig. 10).

The role of MMPs in the normal brain development is gradually becoming apparent (Dzwonek et al., 2004; Luo, 2005; Ethell and Ethell, 2007). However, little is known concerning the effects of MMPs on dendritic spine development, even though both their ECM and non-ECM substrates in the brain have been found to be important for spine formation and remodeling (Ethell and Pasquale, 2005). Recently, MMP-7 (Bilousova et al., 2006), MMP-9 (Meighan et al., 2006; Nagy et al., 2006), and MMP-24 (Monea et al., 2006) were shown to be involved in dendritic filopodia elongation or synaptic remodeling. Particularly, MMP-9–deficient mice show impaired LTP and behavioral impairments in hippocampus-dependent associative learning (Nagy et al., 2006), suggesting the potential importance of MMP on dendritic spine development.

Although mutant mice lacking individual MMPs have been generated (Itoh et al., 1997; Vu et al., 1998), no obvious defects in embryogenesis have been reported. In particular, MMP-2–deficient mice seemed to be healthy and fertile (Itoh et al., 1997), although they exhibited defects in bone metabolism (Inoue et al., 2006). We found that MMP-2–deficient mice seemed to have an increased number of cells in the cerebral cortex, especially in layers 2–3 (Fig. S4). Similar findings have been reported in the cerebellar cortex of MMP-9–deficient mice, which showed an abnormal accumulation of granular precursors in the external granular layer (Vaillant et al., 2003). Thus, our findings on MMP-2–deficient mice deserve more careful and detailed study in the future.

In summary, we have defined a physiological mechanism for the proteolytic processing of ICAM-5 by MMP-2 and -9, and the importance of its cleavage on regulation of dendritic spine development. Our results will help elucidate the functions of both MMPs and adhesion molecules on dendritic development, which is still poorly understood.

Materials and methods

Reagents and antibodies

AMPA, DNQX, gelatin, MK-801, NMDA, and poly-l-lysine were obtained from Sigma-Aldrich. Cytochalasin D, Latrunculin A, GM6001, GM6001 Neg. Ctrl, MMP-2/MMP-9 inhibitor II, and MMP-9 inhibitor I were obtained from Calbiochem. ProMMP-2 and -9 were obtained from Roche. CTT and $CTT_{W/A}$ peptides were gifts from E. Koivunen (Division of Biochemistry, University of Helsinki, Helsinki, Finland; Koivunen et al., 1999).

The pAb anti–ICAM-5cp against the cytoplasmic tail of mouse ICAM-5 was a gift from Y. Yoshihara (Brain Science Institute/Institute of Physical and Chemical Research, Wako City, Japan). The pAb 1000J and the mAb 127E, both against the ectodomain of rat ICAM-5, were gifts from P. Kilgannon (ICOS Corporation, Seattle, WA). The anti-L1CAM mAb, anti–MAP-2 mAb, and the anti-PSD95 mAb and pAb were obtained from Abcam. The anti-actin pAb was obtained from Sigma-Aldrich. The pAbs against MMP-2 and -9 were obtained from Santa Cruz Biotechnology, Inc., and Chemicon, respectively. A mAb negative control was also obtained from Chemicon. Peroxidase-conjugated anti-mouse, anti-rabbit, and anti-human pAbs were obtained from GE Healthcare. Alexa488-, Cy3-, or Cy5-conjugated anti-mouse and anti-rabbit pAbs and Cy3-conjugated phalloidin were obtained from Invitrogen.

Animals

MMP-2–, MMP-9–, and ICAM-5–deficient mice were generated by gene targeting (Itoh et al., 1997; Vu et al., 1998; Nakamura et al., 2001). All animals were backcrossed at least six generations into a homogenous C57BL/6 genetic background and were bred as homozygous lines. Mice deficient in both MMP-2 and -9 were obtained by intercrossing mice that were heterozygous for both mutations. All experiments were approved by and performed according to the guidelines of the local animal ethical committee.

Cell culture

Paju-Mock, Paju-ICAM-5-fl, and Paju-ICAM-5-ΔCP cell lines and hippocampal neurons were prepared as described earlier (Nyman-Huttunen et al., 2006). The CHO cell line stably expressing ICAM-5 D1- 4-Fc recombinant protein, a gift from J. Casasnovas (Universidad Autonoma, Madrid, Spain), was grown as recommended (Casasnovas et al., 1998).

Cell stimulation and sICAM-5 detection

During the 3-wk period of in vitro cultivation of hippocampal neurons, the culture media were replaced with HBSS with 1.8 mM $CaCl_2$ buffer for 16 h on days 3, 7, 14, and 21. The 14-DIV hippocampal neurons were treated for 16 h with 5 μM NMDA or AMPA, with or without a 2-h pretreatment with 20 μM MK-801 or DNQX, respectively, in HBSS/Ca^{2+} buffer. When MMP inhibitors were applied, 20–25 μM chemical inhibitors or 100 μM peptide inhibitors were used together with NMDA. Paju-ICAM-5-fl and Paju-ICAM-5-ΔCP cells were incubated in serum-free culture media for 18 h. Then, 1-ml aliquots of the conditioned culture media were concentrated 20-fold by Vivaspin centrifugal concentrators (Sartorius Ltd.), and the cells were stripped off. All samples were suspended in Laemmli sample buffer for Western blotting.

RNA interference

9-DIV rat hippocampal neurons were transfected with 50 nM predesigned siRNAs against rat MMP-2, MMP-9, or negative control siRNA (Ambion) using Lipofectamine RNAiMAX reagent (Invitrogen) for 48 h. The culture media were changed into HBSS/Ca^{2+} buffer for 16 h and then collected and concentrated for Western blotting.

Crude brain membrane preparations

Forebrains from the postnatal 1 d ($n = 4$), 1 wk ($n = 2$), and 10 wk ($n = 2$) MMP-deficient or WT mice were homogenized with buffer containing 0.32 M sucrose, 10 mM Hepes, pH 7.4, 2 mM EDTA, 50 mM NaF, 1 mM Na_2VO_4, and 1× protease cocktail inhibitors, using a glass-teflon homogenizer. The homogenates were then centrifuged at 1,000 *g*, and the supernatants were centrifuged at 50,000 rpm to separate the membrane fractions from the soluble fractions. The membrane fractions were suspended in lysis buffer (1% Triton X-100, 50 mM Hepes, pH 7.4, 2 mM EDTA, and protease/phosphatase inhibitors). For Western blotting, 20 μg of protein from each sample was suspended in Laemmli sample buffer.

Subcellular fractionations

14-DIV hippocampal neurons were either left untreated or treated with 20 μM NMDA for 60 min, and cells were then lysed in lysis buffer. Lysates were centrifuged at 5,000 rpm to get rid of the nuclear fractions, and the supernatants were further centrifuged at 100,000 rpm for 2 h at +2°C to separate the cytoskeletal fractions from the soluble fractions, and each sample was suspended in Laemmli sample buffer for Western blotting.

Recombinant protein purification

Recombinant human ICAM-5 D1-4-Fc and mouse ICAM-5 D1-9-Fc proteins were purified from cell culture supernatants by affinity chromatography with protein A–Sepharose and ÄKTAprime system (GE Healthcare).

Carl_G_190x270_mm_blokki_FINAL.indd 350 06-Aug-23 1:54:15 PM

In vitro cleavage and detection of recombinant ICAM-5-Fc protein
ProMMP-2 and -9 were activated with p-aminophenylmercuric acetate and trypsin, respectively, and 40 ng of activated enzymes was incubated with 2 μg ICAM-5 D1-9-Fc protein in 50 μl enzyme buffer (20 mM Hepes, 150 mM NaCl, 0.2 mM $CaCl_2$, 1 mM $MnCl_2$, and 1 μM $ZnCl_2$) at 37°C for 18 h. 5 μl of the enzyme-substrate mixtures were suspended in sample buffer.

Western blotting
Samples were separated by 4–12% SDS-PAGE (Invitrogen) and transferred to nitrocellulose membranes (Whatman GmbH). After blocking, membranes were incubated with anti–ICAM-5 pAb 1000J, anti–ICAM-5cp pAb, anti-L1CAM mAb, anti-actin pAb, or horseradish peroxidase–conjugated anti-human pAb, respectively, followed by peroxidase-conjugated secondary antibodies. Membranes were washed with TBS and 0.05% Tween 20 after each incubation and developed with an ECL kit (GE Healthcare). Band intensity was quantified by the software Tina 2.09c (Raytest).

Gelatinase zymography
20 μl of 60-fold–concentrated serum-free cell culture media or 50 μg of protein from brain membrane fractions was suspended in sample buffer and separated by 8% SDS—PAGE containing 0.2% gelatin. Gels were then washed with 2.5% Triton X-100 to remove SDS and incubated in substrate buffer (50 mM Tris, pH 8, and 5 mM $CaCl_2$) for 18 h at 37°C, followed by staining with 0.5% Coomassie blue.

Mass spectrometry
About 1 μg ICAM-5 D1-9-Fc fragments after the MMP-2 or -9 digestion were separated by 4–12% SDS-PAGE (Invitrogen), silver stained, and analyzed in the Protein Chemistry Unit of the Institute of Biotechnology, University of Helsinki. The bands of interest were cut out, reduced with dithiothreitol, alkylated with iodoacetamide, and "in-gel" digested with trypsin (Sequencing Grade Modified Trypsin; V5111; Promega). The recovered peptides were, after desalting using μ-C18 ZipTip (Millipore), subjected to MALDI-TOF mass spectrometric analysis. MALDI-TOF mass spectra for mass fingerprinting and MALDI-TOF/TOF mass spectra for identification by fragment ion analysis were obtained using an Ultraflex TOF/TOF instrument (Bruker-Daltonik GmbH). Protein identification with the generated data was performed using Mascot Peptide Mass Fingerprint and MS/MS Ion Search programs.

Flow cytometry
Paju-Mock, Paju-ICAM-5-fl, or Paju-ICAM-5-ΔCP cells were incubated with 5 μg/ml mAb TL-3 and then with Alexa488-conjugated anti-mouse pAb (Invitrogen). Cells were washed with PBS after each incubation. Samples were analyzed with FACScan and CellQuest software (Becton Dickinson).

Immunofluorescence microscopy
Hippocampal neurons were transfected with pEGFP-N1 plasmid using Lipofectamine 2000 reagent (Invitrogen) at 8–9 DIV and cultured until 12–17 DIV. For filopodia elongation assay, the 9-DIV neurons were treated twice with 10 μg/ml of recombinant ICAM-5 D1-4-Fc protein or control mIgG for 72 h. The 10–12-DIV neurons were then fixed with 4% paraformaldehyde and permeabilized with 0.1% Triton X-100. After blocking with 2% BSA in PBS, neurons were stained with pAb anti–ICAM-5cp plus Alexa488- or Cy3-conjugated anti-rabbit IgG, Cy3-conjugated phalloidin, anti-PSD95 mAb, or anti-MAP-2 mAb plus Cy5-conjugated anti-mouse IgG. The 17-DIV neurons were left untreated or treated with 5 μM NMDA with or without a 2-h pretreatment with 20 μM MK801 or MMP inhibitors in HBSS/Ca^{2+} buffer for 6 h. The neurons were fixed, permeabilized, and blocked afterward, and stained with mAb 127E plus Cy3-conjugated anti-mouse IgG and anti-PSD95 pAb plus Cy5-conjugated anti-rabbit IgG. The fluorescent images were taken with a confocal laser-scanning microscope under 63× magnification (TCS SP2 AOBS, HCX PL APO 63×O/1.4-0.6; Leica) using a charge-coupled device camera (Leica) and the LCSLite software. Four to five neurons per sample were randomly imaged for each experiment. At least three proximal dendritic segments (~60 μm per segment) were analyzed for each neuron. Dendritic filopodia (>2 μm long with pointy tip), thin spines (0.5–2.5 μm long with bulbous tip and <0.1 μm thick in neck), or mushroom-shaped spines (0.5–2.0 μm long and 0.3–0.6 μm wide in head) were quantified and presented as numbers per 100 μm dendritic length. For live imaging, 14-DIV EGFP-transfected neurons were treated with 20 μM NMDA in HBSS/Ca^{2+} buffer, with or without pretreatment with 20 μM MK801 for 1 h, in 5% CO_2/10% O_2 at 37°C, and monitored with an inverted fluorescent microscope under 60× magnification (IX-71; UPlanSApo 60×W/1.2; Olympus) using an electron multiplying charge-coupled device camera (DV885; Andor Technology) and the TillVision software (Till Photonics GmbH). Images were processed with Photoshop and ImagePro plus. Pearson's coefficients were used for colocalization analysis.

Histology
Brains from 8-wk-old mice were fixed with 4% paraformaldehyde in PBS and embedded in paraffin wax. Coronal paraffin sections 10 μm thick were cut and mounted on glass slides. Brain sections were stained with cresyl violet and visualized with a light microscope (IX71; Olympus). Images were processed with Photoshop (Adobe).

Statistical analysis
t test was used to compare different groups of data.

Online supplemental material
Fig. S1 shows that NMDA increases the expression and activities of MMP-2 and -9. Fig. S2 shows peptide mass mapping of MMP-cleaved ICAM-5-Fc proteins. Fig. S3 shows flow cytometry analysis of transfected Paju cell lines. Fig. S4 shows abnormal cortical and hippocampal development in MMP-2–deficient mice. Online supplemental material is available at http://www.jcb.org/cgi/content/full/jcb.200612097/DC1.

We thank Dr. Yoshihiro Yoshihara for providing the anti–ICAM-5cp pAb; Dr. Patrick Kilgannon for rat ICAM-5 mAbs and pAb 1000J; Dr. Erkki Koivunen for MMP-inhibitory peptides; Dr. Jose Casasnovas for CHO cell lines; Dr. Nisse Kalkkinen for peptide mass mapping; Seija Lehto, Leena Kuoppasalmi, Outi Nikkilä, Erja Huttu, and Maria Aatonen for technical assistance; and Yvonne Heinilä for secretarial help.

This study was supported by the Sigrid Jusélius Foundation, the Academy of Finland, the Finnish Cultural Foundation, the Magnus Ehrnrooth Foundation, the Finnish Cancer Society, the Liv och Hälsa Foundation, and the Institute for the Promotion of Innovation through Science and Technology in Flanders (IWT-Vlaanderen).

Submitted: 18 December 2006
Accepted: 13 July 2007

References

Ayoub, A.E., T.Q. Cai, R.A. Kaplan, and J. Luo. 2005. Developmental expression of matrix metalloproteinases 2 and 9 and their potential role in the histogenesis of the cerebellar cortex. *J. Comp. Neurol.* 481:403–415.

Benson, D.L., Y. Yoshihara, and K. Mori. 1998. Polarized distribution and cell type-specific localization of telencephalin, an intercellular adhesion molecule. *J. Neurosci. Res.* 52:43–53.

Bilousova, T.V., D.A. Rusakov, D.W. Ethell, and I.M. Ethell. 2006. Matrix metalloproteinase-7 disrupts dendritic spines in hippocampal neurons through NMDA receptor activation. *J. Neurochem.* 97:44–56.

Borusiak, P., P. Gerner, C. Brandt, P. Kilgannon, and P. Rieckmann. 2005. Soluble telencephalin in the serum of children after febrile seizures. *J. Neurol.* 252:493–494.

Calabrese, B., M.S. Wilson, and S. Halpain. 2006. Development and regulation of dendritic spine synapses. *Physiology (Bethesda).* 21:38–47.

Casasnovas, J.M., T. Stehle, J.H. Liu, J.H. Wang, and T.A. Springer. 1998. A dimeric crystal structure for the N-terminal two domains of intercellular adhesion molecule-1. *Proc. Natl. Acad. Sci. USA.* 95:4134–4139.

Chakraborti, S., M. Mandal, S. Das, A. Mandal, and T. Chakraborti. 2003. Regulation of matrix metalloproteinases: an overview. *Mol. Cell. Biochem.* 253:269–285.

Dityatev, A., G. Dityateva, V. Sytnyk, M. Delling, N. Toni, I. Nikonenko, D. Muller, and M. Schachner. 2004. Polysialylated neural cell adhesion molecule promotes remodeling and formation of hippocampal synapses. *J. Neurosci.* 24:9372–9382.

Dzwonek, J., M. Rylski, and L. Kaczmarek. 2004. Matrix metalloproteinases and their endogenous inhibitors in neuronal physiology of the adult brain. *FEBS Lett.* 567:129–135.

Esparza, J., M. Kruse, J. Lee, M. Michaud, and J.A. Madri. 2004. MMP-2 null mice exhibit an early onset and severe experimental autoimmune encephalomyelitis due to an increase in MMP-9 expression and activity. *FASEB J.* 18:1682–1691.

Ethell, I.M., and E.B. Pasquale. 2005. Molecular mechanisms of dendritic spine development and remodeling. *Prog. Neurobiol.* 75:161–205.

Ethell, I.M., and D.W. Ethell. 2007. Matrix metalloproteinases in brain development and remodeling: synaptic functions and targets. *J. Neurosci. Res.* 10.1002/jnr.21273.

Carl_G_190x270_mm_blokki_FINAL.indd 351 06-Aug-23 1:54:15 PM

Ethell, I.M., F. Irie, M.S. Kalo, J.R. Couchman, E.B. Pasquale, and Y. Yamaguchi. 2001. EphB/syndecan-2 signaling in dendritic spine morphogenesis. *Neuron.* 31:1001–1013.

Fischer, M., S. Kaech, U. Wagner, H. Brinkhaus, and A. Matus. 2000. Glutamate receptors regulate actin-based plasticity in dendritic spines. *Nat. Neurosci.* 3:887–894.

Gahmberg, C.G., L. Valmu, S. Fagerholm, P. Kotovuori, E. Ihanus, L. Tian, and T. Pessa-Morikawa. 1998. Leukocyte integrins and inflammation. *Cell. Mol. Life Sci.* 54:549–555.

Gerrow , K., and A. El-Husseini. 2006. Cell adhesion molecules at the synapse. *Front. Biosci.* 11:2400–2419.

Guo, H., N. Tong, T. Turner, L.G. Epstein, M.P. McDermott, P. Kilgannon, and H.A. Gelbard. 2000. Release of the neuronal glycoprotein ICAM-5 in serum after hypoxic-ischemic injury. *Ann. Neurol.* 48:590–602.

Hering, H., and M. Sheng. 2001. Dendritic spines: structure, dynamics and regulation. *Nat. Rev. Neurosci.* 2:880–888.

Husi, H., M.A. Ward, J.S. Choudhary, W.P. Blackstock, and S.G. Grant. 2000. Proteomic analysis of NMDA receptor-adhesion protein signaling complexes. *Nat. Neurosci.* 3:661–669.

Inoue, K., Y. Mikuni-Takagaki, K. Oikawa, T. Itoh, M. Inada, T. Noguchi, J.S. Park, T. Onodera, S.M. Krane, M. Noda, and S. Itohara. 2006. A crucial role for matrix metalloproteinase 2 in osteocytic canalicular formation and bone metabolism. *J. Biol. Chem.* 281:33814–33824.

Itoh, T., T. Ikeda, H. Gomi, S. Nakao, T. Suzuki, and S. Itohara. 1997. Unaltered secretion of beta-amyloid precursor protein in gelatinase A (matrix metalloproteinase 2)-deficient mice. *J. Biol. Chem.* 272:22389–22392.

Kasai, H., M. Matsuzaki, J. Noguchi, N. Yasumatsu, and H. Nakahara. 2003. Structure-stability-function relationships of dendritic spines. *Trends Neurosci.* 26:360–368.

Koivunen, E., W. Arap, H. Valtanen, A. Rainisalo, O.P. Medina, P. Heikkila, C. Kantor, C.G. Gahmberg, T. Salo, Y.T. Konttinen, et al. 1999. Tumor targeting with a selective gelatinase inhibitor. *Nat. Biotechnol.* 17:768–774.

Lindsberg, P.J., J. Launes, L. Tian, H. Valimaa, V. Subramanian, J. Siren, L. Hokkanen, T. Hyypia, O. Carpen, and C.G. Gahmberg. 2002. Release of soluble ICAM-5, a neuronal adhesion molecule, in acute encephalitis. *Neurology.* 58:446–451.

Liu, W.S., C. Pesold, M.A. Rodriguez, G. Carboni, J. Auta, P. Lacor, J. Larson, B.G. Condie, A. Guidotti, and E. Costa. 2001. Down-regulation of dendritic spine and glutamic acid decarboxylase 67 expressions in the reelin haploinsufficient heterozygous reeler mouse. *Proc. Natl. Acad. Sci. USA.* 98:3477–3482.

Luo, J. 2005. The role of matrix metalloproteinases in the morphogenesis of the cerebellar cortex. *Cerebellum.* 4:239–245.

Malemud, C.J. 2006. Matrix metalloproteinases (MMPs) in health and disease: an overview. *Front. Biosci.* 11:1696–1701.

Matsuno, H., S. Okabe, M. Mishina, T. Yanagida, K. Mori, and Y. Yoshihara. 2006. Telencephalin slows spine maturation. *J. Neurosci.* 26:1776–1786.

Matsuzaki, M., N. Honkura, G.C. Ellis-Davies, and H. Kasai. 2004. Structural basis of long-term potentiation in single dendritic spines. *Nature.* 429:761–766.

Matus, A. 2000. Actin-based plasticity in dendritic spines. *Science.* 290:754–758.

Meighan, S.E., P.C. Meighan, P. Choudhury, C.J. Davis, M.L. Olson, P.A. Zornes, J.W. Wright, and J.W. Harding. 2006. Effects of extracellular matrix-degrading proteases matrix metalloproteinases 3 and 9 on spatial learning and synaptic plasticity. *J. Neurochem.* 96:1227–1241.

Mitsui, S., M. Saito, K. Hayashi, K. Mori, and Y. Yoshihara. 2005. A novel phenylalanine-based targeting signal directs telencephalin to neuronal dendrites. *J. Neurosci.* 25:1122–1131.

Monea, S., B.A. Jordan, S. Srivastava, S. DeSouza, and E.B. Ziff. 2006. Membrane localization of membrane type 5 matrix metalloproteinase by AMPA receptor binding protein and cleavage of cadherins. *J. Neurosci.* 26:2300–2312.

Nagy, V., O. Bozdagi, A. Matynia, M. Balcerzyk, P. Okulski, J. Dzwonek, R.M. Costa, A.J. Silva, L. Kaczmarek, and G.W. Huntley. 2006. Matrix metalloproteinase-9 is required for hippocampal late-phase long-term potentiation and memory. *J. Neurosci.* 26:1923–1934.

Nakagawa, T., J.A. Engler, and M. Sheng. 2004. The dynamic turnover and functional roles of alpha-actinin in dendritic spines. *Neuropharmacology.* 47:734–745.

Nakamura, K., T. Manabe, M. Watanabe, T. Mamiya, R. Ichikawa, Y. Kiyama, M. Sanbo, T. Yagi, Y. Inoue, T. Nabeshima, et al. 2001. Enhancement of hippocampal LTP, reference memory and sensorimotor gating in mutant mice lacking a telencephalon-specific cell adhesion molecule. *Eur. J. Neurosci.* 13:179–189.

Nyman-Huttunen, H., L. Tian, L. Ning, and C.G. Gahmberg. 2006. α-Actinin-dependent cytoskeletal anchorage is important for ICAM-5-mediated neuritic outgrowth. *J. Cell Sci.* 119:3057–3066.

Oertner, T.G., and A. Matus. 2005. Calcium regulation of actin dynamics in dendritic spines. *Cell Calcium.* 37:477–482.

Oray, S., A. Majewska, and M. Sur. 2004. Dendritic spine dynamics are regulated by monocular deprivation and extracellular matrix degradation. *Neuron.* 44:1021–1030.

Portera-Cailliau, C., D.T. Pan, and R. Yuste. 2003. Activity-regulated dynamic behavior of early dendritic protrusions: evidence for different types of dendritic filopodia. *J. Neurosci.* 23:7129–7142.

Scott, E.K., and L. Luo. 2001. How do dendrites take their shape? *Nat. Neurosci.* 4:359–365.

Shi, Y., and I.M. Ethell. 2006. Integrins control dendritic spine plasticity in hippocampal neurons through NMDA receptor and Ca^{2+}/calmodulin-dependent protein kinase II-mediated actin reorganization. *J. Neurosci.* 26:1813–1822.

Star, E.N., D.J. Kwiatkowski, and V.N. Murthy. 2002. Rapid turnover of actin in dendritic spines and its regulation by activity. *Nat. Neurosci.* 5:239–246.

Szklarczyk, A., J. Lapinska, M. Rylski, R.D. McKay, and L. Kaczmarek. 2002. Matrix metalloproteinase-9 undergoes expression and activation during dendritic remodeling in adult hippocampus. *J. Neurosci.* 22:920–930.

Tada, T., and M. Sheng. 2006. Molecular mechanisms of dendritic spine morphogenesis. *Curr. Opin. Neurobiol.* 16:95–101.

Tian, L., H. Nyman, P. Kilgannon, Y. Yoshihara, K. Mori, L.C. Andersson, S. Kaukinen, H. Rauvala, W.M. Gallatin, and C.G. Gahmberg. 2000. Intercellular adhesion molecule-5 induces dendritic outgrowth by homophilic adhesion. *J. Cell Biol.* 150:243–252.

Togashi, H., K. Abe, A. Mizoguchi, K. Takaoka, O. Chisaka, and M. Takeichi. 2002. Cadherin regulates dendritic spine morphogenesis. *Neuron.* 35:77–89.

Vaillant, C., C. Meissirel, M. Mutin, M.F. Belin, L.R. Lund, and N. Thomasset. 2003. MMP-9 deficiency affects axonal outgrowth, migration, and apoptosis in the developing cerebellum. *Mol. Cell. Neurosci.* 24:395–408.

Vu, T.H., J.M. Shipley, G. Bergers, J.E. Berger, J.A. Helms, D. Hanahan, S.D. Shapiro, R.M. Senior, and Z. Werb. 1998. MMP-9/gelatinase B is a key regulator of growth plate angiogenesis and apoptosis of hypertrophic chondrocytes. *Cell.* 93:411–422.

Washbourne, P., A. Dityatev, P. Scheiffele, T. Biederer, J.A. Weiner, K.S. Christopherson, and A. El-Husseini. 2004. Cell adhesion molecules in synapse formation. *J. Neurosci.* 24:9244–9249.

Wyszynski, M., J. Lin, A. Rao, E. Nigh, A.H. Beggs, A.M. Craig, and M. Sheng. 1997. Competitive binding of alpha-actinin and calmodulin to the NMDA receptor. *Nature.* 385:439–442.

Yoshihara, Y., S. Oka, Y. Nemoto, Y. Watanabe, S. Nagata, H. Kagamiyama, and K. Mori. 1994. An ICAM-related neuronal glycoprotein, telencephalin, with brain segment-specific expression. *Neuron.* 12:541–553.

Yuste, R., and T. Bonhoeffer. 2004. Genesis of dendritic spines: insights from ultrastructural and imaging studies. *Nat. Rev. Neurosci.* 5:24–34.

Carl_G_190x270_mm_blokki_FINAL.indd 352 06-Aug-23 1:54:16 PM

NIH Public Access
Author Manuscript
Science. Author manuscript; available in PMC 2009 September 28.

Published in final edited form as:
Science. 2008 November 14; 322(5904): 1101–1104. doi:10.1126/science.1165218.

Del-1 is an endogenous inhibitor of leukocyte-endothelial adhesion limiting inflammatory cell recruitment&

Eun Young Choi[1,*], **Emmanouil Chavakis**[2,*], **Marcus A. Czabanka**[3,#], **Harald Langer**[1,#], **Line Fraemohs**[4], **Matina Economopoulou**[5], **Ramendra K. Kundu**[6], **Alessia Orlandi**[2], **Ying Yi Zheng**[1], **DaRue A. Prieto**[7], **Christie M. Ballantyne**[8], **Stephanie L. Constant**[9], **William C. Aird**[10], **Thalia Papayannopoulou**[11], **Carl G. Gahmberg**[12], **Mark C. Udey**[13], **Peter Vajkoczy**[3], **Thomas Quertermous**[6], **Stefanie Dimmeler**[2], **Christian Weber**[4], and **Triantafyllos Chavakis**[1,†]

[1]Experimental Immunology Branch, Center for Cancer Research, NCI, NIH, Bethesda, MD [2]Molecular Cardiology, Dept. of Internal Medicine III, J.W. Goethe University Frankfurt, Frankfurt, Germany [3]Department of Neurosurgery, Charite Universitätsmedizin Berlin, Berlin, Germany [4]Institute for Molecular Cardiovascular Research, RWTH University Hospital, Aachen, Germany [5]Laboratory of Cellular Oncology, Center for Cancer Research, NCI, NIH, Bethesda, MD [6]Division of Cardiovascular Medicine, Stanford University School of Medicine, Palo Alto, CA [7]Laboratory of Proteomics and Analytical Technologies, SAIC-Frederick Inc., NCI at Frederick, Frederick, MD [8]Baylor College of Medicine and Center for Cardiovascular Disease Prevention, Methodist DeBakey Heart Center, Houston, TX [9]Department of Microbiology, Immunology and Tropical Medicine, George Washington University, Washington, DC [10]Molecular and Vascular Medicine, BIDMC, Harvard Medical School, Boston, MA [11]Department of Medicine/Hematology, University of Washington, Seattle, WA [12]Division of Biochemistry, Faculty of Biosciences, University of Helsinki, Finland [13]Dermatology Branch, Center for Cancer Research, NCI, NIH, Bethesda, MD

Abstract

Leukocyte recruitment to sites of infection or inflammation requires multiple adhesive events. While numerous players promoting leukocyte-endothelial interactions have been characterized, functionally important endogenous inhibitors of leukocyte adhesion have not been identified. Here, we describe the endothelial-derived secreted molecule, developmental endothelial locus-1 (Del-1), as an anti-adhesive factor that interferes with the integrin LFA-1-dependent leukocyte-endothelial adhesion. Endothelial Del-1-deficiency increased LFA-1-dependent leukocyte adhesion *in vitro* and *in vivo*. Del-1-/-mice displayed significantly higher neutrophil accumulation in LPS-induced lung inflammation *in vivo*, which was reversed in Del-1/LFA-1-double deficient mice. Thus, Del-1 is an endogenous inhibitor of inflammatory cell recruitment and could provide a basis for targeting leukocyte-endothelial interactions in disease.

Leukocyte extravasation is integral to the response to infection or injury and to inflammation and autoimmunity. Leukocyte recruitment comprises a well coordinated cascade of adhesive events including selectin-mediated rolling, firm adhesion of leukocytes to endothelial cells and

&This manuscript has been accepted for publication in *Science*. This version has not undergone final editing. Please refer to the complete version of record at http://www.sciencemag.org/. The manuscript may not be reproduced or used in any manner that does not fall within the fair use provisions of the Copyright Act without the prior, written permission of AAAS.

†To whom correspondence should be addressed chavakist@mail.nih.gov.
*EYC and EC contributed equally
#MAC and HL contributed equally

NIH-PA Author Manuscript
NIH-PA Author Manuscript
NIH-PA Author Manuscript

their subsequent transendothelial migration. The interaction between LFA-1 (αLβ2, CD11a/CD18) and endothelial ICAM-1 is crucial during firm endothelial adhesion of leukocytes (1-5). Whereas numerous adhesion receptors promoting inflammatory cell recruitment have been identified, very little information exists about endogenous inhibitors of the leukocyte adhesion cascade (1-7). Developmental endothelial locus-1 (Del-1) is a glycoprotein that is secreted by endothelial cells and can associate with the endothelial cell surface and the extracellular matrix (8-10). Del-1 is regulated upon hypoxia or vascular injury and has been implicated in vascular remodelling during angiogenesis (10-12). Here, we sought to determine whether endothelial-derived Del-1 participates in leukocyte-endothelial interactions. RT-PCR analysis revealed Del-1 mRNA predominantly in the brain and lung, with no expression in liver, spleen, or whole blood (Fig. 1A and fig. S1A). Del-1 was expressed in WT but not in Del-1-/- murine lung endothelial cells (Fig. 1B, *9*). Immunohistochemistry of lung tissues demonstrated the presence of Del-1 in vessels, as observed by co-staining with the endothelial marker PECAM-1 (fig. S1B).

To determine whether Del-1 participates in leukocyte recruitment interactions, we studied adhesion of primary neutrophils to immobilized Del-1. Mouse neutrophils specifically bound to Del-1 under static conditions. Adhesion was inhibited by a blocking monoclonal antibody (mAb) to CD11a (αL-integrin subunit), but not by antibodies to αv-integrin or β1-integrin (Fig. 1C), suggesting that LFA-1 mediates the interaction of neutrophils with Del-1. Consistently, LFA-1-/- neutrophils displayed reduced adhesion to Del-1 (Fig. 1C). The residual, LFA-1-independent binding of neutrophils to Del-1 was blocked by mAb to Mac-1 (fig. S2A), consistent with the fact that LFA-1 and Mac-1 are closely related and share several ligands (13). In addition, αL-transfected but not vector-transfected J-β_2.7 cells specifically bound to immobilized Del-1 (Fig. 1D), whereas a direct interaction between Del-1 and the ligand-binding I-domain of LFA-1, locked in the open high-affinity conformation, was observed (Fig. 1E and fig. S2B). These findings indicate that Del-1 is a ligand of LFA-1 integrin.

To address whether Del-1 participates in leukocyte-endothelial interactions, we studied neutrophil and monocyte adhesion to WT and Del-1-/- endothelial cells (14,15). Contrary to our prediction, Del-1-/- endothelial cells promoted significantly higher neutrophil and monocyte adhesion. LFA-1-deficiency on leukocytes and mAb to LFA-1 abolished the enhanced adhesion to Del-1-/- endothelium (Fig. 2A and fig. S3). Thus, enhanced inflammatory cell adhesion to Del-1-/- endothelium is specifically mediated by LFA-1 on leukocytes.

To understand the unexpected inhibitory role of Del-1 in leukocyte-endothelial adhesion, we addressed whether soluble Del-1 interfered with the interaction of LFA-1 with its major ligand, ICAM-1. Mn^{2+} -induced binding of ICAM-1-Fc to murine leukocytes in solution was significantly inhibited by soluble Del-1 (Fig. 2B). Moreover, soluble Del-1 inhibited the LFA-1-dependent adhesion of WT neutrophils to immobilized ICAM-1 under physiologic flow conditions, whereas soluble Del-1 did not affect the weaker adhesion of LFA-1-/- neutrophils to ICAM-1 (Fig. 2C).

The finding that endothelial Del-1 antagonizes LFA-1-dependent adhesion (Fig. 2A) appeared to be discordant with the finding that immobilized Del-1 promoted leukocyte adhesion under static conditions (Fig. 1C). We therefore assessed the ability of Del-1 and ICAM-1 to promote adhesion when co-immobilized with P-selectin and the chemokine MIP-2 under physiologic flow conditions at low and high shear rate (0.8 and 2 dynes/cm^2). In this system leukocytes first roll on selectin and then arrest on the integrin ligand. Whereas ICAM-1 promoted robust firm adhesion of neutrophils under both shear rates, Del-1 promoted only weak adhesion under the lower shear rate and almost none at the higher shear rate (Fig. 2D). We then analyzed how the presence of plate-bound Del-1 would affect adhesion of neutrophils to ICAM-1 under flow. Increasing concentrations of Del-1 co-immobilized with ICAM-1, P-selectin and MIP-2

significantly inhibited neutrophil adhesion to ICAM-1 (Fig. 2E). Thus, although being a ligand of LFA-1, Del-1 does not promote firm leukocyte adhesion under flow but interferes with leukocyte adhesion to endothelial ICAM-1.

We then assessed the ability of soluble Del-1 expressed as an Fc fusion protein to inhibit neutrophil recruitment *in vivo* in acute thioglycollate-induced peritonitis (14). Intravenous administration of Del-1-Fc 30 min prior to thioglycollate injection significantly reduced neutrophil accumulation, as compared to Fc control protein (Fig. 2F). Similarly, ICAM-1-Fc reduced neutrophil recruitment into the peritoneum (Fig. 2F).

To provide further evidence for the role of Del-1 in inflammatory cell recruitment *in vivo*, we performed intravital microscopy using the dorsal skinfold chamber model (16). Del-1-/- mice displayed increased numbers of leukocytes adherent to postcapillary venules both at baseline and upon TNF-α stimulation (Fig. 3A and B). Besides firm arrest, the interaction between LFA-1 and ICAM-1 contributes to slow rolling processes (17). A significant decrease in rolling velocity accompanied by an increase in the fraction of slow rolling leukocytes was observed in Del-1-/- mice (Fig. 3C and 3D).

We further studied whether Del-1 could regulate inflammatory cell recruitment *in vivo*, by performing LPS-induced lung inflammation. Del-1-/- mice displayed significantly higher accumulation of neutrophils in the bronchoalveolar lavage (BAL) fluid, as compared to WT mice (Fig. 4A). LFA-1-/- mice displayed reduced neutrophil accumulation in the BAL upon LPS-induced lung inflammation (Fig. 4A), consistent with a previous report (18). The increased neutrophil recruitment *in vivo* due to Del-1 deficiency required the presence of LFA-1, as neutrophil accumulation in the BAL in Del-1-/-LFA-1-/- mice equaled accumulation of these cells in LFA-1-/- mice (Fig. 4A). The increased leukocyte recruitment due to Del-1 deficiency could not be attributed to an alteration in peripheral blood counts, since constitutive leukocyte numbers were comparable in WT and Del-1-/- mice (fig. S4). In addition, i.v. administration of soluble Del-1 efficiently reversed the increased neutrophil recruitment in Del-1-/- mice (Fig. 4B). Furthermore, we found that Del-1-deficiency resulted in an upregulation of baseline ICAM-1 protein expression by lung endothelial cells, which was overridden upon TNF-α stimulation, whereas VCAM-1 expression was unaffected (fig. S5). No significant increase in ICAM-1 expression, under baseline or inflammatory conditions, was found in Del-1-/- lungs (fig. S6), suggesting that altered ICAM-1 expression is not involved in the increased leukocyte recruitment to Del-1-/- lungs. Moreover, whereas the increased neutrophil recruitment to the lung upon Del-1-deficiency was completely reversed by leukocyte LFA-1-deficiency (Fig. 4A), inhibition of ICAM-1 by a blocking mAb (18,20) decreased neutrophil recruitment by the same extent in both WT and Del-1-/- mice (Fig. 4C), implying an involvement of other LFA-1 ligands. These findings suggest that Del-1 deficiency enhances LFA-1-dependent leukocyte recruitment *in vivo*.

We found Del-1 to act in an anti-inflammatory fashion, however the expression of Del-1 in inflammation has not been previously elucidated. We therefore analyzed Del-1 mRNA expression in the lung and in endothelial cells upon inflammatory stimulation. Upon LPS administration, lung Del-1 mRNA was significantly reduced (Fig. 4D). Likewise, TNF-α stimulation of endothelial cells induced a significant decrease in Del-1 expression (fig. S7).

Endogenous inhibitors exist in many aspects of inflammation and immunity (21,22), attenuating exuberant inflammatory and immune activation. To date, no endogenous inhibitor was known in the leukocyte adhesion cascade, a central paradigm of inflammation and immunity. Here, endothelial-derived Del-1 was identified to intercept LFA-1-dependent leukocyte-endothelial interactions. Given the importance of LFA-1-dependent leukocyte recruitment in several inflammatory and autoimmune disorders (13,23-25), Del-1 may provide

a platform for designing novel attractive therapeutic modalities to target leukocyte-endothelial interactions in disease.

Supplementary Material

Refer to Web version on PubMed Central for supplementary material.

Acknowledgments

We thank X. Feng and M. Sardy for generating the Del-1-Fc protein, N. Hogg for the antibody mAb24, Valentis Inc. for recombinant Del-1 and the antibody to mouse Del-1, T. Veenstra for help with mass spectrometry, D. Winkler for help with genotyping, I. Okwumabua for technical assistance and D. Singer for critically reading the manuscript. This research was supported by the Intramural Research Program of the NIH, NCI (T.C. and M.U.), by NIH grants AI067254 (S.C.), RO1 HL082927 (W.C.A), and by the Deutsche Forschungsgemeinschaft (FOR809, TP6 to C.W.; and TR-SFB23; Exc 147/1 to S.D. and E.C.). A patent application on the anti-inflammatory actions of Del-1 has been filed.

References and Notes

1. Springer TA. Cell 1994;76:301. [PubMed: 7507411]
2. Hogg N, Laschinger M, Giles K, McDowall A. J Cell Sci 2003;116:4695. [PubMed: 14600256]
3. Vestweber D. Immunol Rev 2007;218:178. [PubMed: 17624953]
4. Imhof BA, Aurrand-Lions M. Nat Rev Immunol 2004;4:432. [PubMed: 15173832]
5. Ley K, Laudanna C, Cybulsky MI, Nourshargh S. Nat Rev Immunol 2007;7:678. [PubMed: 17717539]
6. Weber C, Fraemohs L, Dejana E. Nat Rev Immunol 2007;7:467. [PubMed: 17525755]
7. Chavakis T, Preissner KT, Herrmann M. Trends Immunol 2007;28:408. [PubMed: 17681885]
8. Hidai C, Kawana M, Kitano H, Kokubun S. Cell Tissue Res 2007;330:83. [PubMed: 17701220]
9. Hidai C, et al. Genes Dev 1998;12:21. [PubMed: 9420328]
10. Ho HK, et al. Circulation 2004;109:1314. [PubMed: 14981004]
11. Penta K, et al. J Biol Chem 1999;274:11101. [PubMed: 10196194]
12. Zhong J, et al. J Clin Invest 2003;112:30. [PubMed: 12840057]
13. Gahmberg CG, et al. Cell Mol Life Sci 1998;54:549. [PubMed: 9676574]
14. Materials and Methods are in the supporting online material.
15. Choi EY, et al. Blood 2008;111:3607. [PubMed: 18239087]
16. Fiedler U, et al. Nat Med 2006;12:235. [PubMed: 16462802]
17. Zarbock A, Lowell CA, Ley K. Immunity 2007;26:773. [PubMed: 17543554]
18. Basit A, et al. Am J Physiol Lung Cell Mol Physiol 2006;291:L200. [PubMed: 16461431]
19. Ding ZM, et al. J Immunol 1999;163:5029. [PubMed: 10528208]
20. Kumasaka T, et al. J Clin Invest 1996;97:2362. [PubMed: 8636417]
21. Parry RV, Riley JL, Ward SG. Trends Immunol 2007;28:161. [PubMed: 17336157]
22. Greenwald RJ, Freeman GJ, Sharpe AH. Annu Rev Immunol 2005;23:515. [PubMed: 15771580]
23. Lebwohl M, et al. N Engl J Med 2003;349:2004. [PubMed: 14627785]
24. Luster AD, Alon R, von Andrian UH. Nat Immunol 2005;6:1182. [PubMed: 16369557]
25. Yonekawa K, Harlan JM. J Leukoc Biol 2005;77:129. [PubMed: 15548573]

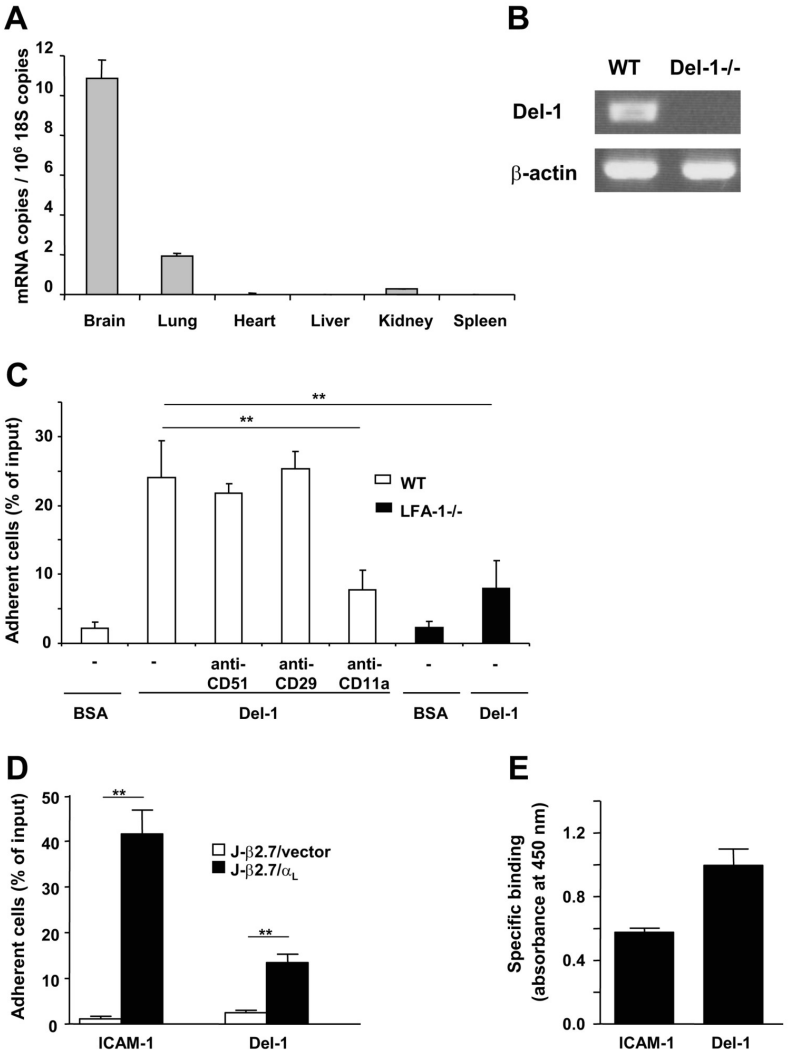

Figure 1. Del-1 is expressed in endothelial cells and interacts with leukocyte LFA-1

(A) Real-time RT-PCR demonstrating the expression of Del-1 mRNA in adult mouse tissues. Del-1 mRNA was normalized against 18S rRNA. (B) RT-PCR in primary lung endothelial cells from WT and Del-1-/- mice. (C) Static adhesion of PMA-stimulated WT (open) or LFA-1-/- (filled) neutrophils to immobilized BSA or mouse Del-1 is shown in the absence (-) or in the presence of mAbs to CD51 (αv-integrin), to CD29 (β1-integrin), or to CD11a (LFA-1). Adhesion is presented as % adherent cells. Data are mean ± SD (n=3). **, $P<0.01$. (D) Adhesion of J-β_2.7 transfectants expressing LFA-1 (J-β_2.7/α_L) or vector (J-β_2.7/vector) to immobilized Del-1 or ICAM-1. Adhesion is presented as % adherent cells. Data are mean ± SEM (n=3). **,

P<0.01. (E) Binding of the LFA-1 I-domain to immobilized Del-1 or ICAM-1. Specific binding is expressed as absorbance at 450 nm. Data are mean ± SEM (n=3).

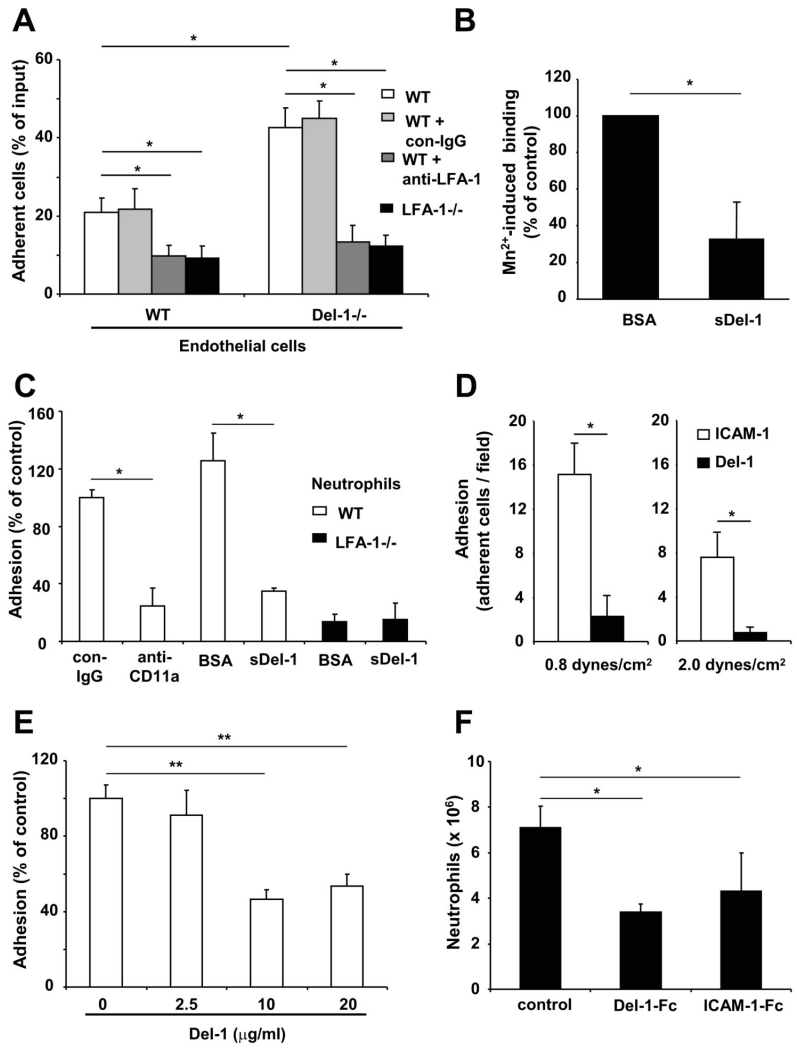

Figure 2. Del-1 interferes with LFA-1-dependent leukocyte adhesion

(A) PMA-induced adhesion of WT neutrophils in the absence (open) or presence of isotype control antibody (light gray) or mAb to LFA-1 (dark gray), or of LFA-1-/- neutrophils (filled) to WT or Del-1-/- lung endothelial cells is shown. Adhesion is presented as % adherent cells. Data are mean ± SD (n=4). *, P<0.05. (B) Binding of soluble ICAM-1-Fc to mouse bone marrow mononuclear cells in the presence of $MnCl_2$. Cells were preincubated with BSA or soluble Del-1. Data are mean ± SEM (n=3). *, P<0.05. (C) Adhesion of WT (open) or LFA-1-/- (filled) neutrophils to immobilized P-selectin, MIP-2 and ICAM-1 under flow (0.8 dyn/cm_2) was studied in the presence of mAb to CD11a or isotype control antibody (each mAb 10 μg/ml), or in the presence of BSA or mouse soluble Del-1 (each at 20 μg/ml). Adhesion is shown

as % of control i.e. adhesion of WT neutrophils in the presence of control antibody. Data are mean ± SEM (n=3). *, P<0.05. (D) Adhesion of WT neutrophils to immobilized P-selectin, MIP-2 and ICAM-1 (open) or Del-1 (filled) was studied at indicated shear rates. Adhesion is shown as number of adherent cells/field. Data are mean ± SEM (n=4). *, P<0.05. (E) Adhesion of WT neutrophils to immobilized P-selectin, MIP-2 and ICAM-1 was studied in the presence of increasing concentrations of Del-1 that was coimmobilized. Adhesion is shown as % of control i.e. adhesion of WT neutrophils in the absence of immobilized Del-1. Data are mean ± SEM (n=6). **, P<0.01. (F) The numbers of neutrophils at 4 h after i.p. injection of thioglycollate in WT mice are shown. Mice were treated 30 min prior to thioglycollate injection with i.v. injection of control Fc protein, Del-1-Fc or ICAM-1-Fc. Data are expressed as absolute numbers of emigrated neutrophils. Data are mean ± SD (n=4 mice/group). *, P<0.05.

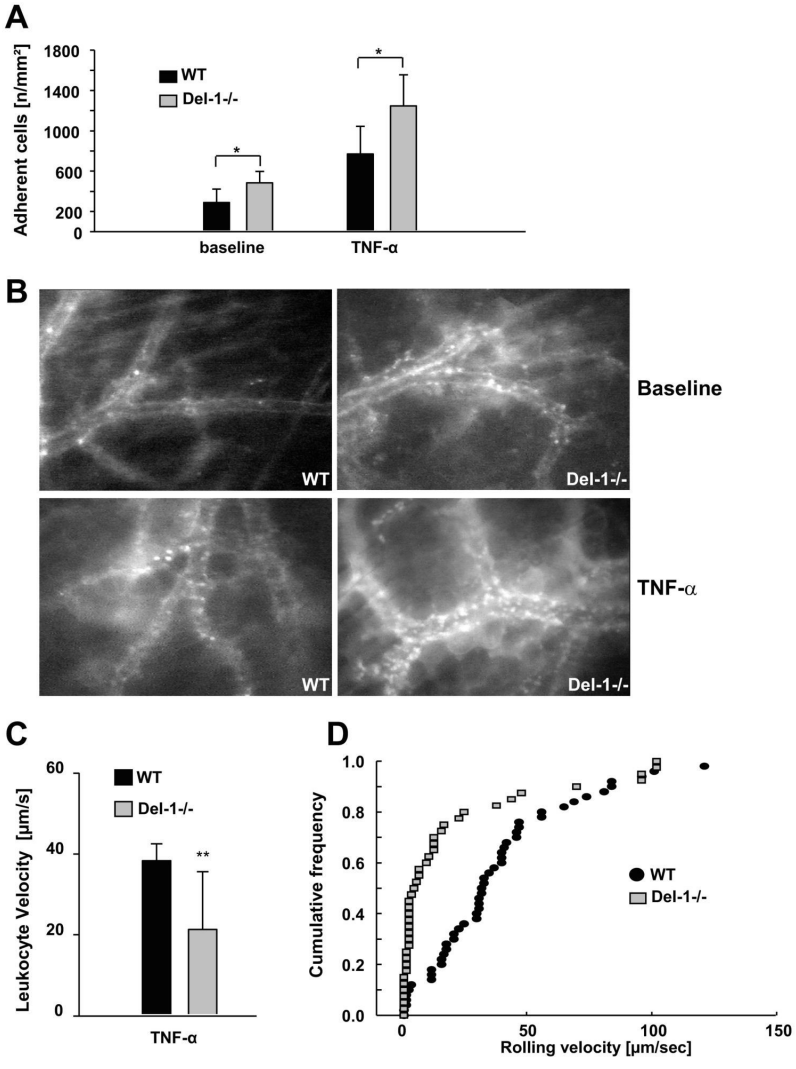

Figure 3. Slow rolling and firm adhesion of inflammatory cells *in vivo* are enhanced due to Del-1 deficiency in the dorsal skinfold chamber model

(A) The number of leukocytes adherent to the endothelium of postcapillary venules were assessed in WT (filled) or Del-1-/- (gray) mice at baseline conditions as well as 2 h after TNF-α superfusion. Adherent leukocytes are shown as number of cells per vessel surface (mm^2). Data are mean ± SD (n=5 mice/group). *, $P<0.05$. (B) Representative images of Rhodamine 6G labeled leukocytes adherent onto the endothelium of postcapillary venules of WT and Del-1-/- mice. (C) The average rolling leukocyte velocities at 2 h after TNF-α superfusion in WT (filled) and Del-1-/- (gray) mice are shown. Data are mean ± SD (n=5 mice/group). **,

P<0.01. (D) The rolling flux fraction at 2 h after TNF-α superfusion in WT (filled circles) and Del-1-/- (gray squares) mice.

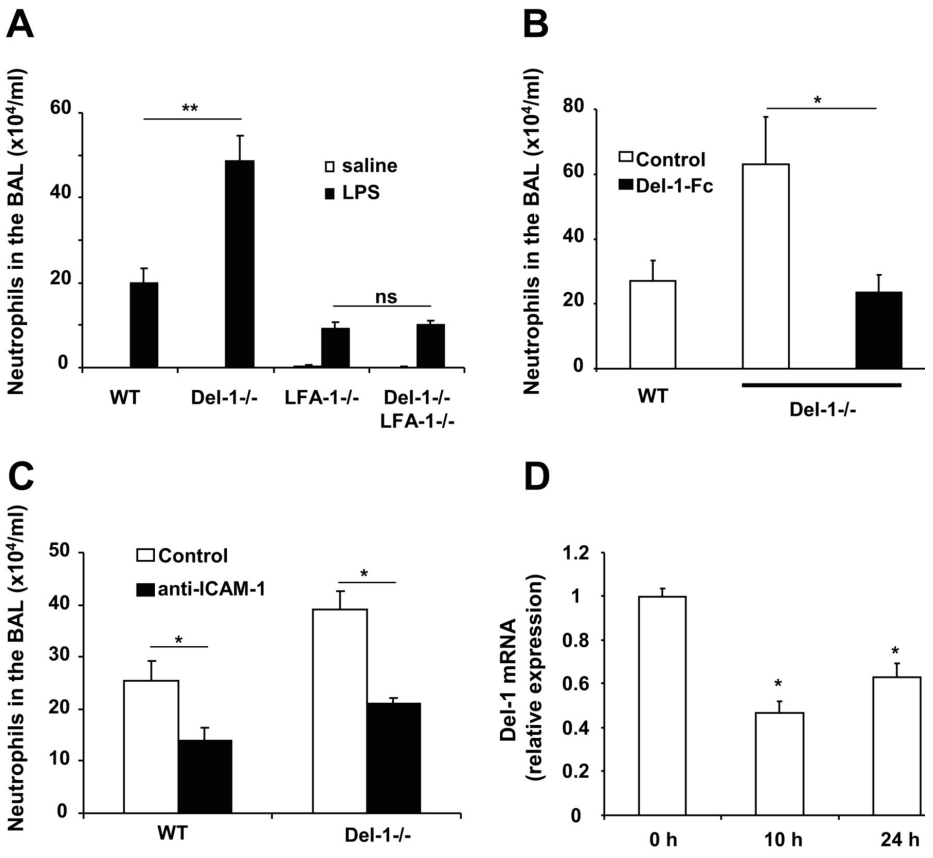

Figure 4. Increased inflammatory cell recruitment *in vivo* due to Del-1 deficiency

(A) The numbers of neutrophils in the BAL fluid in WT, Del-1-/-, LFA-1-/- or Del-1-/-LFA-1-/- mice are shown at 24 h after nasal administration of saline (open) or LPS (filled). Neutrophil recruitment upon saline inhalation was negligible. Data are expressed as absolute numbers and are mean ± SEM (n=11-16 mice/group). **, P<0.01; ns, not significant. (B) Thirty min prior to LPS administration WT or Del-1-/- mice received i.v. injections of BSA (control, open bars) or Del-1-Fc (filled bar) (each at 90 μg/mouse). Data are expressed as absolute numbers and are mean ± SEM (n=4-11 mice/group). *, P<0.05. (C) Thirty min prior to LPS administration WT or Del-1-/- mice received i.v. injections of isotype control IgG (open) or anti-ICAM-1 (filled) (each at 85 μg/mouse). Data are expressed as absolute numbers and are mean ± SEM (n=8-9 mice/group). *, P<0.05. (D) The expression of Del-1 mRNA in mouse lungs at 0 h, 10 h or 24 h post intranasal LPS administration was analyzed by semiquantitative RT-PCR. The data are shown as relative expression. The ratio of Del-1 mRNA / actin mRNA at 0 h was set as 1. Data are mean ± SEM (n=4). *, P<0.05 as compared to 0 h.

Carl_G_190x270_mm_blokki_FINAL.indd 363 06-Aug-23 1:54:19 PM

Carl_G_190x270_mm_blokki_FINAL.indd 364 06-Aug-23 1:54:19 PM

Part V

REGULATION OF INTEGRIN ACTIVITY BY PHOSPHORYLATION

Carl_G_190x270_mm_blokki_FINAL.indd 365 06-Aug-23 1:54:19 PM

Introduction

The integrins are normally inactive, and need activation signals to become active. A major scientific problem is the regulation of integrin activity. A detailed understanding of integrin regulation, could enable the development of specific drugs, which would affect integrin dependent binding of cells and integrin signalling.

Structural studies showed that in resting cells, the integrin ligand binding head is turned towards the membrane, and the integrin straightens out on activation. Further activation results in opening of the binding site. Several articles deal with structural information on integrins (1-8). The regulation of integrin activity is an important issue, and blood cell integrins are excellent models, because cells like leukocytes and platelets are normally resting, but can easily be activated. Integrins are activated, either through inside-out, or outside-in signalling. In the former case, receptors like chemokine receptors signal to the integrins by intracellular signalling routes, and in the latter case, ligands bind to integrins from the outside, and induce activation. In Part III, I described how we identified and characterized integrins. We used cellular activation using phorbol esters, followed by immune precipitation with monoclonal antibodies to cell surface molecules. Because the cellular receptors for phorbol esters are protein kinase Cs, there was a definitive possibility that the integrins themselves become phosphorylated upon activation. This indeed turned out to be the case. Even more important, the integrin phosphorylations turned out to be pivotal for the regulation of integrin activity.

Early work showed that the leukocyte β2 integrin α-chains were phosphorylated in resting cells, and the β-chains became phosphorylated only after activation (9,10). Therefore, early phosphorylation studies focussed on the β2-chain. Serine-756 was phosphorylated upon activation with phorbol esters, but mutation of the residue to alanine did not affect adhesion. Mutation of threonines 758-760 abrogated cell adhesion, but no phosphorylation on these residues was initially observed (11). Therefore, further studies on phosphorylation did not seem very exciting. Subsequent studies showed, however, that integrin phosphorylation is complex, and functionally important.

Comments on Papers 43 to 52

An important breakthrough in the elucidation of mechanisms how integrin activity is regulated occurred, when we found that when phosphatase activity is inhibited by the phosphatase inhibitor okadaic acid, the β2-polypeptide was phosphorylated not only on serine, but also on threonine (Paper 43). We observed the threonine phosphorylation both after activation with phorbol esters and CD3 antibodies. The β-chain phosphorylation correlated with increased binding to the cytoskeleton (12). Further work showed that the phosphorylation mainly

Carl_G_190x270_mm_blokki_FINAL.indd 366 06-Aug-23 1:54:19 PM

occurred on two threonines, and the mean stoichiometry of phosphorylation per phosphorylated residue was about 30% (13). Thus, the threonine phosphorylation was substantial. My graduate student Susanna Fagerholm then went to P. Cohen´s laboratory in Dundee to study the phosphorylation of the β2 cytoplasmic domain using purified protein kinase Cs. It turned out that S745, and T758 and T759 were phosphorylated by several protein kinase Cs, but not S756 (Paper 44). Thus, S756, which is strongly phosphorylated *in vivo* must be phosphorylated by some kinase that is activated through protein kinase Cs. Protein kinases are counteracted by phosphatases and for β1 integrins the β chain threonine phosphatase has been identified as PPM1F (14). No phosphatase has yet been identified for the β2-chain. We then made the finding that phospho-T758, bound the 14-3-3ζ protein. 14-3-3 proteins are dimers that bind to phosphorylated amino acids in proteins. We then showed that T758 was the major residue phosphorylated after CD3 stimulation, and no phosphorylation occurred on S756 (Paper 45). In phorbol ester stimulated cells S745 was weakly labelled and S756 strongly. As in β2, the first threonine in the threonine triplet of β7 was phosphorylated after stimulation. To directly show that the phospho-T758 is involved in integrin signalling, we made a membrane permeable peptide covering the phosphorylated site. It stimulated T cell adhesion and the small GTPases Rac-1 and Cdc-42 (15). Further work showed that signalling from phospho-T758 occurred through 14-3-3ζ and Tiam1 to Rac-1 (16). Rac-1 interacts with the actin cytoskeleton, and the signalling route may be important for integrin clustering and increase in avidity. It is important to note that the β2 cytoplasmic tail phosphorylated at T758 can form a complex simultaneously with 14-3-3ζ and talin (17). This could enable a simultaneous increase in integrin avidity and affinity. 14-3-3ζ binds to the TST sequence of β3 in platelets, and also to the Src tyrosine kinase (18).

The integrin α-chains are constitutively phosphorylated, and inhibition of phosphatase activity increased the phosphorylation, indicating that also there is turnover of the phosphate. Tiina Hilden determined the phosphorylation site in the α-chain of LFA-1, and it turned out to be at S1140. Surprisingly, its mutation to alanine, completely abrogated T cell adhesion (Paper 46). Similar findings were obtained for Mac-1 (S1126) (Paper 47) and αXβ2 (S1158) (19). The αD chain has not yet been studied in this respect.

The T758 site in the β2 chain forms part of the filamin binding region in β2. Susanna Fagerholm and others in my group found that binding of filamin took place to an unphoshorylated β2 cytoplasmic peptide,but phosphorylation of T758 inhibited filamin binding. Binding of the talin head domain was unaffected by phosphorylation, but in the presence of 14-3-3ζ proteins, talin binding was inhibited. Crystallographic studies by Jari Ylänne showed that the β2 peptide readily fitted into the filamin pocket, but when phosphorylated on T758, there was no room for the peptide in the pocket. The phosphorylated peptide bound to the 14-3-3ζ protein and the phosphate interacted with arginines 56 and 127 in 14-3-3ζ (Paper 48).

An important development occurred, when we showed that the S1140A mutation in LFA-1, in fact inhibited the β2 phosphorylation on T758, resulting in block of adhesion, binding of α-actinin, and inhibition of cell migration on an ICAM-1 surface (Paper 49). Currently, we do not know how the α-chain phosphorylation regulates the β-chain phosphorylation on T758. The simplest explanation would be that the negative charge on the α-chains results in repulsion from the cytoplasmic domain of β2, enabling access of the kinase, which phosphorylates β2. When both chains are phosphorylated interactions with 14-3-3ζ, talin and kindlin can take place.

Carl_G_190x270_mm_blokki_FINAL.indd 367 06-Aug-23 1:54:19 PM

Leukocyte integrins communicate with each other. Porter and Hogg showed that activation of LFA-1 on T cells decreased α4β1 and α5β1 functions, but the mechanism remained unclear (20). The α4β1 integrin binds to VCAM-1, and the active integrin is phosphorylated on T788/789 in β1. Activation of LFA-1 through the T cell receptor or the SDF-1 chemokine, resulted in phosphorylation of T758. This resulted in signalling through the 14-3-3ζ /Tiam-1/ Rac-1 pathway to α4β1 and dephosphorylation of β1, resulting in its inactivation (Paper 50). In subsequent studies, we showed that monoclonal antibodies to LFA-1, which activated the integrin, and antibodies, which signalled to α4β1, induced phosphorylation of T758 in β2, and inactivated α4β1 by dephosphorylation. This means that the effect of antibodies, may sometimes be due to integrins not directly targeted by the antibodies, but altered by intracellular signalling (Paper 51). For more details see our recently written a review on integrin phosphorylation (Paper 52).

References

1. Lee, J.-O., Rieu, P., Arnaout, M.A. and Liddington, R. (1995) Crystal structure of the A domain from the α subunit of integrin CR3 (CD11b/CD18) *Cell* **80**, 631-638.
2. Xiong, J.-P., Stehle, T., Diefenbach, B., Zhang, R., Dunker, R., Scott, D.I., Joachimiak, A., Goodman, S.L. and Arnaout, M.A. (2001) Crystal structure of the extracellular segment of integrin αVβ3. *Science* **294**, 339-345.
3. Vinogradova, O., Velyvis, A., Velyviene, A., Hu, B., Haas, T.A., Plow, E.F. and Qin, J. (2002) A structural mechanism of integrin αIIbβ3 inside-out activation as regulated by its cytoplasmic face. *Cell* **110**. 587-597.
4. Nishida, N., Xie, C., Shimaoka, M., Cheng, Y., Walz, T. and Springer, T.A. (2006) Activation of leukocyte beta2 integrins by conversion from bent to extended conformations. *Immunity* **25**, 583-594.
5. Luo, B.H., Carman, C.V. and Springer, T.A. (2007) Structural basis of integrin regulation and signaling. *Ann. Rev. Immunol*. **25**, 619-647.
6. Xiong, J.-P., Mahalingham, B., Alonso, J.L., Borrelli, L.A., Rui, X., Anand, S., Hyman, T.R., Rysiok, T., Muller-Pompalla, D., Goodman, S.L. and Arnaout, M.A. (2009) Crystal structure of the complete integrin alphaVbeta3 ectodomain plus an alpha/beta transmembrane fragment. *J. Cell Biol*. **186**, 589-600.
7. Xie, C., Zhu, J., Chen, X., Nishida, N. and Springer, T.A. (2010) Structure of an integrin with an alphaI domain, complement receptor type 4. *EMBO J*. **29**, 666-679.
8. Springer, T.A. and Sen, M. (2016) Leukocyte integrin αLβ2 headpiece structures: the αI domain, the pocket for the internal ligand, and concerted movements of its loops. *Proc. Natl. Acad. Sci. USA*. **113**, 2940-2945.
9. Chatila, T.A., Geha, R.S. and Arnaout, M.A. (1989) Constitutive and stimulus-induced phosphorylation of CD11/CD18 leukocyte adhesion molecules. *J. Cell Biol*. **109**, 3435-3444.
10. Buyon, J.P., Slade, S.G., Reibman, J., Abramson, J.B., Philips, M.R., Weissmann, G. and Winchester, R. (1990) Constitutive and induced phosphorylation of the α- and β-chains of the CD11/CD18 leukocyte integrin family. *J. Immunol*. **144**, 191-197.
11. Hibbs, M.L., Jakes, S., Stacker, S.T., Wallace, R.W. and Springer, T.A. (1991) The cytoplasmic domain of the integrin lymphocyte function-associated antigen-1 β

subunit: sites required for binding to intercellular adhesion molecule 1 and the phorbol ester-stimulated phosphorylation site. *J. Exp. Med*. **174**, 1227-1238.
12. Valmu, L., Fagerholm, S., Suila, H. and Gahmberg, C.G. (1999) The cytoskeletal association of CD11/CD18 leukocyte integrins in phorbol ester activated T cells correlates with CD18 phosphorylarion. *Eur. J. Immunol*. **29**, 2107-2118.
13. Valmu, L., Hilden, T.J., van Willigen, G. and Gahmberg, C.G. (1999) Characterization of β2 (CD18) integrin phosphorylation in phorbol ester-activated T lymphocytes. *Biochem. J*. **339**, 119-125.
14. Grimm, T.M., Dierdorf, N.I., Betz, K., Paone, C. and Hauck, C.R. (2020) PPM1F controls integrin activity via a conserved phospho-switch. *J. Cell Biol*. **219**, e202001057.
15. Nurmi, S.M., Autero, M., Raunio, A.K., Gahmberg, C.G. and Fagerholm, S.C. (2007) Phosphorylation of the LFA-1 integrin β2-chain on Thr-758 leads to adhesion, Rac-1/Cdc42 activation, and stimulation of CD69 expression in human T cells. *J. Biol. Chem*. **282**, 968-975.
16. Grönholm, M., Jahan, F., Marchesan, S., Karvonen, U., Aatonen, M., Narumanchi, S. and Gahmberg, C.G. (2011) TCR-induced activation of LFA-1 involves signaling through Tiam1. *J. Immunol*. **187**, 3613-3619.
17. Chatterjee, D., Zhiping, L.L., Tan, S.-M. and Bhattacharjya, S. (2016) Interaction analyses of the integrin β2 cytoplasmic tail with the F3 FERM domain of talin and 14-3-3ζ reveal a ternary complex with phosphorylated tail. *J. Mol. Biol*. **428**, 4129-4142.
18. Shen, C., Liu, M., Xu, R., Wang, G., Li, J., Chen, P., Ma, W., Mwangi, J., Lu, Q., Duan, Z., Zhang, Z., Dahmani, F.Z., Mackeigan, D.T., Ni, H. and Lai, R. (2020) The 14-3-3ζ-c-Src-integri-β3 complex is vital for platelet activation. *Blood* **136**, 974-988.
19. Uotila, L.M., Aatonen, M. and Gahmberg, C.G. (2013) Integrin CD11c/CD18 α-chain phosphorylation is functionally important. *J. Biol. Chem*. **288**, 33494-33499.
20. Porter, J.C. and Hogg, N. (1997) Integrin cross talk: activation of lymphocyte function-associated antigen-1 on human T cells alters α4β1- and α5β1-mediated function. *J. Cell Biol*. **138**, 1437-1447.

Carl_G_190x270_mm_blokki_FINAL.indd 369 06-Aug-23 1:54:19 PM

The Journal of Immunology
RESEARCH ARTICLE | AUGUST 01 1995

Treatment with Okadaic Acid Reveals Strong Threonine Phosphorylation of CD18 After Activation of CD11/CD18 Leukocyte Integrins with Phorbol Esters or CD3 Antibodies[1]

Leena Valmu and Carl G. Gahmberg[2]

Department of Biosciences, Division of Biochemistry, University of Helsinki, Finland

The CD11/CD18 leukocyte integrins comprise three heterodimers involved in leukocyte adhesion. CD11/CD18 avidity may be regulated intracellularly, and the CD18 polypeptide has previously been shown to become phosphorylated in leukocytes after phorbol ester stimulation. The importance of phosphorylation in the regulation of CD11/CD18 avidity has, however, remained unclear. We have now activated T cells using phorbol esters, CD3, and CD44 Abs. Both phorbol ester and CD3 treatment activated protein kinase C. CD18 was shown to become more stably phosphorylated after phorbol ester treatment and more transiently so after CD3 stimulation. The phosphorylation was strongly augmented by okadaic acid, a serine/threonine phosphatase inhibitor. While phorbol ester treatment caused phosphorylation mainly on serine, in okadaic acid-pretreated cells, both phorbol ester treatment as well as CD3 stimulation revealed strong threonine phosphorylation. Since earlier mutational studies have demonstrated the functional importance of cytoplasmic threonine residues in CD18, the threonine phosphorylation reported here indicates the role of threonine phosphorylation in the regulation of CD11/CD18 avidity. *The Journal of Immunology,* 1995, 155: 1175–1183.

Leukocyte adhesion is of pivotal importance in leukocyte physiology (1, 2). Leukocytes adhere to each other, as well as to other cells, by strictly regulated interactions of adhesion proteins (3, 4). However, the regulation of leukocyte adhesion is still poorly understood.

The CD11/CD18 leukocyte adhesion proteins are members of a family of cell-cell adhesion molecules known as integrins. These β_2 leukocyte integrins share a common β subunit (CD18), and have distinct α subunits (CD11a, CD11b, CD11c). Three cellular ligands for CD11/CD18 have been described: ICAM-1 (CD54), ICAM-2 (CD102), and ICAM-3 (CD50) (5–10). The CD11/CD18 integrins are not constitutively avid for ICAMs, but the interaction with ICAMs requires an activation of CD11/CD18. This activation event can, in T cells for example, be initiated by intracellular signals generated by the T cell receptor complex after the recognition of Ag. Activation of CD11/CD18 can be triggered artificially by addition of phorbol esters (11, 12), some CD11/CD18 antibodies (13–15), or through ligand stimulation (16, 17). The CD11/CD18 activation has also been shown to be induced by specific mAbs against some surface antigens such as CD3 (18, 19), CD2 (19), CD43 (20), and CD44 (21).

The finding that phorbol esters, which are potent activators of protein kinase C (PKC),[3] could induce leukocyte adhesion, and hence the high avidity state of CD11/CD18, led to the speculation of a role of CD11/CD18 phosphorylation in the activation of leukocyte integrins. Indeed, several reports have demonstrated changes in the phosphorylation status of the CD11/CD18 complex in phorbol ester-activated cells (22–25). Constitutive phosphorylation of CD11 was reported, as well as phorbol ester-induced phosphorylation of the CD18 polypeptide in mononuclear leukocytes (22, 24, 25), monocytes (23), and neutrophils (23, 24). The induced phosphorylation of CD18 was shown to occur mainly on serine, both in CD18 immunoprecipitated from in vivo ^{32}P-labeled monocytes (23), as well as in CD18 phosphorylated in vitro by PKC (25).

Received for publication March 22, 1995. Accepted for publication May 17, 1995.

The costs of publication of this article were defrayed in part by the payment of page charges. This article must therefore be hereby marked *advertisement* in accordance with 18 U.S.C. Section 1734 solely to indicate this fact.

[1] This study was supported by the Academy of Finland, the Sigrid Jusélius Foundation, the Finnish Cancer Society, the University of Helsinki, and the Magnus Ehrnrooth Foundation.

[2] Address correspondence and reprint requests to Dr. Carl G. Gahmberg, Department of Biosciences, Division of Biochemistry, P.O. Box 56 (Viikinkaari 5), 00014 University of Helsinki, Finland.

[3] Abbreviations used in this paper: PKC, protein kinase C; PDBu, phorbol 12,13-dibutyrate; RC, resting cell.

Copyright © 1995 by The American Association of Immunologists

0022-1767/95/$02.00

Carl_G_190x270_mm_blokki_FINAL.indd 370 06-Aug-23 1:54:20 PM

The importance of the CD18 chain, and especially its cytoplasmic domain in CD11/CD18 activation, was further illustrated (26). When the cytoplasmic domain of CD18 was deleted, the CD11/CD18 complex lost its ability to become activated by phorbol esters. However, when putative phosphorylation sites were mutated (27), the importance of CD18 phosphorylation in CD11/CD18 activation became questionable. The major phosphorylation site on the CD18 polypeptide was found to be Ser-756. When this serine residue was mutated, the apparently unphosphorylated CD11/CD18 molecules retained their ability to become activated by phorbol esters. Therefore, it was concluded that the phosphorylation of Ser-756 on CD18 was not essential in the activation of CD11/CD18 integrins. In the same study (27), however, it was noted that mutation of the putative threonine phosphorylation sites in CD18 caused a dramatic decrease in integrin adhesive function. But since the phosphothreonine level observed in phorbol ester-activated, ^{32}P-labeled CD18 molecules was only minimal (23, 27), no significance was imposed on this observation.

As the importance of CD18 phosphorylation has remained unclear, and most studies had been carried out with phorbol esters, a nonphysiologic activator of cells, we have now expanded the study of CD18 phosphorylation by using CD3 and CD44 stimulation. The involvement of protein kinases and phosphatases in the homotypic T cell aggregation caused by these agents was studied using specific inhibitors as well as by direct PKC activity measurement. A minimal and transient CD18 phosphorylation was detected in CD3 stimulated T cells in contrast to a long-lasting phosphorylation caused by phorbol esters. By using the phosphatase inhibitor, okadaic acid, the phosphorylation of CD18 caused by these agents was greatly increased. Most interestingly, the inhibition of phosphatase activity resulted in strong threonine phosphorylation in CD18 in phorbol ester- and CD3-stimulated T cells. Because of the reported fundamental importance of the cytoplasmic threonine residues of CD18 in the function of CD11/CD18 integrins (27, 28), it is possible that the threonine phosphorylation of CD18 is essential in leukocyte adhesion induced through CD3 or by phorbol esters.

Materials and Methods

Reagents

Ficoll-Hypaque was purchased from Pharmacia Biotech AB (Uppsala, Sweden). Phosphate-free MEM and RPMI 1640 were from Sigma Chemical Co. (St. Louis, MO). FCS, L-glutamine and penicillin-streptomycin for cell isolation and culture were obtained from Biological Industries (Kibbutz Bet HaEmek, Israel), whereas phosphate-free penicillin-streptomycin for ^{32}P-radiolabeling was from Life Technologies (Grand Island, NY). *o*-Phospho-DL-serine, *o*-phospho-DL-threonine, and *o*-phospho-DL-tyrosine, as well as PMSF, sodium orthovanadate, BSA, deoxycholic acid, leupeptin, and aprotinin were purchased from Sigma Chemical Co. Ninhydrin and sodium fluoride were from Merck (Darmstadt, Germany). Triton X-100 and SDS were from BDH Chemicals Ltd. (Poole, United Kingdom). DE-52 cellulose was purchased from Whatman (Maidstone, United Kingdom). Polyvinylidene difluoride membranes were from Millipore (Bedford, MA). The phorbol diester PDBu (Sigma) and staurosporine (Sigma) were dissolved in dimethylsulfoxide and okadaic acid (Sigma) in ethanol. The Protein Kinase C Enzyme Assay System, as well as [^{32}P]orthophosphate (carrier free in aqueous solution, 10 mCi/ml, 5000 Ci/mmol), [γ-^{32}P]ATP (in aqueous solution 10 mCi/ml, >5000 Ci/mmol), and the [^{14}C]methylated protein standards were purchased from the Radiochemical Centre (Amersham, United Kingdom).

Antibodies

mAb R7E4 against the CD18-subunit of CD11/CD18 has been described previously (29). mAb OKT3, which reacts with CD3, was used in the form of ascites fluid produced by hybridoma cells (Clone CRL 8001; American Type Culture Collection, Rockville, MD). mAb B-G15 against CD44 was obtained from Innotest (Besançon, France). Mouse IgG1, which was used as a negative control, was purchased from Dako (Glostrup, Denmark).

Cells

Heparinized blood of healthy donors was obtained from the Finnish Red Cross Blood Transfusion Service, Helsinki, Finland. Mononuclear leukocytes were isolated by Ficoll-Hypaque gradient centrifugation. T cells were further enriched using nylon wool columns. Enriched T cells were suspended in RPMI 1640 medium supplemented with 10% FCS, L-glutamine, and antibiotics to a density of 1×10^6 cells/ml, and left in culture overnight at 37°C.

Aggregation assay

Aggregation of enriched T cells was assayed essentially as described (11). Briefly, cells were suspended in RPMI 1640 supplemented with 10% FCS and 50 mM HEPES to a density of 20×10^6 cells/ml. Samples were treated under constant agitation with either PDBu (200 nM), mAb OKT3 (1:200 dilution of ascites fluid), mAb B-G15 (50 μg/ml), or mouse IgG1 (10 μg/ml) for indicated time periods. In some experiments, the cells were preincubated in the presence of mAb R7E4 (50 μg/ml) for 15 min, or in the presence of staurosporine (5 μM) or okadaic acid (1.5 μM) for 20 min, before the addition of PDBu or mAbs. The percentage of aggregated cells was determined by immediately counting single cells in four aliquots of each sample in a hemocytometer. The results are representative of four separate experiments.

Protein kinase C activity assay

PKC was partially purified from membrane fractions of enriched T cells treated with either PDBu, mAb OKT3, or mAb B-G15. Briefly, cells (2×10^7) were treated with either PDBu (200 nM), mAb OKT3 (1:200 dilution of ascites fluid), mAb B-G15 (50 μg/ml), or left untreated. The activation was stopped after indicated times by adding ice-cold 2-mM EDTA/TBS. The cells were then sonicated in buffer I (20 mM Tris, 0.25 M sucrose, 10 mM EGTA, 2 mM EDTA, 0.5 mM PMSF, 10 μg/ml leupeptin, and 10 μg/ml aprotinin, pH 7.5) and centrifuged at 100,000 × *g* for 30 min at 2°C. The membrane-containing pellets were solubilized in the same buffer supplemented with 1% Nonidet P-40 and applied to 1 ml of DE-52 columns equilibrated with buffer II (20 mM Tris, 50 mM β-mercaptoethanol, 1 mM EGTA, 2 mM EDTA, and protease inhibitors, pH 7.5). Columns were washed with buffer II, buffer III (20 mM Tris, 50 mM β-mercaptoethanol, 1 mM EGTA, and 1 mM EDTA, pH 7.5) and buffer III, containing 30 mM NaCl. PKC was eluted with 1.5 ml of buffer III, containing 240 mM NaCl, and was used for the in vitro measurements of PKC activities using the Protein Kinase C Enzyme Assay System.

^{32}P radiolabeling and cell activation

Cells were washed with phosphate-free MEM and suspended in the same medium supplemented with 5% dialyzed FCS, 10 mM HEPES, L-glutamine, and antibiotics to a density of 20 to 50 × 10^6 cells/ml. After preincubation for 45 min at 37°C, 2 mCi of [^{32}P]orthophosphate was added. Cells were labeled at 37°C for 3 h. The cell suspension was then divided into equal aliquots, which were activated with either PDBu, OKT3, or B-G15 for indicated times. Control samples were left untreated. The activation was stopped by adding ice-cold 10 mM EDTA/

Carl_G_190x270_mm_blokki_FINAL.indd 371 06-Aug-23 1:54:20 PM

PBS. Cells were washed once with ice-cold 2 mM EDTA/PBS, and lysed at 0°C for 15 min in 1% Triton X-100, 10 mM sodium phosphate, 10 mM sodium pyrophosphate, 50 mM sodium fluoride, 1 mM sodium orthovanadate, 10 mM EDTA, 350 mM NaCl, 2mM PMSF, 10 μg/ml leupeptin, and 10 μg/ml aprotinin, pH 7.4. Cell lysates were centrifuged at 60,000 × *g* for 30 min at 2°C and the supernatants were used for immunoprecipitations.

Immunoprecipitation

During immunoprecipitations, the concentration of NaCl in the reaction mixture was maintained at 350 mM and the reaction mixture was supplemented with a "detergent cocktail" containing 0.2% SDS, 1% Triton X-100, 0.5% deoxycholic acid, and 10 μg/ml of BSA in PBS. This detergent mixture constituted one-third of the total volume of the reaction mixture during immunoprecipitation. The immunoprecipitations were done using the staphylococcal protein A technique essentially as described (30).

SDS-PAGE and fluorography

SDS-PAGE was performed according to Laemmli (31), using an 8% acrylamide concentration. The gels were treated for fluorography (32) and exposed to Kodak X-Omat AR film (Eastman Kodak, Rochester, NY) using Dupont Quanta III intensifying screens.

Phosphoamino acid analysis

The CD11/CD18 complexes immunoprecipitated from ^{32}P-labeled cells were electrophoresed on SDS-PAGE and blotted onto polyvinylidene difluoride membranes, which then were subjected to autoradiography. The region in the membrane corresponding to CD18 was excised and subjected to hydrolysis in 6 N HCl for 2 h at 110°C. The hydrolysate was lyophilized and standard phosphoamino acids were added. Phosphoamino acids were separated using two-dimensional electrophoresis on a 20 × 20-cm cellulose plate (33). The plate was dried and standard amino acids were visualized by staining with ninhydrin. The plate was exposed to Kodak X-Omat AR film using a Kodak X-Omat regular intensifying screen. The amounts of radioactivity in phosphoamino acids were quantified using a phosphoimager, Fuji BAS 1000 (Tokyo, Japan).

Results

Staurosporine and okadaic acid inhibit T cell aggregation stimulated by phorbol esters and CD3 antibody

Several reports have previously demonstrated the adhesion-promoting effect of phorbol esters (11, 12), as well as that of CD3 (18, 19) and CD44 Abs (21). PDBu, OKT3, and B-G15 were all effective in promoting homotypic T cell aggregation, mediated by CD11/CD18 integrins as shown by the blocking effect of the CD18 Ab (Fig. 1).

To further investigate the role of protein kinases and phosphatases in T cell aggregation, we tested the influence of specific inhibitors upon aggregation. Staurosporine, an inhibitor of PKC, was able to inhibit PDBu stimulated aggregation (Fig. 2*A*), as well as the aggregation induced by OKT3 (Fig. 2*B*). In contrast, it had no effect on the aggregation caused by B-G15 (Fig. 2*C*). Incubation of unstimulated cells with staurosporine had no significant effect on T cell aggregation (Fig. 2), and it did not affect cell viability (data not shown). These results indicate the involvement of protein kinases, possibly PKC, in the induction of T cell aggregation caused by phorbol esters or CD3 stimulation, but not in that caused by CD44 stimulation.

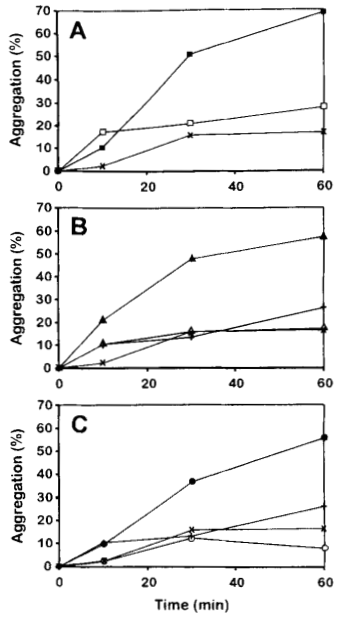

FIGURE 1. T cell aggregation induced by PDBu, OKT3, and B-G15. *A*, T cells were treated with 200 nM of PDBu (■) for indicated times, and the percentage of aggregated cells was determined by counting single cells. (□) cells were pretreated with the CD18 mAb R7E4 before adding PDBu. Resting cells (×) were left untreated. In *B*, T cells were treated with OKT3 without (▲) or with mAb R7E4 (△) and in *C*, with B-G15 without (●) or with R7E4 (○). Control cells (+) were treated with 10 μg/ml of mouse IgG1.

The effect of okadaic acid, an inhibitor of the serine/threonine phosphatases PP1 and PP2A, on T cell aggregation was studied. At 1.5 μM concentration it was shown to inhibit the T cell aggregation induced by all the reagents mentioned above (Fig. 3, *A–C*). Okadaic acid treatment alone had no effect on T cell aggregation (Fig. 3) or their viability (data not shown). The experiments shown in Figures 1 through 3 have been repeated at least four times with closely similar results.

Protein kinase C activity is increased in phorbol ester and CD3 stimulated T cells

The above results suggested a role of PKC in the induction of T cell aggregation. We further studied this possibility by analyzing the PKC activity of T cell membranes after phorbol ester treatment, as well as after CD3 and CD44 stimulation (Fig. 4). As seen in Figure 4*A*, activation of T cells with PDBu increased PKC activity about fourfold compared with that of resting cells. PKC activity remained high up to 30 min. Stimulation of T cells by OKT3 caused

Carl_G_190x270_mm_blokki_FINAL.indd 372 06-Aug-23 1:54:20 PM

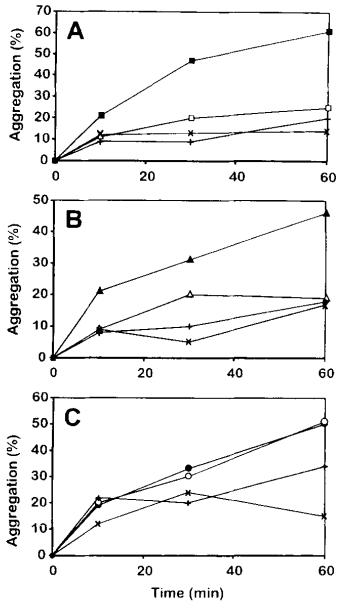

FIGURE 2. Effect of staurosporine on the T cell aggregation induced by PDBu, OKT3, and B-G15. In *A*, T cells were activated with PDBu in the absence (■) or presence (□) of 5 μM of staurosporine; in *B*, with OKT3 in the absence (▲) or presence (△) of staurosporine; and in *C*, with B-G15 in the absence (●) or presence (○) of staurosporine. Control cells (+) were incubated with staurosporine alone, and resting cells (×) were left untreated.

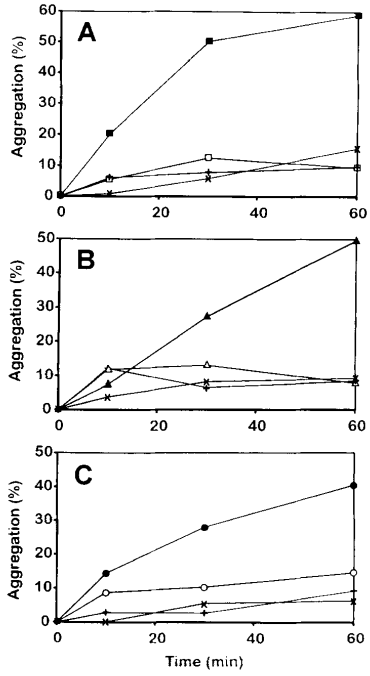

FIGURE 3. Effect of okadaic acid on the T cell aggregation induced by PDBu, OKT3, and B-G15. In *A*, T cells were activated with PDBu in the absence (■) or presence (□) of 1.5 μM of okadaic acid; in *B*, with OKT3 in the absence (▲) or presence (△) of okadaic acid; and in *C*, with B-G15 in the absence (●) or presence (○) of okadaic acid. Control cells (+) were treated with okadaic acid alone, and resting cells (×) were left untreated.

a transient increase in PKC activity (Fig. 4*B*), peaking at 5 min and returning to the basal level at 20 min. When PKC activity was determined in B-G15-stimulated T cells, no increase was detected (Fig. 4*C*). The results were repeatable in four separate experiments.

Phosphorylation of the CD18 is strongly augmented by okadaic acid in T cells activated with either phorbol esters or CD3 antibody

The phosphorylation of the CD11/CD18 polypeptides was studied in phorbol ester (Fig. 5*A*)-, CD3 Ab (Fig. 5*C*)-, and CD44 Ab (Fig. 5*E*)-stimulated T cells. The CD11/CD18 heterodimers were immunoprecipitated from resting and activated ^{32}P-labeled T cells using the mAb R7E4. The CD11 polypeptides were constitutively phosphorylated, and no obvious changes were observed upon stimulation. However, Figure 5*A* shows that activation of cells with 200 nM of PDBu induced phosphorylation of the CD18 chain, as previously reported (22–25). Maximal phosphorylation of CD18 was achieved already in 5 to 10 min. We observed a small and transient CD18 phosphorylation in OKT3-activated cells (Fig. 5*C*). The CD18 phosphorylation was weakly detectable after 5 min of activation, and disappeared after 10 min. In contrast to PDBu- and OKT3-treated cells, in T cells activated with B-G15, no CD18 phosphorylation was seen (Fig. 5*E*).

The possible involvement of phosphatases in CD11/CD18 integrin activation, and particularly in CD18 phosphorylation, was then studied using the serine/threonine phosphatase inhibitor, okadaic acid. ^{32}P-labeled T cells were preincubated with 1.5 μM of okadaic acid for 20 min before activating the cells with either PDBu, OKT3, or B-G15. Resting cells (RC) were incubated with okadaic acid alone. CD11/CD18 integrins were then immunoprecipitated. Okadaic acid treatment greatly enhanced the phosphorylation of the CD18 polypeptide induced by PDBu (Fig. 5*B*). The phosphorylation of CD18 was already increased after 2.5 min of activation, and it increased up to 30 min. It is worth noticing that the okadaic

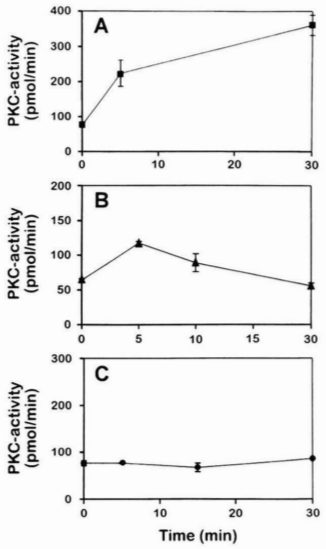

FIGURE 4. PKC activity in activated T cells. T cells were activated with either PDBu (A), OKT3 (B), or B-G15 (C), and PKC activity in the membrane fractions was measured at indicated times. The kinase activity is expressed as picomoles of phosphate incorporated into synthetic substrate per minute.

acid treatment alone caused no or minimal phosphorylation of the CD18 chain (Fig. 5, *B*, *D*, and *F*, RC). In OKT3-stimulated, okadaic acid-treated cells, the CD18 polypeptide was also clearly phosphorylated (Fig. 5*D*). The phosphorylation was already detectable after 2.5 min of activation and increased up to 30 min. No detectable CD18 phosphorylation was seen in B-G15-activated, okadaic acid-treated cells (Fig. 5*F*).

Okadaic acid treatment reveals threonine phosphorylation in CD18 after phorbol ester or CD3 stimulation

The strong increase in CD18 phosphorylation observed after okadaic acid treatment indicated the possibility of qualitative changes in phosphorylation. The CD11/CD18 heterodimers were immunoprecipitated from activated ^{32}P-labeled T cells, and the CD18 polypeptides were isolated and subjected to phosphoamino acid analysis. Phosphorylated amino acids were analyzed by two-dimensional, thin layer electrophoresis (Fig. 6). The phosphorylation of CD18 in T cells occurred primarily on serine residues after PDBu activation (Fig. 6*A*). These results agree with previous reports on phosphorylated amino acids of CD18 after phorbol ester stimulation in monocytes (23) and B lymphoblastoid cells (27).

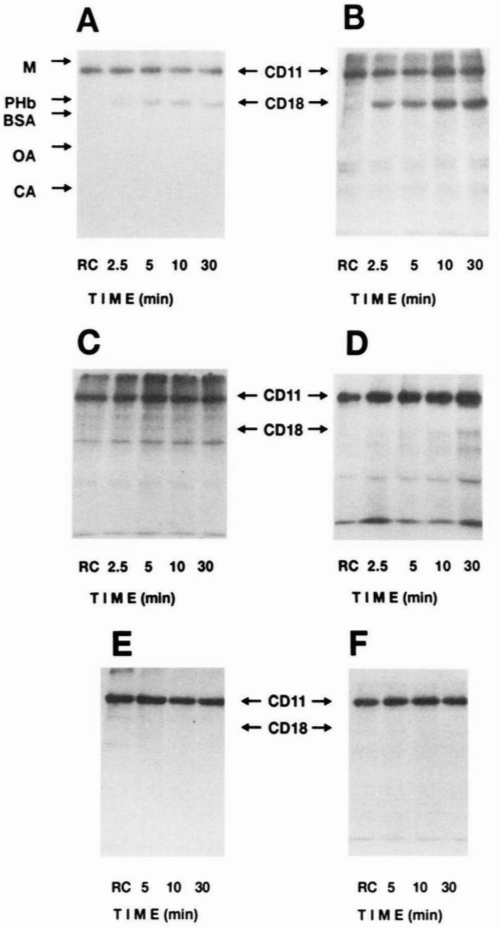

FIGURE 5. Phosphorylation of CD11/CD18 integrins. Autoradiographs of ^{32}P-labeled CD11/CD18 molecules immunoprecipitated from PDBu (*A* and *B*)-, OKT3 (*C* and *D*)-, and B-G15 (*E* and *F*)-activated T cells, which had been either pretreated with 1.5 μM of okadaic acid (*B*, *D*, and *F*) or not (*A*, *C*, and *E*). Resting cells (RC) not treated with activating agents (*A*, *C*, and *E*) or with okadaic acid only (*B*, *D*, and *F*). Activation times are indicated. The molecular masses of the standard proteins are: M, myosin = 200 kDa; PH_b, phosphorylase B = 92.5 kDa; BSA = 68 kDa; OA, ovalbumin = 46 kDa; CA, carbonic anhydrase = 30 kDa.

Interestingly, threonine phosphorylation was strongly increased both in PDBu (Fig. 6*B*)- and OKT3 (Fig. 6*C*)-stimulated T cells preincubated with okadaic acid. After okadaic acid pretreatment and activation with PDBu for 30 min, as much as 29% of the total phosphorylation of CD18 occurred on threonine residues (Fig. 6*B*). Similar results were obtained already at 10 min after activation with

Carl_G_190x270_mm_blokki_FINAL.indd 374 06-Aug-23 1:54:20 PM

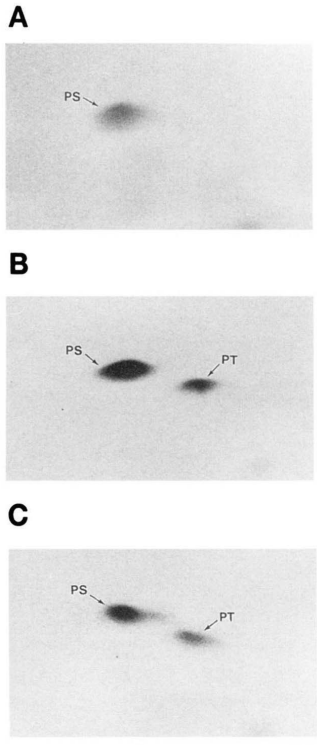

FIGURE 6. Phosphorylated amino acids of CD18. Phosphoamino acid analysis of phosphorylated CD18 polypeptides of CD11/CD18 integrins immunoprecipitated from either PDBu-activated (*A*), okadaic acid-pretreated and PDBu-activated (*B*), or okadaic acid-pretreated and OKT3-activated (*C*) ^{32}P-labeled T cells.

OKT3 (Fig. 6*C*). Here, the amount of phosphothreonine was 37% of the total incorporated ^{32}P in CD18.

Discussion

Several earlier reports have demonstrated phosphorylation of CD18 in phorbol ester activated-leukocytes (22–25). Although a positive correlation between cell adhesion and CD18 phosphorylation was observed, the role of phosphorylation in the regulation of leukocyte adhesion has remained unsettled. In fact, when mutations of the putative phosphorylation sites of CD18 were carried out, the importance of phorbol ester-stimulated CD18 phosphorylation became doubtful (27).

Since phorbol esters, which are potent activators of PKC, could stimulate leukocyte adhesion (11, 12), the possibility arose that PKC is pivotal in the induction of the high avidity state of CD11/CD18. We had earlier shown that purified PKC is able to phosphorylate CD18 on serine (25). We therefore directly measured PKC activity in stimulated T cells. Phorbol ester treatment induced long-lasting PKC activation, whereas stimulation of T cells by CD3 antibody caused a transient increase in PKC activity, as previously described (34). The activity of PKC was not increased after CD44 stimulation. Furthermore, the protein kinase inhibitor staurosporine was shown to inhibit the aggregation stimulated by phorbol esters and CD3. These findings agree well with previous studies on T lymphocytes (18). It should be noted that staurosporine is relatively unspecific, and it may affect several different types of kinases. Staurosporine had no effect on the aggregation caused by mAb against CD44 Ag, and neither was staurosporine alone able to induce aggregation of T cells, as reportedly happened with B cells (35). This difference may be due to the existence of cell-specific isoforms of PKC showing different activation and inhibition properties in different types of leukocytes.

The CD11 polypeptide was constitutively phosphorylated in T cells, and stimulation with either of the activating agents induced no change in its phosphorylation. As previously reported (22–25), the phosphorylation of CD18 was induced by phorbol ester activation. Contrary to previous reports showing no detectable phosphorylation of CD18 in CD3-stimulated T cells (36), we now observed a weak and transient CD18 phosphorylation. No CD18 phosphorylation could be seen, however, in T cells treated with CD44 Ab, but weak and undetectable CD44-induced phosphorylation obviously cannot be excluded. It can be concluded, therefore, that the phosphorylation of the CD18 polypeptide correlates well with induced PKC activity after phorbol ester and CD3 stimulation, and with the extensive aggregation of T cells caused by these agents. However, it seems evident that the aggregation caused by CD44 stimulation is induced by some other mechanism, which does not necessarily involve PKC activation or CD18 phosphorylation.

The involvement of phosphatases in the regulation of CD11/CD18 activation was studied using okadaic acid, an inhibitor of the serine/threonine phosphatases PP1 and PP2A. The ability of okadaic acid to induce stimulus-independent CD18 phosphorylation in neutrophils has previously been reported (37). Here we have shown that, in T cells, okadaic acid treatment alone was incapable of inducing detectable CD18 phosphorylation. But on the other hand, okadaic acid strongly increased the phosphorylation of CD18 induced by phorbol esters or CD3 Ab. These results indicate that phosphorylation/dephosphorylation reactions continuously take place in CD18, but are not observed without the use of phosphatase inhibitors. Since phosphorylation was not induced by okadaic acid treatment alone, it seems obvious that positive signals, i.e., activation of protein kinases, are necessary. It is reasonable to believe that PKC plays an important role. However, the CD18 phosphorylation in CD3-stimulated T cells increased after the PKC activity had declined (Fig. 5*D*).

Carl_G_190x270_mm_blokki_FINAL.indd 375 06-Aug-23 1:54:20 PM

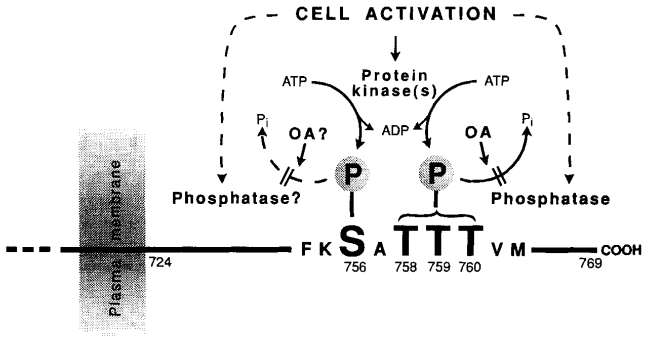

FIGURE 7. A schematic, partially hypothetical picture of phosphorylation events in CD18 after phorbol ester or CD3 stimulation. Protein kinase(s) phosphorylate serine-756 and one or more threonines. Whether phosphatases need to be activated is not known (dashed lines). Okadaic acid (OA) inhibits the dephosphorylation of threonine, but whether it also affects serine phosphorylation is not known. The phosphorylation of Ser-756 is more stable, whereas the phosphorylation of threonine residues is seen only after treatment with okadaic acid.

This indicates the possibility of involvement of some additional protein kinases.

We do not know which phosphatase is involved in the dephosphorylation of the CD18 polypeptide, since the concentration of okadaic acid used (1.5 μM) is known to inhibit both phosphatases PP1 and PP2A (38). These two phosphatases are the two major cellular protein serine/threonine phosphatases (39). In principle one could try to use different concentrations of okadaic acid to identify the phosphatase involved, but because okadaic acid predominately accumulates in cell membranes, where PP1 is more abundant than PP2A (39), definitive conclusions are difficult to draw. More convincing evidence of the involvement of either phosphatase could only be obtained by in vitro dephosphorylation studies.

In phorbol ester- and CD3-stimulated T cells, the inhibition of phosphatase activity induced significant phosphorylation of threonine residues in CD18 in addition to serine. Most probably the phosphorylation occurred on one or more of the three threonine residues (T758–T760) in CD18. We have not, however, excluded the possibility that cell surface threonines in CD18 are phosphorylated. Phorbol ester activation of T cells alone revealed mainly serine phosphorylation, as previously described in monocytes (23) and B lymphoblastoid cells (27). In these reports, minimal amounts of phosphothreonine were detectable. Threonine phosphorylation is interesting in relation to the importance of cytoplasmic threonine residues of CD18 for the function of CD11/CD18 integrins (27, 28). When the putative phosphorylation sites of CD18 were mutated, Ser-756 (Fig. 7) was found to be the major phosphorylation site phosphorylated in response to phorbol esters (27). When this serine residue was mutated to cysteine, phosphorylation of CD18 was not detected, but the CD11/CD18 complex retained the capacity to be activated by phorbol esters and to bind to its counter-receptor. Therefore, it was concluded that the phosphorylation of Ser-756 was not essential in the regulation of CD11/CD18 avidity. Additional results revealed, however, that when the three threonines (T758-T760) were mutated to alanines, the binding of CD11/CD18 to ICAM-1 was essentially abolished. When these threonine residues were mutated one by one, the ability of the integrins to become activated by phorbol esters decreased. It should also be noted that, when Thr-758 was mutated, phosphorylation on serine residues was no longer detected. The effect of this mutation was explained by a change in the kinase binding site that affected phosphorylation at Ser-756.

In a more recent report, the importance of the cytoplasmic domain of CD18, and within it particularly the TTT (758–760) region, was further emphasized. Chimeric integrins were constructed composed of the cytoplasmic domains of CD11/CD18 and the extracellular domains of the platelet integrin GPIIb/IIIa (28). Mutation of the three threonine residues strongly decreased the adhesiveness of the chimeric integrins. Furthermore, the importance of the threonine residues in integrin/cytoskeleton associations was demonstrated. A role for the cytoskeleton in the regulation of CD11/CD18 integrin has earlier been postulated (36, 40). Now, it seems evident that the cytoplasmic threonine residues of the CD18 molecule are involved in the association of CD11/CD18 with the cytoskeleton, and thus in the activation of CD11/CD18 integrins. Threonine phosphorylation could be important in such interactions.

The ability of okadaic acid to inhibit, rather than induce, T cell aggregation suggests an important role of phosphatases in T cell aggregation. Possibly, both protein kinase and protein phosphatase activities are needed for adhesion.

Carl_G_190x270_mm_blokki_FINAL.indd 376 06-Aug-23 1:54:20 PM

In Figure 7 a schematic view of CD18 cytoplasmic phosphorylation is presented. The phosphorylation at Ser-756 is relatively stable, whereas the threonine phosphorylation of residues 758–760 is more labile. Activation of cell adhesion using agents like phorbol esters or CD3 Abs activates one or more serine/threonine protein kinases. Whether serine/threonine phosphatases are activated is not known. However, phorbol esters have been shown in two earlier reports to activate phosphatase activity in mammalian cells (41, 42). Hence, it is possible that the phosphatase activity that dephosphorylates CD18 could also be modulated by the agents inducing leukocyte adhesion. We do not know whether some serine dephosphorylation of CD18 occurs, which can be affected by okadaic acid, but threonine dephosphorylation is certainly inhibited. Fast dephosphorylation of the threonine residues by phosphatases has previously led to an underestimation of the importance of the CD18 phosphorylation in the regulation of CD11/CD18 avidity. Okadaic acid has in some other cases also been shown to increase preferentially the phosphothreonine content of metabolically labeled proteins (39).

It can be concluded that both protein kinase and protein phosphatase activities are needed for the induction of T cell aggregation by either phorbol esters or CD3 Ab. In the presence of okadaic acid, these agents were shown to induce strong phosphorylation of CD18 threonine(s). This threonine phosphorylation most probably takes place during T cell stimulation through CD3, but because of phosphatase activity it is hard to demonstrate this in the absence of phosphatase inhibitors. We think that it is important for CD11/CD18 function.

Acknowledgments

The authors thank Leena Kuoppasalmi and Aili Grundström for skillful technical assistance, Dr. Matias Bergman for assistance with the phosphoimager, and Dr. Claudine Vermot-Desroches for the mAb B-G15.

References

1. Springer, T. A. 1990. Adhesion receptors of the immune system. *Nature 346:425.*
2. Patarroyo, M., J. Prieto, J. Rincon, T. Timonen, C. Lundberg, L. Lindbom, B. Asjo, and C. G. Gahmberg. 1990. Leukocyte-cell adhesion: a molecular process fundamental in leukocyte physiology. *Immunol. Rev. 114:67.*
3. Arnaout, M. A. 1990. Structure and function of the leukocyte adhesion molecules CD11/CD18. *Blood 75:1037.*
4. Diamond, M. S., and T. A. Springer. 1994. The dynamic regulation of integrin adhesiveness. *Curr. Biol. 4:506.*
5. Marlin, S. D., and T. A. Springer. 1987. Purified intracellular adhesion molecule-1 (ICAM-1) is a ligand for lymphocyte function associated antigen-1 (LFA-1). *Cell 51:813.*
6. Patarroyo, M., E. A. Clark, J. Prieto, C. Kantor, and C. G. Gahmberg. 1987. Identification of a novel adhesion molecule in human leukocytes by monoclonal antibody LB-2. *FEBS Lett. 210:127.*
7. Nortamo, P., R. Salcedo, T. Timonen, M. Patarroyo, and C. G. Gahmberg. 1991. A monoclonal antibody to the human leukocyte adhesion molecule intercellular adhesion molecule-2: cellular distribution and molecular characterization of the antigen. *J. Immunol. 146:2530.*
8. De Fougerolles, A. R., S. A. Stacker, R. Schwarting, and T. A. Springer. 1991. Characterization of ICAM-2 and evidence for a third counter-receptor for LFA-1. *J. Exp. Med. 174:253.*
9. De Fougerolles, A. R., and T. A. Springer. 1992. Intercellular adhesion molecule 3, a third adhesion counter-receptor for lymphocyte function-associated molecule 1 on resting lymphocytes. *J. Exp. Med. 175:185.*
10. Fawcett, J., C. L. L. Holness, L. A. Needham, H. Turley, K. C. Gatler, D. Y. Mason, and D. L. Simmons. 1992. Molecular cloning of ICAM-3, a third ligand for LFA-1, constitutively expressed on resting leukocytes. *Nature 360:481.*
11. Patarroyo, M., P. G. Beatty, J. W. Fabre, and C. G. Gahmberg. 1985. Identification of a cell-surface protein complex mediating phorbol ester-induced adhesion (binding) among human mononuclear leukocytes. *Scand. J. Immunol. 22:171.*
12. Rothlein, R., and T. A. Springer. 1986. The requirement for lymphocyte function associated antigen 1 in homotypic leukocyte adhesion stimulated by phorbol esters. *J. Exp. Med. 163:1132.*
13. Keizer, G. D., W. Visser, M. Vliem, and C. G. Figdor. 1988. A monoclonal antibody (NKI-L16) directed against a unique epitope on the α-chain of human leukocyte function-associated antigen 1 induces homotypic cell-cell interactions. *J. Immunol. 140:1393.*
14. Landis, R. C., R. I. Bennett, and N. Hogg. 1993. A novel LFA-1 activation epitope maps to the I domain. *J. Cell Biol. 120:1519.*
15. Robinson, M. K., D. Andrew, H. Rosen, D. Brown, S. Ortlepp, P. Stephens, and E. C. Butcher. 1992. Antibody against the Leu-CAM β-chain (CD18) promotes both LFA-1 and CR3-dependent adhesion events. *J. Immunol. 148:1080.*
16. Damle, N. K., K. Klussman, and A. Aruffo. 1992. Intercellular adhesion molecule-2, a second counter receptor for CD11a/CD18 (leukocyte function-associated antigen-1) provides a costimulatory signal for T cell receptor-initiated activation of human T cells. *J. Immunol. 148:665.*
17. Li, R., P. Nortamo, C. Kantor, P. Kovanen, T. Timonen, and C. G. Gahmberg. 1993. A leukocyte integrin binding peptide from intercellular adhesion molecule-2 stimulates T cell adhesion and natural killer cell activity. *J. Biol. Chem. 268:21474.*
18. Dustin, M. L., and T. A. Springer. 1989. T-cell receptor cross-linking transiently stimulates adhesiveness through LFA-1. *Nature 341:619.*
19. van Kooyk, Y., P. van de Wiel-van Kemenade, P. Weder, T. W. Kuijpers, and C. G. Figdor. 1989. Enhancement of LFA-1 mediated cell adhesion by triggering through CD2 or CD3 on T lymphocytes. *Nature 342:811.*
20. Axelsson, B., R. Youseffi-Etemad, S. Hammarström, and P. Perlmann. 1988. Induction of aggregation and enhancement of proliferation and IL-2 secretion in human T cells by antibodies to CD43. *J. Immunol. 141:2912.*
21. Koopman, G., Y. van Kooyk, M. de Graaff, C. J. L. M. Meyer, C. G. Figdor, and S. T. Pals. 1990. Triggering of CD44 antigen on T lymphocytes promotes T cell adhesion through the LFA-1 pathway. *J. Immunol. 145:3589.*
22. Hara, T., and S. M. Fu. 1986. Phosphorylation of α,β subunits of 180/100-Kd polypeptides (LFA-1) and related antigens. In *Leukocyte Typing II*, Vol 3: *Human Myeloid and Hematopoietic Cells*. E. L. Reinherz, B. F. Haynes, L. M. Nadler, and I. D. Bernstein, eds. Springer-Verlag, New York, p. 77.
23. Chatila, T. A., R. S. Geha, and M. A. Arnaout. 1989. Constitutive and stimulus-induced phosphorylation of CD11/CD18 leukocyte adhesion molecules. *J. Cell Biol. 109:3435.*
24. Buyon, J. P., S. G. Slade, J. Reibman, S. B. Abramson, M. R. Philips, G. Weissmann, and R. Winchester. 1990. Constitutive and induced phosphorylation of the α- and β-chains of the CD11/CD18 leukocyte integrin family. *J. Immunol. 144:191.*
25. Valmu, L., M. Autero, P. Siljander, M. Patarroyo, and C. G. Gahmberg. 1991. Phosphorylation of the β-subunit of CD11/CD18 integrins by protein kinase C correlates with leukocyte adhesion. *Eur. J. Immunol. 21:2857.*
26. Hibbs, M. L., H. Xu, S. A. Stacker, and T. A. Springer. 1991. Regulation of adhesion to ICAM-1 by the cytoplasmic domain of LFA-1 integrin β subunit. *Science 251:1611.*

27. Hibbs, M. L., S. Jakes, S. T. Stacker, R. W. Wallace, and T. A. Springer. 1991. The cytoplasmic domain of the integrin lymphocyte function-associated antigen-1 β subunit: sites required for binding to intercellular adhesion molecule 1 and the phorbol ester-stimulated phosphorylation site. *J. Exp. Med. 174:1227.*
28. Peter, K., and T. E. O'Toole. 1995. Modulation of cell adhesion by changes in $\alpha_L\beta_2$ (LFA-1, CD11a/CD18) cytoplasmic domain/cytoskeleton interaction. *J. Exp. Med. 181:315.*
29. Nortamo, P., M. Patarroyo, C. Kantor, J. Suopanki, and C. G. Gahmberg. 1988. Immunological mapping of the human leukocyte adhesion glykoprotein GP90 (CD18) by monoclonal antibodies. *Scand. J. Immunol. 28:537.*
30. Gahmberg, C. G., and L. C. Andersson. 1978. Leukocyte surface origin of human α1-acid glycoprotein (orosomucoid). *J. Exp. Med. 148:507.*
31. Laemmli, U. K. 1970. Cleavage of structural proteins during the assembly of the head of bacteriophage T4. *Nature 227:680.*
32. Bonner, W. M., and R. A. Laskey. 1974. A film detection method for tritium-labelled proteins and nucleic acids in polyacrylamide gels. *Eur. J. Biochem. 46:83.*
33. Hunter, T., and Sefton, B. M. 1980. Transforming gene product of Rous sarcoma virus phosphorylates tyrosine. *Proc. Natl. Acad. Sci. 77:1311.*
34. Szamel, M., F. Bartels, and K. Resch. 1993. Cyclosporin A inhibits T cell receptor-induced interleukin-2 synthesis of human T lymphocytes by selectively preventing a transmembrane signal transduction pathway leading to sustained activation of a protein kinase C isoenzyme, protein kinase C-β. *Eur. J. Immunol. 23:3072.*
35. Hedman, H., and E. Lundgren. 1992. Regulation of LFA-1 avidity in human B cells: requirements for dephosphorylation events for high avidity ICAM-1 binding. *J. Immunol. 149:2295.*
36. Pardi, R., L. Inverardi, C. Rugarli, and J. R. Bender. 1992. Antigen-receptor complex stimulation triggers protein kinase C-dependent CD11a/CD18-cytoskeleton association in T lymphocytes. *J. Cell Biol. 116:1211.*
37. Merrill, J. T., R. J. Winchester, and J. P. Buyon. 1994. Dynamic state of β2 integrin phosphorylation: regulation of neutrophil aggregation involves a phosphatase-dependent pathway. *Clin. Immunol. Immunopathol. 71:216.*
38. Cohen, P., C. F. B. Holmes, and Y. Tsukitani. 1990. Okadaic acid: a new probe for the study of cellular regulation. *Trends Biochem. Sci. 15:98.*
39. Shenolikar, S. 1994. Protein serine/threonine phosphatases—new avenues for cell regulation. *Annu. Rev. Cell Biol. 10:55.*
40. Haverstick, D., H. Sakai, and L. Gray. 1992. Lymphocyte adhesion can be regulated by cytoskeleton-associated, PMA-induced capping of surface receptors. *Am. J. Physiol. 262:C916.*
41. Feuerstein, N., and H. L. Cooper. 1984. Rapid phosphorylation-dephosphorylation of specific proteins induced by phorbol ester in HL-60 cells. *J. Biol. Chem. 259:2782.*
42. Boyle, W. J., T. Smeal, L. H. K. Defize, P. Angel, J. R. Woodgett, M. Karin, and T. Hunter. 1991. Activation of protein kinase C decreases phosphorylation of c-Jun at sites that negatively regulate its DNA-binding activity. *Cell 64:573.*

THE JOURNAL OF BIOLOGICAL CHEMISTRY
Vol. 277, No. 3, Issue of January 18, pp. 1728–1738, 2002
Printed in U.S.A.
© 2002 by The American Society for Biochemistry and Molecular Biology, Inc.

Phosphorylation of the Cytoplasmic Domain of the Integrin CD18 Chain by Protein Kinase C Isoforms in Leukocytes*

Received for publication, July 20, 2001, and in revised form, November 2, 2001
Published, JBC Papers in Press, November 7, 2001, DOI 10.1074/jbc.M106856200

Susanna Fagerholm‡§¶, Nick Morrice‡, Carl G. Gahmberg§¶‖, and Philip Cohen‡

From the ‡MRC Protein Phosphorylation Unit, MSI/WTB Complex, University of Dundee, Dow Street, Dundee DD1 5EH, Scotland, United Kingdom and §Division of Biochemistry, Department of Biosciences, PB 56, University of Helsinki, 00014 Helsinki, Finland

The CD11/CD18 (β_2) integrins are leukocyte-specific adhesion receptors, and their ability to bind ligands on other cells can be activated by extracellular stimuli. During cell activation, the CD18 chain is known to become phosphorylated on serine and functionally important threonine residues located in the intracellular C-terminal tail. Here, we identify catalytic domain fragments of protein kinase C (PKC) δ and PKCβI/II as the major protein kinases in leukocyte extracts that phosphorylate a peptide corresponding to the cytoplasmic tail of the integrin CD18 chain. The sites phosphorylated *in vitro* were identified as Ser-745 and Thr-758. PKCα and PKCη also phosphorylated these residues, and PKCα additionally phosphorylated Thr-760. Ser-745, a novel site, was shown to become phosphorylated in T cells in response to phorbol ester stimulation. Ser-756, a residue not phosphorylated by PKC isoforms, also became phosphorylated in T cells after phorbol ester stimulation. When leukocyte extracts were subjected to affinity chromatography on agarose to which residues 751–761 of the CD18 chain phosphorylated at Thr-758 were bound covalently, the only proteins that bound specifically were identified as isoforms of 14-3-3 proteins. Thus, PKC-mediated phosphorylation of CD18 after cell stimulation could lead to the recruitment of 14-3-3 proteins to the activated integrin, which may play a role in regulating its adhesive state or ability to signal.

The CD11/CD18 integrins (β_2 integrins) are leukocyte-specific members of the integrin superfamily of heterodimeric cell surface receptors involved in adhesion to the extracellular matrix and to cells. The four different CD11/CD18 integrins (1–2) share a common β chain (CD18) but have different α chains (CD11a–d) and different cell distribution and ligands. CD11/CD18 integrins are unable to bind their ligands, the intercellular adhesion molecules (ICAMs)[1] in resting cells, but instead need an activating signal for conversion to an adhesive state (2, 3). In addition to extracellular activation with divalent cations (4), ligands (5–7), or certain monoclonal antibodies to the extracellular domains (8–10), the integrins can also be activated by intracellular signaling, so-called inside-out signaling. This is induced by triggering the T cell receptor (3, 11) or other leukocyte surface receptors (11–13), or by direct activation of PKC by tumor-promoting phorbol esters (14, 15). The molecular basis for activation is still poorly understood; however, it is thought to involve changes in avidity via surface redistribution of the integrin (16–19) and perhaps signaling mediated conformational changes of the integrin extracellular domain (20). Several signaling pathways have been implicated in the activation process, including those that modulate protein kinase C (PKC) (21), phosphoinositide 3-kinase (PI 3-kinase) (22), mitogen-activated protein kinase (23), the small GTP-binding protein Rap1 (21), protein phosphatases (24, 25), and the calcium-binding proteins calpain (26) and calmodulin (27). The cytoplasmic domain of the CD18 chain is necessary for the regulation of adhesion (16, 28, 29), and interestingly, both phorbol esters and CD3 ligation induce CD18 phosphorylation on Ser (30–32) and Thr (25) residues. Thr phosphorylation is more transient than Ser phosphorylation. The Thr phosphorylation may regulate the adhesive state of the integrin, because mutation of three consecutive threonines in the integrin chain (Thr-758, Thr-759, and Thr-760) reduce integrin binding to ICAM-1 (29) and cytoskeletal association (16) of the integrin molecules. Additionally, phosphorylated integrin molecules preferentially partition with the actin cytoskeleton (33), indicating that phosphorylation of integrins could regulate integrin-cytoskeleton interactions.

In addition to their adhesive properties, the integrins are also involved in activating intracellular signaling pathways and can thus mediate bi-directional signaling across the plasma membrane. In fibroblasts they form focal adhesion complexes with cytoskeletal elements and a wide range of signaling molecules (34). In leukocytes these signaling complexes are believed to be more transient, because leukocytes are involved in relatively short lived interactions with other cells. Several cytoskeletal and signaling molecules have been shown to interact with the CD18 cytoplasmic tail, including the actin-binding proteins talin (33, 35), filamin (36), and α-actinin (37, 38), the adaptor proteins Rack1 (receptor for activated PKC) (39) and cytohesin (40), and the transcription factor Jun activation domain-binding protein (41).

* This work was supported in part by the UK Medical Research Council (to P. C.), The Royal Society (to P. C.), the Academy of Finland, and the Sigrid Juselius Foundation (to C. G.). The costs of publication of this article were defrayed in part by the payment of page charges. This article must therefore be hereby marked "*advertisement*" in accordance with 18 U.S.C. Section 1734 solely to indicate this fact.

¶ Recipient of a postgraduate research studentship from the Oskari Huttunen Foundation. To whom correspondence may be addressed: Dept. of Biosciences, Division of Biochemistry, P. O. Box 56 (Viikinkaari 5), FIN-00014 University of Helsinki, 00014 Helsinki, Finland. Tel.: 358-9-191-59029; Fax: 358-9-191-59068; E-mail: susanna.fagerholm@helsinki.fi.

‖ To whom correspondence may be addressed: Dept. of Biosciences, Division of Biochemistry, P. O. Box 56 (Viikinkaari 5), FIN-00014 University of Helsinki, 00014 Helsinki, Finland. Tel.: 358-9-191-59029; Fax: 358-9-191-59068; E-mail: carl.gahmberg@helsinki.fi.

[1] The abbreviations used are: ICAM, intercellular adhesion molecule; PKC, protein kinase C; Rack1, receptor for activated C kinase; PDBu, phorbol 12,13-dibutyrate; PI 3-kinase, phosphoinositide 3-kinase; JAB1, Jun activation domain-binding protein 1; PKI, the specific peptide inhibitor of cAMP-dependent protein kinase (TTYADFIASGRTGRRNAIHD); PEG, polyethylene glycol; PVDF, polyvinylidene difluoride; BisTris, 2-[bis(2-hydroxyethyl)amino]-2-(hydroxymethyl)propane-1,3-diol.

This paper is available on line at http://www.jbc.org

This is an Open Access article under the CC BY license.

Carl_G_190x270_mm_blokki_FINAL.indd 379 06-Aug-23 1:54:21 PM

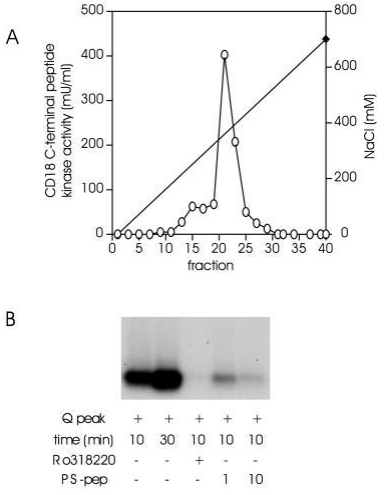

FIG. 1. **A kinase activity that phosphorylates the C-terminal integrin peptide is found in leukocyte lysates.** *A,* the CD18 peptide was phosphorylated for 10 min by fractions from the initial MonoQ column as described under "Experimental Procedures." *B,* the peak fraction from the initial MonoQ column (*Q peak*) was used to phosphorylate the CD18 C-terminal peptide in the presence or absence of 100 nM Ro 318220 or 1 or 10 μM PKC pseudosubstrate inhibitor peptide (*PS-pep*) for the times indicated. The peptide was subjected to SDS-PAGE and transferred to a PVDF membrane, and the radioactive band was detected by autoradiography.

In this study, we present evidence that PKC isoforms are the major protein kinases that phosphorylate the C terminus of the integrin CD18 chain in leukocytes. Ser-745 is identified as a novel phosphorylation site in the integrin cytoplasmic domain. Additionally, we show that a Thr-758-phosphorylated integrin peptide can interact with 14-3-3 proteins in leukocyte lysates and thus potentially initiate signaling complex formation "downstream" of the phosphorylated integrin molecules.

EXPERIMENTAL PROCEDURES

Materials—PKI, the specific peptide inhibitor of cAMP-dependent protein kinase (TTYADFIASGRTGRRNAIHD), was synthesized by F. B. Caudwell in the MRC Protein Phosphorylation Unit and the other peptides by G. Bloomberg (University of Bristol, UK). Hitrap Q, Hitrap heparin, MonoQ, and gel filtration columns, protein G-Sepharose, and [^{32}P]-orthophosphate were purchased from Amersham Biosciences. Vinylsulfone-activated agarose and the calcium ionophore A23187 were from Sigma. Phosphocellulose P-81 paper was from Whatman. Okadaic acid, phorbol 12,13-dibutyrate (PDBu), Ro 318220, Go-6983, W-7, trifluoperazine, PD 98059, and calpeptin were from Calbiochem. PKC pseudosubstrate inhibitor peptide was from Biomol (Plymouth Meeting, PA), and the PKC enzyme panel kit was from Panvera (Madison, WI). Complete protease inhibitor mixture tablets and sequencing grade trypsin were from Roche Molecular Biochemicals. Microcystin-LR was provided by L. Lawton (Robert Gordons University, Aberdeen, UK). Sequelon arylamine membranes were from Milligen (Bedford, USA). Acetonitrile and trifluoroacetic acid were from Rathburn Chemicals (Walkerburn, Peebleshire, Scotland, UK).

Antibodies—Two phosphopeptides were synthesized corresponding to residues 740–751 and 751–761 of the integrin CD18 chain (CKEKLKpSQWNNDN and CNPLFKpSATTTV, where pS is phosphoserine), with an N-terminal cysteine added for coupling, and conjugated to keyhole limpet hemocyanin as in Ref. 42. The complex was injected into sheep at the Scottish Antibody Production Unit (Carluke, Scotland). The antiserum was passed through agarose to which the relevant phosphorylated peptide had been coupled covalently, and the phosphospecific antibodies were eluted with 0.1 M glycine, pH 2.4, immediately adjusted to pH 8.0 with Tris-HCl, and stored at 4 °C. This was carried out by Dr. J. Leitch and C. Clark in our laboratory. The CD18 integrin antibodies R7E4 and R2E7B have been described previously (14, 43). The monoclonal antibody OKT3, which reacts with CD3, was used in the form of ascites fluid produced by hybridoma cells (clone CRL 8001, American Type Culture Collection, Manassas, VA). PKC isozyme-specific antibodies were from Transduction laboratories (Lexington, KY). The broadly reactive 14-3-3β (K-19) antibody was from Santa Cruz Biotechnology (Santa Cruz, CA).

Protein Kinase Assay—Protein kinases were assayed using a peptide corresponding to the integrin CD18 C terminus (RRFEK EKLKS QWNND NPLFK SATTT VMNPK FAES). Recombinant PKC isoforms and activity eluting from column fractions were measured at 30 °C in

Specific activity (mU/mg)	Yield (%)			Specific activity (mU/mg)	Yield (%)
		Human leukocyte lysate			
		↓			
		10-20% PEG precipitation			
		↓			
487	100	Hitrap Q pH 7.5			
		↓			
2805	33	Hitrap heparin pH 6.5	Heparin flowthrough	680	67
		↓	↓		
8318	25	MonoQ pH 6.5	MonoQ pH 6.5	2014	35
		↓	↓		
6673	10	MonoQ pH 7.7	MonoQ pH 7.7	3571	26
		↓	↓		
50000	6	Gelfiltration	Protamine agarose	5300 (F2) 15300 (F3)	6 7

FIG. 2. **Protocol for the purification of the major CD18 kinase activities in leukocyte lysates.** The specific activity and overall yield from Hitrap Q pH 7.5 is shown.

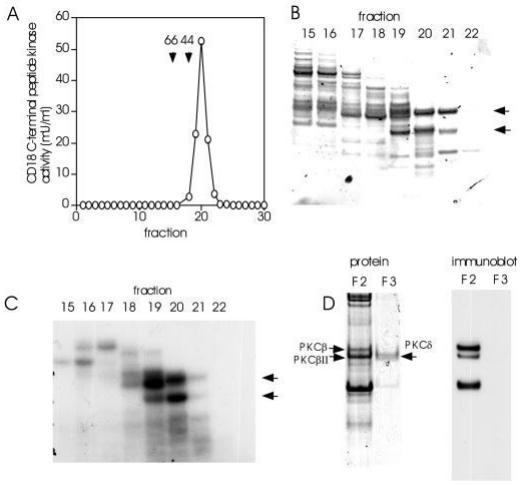

FIG. 3. **Purification of the integrin kinase activity.** *A,* fractions from the final gel filtration column were assayed for CD18 C-terminal peptide kinase activity (*open circles*). The elution position of the standard marker proteins bovine serum albumin (66 kDa) and ovalbumin (44 kDa) are shown. *B,* aliquots of indicated fractions from *A* were subjected to SDS-PAGE and stained with Coomassie Blue. The two protein staining bands that coeluted with the activity are marked. *C,* same as *B*, except that the fractions were incubated for 30 min with 10 mM magnesium acetate, 0.1 mM [γ-^{32}P]ATP (10^6 cpm per nmol) in the standard integrin kinase buffer, and the gel was autoradiographed after electrophoresis. The two major ^{32}P-labeled bands indicated by *arrows* comigrated with the major protein staining bands in *B*. *D,* fractions 2 and 3 (*F2* and *F3*) from the final protamine-agarose column (see "Experimental Procedures"), containing 46 and 54% of the kinase activity, respectively, were subjected to SDS-PAGE and either stained with Coomassie Blue (*left-hand panels*) or transferred to nitrocellulose membranes and immunoblotted with an antibody raised against the PKCα catalytic domain (*right-hand panels*). The bands identified as PKCβ and PKCδ are indicated.

Carl_G_190x270_mm_blokki_FINAL.indd 380 06-Aug-23 1:54:21 PM

TABLE I

Identification of the 42-kDa band in Fig. 3, B and D*, as the catalytic domain of PKC*δ

Tryptic peptides from the 42-kDa autophosphorylating bands in Fig. 3, B and *D*, were analyzed on a Perspective Biosystems Elite STR matrix-assisted laser desorption-time of flight mass spectrometer as described under "Experimental Procedures." The tryptic ions were scanned against the Swiss-Prot and Genpep databases using the SF-FIT program of Protein Prospector. The table summarizes the peptides from the integrin kinase that matched the PKC sequence.

Mass measured	Theoretical	Residue no.	Peptide sequence
727.3920	727.3779	395–399	(R)FELYR(A)
771.4979	771.4980	313–319	(K)VLLGELK(G)
788.4502	788.4459	549–554	(K)IHPFFK(T)
801.4859	801.4834	541–548	(R)LGVTGNIK(I)
806.4185	806.4048	287–293	(K)IWEGSSK(C)
827.4313	827.4303	322–328	(R)GEYFAIK(A)
940.5089	940.5005	393–399	(K)GRFELYR(A)
951.4622	951.4536	447–454	(K)ENIFGESR(A)
984.4967	984.4903	512–519	(R)VDTPHYPR(W)
1019.5520	1019.5526	532–539	(K)LFEREPTK(R)
1040.5577	1040.5529	320–328	(K)GRGEYFAIK(A)
1117.6279	1117.6257	555–563	(K)TINWTLLEK(R)
1139.6608	1139.6465	322–331	(R)GEYFAIKALK(K)
1139.6608	1139.6689	565–573	(R)RLEPPFRPK(V)
1175.6549	1175.6537	532–540	(K)LFEREPTKR(L)
1273.7272	1273.7268	555–564	(K)TINWTLLEKR(R)
1306.6292	1306.6367	294–303	(K)CNINNFIFHK(V)
1313.7294	1313.7429	423–433	(R)DLKLDNVLLDR(D)
1507.8137	1507.8233	426–438	(K)LDNVLLDRDGHIK(I)
1648.7255	1648.7131	579–591	(R)DYSNFDQEFLNEK(A)
1863.9796	1864.0292	423–438	(R)DLKLDNVLLDRDGHIK(I)
1873.7881	1873.8238	269–286	(K)KTGVAGEDMQDNSGTYGK(I)[a]
1873.7881	1873.8577	439–454	(K)IADFGMCKENIFGESR(A)
1879.8483	1879.8669	333–348	(K)DVVLIDDVECTMVEK(R)
2035.9658	2035.9680	333–349	(K)DVVLIDDVECTMVEKR(V)
2086.9836	2087.0094	400–417	(R)ATFYAAEIMCGLQFLHSK(G)
2103.0381	2103.0043	400–417	(R)ATFYAAEIMCGLQFLHSK(G)[a,b]
2417.2460	2417.2903	350–370	(R)VLTLAAENPFLTHLICTFQTK(D)
983.5844	983.5678	566–573	(R)LEPPFRPK(V)[b]

[a] Methionine sulfone derivative is indicated.
[b] Peptides only were detected in the protamine-agarose eluate.

an assay containing 50 mM Tris-HCl, pH 7.5, 0.1 mM EGTA, 100 μg/ml peptide, 2.5 μM PKI, 10 mM magnesium acetate, 0.1 mM [γ-^{32}P]ATP (10^6 cpm/nmol). One unit of activity was that amount that catalyzed the incorporation of 1 nmol of phosphate into the synthetic peptide in 1 min.

Preparation of Leukocyte Lysates and Purification of Integrin Kinase Activities—Human leukocytes were isolated from buffy coat pools by centrifuging for 20 min at 1500 × *g*. The leukocyte layer was then subjected to Ficoll gradient centrifugation and washed with phosphate-buffered saline. The cells were lysed in 50 mM Tris-HCl, pH 7.5, 1 mM EDTA, 1 mM EGTA, 1% Triton X-100, 1 mM sodium orthovanadate, 10 mM sodium glycerophosphate, 50 mM NaF, 5 mM sodium pyrophosphate, 0.27 M sucrose, 2 μM microcystin, 0.1% 2-mercaptoethanol, 1 mM benzamidine, and protease inhibitor mixture. The lysates were frozen in liquid nitrogen and stored in aliquots at −80 °C. The lysates (12 g of protein) were fractionated from 10 to 20% polyethylene glycol 6000 (PEG). After stirring for 3 h at 4 °C, the 20% PEG suspension was centrifuged for 30 min at 7000 × *g*, the supernatant discarded, and the pellet redissolved in 50 ml of buffer A (50 mM Tris-HCl, pH 7.5, 0.1 mM EGTA, 0.1% (v/v) 2-mercaptoethanol, 5% (v/v) glycerol, 0.03% (w/v) Brij 35). The solution was applied to a 5-ml Hitrap Q column equilibrated in buffer A. After washing with equilibration buffer, the column was developed with a linear salt gradient to 0.7 M NaCl in the same buffer. One major peak of activity was detected eluting at 0.3–0.4 M NaCl, which was pooled, diluted 5-fold in buffer B (50 mM BisTris, pH 6.5, 5% (v/v) glycerol, 0.1% (v/v) 2-mercaptoethanol, 1 mM EGTA, 0.03% (w/v) Brij 35), and applied to a 1-ml Hitrap heparin column equilibrated in buffer B. After washing until no protein could be detected in the eluate, the column was developed with a linear salt gradient to 1 M NaCl. One major peak of activity was detected, eluting at 0.2 M NaCl. This was pooled, diluted in buffer B, and applied to a 1-ml MonoQ column, which was developed with a linear salt gradient to 0.7 M NaCl. The most active fractions, eluting at 0.3 M NaCl were pooled, diluted with buffer C (50 mM Tris-HCl, pH 7.7, 0.1 mM EGTA, 0.1% (v/v) 2-mercaptoethanol, 5% (v/v) glycerol, 0.03% (w/v) Brij 35), and applied to a 1-ml MonoQ column, which was developed with a linear salt gradient to 1 M NaCl. The most active fractions, eluting at 0.3 M NaCl were pooled, concentrated to 25 μl with Vivaspin columns, and subjected to gel filtration on Superdex 200 (30 × 0.32 cm) equilibrated in buffer A plus 0.15 M NaCl. Fractions of 50 μl were collected.

The flow-through from the Hitrap-heparin column was chromatographed successively on 1-ml MonoQ columns equilibrated in buffer B and buffer C, respectively, as described above. A single major activity peak was detected eluting at 0.3 M NaCl in buffer B and 0.35 M in buffer C. The activity was then chromatographed on a 2-ml protamine-agarose column equilibrated in buffer A. The column was washed with 5 ml of buffer A plus 200 mM NaCl and then with buffer A plus 1 M NaCl. Four fractions, each of 6 ml, were collected.

Identification of Proteins by Mass Spectrometry and Phosphoamino Acid Analysis—Proteins of interest were excised from SDS-polyacrylamide gels, digested with trypsin, and identified using a Perspective Biosystems (Framingham, MA) Elite STR matrix-assisted laser desorption-time of flight-mass spectrometer as described previously (46). Phosphoamino acid analysis of integrin CD18 C terminus was also performed as described (47).

Isolation of CD11/CD18 Integrins from Lymphocyte Lysates—Integrins were affinity-purified from human leukocytes using R7E4 columns as described previously (48) and were at least 90% pure as monitored by SDS-polyacrylamide gel electrophoresis and Coomassie Blue staining.

Subcellular Fractionation—Fractionation of cells into soluble and cytoskeletal fractions was done after lysis in the presence of Triton X-100 as described (27).

Peptide Affinity Chromatography—The phosphorylated and unphosphorylated forms of the peptides CNPLFKpSATTTV and CLFKSApTTTVMN corresponding to the sequences surrounding phosphorylated Ser-756 and Thr-758, respectively (where pS and pT indicate phosphoserine and phosphothreonine), were coupled to vinylsulfone-activated agarose via the N-terminal cysteine residue. The cytosol and solubilized cytoskeletal fractions (0.5–1 mg of protein) were then subjected to affinity chromatography on each peptide-agarose column as described (33).

Immunoblotting—For detection of the CD11/CD18 integrin with phospho-specific antibodies, the integrin was first immunoprecipitated from 2.0 to 2.5 mg of lysate protein with 20 μg of R7E4 coupled

Carl_G_190x270_mm_blokki_FINAL.indd 381 06-Aug-23 1:54:22 PM

TABLE II
Identification of the proteins in Fig. 3D as the catalytic domain of PKCβ/βII

Tryptic peptides from the autophosphorylating 45-kDa doublet in the 1st lane *of Fig 3D* were analyzed by mass fingerprinting. The table summarizes the peptides from the integrin kinase that matched the PKC sequences.

Mass measured	Theoretical	Residue no.	Peptide sequence
PKCβ (pool 1 upper band)			
570.2999	570.3040	455–458	(R)FFTR(H)
806.4152	806.3949	419–424	(K)EHAFFR(Y)
865.3986	865.3804	448–454	(R)NAENFDR(F)
974.4582	974.4366	407–415	(R)LGCGPEGER(D)
984.5165	984.5301	397–405	(K)GLMTKHPGK(R)[a]
1099.6324	1099.5301	435–443	(K)EIQPPYKPK(A)
1162.6154	1162.5744	313–322	(K)ENIWDGVTTK(T)
1162.6154	1162.6009	416–424	(R)DIKEHAFFR(Y)
1227.7244	1227.7101	434–443	(R)KEIQPPYKPK(A)
1251.6493	1251.6374	425–433	(R)YIDWEKLER(K)
1397.7617	1397.7503	162–173	(K)LTDFNFLMVLGK(G)
1413.7627	1413.7452	162–173	(K)LTDFNFLMVLGK(G)[a]
1470.7443	1470.7263	292–304	(K)LDNMLDSEGHIK(I)
1826.9299	1826.9322	289–304	(R)DLKLDNMLDSEGHIK(I)
2229.0717	2229.1338	1–20	(−)RDAKNLVPMDPNGLSDPYVK(L)
2632.2489	2632.2692	239–260	(R)LYFVMEYVNGGDLMYHIQQVGF(F)
2648.2569	2648.2641	239–260	(R)LYFVMEYVNGGDLMYHIQQVGF(F)[a]
2656.3370	2656.3744	216–238	(R)VLALPGKPPFLQLHSCFQTMDR(L)
PKCβII (pool 1 lower band)			
570.2999	570.3040	632–635	(R)FFTR(H)
806.4152	806.3949	596–601	(K)EHAFFR(Y)
865.3986	865.3804	625–631	(R)NAENFDR(F)
974.4582	974.4366	584–592	(R)LGCGPEGER(D)
984.5165	984.5301	574–582	(K)GLMTKHPGK(R)[a]
1099.6324	1099.6152	612–620	(K)EIQPPYKPK(A)
1162.6154	1162.5744	490–499	(K)ENIWDGVTTK(T)
1162.6154	1162.6009	593–601	(R)DIKEHIFFR(Y)
1227.7244	1227.7101	611–620	(R)KEIQPPYKPK(I)
1251.6493	1251.6374	602–610	(R)YIDWEKLER(K)
1397.7617	1397.7503	339–350	(K)LTDFNFLMVLGK(G)
1413.7627	1413.7452	339–350	(K)LTDFNFLMVLGK(G)[a]
1470.7443	1470.7263	469–481	(K)LDNVMLDSEGHIK(I)
1826.9299	1826.9322	466–481	(R)DLKLDNVMLDSEGHIK(I)
2632.2489	2632.2632	416–437	(R)LYFVMEYVNGGDLMYHIQQVRR(F)
2648.2569	2648.2641	416–437	(R)LYFVMEYVNGGDLMYHIQQVRR(F)[a]
2656.3370	2656.3744	393–415	(R)VLALPGKPPFLTQLHSCFQTMDR(L)

[a] A methionine-sulfone derivative is indicated.

noncovalently to protein G-Sepharose. Bound proteins were eluted with 1% SDS, then subjected to polyacrylamide gel electrophoresis, and transferred to nitrocellulose, and the phosphorylated integrin was immunoblotted and detected using the ECL chemiluminescence detection system (Amersham Biosciences). The phosphospecific antibody that recognizes CD18 phosphorylated at Ser-745 was used at 2 μg/ml in the presence of 5 μg/ml unphosphorylated peptide conjugated to keyhole limpet hemocyanin. The Ser-756 phosphospecific antibody was used at the same concentration but in the presence of 25 μg/ml unphosphorylated peptide conjugated to keyhole limpet hemocyanin. Incubation with both antibodies was carried out overnight in 4 °C. The antibody R2E7B which recognizes phosphorylated and unphosphorylated CD18 equally well was used at 1:5000 dilution. The antibody against the PKCα catalytic domain, which also reacts with PKCβ isoforms, was used as a dilution of 1:1000. An antibody that recognizes all 14-3-3 isoforms was used at 1 μg/ml.

RESULTS

Identification of the Major Protein Kinases in Human Leukocyte Lysates That Phosphorylate the C Terminus of the Integrin CD18 Chain—To identify the major CD18 kinases, human leukocyte lysates were initially fractionated on MonoQ. All the activity was retained by the column and eluted as one major peak (Fig. 1*A*), which was pooled and chromatographed on heparin-Sepharose. At this step, 80% of the activity was not retained by the column, whereas 20% was bound. The activity present in both fractions was then further purified as described under "Experimental Procedures." A flow chart of the overall purification protocol is shown in Fig. 2.

The activity that was retained by heparin-Sepharose eluted as a single peak with an apparent molecular mass of 40 kDa at the final gel filtration step (Fig. 3*A*). SDS-PAGE revealed two major proteins, whose elution position correlated with activity (Fig. 3*B*). When the fractions were incubated with Mg[γ-^{32}P]ATP, both proteins became phosphorylated (Fig. 3*C*), suggesting that they might be protein kinases capable of autophosphorylation. The bands were excised and subjected to tryptic mass fingerprinting, which revealed that they both corresponded to the δ-isoform of PKC. All the peptides detected were located in the catalytic domain of PKCδ (Table I). This observation and the apparent molecular mass of the purified protein (which is much smaller than full-length PKCδ) indicated that it represented an active proteolytic fragment. Such fragments are known to be active in the absence of phospholipids and diacylglycerol, which are required for the activity of full-length PKCδ. This explains why these active fragments were detected, because the assays did not contain the cofactors essential for the activation of PKC isoforms.

The activity that was not retained by heparin-Sepharose was purified by chromatography on MonoQ at two different pH values and finally on protamine-agarose. SDS-PAGE of the activity initially eluted at 1 M NaCl (accounting for 46% of the activity) showed five protein-staining bands (Fig. 3*D*) of which the three most rapidly migrating (apparent molecular masses, of 44, 42, and 30 kDa) became phosphorylated upon incubation with Mg[γ-^{32}P]ATP (data not shown). The 44- and 42-kDa bands were identified as the catalytic domains of PKCβ and PKCβII, respectively, by tryptic mass fingerprinting (Table II), whereas the 30-kDa band appeared to be a mixture of several proteins, none of which was a protein kinase (data not shown). This was confirmed by immunoblotting with an antibody that

Carl_G_190x270_mm_blokki_FINAL.indd 382 06-Aug-23 1:54:22 PM

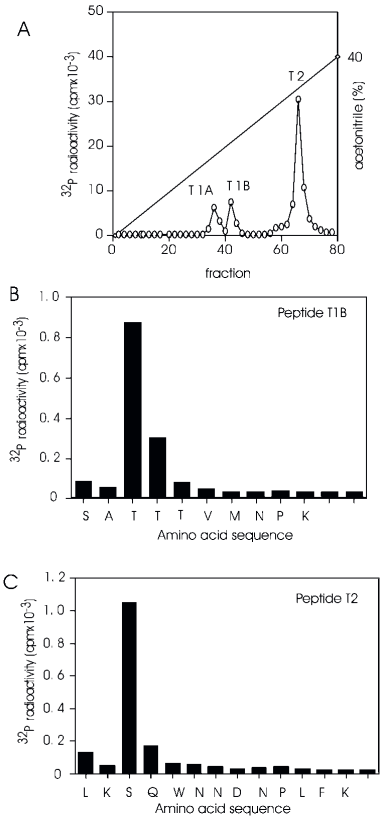

FIG. 4. **Identification of the phosphorylation sites in the integrin C-terminal peptide phosphorylated by PKCδ.** *A*, the integrin peptide was phosphorylated for 10 min with the catalytic domain of PKCδ purified from the leukocyte lysates and then subjected to tryptic digestion (see "Experimental Procedures"). The digest was applied to a Vydac C_{18} column equilibrated in 0.1% (v/v) trifluoroacetic acid and the column developed with an acetonitrile gradient (*straight line*). The flow rate was 1 ml/min, and 0.5-ml fractions were collected and analyzed for ^{32}P radioactivity (*open circles*) by Cerenkov counting. The major ^{32}P tryptic phosphopeptides (*T1A, T1B*, and *T2*) were identified as described in the text. The phosphopeptides T1B and T2 were sequenced by Edman degradation using an Applied Biosystems 42A protein sequencer (*B* and *C*). ^{32}P radioactivity released after each cycle was measured in a separate experiment by solid phase Edman degradation of the peptides coupled to a Sequelon arylamine membrane as described previously (67). Peptide T1A gave the same result as T1B (not shown). The amino acid sequence is shown using the single letter code for amino acids.

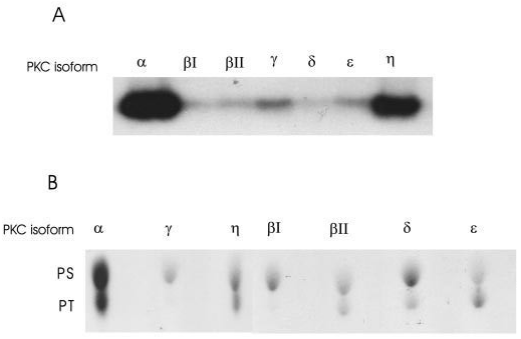

FIG. 5. **Phosphorylation of the C-terminal integrin peptide by PKC isoforms.** *A*, the integrin peptide was phosphorylated for 10 min at 30 °C with [γ-^{32}P]ATP (10^6 cpm per nmol) and the indicated PKC isoforms (each at 3 units/ml). One unit of activity, was that amount which catalyzed the incorporation of 1 nmol of phosphorylate into the standard substrate (histone H3 for PKCα, -βI, -βII, -γ, and a PKCε-substrate peptide for PKCδ, -ε, and -η) in 1 min. Lipids and calcium ions were included as recommended by the supplier. The phosphorylated peptides were subjected to SDS-PAGE, transferred to PVDF membranes, and subjected to autoradiography. *B*, the phosphorylated substrates were excised from the PVDF membrane, partially hydrolyzed in 6 N HCl, and phosphoamino acids resolved by thin layer chromatography (see "Experimental Procedures"). *PS*, phosphoserine; *PT*, phosphothreonine.

recognizes the catalytic domains of PKCα and PKCβ.

More prolonged elution of the protamine-agarose column with 1 M NaCl eluted 54% of the activity. This fraction contained a single protein of apparent molecular mass 42 kDa that was identified as the catalytic domain of PKCδ by tryptic mass fingerprinting (Table I). This indicated that PKCδ was only partially retained by heparin-Sepharose.

To establish that PKC isoforms accounted for all the activity eluted from the initial MonoQ column (Fig. 1*A*), the following additional experiments were performed. First, the activity from this column was shown to be inhibited by 100 nM Ro 318220, a potent inhibitor of conventional PKC isoforms, as well as several other protein kinases (49). Second, the activity was strongly suppressed by a pseudosubstrate peptide, which is believed to be a specific inhibitor of PKC (Fig. 1*B*).

Identification of Residues in the C Terminus of Integrin CD18 Phosphorylated by PKC Isoforms—The C-terminal peptide was phosphorylated with the purified catalytic domain of PKCδ and digested with trypsin. The resulting phosphopeptides were then chromatographed on a Vydac C_{18} column (Hesperia, CA), which resolved three ^{32}P-labeled tryptic peptides, termed T1A, T1B, and T2 (Fig. 4*A*). Each peptide was identified by a combination of Edman sequencing, solid phase sequencing, and mass spectrometry, as described previously (50). Peptides T1A and T2B both corresponded to residues 756–765 of the CD18 chain (SATTTVMNPK) phosphorylated at Thr-758 (Fig. 4*B*), whereas peptide T2 corresponded to residues 743–755 (LKSQWNNDNPLFK) phosphorylated at Ser-745 (Fig. 4*C*).

Phosphorylation of the CD18 C Terminus by Different PKC Isoforms—PKC isoforms have been reported to differ slightly in substrate specificity (51). We therefore examined the ability of seven different PKC isoforms to phosphorylate the C terminus. PKCα was the most active of the conventional PKC isoforms, and PKCη was the most active novel PKC toward the C terminus of CD18 (Fig. 5*A*). PKCβI and PKCγ phosphorylated the peptide almost exclusively on serine, whereas PKCα, -βII, -δ, and -η phosphorylated both serine and threonine. PKCε was the only PKC isoform that preferred threonine to serine (Fig. 5*B*). The sites on the CD18 peptide phosphorylated by PKCη were the same as those phosphorylated by PKCδ, namely Ser-745 and Thr-758 (data not shown). PKCα phosphorylated the CD18 peptide at a cluster of three tryptic peptides, T1, T2, and T3, as well as another peptide T4 (Fig. 6*A*). Peptides T1 and T2 corresponded to peptides T1A and T1B in Fig. 3 and were predominantly phosphorylated at Thr-758 (Fig. 6, *B* and *C*). Interestingly, peptide T3 consisted of the same peptide phosphorylated predominantly at Thr-760 (Fig. 6*D*). Peptide T4 corresponded to peptide T2 in Fig. 3 and was phosphorylated at Ser-745 as expected (Fig. 6*E*).

Phosphorylation of the CD18 Chain in Vivo—It has been shown previously (25, 30–32) that PDBu in conjunction with

Carl_G_190x270_mm_blokki_FINAL.indd 383 06-Aug-23 1:54:23 PM

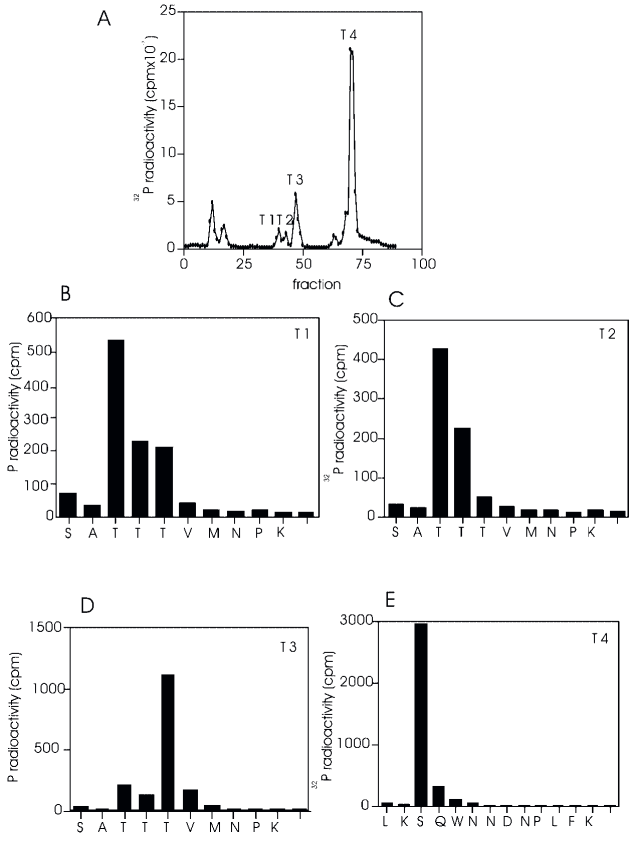

FIG. 6. **Identification of the residues in the C-terminal integrin peptide phosphorylated by PKC*α*.** *A,* the integrin peptide was phosphorylated for 60 min at 30 °C with PKCα, subjected to tryptic digestion, and applied to a Vydac C_{18} column as in Fig. 3. The major ^{32}P-labeled tryptic peptides (*T1, T2, T3,* and *T4*) were identified as described in the text. *B–E,* the phosphopeptides were analyzed by Edman and solid phase sequencing, and ^{32}P radioactivity released after each cycle was measured to identify the sites of phosphorylation.

the phosphatase inhibitor okadaic acid induces phosphorylation of the integrin CD18 chain in T cells, whereas the CD11 chain is phosphorylated constitutively. We confirmed these findings in the present study and also found that the phosphorylation of CD18 was prevented by 1 μM Ro 318220 and 0.5 μM of a related compound, Go-6983 (data not shown).

To identify the residues at the C terminus of CD18 whose phosphorylation is induced by PDBu, we raised phospho-specific antibodies capable of recognizing CD18 only when phosphorylated at Ser-745. We also raised phospho-specific antibodies that should recognize CD18 when phosphorylated at Ser-756, because this site has also been reported to become phosphorylated in response to PDBu, as judged by phosphopeptide mapping (44) and mutagenesis (29). We have been unable, thus far, to generate phospho-specific antibodies that recognize CD18 phosphorylated at Thr-758 and Thr-760 and which are sufficiently sensitive to detect the phosphorylation of these residues in cells. However, based on phosphopeptide mapping, it has been reported previously that two of the three threonine residues Thr-758, Thr-759, and Thr-760 become phosphorylated after stimulation with PDBu and okadaic acid (25, 44).

The antibody raised against the peptide 740–751 phosphorylated at Ser-745 was tested for recognition of the phosphopeptide immunogen and the unphosphorylated peptide in the presence of unphosphorylated peptide to block any antibodies present that recognize both the phosphorylated and unphosphorylated forms of the peptide. These experiments demonstrated that, under these conditions, the antibody only recognized the phosphopeptide and not the unphosphorylated peptide (Fig. 7*A*). Additionally, it only recognized the CD18 protein after phosphorylation by PKCβ *in vitro* (Fig. 7*B*). Recognition by the antibody was prevented by preincubation with the phosphopeptide immunogen but not by the unphosphorylated form of the peptide or the Ser-756 phosphopeptide (Fig. 7*B*). The specificity of the antibody raised against the peptide comprising residues 751–761 phosphorylated at Ser-756 was established in an analogous manner. However, as protein kinases capable of phosphorylating CD18 at Ser-756 have not yet been identified, specificity was established using the phosphopeptide immunogen (Fig. 8*A*). The phospho-specific antibody toward Ser-756 did not recognize the CD18 chain phosphorylated at Ser-745 by PKCβ (Fig. 7*B*).

These antibodies were then used to demonstrate that Ser-745 (Fig. 7*C*) and Ser-756 (Fig. 8*B*) both become phosphorylated when T cells are exposed to PDBu. No other unspecific bands were seen on the gels (not shown). Phosphorylation of Ser-745 could be detected in the presence of PDBu alone, but the phosphorylation was increased when cells were stimulated with PDBu and okadaic acid in the presence of OKT3, a stimulating antibody raised against the CD3 component of the T cell receptor. Phosphorylation of either site was inhibited by 1 μM Ro 318220 (Figs. 7*C* and 8*D*). The phosphorylation of Ser-756 could be detected readily after stimulation with high (200 nM) PDBu and OKT3 in the absence of okadaic acid, but OKT3

Carl_G_190x270_mm_blokki_FINAL.indd 384 06-Aug-23 1:54:23 PM

alone in the presence or absence of okadaic acid did not induce Ser-756 phosphorylation (Fig. 8*B*). Ser-756 phosphorylation can also be induced to similar levels by low (10 nM) PDBu in the presence of the calcium ionophore A12387 (Fig. 8*C*). Because no PKC isoform tested was able to phosphorylate CD18 at Ser-756 *in vitro*, this suggested that the phosphorylation of Ser-756 was likely to be catalyzed by another protein kinase activated directly or indirectly by a PKC isoform. To try and identify the signaling pathway in which this putative kinase was located, we examined the effect of inhibitors of other protein kinases on the phosphorylation of Ser-756 *in vivo*. Interestingly, the phosphorylation of Ser-756 was found to be suppressed by W-7, a calmodulin antagonist (Fig. 8*D*), but not by PD 98059, an inhibitor of the classical mitogen-activated protein kinase pathway, or by calpeptin, an inhibitor of the calcium-dependent proteinase calpain. Trifluoperazine, another calmodulin antagonist, was also found to suppress phorbol ester-induced Ser-756 phosphorylation (data not shown). Both the phosphorylation of Ser-756 induced by high concentrations of phorbol ester alone and the phosphorylation induced by low levels of phorbol ester in conjunction with the calcium ionophore A23187 were greatly suppressed by W-7 as well as the PKC inhibitor Ro 318220 (Fig. 8*E*). These observations indicate that calmodulin may be involved in regulating Ser-756 phosphorylation *in vivo*.

A Thr-758-phosphorylated CD18 Peptide Binds 14-3-3 Proteins from Leukocyte Lysates—To identify potential functions for the phosphorylation of the CD18 C terminus, we investigated whether proteins in T cell lysates were capable of binding to the C terminus when phosphorylated at particular sites. These experiments showed that two proteins of apparent molecular mass 30 and 28 kDa bound specifically to the C-terminal peptide phosphorylated at Thr-758. In contrast, these proteins did not bind to the unphosphorylated C-terminal peptide or to the peptide phosphorylated at Ser-756 (Fig. 9*A*). The 30- and 28-kDa bands were excised and identified by tryptic mass fingerprinting as 14-3-3$\alpha\beta$ and 14-3-3$\delta\zeta$, respectively (Table III). These results were confirmed by immunoblotting with an antibody that recognizes all 14-3-3 isoforms (Fig. 9*B*). The presence of 14-3-3 proteins binding to the C-terminal peptide could also be detected in the cytoskeletal fraction of leukocytes, where the major part of the phosphorylated integrins reside (Fig. 9*C*).

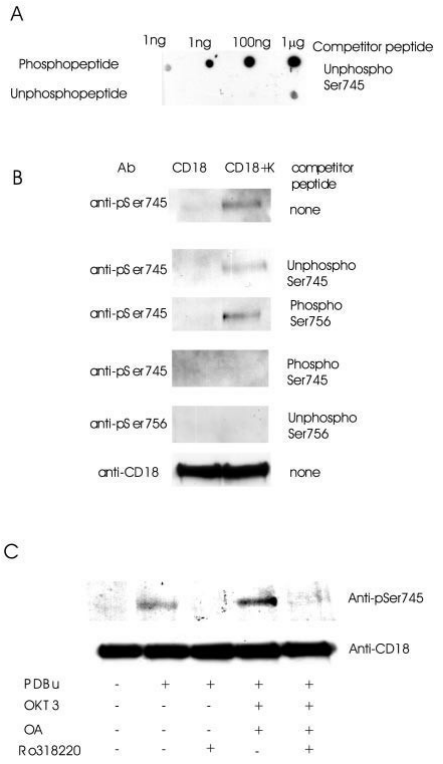

FIG. 7. **Ser-745 is phosphorylated in human T cells.** *A,* the phosphorylated and unphosphorylated forms of the peptide comprising residues 740–751 of CD18 (phosphorylated at Ser-745) were conjugated to keyhole limpet hemocyanin and spotted onto nitrocellulose membranes in the amounts indicated. The membranes were then immunoblotted with an antibody raised against the phosphorylated peptide that had been incubated with the unphosphorylated form of the peptide 740–751 (25 μg/ml). *B,* purified CD18 (1 μg/lane) was phosphorylated for 60 min *in vitro* with purified PKCβ (*CD18+K*) or without kinase (*CD18*). Aliquots of the reaction were subjected to SDS-PAGE, transferred to nitrocellulose, and immunoblotted with antibodies that recognize CD18 phosphorylated at Ser-745 (*anti-pSer745*) or Ser-756 (*anti-pSer756*). The antibodies were first preincubated with or without the indicated peptide antigens (5 μg/ml). The peptides comprised residues 740–751 of CD18 (phosphorylated at Ser-745) and residues 751–761 (phosphorylated at Ser-756) or the unphosphorylated form of the peptide 740–751. The *lowest panel* shows immunoblotting with R2E7B, a CD18-antibody that recognizes the phosphorylated and unphosphorylated forms of CD18 equally well. *C,* human T cells were preincubated for 30 min with or without 1.5 μM okadaic acid (*OA*) or 1 μM Ro 318220, activated with 200 nM PDBu (*PDBu*) or 1:200 dilution of OKT3 (the antibody against the CD3 component of the T cell receptor), and lysed, and the CD11/CD18 complex immunoprecipitated, subjected to SDS-PAGE, and immunoblotted with the phospho-specific antibody that recognizes CD18 phosphorylated at Ser-745 (*anti-pSer745*) in the presence of the unphosphorylated peptide (5 μg/ml). The immunoblots were stripped and reprobed with a CD18-specific antibody (*anti-CD18*) to confirm equal loading.

DISCUSSION

The phosphorylation of integrin cytoplasmic domains has been proposed as a way of regulating integrin activity and/or interaction with cytoplasmic proteins and cell signaling. For example, tyrosine phosphorylation of the integrin β_3 cytoplasmic tail leads to association with Shc (52), an adaptor protein involved in activation of the classical mitogen-activated protein kinase cascade. Tyrosine phosphorylation of the integrin β_3 cytoplasmic tail might also regulate its binding to cytoskeletal elements (53). On the other hand, threonine phosphorylation of β_3 integrins is reported to prevent Shc from binding to the tyrosine-phosphorylated integrin (54).

In contrast to the β_1 and β_3 integrins, the CD18 integrin polypeptide (also called the β_2 integrin) lacks two of the three tyrosines in the conserved NPXY motifs found in the integrin β_1 and β_3 chains. However, the CD18 integrins have been shown to become phosphorylated on serine and threonine residues in cells after stimulation with phorbol ester (30–32) or T cell receptor engagement (25). The role of these phosphorylation events is not yet understood.

To identify the protein kinases that phosphorylate CD18, we purified and identified the major activities in T cell extracts that phosphorylate a synthetic peptide corresponding to most of the cytoplasmic domain of the integrin CD18 chain. The protein kinases detected were found to be active proteolytic fragments of PKCβ and PKCδ, which are known to be cleaved intracellularly from the native enzymes by proteases, such as calpain (55, 56). The native forms of these and other PKC isoforms were presumably not detected because they are only active in the presence of one or more cofactors, *i.e.* calcium ions, phospholipids, and diacylglycerol or phorbol esters (57, 58), and it is possible that other PKC isoforms are cleaved proteolyti-

Carl_G_190x270_mm_blokki_FINAL.indd 385 06-Aug-23 1:54:24 PM

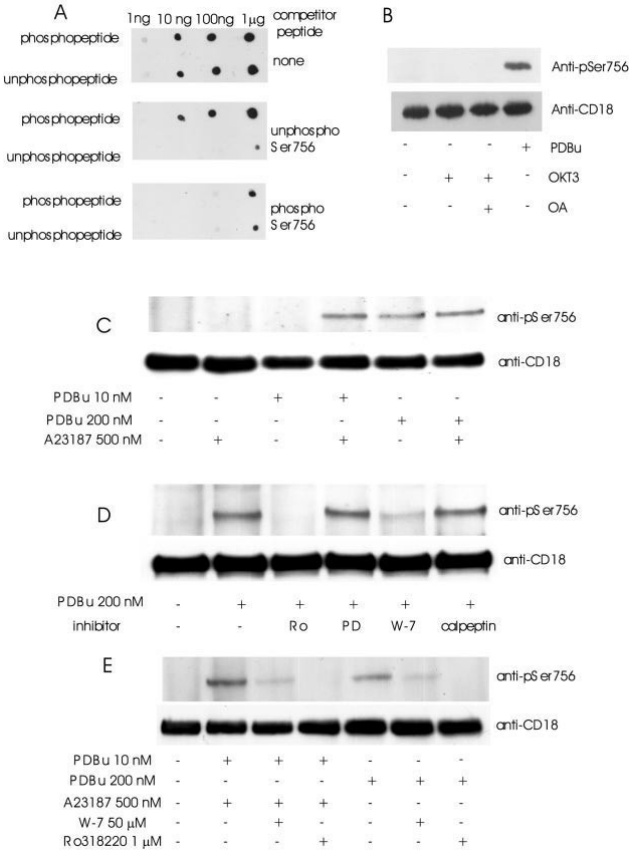

FIG. 8. **Ser-756 phosphorylation is induced by low concentrations of PDBu in the presence of calcium ionophore and inhibited by the calmodulin antagonist W-7.** *A,* the phosphorylated and unphosphorylated forms of the peptide comprising residues 751–761 of CD18 (phosphorylated at Ser-756) were conjugated to keyhole limpet hemocyanin and spotted onto nitrocellulose membranes in the amounts indicated. The membranes were then immunoblotted with an antibody raised against the phosphorylated peptide that had been incubated without additions (none), with the unphosphorylated form of the peptide 751–761, or with the phosphorylated form of the same peptide (each at 100 μg/ml). The figure shows that the antibody only became phospho-specific after incubation with the unphosphorylated peptide. All subsequent experiments with this antibody were therefore performed in the presence of excess unphosphopeptide (25 μg/ml). *B,* the experiment was carried out as in Fig. 7*B* except that the anti-pSer-756 antibody replaced the anti-phospho-Ser-745 antibody. T cells were preincubated with or without 1.5 μM okadaic acid before activation with 1:200 dilution of OKT3 or 200 nM PDBu. *C,* same as *B*, except that T cells were stimulated with or without 10 or 200 nM PDBu in the presence or absence of 500 nM A23187. *D,* same as *B,* except that the T cells were stimulated in the presence or absence of PDBu with or without Ro 318220 (5 μM, *Ro*), PD 98059 (50 μM, *PD*), W-7 (50 μM), or calpeptin (100 μg/ml). *E,* same as *B*, except that the cells were preincubated with or without the indicated concentrations of W-7 or Ro 318220 and stimulated with 10 nM PDBu and 500 nM A23187 or with 200 nM PDBu.

cally to a lesser extent than PKCβ and PKCδ and thus not detected under our assay conditions. This led us to discover that many of the known PKC isoforms are capable of phosphorylating CD18 *in vitro,* and indeed two them, PKCα and PKCη, appeared to be very active toward CD18 (Fig. 4). At present, we cannot say which PKC isoforms are the main kinases phosphorylating CD18 *in vivo*. The residues on CD18 phosphorylated by PKCβ, PKCδ, and PKCη were Ser-745 and Thr-758. Interestingly, however, PKCα phosphorylated CD18 on Thr-760 as well as Thr-758. It may also phosphorylate Thr-759 (Fig. 5, *B* and *C*), but this has not yet been shown definitively.

The finding that the major serine residue phosphorylated by PKC isoforms *in vitro* was Ser-745 was somewhat surprising, because the major site in the C-terminal domain that becomes phosphorylated in response to phorbol esters is Ser-756 (29), which is not phosphorylated by any PKC isoform *in vitro*. However, the PDBu-induced phosphorylation of CD18 at Ser-756 is prevented by inhibitors of PKC (Fig. 8), suggesting that Ser-756 is phosphorylated by a protein kinase that is activated by a PKC isoform. Alternatively, a PKC isoform may inhibit a protein phosphatase that dephosphorylates Ser-756 in cells. Interestingly, we found that the phosphorylation of Ser-756 induced by low concentrations of PDBu only occurred in the presence of the calcium ionophore A23187, a phenomenon reported previously (59) for total CD18 phosphorylation. Moreover, the phosphorylation of Ser-756 induced by low concentrations of PDBu and A23187, or high concentrations of PDBu in the absence of A23187, was suppressed by the calmodulin antagonist W-7. This raises the possibility that a PKC-activated Ser-756 kinase might also be dependent on calcium ions and calmodulin. The phosphorylation of Ser-756 does not seem to be important in adhesion, because its mutation to alanine

Carl_G_190x270_mm_blokki_FINAL.indd 386 06-Aug-23 1:54:24 PM

has no effect on phorbol ester-induced binding of CD18 to ICAM-1, a major ligand of the integrin (29). However, we have shown previously that calmodulin antagonists are strong suppressors of PDBu-induced T cell aggregation (27). Because a calmodulin antagonist also reduces Ser-756 phosphorylation, it is possible that Ser-756 phosphorylation plays a role in these events.

Based on phosphopeptide mapping, it has been reported previously (44) that two of the three threonine residues Thr-758, Thr-759, and Thr-760 become phosphorylated when T cells are stimulated with PDBu, although the protein phosphatase inhibitor okadaic acid also had to be added to the cells. The cytoplasmic domain also becomes phosphorylated on a threonine residue(s) when the T cell receptor is activated (25). In the present study, we have shown that Ser-745 becomes phosphorylated, albeit somewhat weakly, when T cells are stimulated with PDBu alone, and that phosphorylation could be increased in the presence of OKT3, an antibody that binds to the CD3 component of the T cell receptor, plus okadaic acid. Because PKC isoforms are the major protein kinase activities in leukocyte lysates responsible for the phosphorylation Ser-745, and the phosphorylation of Ser-745 is inhibited by Ro 318220 *in vivo*, it would appear that a PKC isoform mediates the phosphorylation of CD18 at Ser-745 in cells. However, since Ro 318220 and Go-6983, which both inhibit CD18 phosphorylation, are not exclusively specific PKC inhibitors, it cannot be completely excluded that another unknown phorbol ester-activated kinase is mediating the phosphorylation of CD18 at Ser-745. It is also possible that Ser-745 becomes phosphorylated more strongly in response to other signals or combinations of signals that have yet to be identified.

The mutation of Ser-745 to Ala, like the mutation of Ser-756 to Ala, has no effect on phorbol ester-induced binding of CD11/CD18 to ICAM-1 (29), indicating that these phosphorylation events may play a different role. Ser-745 is not conserved in the β_1 or β_3 integrins, and it may thus play a role in CD11/CD18-specific signaling events. The stoichiometry of CD18 integrin phosphorylation *in vivo* after phorbol ester treatment in the presence of okadaic acid has been determined as 0.92 mol per mol of protein (44). Because Ser-756, Ser-745, and Thr-758/Thr-759/Thr-760 phosphorylation take place under these conditions, each of these sites is clearly phosphorylated to only a low stoichiometry. However, this does not exclude them playing important roles physiologically if, by analogy with receptor tyrosine phosphorylation, their function is to recruit other signaling molecules to the plasma membrane.

PKC has been implicated previously in the regulation of integrin function. PKCα associates with β_1 integrins and regulates their internalization (60), whereas PKCϵ has been implicated in the regulation of integrin-dependent cell spreading (61, 62). Interestingly, the PKC isoforms α, βI, βII, and δ, but not PKCζ, activate integrin-mediated adhesion to ICAM-1 in a model system (21). Moreover, the receptor for activated PKC (Rack1), a PKCβ-interacting protein that is believed to regulate its localization and substrate specificity (63, 64), interacts with the membrane-proximal part of the integrin CD18 cytoplasmic tail in phorbol ester-activated leukocytes (39). An attractive hypothesis is that the binding of Rack1 to the integrin cytoplasmic tail could recruit active PKCβ to the integrin and allow it to phosphorylate Ser-745 and Thr-758.

To investigate the functions of the C-terminal phosphorylation on CD18, we initially studied whether proteins present in the cytoplasm of T cells bound to the C-terminal peptide when it was phosphorylated at particular sites. This led us to find that the C terminus of CD18 binds specifically to 14-3-3 proteins when it is phosphorylated at Thr-758. The 14-3-3 proteins

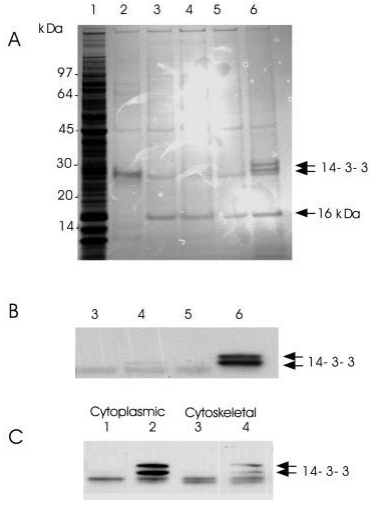

FIG. 9. **14-3-3 proteins bind to a Thr-758-phosphorylated integrin C-terminal peptide but not to a Ser-756-phosphorylated peptide.** Human leukocyte lysates (*A* and *B*) or cytoplasmic and cytoskeletal fractions (*C*) were subjected to affinity chromatography on agarose to which the peptides indicated below had been attached covalently (see "Experimental Procedures"). The protein bound to each column was eluted with SDS, subjected to SDS-PAGE, and either stained with Coomassie Blue (*A*) or transferred to nitrocellulose and immunoblotted with an antibody that recognizes all 14-3-3 isoforms (*B* and *C*). *A, lane 1*, leukocyte lysate; *lane 2*, eluate from a control protein G-Sepharose column; *lane 3*, eluate from agarose to which the unphosphorylated peptide 751–761 had been bound; *lane 4*, eluate from agarose to which the peptide 751–761 phosphorylated at Ser-756 had been bound; *lane 5,* eluate from agarose to which the unphosphorylated peptide 753–763 had been bound; *lane 6*, eluate from agarose to which the peptide 753–763 phosphorylated at Thr-758 had been bound. *B,* fractions 3–6 from *A* were electrophoresed and immunoblotted with an anti-14-3-3 antibody. *C,* same as *B*, except that cytoplasmic (*lanes 1* and *2*) and cytoskeletal (*lanes 3* and *4*) fractions were subjected to affinity chromatography on agarose to which the unphosphorylated form of the peptide 753–763 (*lanes 1* and *3*) or the same peptide phosphorylated at Thr-758 (*lanes 2* and *4*) had been bound.

were recruited both from the soluble and, importantly, from the cytoskeletal fractions of leukocytes, where most of the phosphorylated integrins have been shown to reside (33). In contrast, the 14-3-3s did not bind to the unphosphorylated C-terminal peptide or the peptide phosphorylated at Ser-756. One additional protein of 16 kDa bound to the C-terminal peptide (Fig. 9*A*), but this was independent of phosphorylation. In coprecipitation studies, we failed to detect 14-3-3 binding to CD18 in activated cells, but this could be due to the low stoichiometry of threonine phosphorylation under these circumstances. Alternatively, the phosphorylation of Ser-756, Thr-759, and/or Thr-760 may interfere with binding of 14-3-3s to the Thr-758-phosphorylated integrins. Further work is clearly needed to evaluate whether 14-3-3 binding to CD18 occurs *in vivo*.

14-3-3s are adaptor proteins that bind to phosphoserine- and phosphothreonine-containing motifs (65) and are known to be involved in regulating a number of signaling molecules (66). They have been shown to dimerize and could thus recruit other signaling proteins to form complexes. The optimal consensus sequence for 14-3-3 binding is R*XX*pS/pT*X*P (65), which does not conform to the sequence surrounding Thr-758. However, other phosphorylated sequences have been shown to interact with 14-3-3 proteins (67, 68). Indeed, recently, 14-3-3β was identified in a yeast two-hybrid screen with β_1 integrins, but

Carl_G_190x270_mm_blokki_FINAL.indd 387 06-Aug-23 1:54:25 PM

TABLE III

Identification of the proteins in Fig. 9 binding to the Thr 758-phosphorylated C terminus of CD18 as 14-3-3 α/β and ζ/δ

Tryptic peptides from the bands marked 14-3-3 in Fig. 9*A* were analyzed by mass fingerprinting. The table summarizes the peptides from the bands that matched the 14-3-3 sequences.

Mass measured	Theoretical	Residue no	Peptide sequence
14-3-3α/β			
816.4441	816.4216	12–18	(K)LAEQAER(Y)
907.5347	907.5253	42–49	(R)NLLSVAYK(N)
948.4447	948.4249	121–127	(K)MKGDYYR(Y)[a]
1124.5695	1124.5523	159–167	(K)EMQPTHPIR(L)[a]
1189.6738	1189.6615	213–222	(K)DSTLIMQLLR(D)
1205.6717	1205.6564	213–222	(K)DSTLIMQLLR(D)[a]
1252.6594	1252.6472	158–167	(K)KEMQPTHPIR(L)[a]
1279.6678	1279.6534	128–139	(R)YLAEVAAGDDKK(G)
1304.6990	1304.6850	104–115	(K)FLIPNASQAESK(V)
1548.7507	1548.7142	28–41	(K)SVTEQGAELSNEER(N)
2041.0070	2040.9878	140–157	(K)GIVDQSQQAYQEAFEISK(K)
2132.0076	2131.9923	194–212	(K)TAFDEAIAELDTLSEESYK(D)
2169.0848	2169.0828	139–157	(K)KGIVDQSQQAYQEAFEISK(K)
2169.0484	2169.0828	140–158	(K)GIVDQSQQAYQEAFEISKK(E)
2317.1906	2317.2120	168–187	(R)LGLALNFSVFYYEILNSPEK(A)
3302.6687	3302.6354	194–222	(K)TAFDEAIAELDTLSEESSYKDSTLIMQLLR(D)
3318.7238	3318.6303	194–22	(K)TAFDEAIAELDTLSEESSYKDSTLIMQLLR(D)[a]
14-3-3ζ/δ			
816.4441	816.4216	14–20	(K)LAEQAER(Y)
907.5347	907.5253	44–51	(R)NLLSVAYK(N)
1124.5695	1124.5523	161–169	(K)EMQPTHPIR(L)[a]
1189.6738	1189.6615	215–224	(K)DSTLIMQLLR(D)
1205.6717	1205.6564	215–224	(K)DSTLIMQLLR(D)[a]
1252.6594	1252.6472	160–169	(K)KEMQPTHPIR(L)[a]
1598.7682	1598.7411	30–43	(K)AVTEQGHELSNEER(N)
1844.8289	1844.8159	14–29	(K)LAEQAERYDDMAAAMK(A)[a]
2159.0168	2159.0257	141–159	(K)QTTVSNSQQAYQEAFEISK(K)
2159.0168	2159.0032	196–214	(K)TAFDEAIAELDTLNEESYK(D)
2317.1906	2317.2120	170–189	(R)LLALNFSVFYYEILNSPEK(A)
3345.5854	3345.6412	196–224	(K)TAFDEAIAELDTLNEESYKDSTLIMQLLR(D)[a]

[a] A methionine-sulfone derivative is indicated.

the interaction was not thought to be phosphorylation-dependent (69).

The TTT motif (Thr-758, Thr-759, and Thr-760) appears to play a pivotal role in integrin regulation. Mutation of these threonines singly or in combination decreases binding to ICAM-1 in response to PDBu (29). In addition, an activating mutation (L732R) that induces phorbol ester responsiveness of CD11a/CD18 integrins in K562 cells that normally do not respond to phorbol esters is abolished by the mutation of Thr-758 to Ala (70). The mutation of the TTT motif also causes defects in post-receptor signaling events, whereby the integrin receptor interacts with the actin cytoskeleton and induces cell spreading (16), and phosphorylated integrins have been shown to associate with the actin cytoskeleton preferentially (33). It is therefore tempting to speculate that threonine phosphorylation of CD18 recruits 14-3-3 proteins to the plasma membrane-cytoskeleton connection and that the 14-3-3s in turn recruit further proteins to regulate cell spreading and/or integrin signaling.

Acknowledgments—We thank David Campbell for technical assistance. We are grateful to Edinburgh and Dundee, UK, Blood Transfusion Services for providing buffy coats.

REFERENCES

1. Springer, T. A. (1990) *Nature* **346,** 425–434
2. Gahmberg, C. G., Tolvanen, M., and Kotovuori, P. (1997) *Eur. J. Biochem.* **245,** 215–232
3. Dustin, M. L., and Springer, T. A. (1989) *Nature* **341,** 619–624
4. Dransfield, I., Cabanas, C., Craig, A., and Hogg, N. (1992) *J. Cell Biol.* **116,** 219–226
5. Cabanas, C., and Hogg, N. (1993) *Proc. Natl. Acad. Sci. U. S. A.* **90,** 5838–5842
6. Li, R., Nortamo, P., Kantor, C., Kovanen, P., Timonen, T., and Gahmberg, C. G. (1993) *J. Biol. Chem.* **268,** 21474–21477
7. Kotovuori, A., Pessa-Morikawa, T., Kotovuori, P., Nortamo, P., and Gahmberg, C. G. (1999) *J. Immunol.* **162,** 6613–6620
8. Keizer, G. D., Visser, W., Vliem, M., and Figdor, C. G. (1988) *J. Immunol.* **140,** 1393–1400
9. Landis, R. C., Bennett, R. I., and Hogg, N. (1993) *J. Cell Biol.* **120,** 1519–1527
10. Robinson, M. K., Andrew, D., Rosen, H., Brown, D., Ortlepp, S., Stephens, P., and Butcher, E. C. (1992) *J. Immunol.* **148,** 1080–1085
11. Van Kooyk, Y., van de Wiel, P., van de Kemanede, P., Weder, P., Kuijpers, T. W., and Figdor, C. G. (1989) *Nature* **342,** 811–813
12. Axelsson, B., Youseffi-Etemad, R., Hammarstrom, S., and Perlmann, P. (1988) *J. Immunol.* **141,** 2912–2917
13. Koopman, G., van Kooyk, Y., de Graaff, M., Meyer, C. J. L., Figdor, C. G., and Pals, S. T. (1990) *J. Immunol.* **145,** 3589–3593
14. Patarroyo, M., Beatty, P. G., Fabre, J. W., and Gahmberg, C. G. (1985) *Scand. J. Immunol.* **22,** 171–182
15. Rothlein, R., and Springer, T. A. (1986) *J. Exp. Med.* **63,** 1132–1149
16. Peter, K., and Toole, T. E. (1995) *J. Exp. Med.* **181,** 315–326
17. Pardi, R., Inverardi, L., Rugarli, C., and Bender, J. R. (1992) *J. Cell Biol.* **116,** 1211–1220
18. Stewart, M. P., Cabanas, C., and Hogg, N. (1996) *J. Immunol.* **156,** 1810–1817
19. Van Kooyk, Y., van Vliet, S. J., and Figdor, C. G. (1999) *J. Biol. Chem.* **274,** 26869–26877
20. Lu, C., Ferzly, M., Takagi, J., and Springer, T. A. (2001) *J. Immunol.* **166,** 5629–5637
21. Katagiri, K., Hattori, M., Minato, N., Irie, S.-K., Takatsu, K., and Kinashi, T. (2000) *Mol. Cell. Biol.* **20,** 1956–1969
22. Nagel, W., Zeitlmann, L., Schilcher, P., Geiger, C., Kolanus, J., and Kolanus, W. (1998) *J. Biol. Chem.* **273,** 14853–14861
23. Rourke, A. M., Shao, H., and Kaye, J. (1998) *J. Immunol.* **161,** 5800–5803
24. Hedman, H., and Lundgren, E. (1992) *J. Immunol.* **149,** 2295–2299
25. Valmu, L., and Gahmberg, C. G. (1995) *J. Immunol.* **155,** 1175–1183
26. Stewart, M. P, McDowall, A., and Hogg, N. (1998) *J. Cell Biol.* **140,** 699–707
27. Fagerholm, S., Prescott, A., Cohen, P., and Gahmberg, C. G. (2001) *FEBS Lett.* **491,** 131–136
28. Hibbs, M. L., Xu, H., Stacker, S. A., and Springer, T. A. (1991) *Science* **251,** 1611–1613
29. Hibbs, M. L., Jakes, S., Stacker, S. A., Wallace, R. W., and Springer, T. A. (1991) *J. Exp. Med.* **174,** 1227–1238
30. Hara, T., and Fu, S. M. (1985) in *Leukocyte Typing II* (Reinherz, E. L., Haynes, B. F., Nadler, L. M., and Bernstein, I. D., eds) Vol. 3, pp. 77–84, Springer-Verlag Inc., New York
31. Chatila, T. A., Geha, R. S., and Arnaout, M. A. (1989) *J. Cell Biol.* **109,** 3435–3444
32. Buyon, J. P., Slade, S. G., Reibman, J., Abramson, S. B., Philips, M. R., Weissman, G., and Winchester, R. (1990) *J. Immunol.* **144,** 191–197
33. Valmu, L., Fagerholm, S., Suila, H., and Gahmberg, C. G. (1999) *Eur. J. Immunol.* **29,** 2107–2118
34. Schoenwaelder, S., and Burridge, K. (1999) *Curr. Opin. Cell Biol.* **11,** 274–286
35. Kupfer, A., Burn, P., and Singer, S. J. (1990) *J. Mol. Cell. Immunol.* **4,** 317–325

Carl_G_190x270_mm_blokki_FINAL.indd 388 06-Aug-23 1:54:25 PM

36. Sharma, C. P, Ezzell, R. M., and Arnaout, M. A. (1995) *J. Immunol.* **154,** 3461–3470
37. Pavalko, F. M., and LaRoche, S. M. (1993) *J. Immunol.* **151,** 3795–3807
38. Sampath, R., Gallagher, P. J., and Pavalko, F. M. (1998) *J. Biol. Chem.* **273,** 33588–33594
39. Lilientahl, J., and Chang, D. D. (1998) *J. Biol. Chem.* **273,** 2379–2383
40. Kolanus, W., Nagel, W., Shiller, B., Zeitlmann, L., Godar, S., Stockinger, H., and Seed, B. (1996) *Cell* **86,** 233–242
41. Bianchi, E., Denti, S., Granata, A., Bossi, G., Geginat, J., Villa, A., Rogge, L., and Pardi, R. (2000) *Nature* **404,** 617–621
42. Harlow, E., and Lane, D. (eds) (1988) *Antibodies: A Laboratory Manual*, pp. 82–83, Cold Spring Harbor Laboratory, Cold Spring Harbor, NY
43. Nortamo, P., Patarroyo, M., Kantor, C., Suopanki, J., and Gahmberg, C. G. (1988) *Scand. J. Immunol.* **28,** 537–546
44. Valmu, L., Hilden, T., van Willigen, G., and Gahmberg, C. G. (1999) *Biochem. J.* **339,** 119–125
45. Deleted in proof
46. Woods, L. Y., Rena, G., Morrice, N., Barthel, A., Becker, W., Guo, S., Unterman, T. G., and Cohen, P. (2001) *Biochem. J.* **355,** 597–607
47. Lawler, S., Fleming, Y., Goedert, M., and Cohen, P. (1998) *Curr. Biol.* **8,** 1387–1390
48. Kantor, C., Suomalainen-Nevanlinna, H., Patarroyo, M., Osterlund, K., Bergman, T., Jornvall, H., Schroder, J., and Gahmberg, C. G. (1988) *Eur. J. Biochem.* **170,** 653–659
49. Davies, S. P., Reddy, H., Caivano, M., and Cohen, P. (2000) *Biochem. J.* **351,** 95–105
50. Stokoe, D., Campbell, D. G., Nakielny, S., Hikada, H., Leevers, S. J., Marshall, C., and Cohen, P. (1993) *EMBO J.* **11,** 3985–3994
51. Olivier, A. R., and Parker, P. J. (1991) *Eur J. Biochem.* **200,** 805–810
52. Cowan, K. J., Law, D. A., and Phillips, D. R. (2000) *J. Biol. Chem.* **275,** 36423–36429
53. Jenkins, A. L., Nannizzi-Alaimo, L., Silver, D., Sellers, J. R., Ginsberg, M. H., Law, D. A., and Phillips, D. R. (1998) *J. Biol. Chem.* **273,** 13878–13885
54. Kirk, R. I., Sanderson, M. R., and Lerea, K. M. (2000) *J. Biol. Chem.* 30901–30906
55. Suzuki, K., Saido, T. C., and Hirai, S. (1992) *Ann. N. Y. Acad. Sci.* **674,** 218–227
56. Pontremoli, S., and Melloni, E. (1989) *Rev. Biol. Cell.* **20,** 161–177
57. Hug, H., and Sarre, T. F. (1993) *Biochem. J.* **291,** 329–343
58. Mellor, H., and Parker, P. J. (1998) *Biochem. J.* **332,** 281–292
59. Valmu, L., Autero, M., Siljander, P., Patarroyo, M., and Gahmberg, C. G. (1991) *Eur. J. Immunol.* **21,** 2857–2862
60. Ng, T., Shima, D., Squire, A., Bastiaens, P. I. H., Gschmeissner, S., Humphries, M., and Parker, P. J. (1999) *EMBO J.* **18,** 3909–3923
61. Haller, H., Lindschau, C., Maasch, C., Olthoff, H., Kurscheid, D., and Luft, F. C. (1998) *Circ. Res.* **82,** 157–165
62. Berrier, A. L., Mastrangelo, A. M., Downward, J., Ginsberg, M., and LaFlamme, S. E. (2000) *J. Cell Biol.* **151,** 1549–1560
63. Ron, D., Chen, C.-H., Caldwell, J., Jamieson, L., Orr, E., and Mochly-Rosen, D. (1994) *Proc. Natl. Acad. Sci. U. S. A.* **91,** 839–843
64. Ron, D., Jiang, Z., Ya, L., Vgts, A., Diamond, I., and Gordon, A. (1999) *J. Biol. Chem.* **274,** 27039–27046
65. Muslin, A. J., Tanner, J. W., Allen, P. M., and Shaw, A. S. (1996) *Cell* **84,** 889–897
66. Baldin, V. (2000) in *Progress in Cell Cycle Research* (Meijer, L., Jezequel, A., and Ducommun, B, eds) Vol. 4, pp. 49–60, Kluwer Academic, Plenum Publishers, New York
67. Yaffe, M. B., Rttinger, K., Volinia, S., Caron, P. R., Aitken, A., Leffers, H. Gamblin, S. J., Smerdon, S. J., and Cantley, L. C. (1997) *Cell* **91,** 961–971
68. Liu, Y.-C., Liu, Y., Elly, C., Yoshida, H., Lipkowitz, S., and Altman, A. (1997) *J. Biol. Chem.* **272,** 9979–9985
69. Han, D. C., Rodriguez, L. G., and Guan, J.-L. (2001) *Oncogene* **20,** 346–357
70. Bleijs, D., van Duijnhoven, G. C. F., van Vliet, S. J., Thijssen, J. P. H., Figdor, C. G., and van Kooyk, Y. (2001) *J. Biol. Chem.* **276,** 10338–10346

Carl_G_190x270_mm_blokki_FINAL.indd 389 06-Aug-23 1:54:26 PM

The Journal of Immunology
RESEARCH ARTICLE | APRIL 15 2003
The Journal of Immunology

Threonine Phosphorylation Sites in the β_2 and β_7 Leukocyte Integrin Polypeptides[1]

Tiina J. Hilden,* Leena Valmu,† Satu Kärkkäinen,* and Carl G. Gahmberg[2]*

The cytoplasmic domains of integrins play a key role in a variety of integrin-mediated events including adhesion, migration, and signaling. The molecular mechanisms that enhance integrin function are still incompletely understood. Because protein kinases are known to be involved in the signaling and the activation of integrins, the role of phosphorylation has been studied by several groups. The β_2 leukocyte integrin subunit has previously been shown to become phosphorylated in leukocytes on cytoplasmic serine and functionally important threonine residues. We have now mapped the phosphorylated threonine residues in activated T cells. After phorbol ester stimulation, all three threonine residues (758–760) of the threonine triplet became phosphorylated but only two at a time. CD3 stimulation leads to a strong threonine phosphorylation of the β_2 integrin, but differed from phorbol ester activation in that phosphorylation occurred only on threonine 758. The other leukocyte-specific integrin, β_7, has also been shown to need the cytoplasmic domain and leukocyte-specific signal transduction elements for integrin activation. Cell activation with phorbol ester, and interestingly, through the TCR-CD3 complex, caused β_7 integrin binding to VCAM-1. Additionally, cell activation led to increased phosphorylation of the β_7 subunit, and phosphoamino acid analysis revealed that threonine residues became phosphorylated after cell activation. Sequence analysis by manual radiosequencing by Edman degradation established that threonine phosphorylation occurred in the same threonine triplet as in β_2 phosphorylation. ***The Journal of Immunology,*** **2003, 170: 4170–4177.**

Integrins are heterodimeric glycoproteins that play diverse roles in cell adhesion and signaling. Integrins of the β_1, β_2, and β_7 subfamilies are critical for leukocyte homing (1, 2). β_2 and β_7 integrins are expressed solely on leukocytes (3, 4). These integrins mediate a number of cell-to-cell interactions by binding to intercellular adhesion molecules, which are expressed on different cells (5). β_2 integrins also bind other molecules like E-selectin (6), type I collagen (7), and fibrinogen (8, 9). The integrin $\alpha_4\beta_7$ is a cell adhesion receptor mainly expressed on lymphocytes, and mediates their homing to the intestine and associated lymphoid tissue, such as Peyer's patches (2). $\alpha_4\beta_7$ is a receptor for the VCAM-1 and the mucosal vascular addressin mucosal addressin cell adhesion molecule-1 on intestinal endothelial cells (10).

The affinity or avidity of integrins for their extracellular ligands is regulated by the activation status of the integrin molecule (5, 11). The different states of activation can be modulated by agents such as phorbol esters (12, 13) or by Abs against the TCR-CD3 complex or other proteins such as CD2 (14, 15). This activation of integrins has been termed inside-out signaling (16, 17). Several integrin families have been shown to undergo activation, among these the β_2 integrins in leukocytes (5) and the β_1 integrins in hemopoietic cells (18). Also, $\alpha_4\beta_7$-dependent binding to ligands has been shown to require prior activation (4).

Reversible phosphorylation of proteins is commonly involved in dynamically regulated cellular reactions, and this mechanism is used by cells both in the regulation of adhesion and in integrin-mediated signal transduction (19, 20). However, it is unclear whether or how phosphorylation of integrins themselves affects these activities, and therefore the phosphorylation status of integrins has been extensively studied. The cytoplasmic domains of the integrin β subunits contain a number of putative phosphorylation sites. The phosphorylation state of β_2 integrins has been reported to change after T cell stimulation by phorbol ester (21–24) or by CD3 ligation (25, 26). The main phorbol ester-induced phosphorylation site was identified as Ser^{756} in the β_2 cytoplasmic domain (27). The activation also induces threonine phosphorylation in β_2, which can be revealed when serine/threonine phosphatases in T cells are inhibited (26). It has been reported previously that two of the three threonine residues (758–760) become phosphorylated after T cell stimulation with phorbol ester (28). Ser^{745} was recently found to be phosphorylated in the β_2 cytoplasmic tail, induced by phorbol ester and strengthened by the use of okadaic acid (OA)[3] and CD3 Ab together with phorbol ester (29). The amino acids $Thr^{758–760}$ and Ser^{745} have been shown to become phosphorylated by protein kinase C (PKC) (2, 26, 29), and Ser^{756} by an unknown kinase (29). The importance of the serine phosphorylations of β_2 integrin activation is questionable, but the threonine triplet has been shown to be vital for the phorbol ester-induced β_2-mediated binding of cells to coated ICAM-1 (27). The threonine triplet has also been shown to be involved in regulating postreceptor events through the β_2 integrins, such as cytoskeletal association and cell spreading (30). Threonine-phosphorylated integrins distribute preferentially to the actin cytoskeleton (31). The linkage to the actin cytoskeleton could occur via actin-binding proteins, such as filamin, which interacts directly with β_2 integrin

*Department of Biosciences, Division of Biochemistry, and †Institute of Biotechnology, University of Helsinki, Helsinki, Finland

Received for publication June 21, 2002. Accepted for publication February 12, 2003.

The costs of publication of this article were defrayed in part by the payment of page charges. This article must therefore be hereby marked *advertisement* in accordance with 18 U.S.C. Section 1734 solely to indicate this fact.

[1] This work was supported by the Academy of Finland, the Sigrid Jusélius Foundation, the Finnish Cancer Society, and the Magnus Ehrnrooth Foundation.

[2] Address correspondence and reprint requests to Dr. Carl G. Gahmberg, Department of Biosciences, Division of Biochemistry, University of Helsinki, P.O. Box 56 (Viikinkaari 5), FIN-00014 Helsinki, Finland. E-mail address: carl.gahmberg@helsinki.fi

[3] Abbreviations used in this paper: OA, okadaic acid; PKC, protein kinase C; PDBu, phorbol 12,13-dibutyrate; MS/MS, tandem mass spectrometry.

Copyright © 2003 by The American Association of Immunologists, Inc.

0022-1767/03/$02.00

Carl_G_190x270_mm_blokki_FINAL.indd 390 06-Aug-23 1:54:27 PM

(32). Filamin has been shown to interact also with β_1 and β_7 integrins, and threonine phosphorylation has been speculated to regulate the interaction, and, subsequently, cell migration (33).

The β_7 subunit shows the closest resemblance to the β_2 integrin phosphorylation sites having both a single serine in the position corresponding to the Ser^{756} as well as a threonine triplet. The similarity between the β_2 and β_7 sequences in this region is intriguing, because $\alpha_4\beta_7$, like β_2 integrins, is expressed only on leukocytes, and the existence of leukocyte-specific signal transduction elements are hypothesized to be involved in activation of both β_2 and β_7 integrins (34). The cytoplasmic domain of β_7 is important in the regulation of integrin function, because truncation of the β_7 subunit cytoplasmic domain resulted in three different activation states of $\alpha_4\beta_7$: inactive, partially active, and fully active receptors (35).

In this study, we have mapped the phosphorylated threonines in the β_2 cytoplasmic domain after T cell activation with OA and phorbol ester. We have also characterized the phosphorylation of β_2 after CD3 ligation. T cell activation through the TCR caused phosphorylation both on serine and threonine residues similarly to phorbol esters, but threonine phosphorylation was dominating. Unlike phorbol ester-induced phosphorylation, only one threonine (Thr^{758}) became phosphorylated after CD3 ligation. Interestingly, the main phorbol ester-induced phosphorylation site Ser^{756} did not become phosphorylated in CD3-activated T cells. Additionally, we have shown that CD3 triggering induced β_7 integrin binding to VCAM-1, and we observed β_2-like threonine phosphorylation in activated β_7 integrins, but mutational analysis showed that the phosphorylated threonine was not needed for adhesion.

Materials and Methods

Reagents and Abs

Phorbol 12,13-dibutyrate (PDBu) was from Sigma-Aldrich (St. Louis, MO), and OA was from Calbiochem-Novabiochem (La Jolla, CA). [^{32}P]Orthophosphate (aqueous solution; 10 mCi/ml; 5000 Ci/mmol) was purchased from the Radiochemical Center (Amersham, U.K.). Recombinant human VCAM-1 was from R&D Systems (Abingdon, U.K.). Sequencing-grade modified trypsin (activity >2; 5 U/mg) was purchased from Promega (Madison, WI).

The mAb R7E4 against the human β_2 subunit of leukocyte integrin has been described previously (36). The mAb OKT3, which reacts with CD3, was used in the form of ascites fluid produced by hybridoma cells (clone CRL 8001; American Type Culture Collection (ATCC), Manassas, VA). The anti-β_7 mAb FIB504 hybridoma was obtained from ATCC. The monoclonal activating Ab against mouse-CD3ϵ and the blocking Ab against mouse α_4-chain were purchased from Southern Biotechnology Associates (Birmingham, AL). The monoclonal blocking Ab against mouse β_2 (LFA-1) was from R&D Systems, and the monoclonal blocking Ab against human β_1 was from Chemicon (Temecula, CA).

PCR mutagenesis of the β_7 subunit

The pBluescript constructs encoding the full-length sequence of mouse β_7 and α_4 were kindly provided by Dr. I. Weissmann (Stanford University, Stanford, CA). The point mutant T782A in mouse β_7 cDNA was generated through a two-reaction PCR strategy (37). The mutant and wild-type constructs were subcloned into the mammalian expression vector pEF-BOS (38) using the unique *Xba*I cloning site. The mutated construct was confirmed by automated DNA sequencing.

Cell lines and cDNA transfection

Buffy coats used for the isolation of T cells were obtained from the Finnish Red Cross Blood Transfusion Service (Helsinki, Finland). T cells were isolated as described previously (28). The murine T cell lymphoma line TK-1 was purchased from ATCC. Cells were grown in RPMI 1640 medium supplemented with 10% FCS, nonessential amino acids, 0.05 mM 2-ME, L-glutamine, and antibiotics.

COS-1 cells were cultured in DMEM supplemented with 10% FCS, L-glutamine, and antibiotics. COS-1 cells were cotransfected with purified α_4 and β_7 subunit cDNAs using the Fugene 6 transfection reagent according to the manufacturer's instructions (Roche, Indianapolis, IN). Flow cytometric analysis was used to quantitate cell surface expression of the transfected COS-1 cells.

Cell adhesion assays

Recombinant soluble human VCAM-1 (0.3 μg/well) was coated on flat-bottom 96-well microtiter plates by overnight incubation at 4°C. The wells were blocked with 3% BSA for 2 h at 37°C. TK-1 cells suspended in binding medium (RPMI 1640, 40 mM HEPES, 0.1% BSA, and 1 mM $MgCl_2$) were stimulated with 200 nM PDBu or anti-CD3 mAb (20 μg/ml or indicated concentrations) and added to each well and allowed to adhere for 30–60 min. In inhibition experiments, TK-1 cells were preincubated for 20 min with OA (1.5 μM). After incubation, unbound cells were removed by gentle washing. The binding was quantitated by counting bound cells under a microscope.

Transfected COS-1 cells suspended in binding medium (DMEM, 10 mM HEPES, 0.1% BSA, and 1 mM $MgCl_2$) were stimulated with 100 nM PDBu and allowed to adhere for 10 min. In inhibition experiments, COS-1 cells were preincubated for 10–15 min with the blocking Ab. After incubation, unbound cells were removed by gentle washing. The binding was quantitated by ELISA.

^{32}P radiolabeling and cell activation

Cell labeling was done as described previously (28), except that TK-1 cells were labeled for 2 h. After labeling, the cells were activated. The cell suspensions were divided into equal aliquots, which were treated with 1.5 μM OA for 25 min at 37°C and/or 200 nM PDBu or 10 μg/ml mouse anti-CD3ϵ mAb for TK-1 cells or 1/200-diluted OKT3 ascites for T cells. Control samples were left untreated. The activation was stopped by adding ice-cold 10 mM EDTA/PBS, and the cells were washed once with ice-cold 2 mM EDTA/PBS. The cells were lysed as described previously (28).

Immunoprecipitation and SDS-PAGE

Cell lysates were precleared with protein G-Sepharose for 45 min at 4°C and incubated with anti-β_7 mAb on ice overnight or with anti-β_2 mAb R7E4 for 2.5 h. Immune complexes were captured on protein G-Sepharose. Sepharose beads were washed exclusively with decreasing detergent and salt concentrations. Bound proteins were eluted with SDS and subjected to SDS-PAGE. SDS-PAGE was performed according to Laemmli (39) and blotted onto polyvinylidene difluoride membranes (Millipore, Bedford, MA).

Phosphoamino acid analysis and phosphopeptide mapping

The phosphorylated integrins were localized using a Fuji BAS 1000 PhosphoImager (Tokyo, Japan), and the regions corresponding to integrins were excised. The filter pieces were subjected to hydrolysis in 6 M HCl for 1.5 h at 110°C or subjected to phosphopeptide mapping. The hydrolysate was lyophilized, and standard phosphoamino acids were added. Phosphoamino acids were separated using the two-dimensional HTLE-7000 electrophoresis system (C.B.S. Scientific, Del Mar, CA) on a 20 × 20-cm cellulose plate. The standard phosphoamino acids were visualized by ninhydrin staining, and ^{32}P-labeled amino acids were visualized using the PhosphoImager.

The existence and purity of the β_7 integrin submitted for further phosphorylation studies was proved by the liquid chromatography (LC)-tandem mass spectrometry (MS/MS) analysis. The immune-precipitated β_7 protein band was cut out from a silver-stained gel and in-gel digested with trypsin. The peptides produced were first separated by reversed-phase capillary-HPLC, and the eluent was directly injected into a quadrupole/time-of-flight mass spectrometer (Micromass, Manchester, U.K.) equipped with an electrospray ionization source. MS/MS spectra of doubly charged precursor ions were acquired. Database searches were conducted by using Mascot MS/MS ion search (http://www.matrixscience.com). Mouse integrin β_7 was identified with the score of 94, and three different peptides with ~7-aa sequence tags were observed. Some trace amounts of IgG were also present in the band, but no other protein with significant score was observed.

For phosphopeptide mapping, the filter pieces were first saturated with polyvinylpyrrolidone 360, and after that, the protein was digested with trypsin at 37°C overnight. The resulting peptides were separated in the first dimension by electrophoresis at pH 8 and in the second dimension by ascending chromatography (40). ^{32}P-Labeled peptides were detected with the PhosphoImager.

Manual radiosequencing of phosphopeptides

The phosphopeptide spots were isolated from the phosphopeptide maps and immobilized on a sequence membrane disc (Millipore). They were subjected to Edman degradation as described (41). Each cycle of degradation consisted of the following: incubation of the disc at 50°C for 10 min

Carl_G_190x270_mm_blokki_FINAL.indd 391 06-Aug-23 1:54:28 PM

with coupling reagent (methanol:water:triethylamine:phenylisothiocyanate; 7:1:1:1, v/v). After the incubation, the reagent was removed. The disc was washed with methanol. Vacuum drying of the disc was followed by trifluoroacetic acid cleavage (50°C for 6 min) of the N-terminal amino acid. The cleaved amino acids were dried and spotted onto a polyvinylidene difluoride membrane. The radioactivities of the spots were visualized with the PhosphoImager and quantified using the Tina 2.09c software (Raytest, Straubenhardt, Germany).

Results

Identification of the phosphorylated threonine residues in the β_2 integrin subunit in OA-pretreated and phorbol ester-activated T cells

We have previously shown that, after activation of T cells by OA pretreatment and PDBu, two of the threonine residues in the threonine triplet 758–760 of the β_2 cytoplasmic domain become phosphorylated (28). In this study, we wanted to map in detail which threonine residues are phosphorylated in T cells. In resting T cells, the β_2 subunit is not phosphorylated and β_2 phosphorylation was induced by treatment with OA and PDBu (Ref. 26; Fig. 1, *A* and *B*). Tryptic phosphopeptide mapping was performed from the ^{32}P-labeled β_2 integrin subunits (Fig. 1*C*). Based on a previously report (28) we identified the spots; the main spot (indicated by y) most likely represents peptides produced by incomplete digestion with trypsin, and the other spot (indicated by ST2) is the peptide with Ser^{756} and two of the threonine residues 758–760 phosphorylated. The ST2-peptide was isolated from the peptide map, and the phosphopeptide was covalently attached to an aryl amine membrane disc and subjected to Edman degradation. The amount of radioactivity that was released into the liquid phase from the trifluoroacetic acid cleavage reaction was quantified (Fig. 1*D*). Ser^{756} became phosphorylated, as observed earlier (27, 29). Additionally, all three threonine residues (758–760) became phosphorylated but only two at a time.

Thr^{758} in the cytoplasmic domain of CD18 is the major phosphorylation site after integrin activation through the TCR

In the presence of OA, CD3 ligation was shown to induce phosphorylation of the β_2 subunit (Fig. 2, *A* and *B*), and phosphoamino acid analysis showed that threonine phosphorylation was strongly increased in OKT3-stimulated T cells preincubated with OA (Fig. 2*C*). About 70% of the total phosphorylation of the β_2 subunit occurred on threonine residues. Interestingly, the amount of threonine phosphorylation in PDBu-stimulated T cells treated with OA was only ~30% (26). Tryptic phosphopeptide mapping was performed from the phosphorylated β_2 subunit (Fig. 2*D*). In the map produced from OA-pretreated OKT3-activated T cells, two main spots were detected. The spot indicated by y is most likely produced by incomplete digestion with trypsin, because the spot becomes weaker when we prolonged the digestion conditions (data not shown). The phosphoamino acid analysis shows that the phosphorylation in the y-spot occurred mainly on threonine residues and only weakly on serine (not shown). The other spot (indicated by T) is the main phosphopeptide produced by β_2 subunit digestion with trypsin. The phosphorylation of the T-spot occurred primarily on threonine residues (data not shown). The T-spot was isolated from a phosphopeptide map and subjected to manual Edman degradation, and the radioactive phosphate release was detected at cycle 3 (Fig. 2*E*). This result indicates that Thr^{758} in the β_2 cytoplasmic domain is the main target of threonine phosphorylation in OKT3- and OA-stimulated T cells. Note that Ser^{756}, the major site that becomes phosphorylated in response to PDBu, is not phosphorylated after CD3 stimulation.

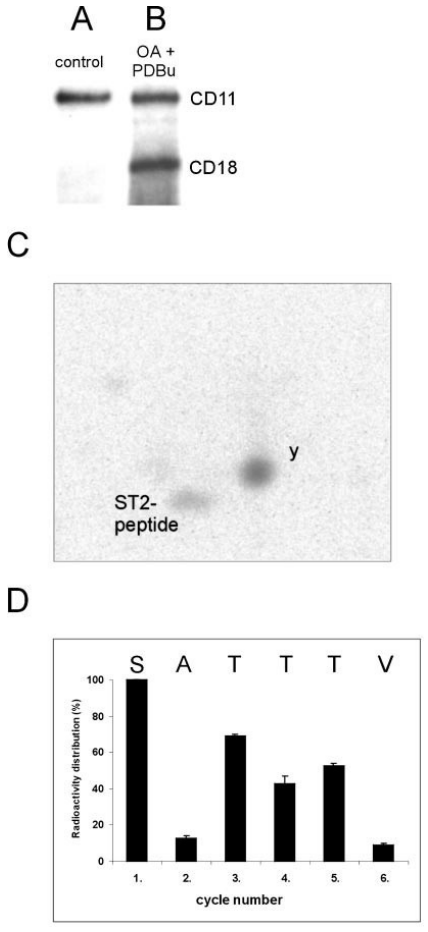

FIGURE 1. Identification of the threonine phosphorylation sites in the β_2 integrin cytoplasmic domain in PDBu-activated T cells. β_2 integrins were immunoprecipitated and electrophoresed on SDS-PAGE from ^{32}P-labeled resting T cells (*A*) or T cells activated with 200 nM PDBu after OA pretreatment (*B*). Phosphorylated β_2 was digested with trypsin. *C,* The tryptic β_2 peptides were run on cellulose plates. The spot indicated y is most likely an incompletely cleaved peptide and the spot indicated ST2-peptide has phosphates on Ser^{756} and on two of the threonines 758–760. *D*, The ST2-peptide was isolated and subjected to radiosequencing by Edman degradation, and the released radioactive phosphorylated amino acids were detected.

CD3 stimulation induces $\alpha_4\beta_7$-mediated adhesion to VCAM-1

TK-1 cells were used, because they express high levels of the $\alpha_4\beta_7$ but do not express very late Ag 4 ($\alpha_4\beta_1$) (42). The β_7-mediated adhesion-promoting effect of phorbol esters has been reported previously (4, 43). In contrast to prior reports, we detected some binding to coated VCAM-1 in the absence of activators (Fig. 3, *A* and *B*). However, 200 nM PDBu treatment resulted in a 3-fold enhancement in binding to coated human VCAM-1 (Fig. 3*A*). The increased binding is mediated by $\alpha_4\beta_7$ as shown by the blocking effect of the anti-β_7 mAb Fib504 and a blocking Ab against the α_4-chain. The Ab against mouse β_2 integrin had no effect on adhesion. Moreover, we wanted to examine whether CD3 ligation

Carl_G_190x270_mm_blokki_FINAL.indd 392 06-Aug-23 1:54:29 PM

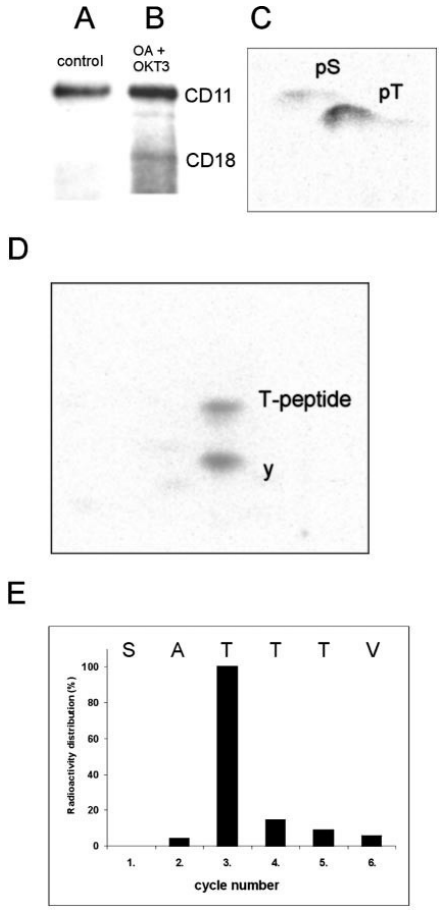

FIGURE 2. Phosphorylation of the β_2 integrin cytoplasmic domain in CD3-stimulated T cells. β_2 integrin was immunoprecipitated from ^{32}P-labeled resting T cells (*A*) or from OKT3-activated T cells, which had been pretreated with 1.5 μM OA (*B*). *C*, Phosphorylated amino acids of the β_2 subunit were analyzed by two-dimensional thin layer electrophoresis. *D*, Tryptic phosphopeptides of the β_2 polypeptide are visualized. The *upper spot* (indicated T-peptide) is the main phosphopeptide produced by trypsin digestion. The phosphorylation occurs only on threonine residue(s). *E*, The phosphorylation site in the T-peptide was identified by manual radiosequencing by Edman degradation.

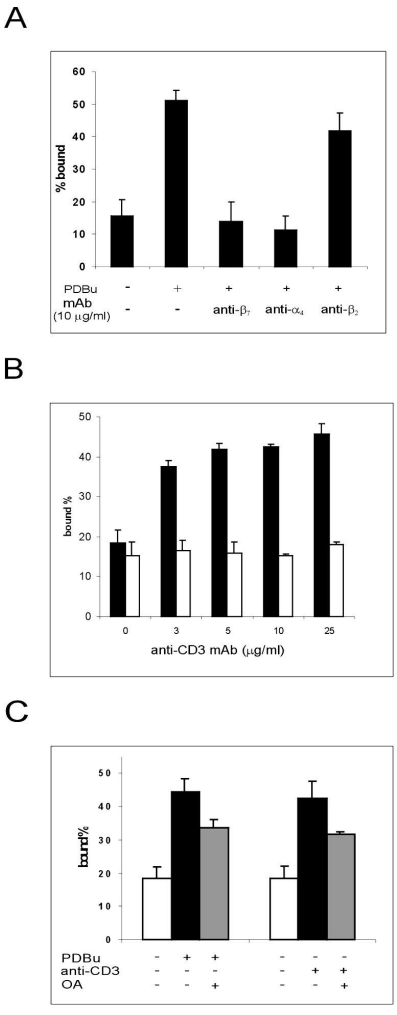

FIGURE 3. Adhesion of TK-1 cells to VCAM-1. *A*, TK-1 cells were activated with 200 nM PDBu in the presence or absence of blocking Ab (10 μg/ml). The control cells were left untreated. The cells bound to coated VCAM-1 (0.3 μg/well) were counted after 30-min incubation. *B*, TK-1 cells were activated with the indicated concentrations of anti-CD3 mAb in the absence (■) or presence (□) of 10 μg/ml Fib504, the blocking Ab against β7. The bound cells were counted after 45 min of activation. *C*, TK-1 cells were treated with 1.5 μM OA for 20 min before cell activation with 200 nM PDBu or 20 μg/ml anti-CD3 mAb. The cells were stimulated for 45 min, and the bound cells were counted. All experiments were repeated at least four times with similar results.

may also lead to β_7 integrin activation. We activated TK-1 cells via the TCR-CD3 complex using different concentrations of anti-CD3ϵ mAb and studied β_7-mediated binding to VCAM-1. As seen in Fig. 3*B*, the anti-CD3 mAb was able to activate TK-1 binding to VCAM-1. The induced adhesion was $\alpha_4\beta_7$ dependent as shown by the inhibition of the adhesion to background levels with Fib504.

We further studied the effect of OA on the $\alpha_4\beta_7$-mediated adhesion to VCAM-1. It was able to inhibit induced adhesion significantly but not totally (Fig. 3*C*).

Cell stimulation leads to increased phosphorylation of β_7 and reveals threonine phosphorylation of β_7

The above result obtained with okadaic acid indicated the involvement of serine/threonine phosphorylation in the regulation of $\alpha_4\beta_7$-dependent functions. The β_7 subunit has a serine residue in position Ser^{779} (corresponding to Ser^{756} in β_2) and a similar triplet of threonines, which have been shown to become phosphorylated in the activated β_2 cytoplasmic domain (Fig. 4). TK-1 cells were labeled with ^{32}P and activated with 10 μg/ml anti-CD3 mAb or 200 nM PDBu or left untreated. Some samples were incubated with 1.5 μM OA before the cell activation. The $\alpha_4\beta_7$ heterodimers were immunoprecipitated and subjected to SDS-PAGE. As shown

FIGURE 4. Comparison of amino acid sequences of the β_2 and β_7 cytoplasmic domains. The amino acid sequence is depicted in the single-letter code. The trypsin cleavage sites in the important area are indicated with arrows. Phosphorylation sites of β_2 are marked with numbers.

in Fig. 5, *A* and *B*, the β_7 subunit is phosphorylated even in unstimulated TK-1 cells. Activation of TK-1 cells with anti-CD3 (Fig. 5*A*) and PDBu (Fig. 5*B*) increased the phosphorylation 15–20%. A stronger enhancement of phosphorylation was observed when cells were incubated with OA before activation. OA pretreatment increased the phosphorylation of β_7 by ~70% in CD3-stimulated TK-1 cells as compared with control and to a similar extent in PDBu-activated cells. In the α_4 subunit, we observed a weak and constitutive phosphorylation.

The enhanced phosphorylation in the β_7 integrin after activation indicated the possibility of qualitative changes in phosphorylation. Thus, we next analyzed phosphorylated amino acids by two-dimensional thin layer electrophoresis (Fig. 5*C*). In unactivated TK-1 cells, the phosphorylation of β_7 occurred primarily on serine. OA alone without activating agent enhanced this serine phosphorylation, but no obvious phosphorylation was observed on threonine residues. Interestingly, threonine phosphorylation was increased in CD3-stimulated, and particularly, in PDBu-stimulated TK-1 cells preincubated with OA.

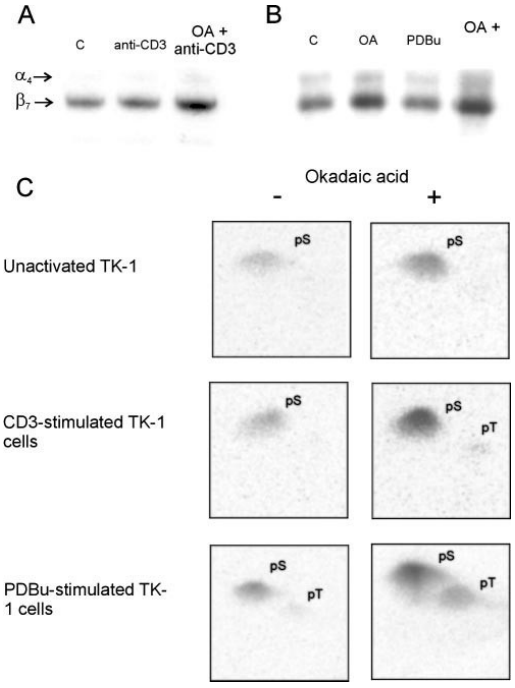

FIGURE 5. Phosphorylation of the β_7 cytoplasmic domain. Autoradiographs of ^{32}P-labeled β_7 integrin immunoprecipitated from CD3-stimulated (*A*) or PDBu-activated TK-1 cells (*B*), which had been either pretreated with 1.5 μM OA or not. The control cells were left untreated. *C*, Phosphoamino acid analysis of phosphorylated β_7 integrin is shown. TK-1 cells were activated with 10 μg/ml anti-CD3 mAb or 200 nM PDBu in the absence or presence of 1.5 μM OA. Control cells were incubated with OA alone or left untreated.

Identification of threonine phosphorylation sites in the β_7 integrin

To determine the threonine phosphorylation site(s) in the β_7 integrin, we made tryptic phosphopeptide maps from unactivated (Fig. 6*A*) and OA-pretreated, PDBu-activated TK-1 cells (Fig. 6*B*). The map from activated cells had one extra spot as compared with the map from unactivated cells (indicated by X). The phosphoamino acid analysis showed that the phosphorylation of this extra spot occurred mainly on threonine residues and a little on serine (not shown). Thus, the spot was isolated and subjected to manual Edman degradation. The amount of released radioactive phosphate was quantitated (Fig. 6*C*). The result shows that the fourth amino acid of the tryptic peptide was phosphorylated. This phosphorylated threonine residue is most likely the first threonine (Thr^{782}) of threonine triplet ($Thr^{782–784}$).

T782/A mutation of β_7 does not affect adhesion in COS-1 cells

We mutated Thr^{782} to Ala and transfected the wild-type and mutated $\alpha_4\beta_7$ integrins into COS-1 cells. Both the wild-type and mutated cells bound to a similar extent to coated VCAM-1 (Fig. 7). The binding of nontransfected cells was due to β_1 integrins.

Discussion

Leukocyte activation initiates intracellular signals, which cause transient activation of leukocyte integrins (13–15). This inside-out signaling is critical for leukocytes, because they must circulate in

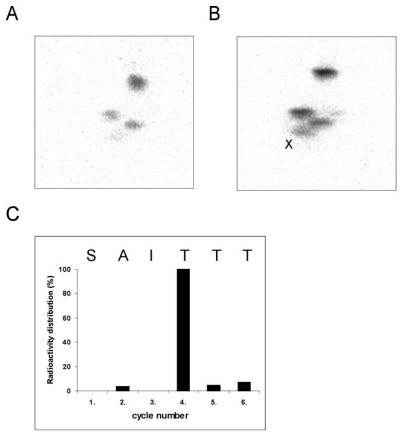

FIGURE 6. Identification of the threonine phosphorylation sites in the β_7 integrin cytoplasmic domain in PDBu-activated TK-1 cells. Tryptic phosphopeptide map of β_7 integrin from unactivated TK-1 cells (*A*) and from OA-pretreated, PDBu-activated TK-1 cells (*B*). *C*, The phosphorylation site of the spot indicated by X, was identified by manual Edman degradation.

Carl_G_190x270_mm_blokki_FINAL.indd 394 06-Aug-23 1:54:30 PM

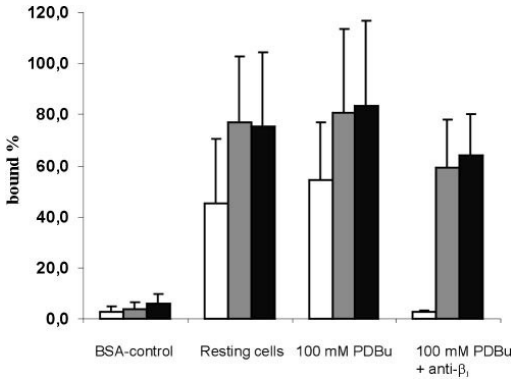

FIGURE 7. Adhesion of COS-1 cells transfected with wild-type and mutant β subunit to VCAM-1. COS-1 cells were transiently transfected with wtβ_7-pEF-BOS (▩) or T782Aβ_7-pEF-BOS (■) or left as control (□). The cells bound to coated VCAM-1 (0.3 μg/well) were counted. All experiments were repeated at least four times with similar results.

a nonadhesive state before targeting and binding at specific sites. In T lymphocytes, the intracellular stimulus can be initiated by the TCR recognizing a foreign Ag on the surface of an APC (44) or by costimulatory molecules often present in the initial contact area between the cells (45). The molecular mechanisms that mediate inside-out signaling of integrins have been studied extensively but are still poorly understood. The avidity changes of integrins are dependent on integrin cytoplasmic tails (27, 34, 35). The cytoplasmic domains of the integrin β subunits expressed on lymphocytes share a number of common features (Fig. 4), which have been shown to be important in integrin activation and functions. Mutation of the three threonine residues in the sequence 758–760 in the β_2 cytoplasmic domain into an alanine triplet caused a dramatic decrease in the leukocyte integrin-mediated adhesion to the ICAM-1 (27). The threonine triplet has also been shown to be involved in regulating postreceptor events through β_2 integrins, like cell spreading (30). Interestingly, the other leukocyte-specific integrin class, β_7, contains a similar threonine triplet in its cytoplasmic domain. Additionally, the single amino acid Phe^{766}, also found in β_7 integrins, is vital for β_2 functions. This residue has been hypothesized to be involved in the lymphocyte-specific signal transduction pathway that is required for activation of both β_2 and β_7 integrins (34).

The phosphorylation of integrin cytoplasmic tails has been proposed as a means of regulating integrin activity. The phosphorylation state of β_2 leukocyte integrins has been reported to change in response to cell stimuli (21–24). The major phosphorylation site has been identified to be Ser^{756} in the β_2 cytoplasmic domain in PDBu-activated T cells (27). A strong threonine phosphorylation of the β_2 subunit was observed by using OA (26). The only threonine residue present in β_2 cytoplasmic domain is the functionally important threonine triplet. We have now shown that all three threonines, $Thr^{758-760}$, act as substrates but only two in a given polypeptide. In contrast, if the T cells were stimulated through the TCR, only the first threonine residue in the threonine triplet became phosphorylated. PKC has been recently shown to be the main β_2 kinase in leukocytes, and many PKC isoforms are capable of phosphorylating the β_2 subunit in vitro (29). The sites phosphorylated by PKCδ and PKCβ were identified as Ser^{745} and Thr^{758}. PKCα additionally phosphorylated Thr^{760}. These results suggest that CD3 stimulation leads to the activation of PKCδ and/or PKCβ, but in contrast, PDBu can also activate other PKC isoforms, indicating that different signaling events take place under different activation conditions.

The β_2 integrin has been observed to bind to ICAM-1 in response to CD3 cross-linking, without affecting the levels of expression of integrins (14, 15). In this study, we have investigated whether inside-out signaling, initiated by CD3 stimulation, can also regulate the β_7 integrin. We showed that brief CD3 stimulation induced $\alpha_4\beta_7$ integrin-mediated binding to VCAM-1. Previous studies have shown that CD3 stimulation increases the expression levels of the β_7 integrin subunit on cell surface (4, 46). However, the effect of CD3 activation on $\alpha_4\beta_7$ adhesion was so rapid that we suggest that CD3 ligation affects the function of $\alpha_4\beta_7$ molecules already present on the cell surface.

In contrast to the β_2 integrin, the β_7 subunit was already phosphorylated in unactivated TK-1 cells. However, the phosphorylation of β_7 occurred only on serine residues in unactivated TK-1 cells. This difference may be due to the properties of different types of cells, because TK-1, as a cell line, is continuously dividing. Cell activation with PDBu or CD3 Ab increased the phosphorylation, but only weak phosphorylation was observed on threonine residues. In PDBu- and CD3-stimulated TK-1 cells, the inhibition of phosphatase activity induced significant phosphorylation of threonine in addition to serine. OA alone enhanced serine phosphorylation, but no phosphorylation was observed on threonine residues. This result indicates the presence of a similar continuous threonine phosphorylation/dephosphorylation cycle in β_7 subunit as in β_2.

The phosphorylation site was determined to be Thr^{782} corresponding to the first threonine of the threonine triplet in β_2. The same site was phosphorylated in the β_2 subunit after cell activation. The phosphorylation site could be on a tryptic peptide next to TTT-peptide, because this peptide also has a threonine residue in position four (Fig. 4). However, this alternative threonine residue is found only in mouse β_7, and it is unlikely that this is the phosphorylated residue.

The role of threonine phosphorylation in the regulation of integrin activity is still unclear. Phosphorylated β_2 integrins have been shown to preferentially associate with the actin cytoskeleton (31), indicating that phosphorylation of integrins could regulate integrin-cytoskeleton interactions. The phosphatase sensitivity of the threonine phosphorylation of leukocyte integrins indicates the possibility of a rapid attachment and detachment of integrins from the cytoskeleton. A possibility is that the cytoskeleton-integrin linkage is mediated by 14-3-3 proteins, which have recently been found to interact specifically with Thr^{758}-phosphorylated β_2 integrins (29). The 14-3-3 proteins could possibly initiate a signaling complex formation, further regulating integrin functions.

The threonine phosphorylation has been speculated to have a role also in other integrins. The β_3 subunit has a Thr-Ser-Thr sequence corresponding to the threonine triplet in β_2. The β_3 integrin was found to be phosphorylated mainly on threonine (47). Threonine phosphorylation was speculated to have a negative role on β_3 integrin inside-out and outside-in signaling (48), possible by inhibiting the binding of tyrosine-phosphorylated integrins to Shc, a signaling protein (49). However, phosphorylation of β_3 integrins has also been speculated to be a major factor in the control of exposure of binding sites for adhesive proteins in the αIIbβ_3 integrin complex (50). Mutation of these threonine residues in the integrin β_3 cytoplasmic domain has been reported to inhibit cell attachment, cell spreading, and extracellular domain conformation changes (51, 52). Threonine phosphorylation of β_1 has not been

Carl_G_190x270_mm_blokki_FINAL.indd 395 06-Aug-23 1:54:30 PM

reported so far, but the VTT sequence in the β_1 integrin cytoplasmic domain has been shown to be important for a number of integrin-dependent functions, including signaling, conformational changes in the extracellular domain, cell attachment, and cell spreading (52, 53). However, the functional importance of the phosphorylated Thr^{782} in β_7 remains unclear, because mutation to alanine did not affect adhesion. This finding does not rule out other possible functions of this phosphorylation and needs further study. Another problem may be that COS-1 cells, being monkey cells, do not possess intracellular interactive molecules normally found in T cells.

Both PDBu and CD3 ligation induce leukocyte integrin phosphorylation also on serine residues (21–23). The main PDBu-induced serine phosphorylation site in β_2 integrin was found to be Ser^{756}, but Ser^{756} is not essential in the activation of β_2 integrins (27). Ser^{756} has been speculated to be involved in so-called post-receptor events, like cell spreading, that are regulated by different signaling events than integrin activation (45). The corresponding serine is not found in β_3, but mutation of the corresponding serine in β_1 integrin (Ser^{785}) to methionine has been shown to promote cell spreading and directed migration, but inhibit cell attachment to laminin (54). In contrast, Ser^{785} mutation to aspartate in β_1, which to some degree mimics a constitutively phosphorylated residue, has been shown to reduce localization at focal contacts (55). Interestingly, Ser^{756} of β_2 is not phosphorylated in CD3-stimulated T cells. However, serine phosphorylation is also observed in β_2 after CD3 stimulation. It has been shown that Ser^{745} becomes phosphorylated when T cells are stimulated with PDBu, and that phosphorylation could be increased in the presence of OKT3 plus OA (29). But OKT3 alone in the presence or absence of OA did not induce Ser^{745} phosphorylation (our unpublished data). In contrast, the stoichiometry of phosphorylation is very low (28), so it is possible that Ser^{745} phosphorylation escapes detection. The role of Ser^{756} and Ser^{745} phosphorylation in β_2 is unknown at present.

In conclusion, we have mapped the phosphorylation sites of leukocyte-specific integrins. The phosphorylation of β_2 integrin occurs on the first threonine of the threonine triplet in OA-pretreated CD3-stimulated T cells. A similar induced threonine phosphorylation was observed in the β_7 integrin. The functional importance of threonine phosphorylation needs further study.

Acknowledgments

We thank Leena Kuoppasalmi for technical assistance, Susanna Fagerholm for helpful discussions, and Dr. I. L. Weissmann (Stanford University) for the murine α_4 and β_7 cDNAs.

References

1. Springer, T. A. 1994. Traffic signals for lymphocyte recirculation and leukocyte emigration: the multistep paradigm. *Cell 76:301.*
2. Butcher, E.C., and L. J. Picker. 1996. Lymphocyte homing and homeostasis. *Science 272:60.*
3. Gahmberg, C. G., L. Valmu, S. Fagerholm, P. Kotovuori, E. Ihanus, L. Tian, and T. Pessa-Morikawa. 1998. Leukocyte integrins and inflammation. *Cell. Mol. Life Sci. 54:549.*
4. Rüegg, C., A. A. Postigo, E. E. Sikorski, E. C. Butcher, R. Pytela, and D. J. Erle. 1992. Role of integrin $\alpha_4\beta_7/\alpha_4\beta_P$ in lymphocyte adherence to fibronectin and VCAM-1 and homotypic cell clustering. *J. Cell Biol. 117:179.*
5. Gahmberg, C. G., M. Tolvanen, and P. Kotovuori. 1997. Leukocyte adhesion: structure and function of human leukocyte β_2-integrin and their cellular ligands. *Eur. J. Biochem. 245:215.*
6. Kotovuori, P., E. Tontti, R. Pigott, M. Shepherd, M. Kiso, A. Hasegawa, R. Renkonen, P. Nortamo, D. C. Altieri, and C. G. Gahmberg. 1993. The vascular E-selectin binds to the leukocyte integrins CD11/CD18. *Glycobiology 3:131.*
7. Garnotel, R., J.-C. Monboisse, A. Randoux, B. Haye, and J. P. Borel. 1995. The binding of type I collagen to lymphocyte function-associated antigen (LFA) 1 integrin triggers the respiratory burst of human polymorphonuclear neutrophils: role of calcium signal and tyrosine phosphorylation of LFA-1. *J. Biol. Chem. 270:27495.*
8. Altieri, D., R. Bader, P. M. Mannucci, and T. S. Edgington. 1988. Oligospecificity of the cellular adhesion receptor MAC-1 encompasses an inducible recognition specificity for fibrinogen. *J. Cell Biol. 107:1893.*
9. Loike, J. D., B. Sodeik, L. Cao, S. Leucona, J. I. Witz, P. A. Detmers, S. D. Wright, and S. C. Silverstein. 1991. CD11c/CD18 on neutrophils recognizes a domain at the N terminus of the Aα chain of fibrinogen. *Proc. Natl. Acad. Sci. USA 88:1044.*
10. Berlin, C., E. L. Berg, M. J. Briskin, D. P. Andrew, P. J. Kilshaw, B. Holzmann, I. L. Weissman, A. Hamann, and E. C. Butcher. 1993. $\alpha_4\beta_7$ integrin mediates lymphocyte binding to the mucosal vascular addressin MadCAM-1. *Cell 74:185.*
11. Springer, T. A. 1990. Adhesion receptors of the immune system. *Nature 346:425.*
12. Patarroyo, M., P. G. Beatty, J. W. Fabre, and C. G. Gahmberg. 1985. Identification of a cell surface protein complex mediating phorbol ester-induced adhesion (binding) among human mononuclear leukocytes *Scand. J. Immunol. 22: 171.*
13. Rothlein, R., and T. A. Springer. 1986. The requirement for lymphocyte function associated antigen 1 in homotypic leukocyte adhesion stimulated by phorbol ester. *J. Exp. Med. 163:1132.*
14. Dustin, M. L., and T. A. Springer. 1989. T-cell receptor cross-linking transiently stimulates adhesiveness though LFA-1. *Nature 341:619.*
15. Van Kooyk, Y., P. van de Wiel-van de Kemenade, P. Weder, T. W. Kuijpers, and C. G. Figdor. 1989. Enhancement of LFA-1-mediated cell adhesion by triggering through CD2 or CD3 on T lymphocytes. *Nature 342:811.*
16. Ginsberg, M. H., X. Du, and E. F. Plow. 1992. Inside-out integrin signalling. *Curr. Opin. Cell Biol. 4:766.*
17. Kolanus, W., and L. Zeitlmann. 1998. Regulation of integrin function by inside-out signaling mechanisms. *Curr. Top. Microbiol. Immunol. 231:33.*
18. Shimizu, Y., G. A. van Seventer, K. J. Horgan, and S. Shaw. 1990. Regulated expression and binding of three VLA (β_1) integrin receptors on T cells. *Nature 345:250.*
19. Parsons, J. T. 1996. Integrin-mediated signalling: regulation by protein tyrosine kinases and small GTP-binding proteins. *Curr. Opin. Cell Biol. 8:146.*
20. Yamada, K., and S. Miyamoto. 1995. Integrin transmembrane signalling and cytoskeletal control. *Curr. Opin. Cell Biol. 7:681.*
21. Hara, T., and S. M. Fu. 1986. Phosphorylation of α,β subunits of 180/100-Kd polypeptides (LFA-1) and related antigens. In *Leukocyte Typing II*, Vol. 3. E. L. Reinherz, B. F. Haynes, L. M. Nadler, and I. D. Bernstein, eds. Springer-Verlag, New York, p. 77.
22. Chatila, T. A., R. S. Geha, and M. A. Arnaout. 1989. Constitutive and stimulus-induced phosphorylation of CD11/CD18 leukocyte adhesion molecules. *J. Cell Biol. 109:3435.*
23. Buyon, J. P., S. G. Slade, J. Reibman, S. B. Abramson, M. R. Philips, G. Weissmann, and R. Winchester. 1990. Constitutive and induced phosphorylation of the α- and β-chains of the CD11/CD18 leukocyte integrin family: relationship to adhesion-dependent functions. *J. Immunol. 144:191.*
24. Valmu, L., M. Autero, P. Siljander, M. Patarroyo, and C. G. Gahmberg. 1991. Phosphorylation of the β-subunit of CD11/CD18 integrins by protein C correlates with leukocyte adhesion. *Eur. J. Immunol. 21:2857.*
25. Pardi, R., L. Inverardi, C. Rugarli, and J. R. Bender. 1992. Antigen-receptor complex stimulation triggers protein kinase C-dependent CD11a/CD18-cytoskeleton association in T lymphocytes. *J. Cell Biol. 116:1211.*
26. Valmu, L., and C. G. Gahmberg. 1995. Treatment with okadaic acid reveals strong threonine phosphorylation of CD18 after activation of CD11/CD18 leukocyte integrins with phorbol esters or CD3 antibodies. *J. Immunol. 155:1175.*
27. Hibbs, M. L., S. Jakes, S. A. Stacker, R. W. Wallace, and T. A. Springer. 1991. The cytoplasmic domain of the integrin lymphocyte function-associated antigen 1 β subunit: sites required for binding to intercellular adhesion molecule 1 and the phorbol ester-stimulated phosphorylation sites. *J. Exp. Med. 174:1227.*
28. Valmu, L., T. J. Hilden, G. van Willigen, and G. C. Gahmberg. 1999. Characterization of β_2 (CD18) integrin phosphorylation in phorbol ester-activated T lymphocytes. *Biochem. J. 339:119.*
29. Fagerholm, S., N. Morrice, C. G. Gahmberg, and P. Cohen. 2002. Phosphorylation of the cytoplasmic domain of the integrin CD18 chain by protein kinase C isoforms in leukocytes. *J. Biol. Chem. 277:1728.*
30. Peter, K., and T. E. O'Toole. 1995. Modulation of cell adhesion by changes in $\alpha_L\beta_2$ (LFA-1, CD11a/CD18) cytoplasmic domain/cytoskeleton interaction. *J. Exp. Med. 181:315.*
31. Valmu, L., S. F. Fagerholm, H. Suila, and C. G. Gahmberg. 1999. The cytoskeletal association of CD11/CD18 leukocyte integrins in phorbol ester-activated cells correlates with CD18 phosphorylation. *Eur. J. Immunol. 29:2107.*
32. Sharma, C. P., R. M. Ezzell, and M. A. Arnaout. 1995. Direct interaction of filamin (ABP-280) with the β_2 integrin subunit CD18. *J. Immunol. 154:3461.*
33. Calderwood, D. A., A. Huttenlocher, W. B. Kiosses, D. M. Rose, D. G. Woodside, M. A. Schwartz, and M. H. Ginsberg. 2001. Increased filamin binding to β-integrin cytoplasmic domains inhibits cell migration. *Nat. Cell. Biol. 3:1060.*
34. Lub, M., S. J. van Vliet, S. P. Oomen, R. A. Pieters, M. Robinson, C. G. Figdor, and Y. van Kooyk. 1997. Cytoplasmic tails of β_1, β_2, and β_7 integrins differentially regulate LFA-1 function in K562 cells. *Mol. Biol. Cell 8:719.*
35. Crowe, D. T., H. Chiu, S. Fong, and I. L. Weissman. 1994. Regulation of the avidity of integrin $\alpha_4\beta_7$ by the β_7 cytoplasmic domain. *J. Biol. Chem. 269:14411.*
36. Nortamo, P., M. Patarroyo, C. Kantor, J. Suopanki, and C. G. Gahmberg. 1988. Immunological mapping of the human leukocyte adhesion glycoprotein gp90 (CD18) by monoclonal antibodies. *Scand. J. Immunol. 28:537.*
37. Mullis, K., F. Faloona, S. Scharf, R. Saiki, G. Horn, and H. Erlich. 1986. Specific enzymatic amplification of DNA in vitro: the polymerase chain reaction. *Cold Spring Harbor Symp. Quant. Biol. 51:263.*
38. Mizushima, S., and S. Nagata. 1990. pEF-BOS, a powerful mammalian expression vector. *Nucleic Acids Res. 18:5322.*
39. Laemmli, U. K. 1970. Cleavage of structural proteins during the assembly of the head of bacteriophage T4. *Nature 227:680.*

Carl_G_190x270_mm_blokki_FINAL.indd 396 06-Aug-23 1:54:32 PM

40. Hunter, T., and B. M. Sefton. 1980. Transforming gene product of Rous sarcoma virus phosphorylates tyrosine. *Proc. Natl. Acad. Sci. USA 77:1311.*
41. Sullivan, S., and T. W. Wong. 1991. A manual sequencing method for identification of phosphorylated amino acid in phosphopeptides. *Anal. Biochem. 197:65.*
42. Holzmann, B., and I. L. Weissman. 1989. Peyer's patch-specific lymphocyte homing receptors consist of a VLA-4-like α chain associated with either of two integrin β chains, one of which is novel. *EMBO J. 8:1735.*
43. Chan, B. M. C., M. J. Elices, E. Murphy, and M. E. Hemler. 1992. Adhesion to vascular cell adhesion molecule 1 and fibronectin. *J. Biol. Chem. 267:8366.*
44. Dustin, M. L., and A. C. Chan. 2000. Signal takes shape in the immune system. *Cell 103:283.*
45. Croft, M., and C. Dubey. 1997. Accessory molecule and costimulation requirements for CD4 T cell response. *Crit. Rev. Immunol. 17:89.*
46. MacKenzie, W. M., D. W. Hoskin, and J. Blay. 2002. Adenosine suppresses $\alpha_4\beta_7$ integrin-mediated adhesion of T lymphocytes to colon adenocarcinoma cells. *Exp. Cell Res. 276:90.*
47. Parise, L. V., A. B. Criss, L. Nannizzi, and M. R. Wardell. 1990. Glycoprotein IIIa is phosphorylated in intact human platelets. *Blood 75:2363.*
48. Lerea, K. M., K. P. Cordero, K. S. Sakariassen, R. I. Kirk, and V. A. Fried. 1999. Phosphorylation sites in the integrin β_3 cytoplasmic domain in intact platelets. *J. Biol. Chem. 274:1914.*
49. Kirk, R. I., M. R. Sanderson, and K. M. Lerea. 2000. Threonine phosphorylation of the β_3 integrin cytoplasmic tail, at a site recognized by PDK1 and Akt/PKB in vitro, regulates Shc binding. *J. Biol. Chem. 275:30901.*
50. van Willigen, G., I. Hers, G. Gorter, and J.-W. N. Akkerman. 1996. Exposure of ligand-binding sites on platelet integrin α_{IIB}/β_3 by phosphorylation of the β_3 subunit. *Biochem. J. 314:769.*
51. Mastrangelo, A. M., S. M. Homan, M. J. Humphries, and S. E. LaFlamme. 1999. Amino acid motif required for isolated β cytoplasmic domains to regulate "in trans" β_1 integrin conformation and function in cell attachment. *J. Cell Sci. 112:217.*
52. Bodeau, A. L., A. L. Berrier, A. M. Mastrangelo, R. Martinez, and S. E. LaFlamme. 2001. A functional comparison of mutations in integrin β cytoplasmic domains: effects on the regulation of tyrosine phosphorylation, cell spreading, cell attachment and β_1 integrin conformation. *J. Cell Sci. 114:2795.*
53. Wennerberg, K., R. Fässler, B. Wärmegård, and S. Johansson. 1998. Mutation analysis of the potential phosphorylation sites in the cytoplasmic domain of integrin β_{1A}. *J. Cell Sci. 111:1117.*
54. Mulrooney, J. P., T. Hong, and L. B. Grabel. 2001. Serine 785 phosphorylation of the β_1 cytoplasmic domain modulates β_{1A}-integrin-dependent functions. *J. Cell Sci. 114:2525.*
55. Barreuther, M. F., and L. B. Grabel. 1996. The role of phosphorylation in modulating β_1 integrin localisation. *Exp. Cell Res. 222:10.*

THE JOURNAL OF CELL BIOLOGY

JCB: ARTICLE

Specific integrin α and β chain phosphorylations regulate LFA-1 activation through affinity-dependent and -independent mechanisms

Susanna C. Fagerholm, Tiina J. Hilden, Susanna M. Nurmi, and Carl G. Gahmberg

Division of Biochemistry, Faculty of Biosciences, University of Helsinki, FIN-00014 Helsinki, Finland

Integrins are adhesion receptors that are crucial to the functions of multicellular organisms. Integrin-mediated adhesion is a complex process that involves both affinity regulation and cytoskeletal coupling, but the molecular mechanisms behind this process have remained incompletely understood. In this study, we report that the phosphorylation of each cytoplasmic domain of the leukocyte function-associated antigen-1 integrin mediates different modes of integrin activation. α Chain phosphorylation on Ser1140 is needed for conformational changes in the integrin after chemokine- or integrin ligand–induced activation or after activation induced by active Rap1 (Rap1V12). In contrast, the β chain Thr758 phosphorylation mediates selective binding to 14-3-3 proteins in response to inside-out activation through the T cell receptor, resulting in cytoskeletal rearrangements. Thus, site-specific phosphorylation of the integrin cytoplasmic domains is important for the dynamic regulation of these complex receptors in cells.

Introduction

The heterodimeric cell surface receptors called integrins are exceptional in that they can function as bidirectional signaling devices, regulating cell adhesion and migration after so-called inside-out signaling, and they can also signal into the cell to regulate growth, differentiation, and apoptosis after ligand binding (Giancotti and Ruoslahti, 1999; Hynes, 2002). The relatively small intracellular domains of integrins are involved in regulating signaling functions. Recently, separation of integrin cytoplasmic domains has been postulated as a mechanism of regulating integrin bidirectional signaling (Vinogradova et al., 2002; Kim et al., 2003; Tadokoro et al., 2003). Proximal events in the regulation of integrin activation and outside-in signaling presumably involve the binding of cytoplasmic molecules to the intracellular tails (Calderwood, 2004).

Dynamic adhesion is especially important in the immune system, where cells need to attach and detach continuously. The leukocyte function-associated antigen-1 (LFA-1) integrin (αLβ2 or CD11a/CD18) is expressed exclusively in leukocytes and is of fundamental importance to the function of the immune system (Springer, 1990; Gahmberg, 1997). LFA-1 mediates cell adhesion under various conditions, e.g., during immunological synapse formation between the T cell and the antigen-presenting cell and during leukocyte emigration from the bloodstream into tissues. Whereas T cell receptor (TCR)–mediated adhesion is slow and sustained, chemokine-induced adhesion is fast and rapidly reversible. Both affinity-dependent and -independent mechanisms have been postulated as being important in the regulation of integrin activation (van Kooyk and Figdor, 2000; Carman and Springer, 2003; Calderwood, 2004). These mechanisms are not mutually exclusive, and different modes of integrin activation may involve different mechanisms working alone or together. For example, TCR-induced activation of LFA-1 has not been shown to involve affinity regulation (conformational changes) in the integrin, but instead has been closely correlated with the spreading phenotype of T cells and actin cytoskeleton rearrangements (Stewart et al., 1996, 1998). In contrast, chemokines mediate rapid conformational changes in LFA-1, as measured by activation epitope expression with mAbs and the measurement of soluble ligand binding to the integrin (Weber et al., 1999; Constantin et al., 2000). Chemokine-induced adhesion also involves the clustering of integrins (Constantin et al., 2000). Ligands can also induce conformational changes and clustering of integrins (Cabanas and Hogg, 1993; Li et al., 1995; Kotovuori et al., 1999; Kim et al., 2004).

S.C. Fagerholm and T.J. Hilden contributed equally to this paper.

Correspondence to Carl G. Gahmberg: carl.gahmberg@helsinki.fi

Abbreviations used in this paper: ICAM, intercellular adhesion molecule; J, Jurkat; LFA-1, leukocyte function-associated antigen-1; sICAM, soluble ICAM; TCR, T cell receptor; wt, wild-type.

© The Rockefeller University Press $8.00
The Journal of Cell Biology, Vol. 171, No. 4, November 21, 2005 705–715
http://www.jcb.org/cgi/doi/10.1083/jcb.200504016

Carl_G_190x270_mm_blokki_FINAL.indd 398 06-Aug-23 1:54:33 PM

Phosphorylation is a common mechanism for the regulation of surface receptor function and has also been reported in integrins, but its role in integrin regulation has remained only partially understood (Fagerholm et al., 2004). LFA-1 is phosphorylated on both the α and β chains, with the α chain being constitutively phosphorylated, whereas β chain phosphorylation becomes detectable after inside-out stimulation of the integrin (Hara and Fu, 1986; Chatila et al., 1989; Valmu and Gahmberg, 1995). The α chain phosphorylation sites have not been mapped, and their functions are completely unknown. In contrast, the β chain phosphorylation sites are known (Hibbs et al., 1991; Fagerholm et al., 2002b; Hilden et al., 2003). The main phosphorylation site after phorbol ester stimulation of cells is Ser756, but this site is not involved in regulating adhesion (Hibbs et al., 1991). The threonine triplet (Thr758–760) in the β2 chain is important for adhesion, interactions with the actin cytoskeleton, and modulation of cell spreading (Hibbs et al., 1991; Peter and O'Toole, 1995). Interestingly, threonine phosphorylation of the β chain has been reported (Valmu and Gahmberg, 1995) and threonine-phosphorylated integrins distribute preferentially to the actin cytoskeleton in cells (Valmu et al., 1999a). Additionally, it has been shown that 14-3-3 proteins from cell lysates interact with a Thr758-phosphorylated β2 integrin peptide in vitro (Fagerholm et al., 2002b), but whether the interaction occurs in vivo or plays a role in adhesion has not been discovered. In this study, we investigated the role of both α and β chain phosphorylations in the regulation of LFA-1–mediated adhesion.

Results

αL is phosphorylated on Ser1140 in T cells

To establish the role of LFA-1 phosphorylation in integrin regulation, we first mapped the phosphorylation sites in αL. Endogenous αL is phosphorylated in both resting ^{32}P-labeled T cells and in cells activated by phorbol ester stimulation or through ligation of the TCR with the antibody OKT3 (Fig. 1 A). The labeled protein band was subjected to trypsin cleavage and phosphopeptide mapping, and only one major spot (radioactive peptide) was detected (Fig. 1 B). The maps from resting cells and from phorbol ester–activated cells were identical (unpublished data), thus no additional sites were phosphorylated after cell activation. Identification of the serine phosphorylation site was made using manual Edman degradation. The radioactive phosphorylated amino acid was detected as the fourth residue in the tryptic αL peptide (Fig. 1 C). This result indicates that Ser1140 in the αL cytoplasmic domain is the target of phosphorylation (Fig. 1 D). To confirm this, we substituted Ser1140 with Ala. COS-1 cells were transiently transfected with wild-type (wt) αL and S1140A-αL, together with wt β2, and cells were labeled with ^{32}P. The LFA-1 protein was immunoprecipitated from cell lysates and subjected to SDS-PAGE analysis and autoradiography. No radioactive labeling was detected in S1140A-αL transfectants (Fig. 1 E). These data demonstrate that Ser1140 is the principal αL phosphorylation site.

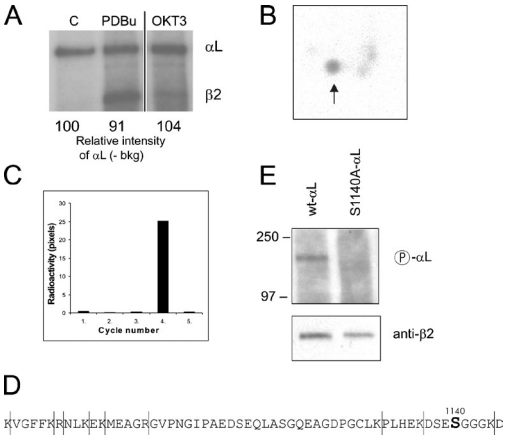

Figure 1. **Ser1140 is the phosphorylation site in the αL chain of LFA-1.** (A) The integrin β chain is phosphorylated only after cell stimulation, whereas the α chain is constitutively phosphorylated. Endogenous integrins were immunoprecipitated from control cells (C) or okadaic acid–pretreated (1.5 μM), PDBu-activated (200 nM; 30 min), or OKT3-activated (10 μg/ml; 60 min) ^{32}P-labeled human T cells and analyzed by SDS-PAGE and autoradiography. The radiolabeled αL bands were also quantified. (B) Phosphopeptide map of ^{32}P-labeled αL digested with trypsin from resting T cells. (C) The main spot in B (arrow) was subjected to Edman degradation. The radioactive phosphorylated amino acid was detected as the fourth residue in the tryptic αL peptide. (D) Sequence of the αL cytoplasmic domains with the Ser1140 phosphorylation site shown in bold. The trypsin cleavage sites in αL are indicated with vertical lines. (E) COS-1 cells were transfected with wt αL or S1140A-αL, together with wt β2, and ^{32}P-labeled LFA-1 was immunoprecipitated and analyzed by SDS-PAGE and autoradiography. No radioactive band was detected in S1140A-αL transfectants. β2 integrins were detected from the same filter by immunoblotting to demonstrate equal loading.

Ser1140 is phosphorylated at a high stoichiometry in resting T cells

To estimate the stoichiometry of αL phosphorylation in leukocytes, we generated a phosphospecific antibody capable of recognizing αL only when it has been phosphorylated on Ser1140. The antibody was αL specific because it failed to react with lysates of Jurkat (J)-β2.7 cells, which are an αL-deficient Jurkat cell line, and reacted with the αL integrin in αL-transfected J-β2.7 cells (Fig. 2 A). This antibody was also tested for recognition of immunoprecipitated LFA-1 from T cells in the presence of blocking αL unphosphopeptide or phosphopeptide (Fig. 2 B). This phosphospecific antibody recognized αL in the presence of competing unphosphorylated peptide (to block any interactions mediated by antibodies that recognize nonphosphorylated forms of the integrins), but in the presence of phosphopeptide no recognition occurred. Specificity was also confirmed by Western blotting of immunoprecipitated αL from cells expressing wt αL and from cells where Ser1140 had been mutated to nonphosphorylatable Ala (Fig. 2 C). The antibody reacted with wt αL, but not with S1140A-mutated αL. Thus, the experiments demonstrated that the antibody is sequence- and phosphospecific.

We used this phosphospecific αL antibody to assess the stoichiometry of αL phosphorylation. The total amount of

Carl_G_190x270_mm_blokki_FINAL.indd 399 06-Aug-23 1:54:33 PM

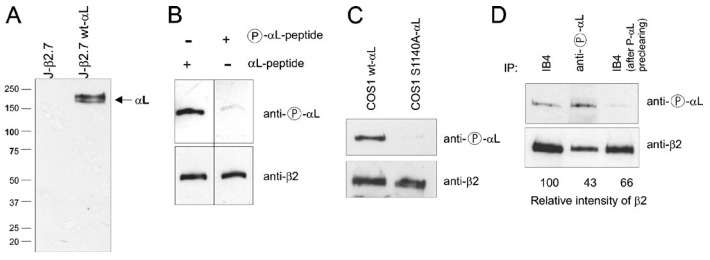

Figure 2. **Characterization of the phosphospecific αL-Ser1140 antibody and assessment of the stoichiometry of αL phosphorylation.** (A) A Ser1140 phosphospecific antibody was made, as described in Materials and methods, and used in a Western blot of cell extracts prepared from J-β2.7 cells and wt αL–transfected J-β2.7 cells. (B) The antibody was tested for recognition of immunoprecipitated LFA-1 from T cells in the presence of 25 μg/ml of blocking unphosphopeptide or 25 μg/ml of phosphopeptide. An immunoprecipitation was made with the IB4 antibody, which recognizes only heterodimeric forms of the β2 integrin. The blots were stripped and reprobed with anti–β2 integrin antibodies (R2E7B) to demonstrate equal loading. (C) wt αL and S1140A-αL integrins were immunoprecipitated from transiently transfected COS-1 cells, and phosphorylated αL was detected by Western blotting. (D) The stoichiometry of the αL phosphorylation was estimated using the phosphospecific αL-Ser1140 antibody. The T cell lysates were immunoprecipitated with either the phosphospecific αL antibody or IB4. The remaining αL from phosphospecific αL immunoprecipitation was immunoprecipitated by IB4. Immunoprecipitates were resolved by SDS-PAGE and phosphorylated αL was detected. β2 detection was used to demonstrate the total amount of integrin in samples. In the Western blot, the phosphospecific antibody was used in the presence of unphosphorylated peptide.

heterodimeric LFA-1 (100%) in T cell lysates was determined by immunoprecipitation with IB4, an antibody that recognizes heterodimeric LFA-1 rather than the monomeric β2 (Fig. 2 D; Wright et al., 1983). The phosphospecific antibody immunoprecipitated ~40% of the total heterodimeric αL from resting T cells (Fig. 2 D). The remaining αL from this lysate was immunoprecipitated with IB4, but no αL phosphorylation was seen in this sample when detected with phosphospecific αL antibody. We conclude that a maximum of 40% of αL is constitutively phosphorylated in T cells.

Mutation of Ser1140 of αL abolishes T cell adhesion to ICAM-1 induced by the activating antibody MEM-83 and MEM-83–induced affinity regulation of LFA-1

We next generated stable J-β2.7 cell transfectants expressing wt αL and S1140A-αL to examine the role of the phosphorylation site in cells (Fig. 3 A). Mutation of Ser1140 to Ala did not affect the heterodimerization or cell surface expression of LFA-1. The phosphospecific αL antibody was used for the characterization of the J-β2.7 cell clones. The αL chain was easily detected in J-β2.7 wt αL cells, whereas no significant staining of αL was seen in J-β2.7 S1140A-αL cells with or without phorbol ester activation (Fig. 3 B).

We went on to study the roles of the αL phosphorylation site in cells that were stimulated with different agonists. The binding of both wt αL and S1140A-αL transfectants to the immobilized ligand intercellular adhesion molecule (ICAM)-1 was increased by TCR ligation and by phorbol ester treatment, as compared with resting cells (Fig. 4 A). In contrast, cells expressing S1140A-αL bound less efficiently to ICAM-1 when activated by MEM-83. It has been speculated that MEM-83 activates LFA-1 binding to ICAM-1 by changing the orientation of the I domain in the αL, which leads to conformational change at the ICAM-1 binding site (Lu et al., 2004). Mg/EGTA also induces a conformational change, probably at the MIDAS and ADMIDAS sites of the I-like domain of the β2 subunit (Shimaoka et al., 2002). Mg/EGTA increased the αL-mutated cell adhesion to ICAM-1, but not as effectively as in wt cells (Fig. 4 A). These results indicate that αL phosphorylation could be involved in LFA-1 conformational changes needed for integrin binding to ligand, but not in integrin activation induced by TCR ligation and phorbol ester stimulation. The latter stimuli lead to increased binding of cells to coated ICAM-1, but previous studies have reported that they did not induce conformational changes in the integrin (Cabanas and Hogg, 1993;

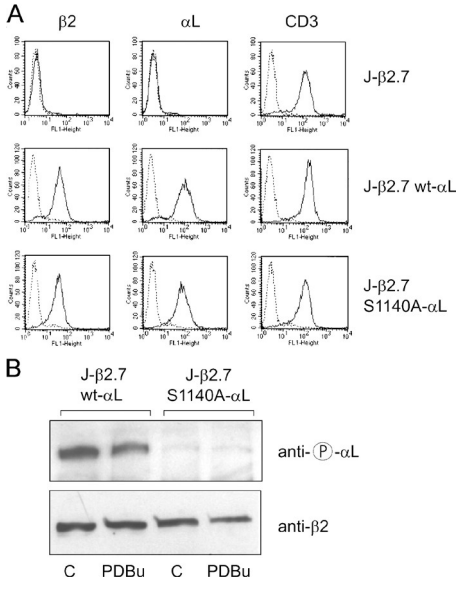

Figure 3. **Mutation of the Ser1140 αL phosphorylation site in J-β2.7 transfectants.** (A) Surface expression of integrin LFA-1 β2 chains (R7E4 antibody staining) and wt and S1140A-αL chains (MEM-83 antibody staining) in J-β2.7 wt cells and J-β2.7 wt αL and J-β2.7 S1140A-αL transfectants was examined by flow cytometry. As a control, the antibody OKT3 was used to detect similar amounts of CD3 in all clones. Dotted lines represent the background fluorescence and solid lines the specific antibody labeling. (B) LFA-1 in S1140A-αL–expressing J-β2.7 cells cannot be phosphorylated on Ser1140, as detected by the phosphospecific antibody against αL. β2 was detected with a blotting antibody to demonstrate equal loading of LFA-1.

Carl_G_190x270_mm_blokki_FINAL.indd 400 06-Aug-23 1:54:34 PM

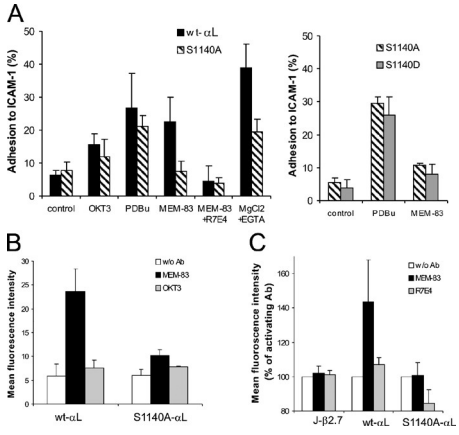

Figure 4. **Effect of mutation of the phosphorylation site in the LFA-1 αL chain on adhesion to ICAM-1 and induction of high-affinity LFA-1.** (A) Mutation of αL chain Ser1140 affects adhesion induced by an activating antibody to LFA-1. J-β2.7 transfectants expressing wt αL or S1140A-αL were allowed to bind to ICAM-1–coated wells without stimulation (control) or after stimulation with 10 μg/ml OKT3, 200 nM PDBu, 5 mM $MgCl_2$/1 mM EGTA, or 10 μg/ml MEM-83 in the presence or absence of the β2-blocking antibody R7E4. (right) Adhesion of S1140A-αL and S1140D-αL–transfected cells to ICAM-1 after phorbol ester or MEM-83 stimulation was compared. (B) Effects of the S1140A mutation on sICAM-1–binding activity of LFA-1. J-β2.7 transfectants were activated with 10 μg/ml MEM-83 or control antibody OKT3 in the presence of 150 μg/ml ICAM-1Fc and binding was determined by flow cytometry. (C) The effects of the S1140A mutation on expression of the αL activation reporter mAb24 were examined. J-β2.7 cells were incubated with mAb24 in the presence of MEM-83 or R7E4, and mAb24 expression was analyzed by flow cytometry. Error bars represent SD.

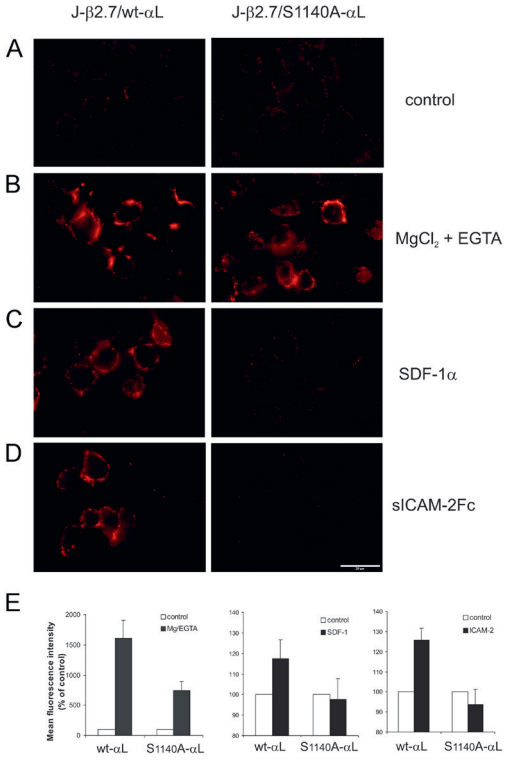

Figure 5. **The Ser1140Ala mutation inhibits mAb24 expression induced by SDF-1 or ICAM-2.** (A) J-β2.7 cells expressing wt αL or S1140A-αL. (B) Cells were activated with 5 mM $MgCl_2$/1 mM EGTA for 30 min. (C) Cells were activated with 3 μg/ml SDF-1α for 2 min; (D) Cells were activated with 10 μg/ml sICAM-2Fc for 30 min, and the high-affinity epitope of LFA-1 was examined by fluorescence microscopy with mAb24. Bar, 20 μm. (E) mAb24 expression was quantified using flow cytometry. Error bars represent SD.

Stewart et al., 1996). Whether a negative charge at position 1140 would be enough to affect adhesion was studied by using a Ser1140Asp mutation (Fig. 4 A, right). The result showed that the S/A and S/D mutations worked similarly.

To further study the mechanisms of the different modes of adhesion, a soluble ICAM-Fc (sICAM-1Fc) binding assay was used to measure the ligand-binding activity. mAb MEM-83 greatly increased the binding of sICAM-1 to wt αL transfectants (Fig. 4 B), whereas TCR stimulation had no effect. Importantly, only minimal sICAM-1 binding was observed for S1140A-αL cells after MEM-83 activation. Affinity modulation of LFA-1 can also be detected using mAb24 (Dransfield and Hogg, 1989). This epitope was not expressed in resting J-β2.7 transfectants, but there was enhanced expression on the wt cells after MEM-83 activation (Fig. 4 C). The S1140A mutation abolished MEM-83–induced expression of the mAb24 epitope (Fig. 4 C). Together, the J-β2.7 cells expressing nonphosphorylatable S1140A-αL mutant show a marked reduction in ICAM-1 binding and expression of the high-affinity form of integrin.

The phosphorylation site in αL is involved in chemokine- and ligand-induced affinity regulation of the integrin

One of the best characterized examples of LFA-1 affinity modulation is the activation of integrin-dependent leukocyte arrest and migration through G protein–coupled receptors for chemokines (Constantin et al., 2000). SDF-1α, a CXC chemokine, has been shown to induce a rapid and transient activation of LFA-1 in J-β2.7 wt αL cells that can be detected by expression of the mAb24 epitope (Weber et al., 1999). To determine whether the S1140A mutation affected chemokine-triggered mAb24 expression, we stimulated J-β2.7 transfectants with SDF-1α and studied the mAb24 epitope by immunofluorescence. No mAb24 staining was seen in nonstimulated cells (Fig. 5 A). Mg/EGTA treatment was used as a positive control to show the ability of transfectants to express the mAb24 epitope (Fig. 5, B and E). After SDF-1α stimulation, clear staining of mAb24 was detected on the wt αL cells, but not on the S1140A-αL–expressing cells (Fig. 5, C and E).

Furthermore, integrin ligands are known to increase adhesion, probably by affinity modulation (Cabanas and Hogg, 1993; Kotovuori et al., 1999). sICAM-2 increased the expression of the mAb24 epitope on wt αL cells, whereas no staining of the S1140A-αL cells was observed (Fig. 5, D and E). Thus, physio-

Carl_G_190x270_mm_blokki_FINAL.indd 401 06-Aug-23 1:54:34 PM

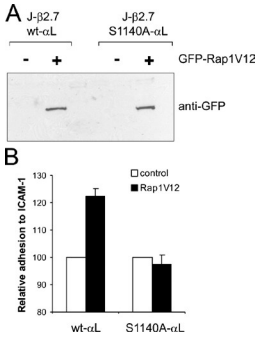

Figure 6. **Rap1V12 is unable to activate the Ser1140Ala-mutated integrin in cells.** (A) The expression levels of GFP-Rap1V12 in J-β2.7 cell transfectants is shown. (B) Adhesion to coated ICAM-1 of the transfectants was measured as described in Materials and methods. Error bars represent SD.

logical activators of the LFA-1 integrin, which have been shown to lead to extracellular conformational changes, are not able to activate integrins with nonphosphorylatable αL chains.

Active Rap1 cannot activate the S1140A-αL–mutated integrin in cells

The small GTPase Rap1 is a potent activator of LFA-1 that is needed in different modes of LFA-1 activation, including activation from the outside of the cell with divalent cations or antibodies (Katagiri et al., 2000, 2002; de Bruyn et al., 2002; Sebzda et al., 2002). Transfection of leukocytes with an active form of Rap1 (Rap1V12) has been shown to increase LFA-1 affinity, as measured by increased ability to bind sICAM-1 (Katagiri et al., 2003). GFP-Rap1V12 was transfected into J-β2.7 cells stably expressing wt αL or S1140A-αL (Fig. 6). The expression level of Rap1V12 in wt αL– and S1140A-αL–expressing J-β2.7 cells was the same (Fig. 6 A). However, Rap1V12 was unable to activate the S1140A mutant, even if increased adhesion of wt αL–expressing cells could be observed after Rap1V12 transfection (Fig. 6 B).

Thr758-phosphorylated β2 binds 14-3-3 in vitro and in vivo

Having established the phosphorylation site in αL and its functional characteristics, we focused on the investigation of the β2 polypeptide phosphorylation. Both phorbol ester activation and TCR ligation induce phosphorylation of the β chain on Thr758 (Hilden et al., 2003), which is the first threonine in the TTT motif that is important for adhesion and cytoskeletal interactions of the LFA-1 and other integrins (Fig. 7 A; Hibbs et al., 1991; Peter and O'Toole, 1995; Fagerholm et al., 2004). 14-3-3 proteins from leukocyte lysates have previously been shown to interact with a synthetic β2 integrin peptide phosphorylated on Thr758 (Fagerholm et al., 2002b), but whether the binding was direct or indirect and whether it occurred in cells was not established. In this study, we examined the binding of purified 14-3-3 proteins to the phosphorylated integrin cytoplasmic peptides. The proteins bound specifically to the phosphorylated, but not to the nonphosphorylated, β2 chain, as examined by peptide affinity chromatography with nonphosphorylated and Thr758-phosphorylated β2 chain peptides (Fig. 7 B). 14-3-3 proteins could be eluted from the affinity column by the peptide ARAApSAPA, which specifically binds to the phosphopeptide-binding groove in 14-3-3 (Moorhead et al., 1999), but not by a control peptide (phospho-αL peptide; Fig. 7 B). This shows that the binding is specific and occurs through the canonical 14-3-3 phosphopeptide binding motif (Fig. 7 B). Phosphorylation

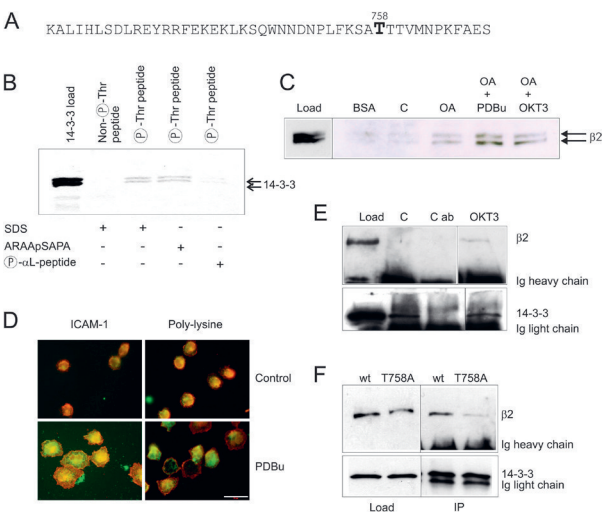

Figure 7. **Specific binding of 14-3-3 proteins to Thr758-phosphorylated β2 integrin in vitro and in vivo.** (A) Sequence of the β2 integrin cytoplasmic domain with the Thr758 phosphorylation site shown in bold. (B) Binding of purified yeast 14-3-3 proteins to Thr758-phosphorylated and nonphosphorylated peptides was assessed by peptide affinity chromatography and Coomassie staining of eluted proteins. Elution was performed with SDS, the ARAApSAPA peptide, or a control peptide (phospho-αL peptide). (C) Binding of β2 integrin from control (C), okadaic acid–pretreated (OA), okadaic acid–pretreated and phorbol ester–activated (OA + PDBu), or TCR-ligated (OA + OKT3) Jurkat cell lysates to 14-3-3–Sepharose or BSA columns. The eluted proteins were detected by Western blotting with β2 integrin antibodies. The two bands detected in the loading control and stimulated cells presumably represent precursor and mature forms of the integrin β chain found in Jurkat cells (Fagerholm et al., 2002a). (D) Coimmunofluorescence of 14-3-3 (green) and β2 integrins (red) in untreated (control) human T cells or in cells activated with phorbol ester (PDBu) on ICAM-1– or poly-lysine–coated coverslips. Bar, 20 μm. (E) Increased binding between 14-3-3 and β2 in TCR-ligated cells. Endogenous 14-3-3 proteins were immunoprecipitated from human T cell lysates with a control antibody (C ab) or a 14-3-3 mAb, and coimmunoprecipitating β2 integrins were detected by Western blotting with β2 integrin antibodies. Immunoprecipitated 14-3-3 proteins were detected with a 14-3-3 blotting antibody to demonstrate equal loading. (F) wt β2 or T758A-β2 transfected COS-1 cell lysates were used in the immunoprecipitation performed as in E.

Carl_G_190x270_mm_blokki_FINAL.indd 402 06-Aug-23 1:54:35 PM

of another major site in the β2 cytoplasmic domain, Ser756, has previously been shown not to mediate 14-3-3 binding (Fagerholm et al., 2002b).

Affinity chromatography with 14-3-3 proteins coupled to Sepharose showed specific interaction between 14-3-3 and β2 integrins, which occurred only when cells had been activated with phorbol ester or TCR ligation (Fig. 7 C). Ligand binding has been shown to cluster integrins on the cell surface (Kim et al., 2004). Indeed, in coimmunofluorescence studies, the 14-3-3 proteins and β2 integrins coclustered in activated T cells spread on ICAM-1, as shown by the increased yellow staining in these cells compared with cells on poly-lysine or nonstimulated cells (Fig. 7 D). Importantly, endogenous 14-3-3 proteins and β2 integrins could be coprecipitated from TCR-stimulated, but not unstimulated, human T cells (Fig. 7 E). To confirm the Thr758-dependent association between 14-3-3 and β2, we transfected COS-1 cells with wt β2 or T758A-mutated β2 and performed coprecipitation experiments with endogenous 14-3-3 proteins. The transfected Thr758Ala-mutated integrin showed reduced association with endogenous 14-3-3 proteins in most coimmunoprecipitation experiments (Fig. 7 F).

Mutation of Thr758 in β2 or blocking of 14-3-3 binding to the β2 chain reduces constitutive COS cell adhesion

Mutation of Thr758 in the β2 chain has previously been shown to affect adhesion of LFA-1 to ICAM-1 when transfected into COS cells, where LFA-1 is constitutively active, and into LAD cells (a B lymphoblastoid cell line lacking LFA-1), where LFA-1 can be activated with phorbol ester (Hibbs et al., 1991). We used the COS cell system to investigate the effect of direct 14-3-3 association with the β2 chain without interfering with activating signals of the integrin and because a T cell model lacking β2 integrins is currently unavailable.

Phorbol ester did not stimulate LFA-1–mediated adhesion to ICAM-1 in this system, but MEM-83 did have a stimulatory effect (Fig. 8 A). As previously reported, the Thr758Ala mutation significantly reduced the constitutive integrin-mediated adhesion of transfected cells to ICAM-1 (Fig. 8 A). MEM-83 could still activate the Thr-mutated integrin, albeit to a lower degree than for wt LFA-1 (Fig. 8 A), showing that activating conformational changes could still occur for the mutated integrin. However, when both Ser1140 and Thr758 were mutated, not even MEM-83 could activate the integrin-mediated adhesion (Fig. 8 A), even if the singly mutated Ser1140Ala-αL together with wt β2 could normally mediate adhesion in COS cells. Because the S1140A-αL–mutated integrin is adhesion deficient in J-β2.7 cells, but not in COS-1 cells, it is clear that these cells are not a useful model for studying LFA-1 function in all cases.

To examine whether the effects of the Thr758 mutation seen were attributable to the blockage of 14-3-3 proteins from binding to the integrin, we cotransfected cells with wt LFA-1 integrins and an EGFP-R18wt construct, which blocks 14-3-3 interactions with its cellular ligands by binding to the phosphopeptide-binding groove in 14-3-3 (Jin et al., 2004). As a control, we used a mutant construct that does not bind to 14-3-3 proteins (R18mut). The level of GFP proteins and cell surface LFA-1 integrins in the EGFP-positive cells was equal in R18wt and R18mut cells, as examined by flow cytometry (unpublished data), Western blotting with an anti-GFP antibody and an LFA-1 blotting antibody (Fig. 8 B), and immunofluorescence (Fig. 8 C). R18wt cotransfected cells showed markedly reduced adherence to ICAM-1 (Fig. 8, C and D). The 14-3-3 proteins have many binding partners among cytoskeletal and signaling proteins that might affect adhesion, and R18 peptides have indeed been shown to alter the cytoskeleton in cells that do not express LFA-1 (Jin et al., 2004). However, when the adhesion of endogenous COS cell integrins to fibronectin was examined there was no difference in adhesion between R18wt and R18mut-transfected cells (Fig. 8 D, right). Thus, it is likely that 14-3-3 binding to the Thr758-phosphorylated integrin mediates the effect of Thr758 on cell adhesion.

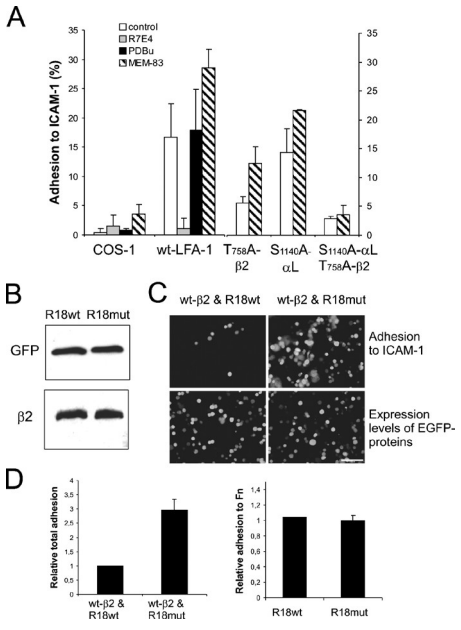

Figure 8. **Effect of the mutation of Thr758 or blocking 14-3-3 binding to the β2 chain on adhesion to ICAM-1.** (A) Mutation of Thr758 of β2 reduces COS cell adhesion to ICAM-1. COS-1 cells were transfected with wt αL or S1140A-αL and wt β2 or Thr758/Ala–mutated β2 integrin cDNA, and cell adhesion to coated ICAM-1 in the presence of PDBu, blocking antibody (R7E4), or stimulating antibody (MEM-83) was examined. (B) Cells were cotransfected with wt LFA-1 integrins and EGFP-R18wt or EGFP-R18mut constructs. Levels of EGFP proteins and LFA-1 in the transfected cells were examined by Western blotting. (C) Adhesion of COS cells was visualized by immunofluorescence of EGFP-expressing cells adhering to ICAM-1–coated plates (top). Bar, 100 μm. (bottom) EGFP levels in the transfected cells. (D, left) Total cells adhering to ICAM-1 were also quantified as described in Materials and methods. (D, right) As a control, the R18wt- and R18mut-transfected cells were also examined for adhesion of endogenous COS cell integrins to fibronectin. Error bars represent SD.

Carl_G_190x270_mm_blokki_FINAL.indd 403 06-Aug-23 1:54:36 PM

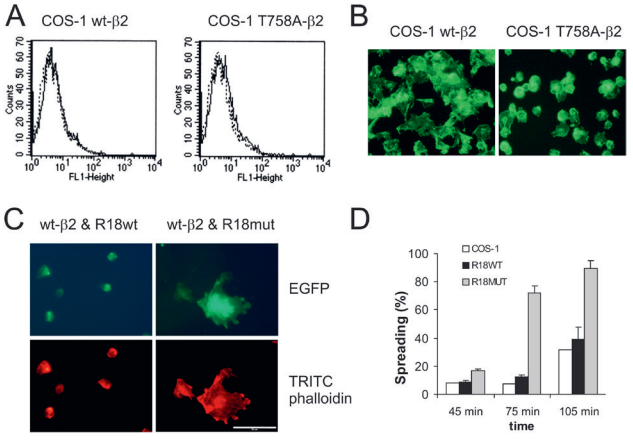

Figure 9. **Blocking the interaction between 14-3-3 and β2 integrins abolishes actin reorganization and cell spreading.** (A) COS cells were transfected with wt β2 or T758A-β2, and the transfected COS cells were examined for mAb24 expression by flow cytometry as in Fig. 3. Dotted lines represent background fluorescence and solid lines represent the mAb24 binding. (B) Cells were allowed to spread on coated ICAM-1. The cells were examined for F-actin by FITC-phalloidin staining. (C) R18wt or R18mut was cotransfected with wt LFA-1 into COS-cells, and cell spreading on ICAM-1 was visualized. Both EGFP (R18) expression and TRITC-phalloidin staining is shown from the same cells. Bar, 50 μm. (D) Spreading was quantified by counting the percentage of spread transfected cells at different time points. Error bars represent SD.

14-3-3 binding to phosphorylated β2 is involved in cytoskeletal rearrangements

Neither the wt LFA-1 nor the Thr758Ala mutant of the β2 chain showed any binding of mAb24 in COS cells (Fig. 9 A). Additionally, phorbol esters and TCR ligation have been reported not to induce sICAM-1 binding or mAb24 expression in T cells, although cell adhesion to coated ICAM-1 can be readily detected (Stewart et al., 1996). In contrast, TCR triggering and phorbol esters have been closely associated with a spreading phenotype of T cells (Stewart et al., 1996). Furthermore, the TTT motif of the integrin has been closely associated with actin reorganization events, but not affinity changes, in integrins (Peter and O'Toole, 1995). Indeed, the Thr758 mutation was shown to significantly reduce cell spreading on ICAM-1 as examined by FITC-phalloidin staining of polymerized actin (Fig. 9 B). In addition, R18wt-transfected cell spreading on ICAM-1 was almost completely abolished (Fig. 9, C and D). Quantitation of transfected cell spreading showed that R18wt and LFA-1 cotransfected cells only spread at later time points, when other untransfected COS-1 cells started spreading unspecifically on ICAM-1 (Fig. 9 D). The mutant R18 construct did not block spreading. These results show that 14-3-3 binding to the phosphorylated β2 integrin is important for integrin effects on the cell cytoskeleton.

A talin head domain construct can activate the Thr758Ala-mutated β2 integrin in cells

The head domain of the large cytoskeletal protein talin has been demonstrated to be a major player in activation of different integrins, including LFA-1 (Kim et al., 2003; Tadokoro et al., 2003). It binds directly to the β chains of integrin cytoplasmic domains and, presumably, induces a separation of the cytoplasmic domains of the α and β chains, which leads to a conformational change in the extracellular domain (Kim et al., 2003; Tadokoro et al., 2003). Thus, we examined whether the effect of the T/A mutation of the β2 chain was attributable to an altered ability of talin to bind to and activate LFA-1.

We cotransfected COS cells with wt or T758A-mutated β2 together with the F2/F3 domains of the talin head domain. The expression levels of LFA-1 and the talin head domain construct were similar in the different transfectants, as measured by Western blotting (Fig. 10 A) and flow cytometry (unpublished data). We saw an increase in LFA-1–mediated adhesion to ICAM-1 in the talin head cotransfected cells as compared with cells without the talin head (Fig. 10 B), although the occurrence of adhesion was somewhat less in T758A-β2–transfected cells than in the wt controls. The talin head domain, like the antibody MEM-83, could activate S1140A-mutated αL in the COS cell system (Fig. 10 B). Thus, in COS-1 cells, affinity-inducing stimuli of the integrin are also functional for S1140A-mutated αL, indicating the possibility that a leukocyte-specific restrictive factor working through the α chain is missing.

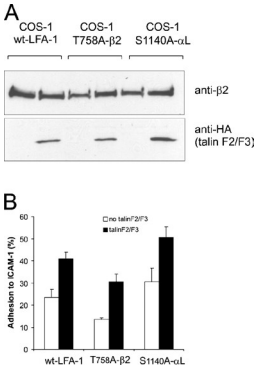

Figure 10. **The head domain of talin can activate the Thr758Ala-mutated β2 integrin.** (A) COS cells were transfected with wt β2 or T758A-β2 or S1140A-αL mutant constructs, together with HA-tagged talin F2/F3 domains, and the level of protein expression was examined by Western blotting with an LFA-1 blotting antibody or an anti-HA antibody. (B) COS cell adhesion of the transfected cells to coated ICAM-1 was examined as described in Materials and methods. Error bars represent SD.

Carl_G_190x270_mm_blokki_FINAL.indd 404 06-Aug-23 1:54:36 PM

Discussion

Phosphorylation of the cytoplasmic domains of LFA-1 was initially reported more than a decade ago (for review see Fagerholm et al., 2004), but the significance of these phosphorylation events in integrin regulation has remained unclear. Threonine phosphorylation of β2 has been reported (Valmu and Gahmberg, 1995; Hilden et al., 2003), and it has also been shown that the threonine triplet in β2 (Thr 758–760) is important for both adhesion and cytoskeletal reorganization mediated by LFA-1 (Hibbs et al., 1991; Peter and O'Toole, 1995). The stoichiometry of the phosphorylation of β2 integrin in phorbol ester–stimulated T cells in the presence of okadaic acid was determined to be 0.92 mol/mol of protein (Valmu et al., 1999b). Because several sites become phosphorylated under these conditions it is clear that each site is phosphorylated at a relatively low level (Fagerholm et al., 2002b; Hilden et al., 2003). However, in comparison with receptor tyrosine phosphorylation, low stoichiometry phosphorylations may still play important biological roles by regulating protein–protein interactions.

αL has been shown to be constitutively phosphorylated in T cells (Hara and Fu, 1986; Chatila et al., 1989), but the phosphorylation site and stoichiometry of αL phosphorylation has not been assessed. We have now mapped the phosphorylation site in the αL cytoplasmic domain to Ser1140 and shown that ∼40% of surface αL was phosphorylated in T cells. A similarly high stoichiometry of phosphorylation already found in resting cells has been shown for the α4 integrin (Han et al., 2001). In analogy with the α4 integrin, where paxillin binding to the nonphosphorylated integrin rather than to the phosphorylated form excludes this adaptor protein from the leading edge of the cell and thus regulates cell migration (Goldfinger et al., 2003), constitutive phosphorylation of the αL tail may play profound roles in spatiotemporal regulation of integrin functions.

By mutating Ser1140, we have shown that the nonphosphorylatable LFA-1 α chain expressed in a T cell line can no longer be activated by agents that have previously been demonstrated to induce high-affinity forms of the integrin; i.e., by an activating antibody (MEM-83); by ligands or chemokines, as detected by adhesion to ICAM-1; by sICAM-1 binding; or by mAb24 that detects the high-affinity form of LFA-1. Thus, phosphorylated Ser1140 is involved in conformational changes occurring in LFA-1 in response to several different affinity-increasing stimuli. One possibility is that the negative charge induced by phosphorylation could facilitate the separation of the integrin cytoplasmic tails, leading to a conformational change in the extracellular domain (Kim et al., 2004; Adair et al., 2005). However, a Ser-Asp mutation did not lead to a different adhesion phenotype compared with the Ser-Ala mutation, indicating that simply substituting a negatively charged amino acid for serine is not enough to mimic phosphorylation. Thus, it is more plausible that the αL phosphorylation site works through selective binding to some cytoplasmic factor.

The small GTPase Rap1 is an important mediator of various modes of LFA-1 activation in leukocytes, including activation by antibodies and divalent cations (Katagiri et al., 2000, 2002; de Bruyn et al., 2002; Sebzda et al., 2002). Importantly, Rap1 has been shown to act through the integrin α chain cytoplasmic domain and to influence integrin affinity for ICAM-1 (Tohyama et al., 2003). Thus, we wanted to examine the effect of active Rap1 (Rap1V12) on the nonphosphorylatable S1140A mutant. Rap1V12 was able to induce binding of wt αL–transfected, but not mutant-αL–transfected, J-β2.7 cells to coated ICAM-1. The mutated αL may be locked in a low-affinity conformation that cannot be activated from outside of the cell by activating antibodies or other activating stimuli that increase integrin affinity for its ligands. However, it can still be activated with phorbol ester and TCR stimulation, which do not (and, if so, only marginally) influence integrin affinity.

Rap1 may be working upstream of the αL phosphorylation, possibly influencing the binding of some cytoplasmic factor to the αL cytoplasmic tail. RapL is a Rap1-binding molecule that can activate LFA-1 and is found in leukocytes (Katagiri et al., 2003). It will be of future interest to study the effect of RapL in this system.

It has previously been reported that the 14-3-3 isoforms αβ and δζ from leukocyte lysates associate specifically with a Thr758-phosphorylated β2 integrin COOH-terminal peptide (Fagerholm et al., 2002b). We discovered that the β2–14-3-3 interaction is direct. Additionally, we have shown that the binding occurs in T cells that have been activated by stimuli that induce phosphorylation of the β2 chain on Thr758, i.e., phorbol ester and TCR engagement. Mutation of Thr758 or blocking of 14-3-3 binding to the β2 integrin by R18 peptides inhibited cell adhesion to ICAM-1. The Thr758 mutation or R18 peptide also inhibited integrin-mediated cell spreading on ICAM-1. Thus, phosphorylation of Thr758, which is induced by inside-out activating stimuli for the integrin, mediates binding to 14-3-3 proteins in cells, and this interaction seems to mediate the effect of the integrin on the cell cytoskeleton. The 14-3-3 proteins are dimers, and both monomers can independently bind to phosphorylated targets either within the same protein or in different proteins (Tzivion and Avruch, 2002; MacKintosh, 2004). It is possible that threonine phosphorylation of CD18 recruits 14-3-3 proteins to the plasma membrane–cytoskeleton connection and that the 14-3-3s in turn recruit other proteins to regulate downstream events.

There are increasing amounts of evidence that talin plays a profound role in activating several integrins, including LFA-1 (Kim et al., 2003; Calderwood, 2004; Smith et al., 2005). The head domain of talin binds to integrin β chains and induces a separation of α and β chain cytoplasmic domains. Therefore, we investigated the ability of the talin head domain construct to activate the β2-T758A mutant. It could still be activated by the talin construct in cells, as measured by increased adhesion of the transfected cells to coated ICAM-1. The talin-binding site in β3 integrins encompasses the first NPXY motif (Tadokoro et al., 2003) and corresponds to residues 747–755 in β2, which precede Thr758. Thus, the mechanism by which Thr758 regulates adhesion is presumably not related to talin.

The cytoskeletal protein α-actinin has been shown to associate with the β2 tail at a membrane-proximal site, whereas the COOH-terminal portion of the tail (residues 748–762) inhibits this interaction (Sampath et al., 1998). Substitution of

Carl_G_190x270_mm_blokki_FINAL.indd 405 06-Aug-23 1:54:37 PM

Thr758 with Ala or with the phosphate-mimic Glu stimulates binding of α-actinin to β2, suggesting that phosphorylation of β2 on Thr758 does not regulate α-actinin binding (Sampath et al., 1998). Additionally, deletion of the α-actinin binding site in β2 does not influence adhesion to ICAM-1. On the other hand, other proteins may bind to the TTT region and, indeed, filamin has been shown to do so (Calderwood et al., 2001). Thus, it is possible that threonine phosphorylation and 14-3-3 binding may regulate such interactions.

LFA-1 is involved in many different immunological adhesion events. It can be activated by different stimuli and is regulated both by conformational changes and by cytoskeletal attachment and clustering. It is now clear that phosphorylation of both the α and β chains plays a role in the molecular mechanisms involved in the different activation events. However, the αL and β2 polypeptides play distinctive roles in integrin activation. The integrin αL chain is constitutively phosphorylated, and this phosphorylation site (Ser1140) seems to be required for adhesion events that involve rapid changes in the conformation and affinity of the integrin heterodimer. In contrast, the β2-Thr758 phosphorylation that is induced after physiological triggering of T cells through the TCR works through interaction with 14-3-3 proteins. This form of adhesion is slower and involves actin reorganization and cell spreading. The contribution of the different phosphorylation events to overall adhesion may depend on the context of adhesion and provides the possibility for regulation of both fast, transient adhesive events and long-term, stable adhesion strengthening.

Materials and methods

Reagents
Phorbol 12,13-dibutyrate (PDBu) was obtained from Sigma-Aldrich. [^{32}P]orthophosphate (aqueous solution, 10 mCi/ml, 5,000 Ci/mmol) was purchased from the Radiochemical Centre (GE Healthcare). Recombinant human ICAM-1, ICAM-1Fc, and ICAM-2Fc were obtained from R&D Systems, and fibronectin was obtained from Calbiochem. Sequencing-grade modified trypsin (activity more than 2.5 U/mg) was purchased from Promega. G418 was purchased from Calbiochem-Novabiochem. SDF-1 was obtained from R&D Systems. The peptides (ARAApSAPA, CLFKSATTTVMN, CLFKSApTTTVMN, and CLKPLHEKDSEpSGGGKD, where pS is phosphoserine and pT is phosphothreonine) were synthetized by Fmoc chemistry (Valmu et al., 1999b).

Antibodies
The mAbs R7E4 and R2E7B against the human β2 subunit of leukocyte integrin have been described previously (Nortamo et al., 1988). The monoclonal activating antibody against CD3, OKT3, was purified from ascites fluid produced by hybridoma cells (clone CRL 8001; American Type Culture Collection). The activating mAb MEM-83 was provided by V. Horejsi (Institute of Molecular Genetics, Prague, Czech Republic). IB4 was a gift from M.A. Arnaout (Massachusetts General Hospital, Boston, MA). mAb24 (β2) was a gift from N. Hogg (Imperial Cancer Research Fund, London, UK). The 14-3-3 antibodies H-8 and K-19, as well as the GFP antibody, were obtained from Santa Cruz Biotechnology, Inc. The HA-tagged talin F2/F3 protein was detected by anti–HA-biotin antibodies (Roche) and streptavidin-HRP (GE Healthcare). To produce antiserum to phospho-αL, the integrin αL chain phosphopeptide CLKPLHEKDSEpSGGGKD was conjugated to keyhole limpet hemocyanin (Harlow and Lane, 1988). The complex was injected into rabbits. The antisera were purified by affinity chromatography using the phosphorylated peptide.

cDNA constructs
The EGFP-R18 and EGFP-R18mut plasmids were gifts from T. Pawson (University of Toronto, Toronto, Canada). The 14-3-3 *Saccharomyces cerevisiae* isoforms BMH1 and BMH2 plasmids in DH5α were gifts from C. MacKintosh (University of Dundee, Nethergate, Dundee, Scotland, UK). The HA-tagged talin F2/F3 construct was a gift from D. Calderwood (Yale University, New Haven, CT). GFP-Rap1V12 was a gift from D. Cantrell (University of Dundee). cDNA coding for full-length human αL was subcloned into the pcDNA3 vector and human β2 was subcloned into the πHM3 vector. Mutants were created using site-directed mutagenesis (Weiner et al., 1994), and the mutated constructs were checked by sequencing.

Cell lines and transfection
Buffy coats used for the isolation of T cells were obtained from the Finnish Red Cross Blood Transfusion Service (Valmu et al., 1999b). The cells were grown in RPMI 1640 medium supplemented with 10% FCS, L-glutamine, and antibiotics. The Jurkat cell clone E6.1 (American Type Culture Collection) was maintained in the same medium.

COS-1 cells were cultured in DME supplemented with 10% FCS, L-glutamine, and antibiotics. COS-1 cells were used for transient expression of wt and mutant β2 integrins. COS-1 cells were cotransfected with purified α- and β-subunit cDNAs with or without EGFP-R18wt, EGFP-R18mut, or talin F2/F3 constructs using the FuGENE 6 transfection reagent according to the manufacturer's instructions (Roche). Flow cytometric analysis was used to quantify cell surface expression of integrins in the transfected COS-1 cells.

The human T lymphoma cell line clone J-β2.7, which lacks the LFA-1 α chains and was derived from Jurkat cells by mutagenesis (Weber et al., 1997), was a gift from N. Hogg. J-β2.7 cells (7.2×10^6 per transfection) were washed, suspended in 0.36 ml PBS, and mixed with 20 μg wt αL or S1140A-αL DNA. Electroporation was performed at 240 V and 950 μF. After 48 h of culture, the medium was supplemented with 0.8 mg/ml G418. LFA-1–expressing cells were enriched using magnetic cell sorting (Miltenyi Biotec GmbH). Alternatively, cells (S1140D-αL and Rap1V12) were transfected with the Optifect system according to the manufacturer's instructions (Invitrogen). Flow cytometric analysis was used to quantify cell-surface expression of integrins in the transfected cells. For both wt αL– and S1140A-αL–expressing J-β2.7 cells, several clones were selected that exhibited comparable levels of surface expression as detected by flow cytometry. In each experiment, we used two independent clones of both wt and αL mutant cells.

Peptide affinity chromatography
The peptides CLFKSATTTVMN and CLFKSApTTTVMN, corresponding to the β2 integrin sequence surrounding the phosphorylated Thr758, were coupled to thiopropyl–Sepharose according to the manufacturer's instructions. His-tagged BMH1 and BMH2 proteins were expressed in *Escherichia coli* DH5α and purified with Ni-NTA columns (Moorhead et al., 1999). Affinity chromatography was performed with 2 μg each of purified 14-3-3 proteins BMH1 and BMH2. After extensive washes, the bound proteins were eluted either with SDS or with 1 mM ARAApSAPA peptide or 1 mM phospho-αL peptide (CLKPLHEKDSEpSGGGKD), and the eluates were run on SDS-PAGE and stained with Coomassie blue.

14-3-3 affinity chromatography
Purified BMH1 and BMH2 or BSA were coupled to Sepharose (Moorhead et al., 1999). Jurkat cells were either left untreated or stimulated with 1.5 μM of okadaic acid, a combination of okadaic acid and the OKT3 antibody (10 μg/ml) against the TCR, or 200 nM PDBu. The cells were lysed as described previously (Valmu et al., 1999b). The lysates were mixed with the affinity matrix for 1 h and washed extensively with 500 mM NaCl. Bound proteins were eluted with SDS and analyzed by Western blotting with the blotting β2 integrin antibody R2E7B.

Coimmunoprecipitation
Human T cells were activated with OKT3 or left untreated. Cells were lysed as described previously (Valmu et al., 1999b) and lysates were precleared with protein G–Sepharose. Immunoprecipitations were made with the 14-3-3 H8 antibody or control antibody (OKT3) coupled to protein G–Sepharose, and the immunoprecipitates were washed four times with lysis buffer. The bound proteins were eluted with SDS and analyzed by Western blotting with a 14-3-3 antibody (K-19) and β2 integrin antibody (R2E7B).

Cell adhesion assays
Recombinant soluble human ICAM-1 or fibronectin (0.3 μg/well) was coated on flat-bottom 96-well microtiter plates by overnight incubation at 4°C. The wells were blocked with 1% dry milk for 1.5 h at 37°C. Cells

Carl_G_190x270_mm_blokki_FINAL.indd 406 06-Aug-23 1:54:37 PM

were suspended in binding medium (DME for COS-1 and RPMI 1640 for J-β2.7 cells, with 40 mM Hepes, 0.1% BSA, and 1–2 mM $MgCl_2$). Cells were stimulated with either 200 nM PDBu or 10 μg/ml OKT3 or MEM-83, added to each well, and allowed to adhere for 20 (COS-1) or 30 (J-β2.7) min at 37°C. In inhibition experiments, cells were preincubated for 15 min with 10 μg/ml of the blocking antibody R7E4. After incubation, unbound cells were removed by gentle washing. The binding was quantified by ELISA.

Immunofluorescence staining

Human T cells or J-β2.7 cells were seeded onto poly-lysine– or ICAM-1–coated coverslips at 5×10^5 cells/slide in culture medium in the presence or absence of activators and incubated for 30–60 min at 37°C. For transfected COS-1 spreading assays, 2×10^5 cells were seeded onto ICAM-1–coated coverslips and incubated for the times indicated in the figure legends. Unbound cells were gently washed away and adherent cells were fixed for 10 min with 1% formaldehyde/PBS. Cells were labeled with FITC- or TRITC-phalloidin in 0.1% saponin/1% FBS/PBS for 20–30 min, or cells were incubated with primary antibodies (mAb24, R7E4, 14-3-3 antibody K19 in PBS, or in saponin buffer) for 30 min, followed by incubation with Cy3-conjugated anti–mouse or FITC-conjugated anti–rabbit antibody. After washing with PBS, coverslips were mounted with Mowiol mounting medium and observed under a fluorescence microscope (model IX71; Olympus) and photographed with a camera (model DP70; Olympus). Images were analyzed and processed using the analySIS program (Soft Imaging System GmbH) and Adobe Photoshop.

^{32}P radiolabeling and cell activation, immunoprecipitation, and SDS-PAGE

^{32}P cell labeling was done as previously described (Valmu et al., 1999b). T cells were labeled overnight and COS-1 cells were labeled for 2 h at 37°C. After labeling, the cells were activated or left untreated. The T cell activation was stopped by adding ice-cold 10 mM EDTA/PBS, and COS-1 cells were detached with 5 mM EDTA/PBS. The cells were washed and lysed as described previously (Valmu et al., 1999b). The intensity of the radiolabeled bands was quantified using the Tina 2.09c software (Raytest). The intensity of the radiolabeled bands was reported as intensity of the band minus background intensity of the lane.

Cell lysates were used for immunoprecipitation with 1–3 μg R7E4 or IB4 for 2.5 h or overnight and coupled to protein G–Sepharose for 30 min at 4°C. The immunoprecipitates were washed extensively with decreasing detergent and salt concentrations. Bound proteins were eluted with 1% SDS, subjected to SDS-PAGE, and blotted onto polyvinylidene fluoride membranes (Millipore). Phosphopeptide mapping and manual radiosequencing of phosphopeptides have been described previously (Hilden et al., 2003).

Flow cytometric analysis

Cells were incubated with PBS containing 20 μg/ml of the indicated antibodies (R7E4, MEM-83, and OKT3) on ice for 30 min. The cells were then washed with PBS and further incubated with FITC-conjugated anti–mouse IgG and subjected to flow cytometric analysis with FACScan (Becton Dickinson). For mAb24 staining, J-β2.7 cells or COS-cells were reacted with 10 μg/ml mAb24 in the presence of the activating antibody 10 μg/ml MEM-83 for 30 min at 37°C. Cells were instantly stained with FITC-conjugated anti–mouse IgG antibodies on ice for 20 min and analyzed by flow cytometry. mAb24 expression was reported as mean fluorescence intensity.

sICAM-1Fc binding assay

J-β2.7 transfectants were incubated in 25 μl RPMI 1640, 40 mM Hepes, and 1 mM $MgCl_2$ in the presence or absence of stimulators and 150 μg/ml ICAM-1Fc at 37°C for 30 min. After removal of the unbound ligand by washing with PBS, the cells were incubated with FITC-conjugated anti–human IgG-Fc–specific antiserum (Jackson ImmunoResearch Laboratories) on ice for 20 min. Cells were analyzed by flow cytometry.

We thank T. Pawson for R18 constructs, C. MacKintosh for BMH1/BMH2-expressing bacteria, D. Calderwood for the talin construct, D. Cantrell for the GFP-Rap1V12 construct, and N. Hogg, V. Horejsi, and M.A. Arnaout for antibodies and cells. We would also like to thank M. Aatonen for expert technical assistance and C. Kantor for assistance with antibody production.

This work was supported by the Academy of Finland, The Sigrid Jusélius Foundation, the Finnish Cancer Society, and the Magnus Ehrnrooth Foundation.

Submitted: 4 April 2005
Accepted: 17 October 2005

References

Adair, B.D., J.-P. Xiong, C. Maddock, S.L. Goodman, M.A. Arnaout, and M. Yeager. 2005. Three-dimensional EM structure of the ectodomain of integrin αVβ3 in a complex with fibronectin. *J. Cell Biol.* 168:1109–1118.

Cabanas, C., and N. Hogg. 1993. Ligand intercellular adhesion molecule 1 has a necessary role in activation of integrin lymphocyte function-associated molecule 1. *Proc. Natl. Acad. Sci. USA.* 90:5838–5842.

Calderwood, D.A. 2004. Integrin activation. *J. Cell Sci.* 117:657–666.

Calderwood, D.A., A. Huttenlocher, W.B. Kiosses, D.M. Rose, D.G. Woodside, M. Schwartz, and M.H. Ginsberg. 2001. Increased filamin binding to β-integrin cytoplasmic domains inhibits cell migration. *Nat. Cell Biol.* 3:1060–1068.

Carman, C.V., and T.A. Springer. 2003. Integrin avidity regulation: are changes in affinity and conformation underemphasized? *Curr. Opin. Cell Biol.* 15:547–556.

Chatila, T.A., R.S. Geha, and M.A. Arnaout. 1989. Constitutive and stimulus-induced phosphorylation of CD11/CD18 leukocyte adhesion molecules. *J. Cell Biol.* 109:3435–3444.

Constantin, G., M. Majeed, C. Giagulli, L. Piccio, J.Y. Kim, E.C. Butcher, and C. Laudanna. 2000. Chemokines trigger immediate beta2 integrin affinity and mobility changes: differential regulation and roles in lymphocyte arrest under flow. *Immunity.* 13:759–769.

de Bruyn, K.M.T., S. Rangarajan, K.A. Reedquist, C.G. Figdor, and J.L. Bos. 2002. The small GTPase Rap1 is required for Mn2+- and antibody-induced LFA-1 and VLA-4-mediated cell adhesion. *J. Biol. Chem.* 277: 29468–29476.

Dransfield, I., and N. Hogg. 1989. Regulated expression of Mg2+ binding epitope on leukocyte integrin alpha subunits. *EMBO J.* 8:3759–3765.

Fagerholm, S., T.J. Hilden, and C.G. Gahmberg. 2002a. Lck tyrosine kinase is important for activation of the CD11a/CD18 integrin in human T lymphocytes. *Eur. J. Immunol.* 32:1670–1678.

Fagerholm, S., N. Morrice, C.G. Gahmberg, and P. Cohen. 2002b. Phosphorylation of the cytoplasmic domain of the integrin CD18 chain by protein kinase C isoforms in leukocytes. *J. Biol. Chem.* 277:1728–1738.

Fagerholm, S., T.J. Hilden, and C.G. Gahmberg. 2004. P marks the spot: site-specific integrin phosphorylation regulates molecular interactions. *Trends Biochem. Sci.* 29:504–512.

Gahmberg, C.G. 1997. Leukocyte adhesion: CD11/CD18 integrins and intercellular adhesion molecules. *Curr. Opin. Cell Biol.* 9:643–650.

Giancotti, F.G., and E. Ruoslahti. 1999. Integrin signaling. *Science.* 285: 1028–1032.

Goldfinger, L.E., J. Han, W.B. Kiosses, A.K. Howe, and M.H. Ginsberg. 2003. Spatial restriction of α4 integrin phosphorylation regulates lamellipodial stability and α4β1-dependent cell migration. *J. Cell Biol.* 162:731–741.

Han, J., S. Liu, D.M. Rose, D.D. Schlaepfer, H. McDonald, and M.H. Ginsberg. 2001. Phosphorylation of the integrin alpha4 cytoplasmic domain regulates paxillin binding. *J. Biol. Chem.* 276:40903–40909.

Hara, T., and S.M. Fu. 1986. Phosphorylation of alpha, beta subunits of 180/100-Kd polypeptides (LFA-1) and related antigens. *In* Leukocyte typing II, Vol. 3, Human myeloid and hematopoietic cells. E.L. Reinherz, B.F. Haynes, L.M. Nadler, and I.D. Bernstein, editors. Springer-Verlag, New York. 77–84.

Harlow, E., and D. Lane, editors. 1988. Synthetic peptides. *In* Antibodies: A Laboratory Manual. Cold Spring Harbor Laboratory Press, Cold Spring Harbor, NY. 82–83.

Hibbs, M.L., S. Jakes, S.A. Stacker, R.W. Wallace, and T.A. Springer. 1991. The cytoplasmic domain of the integrin lymphocyte function-associated antigen 1 β subunit: sites required for binding to intercellular adhesion molecule 1 and the phorbol ester–stimulated phosphorylation site. *J. Exp. Med.* 174:1227–1238.

Hilden, T.J., L. Valmu, S. Kärkkäinen, and C.G. Gahmberg. 2003. Threonine phosphorylation sites in the β2 and β7 leukocyte integrin polypeptides. *J. Immunol.* 170:4170–4177.

Hynes, R.O. 2002. Integrins: bidirectional, allosteric signaling machines. *Cell.* 110:673–687.

Jin, J., F.D. Smith, C. Stark, C.D. Wells, J.P. Fawcett, S. Kulkarni, P. Metalnikov, P. O'Donnell, P. Taylor, L. Taylor, et al. 2004. Proteomic, functional and domain-based analysis of in vivo 14-3-3 binding proteins involved in cytoskeletal regulation and cellular organization. *Curr. Biol.* 14:1436–1450.

Katagiri, K., M. Hattori, N. Minato, S. Irie, K. Takatsu, and T. Kinashi. 2000. Rap1 is a potent activation signal for leukocyte function-associated antigen 1 distinct from protein kinase C and phosphatidylinositol-3-OH kinase. *Mol. Cell. Biol.* 20:1956–1969.

Katagiri, K., M. Hattori, N. Minato, and T. Kinashi. 2002. Rap1 functions as a

Carl_G_190x270_mm_blokki_FINAL.indd 407 06-Aug-23 1:54:38 PM

key regulator of T-cell and antigen-presenting cell interactions and modulates T-cell responses. *Mol. Cell. Biol.* 22:1001–1015.

Katagiri, K., A. Maeda, M. Shimonaka, and T. Kinashi. 2003. RAPL, a Rap-1 binding molecule that mediates Rap1-induced adhesion through spatial regulation of LFA-1. *Nat. Immunol.* 4:741–748.

Kim, M., C.V. Carman, and T.A. Springer. 2003. Bidirectional transmembrane signaling by cytoplasmic domain separation in integrins. *Science.* 301:1720–1725.

Kim, M., C.V. Carman, W. Yang, A. Salas, and T.A. Springer. 2004. The primacy of affinity over clustering in regulation of adhesiveness of the integrin $\alpha_L\beta_2$. *J. Cell Biol.* 167:1241–1253.

Kotovuori, A., T. Pessa-Morikawa, P. Kotovuori, P. Nortamo, and C.G. Gahmberg. 1999. ICAM-2 and a peptide from its binding domain are efficient activators of leukocyte adhesion and integrin affinity. *J. Immunol.* 162:6613–6620.

Li, R., J. Xie, C. Kantor, V. Koistinen, D.C. Altieri, P. Nortamo, and C.G. Gahmberg. 1995. A peptide derived from the intercellular adhesion molecule-2 regulates the avidity of the leukocyte integrins CD11b/CD18 and CD11c/CD18. *J. Cell Biol.* 129:1143–1153.

Lu, C., M. Shimaoka, A. Salaz, and T.A. Springer. 2004. The binding sites for competitive antagonistic, allosteric antagonistic, and agonistic antibodies to the I domain of integrin LFA-1. *J. Immunol.* 173:3972–3978.

MacKintosh, C. 2004. Dynamic interactions between 14-3-3 proteins and phosphoproteins regulate diverse cellular processes. *Biochem. J.* 381:329–342.

Moorhead, G., P. Douglas, V. Cotelle, J. Harthill, N. Morrice, S. Meek, U. Deiting, M. Stitt, M. Scarabel, A. Aitken, and C. MacKintosh. 1999. Phosphorylation-dependent interactions between enzymes of plant metabolism and 14-3-3 proteins. *Plant J.* 18:1–12.

Nortamo, P., M. Patarroyo, C. Kantor, J. Suopanki, and C.G. Gahmberg. 1988. Immunological mapping of the human leukocyte adhesion glycoprotein GP90 (D18) by monoclonal antibodies. *Scand. J. Immunol.* 28:537–546.

Peter, K., and T.E. O'Toole. 1995. Modulation of cell adhesion by changes in $\alpha_L\beta_2$ (LFA-1, CD11a/CD18) cytoplasmic domain/cytoskeleton interaction. *J. Exp. Med.* 181:315–326.

Sampath, R., P.J. Gallagher, and F.M. Pavalko. 1998. Cytoskeletal interactions with the leukocyte integrin β2 cytoplasmic tail. *J. Biol. Chem.* 273:33588–33594.

Sebzda, E., M. Bracke, T. Tugal, N. Hogg, and D.A. Cantrell. 2002. Rap1A positively regulates T cells via integrin activation rather than inhibiting lymphocyte signaling. *Nat. Immunol.* 3:251–258.

Shimaoka, M., J. Takagi, and T.A. Springer. 2002. Conformational regulation of integrin structure and function. *Annu. Rev. Biophys. Biomol. Struct.* 31:485–516.

Smith, A., Y.R. Carrasco, P. Stanley, N. Kieffer, F.D. Batista, and N. Hogg. 2005. A talin-dependent LFA-1 focal zone is formed by rapidly migrating T lymphocytes. *J. Cell Biol.* 170:141–151.

Springer, T.A. 1990. Adhesion receptors of the immune system. *Nature.* 346: 425–434.

Stewart, M.P., C. Cabanas, and N. Hogg. 1996. T cell adhesion to intercellular adhesion molecule-1 (ICAM-1) is controlled by cell spreading and the activation of integrin LFA-1. *J. Immunol.* 156:1810–1817.

Stewart, M.P., A. McDowall, and N. Hogg. 1998. LFA-1–mediated adhesion is regulated by cytoskeletal restraint and by a Ca^{2+}-dependent protease, calpain. *J. Cell Biol.* 140:699–707.

Tadokoro, S., S.J. Shattil, K. Eto, V. Tai, R.C. Liddington, J.M. de Pereda, M.H. Ginsberg, and D.A. Calderwood. 2003. Talin binding to integrin beta tails: a final common step in integrin activation. *Science.* 302:103–106.

Tohyama, Y., K. Katagiri, R. Pardi, C. Lu, T.A. Springer, and T. Kinashi. 2003. The critical cytoplasmic regions of the alphaL/beta2 integrin in Rap1-induced adhesion and migration. *Mol. Biol. Cell.* 14:2570–2582.

Tzivion, G., and J. Avruch. 2002. 14-3-3 proteins: active cofactors in cellular regulation by serine/threonine phosphorylation. *J. Biol. Chem.* 277:3061–3064.

Valmu, L., and C.G. Gahmberg. 1995. Treatment with okadaic acid reveals strong threonine phosphorylation of CD18 after activation of CD11/CD18 leukocyte integrins with phorbol ester or CD3 antibodies. *J. Immunol.* 155:1175–1183.

Valmu, L., S. Fagerholm, H. Suila, and C.G. Gahmberg. 1999a. The cytoskeletal association of CD11/CD18 leukocyte integrins in phorbol ester-activated T cells correlates with CD18 phosphorylation. *Eur. J. Immunol.* 29:2107–2118.

Valmu, L., T.J. Hilden, G. van Willigen, and C.G. Gahmberg. 1999b. Characterization of β2 (CD18) integrin phosphorylation in phorbol ester-activated T lymphocytes. *Biochem. J.* 339:119–125.

van Kooyk, Y., and C.G. Figdor. 2000. Avidity regulation of integrins: the driving force in leukocyte adhesion. *Curr. Opin. Cell Biol.* 12:542–547.

Vinogradova, O., A. Velyvis, A. Velyviene, B. Hu, T. Haas, E. Plow, and J. Qin. 2002. A structural mechanism of integrin alpha(IIb)beta(3) "inside-out" activation as regulated by its cytoplasmic face. *Cell.* 110:587–597.

Weber, K.S., M.R. York, T.A. Springer, and L.B. Klickstein. 1997. Characterization of lymphocyte function-associated antigen 1 (LFA-1)-deficient T cell lines: the alphaL and beta2 subunits are interdependent for cell surface expression. *J. Immunol.* 158:273–279.

Weber, K.S.C., L.B. Klickstein, and C. Weber. 1999. Specific activation of leukocyte beta2 integrins lymphocyte function-associated antigen-1 and Mac-1 by chemokines mediated by distinct pathways via the alpha subunit cytoplasmic domains. *Mol. Biol. Cell.* 10:861–873.

Weiner, M.P., G.L. Costa, W. Schoettlin, J. Cline, E. Mather, and J.C. Bauer. 1994. Site-directed mutagenesis of double-stranded DNA by the polymerase chain reaction. *Gene.* 151:119–123.

Wright, S.D., P.E. Rao, W.C. van Voorhis, L.S. Craigmyle, K. Iida, M.A. Talle, E.F. Westerberg, G. Goldstein, and S.C. Silverstein. 1983. Identification of the C3bi receptor of human monocytes and macrophages by using monoclonal antibodies. *Proc. Natl. Acad. Sci. USA.* 80:5699–5703.

Carl_G_190x270_mm_blokki_FINAL.indd 408 06-Aug-23 1:54:39 PM

IMMUNOBIOLOGY

α-Chain phosphorylation of the human leukocyte CD11b/CD18 (Mac-1) integrin is pivotal for integrin activation to bind ICAMs and leukocyte extravasation

Susanna C. Fagerholm, Minna Varis, Michael Stefanidakis, Tiina J. Hilden, and Carl G. Gahmberg

The promiscuous CD11b/CD18 (Mac-1) integrin has important roles in regulating many immunologic functions such as leukocyte adhesion and emigration from the bloodstream via interactions with the endothelial ligands ICAM-1 and ICAM-2, iC3b-mediated phagocytosis, and apoptosis. However, the mechanisms for Mac-1 inside-out activation have remained poorly understood. Phosphorylation of integrin cytoplasmic domains is emerging as an important mechanism of regulating integrin functions. Here, we have studied phosphorylation of human CD11b, which takes place on the cytoplasmic Ser1126 in neutrophils. We show that mutation of the serine phosphorylation site leads to inability of Mac-1 to become activated to bind the cellular ligands ICAM-1 and ICAM-2. However, CD11b-mutant cells are fully capable of binding other studied CD11b ligands (ie, iC3b and denatured BSA). Activation epitopes expressed in the extracellular domain of the integrin and affinity for soluble ICAM ligands were decreased for the mutated integrin. Additionally, the mutation resulted in inhibition of chemokine-induced migration in a transendothelial assay in vitro and significantly reduced the accumulation of intravenously administered cells in the spleen and lungs of Balb/c mice. These results characterize a novel selective mechanism of Mac-1–integrin activation, which mediates leukocyte emigration from the bloodstream to the tissues. (Blood. 2006;108:3379-3386)

© 2006 by The American Society of Hematology

Introduction

The large family of heterodimeric cell surface receptors called integrins mediates adhesion to diverse ligands in the extracellular matrix, on other cells, as well as in solution. The 4 members of the CD11/CD18 family of integrins are exclusively expressed on leukocytes, and they mediate many important immunobiologic functions.[1,2] Such functions include the recruitment of leukocytes to inflammatory sites through interactions with intercellular adhesion molecules (ICAMs) expressed on endothelium. Human patients with defective CD18 integrins have a disease known as leukocyte adhesion deficiency (LAD-I), which is associated with recurrent bacterial infections that the immune system fails to clear, as well as massive leukocytosis.[3]

The Mac-1 integrin (also called αMβ2 or CD11b/CD18) is a member of the CD18 integrin family. It is expressed mainly on cells of the myeloid lineage, such as monocytes and neutrophils, but is also found on T cells. This integrin is involved in phagocytosis, adhesion to, and migration through the endothelium as well as other functions, such as regulation of apoptosis and degranulation.[1,2] In line with its many functions, Mac-1 is the most promiscuous integrin of the CD18 family. It binds to a wide range of ligands, including the blood coagulation protein fibrinogen,[4] the adhesion ligands intercellular adhesion molecule-1 and -2 (ICAM-1 and -2)[5,6] and the complement protein iC3b.[7] More recently discovered partners for Mac-1 include, for example, the LDL-receptor–related protein[8] and the matrix metalloproteinase MMP9.[9]

Lately, important development has been made in the understanding of the structure and function of the integrin receptors; however, their regulation is still incompletely understood. Leukocyte integrins on resting cells are not able to bind their ligands, but, when the cell has received an activating stimulus, for example, by chemokines displayed on or released from the activated endothelium, an intracellular signaling cascade is initiated which mediates a change in the integrin to make it adhesive. This process is called "inside-out" signaling or "activation," and it affects both the structure of the extracellular domains to increase affinity for ligands, as well as integrin clustering in the cell membrane and altered cytoskeletal contacts.[10-12]

The ligands of Mac-1 bind to different sites in the integrin extracellular domains, the so-called inserted or I domain in CD11b being an important binding site for ligands.[12] Also the CD18 I-like domain contains ligand-binding sites, and, additionally, it is involved in regulating I domain conformational changes.[12] Unlike another CD18 family member, LFA-1 (CD11a/CD18), Mac-1 has not been much studied for inside-out signaling, and proximal events in Mac-1 integrin activation are poorly understood.

The inside-out activation of the LFA-1 integrin has been extensively studied, and several proximal elements for its activation have been identified.[11,13,14] It has recently been shown that adhesion through LFA-1 in T cells is regulated by phosphorylation

From the Division of Biochemistry, Faculty of Biosciences, University of Helsinki, Finland.

Submitted March 29, 2006; accepted June 30, 2006. Prepublished online as *Blood* First Edition Paper, July 20, 2006; DOI 10.1182/blood-2006-03-013557.

Supported by the Academy of Finland, The Sigrid Jusélius Foundation, the Finnish Cancer Society, and the Magnus Ehrnrooth Foundation.

The authors declare no competing financial interests.

S.C.F. designed and performed the research and wrote the paper; M.V. performed the research and wrote the paper; M.S. and T.J.H. designed and performed part of the research; and C.G.G. obtained most of the research funding and participated in planning the research and writing the paper.

S.C.F. and M.V. contributed equally to this work.

Reprints: Carl G. Gahmberg, Division of Biochemistry, Faculty of Biosciences, PB56 (Viikinkaari 5), 00014 University of Helsinki, Helsinki, Finland; e-mail: carl.gahmberg@helsinki.fi.

The publication costs of this article were defrayed in part by page charge payment. Therefore, and solely to indicate this fact, this article is hereby marked "advertisement" in accordance with 18 USC section 1734.

© 2006 by The American Society of Hematology

Carl_G_190x270_mm_blokki_FINAL.indd 409 06-Aug-23 1:54:39 PM

of both its intracellular domains.[14] The CD11a phosphorylation site (Ser1140) is constitutively phosphorylated and is necessary for chemokine- and ligand-induced integrin activation, which involves changes in the conformation/affinity in individual integrin molecules.[14] As CD11a, also CD11b has been previously shown to be constitutively phosphorylated on serine in resting leukocytes.[15,16] Indeed, there is only one serine residue in the CD11b cytoplasmic domain (Ser1126). To investigate the possibility that the CD11b phosphorylation site is involved in adhesion regulation, we have mutated the CD11b phosphorylation site and investigated adhesion to diverse Mac-1 ligands after activation, as well as integrin-mediated functions in vivo.

Materials and methods

Reagents

Phorbol 12,13-dibutyrate (PDBu) and bovine serum albumin (BSA) were obtained from Sigma-Aldrich (Zwijndrecht, the Netherlands). Human serum albumin (HSA) was from the Central Laboratory, Blood Transfusion Service, Swiss Red Cross, Bern, Switzerland. Recombinant human ICAM-1, ICAM-2-Fc, and SDF-1α were purchased from R&D Systems (Minneapolis, MN), human complement iC3b from Calbiochem (La Jolla, CA). Optifect and OptiMEM I Reduced Serum Medium were obtained from Invitrogen (Carlsbad, CA). The CD11b cytoplasmic domain peptides (KLGFFKRQYKDMMSEGGPPGAEPQ [BP] and KLGFFKRQYKDMMpSEGGPPGAEPQ [PP], where pS marks phosphoserine) were synthesized by Fmoc chemistry and checked by mass spectrometry.[17]

Monoclonal antibodies

MEM170 (anti-CD11b) was a gift from Dr V. Horejsi (Institute of Molecular Genetics, Prague, Czech Republic). The human leukocyte integrin CD18 chain antibody R7E4 has been reported previously.[18] IB4, a CD18 antibody that recognizes CD11/CD18 heterodimers, was a gift from M.A. Arnaout (Massachusetts General Hospital, Boston, MA). mAb24 (anti-CD18) was a gift from N. Hogg (Imperial Cancer Research Fund, London, United Kingdom). KIM127 (anti-CD18) was a kind gift from M. Robinson (Celltech, Slough, United Kingdom). CBRM1/5 was from Santa Cruz Biotechnology (Santa Cruz, CA). CD11b phosphospecific antibodies were rabbit polyclonal antibodies made as described.[14] The CD11b cytoplasmic domain peptide KLGFFKRQYKDMMpSEGGPPGAEPQ was used as an antigen.

cDNA constructs

The cDNA for full-length CD11b was subcloned into pcDNA3. The S1126A mutation was made by site-directed mutagenesis.[19] Both constructs were checked by sequencing.

Transfections and cell lines

The human T-cell lymphoma cell line clone J-β2.7, which lacks CD11 chains,[20] was a gift from N. Hogg. Wt-CD11b and S1126A-CD11b pcDNA3 were transfected into the J-β2.7 cells using the Optifect transfection reagent according to the manufacturer's instructions. Transfected Jurkat cells were purified using magnetic cell sorting (MACS) columns (Miltenyi Biotech, Surrey, United Kingdom), using the antibodies MEM170 or IB4. The integrin expression and the condition of transfectants were analyzed by flow cytometry. Wt-CD11a-Jβ2.7 and S1140A-CD11a-Jβ2.7 cells have been described.[14] The HMEC-1 endothelial cells were grown as described previously.[9] Human neutrophils were isolated as previously described.[9]

Flow cytometry and adhesion assays

The flow cytometry assays to detect surface expressed integrins were done as described,[14] using IB4 and MEM170 antibodies. Cell adhesion assays were performed as reported,[14] except for modifications as follows. For the adhesion assay with denatured BSA, the protein was denatured for 5 minutes in 95°C and was coated at 10 μg/mL or 1 mg/mL. The adhesion medium was RPMI1640, 40 mM HEPES, 0.1% BSA, 2 mM $CaCl_2$. Three percent HSA was used as a blocking agent for at least 2 hours. Cells were stimulated with either 100 nM PDBu or 5 mM $MgCl_2$/1 mM EGTA, and the R7E4 inhibition of adhesion was made at 10 μg/mL mAb concentration for 30 minutes at 37°C. For mAb24, KIM127, and CBRM1/5 reporter antibody assays, transfected J-β2.7 cells were reacted with mAb24 or KIM127 (5 μg/mL) in the presence of activators for 20 minutes at 37°C. Cells were instantly stained with Alexa-fluor–conjugated anti–mouse IgG Abs on ice for 20 minutes and analyzed by flow cytometry. mAb24, KIM127, and CBRM1/5 expression was reported as mean fluorescence intensity.

Soluble ICAM-2Fc and iC3b binding assays

J-β2.7 transfectants were incubated in 25 μL RPMI 1640, 40 mM HEPES, 1 mM $MgCl_2$ in the presence of 200 μg/mL ICAM-2Fc or iC3b at 37°C for 10 minutes. After removal of the unbound ligand by washing with PBS, the cells were incubated with either FITC-conjugated anti–human IgG-Fc–specific antiserum (for ICAM-2-Fc) (Jackson Immunoresearch Laboratories, West Grove, PA) or FITC-conjugated C3c antibody, which recognizes iC3b (Dako, Glostrup, Denmark) on ice for 20 minutes. Cells were analyzed by flow cytometry. The fluorescence was compared with integrin expression levels and reported as the percentage of MEM170 staining.

Transendothelial migration assay

HMEC-1 cells were cultured for 5 days (until confluent) on gelatin (0.5% in PBS) coated Transwell membranes (8-μm pore size; Costar, Bucks, United Kingdom) in RPMI 1640, 10% FCS, 1% penicillin/streptomycin/L-glutamine. The endothelium was activated with SDF-1α at a concentration of 100 ng/mL for 4 hours. Jβ2.7 tranfectants (1×10^6cells/well) were pipetted onto the endothelial cell layer in 100 μL volume and left to migrate for 4 hours. Migrated cells were collected from the wells and counted.

Cell dissemination in vivo

Animal experiments were approved by the ethics committee of the University of Helsinki. Jβ2.7 cells were labeled with ^{125}I by the lactoperoxidase method[21] and intravenously injected into Balb/c mice (n = 3 per group). Mice were killed 1 hour after inoculation, and organs were harvested, weighed, and the radioactivities were determined using a Wallac-LKB γ-counter.

Results

Ser1126 phosphorylation of CD11b in human neutrophils

We have recently reported that the phosphorylation of CD11a on Ser1140 in the cytoplasmic domain mediates integrin activation by affinity regulation.[14] The CD11b-chain of the integrin has previously been shown to be phosphorylated on serine in resting cells.[15] To study phosphorylation of Ser1126 in cells, we made a polyclonal phosphospecific antibody to pSer1126-CD11b. The antibody was purified using the phosphopeptide antigen and tested on lysates from nontransfected COS cells and cells transfected with wild-type CD11b (Figure 1A). The antibody recognized CD11b specifically and did not recognize any proteins from nontransfected cells. In addition, in a dot blot, it recognized the phosphopeptide much better than the unphosphopeptide (not shown). To investigate phosphorylation of CD11b in human leukocytes, the CD11b polypeptide was immunoprecipitated from neutrophil lysates. Used as such, the antibody recognized CD11b in Western blots (Figure 1B). To block any antibody that recognized the unphosphorylated form of the integrin, the antibody was treated with the unphosphopeptide. This led to a significant decrease in binding to CD11b;

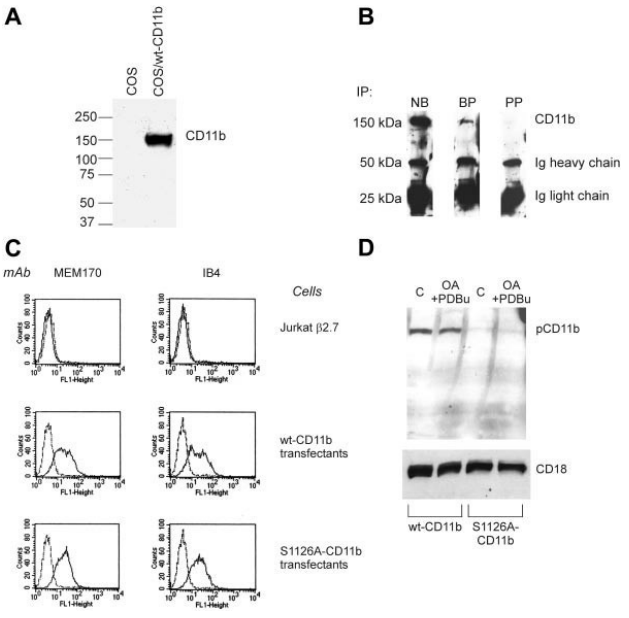

Figure 1. CD11b is phosphorylated on Ser1126 in neutrophils. (A) COS cells were transfected with wt Mac-1 or left untransfected. Cell lysates were analyzed by Western blotting with the pCD11b antibody. (B) Western blot of CD11b/CD18 integrin immunoprecipitated from lysed peripheral blood neutrophils detected with pAb P-CD11b. NB indicates no blocking peptide present; BP, blocking peptide present, PP, CD11b phosphopeptide present. (C) Fluorescence-activated cell sorting (FACS) analysis of transfectants shows that Mac-1 heterodimers are not expressed on untransfected Jβ2.7 cells (2 top panels). The expression level of wt Mac-1 is comparable to that of the S1126A–Mac-1 transfectants (2 bottom panels). MEM170, CD11b-antibody; IB4, CD18-antibody. (D) Wt and S1126A-CD11b–transfected Jβ2.7 cells were pretreated with 1.5 μM okadaic acid (OA) and activated with 200 nM PDBu for 30 minutes or left untreated (C). Lysates from cells were analyzed by Western blotting with the pCD11b antibody (top). CD18 is shown as a loading control (bottom). Dotted lines represent the background fluorescence.

however, the antibody still recognized the CD11b chain, indicating that it is phosphospecific, and that CD11b is indeed phosphorylated on Ser1126 in neutrophils (Figure 1B). Treatment of the phosphospecific antibody with the phosphopeptide antigen before Western blotting completely abolished recognition of CD11b.

Mutation of the Ser1126 phosphorylation site does not influence cell-surface expression of integrin heterodimers

To examine the effect of phosphorylation of Ser1126 on integrin activation, we mutated the serine to alanine and made stable transfectants of Jβ2.7 cells. The transfectants were examined for surface expression of integrin heterodimers (Figure 1C). Mutation of the serine in the CD11b cytoplasmic domain did not influence surface expression of the integrin heterodimers, as examined by flow cytometry with a CD11b and a CD18 antibody (Figure 1C). In addition, the heterodimers formed normally, because they could be immunoprecipitated with the IB4 antibody that only recognizes heterodimeric integrins (not shown). Thus, both wild-type and S1126A-mutated CD11b integrins were normally expressed on the surface of the leukocytes.

The Ser1126-phosphospecific antibody was then used to characterize CD11b from wt CD11b and S1126A-CD11b–stable transfectants (Figure 1D). The antibody recognized wt CD11b but not the S1126A-CD11b protein, confirming that CD11b was phosphorylated on Ser1126 in wt but not in mutant cells. Treatment of cells with a combination of okadaic acid and phorbol ester did not increase Ser1126 phosphorylation in cells (Figure 1D).

Adhesion to ICAM-1 and ICAM-2 is abolished for S1126A-CD11b

Using the wild-type and phosphorylation-site mutant cells, we first examined the Mac-1 integrin–mediated adhesion to the ligands ICAM-1 and ICAM-2. Using different amounts of coated ICAM-1, we determined a concentration that was in the steep portion of the dose-dependence curve (6 μg/mL) (Figure 2A), which was then

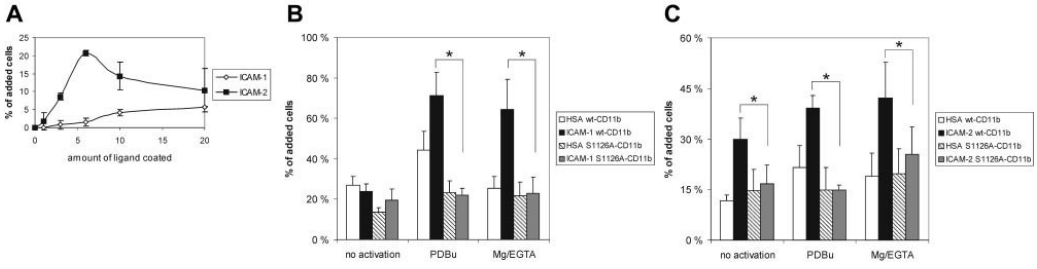

Figure 2. Mac-1 adhesion to ICAM-1 and ICAM-2 is attenuated when serine 1126 is mutated to alanine. (A) Jβ2.7 transfectants expressing wt CD11b were allowed to bind to wells coated with ICAM-1 or ICAM-2 at different ligand concentrations (microgram per milliliter of coated ligand) for 30 minutes. (B) Jβ2.7 transfectants expressing wt CD11b or S1126A-CD11b were allowed to bind to ICAM-1–coated wells (6 μg/mL coated ligand) without stimulation (control) or after stimulation with 100 nM PDBu or 5 mM $MgCl_2$/1 mM EGTA for 30 minutes. Significant differences ($P \leq .02$ for Mg/EGTA samples and $P \leq .002$ for PDBu samples) in bracketed comparisons are indicated by a single asterisk. (C) As in panel B, except that ICAM-2 was used as the coated ligand. Significant differences ($P \leq .05$ for unstimulated and Mg/EGTA-stimulated samples, $P < .001$ for

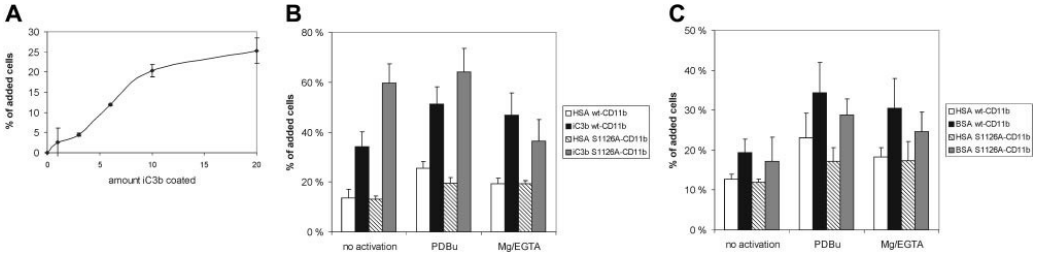

Figure 3. Mac-1 binding to iC3b and denatured BSA is not affected by the S1126A mutation. (A) Jβ2.7 transfectants expressing wt CD11b were allowed to bind to wells coated with iC3b at different ligand concentrations (microgram per milliliter of ligand used for coating) for 30 minutes. (B) Adhesion of transfected cells to coated iC3b (6 μg/mL) with or without activation was performed as described in "Materials and methods." (C) As in panel B, except that denatured BSA (1 mg/mL) was used as a ligand. Error bars represent SD.

used under different stimulatory conditions. Wt CD11b-transfected cells bound to coated ICAM-1 when cells were treated with phorbol ester (Figure 2B), an activating inside-out stimulus for integrins. In addition, adhesion was activated with Mg/EGTA, which bypasses intracellular signaling events and directly influences the extracellular domains of the integrin.[12] The specificity of adhesion was shown by using nontransfected Jβ2.7 cells, which did not adhere to coated ICAM-1, and by blocking adhesion with the CD18 antibody R7E4 (not shown). When adhesion by S1126A-CD11b–transfected cells was examined, it was revealed that mutation of the CD11b phosphorylation site completely abolished activation of Mac-1 in response to phorbol ester and Mg/EGTA stimuli (Figure 2B).

ICAM-2 is another ICAM-family member that binds to Mac-1.[6] Thus, we measured Mac-1 integrin adhesion to coated ICAM-2 and noted a similar phenotype for activation as for ICAM-1 binding; that is, the phosphorylation site mutant could not bind after cell activation with phorbol ester (Figure 2C), even at a concentration which was optimal for wt CD11b-transfected cell binding (6 μg/mL) (Figure 2A). Very weak adhesion of S1126A mutant cells was observed to ICAM-2 after activation of cells with Mg^{2+}/EGTA.

Adhesion to iC3b is normal for S1126A-CD11b

Mac-1 can bind to several other ligands than ICAM-1 and ICAM-2. One of the most important CD11b ligands is iC3b.[7] Therefore, we measured adhesion of wt- and S1126A-CD11b–transfected cells to coated iC3b, at a ligand concentration which was in the steep part of the dose-dependence curve (Figure 3A), and therefore not saturated. Interestingly, we found that the wt CD11b and S1126A-CD11b cells bound at least equally well to iC3b (Figure 3B).

Denatured BSA has been previously shown to bind mainly to the Mac-1 α-I domain.[22] To obtain information about the potential extracellular structures that are regulated by the S1126A-mutated CD11b, we used denatured BSA as a ligand. Binding of cells to coated, denatured BSA does not follow a normal dose-dependence curve, as has been reported previously[23] (results not shown). We used 2 different concentrations of denatured BSA in our assays, 1 mg/mL, which has been previously used to show the complete dependence of the I domain for Mac-1 adhesion,[22] and 10 μg/mL, a much lower concentration, in the same range as the other ligands used. Importantly, phorbol esters and Mg/EGTA treatment could activate S1126A-CD11b–transfected cell binding to denatured BSA, coated at either 1 mg/mL (Figure 3C), or 10 μg/mL (not shown). These results indicate that the Ser1126 mutation may not affect the conformation of the α-I domain of CD11b, at least not in a way that influences binding to denatured BSA.

Activation epitopes in the extracellular domains are influenced by the S1126A-CD11b mutation

We next examined whether the adhesion-deficient phenotype of the Mac-1 phosphorylation site mutant was due to an inability to undergo conformational changes in response to inside-out stimulation. Indeed, using mAb24, an antibody against an activation epitope in the β-I domain,[24] we saw a reduced amount of mAb24 binding to the integrin extracellular domain in PDBu-treated cells but not to cells treated with Mg/EGTA, as compared with the wild-type CD11b-transfected cells (Figure 4A).

KIM127 is a reporter antibody for the active form of the integrin, which binds to the cysteine-rich repeat 2 in the extracellular region of the CD18 chain, and the binding correlates with the

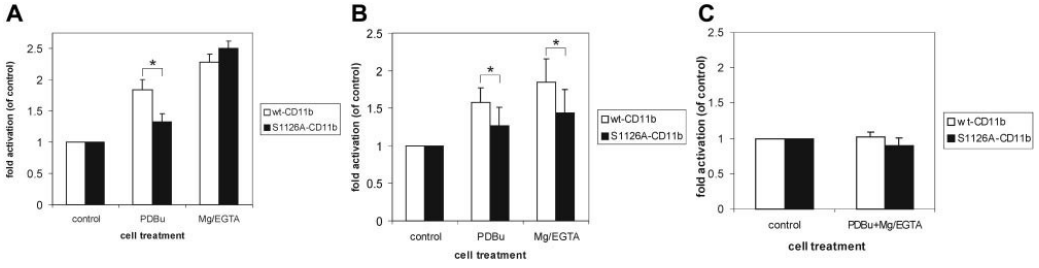

Figure 4. The S1126A mutation gives rise to modifications in activation epitopes. (A) The effects of the S1126A-CD11b mutation on expression of the CD18 activation reporter mAb24 were examined. Jβ2.7 cells were incubated with mAb24 (5 μg/mL) in the presence of phorbol ester (100 nM) or 5 mM Mg^{2+}/1 mM EGTA, and mAb24 expression was analyzed by flow cytometry. Significant differences ($P \leq .01$) in bracketed comparisons are indicated by a single asterisk. (B) As in panel A, except that KIM127 (5 μg/mL) was used instead of mAb24. Significant differences ($P \leq .05$) in bracketed comparisons are indicated by a single asterisk. (C) As in panels A and B, except that

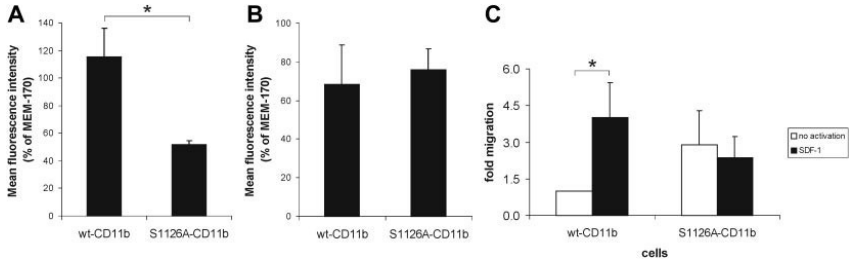

Figure 5. S1126A-mutated integrins have lower affinity for a soluble ICAM ligand, and migration through SDF-1–activated endothelium is attenuated. (A) The effect of the S1126A mutation on soluble ICAM-2 binding of Mac-1 was determined. Jβ2.7 transfectants were incubated with 200 μg/mL ICAM-2Fc, and binding was determined by flow cytometry. (B) Jβ2.7 transfectants were incubated with 200 μg/mL iC3b, and binding was determined by flow cytometry. (C) Transendothelial migration through nonstimulated or SDF-1α–activated endothelium was determined as described in "Materials and methods." Significant differences ($P \leq .02$) in bracketed comparisons are indicated by a single asterisk. Error bars represent SD.

extension of the integrin extracellular domain.[25,26] In contrast to mAb24, the KIM127 epitope showed decreased expression both in Mg/EGTA- and PDBu-treated cells for the phosphorylation site mutant as compared with wt CD11b cells. This result further indicates that the CD18 chain extracellular domain adopts a different conformation for the phosphorylation site mutant (Figure 4B).

The CBRM1/5 antibody has been reported to detect the "open" form of the I domain in CD11b. However, we could not detect any binding of CBRM1/5 to either wt or S1126A mutant cells either on unstimulated or phorbol ester–stimulated cells in the presence of magnesium (Figure 4C), indicating that in Jβ2.7 cells, the I domain of CD11b is in the "closed" conformation.

To compare the LFA-1 mutant with the Mac-1 mutant, we performed the same experiment for wild-type and S1140A–LFA-1 cells. KIM127 expression in these cells was normal in response to PDBu and Mg stimulation (not shown), showing that the extracellular domains of these 2 integrins of the same family are regulated differently.

Integrin affinity for ICAM ligands is reduced, and SDF-1α cannot activate migration through endothelium for the phosphorylation site mutant

On the basis of the activation epitope studies, we concluded that the mutant integrin could not undergo normal conformational changes in response to activation. Conformational changes of integrin extracellular domains have clearly been linked to affinity regulation of individual integrin molecules. To further study the mechanism of the decreased adhesion of mutant Mac-1 integrins to ICAMs, we investigated the affinity of Mac-1 for its ICAM ligands. For this, we used a soluble ligand binding assay.[14] The binding of sICAM-1 to the cells is of low affinity and was below the detection limit in our assay. However, sICAM-2 bound well to the transfected cell and was thus used in our studies. Indeed, sICAM-2Fc bound well to wt CD11b-transfected Jβ2.7 cells (Figure 5A). Much weaker binding could be detected for S1126A-CD11b–transfected Jβ2.7 cells (Figure 5A). These results show that the affinity (or possibly, partially avidity) of the mutant Mac-1 integrin for ICAM ligands is lower than for the wild-type integrin. In contrast, the high affinity (binding) for iC3b was preserved for the S1126A-CD11b cells, as compared with wt CD11b-transfected cells, in good agreement with the adhesion results (Figure 5B).

One of the best characterized examples of integrin affinity modulation in a physiologic setting is the activation of integrin-dependent leukocyte arrest and migration through G protein–coupled receptors for chemokines.[27] Therefore, we investigated the migration of wild-type and mutant CD11b-transfected cells through an SDF1α-stimulated endothelial cell layer in vitro. Wild-type cells were stimulated to migrate through endothelium activated with SDF-1α (Figure 5C). In contrast, no effect on migration could be seen in the presence of SDF-1α for mutant CD11b-transfected cells, but the basal migration was higher (Figure 5C).

Phosphorylation site mutation inhibits extravasation in vivo

To study the effect of the phosphorylation site mutant in a more physiologic setting, we examined cell extravasation in an in vivo model. ^{125}I surface-labeled wt CD11b-Jβ2.7 and S1126A-CD11b-Jβ2.7 cells were injected into mice. The results showed that the phosphorylation site mutation of CD11b resulted in an increased amount of cells remaining in the peripheral circulation (Table 1). In addition, the infiltration to the lungs and spleen was dramatically reduced for the phosphorylation site mutant, whereas infiltration to other studied organs was not significantly affected. Thus, we conclude that the phosphorylation site mutation affects in vivo migration of leukocytes to target organs, presumably by interfering with Mac-1 integrin interactions with ICAM ligands on endothelium.

Discussion

In the present study, we demonstrate that phosphorylation of CD11b on the cytoplasmic Ser1126 is a major factor in the regulation of ICAM ligand binding and cellular extravasation. The major findings are as follows: (1) CD11b is phosphorylated on Ser1126 in resting human neutrophils, (2) mutation of the phosphorylation site leads to an inability of the integrin to become activated

Table 1. Effect of the CD11b phosphorylation site mutant on leukocyte extravasation in vivo

Organ	Percentage of injected dose/g tissue	
	Wt CD11b/Jβ2.7	S1126A-CD11b/Jβ2.7
Blood	30 ± 4.7	42.2 ± 2.46
Heart	17.1 ± 5.5	18.38 ± 4.98
Liver	12.23 ± 2.16	15.35 ± 8.93
Kidney	26.46 ± 2.32	24.14 ± 10.13
Lungs	100.24 ± 37.75	6.02 ± 1.93
Muscle	4.88 ± 2.98	2.04 ± 0.62
Femur	10.96 ± 1.62	12.59 ± 3.18
Brain	0.89 ± 0.37	0.099 ± 0.003
Spleen	20.9 ± 4.4	2.07 ± 0.16

^{125}I-surface-labeled wt and S1126A mutant cells were intravenously administered into Balb/c mice. At 1 hour after inoculation, mice were killed, and organs were harvested, weighed, and γ-counted. The result is given as mean ± SD (n = 3).

to bind ICAM-ligands, (3) the affinity for ICAMs of the mutated integrin is lower than that of the wild-type integrin, and (4) the phosphorylation site regulates chemokine-induced activation of migration through endothelium and severely diminishes in vivo dissemination of human leukocytes to lungs and spleen in a mouse model.

The Mac-1 integrin is involved in many different immunologic adhesion events to diverse ligands. It is now clear that phosphorylation of the α-chain plays a major role in the molecular mechanisms involved in certain selective activation events. The integrin CD11b chain is constitutively phosphorylated on Ser1126, and this phosphorylation site is required for adhesion events to ICAMs, as measured by a solid-phase adhesion assay. One major mechanism of regulating adhesion is through changes in the conformation of the extracellular domains of the integrin, thereby influencing its affinity for ligands. Several models for global conformational changes flowing through the integrin have been postulated, including the "switchblade"[28] and "deadbolt" models.[29] We have now shown that the CD11b cytoplasmic domain is indeed involved in controlling the global conformation of the integrin extracellular domain. Phorbol esters have been previously reported to change the conformation of the Mac-1 extracellular domain into the active conformation (with the open I domain, detected with the CBRM1/5 antibody).[30]

However, phorbol esters could not activate the phosphorylation site mutant, as measured by a solid-phase adhesion assay to ICAM-1 and ICAM-2 and by measuring the activation epitopes mAb24 and KIM127 in the extracellular domain of the β-chain. In the Jβ2.7-transfected cells, we could not detect any binding of the CBRM1/5 antibody during any stimulatory conditions for the wt or mutant cells. Phorbol esters have been reported to affect valency regulation of integrins, and it is possible that this clustering is involved in the regulation of Mac-1 by the Ser1126 phosphorylation site.

Mg^{2+} is thought to influence affinity of integrins by binding to the β-I–like domain MIDAS and ADMIDAS sites and thus changes the conformation of the β-I–like domain directly.[12] We could see an increase in binding of mAb24 to the mutant integrin after Mg^{2+} stimulation. However, this change in conformation is apparently not enough to induce adhesion to coated ICAM-1, probably because the conformational changes cannot be further transmitted through the integrin. In addition, with another reporter antibody, KIM127, which primarily reports "extension" of the bent β2 integrins,[25,26] we could see a decrease in activation after Mg^{2+} stimulation for the phosphorylation site mutant. These findings implicate that the mutant integrin extracellular domain is incapable of undergoing correct global conformational changes in response to phorbol ester or Mg^{2+} stimulation. It seems, however, that the mutation affects the flow of conformational changes in the integrin extracellular domains in such a way that binding only to certain ligands are affected. These results indicate that the mutant integrin adopts a conformation nonfavorable for ICAM-1 binding. This is further supported by its decreased binding of soluble ICAM-2, although the soluble ligand binding assay both for ICAM-2 and iC3b may partially measure also avidity of the interaction. Previously published results have shown that only certain antibodies, but not others, are capable of immunoprecipitating the phosphorylated form of CD11b,[31] indicating that the phosphorylated species has a different conformation than the nonphosphorylated molecule, and that different pools of Mac-1 are capable of becoming activated to bind different ligands. Thus, constitutive phosphorylation of CD11b may profoundly regulate the function of this molecule, maybe by regulating the interaction with some integrin-activating factor in cells. One possible scenario could also be that cell activation results in modification of this factor and thereafter allows its interaction only with the phosphorylated integrin. Alternatively, the phosphorylation of CD11b is required for Mac-1 activation, but the activation may require binding of factors also to the β-chain, which occurs only after cell stimulation. When these 2 requirements are met (CD11b is phosphorylated and the β-chain has bound the activating factor), conformational changes are transmitted to the integrin extracellular domain, resulting in ICAM binding. In analogy, the α4-integrin is also constitutively phosphorylated. In its phosphorylated form it cannot bind paxillin, and this process excludes paxillin from the leading edge of the cell and regulates cell migration.[32]

Unfortunately, the phosphospecific antibody used in this study did not immunoprecipitate CD11b and, thus, could not be used to determine the stoichiometry of phosphorylation of CD11b on Ser1126; however, the stoichiometry of phosphorylation of the related integrin αL-chain has been reported to be rather high, in the range of 40%.[14] In addition, using 2-dimensional gel electrophoresis, it was reported that alkaline phosphatase treatment shifted the single, broad band of CD11b to a more basic form, indicating that also CD11b is phosphorylated at a high stoichiometry.[15]

The binding of Mac-1 to the ligand iC3b was not negatively affected by the phosphorylation site mutation; actually, there was more constitutive binding to iC3b for the S1126A-CD11b–transfected cells. Indeed, iC3b binding sites are present in different parts of Mac-1, that is, the α-I domain,[33,34] the β-propeller in CD11b,[22] and the β-I–like domain in CD18.[35] A combination of all these sites may give rise to the strong binding between Mac-1 and iC3b and probably explains why the binding to iC3b is not affected by CD11b phosphorylation. Probably the I domain is not the most essential iC3b binding site in the Jβ2.7 cell system, because it seems to be in the closed conformation, both in the wild-type and mutant integrin, also during stimulatory conditions. Instead, the β-I–like domain may be important for iC3b binding, because this domain has binding sites for both ICAM and iC3b; however, the amino acid residues responsible for binding are different for the 2 ligands, and it is possible that the phosphorylation site mutant exposes only the iC3b binding sites. We also investigated the binding of the transfected cells to other ligands with broad recognition footprints, that is, fibrinogen and Factor X[22,36]; unfortunately, these bound to untransfected Jβ2.7 cells as well as to CD11b-transfected cells and could therefore not be used to investigate the binding of Mac-1 and the phosphorylation site mutant.

These results show that we have identified a major proximal regulatory event for Mac-1–mediated adhesion. It is clear that the activation of Mac-1 can be regulated in different ways, resulting in specific ligand binding. In addition, the CD11b phosphorylation site is unique for this integrin, showing that regulation of integrin activation is a complex process, evidently not regulated in the same way for all integrins. However, together with the recently reported LFA-1 integrin regulation by phosphorylation on Ser1140 in the CD11a chain,[14] these experiments strengthen the notion that integrin α-chain phosphorylation could be a more general mechanism of regulating integrin affinity. CD11a phosphorylation on Ser1140 regulates adhesion to ICAM-1 only during certain stimulatory conditions (by chemokines, ligands, or activating antibodies) but not others (phorbol ester and T-cell receptor stimulation).[14] However, CD11b phosphorylation on Ser1126 regulates all tested ways of activation of adhesion to ICAM-1. This implicates that affinity regulation is the major regulatory mechanism for Mac-1–

Carl_G_190x270_mm_blokki_FINAL.indd 414 06-Aug-23 1:54:41 PM

mediated adhesion, whereas LFA-1 uses either affinity or valency regulation, depending on the mode of activation.

Extravasation of leukocytes into the tissues is an important step in the defense against infections. However, this process may also cause serious tissue damage, for example, in autoimmune diseases, allograft rejection, and postischemic tissue destruction after myocardial infarction. CD11/CD18 integrin–ICAM interactions are necessary and sufficient for leukocyte arrest and transmigration through endothelium.[1,2] Recently, it has been shown that dynamic shifts in β2-integrin affinity for ligands is a main mechanism involved in the regulation of leukocyte rolling, arrest, and transendothelial migration.[37-39] One of the changes that happens in the transition from nonadherent, free leukocytes to rolling and firmly adherent leukocytes after chemokine stimulation is the expression of the KIM127 activation epitope.[40,41] Both integrin affinity for ICAMs and the KIM127 epitope were down-regulated for the phosphorylation site mutant, and cells expressing the CD11b phosphorylation site mutant were deficient in chemokine-stimulated migration across an endothelial cell layer in vitro. Basal migration, however, was even higher than for the wild-type integrin-expressing cells. This static migration assay that is conducted without flow, evidently allows the cells to attach and detach more easily during the cell migration process, because of the lower affinity of the integrin for its ICAM ligands.

To study migration in a more physiologic setting, in which the blood flow will influence migration of cells through endothelium, the wild-type and mutant integrin-transfected Jβ2.7 cells were intravenously administered to Balb/c mice. Here, we took advantage of the fact that human β2-integrins have been shown to bind to murine ICAM-1 and ICAM-2.[42,43] Indeed, the S1126 mutation dramatically decreased the extravasation of the cells to the spleen and lungs. These results show that the CD11b phosphorylation site is important in the regulation of in vivo migration of leukocytes through endothelium, through regulation of Mac-1 integrin affinity for ICAM-ligands. This is potentially useful in the therapeutic targeting of specific Mac-1 integrin functions, that is, adhesion to endothelial cells via ICAM-1 and ICAM-2, while leaving other functions intact, such as adhesion to foreign organisms coated with iC3b.

Acknowledgments

We thank M. Robinson, N. Hogg, V. Horejsi, and M.A. Arnaout for antibodies and cells and M. Aatonen and S. Kaukinen for expert technical assistance.

References

1. Springer TA. Adhesion receptors of the immune system. Nature. 1990;346:425-434.
2. Gahmberg CG. Leukocyte adhesion: CD11/CD18 integrins and intercellular adhesion molecules. Curr Opin Cell Biol. 1997;9:643-650.
3. Hogg N, Bates PA. Genetic analysis of integrin function in man: LAD-1 and other syndromes. Matrix Biol. 2000;19:211-222.
4. Wright SD, Weitz JI, Huang AJ, Levin SM, Silverstein SC, Loike JD. Complement receptor type 3 (CD11b/CD18) of human polymorphonuclear leukocytes recognizes fibrinogen. Proc Natl Acad Sci U S A.1988;85:7734-7738.
5. Diamond MS, Staunton DE, de Fougerolles AR, et al. ICAM-1 (CD54): a counter-receptor for Mac-1. J Cell Biol. 1990;111:3129-3139.
6. Xie J, Li R, Kotovuori P, et al. Intercellular adhesion molecule 2 (CD102) binds to the leukocyte integrin CD11b/CD18 through the A domain. J Immunol. 1995;155:3619-3628.
7. Beller DI, Springer TA, Schreiber RD. Anti-Mac-1 selectively inhibits the mouse and human type three complement receptor. J Exp Med. 1982; 156:1000-1009.
8. Spijkers PP, da Costa Martins P, Westein E, Gahmberg CG, Zwaginga JJ, Lenting PJ. LDL-receptor-related protein regulates beta2-integrin-mediated leukocyte adhesion. Blood. 2005;105: 170-177.
9. Stefanidakis M, Ruohtula T, Borregaard N, Gahmberg CG, Koivunen E. Identification of a negatively charged peptide motif within the catalytic domain of progelatinases that mediates binding to leukocyte beta 2 integrins. J Biol Chem. 2003;278:34674-34684.
10. van Kooyk Y, Figdor CG. Avidity regulation of integrins: the driving force in leukocyte adhesion. Curr Opin Cell Biol. 2000;12:542-547.
11. Kim M, Carman CV, Springer TA. Bidirectional transmembrane signaling by cytoplasmic domain separation in integrins. Science. 2003;301:1720-1725.
12. Shimaoka M, Takagi J, Springer TA. Conformational regulation of integrin structure and function. Annu Rev Biophys Biomol Struct. 2002;31:485-516.
13. Katagiri K, Maeda A, Shimonaka M, Kinashi T. RAPL, a Rap-1 binding molecule that mediates Rap1-induced adhesion through spatial regulation of LFA-1. Nat Immunol. 2003;4:741-748.
14. Fagerholm SC, Hilden TJ, Nurmi SM, Gahmberg CG. Specific integrin alpha and beta chain phosphorylations regulate LFA-1 activation through affinity-dependent and independent mechanisms. J Cell Biol. 2005;171:705-715.
15. Chatila TA, Geha RS, Arnaout MA. Constitutive and stimulus-induced phosphorylation of CD11/CD18 leukocyte adhesion molecules. J Cell Biol. 1989;109:3435-3444.
16. Fagerholm SC, Hilden TJ, Gahmberg CG. P marks the spot: site-specific integrin phosphorylation regulates molecular interactions. Trends Biochem Sci. 2004;29:504-512.
17. Valmu L, Hilden TJ, van Willigen G, Gahmberg CG. Characterization of β2 (CD18) integrin phosphorylation in phorbol ester-activated T lymphocytes. Biochem J. 1999;339:119-125.
18. Nortamo P, Patarroyo M, Kantor C, Suopanki J, Gahmberg CG. Immunological mapping of the human leukocyte adhesion glycoprotein GP90 (D18) by monoclonal antibodies. Scand J Immunol. 1988;28:537-546.
19. Weiner MP, Costa GL, Schoettlin W, Cline J, Mather E, Bauer JC. Site-directed mutagenesis of double-stranded DNA by the polymerase chain reaction. Gene. 1994;151:119-123.
20. Weber KS, York MR, Springer TA, Klickstein LB. Characterization of lymphocyte function-associated antigen 1 (LFA-1)-deficient T cell lines: the alphaL and beta2 subunits are interdependent for cell surface expression. J Immunol. 1997;158: 273-279.
21. Hubbard AL, Cohn ZA. The enzymatic iodination of the red cell membrane. J Cell Biol. 1972;55: 390-405.
22. Yalamanchili P, Lu C, Oxvig C, Springer TA. Folding and function of I domain-deleted Mac.1 and lymphocyte function-associated antigen-1. J Biol Chem. 2000;275:21877-21882.
23. Brevig T, Holst B, Ademovic Z, et al. The recognition of adsorbed and denatured proteins of different topographies by beta2 integrins and effects on leukocyte adhesion and activation. Biomaterials. 2005;26:3039-3053.
24. Dransfield I, Hogg N. Regulated expression of Mg2+ binding epitope on leukocyte integrin alpha subunits. EMBO J. 1989;8:3759-3765.
25. Beglova N, Blacklow SC, Takagi J, Springer TA. Cysteine-rich module structure reveals a fulcrum for integrin rearrangement upon activation. Nat Struct Biol. 2002;9:282-287.
26. Salas A, Shimaoka M, Kogan AN, Harwood C, von Andrian U, Springer TA. Rolling adhesion through an extended conformation of integrin alphaLbeta2 and relation to alpha I and beta I-like domain interaction. Immunity. 2004;20:393-406.
27. Constantin G, Majeed M, Giagulli C, et al. Chemokines trigger immediate beta2 integrin affinity and mobility changes: differential regulation and roles in lymphocyte arrest under flow. Immunity. 2000;13:759-769.
28. Takagi J, Petre BM, Walz T, Springer TA. Global conformational rearrangements in integrin extracellular domains in outside-in and inside-out signaling. Cell. 2002;110:599-611.
29. Xiong JP, Stehle T, Goodman SL, Arnaout MA. New insights into the structural basis of integrin activation. Blood. 2003;102:1155-1159.
30. Diamond MS, Springer TA. A subpopulation of Mac-1 (CD11b/CD18) molecules mediates neutrophil adhesion to ICAM-1 and fibrinogen. J Cell Biol. 1993;120:545-556.
31. Buyon JP, Slade SG, Reibman J, et al. Constitutive and induced phosphorylation of the alpha- and beta-chains of the CD11/CD18 leukocyte integrin family. Relationship to adhesion-dependent functions. J Immunol. 1990;144:191-197.
32. Han J, Liu S, Rose DM, Schlaepfer DD, McDonald H, Ginsberg MH. Phosphorylation of the integrin alpha4 cytoplasmic domain regulates paxillin binding. J Biol Chem. 2001;276:40903-40909.
33. Ueda T, Rieu P, Brayer J, Arnaout MA. Identification of the complement iC3b binding site in the beta 2 integrin CR3 (CD11b/CD18). Proc Natl Acad Sci U S A. 1994;91:10680-10684.
34. Ustinov VA, Plow EF. Identity of the amino acid residues involved in C3bi binding to the I-domain

Carl_G_190x270_mm_blokki_FINAL.indd 415 06-Aug-23 1:54:42 PM

supports a mosaic model to explain the broad ligand repertoire of integrin alpha M beta 2. Biochemistry. 2005;44:4357-4364.

35. Xiong YM, Haas TA, Zhang L. Identification of functional segments within the β2I-domain of integrin αMβ2. J Biol Chem. 2002;277:46639-46644.
36. Lishko VK, Podolnikova NP, Yakubenko VP, et al. Multiple binding sites in fibrinogen for integrin alphaMbeta2 (Mac-1). J Biol Chem. 2004;279:44897-44906.
37. Salas A, Shimaoka M, Chen S, Carman CV, Springer T. Transition from rolling to firm adhesion is regulated by the conformation of the I domain of the integrin lymphocyte function-associated antigen-1. J Biol Chem. 2002;277:50255-50262.
38. Lum AF, Green CE, Lee GR, Staunton DE, Simon SI. Dynamic regulation of LFA-1 activation and neutrophil arrest on intercellular adhesion molecule 1 (ICAM-1) in shear flow. J Biol Chem. 2002;277:20660-20670.
39. Green CE, Schaff UY, Sarantos MR, Lum AF, Staunton DE, Simon SI. Dynamic shifts in LFA-1 affinity regulate neutrophil rolling, arrest, and transmigration on inflamed endothelium. Blood. 2006;107:2101-2111.
40. Salas A, Shimaoka M, Kogan AN, Harwood C, von Andrian UH, Springer TA. Rolling adhesion through an extended conformation of integrin alphaLbeta2 and relation to alpha I and beta I-like domain interaction. Immunity. 2004;20:393-406.
41. Shamri R, Grabovsky V, Gauguet JM, et al. Lymphocyte arrest requires instantaneous induction of an extended LFA-1 conformation mediated by endothelium-bound chemokines. Nat Immunol. 2005;6:497-506.
42. Johnston SC, Dustin ML, Hibbs ML, Springer TA. On the species specificity of the interaction of LFA-1 with intercellular adhesion molecules. J Immunol. 1990;145:1181-1187.
43. Xu H, Tong IL, De Fougerolles AR, Springer TA. Isolation, characterization, and expression of mouse ICAM-2 complementary and genomic DNA. J Immunol. 1992;149:2650-2655.

IMMUNOBIOLOGY

β2 integrin phosphorylation on Thr758 acts as a molecular switch to regulate 14-3-3 and filamin binding

*Heikki Takala,[1] *Elisa Nurminen,[1] *Susanna M. Nurmi,[2] Maria Aatonen,[2] Tomas Strandin,[3] Maarit Takatalo,[2] Tiila Kiema,[4] Carl G. Gahmberg,[2] Jari Ylänne,[1] and Susanna C. Fagerholm[2,5]

[1]Department of Biological and Environmental Science and Nanoscience Center, University of Jyväskylä, Jyväskylä, Finland; [2]Faculty of Biosciences, Division of Biochemistry, and [3]Peptide and Protein Laboratory, Haartman Institute, University of Helsinki, Helsinki, Finland; [4]Department of Biochemistry, University of Oulu, Oulu, Finland; and [5]Section of Immunology, Division of Pathology and Neuroscience, Ninewells Hospital and Medical School, University of Dundee, Dundee, United Kingdom

Leukocyte integrins of the β2 family are essential for immune cell-cell adhesion. In activated cells, β2 integrins are phosphorylated on the cytoplasmic Thr758, leading to 14-3-3 protein recruitment to the β2 integrin. The mutation of this phosphorylation site impairs cell adhesion, actin reorganization, and cell spreading. Thr758 is contained in a Thr triplet of β2 that also mediates binding to filamin. Here, we investigated the binding of filamin, talin, and 14-3-3 proteins to phosphorylated and unphosphorylated β2 integrins by biochemical methods and x-ray crystallography. 14-3-3 proteins bound only to the phosphorylated integrin cytoplasmic peptide, with a high affinity (K_d, 261 nM), whereas filamin bound only the unphosphorylated integrin cytoplasmic peptide (K_d, 0.5 mM). Phosphorylation did not regulate talin binding to β2 directly, but 14-3-3 was able to outcompete talin for the binding to phosphorylated β2 integrin. X-ray crystallographic data clearly explained how phosphorylation eliminated filamin binding and induced 14-3-3 protein binding. Filamin knockdown in T cells led to an increase in stimulated cell adhesion to ICAM-1–coated surfaces. Our results suggest that the phosphorylation of β2 integrins on Thr758 acts as a molecular switch to inhibit filamin binding and allow 14-3-3 protein binding to the integrin cytoplasmic domain, thereby modulating T-cell adhesion. (Blood. 2008; 112:1853-1862)

Introduction

Integrins are heterodimeric plasma membrane receptors that mediate binding to the extracellular matrix and to ligands present on the surface of other cells. Their function is tightly regulated; they bind ligands only after activation. Modulation of integrin activity occurs through tightly regulated interactions between cytoplasmic molecules and integrin intracellular tails. Factors binding to integrin cytoplasmic domains regulating integrin adhesiveness include the cytoskeletal proteins talin[1,2] and filamin,[3] and the 14-3-3 proteins, which are molecular adaptors that bind to phosphorylated serine or threonine (pSer/pThr) containing polypeptide sequences.[4]

The β2 integrins are expressed exclusively on leukocytes and bind ICAM molecules on other leukocytes and endothelial cells after cell activation.[5,6] Talin binds to β2 integrins in vitro and in cells and is involved in activating the β2 integrins, resulting in binding to ICAMs.[1,4,7-9] The β2 integrin polypeptide chain is phosphorylated on the intracellular domain on several residues after cell stimulation with various agents.[10] Thr758 is a physiologically important amino acid residue in the β2 cytoplasmic tail, and becomes phosphorylated after T-cell stimulation with T-cell receptor (TCR) antibodies or with phorbol esters.[11-13] After its phosphorylation, β2 binds to 14-3-3 proteins both in vitro and in cells.[4] Blocking of this interaction with a β2 Thr758 to Ala mutation, or by expression of constructs that bind to 14-3-3 proteins and block their interactions with target proteins, leads to abrogation of actin cytoskeleton rearrangements, cell spreading, and adhesion to ICAM ligands.[4] β2-Thr758 phosphorylation leads to the activation of the actin cytoskeleton modulators, Rac1/Cdc42, in cells.[13]

The region in the β2 cytoplasmic tail that binds 14-3-3 proteins has been reported to interact with filamin in other integrins,[14] and for the strong filamin-binder β7 integrin, phosphorylation mimicking substitutions of 3 threonine residues (TTT) reduces filamin affinity.[3] Filamin has been reported to associate with β2 integrins in vivo[15,16] and it binds a β2 integrin peptide containing the TTT sequence in vitro.[7] The filamin-integrin cytoplasmic tail interaction negatively regulates talin binding and talin-dependent integrin activation[3]; it also regulates cell migration.[14]

In this study, we investigated the binding of the β2 integrin cytoplasmic domain to filamin, talin, and 14-3-3. We show that the β2 Thr758 phosphorylation abrogates filamin binding but is required for 14-3-3 binding. Phosphorylation does not directly regulate talin binding to β2 integrin, but 14-3-3 can outcompete talin for binding to phosphorylated β2 integrin. Filamin knockdown by siRNA increases cell adhesion to ICAM-1, indicating that filamin plays a negative role in regulating adhesion. We solved the crystal structures of Thr758-phosphorylated β2 peptide/14-3-3 complex and unphosphorylated β2 peptide/filamin complex. These structures show that the interaction sites are mostly overlapping and explain how β2 phosphorylation switches the binding specificity between filamin and 14-3-3.

Submitted December 11, 2007; accepted April 22, 2008. Prepublished online as *Blood* First Edition paper, June 12, 2008; DOI 10.1182/blood-2007-12-127795.

*H.T., E.N., and S.M.N. contributed equally to this work.

The publication costs of this article were defrayed in part by page charge payment. Therefore, and solely to indicate this fact, this article is hereby marked "advertisement" in accordance with 18 USC section 1734.

© 2008 by The American Society of Hematology

Carl_G_190x270_mm_blokki_FINAL.indd 417 06-Aug-23 1:54:43 PM

Table 1. Peptides used in experiments

Peptide name	Sequence*	Source
pαL	CLKPLHEKDSEpSGGGKD	In house
	ARAApSAPA	In house
β2-35	^{734}CRRFEKEKLKSQWNNDNPLFKSATTTVMNPKFAES^{769}	In house
β2-35A	^{734}CRRFEKEKLKSQWNNDNPLFKSAATTVMNPKFAES^{769}	In house
β2-35pT	^{734}CRRFEKEKLKSQWNNDNPLFKSApTTTVMNPKFAES^{769}	In house
β2-12	CLFKSATTTVMN	In house
β2-21	^{745}SQWNNDNPLFKSATTTVMNPK^{765}	EZBiolab
β2-10pT	^{755}KSApTTTVMNP^{764}	Haartman Institute, University of Helsinki

EZBiolab (Westfield, IN).
*pT is phosphothreonine and pS is phosphoserine.

Methods

Materials

The peptides β2-35, β2-35A, β2-35pT, β2-12, ARAApSAPA, and pαL (Table 1) were synthesized by Fmoc chemistry as in Valmu et al.[7] The α-actinin antibody (MAB1682) and the filamin antibody (MAB1678) were from Chemicon (Temecula, CA), the 14-3-3 blotting antibody (K-19) was from Santa Cruz Biotechnology (Santa Cruz, CA), and the actin antibody (A5060) was from Sigma-Aldrich (St Louis, MO). The pThr758-β2 antibody and the R2E7B antibody to β2 have been described previously.[13,17] Predesigned siRNAs for filamin A (siGenome smart pool, M-012579-00) and controls cyclophilin B (siGLO, D-001610-01-05) and nontargeting siRNA (D-001210-02-05) were from Dharmacon (Lafayette, CO).

Peptide affinity chromatography

Peptides (β2-35, β2-35A, β2-35pT, and pαL) were coupled to vinyl sulphon–activated agarose. T cells were isolated from buffy coats as described[16] and lysed in 1% Tx-100, 10 mM sodium phosphate, pH 7.4, 50 mM NaCl, 10 mM EDTA, 50 mM NaF, and protease inhibitor cocktail. In some experiments, the T-cell lysates were pretreated with the peptide ARAApSAPA (10 μM). Peptide affinity chromatography with the T-cell lysates was performed as in Valmu et al.[16] The competition assay between purified 14-3-3ζ and talin was performed in 1% Tx-100, 150 mM NaCl, 50 mM NaF, 10 mM EDTA, 50 mM Tris, pH 7.4. Proteins were incubated for 30 minutes with 10 μL peptide-coupled agarose. The samples were then washed 5 times with buffer, and eluted with NuPAGE LDS Sample Buffer (Invitrogen, Frederick, MD) at 70°C for 10 minutes.

Transfection with siRNA

The Jurkat cell clone E6.1 (ATCC, Manassas, VA) was maintained in RPMI 1640 medium supplemented with 10% FBS, L-glutamine, and antibiotics. Jurkat E6.1 cells (1.0×10^6 per transfection) were washed with PBS, suspended in 0.1 mL siPORT siRNA electroporation buffer (Ambion, Austin, TX), and mixed with 200 nM siCONTROL Non-Targeting no. 2, siGLO Cyclophilin B, and siGENOME SMART pool human filamin A (FLNa) siRNAs (Dharmacon). Electroporation was performed twice at 325 V, 175 Ω, and 1 μF with pulse width of 0.2 ms and pulse interval of 2 seconds. Cells were grown for 4 days.

Cell stimulation, lysis, SDS–polyacrylamide gel electrophoresis, and Western blot

For pThr758-detection, T cells were isolated from buffy coats as described.[16] They were left untreated or preincubated with 1.5 μM okadaic acid and stimulated for 30 minutes with either 200 mM protein kinase C stimulating phorbol ester, phorbol 12,13-dibuturate (PDBu; Sigma-Aldrich), or 10 μg/mL of the T-cell receptor stimulating antibody OKT3 (clone CRL 8001; ATCC). After cell lysis, extracts were run on SDS–polyacrylamide gel electrophoresis (PAGE) and detected with the pThr758 polyclonal antibody as described.[13] Membranes were stripped and reprobed with a β2 integrin blotting antibody (R2E7B) to confirm equal loading.

For detection of filamin knockdown, 10^6 siRNA-treated cells were centrifuged and the pellet was washed once with PBS. The cells were lysed in NET-buffer (20 mM Tris-HCl pH 8.0, 150 mM NaCl, 1 mM EDTA, 1% Triton X-100) including protease inhibitors (Complete; Roche, Indianapolis, IN). Cell extracts were analyzed by Western blotting and detected with Amersham Biosciences (Arlington Heights, IL) HRP-labeled secondary antibodies (na931v and na934v) and Pierce enhanced chemiluminescence (ECL) Western Blotting Substrate (32106; Rockford, IL). The FLNa knockdown levels were detected with mouse antibody (mab) against FLNa, and the loading was controlled with polyclonal antibody against actin. The expression levels were quantified from scanned films using TINA 2.0 software.

For detection of proteins bound to peptide columns in the peptide affinity chromatography experiments, eluates were subjected to Western blotting with anti-FLNa (Raytest, Straubenhardt, Germany) or with α-actinin or 14-3-3 antibodies and detected by ECL or were subjected to staining with Simply Blue Safe Stain (Invitrogen).

Adhesion assay

Recombinant soluble human ICAM-1 (0.3 μg/well; R&D Systems, Minneapolis, MN) was coated on flat-bottom 96-well microtiter plates (Nunc, Rochester, NY) by overnight incubation at 4°C. The wells were blocked with 1% dry milk for 1.3 hours at 37°C. Cells were suspended in binding medium (RPMI with 40 mM HEPES, 0.1% BSA, 2 mM $MgCl_2$) and stimulated with 200 nM PDBu or left untreated, added to each well, and allowed to adhere for 30 minutes at 37°C. After incubation, unbound cells were removed by gentle washing. The bound cells (or the total amount of added cells without washing) were lysed in 100 μL per well 0.3 mg/mL *p*-nitrophenylphosphate (Calbiochem, San Diego, CA) containing lysis buffer (1% Triton X-100, 50 mM sodium acetate, pH 5.0) and incubated for 45 minutes at 37°C. The reaction was terminated by adding 50 μL per well of 1 M NaOH and the absorbance at 405 nm was measured.

Protein production and purification

The human filamin A immunoglobulin-like domain 21 (IgFLNa21) was expressed and purified as previously described.[3] The bovine 14-3-3ζ cDNA, which encodes a protein 100% identical with the human protein, in pET-15b plasmid (Novagen, Madison, WI) was a generous gift from Dr R. C. Liddington (Burnham Institute for Medical Research, La Jolla, CA). The recombinant protein contained a thrombin digestion site between 14-3-3ζ sequence and an N-terminal His_6 tag.[18] Protein expression in *Escherichia coli* BL21 (DE3) was induced for 3 hours at 37°C in the presence of 0.4 mM IPTG. The cells were disrupted by sonication and soluble proteins were then separated by centrifugation (36 900*g* for 30 minutes at 4°C). The 14-3-3 fusion protein was purified by a Ni-NTA agarose column (Qiagen, Valencia, CA),[19,20] and after overnight thrombin (GE Healthcare, Little Chalfont, United Kingdom) digestion at 23°C the 14-3-3ζ part was eluted. The sample was further purified by HiTrap Q ion exchange chromatography (Amersham Biosciences) in 20 mM Tris-HCl, pH 8.0, with NaCl gradient elution. Final purification was achieved by gel filtration in a Superdex G75

Carl_G_190x270_mm_blokki_FINAL.indd 418 06-Aug-23 1:54:43 PM

24 mm × 600 mm column (Amersham Biosciences) in 20 mM Tris-HCl, pH 7.5, 1 mM EDTA, 1 mM DTT. The pGEX2 plasmid encoding mouse talin F2/F3 head domain (residues 206-405)[21] was a generous gift from Dr D. A. Calderwood (Yale University, New Haven, CT). The fusion protein was expressed in *E coli* BL21 Gold in the presence of 4 mM IPTG. The cells were disrupted with a French press and the soluble proteins were separated by centrifugation (36 900*g* for 30 minutes at 4°C). The fusion protein was purified by glutathione Sepharose column (GE Healthcare), and after overnight digestion with 500 U thrombin (GE Healthcare) at 23°C the talin part was eluted. For surface plasmon resonance experiments, the remaining thrombin traces were removed using a *p*-aminobenzamidine column (Sigma-Aldrich). Protein was further purified by gel filtration in a Superdex G75 24 mm × 600 mm column (Amersham Biosciences) in 150 mM NaCl, 20 mM Tris-HCl, pH 7.5.

Quantitative interaction analysis

The real-time binding of 14-3-3ζ, talin, and IgFLNa21 to β2 integrin peptides was analyzed by surface plasmon resonance (SPR) using the Biacore system (Biacore, Uppsala, Sweden). In this system, the binding of soluble analytes to immobilized ligands was measured in arbitrary units (resonance units [RU]). The phosphorylated (β2-35p) and unphosphorylated (β2-35) β2 integrin peptides were coupled to the matrix of a CM5 sensor chip by amine coupling chemistry. Serial dilutions of 14-3-3, talin F2/F3, or IgFLNa21 in running buffer (10 mM HEPES, pH 7.5, 150 mM NaCl, 3 mM EDTA, 0.005% p20 in the case of 14-3-3; 20 mM Tris-HCl, pH 8.0, 100 mM NaCl, 1 mM DTT in the case of IgFLNa21; and 20 mM Tris-HCl, pH 8.0, 150 mM NaCl, 1 mM EDTA, 1 mM DTT in the case of talin) were injected over the peptide surfaces at a flow rate of 20 μL/min. Binding to an empty negative control surface was subtracted from the obtained sensorgrams. The equilibrium rate constants (K_d values) were calculated using a Langmuir model with the Biacore evaluation software 3.1 provided by the manufacturer for the 14-3-3–β2 and talin–β2 integrin interaction. For the filamin–β2 integrin interactions, which did not fit the Langmuir model, we used an equilibrium binding analysis with Sigmaplot (Systat Software, San Jose, CA). In both interactions, a simple 1:1 interaction was assumed.

Protein crystallography

An equimolar mixture of 1 mM human IgFLNa21 and the β2 integrin peptide β2-21 (Table 1) was crystallized in 1.6 M $(NH_4)_2SO_4$, 0.2 M $NaCH_3COO$, pH 4.6. The crystals were flash frozen in liquid nitrogen in 30% ethylene glycol containing crystallization solution. The diffraction data were collected at 100 K at the European Synchrotron Radiation Facility (Grenoble, France) beamline ID23-1.

The bovine 14-3-3ζ protein (8-10 mg/mL) was crystallized by the hanging drop vapor diffusion method with similar conditions as described in Liu et al[22] (18%-19% PEG3350, 100 mM Tris-HCl, pH 8.5, 10 mM $CaCl_2$, 1 mM $NiCl_2$ at 4°C). The grown 14-3-3ζ crystals were soaked with surplus β2 cytoplasmic integrin phosphopeptide β2-10pT (Table 1). Crystals were transferred in 3 steps into cryoprotectant solution (5%-15% ethylene glycol, 19%-23% PEG3350, 100 mM Tris-HCl, pH 8.5, 10 mM $CaCl_2$, 1 mM $NiCl_2$) and flash frozen in liquid nitrogen.[23] The diffraction data were collected at 100 K at the European Synchrotron Radiation Facility beamline ID14-3.

The data were processed and scaled with the XDS program package (Max Planck Institute for Medical Research, Heidelberg, Germany).[24] Both of the structures were solved by molecular replacement with Phaser (University of Cambridge, Cambridge, United Kingdom).[25] Protein Data Bank (PDB) entry 1A4O[21,22,26] was used as the search model for 14-3-3ζ and PDB entry 2BRQ[3] for IgFLNa21. Peptide backbone of the IgFLNa/β2 structure was built with the program ARP/wARP version 6.1 (European Molecular Biology Laboratory, Hamburg, Germany).[27] The structures were refined with Refmac5[28] (CCP4, Daresbury Laboratory, Warrington, United Kingdom) and the molecular graphics program O (DatOno AB, Uppsala, Sweden).[29] Water molecules were added to the IgFLNa/β2 structure with the program ARP/wARP. Because of hemihedral twinning (twinning fraction 0.306) 14-3-3ζ refinement was further continued with CNS 1.2 program package[30] (Yale University, New Haven, CT) using strict NCS restraints. Structure figures were generated using PyMOL (DeLano Scientific, San Carlos, CA).

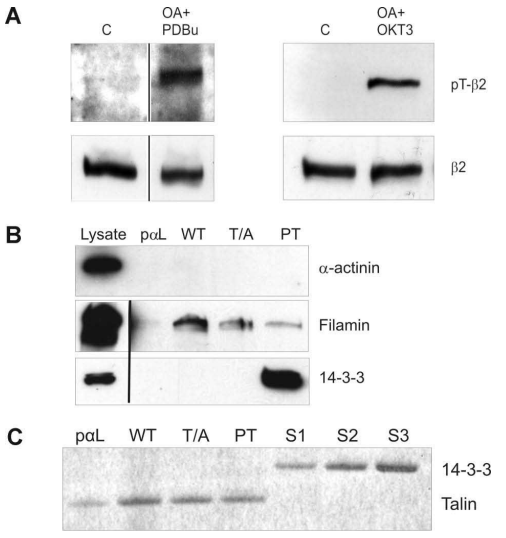

Figure 1. Analysis of β2-phosphorylation status in stimulated T cells and peptide affinity chromatography with phosphorylated and nonphosphorylated β2 cytoplasmic peptides. (A) β2 integrins are phosphorylated on Thr758 in T cells after phorbol ester and TCR ligation. Isolated human T cells were either nonstimulated (C) or preincubated with okadaic acid (OA) and stimulated with PDBu or OKT3. The cells were lysed and extracts subjected to Western blotting with the pThr758-specific antibody (pT-β2) or with the R2E7B antibody (β2). Vertical lines have been inserted to indicate a repositioned gel lane. (B) Binding of filamin and 14-3-3 to a phosphorylated control peptide (pαL), β2-35 (WT), β2-35A (T/A), and β2-35pT (PT) peptide affinity columns. The lysates and the bound materials were analyzed by Western blotting with α-actinin, 14-3-3, and filamin antibodies. Vertical lines have been inserted to indicate a repositioned gel lane. (C) Binding of purified talin head domain and 14-3-3ζ to peptide affinity columns. Talin head fragment (44 nM) binds to all β2 integrin peptides (WT, T/A, PT) in a similar way, thus indicating that talin binding is independent of β2 integrin Thr758. The control peptide (pαL) binding is much weaker, which implies specific binding. The binding of talin to PT is completely outcompeted when a similar molar amount of 14-3-3ζ was added in the incubation volume. The concentrations of the 14-3-3 added were 36 nM (S1), 71 nM (S2), and 143 nM (S3), and 44 nM talin was present in each column.

Results

Characterization of the effect of phosphorylation of Thr758 on 14-3-3, filamin, and talin binding to the β2-cytoplasmic peptide

The TTT motif in integrin β chain cytoplasmic domains is important for integrin regulation, and both β7 and β2 integrins become phosphorylated on this motif in leukocytes.[11-13] Using a recently developed anti-pThr758 rabbit polyclonal antibody,[13] we investigated the phosphorylation status of β2 integrins in T cells. As previously reported, β2 integrins indeed become phosphorylated on the cytoplasmic Thr758 after stimulation of cells with TCR antibodies or with phorbol ester (Figure 1A). These are stimuli that are well known to lead to increased binding of T cells to the β2 integrin ligand ICAM-1.[31]

The TTT-containing region of the integrin β-chains is important for the binding of cytoplasmic molecules filamin[3] and 14-3-3 proteins to the β2 integrin intracellular domain.[4,32] To investigate the effect of phosphorylation of Thr758 on filamin and 14-3-3

protein interaction with the integrin cytoplasmic domain, we synthesized unphosphorylated and Thr758-phosphorylated integrin cytoplasmic domain peptides, as well as peptides with Thr758 mutated to alanine (Table 1). As expected, 14-3-3 proteins from T-cell lysates interacted only with pThr758 peptides and not at all with the unphosphorylated or Thr758Ala-mutated β2 peptide (Figure 1B). In contrast, filamin from cell lysates interacted well with the unphosphorylated peptide, but binding was significantly weaker to the phosphorylated peptide (Figure 1B). We could not detect binding of α-actinin, another protein that has been reported to bind to β2 integrin peptides and interact with β2 integrin in vivo,[33] to any of the peptides (Figure 1B).

Talin, a major player in integrin activation, binds β2 integrins in vitro and in cells.[1,7] The talin head domain can activate both the wt-β2 and Thr758Ala-β2 integrins in cells.[4] Next, we assessed the role of Thr758 phosphorylation in talin binding to the integrin. We could not detect any full-length talin from T-cell lysates binding to the integrin peptides (data not shown). Thus, we instead examined binding of the main integrin-binding domain of talin, purified talin F2/F3 domains, to the β2 integrin peptides. As expected, because the talin-binding site in integrins does not overlap with Thr758,[21,34] phosphorylation of Thr758 did not influence talin binding to the integrin (Figure 1C). However, the phosphorylation indirectly influences talin binding, as addition of 14-3-3 led to detachment of talin from the phosphorylated integrin peptide (Figure 1C). This result suggests that 14-3-3– and talin-binding sites in the integrin are partially overlapping.

Affinity measurement of 14-3-3–β2, talin-β2, and filamin-β2 interactions

To measure the affinity of the studied protein-protein interactions, we performed surface plasmon resonance (Biacore) measurements. The peptides β2-35 and β2-35pT were coupled to individual flow cells of the Biacore sensor chip CM5, and different concentrations of the 14-3-3 protein, IgFLNa21, or talinF2/F3 were added in the solution. The 14-3-3 protein interacted with the phosphorylated but not the unphosphorylated β2 peptide, as expected. The interaction was very strong: the K_d was of the order of 260 nM (Figure 2A), which is comparable to other 14-3-3 interactions with their phosphorylated target sequences. Talin F2/F3 interacted with similar affinity with both the unphosphorylated and phosphorylated β2 peptide (K_d, 11 and 12.5 nM, respectively) (Figure 2B). The main integrin-binding site of filamin A, immunoglobulin domain 21 (IgFLNa21), interacted only with the nonphosphorylated β2 peptide, and the interaction was considerably weaker than for the 14-3-3 and talin interactions, in the range of 0.5 mM (Figure 2C). Nevertheless, the interaction of full-length filamin from T-cell lysates with the unphosphorylated β2 peptide was readily detected in our assays even if abundant amounts of 14-3-3 was present (Figure 1B), indicating that 14-3-3 could not outcompete filamin binding to the unphosphorylated integrin.

To further investigate whether the stronger affinity of the 14-3-3–β2 integrin interaction would mean that 14-3-3 would outcompete the filamin binding to the β2 integrin, we performed further experiments. The binding ability of 14-3-3 proteins in T-cell lysates was blocked by preincubation with the 14-3-3–binding peptide ARAApSAPA. This peptide binds to the 14-3-3 phosphate–binding groove and prevents the protein from interacting with phosphorylated targets, including β2 integrin.[4] As expected, treatment of T-cell lysate with this peptide indeed significantly inhibited 14-3-3 binding to the phosphorylated β2 integrin peptide (Figure 2D). However, filamin binding was not significantly increased either to the nonphosphorylated or the phosphorylated β2 peptide (Figure 2D). This result implicates that it is not 14-3-3 binding but phosphorylation of β2 integrin that regulates the filamin interaction with the integrin. Taken together, both our peptide affinity chromatography results and Biacore results suggest that phosphorylation of Thr758 inhibits β2 integrin binding to filamin and enables its interaction with 14-3-3 proteins. We also showed that 14-3-3 competes with talin binding to the Thr758-phosphorylated β2 integrin tail.

Structures of filamin/β2 and 14-3-3/phospho-β2 complexes

To understand the structural basis of the β2 integrin cytoplasmic domain binding to filamin and 14-3-3 we cocrystallized the β2 peptide with IgFLNa21 and soaked the β2 phosphopeptide in crystals of 14-3-3ζ. The IgFLNa-β2 peptide crystals belong to space group $P2_13$ and diffracted to 2.2-Å resolution. The structure was solved by molecular replacement using the previously solved IgFLNa21 (chain A from Protein Data Bank id 2BRQ) as the search model. Data collection and refinement statistics are shown in Table 2. In addition to the search model, electron density of the β2 peptide was observed next to the β-strand C of IgFLNa21, and 11 residues of the peptide could be built in the final model (Figure 3A-C). In the current crystal, the IgFLNa21 structure was otherwise identical (root-mean-square deviation for 86 Cα atoms 0.48 Å) with the previously published structure except that the residues of the DE loop were missing in the electron density map and could not be included in the final model (Figure 3C,D). The final refinement R-values were slightly higher (R = 24.3% and Rfree = 27.8%) than in an average 2.2-Å structure in the PDB database (R_{ave} = 20.3% and $Rfree_{ave}$ = 25.3%), which is apparently caused by the disorder in the DE loop. The β2 peptide bound to IgFLNa21 in a very similar way as the β7 peptide,[3] forming a hydrogen-bonded β-strand next to the strand C of IgFLNa21 and interacting hydrophobically with the side chains of strand D (Figure 3C,D). The main hydrophobic contacts are mediated by the side chain methyl groups of Thr758 and Thr760 in β2. As Thr758 resides in a hydrophobic site of IgFLNa21, it is most probable that addition of a negatively charged phosphate group to this residue strongly disfavors its interaction. Thus, the structure of IgFLNa21/β2 peptide complex explains why Thr758-phosphorylated β2 integrin is not able to interact with filamin.

The 14-3-3ζ crystallized in the space group $P6_5$ and data up to 2.5-Å resolution were used for structure calculations (Table 2). The cumulative intensity distribution of the diffraction data indicated that the best crystals were merohedral twins with a twinning fraction of 0.306. Nontwinned crystals were not found. Despite this, the structure could be solved and the electron density maps could be clearly interpreted to yield a good quality model (R = 22.7% and R_{free} = 27.3%; Table 2). The soaked β2 phosphopeptide was bound in all 4 14-3-3ζ monomers of the asymmetric unit, and noncrystallographic restrains were used in the final refinements (Figure 4). The phosphopeptide was bound to the well-characterized binding pocket between α-helices E and F of each 14-3-3 molecules.[35] The main electrostatic interactions were between Thr758 phosphate group of the β2 peptide and 14-3-3ζ Arg residues 56 and 127, which form a typical basic batch in the binding site (Figures 4A,5). A hydrogen bond was observed between the phosphate group and Tyr128 of 14-3-3 (Figure 5A,B). The side chain of Ser756 formed hydrogen bonds with Trp228 and Glu180 (Figure 5A,B). The interaction features between β2 phosphopeptide and 14-3-3ζ were very similar to other published

Carl_G_190x270_mm_blokki_FINAL.indd 420 06-Aug-23 1:54:44 PM

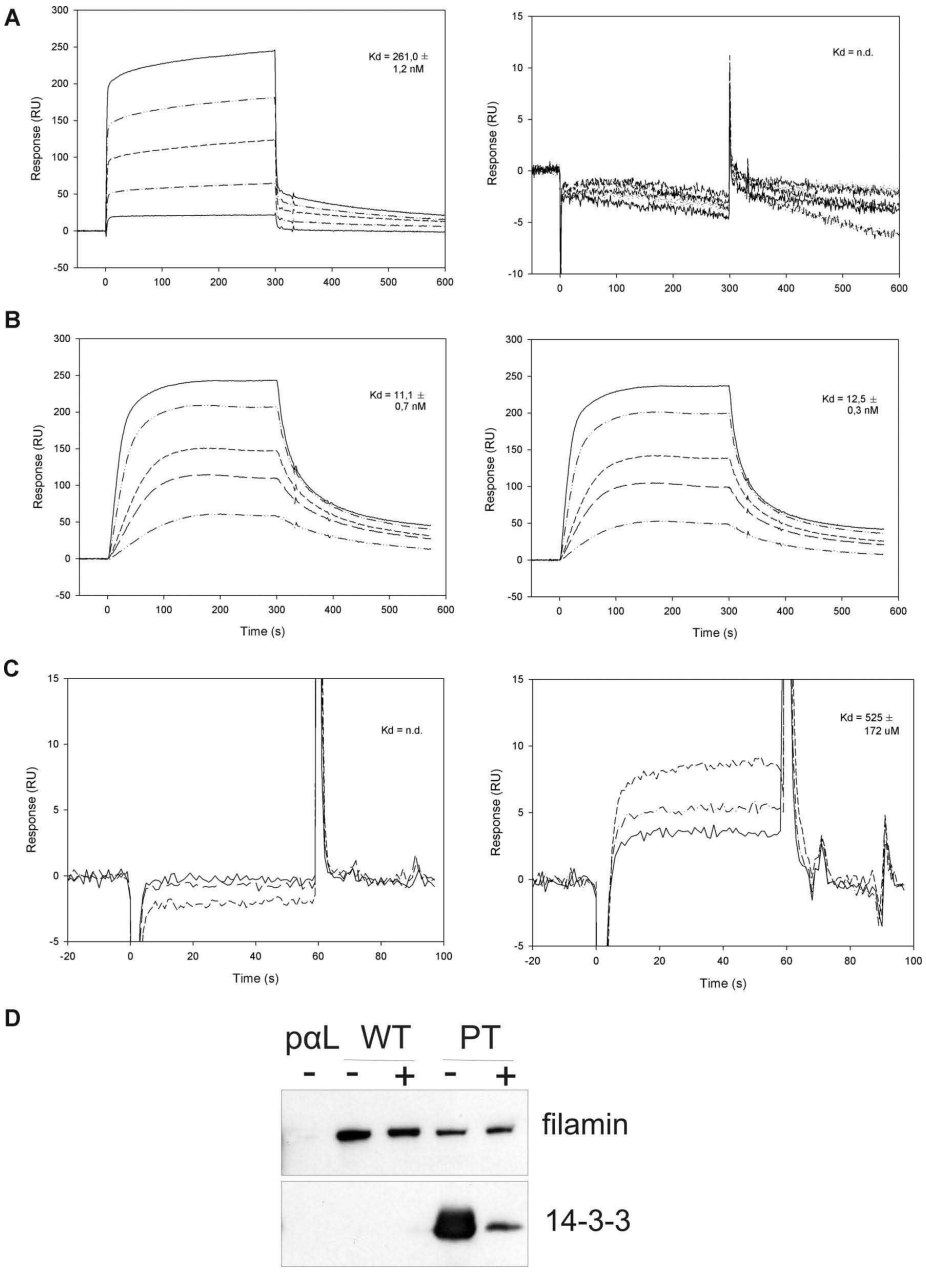

Figure 2. Surface plasmon resonance and competition studies of 14-3-3, talin, and filamin interactions with β2 cytoplasmic peptides. (A) Surface plasmon resonance (Biacore) sensorgrams of 14-3-3 binding to the phosphorylated (pT) and unphosphorylated (T) β2 peptide. The 14-3-3 concentrations used were 40, 160, 320, 640, and 1000 nM. (B) Surface plasmon resonance (Biacore) sensorgrams of talinF2/F3 binding to the phosphorylated (pT) and unphosphorylated (T) β2 peptide. The concentrations of talin used were 4, 10, 20, 40, and 60 nM. (C) Surface plasmon resonance (Biacore) sensorgrams of IgFLNa21 binding to the phosphorylated (pT) and unphosphorylated (T) β2 peptide. The concentrations of FLN used were 100, 200, and 400 μM. (D) Binding of filamin and 14-3-3 from ARAApSAPA-treated lysates to integrin peptide affinity columns. ARAApSAPA significantly reduced the interaction between 14-3-3 and β2 integrin peptide. The binding of filamin to wt integrin peptide or to the pT integrin peptide is not significantly increased in ARAApSAPA-treated lysates. Equal loading was confirmed by Western blotting of 14-3-3 from lysates (not shown). − indicates no ARAApSAPA treatment; +, 10 μM ARAApSAPA treatment.

Table 2. Crystallographic data collection and refinement statistics

	IgFLNa21 / β2	14-3-3ζ / phospho-β2
Data collection		
Beamline	ESRF ID23-1	ESRF ID14-3
Wavelength, Å	0.98	0.93
Space group	$P2_13$	$P6_5$
Cell dimensions		
a, b, c, Å	78.72, 78.72, 78,72	94.92, 94.92, 233.6
α, β, γ, °	90, 90, 90	90, 90, 120
Resolution range, Å	45.5-2.20 (2.26-2.20)†	47.6-2.5 (2.59-2.50)†
R_{sym}*, %	6.8 (43.1)	9.0 (53.4)
$I/\sigma I$	25.4 (6.2)	16.9 (4.91)
Completeness, %	99.8 (100)	99.9 (99.9)
Redundancy	14 (14.2)	9.00 (8.94)
Refinement		
Resolution range, Å	45.45-2.2 (2.26-2.20)	47.6-2.50 (2.59-2.50)
No. of reflections		
Refinement	7633 (555)	39003 (3889)
Test set	849 (62)	1967 (181)
R_{cryst}/R_{free}, %	24.7/27.8 (30.2/31.9)	22.8/27.3 (39.8/40.8)
No. of atoms		
Protein	718	7446
Heterogen	6	44
Solvent	19	155
Rms differences		
Bond lengths, Å	0.02	0.02
Bond angles, °	1.89	1.17
Average B-factor, Å^2		65.1
Protein	41	65.7
Peptide	54.6	67.8
Solvent	44.5	33.4
B-factor from Wilson plot, Å^2	51.4	47.0
Amino acids in Ramachandran diagram, %		
In most favored regions	93.3	87.3
In additional allowed regions	5.3	11.9
In generously allowed regions	1.3	0.8

*R factor $= \frac{\sum||F_{obs}|-|F_{calc}||}{\sum|F_{obs}|}$, where F_{obs} is observed and F_{calc} is calculated structure factor.

†Values of the last resolution shell in parentheses.

phosphopeptide/14-3-3 structures where the phosphate group has been shown to be the key determinant for binding.[35]

Filamin knockdown increases activated Jurkat cell adhesion to ICAM-1

Blocking 14-3-3 binding to β2 by a Thr758Ala mutation or by 14-3-3 blocking (R18) constructs inhibits β2 integrin–dependent binding to ICAM-1.[4] To investigate the role of filamin binding in regulating β2 integrin–mediated adhesion, we performed knockdown experiments (siRNA) of filamin in Jurkat cells (Figure 6A). Filamin knockdown did not influence basal adhesion to ICAM-1 (not shown). However, it increased binding of PDBu-stimulated Jurkat cells to ICAM-1 (Figure 6B). Thus, filamin plays an inhibitory role in regulating T-cell adhesion to ICAM-1.

Discussion

In this article, we have investigated the binding of 3 cytoplasmic proteins, the pSer/pThr-binding adaptor protein 14-3-3 and the large cytoskeletal proteins talin and filamin, to the unphosphorylated and phosphorylated β2 integrin cytoplasmic tails. The main findings are that the phosphorylation of β2 on the physiologically relevant Thr758 leads to impairment of filamin interaction and binding of 14-3-3, thus acting as a "molecular switch" for these protein-protein interactions, and that 14-3-3 can outcompete talin for binding to the β2 integrin in its phosphorylated state.

IgFLNa21 has been shown to be the main interaction site in filamin A for β1 and β7 integrins.[3] Here we report the structure of IgFLNa21 with a peptide from the β2 cytoplasmic tail. The interaction is very similar to the previously reported IgFLNa21/β7 integrin complex.[3] The main difference of the 2 structures derives from the fact that the TTT motif is one residue earlier in β2 than in β7. Because of this, the main hydrophobic interaction with the Phe2285 of FLNa is mediated by Thr758 in β2 instead of Ile782 in β7. The methyl group of Thr758 points toward the interface, whereas the hydroxyl group is partially exposed. Based on the structure, it is apparent that the addition of a phosphate group to Thr758 would be very unfavorable for the β2-IgFLNA21 interaction. We could also show this in phosphopeptide affinity chromatography and in surface plasmon resonance assays. To the best of our knowledge, this is the first report where the inhibitory effect of integrin phosphorylation on filamin binding has been directly demonstrated. In an earlier study, phosphate mimicking Thr to Glu mutations were used in the β7 integrin.[3]

We showed here that 14-3-3 bound only to Thr758-phosphorylated β2. This is in line with the general principle that most 14-3-3 interactions are dependent on phosphorylation. The β2 sequence is quite close to the mode 1 14-3-3–binding consensus motif RSXpS/TXP[37] (Figure 7A). The structure of the pThr758 β2/14-3-3 complex revealed that the phosphate group is the major determinant of the interaction. There are only few other side chain interactions between β2 and IgFLNa21 in the complex. Again, this is very similar to other 14-3-3 complexes (Figure 7B).

When we compare the conformation of the β2 peptide bound to 14-3-3 and to filamin, we see that they are very different (Figure 7C). Both of them are extended, but the peptide does not form a β-strand in the 14-3-3 complex as seen in the filamin complex. This indicates that the integrin cytoplasmic tail can adopt different conformations depending of its binding partner. In the crystal structures, we see only those parts of the cytoplasmic tail peptides that are in direct contacts, whereas the other regions apparently are disordered. It is possible that integrin β tails are disordered also in vivo, unless they are in contact with other molecules.

We have now shown that inhibition of filamin binding to β2 integrins by filamin "knockdown" leads to an increase in stimulated T-cell adhesion to ICAM-1. In combination with previously reported results showing that inhibition of 14-3-3 binding to β2 dramatically reduces adhesion,[4] this result shows that the phosphorylation of Thr758 is an important molecular switch that regulates adhesion. We have previously shown that a Thr758-phosphorylated β2 peptide, which was introduced into cells with the aid of a hydrophobic penetratin sequence, activated cell adhesion and further signaling to the actin regulating small G-proteins Rac1 and Cdc42.[13] Thus, phosphorylation of β2 on Thr758, which occurs after cell stimulation, leads to a detachment of filamin and a binding of 14-3-3 to the β2 tail, and the combination of further downstream molecular events leads to increased cell adhesion.

Talin is an important regulator of αLβ2 integrins in T cells stimulated through the T-cell receptor.[8] We found that phosphorylation of β2 integrin does not directly affect binding of talin to the integrin. However, it appears that 14-3-3 binding to the phosphorylated integrin may lead to detachment of talin from the integrin tail. The talin-binding site in the β3 integrin[21] and the 14-3-3–binding

Carl_G_190x270_mm_blokki_FINAL.indd 422 06-Aug-23 1:54:45 PM

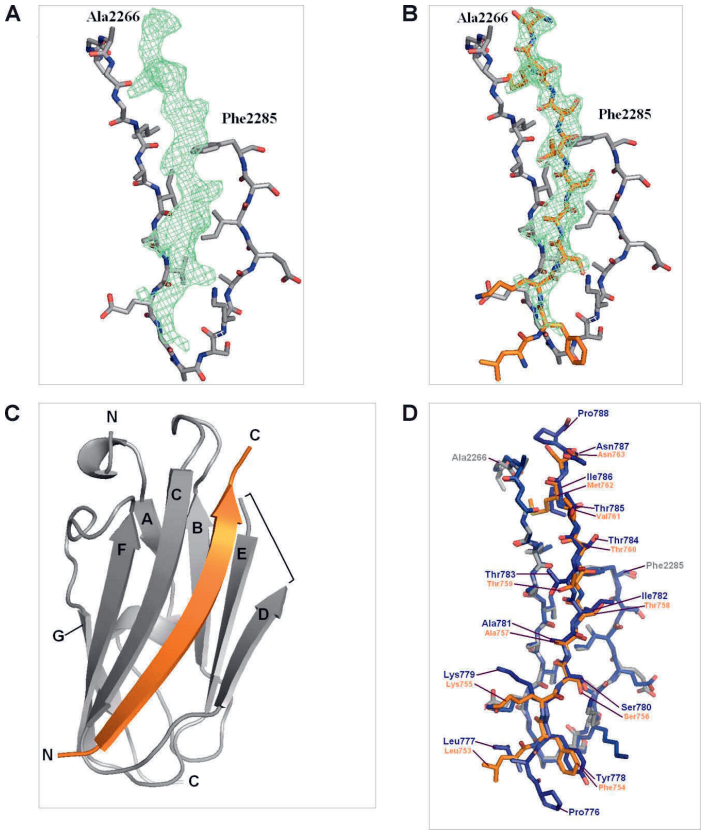

Figure 3. Crystal structure of IgFLNa21/β2 complex. (A) Electron density map ($F_o - F_c$) of the β2 peptide calculated from the final model without the peptide, shown at $\sigma = 2$. Only β-strands C and D of IgFLNa21 are shown for clarity. (B) The final model of the peptide (orange) built in the electron density map. (C) Overall structure of the IgFLNa21 (gray) and the peptide shown as ribbon diagram. N and C termini are indicated and the β-strands are named. The loop between β-strands D and E that is missing from the final model is indicated with a bracket. (D) Comparison of IgFLNa21/β7 (blue) (PDB entry 2BRQ) and IgFLNa21/β2 (gray and orange) complexes. The numbering of integrin residues is shown.

site in β2 (this study) show only one amino acid overlap, but that might be enough to prevent the simultaneous binding of these 2 molecules to phosphorylated integrin tails (Figure 7D). One could envision a sequential model by which these proteins influence αLβ2 integrin–mediated adhesion. Filamin is bound to the integrin in resting cells (where β2 is unphosphorylated) and plays an inhibitory role in integrin activation. Talin is directly involved in β2 integrin activation by regulating both integrin affinity and clustering,[8] and talin and filamin may compete for the β2 integrin, as has been described for the β7 integrin.[3] The importance of talin in β2 integrin–mediated cell-cell binding is especially pronounced at early stages (30 seconds to 5 minutes) after T-cell receptor stimulation, although whether there is a constitutive or stimulated association between talin and αLβ2 is not known.[8] 14-3-3 does not bind to the integrin until the β2-chain becomes phosphorylated at Thr758, at later time points after TCR stimulation.[11] At these later time points, the contact between T-cell and antigen-presenting cell matures and talin is no longer crucial for adhesion.[8] Phosphorylation of Thr758 directly inhibits filamin binding, and indirectly inhibits talin binding to the β2 integrin. The phosphorylated integrin/14-3-3 complex then mediates actin reorganization downstream of the integrin, strengthening the cell-cell contact.

The 14-3-3 proteins are involved in many cellular processes but do not have any enzymatic activity. There are at least 2 possible mechanisms by which 14-3-3s can function in signaling. As they are dimers, either they can work as scaffolding proteins that bind to 2 phosphorylated ligands simultaneously, or they can function as allosteric modulators that stabilize further interactions of the ligand. In β2 integrin signaling, both of these mechanisms are possible. Because the 2 phosphopeptide-binding grooves in the 14-3-3 dimer are quite close to each other (the distance between the 2 phosphate groups is about 30 Å) and the binding pockets are partly covered, 2 folded domains cannot fit in the binding pocket simultaneously. However, 2 extended peptides such as integrin cytoplasmic tails could bind the 14-3-3 dimer simultaneously. Thus, 14-3-3 could act by inducing integrin clustering, in a similar way that has been observed for 14-3-3s to induce hexamer formation of a P-type H^+-ATPase.[38] On the other hand, 14-3-3 could induce some further interactions of the integrin cytoplasmic domain, for instance by favoring certain conformations of the tail. It is apparent that Rac1/Cdc42 activation is downstream of 14-3-3–integrin interaction.[13] However, the intermediate steps between 14-3-3 and these small G-proteins are currently not known.

Do other integrins bind to 14-3-3 or is the binding mechanism described here specific for β2 integrins? When we compared other integrin cytoplasmic tail sequences to the region surrounding Thr758 of β2, we found that Thr777 of β3 (or Thr751 without signal peptide) and Thr766 of β6 locate in a very similar consensus position as Thr758 of β2, resembling the mode 1 14-3-3–binding phosphopeptide sequence. The β3 integrin has been reported to be phosphorylated on Thr777 in cells.[39-41] β1, β7, and β5 sequences

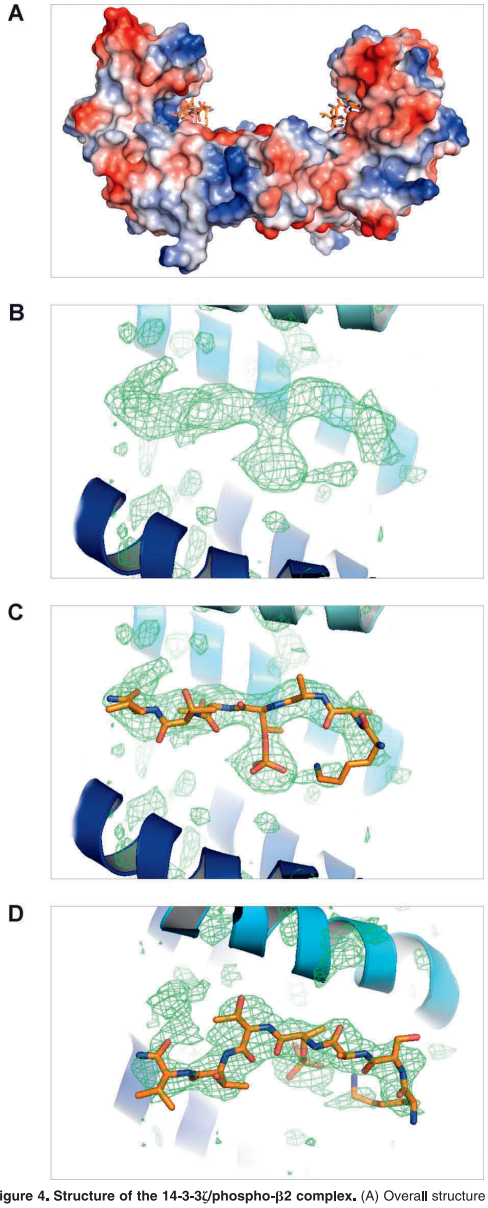

Figure 4. Structure of the 14-3-3ζ/phospho-β2 complex. (A) Overall structure of the 14-3-3ζ dimer and 2 peptides. The protein is shown as a surface representation colored according to surface charge as implemented in PyMOL. (B) The difference electron density map ($F_o - F_c$) of the β2 phosphopeptide calculated from the final model without the peptide, shown at $\sigma = 2$. The α-helices E and H of 14-3-3 are located below and above the peptide, respectively, and shown as a ribbon diagram. (C) Same as panel B, but the final model of the peptide is also shown. (D) The same as panel C, but shown from above.

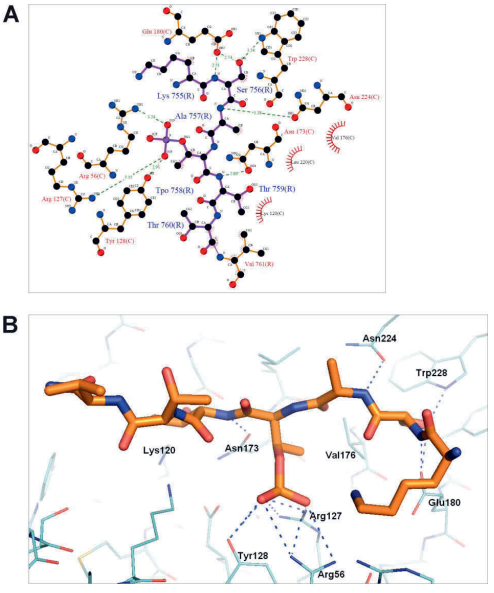

Figure 5. Details of the 14-3-3ζ–phospho-β2 interaction. (A) An illustration of the atomic interactions between the protein and peptide. Hydrogen bonds are shown as dashed lines with distances and atoms participating in hydrophobic interactions marked. The figure was generated by the program Ligplot (University College London, London, United Kingdom).[36] (B) The hydrogen bonds indicated in panel A are shown in the actual model. Note that only the pThr758 (marked Tpo in A) and Ser756 have side chain hydrogen bonds with the protein.

have some resemblance to the mode 2 14-3-3–binding motif (Figure 8B). Of these, both β1 and β7 integrins are known to be phosphorylated in cells.[12,42] There is conflicting evidence about the involvement of 14-3-3 proteins in β1 integrin–mediated adhesion.[4,43,44] To our knowledge, however, the direct effects of β1 phosphorylation on 14-3-3 interactions have not been studied. The sequence comparisons suggest that many phosphorylated β integrin tails may interact with 14-3-3 in a similar way to the Thr758-phosphorylated β2.

Only limited structural information is available on integrin β tails. Nuclear magnetic resonance (NMR) methods have given an overall picture of the conformational flexibility of integrin tails.[45,46] Crystal structures of the integrin/talin[21] and integrin/filamin complexes[3] are available as well as detailed NMR data of the integrin-talin interaction.[34] In this paper, we have described the structure of 14-3-3 with the integrin cytoplasmic tail phosphopeptide and a second integrin/filamin complex. It reveals that the phosphorylation of Thr758 in β2 switches the binding between filamin and 14-3-3. We believe that this is an important new concept of integrin function.

Acknowledgments

The coordinates have been deposited to PDB under codes 2V7D (14-3-3ζ/β2 complex) and 2JF1 (IgFLNa21/β2 complex). We acknowledge the European Synchrotron Radiation Facility for provision of synchrotron radiation facilities, and we thank Dr Didier Nurizzo and Dr Joanna Timmins for assistance in using beamlines ID23-1 and ID14-3.

This study has been supported by Academy of Finland grants 105211, 114717 (J.Y.), and 210390 (C.G.G.); the Sigrid Jusélius Foundation (C.G.G.); the Finnish Cancer Society (C.G.G.); the Finnish Medical Association (C.G.G.); Magnus Ehrnrooth

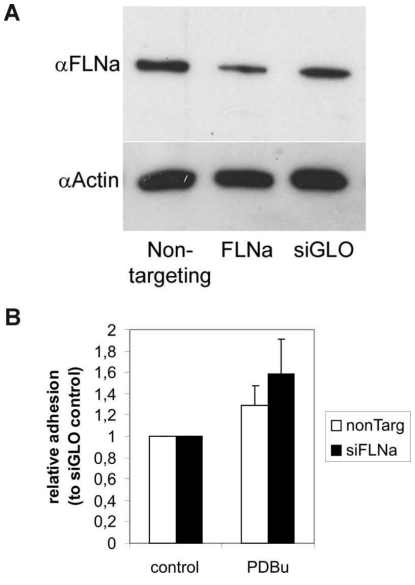

Figure 6. Effect of filamin knockdown on β2 integrin–dependent T-cell adhesion to coated ICAM-1. (A) Jurkat T cells were transfected with siGENOME SMART pool human filamin A (FLNa) siRNAs or control siRNAs. Filamin knockdown with filamin-specific siRNAs, but not control siRNAs, resulted in knockdown of filamin protein levels, as shown by Western blotting of corresponding cell extracts with antifilamin antibodies. The blot was stripped and reprobed with actin antibodies to show equal loading. (B) siRNA-transfected cells were left untreated or stimulated with 200 nM PDBu and cell binding to coated ICAM-1 was assayed for as described in "Adhesion assay." Treatment of cells with FLNa siRNAs, but not control siRNAs, increased the stimulated cell binding to ICAM-1 ($P < .05$ for PDBu-stimulated samples). The experiment was repeated 9 times with similar results. Error bars represent SD.

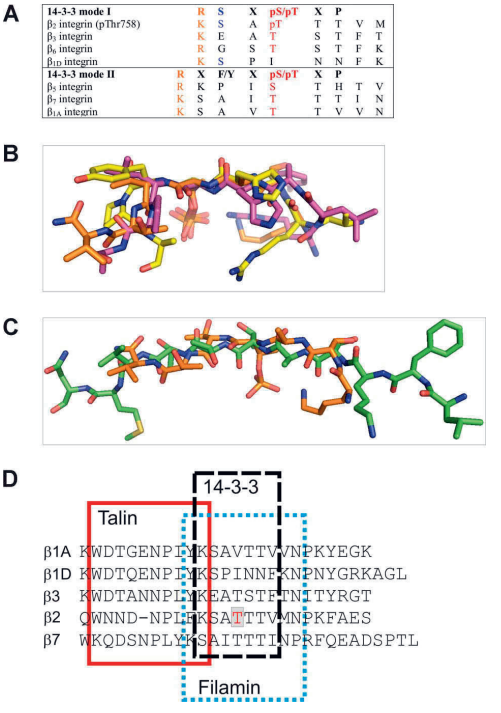

Figure 7. Comparison of 14-3-3–binding peptides and integrins. (A) Alignment of mode 1 and mode 2 14-3-3–binding consensus sequences with integrin sequences. (B) Superimposition of our 14-3-3 bound β2 (orange) with mode 1 (PDB entry 1QJB, purple) and mode 2 (PDB entry 1QJA, yellow) peptide structures. The only common features are the Arg/Lys and the pThr/pSer indicated in red in panel A. (C) Superimposition of β2 peptides in 14-3-3–binding conformation (orange) and IgFLNa21-binding conformation (green) shows that in both complexes the peptides are extended, but the side chain orientations differ markedly. (D) Sequence alignment of talin-, filamin-, and 14-3-3–binding sites in different integrin β-chains. The binding sites are based on the β3-talin complex structure 1MIZ[21] and our current structures (β2/14-3-3 and β2/filamin).

Foundation (S.C.F.); the Liv och Halsa foundation (S.C.F., C.G.G.); and the Ruth and Nils-Erik Stenback foundation grants (S.C.F.; all Helsinki, Finland).

Authorship

Contribution: H.T. performed research, analyzed data, and contributed to writing the paper; E.N., S.M.N., M.A., T.S., T.K., and M.T. performed research and analyzed data; C.G.G. contributed to design of research and writing the paper; and J.Y. and S.C.F. designed research, analyzed data, and wrote the paper.

Conflict-of-interest disclosure: The authors declare no competing financial interests.

Correspondence: Susanna Fagerholm, Section of Immunology, Division of Pathology and Neuroscience, Ninewells Hospital and Medical School, Dundee University, DD1 9SY, Dundee, United Kingdom; e-mail: s.c.fagerholm@dundee.ac.uk; or Jari Ylänne, Department of Environmental and Biological Science and Nanoscience Center, University of Jyäskylä, PO Box 35, 40014 Jyväskylä, Finland; e-mail: jylanne@bytl.jyu.fi.

References

1. Kim M, Carman CV, Springer TA. Bidirectional transmembrane signaling by cytoplasmic domain separation in integrins. Science. 2003;301:1720-1725.
2. Tadokoro S, Shattil SJ, Eto K, et al. Talin binding to integrin beta tails: a final common step in integrin activation. Science. 2003;302:103-106.
3. Kiema T, Lad Y, Jiang P, et al. The molecular basis of filamin binding to integrins and competition with talin. Mol Cell. 2006;21:337-347.
4. Fagerholm SC, Hilden TJ, Nurmi SM, Gahmberg CG. Specific integrin alpha and beta chain phosphorylations regulate LFA-1 activation through affinity-dependent and -independent mechanisms. J Cell Biol. 2005;171:705-715.
5. Springer TA. Traffic signals for lymphocyte recirculation and leukocyte emigration: the multistep paradigm. Cell. 1994;76:301-314.
6. Gahmberg CG. Leukocyte adhesion: CD11/CD18 integrins and intercellular adhesion molecules. Curr Opin Cell Biol. 1997;9:643-650.
7. Valmu L, Hilden TJ, van Willigen G, Gahmberg CG. Characterization of beta2 (CD18) integrin phosphorylation in phorbol ester-activated T lymphocytes. Biochem J. 1999;339(pt 1):119-125.
8. Simonson WT, Franco SJ, Huttenlocher A. Talin1 regulates TCR-mediated LFA-1 function. J Immunol. 2006;177:7707-7714.
9. Li YF, Tang RH, Puan KJ, Law SK, Tan SM. The cytosolic protein talin induces an intermediate affinity integrin {alpha}Lbeta2. J Biol Chem. 2007; 282:24310-24319.
10. Fagerholm SC, Hilden TJ, Gahmberg CG. P marks the spot: site-specific integrin phosphorylation regulates molecular interactions. Trends Biochem Sci. 2004;29:504-512.
11. Valmu L, Gahmberg CG. Treatment with okadaic acid reveals strong threonine phosphorylation of CD18 after activation of CD11/CD18 leukocyte

integrins with phorbol esters or CD3 antibodies. J Immunol. 1995;155:1175-1183.

12. Hilden TJ, Valmu L, Karkkainen S, Gahmberg CG. Threonine phosphorylation sites in the beta 2 and beta 7 leukocyte integrin polypeptides. J Immunol. 2003;170:4170-4177.
13. Nurmi SM, Autero M, Raunio AK, Gahmberg CG, Fagerholm SC. Phosphorylation of the LFA-1 integrin beta2-chain on Thr-758 leads to adhesion, Rac-1/Cdc42 activation, and stimulation of CD69 expression in human T cells. J Biol Chem. 2007; 282:968-975.
14. Calderwood DA, Huttenlocher A, Kiosses WB, et al. Increased filamin binding to beta-integrin cytoplasmic domains inhibits cell migration. Nat Cell Biol. 2001;3:1060-1068.
15. Sharma CP, Ezzell RM, Arnaout MA. Direct interaction of filamin (ABP-280) with the beta 2-integrin subunit CD18. J Immunol. 1995;154: 3461-3470.
16. Valmu L, Fagerholm S, Suila H, Gahmberg CG. The cytoskeletal association of CD11/CD18 leukocyte integrins in phorbol ester-activated cells correlates with CD18 phosphorylation. Eur J Immunol. 1999;29:2107-2118.
17. Nortamo P, Patarroyo M, Kantor C, Suopanki J, Gahmberg CG. Immunological mapping of the human leucocyte adhesion glycoprotein gp90 (CD18) by monoclonal antibodies. Scand J Immunol. 1988;28:537-546.
18. Rosenberg AH, Lade BN, Chui DS, Lin SW, Dunn JJ, Studier FW. Vectors for selective expression of cloned DNAs by T7 RNA polymerase. Gene. 1987;56:125-135.
19. Fu H, Coburn J, Collier RJ. The eukaryotic host factor that activates exoenzyme S of Pseudomonas aeruginosa is a member of the 14-3-3 protein family. Proc Natl Acad Sci U S A. 1993;90:2320-2324.
20. Moorhead G, Douglas P, Cotelle V, et al. Phosphorylation-dependent interactions between enzymes of plant metabolism and 14-3-3 proteins. Plant J. 1999;18:1-12.
21. García-Alvarez B, de Pereda JM, Calderwood DA, et al. Structural determinants of integrin recognition by talin. Mol Cell. 2003;11:49-58.
22. Liu D, Bienkowska J, Petosa C, Collier RJ, Fu H, Liddington R. Crystal structure of the zeta isoform of the 14-3-3 protein. Nature. 1995;376:191-194.
23. Petosa C, Masters SC, Bankston LA, et al. 14-3-3zeta binds a phosphorylated Raf peptide and an unphosphorylated peptide via its conserved amphipathic groove. J Biol Chem. 1998;273:16305-16310.
24. Kabsch WJ. Automatic processing of rotation diffraction data from crystals of initially unknown symmetry and cell constants. J Appl Crystallogr. 1993;26:795-800.
25. Storoni LC, McCoy AJ, Read RJ. Likelihood-enhanced fast rotation functions. Acta Crystallogr D Biol Crystallogr. 2004;60:432-438.
26. Research Collaboratory for Structural Bioinformatics. Protein Data Bank. http://www.rcsb.org/pdb. Accessed July 20, 2008.
27. Perrakis A, Morris R, Lamzin VS. Automated protein model building combined with iterative structure refinement. Nat Struct Biol. 1999;6:458-463.
28. Murshudov GN, Vagin AA, Dodson EJ. Refinement of macromolecular structures by the maximum-likelihood method. Acta Crystallogr D Biol Crystallogr. 1997;53:240-255.
29. Jones TA, Zou JY, Cowan SW, Kjeldgaard M. Improved methods for building protein models in electron density maps and the location of errors in these models. Acta Crystallogr A. 1991;47(pt 2):110-119.
30. Brünger AT, Adams PD, Clore GM, et al. Crystallography & NMR system: a new software suite for macromolecular structure determination. Acta Crystallogr D Biol Crystallogr. 1998;54:905-921.
31. Dustin ML, Springer TA. T-cell receptor cross-linking transiently stimulates adhesiveness through LFA-1. Nature. 1989;341:619-624.
32. Fagerholm S, Morrice N, Gahmberg CG, Cohen P. Phosphorylation of the cytoplasmic domain of the integrin CD18 chain by protein kinase C isoforms in leukocytes. J Biol Chem. 2002;277: 1728-1738.
33. Pavalko FM, LaRoche SM. Activation of human neutrophils induces an interaction between the integrin beta 2-subunit (CD18) and the actin binding protein alpha-actinin. J Immunol. 1993;151: 3795-3807.
34. Wegener KL, Partridge AW, Han J, et al. Structural basis of integrin activation by talin. Cell. 2007;128:171-182.
35. Gardino AK, Smerdon SJ, Yaffe MB. Structural determinants of 14-3-3 binding specificities and regulation of subcellular localization of 14-3-3-ligand complexes: a comparison of the X-ray crystal structures of all human 14-3-3 isoforms. Semin Cancer Biol. 2006;16:173-182.
36. Wallace AC, Laskowski RA, Thornton JM. LIGPLOT: a program to generate schematic diagrams of protein-ligand interactions. Protein Eng. 1995;8:127-134.
37. Yaffe MB, Rittinger K, Volinia S, et al. The structural basis for 14-3-3:phosphopeptide binding specificity. Cell. 1997;91:961-971.
38. Ottmann C, Marco S, Jaspert N, et al. Structure of a 14-3-3 coordinated hexamer of the plant plasma membrane H+ -ATPase by combining X-ray crystallography and electron cryomicroscopy. Mol Cell. 2007;25:427-440.
39. Parise LV, Criss AB, Nannizzi L, Wardell MR. Glycoprotein IIIa is phosphorylated in intact human platelets. Blood. 1990;75:2363-2368.
40. van Willigen G, Hers I, Gorter G, Akkerman JW. Exposure of ligand-binding sites on platelet integrin alpha IIB/beta 3 by phosphorylation of the beta 3 subunit. Biochem J. 1996;314(pt 3):769-779.
41. Lerea KM, Cordero KP, Sakariassen KS, Kirk RI, Fried VA. Phosphorylation sites in the integrin beta3 cytoplasmic domain in intact platelets. J Biol Chem. 1999;274:1914-1919.
42. Kim SM, Kwon MS, Park CS, et al. Modulation of Thr phosphorylation of integrin beta1 during muscle differentiation. J Biol Chem. 2004;279: 7082-7090.
43. Han DC, Rodriguez LG, Guan JL. Identification of a novel interaction between integrin beta1 and 14-3-3beta. Oncogene. 2001;20:346-357.
44. Rodriguez LG, Guan JL. 14-3-3 regulation of cell spreading and migration requires a functional amphipathic groove. J Cell Physiol. 2005;202:285-294.
45. Vinogradova O, Velyvis A, Velyviene A, et al. A structural mechanism of integrin alpha(IIb)beta(3) "inside-out" activation as regulated by its cytoplasmic face. Cell. 2002;110:587-597.
46. Vinogradova O, Vaynberg J, Kong X, Haas TA, Plow EF, Qin J. Membrane-mediated structural transitions at the cytoplasmic face during integrin activation. Proc Natl Acad Sci U S A. 2004;101: 4094-4099.

JBC ARTICLE

Phosphorylation of the α-chain in the integrin LFA-1 enables β2-chain phosphorylation and α-actinin binding required for cell adhesion

Received for publication, June 6, 2018, and in revised form, June 11, 2018 Published, Papers in Press, June 14, 2018, DOI 10.1074/jbc.RA118.004318

Farhana Jahan, Sudarrshan Madhavan, Taisia Rolova, Larisa Viazmina, Mikaela Grönholm[1,2], and Carl G. Gahmberg[1,3]

From the Faculty of Biological and Environmental Sciences, Molecular and Integrative Biosciences Research Program, University of Helsinki, Helsinki 00014 UH, Finland

Edited by Wolfgang Peti

The integrin leukocyte function–associated antigen-1 (LFA-1) plays a pivotal role in leukocyte adhesion and migration, but the mechanism(s) by which this integrin is regulated has remained incompletely understood. LFA-1 integrin activity requires phosphorylation of its β2-chain and interactions of its cytoplasmic tail with various cellular proteins. The α-chain is constitutively phosphorylated and necessary for cellular adhesion, but how the α-chain regulates adhesion has remained enigmatic. We now show that substitution of the α-chain phosphorylation site (S1140A) in T cells inhibits the phosphorylation of the functionally important Thr-758 in the β2-chain, binding of α-actinin and 14-3-3 protein, and expression of an integrin-activating epitope after treatment with the stromal cell–derived factor-1α. The presence of this substitution resulted in a loss of cell adhesion and directional cell migration. Moreover, LFA-1 activation through the T-cell receptor in cells expressing the S1140A LFA-1 variant resulted in less Thr-758 phosphorylation, α-actinin and talin binding, and cell adhesion. The finding that the LFA-1 α-chain regulates adhesion through the β-chain via specific phosphorylation at Ser-1140 in the α-chain has not been previously reported and emphasizes that both chains are involved in the regulation of LFA-1 integrin activity.

Integrins are transmembrane heterodimeric receptors that communicate in two directions across the plasma membrane and mediate interactions with other cells and the extracellular environment (1). Integrins can bind ligands, resulting in outside-in signaling, whereas inside-out signaling is initiated by ligand binding to nonintegrin receptors, such as chemokine receptors or the T-cell receptor (TCR),[4] which activate integrins through intracellular signaling (2, 3). The family of leukocyte-specific β2-integrins consists of four members that have a common β2-chain (CD18) and one of the α-chains (αL, CD11a; αM, CD11b; αX, CD11c; and αD, CD11d). The leukocyte function-associated antigen-1 heterodimer (LFA-1, αLβ2, CD11a/CD18) is primarily expressed on lymphocytes and binds to intercellular adhesion molecules (ICAMs). Mac-1 (macrophage 1 antigen, αMβ2, CD11b/CD18) is enriched in the myeloid lineage and is able to bind numerous ligands, among them ICAMs and complement protein iC3b. Complement receptor 4 (CR4, αXβ2, CD11c/CD18, p150,95) is expressed in monocytes, macrophages, and dendritic cells, as well as in some subsets of activated T and B cells. It is also capable of binding various ligands, including extracellular matrix molecules, cellular and soluble ligands, and denatured proteins (4, 5).

Integrins exist in at least three different conformations: closed, extended, and extended open, each of which possesses different ligand binding affinities and localization in cells. Integrins can modulate their adhesive properties within seconds. The activity of the integrins is for the main part regulated by the binding of different proteins to the cytoplasmic tails, which is mediated by integrin phosphorylation, clustering, and receptor cross-talk (6, 7).

The leukocyte integrin α-chains are constitutively phosphorylated, whereas the β2-chain becomes phosphorylated after activation through chemokines, the TCR, or phorbol esters (8–12). The integrin cytoplasmic domains are short and devoid of catalytic activity. Only a few cytoplasmic proteins have been found to specifically bind to the integrin α-chain cytoplasmic tails (13), whereas signaling, adaptor, and cytoskeletal linker proteins, including talin, kindlins, filamin, α-actinin, and 14-3-3 proteins, bind to the β2-integrin tails (14). The integrin β-chain cytoplasmic domains contain three conserved regions: the two NP*X*(Y/F) sequences and the serine/threonine sequence between them. Mutation of the β2-chain threonines abrogated cell adhesion, but initial experiments did not reveal phosphorylation of these (15). By using the phosphatase inhi-

This work was supported by the Academy of Finland, the Sigrid Jusélius Foundation, the Medicinska Understödsföreningen Liv och Hälsa, the Finska Läkaresällskapet, the Wilhelm and Else Stockmann Foundation, the Ruth och Nils-Erik Stenbäck Foundation, and the Magnus Ehrnrooth Foundation. The authors declare that they have no conflicts of interest with the contents of this article.

This article contains Videos S1 and S2.

[1] These authors contributed equally to this work.

[2] To whom correspondence may be addressed: Faculty of Biological and Environmental Sciences, Molecular and Integrative Biosciences Research Program, University of Helsinki, Helsinki, 00014 UH, Finland. Tel.: 358504486383; E-mail: mikaela.gronholm@helsinki.fi.

[3] To whom correspondence may be addressed: Faculty of Biological and Environmental Sciences, Molecular and Integrative Biosciences Research Program, University of Helsinki, Helsinki 00014 UH, Finland. Tel.: 358505399439; E-mail: carl.gahmberg@helsinki.fi.

[4] The abbreviations used are: TCR, T-cell receptor; LFA-1, leukocyte function-associated antigen-1; ICAM, intercellular adhesion molecule; PKC, protein kinase C; SDF, stromal cell–derived factor; PMA, phorbol 12-myristate 13-acetate; APC, allophycocyanin.

© 2018 Jahan et al. Published under exclusive license by The American Society for Biochemistry and Molecular Biology, Inc.
This is an Open Access article under the CC BY license.

Carl_G_190x270_mm_blokki_FINAL.indd 427 06-Aug-23 1:54:47 PM

bitor okadaic acid, strong threonine phosphorylation was observed after activation (9–11). The β2-chain is phosphorylated by protein kinase C (PKC) enzymes (16). The phosphorylation of Thr-758 on β2 leads to release of bound filamin and promotes binding of 14-3-3 proteins. Talin can bind both to the Thr-758 phosphorylated and unphosphorylated chain (17). The regulation of the association between α-actinin and the β2-chain is currently poorly understood, but it has been shown that α-actinin binding is enhanced by the activation of neutrophils and T cells (18, 19).

The leukocyte β2-integrin α-chains are phosphorylated on Ser-1140 (αL), Ser-1126 (αM), and Ser-1158 (αX) (see Fig. 1*A*), whereas αD phosphorylation has not been studied. The α-chain phosphorylation is important for leukocyte adhesion and intracellular signaling (20–22), but the mechanism(s) has remained unknown. We have now focused on the LFA-1 integrin and show that through the phosphorylation of the α-chain, it regulates the phosphorylation, conformation, and protein binding to the β2-chain in a specific manner. When cells expressed the LFA-1 S1140A mutation, there was no phosphorylation of the β2-chain on Thr-758, but there was a loss of both α-actinin and 14-3-3 binding and the presence of the integrin activation-reporter epitope L16 upon treatment with the chemokine stromal cell–derived factor-1α (SDF-1α). Binding of filamin increased. These mutant cells displayed abrogated cell adhesion to the LFA-1 ligand ICAM-1 and impaired directional migration. When LFA-1 S1140A mutated cells were activated through the TCR, the β2 phosphorylation and the binding of α-actinin to β2 decreased as compared with WT cells, whereas the presence of the activation epitope L16 was reduced only slightly as compared with WT cells. This decreased cell adhesion to ICAM-1. The results indicate an important role for integrin α-chains in the modulation of leukocyte functions by regulating β-chain phosphorylation, which results in altered cytoplasmic protein interactions, followed by changes in adhesion and migration.

Results

Phosphorylation of the LFA-1 α-chain regulates the phosphorylation of the β2-chain on Thr-758

Cytoplasmic protein interactions with the integrin β2-chain have been extensively studied, but the regulation of these has remained incompletely understood. We now show how the α-chain of LFA-1 regulates integrin functions by affecting the β2-chain. We used the Jβ2.7 human Jurkat T cell line expressing equal amounts of WT LFA-1 or LFA-1 containing the mutation S1140A at the known α-chain phosphorylation site (Fig. 1*B*). We have previously shown that this is the only phosphorylation site on the αL-chain and that a significant subset (~40%) of αL Ser-1140 is phosphorylated in both activated and nonactivated cells (9, 20). When the phosphorylation site serine was substituted by alanine, phosphorylation could not be recognized by a Ser(P)-1140–specific antibody (Fig. 1*C*). Cells expressing WT LFA-1 could bind ICAM-1 after activation by chemokines such as SDF-1α or through the TCR. Cells expressing the αL S1140A mutant were unable to bind ICAM-1 after SDF-1α activation and showed much reduced binding after activation with anti-CD3 (Fig. 1*D*). WT cells aggregated on an SDF-1α–coated surface and SDF-1α–activated cells spread on ICAM-1, which was not seen with cells expressing the LFA-1 S1140A mutant (Fig. 1*E*).

Phosphorylation of the β2-chain Thr-758 is seen only after activation, *e.g.* by SDF-1α or through the TCR (9–11). In LFA-1 WT expressing cells, there was no phosphorylation of Thr-758 on the β2-chain without activation, but after treatment with SDF-1α or TCR, a strong label was seen. Importantly, no phosphorylation occurred on β2 Thr-758 in cells expressing the αL S1140A mutant α-chain activated with SDF-1α. In cells activated through the TCR, a significantly weaker labeling of the Thr-758 was obtained in mutant cells as compared with WT cells (Fig. 1, *F* and *G*).

Phosphorylation of Ser-1140 on the LFA-1 α-chain affects the binding of cytoskeletal proteins to the β2-chain

We further tested whether the α-chain mutation affects the interaction with proteins known to bind to the β2-chain and to be involved in cell adhesion. Fig. 2*A* shows immunoprecipitations from Jurkat cells under three conditions; nonactivated, SDF-1α–activated, or anti-CD3–activated cells. Western blots of supernatants showed equal amounts of proteins in WT and S1140A-expressing cells. Proteins coprecipitated with LFA-1 in the WT and mutant cell line are shown in the IP IB4 lane and quantified from three separate experiments as shown below (Fig. 2*B*). A significantly reduced binding of α-actinin and 14-3-3 was seen in SDF-1α–activated mutant cells compared with WT cells. Talin binding was consistently reduced, but not significantly. Filamin binding was increased. Activation of the TCR by anti-CD3 resulted in a significant reduction in talin binding. α-Actinin and 14-3-3 binding was reduced, but not significantly (Fig. 2, *A* and *B*).

The most significant difference between αL WT and S1140A-expressing cells after SDF-1α was seen for α-actinin binding to β2. The α-actinin–binding site on the LFA-1 integrin has been mapped to the β2-chain amino acids 736–745, partly overlapping with the talin membrane-proximal binding site (23) (Fig. 1*A*). To verify that there is no α-actinin-binding site on αL, synthetic peptides of the cytoplasmic chains of αL, αL/Ser(P)-1140, β2, or β2/Thr(P)-758 were linked to Sepharose beads, and Jurkat cell lysates were added. Bound proteins were separated by SDS-PAGE and analyzed by immunoblotting for α-actinin, 14-3-3, and talin (Fig. 2*C*). In another experiment, peptides were spotted on a nitrocellulose membrane, and purified α-actinin was added. After extensive washing, protein binding was determined with specific antibodies. Experiments verified that α-actinin binds to the β2 or β2/Thr(P)-758 peptides but not to αL or αL/Ser(P)-1140 (Fig. 2*D*).

To study the differences in LFA-1-mediated adhesion complex formation in cells adhering to the ligand, the complexes from Jurkat cells binding to coated ICAM-1 or poly-L-lysine were purified, and their protein content was analyzed. Proteins found in the adhesion sites of LFA-1 WT-expressing cells and bound to ICAM-1 included the integrin β2 and αL chains, α-actinin, 14-3-3, and talin, after both SDF-1α and anti-CD3 activation. In contrast, ICAM-1 adhesion complexes from LFA-1 S1140A-expressing cells contained none of the proteins

Carl_G_190x270_mm_blokki_FINAL.indd 428 06-Aug-23 1:54:48 PM

Integrin α-chain regulates the β-chain

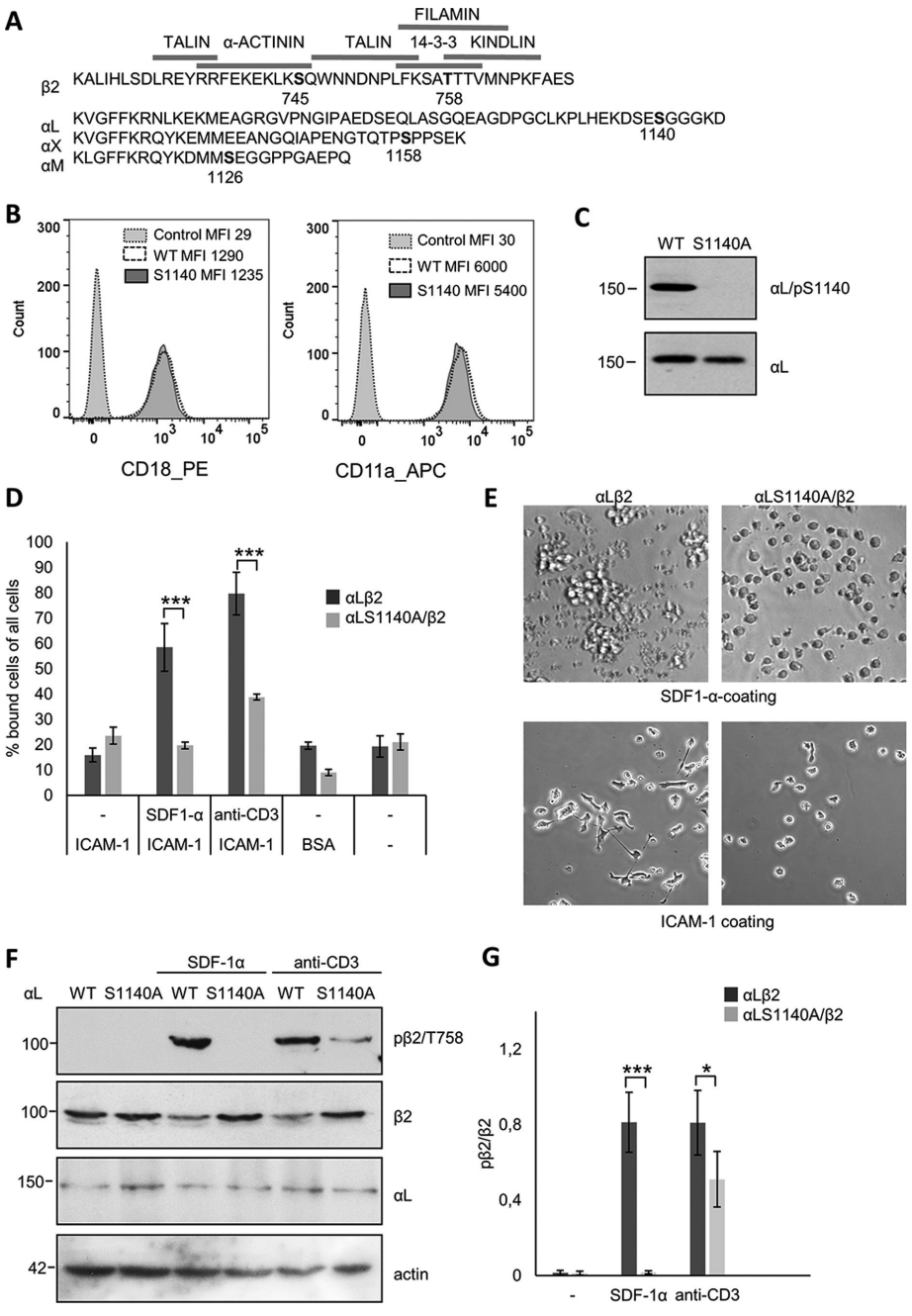

Carl_G_190x270_mm_blokki_FINAL.indd 429 06-Aug-23 1:54:48 PM

found in WT LFA-1–expressing cells activated with SDF-1α, indicating that stable adhesion complexes were not formed (Fig. 2*E*). Instead, these proteins were detected in the Western blotting of unbound cells (Fig. 2*F*). After anti-CD3 activation of S1140A-expressing cells, the same proteins were present in the ICAM-1 adhesion complexes, although less than in WT LFA-1–expressing cells. The proteins in the adhesion complexes were quantified from three separate experiments (Fig. 2*G*). This result indicates that Jβ2.7 LFA-1 S1140A-expressing cells can be at least partly activated to bind ligand by anti-CD3, which is not the case for SDF-1α activation (Figs. 1, *D* and *E*, and 2*E*). Jβ2.7 Jurkat cells lacking LFA-1 expression did not bind to ICAM-1, which indicates that binding takes place solely through LFA-1 (not shown).

A negative charge on both the α- and β2-chain phosphorylation sites increases binding of α-actinin to LFA-1

We were not able to transfect Jβ2.7 cells with the αL S1140D mutant and therefore used COS7 cells, which have been shown to express functional heterodimeric integrins on their cell surface after transfection with β2-integrins (24). The αL-chain is phosphorylated in COS7 cells on Ser-1140 (20). COS7 cells do not contain the SDF-1α receptor or TCR, but integrins can be activated by phorbol esters. PMA activation of COS7 cells transfected with WT LFA-1 led to increased Thr-758 phosphorylation on β2 (Fig. 3*A*) and increased α-actinin and 14-3-3 binding (Fig. 3*B*). COS7 cells were then transfected with WT αL, the nonphosphorylatable S1140A or the S1140D mutant that mimics phosphorylated Ser-1140. β2 Thr-758 was phosphorylated in cells expressing the S1140D mutant but not in cells expressing S1140A (Fig. 3*A*). Lysates from PMA-activated cells were immunoprecipitated with the LFA-1 antibody IB4, and the precipitates were immunoblotted for α-actinin, β2, and αL. Binding of α-actinin to LFA-1 was reduced in LFA-1 S1140A-expressing cells in accordance with the results from Jβ2.7 cells. The LFA-1 S1140D mutation resembled that of WT LFA-1 phosphorylated on Ser-1140, supporting the model that the negative charge on the α-chain is important for β2 Thr-758 phosphorylation, enabling stronger α-actinin binding (Fig. 3*C*). Mutation of Thr-758 to alanine resulted in decreased binding of α-actinin (Fig. 3*D*). Cells expressing β2 T758D and the S1140A αL-chain were able to bind α-actinin; however, binding was further increased when a negative charge was present on both chains, represented by cells expressing αL WT Ser-1140 and β2 T758D. αL S1140D-expressing cells did not bind α-actinin without PMA activation (Fig. 3*E*). This verifies that the negative charge on the αL-chain Ser-1140 is important for β2 Thr-758 phosphorylation and for increased α-actinin binding, which requires the phosphorylated β2 Thr-758.

We then extended the study to another α-chain, αXβ2. This integrin is expressed in myeloid cells. We therefore stably expressed αXβ2 in the myeloid/erythroleukemic cell line K562. Activation of these cells with SDF-1α resulted in phosphorylation of β2 Thr-758 in WT αXβ2-expressing cells, whereas no phosphorylation of β2 Thr-758 was detected in cells expressing the α-chain phosphorylation mutant αX S1158A (Fig. 3*F*). This result further emphasizes the role of α-chain phosphorylation for β2-chain phosphorylation. The double band could mean that some β2-chains are phosphorylated on additional sites (16).

Phosphorylation of αL affects the cellular localization of α-actinin and the activation epitope of LFA-1

We next studied whether there is a difference in the localization of α-actinin in cells expressing LFA-1 WT or S1140A. The cells were activated with SDF-1α or anti-CD3 and allowed to adhere to ICAM-1, fixed, and stained for β2, for α-actinin, or by phalloidin (Fig. 4, *A*, and *B*). In cells expressing WT LFA-1, α-actinin localized to the membrane and ruffling edges and colocalized with β2 and phalloidin both in SDF-1α and anti-CD3 activated cells (Pearson's correlation coefficient for β2 and α-actinin at the membrane was 0.78 for SDF-1α and 0.70 for anti-CD3 activation). Colocalization was also seen in anti-CD3–activated cells expressing the S1140A mutant, but less in mutant cells activated with SDF-1α where α-actinin staining was more diffused (Pearson's correlation coefficient for β2 and α-actinin at the membrane was 0.47 for SDF-1α and 0.69 for anti-CD3 activation).

The effect of αL S1140A phosphorylation on LFA-1 activation was next identified by labeling cells with the NKI-L16 antibody recognizing the fully active epitope L16 of LFA-1 (25). Cells expressing the WT LFA-1 activated with SDF-1α were strongly positive for the L16 epitope, which was not detected in the S1140A-expressing cells. In contrast, L16 positivity was detected after anti-CD3 activation of S1140A-expressing cells (Fig. 4, *C* and *D*).

Phosphorylation of the LFA-1 α- and β-chains and binding of α-actinin are needed for chemotaxis

The linking of integrins to the actin cytoskeleton by α-actinin is important for cell adhesion and migration (26). Cell adhesion was studied by transfecting Jurkat cells expressing LFA-1 with a β2-peptide containing the α-actinin–binding site of β2, which blocks the interaction between α-actinin and the β2-chain but does not affect talin binding (19). Static adhesion to ICAM-1 was inhibited by β2-peptide transfection into cells activated by SDF-1α, but not by the control peptide (Fig. 5*A*). To analyze the role of the α-actinin/integrin interaction in migration, Jurkat

Figure 1. Phosphorylation of Ser-1140 on αL regulates phosphorylation of β2 on Thr-758. *A*, amino acid sequence of the β2, αL, αM, and αX chains with the known phosphorylation sites in bold and the binding domains of talin, α-actinin, kindling, and 14-3-3 indicated. *B*, Jβ2.7 cells lacking αL expression (control) or expressing LFA-1 WT or S1140A were stained with β2 (CD18-PE) or αL (CD11a-APC) and analyzed by flow cytometry. Mean fluorescence intensity (*MFI*) is shown for each graph. *C*, Jβ2.7 cells expressing αL WT or S1140A were analyzed by Western blotting and immunoblotted with αL/pS1140 or αL antibodies. *D*, Jβ2.7 cells expressing αL WT or S1140A were activated with SDF-1α or anti-CD3 and allowed to adhere to ICAM-1, and bound cells were quantified. *E*, in the *upper panels*, Jβ2.7 cells expressing αL WT or αL S1140A were allowed to adhere to a SDF-1α–coated surface. In the *lower panels*, SDF-1α–activated cells were allowed to adhere to ICAM-1 and spread for 1 h. *F*, lysates of Jβ2.7 cells expressing αL WT or S1140A were activated with SDF-1α or anti-CD3, analyzed by SDS-PAGE, and immunoblotted with β2/Thr(P)-758, β2, αL, or actin as a loading control. *G*, the amount of β2/Thr(P)-758 per β2 was quantified from five separate experiments. Molecular mass markers (kDa) are shown to the *left* of the blots. *, $p < 0.05$; ***, $p < 0.005$.

Carl_G_190x270_mm_blokki_FINAL.indd 430 06-Aug-23 1:54:48 PM

Integrin α-chain regulates the β-chain

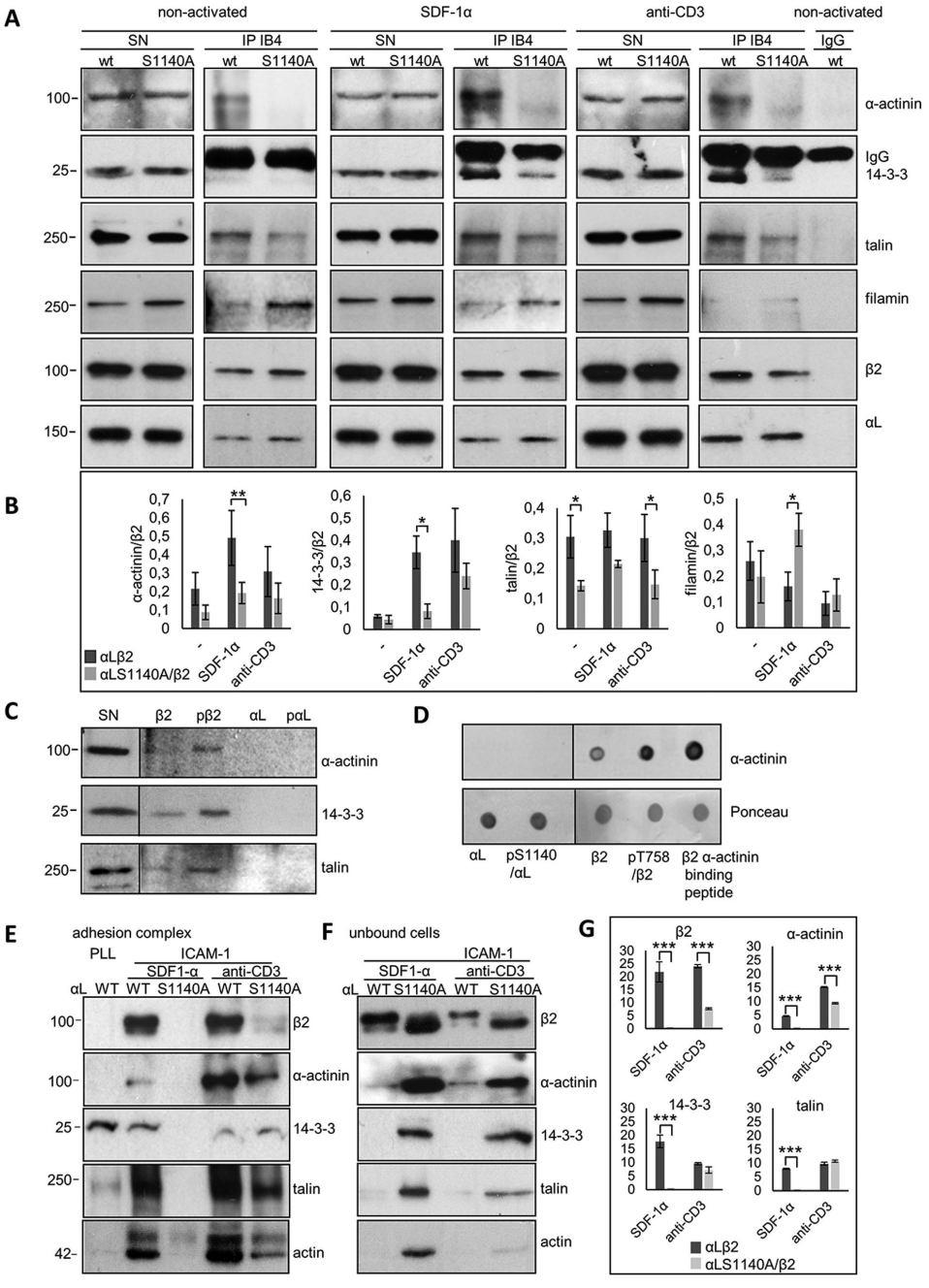

Carl_G_190x270_mm_blokki_FINAL.indd 431 06-Aug-23 1:54:48 PM

cells expressing WT LFA-1 or LFA-1 S1140A were allowed to migrate over an ICAM-1–coated surface toward SDF-1α. In the mutant cells, with reduced interaction between the integrin and α-actinin, directional migration was impaired (Fig. 5*B* and videos S1 and S2). Cells transfected with the β2 peptide, but not the control peptide, were also unable to migrate (Fig. 5*B*). Mutant cells were not able to strongly adhere to ICAM-1 and could be washed off by pipetting, which was not the case for WT cells. The mutant cells formed extensions but did not spread or become polarized to the same extent as WT cells and were not able to move toward the chemokine gradient. Instead they ruffled in different directions, but the cell body remained stationary (Fig. 5, *C* and *D*). Both the accumulated and euclidean distances, as well as directionality, were reduced in cells with impaired α-actinin–integrin binding (Fig. 5*E*).

Discussion

Integrin activity has to be tightly regulated to allow rapid and precise changes between different activation states. The roles of the β-chain cytoplasmic tails have been extensively studied and shown to be essential for integrin function. Chemokines, such as SDF-1α, bind to their receptors resulting in phospholipase C activation followed by signaling through CalDag, Rap1, and RapL (27). The proximal signaling events from the TCR are different and include the Lck tyrosine kinase (28), which then phosphorylates the ZAP-70 kinase, and phospholipase Cγ (27). PKC enzymes then become activated in both pathways and phosphorylate Thr-758 on β2. Phosphorylation of the β2-chain is known to regulate the affinity for different binding proteins (7). Filamin binds primarily to the unphosphorylated β2-chain, whereas β2 phosphorylated on Thr-758 binds 14-3-3 proteins and initiates intracellular signaling through Tiam1–Rac1 and inhibitory signaling to α4β1 (12, 17, 29, 30).

Previous work indicates a regulatory role for the membrane-proximal part of α-chain cytoplasmic domains in integrin regulation. The proximal portions of both α and β cytoplasmic domains are α-helical and associate with each other (31). The GFFKR motif in the α-chain is well conserved and is important in keeping the integrins in a nonadhesive state by interacting by ionic bonds with the β-chain. When this motif is deleted or mutated, integrins become active (32–37). Binding of talin can perturb the membrane-proximal association, disrupting the intersubunit interactions, which results in activation (38, 39). In fact, most of the known negative regulators of integrins bind to the conserved membrane-proximal site (40–42).

The α-chain membrane distal regions vary in lengths and sequences, and their roles in integrin activation have been less defined. Deletion of the membrane distal regions of some α-chains affects cell adhesion and spreading, but similar deletions in other α-chains have no effect on adhesion (15, 43–49). This shows that there are different regulatory roles of the membrane distal regions among different integrins. Interestingly, deletion of the αL membrane distal part diminishes talin- and kindlin-induced integrin conformational change and ligand binding (50). We have previously shown that β2-integrin α-chain phosphorylation is needed for adhesion after activation induced by chemokine, ligand, or active Rap1 (20–22). The regulatory mechanisms have not been known. We now show that phosphorylation of the α-chain of LFA-1 is needed for β2-chain phosphorylation and its protein interactions.

A significant part of the LFA-1 α-chain is phosphorylated on the single site Ser-1140 (9, 20), and mutation of the serine residue to alanine inhibited or reduced phosphorylation of Thr-758 in the β2-chain. Treatment with the phosphatase inhibitor okadaic acid increased α-chain phosphorylation (9), indicating that there is a cycle of phosphorylation and dephosphorylation events of the α-chain. This could, in turn, regulate the phosphorylation of Thr-758 of the β2-chain, enabling rapid cell adhesion and deadhesion for example during movement. We extended the study to include another α-chain, αX, which is known to be phosphorylated on Ser-1158 (22). Phosphorylation of β2 Thr-758 was impaired also in myeloid/erythroid K562 cells expressing αX S1158A.

Although activation of cells with both SDF-1α and through the TCR results in phosphorylation of Thr-758 on β2, differences were seen between the LFA-1 WT and S1140A-expressing cells. LFA-1 β2 could not be phosphorylated on Thr-758, nor bind to ICAM-1 in mutant cells activated with the chemokine, but showed only a reduced phosphorylation compared with WT after anti-CD3 activation. This reflects the differences in signaling downstream of the TCR and chemokine receptor and indicates that additional factors play a role in the regulation of β2 phosphorylation. In WT expressing cells, Thr-758 on β2 is readily phosphorylated upon SDF-1α treatment, and S1140D is functionally similar evidently because of the negative charge at position Ser-1140.

The S1140A α-chain phosphorylation mutation markedly decreased α-actinin binding to the β2-chain and impaired cell migration toward the SDF-1α chemokine. Decreased binding was also seen with 14-3-3 and an increase in binding of filamin, which is most likely a cause of decreased Thr-758 phosphorylation in the mutant cell line. There was also a decrease in talin binding in the mutant cells activated with anti-CD3. Because the most prominent difference in binding was seen with α-actinin, we investigated this further. α-Actinin is essential for cell migration (26). Phosphorylation of both αL and β2 regulated the binding between α-actinin and LFA-1. The strongest binding occurred when both αL Ser-1140 and β2 Thr-758 were phosphorylated.

Figure 2. α-Chain phosphorylation regulates binding of cytoplasmic interaction partners to β2 differently. *A*, lysates of Jβ2.7 cells expressing αL WT or S1140A were not treated or activated with SDF-1α or anti-CD3, immunoprecipitated with the LFA-1 antibody IB4, and immunoblotted for α-actinin, 14-3-3, talin, filamin, β2, or αL. *B*, the amount of coprecipitated proteins per immunoprecipitated β2 was quantified from three separate experiments. *C*, full-length cytoplasmic peptides of αL, αL/Ser(P)-1140, β2, or β2/Thr(P)-758 were bound to beads and Jurkat cell lysate added. Bound proteins were analyzed by immunoblotting with indicated antibodies. *D*, peptides were spotted on nitrocellulose, and purified α-actinin was added. After washing, binding was assessed with the α-actinin antibody. *E* and *F*, Jβ2.7 cells expressing αL or αL S1140A were allowed to adhere on poly-L-lysine or ICAM-1 and adhesion complexes (*E*) or unbound cells (*F*) collected, and lysates were analyzed by immunoblotting using indicated antibodies. *G*, the amount of protein found in the adhesion complexes was quantified from three separate experiments. *SN*, supernatant. Molecular mass markers (kDa) are shown to the *left* of the blots. *Lines* depict borders between two separate gels. *, $p < 0.05$; **, $p < 0.01$.

Carl_G_190x270_mm_blokki_FINAL.indd 432 06-Aug-23 1:54:49 PM

Integrin α-chain regulates the β-chain

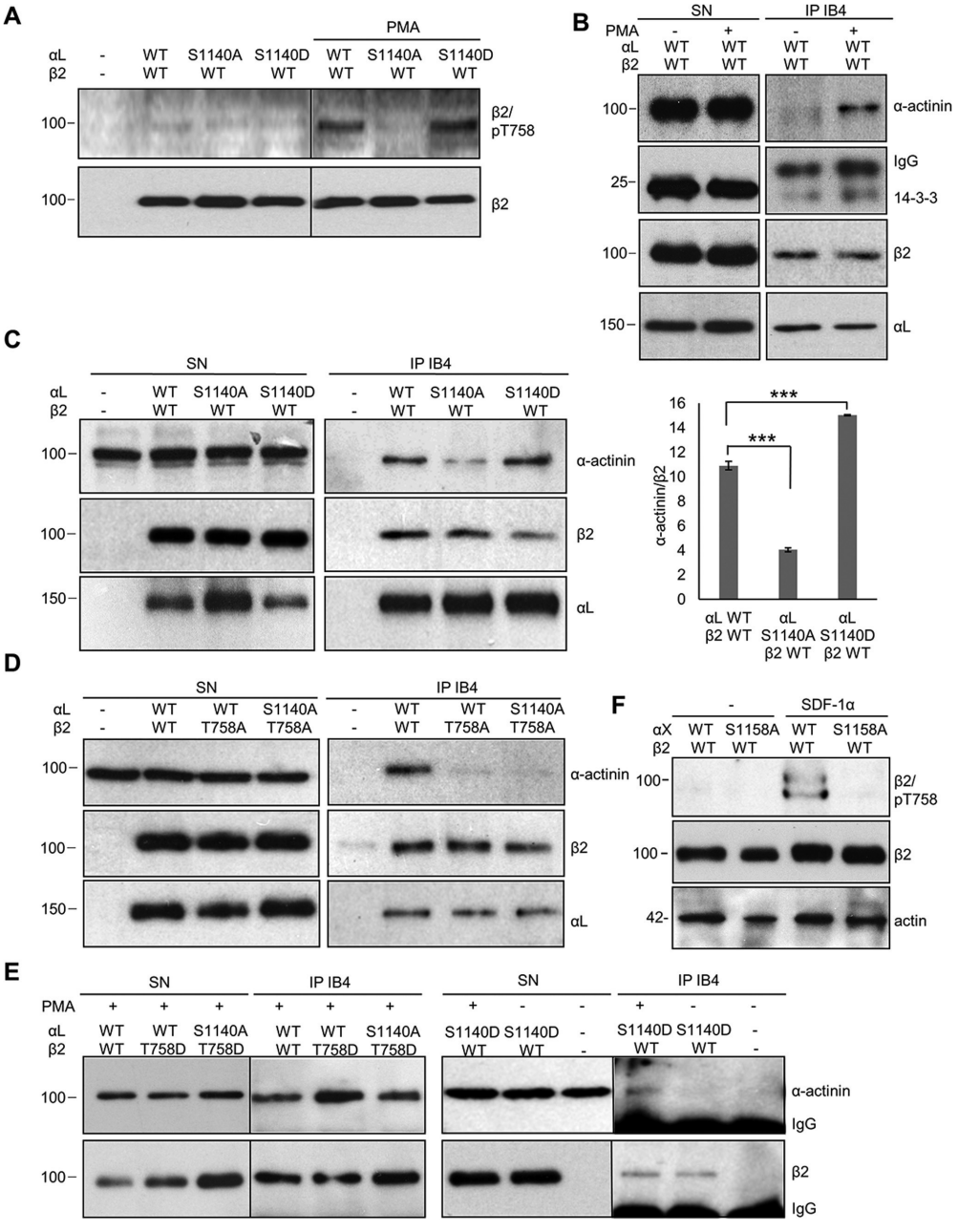

Carl_G_190x270_mm_blokki_FINAL.indd 433 06-Aug-23 1:54:49 PM

A negative charge on the αL-chain, either by Ser-1140 phosphorylation or by expressing the S1140D mutant, was needed to enable phosphorylation of the β2 Thr-758. α-Actinin was able to bind the β2-chain also without α-chain phosphorylation only if there was a negative charge on Thr-758, as in the β2 T758D mutant, which could override the S1140A mutation and bind α-actinin. Binding was, however, stronger with a negative charge on both chains, indicating that the α-chain also directly regulates α-actinin binding. The αL cytoplasmic tail forms a triple-helical structure. Helix 3 makes contacts with both helices 1 and 2, and helices 1 and 3 are in contact with the β2-tail. Interestingly, Ser-1140 is located in helix 3 at the negatively charged surface of the αL tail, and its phosphorylation can enhance the negative charge of this surface (51). We conclude that αL Ser-1140 phosphorylation is required for β2 Thr-758 phosphorylation, possibly by making the site accessible to PKC enzymes, and as the chains move apart allowing new cytoskeletal interactions, as shown by increased α-actinin binding. This, in turn, would have an effect on cytoskeleton-mediated processes in cells.

We show that LFA-1 S1140A-expressing cells with impaired α-actinin binding exhibited impaired directional migration toward the SDF-1α chemokine. Cells expressing the LFA-1 S1140A mutant had a rounded and less polarized morphology compared with WT expressing cells. The same could be seen with cells where the β2-α-actinin interaction was disrupted by a peptide corresponding to the α-actinin– binding site on β2. This peptide has shown selectivity in binding α-actinin and not talin, although it contains part of the talin membrane-proximal site (19). Impaired migration in S1140A-expressing cells appears to be a result of the lack of α-actinin linking β2 to the cytoskeleton, which is known to be important for cell migration. A conserved region (residues 733–742) in the β2 cytoplasmic domain is critical for its cytoskeletal association (34). This region overlaps with the mapped α-actinin site (residues 736–746). Furthermore, a regulatory domain in β2 between residues 748–762 inhibits the constitutive association of the β2 tail with α-actinin (23). This sequence contains both the Thr-758 phosphorylation site and binding sites for talin and 14-3-3. Phosphorylation of Ser-1140 on αL and Thr-758 on β2 may release the inhibitory structure of the β2-chain, resulting in α-actinin binding, activation of the integrin binding site as shown with the NKI-L16 antibody, and migration of cells. We cannot, however, rule out the possibility that the reduced migration of LFA-1 S1140A-expressing cells is due to impaired binding of other proteins to the α-chain. Cells lacking α-actinin have a decreased ability to translocate but adhere more strongly to ICAM-1 (19). In our migration experiment, the LFA-1 S1140A-expressing cells were able to weakly adhere and make membrane projections but did not migrate toward the chemokine. This indicates that α-actinin may link the active integrin to the cytoskeleton to mediate directional migration.

At the leading edge, adhesions are constantly turned over, and the cell membrane attaches and then detaches from ICAM-1 when making new ligand contacts. Phosphorylation–dephosphorylation of αL Ser-1140 and αX Ser-1158 could provide a fast way of regulating integrin–α-actinin cytoskeleton linkage, dynamic adhesion, and migration. Our data establish an essential role for the α-chain cytoplasmic domain phosphorylation in the regulation of the β-chain and thus integrin activity.

Experimental procedures

Reagents and antibodies

Human ICAM-1–Fc and SDF-1α were from R&D Systems (Minneapolis, MN). The following antibodies were used: MHM24 (Developmental Studies Hybridoma Bank (DSHB), Iowa City, IA), anti-CD3 (Immunotools, Friesoythe, Germany), anti-talin 8d4 (Sigma–Aldrich), mouse anti–α-actinin clone AT6/172 and anti-filamin mAb 1678 (Merck Millipore), rabbit anti-α-actinin EP2527Y (Abcam, Cambridge, UK), pan anti-14-3-3 (Santa Cruz Biotechnology, Dallas, TX); a polyclonal rabbit antiserum against the β2-chain phosphorylated on Thr-758 was produced by GenicBio Ltd. (Shanghai, China), and NKI-L16 was from Acris Antibodies. The R2E7B antibody against human β2 was previously described (52). IB4, which recognizes the heterodimeric forms of β2-integrins, was a gift from M. Arnaout (Massachusetts General Hospital, Boston, MA). Okadaic acid (CAS 78111-17-8) was from Santa Cruz Biotechnology, and horseradish peroxidase–linked antibodies against mouse and rabbit IgG were from Cell Signaling (Danvers, MA). APC-conjugated mouse secondary antibody was from Immunotools. CD11a-APC– and CD18-PE–conjugated antibodies were from BD Biosciences.

Cell cultures, immunoprecipitation, and immunoblotting

COS7 cells were cultured in Dulbecco's modified Eagle's medium and the human T-cell lymphoma cell line Jβ2.7, which lacks the αL-chain (53), was grown in RPMI 1640 supplemented with 10% FBS, 2 mM L-glutamine, and 100 units/ml penicillin/streptomycin. Jβ2.7 cells expressing WT αL or S1140A αL together with β2 have been described (7). K562 cells stably expressing WT αX or αX S1158A together with β2 have been previously described (22). K562 cells were cultured in RPMI medium supplemented with 0.5 mg/ml G418 (Calbiochem/Merck Millipore), 10% FBS, 2 mM L-glutamine, and 100

Figure 3. Phosphorylations (negative charges) on both the α- and the β2-chains regulate α-actinin binding to LFA-1. *A*, COS7 cells were transfected with WT αL, αL/S1140A, or αL/S1140D together with WT β2 and cells activated with PMA or left untreated. Lysates were immunoblotted for β2/Thr(P)-758 or β2, showing that PMA activation increases β2 Thr-758 phosphorylation in WT αL and αL/S1140D-expressing cells. *B*, lysates of PMA-activated cells expressing WT LFA-1 were immunoprecipitated with the LFA-1 antibody IB4, and precipitates were immunoblotted for α-actinin, 14-3-3, β2, or αL. *C*, COS7 cells were transfected with the αL WT, or the S1140A or S1140D mutant, and β2 and lysates were immunoprecipitated with the LFA-1 antibody IB4, and precipitates were immunoblotted for α-actinin, β2, or αL. The amount of coprecipitated α-actinin per immunoprecipitated β2 was quantified from three separate experiments. *D*, COS7 cells were transfected with LFA-1 WT or the phosphorylation mutants αL/S1140A or β2/T758A; lysates were immunoprecipitated with IB4; and precipitates were immunoblotted for α-actinin, β2, or αL. *E*, COS7 cells were transfected with the WT αL, αL/S1140A, or αL/S1140D and WT β2 or β2/T758D; activated with PMA; or left untreated and analyzed as above. *F*, K562 cells were transfected with αX WT or the phosphorylation mutant S1158A and β2, and lysates were immunoblotted with β2/Thr(P)-758 or β2. The amount of β2/Thr(P)-758 per β2 was quantified from three separate experiments. *SN*, supernatant. Molecular mass markers (kDa) are shown to the *left* of the blots. ***, $p < 0.005$.

Carl_G_190x270_mm_blokki_FINAL.indd 434 06-Aug-23 1:54:50 PM

Integrin α-chain regulates the β-chain

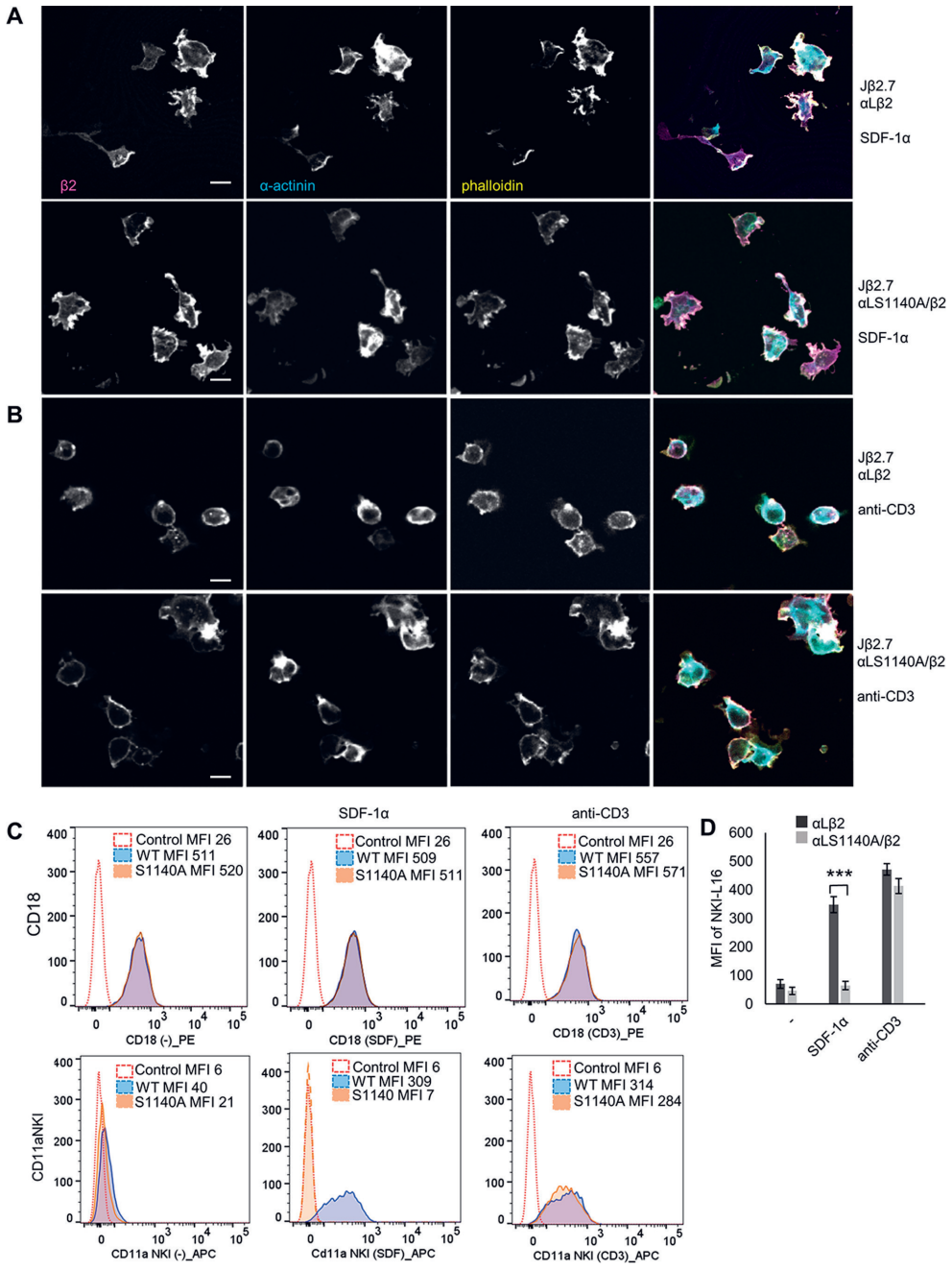

ASBMB

Carl_G_190x270_mm_blokki_FINAL.indd 435 06-Aug-23 1:54:50 PM

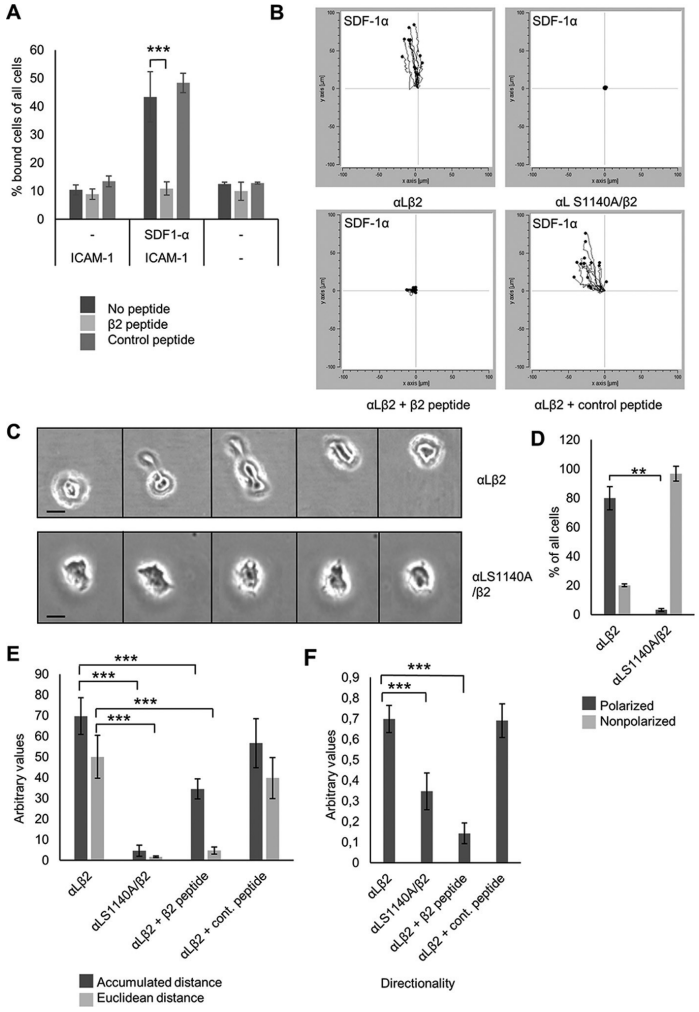

Figure 5. Phosphorylation of αL and α-actinin binding affect cell migration toward the chemokine SDF-1α. *A*, Jβ2.7 cells expressing αL WT or S1140A with or without SDF-1α activation transfected with the β2-peptide or control peptide were allowed adhere on ICAM-1, and bound cells were quantified. *B*, Jβ2.7 cells expressing αL WT or S1140A were allowed to migrate over an ICAM-1 covered surface toward the chemokine SDF-1α. Tracks of 15 migrating cells of one representative experiment are shown. *C*, bright-field images of migrating Jβ2.7 cells expressing αL WT or S1140A at five different time points (pictures taken at 30-min intervals). The *scale bar* represents 10 μm. *D*, quantification of polarized and nonpolarized cells from 20 screens. *E* and *F*, accumulated and euclidean distance (*E*) and directionality of migration (*F*) were quantified by a chemotaxis and migration tool for 50 cells from three experiments. **, $p < 0.01$; ***, $p < 0.005$.

units/ml penicillin-streptomycin. The cells were treated with SDF-1α (50 ng/ml) for 20 min, anti-CD3 (10 μg/ml) for 30 min or left untreated. For immunoblotting with the Thr(P)-758/β2 antibody, cells were treated with 1 μg/ml of okadaic acid for 5 min. Cells were washed once with cold PBS, lysed on ice in 2% immunoprecipitation assay buffer (50 mM Tris-HCl, pH 7.8, 150 mM NaCl, 1% Triton X-100, 1% Nonidet P-40, 15 mM $MgCl_2$, and 5 mM EDTA) with protease and phosphatase inhib-

Figure 4. Phosphorylation of αL affects α-actinin localization. Jβ2.7 cells expressing αL WT or S1140A were activated with SDF-1α (*A*) or anti-CD3 (*B*), allowed to adhere to ICAM-1, fixed, and stained for β2, α-actinin, and phalloidin. The *scale bar* represents 10 μm (*C*). Jβ2.7 cells lacking αL expression (control) or cells expressing αL WT or S1140A were left untreated or activated with SDF-1α or anti-CD3. The cells were stained for β2 (CD18-PE) or NKI-L16–APC recognizing the activated form of the integrin and analyzed by flow cytometry. Mean fluorescence intensity (*MFI*) is shown for each graph and quantification of mean fluorescence intensity from three separate experiments (*D*). ***, $p < 0.005$.

Carl_G_190x270_mm_blokki_FINAL.indd 436 06-Aug-23 1:54:50 PM

itors (Roche Applied Science) for 30 min. Lysates were centrifuged at 20,000 × *g* for 1 h at 4 °C. Prewashed protein G-Sepharose beads were added for 2 h at 4 °C. The unbound fraction was mixed with IB4 or α-actinin antibody overnight at 4 °C, and protein G-Sepharose beads for another 2 h at 4 °C. The beads were washed three times with 1% immunoprecipitation assay buffer (50 mM Tris-HCl, pH 7.8, 150 mM NaCl, 0.5% Triton X-100, 0.5% Nonidet P-40, 15 mM $MgCl_2$, and 5 mM EDTA), and bound proteins were eluted with Laemmli sample buffer, separated on SDS-PAGE, immunoblotted, and detected using ECL (Pierce). The figures show one representative picture of at least three experiments. The amount of coprecipitated proteins per immunoprecipitated β2 was quantified from three separate experiments by ImageJ. For the calculation of *p* values, one-way analysis of variance (Bonferroni post hoc) or unpaired Student's *t* test was used. The mean standard deviations are given in the figures.

Adhesion complex isolation

Integrin adhesion complexes were isolated as previously described (54). Briefly, the Jurkat Jβ2.7 cells (5 × 10^6/2.5 ml) activated with SDF-1α for 15 min or anti-CD3 for 30 min were allowed to adhere on ICAM-1 (3 μg/ml) or poly-L-lysine–coated (0.01%) 6-cm plates for 1 h. The cells were washed once with prewarmed RPMI 1640 and 6 mM dimethyl 3,3′-dithiobispropionimidate cross-linker (Fisher Scientific) was added for 15 min in the incubator. 3,3′-Dithiobispropionimidate was quenched with 1 M Tris-HCl, pH 8, for 5 min at room temperature. The cells were carefully washed once with ice-cold PBS and once with modified radioimmune precipitation assay buffer (50 mM Tris-HCl, pH 7.6, 150 mM NaCl, 5 mM disodium EDTA, pH 8,0, 5% SDS, 1% Triton X-100, 1% sodium deoxy cholate). 100 μl of adhesion recovery solution (125 mM Tris-HCl, pH 6.8, 1% SDS, 150 mM DTT) was added, and adhesion complexes were scraped off and collected. Four volumes of −20 °C acetone were added to each sample, which were stored at −80 °C. Precipitated proteins were centrifuged for 20 min at 160,00 × *g*, and the pellets were resuspended in reducing Laemmli sample buffer and heated at 85 °C for 5 min.

Cell transfections

αL was subcloned into the pcDNA3.1 vector (Thermo Scientific). β2 in the pcDNA3.1 vector was from Addgene (Cambridge, MA) (plasmid 8640 (55); the αX WT and αX S1158A mutant in the pcDM8 vector have been described (22). The mutations S1140A and S1140D in αL were introduced by site-directed mutagenesis (56). All constructs were checked by sequencing. COS7 cells were transiently cotransfected using FuGENE HD transfection reagent according to the manufacturer's instructions (Promega, Madison, WI) and harvested 48 h after the transfection.

The α-actinin–binding site-containing the β2 peptide HLSDLREYRRFEKEKLKSC and the β2 cytoplasmic chain peptides with and without phosphate on Thr-758 C-NNDNPLFKSA(pT)-TTVMNPK and C-NNDNPLFKSATTTVMNPK were obtained from GenicBio Ltd. (Shanghai, China). As a control, the P621 peptide VDVDSDGSTDLVIGA was used. The β2 peptide containing the α-actinin–binding site or the control peptide P621 was transfected into Jβ2.7 expressing LFA-1 WT using Pro-Ject protein transfection reagent kit according to the manufacturer's instructions (Thermo Scientific). Briefly, 5 μg of peptide in 50 μl of PBS was added to 10 μl of the dried Pierce reagent tube, incubated for 5 min at room temperature, and added to 500,000 cells/ml in RPMI 1640 without serum in a six-well plate. After 4 h, the cells were washed twice with PBS and stored in RPMI 1640.

Immunofluorescence

Jurkat Jβ2.7 cells were activated with SDF-1α (50 ng/ml) for 20 min or anti-CD3 (10 μg/ml) for 30 min and allowed to adhere on ICAM-1 (6 μg/ml) coated 8-well Ibidi chambers (μ-Slide 8-well, ibiTreat) for 30 min and fixed in 4% formaldehyde for 20 min at 37 °C. The plates were washed twice with PBS. The cells were stained with primary antibodies against β2 (R2E7B) and α-actinin (EP2527Y) and Alexa Fluor 488 or 633 secondary antibodies or TRITC-phalloidin (Invitrogen), washed, and mounted with Prolong Gold antifade reagent (Thermo Scientific). The Images were acquired using a Leica TCS SP8 STED 3X CW 3D confocal microscope (Wetzlar, Germany) with the HC PL Apo 20×/0.75 IMM CORR CS_2 (glycerol) objective at room temperature and analyzed with Leica Application Suite and Fiji (National Institutes of Health). For colocalization studies, confocal images were automatically analyzed, and individual cells were manually selected as region of interest.

Flow cytometry

Jurkat Jβ2.7 cells were activated with SDF-1α (100 ng/ml) or anti-CD3 (10 μg/ml) or left untreated. 1 × 10^6 cells per treatment were incubated with NKI-L16 (1:100) or CD18-PE in Hepes buffer on ice for an hour. APC-conjugated goat anti-mouse was used as the secondary antibody. Flow data were acquired using an LSR II flow cytometer (Becton Dickinson) and analyzed using BD FACSDiva software.

Peptide affinity chromatography and dot blot

Sepharose-conjugated lyophilized peptides αL: C-KVGFFKRNLKEKMEAGRGVPNGIPAEDSELASGQEAGDPGCLKPLHEKDSESGGGKD; phospho-αL: C-KVGFFKRNLKEKMEAGRGVPNGIPAEDSEQLASGQEAGDPGCLKPLHEKDSEpSGGGKD; β2: C-KALIHLSDLREYRRFE-KEKLKSQWNNDNPLFKSATTTVMNPKFAES; and phospho-β2: C-KALIHLSDLREYRRF-EKEKLKSQWNNDNPLFKSApTTTVMNPKFAES (GenicBio Ltd., Shanghai, China) were dissolved in PBS with 0.01% Triton X-100. 150 million Jurkat JE6.1 cells were lysed with 2% immunoprecipitation buffer and added to peptide-conjugated beads for 8–12 h on a rotator at 4 °C. The samples were washed four times with 1% immunoprecipitation buffer, and bound proteins were detected by immunoblotting. For dot-blot analyses, 5 μg of free peptides were spotted on a nitrocellulose membrane; filters were blocked with 5% milk for 1 h. 5 μg of human α-actinin protein (Sigma–Aldrich, A9776) was added on the peptide spots. The membranes were incubated for 2 h on a shaker in coupling buffer (50 mM Tris, 5 mM EDTA, pH 8.3), washed twice with TBS, and bound α-actinin was detected with the EP2527Y antibody.

ASBMB

Carl_G_190x270_mm_blokki_FINAL.indd 437 06-Aug-23 1:54:51 PM

Cell adhesion and migration assays

For static adhesion assays, soluble ICAM-1 (6 μg/ml) was coated on flat-bottomed 96-well microtiter plates (NUNC MaxiSorp, Thermo Scientific) overnight at 4 °C. The plates were then washed twice with PBS and blocked with 1% heat-denatured BSA for 1 h. 200,000 Jβ2.7 cells expressing LFA-1 WT or αL S1140A/β2 with or without activation with SDF-1α (50 ng/ml) for 20 min or anti-CD3 (10 μg/ml) for 30 min were allowed to adhere for 30 min. Unbound cells were removed by washing three times in PBS, and the bound cells were lysed and detected using *p*-nitrophenyl phosphate substrate tablets (Sigma–Aldrich, S0942) dissolved in buffer (50 mM $NaCH_3COO$, pH 5, 1% Triton X-100) at a concentration of 3 mg/ml. 100 μl of substrate solution was added to each well containing lysate and incubated for 45 min at 37 °C. The reaction was stopped with 1 M NaOH, and the reactivity was detected by measuring absorbance at 405 nm.

For the chemotactic cell migration assay, μ-slide chemotaxis chambers (Ibidi, Germany) were used. The assays were performed according to the manufacturer's instructions. Briefly, the μ-Slide chemotaxis slides were coated with 6 μg/ml ICAM-1 at 37 °C for 1 h and washed with PBS. 6 μl of cells at a concentration of 3×10^6 cells/ml were seeded in the center chamber of a μ-slide. Two reservoirs were filled with 60 μl of serum-free RPMI 1640. One of the filling ports was filled with 10 μl of chemoattractant SDF-1α (1 μg/ml) solution by removing 10 μl of medium from the other port on the same side of the device. Cell migration was recorded by mounting the μ-Slide on the stage of an inverted microscope in a cell incubator. For the trajectory analysis, pictures were taken every 4 min for 4 h using the Cell-IQ high content screening microscope (×10 lens) (Chip-Man Technologies Ltd., Tampere, Finland). The cells were tracked with the Fiji ImageJ manual tracking program (National Institutes of Health), tracks of 15 cells from one representative experiment are shown in the figure, and tracks of 50 cells each from three separate experiments were analyzed with the Chemotaxis and Migration Tools software (Ibidi for ImageJ). Statistical analyses were performed using one-way analysis of variance (Bonferroni post hoc) or unpaired Student's *t* test. Mean standard deviations are included in figures.

Author contributions—F. J., S. M., M. G., and C. G. G. conceptualization; F. J., S. M., T. R., L. V., M. G., and C. G. G. data curation; F. J., S. M., T. R., L. V., M. G., and C. G. G. formal analysis; F. J., S. M., T. R., L. V., M. G., and C. G. G. methodology; F. J., M. G., and C. G. G. writing-original draft; F. J., S. M., T. R., M. G., and C. G. G. writing-review and editing; M. G. and C. G. G. supervision; M. G. and C. G. G. funding acquisition; M. G. and C. G. G. investigation; M. G. and C. G. G. project administration; C. G. G. resources.

References

1. Hynes, R. O. (2002) Integrins: Bidirectional, allosteric signaling machines. *Cell* **110,** 673–687 CrossRef Medline
2. Gahmberg, C. G., Fagerholm, S. C., Nurmi, S. M., Chavakis, T., Marchesan, S., and Grönholm, M. (2009) Regulation of integrin activity and signalling. *Biochim. Biophys. Acta* **1790,** 431–444 CrossRef Medline
3. Hogg, N., Patzak, I., and Willenbrock, F. (2011) The insider's guide to leukocyte integrin signalling and function. *Nat. Rev. Immunol.* **11,** 416–426 CrossRef Medline
4. Gahmberg, C. G., Tolvanen, M., and Kotovuori, P. (1997) Leukocyte adhesion: structure and function of human leukocyte β2-integrins and their cellular ligands. *Eur. J. Biochem.* **245,** 215–232 CrossRef Medline
5. Tan, S. (2012) The leucocyte β2 (CD18) integrins: the structure, functional regulation and signalling properties. *Biosci. Rep.* **32,** 241–269 CrossRef Medline
6. Luo, B.-H., Carman, C. V., and Springer, T. A. (2007) Structural basis of integrin regulation and signaling. *Annu. Rev. Immunol.* **25,** 619–647 CrossRef Medline
7. Gahmberg, C. G., Grönholm, M., and Uotila, L. M. (2014) Regulation of integrin activity by phosphorylation. *Adv. Exp. Med. Biol.* **819,** 85–96 CrossRef Medline
8. Chatila, T. A., Geha, R. S., and Arnaout, M. A. (1989) Constitutive and stimulus-induced phosphorylation of CD11/CD18 leukocyte adhesion molecules. *J. Cell Biol.* **109,** 3435–3444 CrossRef Medline
9. Valmu, L., and Gahmberg, C. G. (1995) Treatment with okadaic acid reveals strong threonine phosphorylation of CD18 after activation of CD11/CD18 leukocyte integrins with phorbol esters or CD3 antibodies. *J. Immunol.* **155,** 1175–1183 Medline
10. Valmu, L., Hilden, T. J., van Willigen, G., and Gahmberg, C. G. (1999) Characterization of β2 (CD18) integrin phosphorylation in phorbol ester-activated T lymphocytes. *Biochem. J.* **339,** 119–125 CrossRef Medline
11. Hilden, T. J., Valmu, L., Kärkkäinen, S., and Gahmberg, C. G. (2003) Threonine phosphorylation sites in the β2 and β7 leukocyte integrin polypeptides. *J. Immunol.* **170,** 4170–4177 CrossRef Medline
12. Uotila, L. M., Jahan, F., Soto Hinojosa, L., Melandri, E., Grönholm, M., and Gahmberg, C. G. (2014) Specific phosphorylations transmit signals from leukocyte β2 to β1 integrins and regulate adhesion. *J. Biol. Chem.* **289,** 32230–32242 CrossRef Medline
13. Abram, C. L., and Lowell, C. A. (2009) The ins and outs of leukocyte integrin signaling. *Annu. Rev. Immunol.* **27,** 339–362 CrossRef Medline
14. Legate, K. R., and Fässler, R. (2009) Mechanisms that regulate adaptor binding to β-integrin cytoplasmic tails. *J. Cell Sci.* **122,** 187–198 CrossRef Medline
15. Hibbs, M. L., Jakes, S., Stacker, S. A., Wallace, R. W., and Springer, T. A. (1991) The cytoplasmic domain of the integrin lymphocyte function-associated antigen 1 β subunit: sites required for binding to intercellular adhesion molecule 1 and the phorbol ester-stimulated phosphorylation site. *J. Exp. Med.* **174,** 1227–1238 CrossRef Medline
16. Fagerholm, S., Morrice, N., Gahmberg, C. G., and Cohen, P. (2002) Phosphorylation of the cytoplasmic domain of the integrin CD18 chain by protein kinase C isoforms in leukocytes. *J. Biol. Chem.* **277,** 1728–1738 CrossRef Medline
17. Takala, H., Nurminen, E., Nurmi, S. M., Aatonen, M., Strandin, T., Takatalo, M., Kiema, T., Gahmberg, C. G., Ylänne, J., and Fagerholm, S. C. (2008) β2 integrin phosphorylation on Thr758 acts as a molecular switch to regulate 14-3-3 and filamin binding. *Blood* **112,** 1853–1862 CrossRef Medline
18. Pavalko, F. M., and LaRoche, S. M. (1993) Activation of human neutrophils induces an interaction between the integrin β2-subunit (CD18) and the actin binding protein α-actinin. *J. Immunol.* **151,** 3795–3807 Medline
19. Stanley, P., Smith, A., McDowall, A., Nicol, A., Zicha, D., and Hogg, N. (2008) Intermediate-affinity LFA-1 binds α-actinin-1 to control migration at the leading edge of the T cell. *EMBO J.* **27,** 62–75 CrossRef Medline
20. Fagerholm, S. C., Hilden, T. J., Nurmi, S. M., and Gahmberg, C. G. (2005) Specific integrin α and β chain phosphorylations regulate LFA-1 activation through affinity-dependent and -independent mechanisms. *J. Cell Biol.* **171,** 705–715 CrossRef Medline
21. Fagerholm, S. C., Varis, M., Stefanidakis, M., Hilden, T. J., and Gahmberg, C. G. (2006) α-Chain phosphorylation of the human leukocyte CD11b/CD18 (Mac-1) integrin is pivotal for integrin activation to bind ICAMs and leukocyte extravasation. *Blood* **108,** 3379–3386 CrossRef Medline
22. Uotila, L. M., Aatonen, M., and Gahmberg, C. G. (2013) Integrin CD11c/CD18 α-chain phosphorylation is functionally important. *J. Biol. Chem.* **288,** 33494–33499 CrossRef Medline
23. Sampath, R., Gallagher, P. J., and Pavalko, F. M. (1998) Cytoskeletal interactions with the leukocyte integrin β2 cytoplasmic tail: activation-depen-

Carl_G_190x270_mm_blokki_FINAL.indd 438 06-Aug-23 1:54:51 PM

dent regulation of associations with talin and α-actinin. *J. Biol. Chem.* **273,** 33588–33594 CrossRef Medline
24. Larson, R. S., Hibbs, M. L., and Springer, T. A. (1990) The leukocyte integrin LFA-1 reconstituted by cDNA transfection in a nonhematopoietic cell line is functionally active and not transiently regulated. *Cell Regul.* **1,** 359–367 CrossRef Medline
25. van Kooyk, Y., Weder, P., Hogervorst, F., Verhoeven, A. J., van Seventer, G., te Velde, A. A., Borst, J., Keizer, G. D., and Figdor, C. G. (1991) Activation of LFA-1 through a Ca^{2+}-dependent epitope stimulates lymphocyte adhesion. *J. Cell Biol.* **112,** 345–354 CrossRef Medline
26. Otey, C. A., and Carpen, O. (2004) α-actinin revisited: a fresh look at an old player. *Cell Motil. Cytoskeleton* **58,** 104–111 CrossRef Medline
27. Kinashi, T. (2005) Intracellular signalling controlling integrin activation in lymphocytes. *Nat. Rev. Immunol.* **5,** 546–559 CrossRef Medline
28. Fagerholm, S., Hilden, T. J., and Gahmberg, C. G. (2002) Lck tyrosine kinase important for activation of the CD11a/CD18-integrins in human T lymphocytes. *Eur. J. Immunol.* **32,** 1670–1678 CrossRef Medline
29. Grönholm, M., Jahan, F., Marchesan, S., Karvonen, U., Aatonen, M., Narumanchi, S., and Gahmberg, C. G. (2011) TCR-induced activation of LFA-1 involves signaling through Tiam1. *J. Immunol.* **187,** 3613–3619 CrossRef Medline
30. Grönholm, M., Jahan, F., Bryushkova, E. A., Madhavan, S., Aglialoro, F., Soto Hinojosa, L., Uotila, L. M., and Gahmberg, C. G. (2016) LFA-1 integrin antibodies inhibit leukocyte α4β1-mediated adhesion by intracellular signaling. *Blood* **128,** 1270–1281 CrossRef Medline
31. Vinogradova, O., Velyvis, A., Velyviene, A., Hu, B., Haas, T., Plow, E., and Qin, J. (2002) A structural mechanism of integrin αIIβ3 "inside-out" activation as regulated by its cytoplasmic face. *Cell* **110,** 587–597 CrossRef Medline
32. O'Toole, T. E., Mandelman, D., Forsyth, J., Shattil, S. J., Plow, E. F., and Ginsberg, M. H. (1991) Modulation of the affinity of integrin αIIbβ3 (GPIIb-IIIa) by the cytoplasmic domain of αIIb. *Science* **254,** 845–847 CrossRef Medline
33. O'Toole, T. E., Katagiri, Y., Faull, R. J., Peter, K., Tamura, R., Quaranta, V., Loftus, J. C., Shattil, S. J., and Ginsberg, M. H. (1994) Integrin cytoplasmic domains mediate inside-out signal transduction. *J. Cell Biol.* **124,** 1047–1059 CrossRef Medline
34. Pardi, R., Bossi, G., Inverardi, L., Rovida, E., and Bender, J. R. (1995) Conserved regions in the cytoplasmic domains of the leukocyte integrin αLβ2 are involved in endoplasmic reticulum retention, dimerization, and cytoskeletal association. *J. Immunol.* **155,** 1252–1263 Medline
35. Hughes, P. E., O'Toole, T. E., Ylänne, J., Shattil, S. J., and Ginsberg, M. H. (1995) The conserved membrane-proximal region of an integrin cytoplasmic domain specifies ligand binding affinity. *J. Biol. Chem.* **270,** 12411–12417 CrossRef Medline
36. Hughes, P. E., Diaz-Gonzalez, F., Leong, L., Wu, C., McDonald, J. A., Shattil, S. J., and Ginsberg, M. H. (1996) Breaking the integrin hinge: A defined structural constraint regulates integrin signaling. *J. Biol. Chem.* **271,** 6571–6574 CrossRef Medline
37. Lu, C. F., and Springer, T. A. (1997) The α subunit cytoplasmic domain regulates the assembly and adhesiveness of integrin lymphocyte function-associated antigen-1. *J. Immunol.* **159,** 268–278 Medline
38. Vinogradova, O., Vaynberg, J., Kong, X., Haas, T. A., Plow, E. F., and Qin, J. (2004) Membrane-mediated structural transitions at the cytoplasmic face during integrin activation. *Proc. Natl. Acad. Sci. U.S.A.* **101,** 4094–4099 CrossRef Medline
39. Li, Y. F., Tang, R. H., Puan, K. J., Law, S. K., and Tan, S. M. (2007) The cytosolic protein talin induces an intermediate affinity integrin αLβ2. *J. Biol. Chem.* **282,** 24310–24319 CrossRef Medline
40. Pouwels, J., Nevo, J., Pellinen, T., Ylänne, J., and Ivaska, J. (2012) Negative regulators of integrin activity. *J. Cell Sci.* **125,** 3271–3280 CrossRef Medline
41. Bouvard, D., Pouwels, J., De Franceschi, N., and Ivaska, J. (2013) Integrin inactivators: balancing cellular functions *in vitro* and *in vivo*. *Nat. Rev. Mol. Cell Biol.* **14,** 430–442 CrossRef Medline
42. Morse, E. M., Brahme, N. N., and Calderwood, D. A. (2014) Integrin cytoplasmic tail interactions. *Biochemistry* **53,** 810–820 CrossRef Medline
43. Kassner, P. D., and Hemler, M. E. (1993) Interchangeable α chain cytoplasmic domains play a positive role in control of cell adhesion mediated by VLA-4, a β1 integrin. *J. Exp. Med.* **178,** 649–660 CrossRef Medline
44. Shaw, L. M., and Mercurio, A. M. (1993) Regulation of α6β1 integrin laminin receptor function by the cytoplasmic domain of the α6 subunit. *J. Cell Biol.* **123,** 1017–1025 CrossRef Medline
45. Filardo, E. J., and Cheresh, D. A. (1994) A β turn in the cytoplasmic tail of the integrin αv subunit influences conformation and ligand binding of αvβ3. *J. Biol. Chem.* **269,** 4641–4647 Medline
46. Kassner, P. D., Alon, R., Springer, T. A., and Hemler, M. E. (1995) Specialized functional properties of the integrin α4 cytoplasmic domain. *Mol. Biol. Cell.* **6,** 661–674 CrossRef Medline
47. Ylänne, J., Huuskonen, J., O'Toole, T. E., Ginsberg, M. H., Virtanen, I., and Gahmberg, C. G. (1995) Mutation of the cytoplasmic domain of the integrin β3 subunit: differential effects on cell spreading, recruitment to adhesion plaques, endocytosis, and phagocytosis. *J. Biol. Chem.* **270,** 9550–9557 CrossRef Medline
48. Yauch, R. L., Felsenfeld, D. P., Kraeft, S. K., Chen, L. B., Sheetz, M. P., and Hemler, M. E. (1997) Mutational evidence for control of cell adhesion through integrin diffusion/clustering, independent of ligand binding. *J. Exp. Med.* **186,** 1347–1355 CrossRef Medline
49. Abair, T. D., Bulus, N., Borza, C., Sundaramoorthy, M., Zent, R., and Pozzi, A. (2008) Functional analysis of the cytoplasmic domain of the integrin α1 subunit in endothelial cells. *Blood* **112,** 3242–3254 CrossRef Medline
50. Liu, J., Wang, Z., Thinn, A. M., Ma, Y. Q., and Zhu, J. (2015) The dual structural roles of the membrane distal region of the α-integrin cytoplasmic tail during integrin inside-out activation. *J. Cell Sci.* **128,** 1718–1731 CrossRef Medline
51. Bhunia, A., Tang, X.-Y., Mohanram, H., Tan, S.-M., and Bhattacharjya, S. (2009) NMR solution conformations and interactions of integrin αLβ2 cytoplasmic tails. *J. Biol. Chem.* **284,** 3873–3884 CrossRef Medline
52. Nortamo, P., Patarroyo, M., Kantor, C., Suopanki, J., and Gahmberg, C. G. (1988) Immunological mapping of the human leucocyte adhesion glycoprotein gp90 (CD18) by monoclonal antibodies. *Scand. J. Immunol.* **28,** 537–546 CrossRef Medline
53. Weber, K. S., York, M. R., Springer, T. A., and Klickstein, L. B. (1997) Characterization of lymphocyte function-associated antigen 1 (LFA-1)-deficient T cell lines: the αL and β2 subunits are interdependent for cell surface expression. *J. Immunol.* **158,** 273–279 Medline
54. Jones, M. C., Humphries, J. D., Byron, A., Millon-Frémillon, A., Robertson, J., Paul, N. R., Ng, D. H. J., Askari, J. A., and Humphries, M. J. (2015) Isolation of integrin-based adhesion complexes. *Curr. Protoc. Cell Biol.* **66,** 9.8.1–9.8.15 Medline
55. Kishimoto, T. K., O'Connor, K., Lee, A., Roberts, T. M., and Springer, T. A. (1987) Cloning of the β subunit of the leukocyte adhesion proteins: Homology to an extracellular matrix receptor defines a novel supergene family. *Cell* **48,** 681–690 CrossRef Medline
56. Weiner, M. P., Costa, G. L., Schoettlin, W., Cline, J., Mathur, E., and Bauer, J. C. (1994) Site-directed mutagenesis of double-stranded DNA by the polymerase chain reaction. *Gene* **151,** 119–123 CrossRef Medline

ASBMB

Carl_G_190x270_mm_blokki_FINAL.indd 439 06-Aug-23 1:54:52 PM

THE JOURNAL OF BIOLOGICAL CHEMISTRY VOL. 289, NO. 46, pp. 32230–32242, November 14, 2014
© 2014 by The American Society for Biochemistry and Molecular Biology, Inc. Published in the U.S.A.

Specific Phosphorylations Transmit Signals from Leukocyte β_2 to β_1 Integrins and Regulate Adhesion*

Received for publication, June 11, 2014, and in revised form, September 24, 2014 Published, JBC Papers in Press, October 2, 2014, DOI 10.1074/jbc.M114.588111

Liisa M. Uotila, Farhana Jahan, Laura Soto Hinojosa, Emiliano Melandri, Mikaela Grönholm[1], and Carl G. Gahmberg[1,2]

From the Division of Biochemistry and Biotechnology, Faculty of Biological and Environmental Sciences, University of Helsinki, 00014 Helsinki, Finland

Background: Integrins regulate leukocyte adhesion in a stepwise manner.
Results: β_2 Integrins can signal to β_1 integrin very late antigen 4 and inhibit ligand binding.
Conclusion: Phosphorylation on both the α and β chains of β_2 integrins are needed, but the signal is transmitted through the β_2 chain, leading to dephosphorylation of β_1.
Significance: Our findings show a mechanism of integrin cross-talk.

The regulation of integrins expressed on leukocytes must be controlled precisely, and members of different integrin subfamilies have to act in concert to ensure the proper traffic of immune cells to sites of inflammation. The activation of β_2 family integrins through the T cell receptor or by chemokines leads to the inactivation of very late antigen 4. The mechanism(s) of this cross-talk has not been known. We have now elucidated in detail how the signals are transmitted from leukocyte function-associated antigen 1 and show that, after its activation, the signaling involves specific phosphorylations of β_2 integrin followed by interactions with cytoplasmic signaling proteins. This results in loss of β_1 phosphorylation and a decrease in very late antigen 4 binding to its ligand vascular cell adhesion molecule 1. Our results show how a member of one integrin family regulates the activity of another integrin. This is important for the understanding of integrin-mediated processes.

Leukocyte extravasation plays a key role in inflammation. The recruitment of leukocytes into inflamed tissue requires leukocyte adhesion to the vascular endothelium as a sequence of events, including the capture of circulating leukocytes and subsequent leukocyte rolling, arrest, firm adhesion, and transmigration. These processes are mediated by adhesion receptors, of which selectins and integrins are of pivotal importance (1, 2).

Integrins are transmembrane heterodimeric receptors that can communicate in two directions across the plasma membrane. Outside-in signaling occurs by binding of ligands or, *e.g.*, activating antibodies to the integrins, whereas inside-out signaling is due to ligand binding to non-integrin receptors (such as chemokine receptors or the T cell receptor), which, through intracellular signaling, convey the message to integrins, resulting in changes in activity. Integrins can exist in at least three different conformations: inactive, extended, and extended open (3–6).

The family of leukocyte-specific β_2 integrins consists of four members. They have a common β chain (β_2, CD18) and one of the α chains (α_L, CD11a; α_M, CD11b; α_X, CD11c; and α_D, CD11d). The leukocyte function-associated antigen 1 heterodimer (LFA-1, $\alpha_L\beta_2$, CD11a/CD18) is primarily expressed in lymphocytes and binds to intercellular adhesion molecules (ICAMs)[3] (7). Mac-1 (macrophage 1 antigen, $\alpha_M\beta_2$, CD11b/CD18) is enriched in the myeloid lineage, and its adhesion activity is promiscuous, showing binding to ICAMs but also to a variety of different molecules. Complement receptor 4 (CR4, $\alpha_X\beta_2$, CD11c/CD18, p150,95) is expressed in monocytes, macrophages, and dendritic cells as well as in some subsets of activated T and B cells. It is able to bind to various ligands, including extracellular matrix molecules (Collagen I), cellular ligands (ICAM-1, ICAM-2, ICAM-4, vascular cell adhesion molecule 1 (VCAM-1)), soluble ligands (iC3b, fibrinogen), and denatured proteins (8, 9). In addition, leukocytes express β_1 integrins, notably the very late antigen 4 (VLA-4, $\alpha_4\beta_1$) integrin. VLA-4 plays an important role in leukocyte adhesion and binds to the endothelial protein VCAM-1 but also to extracellular matrix proteins such as fibronectin (2, 10, 11).

The integrin cytoplasmic domains are short and devoid of catalytic activity. However, integrin function is regulated by protein interactions with the cytoplasmic domains. Many adaptor proteins, including filamin, α-actinin, and 14-3-3 protein family members, compete for the relatively few binding sites on the integrin tails. Talin and the kindlin family of proteins are considered to be important in the final stages of activation (1, 6, 12, 13).

LFA-1 and VLA-4 mediate distinct steps in the adhesion cascade. VLA-4 is the predominant integrin regulating rolling, and it participates in adhesion strengthening, whereas LFA-1 is needed for firm adhesion and migration (2). Importantly, integ-

This is an open access article under the CC BY license.

* This study was supported by the Academy of Finland, by the Sigrid Jusélius Foundation, by the Medicinska Understödsföreningen Liv och Hälsa, by Finska Läkaresällskapet, by the Wilhelm and Else Stockmann Foundation, and by the Magnus Ehrnrooth Foundation.
[1] Both authors contributed equally to this work.
[2] To whom correspondence should be addressed: Div. of Biochemistry and Biotechnology, Faculty of Biological and Environmental Sciences, Viikinkaari 5 D (P.O. Box 56), 00014 University of Helsinki, Helsinki, Finland. Tel.: 358-50-4486388; E-mail: carl.gahmberg@helsinki.fi.

[3] The abbreviation used is: ICAM, intercellular adhesion molecule; HMEC, human mammary epithelial cells.

Carl_G_190x270_mm_blokki_FINAL.indd 440 06-Aug-23 1:54:53 PM

rins have the ability to modulate their adhesive properties within seconds after chemokine stimulation (14).

Little is known about how integrins act in concert. Some earlier studies have shown that LFA-1 may regulate VLA-4 activity in T cells, but the mechanisms have remained largely unknown (15). We have shown previously that integrin phosphorylations are essential in the regulation of β_2 integrin activity (6, 16–18). Phosphorylation of Thr-758 in the β_2 chain leads to 14-3-3 binding, recruitment of T cell lymphoma invasion and metastasis 1 (Tiam1) protein, and up-regulation of Ras-related C3 botulinum toxin substrate 1 (Rac1) (19).

We now show that LFA-1 and CR4 α chain phosphorylation is needed for chemokine-induced cross-talk to VLA-4. In contrast, signaling through the T cell receptor and outside-in activation do not need α chain phosphorylation. However, after both inside-out and outside-in activations, signaling is transmitted through β_2 chain phosphorylation and the 14-3-3/Tiam1/Rac1 pathway. This results in the inhibition of β_1 phosphorylation, VLA-4 binding to filamin, and inactivation of VLA-4.

EXPERIMENTAL PROCEDURES

Reagents and Antibodies—The peptides (CLFKSATTTVMN and CLFKSApTTTVMN, in which pT is phospho-threonine) were synthesized by TAG Copenhagen A/S (Copenhagen, Denmark). The antagonist of 14-3-3 proteins, the R18 peptide PHCVPRDLSWLDLEANMCLP, was from TOCRIS Bioscience (Ellisville, MO), and, as a control, the P621 peptide VDVDSDGSTDLVIGA was used. VCAM-1-Fc, ICAM-1-Fc, and SDF-1α were from R&D Systems (Minneapolis, MN). The mAbs R2E7B and R7E4 against the human β_2 subunit of leukocyte integrin and polyclonal antiserum against the β_2 chain phosphorylated on Thr-758 have been described previously (20, 21). IB4, which recognizes the heterodimeric forms of β_2 integrins, was a gift from M. Arnaout (Massachusetts General Hospital, Boston, MA). The β_2 integrin antibodies KIM127 and mAb24 were gifts from M. Robinson (Celltech, Slough, UK) and N. Hogg (Imperial Cancer Research Fund, London, UK), respectively. The β_2 chain binding, activating antibody CBR LFA-1/2 was from Timothy Springer (Harvard Medical School). The following antibodies were also used: anti-CD3 (MEM 57, ImmunoTools, Friesoythe, Germany), pan 14-3-3 (clone K-19, Santa Cruz Biotechnology, Santa Cruz, CA), 14-3-3ζ (Thermo Scientific, Waltham, MA), talin 8d4 (Sigma-Aldrich, St. Louis, MO), filamin (Chemicon/Merck, Billerica, MA), integrin α_4 2B4 (R&D Systems), PA5-20599 (Thermo Fisher Scientific), 4600S (Cell Signaling Technology), α_4-phospho-988 (Millipore/Merck), integrin β_1 (Mab 13, BD Biosciences), phospho-β_1 Thr-788/789 (Abcam, Cambridge, UK), and VCAM-1 (B-K9, Diaclone, Besançon, France). Phalloidin was from Invitrogen, and HRP-linked antibodies against mouse and rabbit Ig were from GE Healthcare. Secondary anti-mouse-allophycocyanin used in flow cytometry was from Beckman Coulter (Brea, CA). The Tiam1 (catalog no. NSC23766) and Rac1 (catalog no. EHT1864) inhibitors were from TOCRIS Bioscience.

Cell Culture and Transfection—Stable transfectants of the K562 cell line (22) expressing WT CR4 or S1158A-$\alpha_X\beta_2$ (CR4 S/A) or empty plasmid have been described previously (23). HMEC cells were a gift from Antti Vaheri (University of Helsinki, Finland) and have been described previously (24). Cells were grown on plates coated with 0.5% gelatin in RPMI 1640 medium supplemented with 10% FBS, 100 units/ml penicillin/streptomycin, and 2 mM L-glutamine. The human T cell lymphoma cell line clone Jβ2.7, which lacks the CD11 chain (25), was a gift from N. Hogg and was grown in RPMI 1640 medium supplemented with 10% FBS, 2 mM L-glutamine, and 100 units/ml penicillin/streptomycin. The Jβ2.7 cell lines expressing LFA-1 WT or the phosphorylation mutant S1140A were produced by virus transductions. HEK293T cells were transiently transfected using the following protocol. 30 μg of DNA (12.5 μg of retroviral vector, 12.5 μg of GAG-Pol, and 5 μg of Env) were mixed with 120 μl of polyethylenimine (Polysciences, Warrington, PA) and DMEM to a total volume of 1.5 ml and incubated for 10 min at room temperature. 1 ml of DMEM with 10% FBS, 2 mM L-glutamine, and 100 units/ml penicillin/streptomycin and 250 μl of the DNA mixture were added to each well. The supernatants were harvested 24 and 48 h after transfection. For transduction, 10^5 Jβ2.7 cells were grown for 4–6 h in the presence of 1 μl of Polybrene (Sigma-Aldrich), after which 1 ml of fresh medium and 1 ml of virus supernatant were added to each well. 24–72 h after transduction, the cells were rinsed and expanded in fresh medium.

Immunoprecipitation—Jβ2.7 cells were activated with 50 ng/ml SDF-1α, 10 μg/ml anti-CD3, CBR LFA-1/2, or left untreated. Cells were lysed on ice for 30 min in 2% radioimmune precipitation assay buffer (50 mM Tris-HCl (pH 7.8), 150 mM NaCl, 1% Triton X-100, 1% Nonidet P-40, 15 mM $MgCl_2$, and 5 mM EDTA) with protease and phosphatase inhibitors (Roche). Cell lysates were centrifuged at 13,400 rpm for 60 min at 4 °C. Lysates were cleared with protein G-Sepharose (GE Healthcare) for 1 h with constant rolling at 4 °C. The precleared supernatants were mixed with CD11/CD18 (IB4) or integrin α_4 (4600S) antibodies or IgG and incubated for 2.5 h at 4 °C with constant shaking. Protein G-Sepharose beads (GE Healthcare) were added for 1 h at 4 °C and washed four times with 1% radioimmune precipitation assay buffer (including 0.5% Triton X-100 and 0.5% Nonidet P-40). Bound proteins were eluted with Laemmli sample buffer and run on SDS-PAGE, and then lysates and immunoprecipitates were analyzed by immunoblotting for 14-3-3 (K-19 or 14-3-3ζ), filamin A (Mab 1678), sharpin, paxillin, integrin β_2 (R2E7B), integrin β_1, phospho-β_1 788/789, integrin α_4, or phospho-α_4 Ser-988. The amount of coprecipitated 14-3-3ζ or filamin per immunoprecipitated β_2 or α_4 was quantified from three experiments by ImageJ and normalized to the level of precipitated β_2.

Cell Adhesion Assays—For adhesion assays with Jβ2.7 cell lines, culture wells were coated with VCAM-1-Fc, and 10,000 cells were added and allowed to adhere for 30 min with or without preincubation with 10 μg/ml α_4-blocking 2B4 or β_1-blocking mAb 13 antibodies for 30 min or SDF-1α (50 ng/ml) for 15 min. Adhered and spread cells were counted from ten screens using an Evos microscope (Invitrogen). For live cell imaging, cells were followed for 10–120 min, and time lapse movies were taken with the Evos microscope. Adhesion assays of K562 cells to VCAM-1 were performed as described previously (23).

Carl_G_190x270_mm_blokki_FINAL.indd 441 06-Aug-23 1:54:53 PM

Briefly, K562 cells transfected with empty plasmid, WT CR4, or S1158A-$\alpha_X\beta_2$ (CR4 S/A) were allowed to bind to VCAM-1-Fc coated on Nunc MaxiSorp 96-well plates (Thermo Fisher Scientific). 100,000 cells were incubated in the wells without treatment or in the presence of antibodies against α_4 (2B4) or β_1 (Mab 13), after which the wells were washed and the bound cells were lysed and detected using phosphatase substrate (Sigma-Aldrich).

Flow Adhesion Assays—For flow adhesion assays, HMEC cells were seeded on flow chamber channels (μ-Slide VI$^{0.4}$, Ibidi GmbH, Martinsried, Germany) coated with 0.5% gelatin and grown until confluency, after which cells were activated with TNF-α (Sigma-Aldrich), 50 ng/ml, overnight. Alternatively, chambers were coated with 6 μg/ml VCAM-1. Jβ2.7 cell lines were stained with carboxyfluorescein diacetate succinimidyl ester (Invitrogen) according to the instructions of the manufacturer and treated with SDF-1α for 10 min or left untreated. The cell suspensions were then injected into a flow system using a silicone tubing loop connected to a multiphaser NE-1000 syringe pump (New Era Pump Systems, Inc., Farmingdale, NY), allowing cells to flow over HMEC-1- or VCAM-1-coated Ibidi microslides VI 0.4. A continuous shear flow rate of 0.3 dynes/cm^2 was used. Adhering cells were monitored by fluorescence microscopy (EVOS fl, Invitrogen), and firmly attached cells were counted at two different time points from eight separate screens.

Migration Assays—For the chemokine-induced migration assays, 5-μm pore size Transwell membranes were incubated with soluble VCAM-1, ICAM-1, or BSA (10 μg/ml or the indicated concentrations) overnight at 4 °C, washed once with PBS, and placed in the wells of a 24-well plate containing 600 μl of buffer (RPMI 1640 medium/10% FBS) with 15 ng/ml SDF-1α. Cells were stained with carboxyfluorescein diacetate succinimidyl ester, calcein blue (eBioscience, San Diego, CA), fluorescein, or eFLuor 670 (eBioscience) according to the instructions of the manufacturer. In some cases, cells were preincubated with 10 μg/ml of the α_4-blocking antibody 2B4 for 15 min at 37 °C. 60,000 cells were placed on the membrane and allowed to migrate toward SDF-1α at 37 °C for 1 h. Migrated cells were collected and counted.

Peptide Transfections—60,000 cells in 100 μl of buffer (RPMI 1640 medium/5% FBS) were transfected in 48-well plates. For transfection, 2 μg of nonphosphorylated or Thr-758-phosphorylated β_2 peptide was incubated for 20 min at room temperature with 1 ml enhancer and 1 ml Turbofect transfection reagent (Fermentas, Thermo Fischer Scientific) in 50 μl of RPMI medium and added to the cells. After incubation, the transfected cells were added to Transwell filters, and migration assays were performed as above. To block the interaction between 14-3-3 proteins and their targets, cells were transfected with the R18 peptide or the control peptide P621 (2 μg/transfection) prior to migration. To inhibit Tiam1, cells were preincubated with the NSC23766 inhibitor (100 μM, TOCRIS Bioscience) for 2 h at 37 °C.

Immunofluorescence and Flow Cytometry—Jβ2.7 cells were treated with 50 ng/ml SDF-1α for 30 min or left untreated and spun down on cytospin glasses or were allowed to adhere to VCAM-1 for 2 h. Cells were fixed in 4% paraformaldehyde and stained for talin (8d4), 14-3-3 ζ, filamin, integrin α_4 (PA5-20599), integrin β_2 (R7E4), the extended form of LFA-1 (KIM127), or the extended open form of LFA-1 (mAb24) and Alexa Fluor secondary antibodies (Invitrogen), and images were acquired by a Leica TCS SP5 MP confocal microscope. For flow cytometry analysis, Jβ2.7 cells were stained with the anti-α_4 antibody 2B4, followed by anti-mouse allophycocyanin. K562 cells were stained with polyclonal anti-α4 PA5–2099 and anti-rabbit Alexa Fluor 488. Surface expression of the α_4 integrin chain was detected with a LSRII flow cytometer (BD Biosciences) and analyzed with FlowJo software (Treestar, Ashland, OR).

Quantifications—Quantifications were done using ImageJ (v10.2) software. The fluorescence intensity of cells stained with mab24 and KIM127 is an average of 100 cells for each condition and cell line done in triplicate. Cell extensions were quantified as extensions longer than the cell body from 10 frames of adhered cells in triplicate. All statistical analyses were performed in Excel with unpaired Student's *t* test. In the figures, the mean ± S.D. is given.

RESULTS

Binding of Jβ2.7 Cells to VCAM-1 through VLA-4 Can Be Blocked by LFA-1—For these studies, we mainly used the Jβ2.7 Jurkat cell line, which contains a mutation in the α_L gene, leading to lack of expression of α_L and, thus, no functional LFA-1 on the cell surface. The cells spread and adhere strongly to VCAM-1 (Fig. 1*A*). The VCAM-1 binding integrin VLA-4 expression on Jβ2.7 cells was verified by flow cytometry (data not shown). By blocking α_4 or β_1, adhesion is inhibited, showing that the cells bind to VCAM-1 through VLA-4 (Fig. 1*A*).

This cell line was used to study how the presence of LFA-1 affects VLA-4 functions. A stable Jβ2.7 cell line expressing the α_L chain of LFA-1 (LFA-1) was produced by virus transduction. The expression of α_L and β_2 was detected by flow cytometry, and binding of LFA-1 to its ligand, ICAM-1, was shown by adhesion to ICAM-1 under flow (data not shown). Therefore, LFA-1 cells express functional LFA-1. To study how the expression of LFA-1 affects VLA-4, Jβ2.7 cells, or LFA-1 cells were allowed to adhere to VCAM-1-coated wells and adhered cells were counted (Fig. 1*B*). Cells were either unactivated or activated by the chemokine stromal cell-derived factor 1α (SDF-1α), which has been shown to activate LFA-1 (26). Cells adhere and spread much faster on VCAM-1 in the absence of activated LFA-1. The presence of SDF-1α -activated LFA-1 leads to a clear reduction of cell adhesion to VCAM-1, pointing to a trans-dominant inhibition of VLA-4 by LFA-1. Inhibition of VCAM-1 binding is not seen after activation with anti-CD2 or anti-CD28, indicating that this inhibition is not a common effect of leukocyte membrane receptors (data not shown).

Inhibition of VCAM-1 binding could also be seen in an adhesion assay under flow on VCAM-1-coated surfaces (Fig. 1*C*) or endothelial cells activated with TNFα (Fig. 1*D*). The bright field image of the cells spreading on VCAM-1 show that fewer LFA-1 cells adhere to and spread on VCAM-1 (Fig. 1*E*). Activation by SDF-1α of JE6.1 Jurkat cells, which express both LFA-1 and VLA-4, also leads to a reduction of VLA-4 binding to VCAM-1 (data not shown).

Carl_G_190x270_mm_blokki_FINAL.indd 442 06-Aug-23 1:54:54 PM

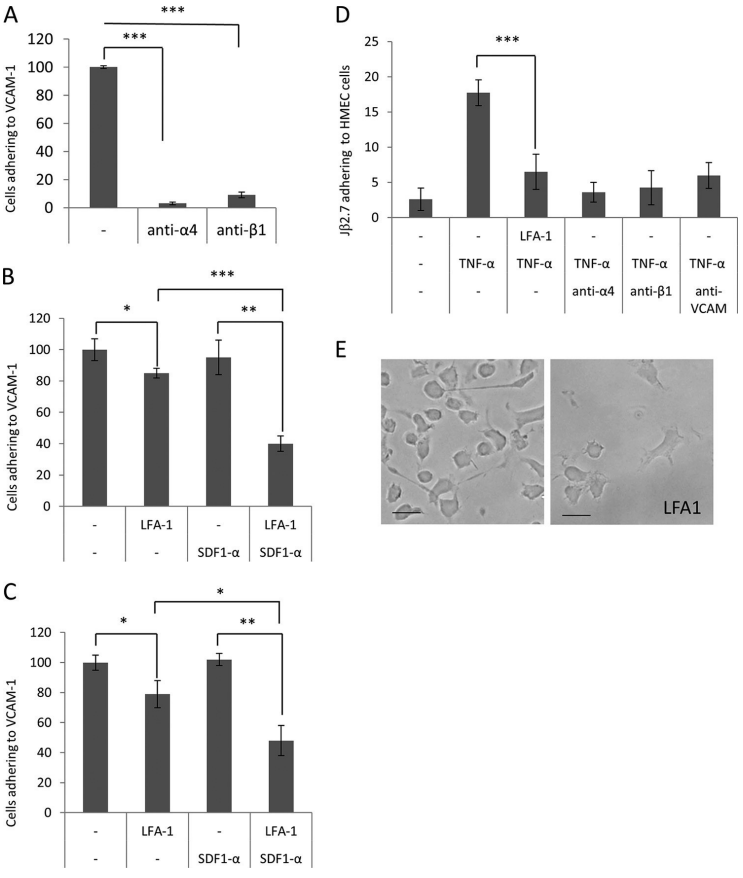

FIGURE 1. **LFA-1 inhibits binding of VLA-4 to VCAM-1.** *A*, Jβ2.7 cells lacking LFA-1 bind VCAM-1 through VLA-4. Jβ2.7 cells were allowed to adhere for 30 min to VCAM-1 with or without α_4-blocking 2B4 or β_1-blocking MEM-13 antibodies under static conditions. An average of adhered cells from ten counted frames in triplicate is shown. *B* and *C*, LFA-1 expression inhibits Jβ2.7 cell binding to VCAM-1. Jβ2.7 cells lacking LFA-1 or expressing LFA-1 were activated with SDF-1α and allowed to adhere to VCAM-1 under static (*B*) or flow (*C*) conditions, and bound cells were quantified as in *A*. *D*, flow adhesion to endothelial cells. Endothelial HMEC cells were cultured to confluence, and Jβ2.7 or Jβ2.7 LFA-1 cells were allowed to bind to TNFα-activated cells under flow. Bound cells were quantified as in *A*. Binding could be inhibited by VLA-4-blocking (2B4 or Mab 13) or VCAM-1-blocking (B-K9) antibodies. *E*, bright field image of Jβ2.7 and Jβ2.7 LFA-1 cells adhering to VCAM-1 for 2 h. *Scale bars* = 20 μm. *, $p < 0.05$; **, $p < 0.01$; ***, $p < 0.001$.

Strong Adhesion between VLA-4 and VCAM-1 Causes Impaired Detachment, Which Can Be Inhibited by LFA-1—Jβ2.7 cells adhere strongly to VCAM-1, and cells bound to VCAM-1 cannot be removed by increasing the flow rate extensively, which is the case with LFA-1 adhesion to ICAM-1 (data not shown). This strong adhesion is also seen in cell migration experiments. Cells were allowed to migrate over Transwell filters coated with VCAM-1 toward SDF-1α present below. Jβ2.7 cells lacking LFA-1 do not migrate over the VCAM-1-coated filters. To detect whether cells stay bound to the filter, they were fluorescently stained with carboxyfluorescein diacetate succinimidyl ester. In cells lacking LFA-1, most cells stay bound to the filter. When cells express LFA-1 or the VCAM-1 interaction is blocked by a VLA-4 blocking antibody, cells migrate through the filters toward SDF-1α. This indicates that LFA-1 inhibits VLA-4 activity, therefore reducing adhesion between VLA-4 and VCAM-1 (Fig. 2*A*).

We next studied the cell morphology of Jβ2.7 cells adhering to VCAM-1 by live cell imaging. Jβ2.7 cells spread on VCAM-1 with long extensions, which are not seen in LFA-1-expressing cells. When Jβ2.7 cells were allowed to adhere and form extensions and then the α4-blocking antibody was added, the extensions disappeared (Fig. 2*B*). To elucidate whether the long extensions are filopodia growing out of the cell body or caused by impaired retraction of adhesion sites, we performed live cell imaging of cells. This clearly showed that the extensions result from strong adhesions that cannot be released as the cells are moving in an opposite direction, therefore leaving a long extension behind (Fig. 2*C*). When cells express SDF-1α-activated LFA-1 or when VLA-4 is blocked by an α_4-blocking antibody,

Carl_G_190x270_mm_blokki_FINAL.indd 443 06-Aug-23 1:54:54 PM

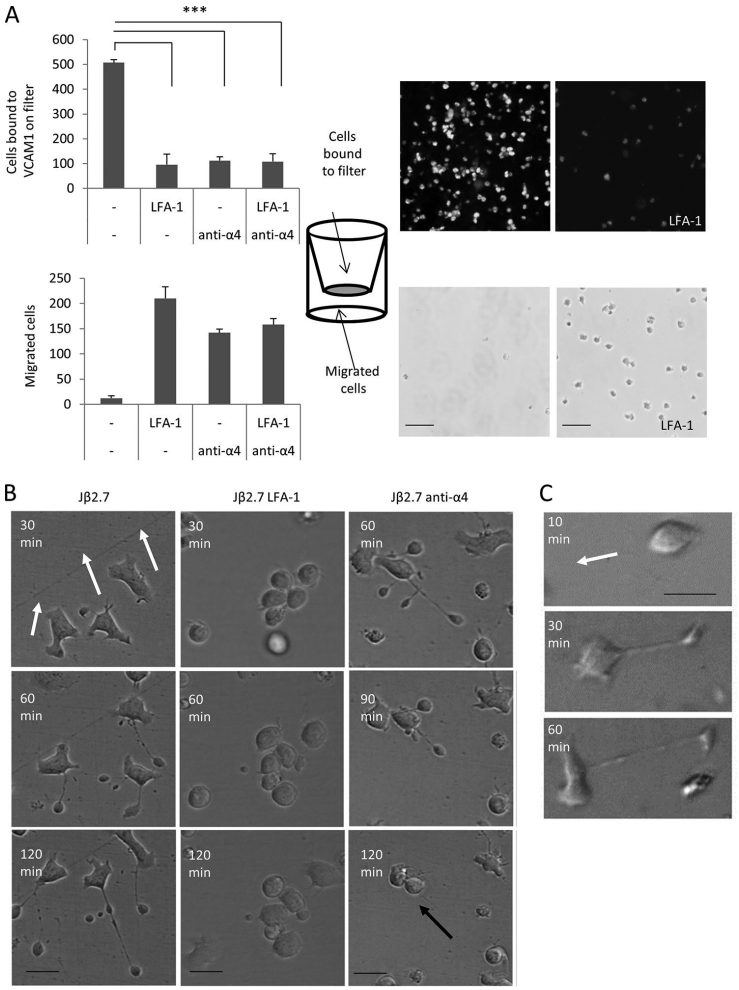

FIGURE 2. **Strong binding between VLA-4 and VCAM-1 causes impaired detachment that can be blocked by LFA-1.** *A*, migration assays over VCAM-1-coated filters. VCAM-1 (10 μg/ml) was applied to Transwell filters, and Jβ2.7 or Jβ2.7 LFA-1 cells with or without VLA-4-blocking antibody (2B4) were allowed to migrate toward SDF-1α. Cells bound to the filter (*top panels*) and migrated cells (*bottom panels*) were counted after 30 min. Cells lacking LFA-1 bind to the filter so strongly that migration is inhibited. This binding can be released by LFA-1 expression or by blocking VLA-4. A representative fluorescence picture of carboxyfluorescein diacetate succinimidyl ester-stained cells on the filter and migrated cells (bright field) is shown. *Scale bars* = 100 μm. *B*, formation of long extensions in Jβ2.7 cells can be inhibited by LFA-1 expression. *Left* and *center columns*, live cell imaging of Jβ2.7 cells lacking LFA-1 or expressing LFA-1 on VCAM-1 after SDF-1α activation was performed. Three frames of the same cells are shown (time points 30, 60, and 120 min). *Right column*, Jβ2.7 cells were allowed to attach to VCAM-1 for 60 min, creating long extensions. Thereafter, anti-α4 was added to the cells, and cells were followed for another 60 min, causing the adhesions to retract. *White arrows* indicate the direction of cell migration, and the *black arrow* indicates retracted extension. *Scale bars* = 20 μm. *C*, the long extensions are caused by impaired retraction of the adhesion sites. Shown are higher magnification of live cell imaging of Jβ2.7 cells migrating on VCAM-1. Three time points (10, 30, and 60 min) are shown. The *arrow* indicates the direction of cell migration. *Scale bar* = 20 μm. ***, $p < 0.001$.

these extensions were not seen, indicating that the strong adhesions between VLA-4 and VCAM-1 cannot be formed (data not shown). LFA-1 needs to be activated to be able to inhibit VLA-4. When LFA-1-expressing cells were allowed to bind to VCAM-1 before the addition of SDF-1α, strong adhesions could not be released, regardless of later activation of LFA-1. This indicates that LFA-1 can block the formation of VLA-4/VCAM-1 interactions, but when the strong adhesions and long extensions have formed, activation of LFA-1 cannot disassociate these.

Phosphorylation of α_L and α_X Is Required for the Inhibition of VLA-4 after Chemokine Activation—To elucidate the mechanisms behind the VLA-4 inhibition, we studied the role of integrin α and β chain signaling and the activation state of

Carl_G_190x270_mm_blokki_FINAL.indd 444 06-Aug-23 1:54:54 PM

LFA-1 needed for cross-talk. We have shown previously that the α chain of LFA-1 is phosphorylated on Ser-1140 and that this modification is needed for conformational changes in the integrin after chemokine activation (17). We therefore made a Jβ2.7 cell line stably expressing the phosphorylation mutant α_L S1140A (LFA-1 S/A). A similar expression of LFA-1 WT and LFA-1 S/A was verified by flow cytometry, and mutated cells showed reduced binding to ICAM-1 compared with WT LFA-1 (Fig. 1, *A* and *C*). We next performed static adhesion assays on VCAM-1 with the three cell lines Jβ2.7, LFA-1, and LFA-1 S/A in the presence of SDF-1α. Bright field images of adhering cells were taken after 30 min. After 2 h, cells were fixed and stained with phalloidin. Less cells adhered to and spread on VCAM-1 in LFA-1 cells, whereas the LFA-1 S/A cells resembled those of Jβ2.7 cells (Fig. 3*A*). Adhered cells and the amount of cells with an extension longer than the cell body were quantified. Although LFA-1 expression reduced VLA-4 adhesion to VCAM-1, the phosphorylation mutant LFA-1S/A was not able to inhibit VLA-4, indicating that a phosphorylated Ser-1140 is essential for inhibition (Fig. 3*B*). We next performed a migration assay. The three cell lines were first stained with different fluorescent markers and mixed before they were allowed to migrate over VCAM-1-coated filters. We first verified that the stains did not affect migration (not shown). In the experiment shown in Fig. 3*C*, Jβ2.7 cells are red, LFA-1 cells are green, and LFA-1 S/A blue. The LFA-1 S/A phosphorylation mutant was not able to release Jβ2.7 cells from the VCAM-1-coated filters as LFA-1 WT did, indicating that phosphorylation of the α chain Ser-1140 is needed for LFA-1-mediated inhibition of VLA-4 in SDF-1α-activated cells (Fig. 3*C*).

The β_2 integrin CR4 ($\alpha_X\beta_2$) is also expressed in leukocytes, and we have shown recently that it is phosphorylated on serine 1158 in the α chain (23). To find out whether the cross-talk is unique to LFA-1, we studied whether CR4 can regulate VLA-4. We used K562 cells that were transfected with WT CR4 or with the α chain phosphorylation mutant α_X-S1158A (CR4 S/A). These cells express α_4, as detected by the anti-α_4 antibody 2B4. Cells stably transfected with WT CR4, CR4 S/A, or empty plasmid were allowed to adhere to VCAM-1 coated on plastic. The mock-transfected K562 cells bound VCAM-1, whereas WT CR4 transfectants showed almost no binding. Expression of CR4 S/A in K562 cells resulted in equal binding as K562 mock cells. Adhesion of mock cells was inhibited to the background level by treatment with anti-α_4 or anti-β_1 antibodies (Fig. 3*D*). In an additional assay, K562 cells stably transfected with WT CR4 or empty plasmid were left to adhere to confluent layers of endothelial cells under flow. More mock-transfected K562 cells bound endothelial cells than WT CR4 transfectants. That is, expression of functional CR4 blocked the adhesion of K562 to endothelial cells (data not shown). We conclude that both β_2 integrins studied, LFA-1 and CR4, can inhibit VLA-4 and that this inhibition requires a phosphorylatable α chain.

Transdominant Inhibition of VLA-4 by LFA-1 Needs an Active LFA-1 and pT758-14-3-3Tiam1 Signaling—It has been shown previously that the LFA-1 S1140A mutant is not fully activated after SDF-1α induction, and the mab24 activation epitope that reveals the extended open conformation of the integrin head domain (27) can be detected only in LFA-1 WT-expressing cells (17). Therefore, we tested additional ways to activate LFA-1, including inside-out activation with anti-CD3 or outside-in activation with soluble ICAM-1 and ICAM-2 (28) or CBR LFA-1/2 (5), a LFA-1-activating antibody. We then performed an adhesion assay to VCAM-1 under static conditions (Fig. 4*A*) or under flow (Fig. 4*B*). LFA-1 was able to reduce VLA-4 binding after each activation. The mutated α chain was able to inhibit VLA-4 when the β_2 integrin was activated with anti-CD3 or by outside-in activation but not by SDF-1α. Therefore, the inhibition of VLA-4 is not directly mediated through the α chain Ser-1140 phosphorylation itself, but the phosphorylation is needed when cells are activated with SDF-1α to fully activate the integrin. We next studied the activation state of LFA-1. Both WT and mutant LFA-1 can be detected with the KIM127 antibody (which recognizes the extended conformation with either a closed or an open headpiece) after SDF-1α activation, indicating that LFA-1 is in an activated extended form (Fig. 4*C*). Only LFA-1, but not LFA-1 S/A, expressed the mab24-epitope, recognizing the extended open headpiece after SDF-1α activation (Fig. 4*D*). When cells were activated with soluble ICAM-1, however, both LFA-1 WT- and LFA-1 S/A-expressing cells were mab24-positive (Fig. 4*E*), indicating that the α_L phosphorylation mutant can be fully activated by outside-in activation and that there is a correlation between the presence of mab24-positive LFA-1 and LFA-1 inhibition of VLA-4. This implies that the fully activated, mab24-positive form of LFA-1 is present and needed for VLA-4 inhibition but does not exclude the possibility that molecules with lower affinity conformation(s) take part in the cross-talk.

LFA-1 inhibited VLA-4 both after inside-out activation by SDF-1α and anti-CD3 and outside-in activation, *e.g.* by the activating antibody CBR LFA-1/2. Interestingly, these activations all lead to the phosphorylation of the LFA-1 β_2-chain on Thr-758 (Fig. 4*F*). We have previously characterized the signaling pathway downstream of Thr-758-phosphorylated LFA-1. The Thr-758-phosphorylated β_2 binds to the adaptor protein 14-3-3, which, in turn, binds to the Rac1 guanine nucleotide exchange factor Tiam1, which activates Rac1 (19). We therefore studied the role of β_2 chain signaling in the LFA-1-mediated inhibition of VLA-4. Jβ2.7 cells lacking LFA-1 were transfected with the phospho-Thr-758 peptide of β_2 ($p\beta_2$), which has been shown to activate the signaling pathway on its own (21). Cells were then allowed to adhere to VCAM-1 under flow, and adhered cells were counted. The presence of the β_2 peptide inhibited VLA-4 activity, indicating that this pathway can mediate LFA-1 inhibition of VLA-4. Cells transfected with the β_2 peptide lacking phosphate showed a slight decrease of VLA-4 activity, which could be caused by the peptide being phosphorylated in the cells. Transfection with a control peptide did not interfere with VLA-4 activity (Fig. 5*A*). The Thr-758-phosphorylated β_2 chain binds to 14-3-3, so we next transfected Jβ2.7 cells lacking LFA-1 with $p\beta_2$ with or without the 14-3-3-blocking peptide R18 or R18 alone. Cells were allowed to adhere to VCAM-1 under flow, and adhered cells were counted. The $p\beta_2$ peptide inhibited VLA-4, and blocking signaling from $p\beta_2$ to 14-3-3 reduced the inhibition. R18 did not affect VLA-4

Carl_G_190x270_mm_blokki_FINAL.indd 445 06-Aug-23 1:54:55 PM

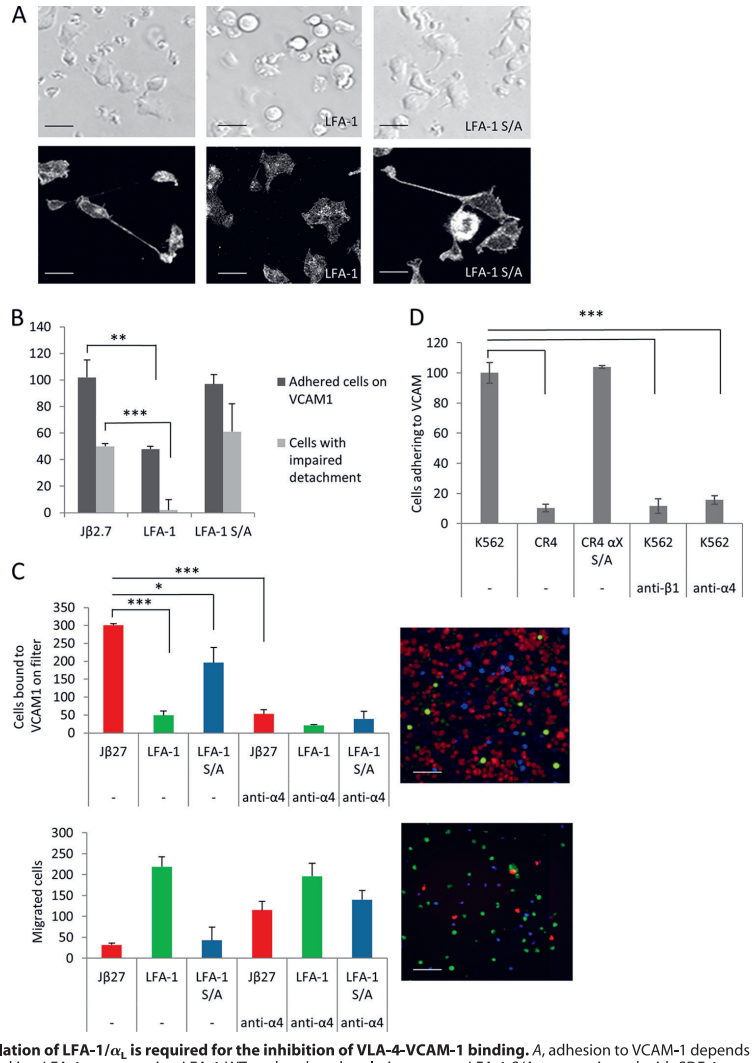

FIGURE 3. **Phosphorylation of LFA-1/α_L is required for the inhibition of VLA-4-VCAM-1 binding.** *A*, adhesion to VCAM-1 depends on a phosphorylatable α_L chain. Jβ2.7 cells lacking LFA-1 or expressing LFA-1 WT or the phosphorylation mutant LFA-1 S/A were activated with SDF-1α and allowed to adhere to VCAM-1 for 30 min (*top row*) or 2 h (*bottom row*). Shown are bright field image of cells (*top row*) or fluorescence image (*bottom row*) of cells fixed and stained with the α_4-antibody. *Scale bar* = 20 μm. *B*, quantification of impaired detachment. Cells were activated with SDF-1α and allowed to adhere to VCAM-1 for 1 h. Adhered cells and cells with long extensions/impaired detachment were quantified from six screens in triplicate. *C*, migration depends on phosphorylation of the α_L chain. The three cell lines were stained with fluorescent dyes (Jβ2.7, *red*; LFA-1, *green*; and LFA-1 S/A, *blue*). Equal amounts of cells were mixed and allowed to migrate toward SDF-1α over a VCAM-1-coated filter with or without the VLA-4-blocking antibody (2B4). Cells attached to the filter and migrated cells were quantified from ten screens in triplicate. An average of experiments are shown in the *left panels*, and a representative fluorescence pictures of one experiment is shown in the *right panels*. *Scale bars* = 100 μm. *D*, CR4 α_X chain phosphorylation inhibits VLA-4/VCAM-1 binding. K562 cells were transfected with empty plasmid (K562), WT CR4 (CR4), or the α_X chain phosphorylation mutant S1158A (CR4 S/A). Cells were allowed to adhere to VCAM-1 with or without the VLA-4-blocking antibodies 2B4 or Mab 13 as described under "Experimental Procedures," and bound cells were detected enzymatically. Cell binding is reported relative to K562 cell binding. *, $p < 0.05$; **, $p < 0.01$; ***, $p < 0.001$.

directly because no effect on VLA-4 to VCAM-1 binding was seen in Jβ2.7 cells lacking LFA-1 (Fig. 5*B*). In the following experiments, we studied the role of Tiam1, which is the next player in the signaling cascade. Jβ2.7 or LFA-1 cells were treated with an inhibitor of Tiam1. Adhesion experiments with VCAM-1 under flow were performed and showed that blocking Tiam1 reduced LFA-1 inhibition of VLA-4 (Fig. 5*C*). This indicates that LFA-1 can inhibit VLA-4 activity through the pT758β_2/14-3-3/Tiam1-pathway. This pathway leads to activation of Rac1 activity. Rac1 has been implicated in VLA-4 reg-

Carl_G_190x270_mm_blokki_FINAL.indd 446 06-Aug-23 1:54:55 PM

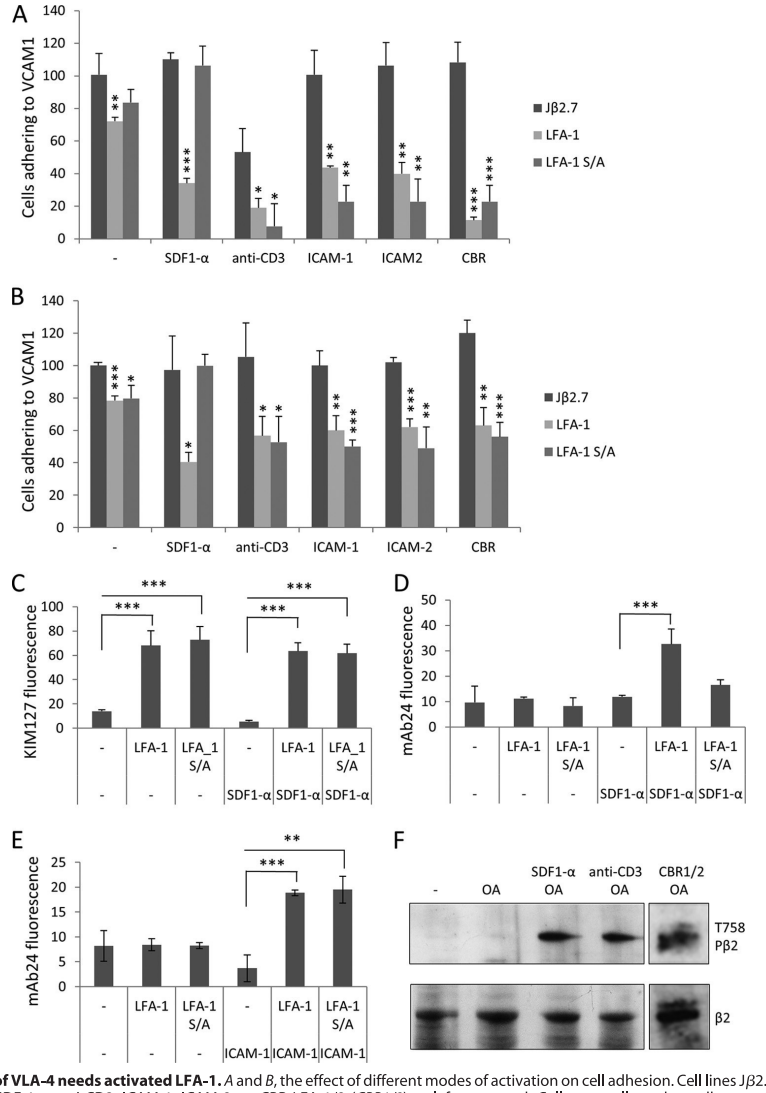

FIGURE 4. **Inhibition of VLA-4 needs activated LFA-1.** *A* and *B*, the effect of different modes of activation on cell adhesion. Cell lines Jβ2.7, LFA-1, or LFA-1 S/A were activated with SDF-1α, anti-CD3, ICAM-1, ICAM-2, or CBR LFA-1/2 (*CBR1/2*) or left untreated. Cells were allowed to adhere to VCAM-1 under static conditions (*A*) or flow (*B*). Bound cells were counted from ten frames in triplicate. Statistical significance is shown for LFA-1 or LFA-1 S/A cells compared with Jβ2.7 cells for each activation. *C–E*, LFA-1 activation epitope expression. The three cell lines were activated with SDF-1α (*C* and *D*) or ICAM-1 (*E*) or left untreated. Cells were spun down on glasses, fixed, and stained with KIM127 (*C*) or mAb24 (*D* and *E*) antibodies toward differently activated forms of LFA-1. Fluorescence intensity was measured by ImageJ. *F*, phosphorylation of the LFA-1 β_2 chain. Jβ2.7 LFA-1 cells were treated with okadaic acid (*OA*) and activated with SDF-1α, anti-CD3, and CBR LFA-1/2 or left untreated. Cells were lysed, the β_2-chain was immunoprecipitated, and the Western blot was stained for phospho-Thr-758-β_2 or β_2. *, $p < 0.05$; **, $p < 0.01$; ***, $p < 0.001$.

ulation, and we therefore blocked Rac1 in the three Jβ2.7 cell lines with the Rac1 inhibitor EHT 1864. Lack of Rac1 activity caused a large reduction of cell adhesion and spreading in all three cell lines, and differences between cell lines were not significant (data not shown).

We have shown previously that 14-3-3 binding to LFA-1 β_2 is induced by phosphorylated Thr-758 (19, 21). We next looked at 14-3-3 binding to β_2 in the different cell lines (Jβ2.7, LFA-1, and LFA-1 S/A) after three different activations: SDF-1α, anti-CD3, and CBR LFA-1/2 (Fig. 5, *D–F*). LFA-1 WT and S/A cells bound equally well to 14-3-3 after anti-CD3 or CBR1/2 activation, but LFA-1 S/A cells showed reduced binding to 14-3-3 after SDF-1α-activation. This is the only condition found where LFA-1 S/A does not inhibit

Carl_G_190x270_mm_blokki_FINAL.indd 447 06-Aug-23 1:54:55 PM

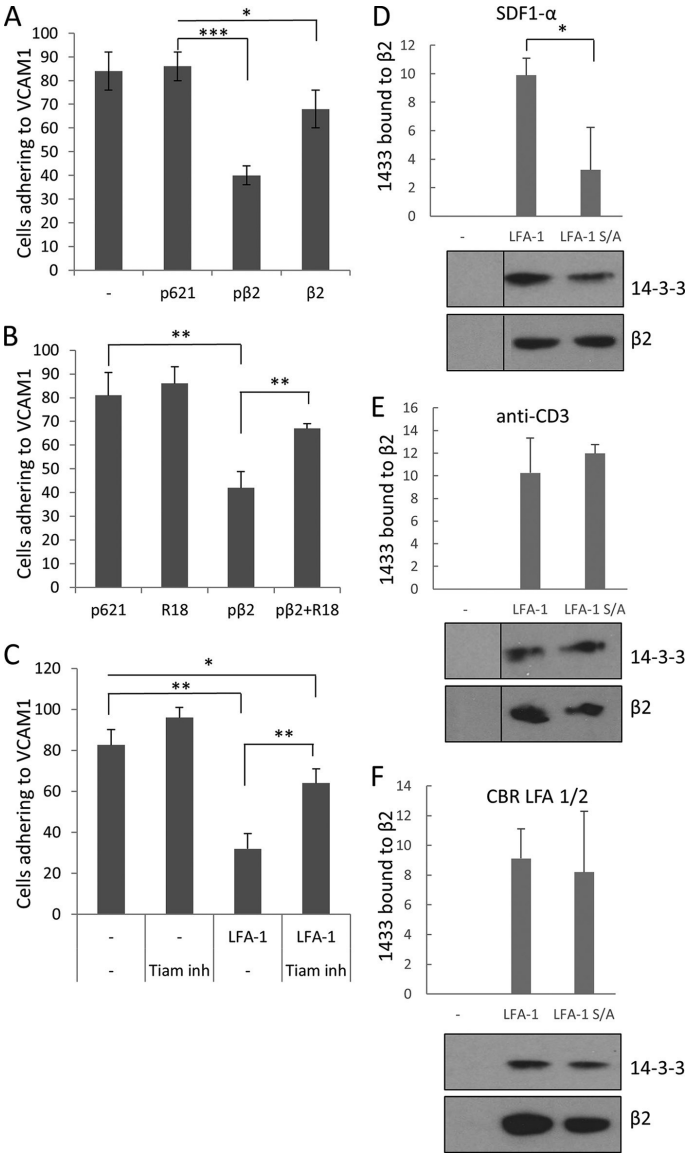

FIGURE 5. **Inhibition of VLA-4 by LFA-1 requires β_2/pThr-758–14-3-3-Tiam1 signaling.** *A*, effect of phospho-β_2 peptide transfection on adhesion. Jβ2.7 cells lacking LFA-1 were transfected with the phospho-Thr-758/β_2 peptide (*pβ2*), the β_2 peptide (*β2*), or a control peptide (*P621*). SDF-1α-activated cells were allowed to adhere to VCAM-1 under flow and counted from ten frames in triplicate. *B*, blocking of the 14-3-3 binding site. Jβ2.7 cells were transfected with pβ_2 or control peptide or pβ_2 together with the 14-3-3-blocking peptide R18. SDF-1α-activated cells were allowed to bind to VCAM-1 under flow and counted as in *A*. *C*, effect of the Tiam inhibitor. Jβ2.7 or LFA-1 cells were treated with the Tiam1 inhibitor for 2 h or left untreated. Cells were allowed to adhere to VCAM-1 under flow, and adhered cells were counted as in *A*. *D*—*F*, the amount of 14-3-3 coimmunoprecipitating with β_2. The three cell lines were activated with SDF-1α, anti-CD3, or CBR LFA-1/2. Cells were lysed, and β_2 was immunoprecipitated. Samples were run on SDS-PAGE, and β_2 and coprecipitated 14-3-3 were detected by antibodies. The amount of coprecipitated protein was normalized to the amount of precipitated β_2 and quantified from three separated experiments. *, $p < 0.05$; **, $p < 0.01$; ***, $p < 0.001$.

Carl_G_190x270_mm_blokki_FINAL.indd 448 06-Aug-23 1:54:55 PM

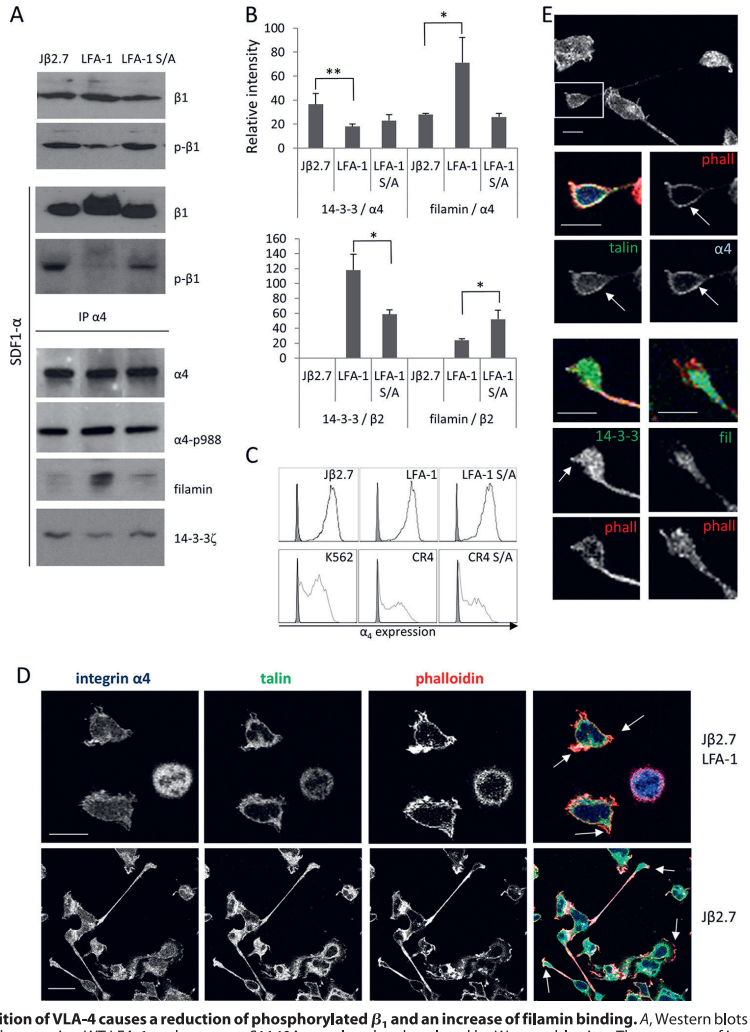

FIGURE 6. **LFA-1 inhibition of VLA-4 causes a reduction of phosphorylated β_1 and an increase of filamin binding.** *A*, Western blots of Jβ2.7 cell lines. Jβ2.7 cells lacking LFA-1 and expressing WT LFA-1 or the mutant S1140A were lysed and analyzed by Western blotting. The amounts of integrin β_1 and phosphorylated Thr-788/Thr-789 β_1 were detected by immunoblotting in cells with or without SDF1-α activation. Lysates were immunoprecipitated by integrin α_4 and immunoblotted to detect α_4, phosphorylated α_4 Ser-988, filamin, or 14-3-3ζ. *B*, the amount of coprecipitated 14-3-3 or filamin per immunoprecipitated β_2 or α_4 was quantified from three experiments. *C*, flow cytometry analysis of Jβ2.7 cells. Jβ2.7 LFA-1 and LFA-1 S/A cells were stained with anti-α_4 antibody (clone 2B4), followed by incubation with anti-mouse allophycocyanin, and detected by flow cytometry. *D*, fluorescence microscopy. Jβ2.7 cells with or without LFA-1 were allowed to adhere to VCAM-1 for 2 h, fixed, and stained for integrin α_4, talin, and phalloidin. *Scale bars* = 20 μm. *E*, the strong adhesion sites of Jβ2.7 cells bound to VCAM-1 stained with integrin α_4, talin, phalloidin (*phall*), 14-3-3, and filamin (*fil*). *Scale bars* = 10 μm. The *arrows* indicate membrane localization of α4, talin, phalloidin, and 14-3-3. *, $p < 0.05$; **, $p < 0.01$.

VLA-4, suggesting that the phosphorylation of Thr-758 and 14-3-3 binding is important for LFA-1-mediated inhibition of VLA-4 after SDF1-α activation.

Activated LFA-1 Affects VLA-4 Phosphorylation and Filamin Binding—We next studied how LFA-1 inhibition affects the VLA-4 molecule. We activated Jβ2.7, LFA-1, or LFA-1S/A cells with SDF-1α, and then cells were lysed and analyzed by immunoblotting. We detected a drastic reduction of VLA-4 β_1 chain phosphorylation on Thr-788/789 in LFA-1 cells compared with Jβ2.7 and LFA-1S/A cells. We next immunoprecipitated the α_4 chain and detected no difference in the amount to α_4, or α_4 phosphorylated on Ser-988. We could, however, see an increased amount of coprecipitated filamin in the LFA-1 cells compared with Jβ2.7 and LFA-1 S/A cells. In contrast, the amount of coprecipitated 14-3-3 was slightly reduced in the LFA-1 cells (Fig. 6*A*). No coprecipitated paxillin or sharpin

Carl_G_190x270_mm_blokki_FINAL.indd 449 06-Aug-23 1:54:56 PM

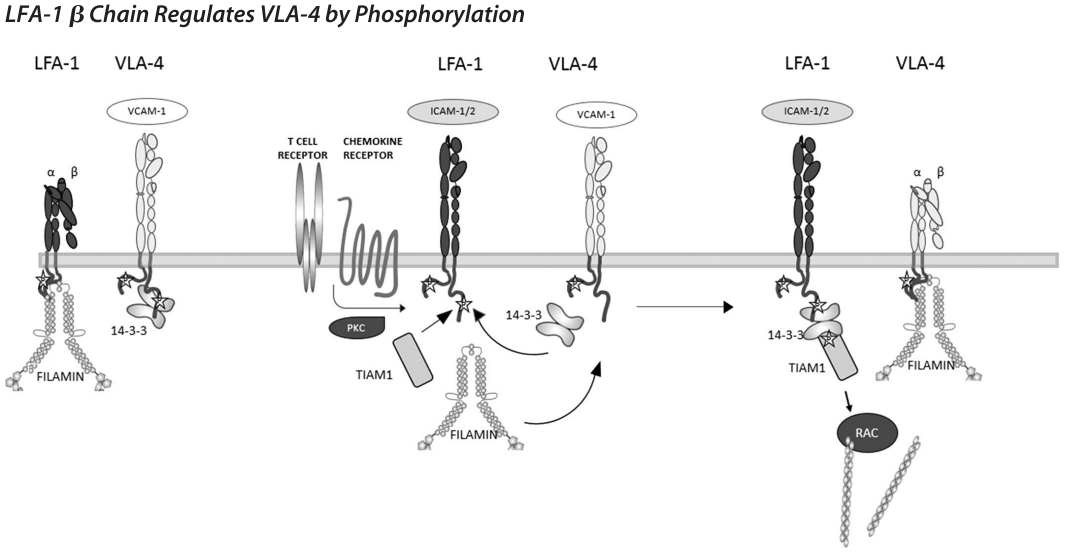

FIGURE 7. **Schematic of the LFA-1-mediated regulation of VLA-4.** When LFA-1 is inactive, VLA-4 binds VCAM-1. In this setting, LFA-1 is bound to filamin, and 14-3-3 is associated with VLA-4, which is phosphorylated on Thr-788/789 on the β_1 chain. When LFA-1 is activated, the β_2 chain is phosphorylated on Thr-758, 14-3-3 and Tiam1 bind, and VLA-4 binding to VCAM-1 is inhibited. Simultaneously, Thr-788/789 phosphorylation on the β_1 chain and 14-3-3 binding are reduced, whereas filamin binding is increased.

(data not shown) could be detected in the three cell lines. The amount of coprecipitated filamin and 14-3-3 relative to the amount of immunoprecipitated α_4 or β_2 was quantified from three experiments (Fig. 6*B*). This shows that, when LFA-1 is activated, more 14-3-3 and less filamin binds, whereas the opposite is true for VLA-4. Talin coprecipitation is not included because we were not able to specifically precipitate talin without an unspecific background (data not shown).

We next studied the expression and distribution of α_4 in Jβ2.7 and LFA-1 cells. Equal amounts of α_4 was seen in all three cell lines, as seen by flow cytometry (Fig. 6*C*) and Western blot analysis (Fig. 6*A*). Immunofluorescence staining of the subcellular localization of α_4, talin, and phalloidin showed that α_4 and talin are present at the membrane at adhesion sites where they colocalize with phalloidin, whereas less α_4 and talin were seen in these structures in LFA-1 cells (Fig. 6*D*, *arrows*). We finally looked at the localization of VLA-4-binding proteins in Jβ2.7 cells. The strong adhesions sites in the cells, which cannot be detached during migration, showed positive integrin α_4, talin, 14-3-3, and phalloidin staining at the membrane. Filamin was also present in the adhesion sites but less at the membrane (Fig. 6*C*, *arrows*).

DISCUSSION

Leukocyte cell adhesion to endothelial cells and transendothelial migration is a dynamic, multistep process in which cells are tethered to and roll on the endothelial cells, after which they adhere to and crawl on the endothelium and finally transmigrate. This complicated sequence of events is mediated by different adhesion molecules on the transmigrating cells, regulated through intracellular signaling, ligand binding, and shear flow and by signals expressed by the endothelium (29, 30).

T cells express several integrins, of which LFA-1 and VLA-4 are particularly important for the adhesion to endothelial cells. They play different roles in this cascade because VLA-4 can mediate cell tethering and rolling as well as firm arrest (31), whereas LFA-1 participates in the formation of strong adhesions and regulates migration over the endothelial surface (1). These interactions are mediated by changes in integrin conformation and affinity. We show that the activation of LFA-1 can inhibit VLA-4 binding to VCAM-1, an earlier step in the adhesion cascade. Cells lacking active LFA-1 adhere strongly to VCAM-1, which impairs migration because of the inability to detach adhesions and retract the trailing edge in the polarized cells. The expression of activated LFA-1 can inhibit this strong adhesion to the same extent as VLA-4 blocking antibodies and allow cells to migrate.

Regulation between different integrin classes in a given leukocyte was first described in 1993 (15). After that, the phenomenon has been reported in other cell types and between different integrin subclasses. Although, in many cases, the outside-in activation through ligand binding of one integrin decreases the activity of another integrin, there are reports that show an opposite effect (32, 33). It has been shown that the activation of LFA-1 can affect VLA-4 activity in T cells (34), but the mechanism has not been known.

We show that an activated LFA-1 is needed for inhibition of VLA-4 (Fig. 7). The downstream signaling from the activated LFA-1 requires the phosphorylation of the β_2 cytoplasmic chain on Thr-758. Both the activation of the T cell receptor and SDF-1α chemokine signaling result in the phosphorylation of Thr-758 in LFA-1 and inhibition of VLA-4. In a similar way, outside-in activation by the natural ligands ICAM-1 and ICAM-2 or the activating antibody CBR LFA-1/2 inhibit

Carl_G_190x270_mm_blokki_FINAL.indd 450 06-Aug-23 1:54:56 PM

VLA-4. Phosphorylation of the β_2 chain is needed for the activation of leukocyte integrins, and the signaling cascade downstream of β_2 integrin phosphorylation, leading to rearrangement of the actin cytoskeleton, has been characterized. T cell receptor-induced activation has been found to result in phosphorylated Thr-758 in β_2, binding of the adaptor protein 14-3-3 and the Rac1 guanine nucleotide exchange factor Tiam1, and, ultimately, to the activation of Rac1, cytoskeleton rearrangements, and integrin clustering (19, 21, 23). Transfection of a Thr-758-phosphorylated β_2 cytoplasmic peptide was enough to initiate this signaling pathway (19), and we now show that it is sufficient to induce a decrease in VLA-4 ligand binding capacity when transfected into LFA-1-negative cells. This has also been shown in another integrin cross-talk setting. The β_3 cytoplasmic tail alone is necessary and sufficient to mediate transdominant inhibition of $\alpha_5\beta_1$. The expression of the isolated β_3 cytoplasmic tail exerts an inhibitory effect upon $\alpha_5\beta_1$-mediated migration, as well as phagocytosis, in a similar way as $\alpha_v\beta_3$ ligation (35). In LFA-1-expressing cells, inhibition of VLA-4 by LFA-1 could be overcome by blocking 14-3-3 binding using the R18 blocking peptide, which inhibits its binding to phospho-β_2 and other molecules of the signaling cascade. Incubation of the cells with the Tiam1 inhibitor, the next player in the pathway, increased VLA-4/VCAM-1 binding back to the basal level.

There is also a slight, but not significant, increase in VCAM-1 binding in cells lacking LFA-1 and treated with the Tiam1 inhibitor. Therefore, we cannot exclude the possibility that the inhibition of Tiam1 may also directly affect VLA-4 binding to VCAM-1 and that the full effect of the increase in VCAM-1 binding is not detectable because of the strong interaction between VLA-4 and VCAM-1 in untreated cells. Blocking Tiam1, however, would lead to less activation of Rac1, which should decrease VCAM-1 binding because Rac1 has been implicated previously in VLA-4 activation (36). It is possible that the signaling pathway downstream of LFA-1, which leads to activation of Rac1, may sequester Rac1 activity away from VLA-4, thereby inhibiting VLA-4. Alternatively, a large proportion of Rac1 is consumed by the LFA-1/Rac1 pathway, resulting in less availability for the VLA-4/Rac1 pathway.

Interestingly, α chain phosphorylation was found to play an essential role in the activation cascade when inside-out activation was triggered with the chemokine SDF-1α but not by other forms of activation. This is not unique for LFA-1 because the CR4-integrin also requires α chain phosphorylation for transdominant inhibition of VLA-4. SDF-1α has also been reported to activate VLA-4-dependent leukocyte adhesion (36, 37). However, according to Manevich *et al.* (37) and our own observations, Jurkat cells (from which the Jβ2.7 cell line is derived) show stronger VLA-4/VCAM-1 adhesion than primary T cells. This indicates that VLA-4 in Jβ2.7 is already in the high-activity conformation and, thus, cannot achieve any higher affinity.

We also show that, under conditions where LFA-1 is able to inhibit VLA-4, there is an increased amount of the mab24-positive conformation of LFA-1, which is not seen in non-activated cells or SDF-1α-activated α chain phosphorylation mutants not mediating inhibition. The mab24-positive integrin corresponds to the high-affinity extended open headpiece conformation (1, 2). The amount of KIM127-positive reactivity, which detects the extended conformation of the integrin, was the same in all activated cells.

The importance of Thr-758 phosphorylation and 14-3-3 binding for VLA-4 inhibition was further shown by coimmunoprecipitations of β_2 and 14-3-3. Cells expressing the LFA-1 α chain phosphorylation mutant S1140A, which cannot mediate inhibition of VLA-4 when activated by SDF-1α, bound 14-3-3 poorly compared with WT LFA-1. On the other hand, LFA-1 S1140A, activated with anti-CD3 or CBR LFA 1/2, binds 14-3-3 equally well, and mediates inhibition of VLA-4.

Like other integrins, VLA-4 activities are also regulated by phosphorylation. The VLA-4 α chain was phosphorylated on Ser-988 in the cell lines studied, regardless of the expression of LFA-1 or its activation. The phosphorylation of β_1 on Thr-788/789 corresponds to the phosphorylation triplet in β_2, including Thr-758. This phosphorylation reduces β_1 association with the actin cytoskeleton (38) and increases pressure-induced cell adhesion in cancer cells (39). Importantly, cells expressing the activated form of LFA-1 showed reduced phosphorylation of β_1 Thr-788/789.

Like β_2, the β_1 cytoplasmic part also interacts with filamin, 14-3-3, and talin (40), but the regulation of these interactions by phosphorylation has not been studied. For β_2, it is known that the bent inactive conformation interacts with filamin and that, upon Thr-758 phosphorylation, binding of 14-3-3 outcompetes filamin binding (18). We showed that, when LFA-1 mediates inhibition of VLA-4, LFA-1 was phosphorylated on Thr-758 and bound to 14-3-3 but not to filamin. Instead, the binding between VLA-4 and filamin was increased, and the binding to 14-3-3 was decreased. VLA-4 binds to 14-3-3 both through the α and β chains, whereas LFA-1 binds only through the β_2 chain. It has recently been shown that the Thr-758 phosphorylated binding motif in the β_2 integrin tail has a much higher affinity for 14-3-3ζ than the corresponding α_4 motif (41). Therefore, Thr-758 phosphorylation of β_2 may reduce binding between VLA-4 and 14-3-3 by binding to 14-3-3 protein, enabling binding of filamin to the β_1 polypeptide. In this way, specific integrin phosphorylations can control cell adhesion and migration by spatial segregation of adaptor-protein binding.

Under several clinical conditions, it would be important to affect leukocyte adhesion and migration into tissues. Modulation of β_2 integrins is currently used in the treatment of autoimmune diseases (32). Our results show that this may affect not only LFA-1 but also VLA-4 and, possibly, other integrins, which must be taken into consideration in the interpretation of the clinical outcome.

Acknowledgments—We thank Leena Kuoppasalmi and Daniela Lopéz Contreras for technical assistance and M. Arnaout, M. Robinson, N. Hogg, and T. A. Springer for antibodies.

REFERENCES

1. Hogg, N., Patzak, I., and Willenbrock, F. (2011) The insider's guide to leukocyte integrin signalling and function. *Nat. Rev. Immunol.* **11,** 416–426
2. Chigaev, A., and Sklar, L. A. (2012) Aspects of VLA-4 and LFA-1 regulation that may contribute to rolling and firm adhesion. *Front. Immunol.* **3,**

Carl_G_190x270_mm_blokki_FINAL.indd 451 06-Aug-23 1:54:57 PM

LFA-1 β Chain Regulates VLA-4 by Phosphorylation

242
3. Butcher, E. C. (1991) Leukocyte-endothelial cell recognition: three (or more) steps to specificity and diversity. *Cell* **67,** 1033–1036
4. Springer, T. A. (1994) Traffic signals for lymphocyte recirculation and leukocyte emigration: the multistep paradigm. *Cell* **76,** 301–314
5. Luo, B. H., Carman, C. V., and Springer, T. A. (2007) Structural basis of integrin regulation and signaling. *Annu. Rev. Immunol.* **25,** 619–647
6. Gahmberg, C. G., Fagerholm, S. C., Nurmi, S. M., Chavakis, T., Marchesan, S., and Grönholm, M. (2009) Regulation of integrin activity and signalling. *Biochim. Biophys. Acta* **1790,** 431–444
7. Gahmberg, C. G. (1997) Leukocyte adhesion: CD11/CD18 integrins and intercellular adhesion molecules. *Curr. Opin. Cell Biol.* **9,** 643–650
8. Tan, S. M. (2012) The leucocyte β2 (CD18) integrins: the structure, functional regulation and signalling properties. *Biosci. Rep.* **32,** 241–269
9. Gahmberg, C. G., Tolvanen, M., and Kotovuori, P. (1997) Leukocyte adhesion: structure and function of human leukocyte β2-integrins and their cellular ligands. *Eur. J. Biochem.* **245,** 215–232
10. Imai, Y., Shimaoka, M., and Kurokawa, M. (2010) Essential roles of VLA-4 in the hematopoietic system. *Int. J. Hematol.* **91,** 569–575
11. Rose, D. M., Alon, R., and Ginsberg, M. H. (2007) Integrin modulation and signaling in leukocyte adhesion and migration. *Immunol. Rev.* **218,** 126–134
12. Das, M., Subbayya Ithychanda, S., Qin, J., and Plow, E. F. (2014) Mechanisms of talin-dependent integrin signaling and crosstalk. *Biochim. Biophys. Acta* **1838,** 579–588
13. Calderwood, D. A., Campbell, I. D., and Critchley, D. R. (2013) Talins and kindlins: partners in integrin-mediated adhesion. *Nat. Rev. Mol. Cell. Biol.* **14,** 503–517
14. Campbell, J. J., Hedrick, J., Zlotnik, A., Siani, M. A., Thompson, D. A., and Butcher, E. C. (1998) Chemokines and the arrest of lymphocytes rolling under flow conditions. *Science* **279,** 381–384
15. van Kooyk, Y., van de Wiel-van Kemenade, E., Weder, P., Huijbens, R. J., and Figdor, C. G. (1993) Lymphocyte function-associated antigen 1 dominates very late antigen 4 in binding of activated T cells to endothelium. *J. Exp. Med.* **177,** 185–190
16. Fagerholm, S. C., Hilden, T. J., and Gahmberg, C. G. (2004) P marks the spot: site-specific integrin phosphorylation regulates molecular interactions. *Trends Biochem. Sci.* **29,** 504–512
17. Fagerholm, S. C., Hilden, T. J., Nurmi, S. M., and Gahmberg, C. G. (2005) Specific integrin α and β chain phosphorylations regulate LFA-1 activation through affinity-dependent and -independent mechanisms. *J. Cell Biol.* **171,** 705–715
18. Takala, H., Nurminen, E., Nurmi, S. M., Aatonen, M., Strandin, T., Takatalo, M., Kiema, T., Gahmberg, C. G., Ylänne, J., and Fagerholm, S. C. (2008) β2 integrin phosphorylation on Thr758 acts as a molecular switch to regulate 14-3-3 and filamin binding. *Blood* **112,** 1853–1862
19. Grönholm, M., Jahan, F., Marchesan, S., Karvonen, U., Aatonen, M., Narumanchi, S., and Gahmberg, C. G. (2011) TCR-induced activation of LFA-1 involves signaling through Tiam1. *J. Immunol.* **187,** 3613–3619
20. Nortamo, P., Patarroyo, M., Kantor, C., Suopanki, J., and Gahmberg, C. G. (1988) Immunological mapping of the human leucocyte adhesion glycoprotein gp90 (CD18) by monoclonal antibodies. *Scand. J. Immunol.* **28,** 537–546
21. Nurmi, S. M., Autero, M., Raunio, A. K., Gahmberg, C. G., and Fagerholm, S. C. (2007) Phosphorylation of the LFA-1 integrin β2-chain on Thr-758 leads to adhesion, Rac-1/Cdc42 activation, and stimulation of CD69 expression in human T cells. *J. Biol. Chem.* **282,** 968–975
22. Andersson, L. C., Nilsson, K., and Gahmberg, C. G. (1979) K562: a human erythroleukemic cell line. *Int. J. Cancer.* **23,** 143–147
23. Uotila, L. M., Aatonen, M., and Gahmberg, C. G. (2013) Integrin CD11c/CD18 α-chain phosphorylation is functionally important. *J. Biol. Chem.* **288,** 33494–33499
24. Ades, E. W., Candal, F. J., Swerlick, R. A., George, V. G., Summers, S., Bosse, D. C., and Lawley, T. J. (1992) HMEC-1: establishment of an immortalized human microvascular endothelial cell line. *J. Invest. Dermatol.* **99,** 683–690
25. Weber, K. S., York, M. R., Springer, T. A., and Klickstein, L. B. (1997) Characterization of lymphocyte function-associated antigen 1 (LFA-1)-deficient T cell lines: the αL and β2 subunits are interdependent for cell surface expression. *J. Immunol.* **158,** 273–279
26. Constantin, G., Majeed, M., Giagulli, C., Piccio, L., Kim, J. Y., Butcher, E. C., and Laudanna, C. (2000) Chemokines trigger immediate β2 integrin affinity and mobility changes: differential regulation and roles in lymphocyte arrest under flow. *Immunity.* **13,** 759–769
27. Dransfield, I., and Hogg, N. (1989) Regulated expression of Mg^{2+} binding epitope on leukocyte integrin α subunits. *EMBO J.* **8,** 3759–3765
28. Kotovuori, A., Pessa-Morikawa, T., Kotovuori, P., Nortamo, P., and Gahmberg, C. G. (1999) ICAM-2 and a peptide from its binding domain are efficient activators of leukocyte adhesion and integrin affinity. *J. Immunol.* **162,** 6613–6620
29. Muller, W. A. (2011) Mechanisms of leukocyte transendothelial migration. *Annu. Rev. Pathol.* **6,** 323–344
30. Shulman, Z., Cohen, S. J., Roediger, B., Kalchenko, V., Jain, R., Grabovsky, V., Klein, E., Shinder, V., Stoler-Barak, L., Feigelson, S. W., Meshel, T., Nurmi, S. M., Goldstein, I., Hartley, O., Gahmberg, C. G., Etzioni, A., Weninger, W., Ben-Baruch, A., and Alon, R. (2012) Transendothelial migration of lymphocytes mediated by intraendothelial vesicle stores rather than by extracellular chemokine depots. *Nat. Immunol.* **13,** 67–76
31. Alon, R., Feigelson, S. W., Manevich, E., Rose, D. M., Schmitz, J., Overby, D. R., Winter, E., Grabovsky, V., Shinder, V., Matthews, B. D., Sokolovsky-Eisenberg, M., Ingber, D. E., Benoit, M., and Ginsberg, M. H. (2005) α4β1-dependent adhesion strengthening under mechanical strain is regulated by paxillin association with the α4-cytoplasmic domain. *J. Cell Biol.* **171,** 1073–1084
32. Gonzalez, A. M., Bhattacharya, R., deHart, G. W., and Jones, J. C. (2010) Transdominant regulation of integrin function: mechanisms of crosstalk. *Cell. Signal.* **22,** 578–583
33. Chan, J. R., Hyduk, S. J., and Cybulsky, M. I. (2000) α 4 β 1 integrin/VCAM-1 interaction activates α L β 2 integrin-mediated adhesion to ICAM-1 in human T cells. *J. Immunol.* **164,** 746–753
34. Porter, J. C., and Hogg, N. (1997) Integrin cross talk: activation of lymphocyte function-associated antigen-1 on human T cells alters α4β1- and α5β1-mediated function. *J. Cell Biol.* **138,** 1437–1447
35. Blystone, S. D., Lindberg, F. P., LaFlamme, S. E., and Brown, E. J. (1995) Integrin β 3 cytoplasmic tail is necessary and sufficient for regulation of α 5 β 1 phagocytosis by α v β 3 and integrin-associated protein. *J. Cell Biol.* **130,** 745–754
36. García-Bernal, D., Wright, N., Sotillo-Mallo, E., Nombela-Arrieta, C., Stein, J. V., Bustelo, X. R., and Teixidó, J. (2005) Vav1 and Rac control chemokine-promoted T lymphocyte adhesion mediated by the integrin α4β1. *Mol. Biol. Cell* **16,** 3223–3235
37. Manevich, E., Grabovsky, V., Feigelson, S. W., and Alon, R. (2007) Talin 1 and paxillin facilitate distinct steps in rapid VLA-4-mediated adhesion strengthening to vascular cell adhesion molecule 1. *J. Biol. Chem.* **282,** 25338–25348
38. Suzuki, K., and Takahashi, K. (2003) Reduced cell adhesion during mitosis by threonine phosphorylation of β1 integrin. *J. Cell. Physiol.* **197,** 297–305
39. Craig, D. H., Gayer, C. P., Schaubert, K. L., Wei, Y., Li, J., Laouar, Y., and Basson, M. D. (2009) Increased extracellular pressure enhances cancer cell integrin-binding affinity through phosphorylation of β1-integrin at threonine 788/789. *Am. J. Physiol. Cell. Physiol.* **296,** C193–C204
40. Legate, K. R., and Fässler, R. (2009) Mechanisms that regulate adaptor binding to β-integrin cytoplasmic tails. *J. Cell Sci.* **122,** 187–198
41. Bonet, R., Vakonakis, I., and Campbell, I. D. (2013) Characterization of 14-3-3-ζ interactions with integrin tails. *J. Mol. Biol.* **425,** 3060–3072

Regular Article

blood

PHAGOCYTES, GRANULOCYTES, AND MYELOPOIESIS

LFA-1 integrin antibodies inhibit leukocyte $\alpha_4\beta_1$–mediated adhesion by intracellular signaling

Mikaela Grönholm,* Farhana Jahan,* Ekaterina A. Bryushkova, Sudarrshan Madhavan, Francesca Aglialoro, Laura Soto Hinojosa, Liisa M. Uotila, and Carl G. Gahmberg

Division of Biochemistry and Biotechnology, Faculty of Biological and Environmental Sciences, University of Helsinki, Helsinki, Finland

Key Points

- Activating and inhibitory antibodies to the LFA-1 integrin inhibit the $\alpha_4\beta_1$ integrin.
- Inhibition occurs by intracellular signaling resulting from integrin phosphorylations.

Binding of intercellular adhesion molecule-1 to the β_2-integrin leukocyte function associated antigen-1 (LFA-1) is known to induce cross-talk to the $\alpha_4\beta_1$ integrin. Using different LFA-1 monoclonal antibodies, we have been able to study the requirement and mechanism of action for the cross-talk in considerable detail. LFA-1-activating antibodies and those inhibitory antibodies that signal to $\alpha_4\beta_1$ induce phosphorylation of Thr-758 on the β_2-chain, which is followed by binding of 14-3-3 proteins and signaling through the G protein exchange factor Tiam1. This results in dephosphorylation of Thr-788/789 on the β_1-chain of $\alpha_4\beta_1$ and loss of binding to its ligand vascular cell adhesion molecule-1. The results show that with LFA-1 antibodies, we can activate LFA-1 and inhibit $\alpha_4\beta_1$, inhibit both LFA-1 and $\alpha_4\beta_1$, inhibit LFA-1 but not $\alpha_4\beta_1$, or not affect LFA-1 or $\alpha_4\beta_1$. These findings are important for the understanding of integrin regulation and for the interpretation of the effect of integrin antibodies and their use in clinical applications. (*Blood*. 2016;128(9):1270-1281)

Introduction

To conduct effective immune surveillance, the host has to be able to recruit leukocytes to specific sites of infection and inflammation. Leukocytes adhere to the vascular endothelium in a sequence of events, including the capture of circulating leukocytes and subsequent leukocyte rolling, arrest, firm adhesion, and transendothelial migration. These processes are tightly regulated and mediated by the selectin and integrin adhesion receptors and their ligands.[1-3]

Integrins are heterodimeric transmembrane receptors. The family of leukocyte-specific β_2 integrins consists of 4 members. They have a common β_2-chain (CD18) and 1 of 4 α-chains: α_L (CD11a), α_M (CD11b), α_X (CD11c), and α_D (CD11d). The leukocyte function-associated antigen-1 heterodimer (LFA-1, $\alpha_L\beta_2$, CD11a/CD18) is primarily expressed in lymphocytes and binds to intercellular adhesion molecules (ICAMs).[4,5] In addition, leukocytes express β_1 integrins, among them $\alpha_4\beta_1$ (very late antigen 4). $\alpha_4\beta_1$ binds to the endothelial protein vascular cell adhesion molecule-1 (VCAM-1), but also to extracellular matrix proteins such as fibronectin.[1]

Integrins can communicate in 2 directions across the plasma membrane. Outside-in signaling occurs by integrin ligand binding, whereas inside-out signaling is activated by ligand binding to nonintegrin receptors, such as chemokine receptors or the T-cell receptor (TCR), which convey signals to integrins through intracellular pathways. This results in changes in integrin activity. Integrins can exist in at least 3 different conformations: inactive bent, extended, and extended open.[6] The integrin cytoplasmic domains are short and devoid of catalytic activity. However, integrin function is regulated by changes in phosphorylation and protein interactions in the cytoplasmic domains.[7-10]

LFA-1 and $\alpha_4\beta_1$ mediate distinct steps in the adhesion cascade. $\alpha_4\beta_1$ mediates rolling and adhesion strengthening, whereas LFA-1 is needed for firm adhesion and migration.[1] Importantly, integrins have the ability to modulate their adhesive properties within seconds after chemokine stimulation.[11] We and others have previously shown that TCR activation, chemokines, and ligands to LFA-1 regulate $\alpha_4\beta_1$ activity in T cells.[12,13] Changes in both the phosphorylation status of β_1 and β_2 chains and the β-chain binding proteins mediate this cross-talk.[13] The signaling pathway from the phosphorylated Thr-758 in the β_2 integrin, followed by 14-3-3 binding, recruitment of T-cell lymphoma invasion and metastasis 1 (Tiam1) protein, and upregulation of Ras-related C3 botulinum toxin substrate 1 (Rac1) was described earlier.[14-16] This leads to dephosphorylation of β_1 Thr-788/789, reduced β_1-14-3-3 binding, increased filamin binding to β_1, and reduced adhesion of cells to VCAM-1.[13]

We have now studied the effect of LFA-1-specific antibodies on cross-talk to $\alpha_4\beta_1$. We show that activating and some blocking LFA-1 antibodies inhibit $\alpha_4\beta_1$-binding to VCAM-1. Other LFA-1 antibodies may inhibit LFA-1 but do not affect $\alpha_4\beta_1$. The cross-talk is a result of intracellular signaling through phospholipases (phospholipase C β [PLCβ] and PLCγ) and protein kinase C (PKC), resulting in phosphorylation of Thr-758 on β_2, signaling through Tiam1, decrease of β_1 phosphorylation, and inhibition of $\alpha_4\beta_1$ adhesion to VCAM-1. To the best of our knowledge, this is the first time it has been shown that antibodies to a leukocyte integrin can regulate another integrin in different ways as a result of intracellular signaling.

Submitted March 11, 2016; accepted July 12, 2016. Prepublished online as *Blood* First Edition paper, July 21, 2016; DOI 10.1182/blood-2016-03-705160.

*M.G. and F.J. contributed equally to this study.

The online version of this article contains a data supplement.

The publication costs of this article were defrayed in part by page charge payment. Therefore, and solely to indicate this fact, this article is hereby marked "advertisement" in accordance with 18 USC section 1734.

© 2016 by The American Society of Hematology

Carl_G_190x270_mm_blokki_FINAL.indd 453 06-Aug-23 1:54:58 PM

Methods

Reagents and antibodies

VCAM-1-Fc, ICAM-1-Fc, fibronectin, and stromal cell-derived factor 1α (SDF-1α) were from R&D Systems (Minneapolis, MN). A polyclonal rabbit antiserum against the β_2-chain phosphorylated on Thr-758 was produced by GenicBio Ltd. (Shanghai, China). CBR LFA-1/2, CBR LFA-1/7, MEM83, and TS2/4 were from T.A. Springer (Boston Children's Hospital, Boston, MA). Other antibodies were 7E4 and R2E7B,[17] MEM48, MEM148, anti-phospho-β_1 Thr-788/789, 12G10-488 (Abcam, Cambridge, United Kingdom), TS1/22, TS1/18, anti-α_4 (Thermo Scientific, Waltham, MA), MHM23 (Dako, Glostrup, Denmark), MHM24 (DSHB, Iowa City, IA), anti-CD3, anti-CD25-PE (ImmunoTools, Friesoythe, Germany), anti-β_1 (MAB13, BD Biosciences, San Jose, CA), anti-PLCβ$_3$, anti-phospho-PLCβ$_3$ Ser-1105, anti-phospho-PLCγ$_1$ Tyr-783 (Cell Signaling, Danvers, MA), anti-talin 8d4, anti-actin (Sigma-Aldrich, St Louis, MO), anti-PLCγ$_1$, anti-14-3-3 (Santa Cruz Biotechnology, Dallas, TX), blocking antibodies to α_4 (2B4, R&D Systems) and α_5 (P1D6, Millipore), horseradish peroxidase–linked Abs against mouse and rabbit IgG (GE Healthcare, Little Chalfont, United Kingdom). Fab fragments of the 7E4 antibody were produced by papain cleavage (10 μg papain/mg antibody; 37°C for 8 h) (Sigma-Aldrich) and purified by Protein G/A sepharose (PGS/PAS, GE Healthcare). Other reagents include Tiam1 (NSC23766, 100 μM) and ras-related C3 botulinum toxin substrate 1 (Rac1) (EHT1864, 10 μM) inhibitors (Biotechne, Minneapolis, MN), Cytochalasin D (Sigma-Aldrich).

Cell cultures, immunoprecipitation, and immunoblotting

The human T-cell lymphoma cell line Jβ2.7, which lacks CD11 chains,[18] was grown in RPMI1640 medium supplemented with 10% FBS, 2 mM L-glutamine, and 100 U/mL penicillin-streptomycin. Jβ2.7 expressing wt LFA-1 has been described.[13] Naive T cells were purified from buffy coats obtained from the Finnish Red Cross Blood Transfusion Service (Helsinki, Finland) by Ficoll-Hypaque gradient centrifugation and nylon-wool columns. T blasts were induced by ImmunoCult human CD3/CD28/CD2 T-cell activator and 30 IU/mL IL-2 in ImmunoCult-XF T Cell Expansion Medium (Stemcell Technologies, Grenoble, France) and used after 96 hours. Jβ2.7 or Jβ2.7/LFA-1 cells or T blasts were incubated with different LFA-1 antibodies for 15 minutes. Cells were washed in cold PBS, lysed on ice in 2% radioimmune precipitation assay buffer[14] with protease and phosphatase inhibitors (Roche, Basel, Switzerland). Lysates were centrifuged at 13,400 rpm for 60 minutes at 4°C. For co-immunoprecipitation, cells were treated with CBR LFA-1/2 or TS2/4 and lysed. Prewashed PGS beads were added for 3 hours at 4°C. The unbound fraction was mixed with α_4 antibody for 1 hour, and PGS beads for another 2 hours at 4°C. Beads were washed 4 times with 1% radioimmune precipitation assay buffer.[14] Equal amounts of protein were analyzed by SDS-PAGE and immunoblotting and detected with ECL (Pierce Biotechnology, IL).

Cell adhesion and migration assays

For the static adhesion assay, culture wells were coated with 6 μg/mL ICAM-1 or 10 μg/mL fibronectin, blocked with 2% BSA, and 10 000 Jβ2.7/LFA-1-cells or T blasts were allowed to adhere for 30 minutes with or without pre-incubation with SDF-1α (50 ng/mL) or indicated antibodies (10 μg/mL except 30 μg/mL 7E4) for 15 minutes. Loose cells were washed off by placing the plate upside-down in PBS for 1 hour, and adhered cells counted from 10 screens using an EVOS microscope (Life Technologies, Carlsbad, CA). Flow adhesion assays were performed in VCAM-1-coated (10 μg/mL) flow chamber channels (μ-SlideVI$^{0.4}$; Ibidi GmbH, Martinsried, Germany), using the multiphaser NE-1000 syringe pump (shear flow rate, 0.3 dynes/cm^2; New Era Pump Systems, Inc., Farmingdale, NY). Attached cells were counted from 6 separate screens. The migration assay was performed over 5 μm pore-size Transwell membranes coated with fibronectin or BSA (5 μg/mL). Cells were incubated with α_4 or α_5 blocking antibody for 10 minutes and an activating (CBR LFA-1/2) or neutral (TS2/4) LFA-1 antibody for 15 minutes. Cells were allowed to migrate toward SDF-1α (25 ng/mL) at 37°C for 1 hour. Migrated cells were collected and counted.

Table 1. LFA-1 specific antibody binding sites and effects on LFA-1 and $\alpha_4\beta_1$ activity

	Chain	Binding site	Lfa-1 activity	α4β1 activity
CBR LFA-1/2	β_2	I-EGF-3	Activating	Inhibiting
MEM48	β_2	I-EGF-3	Activating	Inhibiting
MEM148	β_2	Hybrid	Activating	Inhibiting
7E4	β_2	Hybrid	Inhibiting	Inhibiting
TS1/18	β_2	β I-LIKE	Inhibiting	Inhibiting
MHM23	β_2	β I-LIKE	Inhibiting	No effect
CBR LFA-1/7	β_2	I-EGF-1	No effect	No effect
MEM83	α_L	α I-domain	Activating	Inhibiting
TS1/22	α_L	α I-domain	Inhibiting	No effect
MHM24	α_L	α I-domain	Inhibiting	Inhibiting
TS2/4	α_L	β propeller	No effect	No effect

Small interfering RNA and Rac1 pulldown

Tiam1 (200 nM; sc-36669) or control siRNA (Santa Cruz Biotechnology) was electroporated into cells with the Neon electroporator (Thermo Fisher Scientific).[14] The active Rac-1 pulldown kit was from Thermo Scientific.

Immunofluorescence

Cells were treated with SDF-1α or antibodies for 15 minutes or left untreated. To cluster $\alpha_4\beta_1$, cells were treated with soluble VCAM-1 (5 μg/mL) and an anti-VCAM-1 antibody (ImmunoTools). Cells were seeded on poly-L-lysine and fixed in 4% paraformaldehyde. Cells were stained with antibodies for 1 hour, and Alexa fluor secondary antibodies 488 or 633 or TRITC-phalloidin, washed in PBS, mounted with Prolong Hold Antifade reagent (Thermo Scientific), and analyzed with a Leica TCS SP5 MP confocal microscope (Wetzlar, Germany) and Leica Application Suite, using a HCX APO 63x/1,30 Corr (glycerol) CS 21 objective in room temperature.

Quantifications

Quantifications were done using ImageJ (v1.50b) software. Fluorescence intensity was quantified as corrected total cell fluorescence. Statistical analyses were performed in Excel with unpaired Student *t* test. Mean standard deviations are included in figures.

Results

LFA-1-specific antibodies affect the activity of $\alpha_4\beta_1$

We have previously shown that activation of LFA-1 through the TCR receptor or chemokine receptors, induces a signaling pathway, leading to the phosphorylation of Thr-758 on the β_2-chain, 14-3-3 and Tiam1 binding,[14-16,19] and downregulation of $\alpha_4\beta_1$ binding to VCAM-1.[13] We have now found that activating and inhibitory antibodies to LFA-1 can regulate this signaling pathway. We collected antibodies to both β_2 and α_L, which have been described to activate, inhibit, or have no effect on LFA-1 ligand binding (Table 1). We first tested their ability to specifically bind LFA-1 on the human Jurkat cell line, Jβ2.7/LFA-1, expressing LFA-1, and, as a control on Jβ2.7 cells, lacking LFA-1 on their cell surface. Antibodies bound to LFA-1 on Jβ2.7/LFA-1 cells, but there was no binding to Jβ2.7 cells, as shown by flow cytometry (supplemental Figure 1, available on the *Blood* Web site). We next assessed the ability of these antibodies to activate or inhibit binding to the LFA-1 ligand ICAM-1 in a static adhesion assay. Jβ2.7/LFA-1 cells (Figure 1A) or CD25-positive T blasts (Figure 1B) were incubated with SDF-1α or the indicated activating antibodies, or incubated with SDF1-α together with blocking or neutral antibodies and ICAM-1-bound cells quantified. Activating but not neutral antibodies increased

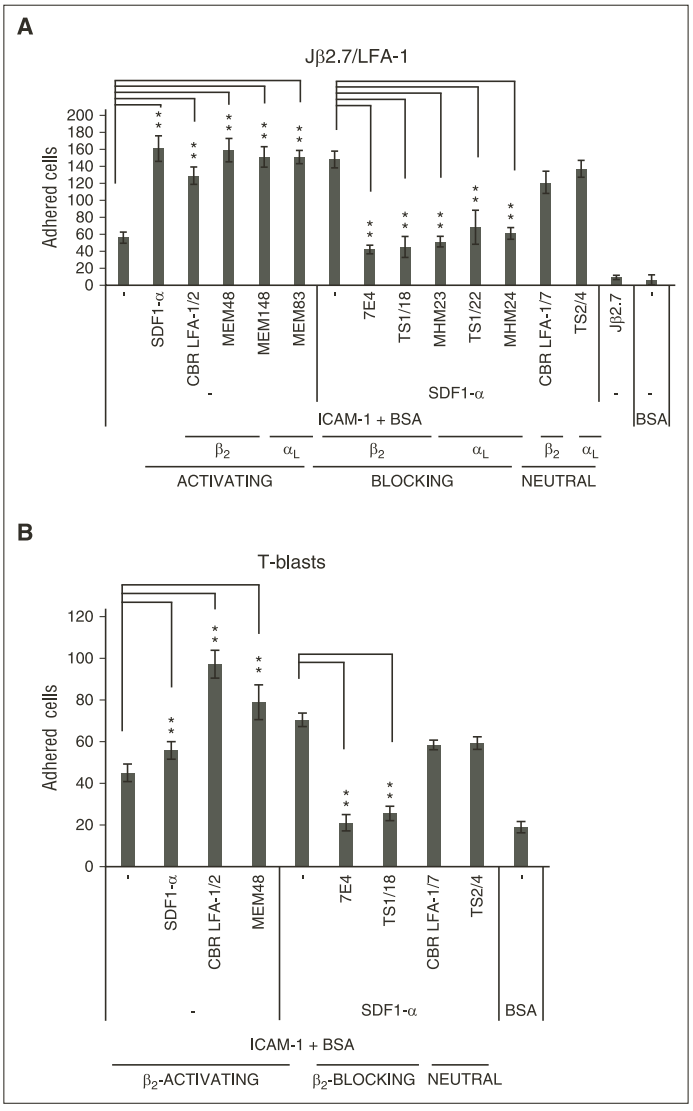

Figure 1. Activating, blocking, and neutral antibodies toward LFA-1 affect binding of Jβ2/LFA-1 cells or T blasts to ICAM-1. (A,B) Static adhesion test to ICAM-1. Jβ2.7/LFA-1 cells (A) or T blasts (B) were activated with the chemokine SDF-1α or activating antibodies or with SDF1-α alone or together with blocking or neutral antibodies. Cells were allowed to bind to an ICAM-1-coated surface, unbound cells washed off, and bound cells counted from 6 screens in triplicate. Amounts of bound cells and standard deviations are shown. $^{**}P < .01$.

binding to ICAM-1, whereas blocking antibodies were able to block the SDF1-α-induced binding to ICAM-1.

The binding of Jβ2.7 cells and T blasts to VCAM-1 is mediated through $\alpha_4\beta_1$, as blocking antibodies to $\alpha_4\beta_1$ abolish VCAM-1-binding.[13] To study the effect of the LFA-1-specific antibodies on $\alpha_4\beta_1$ activity, cells were treated with different antibodies, and the amount of cells adhering to VCAM-1 under flow quantified. Incubation with the activating antibodies to β_2 and α_L leads to a decrease of Jβ2.7/LFA-1 cells binding to VCAM-1. This was LFA-1-dependent, as Jβ2.7 cells lacking LFA-1 showed no changes in VCAM-1 binding (Figure 2A). Next, we tested how blocking antibodies to β_2 or α_L affected $\alpha_4\beta_1$ binding to VCAM-1, expecting to see no effect on $\alpha_4\beta_1$ activity. The blocking antibodies MHM23 and TS1/22 did not affect adhesion to VCAM-1, but incubation of Jβ2.7/LFA-1 cells with the β_2 blocking antibody 7E4 resulted in a strong decrease of $\alpha_4\beta_1$ binding to VCAM-1. A smaller effect was seen with the β_2 blocking TS1/18 and the α_L blocking antibody MHM24. Incubation with neutral antibodies did not affect VCAM-1 binding. To test that the lack of effect of neutral antibodies was not caused by insufficient amounts of antibody, we tested increasing amounts of neutral antibodies CBR LFA-1/7 or TS2/4, with no change in VCAM-1 binding. Higher concentrations of blocking antibodies than the ones used did not change their effect on cells significantly, as shown for 7E4 (Figure 2B). The inhibitory effect of 7E4 on $\alpha_4\beta_1$ activity was not caused by crosslinking of

Carl_G_190x270_mm_blokki_FINAL.indd 455 06-Aug-23 1:54:59 PM

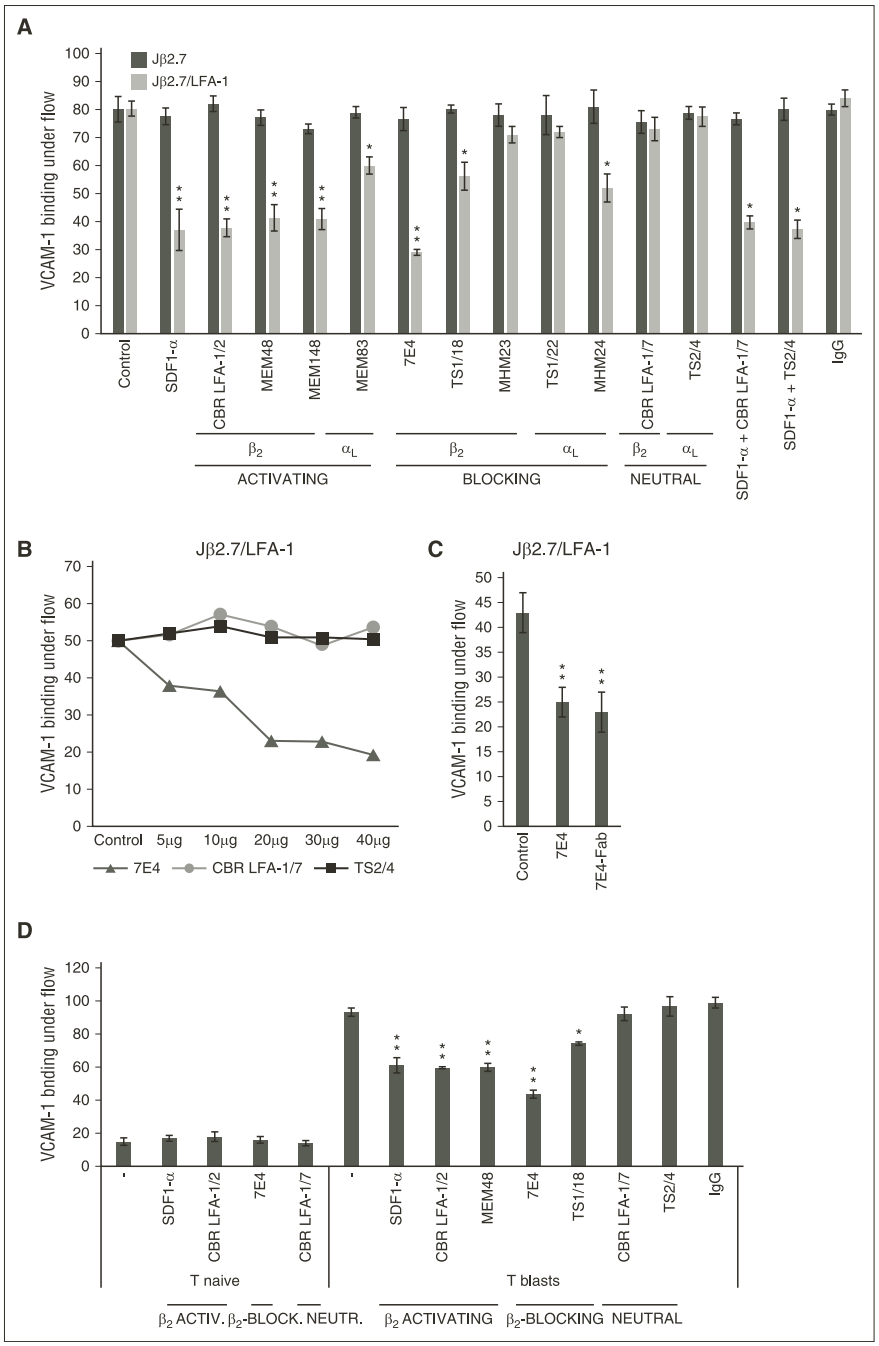

Figure 2. Treatment of Jβ2/LFA-1 cells or T blasts with activating or blocking antibodies leads to transdominant inhibition of $\alpha_4\beta_1$. Jβ2.7 or Jβ2.7/LFA-1 cells (A) or naive T cells or T blasts (D) were treated with SDF1-α, indicated LFA-1 antibodies, or left untreated. (B) Jβ2.7/LFA-1 cells were treated with different concentrations of the LFA-1 blocking antibody 7E4 or the neutral antibodies CBR LFA-1/7 or TS2/4. (C) Jβ2.7/LFA-1 cells were treated with the 7E4 antibody or an equal molar amount of the Fab fragment of the antibody. Adhesion to VCAM-1 under flow was quantified from 6 screens in triplicate. Amounts of bound cells and standard deviations shown. $^*P < .05$; $^{**}P < .01$, compared with untreated control of the same cell type.

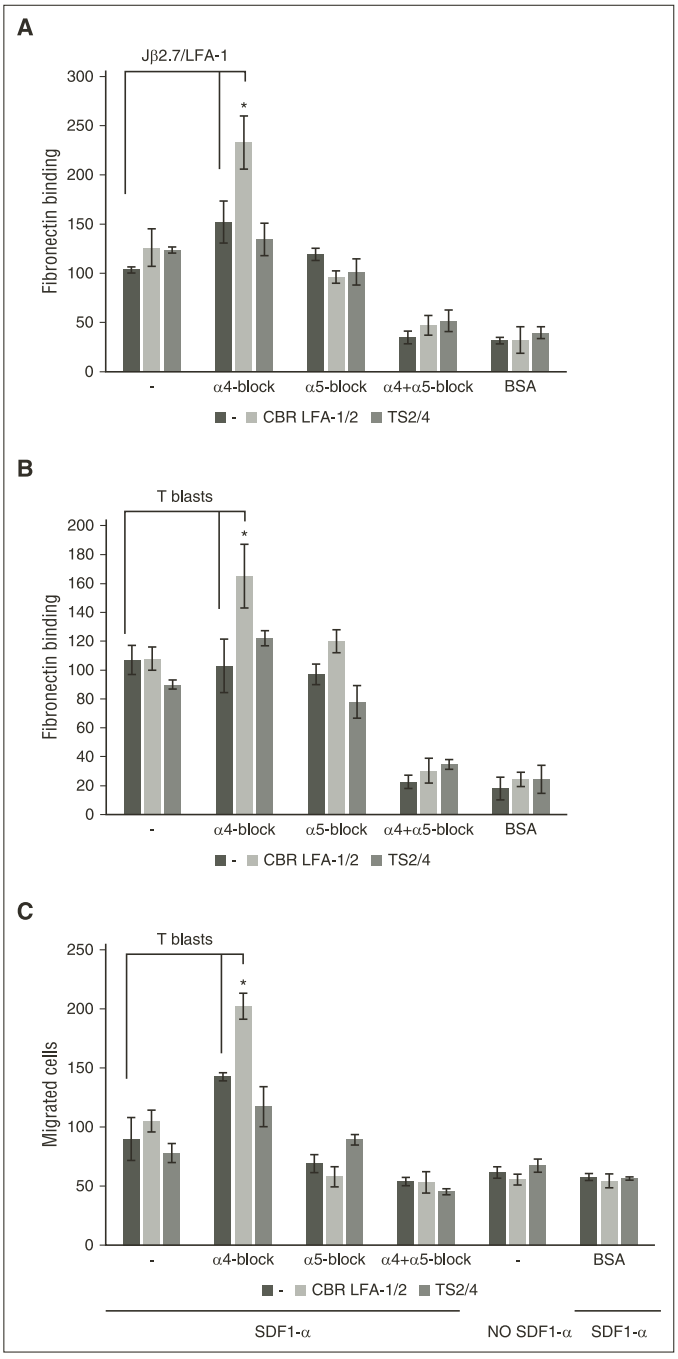

Figure 3. Treatment of Jβ2/LFA-1 cells or T blasts with activating or blocking antibodies enhances $\alpha_5\beta_1$ and does not reduce $\alpha_4\beta_1$ adhesion and migration on fibronectin. Jβ2.7/LFA-1 cells (A) or T blasts (B) were treated with α_4 or α_5 blocking antibodies and the LFA-1 activating antibody CBR LFA-1/2 or neutral antibody TS2/4 or left untreated. Cells were allowed to adhere to fibronectin, unbound cells washed off, and bound cells quantified from 6 screens in triplicate. Amounts of bound cells and standard deviations are shown. (C) T blasts were treated as earlier and allowed to migrate over a fibronectin-coated filter for 1 hour. Migrated cells were quantified from 3 independent experiments. *$P < .05$.

LFA-1 molecules, as purified monovalent Fab fragments of the 7E4 antibody caused inhibition of VCAM-1-binding equally well as the full antibody (Figure 2C). We also tested a set of antibodies on human T cells and T blasts (Figure 2D). Naive T cells bound poorly to VCAM-1 under flow. A similar pattern of $\alpha_4\beta_1$ inhibition as in Jβ2.7/LFA-1 cells was seen for T blasts. The results show that

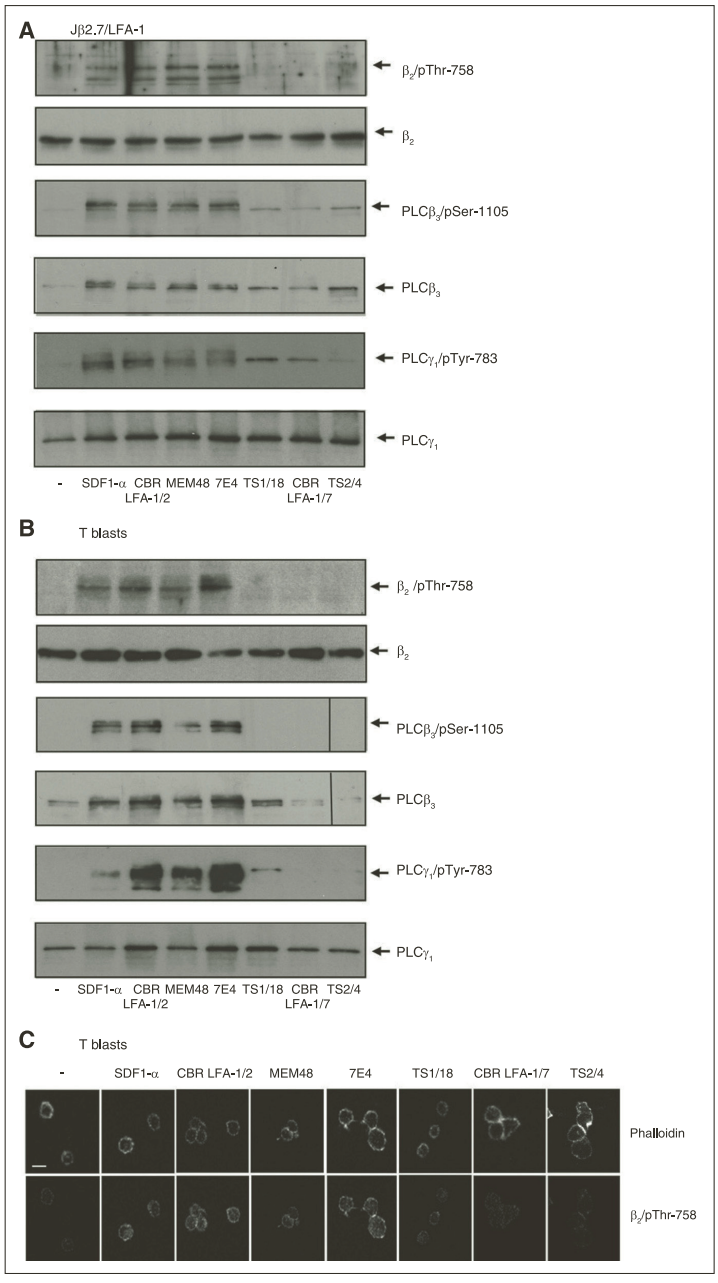

Figure 4. Treatment of Jβ2.7/LFA-1 cells or T blasts with activating or blocking antibodies results in phosphorylation of β_2, PLCβ_3, and PLCγ_1. Jβ2.7/LFA-1 cells (A) or T blasts (B) were treated with SDF1-α, antibodies or left untreated. Cells were lysed and analyzed by western blotting, with the specific antibodies indicated to the right. (C) T blasts were allowed to settle on poly-L-lysine, were treated with SDF-1α, the indicated antibodies, or left untreated. Cells were fixed and stained with phalloidin or the β_2/pThr-758 antiserum. Scale bar represents 10 μM.

specific antibodies to LFA-1 can affect the activity of $\alpha_4\beta_1$ in the same cell. Blocking ICAM-1 or ICAM-2 with specific antibodies did not affect the cross-talk between LFA-1 and $\alpha_4\beta_1$ initiated by LFA-1 antibodies (supplemental Figure 2A), and the presence of Mg^{2+} was not a prerequisite for cross-talk, as cells in PBS containing Ca^{2+} but no Mg^{2+} bound less to VCAM-1 when LFA-1 was activated. The most efficient transdominant inhibition of $\alpha_4\beta_1$ was seen with PBS containing Mg^{2+} but lacking Ca^{2+}, which may be a result of the inhibitory effect of Ca^{2+} on LFA-1[20] (supplemental Figure 2B).

Integrins $\alpha_4\beta_1$ and $\alpha_5\beta_1$ on T cells bind fibronectin. Cells were incubated with blocking antibodies to α_4 or α_5 before LFA-1 antibodies and allowed to adhere to fibronectin. LFA-1-mediated inhibition of

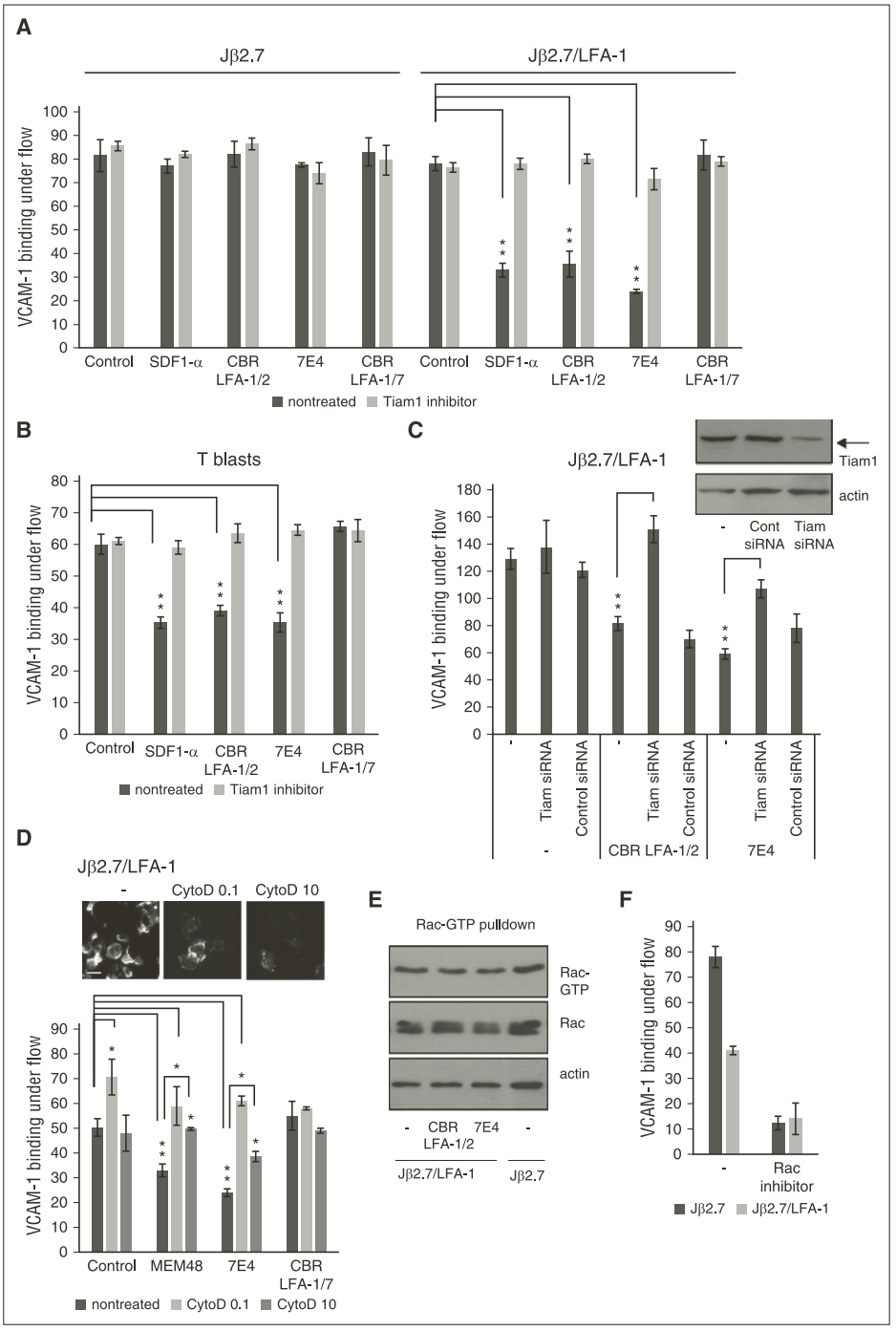

Figure 5. Inhibitory signaling from LFA-1 to $\alpha_4\beta_1$ in Jβ2.7/LFA-1 cells or T blasts requires Tiam1 and an intact cytoskeleton. (A) Jβ2.7 or Jβ2.7/LFA-1 cells or (B) T blasts were treated with SDF1-α, the LFA-1 activating (CBR LFA-1/2), blocking (7E4), or neutral (CBR LFA-1/7) antibodies with or without a Tiam1 inhibitor. (C) Jβ2.7/LFA-1 cells transfected with Tiam1 siRNA or control siRNA and treated with activating (CBR LFA-1/2) or blocking (7E4) antibodies. (D) Jβ2.7/LFA-1 cells were treated with

$\alpha_4\beta_1$ is specific for VCAM-1 binding, as cells with activated LFA-1 bound equally well to fibronectin after blocking $\alpha_5\beta_1$. Cells with active LFA-1, however, increased binding to fibronectin mediated by $\alpha_5\beta_1$ (Figure 3A-B). The same could be seen in a migration assay over fibronectin-coated transwell filters toward SDF1-α (Figure 3C). Activation of $\alpha_5\beta_1$ after blocking $\alpha_4\beta_1$ has previously been shown.[21] Whether the increased binding of $\alpha_5\beta_1$ to fibronectin is mediated by LFA-1 or a consequence of $\alpha_4\beta_1$ inhibition by LFA-1 is not known.

Antibodies to LFA-1 cause changes in β_2 and PLC phosphorylation

LFA-1-mediated inhibition of $\alpha_4\beta_1$ activity in anti-CD3 or SDF1-α-activated T cells includes β_2-chain phosphorylation on Thr-758.[13] After SDF1-α activation, phospho-Thr-758 could be detected in cell lysates (100 kDa) and by immunofluorescence with a phospho-specific antiserum (supplemental Figure 3A-B). The additional band in β_2 pThr-758 (Figure 4A) may be intracellular β_2. Jβ2.7 cells showed no reactivity with the phospho-Thr-758-antiserum, indicating that it is LFA-1-specific. Cells incubated with activating antibodies, but also with the blocking antibody 7E4, were phosphorylated on Thr-758. This could not be seen with the blocking antibody TS1/18 or the neutral antibodies (Figure 4A-B). Phosphorylation of β_2 Thr-758 was also seen by immunofluorescence of cells allowed to settle on poly-L-lysine and stained for Thr-758 and phalloidin after incubation with β_2-activating antibodies or 7E4 (Figure 4C).

SDF1-α can activate PLCβ$_3$ and PLCγ$_1$.[22] PLC catalyzes the cleavage of PIP_2 into diacylglycerol, which results in the activation of PKC, which in turn phosphorylates Thr-758 on β_2.[19] We therefore tested whether PLCs are activated after LFA-1 antibody treatments. Incubating cells with the β_2-activating antibodies or the blocking antibody 7E4 resulted in increased phosphorylation of PLCβ$_3$ on Ser-1105 and PLCγ$_1$ on Tyr-783, indicating that they are activated. Lower amounts of phosphorylated PLC was also seen after other antibody incubations, especially in Jβ2.7/LFA-1 cells. These results indicate that incubation of cells with activating antibodies to LFA-1 or the blocking antibody 7E4 leads to PLC activation and β_2 Thr-758 phosphorylation (Figure 4A-B). A difference in the total amount of PLCβ$_3$ was present both in the soluble and pellet fractions. The amount of PLCβ$_3$ remained low in control cells after MG132 or leupeptin treatment. Cells treated with 7E4 showed more PLCβ$_3$, and the amount remained unchanged after MG132 treatment, but leupeptin reduced the amount to similar levels as in untreated cells. This could indicate that calpain regulates a pathway that leads to increased PLCβ$_3$ levels after LFA-1 activation and cross-talk signaling to $\alpha_4\beta_1$ (supplemental Figure 4A).

Inhibition of $\alpha_4\beta_1$ by LFA-1 antibodies requires signaling through Tiam1

Phosphorylation of Thr-758 on β_2 leads to the binding of 14-3-3 and signaling through Tiam1 and Rac1.[14] Cells were incubated with LFA-1 antibodies with or without pretreatment with the Tiam1 inhibitor. The reduction of binding seen with CBR LFA-1/2 or 7E4 was reversed by the inhibition of Tiam1. (Figure 5A-B). Because the Tiam1 inhibitor also can inhibit TrioN, we transfected Jβ2.7/LFA-1 cells with siRNA for Tiam1 or a control. Tiam1 siRNA reduced Tiam1 to 35% of untreated cells and caused a reduction of cross-talk to $\alpha_4\beta_1$ (Figure 5C).

Treatment of cells with low concentration of cytochalasin D partly reversed the inhibition of VCAM-1 binding seen with MEM48 and 7E4 (Figure 5D). This indicates that an intact cytoskeleton is required for the cross-talk between LFA-1 and $\alpha_4\beta_1$ or is a result of increased mobility of integrins.[23] The amount of active Rac1 in antibody-treated cells was not changed (Figure 5E). Rac1 has been implicated in the regulation of $\alpha_4\beta_1$ activity.[24] We saw that Rac1 inhibition decreased binding to VCAM-1 also in Jβ2.7 cells lacking LFA-1. Therefore, we were unable to study the role of LFA-1 antibodies on $\alpha_4\beta_1$ in cells with inactive Rac1 (Figure 5F).

Antibodies to LFA-1 affect β_1 phosphorylation and activation

We next studied the phosphorylation and activation state of $\alpha_4\beta_1$. Cells were treated with LFA-1 antibodies, and the phosphorylation state of β_1 studied using a phospho-specific Thr-788/789 antiserum. The phosphorylation was reduced by activating LFA-1 antibodies or the blocking antibodies 7E4 and TS1/18, but not by neutral antibodies (Figure 6A). In cells treated with the Tiam1 inhibitor before CBR LFA-1/2, the amount of β_1 phosphorylation was not reduced (Figure 6B), whereas cells treated with 0.1 μg/mL cytochalasin D before LFA-1/2 showed an intermediate amount of phosphorylated β_1 (Figure 6C). Activating and blocking antibodies toward LFA-1 caused a reduction in the intensity of 12G10 staining, indicating that there is less active β_1 in the cells. There were no changes in α_4 clustering on the cell surface of antibody-treated cells (Figure 6D-E).

In co-immunoprecipitation experiments, more talin was bound to α_4-complexes in cells treated with the LFA-1 activating antibody CBR LFA-1/2 than in cells treated with the neutral antibody TS2/4. Both the 225- and the 190-kDa talin fragments were coprecipitated. Weak talin binding was seen in β_2 complexes of TS2/4-treated cells. More 14-3-3 bound to β_2 from CBR LFA-1/2 activated cells and less to the TS2/4-treated cells, whereas the opposite was seen in α_4-complexes (Figure 6F).[13]

The blocking antibodies 7E4 and TS1/18 regulate $\alpha_4\beta_1$ activity through the same pathway, but with different intensity

7E4 was most potent in inhibiting $\alpha_4\beta_1$ activity, whereas the TS1/18 antibody showed an intermediate effect. Incubation of cells with 7E4 lead to the phosphorylation of PLC and Thr-758 on β_2, and a Tiam1-dependent decrease in $\alpha_4\beta_1$ phosphorylation of Thr-788/789 on β_1, 12G10 reactivity, and VCAM-1 binding. We also saw a reduction in β1 phosphorylation, 12G10 reactivity, and VCAM-1 binding with TS1/18 treatment, but it was not as strong as with activating antibodies or 7E4. Although no phosphorylation of Thr-758 was detected with shorter exposures (Figure 4B-C), with long exposures a weaker phospho-Thr-758 signal could be detected after TS1/18 treatment, which may be enough to initiate inhibitory signaling (supplemental Figure 4B). Blocking Tiam1 partly restored VCAM-1 binding, supporting signaling through Tiam1 for $\alpha_4\beta_1$ inhibition (supplemental Figure 4C).

Figure 5 (continued) cytochalasin D (0.1 or 10 μg/mL) and LFA-1 activating (MEM48), blocking (7E4), or neutral (CBR LFA-1/7) antibodies. Adhesion to VCAM-1 under flow was quantified from 6 screens in triplicate. Amounts of bound cells and standard deviations are shown. Phalloidin staining of F-actin of Jβ2.7/LFA cells treated with 0.1 or 10 μg/mL cytochalasin D. Scale bar represents 10 μM. (E) Jβ2.7 or Jβ2.7/LFA-1 cells treated with LFA-1 activating antibody (CBR LFA-1/2) or blocking antibody (7E4) were lysed and Rac-GTP pulled down from lysates. Immunoblot shows Rac-GTP from pulldown and total Rac or actin from cell lysates. (F) Jβ2.7 or Jβ2.7/LFA-1 cells were incubated with the Rac inhibitor or left untreated and with the LFA-1 activating antibody (CBR LFA-1/2), and cells adhering to VCAM-1 under flow quantified as earlier. $^*P < .05$; $^{**}P < .01$.

Carl_G_190x270_mm_blokki_FINAL.indd 460 06-Aug-23 1:55:00 PM

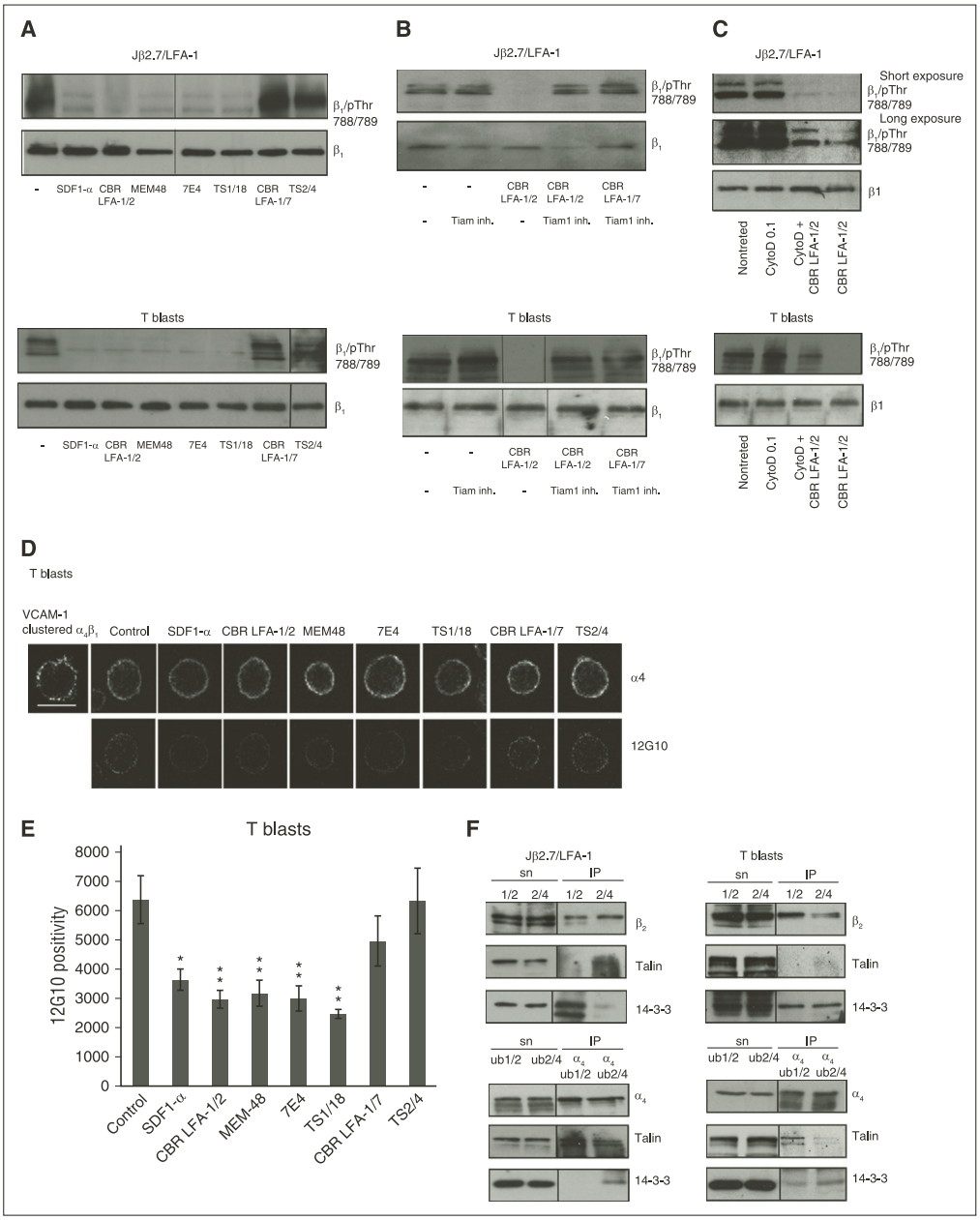

Figure 6. Antibody treatment of LFA-1 on Jβ2.7 cells or T blasts leads to changes in integrin β_1-phosphorylation, activation epitope, and protein complexes. (A) Jβ2.7/LFA-1 cells or T blasts were treated with SDF1-α or antibodies to LFA-1. Cells were lysed and analyzed by western blotting for β_1/pThr-788/789 or β_1. (B) Cells were preincubated with Tiam1 inhibitor or (C) cytochalasin D (0.1 μg/mL) (C) and LFA-1 antibodies CBR LFA-1/2 or CBR LFA-1/7, and lysates analyzed as earlier. (D) T blasts were treated as earlier, allowed to adhere on poly-L-lysine, and fixed before immunofluorescence staining with an α_4 antibody or the antibody for activated integrin β_1 (12G10-488). $\alpha_4\beta_1$ clustered by soluble VCAM-1 and VCAM-1 antibody. (E) Positive pixels from 50 cells stained with 12G10-488 were quantified using ImageJ. Standard deviations shown and statistical significance compared with control. $^*P < .05$; $^{**}P < .01$. Scale bar represents 10 μM. (F) Jβ2.7/LFA-1 cells or T blasts were lysed, immunoprecipitated with the activating CBR LFA-1/2 (1/2) or neutral TS2/4 (2/4) antibody, and immunoblotted for β_2, talin or 14-3-3. The unbound fraction of the CBR LFA-1/2 (ub1/2) and TS2/4 (ub2/4) precipitates were further immunoprecipitated with α_4 antibody and immunoblotted for α_4, talin, and 14-3-3.

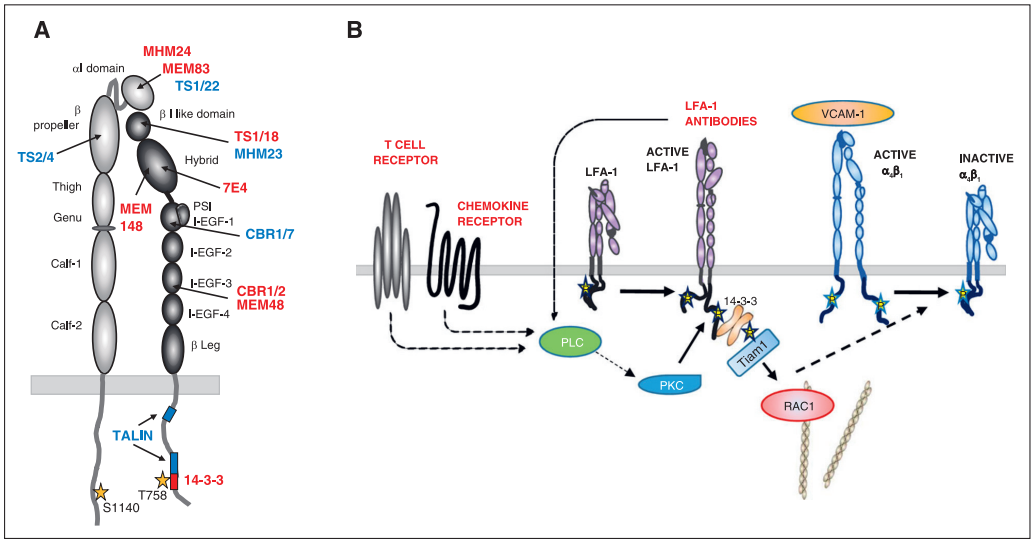

Figure 7. Schematic figure of LFA-1-specific antibody binding sites and the cross-talk from LFA-1 to $\alpha_4\beta_1$. (A) A schematic picture of LFA-1 α_L and β_2-chains, with the binding sites of the antibodies used. Antibodies in red induce the inhibitory signal to $\alpha_4\beta_1$; antibodies in blue do not affect $\alpha_4\beta_1$ activity. Binding site for talin and 14-3-3 indicated on the β_2 chain. (B) Activation from the T-cell receptor, through chemokines or by LFA-1 antibodies, results in PLC and PKC activation and phosphorylation of Thr-758 in β_2, followed by binding of 14-3-3 and Tiam1 and activation of Rac1. The signal is further transferred to $\alpha_4\beta_1$, resulting in dephosphorylation of Thr-788/789 and loss of activity and ligand binding.

Discussion

Interactions between integrins and their ligands are involved in many pathological conditions, including autoimmune diseases, allograft rejection, and cancer. Blocking LFA-1 and $\alpha_4\beta_1$ ligand interactions is a potential target for disease interventions. Antibodies, peptides, and small molecules toward these integrins have been used to control inflammation and autoimmune diseases as well as metastasis.[25,26] We now show that antibodies that bind specifically to LFA-1 can regulate the activity not only of LFA-1 but also another integrin, $\alpha_4\beta_1$. This is important to know when studying integrin antibody effects on cells, but also when designing treatment strategies aiming at a specific integrin.

Leukocytes circulating in the blood are nonadhesive and express inactive forms of the adhesion receptors LFA-1 or $\alpha_4\beta_1$. As they reach the inflammatory site, these integrins are activated in a highly regulated manner to allow for the sequential steps of cell rolling, adhesion, firm adhesion, and transmigration over endothelial cells. Cross-talk between LFA-1 and $\alpha_4\beta_1$ allows the controlled progression of leukocyte adhesion and migration in this stepwise manner.[12,13,21] At an early stage, $\alpha_4\beta_1$ mediates rolling and simultaneously may provide activation signals required for firm adhesion enhancing LFA-1 binding to ICAM-1.[27,28] Next, the transition from firm adhesion to a migratory phenotype is initiated by LFA-1-mediated transdominant inhibition of $\alpha_4\beta_1$.[13,21] Adhesion of T cells via β_2 integrins not only decreases $\alpha_4\beta_1$ integrin-mediated adhesion but also enhances $\alpha_5\beta_1$ integrin-mediated transmigration (Figure 3).[21] We have previously shown that the *trans*-dominant inhibition of $\alpha_4\beta_1$ by LFA-1 mediated by intracellular signaling requires an active form of LFA-1 and changes in β_1- and β_2-chain phosphorylations and protein interactions.[13] We now show that this cross-talk can be initiated not only by inside-out activation or ligand binding of LFA-1 but also by specific antibodies.

Antibodies shown to activate LFA-1 ligand binding and an active conformation initiate an inhibitory signal to $\alpha_4\beta_1$, which could not be seen with neutral antibodies. Antibodies that have been shown to inactivate LFA-1 ligand binding show different outcomes, evidently depending on the binding site on the extracellular domains. The LFA-1 antibodies that we have used have been well-characterized and their binding sites carefully mapped (Figure 7).

Antibodies that map to the α_L I-domain or the β I-like domain are normally inhibitory. Antibodies that bind more C-terminally are often neutral or activating.[29] The neutral antibody CBR LFA-1/7 binds to the first I-EGF-domain on β_2[30] and TS2/4 to the β-propeller on α_L.[31,32] The LFA-1 stalk region provides a crucial link between changes in the transmembrane and cytoplasmic domains and conformational movements in the ligand binding site. Several antibodies that activate ligand binding map to this region. In our experiments, the β_2 activating antibodies CBR LFA-1/2, MEM48, and MEM148, as well as the α_L activating antibody MEM83, reduced $\alpha_4\beta_1$ binding to VCAM-1. CBR LFA-1/2[33] and MEM48[34] bind to overlapping epitopes including residues 534, 536, 541, 543, and 546 in the I-EGF-3 repeat.[29,30] CBR LFA-1/2 and MEM48 have been suggested to act as a wedge to keep the α- and β-subunits apart, and thus induce an extended form of β_2 altering the ligand binding part.[30,35] This change in conformation also affects protein interactions with the β_2 cytoplasmic domain and may induce Thr-758 phosphorylation. MEM148 binds to the hybrid domain in β_2 and recognizes an activation epitope, residue Pro-374, on the β_2 hybrid domain facing the α-subunit β-propeller (ie, the inner face of the hybrid domain), and it stabilizes hybrid domain swing out and increases affinity toward ligand.[36-38]

7E4 binds to the hybrid domain, but in contrast to MEM148, it is inhibitory.[17] It binds to residue Val-385 on a loop on the outer face of the hybrid domain at the interphase with the β I-like domain, which is remodeled on hybrid domain swingout to the open conformation.[39,40]

The antibody TS1/18[31] binds to the β I-like domain, blocks ligand binding,[29,30] and induces a closed head piece.[36,41] The epitope maps to the residues that are adjacent in the α1 and α7 helices of the β I-like domain (Arg-133, Gln-332). The β_2 blocking antibody MHM23[42] binds to Glu-175 in the loop between the β2 and β3 strands in the β I-like domain, but it does not inhibit $\alpha_4\beta_1$. Both 7E4 and TS1/18 localize to regions that are significantly altered when shifting to the open head piece. Binding of these antibodies stabilizes the closed head piece[36] and may simultaneously cause structural changes that result in intracellular signaling, similar to that seen with activating antibodies. Therefore, an antibody can be both inhibitory when it comes to ligand binding and activating when it comes to intracellular signaling.

Two of the α_L blocking antibodies, TS1/22[31,43] and MHM24,[42] bind to the α-chain I domain. TS1/22 does not affect $\alpha_4\beta_1$ activity, whereas MHM24 shows a small reduction in $\alpha_4\beta_1$ activity. The α_L activating antibody MEM83 also binds to the α-chain I-domain and inhibits $\alpha_4\beta_1$ activity, but less than other activating antibodies. The epitopes of MEM83 and MHM24 are in close proximity, MEM83 was mapped to the β3–α2 loop and the α4 helix residues 153 to 183 and 217 to 248 and MHM24 to the α–-α4 loops containing residues 197 to 201. TS1/22 maps more C-terminal to the β5–α6 loop and the short α6 helix residues 266 to 270.[43]

The murine antibody MHM24 has been humanized (efalizumab) (Raptiva, Genentech)[44] for treating psoriasis[45] and can inhibit the extravasation and of T lymphocytes.[46] It is of interest to note that according to our studies, MHM24 does not only inhibit ICAM-1 binding but also significantly reduces $\alpha_4\beta_1$ binding to VCAM-1. Thus, the 2 important integrins in transmigration are inhibited.

Antibodies that initiate cross-talk to $\alpha_4\beta_1$ cause phosphorylation of Thr-758 on β_2. The mechanism by which antibody binding leads to the phosphorylation of the β_2 cytoplasmic tail is only partially understood, but we show that PLC enzymes are activated. The resulting diacylglycerol is known to activate PKCs, the kinases phosphorylating Thr-758.[19] Antibodies to LFA-1 may cause structural changes in the integrin, which transfer signals into the cell, activating PLC, and thus PKC.

The reduced binding of $\alpha_4\beta_1$ to VCAM-1 indicates a change in affinity. Cross-talk between integrins have previously been shown to require an intact cytoskeleton,[47] and we confirm this, using cytochalasin D. Future studies of different subsets of recently activated effector lymphocytes will shed light on the environmental settings in which this cross-talk takes place.

Here we show that modifying LFA-1 activity by LFA-1-specific antibodies will not only affect LFA-1 ligand binding but concomitantly may change the activity of $\alpha_4\beta_1$. We now have antibodies to LFA-1, which enable us to activate LFA-1 and block $\alpha_4\beta_1$, inhibit both integrins, or only block LFA-1. The findings may make it possible to develop specific pharmaceuticals of high specificity.

Acknowledgments

This study was supported by research funding from the Academy of Finland, the Sigrid Jusélius Foundation, the Medicinska Understödsföreningen Liv och Hälsa, the Finska Läkaresällskapet, the Wilhelm and Else Stockmann Foundation, the Ruth och Nils-Erik Stenbäck Foundation and the Magnus Ehrnrooth Foundation (C.G.G., M.G., and F.J.).

Authorship

Contribution: F.J., E.A.B., M.G., S.M., F.A, L.S.H., and L.M.U. performed the experiments; F.J. supervised the students; and M.G. and C.G.G. planned the experiments, analyzed the data, and wrote the article.

Conflict-of-interest disclosure: The authors declare no competing financial interests.

Correspondence: Carl G. Gahmberg, Division of Biochemistry and Biotechnology, Faculty of Biological and Environmental Sciences, Viikinkaari 9 C (P.O. Box 56), 00014 University of Helsinki, Helsinki, Finland; e-mail: carl.gahmberg@helsinki.fi.

References

1. Chigaev A, Sklar LA. Aspects of VLA-4 and LFA-1 regulation that may contribute to rolling and firm adhesion. *Front Immunol.* 2012;3(August):242.
2. Springer TA. Traffic signals for lymphocyte recirculation and leukocyte emigration: the multistep paradigm. *Cell.* 1994;76(2):301-314.
3. Butcher EC. Leukocyte-endothelial cell recognition: three (or more) steps to specificity and diversity. *Cell.* 1991;67(6):1033-1036.
4. Gahmberg CG, Tolvanen M, Kotovuori P. Leukocyte adhesion–structure and function of human leukocyte beta2-integrins and their cellular ligands. *Eur J Biochem.* 1997;245(2):215-232.
5. Springer TA. Adhesion receptors of the immune system. *Nature.* 1990;346(6283):425-434.
6. Luo B-H, Carman CV, Springer TA. Structural basis of integrin regulation and signaling. *Annu Rev Immunol.* 2007;25:619-647.
7. Gahmberg CG, Fagerholm SC, Nurmi SM, Chavakis T, Marchesan S, Grönholm M. Regulation of integrin activity and signalling. *Biochim Biophys Acta.* 2009;1790(6):431-444.
8. Hogg N, Patzak I, Willenbrock F. The insider's guide to leukocyte integrin signalling and function. *Nat Rev Immunol.* 2011;11(6):416-426.
9. Legate KR, Fässler R. Mechanisms that regulate adaptor binding to beta-integrin cytoplasmic tails. *J Cell Sci.* 2009;122(Pt 2):187-198.
10. Takala H, Nurminen E, Nurmi SM, et al. Beta2 integrin phosphorylation on Thr758 acts as a molecular switch to regulate 14-3-3 and filamin binding. *Blood.* 2008;112(5):1853-1862.
11. Campbell JJ, Hedrick J, Zlotnik A, Siani MA, Thompson DA, Butcher EC. Chemokines and the arrest of lymphocytes rolling under flow conditions. *Science.* 1998;279(5349):381-384.
12. van Kooyk Y, van de Wiel-van Kemenade E, Weder P, Huijbens RJ, Figdor CG. Lymphocyte function-associated antigen 1 dominates very late antigen 4 in binding of activated T cells to endothelium. *J Exp Med.* 1993;177(1):185-190.
13. Uotila LM, Jahan F, Soto Hinojosa L, Melandri E, Grönholm M, Gahmberg CG. Specific phosphorylations transmit signals from leukocyte β2 to β1 integrins and regulate adhesion. *J Biol Chem.* 2014;289(46):32230-32242.
14. Grönholm M, Jahan F, Marchesan S, et al. TCR-induced activation of LFA-1 involves signaling through Tiam1. *J Immunol.* 2011;187(7):3613-3619.
15. Nurmi SM, Autero M, Raunio AK, Gahmberg CG, Fagerholm SC. Phosphorylation of the LFA-1 integrin beta2-chain on Thr-758 leads to adhesion, Rac-1/Cdc42 activation, and stimulation of CD69 expression in human T cells. *J Biol Chem.* 2007;282(2):968-975.
16. Fagerholm SC, Hilden TJ, Nurmi SM, Gahmberg CG. Specific integrin α and β chain phosphorylations regulate LFA-1 activation through affinity-dependent and -independent mechanisms. *J Cell Biol.* 2005;171(4):705-715.
17. Nortamo P, Patarroyo M, Kantor C, Suopanki J, Gahmberg CG. Immunological mapping of the human leucocyte adhesion glycoprotein gp90 (CD18) by monoclonal antibodies. *Scand J Immunol.* 1988;28(5):537-546.
18. Weber KS, York MR, Springer TA, Klickstein LB. Characterization of lymphocyte function-associated antigen 1 (LFA-1)-deficient T cell lines: the alphaL and beta2 subunits are interdependent for cell surface expression. *J Immunol.* 1997;158(1):273-279.
19. Fagerholm S, Morrice N, Gahmberg CG, Cohen P. Phosphorylation of the cytoplasmic domain of the integrin CD18 chain by protein kinase C isoforms in leukocytes. *J Biol Chem.* 2002;277(3):1728-1738.
20. Day ES, Osborn L, Whitty A. Effect of divalent cations on the affinity and selectivity of alpha4 integrins towards the integrin ligands vascular cell adhesion molecule-1 and mucosal addressin cell

adhesion molecule-1: Ca2+ activation of integrin alpha4beta1 confers a distinct ligand specificity. *Cell Commun Adhes.* 2002;9(4):205-219.

21. Porter JC, Hogg N. Integrin cross talk: activation of lymphocyte function-associated antigen-1 on human T cells alters $\alpha 4\beta 1$- and $\alpha 5\beta 1$-mediated function. *J Cell Biol.* 1997;138(6):1437-1447.
22. Kremer KN, Clift IC, Miamen AG, et al. Stromal cell-derived factor-1 signaling via the CXCR4-TCR heterodimer requires phospholipase C-$\beta 3$ and phospholipase C-$\gamma 1$ for distinct cellular responses. *J Immunol.* 2011;187(3):1440-1447.
23. van Kooyk Y, Figdor CG. Avidity regulation of integrins: the driving force in leukocyte adhesion. *Curr Opin Cell Biol.* 2000;12(5):542-547.
24. Garcia-Bernal D, Wright N, Sotillo-Mallo E, et al. Vav1 and Rac control chemokine-promoted T lymphocyte adhesion mediated by the integrin alpha4beta1. *Mol Biol Cell.* 2005;16(7): 3223-3235.
25. Yusuf-Makagiansar H, Anderson ME, Yakovleva TV, Murray JS, Siahaan TJ. Inhibition of LFA-1/ICAM-1 and VLA-4/VCAM-1 as a therapeutic approach to inflammation and autoimmune diseases. *Med Res Rev.* 2002;22(2):146-167.
26. Hilden TJ, Nurmi SM, Fagerholm SC, Gahmberg CG. Interfering with leukocyte integrin activation–a novel concept in the development of anti-inflammatory drugs. *Ann Med.* 2006;38(7): 503-511.
27. May AE, Neumann FJ, Schömig A, Preissner KT. VLA-4 (alpha(4)beta(1)) engagement defines a novel activation pathway for beta(2) integrin-dependent leukocyte adhesion involving the urokinase receptor. *Blood.* 2000;96(2):506-513.
28. Chan JR, Hyduk SJ, Cybulsky MI. α 4 β 1 integrin/VCAM-1 interaction activates α L β 2 integrin-mediated adhesion to ICAM-1 in human T cells. *J Immunol.* 2000;164(2):746-753.
29. Huang C, Zang Q, Takagi J, Springer TA. Structural and functional studies with antibodies to the integrin beta 2 subunit. A model for the I-like domain. *J Biol Chem.* 2000;275(28): 21514-21524.
30. Lu C, Ferzly M, Takagi J, Springer TA. Epitope mapping of antibodies to the C-terminal region of the integrin beta 2 subunit reveals regions that become exposed upon receptor activation. *J Immunol.* 2001;166(9):5629-5637.
31. Sanchez-Madrid F, Krensky AM, Ware CF, et al. Three distinct antigens associated with human T-lymphocyte-mediated cytolysis: LFA-1, LFA-2, and LFA-3. *Proc Natl Acad Sci USA.* 1982;79(23): 7489-7493.
32. Huang C, Springer TA. Folding of the β-propeller domain of the integrin alphaL subunit is independent of the I domain and dependent on the $\beta 2$ subunit. *Proc Natl Acad Sci USA.* 1997;94(7):3162-3167.
33. Petruzzelli L, Maduzia L, Springer TA. Activation of lymphocyte function-associated molecule-1 (CD11a/CD18) and Mac-1 (CD11b/CD18) mimicked by an antibody directed against CD18. *J Immunol.* 1995;155(2):854-866.
34. Bazil V, Stefanová I, Hilgert I, Kristofová H, Vaněk S, Horejsí V. Monoclonal antibodies against human leucocyte antigens. IV. Antibodies against subunits of the LFA-1 (CD11a/CD18) leucocyte-adhesion glycoprotein. *Folia Biol (Praha).* 1990; 36(1):41-50.
35. Nishida N, Xie C, Shimaoka M, Cheng Y, Walz T, Springer TA. Activation of leukocyte beta2 integrins by conversion from bent to extended conformations. *Immunity.* 2006;25(4):583-594.
36. Chen X, Xie C, Nishida N, Li Z, Walz T, Springer TA. Requirement of open headpiece conformation for activation of leukocyte integrin alphaXbeta2. *Proc Natl Acad Sci USA.* 2010;107(33): 14727-14732.
37. Drbal K, Angelisová P, Cerný J, Hilgert I, Horejsí V. A novel anti-CD18 mAb recognizes an activation-related epitope and induces a high-affinity conformation in leukocyte integrins. *Immunobiology.* 2001;203(4):687-698.
38. Tang R-H, Tng E, Law SKA, Tan S-M. Epitope mapping of monoclonal antibody to integrin alphaL beta2 hybrid domain suggests different requirements of affinity states for intercellular adhesion molecules (ICAM)-1 and ICAM-3 binding. *J Biol Chem.* 2005;280(32):29208-29216.
39. Tan SM, Robinson MK, Drbal K, van Kooyk Y, Shaw JM, Law SK. The N-terminal region and the mid-region complex of the integrin β 2 subunit. *J Biol Chem.* 2001;276(39):36370-36376.
40. Tng E, Tan SM, Ranganathan S, Cheng M, Law SKA. The integrin α L β 2 hybrid domain serves as a link for the propagation of activation signal from its stalk regions to the I-like domain. *J Biol Chem.* 2004;279(52):54334-54339.
41. Beals CR, Edwards AC, Gottschalk RJ, Kuijpers TW, Staunton DE. CD18 activation epitopes induced by leukocyte activation. *J Immunol.* 2001; 167(11):6113-6122.
42. Hildreth JE, Gotch FM, Hildreth PD, McMichael AJ. A human lymphocyte-associated antigen involved in cell-mediated lympholysis. *Eur J Immunol.* 1983;13(3):202-208.
43. Lu C, Shimaoka M, Salas A, Springer TA. The binding sites for competitive antagonistic, allosteric antagonistic, and agonistic antibodies to the I domain of integrin LFA-1. *J Immunol.* 2004;173(6):3972-3978.
44. Werther WA, Gonzalez TN, O'Connor SJ, et al. Humanization of an anti-lymphocyte function-associated antigen (LFA)-1 monoclonal antibody and reengineering of the humanized antibody for binding to rhesus LFA-1. *J Immunol.* 1996; 157(11):4986-4995.
45. Gottlieb A, Krueger JG, Bright R, et al. Effects of administration of a single dose of a humanized monoclonal antibody to CD11a on the immunobiology and clinical activity of psoriasis. *J Am Acad Dermatol.* 2000;42(3):428-435.
46. Jullien D, Prinz JC, Langley RGB, et al. T-cell modulation for the treatment of chronic plaque psoriasis with efalizumab (Raptiva): mechanisms of action. *Dermatology.* 2004;208(4):297-306.
47. Leitinger B, Hogg N. Effects of I domain deletion on the function of the beta2 integrin lymphocyte function-associated antigen-1. *Mol Biol Cell.* 2000;11(2):677-690.

Trends in
Biochemical Sciences

CellPress
OPEN ACCESS

Review

How integrin phosphorylations regulate cell adhesion and signaling

Carl G. Gahmberg [1,*] and Mikaela Grönholm [1,2]

Cell adhesion is essential for the formation of organs, cellular migration, and interaction with target cells and the extracellular matrix. Integrins are large protein α/β-chain heterodimers and form a major family of cell adhesion molecules. Recent research has dramatically increased our knowledge of how integrin phosphorylations regulate integrin activity. Phosphorylations determine the signaling complexes formed on the cytoplasmic tails, regulating downstream signaling. α-Chain phosphorylation is necessary for inducing β-chain phosphorylation in LFA-1, and the crosstalk from one integrin to another activating or inactivating its function is in part mediated by phosphorylation of β-chains. The severe acute respiratory syndrome coronavirus 2 (SARS-CoV-2) virus receptor angiotensin-converting enzyme 2 (ACE2) and possible integrin coreceptors may crosstalk and induce a phosphorylation switch and autophagy.

Highlights

Integrins are transmembrane proteins involved in cell–cell and cell–matrix communication.

Recent studies show how integrin phosphorylations regulate integrin activity.

Phosphorylation of both integrin α- and β-chains are emerging as being critical for activity.

Phosphorylation of integrin β-chains enables kindlin binding by the assistance of talin, resulting in cell adhesion.

Crosstalk between integrins and other receptors may occur by phosphorylation switches.

Cell adhesion functions by cooperation between extracellular and intracellular molecules

A variety of adhesion molecules bind cells to each other and mediate both cell–cell and cell–matrix communication. The adhesion molecules form molecular families, which include the integrins, cadherins, immunoglobulin superfamily molecules, and selectins. While earlier reviews dealt with integrins and their interactions with cytoplasmic interactors [1–8], recent studies have increased our understanding of integrin-mediated adhesion and signaling. This includes how specific integrin phosphorylations regulate cell adhesion and signaling by enabling specific and dynamic interactions between integrins and intracellular interactors.

Herein, we first briefly review what integrins are and their extracellular and cytoplasmic interacting proteins. We then focus on recent studies that show how specific phosphorylations of integrin cytoplasmic tails regulate their activity by mediating interactions with key intracellular proteins including 14-3-3ζ, talin, and kindlins, but also abrogating interactions with inhibitory proteins such as filamin A.

Integrins are important adhesion molecules regulated in a dynamic manner

The integrins are protein heterodimers consisting of α- and β-chains, which form integrin subfamilies. They are type I membrane glycoproteins with large extracellular domains, single transmembrane domains, and relatively short intracellular tails. Integrins can be activated by inside-out or outside-in activation. In inside-out integrin activation, signals originate from non-integrin receptors, which transmit signals to the integrins. In outside-in activation, ligands bind to the external integrin domains and signal into the cells. The most detailed information on integrin inside-out activation comes from leukocytes and platelets as model cells, but platelets have also provided important information on outside-in activation [2,3,7,8].

Some integrin α-chains contain an inserted I domain acting as the ligand-binding site, or the binding site may be formed by a combination of the α- and β-chains and form an integrin 'head.' In the

[1]Molecular and Integrative Biosciences Research Programme, University of Helsinki, Viikinkaari 9 C, 00014 Helsinki, Finland
[2]Faculty of Pharmacy, University of Helsinki, Viikinkaari 5E, 00014 Helsinki, Finland

*Correspondence:
carl.gahmberg@helsinki.fi
(C.G. Gahmberg).

© 2021 The Authors. Published by Elsevier Ltd. This is an open access article under the CC BY-NC-ND license (http://creativecommons.org/licenses/by-nc-nd/4.0/).

Carl_G_190x270_mm_blokki_FINAL.indd 465 06-Aug-23 1:55:02 PM

CellPress
OPEN ACCESS

Trends in Biochemical Sciences

resting state, the integrin ligand-binding head faces the membrane, and the intracellular tails are clasped. Upon activation, the integrin stalk extends, the ligand-binding site opens, and the intracellular integrin tails separate [2,9]. The different integrin conformations enable adjustments in cell adhesion and signaling.

Extracellular interactions

Integrin ligands include extracellular molecules such as fibronectin, laminins, fibrinogen, and collagens. Several integrins, including $\alpha_5\beta_1$, $\alpha_V\beta_3$, and $\alpha_{IIb}\beta_3$, recognize an RGD sequence found in fibronectin, fibrinogen, and several other proteins [10], but also in some virus proteins, among them the SARS-CoV-2 spike protein [11,12]. The major lymphocyte integrins, LFA-1 ($\alpha_L\beta_2$; CD11a/CD18) and VLA-4 ($\alpha_4\beta_1$; CD49d/CD29), bind to the cellular ligands intercellular adhesion molecules 1–5 (ICAM1–5) and the vascular cell adhesion molecule 1 (VCAM-1), respectively. Integrins are inhibited by antibodies, RGD, and other ligand-derived peptides and snake venom peptides such as echistatin. Del-1 is a natural inhibitor of LFA-1 [13].

Intracellular interactions

A number of cytoplasmic components regulate the interactions of integrins with the cytoskeleton, enabling changes in both ligand-binding **avidity** (see Glossary), due to integrin clustering, or allosteric alterations, affecting integrin ligand **affinity** [6]. Integrins are also regulated by mechanotransduction. Here, bonds are formed between integrins and extracellular or cellular ligands, which generate activation by inducing interactions between the integrin tails and cytoplasmic proteins [14,15].

The integrin β-chain cytoplasmic domains are homologous, containing conserved regions (Figure 1). The β-chains are important in integrin activity regulation by interacting with cytoplasmic proteins, some of which are shared by different β-chains, such as talin, and some are unique for a particular β-chain. By contrast, the α-chain tails show low homology. They contain a common GFFKR sequence close to the membrane, however, and its deletion activates integrins, probably due to unclasping of the integrin tails. The α-chain-binding proteins include calreticulin, RapL, paxillin, and SHARPIN [16], but they do not appear to be shared by all α-chains [8]. In fact, SHARPIN also binds to integrin β-chains [17].

Several proteins bind to the integrin cytoplasmic domains; most of those identified bind to integrin β-chains and a few to α-chains. LFA-1 is shown as an example in Figure 2. The best-known cytoplasmic binding proteins are filamin A, DOK1, talin-1, 14-3-3ζ, α-actinin, and kindlin-3. Many of the LFA-1 intracellular binding proteins also bind to other integrins.

Negative regulators of integrins

The filamins are large 280 kDa proteins containing two actin-binding domains followed by 24 immunoglobulin-like repeats [18]. Filamin A is an important negative regulator of integrins, among them LFA-1 and $\alpha_{IIb}\beta_3$, and its binding to integrins has been studied in detail [19]. It is phosphorylated on Ser2152 by the Ndr2 kinase, which promotes its dissociation from LFA-1 [20]. Filamin A seems to have many different functions, and mutations in it may result in cardiovascular malformations and skeletal dysplasia [21].

Like filamin A, Dok1 is an integrin inhibitor [22], and it may be more important in neutrophil and platelet adhesion than in T cell adhesion. It was observed bound with high affinity to the tyrosine phosphorylated proximal NPLY sequence in β_3 and competed with talin for binding [23]. Dok1 bound weakly to β_2 cytoplasmic peptides, but peptides phosphorylated at S756 showed stronger binding. The result suggests that in β_2-integrins, there may occur a phosphorylation

Glossary

Affinity: the binding strength of an individual molecule.
Avidity: increased avidity means that several interacting molecules together increase binding strength.
Constitutively phosphorylated: phosphorylation that is present without the preceding activation.
Crosstalk: the ability to connect some function from one molecule to another.
G protein: a protein regulated by GTP–GDP exchange.
Immunological synapse: an interface between an antigen-presenting cell and a lymphocyte.
LAD-I: leukocyte adhesion deficiency type I is a genetic disorder due to lack of functioning β_2-integrins.
LAD-III: leukocyte adhesion deficiency type III is a genetic disorder due to lack of kindlin-3 function.
Protein kinases: enzymes that phosphorylate proteins on tyrosine, serine, or threonine.
Protein phosphatase: enzyme that hydrolyses the linkage between a protein and phosphate.

Carl_G_190x270_mm_blokki_FINAL.indd 466 06-Aug-23 1:55:03 PM

Trends in Biochemical Sciences

CellPress
OPEN ACCESS

αL KVGFFKRNLKEKMEAGRGVPNGIPAEDSEQLASGQEAGDPGGCLKPLHEKDSES(1140)GGGKD
αM KLGFFKRQYKDMMS(1126)EGGPPGAEPQ
αX KVGFFKRQYKEMMEEANGQIAPENGTQTPS(1158)PPSEK
αD KLGFFKRHYKEMLEDKPEDTATFSGDDFSCVAPNVPLS
αV RMGFFKRVRPPQEEQEREQLQPHENGEGNSET
αE KCGFFKRKYQQLNLESIRKAQLKSENLLEEEN
α1 KIGFFKRPLKKKMEK
α2 KLGFFKRKYEKMTKNPDEIDETTELSS
αIIb KVGFFKRNRPPLEEDDEEGE
α3 KCGFFKRARTRALYEAKRQKAEMKSQPSETERLTDDY
α4 KAGFFKRQYKSILQEENRRDS(988)WSYINSKSNDD
α5 KLGFFKRSLPYGTAMEKAQLKPPATSDA
α6 KCGFFKRNKKDHYDATYHKAEIHAQPSDKERLTSDA
α7 KCGFFHRSSQSSSFPTNYHRACLAVQPSAMEGGPGTVGWSSNGSTPRPPCPSTMR
α8 KCFFDRARPPQEDMTDREQLTNDKTPEA
α9 KMGFFRRRYKEIIEAEKNRKENEDSWDWVQKNQ
α10 KLGFFAHKKIPEEKREEKLEQ
α11 KLGFFRSARRRREPGLDPTPKVLE

β1 KLLMIIHDRREFAKFEKEKMNAKWDTGENPIYKSAVT(788)TVVNPKYEGK
β2 KALIHLSDLREY(735)RRFEKEKLKS(745)QWNNDNPLFKS(756)AT(758)TTVMNPKFAES
β3 KLLITIHDRKEFAKFEEERARAKWDTANNPLY(747)KEATS(752)T(753)FTNITY(759)RGT
β5 KLLVTIHDRREFAKQS(759)ERS(762)RARYEMASNPLYRKPISTHTVDFTFNKFNKSYNGTVD
β6 KLLSSFHDRKEVAKFEAERSKAKWQTGTNPLYRGSTSTFKNVTYKHREKQKVDLSTDC
β7 RLSVEIYDRREYSRFEKEQQQLNWKQDSNPLYKSAIT(782)TTINPRFQEADSPTL
β8 RQVILQWNSNKIKSSSDYRVSASKKDKLILQSVCTRAVTYRREKPREIKDISKLNAHETFRCNF

ACE2 KARSGENPY(781)AS(783)IDISKGENNPGFQNTDDVQTSF

Trends in Biochemical Sciences

Figure 1. The sequences of the human integrin and the angiotensin-converting enzyme 2 (ACE2) severe acute respiratory syndrome coronavirus 2 receptor cytoplasmic tails. The known phosphorylation sites are marked in red. The important NPXY/F sequences are marked in blue. The β_4 tail is longer than the tails of the other β-chains, and is not shown.

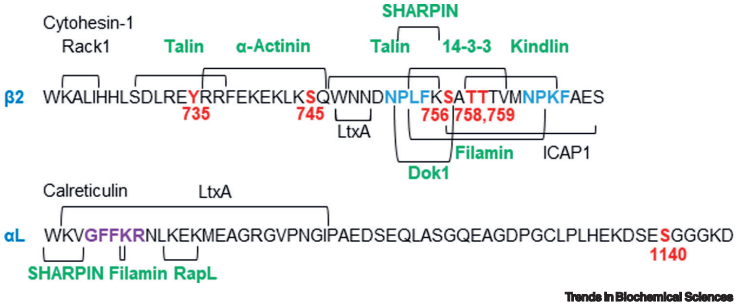

Trends in Biochemical Sciences

Figure 2. Binding sites on the LFA-1 αL and β_2 cytoplasmic tails for important interacting proteins. Talin binds to two sites on the β_2 tail, one of which is the important proximal NPLF sequence. Filamin binds to a stretch covering part of the NPLF and NPKF sequences and the important TTT sequence between them. When T758 is phosphorylated, filamin is released, and 14-3-3ζ binds to the phosphorylated residue. In β_2, Dok1 binds to the phosphorylated S756, but when T758 is phosphorylated, it is released. Kindlin binds to the sequence from T758 to the end of the distal NPKF sequence. Its binding needs cooperation by talin and phosphorylation on T758. SHARPIN binds to the α-chain and probably to the proximal NPLF sequence in β-tails, as has been shown for β_1 (NPIY). The phosphorylation sites are marked in red. The most studied interacting proteins are marked in green.

Carl_G_190x270_mm_blokki_FINAL.indd 467 06-Aug-23 1:55:03 PM

CellPress
OPEN ACCESS

Trends in Biochemical Sciences

switch that regulates Dok1 binding [24]. In the neutrophil $\alpha_M\beta_2$ integrin, the small **G protein** Rap1 bound to the phosphorylated S756 and may compete with Dok1 binding and release the inhibition [25].

SHARPIN is another negative regulator of some integrins, but less is known about how it regulates adhesion. This may be due to its interaction with the proximal NPXY/F sequence in integrin β-chains, where it competed with talin binding [17].

Positive regulators of integrins

The dimeric 14-3-3 proteins bind with high affinity to phosphorylated serine and threonine residues in proteins [26]. 14-3-3ζ is important in blood cell adhesion, and it binds to phosphorylated integrin β-chains [27].

Talin-1 and -2 are important components involved in integrin regulation [28]. Their 4.1-ezrin-radixin-moesin (FERM) domain binds to two sites on the β-chain cytoplasmic tails, including the proximal NPXY/F sequence (Figure 1). The talin rod binds to the cytoskeleton. Absence of talin is lethal [29].

Three kindlin molecules are present in mammals [30]. Kindlin-3 is expressed in hematopoietic cells, and lack of a functional molecule results in the leukocyte adhesion deficiency type III (**LAD-III)** syndrome, characterized by defective adhesion of blood cells [31–33]. Active kindlin-3 is a dimer [34–36], and its phosphorylation on S484 is induced by integrin-linked kinase (ILK)-stimulated **protein kinase** C α (PKCα), and it is required for activity [37].

Filamin A, 14-3-3ζ, kindlins, and talins together form an important integrin regulatory assembly, which depends on integrin phosphorylation as described later. Several other cytoplasmic proteins bind to the integrin cytoplasmic domains, but because the possible role of integrin phosphorylation on their activity is less understood, we do not focus on them. The reader is referred to reviews covering cytoplasmic proteins [5,8,38].

Site-specific integrin phosphorylations regulate integrin activity

In this review, we aim to explain how integrin activity is regulated by integrin phosphorylation. Protein kinases and phosphatases induce specific integrin phosphorylations and dephosphorylations, enabling the integrins to regulate dynamic interactions with cytoplasmic proteins to achieve changes in adhesion and signaling. A dramatic development in our understanding of integrin regulation has occurred during the past few years, and integrin phosphorylation has turned out to be of fundamental importance.

Integrins are phosphorylated at specific sites

Early work on integrin phosphorylation was initiated by the fact that PKC activation by phorbol esters induced integrin-dependent leukocyte adhesion [39]. Phosphorylation sites were first determined by labelling of cells with radioactive ^{32}P-phosphate, followed by immune precipitation with anti-integrin antibodies and Edman degradation of the isolated integrin chains [40]. Later phosphospecific antibodies have been used both against phosphorylated serine/phosphorylated threonine (pS/pT) sites and phosphotyrosine [41,42]. Antibodies are convenient to use, but their specificity must be carefully checked. Currently, mass spectrometry is the preferred technique to identify phosphorylation sites [43].

LFA-1 has been a favorite study object because of its importance in T cells. The α-chain of LFA-1 is **constitutively phosphorylated** in resting cells, but the phosphorylation is constantly turning

Carl_G_190x270_mm_blokki_FINAL.indd 468 06-Aug-23 1:55:03 PM

Trends in Biochemical Sciences

CellPress
OPEN ACCESS

over. Activation results in β_2-chain phosphorylation. The integrin β_2-phosphorylation site was initially observed on S756, but the S756A mutation did not affect T cell adhesion [44]. Later work showed phosphorylation of the functionally important T758-T759 residues, but to observe it, it was necessary to inhibit **protein phosphatase** activity [40,45]. A similar finding was reported for T788-T789 in β_1-integrins [46]. The single α-chain phosphorylation sites of LFA-1, Mac-1 ($\alpha_M\beta_2$; CD11b/CD18), and $\alpha_X\beta_2$ (CD11c/CD18) were found to be essential for cell adhesion and cellular movement [47–49]. Importantly, α-chain phosphorylation enabled LFA-1 β-chain phosphorylation, including opening of the cytoplasmic clasp, allowing binding of cytoplasmic integrin regulatory proteins [41]. Structural and functional studies have now shown how molecular complexes are formed on the phosphorylated β-chain and how adhesion and signaling take place. The Mac-1, $\alpha_X\beta_2$, and $\alpha_D\beta_2$ integrins have not yet been studied in this respect.

$\alpha_{IIb}\beta_3$ is the major platelet integrin, and it is an important model for studies on outside-in integrin activation [50]. Important sites in the β-chains are the two NPXY sequences, which flank the conserved serine/threonines (Figure 1). The mutation Y747A in β_3 inhibited the uptake of fibrinogen-coated particles and cell spreading of $\alpha_{IIb}\beta_3$ transfected Chinese hamster ovary cells, and the Y759A mutation likewise inhibited fibrinogen uptake, but had less effect on cell spreading [51]. Sarcoma virus kinase (Src) phosphorylated both Y747 and Y759 in β_3 [52,53].

Inside-out signaling results in integrin phosphorylation

To get a more general understanding of integrin-dependent cell adhesion, we must compromise and combine results obtained with different cell, signaling, and adhesion models. The β_1-, β_2-, and β_3-integrins are best known, and many of the regulatory mechanisms appear similar in the different integrin families. A few protein kinases and phosphatases have been identified to be involved in integrin phosphorylation, but here much additional work is needed [27,54].

Activation of the T cell receptor (TCR) [55,56] and chemokine receptors results in β_2-integrin activation [41,57]. Figure 3 shows a simplified map of the signaling routes in inside-out activation of LFA-1. Signaling starts from the initial binding of an agonist to the TCR in the **immunological synapse**, activation of lymphocyte-specific protein tyrosine kinase (Lck), followed by activation of downstream signaling molecules.

An excellent example of integrin activation in T cells with large clinical implications is how the commonly used immunosuppressive drugs cyclosporine and FK506 inhibit the phosphorylation and the subsequent activation of LFA-1. Until recently, these drugs were only known to inhibit the dephosphorylation of nuclear factor of activated T cells (NFAT) proteins and transcription. Recent studies have shown, however, that they also inhibit T cell adhesion by inhibiting the phosphatase calcineurin [58]. Calcineurin normally dephosphorylates the inhibitory phosphorylated S59 on Lck kinase and activates it. This results in signaling to LFA-1 and β_2-chain phosphorylation [58]. Using a transgenic mouse model that expresses Lck-S59A, Otsuka *et al.* [59] found that the calcineurin inhibitors suppressed acute graft-versus-host disease via NFAT-independent inhibition of TCR signaling and T758 phosphorylation of β_2.

Like activation through the TCR, several chemokines activate leukocyte integrins. They bind to trimeric G protein receptors, which dissociate and activate phospholipase C β_2 (PLCβ_2) and PLCβ_3, which generate diacyl glycerol (DAG) and inositol trisphosphate. The chemokine induced activation also resulted in T758 phosphorylation [41]. ILK may be important for the activation of PKCα and its membrane targeting [60].

Carl_G_190x270_mm_blokki_FINAL.indd 469 06-Aug-23 1:55:04 PM

CellPress
OPEN ACCESS

Trends in Biochemical Sciences

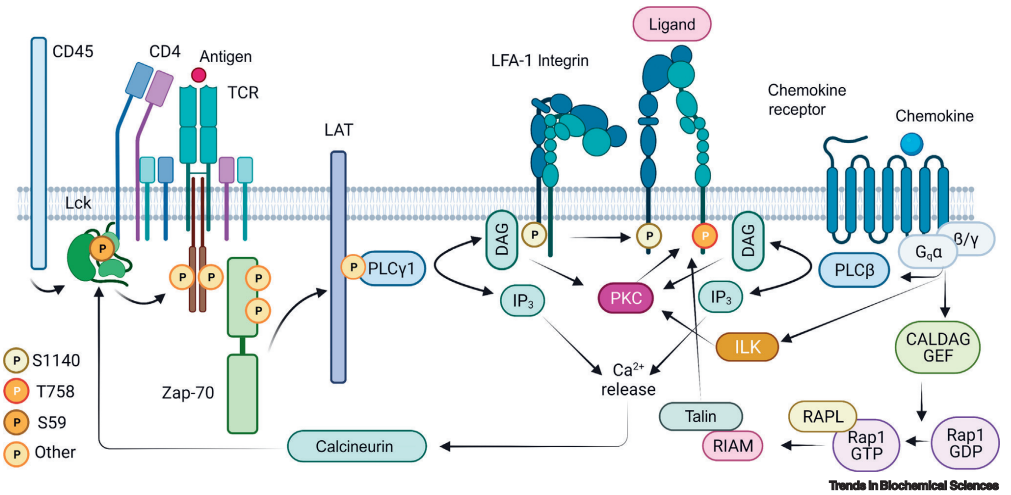

Figure 3. A simplified drawing of the inside-out signalling from the T cell receptor (TCR) and chemokine receptors to LFA-1. The tyrosine kinase Lck is activated after TCR activation by specific phosphorylations and dephosphorylation. The CD45 tyrosine phosphatase dephosphorylates the phosphorylated C-terminal tyrosine in Lck in the immunological synapse. The active Lck then phosphorylates the ZAP-70 kinase, which in turn phosphorylates the LAT adaptor protein. This activates phospholipase C γ1 (PLCγ1), resulting in the generation of diacyl glycerol (DAG) and inositol trisphosphate (IP_3). DAG activates protein kinase C (PKC) kinases, which phosphorylate the β_2 chain on T758 and less on T759. IP_3 stimulates Ca^{2+} release, which activates the calcineurin phosphatase, which removes the phosphate on S59 in previously inactive Lck molecules and further activates the kinase. Chemokine receptor activation results in activation of PLCβ and generates DAG and IP_3. This results in the activation of the small G protein Rap1. Rap1 in turn interacts with the Rap1-interacting adaptor molecule (RIAM), which binds to talin, and induces talin binding to the integrin β-chain [58]. PKC is activated downstream of DAG and integrin-linked kinase (ILK). The signalling results in integrin conformational changes, release and binding of cytosolic proteins, and integrin activation.

The interactions of cytoplasmic proteins with integrins are regulated by integrin phosphorylation

LFA-1 integrin as a model for adhesion studies

Let us now look in detail how integrin activity is regulated and use the T cell LFA-1 integrin as a model (Figure 4). The α-chain phosphorylation on S1140 is required for β-chain phosphorylation on T758 [41]. For example, when cells migrate towards a chemokine source, there must be a continuous adhesion and deadhesion to the substrate, and these events may be a consequence of α-chain phosphorylation turnover, which in turn regulates β-chain T758 phosphorylation and activates adhesion. The phosphorylation of T758 takes place by activated PKCs [27], but they must get access to their substrate in the β-chain. The Ca^{2+}/calmodulin-dependent protein kinase II (CaMKII) has also been implicated in β-chain phosphorylation [61].

A separation of the clasped integrin tails upon activation was observed by electron microscopy and Förster resonance energy transfer (FRET) analysis [8]. α-Actinin binds to the cytoplasmic domain of LFA-1 with the intermediate-affinity extended conformation [62,63]. It bound well to the activated wild-type (WT) LFA-1 integrin, whereas the α-chain S1140A mutation inhibited binding, indicating steric hindrance in the clasped tail [41]. The separation of the cytoplasmic tails only occurred when both integrin chains were phosphorylated, the α-chain on S1140 and the β-chain on T758. The chain separation could be due to repulsion between the negatively charged α- and β-tails, but we cannot exclude that integrin tail binding proteins can be involved

Carl_G_190x270_mm_blokki_FINAL.indd 470 06-Aug-23 1:55:04 PM

Trends in Biochemical Sciences

CellPress
OPEN ACCESS

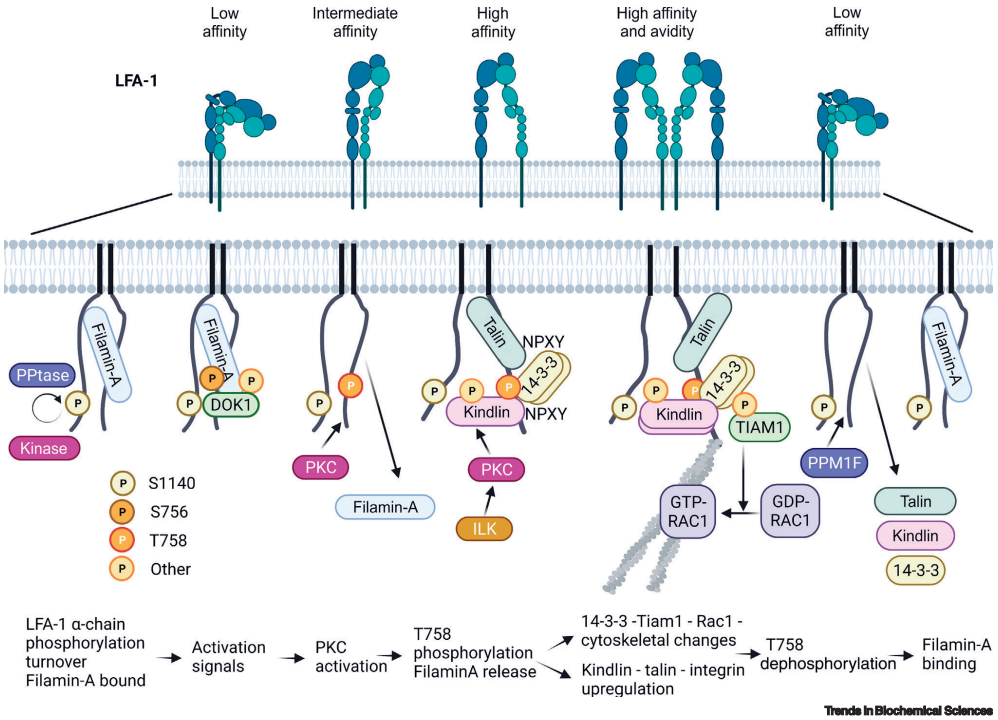

Figure 4. A detailed view of LFA-1 integrin activation. The upper part of the figure shows (from left) the inactive integrin with the head turned towards the lipid bilayer, the extended intermediate affinity integrin, the fully active integrin, the clustered high-affinity–high-avidity complex, and the inactivated integrin. The middle part shows that in the resting state, the LFA-1 α-chain is phosphorylated on S1140, but there is a turnover of the phosphate. The α-chain kinase(s) and phosphatase(s) [PPtase(s)] are not known. A filamin A molecule is bound to the β_2 tail. When the T cell is activated by phorbol esters, both S756 and T758 are phosphorylated. Dok1 can bind to the phosphorylated S756, but T758 phosphorylation outcompetes Dok1 binding because 14-3-3ζ binds to phosphorylated T758 with high affinity. Activation through the T cell receptor (TCR) targets T758 phosphorylation by protein kinase C (PKC). The S1140 phosphorylation is required for T758 phosphorylation. The phosphorylations facilitate binding of interacting proteins, and the tails move apart. Upon T758 phosphorylation, filamin A is released and replaced by 14-3-3ζ. Talin binds to two sites on β_2; one is close to the membrane, and the other is the proximal NPXY sequence. Integrin-linked kinase (ILK) is required for membrane targeting of PKC and stimulates the phosphorylation of kindlin-3, which dimerizes. The T758 phosphorylation enables kindlin-3 binding to the distal NPXY sequence with the help of talin, but a portion of the kindlin molecules could interact with the β_2-chain through 14-3-3ζ. These events upregulate LFA-1 affinity. The 14-3-3ζ/Tiam-1/Rac1 complex and α-actinin interact with the cytoskeleton and increase binding avidity by clustering the integrins on the plasma membrane. Finally, the PPM1F PPtase cleaves off the phosphate from T758 and releases the 14-3-3ζ/Tiam-1/Rac1 and talin/kindlin complexes, filamin returns to its binding site, and the integrin is inactivated. At bottom is a simplified drawing of the sequence of events. Note that the 14-3-3ζ-Tiam-1-Rac1 and kindlin–talin complexes can occur on the same β-tail, which enables both changes in integrin avidity and affinity.

in chain separation. The unclasping of the cytoplasmic domain then makes binding possible of the key components 14-3-3ζ, talin, and kindlin to the β tails.

Phosphorylation of LFA-1 β-chain promotes 14-3-3ζ binding

In resting cells, filamin A bound to the β_2-chain and inhibited cell adhesion [19]. When T758 was phosphorylated, 14-3-3ζ bound with high affinity and inhibited filamin A binding. The β_2-tail forms a loop, and whereas 14-3-3ζ readily fitted into the loop, the filamin A domain did not due to steric hindrance by pT758 [64]. The interaction with 14-3-3ζ did not affect talin binding. The dimeric

Carl_G_190x270_mm_blokki_FINAL.indd 471 06-Aug-23 1:55:05 PM

CellPress
OPEN ACCESS

Trends in Biochemical Sciences

14-3-3ζ in turn bound to the Tiam1 adaptor protein, which further activated the small G protein Rac-1, which regulates the organization of the actin cytoskeleton [65].

Unclasping of LFA-1 cytoplasmic tails after β-chain phosphorylation

Talins and kindlins must cooperate to induce the integrin conformational changes, resulting in increased adhesion. In experiments with neutrophils, a portion of kindlin-3 molecules was recruited to the plasma membrane before the rolling-induced cellular arrest of leukocytes and the appearance of small clusters of highly active β_2-integrins [66]. Kindlin activity was induced before integrin-mediated adhesion was upregulated.

Kindlins bind to the TTTVMNPKF peptide sequence in β_2 (Figure 2); it covers both the important T758 site and the distal NPKF sequence. Indeed, when the T758-760/AAA mutated β_2 was expressed in mice, FRET analysis indicated a loss of kindlin-3 association with the β_2 chain [67]. The mice were healthy but showed an accumulation of leukocytes in the blood, fewer T cells in lymph nodes, decreased cell adhesion, and less spreading of T cells. The results support the concept that β_2-chain phosphorylation is important for leukocyte functions *in vivo*.

To further test if the phosphorylation of the threonine residues affects kindlin binding, various peptides were used, and the homologous integrin β_1 was used as a model [68]. In integrin β_1, residues T788-T789 correspond to T758-T759 in β_2. Kindlin-2 bound to the unphosphorylated WT β_1-peptide covering residues 762–798 *in vitro*, whereas a peptide containing pT788/pT789 showed no binding. Importantly, in the presence of the talin F3 domain, kindlin-2 bound to the integrin β_1 pT788/pT789 and required the intact distal NPKY motif for binding. The results are explained by the fact that although talin and kindlin do not directly interact with each other, talin reorients the integrin tail so that kindlin now can bind. A prerequisite for kindlin binding *in vivo* is thus that the T788/T789 residues in β_1 are phosphorylated [68]. The phosphorylated integrin outcompeted the binding of filamin A.

Further proof for the importance of T788/T789 phosphorylation for kindlin binding was obtained using GFP–kindlin-2. It strongly colocalized with the phosphomimicking T788D/T789D (threonines replaced by negative aspartic acids) β_1-integrin in intact cells [68]. The results support earlier results, which showed that T788/T789 must be phosphorylated for activation of β_1 [69]. Kindlin-2 has been shown to bind to the distal NITY sequence in β_3, and its tyrosine phosphorylation inhibited adhesion [70]. This finding strengthens the concept that an intact distal NPXY sequence is required to promote adhesion.

Very recent studies showed that kindlin-3 disrupted the association of the integrin β_2 tails and the subunit clasp and in this way contributed to integrin activation [71]. An interesting possibility is that a fraction of kindlin-3 molecules in hematopoietic cells could bind to the phosphorylated T758 residues in β_2 through 14-3-3ζ. It has been shown that 5–10% of the normal levels of kindlin-3 suffices for its basal functions in mice [72]. Therefore, the 14-3-3ζ-Tiam-1–Rac-1 pathway would not exclude binding of kindlin-3. The 14-3-3ζ proteins are dimers and could bind both phosphorylated T/S residues in integrin β-chains and phosphorylated kindlin-3. Kindlin-3 is phosphorylated at several sites, but the double-mutant T482/S484-AA in kindlin-3 inhibited adhesion of T lymphocytes, which shows that phosphorylation of kindlin-3 is functionally important [37,73].

Structural studies confirm that the β_2 phosphorylated cytoplasmic tail simultaneously can bind both the talin FERM domain and 14-3-3ζ [74]. Using single-protein analysis, it is now established that the β_1 tail, talin, and kindlin form a molecular complex and that the distances between the measured binding sites on individual integrins match the known binding sites [75]. These findings

Carl_G_190x270_mm_blokki_FINAL.indd 472 06-Aug-23 1:55:05 PM

Trends in Biochemical Sciences

CellPress
OPEN ACCESS

indicate that single integrins can both cluster and change conformation by two different downstream events, originating from the threonines between the NPXY/F sequences. The talin/kindlin- and 14-3-3ζ/Tiam-1/Rac-1-induced structural changes greatly advance our understanding of how adhesion takes place.

Dephosphorylation of the β-chain allows filamin binding

The phosphorylated T788/T789 residues in β_1 are dephosphorylated by the PPM1F phosphatase, regaining filamin A binding and abrogating adhesion [68]. PPM1F-knockout cells, which express increased levels of the pT788/pT789 β_1-integrin, showed an accumulation of kindlin-2 with β_1. Overexpression of PPM1F impaired talin recruitment to the integrin tail. WT cells showed clustering of GFP-filamin A with β_1, whereas overexpression of inactive PPM1F showed no codistribution [70]. The results indicate that PPM1F activity towards T788/T789 is important for integrin/filamin A association. Currently, we do not know whether PPM1F is involved in the regulation of other integrins than β_1-integrins, but due to the high homology of β-chains, it is highly probable. We do not know how PPM1F is regulated, but it certainly plays an important role at least in the regulation of β_1-integrin activity.

Integrin serine/threonine phosphorylation has general significance

In addition to the β_1- and β_2-integrins, the possible involvement of serine/threonine phosphorylation for the activity of other integrins has been studied to some extent. For example, treatment of platelets with the phosphatase inhibitor calyculin A resulted in phosphorylation of T751 and T753 in β_3 [76]; the phosphorylation inhibited outside-in signaling. By use of a β_3 T753 phosphorylated cytoplasmic peptide, it was shown that the tyrosine phosphorylation by Src was not affected by the T753 phosphorylation. Rather, the T753 phosphorylation inhibited the binding of the adaptor protein SHC (SH2-domain-containing transforming protein C1). *In vitro* experiments showed that the PDK1 and/or Akt/PKB kinases could phosphorylate T753 [77]. Additionally, the β_5 chain in the $\alpha_V\beta_5$ integrin contains a SERS motif, and S759 and S762 in the motif were phosphorylated by the p21-activated kinase 4. Mutation of both residues to alanine abrogated cell migration [78].

Little is known about α-chain phosphorylation. The α-chain of VLA-4 was found to be phosphorylated on S988 by protein kinase A, and the phosphorylation displaced paxillin from the integrin, resulting in integrin activation [79–81].

Outside-in signaling through the platelet integrin $\alpha_{IIb}\beta_3$ involves both tyrosine and serine/threonine phosphorylations

The platelet integrin $\alpha_{IIb}\beta_3$ is an important model for outside-in integrin activation. Patients with Glanzmann thrombasthenia, who lack a functional $\alpha_{IIb}\beta_3$ integrin, develop serious bleeding due to absence or mutations in the integrin [82].

One should bear in mind that inside-out and outside-in activations are intimately connected. When integrins have been activated through inside-out activation, ligands bind and in turn may activate outside-in activation.

Src is the major tyrosine kinase in platelets, and it bound to the integrin β_3 chain C-terminal sequence RGT through its SH3-domain and phosphorylated it [83]. Integrin clustering enabled transphosphorylation of Src molecules and subsequent spleen tyrosine kinase (Syk) and focal adhesion kinase (FAK) tyrosine kinase activations. Like Lck, Src is autoinhibited by C-terminal tyrosine phosphorylation, and it is activated by tyrosine phosphatases such as protein tyrosine phosphatase IB [84]. Downstream of Src phosphorylation, Syk and FAK phosphorylate signaling molecules, among them PKCs and PLCs or α-actinin, respectively. Recent studies showed that,

Carl_G_190x270_mm_blokki_FINAL.indd 473 06-Aug-23 1:55:06 PM

CellPress
OPEN ACCESS

Trends in Biochemical Sciences

upon activation with fibrinogen, a 14-3-3ζ/Src/β3 complex was formed through binding to the KEATSTF sequence of β_3 [85]. Interestingly, a myristylated KEATSTF peptide, which was taken up by cells, inhibited the β_3 outside-in signaling and platelet aggregation. The result indicates that it could be possible to develop drugs that interfere with functions associated with specific integrin phosphorylation sites.

Defects in integrin phosphorylation-mediated signaling could be less severe than total loss of integrins or adaptors

Deletion of the β_2-integrin gene results in leukocyte adhesion deficiency type I (**LAD-I)**, which is characterized by several deficiencies, including antibody production, T cell cytotoxicity, and chemotaxis [86]. To the best of our knowledge, no mutations of the human leukocyte integrin phosphorylation sites have been described in patients. Experimental results indicate that such mutations would be less severe than a total loss of integrin activity. Mutations in adaptor and signaling molecules may not wipe out all effects connected to a specific integrin, on the one hand, but could, on the other hand, affect the functions of several integrins. One example is the absence of a functional kindlin-3, which results in LAD-III [31–33]. In addition to defects in leukocyte cell adhesion-related functions, leukocyte development was impaired. Another example is deficiency in filamin function.

Phosphorylation is important in integrin crosstalk and may affect integrin/SARS-CoV-2 receptor ACE2 interaction

Crosstalk between integrins is well documented and depends on phosphorylation. For example, activated LFA-1 crosstalked with VLA-4 [87,88]. When LFA-1 was targeted with activating LFA-1 antibodies or ICAM-1, T758 in β_2 was phosphorylated, resulting in intracellular signaling, dephosphorylation of β_1, and inactivation of VLA-4 [89]. The two integrins have similar regulatory characteristics, and it is possible that the integrins simply exchange the β-chain-binding proteins, resulting in activation of one integrin and inactivation of the other. Monoclonal antibodies are used in the clinics to inhibit specific integrins, but we should now be aware of that by blocking the activity of one integrin, the activity of another integrin may change. Interestingly, T lymphocytes can migrate upstream of blood flow by binding of LFA-1 to ICAM-1, whereas they migrate downstream by VLA-4 interaction with VCAM-1 [90,91]. The ability to migrate upstream is preserved after the flow is terminated, due to integrin crosstalk between VLA-4 and LFA-1 [92].

The major receptor for the SARS-CoV-2 virus is angiotensin-converting enzyme 2 (ACE2) [93]. Its cytoplasmic domain contains short linear motifs with potential roles in endocytosis and autophagy [11]. ACE2 is present in the kidney and heart, but less in the lungs, where SARS-CoV-2 induces severe damage. This fact indicates that there may be alternative receptors for the virus in some tissues. One such receptor is neuropilin-1, which shows strong expression in the olfactory epithelium [94]. Integrins act as receptors for several viruses [95]. The SARS-CoV-2 virus spike protein contains an RGD sequence to which integrins expressed on lung epithelial cells can bind; these include $\alpha_V\beta_3$ and β_1 integrins such as $\alpha_4\beta_1$ [96–98]. β_1 and β_3 integrins could act as a coreceptor for SARS-CoV-2 [12,98], but they could also function as separate receptors in the lung and facilitate virus uptake by a phosphorylation switch [12,97]. In the immunological synapse, the binding specificity comes from the TCR–antigen interactions, but LFA-1–ICAM-1 interaction is important in strengthening the interaction [99]. In a corresponding way, integrins could strengthen the SARS-CoV-2–receptor interaction.

Previous work has shown a function for integrins and their NPXY motifs in both trafficking and autophagy [100,101]. The cytoplasmic tails of both ACE2 and integrin β_3 contain motifs that may participate in the internalization of the virus and its interactions with the autophagy

Carl_G_190x270_mm_blokki_FINAL.indd 474 06-Aug-23 1:55:06 PM

Trends in Biochemical Sciences

CellPress
OPEN ACCESS

pathway (Figure 5). The β_3 cytoplasmic domain bound the autophagy-related protein 8 (ATG8) domains and required phosphorylation [14]. Phosphorylation of S752 in β_3 strengthened binding to all ATG8 domains, whereas T753 phosphorylation enhanced binding to one of the tested ATG8 domains, but not to the others. Phosphorylation of Y759 improved binding in all cases, and double phosphorylation on T753 and Y759 promoted ATG8 binding. The C-terminus of ACE2 is similar to integrin β-tails containing NPYA and NPGF sequences and serine residues between them (Figures 1 and 5). SH2 domain-containing tyrosine kinases showed binding to the ACE2 cytoplasmic domain, and pY781 disabled the interaction, while pS783 increased the affinity about twofold. The results indicate that the cytoplasmic domains of the ACE2 and integrins may regulate SARS-CoV-2 endocytosis and autophagy, but further work on the role of these proteins as links between pathogen infection and autophagy is required.

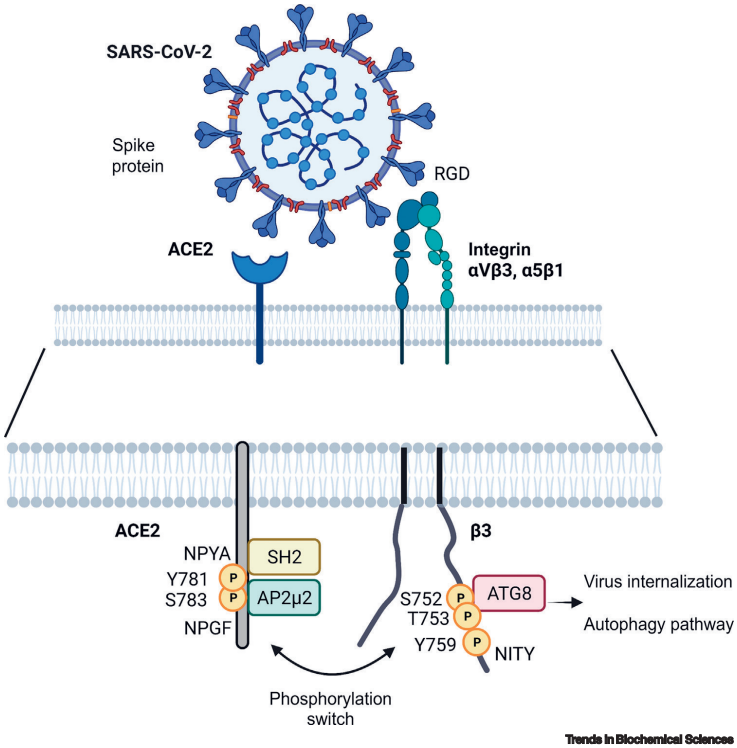

Figure 5. Binding of severe acute respiratory syndrome coronavirus 2 (SARS-CoV-2) to its receptors and possible crosstalk between integrins and the angiotensin-converting enzyme 2 (ACE2) receptor. The ACE2 receptor has been studied extensively and is strongly expressed in the upper airways, but not much in the lungs, where the most serious complications occur. Phosphorylated Y781 acts as a binding site for Src family kinases through their SH2-domains, and its phosphorylation inhibited the binding of the clathrin adaptor AP2μ2, whereas phosphorylation of S783 enhanced the binding [14]. It could act as a binding switch. β_1- and β_3-integrins are expressed in the lungs and can bind SARS-CoV-2 through the RGD motif in the virus spike. These integrins could act as coreceptors or as primary receptors, and they could bind autophagy-related protein 8 (ATG8) domains when phosphorylated on S752 or T753. The similarities between ACE2 and β_1- and β_3-cytoplasmic tails could induce phosphorylation switches such as those seen between LFA-1 and VLA-4 in T cells.

Carl_G_190x270_mm_blokki_FINAL.indd 475 06-Aug-23 1:55:07 PM

CellPress
OPEN ACCESS

Trends in Biochemical Sciences

Concluding remarks

Cell adhesion is of pivotal importance for the development of organs, immunity against foreign microbes, metastasis from malignant tumors, restriction of excessive activity of T cells and macrophages towards own tissues, and clotting of platelets. Integrins constitute an important family of adhesion proteins, and their activity must be dynamically regulated to enable fast changes in activity. Several cytoplasmic proteins bind to the integrin cytoplasmic tails and affect their activity. Among them, 14-3-3ζ, talins, and kindlins are important activators, whereas filamin A and Dok-1 are inhibitory. Although relatively little is known about the protein kinases and phosphatases involved, they are responsible for specific integrin phosphorylations on both the α- and β-chains and regulate the interactions between the integrins and the cytoplasmic adaptors and thus adhesion. Monoclonal antibodies have been used to inhibit cell adhesion of leukocytes, but their clinical use has often been disappointing due to unwanted side effects. In the future, it should be possible to develop drugs that specifically target integrin phosphorylation sites and have more restricted effects (see Outstanding questions).

Outstanding questions

Which protein kinases and phosphatases, in addition to the few known, affect cell adhesion?

Are some integrins regulated in very different ways, or are the mechanisms for the most part similar?

What are the structures of integrin–adaptor complexes like? How are their dynamics regulated?

Will it be possible to develop drugs targeting the integrin phosphorylation sites?

Which additional cytoplasmic proteins will turn out to be important in adhesion?

Does cytoplasmic glycosylation regulate adhesion by competing with phosphorylation?

Acknowledgments

These studies were supported by grants from the Finnish Medical Association, the Finnish Society of Science and Letters, the Wilhelm and Else Stockmann Foundation, the Magnus Ehrnrooth Foundation, and the Medicinska Understödsföreningen Liv och Hälsa Foundation. Figures 3–5 were created with BioRender. Figure 5 was adapted from "SARS-CoV-2 Spike Protein Conformations" from BioRender.com (2021).

Author contributions

Both authors wrote the text and planned the figures.

Declaration of interests

The authors have no conflict of interest.

References

1. Hynes, R.O. (2002) Integrins: Bidirectional, allosteric signalling machines. *Cell* 110, 673–687
2. Arnaout, M.A. *et al.* (2005) Integrin structure, allostery, and bidirectional signalling. *Annu. Rev. Cell Dev. Biol.* 21, 381–410
3. Hogg, N. *et al.* (2011) The insider's guide to leukocyte integrin signalling and function. *Nat. Rev. Immunol.* 11, 416–426
4. Calderwood, D.A. *et al.* (2013) Talins and kindlins: Partners in integrin-mediated adhesion. *Nat. Rev. Mol. Cell Biol.* 14, 503–517
5. Gahmberg, C.G. *et al.* (2019) Regulation of cell adhesion: A collaborative effort of integrins, their ligands, cytoplasmic actors and phosphorylation. *Q. Rev. Biophys.* 52, e10
6. Bachmann, M. *et al.* (2019) Cell adhesion by integrins. *Physiol. Rev.* 99, 1655–1699
7. Nolte, M.A. and Margadant, C. (2020) Activation and suppression of hematopoietic integrins in hemostasis and immunity. *Blood* 135, 7–16
8. Abram, C.L. and Lowell, C.A. (2009) The ins and outs of leukocyte integrin signaling. *Annu. Rev. Immunol.* 27, 339–362
9. Kim, M. *et al.* (2003) Bidirectional transmembrane signaling by cytoplasmic domain separation in integrins. *Science* 301, 1720–1725
10. Pierschbacher, M.D. and Ruoslahti, E. (1984) Cell attachment activity of fibronectin can be duplicated by small synthetic fragments of the molecule. *Nature* 309, 30–33
11. Mészaros, B. *et al.* (2021) Short linear motif candidates in the cell entry system used by SARS-CoV-2 and their potential therapeutic implications. *Sci. Signal.* 14, eabd0334
12. Kliche, J. *et al.* (2021) Cytoplasmic short linear motifs in ACE2 and integrin β3 link SARS-CoV-2 host cell receptors to mediators of endocytosis and autophagy. *Sci. Signal.* 14, eabf1117
13. Choi, E.Y. *et al.* (2008) Del-1, an endogenous leukocyte-endothelial adhesion inhibitor, limits inflammatory cell recruitment. *Science* 322, 1101–1104
14. Nordenfelt, P. *et al.* (2016) Coordinated integrin activation by actin-dependent force during T-cell migration. *Nat. Commun.* 7, 13119
15. Sun, Z. *et al.* (2019) Integrin activation by talin, kindlin and mechanical forces. *Nat. Cell Biol.* 21, 25–31
16. Rantala, J.K. *et al.* (2011) SHARPIN is an endogenous inhibitor of β_1-integrin activation. *Nat. Cell Biol.* 13, 1315–1324
17. Gao, J. *et al.* (2019) Sharpin suppresses β_1-integrin activation by complexing with the β_1 tail and kindlin-1. *Cell Commun. Signal.* 17, 101
18. Stossel, T.P. *et al.* (2001) Filamins as integrators of cell mechanics and signalling. *Nat. Rev. Mol. Cell Biol.* 2, 138–145
19. Kiema, T. *et al.* (2006) The molecular basis of filamin binding to integrins and competition with talin. *Mol. Cell* 21, 337–347
20. Waldt, N. *et al.* (2018) Filamin A phosphorylation at serine 2152 by the serine/threonine kinase Ndr2 controls TCR-induced LFA-1 activation in T cells. *Front. Immunol.* 9, 2852
21. Sasaki, E. *et al.* (2019) A review on filamin A mutations and associated lung disease. *Eur. J. Pediatr.* 178, 121–129
22. Yasuda, T. *et al.* (2007) Dok-1 and Dok-2 are negative regulators of T cell receptor signaling. *Int. Immunol.* 19, 487–495
23. Oxley, C.L. *et al.* (2008) An integrin phosphorylation switch. The effect of β3 integrin tail phosphorylation on Dok1 and talin binding. *J. Biol. Chem.* 283, 5420–5426
24. Gupta, S. *et al.* (2015) An alternative phosphorylation switch in integrin β2 (CD18) tail for Dok1 binding. *Sci. Rep.* 5, 11630
25. Lim, J. *et al.* (2011) Ser756 of β2 integrin controls Rap1 activity during inside-out activation of αMβ2. *Biochem. J.* 437, 461–467
26. Muslin, A.J. *et al.* (1996) Interaction of 14-3-3 with signaling proteins is mediated by the recognition of phosphoserine. *Cell* 84, 889–897
27. Fagerholm, S. *et al.* (2002) Phosphorylation of the cytoplasmic domain of the integrin CD18 chain by protein kinase C isoforms in leukocytes. *J. Biol. Chem.* 277, 1728–1738

Carl_G_190x270_mm_blokki_FINAL.indd 476 06-Aug-23 1:55:07 PM

Trends in Biochemical Sciences

CellPress
OPEN ACCESS

28. Klapholz, B. and Brown, N.H. (2017) Talin- the master of integrin adhesions. *J. Cell Sci.* 130, 2435–2446
29. Monkley, S.J. *et al.* (2000) Disruption of the talin gene arrests mouse development at the gastrulation stage. *Dev. Dyn.* 219, 560–574
30. Ussar, S. *et al.* (2006) The Kindlins: subcellular localization and expression during murine development. *Exp. Cell Res.* 312, 3142–3151
31. Malinin, N.L. *et al.* (2009) A point mutation in KINDLIN3 ablates activation of three integrin subfamilies in humans. *Nat. Med.* 15, 313–318
32. Moser, M. *et al.* (2009) Kindlin-3 is required for β2 integrin-mediated leukocyte adhesion to endothelial cells. *Nat. Med.* 15, 300–305
33. Svensson, L. *et al.* (2009) Leukocyte adhesion deficiency-III is caused by mutations in KINDLIN3 affecting integrin activation. *Nat. Med.* 15, 306–312
34. Li, H. *et al.* (2017) Structural basis of kindlin-mediated integrin recognition and activation. *Proc. Natl. Acad. Sci. U. S. A.* 114, 9349–9354
35. Kadry, Y.A. *et al.* (2020) Differences in self-association between kindlin-2 and kindlin-3 are associated with differential integrin binding. *J. Biol. Chem.* 295, 11161–11173
36. Bu, W. *et al.* (2020) Structural basis of human full-length kindlin-3 homotrimer in an auto-inhibited state. *PLoS Biol.* 18, e3000755
37. Bialkowska, K. *et al.* (2020) Site-specific phosphorylation regulates the functions of kindlin-3 in a variety of cells. *Life Sci.* 3, e201900594
38. Fagerholm, S.C. *et al.* (2019) Beta2-integrins and interacting proteins in leukocyte trafficking, immune suppression, and immunodeficiency disease. *Front. Immunol.* 10, 254
39. Patarroyo, M. *et al.* (1985) Identification of a cell surface protein complex mediating phorbol ester-induced adhesion (binding) among human mononuclear leukocytes. *Scand. J. Immunol.* 22, 171–182
40. Hilden, T.J. *et al.* (2003) Threonine phosphorylation sites in the β2 and β7 leukocyte integrin polypeptides. *J. Immunol.* 170, 4170–4177
41. Jahan, F. *et al.* (2018) Phosphorylation of the α-chain in the integrin LFA-1 enables β2-chain phosphorylation and α-actinin binding required for cell adhesion. *J. Biol. Chem.* 293, 12318–12330
42. Johnson, S.A. and Hunter, T. (2005) Kinomics: Methods for deciphering the kinome. *Nat. Methods* 2, 17–25
43. Robertson, J. *et al.* (2015) Defining the phospho-adhesome through the phosphoproteomic analysis of integrin signalling. *Nat. Commun.* 6, 6265
44. Hibbs, M.L. *et al.* (1991) The cytoplasmic domain of the integrin lymphocyte function-associated antigen 1 β subunit: Sites required for binding to intercellular adhesion molecule 1 and the phorbol ester-stimulated phosphorylation site. *J. Exp. Med.* 174, 1227–1238
45. Valmu, L. and Gahmberg, C.G. (1995) Treatment with okadaic acid reveals strong threonine phosphorylation of CD18 after activation of CD11/CD18 integrin with phorbol ester or CD3 antibodies. *J. Immunol.* 155, 1175–1183
46. Nilsson, S. *et al.* (2006) Threonine 788 in integrin subunit β1 regulates integrin activation. *Exp. Cell Res.* 312, 844–853
47. Fagerholm, S.C. *et al.* (2005) Specific integrin α and β chain phosphorylations regulate LFA-1 activation through affinity-dependent and -independent mechanisms. *J. Cell Biol.* 171, 705–715
48. Fagerholm, S.C. *et al.* (2006) α-chain phosphorylation of the human leukocyte CD11b/CD18 (Mac-1) integrin is pivotal for integrin activation to bind ICAMs and leukocyte extravasation in vivo. *Blood* 108, 3379–3386
49. Uotila, L.M. *et al.* (2013) Integrin CD11c/CD18 α-chain phosphorylation is functionally important. *J. Biol. Chem.* 288, 33494–33499
50. Durrant, T.N. *et al.* (2017) Integrin αIIbβ3 outside-in signaling. *Blood* 130, 1607–1619
51. Ylänne, J. *et al.* (1995) Mutation of the cytoplasmic domain of the integrin beta3 subunit. Differential effects on cell spreading, recruitment to adhesion plaques, endocytosis and phagocytosis. *J. Biol. Chem.* 270, 9550–9557
52. Law, D.A. *et al.* (1996) Outside-in integrin signal transduction. αIIbβ3-(GP-IIIa) tyrosine phosphorylation induced by platelet aggregation. *J. Biol. Chem.* 271, 10811–10815
53. Obergfell, A. *et al.* (2002) Coordinate interactions of Csk, Src, and Syk kinases with αIIbβ3 initiate integrin signaling to the cytoskeleton. *J. Cell Biol.* 157, 265–275
54. Young, K.A. *et al.* (2021) Protein tyrosine phosphatases in cell adhesion. *Biochem. J.* 478, 1061–1083
55. Dustin, M.L. and Springer, T.A. (1989) T-cell receptor cross-linking transiently stimulates adhesiveness through LFA-1. *Nature* 341, 619–624
56. van Kooyk, Y. *et al.* (1989) Enhancement of LFA-1 mediated cell adhesion by triggering through CD2 or CD3 on T lymphocytes. *Nature* 342, 811–813
57. Courtney, A.H. *et al.* (2017) TCR signalling: Mechanisms of initiation and propagation. *Trends Biochem. Sci.* 43, 108–123
58. Dutta, D. *et al.* (2017) Recruitment of calcineurin to the TCR positively regulates T cell activation. *Nat. Immunol.* 18, 196–204
59. Otsuka, S. *et al.* (2021) Calcineurin inhibitors suppress acute graft-versus-host disease via NFAT-independent inhibition of T cell receptor signaling. *J. Clin. Invest.* 131, e147683
60. Margraf, A. *et al.* (2020) The integrin linked kinase is required for chemokine-triggered high affinity conformation of neutrophil β_2-integrin LFA-1. *Blood* 136, 2200–2205
61. Takahashi, K. (2001) The linkage between beta1 integrin and the actin cytoskeleton is differentially regulated by tyrosine and serine/threonine phosphorylation of beta1 integrin in normal and cancerous human breast cells. *BMC Cell Biol.* 2, 23
62. Pavalko, F.M. and LaRoche, S.M. (1993) Activation of human neutrophils induces an interaction between the integrin β2-subunit (CD18) and the actin binding protein α-actinin. *J. Immunol.* 151, 3795–3807
63. Stanley, P. *et al.* (2008) Intermediate-affinity LFA-1 binds α-actinin-1 to control migration at the leading edge of the T cell. *EMBO J.* 27, 62–75
64. Takala, H. *et al.* (2008) β2 integrin phosphorylation on Thr758 acts as a molecular switch to regulate 14-3-3 and filamin binding. *Blood* 112, 1853–1862
65. Grönholm, M. *et al.* (2011) TCR-induced activation of LFA-1 involves signaling through Tiam1. *J. Immunol.* 187, 3613–3619
66. Wen, L. *et al.* (2021) Kindlin-3 recruitment to the plasma membrane precedes high-affinity β2-integrin and neutrophil arrest from rolling. *Blood* 137, 29–38
67. Morrison, V.L. *et al.* (2013) The β2 integrin-kindlin-3 interaction is essential for T-cell homing but dispensable for T-cell activation in vivo. *Blood* 122, 1428–1436
68. Grimm, T.M. *et al.* (2020) PPM1F controls integrin activity via a conserved phospho-switch. *J. Cell Biol.* 219, e202001057
69. Wennerberg, K. *et al.* (1998) Mutational analysis of the potential phosphorylation sites in the cytoplasmic domain of integrin beta1A. Requirement for threonines 788-789 in receptor activation. *J. Cell Sci.* 111, 1117–1126
70. Bledzka, K. *et al.* (2010) Tyrosine phosphorylation of integrin β3 regulates kindlin-2 binding and integrin activation. *J. Biol. Chem.* 285, 30370–30374
71. Kondo, N. *et al.* (2021) Kindlin-3 disrupts an intersubunit association in the integrin LFA1 to trigger positive feedback activation by Rap1 and talin1. *Sci. Signal.* 14, eabf2184
72. Klapproth, S. *et al.* (2015) Minimal amounts of kindlin-3 suffice for basal platelet and leukocyte functions in mice. *Blood* 126, 2592–2600
73. Bialkowska, K. *et al.* (2021) Phosphorylation of kindlins and the control of integrin function. *Cells* 10, 825
74. Chatterjee, D. *et al.* (2016) Interaction analyses of the integrin β2 cytoplasmic tail with the F3 FERM domain of talin and 14-3-3 ζ reveal a ternary complex with phosphorylated tail. *J. Mol. Biol.* 428, 4129–4142
75. Fischer, L.S. *et al.* (2021) Quantitative single-protein imaging reveals molecular complex formation of integrin, talin, and kindlin during cell adhesion. *Nat. Commun.* 12, 919
76. Lerea, K.M. *et al.* (1999) Phosphorylation sites in the integrin β3 cytoplasmic domain in intact platelets. *J. Biol. Chem.* 274, 1914–1919

Carl_G_190x270_mm_blokki_FINAL.indd 477 06-Aug-23 1:55:08 PM

CellPress
OPEN ACCESS

Trends in Biochemical Sciences

77. Kirk, R.I. *et al.* (2000) Threonine phosphorylation of the β3 integrin cytoplasmic tail, at a site recognized by PDK1 and Akt/PKB in vitro, regulates Shc binding. *J. Biol. Chem.* 275, 30901–30906
78. Li, Z. *et al.* (2010) p21-activated kinase 4 phosphorylation of integrin β5 Ser-759 and Ser-762 regulates cell migration. *J. Biol. Chem.* 285, 23699–23710
79. Han, J. *et al.* (2001) Phosphorylation of the integrin alpha 4 cytoplasmic domain regulates paxillin binding. *J. Biol. Chem.* 276, 40903–40909
80. Han, J. *et al.* (2003) Integrin alpha 4 beta 1-dependent T cell migration requires both phosphorylation and dephosphorylation of the alpha 4 cytoplasmic domain to regulate the reversible binding of paxillin. *J. Biol. Chem.* 278, 34845–34853
81. Goldfinger, L.E. *et al.* (2003) Spatial restriction of α4 integrin phosphorylation regulates lamellipodial stability and α4β1-dependent cell migration. *J. Cell Biol.* 162, 731–741
82. Botero, J.P. *et al.* (2020) Glanzmann thrombasthenia: Genetic basis and clinical correlates. *Haematologica* 105, 888–894
83. Wu, Y. *et al.* (2015) The tyrosine kinase c-Src specifically binds to the active integrin αIIbβ3 to initiate outside-in signaling in platelets. *J. Biol. Chem.* 290, 15825–15834
84. Arias-Romero, L.E. (2009) Activation of Src by protein tyrosine phosphatase 1 B is required for ErbB2 transformation of human breast epithelial cells. *Cancer Res.* 69, 4582–4588
85. Shen, C. *et al.* (2020) The 14-3-3ζ-c-Src-integrin-β3 complex is vital for platelet activation. *Blood* 136, 974–988
86. Springer, T.A. *et al.* (1984) Inherited deficiency of the MAC-1, LFA-1, P150,95 glycoprotein family and its molecular basis. *J. Exp. Med.* 160, 1901–1918
87. Porter, K. and Hogg, N. (1997) Integrin cross-talk: Activation of lymphocyte function-associated antigen-1 on human T cells alters α4β1- and α5β1-mediated function. *J. Cell Biol.* 138, 1437–1447
88. Uotila, L.M. *et al.* (2014) Specific phosphorylations transmit signals from leukocyte β2- to β1-integrins and regulate adhesion. *J. Biol. Chem.* 289, 32230–32242
89. Grönholm, M. *et al.* (2016) LFA-1 integrin antibodies inhibit leukocyte α4β1-mediated adhesion by intracellular signaling. *Blood* 128, 1270–1281
90. Homung, A. *et al.* (2020) A bistable mechanism mediated by integrins controls mechanotaxis of leukocytes. *Biophys. J.* 118, 565–577
91. Roy, N.A. *et al.* (2020) LFA-1 signals to promote actin polymerization and upstream migration in T cells. *J. Cell Sci.* 133, jcs248328
92. Kim, S.H.J. and Hammer, D.A. (2019) Integrin crosstalk allows CD4+ T lymphocytes to continue migrating in the upstream direction after flow. *Integr. Biol.* 11, 384–393
93. Hikmet, F. *et al.* (2020) The protein expression profile of ACE2 in human tissues. *Mol. Syst. Biol.* 16, e9610
94. Cantuti-Castelvetri, L. *et al.* (2020) Neuropilin-1 facilitates SARS-CoV-2 cell entry and provides a possible pathway into the central nervous system. *Science* 370, 856–860
95. Stewart, P.L and Nemerow, G.R. (2007) Cell integrins: Commonly used receptors for diverse viral pathogens. *Trends Microbiol.* 15, 500–507
96. Makowski, L. *et al.* (2021) Biological and clinical consequences of integrin binding via a rogue RGD motif in the SARS CoV-2 spike protein. *Viruses* 13, 146
97. Calver, J. *et al.* (2021) The novel coronavirus SARS-CoV-2 binds RGD integrins and upregulates avb3 integrins in Covid-19 infected lungs. *Thorax* 76, S31
98. Park, E.J. *et al.* (2021) The spike glycoprotein of SARS-CoV-2 binds to β1 integrins expressed on the surface of lung epithelial cells. *Viruses* 13, 645
99. Bromley, S.K. *et al.* (2001) The immunological synapse. *Annu. Rev. Immunol.* 19, 375–396
100. Moreno-Layseca, P. *et al.* (2019) Integrin trafficking in cells and tissues. *Nat. Cell Biol.* 21, 122–132
101. Vlahakis, A. and Debnath, J. (2017) The interconnections between autophagy and integrin-mediated cell adhesion. *J. Mol. Biol.* 429, 515–530

Carl_G_190x270_mm_blokki_FINAL.indd 478 06-Aug-23 1:55:09 PM

Carl_G_190x270_mm_blokki_FINAL.indd 479 06-Aug-23 1:55:09 PM

Carl_G_190x270_mm_blokki_FINAL.indd 480 06-Aug-23 1:55:09 PM

Part VI

ADDITIONAL INTERACTIONS OF LEUKOCYTE INTEGRINS

Carl_G_190x270_mm_blokki_FINAL.indd 481 06-Aug-23 1:55:09 PM

Introduction

The interactions of leukocyte integrins with ICAMs are of pivotal importance for cell adhesion, but in addition, the integrins participate in forming other molecular complexes. Many such complexes are functionally and structurally important. Much of our work here is in collaboration with other research groups.

Comments on Papers 53 to 55

It has become increasingly evident that matrix metalloproteases (MMP) interact with integrins, and therefore the use of MMP inhibitors could be important in inhibition of tumour growth and metastatic dissemination. In collaboration with several groups, we showed that the peptides containing the HWGF sequence are potent inhibitors of MMP-2 and MMP-9 (Paper 53). The peptides inhibited the migration of endothelial cells and tumour cells. The peptides also inhibited tumour cell growth and survival in animal models. Using the Mac-1 I domain as bait, we identified the (D/E)(D/E)(G/L)W motif as and a potent inhibitor of Mac-1 and LFA-1 (1). We showed that the purified integrins bound to the MMP-2 and MMP-9 progelatinases and that the negatively charged sequences in the catalytic domains of the proteases form β2 integrin binding sites. Further studies showed that a complex of Mac-1 and the MMP-9 progelatinase localized to intracellular granules in resting neutrophils, but upon cellular activation, the complex was translocated to the cell surface. A DDGW containing peptide inhibited neutrophil migration (2).

In collaboration with Dutch scientists, we found that the LDL-receptor-related protein (LRP) associated with β2 integrins at the cell surface. LRP bound to Mac-1 and to the I domains of the Mac-1 and LFA-1 integrins with rather high affinity. Interestingly, absence of LRP abrogated β2 integrin-dependent adhesion to endothelial cells (3). This interaction could be especially important for the function of monocytes and macrophages in atherosclerotic plaques.

As noted above some peptides may activate integrins. In the presence of an RGD containing peptide, we looked for additional αIIbβ3 integrin recognition sequences. A peptide mimetic of von Willebrand factor, VPW, turned out to be an efficient activator of αIIbβ3. The VPW peptide activated the Syk tyrosine kinase. In a von Willebrand factor deficient individual, VPW addition increased the binding of platelets to fibrinogen (4). The P-selectin glycoprotein ligand 1 on neutrophils interacted with von Willebrand factor, and the binding was increased by treatment of the cells with phorbol esters. In addition to the I domains of Mac-1 and LFA-1, the I domain of αX also bound to the von Willebrand factor. Thus, the factor can function as an adhesive protein layer for different blood cells (5).

Carl_G_190x270_mm_blokki_FINAL.indd 482 06-Aug-23 1:55:09 PM

High-mobility group box 1 (HMGB1) (amphoterin) mediates inflammatory events. We were involved in studying the mechanism how the nuclear protein acts. HMGB1 promoted neutrophil recruitment, which was Mac-1 dependent. The recruitment was prevented in mice lacking Mac-1, but not in those lacking LFA-1. The neutrophils needed the presence of the receptor for advanced glycation end products (RAGE). HMGB1 activated the interaction between Mac-1 and RAGE. This is an additional example of how leukocyte integrins are involved in complex interactions between leukocytes and surrounding tissues (Paper 54).

Chemokines are important activators of integrin dependable blood cell adhesion and migration, and are stored on vascular endothelial cells. These are important in activation of leukocyte integrins under a variety of conditions. However, it turned out that effector lymphocytes of the type 1 helper T cell and type 1 cytotoxic T cell expressed integrins that bypassed chemokine signals. The transendothelial migration of these cells was promoted by chemokines, which were stored in endothelial intracellular granules. The chemokines were released within tight endothelial-lymphocyte synapses (Paper 55). Thus, integrins utilize locally secreted chemokines either in the blood stream or later during extravascular migration.

References

1. Stefanidakis, M., Björklund, M., Ihanus, E., Gahmberg, C.G. and Koivunen, E. (2003) Identification of a negatively charged peptide motif within the catalytic domain of progelatinases that mediates binding to leukocyte β2 integrins. *J. Biol. Chem*. **278**, 34674-34684.
2. Stefanidakis, M., Ruohtula, T., Borregaard, N., Gahmberg, C.G. and Koivunen, E. (2000) Intracellular and cell surface localization of a complex between αMβ2 integrin and promatrix metalloproteinase-9 progelatinase in neutrophils. *J. Immunol*. **172**, 7060-7068.
3. Spijkers, P.P.E.M., da Costa Martins, P., Westein, E., Gahmberg, C.G., Zwaginga, J.J. and Lenting, P.J. (2005) LDL-receptor-related protein regulates β2 integrin-mediated leukocyte adhesion. *Blood* **105**, 170-177.
4. Litjens, P.E.M.H., van Willigen, G., Weeterings, C., Ijsseldijk, M.J.W., van Lier, M., Koivunen, E., Gahmberg, C.G. and Akkerman, J.W.N. (2005) A tripeptide mimetic of von Willebrand factor residues 981-983 enhances platelet adhesion to fibrinogen by signaling through integrin αIIbβ3. *J. Thromb. Haemost*. **3**, 1274-1283.
5. Pendu, R., Terraube, V., Christophe, O.D., Gahmberg, C.G., de Groot, P.G., Lenting, P.J. and Denis, C.V. (2006) P-selectin glycoprotein ligand 1 and β2-integrins cooperate in the adhesion of leukocytes to von Willebrand factor. *Blood* **108**, 3746-3752.

Carl_G_190x270_mm_blokki_FINAL.indd 483 06-Aug-23 1:55:09 PM

© 1999 Nature America Inc. • http://biotech.nature.com

RESEARCH

Tumor targeting with a selective gelatinase inhibitor

Erkki Koivunen[1]*, Wadih Arap[2], Heli Valtanen[1], Aija Rainisalo[1],Oula Penate Medina[1], Pia Heikkilä[3], Carmela Kantor[1], Carl G. Gahmberg[1], Tuula Salo[4], Yrjö T. Konttinen[5], Timo Sorsa[3], Erkki Ruoslahti[2], and Renata Pasqualini[2]*

Department of Biosciences, Division of Biochemistry, Viikinkaari 5, University of Helsinki, FIN-00014, Finland. [2]The Burnham Institute, 10901 North Torrey Pines Rd., La Jolla, CA 92037. [3]Department of Periodontology, University of Helsinki, FIN-00014, Finland. [4]Department of Diagnostics and Oral Medicine, University of Oulu, FIN-90401, Finland. [5]Department of Anatomy, University of Helsinki, FIN-00014, Finland
**Corresponding authors (e-mail: erkki.koivunen@helsinki.fi* and *pasqualini@burnham-inst.org)).*

Received 5 April 1999; accepted 28 May 1999

Several lines of evidence suggest that tumor growth, angiogenesis, and metastasis are dependent on matrix metalloproteinase (MMP) activity. However, the lack of inhibitors specific for the type IV collagenase/gelatinase family of MMPs has thus far prevented the selective targeting of MMP-2 (gelatinase A) and MMP-9 (gelatinase B) for therapeutic intervention in cancer. Here, we describe the isolation of specific gelatinase inhibitors from phage display peptide libraries. We show that cyclic peptides containing the sequence HWGF are potent and selective inhibitors of MMP-2 and MMP-9 but not of several other MMP family members. Our prototype synthetic peptide, CTTHWGFTLC, inhibits the migration of human endothelial cells and tumor cells. Moreover, it prevents tumor growth and invasion in animal models and improves survival of mice bearing human tumors. Finally, we show that CTTHWGFTLC–displaying phage specifically target angiogenic blood vessels in vivo. Selective gelatinase inhibitors may prove useful in tumor targeting and anticancer therapies.

Keywords: phage display, matrix metalloproteinase, tumor targeting, angiogenesis, cancer therapy

Matrix metalloproteinases (MMPs) are a family of enzymes capable of degrading the constituents of the extracellular matrix and the basement membrane. This protein family includes collagenases, gelatinases, stromelysins, and membrane-type MMPs (MT-MMPs). MMPs play major roles in tissue remodeling and cell migration during morphogenesis and wound healing[1]. In cancer, MMP levels can be abnormally elevated, possibly enabling tumor cells to invade the extracellular matrix and generate metastases at sites distant from the primary tumor[2]. Indeed, high MMP levels are associated with poor prognosis in cancer patients[3].

The two MMPs most closely correlated with metastatic potential are the 72 kDa MMP-2 (gelatinase A) and the 92 kDa MMP-9 (gelatinase B). Both degrade denatured collagens and type IV collagen present in the basement membrane and are therefore designated type IV collagenases/gelatinases[4]. Metastatic tumor cell lines express higher levels of gelatinases than nonmetastatic counterparts[5,6]. Gelatinases are also produced by nonmalignant cells present in a tumor, such as mesenchymal cells[7,8] and tumor-infiltrating macrophages[9,10]; gelatinases produced by endothelial cells play a role in angiogenesis[11–13]. The growth of a solid tumor is largely dependent on nutrients provided by the vasculature recruited by the tumor through angiogenesis. The formation of new capillaries by endothelial cells requires migration of endothelial cells and extensive remodeling of the tissue, a process that requires gelatinases and other proteinases[11–14]. In animal models, generic MMP inhibitors prevent tumor dissemination and formation of metastases[15–19]. Antiangiogenic properties of gelatinase inhibitors may contribute to this outcome.

Because gelatinases and other MMPs are potential targets for therapeutic intervention in cancer, there has been much interest in developing synthetic MMP inhibitors. MMPs are generally inhibited by compounds containing reactive zinc-chelating groups, such as thiol or hydroxamate[20,21]. Despite extensive research, no inhibitors specific for the gelatinases have been described to date; the most potent gelatinase inhibitors also inhibit several other MMP family members[20–22].

Here, we use libraries of random peptides to isolate selective gelatinase inhibitors. We describe a novel class of cyclic peptides containing an HWGF motif that are specific inhibitors of MMP-2 and MMP-9. We show that (1) the cyclic decapeptide CTTHWGFTLC specifically inhibits the activities of these enzymes, (2) suppresses migration of both tumor cells and endothelial cells in vitro, (3) homes to tumor vasculature in vivo, and (4) prevents the growth and invasion of tumors in mice. These data indicate that CTTHWGFTLC peptide and, possibly, HWGF–derived peptidomimetics have potential as anticancer agents.

Results

Isolation of cyclic peptides binding to MMP-9. We selected potential peptide inhibitors of chemically activated MMP-9 from a collection of cyclic, degenerate $CX_{5-8}C$ peptides displayed on filamentous phage. Pronounced enrichment in phage binding to MMP-9 in relation to bovine serum albumin (BSA; control protein) was detected (50-fold in the second and 200-fold in the third round of panning). Sequencing of the peptide insert in selected phage revealed three classes of MMP-9 binding motifs: CLRSGXGC, CXXHWGFXXC, and CXPXC.

Most of the clones selected and analyzed by sequencing consisted of a highly conserved CLRSGXGC motif, in which X was preferentially a basic residue such as arginine, lysine, or histidine (Table 1). The most frequent sequence was CLRSGRGC, which has been previously identified as an echovirus 22-binding motif[23]. Surprisingly, the

Carl_G_190x270_mm_blokki_FINAL.indd 484 06-Aug-23 1:55:09 PM

© 1999 Nature America Inc. • http://biotech.nature.com

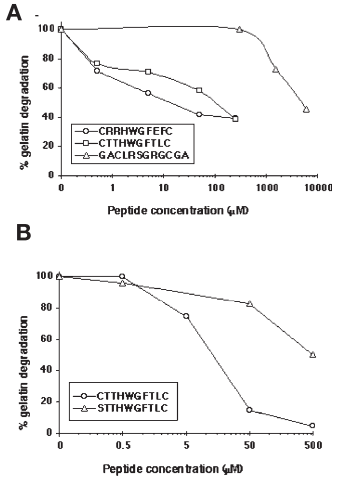

Figure 1. Inhibition of [^{125}I]-gelatin degradation by peptides derived from phage display libraries. APMA-activated MMP-9 (A) or MMP-2 (B) were preincubated with synthetic peptides at the concentrations indicated for 1 h before adding [^{125}I]-gelatin substrate. After gelatinolysis for 1 h, the counts released into the supernatant were determined. The results are means from duplicate measurements.

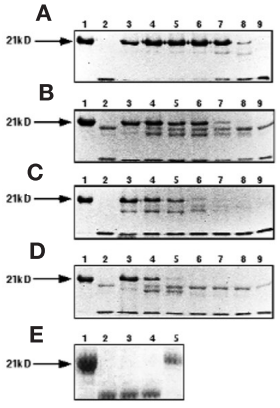

Figure 2. CTTHWGFTLC and CRRHWGFEFC peptides inhibit MMP-2 but not MT1-MMP. After a 1 h pretreatment with the peptides, APMA-activated MMPs were incubated with casein for 2 h. Shown are the Coomassie brilliant blue-staining of the 21 kDa β-casein protein (lane 1) and its fragments (lanes 2–9) resolved by SDS-PAGE. MMPs are shown as follows: (A) and (C), MMP-2; (B) and (D), proMMP-2; and (E), MT1-MMP. In (A) and (B), the CTTHWGFTLC peptide was used at 0, 75, 50, 25, 10, 5, 1, and 0.5 μM (lanes 2–9); in (C) and (D), the CRRHWGFEFC peptide was used at 0, 250, 100, 50, 25, 10, 1, and 0.5 μM (lanes 2–9); in (E), the concentration of the CTTHWGFTLC peptide was 0, 100, and 200 μM (lanes 2–4). The concentration of clodronate was 100 μM (lane 5).

sequence LRSGRG is also found in the hemopexin terminal domain of MMP-9 itself, which has been shown to be important for the ability of the protein to dimerize[24]. Given that we have now independently isolated the motif CLRSGXGC by panning on purified MMP-9, these results suggest that the LRSGRG sequence could be involved in the dimerization of the enzyme and that echovirus 22 may bind MMP-9 through the dimer interface[23].

In addition, three MMP-9–binding peptides were derived from the CX_9 library, which was designed to express an unpaired cysteine residue. Each of these peptides contained a second cysteine and occurred as a cyclic motif CXXHWGFXXC. To induce further constraints on peptide conformation, we designed a library that presents random tetrapeptides (and thus also HWGF) containing four cysteine residues (general structure: $CX_3CX_4CX_2C$). The bicyclic peptides in this library have three potential alternatives for the arrangement of the disulfide bonds, not including a possible disulfide bond with cysteines of the host phage pIII protein. Panning of this library on MMP-9 yielded YGF, WGF, and FGF motifs, which are similar to the HWGF consensus.

We also constructed and screened a related bicyclic $CX_3CX_3CX_3C$ library, where the cysteines were separated from one another by a tripeptide. The sequences that bound to MMP-9 from this library did not show a clear consensus except that a proline residue was present at the central position of the peptide. The common structure was $CX_3CXPXCX_3C$.

HWGF-containing cyclic peptides are specific inhibitors of MMP-2 and MMP-9. We synthesized cyclic peptides corresponding to the frequently observed motifs and tested the metalloproteinase inhibitory activity of the peptides. Two peptides containing the HWGF motif, CRRHWGFEFC and CTTHWGFTLC, were potent inhibitors of MMP-9. In a [^{125}I]-gelatin degradation assay, CRRHWGFEFC was more active than CTTHWGFTLC and inhibited aminophenyl mercuric acetate (APMA)-activated MMP-9 with an IC_{50} of 10 μM (Fig. 1A). GACLRSGRGCGA, which contains the LRSGXG motif, was 1,000-fold less active than the HWGF–containing peptides and only inhibited MMP-9 at concentrations >1 mM. We also synthesized the CIPMCIPDCISWC peptide selected from the $CX_3CX_3CX_3$ library, but this peptide lacked any inhibitory activity (data not shown). Interestingly, the peptides

Table 1. Phage sequences bound to MMP-9.

CX_6C	CX_9	$CX_3CX_4CX_2C$	$CX_3CX_3CX_3C$
CLRSGRGC (10)	CRRHWGFEFC	CQAWCMYGFCGDC (17)	CISMCIPDCISWC (9)
CLRSGRGC (4)	CTTHWGFTLC	CVGVCTYGFCIEC (3)	CLALCTPDCWWYC
CLRSGRGC (2)	CSLHWGFWWC	CRPVCLWGFCITC (3)	CVWLCGPDCWQYC
CLRSGRGC (2)		CDSVCRWGFCLFC (2)	CFWLCAPMCSLVC
CLRSGRGC		CSDICVWGFCVEC (2)	CFWQCAPMCSLVC
CLRSGRGC		CDSFCVYGFCYEC	CVQMCMPACFHLC
CLRSGKGC (5)		CATFCRFGFCYSC	CWVACTPACFLIC
CLRNGKGC			CYNLCSPSCWEYC
CLRSGHGC (3)			CFSWCSPSCWSVC
CLRSGTGC			CYIACLPGCVMLC
CLRSGLGC			

Phage libraries from which the sequences are derived are indicated above (C, cysteine; X, any amino acid).
Amino acid residues that are characteristic for each binding motif are shown in bold.
The number of isolated nucleotide sequences encoding each peptide is indicated in parenthesis.

Carl_G_190x270_mm_blokki_FINAL.indd 485 06-Aug-23 1:55:10 PM

© 1999 Nature America Inc. • http://biotech.nature.com

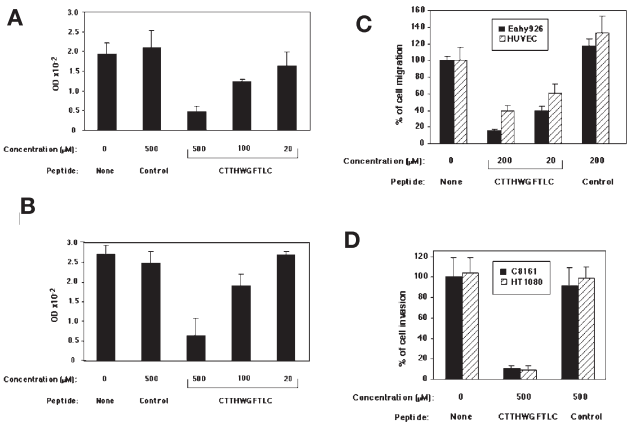

Figure 3. Inhibition of cell migration by the gelatinase inhibitor CTTHWGFTLC. Cells were plated on Transwell or Matrigel filters in the presence or absence of the CTTHWGFTLC or control (CRAVRALWRC) peptides as indicated, and allowed to migrate for 16–24 h. Transwell migration is shown for the following cell lines: (A) HT1080 (t test, p = 0.002); (B) C8161 (t test, p = 0.003); (C) Eahy926 and HUVEC (t test, p = 0.002). In (D), Matrigel invasion is shown for HT1080 and C8161 (t test, p = 0.002). Cells that traversed to the underside of the filter were stained. In (A) and (B), the filter area was scanned; in (C) and (D), the cells were counted microscopically. In each case, data represent mean ± standard deviation; n = 3.

selected by panning on MMP-9 also strongly inhibited the closely related gelatinase MMP-2. In the gelatin degradation assay, CTTHWGFTLC inhibited MMP-2 with an IC_{50} of 10 μM (Fig. 1B). The GACLRSGRGCGA peptide was a poor inhibitor of MMP-2 and only partially inhibited at 1 mM (data not shown). It appears that CRRHWGFEFC preferentially inhibited the activity of MMP-9 relative to the activity of MMP-2 whereas the CTTHWGFTLC peptide preferentially inhibited the activity of MMP-2 relative to the activity of MMP-9 (Fig. 1). Because the CRRHWGFEFC peptide tends to precipitate, we chose to proceed with the soluble CTTHWGFTLC peptide for in vitro and in vivo studies.

To determine whether the cyclic disulfide-bonded structure of CTTHWGFTLC is important for its inhibitory activity, we synthesized a linear version of the peptide, where the cysteine residues were replaced by serine residues. The resulting peptide, STTHWGFTLS, has a 10-fold lower activity compared with the cyclic peptide (Fig. 1B). Loss of inhibitory activity was also observed when the cysteine residues of the CRRHWGFEFC peptide were chemically reduced and alkylated (data not shown).

To show that the inhibitory effect of the peptides on MMP-2 and MMP-9 is not restricted to any particular substrate used, we analyzed casein degradation by SDS gel electrophoresis. The two HWGF–containing peptides were equally effective in preventing degradation of casein and gelatin. For MMP-2, the CTTHWGFTLC and CRRHWGFEFC peptides had IC_{50} values of 5 μM and 25 μM, respectively (Figs. 2A–D). Caseinolysis by MMP-9 was similarly inhibited by the peptides at low micromolar concentrations except that CRRHWGFEFC was a slightly more potent inhibitor of MMP-9 than CTTHWGFTLC (data not shown). The potency of these peptides was not dependent on the chemical activation of MMP-2 and MMP-9 by APMA. Thus, the peptides blocked untreated proMMP, which normally autoactivates when incubated with casein or gelatin (Fig. 2B and D).

We next studied whether the CTTHWGFTLC. peptide inhibits other members of the MMP family or other classes of proteinases. In concentrations up to 500 μM, the CTTHWGFTLC peptide showed no effect on membrane type I matrix metalloproteinase (MT1-MMP) (Fig. 2E and data not shown). Moreover, MMP-8 and MMP-13 were not inhibited at CTTHGFTLC peptide concentrations of 50, 150, and 500 μM (data not shown). The general MMP antagonists clodronate and chemically modified tetracyline-8 (CMT-8) used as controls nearly completely inhibited all of the MMPs studied. At 500 μM, CTTHWGFTLC did not block peptidolytic activity of several serine proteinases such as trypsin-2, several human serine proteinases such as trypsin-2, neutrophil elastase, or cathepsin G (data not shown).

Inhibition of cell migration by CTTHWGFTLC. The cyclic CTTHWGFTLC peptide inhibited the migration of various cell lines in vitro. In a Transwell assay, which measures random cell migration, the peptide prevented the motility of HT1080 fibrosarcoma cells in a dose-dependent manner. Over 80% inhibition was observed at a peptide concentration of 500 μM. Three unrelated control peptides (CQWNNDNPLFKEAEEEVMNPKFAES, CRAVRALWRC, and EVGTGSCNLECVSTNPLSGTEQ) had no effect on cell migration at a concentration of 500 μM (Fig. 3A). The linear STTHWGFTLS peptide was also ineffective at 500 μM in the migration assay (data not shown). CTTHWGFTLC was not toxic to the cells, as cell viability did not decrease even when the cells were cultured as long as two days in the presence of peptide. Initial attachment and spreading of the cells on fibronectin, collagen type IV, or Matrigel substrata were not affected by the peptide.

CTTHWGFTLC also blocked random migration of other tumor cells studied, including C8161 melanoma, SKOV-3 ovarian carcinoma, and KS1767 Kaposi's sarcoma cell lines. Figure 3B shows the results obtained using C8161 cells. The maximal inhibition (80%) was seen at a peptide concentration of 500 μM. The control peptides did not affect cell migration.

We next studied the effect of CTTHWGFTLC on random migration of human endothelial cells in the Transwell assay (Fig. 3C). At a concentration of 200 μM, the peptide inhibited 85% of human Eahy926 and 60% of human umbilical vein endothelial cell (HUVEC) migration. Partial inhibition was observed at peptide concentrations as low as 20 μM. The CRAVRALWRC peptide did not affect endothelial cell migration. The CTTHWGFTLC peptide also appears to inhibit mouse gelatinases because it can partially block the migration of mouse endothelial cells in vitro. However, preliminary results suggest that CTTHWGFTLC targets human cells better than mouse cells (data not shown).

Matrigel invasion of HT1080 and C8161 cells was also suppressed by the CTTHWGFTLC peptide. Maximal inhibition was 90% at 500 μM, the highest concentration studied (Fig. 3D). None of the control peptides affected Matrigel invasion. Results were similar for both cell lines.

Prevention of tumorigenesis and inhibition of tumor growth. We next tested whether the CTTHWGFTLC peptide inhibited the establishment and growth of tumors in vivo. Injecting tumor cells preincubated with the peptide delayed formation of MDA-MB-435-derived breast carcinomas, and the tumors that arose were significantly smaller than those in the control group (Fig. 4A).

Then we tested whether the CTTHWGFTLC peptide could prevent growth of established tumors in immunodeficient mice. Doses and schedules used in pilot experiments were as follows: 100 μg daily, 200 μg twice a week, and 50, 100, 200, or 500 μg once a week. Dose dependency was generally observed (data not shown); the dose, schedule, and route of administration for each particular

Carl_G_190x270_mm_blokki_FINAL.indd 486 06-Aug-23 1:55:10 PM

© 1999 Nature America Inc. • http://biotech.nature.com

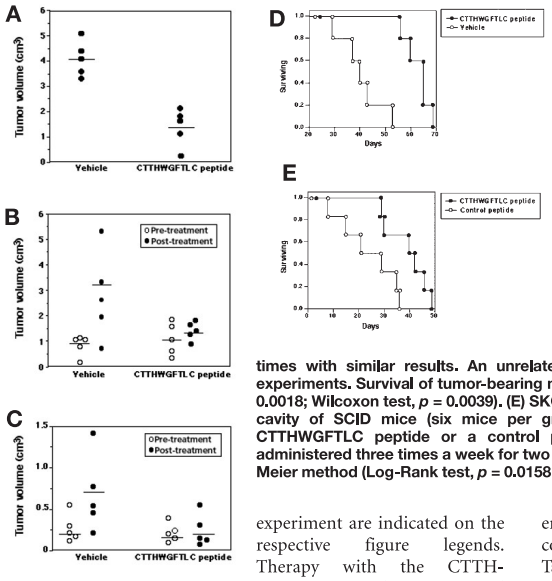

Figure 4. CTTHWGFTLC inhibits tumor growth in mouse models. (A) MDA-MB-435 breast carcinoma cells were preincubated with the . CTTHWGFTLC peptide (100 μg) or vehicle alone (DMEM) and injected subcutaneously (s.c.) into nude mice (five mice per group). Data represent tumor volumes at 5 weeks (t test, $p = 0.002$). (B) MDA-MB-435–derived breast carcinomas were established in the mammary fat pad nude mice (five mice per group). The CTTHWGFTLC peptide or a control peptide (GACFSIAHECGA) were injected into the subcutaneous tissue adjacent to the tumor. Peptides (200 μg per mouse) were administered three times a week for three weeks. Data represent the tumor volumes after nine 9 treatments (t test, $p < 0.05$). (C) Mice bearing established KS1767-derived Kaposi's sarcomas (five mice per group) were treated with the CTTHWGFTLC peptide or a control peptide (GACFSIAHECEA) injected intraperitoneally (i.p.). Peptides (100 μg/mouse) were administered three times a week for four weeks. Data represent the tumor volumes after 12 treatments (t test, $p < 0.05$). (D) SKOV-3 ovarian carcinoma cells were preincubated with the CTTHWGFTLC peptide (200 μg) or vehicle alone (DMEM) and administered i.p. into SCID mice (five mice per group). The experiment was repeated four times with similar results. An unrelated peptide (CVRLNSLAC) was used as a control in two of the experiments. Survival of tumor-bearing mice was analyzed by the Kaplan-Meier method (Log-Rank test, $p = 0.0018$; Wilcoxon test, $p = 0.0039$). (E) SKOV-3–derived ovarian carcinomas were established in the peritoneal cavity of SCID mice (six mice per group). After 24 h, mice were treated intraperitoneally with the CTTHWGFTLC peptide or a control peptide (GACFSIAHECGA). Peptides (200 μg per mouse) were administered three times a week for two weeks. Survival of tumor-bearing mice was analyzed by the Kaplan-Meier method (Log-Rank test, $p = 0.0158$; Wilcoxon test, $p = 0.0242$).

experiment are indicated on the respective figure legends. Therapy with the CTTHWGFTLC peptide was initiated on established tumors in nude mice. The tumors ranged in volumes from 200 to 1,000 mm^3. In the MDA-MB-435 breast carcinoma model, the CTTHWGFTLC peptide or a control peptide (GACFSIAHECGA) were injected into the subcutaneous (s.c.) tissue adjacent to the tumor. The volumes of tumors treated with CTTHWGFTLC remained stable, whereas the tumors treated with the control peptide progressed, reaching up to five times the initial volume at the end of the experiment (Fig. 4B). The CTTHWGFTLC peptide also delayed tumor growth when administered intraperitoneally; KS1767-derived Kaposi's sarcomas grew more slowly in mice treated with intraperitoneal (i.p.) injections of CTTHWGFTLC peptide than the control mice treated with the vehicle alone (Fig. 4C). In addition, establishment and growth of SKOV-3–derived ovarian carcinomas were also inhibited when the CTTHWGFTLC peptide was coinjected with the cells into the peritoneal cavity of severe combined immune-deficient (SCID) mice. These mice often had less tumor-associated ascites, which generally correlated with survival (data not shown). CTTHWGFTLC increased the survival of the mice bearing SKOV-3 tumors as compared with the control group, which received a control cyclic peptide (Fig. 4D). Similarly, the survival of SCID mice bearing i.p. SKOV-3 tumors also improved upon treatment with CTTHWGFTLC (Fig. 4E). In two independent experiments, four (67%) of six and three (60%) of five of the peptide-treated mice were alive at the time all the control mice had died from their tumor burden.

Targeting of CTTHWGFTLC phage into tumors. Because the CTTHWGFTLC peptide inhibited endothelial cell migration, and gelatinases are known to be overexpressed in angiogenic vasculature[11,25], we reasoned that the antitumor activity of CTTHWGFTLC could be partially due to its binding and inhibition of gelatinases in the tumor vasculature. Phage that express peptides capable of binding to endothelial receptors in angiogenic vasculature home to tumors[26,27]. Therefore, we examined the tumor-homing ability of the phage displaying CTTHWGFTLC following intravenous (i.v.) injection into mice (Fig. 5). After perfusion, an average of 10-fold more of the CTTHWGFTLC phage accumulated in the tumors compared with controls (insertless phage or unselected phage library). Also, an average of 10-fold more of the CTTHWGFTLC phage were recovered from tumor tissue than from brain tissue, which served as a control tissue containing abundant normal vasculature (Fig. 5A). Taking into account these differences, and also the lower background of the CTTHWGFTLC phage in the normal organs, the overall tumor selectivity of the CTTHWGFTLC phage is estimated to be at least 40-fold or higher. Moreover, the homing of the CTTHWGPTLC phage into the tumors was specific, as it could be substantially inhibited upon coinjection of the cognate peptide (CTTHWGFTLC); coinjection of an unrelated cyclic peptide (CARAC) had no appreciable effect (Fig. 5B). No difference in bacterial infectivity between CTTHWGFTLC phage and insertless control phage was detected (data not shown).

To further show specificity, we have performed additional experiments in which phage with no insert and a different selectable marker (ampicillin instead of tetracycline) are coinjected with the CTTHWGFTLC phage and serve as an internal control in the homing experiments. The results showed that over 10-fold more CTTHWGFTLC phage than ampicillin phage accumulated in the tumor. In contrast, slightly more ampicillin phage than the CTTHWGFTLC phage were recovered from several control organs tested including brain, kidney, and pancreas. An RGD-4C phage was included as a positive tumor-targeting control[26,27]. The tumor homing of CTTHWGFTLC phage was 1.6-fold more selective than that of RGD-4C phage, at least in this system (Fig. 5C).

Discussion

The data presented here support the concept that gelatinase activity is important for migration of both the tumor and endothelial cells. The CTTHWGFTLC peptide inhibited the in vitro migration of all five human tumor cell lines and both endothelial cell lines studied. In mouse models, the peptide showed potent antitumor activity, prevented invasive growth of three different human tumor xenografts, and increased the survival of tumor-bearing animals. The CTTHWGFTLC peptide did not produce any apparent toxicity in either of the mouse models used in this study. Nonspecific MMP inhibitors affect several members of the MMP family, causing side effects during antitumor therapy[22,28] because of disruption of numerous physiological processes[1,4,29]. In contrast, CTTHWGFTLC inhibited only gelatinases and had minimal or no effect on the MMP family members MMP-8, MMP-13, and MT1-MMP, or on serine proteinases trypsin-2 (ref. 30), elastase, and cathepsin G (ref. 31), which can activate proMMPs. Specific inhibition of proMMP-2 and

Carl_G_190x270_mm_blokki_FINAL.indd 487 06-Aug-23 1:55:11 PM

© 1999 Nature America Inc. • http://biotech.nature.com

proMMP-9 by CTTHWGFTLC has also been observed by gelatin zymography (O.P.M. et al., unpublished data).

The CTTHWGFTLC peptide and the other HWGF–containing peptides isolated in this study lack the typical gelatinase substrate sequence leucine-glycine[4]. Thus, although the inhibitory mechanism of the CTTHWGFTLC peptide is still unclear, it is tempting to speculate that the tryptophan residue in the HWGF motif may bind to the hydrophobic pocket of the substrate cleft in the enzyme[32] and that the histidine residue may act as a ligand for the catalytic zinc ion. Interestingly, histidine-containing tetrapeptide inhibitors of gelatinases have been isolated by a combinatorial library approach[33], and it is possible that the HWGF motif functions analogously to the histidine-containing peptidomimetics. However, full understanding of the inhibitory biochemical mechanism awaits the elucidation of the x-ray crystal structures of MMP-2 or MMP-9/CTTHWGFTLC peptide complexes.

One use for phage peptide libraries has been to search for optimal substrate sequences for proteases[34–36]. However, in contrast to the strategy used here, that method favors the isolation of substrates rather than inhibitors[34]. Peptides that bind to chymotrypsin and trypsin recently have been recovered from random phage-displayed libraries, but the isolated peptides also contained identifiable protease substrate sequences[37,38]. The cyclic conformation is critical for the activity of the CTTHWGFTLC peptide, and libraries that express cyclic peptides may be particularly well suited for identifying peptide inhibitors for metalloproteinases.

Inhibitors of MMPs can reduce the invasiveness and migratory capacity of tumor cells[15–22,39,40]. However, the identification of MMPs that are important for cell migration has been difficult because of the lack of specific inhibitors for the individual members of the MMP family. MMP-2 and MMP-9 are expressed in tumors, and both have been associated with tumor cell invasiveness and lung metastases in mouse models[15–19,39]. In particular, MMP-9 appears to be important for invasion of the blood vessel wall (intravasation), as only cells expressing MMP-9 were able to intravasate in a chicken model[40]. Our experiments with peptides possessing specific gelatinase-inhibitory activities suggest that MMP-2, MMP-9, or perhaps both play a key role in tumor and endothelial cell migration. Of course, we cannot entirely rule out the possibility that targets other than gelatinases might exist in vivo.

In addition to its effects on cell migration, the antitumor activity of CTTHWGFTLC is also likely to depend on its ability to inhibit angiogenesis in tumors. Tumors must recruit blood vessels to support their progressive growth, and it has been shown that inhibitors of MMPs can inhibit angiogenesis[15–22]. Tumor angiogenesis is reduced in mice where the gene for MMP-2 has been deleted[41]. Moreover, the corresponding deficiency of MMP-9 in mice results in a vascularization disorder of the skeletal growth plate[13]. Although the precise molecular role of MMP-9 in tumor angiogenesis is not yet known, it has been proposed that a complex between MMP-2 and the αvβ3 integrin mediates migration of endothelial cells and invasivity of tumor cell lines[11,25].

It should be noted that the CTTHWGFTLC–displaying phage has at least a comparable tumor-homing specificity to phage displaying a peptide ligand to αv integrins[26,27] (Fig. 5C). This pronounced ability of the CTTHWGFTLC–displaying phage to home into tumors shows that gelatinases are not only present on the luminal endothelial surface of tumor blood vessels[11] but can also be targeted by circulating ligands[26,27,42]. In fact, the full relevance of proteases as endothelial cell receptors in nonproliferating blood vessels[43] or in proliferating blood vessels (R.P. et al., unpublished data) is now being increasingly realized by techniques such as in vivo phage display[44].

Novel gelatinase inhibitors such as CTTHWGFTLC have two levels of specificity. First, they specifically inhibit MMP-2 and MMP-9; second, they selectively target tumors because these enzymes are overexpressed and accessible for homing in the tumor vasculature. Overall, this resulted in delayed tumor growth and, ultimately, in an increased survival of tumor-bearing mice. The combination of tumor targeting, antiangiogenic, and anti-invasive properties of the CTTHWGFTLC peptide render it a potential lead compound for the development of peptidomimetic anticancer agents. Because it is unlikely that the non-HWGF motif residues (i.e., T2, T3, T8, and L9) are the optimal amino acids, one can expect that reselection of a CX_2HWGFX_2C secondary library on MMP-9 will yield peptides with greater potency. These studies are currently under way.

Experimental protocol

Proteinases. ProMMP-9 was purified from human neutrophils and proMMP-2 from serum-free culture medium of human gingival fibroblasts, followed by activation of the proenzyme forms with APMA as described[30]. MMP-8, elastase, and cathepsin G were purified from a neutrophil lysate[45]. MMP-13 was obtained from Drs. Vera Knauper and Gillian Murphy

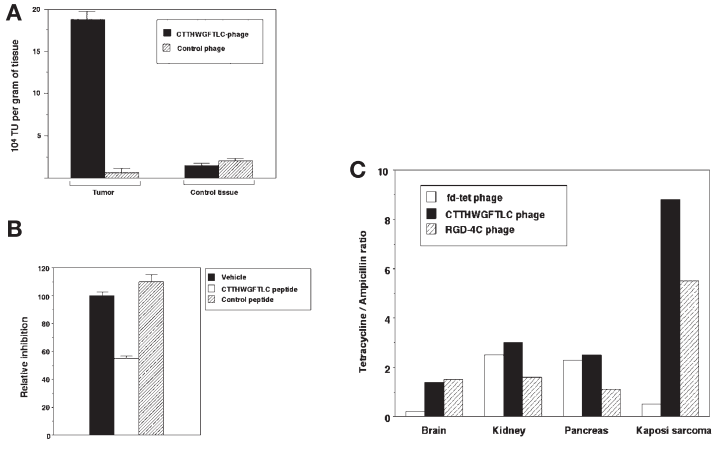

Figure 5. Targeting of CTTHWGFTLC phage into KS1767-derived Kaposi's sarcomas. Phage (10^9 transducing units [TU]) were injected into the tail vein of mice bearing size-matched KS1767-derived tumors (approximately 1,000 mm^3) and recovered after perfusion. (A) Recovery of CTTHWGFTLC phage or insertless phage (negative control) from the tumor or control tissue (brain). Data represent mean ± standard error of the mean (SEM); $n = 3$ (t test, $p = 0.001$). (B) Inhibition of the CTTHWGFTLC phage by the corresponding soluble peptide. CTTHWGFTLC phage (10^8 TU) were coinjected with vehicle alone, 200 μg of the CTTHWGFTLC peptide, or 200 μg of a control cyclic peptide (CARAC). Recovery of CTTHWGFTLC phage was set to 100%. Data represent mean ± SEM; $n = 3$ (t test, $p = 0.002$). (C) Comparison of targeting efficiencies of the CTTHWGFTLC, RGD-4C and insertless phage. Recovery of phage is shown as a ratio of number of colonies on tetracycline versus ampicillin plates. The results show mean values from duplicate platings.

Carl_G_190x270_mm_blokki_FINAL.indd 488 06-Aug-23 1:55:12 PM

© 1999 Nature America Inc. • http://biotech.nature.com

(Strangeways Research Laboratories, Cambridge, UK). MT1-MMP was kindly provided by Dr. Horst Will (InVitro Tek, Berlin, Germany). Trypsin-2 was purified from the conditioned medium of human COLO 205 colon carcinoma cells[46].

Peptide synthesis. Peptides were synthesized on an Applied Biosystems model 433A (Foster City, CA) using Fmoc-chemistry. Oxidation of the disulfide bonds was carried out by mixing the peptides with 20% dimethyl sulfoxide in 5% acetic acid (pH 6.0) overnight at room temperature, after which the peptides were purified by reverse-phase HPLC[47]. The cyclic peptide CARAC was obtained commercially (Anaspec, San Jose, CA). The identity of the peptides was verified by matrix-assisted laser desorption/ionization time-of-flight (MALDI-TOF) mass spectrometry. Each peptide was dissolved at a concentration of 10 mg/ml in H_2O, stored at -20°C, and diluted immediately before use.

Phage display peptide libraries. Preparation of the CX_5C, CX_6C, CX_7C and CX_9 libraries has been described[48]. The $CX_3CX_3CX_3C$ and $CX_5CX_4CX_2C$ libraries were prepared by a slightly modified procedure. Briefly, 20 μg of the synthetic oligonucleotides coding for random amino acids was made double stranded by annealing 40 μg of the primer 5-TTCTGCCCCAGCGGCCCCA-CA-3′ in a volume of 100 μl at 65°C and slowly cooling to room temperature. Primer extension was done by incubating the annealed oligonucleotides with 29 units of Sequenase 2.0 DNA polymerase (Amersham, Arlington Heights, IL) for 60 min at 37°C in a reaction volume of 250 μl containing 10 mM deoxynucleotides and 5 mM dithiothreitol. The double-stranded oligonucleotides were purified using a QIAquick nucleotide removal kit according to the instructions of the manufacturer (QIAGEN, Gmbh, Hilden, Germany) and eluted from each QIAquick column by two 50 μl washes with H_2O. The oligonucleotides were digested with *BglI* for 2 h at 37°C, purified again as above, and ligated into the fUSE5 vector[49]. The plasmids were transfected into MC1061 *Escherichia coli* by 200 individual electroporations, yielding primary libraries containing 5 x 10^7 recombinants.

Selection of MMP-9–binding phage. APMA-activated MMP-9 (100 μg/ml) was coated on microtiter wells overnight at 4°C. Wells were then saturated with 5% BSA. In the first panning, the libraries were incubated overnight at 4°C in 50 mM TBS buffer (Tris-HCl/0.1 M NaCl, pH 7.5) containing 1% BSA. After extensive washing, the bound phage were eluted with a low pH buffer[48,49]. In subsequent pannings, the amplified phage were allowed to bind for 1 h at 22°C. Randomly selected clones were amplified overnight and sequenced using a Sequenase 2.0 kit (Amersham). The binding of each clone to MMP-9 was verified by an attachment assay, in which the cloned phage were incubated for 60 min in MMP-coated or BSA-blocked microtiter wells. The wells were washed five times with TBS containing 0.5% Tween-20. The bound phage were quantified by adding 50 ng/well of anti-M13 antibody (Pharmacia, Uppsala, Sweden) labeled with a Europium-chelate (Wallac, Turku, Finland). After a 45 min incubation and washing, the fluorescence of the chelate was measured with a fluorometer (Model 1230 Arcus, Wallac).

Enzyme inhibition assays. To determine the inhibitory activity of the synthetic peptides, purified MMPs (50–100 ng) were preincubated for 60 min with peptides at concentrations indicated in the text. Clodronate[50] (Leiras-Schering, Turku, Finland) and CMT-8 (ref. 39) (Collagenex, Newtown, PA) served as control MMP inhibitors, both being capable of inhibiting all MMPs studied. The substrates, a 21 kDa β-casein (52 mM) or [^{125}I]-gelatin, were incubated for 1 or 2 h at 22°C. Degradation of casein was analyzed by SDS gel electrophoresis essentially as described[30]. The degradation of [^{125}I]-gelatin was determined by counting radioactivity in the supernatant after precipitation of undegraded gelatin with 20% trichloroacetic acid[30]. To test the effect on serine proteinases, the peptides were preincubated with human trypsin-2, cathepsin G, or leukocyte elastase for 60 min. The activities of the proteinases were then determined using the chromogenic substrate S-2222 (KabiVitrum, Stockholm, Sweden), succinyl-Ala-Ala-Ala-pNA (Sigma, St. Louis, MO) and N-succinyl-Ala-Ala-Pro-Phe-pNA (Sigma) essentially as described[30,45,46].

Cell culture. All cell lines used in this study were of human origin unless otherwise indicated. The SKOV-3 ovarian carcinoma, HT1080 fibrosarcoma, and HUVECs were commercially obtained (American Type Culture Collection, Rockville, MD). The Eahy926 cell line is a HUVEC derivative[51]. KS6717 is a Kaposi's sarcoma–derived cell line that induces angiogenic tumors in animals[52]. The MDA-MB-435 breast carcinoma and C8161 melanoma cell lines were previously described[26,27]. HUVECs were grown in RPMI 1640 medium containing penicillin (100 U/ml), streptomycin (100 μg/ml), 10 mM HEPES, 30 μg/ml endothelial cell growth supplement (Biomedical Technologies, Stoughton, MA), and 20% fetal calf serum (FCS). All other cell lines were cultured in 10% FCS/DMEM containing antibiotics. Cells were harvested with trypsin-EDTA (endothelial cells) or EDTA alone (other cells), washed, and resuspended in complete media.

Cell migration assays. Random cell migration was studied using 8.0 μM pore size and 6.5 mm diameter Transwell filters (Costar, Cambridge, MA). The Transwell filters were equilibrated in serum-containing medium for 2 h before use. Tumor cell invasion was studied using 6.4 mm filters precoated with Matrigel (Becton Dickinson, Bedford, MA) and equilibrated in serum-containing medium. Sum-containing media (750 μl) were added to the lower compartments of the migration filters. For random migration assays, cells were preincubated for 2 h in the presence of peptides at the concentrations indicated in the text, and 2 x 10^4 cells in a volume of 100 μl were plated per Transwell filter. For Matrigel invasion, 10^5 cells were plated per well in a 500 μl volume of serum-containing media in the presence or absence of peptides. Cells were cultured for 16–20 h at 37°C in 5% CO_2, and were then fixed by immersing the filters in methanol for 15 min. Filters were washed once with water, stained in 0.1% toluidene blue for 5 min, and finally washed until cell staining became visible. Cells were removed from the upper surface of the membrane with a cotton swab. Cells migrated on the underside of the membrane were either counted microscopically or quantified by scanning.

Cell viability. To assess the effect of the CTTHWGFTLC peptide on cell viability, 10^5 cells were plated in 24-well plates in 1 ml of medium containing 10% FCS and 500 μM of CTTHWGFTLC or an unrelated control peptide. After culturing for 20 or 40 h, the viability was determined by trypan blue exclusion, or with the MTT reagent according to the instructions of the manufacturer (Sigma). For cell adhesion studies, microtiter wells were coated with fibronectin (Sigma), type IV collagen (Sigma), or Matrigel, followed by blocking with BSA. Cells (10^5 cells/well) were incubated together with 500 μM of CTTHWGFTLC or a control peptide (GRGESP) in serum-free medium for 1 h. After washing twice with phosphate-buffered saline, the bound cells were stained with crystal violet (Sigma).

Treatment of mice bearing human tumor xenografts with CTTHWGFTLC peptide. All animal studies were approved by the Animal Care and Use Committee of the Burnham Institute (La Jolla, CA). Human tumor xenografts were established in mice by administering 10^6 tumor cells per mouse in a 200 μl volume of serum-free DMEM. KS1767 and MDA-MB-435 cells were injected into the fat mammary pad of athymic, female, nude/nude Balb/c mice (Harlan, Sprague-Dawley, San Diego, CA). SKOV-3 cells were injected into the peritoneal cavity of female SCID/SCID mice (Harlan-Sprague-Dawley).

Three-dimensional caliper measurements were taken weekly and the tumor volumes were calculated[26,27]; in the experiments performed with the i.p. model of ovarian carcinoma SKOV-3 cells, mouse survival was followed. To study the effect of CTTHWGFTLC on tumor implantation, CTTHWGFTLC peptide was premixed with the tumor cells ex vivo, prior to the cell implantation. Alternatively, CTTHWGFTLC or control peptides were administered to established tumors either as a systemic (i.p.) or as a local (s.c.) treatment. Statistical differences in the tumor volumes and in the phage homing to tumors were determined by the Student's t-test; statistical differences in the Kaplan-Meier survival were determined by Log-Rank and Wilcoxon tests.

Tumor targeting of CTTHWGFTLC–displaying phage in vivo. In vivo targeting experiments with phage were performed as described[26,27,44]. Mice bearing KS1767 xenografts were injected intravenously through the tail vein with 10^8 transducing units of the CTTHWGFTLC phage in a 200 μl volume of DMEM in the presence or absence of 200 μg of the CTTHWGFTLC peptide. The phage were allowed to circulate for 3 min, and the animals were perfused through the heart with 5 ml of DMEM. The tumor and brain were dissected from each mouse, weighed, and homogenized. The tissue homogenates were washed three times with ice-cold DMEM containing a proteinase inhibitor cocktail and 0.1% BSA. Bound phage were rescued by mixing the homogenates with 1 ml of concentrated K91kan bacteria for 1 h at room temperature. The mixture was then diluted 1:10 in LB medium and incubated for another 15 min, after which aliquots were plated on agar plates. In other experiments, phage with no insert and a different selectable marker (ampicillin instead of tetracycline) were coinjected at the same input in all animals as an internal control as described[26,27,44].

Acknowledgments

We thank Drs. Guy Salvesen and Jeffrey W. Smith for critical reading of the manuscript, and Dr. Daniel Rajotte and Jason A. Hoffman for helpful suggestions. This work was supported by grant CA74238 (E.R.) and Cancer Center Support grant CA30199 from the National Cancer Institute, grants DAMD17-98-1-8041 (R.P.) and DAMD17-98-1-8164 (W.A.) from the Department of Defense, and grants from the Academy of Finland, Finnish Dental Society, Finnish Cancer Society, and Sigrid Juselius Foundation (E.K. and C.G.G.). W.A. is the recipient of a CaP CURE award.

Carl_G_190x270_mm_blokki_FINAL.indd 489 06-Aug-23 1:55:12 PM

© 1999 Nature America Inc. • http://biotech.nature.com

1. Birkendal-Hansen, H. Proteolytic remodeling of extracellular matrix. *Curr. Opin. Cell Biol.* **7,** 728–735 (1995).
2. Stetler-Stevenson, W.G., Aznavoorian, S. & Liotta, L.A. Tumor cell interactions with the extracellular matrix during invasion and metastasis. *Annu. Rev. Cell Biol.* **9,** 541–573 (1993).
3. Murray, G.I., Duncan, M.E., O'Neil, P., Melvin, W.T. & Fothergill, J.E. Matrix metalloproteinase-1 is associated with poor prognosis in colorectal cancer. *Nat. Med.* **2,** 461–462 (1996).
4. Murphy, G. & Crabbe, T. Gelatinases A and B. *Methods Enzymol.* **248,** 470–484 (1995).
5. Liotta, L.A. *et al*. Metastatic potential correlates with enzyme derived from a metastatic murine tumor. *Nature* **284,** 67–68 (1980).
6. Karakiulakis, G. *et al*. Increased type IV collagen-degrading activity in metastases originating from primary tumors of the human colon. *Invasion & Metastasis* **17,** 158–168 1997.
7. Pyke, C., Ralfkiaer, E., Tryggvason, K. & Dano, K. Messenger RNA for two type IV collagenases is located in stromal cells in human colon cancer. *Am. J. Pathol.* **142,** 359–365 (1993).
8. Sugiura, Y., Shimada, H., Seeger, R.C., Laung, W.E. & DeClerck, Y.A Matrix metalloproteinases-2 and -9 are expressed in human neuroblastoma: contribution of stromal cells to their production and correlation with metastasis. *Cancer Res.* **58,** 2209–2216 (1998).
9. Wilhelm, S.M. *et al*. SV40-transformed human lung fibroblasts secrete a 92 kDa type IV collagenase which is identical to that secreted by normal human macrophages. *J. Biol. Chem.* **264,** 17213–17221 (1989).
10. Heppner, K.J., Matrisian, L.M., Jensen, R.A. & Rodgers, W.H. Expression of most matrix metalloproteinase family members in breast cancer represents a tumor-induced response. *Am. J. Pathol.* **149,** 273–282 (1996).
11. Brooks, P.C. *et al*. Localization of matrix metalloproteinase MMP-2 to the surface of invasive cells by interaction with integrin $\alpha v\beta 3$. *Cell* **85,** 683–693 (1996).
12. Haas, T.L., Davis, S.J. & Madri, J.A. Three-dimensional type I collagen lattices induce coordinate expression of matrix metalloproteinases MT1-MMP and MMP-2 in microvascular endothelial cells. *J. Biol. Chem.* **273,** 3604–3610 (1998).
13. Vu, T.H. *et al*. MMP-9/gelatinase B is a key regulator of growth plate angiogenesis and apoptosis of hypertrophic chondrocytes. *Cell* **93,** 411–422 (1998).
14. Hanahan, D. & Folkman, J. Patterns and emerging mechanisms of the angiogenic switch during tumorigenesis. *Cell* **86,** 353–364 (1996).
15. Davies, B., Brown, P.D., East, N., Crimmin, M.J. & Balkwill, F.R.A synthetic matrix metalloproteinase inhibitor decreases tumor burden and prolongs survival of mice bearing human ovarian carcinoma xenografts. *Cancer Res.* **53,** 2087–2091 (1993).
16. Taraboletti, G. *et al*. Inhibition of angiogenesis and murine hemangioma growth by batimastat, a synthetic inhibitor of matrix metalloproteinases. *J. Natl. Cancer Inst.* **87,** 293–298 (1995).
17. Volpert, O.V. *et al*. Captopril inhibits angiogenesis and slows the growth of experimental tumors in rats. *J. Clin. Invest.* **98,** 671–679 (1996).
18. Anderson, I.C., Shipp, M.A., Docherty, A.J.P. & Teicher, B.A. Combination therapy including a gelatinase inhibitor and a cytotoxic agent reduced local invasion and metastasis of murine Lewis lung carcinoma. *Cancer Res.* **56,** 715–710 (1996).
19. Ecclels, S.A. *et al*. Control of lymphatic and hematogenous metastasis of a rat mammary carcinoma by the matrix metalloproteinase inhibitor batimastat (BB-94). *Cancer Res.* **56,** 2815–2822 (1996).
20. Talbot, D.C. & Brown, P.D. Experimental and clinical studies on the use of matrix metalloproteinase inhibitors for the treatment of cancer. *Eur. J. Cancer* **32,** 2528–2533 (1996).
21. Beckett, R.P., Davidson, A.H., Drummond, A.H., Huxley, P. & Whittaker, M. Recent advances in matrix metalloproteinase inhibitor research. *Drug Design Today* **1,** 16–26 (1996).
22. Santos, O., McDermott, C.D., Daniels, R.G. & Appelt, K. Rodent pharmacokinetic and anti-tumor efficacy studies with a series of synthetic inhibitors of matrix metalloproteinases. *Clin. Exp. Metastasis* **15,** 499–508 (1997).
23. Pulli, T., Koivunen, E. & Hyypia, T. Cell-surface interactions of echovirus 22. *J. Biol. Chem.* **272,** 21176–21180 (1997).
24. Goldberg, G.I., Strongin, A., Collier, I.E., Genrich, L.T. & Marmer, B.L. Interaction of 92-kDa type IV collagenase with the tissue inhibitor of metalloproteinases prevents dimerization, complex formation with interstitial collagenase, and activation of the proenzyme with stromelysin. *J. Biol. Chem.* **267,** 4583–4591 (1992).
25. Brooks, P.C., Silletti, S., von Schalscha, T.L., Friedlander, M. & Cheresh, D.A. Disruption of angiogenesis by PEX, a noncatalytic metalloproteinase fragment with integrin binding activity. *Cell* **92,** 391–400 (1998).
26. Pasqualini, R., Koivunen, E. & Ruoslahti, E. αv integrins as receptors for tumor targeting by circulating ligands. *Nat. Biotechnol.* **245,** 346–369 (1997).
27. Arap, W., Pasqualini, R. & Ruoslahti, E. Cancer treatment by targeted drug delivery to tumor vasculature in a mouse model. *Science* **279,** 377–380 (1998).
28. Wojtowicz-Praga, S. *et al*. Phase I trial of Marimastat, a novel matrix metalloproteinase inhibitor, administered orally to patients with advanced lung cancer. *J. Clin. Oncol.* **16,** 2150–2156 (1998).
29. Goetzl, E.J., Banda, M.J. & Leppert, D. Matrix metalloproteinases in immunity. *J. Immunol.* **156,** 1–4 (1996).
30. Sorsa, T. *et al*. Activation of type IV procollagenases by human tumor-associated trypsin-2. *J. Biol. Chem.* **272,** 21067–21074 (1997).
31. Nagase, H., Enghild, J.J., Suzuki, K. & Salvesen, G. Stepwise activation mechanisms of the precursor of matrix metalloproteinase 3 (stromelysin) by proteinases and (4-aminophenyl) mercuric acetate. *Biochemistry* **29,** 5783–5790 (1990).
32. Stocker, W. & Bode, W. Structural features of a superfamily of zinc-endopeptidases: the metzincins. *Curr. Opin. Struct. Biol.* **5,** 383–390 (1995).
33. Ferry, G., Boutin, J.A., Atassi, G., Fauchere, J.-L. & Tucker, G.C. Selection of histidine-containing inhibitor of gelatinases through deconvolution of combinatorial tetrapeptide libraries. *Molecular Diversity* **2,** 135–146 (1996).
34. Matthews, D.J. & Wells, J.A. Substrate phage: selection of protease substrates by monovalent display. *Science* **260,** 1113–1117 (1993).
35. Ke, S.H. *et al*. Distinguishing the specificities of closely related proteases. Role of P3 in substrate and inhibitor discrimination between tissue type plasminogen activator and urokinase. *J. Biol. Chem.* **272,** 16603–16609 (1997).
36. Smith M.M., Shi, L. & Navre, M. Rapid identification of highly active and selective substrates for stromelysin and matrilysin using bacteriophage peptide display libraries. *J. Biol. Chem.* **270,** 6440–6449 (1995).
37. Krook, M., Lindbladh, C., Eriksen, J.A. & Mosbach, K. Selection of a cyclic non-apeptide inhibitor to α-chymotrypsin using a phage display peptide library. *Molecular Diversity* **3,** 149–159 (1998).
38. Rui, F., Jie, Q., Zhi-bin, L., Hui, Z., Wei, L. & Jiacong, S. Selection of trypsin inhibitors in a phage peptide library. *Biochem. Biophys. Res. Commun.* **220,** 53–56 (1996).
39. Seftor, R.E.B. *et al*. Chemically modified tetracyclines inhibit human melanoma cell invasion and metastasis. *Clin. Exp. Metastasis* **16,** 217–225 (1998).
40. Kim, J., Yu, W., Kovalski, K. & Ossowski, L. Requirement for specific proteases in cancer cell intravasation as revealed by a novel semiquantitative PCR-based assay. *Cell* **94,** 353–362 (1998).
41. Itoh, T. *et al*. Reduced angiogenesis and tumor progression in gelatinase A-deficient mice. *Cancer Res.* **58,** 1048–1051 (1998).
42. Arap, W., Pasqualini., R. & Ruoslahti, E. Chemotherapy targeted to tumor vasculature. *Current Opinion in Oncology* **10,** 560–565 (1998).
43. Rajotte, D. & Ruoslahti, E. Membrane dipeptidase is the receptor for a lung-targeting peptide identified by in vivo phage display. *J. Biol. Chem.* **274,** 11593–11598 (1999).
44. Pasqualini, R., Arap, W., Rajotte, D. & Ruoslahti, E. in *Phage display of proteins and peptides* (eds Barbas, C., Burton, D., Silverman, G., & Scott, J.) (Cold Spring Harbor Laboratory Press, New York, 1999). In press.
45. Sorsa, T. *et al*. Effects of tetracyclines on neutrophil, gingival, and salivary collagenases. A functional and Western blot assessment with special reference to their cellular sources in periodontal diseases. *Ann. N.Y. Acad. Sci.* **732,** 112–131 (1994).
46. Koivunen, E. *et al*. Human colon carcinoma, fibrosarcoma and leukemia cell lines produce tumor-associated trypsinogen. *Int. J. Cancer* **47,** 592–596 (1991).
47. Domingo, G.J., Leatherbarrow, R.J., Freeman, N., Patel, S. & Weir, M. Synthesis of a mixture of cyclic peptides based on the Bowman-Birk reactive site loop to screen for serine protease inhibitors. *International Journal of Peptide and Protein Research* **46,** 79–87 (1995).
48. Koivunen, E., Wang, B. & Ruoslahti, E.. Phage libraries displaying cyclic peptides with different ring sizes: ligand specificities of of the RGD-directed integrins. *Bio/Technology* **13,** 265–270 (1995).
49. Smith, G.P. & Scott, J.K. Libraries of peptides and proteins displayed in filamentous phage. *Methods Enzymol.* **217,** 228–257 (1993).
50. Teronen, O. *et al*. Human neutrophil collagenase MMP-8 in peri-implant sulcus fluid and its inhibition by clodronate. *J. Dent. Res.* **76,** 1529–1537 (1997).
51. Edgell, C.-J.S., McDonald, C.C. & Graham, J.B. Permanent cell line expressing human factor VIII-related antigen established by hybridization. *Proc. Natl. Acad. Sci. USA* **80,** 3734–3737 (1983).
52. Herndier, B.G. *et al*. Characterization of a human Kaposi's sarcoma cell line that induces angiogenic tumors in animals. *AIDS* **8,** 575–581 (1996).

Carl_G_190x270_mm_blokki_FINAL.indd 490 06-Aug-23 1:55:13 PM

The EMBO Journal (2007) 26, 1129–1139 | © 2007 European Molecular Biology Organization | All Rights Reserved 0261-4189/07
www.embojournal.org

THE EMBO JOURNAL

A novel pathway of HMGB1-mediated inflammatory cell recruitment that requires Mac-1-integrin

Valeria V Orlova[1], Eun Young Choi[1], Changping Xie[2], Emmanouil Chavakis[3], Angelika Bierhaus[2], Eveliina Ihanus[4], Christie M Ballantyne[5], Carl G Gahmberg[4], Marco E Bianchi[6], Peter P Nawroth[2] and Triantafyllos Chavakis[1,*]

[1]Experimental Immunology Branch, NCI, NIH, Bethesda, MD, USA, [2]Department of Internal Medicine I, University Heidelberg, Heidelberg, Germany, [3]Molecular Cardiology, Department of Internal Medicine III, University of Frankfurt, Frankfurt, Germany, [4]Division of Biochemistry, Faculty of Biosciences, University of Helsinki, Finland, [5]Section of Atherosclerosis and Lipoprotein Research, Department of Medicine, Baylor College of Medicine and Center for Cardiovascular Disease Prevention, Methodist DeBakey Heart Center, Houston, TX, USA and [6]Faculty of Medicine, San Raffaele University, Milano, Italy

High-mobility group box 1 (HMGB1) is released extracellularly upon cell necrosis acting as a mediator in tissue injury and inflammation. However, the molecular mechanisms for the proinflammatory effect of HMGB1 are poorly understood. Here, we define a novel function of HMGB1 in promoting Mac-1-dependent neutrophil recruitment. HMGB1 administration induced rapid neutrophil recruitment *in vivo*. HMGB1-mediated recruitment was prevented in mice deficient in the β2-integrin Mac-1 but not in those deficient in LFA-1. As observed by bone marrow chimera experiments, Mac-1-dependent neutrophil recruitment induced by HMGB1 required the presence of receptor for advanced glycation end products (RAGE) on neutrophils but not on endothelial cells. *In vitro*, HMGB1 enhanced the interaction between Mac-1 and RAGE. Consistently, HMGB1 activated Mac-1 as well as Mac-1-mediated adhesive and migratory functions of neutrophils in a RAGE-dependent manner. Moreover, HMGB1-induced activation of nuclear factor-κB in neutrophils required both Mac-1 and RAGE. Together, a novel HMGB1-dependent pathway for inflammatory cell recruitment and activation that requires the functional interplay between Mac-1 and RAGE is described here.

The EMBO Journal (2007) **26,** 1129–1139. doi:10.1038/sj.emboj.7601552; Published online 1 February 2007
Subject Categories: immunology
Keywords: adhesion; inflammation; integrins; neutrophils

*Corresponding author. Experimental Immunology Branch, NCI, NIH, 10 Center Drive, Rm 4B17, Bethesda, MD 20892, USA.
Tel.: +1 301 451 2104; Fax: +1 301 496 0887;
E-mail: chavakist@mail.nih.gov

Received: 27 July 2006; accepted: 19 December 2006; published online: 1 February 2007

Introduction

Leukocyte recruitment as an integral part of inflammatory processes requires multistep adhesive and signaling events including selectin-dependent rolling, chemokine-dependent leukocyte activation, and integrin-mediated firm adhesion and diapedesis (Springer, 1994). During firm endothelial adhesion of leukocytes, leukocyte β2-integrins, LFA-1 (αLβ2, CD11a/CD18), Mac-1 (αMβ2, CD11b/CD18), and p150,95 (αXβ2, CD11c/CD18), as well as β1-integrins interact with endothelial counterligands such as ICAM-1, surface-associated fibrinogen (FBG) or VCAM-1 (Gahmberg, 1997; Plow *et al*, 2000; Hogg *et al*, 2003). Among leukocyte integrins, Mac-1 plays an important role in innate immunity, as it may regulate inflammatory cell recruitment as well as pathogen recognition, phagocytosis, and neutrophil survival (Ehlers, 2000; Mayadas and Cullere, 2005). Interestingly, Mac-1 ligation on leukocytes may lead to activation of nuclear factor-κB (NF-κB) (Sitrin *et al*, 1998) and the activation of the consequent gene expression (Rezzonico *et al*, 2001), although the underlying mechanisms are poorly understood. The role of Mac-1 in innate immunity is in line with its propensity to be a highly versatile multiligand receptor (Ehlers, 2000) interacting with numerous ligands and counter-receptors. In addition, the functions of Mac-1 may be regulated by interactions in *cis*, that is, on the same leukocyte surface with other receptors, such as the FcγRIII or the urokinase receptor (Zhou *et al*, 1993; Tang *et al*, 1997; Petty *et al*, 2002; Mayadas and Cullere, 2005). Interestingly, although Mac-1 is notorious for interacting in *trans* with different cellular counter-receptors or matrix proteins, only a few membrane partners of Mac-1 in *cis* are identified that may regulate its activity (Ehlers, 2000; Petty *et al*, 2002).

High-mobility group box 1 (HMGB1), also named amphoterin, is a nuclear protein loosely bound to DNA that stabilizes nucleosome formation and regulates transcription (Dumitriu *et al*, 2005b; Lotze and Tracey, 2005). Emerging evidence has demonstrated an important role for extracellular HMGB1 as a very potent inflammatory mediator (Wang *et al*, 1999; Scaffidi *et al*, 2002; Dumitriu *et al*, 2005b; Lotze and Tracey, 2005). HMGB1 can be secreted into the extracellular space by activated macrophages and mature dendritic cells by an active process that may require the acetylation of the molecule in the nucleus (Bonaldi *et al*, 2003). Alternatively, HMGB1 is passively released by necrotic, but not apoptotic cells (Scaffidi *et al*, 2002), thereby representing a signal for tissue damage. Extracellular HMGB1 may interact with toll-like receptors (TLR) and/or RAGE (receptor for advanced glycation end products) (Dumitriu *et al*, 2005b; Lotze and Tracey, 2005). In particular, an interaction between HMGB1 and TLR-2 or TLR-4 has been demonstrated that may mediate the proinflammatory actions of HMGB1 (Park *et al*, 2004, 2006). On the other hand, RAGE is a multiligand receptor on vascular cells that plays a key role in inflammatory processes,

©2007 European Molecular Biology Organization

Carl_G_190x270_mm_blokki_FINAL.indd 491 06-Aug-23 1:55:14 PM

especially at sites where its ligands accumulate (Schmidt *et al*, 2001; Chavakis *et al*, 2004). RAGE ligation may activate a range of signaling pathways including MAP kinases, rho GTPases, as well as activation of NF-κB (Schmidt *et al*, 2001; Yan *et al*, 2003). Recently, we established that endothelial RAGE interacts also with Mac-1 on leukocytes (Chavakis *et al*, 2003).

Extracellular HMGB1 evokes a strong inflammatory response; it stimulates the release of multiple proinflammatory cytokines such as tumor necrosis factor (TNF) and interleukins in macrophages and neutrophils (Andersson *et al*, 2000) and induces the expression of adhesion molecules on endothelial cells, such as VCAM-1 and selectins, as well as it enhances dendritic cell maturation (Dumitriu *et al*, 2005a, b; Lotze and Tracey, 2005). Robust leukocyte recruitment is a prominent hallmark associated with HMGB1-mediated inflammation (Dumitriu *et al*, 2005b; Lotze and Tracey, 2005). As observed in studies that entailed HMGB1 blockade *in vivo*, HMGB1 is important in the pathogenesis of sepsis (Wang *et al*, 1999; Yang *et al*, 2000), as well as in arthritis (Yang *et al*, 2005). Recent studies also indicated that HMGB1 may mediate inflammatory cell recruitment in acute hepatic necrosis (Tsung *et al*, 2005) and in acute lung injury (Kim *et al*, 2005; Lin *et al*, 2005). However, the molecular mechanisms underlying this proinflammatory function of HMGB1 remain to be clarified. In particular, it is not established yet whether HMGB1 affects extravasation-related functions of leukocytes, such as adhesion and migration. Here, we identify a novel pathway for HMGB1-mediated neutrophil recruitment that requires the functional interplay between RAGE and the β2-integrin Mac-1.

Results

HMGB1-mediated neutrophil recruitment in vivo requires Mac-1

We first studied whether HMGB1 administration can elicit rapid inflammatory cell recruitment *in vivo*. Interestingly, intraperitoneally (i.p.) injection of HMGB1 resulted in a rapid (4 h) recruitment of leukocytes (mostly neutrophils) into the peritoneum (Figure 1A). As a comparison, we studied thioglycollate-induced peritonitis (Figure 1B) (Chavakis *et al*, 2002, 2003). The HMGB1-mediated effect on neutrophil recruitment was reduced in RAGE-deficient mice (Figure 1A). In addition, HMGB1-induced neutrophil emigration to the peritoneum was blocked by systemic pretreatment of wild-type mice with soluble RAGE 1 h before HMGB1 injection (data not shown). Whereas thioglycollate-induced neutrophil infiltration was blocked by blocking monoclonal antibody (mAb) against LFA-1 and, to a less extent, by blocking mAb against Mac-1, HMGB1-mediated neutrophil emigration to the peritoneum was only blocked by blocking mAb to Mac-1, but not affected by antibody against LFA-1 (Figure 1B). To define further the underlying mechanisms of HMGB1-mediated neutrophil extravasation, we engaged mice deficient in Mac-1 or LFA-1. Consistent with the antibody inhibition studies, HMGB1-induced neutrophil emigration was decreased in Mac-1-deficient mice but not in LFA-1-deficient mice (Figure 1C). In contrast, thioglycollate-induced peritonitis was prevented in LFA-1-deficient mice (Figure 1D), consistent with previous reports showing an important role of LFA-1 in thioglycollate-induced peritonitis (Coxon *et al*, 1996; Lu *et al*, 1997; Berlin-Rufenach *et al*, 1999; Ding *et al*, 1999). Together, these findings suggest that HMGB1 stimulates neutrophil recruitment *in vivo* and that this process requires Mac-1 as well as RAGE.

RAGE is expressed on both endothelial cells and hematopoietic cells including neutrophils (Collison *et al*, 2002; Yan *et al*, 2003). Endothelial RAGE can interact with leukocyte Mac-1 in *trans* (Supplementary Figure 1, and Chavakis *et al*, 2003). To differentiate whether endothelial- or neutrophil-associated RAGE was required for the activity of HMGB1 to stimulate inflammatory cell recruitment *in vivo*, we performed bone marrow transplantation experiments. In particular, wild-type mice received irradiation and were then reconstituted with bone marrow from either wild-type or RAGE-deficient mice (wt→wt and RAGE−/−→wt, respectively). In the reverse experiment, irradiated RAGE−/− mice were reconstituted with bone marrow from wild-type mice (wt→RAGE−/−). Interestingly, the decrease in HMGB1-induced neutrophil extravasation observed in RAGE−/− mice as compared to wild-type mice (Figure 1A) could be reversed in the wt→RAGE−/− group, that is, by restoring the expression of RAGE on neutrophils (Figure 1E). In contrast, HMGB1-induced neutrophil recruitment into the peritoneum was prevented in the RAGE−/−→wt group as compared to the wt→wt group (Figure 1E). The degree of reduction in HMGB1-induced neutrophil recruitment into the peritoneum owing to the hematopoietic-specific absence of RAGE was comparable to the degree of decrease of HMGB1-induced neutrophil emigration in RAGE-deficient mice (Figure 1A). Taken together, these results indicate that Mac-1 and neutrophil RAGE but not endothelial RAGE are required for the HMGB1-induced recruitment of neutrophils *in vivo*.

HMGB1 stimulates Mac-1-dependent leukocyte adhesion

As these observations suggested a role for HMGB1 in Mac-1-dependent leukocyte extravasation, we studied whether HMGB1 can affect neutrophil adhesion. Interestingly, Mac-1-dependent neutrophil adhesion to FBG was stimulated three-fold by HMGB1. Whereas adhesion of RAGE-deficient neutrophils to FBG was comparable to the adhesion of wild-type neutrophils, the stimulatory effect of HMGB1 on Mac-1-dependent neutrophil adhesion to FBG was abolished in the absence of RAGE (Figure 2A). Additionally, HMGB1 induced spreading of wild-type but not RAGE-deficient neutrophils on FBG (Figure 2B). In contrast, PMA-induced adhesion and spreading of neutrophils to FBG was not affected by RAGE deficiency (not shown). Moreover, Mac-1−/− neutrophils failed to adhere to FBG and HMGB1 did not stimulate the adhesion of Mac-1−/− neutrophils to FBG, whereas HMGB1 enhanced the FBG adhesion of LFA-1−/− neutrophils (Figure 2C). Thus, HMGB1 stimulates the Mac-1-dependent adhesion of neutrophils to FBG in a RAGE-dependent manner.

Next, the effect of HMGB1 on the adhesion of neutrophils to immobilized ICAM-1, the major endothelial counter-receptor of leukocyte β2-integrins, was studied. Neutrophil adhesion to ICAM-1 is mediated by both Mac-1 and LFA-1 (Gahmberg, 1997; Hogg *et al*, 2003), and in the absence of HMGB1 neutrophil adhesion to ICAM-1 was blocked by inhibitory mAb to either Mac-1 or LFA-1 (Figure 2D). Both

 ©2007 European Molecular Biology Organization

Carl_G_190x270_mm_blokki_FINAL.indd 492 06-Aug-23 1:55:14 PM

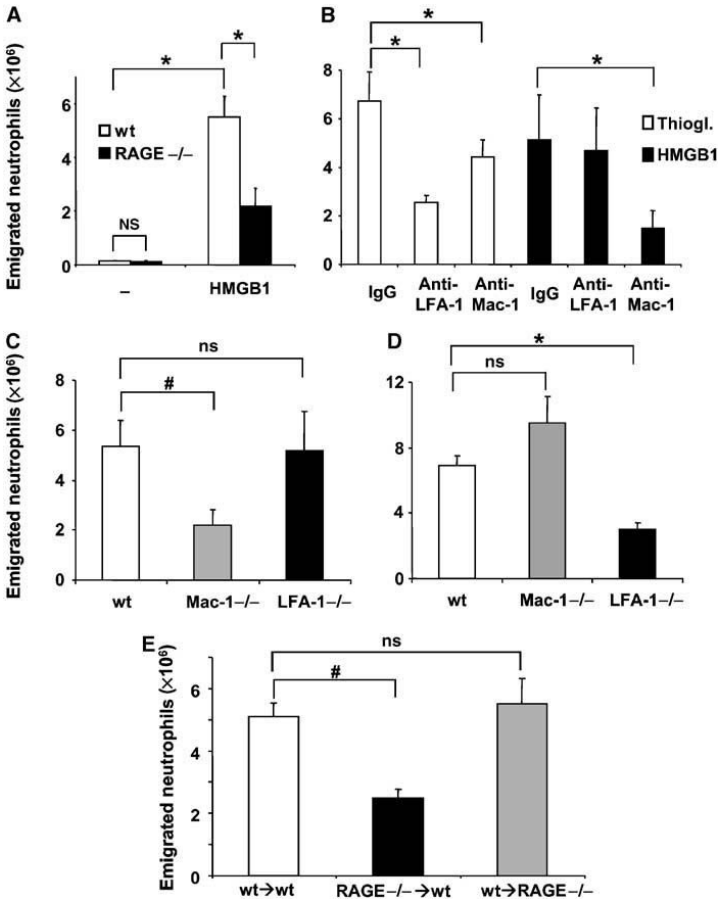

Figure 1 HMGB1-mediated inflammatory cell recruitment *in vivo*. (**A**) The number of neutrophils in wild-type (open bars) or RAGE−/− (filled bars) mice is shown 4 h after the i.p. injection of buffer (–) or HMGB1 (10 μg). (**B**) Sixty minutes before thioglycollate (open bars) or HMGB1 (filled bars) administration, wild-type mice were treated with isotype control mAb, with a blocking mAb against LFA-1 or with a blocking mAb against Mac-1 (each 100 μg). (**C**) HMGB1 induced peritonitis in wild-type, Mac-1−/−, and LFA-1−/− mice. (**D**) Thioglycollate induced peritonitis in wild-type, Mac-1−/−, and LFA-1−/− mice. (**E**) HMGB1 induced peritonitis in sublethally irradiated wild-type mice reconstituted with bone marrow cells from wild-type mice (wt→wt), sublethally irradiated wild-type mice reconstituted with bone marrow cells from RAGE−/− mice (RAGE−/−→wt) and sublethally irradiated RAGE−/−mice reconstituted with bone marrow cells from wild type (wt→RAGE−/−). Data are expressed as absolute numbers of emigrated neutrophils into the peritoneum. $^{*}P<0.01$; $^{\#}P<0.05$; ns: not significant. Data are mean±s.d. ($n=3$–6 mice/group).

Mac-1- and LFA-1-deficient neutrophils displayed decreased adhesion to immobilized ICAM-1 (Figure 2C). HMGB1 increased adhesion of wild-type neutrophils to ICAM-1 and the HMGB1-induced effect was absent in RAGE−/− neutrophils (not shown). Moreover, the HMGB1-induced upregulation of ICAM-1 adhesion was mediated by Mac-1 but not LFA-1, as evidenced by the following observations: (i) ICAM-1 adhesion of wild-type neutrophils in the presence of HMGB1 was prevented by inhibitory mAb to Mac-1 but was not affected by inhibitory mAb to LFA-1. (ii) The HMGB1-induced stimulation of neutrophil adhesion to ICAM-1 was absent in Mac-1-deficient neutrophils. In contrast, HMGB1 increased adhesion of LFA-1-deficient neutrophils to ICAM-1. This HMGB1-induced increase in ICAM-1 adhesion of LFA-1-deficient neutrophils was prevented by inhibitory mAb to Mac-1 but not mAb to LFA-1 (Figure 2D). Moreover, although soluble RAGE did not affect the adhesion of neutrophils to ICAM-1 in the absence of HMGB1, it blocked the HMGB1-induced upregulation of wild-type or LFA-1-deficient neutrophils (Figure 2D). Furthermore, the effect of HMGB1 to stimulate Mac-1-dependent adhesion of neutrophils to FBG or ICAM-1 was dose-dependent (1–250 ng/ml; data not shown). HMGB1 was active in stimulating Mac-1-dependent adhesion independent of whether it was pre-incubated with the neutrophils and then washed away before the adhesion assay or whether it was co-incubated with the neutrophils during the course of the adhesion assay, indicating that HMGB1 primary acts on the neutrophils. Finally, adhesion of wild-type neutrophils to immobilized fibronectin (FN), which is mediated by VLA-4, was not stimulated by HMGB1 (data not shown).

©2007 European Molecular Biology Organization

Carl_G_190x270_mm_blokki_FINAL.indd 493 06-Aug-23 1:55:15 PM

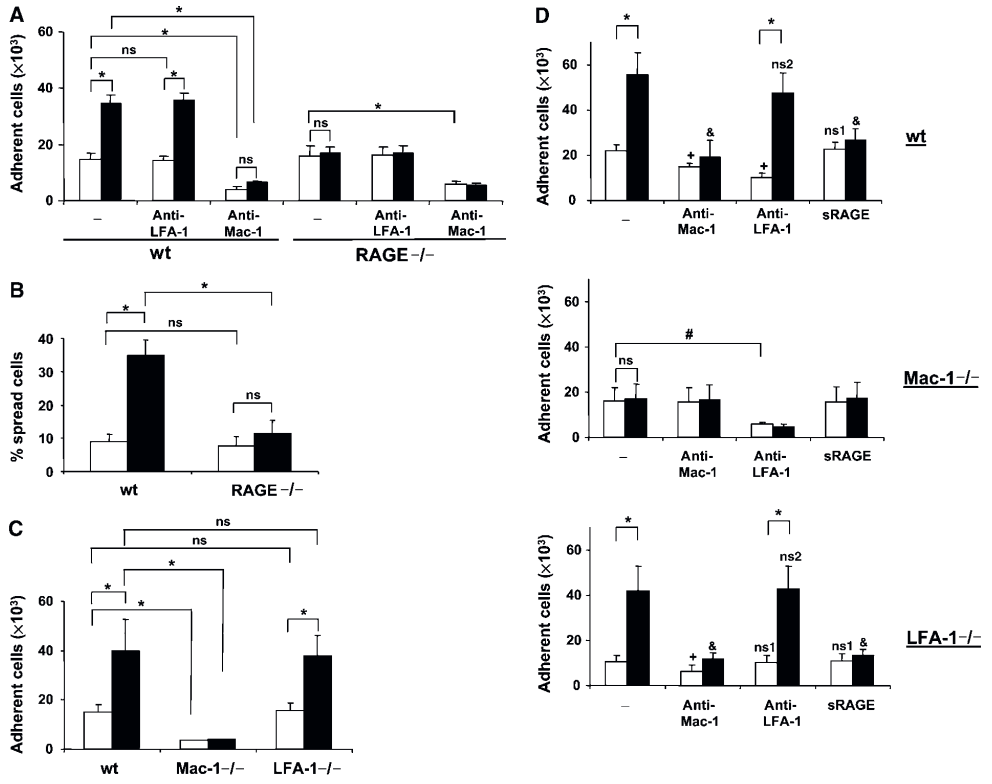

Figure 2 HMGB1-stimulated adhesion of mouse neutrophils. (**A**) Adhesion of wild-type or RAGE−/− neutrophils to immobilized FBG in the absence (open bars) or presence of HMGB1 (filled bars, 100 ng/ml) is shown without (−) or with mAb to LFA-1 or mAb to Mac-1 (each at 20 μg/ml). Cell adhesion is represented as number of adherent cells. (**B**) Spreading of wild-type or RAGE−/− neutrophils on immobilized FBG in the absence (open bars) or presence of HMGB1 (filled bars, 100 ng/ml). Data are represented as % spread cells. (**C**) Adhesion of wild-type, Mac-1−/−, or LFA-1−/− neutrophils to immobilized FBG in the absence (open bars) or presence of HMGB1 (filled bars, 100 ng/ml) is shown. Cell adhesion is represented as number of adherent cells. In (A), (B), and (C), $^{*}P<0.01$; ns: not significant. (**D**) Adhesion of wild-type, Mac-1−/−, or LFA-1−/− neutrophils to immobilized ICAM-1 is shown in the absence (open bars) or presence of HMGB1 (100 ng/ml, filled bars) without (−) or with mAb to Mac-1, mAb to LFA-1, or soluble RAGE (each at 20 μg/ml). Cell adhesion is represented as number of adherent cells. In (D), $^{*}P<0.01$; $^{\#}P<0.05$; ns: not significant; $^{+}P<0.05$ as compared to adhesion in the absence of HMGB1 (open bars) and in the absence of competitors (−); ns1: not significant as compared to adhesion in the absence of HMGB1 (open bars) and in the absence of competitors (−); $^{\&}P<0.01$ as compared to adhesion in the presence of HMGB1 (filled bars) and in the absence of competitors (−); ns2: not significant as compared to adhesion in the presence of HMGB1 (filled bars) and in the absence of competitors (−). Data are mean±s.d. of three independent experiments each performed in triplicate.

Our data indicate that HMGB1 activates Mac-1 in a RAGE-dependent manner. Studies on Mac-1 activation are more feasible to perform with human Mac-1 owing to the availability of both purified human Mac-1 as well as of well-characterized antibodies against human Mac-1. First, we investigated whether HMGB1 also stimulates Mac-1-dependent adhesion of human leukocytes. Consistent with the data obtained from mouse neutrophils, HMGB1 stimulated the Mac-1-dependent adhesion of myelomonocytic THP-1 cells to immobilized FBG or ICAM-1 by three-fold (Figure 3A and B). The effect of HMGB1 was also dose-dependent (1–250 ng/ml; data not shown). HMGB1-induced Mac-1-dependent adhesion of THP-1 cells to FBG or ICAM-1 was prevented in the presence of antibody to HMGB1 or soluble RAGE. In addition, the HMGB1-induced increase of ICAM-1 adhesion of THP-1 was prevented by inhibitory mAb to Mac-1 but was not affected by inhibitory mAb to LFA-1 (Figure 3B). In contrast, PMA or monocyte chemoattractant protein-1 (MCP-1)- stimulated adhesion of THP1 cells to ICAM-1 was blocked by both antibodies to Mac-1 and LFA-1 (data not shown). Adhesion of THP-1 cells to FN was predominantly mediated by VLA-4 and was not affected by the presence of HMGB1, soluble RAGE or antibody to HMGB1 (Figure 3C). Similar results were also obtained in experiments performed with human neutrophils isolated from peripheral blood (Supplementary Figure 2). These experiments indicate that HMGB1 stimulates Mac-1-dependent adhesive events in human leukocytes in a RAGE-dependent manner.

Chemotactic activity of HMGB1 on neutrophils

To assess further HMGB1 as a pro-adhesive/pro-chemotactic factor, we studied whether HMGB1 stimulates lamellipodium

 ©2007 European Molecular Biology Organization

Carl_G_190x270_mm_blokki_FINAL.indd 494 06-Aug-23 1:55:15 PM

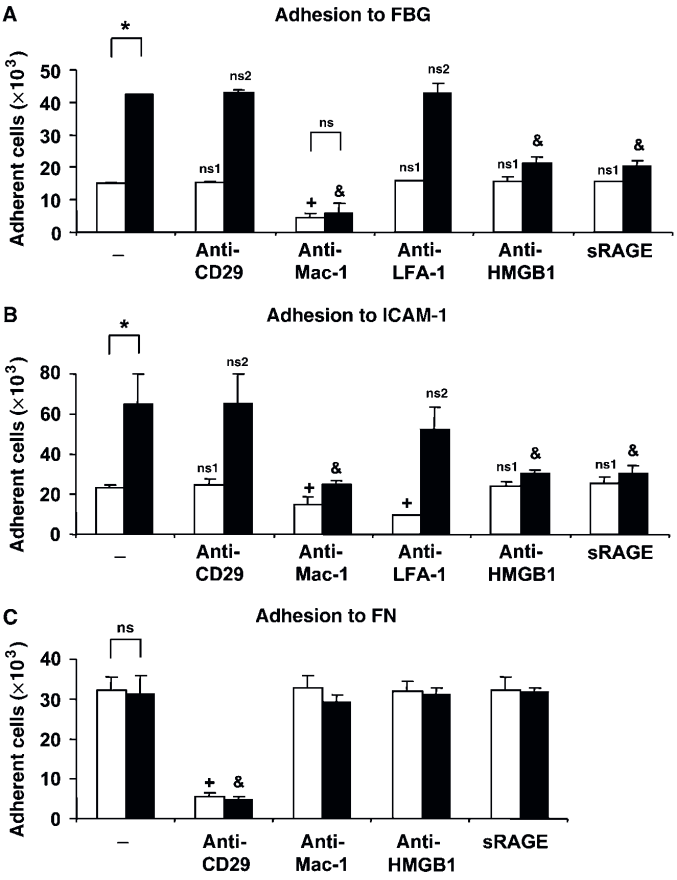

Figure 3 HMGB1-mediated adhesion of human leukocytes. (A, B) Adhesion of THP1 cells to immobilized FBG (**A**) or immobilized ICAM-1 (**B**) is shown in the absence (open bars) or presence of HMGB1 (100 ng/ml, filled bars), without (−) or with mAb to CD29, mAb to Mac-1, mAb to LFA-1, antibody to HMGB1 or soluble RAGE (each at 20 μg/ml). (**C**) Adhesion of THP-1 cells to immobilized FN is shown in the absence (open bars) or presence of HMGB1 (100 ng/ml, filled bars) without (−) or with mAb to CD29, mAb to Mac-1, antibody to HMGB1 or soluble RAGE (each at 20 μg/ml). Cell adhesion is represented as number of adherent cells. $^{*}P<0.01$; ns: not significant; $^{+}P<0.05$ as compared to adhesion in the absence of HMGB1 (open bars) and in the absence of competitors (−); ns1: not significant as compared to adhesion in the absence of HMGB1 (open bars) and in the absence of competitors (−); $^{\&}P<0.01$ as compared to adhesion in the presence of HMGB1 (filled bars) and in the absence of competitors (−); ns2: not significant as compared to adhesion in the presence of HMGB1 (filled bars) and in the absence of competitors (−). Data are mean ± s.d. of three independent experiments each performed in triplicate.

formation. Similar to MCP-1 (not shown and Cambien *et al*, 2001), HMGB1 induced the polarization of THP-1 cells adhering onto FBG. This shape change corresponded with the enrichment of F-actin at the leading edge, indicating that HMGB1-induced lamellipodium formation in these cells. Moreover, consistent with previous reports (Mocsai *et al*, 2002; Schymeinsky *et al*, 2005), the non-receptor protein tyrosine kinase syk was also redistributed at the site of lamellipodium formation and colocalized with F-actin upon stimulation with HMGB1 (Figure 4A). Thus, HMGB1 resembles chemotactic factors in that it induces lamellipodium formation.

In addition, HMGB1 induced chemotaxis of mouse and human neutrophils. The chemotactic effect of HMGB1 on mouse and human neutrophils was comparable to the effects of MIP-2 and IL-8 on mouse and human neutrophils, respectively (Figure 4B and D). The chemotactic effect of HMGB1 on neutrophils required both Mac-1 and RAGE, as HMGB1 failed to induce chemotaxis of Mac-1−/− and RAGE−/− neutrophils (Figure 4C). Consistently, HMGB1-induced chemotaxis of human neutrophils was blocked by soluble RAGE and an inhibitory mAb to Mac-1 but not by inhibitory mAb to LFA-1 (Figure 4D).

As β2-integrins and Mac-1 also play an important role in neutrophil transendothelial migration, we then investigated whether HMGB1 might affect this process. In a transwell assay, HMGB1 significantly stimulated the transmigration of human neutrophils through a monolayer of human umbilical vein endothelial cells (HUVEC) and this effect was blocked by mAb against Mac-1 but not by mAb against LFA-1. In

©2007 European Molecular Biology Organization

Carl_G_190x270_mm_blokki_FINAL.indd 495 06-Aug-23 1:55:15 PM

addition, HMGB1-induced transendothelial migration of neutrophils was inhibited by soluble RAGE or antibody to HMGB1. In contrast, IL-8-stimulated transmigration through cultured endothelial cells was blocked by mAb to Mac-1 as well as mAb to LFA-1, and was not affected by soluble RAGE or antibody to HMGB1 (Figure 4E). Similar results were obtained with THP-1 cells (not shown). Thus, HMGB1 exerts a chemotactic activity on neutrophils, inducing Mac-1-mediated chemotaxis and transendothelial migration in a RAGE-dependent manner.

HMGB1 increases Mac-1 activity in a RAGE-dependent manner

Our data so far suggested that HMGB1 stimulates Mac-1-mediated adhesiveness in a RAGE-dependent manner. Activation of integrin-mediated adhesiveness takes place at the level of avidity or valency (receptor density on the adhesive surface) as well as at the level of affinity for the individual ligand (Carman and Springer, 2003). We found that HMGB1-induced adhesion and spreading of THP-1 cells onto FBG-coated slides was associated with the polarization of Mac-1 to the leading edge of the THP-1 cells, as opposed to the diffuse staining on the cell surface in non-stimulated cells. In addition, we observed a strong colocalization of RAGE with Mac-1 at the leading edge of spreading THP-1 cells upon HMGB1 stimulation (Figure 5A).

Increases in the affinity of integrins are associated with conformational changes leading to increased exposure of activation-dependent epitopes on the integrin (Carman and Springer, 2003; Hogg *et al*, 2003). Activation of Mac-1 on the cell surface can be measured by the binding of the mAb CBRM1/5 that recognizes an activation-dependent epitope on the integrin. Activation of THP-1 cells and neutrophils with HMGB1 resulted in increased exposure of the CBRM1/5 epitope on Mac-1 (Figure 5B, data with THP-1 cells not shown). The total expression of Mac-1 remained unchanged by this short-term stimulation with HMGB1. The HMGB1-induced exposure of the CBRM1/5 epitope on Mac-1 was abolished by soluble RAGE (data not shown).

HMGB1 stimulates the interaction between Mac-1 and RAGE

The previous observations indicated that HMGB1 induces increased colocalization of Mac-1 with RAGE on the membrane of the inflammatory cell. Therefore, we continued to investigate the underlying mechanisms. In a purified system, HMGB1 did not influence the binding of FBG or ICAM-1 to immobilized Mac-1 or the binding of ICAM-1 to LFA-1 (Figure 6A and B). From these data, we can exclude that HMGB1

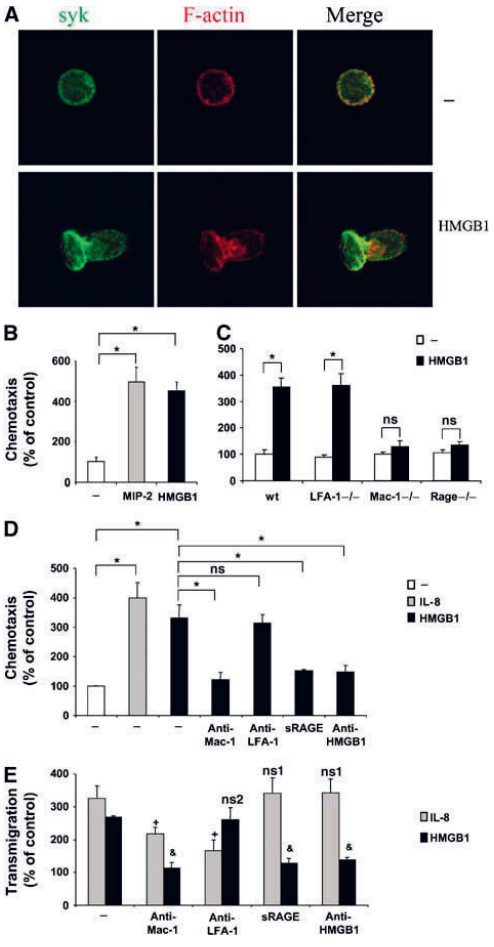

Figure 4 HMGB1-mediated chemotaxis and transendothelial migration of leukocytes. (**A**) Immunofluorescence for Syk (green) or F-actin (red) was performed followed by confocal microscopy. Representative immunofluorescence of THP-1 cells that were incubated in the absence (−) or presence of HMGB1 (50 ng/ml) for 30 min is shown. Double-stained images were merged. HMGB1 induced the enrichment of F-actin and Syk staining at the leading edge of the cell. (**B**) Chemotaxis of wild-type mouse neutrophils towards no chemoattractant (open bar), 50 ng/ml MIP-2 (gray bar) or 50 ng/ml HMGB1 (filled bar) is shown. (**C**) Chemotaxis of wild-type, LFA-1−/−, Mac-1−/−, and RAGE−/− mouse neutrophils towards no chemoattractant (open bars), or 50 ng/ml HMGB1 (filled bars) is shown. (**D**) Chemotaxis of human neutrophils towards no chemoattractant (open bar), 50 ng/ml IL-8 (gray bar) or 50 ng/ml HMGB1 (filled bars) is shown in the absence (−) or presence of blocking mAb to Mac-1, mAb to LFA-1, soluble RAGE, or antibody to HMGB1 (each at 20 μg/ml). In (B), (C), and (D), chemotaxis data are shown as percent of control. In (B) and (C), chemotaxis of wild-type mouse neutrophils in the absence of stimuli or competitors represents the 100% control; in (D) chemotaxis of human neutrophils in the absence of stimuli or competitors represents the 100% control. $^{*}P<0.02$; ns: not significant. (**E**) The transmigration of human neutrophils towards 50 ng/ml IL-8 (gray bars) or 50 ng/ml HMGB1 (filled bars) across HUVEC is shown in the absence (−) or presence of blocking mAb to Mac-1, mAb to LFA-1, soluble RAGE, or antibody to HMGB1 (each at 20 μg/ml). Transmigration is represented as percent of control. Transmigration through HUVEC in the absence of stimuli or competitors represents the 100% control. $^{+}P<0.01$ as compared to transmigration towards IL-8 (gray bars) and in the absence of competitors (−); ns1: not significant as compared to transmigration towards IL-8 (gray bars) and in the absence of competitors (−); $^{\&}P<0.01$ as compared to transmigration towards HMGB1 (filled bars) and in the absence of competitors (−); ns2: not significant as compared to transmigration towards HMGB1 (filled bars) and in the absence of competitors (−). Data are mean ± s.d. of three independent experiments each performed in triplicate.

©2007 European Molecular Biology Organization

Carl_G_190x270_mm_blokki_FINAL.indd 496 06-Aug-23 1:55:16 PM

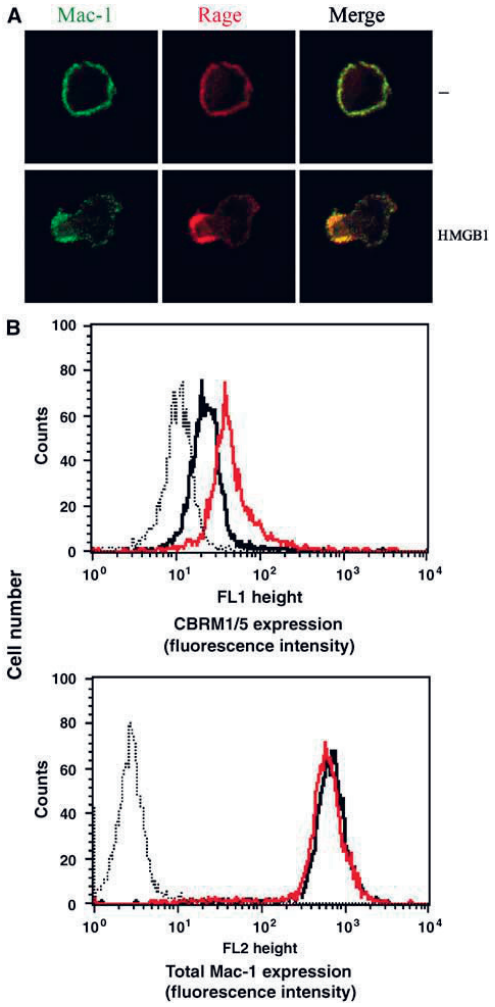

Figure 5 HMGB1-dependent activation of Mac-1. (**A**) Immunofluorescence for Mac-1 and RAGE was performed followed by confocal microscopy. Representative immunofluorescence of THP-1 cells that were incubated in the absence (−) or presence of HMGB1 (100 ng/ml) on FBG for 30 min is shown. Double-stained images were merged. (**B**) Human neutrophils were incubated in the absence (black curves) or presence of HMGB1 (100 ng/ml, red curves) for 20 min. Surface expression of an activation-dependent epitope (CBRM1/5) on Mac-1 was quantitated by FACS analysis. For comparison, quantitative cell surface expression of Mac-1 was analyzed using an antibody, which recognizes an epitope irrespective of the activation state of the integrin. Nonspecific fluorescence was determined using isotype-matched mouse-IgG (dotted thin curves).

directly acts on the interaction of Mac-1 with its ligands FBG or ICAM-1. Interestingly, HMGB1 augmented the interaction between RAGE and immobilized Mac-1 (Figure 6C). HMGB1 interacted specifically and dose-dependently only with RAGE but not with Mac-1 (Figure 6D and Supplementary Figure 3). In addition, HMGB1 bound to wild-type neutrophils but not to RAGE−/− neutrophils (data not shown).

The augmented Mac-1-dependent adhesion of neutrophils or THP-1 cells to FBG or ICAM-1 in the presence of HMGB1 could therefore be attributed to an HMGB1-mediated increase in the interaction between RAGE and Mac-1 in *cis* on the membrane of the inflammatory cell that then results in increased activity of Mac-1. To address this hypothesis, we have studied the adhesion of CHO cells transfected with Mac-1, RAGE, or both receptors. HMGB1 stimulated the adhesion of Mac-1-transfected CHO cells but not mock-transfected cells (cells transfected with the vector alone) to immobilized RAGE (Figure 6E). Mac-1-transfected cells but not mock- or RAGE-transfected cells adhered to immobilized FBG or ICAM-1 (Figure 6F, ICAM-1 adhesion data not shown). Whereas HMGB1 did not alter the adhesion of Mac-1 transfected CHO cells to immobilized FBG or ICAM-1, the adhesion of CHO cells cotransfected with Mac-1 and RAGE was stimulated by HMGB1 (Figure 6F). Thus, the presence of RAGE on the cell surface is essential for the effect of HMGB1 to enhance Mac-1-dependent adhesion to the ligands of the integrin.

HMGB1-induced activation of the transcription factor NF-κB requires both RAGE and Mac-1

Our findings up to this point suggested that HMGB1 stimulates the functional cooperation between RAGE and Mac-1. However, it is conceivable that such a cooperation between RAGE and Mac-1 on the surface of inflammatory cells may affect RAGE-dependent signaling. NF-κB activation is a well-established downstream signaling event of RAGE ligation (Schmidt *et al*, 2001; Chavakis *et al*, 2004). Notably, among β2-integrins, it is especially Mac-1 that has been linked to NF-κB activation (Schmal *et al*, 1998; Sitrin *et al*, 1998; Shi *et al*, 2001); however, the underlying mechanisms are poorly understood. By engaging neutrophils from Mac-1-, LFA-1-, and RAGE-deficient mice, we found that HMGB1-induced NF-κB activation was diminished by the absence of either RAGE or Mac-1 but not of LFA-1, whereas TNF-α-induced NF-κB activation was not affected by the deficiency of any of these receptors (Figure 7). Similarly, HMGB1-induced NF-κB activation in THP-1 cells could be blocked by soluble RAGE, antibody to HMGB1, and mAb to Mac-1 but not by mAb to LFA-1 (Supplementary Figure 4). Thus, HMGB1-induced NF-κB activation requires both RAGE and Mac-1.

Discussion

It has become apparent in recent years that HMGB1 is instrumental in mediating a response to tissue damage or infection. HMGB1 is released by necrotic cells or actively secreted by cells of the innate immune system upon infectious and proinflammatory stimuli and triggers a strong inflammatory response (Dumitriu *et al*, 2005b; Lotze and Tracey, 2005). To date, the underlying mechanisms of HMGB1-mediated inflammatory cell recruitment are poorly defined. The present report demonstrates that HMGB1 induces inflammatory cell recruitment by regulating adhesive and migratory functions of neutrophils. This novel HMGB1-dependent pathway requires the lateral interplay between RAGE and the integrin Mac-1 and may constitute a major mechanism for inflammatory cell recruitment in innate immunity and after tissue injury.

©2007 European Molecular Biology Organization

Carl_G_190x270_mm_blokki_FINAL.indd 497 06-Aug-23 1:55:16 PM

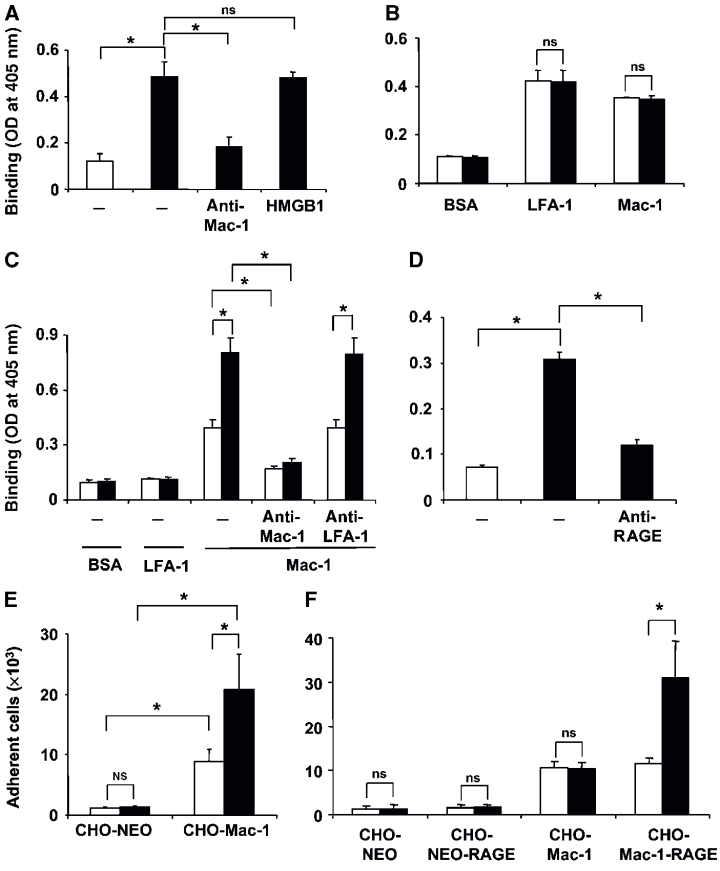

Figure 6 Influence of HMGB1 on the binding interactions between RAGE and Mac-1. (**A**) The binding of FBG to immobilized BSA (open bar) or immobilized Mac-1 (filled bars) is shown in the absence (−) or presence of mAb to Mac-1 or in the presence of HMGB1 (100 ng/ml). (**B**) The binding of ICAM-1 to immobilized BSA, LFA-1, or Mac-1 is shown in the absence (open bars) or presence of HMGB1 (100 ng/ml). (**C**) The binding of RAGE to immobilized BSA, LFA-1, or Mac-1 is shown in the absence (open bars) or presence of HMGB1 (100 ng/ml, filled bars). Binding of RAGE to Mac-1 was studied without (−) or with mAb to Mac-1 or mAb to LFA-1 (each at 20 μg/ml). (**D**) The binding of HMGB1 (0.1 μg/ml) to immobilized BSA (open bar) or immobilized RAGE (filled bars) is shown in the absence (−) or presence of antibody to RAGE (20 μg/ml). Binding is expressed as absorbance at 405 nm. (**E**) The adhesion of mock-transfected CHO cells (CHO-NEO) or CHO cells transfected with Mac-1 to immobilized RAGE is shown in the absence (open bars) or presence of HMGB1 (100 ng/ml, filled bars). (**F**) The adhesion of CHO-NEO cells, CHO-NEO cells transfected with RAGE, CHO-cells transfected with Mac-1 or CHO-cells transfected with both RAGE and Mac-1 to immobilized FBG is shown in the absence (open bars) or presence of HMGB1 (100 ng/ml, filled bars). Cell adhesion is represented as number of adherent cells. $^*P<0.01$; ns: not significant. Data are mean ± s.d. of three independent experiments each performed in triplicate.

The following features are consistent with a pro-adhesive and pro-chemotactic effect of HMGB1 for inflammatory cells: (i) *in vitro* studies demonstrated that HMGB1 specifically promoted Mac-1-but not LFA-1-mediated adhesion of neutrophils to ICAM-1 or FBG in a RAGE-dependent manner, as the effect of HMGB1 was absent in Mac-1- and RAGE-deficient neutrophils. By using Mac-1-RAGE cotransfectants, we verified that HMGB1-induced adhesion to immobilized Mac-1 ligands requires both Mac-1 and RAGE. Additionally, HMGB1 acted chemotactically, as it induced lamellipodium formation, chemotaxis and transendothelial migration of neutrophils in a Mac-1- and RAGE-dependent manner, consistent with a previous report that antibodies to HMGB1 reduced monocyte transendothelial migration *in vitro* (Rouhiainen *et al*, 2004). The stimulation of Mac-1-dependent adhesive and migratory events was accompanied by the activation of Mac-1 by HMGB1. In particular, HMGB1 increased the direct binding between RAGE and Mac-1 in a purified system; it also induced the colocalization of RAGE with Mac-1 at the leading edge of the leukocyte. Furthermore, HMGB1 stimulated the exposure of an activation-dependent epitope on Mac-1 in a RAGE-dependent manner. (ii) *In vivo*, HMGB1 administration triggered acute neutrophil recruitment. This process required Mac-1, as evidenced by the diminished HMGB1-mediated neutrophil recruitment in Mac-1−/− mice, whereas the HMGB1-mediated response in LFA-1−/− mice was normal. Bone marrow chimera experiments indicated that RAGE on the surface of neutrophils, but not endothelial cell

 ©2007 European Molecular Biology Organization

Carl_G_190x270_mm_blokki_FINAL.indd 498 06-Aug-23 1:55:17 PM

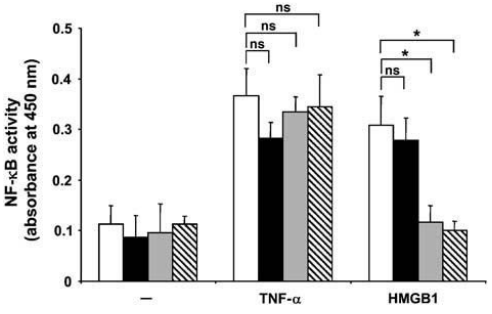

Figure 7 HMGB1-mediated NF-κB activation requires both RAGE and Mac-1. The activity of NF-κB was measured by ELISA in wt (open bars), LFA-1−/− (filled bars), Mac-1−/− (gray bars), or RAGE−/− (hatched bars) mouse neutrophils that were stimulated in the absence (−) or presence of TNF-α (10 ng/ml) or HMGB1 (20 ng/ml), as indicated. NF-κB activity is presented as absorbance at 450 nm. $^*P<0.02$; ns: not significant. Data are mean±s.d. of three independent experiments each performed in triplicate.

RAGE, was required for the HMGB1-induced neutrophil recruitment. Based on these findings, we postulate that HMGB1 mediates inflammatory cell recruitment by stimulating the interaction between RAGE and Mac-1 on the surface of the leukocyte, thereby activating Mac-1-dependent adhesive and migratory phenomena in a RAGE-dependent manner. However, we cannot exclude that indirect effects, such as HMGB1-induced gene expression, may also contribute to HMGB1-mediated neutrophil recruitment *in vivo*.

The lateral interaction of Mac-1 with RAGE triggered by HMGB1 on the leukocyte surface shares similarities with previously identified lateral interactions of Mac-1 with the urokinase receptor or FcγRIII that can regulate the activity of the integrin (Tang *et al*, 1997; Chavakis *et al*, 1999; Ross, 2002). In particular, although ligation of FcγR alone is usually sufficient to trigger activation such as phagocytosis, oxidative burst, and generation of various proinflammatory signals, this activity of FcγR is augmented further by the cooperative input from a synergistic Mac-1/FcγR complex, and vice versa Mac-1-dependent responses may be regulated by FcγR (Tang *et al*, 1997). In accordance, RAGE and Mac-1 are capable of triggering proinflammatory responses alone (Schmidt *et al*, 2001; Chavakis *et al*, 2004; Mayadas and Cullere, 2005); however, the functional synergism between them may result in a potentiation of the HMGB1-dependent inflammatory cell recruitment. Although the ability to react rapidly to injury or an infectious challenge is important, it is equally important that the response is in proportion to the magnitude of the threat (Ehlers, 2000). Thus, the existence of interactions between Mac-1 and FcγR or RAGE may serve to 'fine-tune' the inflammatory response. Nevertheless, additional studies will be necessary to identify the exact structural requirements of the HMGB1-induced interaction of Mac-1 with RAGE in *cis*.

It was previously reported that NF-κB activation is a downstream event of the interaction of RAGE with its ligands (Schmidt *et al*, 2001; Chavakis *et al*, 2004). Interestingly, HMGB1-induced NF-κB activation in neutrophils required both RAGE and Mac-1. However, we cannot exclude that the recently described binding of HMGB1 to TLR-2 and -4 (Park *et al*, 2004, 2006; Lotze and Tracey, 2005; Dumitriu *et al*, 2005b) may also contribute to NF-κB activation or other HMGB1-related functions.

Previously, ligation of Mac-1 resulted in NF-κB activation in an IRAK-1-dependent manner; however, in contrast to Toll/IL-1 receptor signaling, Mac-1-dependent NF-κB activation is MyD88-independent (Shi *et al*, 2001). Although the exact pathways leading to NF-κB activation downstream of both RAGE and Mac-1 ligation still have undefined signaling intermediates, our data indicate that these two receptors may cooperate on the leukocyte surface in order to mediate NF-κB activation. Interestingly, the propensity of Mac-1 to mediate NF-κB activation in neutrophils is consistent with the role of Mac-1 to regulate apoptosis and survival of these cells as described previously (Mayadas and Cullere, 2005).

The pathway described here for HMGB1-mediated inflammatory cell recruitment is consistent with the role of both multiligand receptors, RAGE and Mac-1, as major receptors in innate immunity. Previously, RAGE-deficient mice were largely protected during cecal ligation and puncture (Liliensiek *et al*, 2004), whereas Mac-1 is important for leukocyte functions such as adhesion, phagocytosis, oxidative burst, and survival (Mayadas and Cullere, 2005). In addition, as opposed to LFA-1, Mac-1 has a remarkably broad capacity and diversity for ligand recognition; in this regard Mac-1 may be the most promiscuous integrin, interacting with cellular adhesion molecules, extracellular matrix proteins, complement iC3b, proteolytic factors, as well as with LPS or other microbial ligands (Ehlers, 2000; Mayadas and Cullere, 2005). Our data suggest that HMGB1 signaling converges on Mac-1 (via RAGE) for integration with signals from other ligands, as a means of fine tuning an immediate response against microbial invaders or tissue injury.

Materials and methods

Materials
Details are available in Supplementary data.

Cell culture
Details are available in Supplementary data.

In vitro ligand–receptor interactions
Binding of biotinylated-FBG or ICAM-1 to immobilized Mac-1 or LFA-1 was performed exactly as described previously (Chavakis *et al*, 2002, 2003; Santoso *et al*, 2002). Alternatively, binding of soluble RAGE (5 μg/ml) to immobilized BSA, LFA-1, or Mac-1, (each 10 μg/ml) was performed as described (Chavakis *et al*, 2003). Binding of HMGB1 to immobilized RAGE or Mac-1 was also studied. Details are available in Supplementary data.

Electrophoretic mobility shift assay for the detection of the activity of NF-κB
Nuclear proteins were harvested as described previously and assayed for transcription factor binding activity using the NF-κB consensus sequence 5-AGTTGAG*GGGACTTTCC*CAGGC-3. Specificity of binding was ascertained by competition with a 160-fold molar excess of unlabeled consensus oligonucleotides (Bierhaus *et al*, 2001; Sotiriou *et al*, 2006).

ELISA for the detection of the activity of NF-κB
Details are available in Supplementary data.

Fluorescence cell adhesion assay
Adhesion experiments were performed as described previously (Chavakis *et al*, 2002, 2003; Xie *et al*, 2006). Details are available in Supplementary data.

©2007 European Molecular Biology Organization

Carl_G_190x270_mm_blokki_FINAL.indd 499 06-Aug-23 1:55:17 PM

Chemotaxis of human and mouse neutrophils
Details are available in Supplementary data.

Transmigration
Transmigration of human neutrophils through an endothelial cell monolayer was performed as described previously (Chavakis *et al*, 2004a; Xie *et al*, 2006). Details are available in Supplementary data.

Binding of Fc-RAGE to mouse neutrophils
Details are available in Supplementary data.

Flow cytometry for the detection of activation-dependent epitopes on Mac-1
These experiments were performed as described previously (Chavakis *et al*, 1999). Details are available in Supplementary data.

Immunofluorescence
Details are available in Supplementary data.

Mice
The generation of RAGE−/− mice, LFA-1−/− mice, and Mac-1−/− was described previously (Lu *et al*, 1997; Ding *et al*, 1999; Liliensiek *et al*, 2004). All mice were backcrossed for at least seven generations to a C57BL/6 background. Wild-type C57BL/6 mice were purchased from Jackson Laboratory (Ben Harbor, Maine). Protocols were approved by the NCI Animal Care and Use Committee.

In vivo peritonitis model
Thioglycollate-induced peritonitis in wild-type, Mac-1−/−, LFA-1−/−, or RAGE−/− mice was performed as described previously (Chavakis *et al*, 2002, 2003, 2004a). Alternatively, mice were injected i.p. with 10 μg of HMGB1. For inhibition studies, 1 h before the injection of thioglycollate, 100 μg of mAb against mouse Mac-1 or LFA-1 were administered i.p. Control mice were treated with the same volume of PBS. To evaluate peritoneal neutrophil recruitment, mice were killed at 4 h following injection of thioglycollate or HMGB1. Thereafter, the peritoneal lavage was collected and the number of emigrated neutrophils was quantitated by FACS analysis by staining for Gr-1 (May *et al*, 1998). Alternatively, the number of the granulocytes was analyzed by a conventional smear with Diffquick staining (Chavakis *et al*, 2002, 2003, 2004a) and both methods provided almost identical results.

Radiation bone marrow chimeras were prepared exactly as described previously (Lumsden *et al*, 2003). Wild-type recipient mice were irradiated with 950 rad and reconstituted with 1.5×10^7 bone marrow cells from RAGE-deficient mice (RAGE−/−→wt) or from wild-type mice (wt→wt) as a control. Additionally, irradiated RAGE−/− mice received bone marrow cells from wild-type mice (wt→RAGE−/−). Reconstitution of leukocyte populations was comparable in these groups (data not shown). Peritonitis experiments were performed 7 weeks after reconstitution.

Statistical analysis
Data were analyzed by analysis of variance with *post hoc* analysis (Bonferroni adjustment) using the SPSS software. *P*-values of <0.05 were regarded as significant.

Supplementary data
Supplementary data are available at *The EMBO Journal* Online (http://www.embojournal.org).

Acknowledgements

We acknowledge Dr M Kruhlak for help with confocal microscopy, G Sanchez and L Stepanyan (Bioqual Inc.) for bone marrow chimera experiments, D Winkler for genotyping, Dr A Mazzoni for help with the isolation of bone marrow cells, S Sharrow, T Adams and L Granger for help with FACS analysis, and Drs JJ Oppenheim and D Segal for critically reading the manuscript. This research was supported by the Intramural Research Program of the NIH, National Cancer Institute (TC) and the Sigrid Jusélius Foundation (CGG). The authors declare no direct financial interest in this study. However, MEB is founder and part owner of HMGBiotech, which produces HMGB1.

References

Andersson U, Wang H, Palmblad K, Aveberger AC, Bloom O, Erlandsson-Harris H, Janson A, Kokkola R, Zhang M, Yang H, Tracey KJ (2000) High mobility group 1 protein (HMG-1) stimulates proinflammatory cytokine synthesis in human monocytes. *J Exp Med* **192:** 565–570

Berlin-Rufenach C, Otto F, Mathies M, Westermann J, Owen MJ, Hamann A, Hogg N (1999) Lymphocyte migration in lymphocyte function-associated antigen (LFA)-1-deficient mice. *J Exp Med* **189:** 1467–1478

Bierhaus A, Schiekofer S, Schwaninger M, Andrassy M, Humpert PM, Chen J, Hong M, Luther T, Henle T, Kloting I, Morcos M, Hofmann M, Tritschler H, Weigle B, Kasper M, Smith M, Perry G, Schmidt AM, Stern DM, Haring HU, Schleicher E, Nawroth PP (2001) Diabetes-associated sustained activation of the transcription factor nuclear factor-κB. *Diabetes* **50:** 2792–2808

Bonaldi T, Talamo F, Scaffidi P, Ferrera D, Porto A, Bachi A, Rubartelli A, Agresti A, Bianchi ME (2003) Monocytic cells hyperacetylate chromatin protein HMGB1 to redirect it towards secretion. *EMBO J* **22:** 5551–5560

Cambien B, Pomeranz M, Schmid-Antomarchi H, Millet MA, Breittmayer V, Rossi B, Schmid-Alliana A (2001) Signal transduction involved in MCP-1-mediated monocytic transendothelial migration. *Blood* **97:** 359–366

Carman CV, Springer TA (2003) Integrin avidity regulation: are changes in affinity and conformation underemphasized? *Curr Opin Cell Biol* **15:** 547–556

Chavakis T, Bierhaus A, Al-Fakhri N, Schneider D, Witte S, Linn T, Nagashima M, Morser J, Arnold B, Preissner KT, Nawroth PP (2003) The pattern recognition receptor (RAGE) is a counterreceptor for leukocyte integrins: a novel pathway for inflammatory cell recruitment. *J Exp Med* **198:** 1507–1515

Chavakis T, Bierhaus A, Nawroth PP (2004) RAGE (receptor for advanced glycation end products): a central player in the inflammatory response. *Microbes Infect* **6:** 1219–1225

Chavakis T, Hussain M, Kanse SM, Peters G, Bretzel RG, Flock JI, Herrmann M, Preissner KT (2002) *Staphylococcus aureus* extracellular adherence protein (Eap) serves as anti-inflammatory factor by inhibiting the recruitment of host leukocytes. *Nat Med* **8:** 687–693

Chavakis T, Keiper T, Matz-Westphal R, Hersemeyer K, Sachs UJ, Nawroth PP, Preissner KT, Santoso S (2004a) The junctional adhesion molecule-C promotes neutrophil transendothelial migration *in vitro* and *in vivo*. *J Biol Chem* **279:** 55602–55608

Chavakis T, May AE, Preissner KT, Kanse SM (1999) Molecular mechanisms of zinc-dependent leukocyte adhesion involving the urokinase receptor and β2-integrins. *Blood* **93:** 2976–2983

Collison KS, Parhar RS, Saleh SS, Meyer BF, Kwaasi AA, Hammami MM, Schmidt AM, Stern DM, Al-Mohanna FA (2002) RAGE-mediated neutrophil dysfunction is evoked by advanced glycation end products (AGEs). *J Leukoc Biol* **71:** 433–444

Coxon A, Rieu P, Barkalow FJ, Askari S, Sharpe AH, von Andrian UH, Arnaout MA, Mayadas TN (1996) A novel role for the beta 2 integrin CD11b/CD18 in neutrophil apoptosis: a homeostatic mechanism in inflammation. *Immunity* **5:** 653–666

Ding ZM, Babensee JE, SimonI SI, Lu H, Perrard JL, Bullard DC, Dai XY, Bromley SK, Dustin ML, Entman ML, Smith CW, Ballantyne CM (1999) Relative contribution of LFA-1 and Mac-1 to neutrophil adhesion and migration. *J Immunol* **163:** 5029–5038

Dumitriu IE, Baruah P, Bianchi ME, Manfredi AA, Rovere-Querini P (2005a) Requirement of HMGB1 and RAGE for the maturation of human plasmacytoid dendritic cells. *Eur J Immunol* **35:** 2184–2190

Dumitriu IE, Baruah P, Manfredi AA, Bianchi ME, Rovere-Querini P (2005b) HMGB1: guiding immunity from within. *Trends Immunol* **26:** 381–387

Ehlers MR (2000) CR3: a general purpose adhesion-recognition receptor essential for innate immunity. *Microbes Infect* **2:** 289–294

 ©2007 European Molecular Biology Organization

Carl_G_190x270_mm_blokki_FINAL.indd 500 06-Aug-23 1:55:18 PM

Gahmberg CG (1997) Leukocyte adhesion: CD11/CD18 integrins and intercellular adhesion molecules. *Curr Opin Cell Biol* **9:** 643–650

Hogg N, Laschinger M, Giles K, McDowall A (2003) T-cell integrins: more than just sticking points. *J Cell Sci* **116:** 4695–4705

Kim JY, Park JS, Strassheim D, Douglas I, Diaz del Valle F, Asehnoune K, Mitra S, Kwak SH, Yamada S, Maruyama I, Ishizaka A, Abraham E (2005) HMGB1 contributes to the development of acute lung injury after hemorrhage. *Am J Physiol Lung Cell Mol Physiol* **288:** L958–L965

Liliensiek B, Weigand MA, Bierhaus A, Nicklas W, Kasper M, Hofer S, Plachky J, Grone HJ, Kurschus FC, Schmidt AM, Yan SD, Martin E, Schleicher E, Stern DM, Hammerling G, Nawroth PP, Arnold B (2004) Receptor for advanced glycation end products (RAGE) regulates sepsis but not the adaptive immune response. *J Clin Invest* **113:** 1641–1650

Lin X, Yang H, Sakuragi T, Hu M, Mantell LL, Hayashi S, Al-Abed Y, Tracey KJ, Ulloa L, Miller EJ (2005) Alpha-chemokine receptor blockade reduces high mobility group box 1 protein-induced lung inflammation and injury and improves survival in sepsis. *Am J Physiol Lung Cell Mol Physiol* **289:** L583–L590

Lotze MT, Tracey KJ (2005) High-mobility group box 1 protein (HMGB1): nuclear weapon in the immune arsenal. *Nat Rev Immunol* **5:** 331–342

Lu H, Smith CW, Perrard CW, Bullard D, Tang L, Shappell SB, Entman ML, Beaudet AL, Ballantyne CM (1997) LFA-1 is sufficient in mediating neutrophil emigration in Mac-1-deficient mice. *J Clin Invest* **99:** 1340–1350

Lumsden JM, Williams JA, Hodes RJ (2003) Differential requirements for expression of CD80/86 and CD40 on B cells for T-dependent antibody responses *in vivo*. *J Immunol* **170:** 781–787

May AE, Kanse SM, Lund LR, Gisler RH, Imhof BA, Preissner KT (1998) Urokinase receptor (CD87) regulates leukocyte recruitment via beta 2 integrins *in vivo*. *J Exp Med* **188:** 1029–1037

Mayadas TN, Cullere X (2005) Neutrophil beta2 integrins: moderators of life or death decisions. *Trends Immunol* **26:** 388–395

Mocsai A, Zhou M, Meng F, Tybulewicz VL, Lowell CA (2002) Syk is required for integrin signaling in neutrophils. *Immunity* **16:** 547–558

Park JS, Gamboni-Robertson F, He Q, Svetkauskaite D, Kim JY, Strassheim D, Sohn JW, Yamada S, Maruyama I, Banerjee A, Ishizaka A, Abraham E (2006) High mobility group box 1 protein interacts with multiple Toll-like receptors. *Am J Physiol Cell Physiol* **290:** C917–C924

Park JS, Svetkauskaite D, He Q, Kim JY, Strassheim D, Ishizaka A, Abraham E (2004) Involvement of toll-like receptors 2 and 4 in cellular activation by high mobility group box 1 protein. *J Biol Chem* **279:** 7370–7377

Petty HR, Worth RG, Todd III RF (2002) Interactions of integrins with their partner proteins in leukocyte membranes. *Immunol Res* **25:** 75–95

Plow EF, Haas TA, Zhang L, Loftus J, Smith JW (2000) Ligand binding to integrins. *J Biol Chem* **275:** 21785–21788

Rezzonico R, Imbert V, Chicheportiche R, Dayer JM (2001) Ligation of CD11b and CD11c beta(2) integrins by antibodies or soluble CD23 induces macrophage inflammatory protein 1alpha (MIP-1alpha) and MIP-1beta production in primary human monocytes through a pathway dependent on nuclear factor-kappaB. *Blood* **97:** 2932–2940

Ross GD (2002) Role of the lectin domain of Mac-1/CR3 (CD11b/CD18) in regulating intercellular adhesion. *Immunol Res* **25:** 219–227

Rouhiainen A, Kuja-Panula J, Wilkman E, Pakkanen J, Stenfors J, Tuominen RK, Lepantalo M, Carpen O, Parkkinen J, Rauvala H (2004) Regulation of monocyte migration by amphoterin (HMGB1). *Blood* **104:** 1174–1182

Santoso S, Sachs UJ, Kroll H, Linder M, Ruf A, Preissner KT, Chavakis T (2002) The junctional adhesion molecule 3 (JAM-3) on human platelets is a counter-receptor for the leukocyte integrin Mac-1. *J Exp Med* **196:** 679–691

Scaffidi P, Misteli T, Bianchi ME (2002) Release of chromatin protein HMGB1 by necrotic cells triggers inflammation. *Nature* **418:** 191–195

Schmal H, Czermak BJ, Lentsch AB, Bless NM, Beck-Schimmer B, Friedl HP, Ward PA (1998) Soluble ICAM-1 activates lung macrophages and enhances lung injury. *J Immunol* **161:** 3685–3693

Schmidt AM, Yan SD, Yan SF, Stern DM (2001) The multiligand receptor RAGE as a progression factor amplifying immune and inflammatory responses. *J Clin Invest* **108:** 949–955

Schymeinsky J, Then C, Walzog B (2005) The non-receptor tyrosine kinase Syk regulates lamellipodium formation and site-directed migration of human leukocytes. *J Cell Physiol* **204:** 614–622

Shi C, Zhang X, Chen Z, Robinson MK, Simon DI (2001) Leukocyte integrin Mac-1 recruits toll/interleukin-1 receptor superfamily signaling intermediates to modulate NF-κB activity. *Circ Res* **89:** 859–865

Sitrin RG, Pan PM, Srikanth S, Todd III RF (1998) Fibrinogen activates NF-kappa B transcription factors in mononuclear phagocytes. *J Immunol* **161:** 1462–1470

Sotiriou SN, Orlova VV, Al-Fakhri N, Ihanus E, Economopoulou M, Isermann B, Bdeir K, Nawroth PP, Preissner KT, Gahmberg CG, Koschinsky ML, Chavakis T (2006) Lipoprotein(a) in atherosclerotic plaques recruits inflammatory cells through interaction with Mac-1 integrin. *FASEB J* **20:** 559–561

Springer TA (1994) Traffic signals for lymphocyte recirculation and leukocyte emigration: The multistep paradigm. *Cell* **76:** 301–314

Tang T, Rosenkranz A, Assmann KJ, Goodman MJ, Gutierrez-Ramos JC, Carroll MC, Cotran RS, Mayadas TN (1997) A role for Mac-1 (CDIIb/CD18) in immune complex-stimulated neutrophil function *in vivo*: Mac-1 deficiency abrogates sustained Fcgamma receptor-dependent neutrophil adhesion and complement-dependent proteinuria in acute glomerulonephritis. *J Exp Med* **186:** 1853–1863

Tsung A, Sahai R, Tanaka H, Nakao A, Fink MP, Lotze MT, Yang H, Li J, Tracey KJ, Geller DA, Billiar TR (2005) The nuclear factor HMGB1 mediates hepatic injury after murine liver ischemia-reperfusion. *J Exp Med* **201:** 1135–1143

Wang H, Bloom O, Zhang M, Vishnubhakat JM, Ombrellino M, Che J, Frazier A, Yang H, Ivanova S, Borovikova L, Manogue KR, Faist E, Abraham E, Andersson J, Andersson U, Molina PE, Abumrad NN, Sama A, Tracey KJ (1999) HMG-1 as a late mediator of endotoxin lethality in mice. *Science* **285:** 248–251

Xie C, Alcaide P, Geisbrecht BV, Schneider D, Herrmann M, Preissner KT, Luscinskas FW, Chavakis T (2006) Suppression of experimental autoimmune encephalomyelitis by extracellular adherence protein of *Staphylococcus aureus*. *J Exp Med* **203:** 985–994

Yan SF, Ramasamy R, Naka Y, Schmidt AM (2003) Glycation, inflammation and RAGE. A scaffold for the macrovascular complications of diabetes and beyond. *Circ Res* **93:** 1159–1169

Yang H, Ochani M, Li J, Qiang X, Tanovic M, Harris HE, Susarla SM, Ulloa L, Wang H, DiRaimo R, Czura CJ, Wang H, Roth J, Warren HS, Fink MP, Fenton MJ, Andersson U, Tracey KJ (2000) Reversing established sepsis with antagonists of endogenous high-mobility group box 1. *Proc Natl Acad Sci USA* **101:** 296–301

Yang H, Wang H, Czura CJ, Tracey KJ (2005) The cytokine activity of HMGB1. *J Leukoc Biol* **78:** 1–8

Zhou M, Todd III RF, van de Winkel JG, Petty HR (1993) Cocapping of the leukoadhesin molecules complement receptor type 3 and lymphocyte function-associated antigen-1 with Fc gamma receptor III on human neutrophils. Possible role of lectin-like interactions. *J Immunol* **150:** 3030–3041

©2007 European Molecular Biology Organization

Carl_G_190x270_mm_blokki_FINAL.indd 501 06-Aug-23 1:55:19 PM

ARTICLES

nature immunology

Transendothelial migration of lymphocytes mediated by intraendothelial vesicle stores rather than by extracellular chemokine depots

Ziv Shulman[1,12], Shmuel J Cohen[1,12], Ben Roediger[2], Vyacheslav Kalchenko[3], Rohit Jain[2], Valentin Grabovsky[1,11], Eugenia Klein[4], Vera Shinder[4], Liat Stoler-Barak[1], Sara W Feigelson[1], Tsipi Meshel[5], Susanna M Nurmi[6], Itamar Goldstein[7], Olivier Hartley[8], Carl G Gahmberg[6], Amos Etzioni[9], Wolfgang Weninger[2,10], Adit Ben-Baruch[5] & Ronen Alon[1]

Chemokines presented by the endothelium are critical for integrin-dependent adhesion and transendothelial migration of naive and memory lymphocytes. Here we found that effector lymphocytes of the type 1 helper T cell (T_H1 cell) and type 1 cytotoxic T cell (T_C1 cell) subtypes expressed adhesive integrins that bypassed chemokine signals and established firm arrests on variably inflamed endothelial barriers. Nevertheless, the transendothelial migration of these lymphocytes strictly depended on signals from guanine nucleotide–binding proteins of the G_i type and was promoted by multiple endothelium-derived inflammatory chemokines, even without outer endothelial surface exposure. Instead, transendothelial migration–promoting endothelial chemokines were stored in vesicles docked on actin fibers beneath the plasma membranes and were locally released within tight lymphocyte-endothelial synapses. Thus, effector T lymphocytes can cross inflamed barriers through contact-guided consumption of intraendothelial chemokines without surface-deposited chemokines or extraendothelial chemokine gradients.

The emigration of circulating leukocytes is tightly regulated by integrin-mediated adhesions and chemokine signals[1,2]. For most circulating leukocytes, including naive and memory lymphocytes, chemokines displayed on vascular endothelial cells seem to critically regulate adhesion, spreading, crawling and the subsequent steps of transendothelial migration (diapedesis)[3]. *In vitro* delineation of these processes has shown that naive and memory peripheral blood T lymphocytes use chemokine-stimulated integrins to crawl on endothelial cell surfaces activated by tumor necrosis factor (TNF); this is a critical step for their subsequent transendothelial migration[4]. The presentation of chemokines on the apical surface of the activated endothelial cell barrier is necessary for both integrin activation and the generation of ventral filopodia by chemokine-responsive T cells. These ventral filopodia have been suggested to probe the endothelial cell for exit cues[4–6] such as basolateral chemokines[4].

Newly activated effector T cells released from lymphoid organs rapidly emigrate to peripheral sites of inflammation[7]. Both effector $CD4^+$ T cells (type 1 helper T cells (T_H1 cells)) and $CD8^+$ T cells (type 1 cytotoxic T cells (T_C1 cells)) activated by antigen or inflammatory cytokines such as interluekin 2 (IL-2), TNF and interferon-γ (IFN-γ) in the lymph nodes return to the circulation after downregulating their early activation marker CD69 (ref. 8) and seem to extravasate from inflamed blood vessels more efficiently than their naive and memory counterparts[9,10]. This enhanced extravasation of effector lymphocytes in nonlymphoid tissues has been attributed to their expression of guanine nucleotide–binding (G) protein–coupled receptors (GPCRs) for inflammatory chemokines[11] and to the acquisition of E- and P-selectin ligands[12] and the activation and memory marker CD44 (ref. 13). However, the precise contribution of integrins and of specific GPCRs to the enhanced extravasation capacity of effector lymphocytes at sites of inflammation has remained unclear.

To address those longstanding questions, we used both *in vivo* and *in vitro* models to delineate the roles of endothelial chemokines in adhesion, crawling and crossing of effector T_H1 and T_C1 cells through different inflamed endothelial barriers under physiological conditions of shear flow. T_H1 and T_C1 lymphocytes attached to inflamed endothelial cells independently of chemokine signals, but the ability of these T cells to send invasive filopodia into inflamed endothelial barriers and initiate transendothelial migration depended on intact downstream signaling machineries of G proteins of the G_i type. The inflammatory

[1]Department of Immunology, Weizmann Institute of Science, Rehovot, Israel. [2]Centenary Institute, Newtown, New South Wales, Australia. [3]Veterinary Resources, Weizmann Institute of Science, Rehovot, Israel. [4]Irving and Cherna Moskowitz Center for Nano and Bio-Nano Imaging, Weizmann Institute of Science, Rehovot, Israel. [5]Department of Cell Research and Immunology, George S. Wise Faculty of Life Sciences, Tel Aviv University, Tel Aviv, Israel. [6]Division of Biochemistry, Faculty of Biosciences, University of Helsinki, Finland. [7]Immunology Program, Cancer Research Center, Chaim Sheba Medical Center, Tel-Hashomer, Ramat-Gan, Israel. [8]Department of Structural Biology and Bioinformatics, Faculty of Medicine, University of Geneva, Switzerland. [9]Department of Pediatrics, Meyer Children Hospital, Rambam Medical Center and the B. Rappaport School of Medicine, Technion, Haifa, Israel. [10]Discipline of Dermatology, Sydney Medical School, University of Sydney, Australia. [11]Deceased. [12]These authors contributed equally to this work. Correspondence should be addressed to R.A. (ronen.alon@weizmann.ac.il).

Received 27 September; accepted 25 October; published online 4 December 2011; doi:10.1038/ni.2173

Carl_G_190x270_mm_blokki_FINAL.indd 502 06-Aug-23 1:55:19 PM

lymphocyte GPCRs CCR2 and, to a lesser extent, CCR1, CCR5 and CXCR3, orchestrated effector lymphocyte transendothelial migration across variably inflamed barriers. The endothelial chemokine ligands to these GPCRs were stored inside vesicles rather than in external depots on and below the endothelial barrier. These chemokine vesicles docked on cortical actin fibers immediately beneath the endothelial cell plasma membranes and released their content at confined points of contact with the crawling and protruding effector lymphocytes. This specialized mechanism of chemokine consumption from intraendothelial stores was 'preferentially' used by subsets of effector and memory T cells with large amounts of adhesive integrins that were able to establish contacts with inflamed endothelia independently of integrin-activating chemokines.

RESULTS

Effector T cells bypass G_i protein signals on inflamed vessels

Pretreatment of naive lymphocytes with pertussis toxin blocks the activation of G_i proteins and totally abrogates their ability to arrest on high endothelial venules[14]. To assess the ability of effector T cells to adhere to and cross variably inflamed endothelial barriers before or after blockade of their G_i protein activation, we expanded populations of ovalbumin (OVA)-specific (OT-I) $CD8^+$ effector T cells in IL-2 and analyzed their ability to firmly stick on inflamed skin vessels induced by sterile inflammation. Pretreatment with pertussis toxin did not lead to less arrest of effector lymphocytes on inflamed skin vessels shortly after injection than that of coinjected sham-treated effector lymphocytes (**Fig. 1a** and **Supplementary Fig. 1** and **Supplementary Video 1**). However, treatment with pertussis toxin affected the ability of effector T cells to remain stably adherent after initial firm sticking, as determined by the mean adhesion duration period, which was ~60% lower than that of sham-treated cells (**Fig. 1a**).

To further explore the finding reported above, we developed a skin model of delayed-type hypersensitivity induced by injection of complete Freund's adjuvant (CFA) into the flanks of mice (**Supplementary Figs. 2** and **3**). Naive spleen T cells did not accumulate in the inflamed skin vessels (**Fig. 1b**). Shortly after injection, both T_H1 and T_C1 effector cells stimulated *ex vivo* via their T cell antigen receptor and the coreceptor CD28 (**Fig. 1c**,**d**) and $CD3^+$ effector T cells generated *in vivo* after immunization of the skin with CFA (**Fig. 1e**) accumulated slowly on the inflamed skin vessels of recipient mice. Such accumulation was much more efficient than that on noninflamed skin vessels (**Fig. 1c**,**e**). Pretreatment of effector lymphocytes with pertussis toxin did not interfere with the initial firm sticking of lymphocytes to the CFA-inflamed skin vessels (**Fig. 1d**). Furthermore, the mean duration of adhesions of effector T cells after sticking was not affected by pretreatment with pertussis toxin (**Fig. 1d**). A fraction of the pertussis toxin–treated effector T cells crawled away from their original arrest sites while resisting detachment by blood shear flow (**Supplementary Video 2**). Consistent with those intravital microscopy results, the number of either *ex vivo*– or *in vivo*–generated effector lymphocytes that accumulated in the inflamed skin vessels after pretreatment with pertussis toxin was only 30% lower than that of sham-treated cells (**Fig. 1c**,**e**). Collectively, these results suggested that on inflamed skin vessels with delayed-type hypersensitivity, effector T cells expressed pertussis toxin–insensitive machineries that supported both normal initial sticking and adhesion strengthening. In contrast, on sterile inflamed skin vessels, effector T cells stuck normally but used pertussis toxin–sensitive machineries for subsequent adhesion strengthening.

Human T_H1 and T_C1 cells bypass chemokine and CD44 signals

To further clarify the molecular basis of how effector T cells arrest and crawl on variably inflamed endothelial barriers independently of G_i protein–triggered chemokine signals, we generated human T_H1 and T_C1 effector lymphocytes by polyclonal stimulation of peripheral blood T lymphocytes, followed by prolonged expansion with IL-2 (ref. 15). The resulting lymphocyte population comprised equal fractions of IFN-γ- and TNF-producing $CD4^+$ and $CD8^+$ T cell subsets, characteristic of T_H1 and T_C1 effector cells, respectively (**Supplementary Fig. 4**). Typical of resting effector cells[16], these T cells had moderate expression of the lymph node–homing receptor CD62L (L-selectin) but lacked the activation marker CD69 (**Fig. 2a**) that is detected on early activated T blasts before they

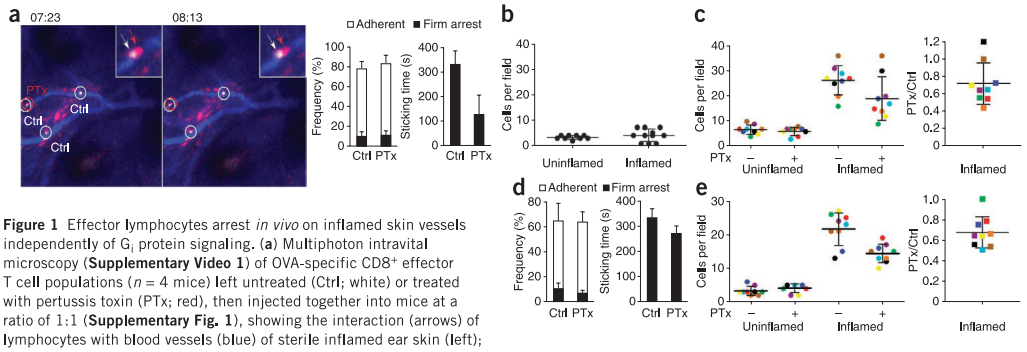

Figure 1 Effector lymphocytes arrest *in vivo* on inflamed skin vessels independently of G_i protein signaling. (**a**) Multiphoton intravital microscopy (**Supplementary Video 1**) of OVA-specific $CD8^+$ effector T cell populations ($n = 4$ mice) left untreated (Ctrl; white) or treated with pertussis toxin (PTx; red), then injected together into mice at a ratio of 1:1 (**Supplementary Fig. 1**), showing the interaction (arrows) of lymphocytes with blood vessels (blue) of sterile inflamed ear skin (left); frequency of T cells that established either unstable or stable (sticking) adhesions (middle); and average sticking time (right). Time, above images (minutes:seconds). (**b**) Accumulation of naive T cells on CFA-inflamed and uninflamed flank skin vessels 1 h after intracardial injection. (**c**) Sham- and pertussis toxin–pretreated $CD3^+$ splenocytes stimulated *ex vivo* that firmly adhered to CFA-inflamed or control skin vessels(left; **Supplementary Fig. 2**), and ratio of sham-treated lymphocytes to pertussis toxin–treated lymphocytes (PTx/Ctrl) that accumulated in individual fields at left (right; colors of squares correspond to circles at left). (**d**) Frequency of sham- and pertussis toxin–treated effector cells generated *in vivo* ($n = 7$ mice) that established either unstable or stable adhesions on CFA-inflamed skin vessels (left; **Supplementary Video 13**), and mean sticking time of untreated and pertussis toxin–treated effector cells (right). (**e**) Sham- and pertussis toxin–pretreated T cells from skin-immunized mice that accumulated on CFA-inflamed or control skin vessels. Field size (**b**,**c**,**e**), 1.5 mm^2. $P = 0.0579$ (**a**) or $P = 0.17$ (**d**; Student's *t*-test). Data are representative of two (**a**,**d**), three (**b**,**e**) or four (**c**) experiments (mean and s.e.m. (**a**,**d**) or mean ± s.e.m. (**b**,**c**,**e**)).

Carl_G_190x270_mm_blokki_FINAL.indd 503 06-Aug-23 1:55:20 PM

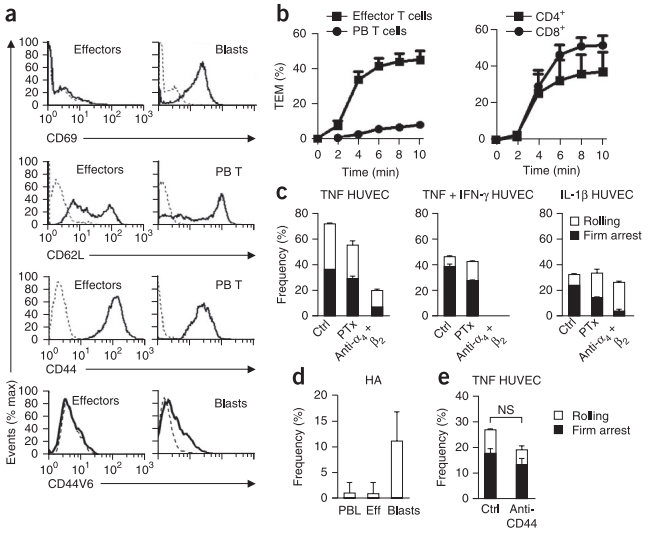

Figure 2 Effector human T lymphocytes arrest on TNF-activated HUVECs independently of chemokine G_i protein signaling. (**a**) Expression of activation and differentiation markers (solid lines) on effector lymphocytes, early T blasts (peripheral blood T cells stimulated for 1 d with antibody to CD3 (anti-CD3) and anti-CD28) or fresh peripheral blood T cells (PB T). Dashed lines, staining with isotype-matched control antibody. CD44V6, splice variant of CD44. (**b**) Frequency of transmigrating T cells in groups of effector or total fresh peripheral blood T cells (left), and of $CD4^+$ or $CD8^+$ effector cells (right), on TNF-activated HUVECs under shear flow (5 dyn/cm^2). (**c**) Frequency of effector T cells pretreated with medium (Ctrl) or with pertussis toxin (PTx) incubated with mAb to α_4 and mAb to β_2 (Anti-α_4 + β_2), then accumulated under shear flow (1.5 dyn/cm^2), that rolled or firmly arrested on HUVECs stimulated with either IL-1β or TNF alone or both TNF and IFN-γ. (**d**) Frequency of peripheral blood lymphocytes (PBL), effector cells (Eff) or T cell blasts stably rolling on high-density hyaluronan (HA) after 1 min of contact with substrate. (**e**) Effect of CD44 blockade with mAb on the frequency of effector T cells that rolled or firmly arrested on TNF-stimulated HUVECs at a shear flow of 1.5 dyn/cm^2. NS, not significant. Data are representative of two (**a**,**c**,**d**) or one of three (**b**) experiments (mean and s.d. of three fields (**b**) or mean and range from two fields (**c**–**e**)).

egress from lymph nodes[8]. Notably, both $CD4^+$ T_H1 and $CD8^+$ T_C1 effector cells readily crossed TNF-stimulated human umbilical vein endothelial cells (HUVECs) under shear flow conditions with much higher efficiency than that of unstimulated primary peripheral blood T cells (**Fig. 2b**). As we observed *in vivo*, prolonged pretreatment of effector T cells with pertussis toxin, which effectively blocked both their integrin activation and chemotactic responses to prototypic inflammatory chemokines (**Supplementary Fig. 5a**,**b**), interfered only mildly with their ability to firmly stick to HUVECs stimulated with either IL-1β or TNF or on HUVECs stimulated with both TNF and IFN-γ (**Fig. 2c** and **Supplementary Fig. 5c**). Pretreatment of T cells with a 'cocktail' of GPCR blockers did not interfere with firm sticking to TNF-stimulated HUVECs (**Supplementary Fig. 5c**). In contrast, blockade of both integrins α_4 and $\alpha_L\beta_2$ (LFA-1) on T cells abolished their firm arrest on HUVEC monolayers stimulated with various cytokines (**Fig. 2c** and **Supplementary Fig. 5c**). Because this chemokine bypass could be attributed to CD44-dependent activation of integrin $\alpha_4\beta_1$ (VLA-4), which has been observed in T cells stimulated via the T cell antigen receptor[13], we determined whether T_H1 or T_C1 effector cells expressed an active isoform of CD44, as measured by their ability to attach to the high-affinity CD44 ligand hyaluronan. Effector T lymphocytes did not establish stable rolling on high-density hyaluronan, in contrast to human $CD69^+$ lymphoblasts activated short term, which expressed the CD44V6 splice variant (**Fig. 2d**). Furthermore, a CD44-blocking monoclonal antibody (mAb) did not interfere with the arrest of effector lymphocytes on inflamed HUVECs (**Fig. 2e**). Collectively, these data suggested that major fractions of effector $CD4^+$ and $CD8^+$ T cells spontaneously expressed adhesive α_4 and β_2 integrins that were able to bypass the requirement for G_i protein signals and CD44 when supporting firm shear-resistant adhesions to cognate endothelial ligands expressed by variably inflamed vascular endothelium.

Integrins on effector cells are conformationally conserved

The chemokine-independent adhesiveness of effector lymphocytes could be attributed to higher binding activity of their VLA-4 and LFA-1. Expression of the β_1, β_2 and α_4 integrin subunits was 3.9-, 3.1- and 2.8-fold higher on effector T cells than on their noneffector peripheral blood counterparts (**Fig. 3a**). However, VLA-4 on effector lymphocytes showed binding saturation to its endothelial ligand VCAM-1 similar to that on peripheral blood T cells (**Fig. 3b** and **Supplementary Fig. 6**). Furthermore, the fraction of spontaneously activated β_1 integrins[17] was similar in effector and noneffector peripheral blood T cells (**Fig. 3c**). In contrast to VLA-4, LFA-1 on both effector cells and peripheral blood T cells did not bind the LFA-1 ligand ICAM-1 at concentrations found to saturate high-affinity LFA-1 subsets[18] (**Fig. 3b**). In addition, the fractions of the β_2 integrin subunit that expressed the KIM127 epitope, which is exposed by β_2 extension, or the 327C epitope, a marker of the open β_2 headpiece[19,20], were nearly identical in effector and noneffector T cells (**Fig. 3c**). As LFA-1 is the exclusive β_2 integrin expressed on effector and peripheral blood T cells (**Supplementary Fig. 5d**), these results further indicated that LFA-1 had a similar activation state on effector T cells and on peripheral blood T cells. Notably, a canonical phosphorylation site in the cytoplasmic tail of the α_L subunit, Ser1140, which facilitates for ICAM-1 binding to LFA-1 (ref. 21), was also similarly phosphorylated in effector and unstimulated peripheral blood T cells (**Fig. 3d**). Furthermore, the β_2 tail residue Thr758, which has been linked to agonist-stimulated associations of LFA-1 with the cortical cytoskeleton[21], was not phosphorylated in either effector and noneffector T cells (data not shown). Notably, the high chemokine-independent adhesiveness developed by LFA-1 and VLA-4 after a short static contact with high-density ICAM-1 or VCAM-1 depended entirely on intact activity of phospholipase C (PLC; **Fig. 3e**), a factor critical to integrin outside-in signaling[22]. The signaling protein PLC-γ1, the main PLC-γ isoform in T cells, was hyperphosphorylated on its key

Carl_G_190x270_mm_blokki_FINAL.indd 504 06-Aug-23 1:55:21 PM

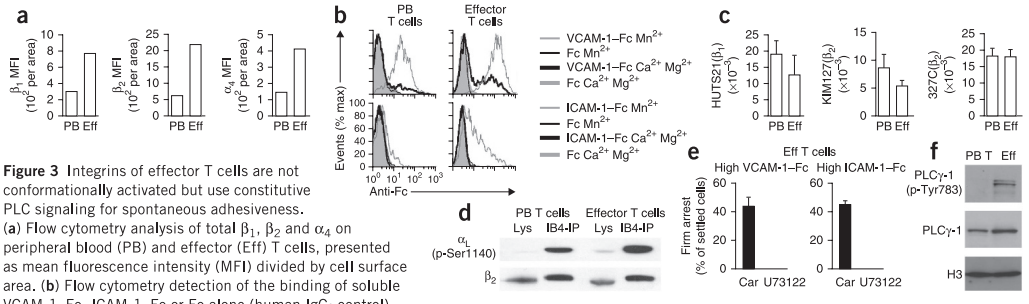

Figure 3 Integrins of effector T cells are not conformationally activated but use constitutive PLC signaling for spontaneous adhesiveness. (**a**) Flow cytometry analysis of total β_1, β_2 and α_4 on peripheral blood (PB) and effector (Eff) T cells, presented as mean fluorescence intensity (MFI) divided by cell surface area. (**b**) Flow cytometry detection of the binding of soluble VCAM-1–Fc, ICAM-1–Fc or Fc alone (human IgG; control) to peripheral blood or effector T cells in control medium (with Ca^{2+} and Mg^{2+}) or Mn^{2+}-supplemented medium. (**c**) Flow cytometry analysis of the activation epitopes β_1 and β_2, which 'report' extended and high-integrin-affinity states, respectively, presented as the MFI of the subunit epitope divided by the MFI of the total corresponding subunit. (**d**) Immunoblot analysis of the phosphorylation of α_L in peripheral blood T cells and effector lymphocytes, assessed with phosphorylation-specific antibody in total lysates or after immunoprecipitation with pan-mAb to β_2. (**e**) Frequency of firmly arrested and spread effector T cells pretreated with the PLC inhibitor U73122 or carrier (Car; DMSO), analyzed on VCAM-1–Fc or ICAM-1–Fc. (**f**) Immunoblot analysis of lysates of peripheral blood and effector T cells, probed with anti-PLCγ-1 or antibody to PLCγ-1 phosphorylated at Tyr783 (p-Tyr783). H3, histone H3. Data are representative of three (**a**,**c**) or two (**b**,**d**,**f**) experiments (mean and s.d. (**c**) or mean and range of two fields (**e**)).

regulatory tyrosine residue Tyr783 in effector T cells before occupancy of integrins by ligands, although it had similar expression in effector and peripheral blood T cells (**Fig. 3f**). Thus, the chemokine-independent adhesiveness of T_H1 and T_C1 effector cells to ICAM-1 and VCAM-1 seemed to result from greater surface densities of LFA-1 and VLA-4 and from hyperactivated PLC-γ1, rather than from preformed conformational activation of individual integrins.

Effector T cell crawling involves integrin outside-in signaling

We next delineated the function of effector integrins in post-arrest spreading, crawling and transendothelial migration across inflamed endothelial barriers under shear flow. Most effector T cells that arrested on TNF-stimulated HUVECs spread and generated many focal dots enriched with activated LFA-1, even after prolonged pretreatment with pertussis toxin (**Fig. 4a**). Scanning electron microscopy (SEM) analysis showed that these pertussis toxin–pretreated lymphocytes had a degree of microvillar collapse almost identical to that of untreated effector cells (**Fig. 4b**). Furthermore, effector T cells arrested on high-density ICAM-1 or VCAM-1 readily underwent microvillar collapse and spreading (83% and 63%, respectively) without exogenous chemokine signals (**Fig. 4c**). In contrast, microvillar collapse, spreading and crawling of unstimulated peripheral blood T cells require *in situ* integrin activation by chemokines displayed on the endothelium[4]. Notably, inhibition of kinases of the Src family in effector cells led to over 50% less spreading on either VCAM-1 or ICAM-1 under shear flow (**Fig. 4d**), whereas their adherence to low-density VCAM-1 or ICAM-1 required potent *in situ* chemokine signals and took place independently of Src kinase activity (**Fig. 4e**). Collectively, these results suggested that both VLA-4 and LFA-1 on effector T cells were able to bypass chemokine-triggered signaling by G_i proteins and used Src kinase signaling when occupied by high-density ligands[23] for spreading under disruptive shear forces.

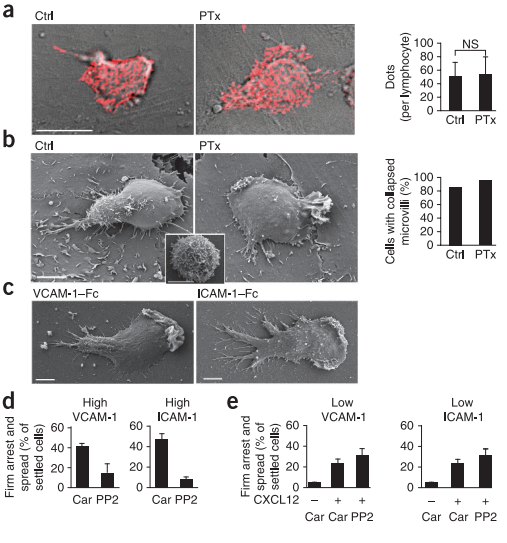

Figure 4 Integrin outside-in Src signals trigger microvillar collapse and spreading of effector lymphocytes on isolated ligands independently of chemokine signals. (**a**) Microscopy (left) of effector lymphocytes pretreated with pertussis toxin or medium, then perfused on TNF-activated HUVECs and fixed after 2 min of crawling, then stained for the high-affinity reporter β_2 (327C; red), and number of dots generated under crawling T cells ($n = 39$). (**b**) SEM of crawling effector lymphocytes (left main images) and intact effector lymphocyte in suspension (left inset), and fractions of adherent lymphocytes with collapsed microvilli (right). (**c**) SEM of effector lymphocytes settled on isolated high-density VCAM-1–Fc (360 sites/μm²) or ICAM-1–Fc (950 sites/μm²), subjected to shear forces of 5 dyn/cm² for 2 min. Scale bars, 6 μm (**a**), 3 μm (**b**) or 4 μm (**c**). (**d**) Firm arrest and spreading of effector lymphocytes treated with the Src family kinase inhibitor PP2 or carrier, settled on ligands (above) and subjected to shear forces of 5 dyn/cm², assessed at 10 min. (**e**) Analysis (as in **d**) of firm arrest and spreading of effector lymphocytes treated with PP2 or carrier, settled on low-density VCAM-1 (40 sites/μm²) or ICAM-1–Fc (80 sites/μm²) and immobilized together with CXCL12 (2 μg/ml). Data are representative of one experiment with 39 cells (**a**) or 40–50 cells each (**b**,**c**) or two experiments (**d**,**e**; mean and s.d. (**a**,**d**,**e**)).

G_i signals are critical for transendothelial migration

Effector T cells initially arrested on TNF-stimulated HUVECs crawled very short distances and rapidly transmigrated at sites close to their

Carl_G_190x270_mm_blokki_FINAL.indd 505 06-Aug-23 1:55:21 PM

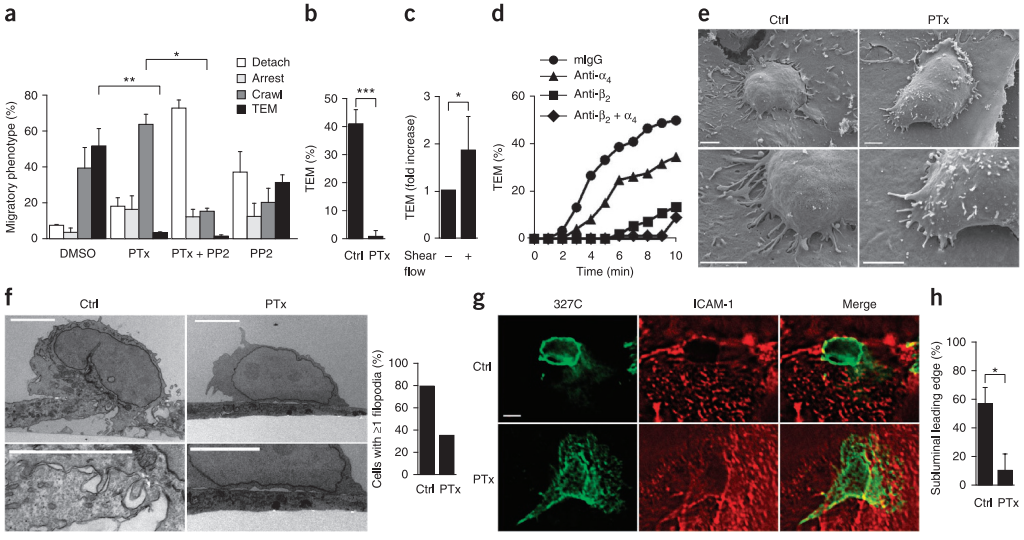

Figure 5 Transendothelial migration but not crawling of effector lymphocytes requires G_i protein signals. (**a**) Adhesion, crawling and transendothelial migration (TEM) of human effector lymphocytes pretreated with pertussis toxin and PP2, analyzed on TNF-activated HUVECs (as in **Fig. 2**). (**b**) Fraction of accumulated $CD3^+$ effector cells from skin-immunized mice, extravasating from CFA-inflamed skin vessels (assessed as in **Fig. 1c**; $n = 4$ mice). (**c**) Transendothelial migration of human effector lymphocytes either settled on TNF-activated HUVECs or subjected to shear flow for 10 min. (**d**) Kinetics of transendothelial migration across TNF-activated HUVECs under shear-free conditions of human effector lymphocytes pretreated with mouse IgG (control) or with mAb to α_4, β_2 or both (key). (**e**,**f**) SEM (**e**) or transmission electron microscopy (**f**) of effector lymphocytes pretreated with medium or pertussis toxin and fixed 4 min after accumulation on TNF-activated HUVECs under flow. Scale bars, 3 μm (**e**) or 2 μm (**f**). Right (**f**), frequency of cells with one or more filopodia-invading endothelial cell. Cells ($n = 29$ and 14) were analyzed in control and pertussis toxin–treated samples, respectively. (**g**) Microscopy of effector lymphocytes fixed during transendothelial migration as in **e** and stained with reporter mAb to β_2 (green) and mAb to ICAM-1 (red). Scale bar, 3 μm. (**h**) Percentage of effector lymphocytes with detectable subluminal leading edge among TNF-activated HUVECs were transiently transfected with eGFP to monitor lymphocyte leading edges during transendothelial migration (**Supplementary Video 5**). $^*P < 0.0014$ and $^{**}P < 0.0003$ (**a**); $^{***}P < 10^{-13}$ (**b**); $^*P < 0.002$ (**c**); $^*P < 0.005$ (**h**; Student's *t*-test). Data are representative of three experiments (**a**,**b**,**d**), 12 paired experiments (**c**) or one experiment with 40–50 cells each (**e**–**h**) mean and s.d. of three fields (**a**–**c**,**h**)).

original sites of arrest, near endothelial cell junctions (**Supplementary Video 3**). This short crawling required intact Src kinase activity (**Fig. 5a**) but was not affected by pertussis toxin–mediated blockade of signaling by G_i proteins (**Supplementary Fig. 7a**,**b**). In contrast, pretreatment with pertussis toxin completely blocked the transendothelial migration of effector lymphocytes across TNF-stimulated HUVEC barriers (**Fig. 5a** and **Supplementary Video 4**). Because this robust transendothelial migration took place without exogenously introduced chemokine gradients, these results indicated that TNF-stimulated HUVECs were able to promote the transendothelial migration of effector lymphocytes in a cell-autonomous manner. Similarly, the ability of mouse $CD3^+$ effector T cells to extravasate CFA-inflamed skin vessels (**Fig. 5b**) and of OT-I effector T cells to extravasate sterile-inflamed skin vessels (**Supplementary Fig. 8** and data not shown) *in vivo* was completely abolished by pretreatment with pertussis toxin. Although endothelial selectins have been suggested to activate LFA-1 on lymphocytes[24], T_H1 and T_C1 cells did not use this alternative chemokine-independent signaling pathway for integrin-mediated crawling or transendothelial migration. Effector T cells derived from a patient with leukocyte adhesion deficiency II that lacked ligand-binding reactivity to E-selectin and therefore were defective in initial attachment to TNF-stimulated HUVEC barriers at physiological shear stresses (data not shown) showed normal shear-resistant, integrin-dependent crawling and transendothelial migration through an E-selectin-expressing barrier once they were arrested on the inflamed endothelium at low shear stress (**Supplementary Fig. 9**).

Although shear stress has been found to be essential for chemokine-stimulated integrin activation and transendothelial migration of peripheral blood T cells[5,25,26], effector lymphocytes crossed endothelial cells even under shear-free conditions, albeit with significantly lower efficacy (**Fig. 5c**). Thus, we were able to determine whether chemotactic G_i protein signals on their own could promote lymphocyte transendothelial migration when the main endothelium-binding lymphocyte integrins were blocked. Blockade of LFA-1 on effector T cells inhibited crossing of the endothelial barrier under these nonstringent, shear-free conditions, whereas blockade of VLA-4 led to only slightly less transendothelial migration of T cells than in the control condition of no blockade (**Fig. 5d**). Thus, both optimal occupancy of endothelial ligands by LFA-1 and serial G_i protein signaling triggered by endothelial chemokines were necessary for successful transendothelial migration of lymphocytes. Notably, during the initial stages of transendothelial migration, effector T cells sent out many invasive filopodia, which were significantly less abundant after treatment with pertussis toxin than without treatment (**Fig. 5e**,**f**). Lymphocytes treated with pertussis toxin did not form characteristic transmigratory rings enriched in activated LFA-1 (**Fig. 5g**) or send a leading edge underneath the endothelium (**Supplementary Video 5** and **Fig. 5h**). Instead, cells treated with pertussis toxin formed multiple, nanometer-scale

Carl_G_190x270_mm_blokki_FINAL.indd 506 06-Aug-23 1:55:22 PM

contacts with the endothelial surface (**Figs. 4a** and **5e**). Thus, although they were dispensable for tight integrin-dependent lymphocyte contacts, G_i protein signals triggered by endothelial chemokines encountered in these contacts were critical for the generation of invasive protrusions by the crawling lymphocytes and for their subsequent diapedesis.

The CCR2 axis in migration across TNF-stimulated endothelium

TNF-stimulated endothelial cells expressed many inflammatory chemokines recognized by cognate receptors such as CCR1, CCR2, CCR5 and CXCR3, and T_H1 and T_C1 effector cells had higher expression of these receptors (**Fig. 6a**). Exposure of effector T cells to GPCR inhibitors indicated that CCR2 on T cells was essential for transendothelial migration across TNF-stimulated HUVECs, including the transcellular route (**Fig. 6b**,**c** and **Supplementary Video 6**). Met-RANTES, a blocker of both CCR1 and CCR5, also led to less lymphocyte transendothelial migration than that of control cells without blockade, but to a much lesser extent than did the CCR2 blocker (**Fig. 6b**). Similarly, transendothelial migration of the small subset of peripheral blood T cells arrested on TNF-stimulated HUVECs also depended on CCR2 (**Supplementary Fig. 10**), consistent with reports on the substantial role of human $CCR2^+$ memory T subsets in inflammatory recall responses[27]. We observed that transendothelial migration also depended on CCR2 for HUVECs stimulated with IL-1β or briefly (4 h) with TNF (data not shown). We next investigated whether ICAM-1 and CCL2 were sufficient for the transendothelial migration of effector T cells without stimulation of HUVECs by TNF or IL-1β. Ectopic coexpression of ICAM-1 and CCL2 in unstimulated HUVECs, which lacked endogenous CCL2 (**Supplementary Fig. 11a**) and had only residual ICAM-1 (ref. 28), was sufficient for transendothelial migration of lymphocytes under shear flow conditions, whereas ectopic expression of ICAM-1 or CCL2 alone did not promote transendothelial migration of lymphocytes (**Fig. 6d**).

TNF-stimulated human dermal microvascular endothelial cells (HDMECs) have higher expression of CCL5 than do HUVECs[29]. Effector T cells required all of the main inflammatory GPCRs (CCR2, CCR1 and CCR5) to cross the HDMEC barrier (**Fig. 6e**), although these GPCRs were not required for the earlier steps of adhesion and shear-resistant crawling of T cells. Thus, although endothelial ICAM-1 and CCL2 were both necessary and sufficient for the transendothelial migration of effector lymphocytes, T_H1 and T_C1 effector cells responded differently to combinations of various endothelium-derived inflammatory chemokines to optimally cross different inflamed endothelial barriers. Once they accumulate at sites of inflammation, effector T cells locally secrete IFN-γ, which in turn stimulates TNF- and/or IL-1β-activated endothelial cells to express the CXCR3-binding inflammatory chemokine CXCL10, in addition to CCL2 and CCL5 (ref. 29). Individual blockade of either CCR2 or CXCR3 or simultaneous blockade of both CCR1 and CCR5 did not block the transendothelial migration of effector T cells, whereas blockade of all four GPCRs abrogated all transendothelial migration (**Fig. 6f**). In contrast, transendothelial migration across HUVECs stimulated with both TNF and IL-4 depended entirely on CCR2 (**Fig. 6g**). Thus, as T_H1 inflammation progressed, the expression of

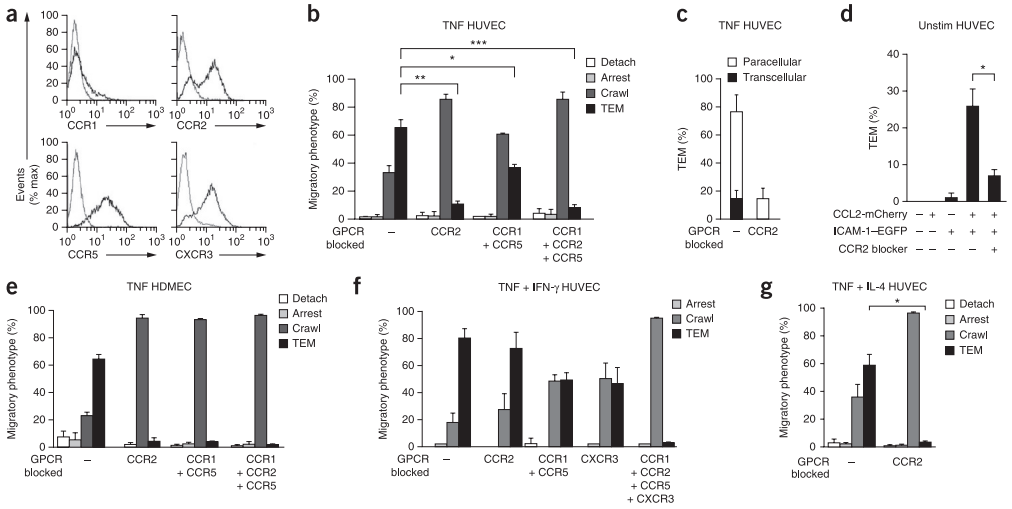

Figure 6 CCR2 on effector lymphocytes is critical for their transendothelial migration through TNF-activated HUVECs and HDMECs. (**a**) Flow cytometry analysis of GPCR expression on effector lymphocytes. (**b**) Migratory phenotypes of effector lymphocytes treated for 30 min with GPCR blockers and perfused over TNF-activated HUVECs. (**c**) Paracellular and transcellular transendothelial migration (occurring at least 5 μm away from endothelial junctions) of effector cells through TNF-activated HUVECs (details, **Supplementary Video 3**). (**d**) Transendothelial migration of effector lymphocytes pretreated with medium or CCR2 blocker and perfused over HUVECs transiently transfected with eGFP or ICAM-1–EGFP alone or together with CCL2-mCherry and left unstimulated (analyzed as in **b**). (**e**) Effect of Met-RANTES (a blocker of CCR1 and CCR5) and CCR2 blocker on effector lymphocyte adhesion and migration through TNF-activated HDMECs (assessed as in **b**). (**f**) Combined effects of inhibitors of CCR1, CCR5, CCR2 and CXCR3 on adhesive and migratory properties of effector T cells interacting with HUVECs costimulated with TNF and IFN-γ (analyzed as in **b**). (**g**) Effect of CCR2 blockade on transendothelial migration of effector lymphocytes through HUVECs stimulated with TNF and IL-4. $^*P < 0.002$; $^{**}P < 0.0001$ and $^{***}P < 0.0001$ (**b**); $^*P < 0.004$ (**d**); $^*P < 0.0002$ (**g**; Student's *t*-test). Data are representative of three (**a**,**b**,**d**–**g**) or two (**c**) experiments (mean and s.d. of migratory phenotypes in three fields (**b**,**d**–**g**); mean and s.d. of transendothelial migration in five fields (**c**)).

Carl_G_190x270_mm_blokki_FINAL.indd 507 06-Aug-23 1:55:22 PM

multiple functionally redundant chemokines by the endothelium took place to further enhance the diapedesis of more T_H1 and T_C1 effector subsets.

Vesicle-stored chemokines drive transendothelial migration

To investigate the role of endothelium-derived CCL2 in the transendothelial migration of effector T cells, we incubated HUVECs with saturating amounts of a CCL2-blocking mAb for the duration of the transendothelial migration assay. Although this blockade eliminated the chemotaxis of effector T cells toward cell-free CCL2, it interfered only slightly with the transendothelial migration of lymphocytes (**Fig. 7a**,**b**), which suggested little accessibility of the blocking antibody to endothelial CCL2. Furthermore, despite its reported ability to tether on glycocalyx heparan sulfates[30], and the abundance of this glycosaminoglycan near paracellular junctions in both resting and inflamed HUVECs (data not shown), we did not detect apical or basolateral CCL2 outside of nonpermeabilized TNF-stimulated HUVECs (**Fig. 7c**). However, we detected abundant CCL2 in the Golgi apparatus and in many scattered vesicles inside the endothelial cell after cell permeabilization (**Fig. 7c**). We also detected small amounts of the CCR5 and CCR1 ligand CCL5 in the Golgi apparatus in stimulated HUVECs (data not shown). To explore the dynamic distribution of these vesicles, we ectopically expressed CCL2 linked to enhanced green fluorescent protein (CCL2-eGFP) in TNF-stimulated HUVECs. CCL2-eGFP but not eGFP was stored in many dynamic vesicles with a distribution nearly identical to that of endogenous immunostained CCL2 (**Fig. 7c** and **Supplementary Fig. 11b**). These vesicles were much smaller than Weibel-Palade bodies and were distinct from early endosomes, because they did not express the recycling endosomal marker Rab11 or early endosomal marker EEA1 (**Supplementary Video 7** and unpublished data), suggesting that they are type 2 granules[31,32].

To further assess whether chemokine storage in those intraendothelial vesicles was critical for the transendothelial migration of lymphocytes, we pretreated TNF-stimulated HUVECs with brefeldin A, a potent inhibitor of vesicle packaging[33]. Brief pretreatment with brefeldin A depleted all CCL2 vesicles without disrupting the actin cytoskeleton (**Fig. 7d**) and blocked all transendothelial migration of lymphocytes across both TNF-stimulated HUVECs and HDMECs without interfering with the earlier GPCR-independent lymphocyte adhesion and crawling steps (**Fig. 7e** and **Supplementary Fig. 12**). Notably, exogenously introduced CCL2 did not restore the transendothelial migration of lymphocytes across endothelial cells treated with brefeldin A (**Fig. 7e**), which demonstrated that CCL2 stored in intraendothelial vesicles was the critical chemotactic element in the transendothelial migration of lymphocytes. Even when we grew TNF-stimulated HUVECs over a heparan sulfate–rich matrix, which could potentially trap CCL2 spontaneously released from the endothelial cells, we did not find a role for CCL2 secreted from the endothelium, as elimination of CCL2-containing vesicles by short pretreatment with brefeldin A still blocked all transendothelial migration (**Fig. 7f**). Notably, the short treatment with brefeldin A did not impair any endothelial functions critical for the transendothelial migration of lymphocytes, because effector T cells readily transmigrated across the brefeldin A–treated TNF-stimulated HUVECs after we overlaid the control exogenous chemokine CXCL12, which avidly adsorbs onto the extracellular surface of TNF-stimulated HUVECs (**Fig. 7e**).

We next investigated whether the additional inflammatory chemokines found to promote transendothelial migration of effector T_H1

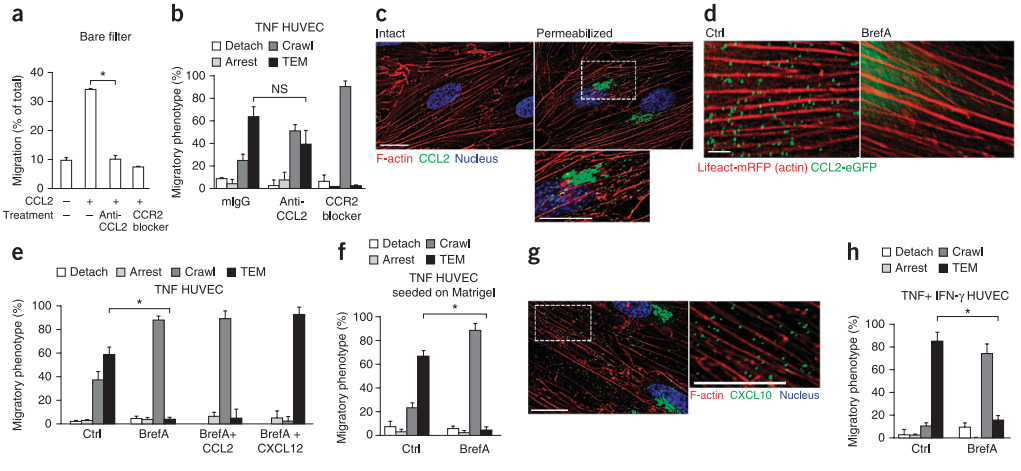

Figure 7 Vesicle-stored CCL2 drives effector lymphocyte transendothelial migration. (**a**) Transwell migration of effector lymphocytes toward CCL2, with or without CCL2-blocking mAb or CCR2 blockade. (**b**) Migratory phenotype of effector lymphocytes pretreated with CCR2 blocker and perfused over HUVECs activated with TNF and pretreated with control mAb (mIgG) or CCL2-blocking mAb (40 μg/ml). (**c**) Microscopy of TNF-activated HUVECs fixed and left intact or further permeabilized and stained with mAb to CCL2 (green). Scale bars, 15 μm. (**d**) Live microscopy of TNF-activated HUVECs transiently transfected with CCL2-eGFP and the actin marker Lifeact-mRFP and treated for 1 h with medium or brefeldin A (BrefA). Scale bar, 3 μm. (**e**) Migratory phenotype of TNF-activated HUVECs pretreated with medium or brefeldin A, and preincubated or not for 5 min with CCL2 or CXCL12 (1 μg/ml), analyzed under shear flow. (**f**) Migration of effector lymphocytes across TNF-activated HUVECs seeded on Matrigel and pretreated with brefeldin A or medium (analyzed as in **e**). (**g**) Microscopy of HUVECs activated with both TNF and IFN-γ, then permeabilized and immunostained for CXCL10 (green). Scale bars, 15 μm. (**h**) Effect of brefeldin A on the transendothelial migration of effector lymphocytes through HUVECs activated with TNF and IFN-γ (assessed as in **e**). $^*P < 0.07$ (**a**); $^*P < 0.00001$ (**e**); $^*P < 0.00005$ (**f**); and $^*P < 0.0002$ (**h**; Student's *t*-test). Data are representative of two (**a**–**c**,**f**–**h**) or three (**d**,**e**) experiments (mean and range of duplicates (**a**); mean and s.d. of three fields of view (**b**,**e**,**f**,**h**)).

Carl_G_190x270_mm_blokki_FINAL.indd 508 06-Aug-23 1:55:23 PM

cells also functioned in a vesicle-stored form rather than in extracellular deposits. As with CCL2, we detected CXCL10, the main CXCR3 ligand produced by HUVECs stimulated with TNF and IFN-γ, solely inside endothelial cells, in the Golgi and in scattered vesicles (**Fig. 7g**). Notably, these cotranscribed chemokines did not localize together in the same vesicles (data not shown). Brief pretreatment of TNF and IFN-γ endothelial cells with brefeldin A eliminated all CXCL10-containing vesicles and abolished both CCR2- and CXCR3-dependent transendothelial migration of lymphocytes (**Fig. 7h**, **Supplementary Fig. 13** and unpublished data). Furthermore, CXCR3-mediated transendothelial migration of lymphocytes was resistant to treatment with mAb to CXCL10 (**Supplementary Fig. 14**). Thus, CCL2 and CXCL10 stored in vesicles were not deposited on the outer apical or the basolateral surfaces of the inflamed endothelial barrier but nevertheless promoted robust CCR2- and CXCR3-dependent transendothelial migration of lymphocytes.

Chemokine vesicles dock beneath apical endothelial membranes

Because the transendothelial migration of lymphocytes across TNF-stimulated endothelial cells involved mainly CCL2 and CCR2, we further analyzed the movement of CCL2-containing vesicles on distinct endothelial cell cytoskeletal elements. Real-time fluorescence microscopy of ectopically expressed CCL2-eGFP and actin labeled with red fluorescent protein (RFP) indicated that most CCL2 vesicles were highly dynamic, whereas 20% of these vesicles remained docked on actin fibers (**Fig. 8a** and **Supplementary Videos 8** and **9**). Correlative SEM and fluorescence microscopy indicated that these endothelial cell actin fibers were located both immediately beneath the apical plasma membrane (**Fig. 8b**) and near paxillin-enriched focal adhesions at the basolateral plasma membrane (**Fig. 8c**). Live imaging suggested that CCL2 vesicles rapidly slid over microtubules and then docked on both apical and basolateral actin fibers (**Fig. 8d** and **Supplementary Videos 8** and **9**). Notably, vesicle docking rather than vesicle transport on microtubules seemed essential for lymphocyte transendothelial migration, because nocodazole-mediated disruption of all microtubules led to more docking of CCL2-containing vesicles on actin fibers than in control conditions without nocodazole (**Fig. 8a–e** and **Supplementary Videos 9** and **10**) but had no effect on CCR2-mediated transendothelial migration of lymphocytes (**Fig. 8f**). Thus, the docking of CCL2-containing vesicles rather than the sliding of vesicles over microtubules was rate limiting for the transendothelial migration of lymphocytes promoted by CCL2 and CCR2. These findings also suggested that CCL2-containing vesicles were biochemically distinct from the microtubule-dependent recycling vesicles enriched for the adhesion molecule CD31 (PECAM-1), which have been linked to the transendothelial migration of monocytes[34]. Mild disruption of the actin cytoskeleton eliminated all docked CCL2-containing vesicles but also impaired endothelial cell integrity and prevented further analysis of lymphocyte transendothelial migration (**Supplementary Video 11**).

SEM analysis showed that lymphocytes crawling on TNF-stimulated endothelial cells 'preferentially' sent their invasive filopodia to

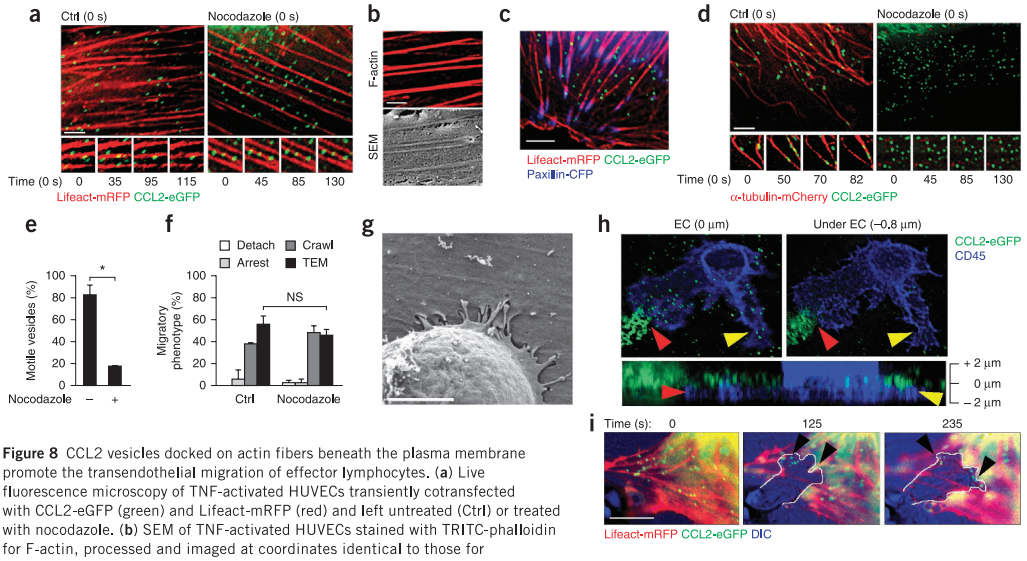

Figure 8 CCL2 vesicles docked on actin fibers beneath the plasma membrane promote the transendothelial migration of effector lymphocytes. (**a**) Live fluorescence microscopy of TNF-activated HUVECs transiently cotransfected with CCL2-eGFP (green) and Lifeact-mRFP (red) and left untreated (Ctrl) or treated with nocodazole. (**b**) SEM of TNF-activated HUVECs stained with TRITC-phalloidin for F-actin, processed and imaged at coordinates identical to those for immunofluorescence. (**c**) Fluorescence microscopy of TNF-HUVECs transfected with CCL2-eGFP, Lifeact-mRFP and paxillin-CFP (blue). (**d**) Live fluorescence microscopy of TNF-activated HUVECs transfected with CCL2-eGFP and microtubule marker α-tubulin–mCherry (red). (**e**) Fraction of motile vesicles in nocodazole-treated HUVECs in **d**. (**f**) Analysis of the transendothelial migration of effector T cells across nocodazole- or medium-treated TNF-activated HUVECs (analyzed as in **Fig. 3a**). (**g**) SEM of effector lymphocyte crawling for 2 min on TNF-activated HUVECs and fixed. (**h**) Visualization of effector lymphocytes transmigrating across CCL2-eGFP-transfected HUVECs fixed and stained with CD45 (blue). Red and yellow arrowheads indicate distinct sublumenal leading edges. Side views of *z*-stacked sections at various distances above and below endothelial cell surface. (**i**) Real-time differential interference contrast (DIC)–fluorescence microscopy of a sublumenal leading edge of a transmigrating lymphocyte. Images containing CCL2-eGFP and Lifeact-mRFP are from **Supplementary Video 12**. Black arrowheads, CCL2 vesicles in immediate contact with leading edges of lymphocytes. Images below **a** and **d** are from time-lapse segments of **Supplementary Video 9**. Scale bars, 3 μm (**a–d**,**g**) or 10 μm (**i**).*$P < 0.0003$ (**e**). Data are representative of three (**a**,**d–f**) or two (**b**,**c**,**g–i**) experiments (mean and s.d. (**e**,**f**)).

Carl_G_190x270_mm_blokki_FINAL.indd 509 06-Aug-23 1:55:23 PM

regions near the actin fibers beneath the apical plasma membrane (**Fig. 8g**), where CCL2-containing vesicles docked. Furthermore, the leading edge of actively transmigrating lymphocytes was closely opposed to endothelial CCL2 vesicles (**Fig. 8h**) and 'preferentially' developed near compartments enriched for CCL2-containing vesicles docked near the endothelial cell plasma membrane engaged by this leading edge (**Fig. 8i** and **Supplementary Video 12**). Collectively, these data suggested that lymphocyte attachments maintained transmigrating lymphocytes near actin-docked chemokine vesicles that were continuously consumed by the lymphocyte's leading edge.

DISCUSSION

Here we have described a previously unknown mechanism of chemokine-mediated transendothelial migration of lymphocytes driven by contact-guided consumption of endothelial stored inflammatory chemokines. This mechanism of transendothelial migration is probably used by subsets of effector lymphocytes with high integrin expression and adhesiveness and can occur even when the availability of cognate chemokine deposition on the outer endothelial interface is low. Thus, we do not think this form of transendothelial migration depends on transcytosis of chemokines from stromal pools[35–37] or on the massive deposition of chemokines produced by the endothelium, which is commonly observed in inflamed high endothelial venules[38].

The chemokine vesicles characterized here may represent the classical 'hot spots' that signal exit cues for crawling T cells and possibly other crawling leukocytes during paracellular, pericellular and transcellular transendothelial migration[2]. We think that the confined release of inflammatory chemokines from endothelial vesicles into nanometer-scale synapses would provide several major advantages to responding effector lymphocytes, such as chemokine protection from rapid dilution by blood flow, secretion in sub-femtoliter volumes in concentration ranges that would probably saturate nearby GPCRs in confined contacts generated by the responding T cell, protection from proteolytic cleavage of chemokines that either inactivates chemokines or generates GPCR-antagonistic fragments[39] and protection from GPCR desensitization. Because only a small fraction of the entire GPCR pool is occupied at any given focal contact, the rest of the GPCRs are protected from desensitization. We predict that this ensures continuous responsiveness of the effector lymphocyte to additional pools of inflammatory chemokines presented beneath the endothelial cell barrier by neighboring stromal cells and infiltrating leukocytes. Similarly confined release of chemokines and contact-guided chemokine consumption by adherent leukocytes could also be used by leukocytes crossing inflamed epithelia and lymphatic vessels[30,40].

Confined release of chemokines at leukocyte-endothelium synapses must involve vesicle fusion events near the endothelial invaginations surrounding the leukocyte-invasive filopodia[6]. To ensure optimal directional transendothelial migration, chemokine vesicle fusion events may take place 'preferentially' at the basolateral endothelial compartments. Alternatively, the local concentration of homogenously released chemokines could remain higher at basolateral compartments protected from extensive dilution by blood flow. Notably, inflammatory chemokine vesicles promote the transendothelial migration of lymphocytes independently of endothelial cell agonists or secretagogues[31] such as histamine (unpublished data). In support of their partitioning in the pool of constitutive Golgi-derived secretory vesicles[41], the transendothelial migration–promoting activities of CCL2 persisted even after inhibition of RalA (unpublished results), a GTPase essential for regulated granule release[42].

Primary inflammatory cytokines such as TNF, IL-1β and IFN-γ have been suggested to promote leukocyte trafficking by triggering endothelial expression of selectins and integrin ligands[43]. Our results extend that view, suggesting that these cytokines also act directly on endothelial barriers to promote endothelial transcription, packaging, transport and confined secretion of multiple inflammatory chemokines that are able to promote robust transendothelial migration of lymphocytes. In highly inflamed sites, neutrophils, monocytes and effector lymphocytes may secrete similar or additional inflammatory chemokines to augment the transendothelial migration of additional circulating effector and memory lymphocytes[44]. However, these extraendothelial attractants would be more prone to proteolytic inactivation by leukocyte, stromal and endothelial proteases[39] and to rapid clearance by decoy intereceptors[45] than their chemokine counterparts stored in the endothelium.

In conclusion, we predict from our data that lymphocyte extravasation at sites of inflammation would be substantially resistant to antibody-mediated chemokine blocking or to interference with chemokine-glycosaminoglycan interactions[46] *in vivo*. Therapeutic intervention in the transendothelial migration of lymphocytes would require the simultaneous blockade of multiple inflammatory GPCRs rather than of their cognate chemokines. Effective intervention may therefore require more upstream interference with signaling via TNF, IL-1β and IFN-γ to vascular endothelial cells to slow the upregulation of integrin ligands critical for the optimal response of recruited effector lymphocytes to chemokines produced in the endothelium.

METHODS

Methods and any associated references are available in the online version of the paper at http://www.nature.com/natureimmunology/.

Note: Supplementary information is available on the Nature Immunology website.

ACKNOWLEDGMENTS

We thank R. Wedlich-Soeldner (Max-Planck Institute for Biochemistry) for Lifeact-mRFP; A. Bershadsky (Weizmann Institute) for α-tubulin–mCherry; B. Geiger (Weizmann Institute) for paxillin-CFP; F. Sanchez-Madrid (Universidad Autónoma de Madrid) for ICAM-1-EGFP; Y. Kloog (Tel-Aviv University) for eGFP-th; R. Pardi (Dibit-Scientific Institute San Raffaele) for Rab11-DsRed; G. Shakhar and M. Fernandez-Borja for discussions, and S. Schwarzbaum for editorial assistance. Supported by The Linda Jacobs Chair in Immune and Stem Cell Research (R.A.), the Israel Science Foundation (R.A.), the Minerva Foundation, the Flight Attendant Medical Research Institute Foundation (R.A.) and the Germany-Israel Science Foundation (R.A.).

AUTHOR CONTRIBUTIONS

Z.S. designed the *in vitro* models, did most of the experiments and wrote parts of the manuscript; S.J.C. designed and did major parts of **Figures 1** and **5b**, and **Supplementary Figures 2** and **3**; B.R., V.K. and R.J. did multiphoton intravital imaging; V.G. and L.S.-B. did flow chamber studies; S.W.F. did flow chamber experiments, biochemistry and data organization; E.K. and V.S. did EM analysis; T.M. did chemokine-GFP cloning; S.M.N. did LFA-1 phosphorylation analysis; I.G. did T_H1-T_C1 analysis; O.H. did GPCR blocker synthesis; C.G.G., A.E., W.W. and A.B.-B. supervised specific parts of the research; and R.A. designed the study, supervised the work and wrote the manuscript.

COMPETING FINANCIAL INTERESTS

The authors declare no competing financial interests.

Published online at http://www.nature.com/natureimmunology/.
Reprints and permissions information is available online at http://www.nature.com/reprints/index.html.

1. Campbell, J.J. & Butcher, E.C. Chemokines in tissue-specific and microenvironment-specific lymphocyte homing. *Curr. Opin. Immunol.* **12**, 336–341 (2000).
2. Ley, K., Laudanna, C., Cybulsky, M.I. & Nourshargh, S. Getting to the site of inflammation: the leukocyte adhesion cascade updated. *Nat. Rev. Immunol.* **7**, 678–689 (2007).

Carl_G_190x270_mm_blokki_FINAL.indd 510 06-Aug-23 1:55:24 PM

3. Thelen, M. & Stein, J.V. How chemokines invite leukocytes to dance. *Nat. Immunol.* **9**, 953–959 (2008).
4. Shulman, Z. *et al.* Lymphocyte crawling and transendothelial migration require chemokine triggering of high-affinity LFA-1 integrin. *Immunity* **30**, 384–396 (2009).
5. Schreiber, T.H., Shinder, V., Cain, D.W., Alon, R. & Sackstein, R. Shear flow-dependent integration of apical and subendothelial chemokines in T-cell transmigration: implications for locomotion and the multistep paradigm. *Blood* **109**, 1381–1386 (2007).
6. Carman, C.V. *et al.* Transcellular diapedesis is initiated by invasive podosomes. *Immunity* **26**, 784–797 (2007).
7. Ravkov, E.V., Myrick, C.M. & Altman, J.D. Immediate early effector functions of virus-specific $CD8^{+}CCR7^{+}$ memory cells in humans defined by HLA and CC chemokine ligand 19 tetramers. *J. Immunol.* **170**, 2461–2468 (2003).
8. Shiow, L.R. *et al.* CD69 acts downstream of interferon-α/β to inhibit S1P1 and lymphocyte egress from lymphoid organs. *Nature* **440**, 540–544 (2006).
9. von Andrian, U.H. & Mackay, C.R. T-cell function and migration. Two sides of the same coin. *N. Engl. J. Med.* **343**, 1020–1034 (2000).
10. Masopust, D. *et al.* Activated primary and memory CD8 T cells migrate to nonlymphoid tissues regardless of site of activation or tissue of origin. *J. Immunol.* **172**, 4875–4882 (2004).
11. Bromley, S.K., Mempel, T.R. & Luster, A.D. Orchestrating the orchestrators: chemokines in control of T cell traffic. *Nat. Immunol.* **9**, 970–980 (2008).
12. Xie, H., Lim, Y.C., Luscinskas, F.W. & Lichtman, A.H. Acquisition of selectin binding and peripheral homing properties by $CD4^{+}$ and $CD8^{+}$ T cells. *J. Exp. Med.* **189**, 1765–1776 (1999).
13. Siegelman, M.H., Stanescu, D. & Estess, P. The CD44-initiated pathway of T-cell extravasation uses VLA-4 but not LFA-1 for firm adhesion. *J. Clin. Invest.* **105**, 683–691 (2000).
14. Warnock, R.A., Askari, S., Butcher, E.C. & von Andrian, U.H. Molecular mechanisms of lymphocyte homing to peripheral lymph nodes. *J. Exp. Med.* **187**, 205–216 (1998).
15. Shulman, Z. & Alon, R. Real-time *in vitro* assays for studying the role of chemokines in lymphocyte transendothelial migration under physiologic flow conditions. *Methods Enzymol.* **461**, 311–332 (2009).
16. McKinstry, K.K. *et al.* Rapid default transition of CD4 T cell effectors to functional memory cells. *J. Exp. Med.* **204**, 2199–2211 (2007).
17. Lim, Y.C. *et al.* α4 β1-integrin activation is necessary for high-efficiency T-cell subset interactions with VCAM-1 under flow. *Microcirculation* **7**, 201–214 (2000).
18. Constantin, G. *et al.* Chemokines trigger immediate β_2 integrin affinity and mobility changes: differential regulation and roles in lymphocyte arrest under flow. *Immunity* **13**, 759–769 (2000).
19. Beals, C.R., Edwards, A.C., Gottschalk, R.J., Kuijpers, T.W. & Staunton, D.E. CD18 activation epitopes induced by leukocyte activation. *J. Immunol.* **167**, 6113–6122 (2001).
20. Bolomini-Vittori, M. *et al.* Regulation of conformer-specific activation of the integrin LFA-1 by a chemokine-triggered Rho signaling module. *Nat. Immunol.* **10**, 185–194 (2009).
21. Fagerholm, S.C., Hilden, T.J., Nurmi, S.M. & Gahmberg, C.G. Specific integrin α and β chain phosphorylations regulate LFA-1 activation through affinity-dependent and -independent mechanisms. *J. Cell Biol.* **171**, 705–715 (2005).
22. Baker, R.G. & Koretzky, G.A. Regulation of T cell integrin function by adapter proteins. *Immunol. Res.* **42**, 132–144 (2008).
23. Hogg, N., Patzak, I. & Willenbrock, F. The insider's guide to leukocyte integrin signalling and function. *Nat. Rev. Immunol.* **11**, 416–426 (2011).
24. Atarashi, K., Hirata, T., Matsumoto, M., Kanemitsu, N. & Miyasaka, M. Rolling of Th1 cells via P-selectin glycoprotein ligand-1 stimulates LFA-1-mediated cell binding to ICAM-1. *J. Immunol.* **174**, 1424–1432 (2005).
25. Cinamon, G., Shinder, V. & Alon, R. Shear forces promote lymphocyte migration across vascular endothelium bearing apical chemokines. *Nat. Immunol.* **2**, 515–522 (2001).
26. Woolf, E. *et al.* Lymph node chemokines promote sustained T lymphocyte motility without triggering stable integrin adhesiveness in the absence of shear forces. *Nat. Immunol.* **8**, 1076–1085 (2007).
27. Zhang, H.H. *et al.* CCR2 identifies a stable population of human effector memory $CD4^{+}$ T cells equipped for rapid recall response. *J. Immunol.* **185**, 6646–6663 (2010).
28. Cinamon, G., Shinder, V., Shamri, R. & Alon, R. Chemoattractant signals and β_2 integrin occupancy at apical endothelial contacts combine with shear stress signals to promote transendothelial neutrophil migration. *J. Immunol.* **173**, 7282–7291 (2004).
29. Hillyer, P., Mordelet, E., Flynn, G. & Male, D. Chemokines, chemokine receptors and adhesion molecules on different human endothelia: discriminating the tissue-specific functions that affect leucocyte migration. *Clin. Exp. Immunol.* **134**, 431–441 (2003).
30. Bao, X. *et al.* Endothelial heparan sulfate controls chemokine presentation in recruitment of lymphocytes and dendritic cells to lymph nodes. *Immunity* **33**, 817–829 (2010).
31. Øynebråten, I., Bakke, O., Brandtzaeg, P., Johansen, F.E. & Haraldsen, G. Rapid chemokine secretion from endothelial cells originates from 2 distinct compartments. *Blood* **104**, 314–320 (2004).
32. Øynebråten, I. *et al.* Characterization of a novel chemokine-containing storage granule in endothelial cells: evidence for preferential exocytosis mediated by protein kinase A and diacylglycerol. *J. Immunol.* **175**, 5358–5369 (2005).
33. Klausner, R.D., Donaldson, J.G. & Lippincott-Schwartz, J. Brefeldin A: insights into the control of membrane traffic and organelle structure. *J. Cell Biol.* **116**, 1071–1080 (1992).
34. Mamdouh, Z., Mikhailov, A. & Muller, W.A. Transcellular migration of leukocytes is mediated by the endothelial lateral border recycling compartment. *J. Exp. Med.* **206**, 2795–2808 (2009).
35. Middleton, J. *et al.* Transcytosis and surface presentation of IL-8 by venular endothelial cells. *Cell* **91**, 385–395 (1997).
36. Palframan, R.T. *et al.* Inflammatory chemokine transport and presentation in HEV: a remote control mechanism for monocyte recruitment to lymph nodes in inflamed tissues. *J. Exp. Med.* **194**, 1361–1373 (2001).
37. Pruenster, M. *et al.* The Duffy antigen receptor for chemokines transports chemokines and supports their promigratory activity. *Nat. Immunol.* **10**, 101–108 (2009).
38. Guarda, G. *et al.* L-selectin-negative CCR7-effector and memory $CD8^{+}$ T cells enter reactive lymph nodes and kill dendritic cells. *Nat. Immunol.* **8**, 743–752 (2007).
39. Wolf, M., Albrecht, S. & Marki, C. Proteolytic processing of chemokines: implications in physiological and pathological conditions. *Int. J. Biochem. Cell Biol.* **40**, 1185–1198 (2008).
40. Sauty, A. *et al.* The T cell-specific CXC chemokines IP-10, Mig, and I-TAC are expressed by activated human bronchial epithelial cells. *J. Immunol.* **162**, 3549–3558 (1999).
41. Park, J.J. & Loh, Y.P. How peptide hormone vesicles are transported to the secretion site for exocytosis. *Mol. Endocrinol.* **22**, 2583–2595 (2008).
42. Rondaij, M.G. *et al.* Guanine exchange factor RalGDS mediates exocytosis of Weibel-Palade bodies from endothelial cells. *Blood* **112**, 56–63 (2008).
43. Pober, J.S. & Sessa, W.C. Evolving functions of endothelial cells in inflammation. *Nat. Rev. Immunol.* **7**, 803–815 (2007).
44. Soehnlein, O., Lindbom, L. & Weber, C. Mechanisms underlying neutrophil-mediated monocyte recruitment. *Blood* **114**, 4613–4623 (2009).
45. Jamieson, T. *et al.* The chemokine receptor D6 limits the inflammatory response *in vivo*. *Nat. Immunol.* **6**, 403–411 (2005).
46. Proudfoot, A.E. The biological relevance of chemokine-proteoglycan interactions. *Biochem. Soc. Trans.* **34**, 422–426 (2006).

Carl_G_190x270_mm_blokki_FINAL.indd 511 06-Aug-23 1:55:24 PM

ONLINE METHODS

Cells. HUVECs and HDMECs were cultured according to the supplier's instructions (Promocell). All *in vitro* experiments with human leukocytes were approved by the Institutional Review Board of the Rambam Medical Center, in accordance with the provisions of the Declaration of Helsinki. Human T cells were isolated from citrate-anticoagulated whole blood of healthy donors by dextran sedimentation and density separation over Ficoll-Hypaque as described[47]. The resulting peripheral blood T cells (>90% $CD3^+$ T cells) were either cultured for 16–18 h before experiments or used for the production of effector lymphocytes by seeding on plates coated with anti-CD3 (OKT3; Biolegend) and anti-CD28 (CD28.2; Biolegend) and culture for 9–12 d with IL-2 (ref. 15). Before experiments, effector lymphocytes were washed and kept overnight in fresh IL-2-containing medium. The generation of mouse effector T cells is described in the **Supplementary Methods**. All animal procedures were approved by the Animal Research Committees at the Weizmann Institute of Science and the University of Sydney Animal Ethics Committee.

GPCR blockers. The CCR2 blocker BMS CCR2 22 (1 μM) was from Tocris Bioscience. The CCR1 and CCR5 blocker Met-RANTES (100 nM) was synthesized[48]. The CXCR3 blocker AMG487 (15 μM) was from Amgen. The CXCR4 blocker AMD3100 (10 μM) was from Sigma-Aldrich. Cells were incubated for 30 min with each blocker and all blockers were left in the medium throughout the assays.

Analysis of T cell migration under shear flow. Unless otherwise indicated, primary HUVECs or HDMECs were plated at confluence on plastic- or glass-bottomed dishes spotted with fibronectin and were stimulated for 20–24 h with IL-1β (2 ng/ml) or TNF (2 ng/ml) alone or together with IFN-γ (2 ng/ml) as described[15]. Endothelial cell–coated plates were assembled in a flow chamber[47] and washed extensively. T cells were perfused over the endothelial cell monolayer in binding medium (Hank's balanced-salt solution containing 2 mg/ml of BSA and 10 mM HEPES, pH 7.4, supplemented with $CaCl_2$ and $MgCl_2$) for 40 s at a force of 1.5 dyn/cm^2 or at 0.75 dyn/cm^2 (accumulation phase) and then left under constant shear (5 dyn/cm^2) for 10 min. Images were either acquired in real time[47] or were recorded at a rate of four frames per minute for analysis of migration with a fluorescence microscope (DeltaVision system, Delta Vision Spectris RT, Applied Precision) equipped with 20× phase-contrast objective and motorized stage. Firm arrests were defined as lymphocytes arrested at a force of 1.5 dyn/cm^2 and remaining stuck for over 10 s when subjected to a force of 5 dyn/cm^2 (refs. 2,47). For analysis of migratory phenotype, T cells accumulated in three fields (~60 cells per field) were individually tracked and categorized as described[25]. The migratory phenotypes was calculated as the fraction of T cells originally accumulated. For blockade of integrin or GPCR signaling, T cells were preincubated with the appropriate blocking mAb (20 μg/ml; 5 min), the Src family kinase inhibitor PP2 (10 μM; 30 min), pertussis toxin (100 ng/ml; 18 h) or the PLC inhibitor U73122 (10 μM; 1 min). For blockade of endothelial chemokines, endothelial cell monolayers were pretreated for 30 min with the appropriate mAb (40 μg/ml), and T cells were perfused in continuous presence of mAb (kept at 2 μg/ml). For selective interference with vesicle production and transport, HUVECs were treated with brefeldin A (5 μg/ml; 1 h), nocodazole (5 μM diluted from 25 mM stock in DMSO; 10 min) or latrunculin A (5 μg/ml; 30 min) in medium containing TNF. For analysis of firm arrest on purified integrin ligands of T cells, Petri dishes were precoated with protein A (20 μg/ml) coated with ICAM-1–Fc (5 μg/ml) or VCAM-1–Fc (2 μg/ml)[47]. For analysis of chemokine-induced arrest, ICAM-1–Fc (1 μg/ml) or VCAM-1–Fc (0.5 μg/ml) was immobilized together with CXCL12 (2 μg/ml) on protein A (1 μg/ml). T cells were settled for 2 min on these various surfaces and exposed for 10 min to shear force (5 dyn/cm^2). Recorded videos were analyzed offline with ImageJ (NIH).

Fluorescence live-cell imaging. CCL2 was cloned into vector encoding eGFP or mCherry. Lifeact-mRFP was a gift from R. Wedlich-Soeldner; α-tubulin-mCherry was a gift from A. Bershadsky; paxillin-CFP was a gift from B. Geiger; ICAM-1-EGFP was a gift from F. Sanchez-Madrid; eGFP-th (a plasmid encoding the C-terminal nine amino acids of H-Ras and used as membranal marker) was gift from Y. Kloog; and Rab11-DsRed was a gift from R. Pardi. HUVEC monolayers were transiently transfected with the AMAXA nucleofection system (Lonza Cologne) and, after 16–40 h, cells were trypsinized, replated and stimulated with TNF. T cell migration was imaged as described above with PlanApo differential interference contrast objectives (60× oil-immersion objective with a numerical aperture of 1.4; 20× objective with a numerical aperture of 0.7). Images were obtained for 10 min at intervals of 15 s. For tracking of mobile CCL2 vesicles that moved or disappeared during the 2-minure recording period, images were acquired at intervals of 5 s and analyzed with the SoftWoRx software. Videos were analyzed offline with ImageJ software.

Fluorescence and electron microscopy of fixed samples. Samples were fixed with PBS containing 4% (wt/vol) paraformaldehyde and 2% (wt/vol) sucrose. For intracellular immunostaining, fixed cells were permeabilized with saponin (0.1% (wt/vol), 5 min), extensively washed, blocked with 10% (vol/vol) goat serum and incubated with either primary fluorescence-labeled mAb or unlabeled mAb, followed by secondary antibody or with the nuclear dye Hoechst 33342 or F-actin probe TRITC (tetramethylrhodamine isothiocyanate)-phalloidin. The DeltaVision system was used for fluorescence microscopy. Images were obtained with a PlanApo (differential interference contrast) objective (60× oil-immersion objective with a numerical aperture of 1.4). Sections were acquired as serial *z* stacks (0.2 μm apart) and were subjected to digital deconvolution and, where indicated, to three-dimensional reconstruction (SoftWoRx, Applied Precision).

For electron microscopy, cells were fixed and processed as described[4]. Correlative fluorescence and SEM of actin fibers was done by fixation and staining of HUVEC monolayers with TRITC-phalloidin. Fluorescent images were acquired with precisely defined coordinates later used for SEM.

Statistical analysis. All data were analyzed by Student's *t*-test. Group comparisons were deemed significant for two-tailed unpaired *P* values < 0.05.

Additional methods. Additional details of all *in vivo* experiments and some *in vitro* assays are in the **Supplementary Methods**.

47. Grabovsky, V. *et al.* Subsecond induction of α4 integrin clustering by immobilized chemokines stimulates leukocyte tethering and rolling on endothelial vascular cell adhesion molecule 1 under flow conditions. *J. Exp. Med.* **192**, 495–506 (2000).
48. Proudfoot, A.E. *et al.* Amino-terminally modified RANTES analogues demonstrate differential effects on RANTES receptors. *J. Biol. Chem.* **274**, 32478–32485 (1999).

doi:10.1038/ni.2173

Carl_G_190x270_mm_blokki_FINAL.indd 512 06-Aug-23 1:55:25 PM

Carl_G_190x270_mm_blokki_FINAL.indd 513 06-Aug-23 1:55:25 PM

Carl_G_190x270_mm_blokki_FINAL.indd 514 06-Aug-23 1:55:25 PM

Part VII

CONCLUDING REMARKS

Carl_G_190x270_mm_blokki_FINAL.indd 515 06-Aug-23 1:55:25 PM

Carl_G_190x270_mm_blokki_FINAL.indd 516 06-Aug-23 1:55:25 PM

It has not been that easy to choose the papers that I comment. Certainly, I have tried to collect for commenting the most important papers. The majority, have been published in good to top journals, but not all of them. Of course, fellow scientists mainly read the established journals and with good reason, but nowadays with advanced searching techniques, the publication forum is perhaps less important. Granting bodies often look for publications in high impact journals and count citations. Nothing can replace peer review by competent evaluators, and that should be encouraged.

I hope that this collection of papers gives a good summary of what I have done, but that it also gives background of the research process. Looking back, it is obvious that the development of new techniques profoundly changed the research during my active time, from the early 1970s to 2020s. SDS gel electrophoresis, monoclonal antibodies, cell surface labelling techniques, DNA sequencing, protein crystallography, protein and peptide mass spectrometry, cell imaging and computer science were all introduced, or greatly improved during the past 50 years. The development has meant that scientists now need to master or at least have some understanding of the various fields. This fact has made it necessary to develop common projects with other research groups, which is very positive. Let us hope that research in the future will further develop, and that the young generation will understand the importance of good basic research. This is necessary for the survival of mankind in an increasingly populated world.

Acknowledgements

I want to thank the Finnish Society of Sciences and Letters for publishing this book. My sincere thanks go to the Permanent Secretary Mats Gyllenberg and the Communications Officer Nadine Nousiainen. Professors Leif Andersson and Sarah Butcher took the time to read the manuscript. I am grateful to Minna Etsalo, who made the layout, which meant a lot of work. Furthermore, I appreciate that the publishers of the articles gave permission to reprint them.

June 5, 2023
Carl G. Gahmberg

Carl_G_190x270_mm_blokki_FINAL.indd 517 06-Aug-23 1:55:25 PM